Scientific and Technical Aerospace Reports

STAR

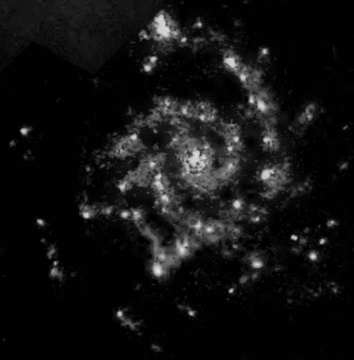

An Abstract Journal

Volume 32, Number 11
November 1994
N94-35226 to N94-36440

The NASA STI Program ... in Profile

Since its founding, NASA has been dedicated to the advancement of aeronautics and space science. The NASA Scientific and Technical Information (STI) Program plays a key part in helping NASA maintain this important role.

The NASA STI Program provides access to the NASA STI Database, the largest collection of aeronautical and space science STI in the world. The Program is also NASA's institutional mechanism for disseminating the results of its research and development activities.

Specialized services that help round out the Program's diverse offerings include creating custom thesauri, translating material to or from 34 foreign languages, building customized databases, organizing and publishing research results ... even providing videos.

For more information about the NASA STI Program, you can:

- **Phone** the NASA Access Help Desk at (301) 621-0390
- **Fax** your question to the NASA Access Help Desk at (301) 621-0134
- **E-mail** your question via the **Internet** to help@sti.nasa.gov
- **Write** to:

NASA Access Help Desk
NASA Center for AeroSpace Information
800 Elkridge Landing Road
Linthicum Heights, MD 21090-2934

Scientific and Technical Aerospace Reports

STAR

Scientific and Technical Aerospace Reports (STAR), is published each month as a major product of the NASA Scientific and Technical Information (STI) Program.

Inside this issue you will find:

- **Front Matter** containing a typical citation and abstract sample explaining the standard format, including codes for ordering reports
- **An Abstract Section** containing citations and abstracts of reports and publications that provide comprehensive coverage of worldwide aerospace-related topics including aeronautics and space science technology. *STAR* lists published and publicly available reports entered into the NASA STI Database during the four weeks preceding publication of this issue. These citations and abstracts are listed by subject categories.
- **An Index Section**
  - Subject
  - Personal author
  - Corporate source
  - Contract number
  - Report number
- **An Appendix** containing a guide for ordering cited reports, registering with the NASA STI Program, and using the available products and services. Additionally, price schedules, phone numbers, and addresses are included in this information packed section.

NASA also sponsors the companion journal, *NASA Open Volumes on Aerospace (NOVA),* which lists abstracts of the open literature on aerospace subjects available worldwide. *NOVA* is for internal NASA use only, available from the NASA Center for AeroSpace Information (CASI).

Entries found in *STAR* are available through the NASA online retrieval service, RECON, and through DIALOG as the Aerospace Database.

The NASA STI Program gathers information through national and international agreements and exchanges and makes this information available to the NASA community and to the public in many forms through various outlets.

For additional information on the NASA STI Program, call the NASA Access Help Desk at (301) 621-0390, or write to:

NASA Center for AeroSpace Information
800 Elkridge Landing Road
Linthicum Heights, Maryland 21090-2934

US ISSN 0036-8741

This publication was prepared by the NASA Center for AeroSpace Information,
800 Elkridge Landing Road, Linthicum Heights, MD 21090-2934, (301) 621-0390.

Volume 32 Number 11 / November1994

TABLE OF CONTENTS

AERONAUTICS For related information see also *Astronautics.*

01 AERONAUTICS (GENERAL) 4189

02 AERODYNAMICS 4189
Includes aerodynamics of bodies, combinations, wings, rotors, and control surfaces; and internal flow in ducts and turbomachinery. For related information see also *34 Fluid Mechanics and Heat Transfer.*

03 AIR TRANSPORTATION AND SAFETY 4191
Includes passenger and cargo air transport operations; and aircraft accidents. For related information see also *16 Space Transportation* and *85 Urban Technology and Transportation.*

04 AIRCRAFT COMMUNICATIONS AND NAVIGATION 4192
Includes digital and voice communication with aircraft; air navigation systems (satellite and ground based); and air traffic control. For related information see also *17 Space Communications, Spacecraft Communications, Command and Tracking* and *32 Communications and Radar.*

05 AIRCRAFT DESIGN, TESTING AND PERFORMANCE 4193
Includes aircraft simulation technology. For related information see also *18 Spacecraft Design, Testing and Performance* and *39 Structural Mechanics.* For land transportation vehicles see *85 Urban Technology and Transportation.*

06 AIRCRAFT INSTRUMENTATION 4198
Includes cockpit and cabin display devices; and flight instruments. For related information see also *19 Spacecraft Instrumentation* and *35 Instrumentation and Photography.*

07 AIRCRAFT PROPULSION AND POWER 4198
Includes prime propulsion systems and systems components, e.g., gas turbine engines and compressors; and onboard auxiliary power plants for aircraft. For related information see also *20 Spacecraft Propulsion and Power, 28 Propellants and Fuels,* and *44 Energy Production and Conversion.*

08 AIRCRAFT STABILITY AND CONTROL 4199
Includes aircraft handling qualities; piloting; flight controls; and autopilots. For related information see also *05 Aircraft Design, Testing and Performance.*

09 RESEARCH AND SUPPORT FACILITIES (AIR) 4200
Includes airports, hangars and runways; aircraft repair and overhaul facilities; wind tunnels; shock tubes; and aircraft engine test stands. For related information see also *14 Ground Support Systems and Facilities (Space).*

ASTRONAUTICS For related information see also *Aeronautics.*

12 ASTRONAUTICS (GENERAL) 4201
For extraterrestrial exploration see *91 Lunar and Planetary Exploration.*

13 ASTRODYNAMICS 4202
Includes powered and free-flight trajectories; and orbital and launching dynamics.

14 GROUND SUPPORT SYSTEMS AND FACILITIES (SPACE) .... N.A.
Includes launch complexes, research and production facilities; ground support equipment, e.g., mobile transporters; and simulators. For related information see also *09 Research and Support Facilities (Air).*

15 LAUNCH VEHICLES AND SPACE VEHICLES 4210
Includes boosters; operating problems of launch/space vehicle systems; and reusable vehicles. For related information see also *20 Spacecraft Propulsion and Power.*

16 SPACE TRANSPORTATION 4211
Includes passenger and cargo space transportation, e.g., shuttle operations; and space rescue techniques. For related information see also *03 Air Transportation and Safety* and *18 Spacecraft Design, Testing and Performance.* For space suits see *54 Man/System Technology and Life Support.*

17 SPACE COMMUNICATIONS, SPACECRAFT COMMUNICATIONS, COMMAND AND TRACKING 4211
Includes telemetry; space communications networks; astronavigation and guidance; and radio blackout. For related information see also *04 Aircraft Communications and Navigation* and *32 Communications and Radar.*

N.A.—No abstracts were assigned to this category for this issue.

18 SPACECRAFT DESIGN, TESTING AND PERFORMANCE 4212
Includes satellites; space platforms; space stations; spacecraft systems and components such as thermal and environmental controls; and attitude controls. For life support systems see *54 Man/System Technology and Life Support.* For related information see also *05 Aircraft Design, Testing and Performance, 39 Structural Mechanics*, and *16 Space Transportation.*

19 SPACECRAFT INSTRUMENTATION 4227
For related information see also *06 Aircraft Instrumentation* and *35 Instrumentation and Photography.*

20 SPACECRAFT PROPULSION AND POWER 4228
Includes main propulsion systems and components, e.g., rocket engines; and spacecraft auxiliary power sources. For related information see also *07 Aircraft Propulsion and Power, 28 Propellants and Fuels, 44 Energy Production and Conversion*, and *15 Launch Vehicles and Space Vehicles.*

CHEMISTRY AND MATERIALS

23 CHEMISTRY AND MATERIALS (GENERAL) 4229

24 COMPOSITE MATERIALS 4232
Includes physical, chemical, and mechanical properties of laminates and other composite materials. For ceramic materials see *27 Nonmetallic Materials.*

25 INORGANIC AND PHYSICAL CHEMISTRY 4235
Includes chemical analysis, e.g., chromatography; combustion theory; electrochemistry; and photochemistry. For related information see also *77 Thermodynamics and Statistical Physics.*

26 METALLIC MATERIALS 4240
Includes physical, chemical, and mechanical properties of metals, e.g., corrosion; and metallurgy.

27 NONMETALLIC MATERIALS 4242
Includes physical, chemical, and mechanical properties of plastics, elastomers, lubricants, polymers, textiles, adhesives, and ceramic materials. For composite materials see *24 Composite Materials.*

28 PROPELLANTS AND FUELS 4247
Includes rocket propellants, igniters and oxidizers; their storage and handling procedures; and aircraft fuels. For related information see also *07 Aircraft Propulsion and Power, 20 Spacecraft Propulsion and Power*, and *44 Energy Production and Conversion.*

29 MATERIALS PROCESSING 4249
Includes space-based development of products and processes for commercial application. For biological materials see *55 Space Biology:*

ENGINEERING For related information see also *Physics.*

31 ENGINEERING (GENERAL) 4249
Includes vacuum technology; control engineering; display engineering; cryogenics; and fire prevention.

32 COMMUNICATIONS AND RADAR 4251
Includes radar; land and global communications; communications theory; and optical communications. For related information see also *04 Aircraft Communications and Navigation* and *17 Space Communications, Spacecraft Communications, Command and Tracking.* For search and rescue see *03 Air Transportation and Safety*, and *16 Space Transportation.*

33 ELECTRONICS AND ELECTRICAL ENGINEERING 4257
Includes test equipment and maintainability; components, e.g., tunnel diodes and transistors; microminiaturization; and integrated circuitry. For related information see also *60 Computer Operations and Hardware* and *76 Solid-State Physics.*

34 FLUID MECHANICS AND HEAT TRANSFER 4262
Includes boundary layers; hydrodynamics; fluidics; mass transfer and ablation cooling. For related information see also *02 Aerodynamics* and *77 Thermodynamics and Statistical Physics.*

35 INSTRUMENTATION AND PHOTOGRAPHY 4268
Includes remote sensors; measuring instruments and gauges; detectors; cameras and photographic supplies; and holography. For aerial photography see *43 Earth Resources and Remote Sensing.* For related information see also *06 Aircraft Instrumentation* and *19 Spacecraft Instrumentation.*

36 LASERS AND MASERS 4270
Includes parametric amplifiers. For related information see also *76 Solid-State Physics.*

37 MECHANICAL ENGINEERING ... 4273
Includes auxiliary systems (nonpower); machine elements and processes; and mechanical equipment.

38 QUALITY ASSURANCE AND RELIABILITY ... 4278
Includes product sampling procedures and techniques; and quality control.

39 STRUCTURAL MECHANICS ... 4278
Includes structural element design and weight analysis; fatigue; and thermal stress. For applications see *05 Aircraft Design, Testing and Performance* and *18 Spacecraft Design, Testing and Performance*.

GEOSCIENCES For related information see also *Space Sciences*.

42 GEOSCIENCES (GENERAL) ... N.A.

43 EARTH RESOURCES AND REMOTE SENSING ... 4281
Includes remote sensing of earth resources by aircraft and spacecraft; photogrammetry; and aerial photography. For instrumentation see *35 Instrumentation and Photography*.

44 ENERGY PRODUCTION AND CONVERSION ... 4281
Includes specific energy conversion systems, e.g., fuel cells; global sources of energy; geophysical conversion; and windpower. For related information see also *07 Aircraft Propulsion and Power, 20 Spacecraft Propulsion and Power,* and *28 Propellants and Fuels.*

45 ENVIRONMENT POLLUTION ... 4284
Includes atmospheric, noise, thermal, and water pollution.

46 GEOPHYSICS ... 4288
Includes aeronomy; upper and lower atmosphere studies; ionospheric and magnetospheric physics; and geomagnetism. For space radiation see *93 Space Radiation.*

47 METEOROLOGY AND CLIMATOLOGY ... 4292
Includes weather forecasting and modification.

48 OCEANOGRAPHY ... 4295
Includes biological, dynamic, and physical oceanography; and marine resources. For related information see also *43 Earth Resources and Remote Sensing.*

LIFE SCIENCES

51 LIFE SCIENCES (GENERAL) ... 4296

52 AEROSPACE MEDICINE ... 4297
Includes physiological factors; biological effects of radiation; and effects of weightlessness on man and animals.

53 BEHAVIORAL SCIENCES ... 4297
Includes psychological factors; individual and group behavior; crew training and evaluation; and psychiatric research.

54 MAN/SYSTEM TECHNOLOGY AND LIFE SUPPORT ... 4298
Includes human engineering; biotechnology; and space suits and protective clothing. For related information see also *16 Space Transportation.*

55 SPACE BIOLOGY ... N.A.
Includes exobiology; planetary biology; and extraterrestrial life.

MATHEMATICAL AND COMPUTER SCIENCES

59 MATHEMATICAL AND COMPUTER SCIENCES (GENERAL) ... 4299

60 COMPUTER OPERATIONS AND HARDWARE ... 4300
Includes hardware for computer graphics, firmware, and data processing. For components see *33 Electronics and Electrical Engineering.*

61 COMPUTER PROGRAMMING AND SOFTWARE ... 4300
Includes computer programs, routines, algorithms, and specific applications, e.g., CAD/CAM.

62 COMPUTER SYSTEMS ... 4310
Includes computer networks and special application computer systems.

63 CYBERNETICS **4311**
Includes feedback and control theory, artificial intelligence, robotics and expert systems. For related information see also *54 Man/System Technology and Life Support.*

64 NUMERICAL ANALYSIS **4313**
Includes iteration, difference equations, and numerical approximation.

65 STATISTICS AND PROBABILITY **4316**
Includes data sampling and smoothing; Monte Carlo method; and stochastic processes.

66 SYSTEMS ANALYSIS **4317**
Includes mathematical modeling; network analysis; and operations research.

67 THEORETICAL MATHEMATICS **4317**
Includes topology and number theory.

PHYSICS For related information see also *Engineering.*

70 PHYSICS (GENERAL) **4317**
For precision time and time interval (PTTI) see *35 Instrumentation and Photography*; for geophysics, astrophysics or solar physics see *46 Geophysics, 90 Astrophysics*, or *92 Solar Physics.*

71 ACOUSTICS **4319**
Includes sound generation, transmission, and attenuation. For noise pollution see *45 Environment Pollution.*

72 ATOMIC AND MOLECULAR PHYSICS **4319**
Includes atomic structure, electron properties, and molecular spectra.

73 NUCLEAR AND HIGH-ENERGY PHYSICS **4330**
Includes elementary and nuclear particles; and reactor theory. For space radiation see *93 Space Radiation.*

74 OPTICS **4332**
Includes light phenomena and optical devices. For lasers see *36 Lasers and Masers.*

75 PLASMA PHYSICS **4335**
Includes magnetohydrodynamics and plasma fusion. For ionospheric plasmas see *46 Geophysics.* For space plasmas see *90 Astrophysics.*

76 SOLID-STATE PHYSICS **4339**
Includes superconductivity. For related information see also *33 Electronics and Electrical Engineering* and *36 Lasers and Masers.*

77 THERMODYNAMICS AND STATISTICAL PHYSICS **4342**
Includes quantum mechanics; theoretical physics; and Bose and Fermi statistics. For related information see also *25 Inorganic and Physical Chemistry* and *34 Fluid Mechanics and Heat Transfer.*

SOCIAL SCIENCES

80 SOCIAL SCIENCES (GENERAL) **4343**
Includes educational matters.

81 ADMINISTRATION AND MANAGEMENT **4343**
Includes management planning and research.

82 DOCUMENTATION AND INFORMATION SCIENCE **4344**
Includes information management; information storage and retrieval technology; technical writing; graphic arts; and micrography. For computer documentation see *61 Computer Programming and Software.*

83 ECONOMICS AND COST ANALYSIS **4347**
Includes cost effectiveness studies.

84 LAW, POLITICAL SCIENCE AND SPACE POLICY **4348**
Includes NASA appropriation hearings; aviation law; space law and policy; international law; international cooperation; and patent policy.

85 URBAN TECHNOLOGY AND TRANSPORTATION **4348**
Includes applications of space technology to urban problems; technology transfer; technology assessment; and surface and mass transportation. For related information see *03 Air Transportation and Safety, 16 Space Transportation,* and *44 Energy Production and Conversion.*

SPACE SCIENCES For related information see also *Geosciences.*

88 SPACE SCIENCES (GENERAL) .... N.A.

89 ASTRONOMY 4349
Includes radio, gamma-ray, and infrared astronomy; and astrometry.

90 ASTROPHYSICS 4350
Includes cosmology; celestial mechanics; space plasmas; and interstellar and interplanetary gases and dust. For related information see also *75 Plasma Physics.*

91 LUNAR AND PLANETARY EXPLORATION 4354
Includes planetology; and manned and unmanned flights. For spacecraft design or space stations see *18 Spacecraft Design, Testing and Performance.*

92 SOLAR PHYSICS 4374
Includes solar activity, solar flares, solar radiation and sunspots. For related information see also *93 Space Radiation.*

93 SPACE RADIATION 4375
Includes cosmic radiation; and inner and outer earth's radiation belts. For biological effects of radiation see *52 Aerospace Medicine.* For theory see *73 Nuclear and High-Energy Physics.*

GENERAL

Includes aeronautical, astronautical, and space science related histories, biographies, and pertinent reports too broad for categorization; histories or broad overviews of NASA programs.

99 GENERAL 4376

SUBJECT INDEX I-1

PERSONAL AUTHOR INDEX I-79

CORPORATE SOURCE INDEX I-89

CONTRACT NUMBER INDEX I-103

REPORT NUMBER INDEX I-107

APPENDIX A-1

TYPICAL CITATION AND ABSTRACT

NASA SPONSORED ⟶ **ON MICROFICHE**

ACCESSION NUMBER →	**N94-12270*#** United Technologies Corp., West Palm Beach, FL. Pratt and Whitney.	← **CORPORATE SOURCE**
TITLE →	**ADVANCED CONTROL FOR AIRBREATHING ENGINES, VOLUME 1: PRATT AND WHITNEY**	
AUTHOR →	J. A. Ralph Jul. 1993 83 p	← **PUBLICATION DATE**
CONTRACT OR GRANT →	(Contract NAS3-25952; RTOP 505-62-61)	
REPORT NUMBERS →	(NASA-CR-189203; E-8006; NAS 1.26:189203) Avail: CASI HC A05/MF A01	← **AVAILABILITY SOURCE AND PRICE CODE**

The application of advanced control concepts to air breathing engines may yield significant improvements in aircraft/engine performance and operability. Screening studies of advanced control concepts for air breathing engines were conducted by three major domestic aircraft engine manufacturers to determine the potential impact of concepts on turbine engine performance and operability. The purpose of the studies was to identify concepts which offered high potential yet may incur high research and development risk. A target suite of proposed advanced control concepts was formulated and evaluated in a two phase study to quantify each concept's impact on desired engine characteristics. To aid in the evaluation specific aircraft/engine combinations were considered: a Military High Performance Fighter mission, a High Speed Civil Transport mission, and a Civil Tiltrotor mission. Each of the advanced control concepts considered in the study are defined and described. The concept potential impact on engine performance was determined. Relevant figures of merit on which to evaluate the concepts are determined. Finally, the concepts are ranked with respect to the target aircraft/engine missions. A final report describing the screening studies was prepared by each engine manufacturer. Volume 1 of these reports describes the studies performed by Pratt & Whitney. Author (revised)

VOLUME 32 NUMBER 11/November 1994

Scientific and Technical Aerospace Reports

A Monthly Publication of the National Aeronautics and Space Administration

01 AERONAUTICS (GENERAL)

N94-35338* National Aeronautics and Space Administration, Washington, DC.
AERONAUTICAL ENGINEERING: A CONTINUING BIBLIOGRAPHY WITH INDEXES (SUPPLEMENT 306)
Jul. 1994 75 p
(NASA-SP-7037(306); NAS 1.21:7037(306)) Avail: CASI HC A04

This bibliography lists 181 reports, articles, and other documents recently introduced into the NASA STI Database. Subject coverage includes the following: design, construction and testing of aircraft and aircraft engines; aircraft components, equipment, and systems; ground support systems; and theoretical and applied aspects of aerodynamics and general fluid dynamics. Author (revised)

N94-35394*# National Aeronautics and Space Administration. Ames Research Center, Moffett Field, CA.
FLIGHT TESTING OF A LUMINESCENT SURFACE PRESSURE SENSOR
B. G. McLachlan, J. H. Bell, J. Espina, J. Gallery, M. Gouterman, C. G. N. Demandante, and L. Bjarke Oct. 1992 28 p
(RTOP 537-03-23)
(NASA-TM-103970; A-92175; NAS 1.15:103970) Avail: CASI HC A03/MF A01

NASA ARC has conducted flight tests of a new type of aerodynamic pressure sensor based on a luminescent surface coating. Flights were conducted at the NASA ARC-Dryden Flight Research Facility. The luminescent pressure sensor is based on a surface coating which, when illuminated with ultraviolet light, emits visible light with an intensity dependent on the local air pressure on the surface. This technique makes it possible to obtain pressure data over the entire surface of an aircraft, as opposed to conventional instrumentation, which can only make measurements at pre-selected points. The objective of the flight tests was to evaluate the effectiveness and practicality of a luminescent pressure sensor in the actual flight environment. A luminescent pressure sensor was installed on a fin, the Flight Test Fixture (FTF), that is attached to the underside of an F-104 aircraft. The response of one particular surface coating was evaluated at low supersonic Mach numbers ($M = 1.0$-1.6) in order to provide an initial estimate of the sensor's capabilities. This memo describes the test approach, the techniques used, and the pressure sensor's behavior under flight conditions. A direct comparison between data provided by the luminescent pressure sensor and that produced by conventional pressure instrumentation shows that the luminescent sensor can provide quantitative data under flight conditions. However, the test results also show that the sensor has a number of limitations which must be addressed if this technique is to prove useful in the flight environment. Author (revised)

02 AERODYNAMICS

Includes aerodynamics of bodies, combinations, wings, rotors, and control surfaces; and internal flow in ducts and turbomachinery.

For related information see also *34 Fluid Mechanics and Heat Transfer.*

N94-35246*# National Aeronautics and Space Administration. Langley Research Center, Hampton, VA.
LANGLEY 14- BY 22-FOOT SUBSONIC TUNNEL TEST ENGINEER'S DATA ACQUISITION AND REDUCTION MANUAL
P. Frank Quinto and Nettie M. Orie Jun. 1994 63 p
(RTOP 535-03-10-02)
(NASA-TM-4563; L-17263; NAS 1.15:4563) Avail: CASI HC A04/MF A01

The Langley 14- by 22-Foot Subsonic Tunnel is used to test a large variety of aircraft and nonaircraft models. To support these investigations, a data acquisition system has been developed that has both static and dynamic capabilities. The static data acquisition and reduction system is described; the hardware and software of this system are explained. The theory and equations used to reduce the data obtained in the wind tunnel are presented; the computer code is not included. Author

N94-35360# Sandia National Labs., Albuquerque, NM.
A REVIEW AND DEVELOPMENT OF CORRELATIONS FOR BASE PRESSURE AND BASE HEATING IN SUPERSONIC FLOW
J. Parker Lamb (Texas Univ., Austin, TX.) and William L. Oberkampf Nov. 1993 79 p
(Contract DE-AC04-94AL-85000)
(SAND93-0280; UC-706) Avail: CASI HC A05/MF A01

A comprehensive review of experimental base pressure and base heating data related to supersonic and hypersonic flight vehicles has been completed. Particular attention was paid to free-flight data as well as wind tunnel data for models without rear sting support. Using theoretically based correlation parameters, a series of internally consistent, empirical prediction equations was developed for planar and axisymmetric geometries (wedges, cones, and cylinders). These equations encompass the speed range from low supersonic to hypersonic flow and laminar and turbulent forebody boundary layers. A wide range of cone and wedge angles and cone bluntness ratios was included in the data base used to develop the correlations. The present investigation also included preliminary studies of the effect of angle of attack and specific-heat ratio of the gas. Author (revised)

N94-35498*# Eloret Corp., Palo Alto, CA.
DEVELOPMENT AND APPLICATION OF COMPUTATIONAL AEROTHERMODYNAMICS FLOWFIELD COMPUTER CODES Final Technical Report, 1 Sep. 1986 - 31 Jan. 1994
Ethiraj Venkatapathy 14 Jul. 1994 124 p
(Contract NCC2-420)
(NASA-CR-196136; NAS 1.26:196136) Avail: CASI HC A06/MF A02

Research was performed in the area of computational modeling and application of hypersonic, high-enthalpy, thermo-chemical nonequilibrium flow (Aerothermodynamics) problems. A number of computational fluid dynamic (CFD) codes were developed and applied to simulate high altitude rocket-plume, the Aeroassist Flight Experiment (AFE), hypersonic base flow for planetary probes, the single expansion ramp model (SERN) connected with the National Aerospace Plane, hypersonic drag devices, hypersonic ramp flows, ballistic range models, shock tunnel facility nozzles, transient and steady flows in the shock tunnel facility, arc-jet flows, thermochemical nonequilibrium flows around simple and complex bodies, axisymmetric ionized flows of interest to re-entry, unsteady shock induced combustion phenomena, high enthalpy pulsed facility simulations, and unsteady shock boundary layer interactions in shock tunnels. Computational modeling involved developing appropriate numerical schemes for the flows on interest and developing, applying, and validating appropriate thermochemical processes. As part of improving the accuracy of the numerical predictions, adaptive grid algorithms were explored, and a user-friendly, self-adaptive code (SAGE) was developed. Aerothermodynamic flows of interest included energy transfer due to strong radiation, and a significant level of effort was spent in developing computational codes for calculating radiation and radiation modeling. In addition, computational tools were developed and applied to predict the radiative heat flux and spectra that reach the model surface. Author

N94-35529 Lehigh Univ., Bethlehem, PA. Dept. of Mechanical Engineering and Mechanics.

UNSTEADY STRUCTURE OF LEADING-EDGE VORTICES ON A DELTA WING Final Report, 1 Nov. 1990 - 31 Oct. 1992

Donald O. Rockwell 22 Mar. 1994 8 p Limited Reproducibility: More than 20% of this document may be affected by microfiche quality
(Grant AF-AFOSR-0005-91)
(AD-A278988; AFOSR-94-0269TR) Avail: Issuing Activity (Defense Technical Information Center (DTIC))

The overall objective of this research program was to characterize the unsteady flow structure on wings having swept edges. Wings were subjected to global control, involving motion of the entire wing and local control, involving perturbations at specified locations on the surface of the wing. New types of experimental facilities and image acquisition and processing techniques have allowed determination of the instantaneous vorticity distributions and streamline patterns of the flow. The occurrence of vortex breakdown and stall and their phase shifts relative to the wing motion and to control at the leading-edges have been interpreted in terms of new flow mechanisms. DTIC

N94-35717 Stanford Univ., CA. Dept. of Aeronautics and Astronautics.

INVESTIGATION OF BURNETT EQUATIONS FOR TWO-DIMENSIONAL HYPERSONIC FLOW Final Report, 1 Nov. 1992 - 31 Oct. 1993

Dean R. Chapman and Robert W. MacCormack Apr. 1994 16 p Limited Reproducibility: More than 20% of this document may be affected by microfiche quality
(Contract F49620-92-J-0012)
(AD-A278942; AFOSR-94-0278TR) Avail: Issuing Activity (Defense Technical Information Center (DTIC))

Two separate areas of investigation are explored of two dimensional flow fields computed from the Burnett and Navier-Stokes equations: evaluation of various forms of Burnett equations from computations of one dimensional hypersonic shock structure and two dimensional flow over a flat plate at zero incidence, and investigation of the interaction at high altitudes of a hypersonic oblique shock impinging on a cowl lip. Among five different formulations of Burnett equations, two were found to exhibit in shock structure a small region of flow wherein the heat flux is physically unreal. Preliminary computations with the three other formulations are made for flow over a flat plate. It is found that the well-known severe overheating, due to oblique shock impingement on a leading edge, decreases significantly as altitude increases, disappearing at Knudsen numbers above about 0.1. DTIC

N94-35826 Naval Postgraduate School, Monterey, CA. Dept. of Mechanical Engineering.

DATA REDUCTION, ANALYSIS AND RESULTS OF LACV-30-07 AIR CUSHION VEHICLE TESTS, FORT STORY, VA, AUGUST - SEPTEMBER 1993

Young S. Shin and Eric Hoy Feb. 1994 521 p Limited Reproducibility: More than 20% of this document may be affected by microfiche quality
(AD-A278859; NPS-ME-94-002) Avail: Issuing Activity (Defense Technical Information Center (DTIC))

The LACV-30-07 Air Cushion Vehicle was instrumented and tested at Fort Story, VA during the months of August-September 1993 by Ed. Thomas, NSWC-Cardrock Division, Annapolis Detachment, Annapolis, MD. The tests include 27 cuts with vehicle speed ranging from 0 to 42 knots and approximate wave height of 0 to 2.5 feet. Two triaxial accelerometers, and a pitch and roll transducer were installed to measure axial, transverse and vertical accelerations and pitch and roll (in degree) of the vehicle. The test results clearly show that the vibration g-amplitude is extremely low (fraction of 1-g level) for air cushion vehicle and air cushion vehicle itself is acting as a super-damper to reduce the wave-induced vibration response amplitude. The vibration amplitude in terms of g-level may not be the controlling factor, but the combined vehicle dominant frequencies, vibration g-level, and duration may be the definite factors that the superconductor magnet must persist. DTIC

N94-35864*# California Univ., San Diego, La Jolla, CA. Dept. of Applied Mechanics and Engineering Sciences.

ON THE VARIOUS FORMS OF THE ENERGY EQUATION FOR A DILUTE, MONATOMIC MIXTURE OF NONREACTING GASES Final Report

Christopher A. Kennedy Jul. 1994 19 p
(Grant NAG1-1193; RTOP 505-59-50-05)
(NASA-CR-4612; NAS 1.26:4612) Avail: CASI HC A03/MF A01

In the case of gas mixtures, the governing equations become rather formidable and a complete listing of the equations in their various forms and methods to evaluate the transport coefficients is difficult to find. This paper seeks to compile common, as well as less well known, results in a single document. Various relationships between equations describing conservation of energy for a dilute, monatomic, nonreacting gas in local equilibrium are provided. The gas is treated as nonrelativistic, not subject to magnetic or electric fields, or radiative effects. Author

N94-35950 Ohio State Univ., Columbus. Dept. of Mechanical Engineering.

EXPANSION EFFECTS ON SUPERSONIC TURBULENT BOUNDARY LAYERS Final Report, 1 Sep. 1991 - 31 Dec. 1993

Stephen A. Arnette, Mo Samimy, and Gregory S. Elliott Feb. 1994 190 p Limited Reproducibility: More than 20% of this document may be affected by microfiche quality
(Grant AF-AFOSR-0412-91)
(AD-A278989; MEMS-94-101; AFOSR-94-0268TR) Avail: Issuing Activity (Defense Technical Information Center (DTIC))

The effects of various expansion regions on the large scale structure of a Mach 3 fully-developed-turbulent boundary layer are investigated. Five cases are studied: 7 deg and 14 deg centered expansions, 7 deg and 14 deg gradual expansions, and the flat plate. Multi-point surface pressure measurements, filtered Rayleigh scattering visualizations, and double-pulse visualizations were employed. Plan view images of the flat plate boundary layer reveal the presence of structures of a very large streamwise, and limited spanwise, extent. These structures were found well above the inner layer, nominally at n/delta = 0.5-1.0. The structures were also found in the expanded boundary layers. Across the expansion, the large scale structures of the outer layer undergo an increase in scale and structure angle. The small scale turbulent motions of the incoming boundary layer are quenched by the expansion, while the large scale structures respond more gradually. Convection velocities from the pressure correlations are reasonable in the incoming boundary layer, but unreasonably high in the expanded boundary layers. Convection velocities from correlations of double-pulse images appear reasonable. The discrepancy between the two results suggests the relationship between the large scale structures and the convecting pressure field is severely altered by the expansions. DTIC

N94-35991*# Eidetics International, Inc., Torrance, CA.

F/A-18 FOREBODY VORTEX CONTROL. VOLUME 1: STATIC TESTS

Brian R. Kramer, Carlos J. Suarez, Gerald N. Malcolm, and Bert F. Ayers Mar. 1994 183 p
(Contract NAS2-13383)
(NASA-CR-4582; A-94056; NAS 1.26:4582) Avail: CASI HC A09/MF A02

A wind tunnel test was conducted on a six percent model of the F/A-18 at the NASA Ames 7 X 10-Foot Low Speed Wind Tunnel. The primary objective of the test was to evaluate several forebody vortex control configurations at high angles of attack in order to determine the most effective method of obtaining well behaved yawing moments, in preparation for the rotary balance test. Both mechanical and pneumatic systems were tested. Single and dual rotating nose tip strakes and a vertical nose strake were tested at different sizes and deflections. A series

of jet blowing configurations were located at various fuselage stations, azimuth angles, and pointing angles ranging from straight aft to 60 deg canted inboard. Slot blowing was investigated for several slot lengths and fuselage stations. The effect of blowing rate was tested for both of these pneumatic systems. The most effective configurations were then further tested with a variation of both sideslip angle and Reynolds number over a range of angles of attack from 0 to 60 deg. It was found that a very robust system can be developed that provides yawing moments at angles of attack up to 60 deg that significantly exceeds that available from 30 deg of rudder deflection (F/A-18 maximum) at 0 deg angle of attack.
Author

N94-35994*# Institute for Computer Applications in Science and Engineering, Hampton, VA.
A THREE DIMENSIONAL MULTIGRID REYNOLDS-AVERAGED NAVIER-STOKES SOLVER FOR UNSTRUCTURED MESHES Final Report
D. J. Mavriplis May 1994 28 p Submitted for publication
(Contract NAS1-19480; RTOP 505-90-52-01)
(NASA-CR-194908; NAS 1.26:194908; ICASE-94-29) Avail: CASI HC A03/MF A01

A three-dimensional unstructured mesh Reynolds averaged Navier-Stokes solver is described. Turbulence is simulated using a single field-equation model. Computational overheads are minimized through the use of a single edge-based data-structure, and efficient multigrid solution technique, and the use of multi-tasking on shared memory multi-processors. The accuracy and efficiency of the code are evaluated by computing two-dimensional flows in three dimensions and comparing with results from a previously validated two-dimensional code which employs the same solution algorithm. The feasibility of computing three-dimensional flows on grids of several million points in less than two hours of wall clock time is demonstrated.
Author

N94-36261# Naval Surface Warfare Center, Bethesda, MD. Ship Systems Directorate.
TIPJET 80-INCH MODEL ROTOR HOVER TEST: TEST NO. 1198 Final Report, Jan. - Dec. 1991
Alan W. Schwartz Sep. 1993 97 p
(Proj. RR22-M59)
(AD-A279680; CDRKNSWC/SSD-93/54) Avail: CASI HC A05/MF A02

An experimental investigation was conducted to examine the aerodynamic properties of a Tipjet integrated pneumatic lift/reaction-drive rotor system in hover. For this rotor system, a single source of compressed air directly powers the rotor as a radial outflow turbine while simultaneously supplying the high velocity jet sheet that produces lift by means of circulation control (CC) along the blades. A sub scale model of such a fully pneumatic Tipjet rotor system was constructed and tested on the hover test facility at the David Taylor Model Basin. The model was tested to identify unique attributes of the integrated lift/drive system including mutual interference between tip nozzle flow and CC jet sheets and the impact of drawing CC supply air from a 'flowing plenum'. Test results are presented for the model is four configurations: CC rotor with tip nozzles closed, rotor locked with nozzles thrusting, tip drive CC rotor with controlled rpm, and tip-jet self drive equilibrium. The basic rotor lifting system, while exhibiting the highest augmentation ratio ever recorded for a CC rotor, suffers an induced power penalty due to the nonlifting region of the blade span where the tip nozzles are located. As expected, an internal pressure drop due to the flow rate in the blade duct was observed. There was no evidence of mutual interference effects between the lift and drive systems. Overall, the rotor exhibited a constant, linear response of lift versus pressure regardless of the slot height or the equilibrium tip speed. Author (revised)

N94-36394*# California Polytechnic State Univ., San Luis Obispo, CA. Dept. of Aeronautical Engineering.
NUMERICAL INVESTIGATION OF MULTI-ELEMENT AIRFOILS Final Technical Report
Russell M. Cummings Oct. 1993 14 p
(Contract NCC2-761)
(NASA-CR-194592; NAS 1.26:194592) Avail: CASI HC A03/MF A01

The flow over multi-element airfoils with flat-plate lift-enhancing tabs was numerically investigated. Tabs ranging in height from 0.25 percent to 1.25 percent of the reference airfoil chord were studied near the trailing edge of the main-element. This two-dimensional numerical simulation employed an incompressible Navier-Stokes solver on a structured, embedded grid topology. New grid refinements were used to improve the accuracy of the solution near the overlapping grid boundaries. The effects of various tabs were studied at a constant Reynolds number on a two-element airfoil with a slotted flap. Both computed and measured results indicated that a tab in the main-element cove improved the maximum lift and lift-to-drag ratio relative to the baseline airfoil without a tab. Computed streamlines revealed that the additional turning caused by the tab may reduce the amount of separated flow on the flap. A three-element airfoil was also studied over a range of Reynolds numbers. For the optimized flap rigging, the computed and measured Reynolds number effects were similar. When the flap was moved from the optimum position, numerical results indicated that a tab may help to reoptimize the airfoil to within 1 percent of the optimum flap case.
Author

N94-35855*# Southampton Univ. (England).
THE SIMULATION OF A PROPULSIVE JET AND FORCE MEASUREMENT USING A MAGNETICALLY SUSPENDED WIND TUNNEL MODEL
K. S. Garbutt and M. J. Goodyer *In* NASA. Langley Research Center, Second International Symposium on Magnetic Suspension Technology, Part 1 May 1994 p 291-305 (For primary document see N94-35836 11-18)
Avail: CASI HC A03/MF A04

N94-35965*# National Aeronautics and Space Administration. Ames Research Center, Moffett Field, CA.
WIND TUNNEL MEASUREMENTS ON A FULL-SCALE F/A-18 WITH A TANGENTIALLY BLOWING SLOT
Wendy R. Lanser *In its* 1993 Technical Paper Contest for Women. Gear Up 2000: Women in Motion Feb. 1994 p 27-36 (For primary document see N94-35961 11-99)
Avail: CASI HC A02/MF A02

03 AIR TRANSPORTATION AND SAFETY

Includes passenger and cargo air transport operations; and aircraft accidents.

For related information see also *16 Space Transportation* and *85 Urban Technology and Transportation.*

N94-35236# Federal Aviation Administration, Oklahoma City, OK. Civil Aeromedical Inst.
A REVIEW OF COMPUTER EVACUATION MODELS AND THEIR DATA NEEDS Final Report
Jeffrey H. Marcus May 1994 14 p
(DOT/FAA/AM-94/11) Avail: CASI HC A03/MF A01

This document reviews the history and current status of computer models of the evacuation of an airliner cabin. Basic concepts upon which evacuation models are based are discussed, followed by a review of the Civil Aeromedical Institute's efforts during the 1970's. A comparison is made of the three models available today (GA Model, AIREVAC, and EXODUS). The report then reviews parameters common to all models, and discusses literature available as a basis for these parameters. Finally, the report briefly discusses validation exercises for evacuation models. Author

N94-35482# National Transportation Safety Board, Washington, DC.
SAFETY STUDY: A REVIEW OF FLIGHTCREW-INVOLVED, MAJOR ACCIDENTS OF US AIR CARRIERS, 1978 THROUGH 1990
Jan. 1994 105 p
(PB94-917001; NTSB/SS-94/01) Avail: CASI HC A06/MF A02

U.S. air carrier operations are extremely safe, and the accident rate has declined in recent years. However, among the wide array of factors cited by the National Transportation Safety Board as causal or contributing to airplane accidents, actions or inactions by the flight crew have been cited in the majority of fatal air carrier accidents. Recognizing that deficiencies in various aspects of the aviation system may adversely influence flight crew performance, the safety board conducted this study to learn more about flight crew performance by evaluating characteristics of the operating environments, crew members, and errors made in major accidents of U.S.

air carriers between 1978 and 1990 in which the flight crew was cited by the board. Characteristics of the operating environments and flight crews were identified from information derived from major investigations of 36 accidents and 1 incident (for convenience, referred to as an accident). The errors identified in the accidents were evaluated in light of the contexts in which they occurred. The safety board aggregated the information examined in this study from its records of individual accident investigations. Although the data were not analyzed for the purpose of determining trends over time, the board did identify patterns in the data. In evaluating the results of the study, the board recognized that major accidents are rare events and that flight crew performance during accidents is subject to the simultaneous influences of many operational context variables. Results of this study need to be viewed from this perspective. Author (revised)

N94-35496# National Transportation Safety Board, Washington, DC. Office of Research and Engineering.
ANNUAL REVIEW OF AIRCRAFT ACCIDENT DATA. US GENERAL AVIATION, CALENDAR YEAR 1992
15 Jun. 1994 85 p
(PB94-181054; NTSB/ARG-94/02) Avail: CASI HC A05/MF A01

This report presents a statistical compilation and review of general aviation accidents which occurred in 1992 in the United States, its territories and possessions, and in international waters. The accidents reported are all those involving U.S. registered aircraft not conducting operations under 14 CFR 121, 14 CFR 127, or 14 CFR 135. This report is divided into five sections: All Accidents; Fatal Accidents: Serious Injury Accidents; Property Damage Accidents; and Midair Collision Accidents. Several tables present accident parameters for 1992 accidents only, and each section includes tabulations which present comparative statistics for 1992 and for the five-year period 1987-1991. Author

N94-35521# National Transportation Safety Board, Washington, DC.
AIRCRAFT ACCIDENT REPORT: UNCONTROLLED COLLISION WITH TERRAIN, AMERICAN INTERNATIONAL AIRWAYS FLIGHT 808, DOUGLAS DC-8-61, N814CK, US NAVAL AIR STATION, GUANTANAMO BAY, CUBA, 18 AUGUST 1993
1994 148 p
(PB94-910406; NTSB/AAR-94/04) Avail: CASI HC A07/MF A02

This report explains the crash of American International Airways Flight 808, a DC-8-61, about 1/4 mile from the approach end of runway 10 at Leeward Point Airfield, U.S. Naval Air Station, Guantanamo Bay, Cuba, on August 18, 1993. The safety issues discussed in the report include flightcrew scheduling, the effects of fatigue on flightcrew performance, training on special airports, and the dissemination of information about special airports. Safety recommendations concerning these issues were made to the Federal Aviation Administration, American International Airways, Inc., and the Department of Defense. Author

N94-35522*# North Carolina State Univ., Raleigh, NC. Dept. of Marine, Earth and Atmospheric Sciences.
NUMERICAL MODELING STUDIES OF WAKE VORTEX TRANSPORT AND EVOLUTION WITHIN THE PLANETARY BOUNDARY LAYER
Semiannual Report, FY 1994
Yuh-Lang Lin, S. Pal Arya, and Michael L. Kaplan 1994 17 p
(Contract NCC1-188)
(NASA-CR-196078; NAS 1.26:196078) Avail: CASI HC A03/MF A01

The proposed research involves four tasks. The first of these is to simulate accurately the turbulent processes in the atmospheric boundary layer. TASS was originally developed to study meso-gamma scale phenomena, such as tornadic storms, microbursts and windshear effects in terminal areas. Simulation of wake vortex evolution, however, will rely on appropriate representation of the physical processes in the surface layer and mixed layer. This involves two parts. First, a specified heat flux boundary condition must be implemented at the surface. Using this boundary condition, simulation results will be compared to experimental data and to other model results for validation. At this point, any necessary changes to the model will be implemented. Next, a surface energy budget parameterization will be added to the model. This will enable calculation of the surface fluxes by accounting for the radiative heat transfer to and from the ground and heat loss to the soil rather than simple specification of the fluxes. The second task involves running TASS with prescribed wake vortices in the initial condition. The vortex models will be supplied by NASA Langley Research Center. Sensitivity tests will be performed on different meteorological environments in the atmospheric boundary layer, which include stable, neutral, and unstable stratifications, calm and severe wind conditions, and dry and wet conditions. Vortex strength may be varied as well. Relevant non-dimensional parameters will include the following: Richardson number or Froude number, Bowen ratio, and height to length scale ratios. The model output will be analyzed and visualized to better understand the transport, decay, and growth rates of the wake vortices. The third task involves running simulations using observed data. MIT Lincoln Labs is currently planning field experiments at the Memphis airport to measure both meteorological conditions and wake vortex characteristics. Once this data becomes available, it can be used to validate the model for vortex behavior under different atmospheric conditions. The fourth task will be to simulate the wake in a more realistic environment covering a wider area. This will involve grid nesting, since high resolution will be required in the wake region but a larger total domain will be used. During the first allocation year, most of the first task will be accomplished. Derived from text

04 AIRCRAFT COMMUNICATIONS AND NAVIGATION

Includes digital and voice communication with aircraft; air navigation systems (satellite and ground based); and air traffic control.

For related information see also *17 Space Communications, Spacecraft Communications, Command and Tracking* and *Communications and Radar.*

N94-36048*# National Aeronautics and Space Administration. Langley Research Center, Hampton, VA.
FINAL-APPROACH SPACING AIDS (FASA) EVALUATION FOR TERMINAL-AREA, TIME-BASED AIR TRAFFIC CONTROL
Leonard Credeur, William R. Capron, Gary W. Lohr, Daniel J. Crawford, Dershuen A. Tang, and William G. Rodgers, Jr. Dec. 1993 193 p
(RTOP 505-64-13-01)
(NASA-TP-3399; L-17260; NAS 1.60:3399) Avail: CASI HC A09/MF A03

A jointly funded (NASA/FAA) real-time simulation study was conducted at NASA Langley Research Center to gather comparative performance data among three candidate final-approach spacing aid (FASA) display formats. Several objective measures of controller performance and their display eye-scan behavior as well as subjective workload and rating questionnaires were used. For each of two representative pattern-speed procedures (a 170-knot procedure and a 210-knot procedure with speed control aiding), data were gathered, via twelve FAA controllers, using four final-controller display format conditions (manual/ARTS 3, graphic marker, DICE countdown, and centerline slot marker). Measured runway separations were more precise with both the graphic marker and DICE countdown formats than with the centerline slot marker and both (graphic and DICE) improved precision relative to the manual/ARTS 3 format. For three separate rating criteria, the subject controllers ranked the FASA formats in the same order: graphic marker, DICE countdown, and centerline slot marker. The increased precision measured with the 210-knot pattern-speed procedure may indicate the potential for the application of speed-control aiding where higher pattern speeds are practical after the base-to-final turn. Also presented are key FASA issues, a rationale for the formats selected for testing, and their description. Author

N94-36184 Air Force Inst. of Tech., Wright-Patterson AFB, OH. School of Engineering.
AN ANALYSIS OF OPERATIONAL SUITABILITY FOR TEST AND EVALUATION OF HIGHLY RELIABLE SYSTEMS M.S. Thesis
James N. Serpa Mar. 1994 52 p Limited Reproducibility: More than 20% of this document may be affected by microfiche quality
(AD-A278573; AFIT/GOR/ENS/94M-13) Avail: Issuing Activity (Defense Technical Information Center (DTIC))

The purpose of this research was to develop a quantitative measure of operational suitability (OS) and determine its applicability in making the test length decision prior to Initial Operational Test and Evaluation (IOT&E). The current approach used by the Air Force Operational Test and Evaluation

Center (AFOTEC) was presented and used to establish the relationships of the test measures. It was established that OS could be represented by a function of operational availability (A(sub O)) and built-in test effectiveness (BE). BE was defined and measures proposed based on the method of data collection. A proposal for predicting A(sub O), BE, and OS to determine the proper test length and sample size was analyzed for several examples of prior information. Multiplicative and additive utility functions were proposed as possible ways to calculate OS. It was shown that probability statements could be made about BE, A(sub O), and OS from the prior information; this analysis revealed the reliance of the results on the prior information.
DTIC

05 AIRCRAFT DESIGN, TESTING AND PERFORMANCE

Includes aircraft simulation technology.

For related information see also *18 Spacecraft Design, Testing and Performance* and *39 Structural Mechanics.*For land transportation vehicles see *85 Urban Technology and Transportation.*

N94-35241*# National Aeronautics and Space Administration. Hugh L. Dryden Flight Research Facility, Edwards, CA.
EVALUATING THE DYNAMIC RESPONSE OF IN-FLIGHT THRUST CALCULATION TECHNIQUES DURING THROTTLE TRANSIENTS
Ronald J. Ray Jun. 1994 27 p Presented at the 7th Biennial Flight Test Conference, Colorado Springs, CO, 20-23 Jun. 1994
(RTOP 505-68-00)
(NASA-TM-4591; H-1990; NAS 1.15:4591; AIAA Paper 94-2115)
Copyright Avail: CASI HC A03/MF A01

New flight test maneuvers and analysis techniques for evaluating the dynamic response of in-flight thrust models during throttle transients have been developed and validated. The approach is based on the aircraft and engine performance relationship between thrust and drag. Two flight test maneuvers, a throttle step and a throttle frequency sweep, were developed and used in the study. Graphical analysis techniques, including a frequency domain analysis method, were also developed and evaluated. They provide quantitative and qualitative results. Four thrust calculation methods were used to demonstrate and validate the test technique. Flight test applications on two high-performance aircraft confirmed the test methods as valid and accurate. These maneuvers and analysis techniques were easy to implement and use. Flight test results indicate the analysis techniques can identify the combined effects of model error and instrumentation response limitations on the calculated thrust value. The methods developed in this report provide an accurate approach for evaluating, validating, or comparing thrust calculation methods for dynamic flight applications. Author

N94-36321# Advisory Group for Aerospace Research and Development, Neuilly-Sur-Seine (France). Flight Mechanics Panel.
RECENT ADVANCES IN LONG RANGE AND LONG ENDURANCE OPERATION OF AIRCRAFT [LES PROGRES RECENTS DANS LE DOMAINE DES OPERATIONS AERIENNES A LONGUE DISTANCE ET DE LONGUE DUREE]
Nov. 1993 317 p In ENGLISH and FRENCH Symposium held in The Hague, Netherlands, 24-27 May 1993
(AGARD-CP-547; ISBN-92-835-0726-6) Copyright Avail: CASI HC A14/MF A03

Over the past few years, the use of aircraft in long range and/or long endurance operations has proved to be a successful use of military resources. Technologies which improve the range and endurance of aircraft have seen considerable advances over the past ten years. Aircraft design for these features has matured considerably while the procedure of air-to-air refuelling has made global deployment and 24+ hour operations a reality. This Symposium attempted to summarize the latest technological advances in the various fields which in a combined manner define the range and endurance of airborne vehicles, i.e.: airframe design technologies, including aerodynamic structures; propulsion technology; the human factors problems associated with these types of missions; and air-to-air refuelling technologies and procedures. For individual titles, see N94-36322 through N94-36347.

N94-36322# Wright Lab., Wright-Patterson AFB, OH.
HIGH ALTITUDE LONG ENDURANCE AIRCRAFT DESIGN STUDIES
V. B. Venkayya and V. A. Tischler *In* AGARD, Recent Advances in Long Range and Long Endurance Operation of Aircraft Nov. 1993 17 p (For primary document see N94-36321 11-05)
Copyright Avail: CASI HC A03/MF A03

This paper presents the results of structural optimization studies made on a High Altitude Long Endurance (HALE) aircraft at Wright Research and Development Center (now Wright Laboratory) during the late eighties. The purpose of this study is to investigate the feasibility of developing an ultralightweight airframe that can operate at high altitudes for extended periods of time in order to provide continuous reconnaissance, surveillance, communications and targeting functions. A variety of structural concepts and material studies were made prior to settling on a twin boom very high aspect ratio wing airframe. The wing and fuselage structures are made of truss substructures covered with skins, both made of high strength, high modulus, lightweight composite materials. Extensive structural optimization studies were conducted in order to obtain a lightweight structure. The large size of the aircraft drove the design to a stiffness critical structure.
Author

N94-36323# Alenia Aeronautica, Turin (Italy). Preliminary Design Dept.
TECHNOLOGICAL CHALLENGES OF HIGH ALTITUDE LONG ENDURANCE UNMANNED CONFIGURATIONS
R. Bargetto and R. Spezzaferro *In* AGARD, Recent Advances in Long Range and Long Endurance Operation of Aircraft Nov. 1993 12 p (For primary document see N94-36321 11-05)
Copyright Avail: CASI HC A03/MF A03

This paper presents the conceptual work performed in Alenia during the recent years for defining some possible configurations for military and civil HALE (High Altitude Long Endurance) aircraft capable of carrying very different kinds of payloads and with mission durations ranging from one to two days. Also in relation to the aircrew fatigue implied by such a long flight time, they all have been conceived as UMA (UnManned Aircraft), achieving in that way a significant reduction of mass and complexity, withstanding the maturity of automatic control system. The aeromechanical aspect of the configurations (i.e aerodynamics, propulsion, structures, systems, weights and performances) will be discussed in detail considering that HALE-UMA type of aircraft have to face some technical challenges in many fields generated by the rather demanding requirements in terms of payload and endurance. Author

N94-36324# Aerospatiale, Toulouse (France). Aircraft Div.
FUTURE SUPERSONIC COMMERCIAL TRANSPORT AIRCRAFT: A TECHNOLOGICAL CHALLENGE FOR LONG HAUL TRAFFIC [AVION DE TRANSPORT SUPERSONIQUE FUTUR: UN DEFI TECHNOLOGIQUE POUR LE VOL LONG COURRIER]
J.-L. Galvani *In* AGARD, Recent Advances in Long Range and Long Endurance Operation of Aircraft Nov. 1993 8 p In FRENCH (For primary document see N94-36321 11-05)
Copyright Avail: CASI HC A02/MF A03

Long haul traffic is a key sector that is constantly increasing. Since Concorde entry into service in 1976, it has tripled and will again double by the end of the century. There is no doubt that this long haul traffic development will create an increasing interest in high speed. The entry into service of a HSCT will enable flight time to be divided at least by 2 on these long routes, and could capture 20 percent to 40 percent of the long range market. To face up this future air transport landscape Aerospatiale, who jointly with British Aerospace has accumulated an unique experience in high speed transport with the Concorde program, is studying a potential successor: the Alliance project cruising at Mach 2. Due to the significant progress in technology already achieved or foreseen in the near future, the entry into service of a second generation supersonic transport can be envisaged as early as 2005. The success of this project is strongly linked to the capability of the aircraft and the engine manufacturers to provide the appropriate technology level to make the airplane environmentally acceptable and economically attractive. A significant effort in R & D is necessary to make available the challenging technologies: new materials, aerodynamics, propulsion.... Considering the level of investment required and the complexity of the problems to be solved, a close collaboration involving industrial partners is necessary on a world wide basis. This collaboration has already started. Following a long experience of bilateral cooperation, Aerospatiale and British Aerospace joined again in 1990 to study together a second generation supersonic aircraft around their respective concepts (AST and Alliance). Both partners are also cooperating with DASA, Boeing, McDonnell Douglas, the Japanese Industries, Alenia and Tupolev within an International Study Group. Author

N94-36325# Naval Air Warfare Center, Warminster, PA. Aircraft Div.
THE CASE FOR SURFACE EFFECT RESEARCH, PLATFORM APPLICATIONS AND TECHNOLOGY DEVELOPMENT OPPORTUNITIES
J. M. L. Reeves *In* AGARD, Recent Advances in Long Range and Long Endurance Operation of Aircraft Nov. 1993 10 p (For primary document see N94-36321 11-05)
Copyright Avail: CASI HC A02/MF A03

This paper commences by defining the conventional understanding of Surface Effect phenomenon and compares theories which show small reductions in drag occur above one span height above the surface. A discussion on reports of pilots who have flown their aircraft in surface effect ensues. From this, a broader understanding of surface effect is developed supported by low speed wind tunnel tests and Russian published technical documentation. The author divides surface effect platforms or, perhaps, better described as Enhanced Performance Low Flying Platforms (EPLFP's) into three distinct categories. Potential applications of surface effect platforms are discussed based on the changing world, the evolving airline industry and airport constraints. Missions and specific mission examples are given. Reasons for the pursuit of rather large platforms are presented as are some of the major technical hurdles which will have to be overcome for them to succeed. Technology opportunities are discussed. A summary concludes the paper. Author

N94-36326# Office National d'Etudes et de Recherches Aerospatiales, Paris (France).
THE FUTURE OF LARGE CAPACITY/LONG RANGE MULTIPURPOSE AIR CARGO FLEETS [L'AVENIR D'AVIONS CARGOS MULTI-ROLES A LARGE CAPACITE ET GRAND RAYON D'ACTION]
Philippe Poisson-Quinton *In* AGARD, Recent Advances in Long Range and Long Endurance Operation of Aircraft Nov. 1993 8 p In FRENCH (For primary document see N94-36321 11-05)
Copyright Avail: CASI HC A02/MF A03

Both commercial and military aspects of Cargo Transport Aviation were discussed at the International Symposium organized by the French Aerospace Academy, held in March 1993 in Strasbourg. This paper summarizes some of the contributions and discussions dealing with the future role of the Air Cargo Transportation in relation to a global international policy of military and humanitarian intervention, including their technical and operational aspects. In a first part, the status of the World's Air Cargo activity is reviewed in terms of the main operational cargo airplanes, their capacity and their range, used both for commercial and military purposes; it includes the family of large cargos developed by Antonov in Ukraine and preliminary designs of huge cargo projects by the Russian laboratory TsAGI for 250 to 500 tons payload, and by NASA with spanloader or conventional schemes for intermodal containers transport. In a second part, the present U.S. Military Airlift forces are analyzed, with some comments on their recent global airlift deployment during the Gulf War. It is concluded that, as regards long term global policy, such existing task forces are totally inadequate to either stop immediately some local conflicts around the world, or to save population, in case of major natural or man-made disasters. That is why a much larger airlift system should be developed on an intergovernmental basis, the main objective would be its 'strategic efficiency' instead of a 'profit earning capacity', as used in commercial aviation. For that purpose, a 'supercargo' can be defined, developed and produced in the framework of an international consensus between the major aeronautical powers. Its size, configuration, operational characteristics and performance must be discussed, and a compromise agreed to cope with the main military and humanitarian missions; but such 'supercargo' airplane would be certainly much larger than the present ones, with two to four times their payload, and a transcontinental range capability; for their development, advantage would be taken of the best technologies that would become available in the next decade, and of the availability of design capability in the world's aircraft industry resulting from the present crisis. A flying wing configuration is suggested as a basis for a preliminary project. Finally, there is certainly a commercial spin-off of such massive supercargo production, if used to compete successfully with the surface transportation systems of large intermodal containers already used on major international markets. Author

N94-36327# Deutsche Aerospace A.G., Munich (Germany). Military Aircraft.
OPTIMISATION OF COMPOSITE AIRCRAFT STRUCTURES BY DIRECT MANUFACTURING APPROACHES
G. Berchtold and J. Klenner *In* AGARD, Recent Advances in Long Range and Long Endurance Operation of Aircraft Nov. 1993 12 p (For primary document see N94-36321 11-05)
Copyright Avail: CASI HC A03/MF A03

The present high performance aircraft designs are increasingly using high strength composite structures, mainly made of unidirectional carbon fiber tapes. But the composite technology is still afflicted with several weak points, e.g. the lack of adequate mechanized tape application techniques for complex compound structures, unsatisfying designs and design methods and missing continuous CAD/CAM-linkage. In this paper we will describe an 'Integrated Tape Laying System' (ITLS) which uses a new tape steering technology for automated manufacturing of complex parts. This system integrates the steering technology's potentials and restrictions completely in the design process to avoid time consuming iteration loops and to optimize the structure. To be able to understand the detailed process a short overview about two different geometry models demonstrated on a typical example will be given. From this the optimal detailed process will be derived, with an important influence from the specific manufacturing technology. Finally some remarks on economic potentials are outlined with their impact on typical composite aircraft parts related to different automated manufacturing techniques. Author (revised)

N94-36328# Dassault Aviation, Saint-Cloud (France). Div. des Etudes Avancees.
LAMINAR FLOW STUDIES AT DASSAULT AVIATION: CALCULATIONS AND FLIGHT TESTS [ETUDES D'ECOULEMENTS LAMINAIRES CHEZ DASSAULT AVIATION: CALCULS ET ESSAIS EN VOL] c34
J. C. Courty, C. Bulgubure, and D. Arnal *In* AGARD, Recent Advances in Long Range and Long Endurance Operation of Aircraft Nov. 1993 14 p In FRENCH (For primary document see N94-36321 11-05)
Copyright Avail: CASI HC A03/MF A03

The tools used at Dassault Aviation to calculate the limits on laminar layers, transition criteria and analyses on linear stability are presented and analyzed as far as their precision but also as far as their effectiveness when they have to be used to optimize the design of aircrafts' wing systems. These calculations were used in the concept of laminar deviation that was tested in the air on a FALCON 50, and in the concept of a wing with an hybrid laminarity that was tested in the air on a FALCON 50 during a second phase, 1987-1990. Author

N94-36329# Technische Univ., Munich (Germany). Inst. of Flight Mechanics and Flight Control.
IMPROVEMENT OF ENDURANCE PERFORMANCE BY PERIODIC OPTIMAL CONTROL OF VARIABLE CAMBER c08
G. Sachs and R. Mehlhorn *In* AGARD, Recent Advances in Long Range and Long Endurance Operation of Aircraft Nov. 1993 7 p (For primary document see N94-36321 11-05)
Copyright Avail: CASI HC A02/MF A03

Other than in classical theory, endurance cruise is considered as an optimal periodic control problem where the state and control variables change in a periodic manner. Variable camber is introduced as a further control in addition to angle of attack and thrust setting. By periodically varying camber in a coordinated process with the two other controls, it is possible to fully exploit its potential of improving the lift/drag ratio for increasing the endurance of aircraft. It is quantitatively shown which gain in endurance performance can be achieved. Results are presented for an idealized engine model showing no control rate limitations as well as for a realistic model with constraints on control rates imposed. The numerical values for the constraints are chosen such that only slow thrust changes are admitted. Author

N94-36330# Westland Helicopters Ltd., Yeovil (England).
EH101: A NEW HELICOPTER CAPABLE OF LONG RANGE MISSIONS
C. J. Battisson and H. E. Tatton-Brown *In* AGARD, Recent Advances in

Long Range and Long Endurance Operation of Aircraft Nov. 1993 10 p (For primary document see N94-36321 11-05)
Copyright Avail: CASI HC A02/MF A03

The EH101 is a new medium helicopter being produced by EH Industries, a company jointly owned by Agusta of Italy and Westland of the UK. The aim of this presentation is to explore the roles in which the EH101 will be called upon to cover long ranges and examine its suitability for these roles. The roles which will be examined fall into the following categories: search and rescue, self-ferry, and special operations. The successful completion of such missions will demand particular capabilities of the crew and the machine. The following aspects of aircraft design will be looked at with respect to the EH101: in-flight refuelling, all-weather capability, maintenance requirements, and crew environment. Because of the wide ranging nature of the subject and the limited time available this is intended to examine only the key points required for these roles and capabilities.
Author (revised)

N94-36331# Eurocopter France, Marignane (France).
THE CONVERTIBLE (HELICOPTER/AIRPLANE) EUROFAR: GENERAL CONSIDERATIONS ON THE TECHNICAL PROGRESS AND ON FUTURE ADVANCES [LE CONVERTIBLE TYPE EUROFAR: VUE D'ENSEMBLE DES AVANCEMENTS TECHNIQUES ET MISSIONS FUTURES]
A. Martini and J. Renaud *In* AGARD, Recent Advances in Long Range and Long Endurance Operation of Aircraft Nov. 1993 7 p In FRENCH (For primary document see N94-36321 11-05)
Copyright Avail: CASI HC A02/MF A03

Until the last few years, the idea of a convertible aircraft did not progress into testing because the available technology did not satisfy the cost/efficiency parameters, and because the need for such an aircraft was not felt. Today, conditions are different. Strategic necessities and technical progress have created an atmosphere in the United States and in Europe where this old dream of engineers may be resurrected. Author

N94-36332# Aerospatiale, Toulouse (France). Aerodynamics Conception Dept.
CALCULATIONS USED TO OPTIMIZE THE INSTALLATION OF CIVIL AIRCRAFT ENGINES [UTILISATION DES METHODES DE CALCUL POUR OPTIMISER L'INSTALLATION MOTRICE DES AVIONS DE TRANSPORT]
X. Monthus, Ph. Colin, Ph. Mogilka, and A. Molbay-Arsan *In* AGARD, Recent Advances in Long Range and Long Endurance Operation of Aircraft Nov. 1993 31 p In FRENCH (For primary document see N94-36321 11-05)
Copyright Avail: CASI HC A03/MF A03

Within the research program on AIRBUS, the Aerodynamics Conception Department of Aerospacial Avions is responsible for the research on the aerodynamics of the reactor's pylon, air inlet (or technical evaluation on the system provided by the constructor) and for the optimization of aerodynamics in the ensemble of the engine installation. This includes studies on minimizing undesirable effects (loss of carrying capacity, increase in drag) due to the interaction between wings, pylon, and engine pod. This article lists the various tools used by the above department in order to fulfill its task: the C.A.O. system, principally conceived for aerodynamics concerns, the surface and volume representation systems as well as the main systems of 3D calculations on complex geometric arrangements. Three recent applications of these methods are presented within the framework of the development of the AIRBUS A330/A340 aircraft, and associated systems: air flow in the zone of pylon/wing intersection; effects due to the size of the engine in comparison to given wing characteristics and modelization of the jet's effect; and orientation of relationship between engine thrust and aircraft. Author

N94-36333# Naval Air Warfare Center, Warminster, PA. Aircraft Div.
PROPULSION SYSTEM SELECTION FOR A HIGH ALTITUDE LONG ENDURANCE AIRCRAFT **c07**
John D. Cyrus and Joseph Franz *In* AGARD, Recent Advances in Long Range and Long Endurance Operation of Aircraft Nov. 1993 7 p (For primary document see N94-36321 11-05)
Copyright Avail: CASI HC A02/MF A03

This paper addresses the major propulsion system options for High Altitude Long Endurance aircraft internal combustion engines, turbine engines and fuel cells. The paper identifies the technology drivers for the vehicle and assesses the secondary equipment requirements for the various system options. Critical technologies and development requirements are addressed in terms of mission capability for both near-term and advanced systems. This AGARDograph was sponsored by the Flight Mechanics Panel.
Author

N94-36334# Rolls-Royce Ltd., Bristol (England).
PROPULSION SYSTEM TECHNOLOGIES FOR LONG RANGE AND LONG ENDURANCE AIRCRAFT **c07**
K. R. Garwood *In* AGARD, Recent Advances in Long Range and Long Endurance Operation of Aircraft Nov. 1993 7 p (For primary document see N94-36321 11-05)
Copyright Avail: CASI HC A02/MF A03

The NATO requirement for increased range and endurance of aircraft is also associated with the necessity to reduce the initial and life cycle costs of these aircraft. Consideration of these conflicting requirements leads to the prioritization of engine technologies for different vehicle types and presented here are views of engine manufacturers addressing these challenges over the range of aircraft. This paper will discuss the prioritization of technologies required for the range of air vehicles and examine how increases in endurance and range affect the balance of technology within each propulsion unit type. It is convenient to group the vehicles in the following way: transport, tanker, AWACS; maritime patrol; combat; and special purpose. Each grouping has the challenges of range or duration subject to its class, although clearly in absolute terms the range of transport vehicles is significantly different from that of a combat aircraft. It is primarily these differences in the groupings that give rise to the differences in technology prioritization. Derived from text

N94-36335# Industrieanlagen-Betriebsgesellschaft m.b.H., Ottobrunn (Germany).
THE STRATO 2C PROPULSION SYSTEM: A LOW COST APPROACH FOR A HIGH ALTITUDE LONG ENDURANCE AIRCRAFT **c07**
H. Toenskoetter *In* AGARD, Recent Advances in Long Range and Long Endurance Operation of Aircraft Nov. 1993 6 p (For primary document see N94-36321 11-05)
Copyright Avail: CASI HC A02/MF A03

For the STRATO 2C - a High Altitude Long Endurance Research Aircraft - a low cost propulsion system was designed and is now under development. The approach to achieve the aim of low development procurement and in-service costs is a compound propulsion system based on a highly supercharged liquid cooled piston engine with charge air inter-cooling and the extensive usage of available components. The concept of the propulsion system and the main components are described. Aspects of controlling the three-stage turbocharger system are discussed. The way to realize the power plant in three years is presented and the test program is addressed. Author

N94-36336# Netherlands Aerospace Medical Centre, Soesterberg. Research Dept.
REVIEW OF HUMAN FACTORS PROBLEMS RELATED TO LONG DISTANCE AND LONG ENDURANCE OPERATION OF AIRCRAFT **c54**
Ries M. Simons and Pierre J. L. Valk *In* AGARD, Recent Advances in Long Range and Long Endurance Operation of Aircraft Nov. 1993 9 p (For primary document see N94-36321 11-05)
Copyright Avail: CASI HC A02/MF A03

Long distance operations are characterized by rapid multiple time-zone changes and long irregular work schedules. Performance and alertness of aircrew engaged in these operations might be affected by circadian disruptions, sleep loss, workload, and cockpit-environmental factors, such as lower pressure, low relative humidity, and constant background noise. Recent literature on the various factors, which contribute to fatigue and reduced alertness of pilots, is reviewed. Author

N94-36337# Deutsche Forschungs- und Versuchsanstalt fuer Luft- und Raumfahrt, Cologne (Germany). Inst. for Aerospace Medicine.
EXTENDED RANGE OPERATIONS: A REVIEW OF RECENT DEVELOPMENTS **c66**
A. Samel and H. M. Wegmann *In* AGARD, Recent Advances in Long Range and Long Endurance Operation of Aircraft Nov. 1993 10 p (For primary document see N94-36321 11-05)
Copyright Avail: CASI HC A02/MF A03

The introduction of long-haul aircraft which can be operated by a 2-crew flight deck over expanded duty hours, raises serious concerns about flight safety. It is a matter of intense discussions between authorities, operator and pilot associations in the USA, in Japan and in Europe whether the legal standards of flight duty limitations presently in force are still adequate or must be modified for minimum crew operations under the changing conditions. In cooperation with various air carriers, different approaches have recently been undertaken by international scientific laboratories to investigate physiological and psychological responses of the human element to the new technology in the cockpit during long-haul operations. In the conventional 3-man cockpit, pre-planned controlled rest on the flight deck has been investigated. In augmented crews, comparison have been made between the 3-man flight deck and the newly introduced 2-crew cockpit. The efficiency of onboard rest facilities has been investigated during long-haul augmented 2-crew operations. Workload, alertness and fatigue are under investigation in single 2-crew operations with non-stop flights of up to 14 hours flight duty time. Because not all of these investigations are completed, scientific contributions for discussions about flight time limitations and rest requirements must still be limited. However, in certain countries, scientific results have already led to recommendations for amendments in the actual legislation. Author

N94-36338# Aerospace Medical Research Labs., Brooks AFB, TX. Sustained Operations Branch.

DETERMINANTS OF SUBJECTIVE FATIGUE FOR C-141 CREWS DURING OPERATION DESERT STORM c52

Jonathan French, Kelly J. Neville, William F. Storm, Roger U. Bisson, and Patricia Boll *In* AGARD, Recent Advances in Long Range and Long Endurance Operation of Aircraft Nov. 1993 12 p (For primary document see N94-36321 11-05)

Copyright Avail: CASI HC A03/MF A03

As aircraft flight endurance capabilities increase, the importance of attenuating fatigue during long duration missions increases. Profile of Mood States (POMS) data were used to document cumulative fatigue and to explore the relationships between mission characteristics and changes in mood of C-141 aircrew members during Operation Desert Storm. In particular, this research assessed the effects of increasing the limit of 30-day cumulative flight for long duration transport crews from 125 to 150 hours. POMS data were collected at the beginning of the legal for alert (LFA) and crew rest (CR) intervals. Correlational analyses were used to compare POMS dimensions (anger, depression, confusion, fatigue, vigor, tension) with 13 flight and sleep schedule variables. During both LFA and CR intervals, 30-day cumulative flight hours were not related to subjective mood dimensions. However, when 30 day cumulative flight hours exceeded 125 hours, POMS vigor was decreased by recent flight and sleep hours. Therefore, attending to recent sleep and flight history may predict decrements in vigor when operational pressures require exceeding the normal cumulative flight hours per month. A first attempt to construct a crew rest equation is proposed that accounts for these factors. This equation is based on a stepwise multiple regression procedure which revealed that vigor and fatigue were best predicted by cumulative 24-hour sleep and 48-hour flight time. In addition to improved crew rest schedules, dedicated crew rest facilities and sleep hygiene instruction are recommended before flying long duration missions. Author

N94-36339# Centre d'Etudes et de Recherches de Medecine Aerospatiale, Bretigny sur Orge (France).

SOME SOLUTIONS TO REDUCE THE HUMAN EFFECTS OF EXTENDED OPERATION TIMES [QUELQUES SOLUTIONS POUR REDUIRE LES EFFETS SUR L'HOMME DES OPERATIONS DE LONGUE DUREE] c52

D. Lagarde and D. Batejat *In* AGARD, Recent Advances in Long Range and Long Endurance Operation of Aircraft Nov. 1993 17 p In FRENCH (For primary document see N94-36321 11-05)

Copyright Avail: CASI HC A03/MF A03

Mostly, in aeronautical environment, the extended operation times assume the continued operations aspect with long duration flights, sometimes transmeridian. In this operations setting, the fast and repeated passing of several time zones is attended with the classical symptomatology of 'jet-lag', intensified by the conditions of the mission. The appearance and the extent of 'jet-lag' are variable according to the flight and the involved subject characteristics; nevertheless, the psychomotor performances decrease is a constant factor of these disorders. In order to investigate with a greater accuracy this aspect in laboratory, the authors present a study model represented by the STRES battery, an ensemble of seven psychomotor tests, recommended by the working group n degrees 12 of the AGARD/NATO, that allows the evaluation of the whole psychomotor register of a subject situated in stress environmental conditions, in a broad meaning. Two examples of these tests to sleep deprivation states are introduced so as to illustrate the sensibility and the interest of implementing this test battery. In view of the disorder's penalizing effect, several authors have postulated solutions in order to suppress or at least to reduce the duration and importance of such symptoms. Thus, some accurate instructions have been recommended relating to the maximum workload condition that can not be exceeded and to the dual aircrew. Others have enjoined to be synchronized with the new time table before departure or to strengthen the social 'zeitgeber' at arrival. Phototherapy, naps, dietetic measures, and physical exercise are also a part of the suggested steps. The pharmacological approach with the use of caffeine, hypnotics, and more recently melatonin have a new lease of interest especially with the appearance of new awakening drugs, as powerful as amphetamines but without their secondary effects. Thus, after the justification of the stimulating drugs' use in the setting of wake sleep rhythms desynchronization, the authors present concisely the modafinil, main representative of this new molecule category. Then, from examples from the laboratory, on occasion of psychomotor performance evaluation with the STRES battery on subjects under sleep deprivation, or on field, they present some results obtained after dispensation of this drug. At the end of this review and of the experimental results, it appears that the extended operation times induce wake-sleep rhythm and psychomotor performances disorders. Numerous possibilities, complementary, exist in order to reduce the observed disorders; none of them appears alone sufficient. Nevertheless, the new awakening drugs appearance, on account of their great efficiency and their whole inocuity, should constitute a major element in biological rhythms resynchronization in the future. Author (revised)

N94-36340# Aerospace Engineering Test Establishment, Cold Lake (Alberta).

FLIGHT TEST CERTIFICATION OF A 480 GALLON COMPOSITE FUEL TANK ON CF-18

Mario B. J. Lagrange *In* AGARD, Recent Advances in Long Range and Long Endurance Operation of Aircraft Nov. 1993 22 p (For primary document see N94-36321 11-05)

Copyright Avail: CASI HC A03/MF A03

The Aerospace Engineering Test Establishment (AETE), as the Canadian Forces (CF) flight test authority, has recently completed flight tests and analysis of a major store certification program to establish an operational flight envelope for the carriage and jettison of a newly designed 480 gallon external fuel tank (EFT) for the CF-18 aircraft. The certification process involved a progressive series of analysis, wind tunnel tests, qualification tests, ground tests, and flight test activities. Most of the preflight activities were performed by the designer, McDonnell Aircraft Company (McAir), while all flight testing was the responsibility of AETE with engineering support from McAir. The progression of events from the qualification testing to the final flight testing recommendations are summarized herein. The primary focus of this paper is on the flying activities such as flutter, loads, stability and control, separation/jettison, and performance. Special instrumentation, flight test techniques, and test concept philosophy are also discussed. This paper highlights various technical problems encountered, such as the near flutter onset condition observed with tanks 50 percent full, the premature failure of the inboard wing spar pylon receptacle discovered after the last maneuvering loads flight, and the localized pitchup phenomena observed during stability and control (S&C) testing. A glance at the increased range and payload capabilities is also included. Overall, the 480 gallon EFT was determined to be a viable option for the CF-18 aircraft. Author

N94-36341# Dassault Aviation, Saint-Cloud (France). Direction Generale Technique.

IN-FLIGHT REFUELING: DASSAULT AVIATION RESEARCH ON THE RAFALE AIRCRAFT [RAVITAILLEMENT EN VOL L'EXPERIENCE DE DASSAULT-AVIATION APPLIQUEE AU RAFALE]

Charles Defreville *In* AGARD, Recent Advances in Long Range and Long Endurance Operation of Aircraft Nov. 1993 11 p In FRENCH

(For primary document see N94-36321 11-05)
Copyright Avail: CASI HC A03/MF A03

The Rafale is the latest combat aircraft built by Dassault Aviation. It is equipped with an in-flight refueling system using a fixed pole. This article relates the important steps taken during its conception and the various technologies that were used: structure, aerodynamics, systems, etc. The second part of the article describes the testing that was conducted in-flight as well as on the ground, making it possible to corroborate the performance of the systems and the flight characteristics of this aircraft.
Transl. by FLS

N94-36342# Frontier Technology, Inc., Beavercreek, OH.
FUTURE TANKER CONSIDERATIONS AND REQUIREMENTS
Lavon Jordan and Michael Krimmer *In* AGARD, Recent Advances in Long Range and Long Endurance Operation of Aircraft Nov. 1993 7 p (For primary document see N94-36321 11-05)
Copyright Avail: CASI HC A02/MF A03

Starting seven years ago, the USAF Aeronautical Systems Center began analyzing future tanker system requirements and developing plans for satisfying these requirements. Frontier Technology, Inc. (FTI) supported the USAF in four of the efforts. Frontier has completed one KC-135 multipoint analysis and is currently doing a second one. The completed effort determined: the pros and cons of hose-drogue refueling and the best fuel pumping rate for the KC-135 using two wing air refueling pods. The current job involves a more in-depth, overall assessment of operational needs, concepts of operation, and alternative wing pods. It emphasizes compatibility with Allied and U.S. Navy aircraft receivers. Frontier Technology is presenting two related papers at this AGARD symposium. This paper covers the rationale and requirements for multipoint refueling. It covers trends and future employment of aerial refueling tankers, as well as the increasing importance of interoperability. Derived from text

N94-36343# Naval Air Warfare Center, Patuxent River, MD. Flight Test and Engineering Group.
AERIAL REFUELING INTEROPERABILITY FROM A RECEIVER FLYING QUALITIES PERSPECTIVE
D. J. Ludwig *In* AGARD, Recent Advances in Long Range and Long Endurance Operation of Aircraft Nov. 1993 7 p (For primary document see N94-36321 11-05)
Copyright Avail: CASI HC A02/MF A03

Over the past decade, there has been increased emphasis on interservice and international operability with respect to aerial refueling (AR). One area concerning interoperability that needs to be considered in light of the increased trend towards large multipoint tankers is receiver flying qualities during AR. This paper stresses the importance of conducting receiver proximity trials to optimize refueling position behind the tanker and providing the pilot with the best receiver flying qualities for AR that can be attained. Receiver flying qualities behind the tanker can be seriously degraded if proper steps to optimize receiver refueling positions are not taken prior to final design. Poor receiver flying qualities in the refueling positions can reduce engagement success rate, increase the amount of training required, increase mishaps, increase refueling cycle time and seriously degrade mission effectiveness of the tanker. There are, of course, many other considerations regarding tanker/receiver compatibility such as airspeed/altitude compatibility, fuel system compatibility, communications, night lighting, etc. But this paper primarily addresses receiver flying qualities and the importance of refueling position behind the tanker as it pertains to flying qualities. Specific programs discussed are Navy trials with the Air Force KC-10 and KC-135 tankers and Navy programs to bring a wing pod tanker capability to the P-3 airplane. Additionally, efforts underway to enhance tanker mission effectiveness of the KC-130 with a variable geometry drogue are discussed and their ramifications explored. Author

N94-36344# McDonnell-Douglas Aerospace, Long Beach, CA. Transport Aircraft.
TANKER SYSTEM AND TECHNOLOGY REQUIREMENTS DEFINITION: A TANKER TECHNOLOGY ROAD MAP
John Koriagin and Berton B. Rund *In* AGARD, Recent Advances in Long Range and Long Endurance Operation of Aircraft Nov. 1993 12 p (For primary document see N94-36321 11-05)
Copyright Avail: CASI HC A03/MF A03

This paper presents a process that leads from comprehensive tanker system requirements analysis to the development of a technology 'road map.' This road map is a matrix listing key technology requirements for future air refueling tanker aircraft capabilities and the current status of research and development activities in these key areas. Generalized examples from material prepared under a U.S. Air Force Contracted Research and Development (CRAD) study are utilized. Multimission capabilities (i.e., tanker, and cargo and passenger transport) are often preferred for these new aircraft. This allows the flexibility of use for many purposes besides that of just air refueling: military cargo and passenger deployments, humanitarian relief, medical air evacuation, executive transport, etc. For this reason these tankers are often referred to as 'tanker/transports' to emphasize these capabilities. In this paper, the term 'tanker' is used to describe what in all likelihood will be a tanker/transport. Author (revised)

N94-36345# Frontier Technology, Inc., Beavercreek, OH.
HOSE-DROGUE VERSUS BOOM RECEPTACLE AIR REFUELING
Donald Copeland and Thomas McConnell *In* AGARD, Recent Advances in Long Range and Long Endurance Operation of Aircraft Nov. 1993 6 p (For primary document see N94-36321 11-05)
Copyright Avail: CASI HC A02/MF A03

The basis of this paper is analyses performed by Frontier Technology, Inc. for the USAF. Frontier has performed evaluations of multiple tanker candidates to supplement and to eventually replace the KC-135 tanker fleet. The analyses included tanker refueling support for six mission areas: theater employment of combat fighter aircraft, intercontinental fighter deployments, extended offshore range of naval carrier operations, intercontinental airlift, North American air defense, and long range nuclear warfare. The characteristic airborne refueling needs of the six missions are somewhat different. The first mission listed, theater employment of combat fighter aircraft, is characteristically different from the other areas in that it stresses the need to refuel more aircraft over shorter periods of time than the other five mission demands except for some situations in air defense support. In theater employment operations the demands of the larger tanker aircraft are stressed the most when waves of aircraft attack during short periods of time in the attempt to overwhelm enemy defenses. This tanker demand is in contrast to that of the nuclear warfare mission which requires large amounts of fuel for a single receiver (bomber) aircraft on a lengthy mission where the precise refueling time is not critical. Author (revised)

N94-36346# Royal Netherlands Air Force, The Hague. Training and Transport Aircraft and Helicopter Div.
THE KDC-10 PROGRAMME OF THE ROYAL NETHERLANDS AIR FORCE
Paul R. Brinkgreve *In* AGARD, Recent Advances in Long Range and Long Endurance Operation of Aircraft Nov. 1993 6 p (For primary document see N94-36321 11-05)
Copyright Avail: CASI HC A02/MF A03

Replacement of the RNLAF F-27 transport fleet, first mooted in 1984, became a serious option a few years later because of a growing need for AAR capacity. Years of discussion and market research resulted in a requirement for (among others) two DC-10 aircraft to be modified into tanker/transport aircraft. The budget was not sufficient to develop new KMD-11 tanker aircraft, nor did it allow buying existing tanker aircraft. On the basis of earlier programs from other countries, involving different aircraft, RNLAF decided that it should be possible to modify two DC-10 aircraft into so-called KDC-10 aircraft. With assistance from McDonnell Douglas Aircraft (MDA), four aircraft were selected on the basis of a number of criteria. These aircraft were studied thoroughly. On the basis of condition and price two Martinair DC10-30 CF aircraft were purchased on 30 June 1992. These will be modified into KDC-10 tanker/transport aircraft. The RNLAF contracted MDA to study feasibility, timetable, and cost of modifying two (Martinair) DC-10-30 CF aircraft into tanker/transport aircraft. The study concluded that the program was feasible within the proposed time frame, given that USAF would cooperate. Also the total cost estimate could be kept within budget. It was not possible to keep the KC-10 Aerial Refuelling Operator (ARO) station, so a new Remote Aerial Refuelling Operator (RARO) station will have to be developed. The design, however, is not completely new as it has been implemented on other aircraft. The RNLAF expects the first KDC-10 aircraft to be in service by January 1995, the second to follow approximately three months later. Based on this, the modification of the first aircraft is scheduled to start on 1 July 1994 and the second in

December 1994. Development of the modification program has already begun. USAF has been requested to assist RNLAF in program management, contracting, and purchasing of certain parts. Author

N94-36347# Aerospace Engineering Test Establishment, Cold Lake (Alberta). Flight Dynamics.
CC-130H(T) TACTICAL AERIAL REFUELLING TANKER DEVELOPMENT FLIGHT TEST PROGRAMME
Andrew Reif and Marc Tremblay *In* AGARD, Recent Advances in Long Range and Long Endurance Operation of Aircraft Nov. 1993 16 p (For primary document see N94-36321 11-05)
Copyright Avail: CASI HC A03/MF A03

This paper describes the development flight test program for the CC-130H(T) Tactical Aerial Refuelling Tanker. The Canadian operational requirement is first described, followed by a detailed discussion of the test item, receiver aircraft, and the ground/flight test method and preliminary results. The development is significant since it represents the first certification of the Flight Refuelling Limited Mk 32B refuelling pods on a Hercules aircraft. Further flight testing to be conducted in the near future are also mentioned. Author

N94-36380*# National Aeronautics and Space Administration. Ames Research Center, Moffett Field, CA.
THE REDUCTION OF TAKEOFF GROUND ROLL BY THE APPLICATION OF A NOSE GEAR JUMP STRUT
Joseph C. Eppel, Martin D. Maisel, J. Greer McClain, and W. Luce May 1994 16 p
(RTOP 505-59-36)
(NASA-TM-108822; A-94082; NAS 1.15:108822) Avail: CASI HC A03/MF A01

A series of flight tests were conducted to evaluate the reduction of takeoff ground roll distance obtainable from a rapid extension of the nose gear strut. The NASA Quiet Short-haul Research Aircraft (QSRA) used for this investigation is a transport-size short take off and landing (STOL) research vehicle with a slightly swept wing that employs the upper surface blowing (USB) concept to attain the high lift levels required for its low-speed, short-field performance. Minor modifications to the conventional nose gear assembly and the addition of a high-pressure pneumatic system and a control system provided the extendable nose gear, or jump strut, capability. The limited flight test program explored the effects of thrust-to-weight ratio, wing loading, storage tank initial pressure, and control valve open time duration on the ground roll distance. The data show that a reduction of takeoff ground roll on the order of 10 percent was achieved with the use of the jump strut, as predicted. Takeoff performance with the jump strut was also found to be essentially independent of the pneumatic supply pressure and was only slightly affected by control valve open time within the range of the parameters examined. Author (revised)

N94-35969*# National Aeronautics and Space Administration. Hugh L. Dryden Flight Research Facility, Edwards, CA.
IN-FLIGHT SIMULATION STUDIES AT THE NASA DRYDEN FLIGHT RESEARCH FACILITY
Mary F. Shafer *In* NASA. Ames Research Center, 1993 Technical Paper Contest for Women. Gear Up 2000: Women in Motion Feb. 1994 p 77-97 (For primary document see N94-35961 11-99)
Avail: CASI HC A03/MF A02

06 AIRCRAFT INSTRUMENTATION

Includes cockpit and cabin display devices; and flight instruments.

For related information see also *19 Spacecraft Instrumentation* and *35 Instrumentation and Photography.*

N94-35344# Radio Technical Commission for Aeronautics, Washington, DC.
MINIMUM PERFORMANCE STANDARDS: AIRBORNE LOW-RANGE RADAR ALTIMETERS
1 Nov. 1974 64 p Supersedes RTCA Paper No. 96-63/DO-123
(RTCA-DO-155) Avail: CASI HC A04/MF A01

Minimum performance standards are set forth for those characteristics of the airborne low-range radar altimeter which are essential for its operation in applications which provide measured height above terrain for clearance and landing data. The potentially diverse range of applications for this equipment precludes the precise definition of the term 'low-range.' It should be recognized that very limited capabilities may suffice in some installations while other installations may require a broader range of altitude (height) data. The maximum range envisioned by system designers at the date of this document is of the order of 2500 feet. The term 'altitude' shall be defined for the purposes of this document as height or distance from the terrain to the altimeter antennas. Compliance with these standards is recommended as a means of assuring that the equipment will satisfactorily perform its intended functions over all conditions normally encountered in routine aeronautical operations. Inasmuch as measured values of radio equipment performance characteristics may be a function of the method of measurement, standard test conditions and methods of tests are also recommended. Derived from text

07 AIRCRAFT PROPULSION AND POWER

Includes prime propulsion systems and systems components, e.g., gas turbine engines and compressors; and onboard auxilliary power plants for aircraft.

For related information see also *20 Spacecraft Propulsion and Power, 28 Propellants and Fuels,* and *44 Energy Production and Conversion.*

N94-35352*# National Aeronautics and Space Administration. Lewis Research Center, Cleveland, OH.
COMPUTATIONAL METHODS FOR HSCT-INLET CONTROLS/CFD INTERDISCIPLINARY RESEARCH
Gary L. Cole, Kevin J. Melcher, Amy K. Chicatelli, Tom T. Hartley, and Joongkee Chung May 1994 13 p Presented at the 30th Joint Propulsion Conference, Indianapolis, IN, 27-29 Jun. 1994; sponsored by AIAA, ASME, SAE, and ASEE
(Contract NCC3-233; NAG3-1450; RTOP 505-62-52)
(NASA-TM-106618; ICOMP-94-10; E-8903; NAS 1.15:106618; AIAA Paper 94-3209) Copyright Avail: CASI HC A03/MF A01

A program aimed at facilitating the use of computational fluid dynamics (CFD) simulations by the controls discipline is presented. The objective is to reduce the development time and cost for propulsion system controls by using CFD simulations to obtain high-fidelity system models for control design and as numerical test beds for control system testing and validation. An interdisciplinary team has been formed to develop analytical and computational tools in three discipline areas: controls, CFD, and computational technology. The controls effort has focused on specifying requirements for an interface between the controls specialist and CFD simulations and a new method for extracting linear, reduced-order control models from CFD simulations. Existing CFD codes are being modified to permit time accurate execution and provide realistic boundary conditions for controls studies. Parallel processing and distributed computing techniques, along with existing system integration software, are being used to reduce CFD execution times and to support the development of an integrated analysis/design system. This paper describes: the initial application for the technology being developed, the high speed civil transport (HSCT) inlet control problem; activities being pursued in each discipline area; and a prototype analysis/design system in place for interactive operation and visualization of a time-accurate HSCT-inlet simulation. Author

N94-35746 Air Force Office of Scientific Research, Bolling AFB, Washington, DC.
AFOSR CONTRACTORS PROPULSION MEETING
M. A. Birkan and J. M. Tishkoff 20 Apr. 1994 338 p Meeting held in Atlantic City, NJ, 14-18 Jun. 1993 Limited Reproducibility: More than 20% of this document may be affected by microfiche quality
(AF Proj. 2308)
(AD-A279028; AFOSR-TR-94-0275) Avail: Issuing Activity (Defense Technical Information Center (DTIC))

Abstracts are given for research in airbreathing combustion, rocket propulsion, and diagnostics in reacting media supported by the Air Force Office of Scientific Research. DTIC

N94-36379*# National Aeronautics and Space Administration. Lewis Research Center, Cleveland, OH.

COMPLIANT METAL ENHANCED CONVECTION COOLED REVERSE-FLOW ANNULAR COMBUSTOR

Marc D. Paskin and Waldo A. Acosta Jun. 1994 24 p Presented at the 30th Joint Propulsion Conference, Indianapolis, IN, 27-29 Jun. 1994; sponsored by AIAA, ASME, SAE, and ASEE Original contains color illustrations
(Contract NAS3-24226; DA Proj. 1L1-62211-A-47-A; RTOP 537-04-20)
(NASA-TM-106626; E-8917; NAS 1.15:106626; ARL-MR-151; AIAA Paper 94-2710) Avail: CASI HC A03/MF A01; 1 functional color page

A joint Army/NASA program was conducted to design, fabricate, and test an advanced, reverse-flow, small gas turbine combustor using a compliant metal enhanced (CME) convection wall cooling concept. The objectives of this effort were to develop a design method (basic design data base and analysis) for the CME cooling technique and tben demonstrate its application to an advanced cycle, small, reverse-flow combustor with 3000 F (1922 K) burner outlet temperature (BOT). The CME concept offers significant improvements in wall cooling effectiveness resulting in a large reduction in cooling air requirements. Therefore, more air is available for control of burner outlet temperature pattern in addition to the benefit of improved efficiency, reduced emissions, and smoke levels. Rig test results demonstrated the benefits and viability of the CME concept meeting or exceeding the aerothermal performance and liner wall temperature characteristics of similar lower temperature-rise combustors, achieving 0.15 pattern factor at 3000 F (1922 K) BOT, while utilizing approximately 80 percent less cooling air than conventional, film-cooled combustion systems. Author (revised)

N94-36333# Naval Air Warfare Center, Warminster, PA. Aircraft Div.

PROPULSION SYSTEM SELECTION FOR A HIGH ALTITUDE LONG ENDURANCE AIRCRAFT

John D. Cyrus and Joseph Franz *In* AGARD, Recent Advances in Long Range and Long Endurance Operation of Aircraft Nov. 1993 7 p
(For primary document see N94-36321 11-05)
Copyright Avail: CASI HC A02/MF A03

N94-36334# Rolls-Royce Ltd., Bristol (England).

PROPULSION SYSTEM TECHNOLOGIES FOR LONG RANGE AND LONG ENDURANCE AIRCRAFT

K. R. Garwood *In* AGARD, Recent Advances in Long Range and Long Endurance Operation of Aircraft Nov. 1993 7 p (For primary document see N94-36321 11-05)
Copyright Avail: CASI HC A02/MF A03

N94-36335# Industrieanlagen-Betriebsgesellschaft m.b.H., Ottobrunn (Germany).

THE STRATO 2C PROPULSION SYSTEM: A LOW COST APPROACH FOR A HIGH ALTITUDE LONG ENDURANCE AIRCRAFT

H. Toenskoetter *In* AGARD, Recent Advances in Long Range and Long Endurance Operation of Aircraft Nov. 1993 6 p (For primary document see N94-36321 11-05)
Copyright Avail: CASI HC A02/MF A03

08 AIRCRAFT STABILITY AND CONTROL

Includes aircraft handling qualities; piloting; flight controls; and autopilots.

For related information see also *05 Aircraft Design, Testing and Performance.*

N94-35258*# National Aeronautics and Space Administration. Hugh L. Dryden Flight Research Facility, Edwards, CA.

FLIGHT TESTING A PROPULSION-CONTROLLED AIRCRAFT EMERGENCY FLIGHT CONTROL SYSTEM ON AN F-15 AIRPLANE

F. W. Burcham, Jr., John Burken, and Trindel A. Maine NASA, Washington Jun. 1994 19 p Presented at the 7th Biennial Flight Test Conference, Colorado Springs, CO, 20-23 Jun. 1994
(RTOP 533-02-34)
(NASA-TM-4590; H-1988; NAS 1.15:4590; AIAA Paper 94-2123)
Copyright Avail: CASI HC A03/MF A01

Flight tests of a propulsion-controlled aircraft (PCA) system on an F-15 airplane have been conducted at the NASA Dryden Flight Research Center. The airplane was flown with all flight control surfaces locked both in the manual throttles-only mode and in an augmented system mode. In the latter mode, pilot thumbwheel commands and aircraft feedback parameters were used to position the throttles. Flight evaluation results showed that the PCA system can be used to land an airplane that has suffered a major flight control system failure safely. The PCA system was used to recover the F-15 airplane from a severe upset condition, descend, and land. Pilots from NASA, U.S. Air Force, U.S. Navy, and McDonnell Douglas Aerospace evaluated the PCA system and were favorably impressed with its capability. Manual throttles-only approaches were unsuccessful. This paper describes the PCA system operation and testing. It also presents flight test results and pilot comments. Author

N94-35796 Air Force Inst. of Tech., Wright-Patterson AFB, OH. School of Engineering.

DIRECT REDUCED ORDER MIXED H2/H INFINITY CONTROL FOR THE SHORT TAKE-OFF AND LANDING/MANEUVER TECHNOLOGY DEMONSTRATOR (STOL/MTD) M.S. Thesis

William C. Reigelsperger, Jr. Mar. 1994 169 p Limited Reproducibility: More than 20% of this document may be affected by microfiche quality
(AD-A278675; AFIT/GAE/ENY/94M-3) Avail: Issuing Activity (Defense Technical Information Center (DTIC))

One of the conclusions from the STOL/MTD program was the need for a multivariable method of designing controllers of low order. This research investigated that problem by studying reduced order mixed H-two/H-infinity control theory applied to the STOL Landing configuration which employs both thrust vectoring and the use of a canard. Model matching techniques were used to obtain responses that met handling qualities criteria and reduced pilot workload by decoupling pitch rate and velocity commands. The time responses were found through nonlinear simulation and showed that the full order designs did match the ideal models very well and had good noise and wind rejection. Singular value analysis showed that the commands were decoupled very well. The reduced order method was mixed H-two/H-infinity optimization. A fourth order controller that had good performance was found by using a performance constraint, and a fourth order controller that provided good margins was found using a robustness constraint. A third order controller was also found with a performance constraint. Recommendations for finding a low order controller, with good performance and robustness are given. DTIC

N94-36384 Purdue Univ., West Lafayette, IN. School of Aeronautics and Astronautics.

AEROSERVOELASTIC TAILORING WITH PIEZOELECTRIC MATERIALS: ACTUATOR OPTIMIZATION STUDIES Final Report, 1 Oct. 1991 - 30 Sep. 1993

Terrence A. Weisshaar and Mario A. Rotea 9 Feb. 1994 48 p Limited Reproducibility: More than 20% of this document may be affected by microfiche quality
(Grant AF-AFOSR-0386-91)
(AD-A278640; Aero-3; AFOSR-94-0263TR) Avail: Issuing Activity (Defense Technical Information Center (DTIC))

This report summarizes aeroservoelastic tailoring studies in which adaptive material actuators are used to control structural deflection of aeroelastic systems. The problem is to furnish enough directed control of a system to make the control of the phenomenon feasible. Specific research problems considered are: choice of the actuator material for effective control; geometric arrangement for active control; and optimum coverage of surface panels for effective control. A specific method of controller design is suggested to determine the limits of control. It is applied to a typical section whose response to random atmospheric turbulence is to be controlled. A finite element method is developed to model actuator and sensor output for plate-like actuators and its use is illustrated for wing-like configurations to demonstrate the benefits of orthotropic material actuators. Finally, the problem of optimum actuators to supply deflection of panels for wing surfaces is examined to determine optimality criteria for such panels and to use strain energy as a guide for efficient use of actuator/host plate combinations. DTIC

N94-36436*# Sterling Software, Inc., Moffett Field, CA.
ALLEVIATION OF WHIRL-FLUTTER ON A JOINED-WING TILT-ROTOR AIRCRAFT CONFIGURATION USING ACTIVE CONTROLS
Johannes M. VanAken 1991 27 p Presented at the International Specialists' Meeting on Rotorcraft Basic Research of the American Helicopter Society, Atlanta, GA, 25-27 Mar. 1991 See also A92-14423
(Contract NCC2-417)
(NASA-CR-196103; NAS 1.26:196103) Avail: CASI HC A03/MF A01

The feasibility of using active controls to delay the onset of whirl-flutter on a joined-wing tilt rotor aircraft was investigated. The CAMRAD/JA code was used to obtain a set of linear differential equations which describe the motion of the joined-wing tilt-rotor aircraft. The hub motions due to wing/body motion is a standard input to CAMRAD/JA and were obtained from a structural dynamics model of a representative joined-wing tilt-rotor aircraft. The CAMRAD/JA output, consisting of the open-loop system matrices, and the airframe free vibration motion were input to a separate program which performed the closed-loop, active control calculations. An eigenvalue analysis was performed to determine the flutter stability of both open- and closed-loop systems. Sensor models, based upon the feedback of pure state variables and based upon hub-mounted sensors, providing physically measurable accelerations, were evaluated. It was shown that the onset of tilt-rotor whirl-flutter could be delayed from 240 to above 270 knots by feeding back vertical and span-wise accelerations, measured at the rotor hub, to the longitudinal cyclic pitch. Time response calculations at a 270-knot cruise condition showed an active cyclic pitch control level of 0.009 deg, which equates to a very acceptable 9 pound active-control force applied at the rotor hub. Author

N94-35873*# National Aeronautics and Space Administration. Langley Research Center, Hampton, VA.
FLUTTER SUPPRESSION DIGITAL CONTROL LAW DESIGN AND TESTING FOR THE AFW WIND TUNNEL MODEL
Vivek Mukhopadhyay *In its* NASA Workshop on Distributed Parameter Modeling and Control of Flexible Aerospace Systems Jun. 1994 p 135-149 (For primary document see N94-35865 11-18)
Avail: CASI HC A03/MF A06

N94-35874*# California Univ., Los Angeles, CA. Dept. of Mechanical, Aerospace and Nuclear Engineering.
SELECTED TOPICS ON THE ACTIVE CONTROL OF HELICOPTER AEROMECHANICAL AND VIBRATION PROBLEMS
Peretz P. Friedmann *In* NASA. Langley Research Center, NASA Workshop on Distributed Parameter Modeling and Control of Flexible Aerospace Systems Jun. 1994 p 151-177 (For primary document see N94-35865 11-18)
(Grant NAG2-477)
Avail: CASI HC A03/MF A06

N94-35875*# Ohio State Univ., Columbus. Dept. of Electrical Engineering.
ROBUST CONTROL DESIGN TECHNIQUES FOR ACTIVE FLUTTER SUPPRESSION
Hitay Ozbay and Glen R. Bachmann *In* NASA. Langley Research Center, NASA Workshop on Distributed Parameter Modeling and Control of Flexible Aerospace Systems Jun. 1994 p 179-191 (For primary document see N94-35865 11-18)
Avail: CASI HC A03/MF A06

N94-35962*# National Aeronautics and Space Administration. Ames Research Center, Moffett Field, CA.
PILOTED SIMULATION STUDY OF TWO TILT-WING CONTROL CONCEPTS
Lourdes G. Birckelbaw and Lloyd D. Corliss *In its* 1993 Technical Paper Contest for Women. Gear Up 2000: Women in Motion Feb. 1994 p 1-12 (For primary document see N94-35961 11-99)
Avail: CASI HC A03/MF A02

N94-35972*# National Aeronautics and Space Administration. Ames Research Center, Moffett Field, CA.
GROUND VIBRATION TEST OF THE XV-15 TILTROTOR RESEARCH AIRCRAFT AND PRETEST PREDICTIONS
Karen Studebaker and Anita Abrego *In its* 1993 Technical Paper Contest for Women. Gear Up 2000: Women in Motion Feb. 1994 p 117-123 (For primary document see N94-35961 11-99)
Avail: CASI HC A02/MF A02

N94-36329# Technische Univ., Munich (Germany). Inst. of Flight Mechanics and Flight Control.
IMPROVEMENT OF ENDURANCE PERFORMANCE BY PERIODIC OPTIMAL CONTROL OF VARIABLE CAMBER
G. Sachs and R. Mehlhorn *In* AGARD, Recent Advances in Long Range and Long Endurance Operation of Aircraft Nov. 1993 7 p (For primary document see N94-36321 11-05)
Copyright Avail: CASI HC A02/MF A03

09 RESEARCH AND SUPPORT FACILITIES (AIR)

Includes airports, hangars and runways; aircraft repair and overhaul facilities; wind tunnels; shock tubes; and aircraft engine test stands.
For related information see also *14 Ground Support Systems and Facilities (Space).*

N94-35267*# Sverdrup Technology, Inc., Brook Park, OH.
HOT CORROSION TEST FACILITY AT THE NASA LEWIS SPECIAL PROJECTS LABORATORY Final Report
Raymond C. Robinson and Michael D. Cuy May 1994 39 p
(Contract NAS3-25266; RTOP 537-04-20)
(NASA-CR-195323; E-8770; NAS 1.26:195323) Avail: CASI HC A03/MF A01

The Hot Corrosion Test Facility (HCTF) at the NASA Lewis Special Projects Laboratory (SPL) is a high-velocity, pressurized burner rig currently used to evaluate the environmental durability of advanced ceramic materials such as SiC and Si3N4. The HCTF uses laboratory service air which is preheated, mixed with jet fuel, and ignited to simulate the conditions of a gas turbine engine. Air, fuel, and water systems are computer-controlled to maintain test conditions which include maximum air flows of 250 kg/hr (550 lbm/hr), pressures of 100-600 kPa (1-6 atm), and gas temperatures exceeding 1500 C (2732 F). The HCTF provides a relatively inexpensive, yet sophisticated means for researchers to study the high-temperature oxidation of advanced materials, and the injection of a salt solution provides the added capability of conducting hot corrosion studies. Author

N94-36437# Wichita State Univ., KS. Aerodynamic Labs.
THREE-DIMENSIONAL FORCE DATA ACQUISITION AND BOUNDARY CORRECTIONS FOR THE WALTER H. BEECH MEMORIAL 7 X 10 FOOT LOW SPEED WIND TUNNEL
Bonnie L. Johnson, James E. Leigh, and Kevin A. Moore Jun. 1993 47 p
(AR93-2) Avail: CASI HC A03/MF A01

The Walter H. Beech Memorial 7 X 10 Foot Low-Speed Wind Tunnel at The Wichita State University has gone through many recent upgrades. One significant major upgrade has been the streamlining of the data acquisition and reduction system. This report covers the upgrades to the software and supersedes previous reports on the data reduction routines for three-dimensional models tested in the wind tunnel. A HP 9000/380 workstation processes the data by reduction and correction equations in a HP BASIC/UX program. For the data to be corrected, model and test section correction constants are required. These constants are used to correct the force and moment data for tunnel boundary and interference effects and to facilitate the reduction of the force and moment data into coefficient form. The data reduction methods and equations needed to calculate the proper model constants are presented as well as examples illustrating the methods. These examples and the methods presented in this report are only for three-dimensional models. Accuracy and rapid processing of data are of high importance in wind tunnel testing; accuracy and speed are achieved in this tunnel through the use of a HP 3852 Data Acquisition System. The final corrected data are presented to the customer in both graphical and tabulated forms in the reference axis or axes of their choice (body, wind, or stability). The on-line system is capable of providing immediate corrected tabulated data and plotted results affording real time monitoring of the test objectives and thus providing the wind tunnel user with an invaluable management tool for the customer's particular

test requirements. Examples of the plotting capability are included.
Author (revised)

12 ASTRONAUTICS (GENERAL)

For extraterrestrial exploration see *91 Lunar and Planetary Exploration.*

N94-35390*# National Aeronautics and Space Administration, Washington, DC.
AEROSPACE SAFETY ADVISORY PANEL Annual Report
Mar. 1993 82 p Original contains color illustrations
(NASA-TM-109840; NAS 1.15:109840) Avail: CASI HC A05/MF A01; 1 functional color page

The Aerospace Safety Advisory Panel (ASAP) provided oversight on the safety aspects of many NASA programs. In addition, ASAP undertook three special studies. At the request of the Administrator, the panel assessed the requirements for an assured crew return vehicle (ACRV) for the space station and reviewed the organization of the safety and mission quality function within NASA. At the behest of Congress, the panel formed an independent, ad hoc working group to examine the safety and reliability of the space shuttle main engine. Section 2 presents findings and recommendations. Section 3 consists of information in support of these findings and recommendations. Appendices A, B, C, and D, respectively, cover the panel membership, the NASA response to the findings and recommendations in the March 1992 report, a chronology of the panel's activities during the reporting period, and the entire ACRV study report.
Derived from text

N94-35510* Jet Propulsion Lab., California Inst. of Tech., Pasadena, CA.
MAGELLAN TO VENUS (Videotape)
Jul. 1990 Videotape: 3 min. 35 sec. playing time, in color, with sound
(NASA-CR-195779; NONP-NASA-VT-94-15918) Avail: CASI VHS A01/BETA A22

This video presents cell animation of the Magellan approach to Venus, orbit insertion, and mapping sequence. CASI

N94-35511* Jet Propulsion Lab., California Inst. of Tech., Pasadena, CA.
PLANETARY ROVER PROGRAM (Videotape)
Jul. 1990 Videotape: 10 min. playing time, in color, with sound
(NASA-CR-196108; NONP-NASA-VT-94-15919) Avail: CASI VHS A01/BETA A22

This video presentation explains the Planetary Rover Program and shows testing in the Arroyo near JPL. CASI

N94-35518# Joint Publications Research Service, Arlington, VA.
JPRS REPORT: SCIENCE AND TECHNOLOGY. CENTRAL EURASIA: SPACE
16 Feb. 1994 39 p Transl. into ENGLISH from various Russian articles
(JPRS-USP-94-001) Avail: CASI HC A03/MF A01

Translated articles cover the following topics: optimization of perturbation maneuver of solar-sail equipped spacecraft near the moon in a geocentric boost problem; model of particle fluxes and averaged energy spectra of solar cosmic rays; forecasting radiation conditions in interplanetary space; depth profiles of dielectric permeability of cryolithosphere of Mars; qualitative analysis of some methods of reducing the asteroid hazards for the earth; origin and current status of the problem of asteroid hazard; probability of asteroids colliding with Earth; description of control associated with placement of spacecraft in vicinity of L(sub 2) point of sun-Earth system via use of lunar gravity; optimal spatial transfer of a spacecraft between the lunar surface and artificial lunar satellite orbit; fly-back booster said to be most promising design for reusable aerospace system; and annual, semiannual, and seasonal variations of total ozone as deduced from TOMS data for the region of St. Petersburg. CASI

N94-35520# Joint Publications Research Service, Arlington, VA.
JPRS REPORT: SCIENCE AND TECHNOLOGY. CENTRAL EURASIA: SPACE
22 Apr. 1994 32 p Transl. into ENGLISH from various Russian articles
(JPRS-USP-94-003) Avail: CASI HC A03/MF A01

Translated articles cover the following topics: influence of aerosol atmosphere on colorimetric characteristics of water surfaces in space observation; allowance for influence of waves and cloud cover in measurements of ocean surface temperature from artificial earth satellites by microwave-spectrometer method; Almaz 1 Spacecraft - 'Okean-I' Program: preliminary results of high-resolution radar observation of oceanic processes, internal waves; Russia's space plans to end of decade; views of value of space program, future of Buran; accomplishments of space program lauded; superiority of reusable aerospace systems; pros and cons of cooperation on Alpha Space Station Project; and nuclear power sources for space, cooperation with U.S. CASI

N94-35827 Mitre Corp., Bedford, MA.
THE EARTH SATELLITE PROGRAM (ESP), VERSION 2.0
R. Callwood and L. M. Gaffney Feb. 1994 111 p Limited Reproducibility: More than 20% of this document may be affected by microfiche quality
(Contract F19628-94-C-0001)
(AD-A278860; MTR-93B0000070-V2) Avail: Issuing Activity (Defense Technical Information Center (DTIC))

The Earth Satellite Program (ESP) version 2.0 is a user-friendly, highly graphical, Macintosh-based program that was developed for the Air Force Milstar program to support satellite constellation and ground site terminal design studies. The computer program generates satellite ground tracks; computes elevation angles, ranges, and range rates; determines outage zones for a constellation of satellites; and generates spot beam projections. Any elliptical Earth-orbit may be accommodated. A fourth-order Runge-Kutta integrator is used to propagate satellite orbits. Perturbations due to the Earth's oblateness (J2 effects), atmospheric drag, and solar radiation pressure are included. This paper contains a user's guide to the program, presents the underlying mathematical models, and includes several sample outputs and the software on diskette. DTIC

N94-36011# Joint Publications Research Service, Arlington, VA.
JPRS REPORT: SCIENCE AND TECHNOLOGY. CENTRAL EURASIA: SPACE
5 Oct. 1993 42 p Transl. into ENGLISH from various Russian articles
(JPRS-USP-93-005) Avail: CASI HC A03/MF A01

Translated articles on the following topics are presented: history and prospects of orbital space station programs; problems involving the study of the effectiveness of aviation/space systems; and development of first Soviet photoreconnaissance satellite Zenit. CASI

N94-36440*# National Aeronautics and Space Administration, Washington, DC.
[THE HISTORY OF SPACE EXPLORATION]
Martin J. Collins (National Air and Space Museum, Washington, DC.) and Sylvia K. Kraemer 1994 8 p Repr. from Space: Discovery and Exploration (Hugh Lauter Levin Associates, Inc., Hong Kong), 1993 p 7-11
(NASA-TM-109886; NAS 1.15:109886; ISBN-0-88363-893-2) Copyright
Avail: CASI HC A02/MF A01

Presented are the acknowledgements and introduction sections of the book 'Space: Discovery and Exploration.' The goal of the book is to address some basic questions of American space history, including how this history compares with previous eras of exploration, why the space program was initiated when it was, and how the U.S. space program developed. In pursuing these questions, the intention is not to provide exhaustive answers, but to point the reader toward a more varied picture of how our venture in space has intersected with American government, politics, business, and science. CASI

N94-35626*# National Aeronautics and Space Administration. Marshall Space Flight Center, Huntsville, AL.
ATLAS SOLAR POINTING OPERATIONS
C. A. Tyler (Teledyne Brown Engineering, Huntsville, AL.) and C. J. Zimmerman *In* NASA. Goddard Space Flight Center, Flight Mechanics/Estimation Theory Symposium, 1994 May 1994 p 271-279
(For primary document see N94-35605 11-13)
(Contract NAS8-41000)
Avail: CASI HC A02/MF A04

13 ASTRODYNAMICS

Includes powered and free-flight trajectories; and orbital and launching dynamics.

N94-35487*# Georgia Inst. of Tech., Atlanta, GA. School of Aerospace Engineering.
THEORY AND COMPUTATION OF OPTIMAL LOW- AND MEDIUM-THRUST TRANSFERS Semiannual Status Report, 7 Jan. - 6 Jul. 1994
C.-H. Chuang 6 Jul. 1994 10 p
(Grant NAG8-921)
(NASA-CR-196077; NAS 1.26:196077) Avail: CASI HC A02/MF A01

This report describes the current state of development of methods for calculating optimal orbital transfers with large numbers of burns. Reported on first is the homotopy-motivated and so-called direction correction method. So far this method has been partially tested with one solver; the final step has yet to be implemented. Second is the patched transfer method. This method is rooted in some simplifying approximations made on the original optimal control problem. The transfer is broken up into single-burn segments, each single-burn solved as a predictor step and the whole problem then solved with a corrector step. Author

N94-35605*# National Aeronautics and Space Administration. Goddard Space Flight Center, Greenbelt, MD.
FLIGHT MECHANICS/ESTIMATION THEORY SYMPOSIUM, 1994
Kathy R. Hartman, ed. Washington May 1994 533 p Symposium held in Greenbelt, MD, 17-19 May 1994
(RTOP 550-00-00)
(NASA-CP-3265; Rept-94B00060; NAS 1.55:3265) Avail: CASI HC A23/MF A04

This conference publication includes 41 papers and abstracts presented at the Flight Mechanics/Estimation Theory Symposium on May 17-19, 1994. Sponsored by the Flight Dynamics Division of Goddard Space Flight Center, this symposium featured technical papers on a wide range of issues related to orbit-attitude prediction, determination and control; attitude sensor calibration; attitude determination error analysis; attitude dynamics; and orbit decay and maneuver strategy. Government, industry, and the academic community participated in the preparation and presentation of these papers. For individual titles, see N94-35606 through N94-35646.

N94-35606*# Air Force Inst. of Tech., Wright-Patterson AFB, OH. Dept. of Aeronautics and Astronautics.
MODAL DECOMPOSITION OF HAMILTONIAN VARIATIONAL EQUATIONS **c64**
William E. Wiesel *In* NASA. Goddard Space Flight Center, Flight Mechanics/Estimation Theory Symposium, 1994 May 1994 p 3-13
(For primary document see N94-35605 11-13)
Avail: CASI HC A03/MF A04

Over any finite arc of trajectory, the variational equations of a Hamiltonian system can be separated into 'normal' modes. This transformation is canonical, and the Lyapunov exponents over the trajectory arc occur as positive/negative pairs for conjugate modes, while the modal vectors remain unit vectors. This decomposition effectively solves the variational equations for any canonical, linear-dependent system. As an example, we study the Voyager I trajectory. In an interplanetary flyby, some of the modal variables increase by very large multiplicative factors, but this means that their conjugate modal variables decrease by those same very large multiplicative vectors. Maneuver strategies for this case are explored, and the minimum delta upsilon maneuver is found. Author

N94-35607*# Jet Propulsion Lab., California Inst. of Tech., Pasadena, CA.
LOW ENCOUNTER SPEED COMET COMA SAMPLE RETURN MISSIONS Abstract Only **c90**
P. Tsou, C. W. Yen, and A. L. Albee *In* NASA. Goddard Space Flight Center, Flight Mechanics/Estimation Theory Symposium, 1994 May 1994 p 15 (For primary document see N94-35605 11-13)
Avail: CASI HC A01/MF A04

Comets, being considered the most primitive bodies in the solar system, command the highest priority among solar-system objects for studying solar nebula evolution and the evolution of life through biogenic elements and compounds. The study of comets, and more especially, of material from them, provides an understanding of the physical, chemical, and mineralogical processes operative in the formation and earliest development of the solar systems. These return samples will provide valuable information on comets and serve as a rosetta stone for the analytical studies conducted on interplanetary dust particles over the past two decades, and will provide much needed extraterrestrial samples for the planetary materials community since the Apollo program. Lander sample return missions require rather complex spacecraft, intricate operations, and costly propulsion systems. By contrast, it is possible to take a highly simplified approach for sample capture and return in the case of a comet. In the past, we have considered Earth free-return trajectory to the comet, in which passive collectors intercept dust and volatiles from the cometary coma. However, standard short period cometary free-return trajectories results in the comet to the spacecraft encounter speeds in the range of 10 km/s. At these speeds the kinetic energy of the capture process can render significant modification of dust structure, change of solid phase as well as the lost of volatiles components. This paper presents a class of new missions with trajectories with significant reduction of encounter speeds by incorporating gravity assists and deep space maneuvering. Low encounter speed cometary flyby sample return will enable a marked increase in the value of the return science. Acquiring thousands of samples from a known comet and thousands of images of a comet nucleus would be space firsts. Applying new approach in flight mechanics to generate a new class of low encounter speed cometary sample return trajectories opens new possibilities in science. A systematic search of trajectories for the first decade of the twenty-first century will be made. The target encounter speed is for less than 7 km/s to short period comets. Author

N94-35608*# National Aeronautics and Space Administration. Goddard Space Flight Center, Greenbelt, MD.
HIGH EARTH ORBIT DESIGN FOR LUNAR ASSISTED SMALL EXPLORER CLASS MISSIONS
M. Mathews (Computer Sciences Corp., Lanham, MD.), M. Hametz (Computer Sciences Corp., Lanham, MD.), J. Cooley, and D. Skillman *In its* Flight Mechanics/Estimation Theory Symposium, 1994 May 1994 p 17-31
(For primary document see N94-35605 11-13)
(Contract NAS5-31500)
Avail: CASI HC A03/MF A04

Small Expendable launch vehicles are capable of injecting modest payloads into high Earth orbits having apogee near the lunar distance. However, lunar and solar perturbations can quickly lower perigee and cause premature reentry. Costly perigee raising maneuvers by the spacecraft are required to maintain the orbit. In addition, the range of inclinations achievable is limited to those of launch sites unless costly spacecraft maneuvers are performed. This study investigates the use of a lunar swingby in a near-Hohmann transfer trajectory to raise perigee into the 8 to 25 solar radius range and reach a wide variety of inclinations without spacecraft maneuvers. It is found that extremely stable orbits can be obtained if the postencounter spacecraft orbital period is one-half of a lunar sidereal revolution and the Earth-vehicle-Moon geometry is within a specified range. Criteria for achieving stable orbits with various perigee heights and ecliptic inclinations are developed, and the sensitivity of the resulting mission orbits to transfer trajectory injection (TTI) errors is examined. It is shown that carefully designed orbits yield lifetimes of several years, with excellent ground station coverage characteristics and minimal eclipses. A phasing loop error correction strategy is considered with the spacecraft propulsion system delta V demand for TTI error correction and a postlunar encounter apogee trim maneuver typically in the 30 to 120 meters per second range. Author

N94-35609*# National Aeronautics and Space Administration. Goddard Space Flight Center, Greenbelt, MD.
OBTAINING COINCIDENT IMAGE OBSERVATIONS FOR MISSION TO PLANET EARTH SCIENCE DATA RETURN **c43**
Lauri Kraft Newman, David C. Folta, and James P. Farrell *In its* Flight Mechanics/Estimation Theory Symposium, 1994 May 1994 p 33-47
(For primary document see N94-35605 11-13)
Avail: CASI HC A03/MF A04

One objective of the Mission to Planet Earth (MTPE) program involves comparing data from various instruments on multiple spacecraft to obtain a total picture of the Earth's systems. To correlate image data from instruments on different spacecraft, these spacecraft must be able to image the same location on the Earth at approximately the same time. Depending on the orbits of the spacecraft involved, complicated operational details must be considered to obtain such observations. If the spacecraft are in similar orbits, close formation flying or synchronization techniques may be used to assure coincident observations. If the orbits are dissimilar, the launch time of the second satellite may need to be restricted in order to align its orbit with that of the first satellite launched. This paper examines strategies for obtaining coincident observations for spacecraft in both similar and dissimilar orbits. Although these calculations may be performed easily for coplanar spacecraft, the non-coplanar case involves additional considerations which are incorporated into the algorithms presented herein. Author

N94-35610*# National Aeronautics and Space Administration. Goddard Space Flight Center, Greenbelt, MD.

AUTOMATED MANEUVER PLANNING USING A FUZZY LOGIC ALGORITHM

D. Conway (Computer Sciences Corp., Lanham, MD.), R. Sperling (Computer Sciences Corp., Lanham, MD.), D. Folta, K. Richon, and R. DeFazio *In its* Flight Mechanics/Estimation Theory Symposium, 1994 May 1994 p 49-62 (For primary document see N94-35605 11-13)
(Contract NAS5-31500)
Avail: CASI HC A03/MF A04

Spacecraft orbital control requires intensive interaction between the analyst and the system used to model the spacecraft trajectory. For orbits with right mission constraints and a large number of maneuvers, this interaction is difficult or expensive to accomplish in a timely manner. Some automation of maneuver planning can reduce these difficulties for maneuver-intensive missions. One approach to this automation is to use fuzzy logic in the control mechanism. Such a prototype system currently under development is discussed. The Tropical Rainfall Measurement Mission (TRMM) is one of several missions that could benefit from automated maneuver planning. TRMM is scheduled for launch in August 1997. The spacecraft is to be maintained in a 350-km circular orbit throughout the 3-year lifetime of the mission, with very small variations in this orbit allowed. Since solar maximum will occur as early as 1999, the solar activity during the TRMM mission will be increasing. The increasing solar activity will result in orbital maneuvers being performed as often as every other day. The results of automated maneuver planning for the TRMM mission will be presented to demonstrate the prototype of the fuzzy logic tool. Author

N94-35611*# Massachusetts Inst. of Tech., Lexington. Lincoln Lab.

REDUCTION PROCEDURES FOR ACCURATE ANALYSIS OF MSX SURVEILLANCE EXPERIMENT DATA

E. Mike Gaposchkin, Mark T. Lane, and Rick I. Abbot *In* NASA. Goddard Space Flight Center, Flight Mechanics/Estimation Theory Symposium, 1994 May 1994 p 63-76 (For primary document see N94-35605 11-13)
(Contract F19628-90-C-0002)
Avail: CASI HC A03/MF A04

Technical challenges of the Midcourse Space Experiment (MSX) science instruments require careful characterization and calibration of these sensors for analysis of surveillance experiment data. Procedures for reduction of Resident Space Object (RSO) detections will be presented which include refinement and calibration of the metric and radiometric (and photometric) data and calculation of a precise MSX ephemeris. Examples will be given which support the reduction, and these are taken from ground-test data similar in characteristics to the MSX sensors and from the IRAS satellite RSO detections. Examples to demonstrate the calculation of a precise ephemeris will be provided from satellites in similar orbits which are equipped with S-band transponders. Author

N94-35612*# National Aeronautics and Space Administration. Goddard Space Flight Center, Greenbelt, MD.

FIXED-HEAD STAR TRACKER ATTITUDE UPDATES ON THE HUBBLE SPACE TELESCOPE **c89**

Matthew S. Nadelman (Computer Sciences Corp., Laurel, MD.), Jeffrey B. Karl (Computer Sciences Corp., Laurel, MD.), and Lou Hallock *In its* Flight Mechanics/Estimation Theory Symposium, 1994 May 1994 p 79-93 (For primary document see N94-35605 11-13)
(Contract NAS5-31500)
Avail: CASI HC A03/MF A04

The Hubble Space Telescope (HST) was launched in April 1990 to begin observing celestial space to the edge of the universe. National Aeronautics and Space Administration (NASA) standard fixed-head star trackers (FHST's) are used operationally onboard the HST to regularly adjust ('update') the spacecraft attitude before the acquisition of guide stars for science observations. During the first 3 months of the mission, the FHST's updated the spacecraft attitude successfully only 85 percent of the time. During the other periods, the trackers were unable to find the selected stars -- either they failed to find any star, or worse, they selected incorrect stars and produced erroneous attitude updates. In July 1990, the HST project office at Goddard Space Flight Center (GSFC) requested that Computer Sciences Corporation (CSC) form an investigative 'tiger' team to examine these FHST update failures. This paper discusses the work of the FHST tiger team, describes the investigations that led the team to identify the sources of the errors, and defines the solutions that were subsequently developed, which ultimately increased the success rate of FHST updates to approximately 98 percent. Author

N94-35613*# National Aeronautics and Space Administration. Goddard Space Flight Center, Greenbelt, MD.

IN-FLIGHT SCALE/DISTORTION CALIBRATION OF THE HUBBLE SPACE TELESCOPE FIXED-HEAD STAR TRACKERS **c74**

R. McCutcheon (Computer Sciences Corp., Laurel, MD.), John J. Boia (Computer Sciences Corp., Laurel, MD.), Martin F. Gakenheimer (Allied-Signal Aerospace Co., Seabrook, MD.), L. Hallock, E. Kimmer, S. Murphy, and Gary L. Welter *In its* Flight Mechanics/Estimation Theory Symposium, 1994 May 1994 p 95-108 (For primary document see N94-35605 11-13)
(Contracts NAS5-31000; NAS5-31500)
Avail: CASI HC A03/MF A04

This paper describes an in-flight scale and distortion calibration procedure that has been developed for the Ball Aerospace Systems Division Fixed-Head Star Trackers (FHST's) used on the Hubble Space Telescope (HST). The FHST is a magnetically focused and deflected imaging sensor that is designed to track stars as faint as m(sub v) = 5.7 over an 8 degree by 8 degree field of view. Raw FHST position measurements are accurate to approximately 200 arcseconds, but this can be improved to 10-15 arcseconds by processing the raw measurements through calibration polynomials that correct for flat field, temperature intensity, and magnetic field effects. The coefficients for these polynomials were initially determined using ground test data. On HST the use of three FHST's is an integral part of the preliminary attitude update procedures required before the acquisition of guide stars for science observations. To this end, FHST-based attitude determination having single-axis errors no worse than 22 arcseconds (1 sigma) is required. In early 1991 it became evident that one of the HST FHST's was experiencing a significant change in its optical scale. By mid-1993 the size of this error had grown to a point that, if not corrected, it would correspond to a maximum position error on the order of 100 arcseconds. Subsequent investigations demonstrated that substantial, uncompensated cubic distortion effects had also developed, the maximum contribution to position errors from the cubic terms being on the order of 30 arcseconds. To ensure accurate FHST-based attitude updates, procedures have been developed to redetermine the FHST scale and distortion calibration coefficients based on in-flight data gathered during normal HST operations. These scale and distortion calibrations have proven very effective operationally, and procedures are in place to monitor FHST calibration changes on a continuing basis. Author

N94-35614*# Computer Sciences Corp., Laurel, MD.

A LONG-BASELINE METHOD FOR HST GYRO DRIFT RATE BIAS CALIBRATION Abstract Only **c35**

John J. Boia, Gary L. Welter, and Martin F. Gakenheimer *In* NASA. Goddard Space Flight Center, Flight Mechanics/Estimation Theory Symposium, 1994 May 1994 p 109 (For primary document see N94-35605 11-13)
(Contract NAS5-31500)
Avail: CASI HC A01/MF A04

The routine on-orbit calibration of the Hubble Space Telescope (HST) rate gyro assemblies (RGA's) has depended on several related algorithms for drift rate bias calibration. The gyros have exhibited time-varying biases, which must be regularly corrected to maintain pointing stability. Currently, gyro drift parameters are uplinked to the spacecraft every 1-2 days for low rate mode and every 7 days for high rate mode. In order to minimize the impact of frequent calibrations on the HST science schedule, we have refined the gyro calibration algorithms and data collection schemes to reduce the amounts of telemetry data and processing time required for accurate bias calibration. We present a review of the evolution of the gyro calibration algorithms, with particular attention to what we have called the long-baseline bias (LBBIAS) technique, and describe the relative success of these methods in maintaining spacecraft stability. Author

N94-35615*# National Aeronautics and Space Administration. Goddard Space Flight Center, Greenbelt, MD.

THE IN-FLIGHT CALIBRATION OF THE HUBBLE SPACE TELESCOPE FINE GUIDANCE SENSORS, 2 (A SUCCESS STORY) c35

Gary L. Welter (Computer Sciences Corp., Laurel, MD.), L. Abramowicz-Reed (Hughes Danbury Optical Systems, Inc., CT.), A. Guha (AKG, Inc., MN.), L. Hallock, and E. Kimmer *In its* Flight Mechanics/Estimation Theory Symposium, 1994 May 1994 p 111-122 (For primary document see N94-35605 11-13)
(Contracts NAS5-31500; NAS5-31786; NAS5-31000)
Avail: CASI HC A03/MF A04

The Hubble Space Telescope's fine guidance sensors (FGS's) are unique in the performance levels being attempted; spacecraft control and astrometric research with accuracies better than 3 milli-arcseconds (mas) are the ultimate goals. This paper presents a review of the in-flight calibration of the sensors, describing both the algorithms used and the results achieved to date. The work was done primarily in support of engineering operations related to spacecraft pointing and control and secondarily in support of the astrometric science calibration effort led by the Space Telescope Astrometry Team. Calibration items of principal interest are distortion, sensor magnification, and relative alignment. An initial in-flight calibration of the FGS's was performed in December 1990; this calibration has been used operationally over the past few years. Followup work demonstrated that significant, unexpected temporal variations in the calibration parameters are occurring; provided good characterization of the variation; and set the stage for a distortion calibration designed to achieve the full design accuracy for one of the FGS's. This full distortion calibration, using data acquired in January 1993, resulted in a solution having single-axis residuals with a standard deviation of 2.5 mas. Scale and alignment calibration results for all of the FGS's have been achieved commensurate with the best ground-based astrometric catalogs (root-mean-square error approximately 25 mas). A calibration monitoring program has been established to allow regular updates of the calibration parameters as needed. Author

N94-35616*# National Aeronautics and Space Administration. Goddard Space Flight Center, Greenbelt, MD.

IN-FLIGHT ESTIMATION OF GYRO NOISE ON THE UPPER ATMOSPHERE RESEARCH SATELLITE (UARS) AND EXTREME ULTRAVIOLET EXPLORER (EUVE) MISSIONS c35

M. Lee, P. Crouse, R. Harman, Terry Leid, W. Davis, and S. Underwood *In its* Flight Mechanics/Estimation Theory Symposium, 1994 May 1994 p 123-137 (For primary document see N94-35605 11-13)
(Contract NAS5-32500)
Avail: CASI HC A03/MF A04

This paper characterizes the low-frequency noise response of the Teledyne dry rotor inertial reference unit (DRIRU) gyroscopes on the Upper Atmosphere Research Satellite (UARS) and the Extreme Ultraviolet Explorer (EUVE). The accuracy of spacecraft attitude estimation algorithms that use gyro data for propagating the spacecraft attitude is sensitive to gyro noise. EUVE gyro data were processed to validate a single-axis gyro noise model, which is used onboard various spacecraft. The paper addresses the potential impact of temperature effects on the gyro noise model and the overall impact on attitude determination accuracy. The power spectral density (PSD) of the gyro noise is estimated from UARS in-flight data by Fast Fourier Transform (FFT). The role of actuator dynamics on the PSD function is also discussed. Author

N94-35617*# National Aeronautics and Space Administration. Goddard Space Flight Center, Greenbelt, MD.

OPERATIONAL SUPPORT FOR UPPER ATMOSPHERE RESEARCH SATELLITE (UARS) ATTITUDE SENSORS c19

M. Lee, A. Garber, M. Lambertson, P. Raina, S. Underwood, and C. Woodruff *In its* Flight Mechanics/Estimation Theory Symposium, 1994 May 1994 p 139-151 (For primary document see N94-35605 11-13)
(Contract NAS5-31500)
Avail: CASI HC A03/MF A04

The Upper Atmosphere Research Satellite (UARS) has several sensors that can provide observations for attitude determination: star trackers, Sun sensors (gimbaled as well as fixed), magnetometers, Earth sensors, and gyroscopes. The accuracy of these observations is important for mission success. Analysts on the Flight Dynamics Facility (FDF) UARS Attitude task monitor these data to evaluate the performance of the sensors taking corrective action when appropriate. Monitoring activities range from examining the data during real-time passes to constructing long-term trend plots. Increasing residuals (differences) between the observed and expected quantities is a prime indicator of sensor problems. Residual increases may be due to alignment shifts and/or degradation in sensor output. Residuals from star tracker data revealed and anomalous behavior that contributes to attitude errors. Compensating for this behavior has significantly reduced the attitude errors. This paper discusses the methods used by the FDF UARS attitude task for maintenance of the attitude sensors, including short- and long-term monitoring, trend analysis, and calibration methods, and presents the results obtained through corrective action. Author

N94-35618*# Computer Sciences Corp., Lanham, MD.

SPACECRAFT ATTITUDE DETERMINATION ACCURACY FROM MISSION EXPERIENCE c18

D. Brasoveanu and J. Hashmall *In* NASA. Goddard Space Flight Center, Flight Mechanics/Estimation Theory Symposium, 1994 May 1994 p 153-166 (For primary document see N94-35605 11-13)
(Contract NAS5-31500)
Avail: CASI HC A03/MF A04

This paper summarizes a compilation of attitude determination accuracies attained by a number of satellites supported by the Goddard Space Flight Center Flight Dynamics Facility. The compilation is designed to assist future mission planners in choosing and placing attitude hardware and selecting the attitude determination algorithms needed to achieve given accuracy requirements. The major goal of the compilation is to indicate realistic accuracies achievable using a given sensor complement based on mission experience. It is expected that the use of actual spacecraft experience will make the study especially useful for mission design. A general description of factors influencing spacecraft attitude accuracy is presented. These factors include determination algorithms, inertial reference unit characteristics, and error sources that can affect measurement accuracy. Possible techniques for mitigating errors are also included. Brief mission descriptions are presented with the attitude accuracies attained, grouped by the sensor pairs used in attitude determination. The accuracies for inactive missions represent a compendium of missions report results, and those for active missions represent measurements of attitude residuals. Both three-axis and spin stabilized missions are included. Special emphasis is given to high-accuracy sensor pairs, such as two fixed-head star trackers (FHST's) and fine Sun sensor plus FHST. Brief descriptions of sensor design and mode of operation are included. Also included are brief mission descriptions and plots summarizing the attitude accuracy attained using various sensor complements. Author

N94-35619*# Jet Propulsion Lab., California Inst. of Tech., Pasadena, CA.

COMPATIBILITY OF TOPEX/POSEIDON TRAJECTORY PROPAGATION WITH JPL AND GSFC/FDF OPERATIONAL SOFTWARE

Ahmed Salama, Michael Nemesure, Joseph Guinn, Dave Bolvin, and Robert Leavitt *In* NASA. Goddard Space Flight Center, Flight Mechanics/Estimation Theory Symposium, 1994 May 1994 p 169-178 (For primary document see N94-35605 11-13)
Avail: CASI HC A02/MF A04

Two independent trajectory software systems are used to perform the TOPEX/Poseidon operational orbit determination and propagation: the Goddard Trajectory Determination System (GTDS) at the GSF/FDF and the Double Precision Trajectory System (DPTRAJ) at JPL. GTDS is used for operational tracking and TDRS-based orbit determination. DPTRAJ is used for ephemeris generation necessary to conduct day-to-day mission operations. This paper describes the DPTRAJ/GTDS trajectory comparison analysis conducted jointly by JPL and GSFC to ensure the compatibility of these two independent trajectory software systems. Author

N94-35620*# National Aeronautics and Space Administration. Goddard Space Flight Center, Greenbelt, MD.

IMPROVED SOLUTION ACCURACY FOR TDRSS-BASED TOPEX/POSEIDON ORBIT DETERMINATION

C. E. Doll, G. D. Mistretta, R. C. Hart, D. H. Oza, D. T. Bolvin, C. M. Cox, M. Nemesure, D. J. Niklewski, and M. V. Samii *In its* Flight Mechanics/Estimation Theory Symposium, 1994 May 1994 p 179-193 (For primary document see N94-35605 11-13)
(Contract NAS5-31500)
Avail: CASI HC A03/MF A04

Orbit determination results are obtained by the Goddard Space Flight Center (GSFC) Flight Dynamics Division (FDD) using a batch-least-squares estimator available in the Goddard Trajectory Determination System (GTDS) and an extended Kalman filter estimation system to process Tracking and Data Relay Satellite (TDRS) System (TDRSS) measurements. GTDS is the operational orbit determination system used by the FDD in support of the Ocean Topography Experiment (TOPEX)/Poseidon spacecraft navigation and health and safety operations. The extended Kalman filter was implemented in an orbit determination analysis prototype system, closely related to the Real-Time Orbit Determination System/Enhanced (RTOD/E) system. In addition, the Precision Orbit Determination (POD) team within the GSFC Space Geodesy Branch generated an independent set of high-accuracy trajectories to support the TOPEX/Poseidon scientific data. These latter solutions use the geodynamics (GEODYN) orbit determination system with laser ranging and Doppler Orbitography and Radiopositioning integrated by satellite (DORIS) tracking measurements. The TOPEX/Poseidon trajectories were estimated for November 7 through November 11, 1992, the timeframe under study. Independent assessments were made of the consistencies of solutions produced by the batch and sequential methods. The batch-least-squares solutions were assessed based on the solution residuals, while the sequential solutions were assessed based on primarily the estimated covariances. The batch-least-squares and sequential orbit solutions were compared with the definitive POD orbit solutions. The solution differences were generally less than 2 meters for the batch-least-squares and less than 13 meters for the sequential estimation solutions. After the sequential estimation solutions were processed with a smoother algorithm, position differences with POD orbit solutions of less than 7 meters were obtained. The differences among the POD, GTDS, and filter/smoother solutions can be traced to differences in modeling and tracking data types, which are being analyzed in detail. Author

N94-35621*# Storm Integration, Inc., San Jose, CA.

IMPLEMENTATION OF A LOW-COST, COMMERCIAL ORBIT DETERMINATION SYSTEM

Jim Corrigan *In* NASA. Goddard Space Flight Center, Flight Mechanics/Estimation Theory Symposium, 1994 May 1994 p 195-209 (For primary document see N94-35605 11-13)
Avail: CASI HC A03/MF A04

This paper describes the implementation and potential applications of a workstation-based orbit determination system developed by Storm Integration, Inc. called the Precision Orbit Determination System (PODS). PODS is offered as a layered product to the commercially-available Satellite Tool Kit (STK) produced by Analytical Graphics, Inc. PODS also incorporates the Workstation/Precision Orbit Determination (WS/POD) product offered by Van Martin System, Inc. The STK graphical user interface is used to access and invoke the PODS capabilities and to display the results. WS/POD is used to compute a best-fit solution to user-supplied tracking data. PODS provides the capability to simultaneously estimate the orbits of up to 99 satellites based on a wide variety of observation types including angles, range, range rate, and Global Positioning System (GPS) data. PODS can also estimate ground facility locations, Earth geopotential model coefficients, solar pressure and atmospheric drag parameters, and observation data biases. All determined data is automatically incorporated into the STK data base, which allows storage, manipulation and export of the data to other applications. PODS is offered in three levels: Standard, Basic GPS and Extended GPS. Standard allows processing of non-GPS observation types for any number of vehicles and facilities. Basic GPS adds processing of GPS pseudo-ranging data to the Standard capabilities. Extended GPS adds the ability to process GPS carrier phase data. Author

N94-35622*# Texas Univ., Austin, TX. Center for Space Research.

TRACKING SYSTEM OPTIONS FOR FUTURE ALTIMETER SATELLITE MISSIONS

G. W. Davis, H. J. Rim, J. C. Ries, and B. D. Tapley *In* NASA. Goddard Space Flight Center, Flight Mechanics/Estimation Theory Symposium, 1994 May 1994 p 211-223 (For primary document see N94-35605 11-13)
(Contract JPL-959737)
Avail: CASI HC A03/MF A04

Follow-on missions to provide continuity in the observation of the sea surface topography once the successful TOPEX/POSEIDON (T/P) oceanographic satellite mission has ended are discussed. Candidates include orbits which follow the ground tracks of T/P GEOSAT or ERS-1. The T/P precision ephemerides, estimated to be near 3 cm root-mean-square, demonstrate the radial orbit accuracy that can be achieved at 1300 km altitude. However, the radial orbit accuracy which can be achieved for a mission at the 800 km altitudes of GEOSAT and ERS-1 has not been established, and achieving an accuracy commensurate with T/P will pose a great challenge. This investigation focuses on the radial orbit accuracy that can be achieved for a mission in the GEOSAT orbit. Emphasis is given to characterizing the effects of force model errors on the estimated radial orbit accuracy, particularly those due to gravity and drag. The importance of global, continuous tracking of the satellite for reduction in these sources of orbit error is demonstrated with simulated GPS tracking data. A gravity tuning experiment is carried out to show how the effects of gravity error may be reduced. Assuming a GPS flight receiver with a full-sky tracking capability, the simulation results indicate that a 5 cm radial orbit accuracy for an altimeter satellite in GEOSAT orbit should be achievable during low-drag atmospheric conditions and after an acceptable tuning of the gravity model. Author

N94-35623*# National Aeronautics and Space Administration. Goddard Space Flight Center, Greenbelt, MD.

IMPROVED SOLUTION ACCURACY FOR LANDSAT-4 (TDRSS-USER) ORBIT DETERMINATION

D. H. Oza (Computer Sciences Corp., Lanham, MD.), D. J. Niklewski (Computer Sciences Corp., Lanham, MD.), C. E. Doll, G. D. Mistretta, and R. C. Hart *In its* Flight Mechanics/Estimation Theory Symposium, 1994 May 1994 p 225-236 (For primary document see N94-35605 11-13)
(Contract NAS5-31500)
Avail: CASI HC A03/MF A04

This paper presents the results of a study to compare the orbit determination accuracy for a Tracking and Data Relay Satellite System (TDRSS) user spacecraft, Landsat-4, obtained using a Prototype Filter Smoother (PFS), with the accuracy of an established batch-least-squares system, the Goddard Trajectory Determination System (GTDS). The results of Landsat-4 orbit determination will provide useful experience for the Earth Observing System (EOS) series of satellites. The Landsat-4 ephemerides were estimated for the January 17-23, 1991, timeframe, during which intensive TDRSS tracking data for Landsat-4 were available. Independent assessments were made of the consistencies (overlap comparisons for the batch case and convariances for the sequential case) of solutions produced by the batch and sequential methods. The filtered and smoothed PFS orbit solutions were compared with the definitive GTDS orbit solutions for Landsat-4; the solution differences were generally less than 15 meters. Author

N94-35624*# National Aeronautics and Space Administration. Goddard Space Flight Center, Greenbelt, MD.

OPTIMUM SATELLITE RELAY POSITIONS WITH APPLICATION TO A TDRS-1 INDIAN OCEAN RELAY

A. H. Jackson and P. Christopher *In its* Flight Mechanics/Estimation Theory Symposium, 1994 May 1994 p 237-251 (For primary document see N94-35605 11-13)
Avail: CASI HC A03/MF A04

An Indian Ocean satellite relay is examined. The relay satellite position is optimized by minimizing the sum of downlink and satellite to satellite link losses. Osculating orbital elements are used for fast intensive orbital computation. Integrated Van Vleck gaseous attenuation and a Crane rain model are used for downlink attenuation. Circular polarization losses on the satellite to satellite link are found dynamically. Space to ground link antenna pointing losses are included as a function of yaw ans spacecraft limits. Relay satellite positions between 90 to 100 degrees East are found attractive for further study. Author

N94-35625*# National Aeronautics and Space Administration. Goddard Space Flight Center, Greenbelt, MD.

TDRSS ONBOARD NAVIGATION SYSTEM (TONS) FLIGHT QUALIFICATION EXPERIMENT

C. J. Gramling, R. C. Hart, D. C. Folta, and A. C. Long *In its* Flight Mechanics/Estimation Theory Symposium, 1994 May 1994 p 253-267 (For primary document see N94-35605 11-13)
(Contract NAS5-31500)
Avail: CASI HC A03/MF A04

The National Aeronautics and Space Administration (NASA) Goddard Space Flight Center (GSFC) is currently developing an operational Tracking and Data Relay Satellite (TDRS) System (TDRSS) Onboard Navigation System (TONS) to provide realtime, autonomous, high-accuracy navigation products to users of TDRSS. A TONS experiment was implemented on the Explorer Platform/Extreme Ultraviolet Explorer (EP/EUVE) spacecraft, launched June 7, 1992, to flight qualify the TONS operational system using TDRSS forward-link communications services. This paper provides a detailed evaluation of the flight hardware, an ultrastable oscillator (USO) and Doppler extractor (DE) card in one of the TDRSS user transponders and the ground-based prototype flight software performance, based on the 1 year of TONS experiment operation. The TONS experiment results are used to project the expected performance of the TONS 1 operational system. TONS 1 processes Doppler data derived from scheduled forward-link S-band services using a sequential estimation algorithm enhanced by a sophisticated process noise model to provide onboard orbit and frequency determination and time maintenance. TONS 1 will be the prime navigation system on the Earth Observing System (EOS)-AM1 spacecraft, currently scheduled for launch in 1998. Inflight evaluation of the USO and DE short-term and long-term stability indicates that the performance is excellent. Analysis of the TONS prototype flight software performance indicates that realtime onboard position accuracies of better than 25 meters root-mean-square are achievable with one tracking contact every one to two orbits for the EP/EUVE 525-kilometer altitude, 28.5 degree inclination orbit. The success of the TONS experiment demonstrates the flight readiness of TONS to support the EOS-AM1 mission. Author

N94-35626*# National Aeronautics and Space Administration. Marshall Space Flight Center, Huntsville, AL.

ATLAS SOLAR POINTING OPERATIONS c12

C. A. Tyler (Teledyne Brown Engineering, Huntsville, AL.) and C. J. Zimmerman *In* NASA. Goddard Space Flight Center, Flight Mechanics/Estimation Theory Symposium, 1994 May 1994 p 271-279 (For primary document see N94-35605 11-13)
(Contract NAS8-41000)
Avail: CASI HC A02/MF A04

The ATLAS-series of Spacelab missions are comprised of a diverse group of scientific instruments including instruments for studying the sun and how the sun's energy changes across an eleven-year solar cycle. The ATLAS solar instruments are located on one or more pallets in the Orbiter payload bay and use the Orbiter as a pointing platform for their examinations of the sun. One of the ATLAS instruments contained a sun sensor which allowed scientists and engineers on the ground to see the pointing error of the sun with respect to the instrument and correct for the error based upon the information coming from the ATLAS 1 and ATLAS 2 missions with particular attention given to identifying the sources of pointing discrepancies of the solar instruments and to describe the crew and ground controller procedures that were developed to correct for these discrepancies. The Orbiter pointing behavior from the ATLAS 1 and ATLAS 2 flights presented in this paper can be applied to future flights which use the Orbiter as a pointing platform. Author (revised)

N94-35627*# Integrated Systems, Inc., Santa Clara, CA.

OVERVIEW OF THE MINIATURE SENSOR TECHNOLOGY INTEGRATION (MSTI) SPACECRAFT ATTITUDE CONTROL SYSTEM c18

Rob McEwen *In* NASA. Goddard Space Flight Center, Flight Mechanics/Estimation Theory Symposium, 1994 May 1994 p 281-295 (For primary document see N94-35605 11-13)
Avail: CASI HC A03/MF A04

Msti2 is a small, 164 kg (362 lb), 3-axis stabilized, low-Earth-orbiting satellite whose mission is missile booster tracking. The spacecraft is actuated by 3 reaction wheels and 12 hot gas thrusters. It carries enough fuel for a projected life of 6 months. The sensor complement consists of a Horizon Sensor, a Sun Sensor, low-rate gyros, and a high rate gyro for despin. The total pointing control error allocation is 6 mRad (.34 Deg), and this is while tracking a target on the Earth's surface. This paper describes the Attitude Control System (ACS) algorithms which include the following: attitude acquisition (despin, Sun and Earth acquisition), attitude determination, attitude control, and linear stability analysis. Author (revised)

N94-35628*# Analytic Sciences Corp., Reston, VA.

A GEOMETRIC MODEL OF A V-SLIT SUN SENSOR CORRECTING FOR SPACECRAFT WOBBLE c19

W. P. McMartin and S. S. Gambhir *In* NASA. Goddard Space Flight Center, Flight Mechanics/Estimation Theory Symposium, 1994 May 1994 p 297-302 (For primary document see N94-35605 11-13)
Avail: CASI HC A02/MF A04

A V-Slit sun sensor is body-mounted on a spin-stabilized spacecraft. During injection from a parking or transfer orbit to some final orbit, the spacecraft may not be dynamically balanced. This may result in wobble about the spacecraft spin axis as the spin axis may not be aligned with the spacecraft's axis of symmetry. While the widely used models in Spacecraft Attitude Determination and Control, edited by Wertz, correct for separation, elevation, and azimuthal mounting biases, spacecraft wobble is not taken into consideration. A geometric approach is used to develop a method for measurement of the sun angle which corrects for the magnitude and phase of spacecraft wobble. The algorithm was implemented using a set of standard mathematical routines for spherical geometry on a unit sphere. Author (revised)

N94-35629*# Integrated Systems, Inc., Santa Clara, CA.

OVERVIEW OF THE MSTI 2 ON-ORBIT ALIGNMENT c18

Christopher A. Rygaard, Fred W. Smith, and M. Michael Briggs *In* NASA. Goddard Space Flight Center, Flight Mechanics/Estimation Theory Symposium, 1994 May 1994 p 303-313 (For primary document see N94-35605 11-13)
Avail: CASI HC A03/MF A04

The Miniature Sensor Technology Integration (MSTI) 2 Spacecraft is a small 3-axis stabilized spacecraft designed to track mid-range missiles and estimate their state vectors. In order to accurately estimate the target state vector, the MSTI 2 spacecraft must have highly accurate knowledge of its own attitude. Errors in its attitude knowledge arise primarily from the errors in its Attitude Control System (ACS) sensors. The ACS sensors on the spacecraft include a scanning Earth Sensor (ES), a Sun Sensor (SS), and two 2-axis gyros. The On-Orbit Alignment (OOA) generated an error map of the ES and estimated the biases of the SS and the misalignment of the gyros. This paper discusses some of the error sources, and the techniques used to reduce the effects of these errors. The payload carried by the MSTI2 spacecraft is a high fidelity camera, which was aimed at the target using gimballed mirrors. By aiming it at a celestial target, the payload was used as a high-accuracy single-axis attitude reference. This attitude reference was compared to the attitude reference of the ACS sensors, and the errors were attributed to the ACS sensors. Author (revised)

N94-35630*# Analytical Engineering Corp., Boulder, CO.

MEASURING ATTITUDE WITH A GRADIOMETER c18

David Sonnabend and Thomas G. Gardner *In* NASA. Goddard Space Flight Center, Flight Mechanics/Estimation Theory Symposium, 1994 May 1994 p 315-329 Prepared for Colorado Univ., Boulder (For primary document see N94-35605 11-13)
Avail: CASI HC A03/MF A04

This paper explores using a gravity gradiometer to measure the attitude of a satellite, given that the gravity field is accurately known. Since gradiometers actually measure a combination of the gradient and attitude rate and acceleration terms, the answer is far from obvious. The paper demonstrates that it can be done and at microradian accuracy. The technique employed is dynamic estimation, based on the momentum biased Euler equations. The satellite is assumed nominally planet pointed, and subject to control, gravity gradient, and partly radom drag torques. The attitude

estimator is unusual. While the standard method of feeding back measurement residuals is used, the feedback gain matrix isn't derived from Kalman theory. instead, it's chosen to minimize a measure of the terminal covariance of the error in the estimate. This depends on the gain matrix and the power spectra of all the process and measurement noises. An integration is required over multiple solutions of Lyapunov equations.
Author (revised)

N94-35631*# Integrated Systems, Inc., Santa Clara, CA.
OVERVIEW OF THE MSTI 2 PROCESSOR-IN-THE-LOOP SIMULATOR
c61
Christopher A. Rygaard *In* NASA. Goddard Space Flight Center, Flight Mechanics/Estimation Theory Symposium, 1994 May 1994 p 331-340 (For primary document see N94-35605 11-13)
Avail: CASI HC A02/MF A04

To thoroughly test the on-board software for the MSTI 2 spacecraft, it was necessary to generate an environment for the software which accurately simulated the on-orbit conditions of the spacecraft. To achieve this, the MSTI 2 Processor-In-the-Loop (PIL) high-fidelity simulator was developed. The entire development was completed in 3 months and required 4 man-months of effort. This paper describes the design and development of this simulator and the methodology employed. Author (revised)

N94-35632*# Madison Guidance, Navigation and Control, Yorktown Heights, NY.
THE CONTROL OF SATELLITES WITH MICROGRAVITY CONSTRAINTS: THE COMET CONTROL SYSTEM **c18**
Walter Grossman and Douglas Freesland *In* NASA. Goddard Space Flight Center, Flight Mechanics/Estimation Theory Symposium, 1994 May 1994 p 341-354 (For primary document see N94-35605 11-13)
Avail: CASI HC A03/MF A04

The COMET attitude determination and control system, using inverse dynamics and a novel torque distribution/momentum management technique, has shown great flexibility, performance, and robustness. Three-axis control with two wheels is an inherent consequence of inverse dynamics control which allows for reduction in spacecraft weight and cost, or alternatively, provides a simple means of failure-redundancy for three-wheel spacecraft. The control system, without modification, has continued to perform well in spite of large changes in spacecraft mass properties and mission orbit altitude that have occurred during development. This flexibility has obviated imposition of early stringent ADACS design constraints and has greatly reduced commonly incurred ADACS modification costs and delay associated with program maturation. Author (revised)

N94-35633*# Cincinnati Univ., OH. Dept. of Aerospace Engineering.
SELF-RESCUE STRATEGIES FOR EVA CREWMEMBERS EQUIPPED WITH THE SAFER BACKPACK **c54**
Trevor Williams and David Baughman *In* NASA. Goddard Space Flight Center, Flight Mechanics/Estimation Theory Symposium, 1994 May 1994 p 357-371 (For primary document see N94-35605 11-13)
Avail: CASI HC A03/MF A04

An extravehicular astronaut who becomes separated from a space station has three options available: grappling the station immediately by means of a 'shepherd's crook' device; rescue by either a second crewmember flying an MMU or a robotic-controlled MMU; or self-rescue by means of a propulsive system. The first option requires very fast response by a tumbling astronaut; the second requires constant availability of an MMU, as well as a rendezvous procedure thousands of feet from the station. This paper will consider the third option, propulsive self-rescue. In particular, the capability of the new Simplified Aid for EVA Rescue (SAFER) propulsive backpack, which is to be tested on STS-64 in Sep. 1994, will be studied. This system possesses an attitude hold function that can automatically detumble an astronaut after separation. On-orbit tests of candidate self-rescue systems have demonstrated the need for such a feature. SAFER has a total delta(v) capability of about 10 fps, to cover both rotations and translations, compared with a possible separation rate of 2.5 fps. But the delta(v) required for self-rescue is critically dependent on the delay before return can be initiated, as a consequence of orbital effects. A very important practical question is then whether the total delta(v) of SAFER is adequate to perform self-rescue for worst case values of separation speed, time to detumble, and time for the astronaut to visually acquire the station. This paper shows that SAFER does indeed have sufficient propellant to carry out self-rescue in all realistic separation cases, as well as in cases which are considerably more severe than anything likely to be encountered in practice. The return trajectories and total delta(v)'s discussed are obtained by means of an 'inertial line-of-sight targeting' scheme, derived in the paper, which allows orbital effects to be corrected by making use of the visual information available to the pilot, namely the line-of-sight direction to the station relative to the stars. Author (revised)

N94-35634*# Massachusetts Inst. of Tech., Lexington. Lincoln Lab.
SPACE SHUTTLE ORBIT DETERMINATION USING EMPIRICAL FORCE MODELING OF ATTITUDE MANEUVERS FOR THE GERMAN MOMS-02/D2 MISSION
C. vonBraun and Christoph Reigber *In* NASA. Goddard Space Flight Center, Flight Mechanics/Estimation Theory Symposium, 1994 May 1994 p 373-384 Sponsored in part by BMFT and Stuttgart Univ. (For primary document see N94-35605 11-13)
Avail: CASI HC A03/MF A04

In the spring of 1993, the MOMS-02 (modular Optoelectronic Multispectral Scanner) camera, as part of the second German Spacelab mission aboard STS-55, successfully took digital threefold stereo images of the surface of the Earth. While the mission is experimental in nature, its primary goals are to produce high quality maps and three-dimensional digital terrain models of the Earth's surface. Considerable improvement in the quality of the terrain model can be attained if information about the position and attitude of the camera is included during the adjustment of the image data. One of the primary sources of error in the Shuttle's position is due to the significant attitude maneuvers conducted during the course of the mission. Various arcs, using actual Tracking and Data Relay Satellite (TDRSS) Doppler data of STS-55, were processed to determine how effectively empirical force modeling could be used to solve for the radial, transverse, and normal components of the orbit perturbations caused by these routine maneuvers. Results are presented in terms of overlap-orbit differences in the three components. Comparisons of these differences, before and after the maneuvers are estimated, show that the quality of an orbit can be greatly enhanced with this technique, even if several maneuvers are present. Finally, a discussion is made of some of the difficulties encountered with this approach, and some ideas for future studies are presented. Author (revised)

N94-35635*# Mitre Corp., Bedford, MA.
APPLICATION OF A MONTE CARLO ACCURACY ASSESSMENT TOOL TO TDRS AND GPS
Michael S. Pavloff *In* NASA. Goddard Space Flight Center, Flight Mechanics/Estimation Theory Symposium, 1994 May 1994 p 385-398 (For primary document see N94-35605 11-13)
Avail: CASI HC A03/MF A04

In support of a NASA study on the application of radio interferometry to satellite orbit determination, MITRE developed a simulation tool for assessing interferometric tracking accuracy. Initially, the tool was applied to the problem of determining optimal interferometric station siting for orbit determination of the Tracking and Data Relay Satellite (TDRS). Subsequently, the Orbit Determination Accuracy Estimator (ODAE) was expanded to model the general batch maximum likelihood orbit determination algorithms of the Goddard Trajectory Determination System (GTDS) with measurement types including not only group and phase delay from radio interferometry, but also range, range rate, angular measurements, and satellite-to-satellite measurements. The user of ODAE specifies the statistical properties of error sources, including inherent observable imprecision, atmospheric delays, station location uncertainty, and measurement biases. Upon Monte Carlo simulation of the orbit determination process, ODAE calculates the statistical properties of the error in the satellite state vector and any other parameters for which a solution was obtained in the orbit determination. This paper presents results from ODAE application to two different problems: (1)determination of optimal geometry for interferometirc tracking of TDRS, and (2) expected orbit determination accuracy for Global Positioning System (GPS) tracking of low-earth orbit (LEO) satellites. Conclusions about optimal ground station locations for TDRS orbit determination by radio interferometry are presented, and the feasibility of GPS-based tracking for IRIDIUM. a LEO mobile satellite communications (MOBILSATCOM) system, is demonstrated. Author (revised)

N94-35636*# National Aeronautics and Space Administration. Goddard Space Flight Center, Greenbelt, MD.

EVALUATION OF SEMIEMPIRICAL ATMOSPHERIC DENSITY MODELS FOR ORBIT DETERMINATION APPLICATIONS

C. M. Cox (Computer Sciences Corp., Lanham, MD.), R. J. Feiertag (Computer Sciences Corp., Lanham, MD.), D. H. Oza (Computer Sciences Corp., Lanham, MD.), and C. E. Doll *In its* Flight Mechanics/Estimation Theory Symposium, 1994 May 1994 p 399-413 (For primary document see N94-35605 11-13)
(Contract NAS5-31500)
Avail: CASI HC A03/MF A04

This paper presents the results of an investigation of the orbit determination performance of the Jacchia-Roberts (JR), mass spectrometer incoherent scatter 1986 (MSIS-86), and drag temperature model (DTM) atmospheric density models. Evaluation of the models was performed to assess the modeling of the total atmospheric density. This study was made generic by using six spacecraft and selecting time periods of study representative of all portions of the 11-year cycle. Performance of the models was measured for multiple spacecraft, representing a selection of orbit geometries from near-equatorial to polar inclinations and altitudes from 400 kilometers to 900 kilometers. The orbit geometries represent typical low earth-orbiting spacecraft supported by the Goddard Space Flight Center (GSFC) Flight Dynamics Division (FDD). The best available modeling and orbit determination techniques using the Goddard Trajectory Determination System (GTDS) were employed to minimize the effects of modeling errors. The latest geopotential model available during the analysis, the Goddard earth model-T3 (GEM-T3), was employed to minimize geopotential model error effects on the drag estimation. Improved-accuracy techniques identified for TOPEX/Poseidon orbit determination analysis were used to improve the Tracking and Data Relay Satellite System (TDRSS)-based orbit determination used for most of the spacecraft chosen for this analysis. This paper shows that during periods of relatively quiet solar flux and geomagnetic activity near the solar minimum, the choice of atmospheric density model used for orbit determination is relatively inconsequential. During typical solar flux conditions near the solar maximum, the differences between the JR, DTM, and MSIS-86 models begin to become apparent. Time periods of extreme solar activity, those in which the daily and 81-day mean solar flux are high and change rapidly, result in significant differences between the models. During periods of high geomagnetic activity, the standard JR model was outperformed by DTM. Modification of the JR model to use a geomagnetic heating delay of 3 hours, as used in DTM, instead of the 6.7-hour delay produced results comparable to or better than the DTM performance, reducing definitive orbit solution ephermeris overlap differences by 30 to 50 percent. The reduction in the overlap differences would be useful for mitigating the impact of geomagnetic storms on orbit prediction. Author

N94-35637*# National Aeronautics and Space Administration. Goddard Space Flight Center, Greenbelt, MD.

FILTER PARAMETER TUNING ANALYSIS FOR OPERATIONAL ORBIT DETERMINATION SUPPORT

J. Dunham (Computer Sciences Corp., Lanham, MD.), C. Cox (Computer Sciences Corp., Lanham, MD.), D. Niklewski (Computer Sciences Corp., Lanham, MD.), G. Mistretta, and R. Hart *In its* Flight Mechanics/Estimation Theory Symposium, 1994 May 1994 p 415-429 (For primary document see N94-35605 11-13)
(Contract NAS5-31500)
Avail: CASI HC A03/MF A04

The use of an extended Kalman filter (EKF) for operational orbit determination support is being considered by the Goddard Space Flight Center (GSFC) Flight Dynamics Division (FDD). To support that investigation, analysis was performed to determine how an EKF can be tuned for operational support of a set of earth-orbiting spacecraft. The objectives of this analysis were to design and test a general purpose scheme for filter tuning, evaluate the solution accuracies, and develop practical methods to test the consistency of the EKF solutions in an operational environment. The filter was found to be easily tuned to produce estimates that were consistent, agreed with results from batch estimation, and compared well among the common parameters estimated for several spacecraft. The analysis indicates that there is not a sharply defined 'best' tunable parameter set, especially when considering only the position estimates over the data arc. The comparison of the EKF estimates for the user spacecraft showed that the filter is capable of high-accuracy results and can easily meet the current accuracy requirements for the spacecraft included in the investigation. The conclusion is that the EKF is a viable option for FDD operational support. Author

N94-35638*# Computer Sciences Corp., Lanham, MD.

COMPARISON OF KALMAN FILTER AND OPTIMAL SMOOTHER ESTIMATES OF SPACECRAFT ATTITUDE **c18**

J. Sedlak *In* NASA. Goddard Space Flight Center, Flight Mechanics/Estimation Theory Symposium, 1994 May 1994 p 431-445 (For primary document see N94-35605 11-13)
(Contract NAS5-31500)
Avail: CASI HC A03/MF A04

Given a valid system model and adequate observability, a Kalman filter will converge toward the true system state with error statistics given by the estimated error covariance matrix. The errors generally do not continue to decrease. Rather, a balance is reached between the gain of information from new measurements and the loss of information during propagation. The errors can be further reduced, however, by a second pass through the data with an optimal smoother. This algorithm obtains the optimally weighted average of forward and backward propagating Kalman filters. It roughly halves the error covariance by including future as well as past measurements in each estimate. This paper investigates whether such benefits actually accrue in the application of an optimal smoother to spacecraft attitude determination. Tests are performed both with actual spacecraft data from the Extreme Ultraviolet Explorer (EUVE) and with simulated data for which the true state vector and noise statistics are exactly known. Author

N94-35639*# Florida Univ., Gainesville, FL. Dept. of Aerospace Engineering, Mechanics and Engineering Science.

ATTITUDE STABILITY OF A SPINNING SPACECRAFT DURING APPENDAGE DEPLOYMENT/RETRACTION **c18**

Norman Fitz-Coy and Wayne Fullerton *In* NASA. Goddard Space Flight Center, Flight Mechanics/Estimation Theory Symposium, 1994 May 1994 p 447-448 (For primary document see N94-35605 11-13)
Avail: CASI HC A01/MF A04

The work presented is motivated by the need for a national satellite rescue policy, not the ad hoc policy now in place. In studying different approaches for a national policy, the issue of capture and stabilization of a tumbling spacecraft must be addressed. For a rescue mission involving a tumbling spacecraft, it may be advantageous to have a rescue vehicle which is compact and 'rigid' during the rendezvous/capture phase. After capture, passive stabilization techniques could be utilized as an efficient means of detumbling the resulting system (i.e., both the rescue vehicle and captures spacecraft). Since the rescue vehicle is initially compact and 'rigid,' significant passive stabilization through energy dissipation can only be achieved through the deployment of flexible appendages. Once stabilization is accomplished, retraction of the appendages before maneuvering the system to its final destination may also prove advantageous. It is therefore of paramount interest that we study the effect of appendage deployment/retraction on the attitude stability of a spacecraft. Particular interest should be paid to appendage retraction, since if this process is destabilizing, passive stabilization as proposed may not be useful. Over the past three decades, it has been an 'on-again-off-again affair' with the problem of spacecraft appendage deployment. In most instances, these studies have been numerical simulations of specific spacecraft configurations for which there were specific concerns. The primary focus of these studies was the behavior of the appendage during deployment; the effects of appendage retraction was considered only in one of these studies. What is missing in the literature is a thorough study of the effects of appendage deployment/retraction on the attitude stability of a spacecraft. This paper presents a rigorous analysis of the stability of a spinning spacecraft during the deployment or the retraction of an appendage. The analysis is simplified such that meaningful insights into the problem can be inferred; it is not overly simplified such that critical dynamical behavior is neglected. The system is analyzed assuming that the spacecraft hub is rigid. The appendage deployment mechanism is modeled as a point mass on a massless rod whose length undergoes prescribed changes. Simplified flexibility effects of the appendage are included. The system is examined for stability by linearizing the equations in terms of small deviations from steady,

noninterfering coning motion. Routh's procedure for analyzing small deviations from steady motion in dynamical systems is utilized in the analysis. The system of equations are nondimensionalized to facilitate parametric studies. The results are presented in terms of a reduced number of nondimensional parameters so that some general conclusions may be drawn. Verification of the linear analysis is presented through numerical simulations of the complete nonlinear, nonautonomous, coupled equations.
Author (revised)

N94-35640*# Computer Sciences Corp., Lanham, MD.
APPLICATION OF STAR IDENTIFICATION USING PATTERN MATCHING TO SPACE GROUND SYSTEMS AT GSFC c89
D. Fink and D. Shoup *In* NASA. Goddard Space Flight Center, Flight Mechanics/Estimation Theory Symposium, 1994 May 1994 p 451-465 (For primary document see N94-35605 11-13)
(Contract NAS5-31500)
Avail: CASI HC A03/MF A04

This paper reports the application of pattern recognition techniques for star identification based on those proposed by Van Bezooijen to space ground systems for near-real-time attitude determination. A prototype was developed using these algorithms, which was used to assess the suitability of these techniques for support of the X-Ray Timing Explorer (XTE), Submillimeter Wave Astronomy Satellite (SWAS), and the Solar and Heliospheric Observatory (SOHO) missions. Experience with the prototype was used to refine specifications for the operational system. Different geometry tests appropriate to the mission requirements of XTE, SWAS, and SOHO were adopted. The applications of these techniques to upcoming mission support of XTE, SWAS, and SOHO are discussed. Author

N94-35641*# National Aeronautics and Space Administration. Goddard Space Flight Center, Greenbelt, MD.
COLOR/MAGNITUDE CALIBRATION FOR NATIONAL AERONAUTICS AND SPACE ADMINISTRATION (NASA) STANDARD FIXED-HEAD STAR TRACKERS (FHST) c17
J. Landis (Computer Sciences Corp., Lanham, MD.), Terry Leid (Computer Sciences Corp., Lanham, MD.), A. Garber (Computer Sciences Corp., Lanham, MD.), and M. Lee *In its* Flight Mechanics/Estimation Theory Symposium, 1994 May 1994 p 467-480 (For primary document see N94-35605 11-13)
(Contract NAS5-31500)
Avail: CASI HC A03/MF A04

This paper characterizes and analyzes the spectral response of Ball Aerospace fixed-head star trackers, (FHST's) currently in use on some three-axis stabilized spacecraft. The FHST output is a function of the frequency and intensity of the incident light and the position of the star image in the field of view. The FHST's on board the Extreme Ultraviolet Explorer (EUVE) have had occasional problems identifying stars with a high B-V value. These problems are characterized by inaccurate intensity counts observed by the tracker. The inaccuracies are due to errors in the observed star magnitude values. These errors are unique to each individual FHST. For this reason, data were also collected and analyzed from the Upper Atmosphere Research Satellite (UARS). As a consequence of this work, the Goddard Space Flight Center (GSFC) Flight Dynamics Division (FDD) hopes to improve the attitude accuracy on these missions and to adopt better star selection procedures for catalogs. Author

N94-35642*# National Aeronautics and Space Administration. Goddard Space Flight Center, Greenbelt, MD.
ADVANTAGES OF ESTIMATING RATE CORRECTIONS DURING DYNAMIC PROPAGATION OF SPACECRAFT RATES: APPLICATIONS TO REAL-TIME ATTITUDE DETERMINATION OF SAMPEX c18
M. S. Challa (Computer Sciences Corp., Lanham, MD.), G. A. Natanson (Computer Sciences Corp., Lanham, MD.), D. F. Baker, and J. K. Deutschmann *In its* Flight Mechanics/Estimation Theory Symposium, 1994 May 1994 p 481-495 (For primary document see N94-35605 11-13)
(Contract NAS5-31500)
Avail: CASI HC A03/MF A04

This paper describes real-time attitude determination results for the Solar, Anomalous, and Magnetospheric Particle Explorer (SAMPEX), a gyroless spacecraft, using a Kalman filter/Euler equation approach denoted the real-time sequential filter (RTSF). The RTSF is an extended Kalman filter whose state vector includes the attitude quaternion and corrections to the rates, which are modeled as Markov processes with small time constants. The rate corrections impart a significant robustness to the RTSF against errors in modeling the environmental and control torques, as well as errors in the initial attitude and rates, while maintaining a small state vector. SAMPLEX flight data from various mission phases are used to demonstrate the robustness of the RTSF against a priori attitude and rate errors of up to 90 deg and 0.5 deg/sec, respectively, as well as a sensitivity of 0.0003 deg/sec in estimating rate corrections in torque computations. In contrast, it is shown that the RTSF attitude estimates without the rate corrections can degrade rapidly. RTSF advantages over single-frame attitude determination algorithms are also demonstrated through (1) substantial improvements in attitude solutions during sun-magnetic field coalignment and (2) magnetic-field-only attitude and rate estimation during the spacecraft's sun-acquisition mode. A robust magnetometer-only attitude-and-rate determination method is also developed to provide for the contingency when both sun data as well as a priori knowledge of the spacecraft state are unavailable. This method includes a deterministic algorithm used to initialize the RTSF with coarse estimates of the spacecraft attitude and rates. The combined algorithm has been found effective, yielding accuracies of 1.5 deg in attitude and 0.01 deg/sec in the rates and convergence times as little as 400 sec. Author

N94-35643*# State Univ. of New York, Buffalo, NY. Dept. of Mechanical and Aerospace Engineering.
MME-BASED ATTITUDE DYNAMICS IDENTIFICATION AND ESTIMATION FOR SAMPEX c18
Juan DePena, John L. Crassidis, Michael D. McPartland, Thomas J. Meyer, and D. Joseph Mook *In* NASA. Goddard Space Flight Center, Flight Mechanics/Estimation Theory Symposium, 1994 May 1994 p 497-511 Sponsored in part by NAS-NRC (For primary document see N94-35605 11-13)
(Grant NAG5-2181)
Avail: CASI HC A03/MF A04

A method is described for obtaining optimal attitude estimation algorithms for spacecraft lacking attitude rate measurement devices (rate gyros), and then demonstrated using actual flight data from the Solar, Anomalous, and Magnetospheric Particle Explorer (SAMPEX) spacecraft. SAMPEX does not have on-board rate sensing, and relies on sun sensors and a three-axis magnetometer for attitude determination. Problems arise since typical attitude estimation is accomplished by filtering measurements of both attitude and attitude rates. Rates are nearly always sampled much more densely than are attitudes. Thus, the absence/loss of rate data normally reduces both the total amount of data available and the sampling density (in time) by a substantial fraction. As a result, the sensitivity of the estimates to model uncertainty and to measurement noise increases. In order to maintain accuracy in the attitude estimates, there is increased need for accurate models of the rotational dynamics. The proposed approach is based on the minimum model error (MME) optimal estimation strategy, which has been successfully applied to estimation of poorly modeled dynamic systems which are relatively sparsely and/or noisily measured. The MME estimates may be used to construct accurate models of the system dynamics (i.e. perform system model identification). Thus, an MME-based approach directly addresses the problems created by absence of attitude rate measurements. Author

N94-35644*# Comissao Nacional de Atividades Espaciais, Sao Jose Dos Campos (Brazil). Attitude Control Group.
A NEW ALGORITHM FOR ATTITUDE-INDEPENDENT MAGNETOMETER CALIBRATION c18
Roberto Alonso and Malcolm D. Shuster *In* NASA. Goddard Space Flight Center, Flight Mechanics/Estimation Theory Symposium, 1994 May 1994 p 513-527 Sponsored in part by Consejo Nacional de Investigaciones Cientificas y Tecnicas (For primary document see N94-35605 11-13)
Avail: CASI HC A03/MF A04

A new algorithm is developed for inflight magnetometer bias determination without knowledge of the attitude. This algorithm combines the fast convergence of a heuristic algorithm currently in use with the correct treatment of the statistics and without discarding data. The algorithm performance is examined using simulated data and compared with previous algorithms. Author

N94-35645*# Hughes Aircraft Co., Los Angeles, CA.
A SIMPLE SUBOPTIMAL LEAST-SQUARES ALGORITHM FOR ATTITUDE DETERMINATION WITH MULTIPLE SENSORS **c18**
Thomas F. Brozenec and Douglas J. Bender *In* NASA. Goddard Space Flight Center, Flight Mechanics/Estimation Theory Symposium, 1994 May 1994 p 529-543 (For primary document see N94-35605 11-13)
Avail: CASI HC A03/MF A04

Three-axis attitude determination is equivalent to finding a coordinate transformation matrix which transforms a set of reference vectors fixed in inertial space to a set of measurement vectors fixed in the spacecraft. The attitude determination problem can be expressed as a constrained optimization problem. The constraint is that a coordinate transformation matrix must be proper, real, and orthogonal. A transformation matrix can be thought of as optimal in the least-squares sense if it maps the measurement vectors to the reference vectors with minimal 2-norm errors and meets the above constraint. This constrained optimization problem is known as Wahba's problem. Several algorithms which solve Wahba's problem exactly have been developed and used. These algorithms, while steadily improving, are all rather complicated. Furthermore, they involve such numerically unstable or sensitive operations as matrix determinant, matrix adjoint, and Newton-Raphson iterations. This paper describes an algorithm which minimizes Wahba's loss function, but without the constraint. When the constraint is ignored, the problem can be solved by a straightforward, numerically stable least-squares algorithm such as QR decomposition. Even though the algorithm does not explicitly take the constraint into account, it still yields a nearly orthogonal matrix for most practical cases; orthogonality only becomes corrupted when the sensor measurements are very noisy, on the same order of magnitude as the attitude rotations. The algorithm can be simplified if the attitude rotations are small enough so that the approximation sin(theta) approximately equals theta holds. We then compare the computational requirements for several well-known algorithms. For the general large-angle case, the QR least-squares algorithm is competitive with all other know algorithms and faster than most. If attitude rotations are small, the least-squares algorithm can be modified to run faster, and this modified algorithm is faster than all but a similarly specialized version of the QUEST algorithm. We also introduce a novel measurement averaging technique which reduces the n-measurement case to the two measurement case for our particular application, a star tracker and earth sensor mounted on an earth-pointed geosynchronous communications satellite. Using this technique, many n-measurement problems reduce to less than or equal to 3 measurements; this reduces the amount of required calculation without significant degradation in accuracy. Finally, we present the results of some tests which compare the least-squares algorithm with the QUEST and FOAM algorithms in the two-measurement case. For our example case, all three algorithms performed with similar accuracy. Author

N94-35646*# Computer Sciences Corp., Lanham, MD.
MOTION MODELS IN ATTITUDE ESTIMATION **c18**
D. Chu, Z. Wheeler, and J. Sedlak *In* NASA. Goddard Space Flight Center, Flight Mechanics/Estimation Theory Symposium, 1994 May 1994 p 545-557 (For primary document see N94-35605 11-13)
(Contract NAS5-31500)
Avail: CASI HC A03/MF A04

Attitude estimator use observations from different times to reduce the effects of noise. If the vehicle is rotating, the attitude at one time needs to be propagated to that at another time. If the vehicle measures its angular velocity, attitude propagating entails integrating a rotational kinematics equation only. If a measured angular velocity is not available, torques can be computed and an additional rotational dynamics equation integrated to give the angular velocity. Initial conditions for either of these integrations come from the estimation process. Sometimes additional quantities, such as gyro and torque parameters, are also solved for. Although the partial derivatives of attitude with respect to initial attitude and gyro parameters are well known, the corresponding partial derivatives with respect to initial angular velocity and torque parameters are less familiar. They can be derived and computed numerically in a way that is analogous to that used for the initial attitude and gyro parameters. Previous papers have demonstrated the feasibility of using dynamics models for attitude estimation but have not provided details of how each angular velocity and torque parameters can be estimated. This tutorial paper provides some of that detail, notably how to compute the state transition matrix when closed form expressions are not available. It also attempts to put dynamics estimation in perspective by showing the progression from constant to gyro-propagated to dynamics-propagated attitude motion models. Readers not already familiar with attitude estimation will find this paper an introduction to the subject, and attitude specialists may appreciate the collection of heretofore scattered results brought together in a single place. Author

N94-35543*# Jet Propulsion Lab., California Inst. of Tech., Pasadena, CA.
THE MARS OBSERVER DIFFERENTIAL ONE-WAY RANGE DEMONSTRATION
P. M. Kroger, J. S. Border, and S. Nandi *In its* The Telecommunications and Data Acquisition Report 15 May 1994 p 1-15 (For primary document see N94-35542 11-32)
(RTOP 310-10-61-90-01)
Avail: CASI HC A03/MF A03

14 GROUND SUPPORT SYSTEMS AND FACILITIES (SPACE)

Includes launch complexes, research and production facilities; ground support equipment, e.g., mobile transporters; and simulators.

For related information see also *09 Research and Support Facilities (Air).*

No abstracts in this category.

15 LAUNCH VEHICLES AND SPACE VEHICLES

Includes boosters; operating problems of launch/space vehicle systems; and reusable vehicles.

For related information see also *20 Spacecraft Propulsion and Power.*

N94-35377# Naval War Coll., Newport, RI.
GEOSTATIONARY SPACE LAUNCH VEHICLES AND THE US DILEMMA
William G. Clapp (Weber State Coll., Ogden, UT.) 17 Jun. 1994 201 p
Avail: CASI HC A10/MF A03

The U.S. commercial space launch program no longer dominates the world and is now playing 'catch-up' with the world's first commercial launch company, Arianespace. The effort to regain the lead in the commercial space launch market has been hindered by declining Department of Defense budgets. President Clinton's space policy prohibits expensive new launch vehicles and limits the Department of Defense to low-cost upgrades of existing launch vehicles. The U.S. government created the space sector and has an obligation to ensure a smooth and effective split from the emerging commercial space program. Until the ties are severed, the Department of Defense must consider commercial space launch interests when making decisions. Ariane has provided an excellent 'bench mark' for the U.S. to base future launch vehicle upgrades. The 198 commercial satellite launches since 1965 have provided a significant amount of data that were used to critically compare space launch vehicles. The dilemma was that U.S. space launch vehicles were found to be economically superior to Ariane for specific military payloads, but were not effective at launching commercial satellites over a wide range of payload weights. Ariane advantages were identified and low-cost recommendations have been made. If the U.S. sets the target of first equaling and then surpassing Ariane, the U.S. could once again dominate the world commercial launch market. Author

16 SPACE TRANSPORTATION

Includes passenger and cargo space transportation, e.g., shuttle operations; and space rescue techniques.

For related information see also *03 Air Transportation and Safety* and *18 Spacecraft Design, Testing and Performance.* For space suits see *54 Man/System Technology and Life Support.*

N94-35251*# Lockheed Engineering and Sciences Co., Houston, TX.
STS-58 SPACE SHUTTLE MISSION REPORT
Robert W. Fricke, Jr. Jan. 1994 40 p Sponsored by NASA. Johnson Space Center
(NASA-TM-109867; NAS 1.15:109867; NSTS-08287) Avail: CASI HC A03/MF A01

The STS-58 Space Shuttle Program Mission Report provides a summary of the payload activities as well as the orbiter, external tank (ET), solid rocket booster (SRB) and redesigned solid rocket motor (RSRM), and the space shuttle main engine (SSME) subsystems performance during the fifty-eighth mission of the space shuttle program and fifteenth flight of the orbiter vehicle Columbia (OV-102). In addition to the orbiter, the flight vehicle consisted of an ET (ET-57); three SSME's, which were designated as serial numbers 2024, 2109, and 2018 in positions 1, 2, and 3, respectively; and two SRB's which were designated BI-061. The lightweight RSRM's that were installed in each SRB were designated as 360L034A for the left SRB and 360W034B for the right SRB. Derived from text

N94-35252*# Lockheed Engineering and Sciences Co., Houston, TX.
STS-51 SPACE SHUTTLE MISSION REPORT
Robert W. Fricke, Jr. Dec. 1993 56 p Sponsored by NASA. Johnson Space Center
(NASA-TM-109866; NAS 1.15:109866; NSTS-08286) Avail: CASI HC A04/MF A01

The STS-51 Space Shuttle Program Mission Report summarizes the payloads as well as the orbiter, external tank (ET), solid rocket booster (SRB), redesigned solid rocket motor (RSRM), and the space shuttle main engine (SSME) systems performance during the fifty-seventh flight of the space shuttle program and seventeenth flight of the orbiter vehicle Discovery (OV-103). In addition to the orbiter, the flight vehicle consisted of an ET designated as ET-59; three SSME's, which were designated as serial numbers 2031, 2034, and 2029 in positions 1, 2, and 3, respectively; and two SRB's which were designated BI-060. The lightweight RSRM's that were installed in each SRB were designated as 360W033A for the left SRB and 360L033B for the right SRB. Derived from text

N94-35523*# National Aeronautics and Space Administration. John F. Kennedy Space Center, Cocoa Beach, FL.
DEBRIS/ICE/TPS ASSESSMENT AND INTEGRATED PHOTOGRAPHIC ANALYSIS FOR SHUTTLE MISSION STS-59 Final Report, 22 Jul. 1993 - 9 Apr. 1994
Gregory N. Katnik, Barry C. Bowen, and J. Bradley Davis Jun. 1994 148 p Original contains color illustrations
(NASA-TM-109203; NAS 1.15:109203) Avail: CASI HC A07/MF A02; 55 functional color pages

A debris/ice/thermal protection system assessment and integrated photographic analysis was conducted for shuttle mission STS-59. Debris inspections of the flight elements and launch pad were performed before and after launch. Icing conditions on the external tank were assessed by the use of computer programs, nomographs, and infrared scanner data during cryogenic loading of the vehicle followed by an on-pad visual inspection. High speed photography of the launch was analyzed to identify ice/debris sources and evaluate potential vehicle damage and/or in-flight anomalies. This report documents the ice/debris/ thermal protection system conditions and integrated photographic analysis of shuttle mission STS-59, and the resulting effect on the Space Shuttle Program. Author

17 SPACE COMM., SPACECRAFT COMM., COMMAND & TRACKING

Includes telemetry; space communications networks; astronavigation and guidance; and radio blackout.

For related information see also *04 Aircraft Communications and Navigation* and *32 Communications and Radar.*

N94-35269*# National Aeronautics and Space Administration. Goddard Space Flight Center, Greenbelt, MD.
CATLAC: CALIBRATION AND VALIDATION ANALYSIS TOOL OF LOCAL AREA COVERAGE FOR THE SeaWIFS MISSION
Robert H. Woodward (General Sciences Corp., Laurel, MD.), Watson W. Gregg, and Frederick S. Patt May 1994 19 p Original contains color illustrations
(RTOP 970-00-00)
(NASA-TM-104603; Rept-94B00079; NAS 1.15:104603) Avail: CASI HC A03/MF A01; 1 functional color page

Calibration and validation Analysis Tool of Local Area Coverage (CATLAC) is an analysis package for selecting and graphically displaying Earth and space targets for calibration and validation activities on a polar orbiting satellite. The package is written in the Interactive Data Language (IDL) and includes a graphical user interface. Although it is designed specifically for the Sea-viewing Wide Field-of-view Sensor (SeaWiFS) mission, the package can be used for analysis on other Earth-viewing missions. An individual can use text or graphical methods in CATLAC to select Earth targets to be scanned by a satellite. Additional onboard calibration activities (such as observations of the moon, or solar irradiance from a solar diffuser), which use data recorder time, can also be specified. All information pertinent to the creation of a command schedule can be written to a file which is read by a command scheduler. The scheduler can be invoked and the Local Area Coverage (LAC) recording periods can be visually verified using CATLAC. The schedule can also be verified by examining record and error files written by the scheduler. Author

N94-35357*# New Mexico State Univ., Las Cruces, NM. Dept. of Electrical and Computer Engineering.
ISSUES IN THE DEVELOPMENT OF A 10 MBPS K=15 VITERBI DECODER Semiannual Status Report, Feb. - Jun. 1994
William P. Osborne 1994 22 p
(Grant NAG5-1491)
(NASA-CR-196083; NAS 1.26:196083) Avail: CASI HC A03/MF A01

The NMSU Telemetry Center, in collaboration with the NASA Microelectronics Center (MRC) at UNM, has completed a study of the feasibility of building a constraint length 15, rate 1/2 Viterbi Decoder (or BVD) to operate at a rate of 10 Mbps. The BVD, if built, would make TDRSS more accessible to all users, small satellites in particular, by providing an additional 2 dB of link margin, relative to the use of the standard constraint length 7 decoder. The study included the following: review of the 1 Mbps BVD built by the Jet Propulsion Laboratory (JPL), currently the only BVD in existence; development of Specifications for the basic processing unit of the BVD (MRC); analytical Determination of performance of large constraint length convolutional codes; investigation of the impact of processor design on the overall system design; and two feasible packaging technologies, proposed by Cincinnati Electronics of Ohio. It was concluded that while the construction of the BVD is feasible, it will require the most advanced packaging technology currently available, and that the project would be best accomplished in an industrial facility. While the size, complexity, and power requirements of the BVD will be extreme, these will impact only the ground station. The spacecraft will incur a minor change in the encoder design, and the increased coding gain will allow a satellite to operate with a smaller antenna. Derived from text

N94-35641*# National Aeronautics and Space Administration. Goddard Space Flight Center, Greenbelt, MD.
COLOR/MAGNITUDE CALIBRATION FOR NATIONAL AERONAUTICS AND SPACE ADMINISTRATION (NASA) STANDARD FIXED-HEAD STAR TRACKERS (FHST)
J. Landis (Computer Sciences Corp., Lanham, MD.), Terry Leid (Computer Sciences Corp., Lanham, MD.), A. Garber (Computer Sciences Corp., Lanham, MD.), and M. Lee *In its* Flight Mechanics/Estimation Theory

Symposium, 1994 May 1994 p 467-480 (For primary document see N94-35605 11-13)
(Contract NAS5-31500)
Avail: CASI HC A03/MF A04

18 SPACECRAFT DESIGN, TESTING AND PERFORMANCE

Includes satellites; space platforms; space stations; spacecraft systems and components such as thermal and environmental controls; and attitude controls.

For life support systems see *54 Man/System Technology and Life Support.* For related information see also *05 Aircraft Design, Testing and Performance, 39 Structural Mechanics,* and *16 Space Transportation.*

N94-35484*# Massachusetts Inst. of Tech., Cambridge. Dept. of Aeronautics and Astronautics.
STRUCTURAL ASSEMBLY DEMONSTRATION EXPERIMENT, PHASE 1 Final Report, Jul. 1981 - Apr. 1982
David L. Akin, Mary L. Bowden, and Rene H. Miller Mar. 1983 69 p
(Contract NAS8-34501)
(NASA-CR-193967; NAS 1.26:193967; SSL-10-83) Avail: CASI HC A04/MF A01

The goal of this phase of the structural assembly and demonstration experiment (SADE) program was to begin to define a shuttle flight experiment that would yield data to compare on-orbit assembly operations of large space structures with neutral buoyancy simulations. In addition, the experiment would be an early demonstration of structural hardware and human capabilities in extravehicular activity (EVA). The objectives of the MIT study, as listed in the statement of work, were: to provide support in establishing a baseline neutral buoyancy testing data base, to develop a correlation technique between neutral buoyancy test results and on-orbit operations, and to prepare the SADE experiment plan (MSFC-PLAN-913). Derived from text

N94-35585 Naval Surface Warfare Center, Dahlgren, VA.
PRELIMINARY STUDY OF SATELLITE ATTITUDE DETERMINATION FOR THE LANDSAT 7 SPACECRAFT
Patrick J. Fell Apr. 1994 18 p Limited Reproducibility: More than 20% of this document may be affected by microfiche quality
(AD-A278876; NSWCDD/TR-94/15) Avail: Issuing Activity (Defense Technical Information Center (DTIC))

This report presents the results of an error analysis for satellite attitude determination for the LANDSAT 7 spacecraft. The purpose of this study was (1) to evaluate the contribution of dual-antenna Global Positioning System (GPS) measurements to spacecraft attitude uncertainty and (2) to determine if spacecraft attitude could be determined to an accuracy that would allow direct mapping from LANDSAT 7 stereo pair imagery. Although preliminary, the results indicate that GPS measurements have the potential to improve spacecraft attitude if certain technical goals can be achieved associated with GPS instrumentation. The usability of stand-alone stereo pairs for direct mapping, satisfying Defense Mapping Agency (DMA) product standards, is questionable due to correlated stellar sensor errors. DTIC

N94-35648# Martin Marietta Astro Space, Philadelphia, PA.
GPHS-RTGs IN SUPPORT OF THE CASSINI MISSION
24 Apr. 1994 90 p
(Contract DE-AC03-91SF-18852)
(DE94-009994; DOE/SF-18852/T38) Avail: CASI HC A05/MF A01

This report is organized by the program task structure as follows: (1) spacecraft integration and liaison; (2) engineering support; (3) safety; (4) qualified unicouple fabrication; (5) ETG fabrication, assembly, and test; (6) ground support equipment (GSE); (7) RTG shipping and launch support; (8) designs, reviews, and mission applications; (9) project management, quality assurance and reliability, contract changes, noncapital contractor acquired government owned property (CAGO) acquisition, and CAGO maintenance; and (10) CAGO acquisition. DOE

N94-35799 Naval Research Lab., Washington, DC.
NAVSPACECOM SPACE SURVEILLANCE SENSOR SYSTEM DIGITAL SIGNAL PROCESSING RECEIVER. VOLUME 3: OPERATING SYSTEM FUNCTIONS Final Report, Oct. 1990 - Sep. 1993
Carolyn F. Bryant, Tamara A. Myers, and Carl J. Morris 6 Apr. 1994 19 p Limited Reproducibility: More than 20% of this document may be affected by microfiche quality
(AD-A278839; NRL/FR/8150-94-9714-Vol-3) Avail: Issuing Activity (Defense Technical Information Center (DTIC))

This is a system description of the Naval Space Command (NAVSPACECOM) Space Surveillance Sensor System Digital Signal Processing Receiver (DSPR). Formerly known as NAVSPASUR, the Space Surveillance system began as an advanced research project in June 1958, was commissioned as an operational Naval command in February 1961, and is operated by NAVSPACECOM's Space Surveillance Processing Center in Dahlgren, Virginia. The DSPR is a real-time radar data acquisition and analysis system. Its function is to detect, with no prior information, all space objects whose orbits cross the continental United States and to compute their subsequent orbits. It provides vital satellite information in support of national defense mission objectives of space intelligence, satellite attack warning, satellite intercept support, and space mission support. This system description was prepared as part of a modernization program that has replaced DSPR hardware for which parts are no longer available. Volume 3 describes the operating system functions required by the applications software. Volume 4 describes the hardware interfaces between the major subsystems of the DSPR and identifies critical timing paths and interrupts between subsystems. Previously published, Volume 1 (NRL/FR/8154-93-9577) presents an overview of the hardware and software of the DSPR system, and Volume 2 (NRL/FR/8154-93-9578) discusses the function and capabilities of individual software and hardware components of each subsystem. DTIC

N94-35801 Naval Research Lab., Washington, DC.
NAVSPACECOM SPACE SURVEILLANCE SENSOR SYSTEM DIGITAL SIGNAL PROCESSING RECEIVER. VOLUME 4: HARDWARE INTERFACES Final Report, Oct. 1990 - Sep. 1993
Carl J. Morris and Carolyn F. Bryant 6 Apr. 1994 35 p Limited Reproducibility: More than 20% of this document may be affected by microfiche quality
(AD-A278845; NRL/FR/8150-94-9715-Vol-4) Avail: Issuing Activity (Defense Technical Information Center (DTIC))

This is a system description of the Naval Space Command (NAVSPACECOM) Space Surveillance Sensor System Digital Signal Processing Receiver (DSPR). Formerly known as NAVSPASUR, the Space Surveillance system began as an advanced research project in June 1958, was commissioned as a operational Naval command in February 1961, and is operated by NAVSPACECOM's Space Surveillance Processing Center in Dahlgren, Virginia. The DSPR is a real-time radar data acquisition and analysis system. Its function is to detect, with no prior information, all space objects whose orbits cross the continental United States and to their subsequent orbits. It provides vital satellite information in support of national defense mission objectives of space intelligence, satellite attack warning, satellite intercept support, and space mission support. This system description was prepared as part of a modernization program that has replaced DSPR hardware for which parts are no longer available. Volume 3 describes the operating system functions required by the applications software. Volume 4 describes the hardware interfaces between the major subsystems of the DSPR and identifies critical timing paths and interrupts between subsystems. Previously published, Volume 1 (NRL/FR/8154-93-9577) presents an overview of the hardware and software of the DSPR system, and Volume 2 (NRL/FR/8154-93-9578) discusses the function and capabilities of individual software and hardware components of each subsystem. DTIC

N94-35836*# National Aeronautics and Space Administration. Langley Research Center, Hampton, VA.
SECOND INTERNATIONAL SYMPOSIUM ON MAGNETIC SUSPENSION TECHNOLOGY, PART 1
Nelson J. Groom, ed. and Colin P. Britcher, ed. May 1994 416 p Symposium held in Seattle, WA, 11-13 Aug. 1993 Sponsored by NASA, Washington

(RTOP 233-03-01-01)
(NASA-CP-3247-Pt-1; L-17369-Pt-1; NAS 1.55:3247-Pt-1) Avail: CASI HC A18/MF A04

In order to examine the state of technology of all areas of magnetic suspension and to review related recent developments in sensors and controls approaches, superconducting magnet technology, and design/implementation practices, the Second International Symposium on Magnetic Suspension Technology was held. The symposium included 18 technical sessions in which 44 papers were presented. The technical sessions covered the areas of bearings, bearing modeling, controls, vibration isolation, micromachines, superconductivity, wind tunnel magnetic suspension systems, magnetically levitated trains (MAGLEV), rotating machinery and energy storage, and applications. A list of attendees appears at the end of the document. For individual titles, see N94-35837 through N94-35863.

N94-35837*# SatCon Technology Corp., Cambridge, MA.
AEROSPACE APPLICATIONS OF MAGNETIC BEARINGS c37
James Downer, James Goldie, Vijay Gondhalekar, and Richard Hockney *In* NASA. Langley Research Center, Second International Symposium on Magnetic Suspension Technology, Part 1 May 1994 p 3-26 (For primary document see N94-35836 11-18)
Avail: CASI HC A03/MF A04

Magnetic bearings have traditionally been considered for use in aerospace applications only where performance advantages have been the primary, if not only, consideration. Conventional wisdom has been that magnetic bearings have certain performance advantages which must be traded off against increased weight, volume, electric power consumption, and system complexity. These perceptions have hampered the use of magnetic bearings in many aerospace applications because weight, volume, and power are almost always primary considerations. This paper will review progress on several active aerospace magnetic bearings programs at SatCon Technology Corporation. The magnetic bearing programs at SatCon cover a broad spectrum of applications including: a magnetically-suspended spacecraft integrated power and attitude control system (IPACS), a magnetically-suspended momentum wheel, magnetic bearings for the gas generator rotor of a turboshaft engine, a vibration-attenuating magnetic bearing system for an airborne telescope, and magnetic bearings for the compressor of a space-rated heat pump system. The emphasis of these programs is to develop magnetic bearing technologies to the point where magnetic bearings can be truly useful, reliable, and well tested components for the aerospace community. Author

N94-35838*# General Electric Co., Schenectady, NY. Control Systems Lab.
NONLINEAR CONTROL OF MAGNETIC BEARINGS c37
A. K. Pradeep and R. Gurumoorthy *In* NASA. Langley Research Center, Second International Symposium on Magnetic Suspension Technology, Part 1 May 1994 p 27-57 (For primary document see N94-35836 11-18)
Avail: CASI HC A03/MF A04

In this paper we present a variety of nonlinear controllers for the magnetic bearing that ensure both stability and robustness. We utilize techniques of discontinuous control to design novel control laws for the magnetic bearing. We present in particular sliding mode controllers, time optimal controllers, winding algorithm based controllers, nested switching controllers, fractional controllers, and synchronous switching controllers for the magnetic bearing. We show existence of solutions to systems governed by discontinuous control laws, and prove stability and robustness of the chosen control laws in a rigorous setting. We design sliding mode observers for the magnetic bearing and prove the convergence of the state estimates to their true values. We present simulation results of the performance of the magnetic bearing subject to the aforementioned control laws, and conclude with comments on design. Author

N94-35839*# Eidgenoessische Technische Hochschule, Zurich (Switzerland). International Center for Magnetic Bearings.
HIGH PERFORMANCE DATA ACQUISITION, IDENTIFICATION, AND MONITORING FOR ACTIVE MAGNETIC BEARINGS c37
Raoul Herzog and Roland Siegwart *In* NASA. Langley Research Center, Second International Symposium on Magnetic Suspension Technology, Part 1 May 1994 p 61-66 (For primary document see N94-35836 11-18)
Avail: CASI HC A02/MF A04

Future active magnetic bearing systems (AMB) must feature easier on-site tuning, higher stiffness and damping, better robustness with respect to undesirable vibrations in housing and foundation, and enhanced monitoring and identification abilities. To get closer to these goals we developed a fast parallel link from the digitally controlled AMB to Matlab, which is used on a host computer for data processing, identification, and controller layout. This enables the magnetic bearing to take its frequency responses without using any additional measurement equipment. These measurements can be used for AMB identification. Author

N94-35840*# Grumman Aerospace Corp., Bethpage, NY.
SYSTEM CONCEPT DEFINITION OF THE GRUMMAN SUPERCONDUCTING ELECTROMAGNETIC SUSPENSION (EMS) MAGLEV DESIGN c37
M. Proise *In* NASA. Langley Research Center, Second International Symposium on Magnetic Suspension Technology, Part 1 May 1994 p 69-76 Sponsored by Corps of Engineers (For primary document see N94-35836 11-18)
Avail: CASI HC A02/MF A04

Grumman, under contract to the Army Corps of Engineers, completed a System Concept Definition (SCD) study to design a high-speed 134 m/s (300 m.p.h.) magnetically levitated (Maglev) transportation system. The primary development goals were to design a Maglev that is safe, reliable, environmentally acceptable, and low-cost. The cost issue was a predominant one, since previous studies have shown that an economically viable Maglev system (one that is attractive to investors for future models of passenger and/or freight transportation) requires a cost that is about $12.4 M/km ($20 Million per mile). The design is based on the electromagnetic suspension (EMS) system using superconducting iron-core magnets mounted along both sides of the vehicle. The EMS system has several advantages compared to the electrodynamic suspension (EDS) Maglev systems such as low stray magnetic fields in the passenger cabin and the surrounding areas, uniform load distribution along the full length of the vehicle, and small pole pitch for smoother propulsion and ride comfort. It is also levitated at all speeds and incorporates a wrap-around design of safer operation. The Grumman design has all the advantages of an EMS system identified above, while eliminating (or significantly improving) drawbacks associated with normal magnet powered EMS systems. Improvements include larger gap clearance, lighter weight, lower number of control servos, and higher off line switching speeds. The design also incorporates vehicle tilt (plus or minus 9 deg) for higher coordinated turn and turn out speed capability. Author

N94-35841*# Thyssen Henschel America, Inc.
TRANSRAPID (THE FIRST HIGH-SPEED MAGLEV TRAIN SYSTEM CERTIFIED READY FOR APPLICATION): DEVELOPMENT STATUS AND PROSPECTS FOR DEPLOYMENT c37
Reinhard F. Luerken *In* NASA. Langley Research Center, Second International Symposium on Magnetic Suspension Technology, Part 1 May 1994 p 77-91 (For primary document see N94-35836 11-18)
Avail: CASI HC A03/MF A04

The Transrapid maglev technology is at the threshold of commercial deployment and technologically all prerequisites for the successful operation of the system in public service are given. In post unification Germany the domestic maglev technology is envisioned to be applied in the Berlin-Hamburg project. At present, a public-private funding concept is being prepared and the lengthy planning process is about to be initiated. In the USA the AMG has presented a program to Americanize the technology and to make it available for commercial use in the U.S. in the very near future. The paramount features of this program are to generate economic development, provide a basis for transportation technology development, create opportunities for U.S. industry, improve the U.S. transportation infrastructure, and improve the environment and traveler safety. Maglev is ready for the U.S.; is the U.S. ready for maglev? Author

N94-35842*# Draper (Charles Stark) Lab., Inc., Cambridge, MA.
CONTROL OF MAGLEV VEHICLES WITH AERODYNAMIC AND GUIDEWAY DISTURBANCES c37
Karl Flueckiger, Steve Mark, Ruth Caswell, and Duncan McCallum *In* NASA. Langley Research Center, Second International Symposium on Magnetic Suspension Technology, Part 1 May 1994 p 93-107 (For primary document see N94-35836 11-18)
Avail: CASI HC A03/MF A04

A modeling, analysis, and control design methodology is presented for maglev vehicle ride quality performance improvement as measured by the Pepler Index. Ride quality enhancement is considered through active control of secondary suspension elements and active aerodynamic surfaces mounted on the train. To analyze and quantify the benefits of active control, the authors have developed a five degree-of-freedom lumped parameter model suitable for describing a large class of maglev vehicles, including both channel and box-beam guideway configurations. Elements of this modeling capability have been recently employed in studies sponsored by the U.S. Department of Transportation (DOT). A perturbation analysis about an operating point, defined by vehicle and average crosswind velocities, yields a suitable linearized state space model for multivariable control system analysis and synthesis. Neglecting passenger compartment noise, the ride quality as quantified by the Pepler Index is readily computed from the system states. A statistical analysis is performed by modeling the crosswind disturbances and guideway variations as filtered white noise, whereby the Pepler Index is established in closed form through the solution to a matrix Lyapunov equation. Data is presented which indicates the anticipated ride quality achieved through various closed-loop control arrangements. Author

N94-35843*# Houston Univ., TX. Center for Superconductivity.
HIGH TEMPERATURE SUPERCONDUCTORS FOR MAGNETIC SUSPENSION APPLICATIONS c33
C. K. McMichael, R. S. Cooley, Q. Y. Chen, K. B. Ma, M. A. Lamb, R. L. Meng, C. W. Chu, and W. K. Chu *In* NASA. Langley Research Center, Second International Symposium on Magnetic Suspension Technology, Part 1 May 1994 p 111-118 (For primary document see N94-35836 11-18)
(Contract MDA972-90-J-1001)
Avail: CASI HC A02/MF A04

High temperature superconductors (HTS) hold the promise for applications in magnetic levitation bearings, vibration damping, and torque coupling. Traditional magnetic suspension systems require active feedback and vibration controls in which power consumption and low frequency vibration are among the major engineering concerns. HTS materials have been demonstrated to be an enabling approach towards such problems due to their flux trapping properties. In our laboratory at TCSUH, we have been conducting a series of experiments to explore various mechanical applications using HTS. We have constructed a 30 lb. model flywheel levitated by a hybrid superconducting magnetic bearing (HSMB). We are also developing a levitated and vibration-dampled platform for high precision instrumentation. These applications would be ideal for space usages where ambient temperature is adequate for HTS to operate properly under greatly reduced cryogenic requirements. We will give a general overview of these potential applications and discuss the operating principles of the HTS devices we have developed. Author (revised)

N94-35844*# Kanazawa Inst. of Tech. (Japan).
MEASUREMENT AND CHARACTERIZATION OF FORCE DYNAMICS IN HIGH T(SUB c) SUPERCONDUCTORS c33
Toshiro Higuchi (Tokyo Univ., Japan.), Allan J. Kelley (Tokyo Univ., Japan.), and Yukio Tsutsui (Yaskawa Electric Mfg. Co. Ltd., Kitakyushu, Japan.) *In* NASA. Langley Research Center, Second International Symposium on Magnetic Suspension Technology, Part 1 May 1994 p 119-132 (For primary document see N94-35836 11-18)
Avail: CASI HC A03/MF A04

Magnetic bearing implementations using more exotic superconducting phenomena have been proliferating in recent years because they have important advantages over conventional implementations. For example, the stable suspension of a six degrees-of-freedom object by superconducting means can be achieved without a control system and with the use of only a single superconductor. It follows that the construction becomes much simpler with decreased need for position sensors and stabilizers. However, it is recognized that the design of superconducting systems can be difficult because important characteristics relating to the 6 degree-of-freedom dynamics of an object suspended magnetically are not readily available and the underlying principles of superconducting phenomena are not yet completely understood. To eliminate some of the guesswork in the design process, this paper proposes a system which can resolve the mechanical properties of suspension by superconductivity and provide position and orientation dependent data about the system's damping, stiffness, and frequency response characteristics. This system employs an actively-controlled magnetically-suspended fine-motion device that can also be used as a six degree-of-freedom force sensor. By attaching the force sensor to a permanent magnet that is being levitated above a superconducting magnet, mechanical characteristics of the superconductor levitation can be extracted. Such information would prove useful for checking the validity of theoretical models and may even give insights into superconducting phenomena. Author (revised)

N94-35845*# North Carolina Univ., Charlotte, NC. Dept. of Electrical Engineering.
MATERIALS FOR EFFICIENT HIGH-FLUX MAGNETIC BEARING ACTUATORS c37
M. E. Williams and D. L. Trumper *In* NASA. Langley Research Center, Second International Symposium on Magnetic Suspension Technology, Part 1 May 1994 p 135-145 (For primary document see N94-35836 11-18)
Avail: CASI HC A03/MF A04

Magnetic bearings have demonstrated the capability for achieving positioning accuracies at the nanometer level in precision motion control stages. This makes possible the positioning of a wafer in six degrees of freedom with the precision necessary for photolithography. To control the position of an object at the nanometer level, a model of the magnetic bearing actuator force-current-airgap relationship must be accurately obtained. Additionally, to reduce thermal effects the design of the actuator should be optimized to achieve maximum power efficiency and flux density. Optimization of the actuator is accomplished by proper pole face sizing and utilizing a magnetic core material which can be magnetized to the highest flux density with low magnetic loss properties. This paper describes the construction of a magnetic bearing calibration fixture designed for experimental measurement of the actuator force characteristics. The results of a material study that review the force properties of nickel-steel, silicon-steel, and cobalt-vanadium-iron, as they apply to magnetic bearing applications are also presented. Author (revised)

N94-35846*# Politecnico di Torino (Italy). Dipt. di Meccanica.
DESIGN, CONSTRUCTION, AND TESTING OF A FIVE ACTIVE AXES MAGNETIC BEARING SYSTEM c37
Cristiana Delprete, Giancarlo Genta, and Stefano Carabelli *In* NASA. Langley Research Center, Second International Symposium on Magnetic Suspension Technology, Part 1 May 1994 p 147-161 Sponsored by Italian Ministry of Univ. and Scientific Research (For primary document see N94-35836 11-18)
Avail: CASI HC A03/MF A04

A high speed electric spindle based on active electromagnetic suspension technology has been designed, built, and tested. The main goal of the research work was the construction of a highly modular unit which can be used for teaching and research purposes. The design of the electromechanical components and of the control unit is described in detail, together with the characterization tests performed on the various subsystems. A description of the preliminary tests on the unit, conducted at speeds not in excess of the first deformation critical speed of the rotor, concludes the work. Author

N94-35847*# Virginia Univ., Charlottesville, VA.
EXPERIMENTAL MEASUREMENT AND CALCULATION OF LOSSES IN PLANAR RADIAL MAGNETIC BEARINGS c37
M. E. F. Kasarda, P. E. Allaire, R. W. Hope, and R. R. Humphris *In* NASA. Langley Research Center, Second International Symposium on Magnetic Suspension Technology, Part 1 May 1994 p 163-174 Sponsored in part by Center for Innovative Technology (For primary document see N94-35836 11-18)
Avail: CASI HC A03/MF A04

The loss mechanisms associated with magnetic bearings have yet to be adequately characterized or modeled analytically and thus pose a problem for the designer of magnetic bearings. This problem is particularly important for aerospace applications where low power consumption of components is critical. Also, losses are expected to be large for high speed operation. The iron losses in magnetic bearings can be divided into eddy current losses and hysteresis losses. While theoretical models for these losses exist for transformer and electric motor applications, they have not been verified for magnetic bearings. This paper presents the results from a low speed experimental test rig and compares them to calculated values from existing theory. Experimental data was taken over a range of 90 to 2,800 rpm for several bias currents and two different pole configurations. With certain assumptions agreement between measured and calculated power losses was within 16 percent for a number of test configurations.

Author (revised)

N94-35848*# Draper (Charles Stark) Lab., Inc., Cambridge, MA. Advanced Computer Architectures Group.

FAULT TOLERANT COMPUTER CONTROL FOR A MAGLEV TRANSPORTATION SYSTEM c37

Jaynarayan H. Lala, Gail A. Nagle, and George Anagnostopoulos *In* NASA. Langley Research Center, Second International Symposium on Magnetic Suspension Technology, Part 1 May 1994 p 177-195 (For primary document see N94-35836 11-18)
(Contract DTFR53-91-C-00043)
Avail: CASI HC A03/MF A04

Magnetically levitated (Maglev) vehicles operating on dedicated guideways at speeds of 500 km/hr are an emerging transportation alternative to short-haul air and high-speed rail. They have the potential to offer a service significantly more dependable than air and with less operating cost than both air and high-speed rail. Maglev transportation derives these benefits by using magnetic forces to suspend a vehicle 8 to 200 mm above the guideway. Magnetic forces are also used for propulsion and guidance. The combination of high speed, short headways, stringent ride quality requirements, and a distributed offboard propulsion system necessitates high levels of automation for the Maglev control and operation. Very high levels of safety and availability will be required for the Maglev control system. This paper describes the mission scenario, functional requirements, and dependability and performance requirements of the Maglev command, control, and communications system. A distributed hierarchical architecture consisting of vehicle on-board computers, wayside zone computers, a central computer facility, and communication links between these entities was synthesized to meet the functional and dependability requirements on the maglev. Two variations of the basic architecture are described: the Smart Vehicle Architecture (SVA) and the Zone Control Architecture (ZCA). Preliminary dependability modeling results are also presented. Author (revised)

N94-35849*# Grumman Aerospace Corp., Bethpage, NY.

SUPERCONDUCTING ELECTROMAGNETIC SUSPENSION (EMS) SYSTEM FOR GRUMMAN MAGLEV CONCEPT c33

Swarn S. Kalsi *In* NASA. Langley Research Center, Second International Symposium on Magnetic Suspension Technology, Part 1 May 1994 p 197-211 (For primary document see N94-35836 11-18)
(Contract DTFR53-92-C-00004)
Avail: CASI HC A03/MF A04

The Grumman developed Electromagnetic Suspension (EMS) Maglev system has the following key characteristics: a large operating airgap--40 mm; levitation at all speeds; both high speed and low speed applications; no deleterious effects on SC coils at low vehicle speeds; low magnetic field at the SC coil--less than 0.35 T; no need to use non-magnetic/non-metallic rebar in the guideway structure; low magnetic field in passenger cabin--approximately 1 G; low forces on the SC coil; employs state-of-the-art NbTi wire; no need for an active magnet quench protection system; and lower weight than a magnet system with copper coils. The EMS Maglev described in this paper does not require development of any new technologies. The system could be built with the existing SC magnet technology. Author (revised)

N94-35850*# Southern California Edison Co., Rosemead, CA.

NATIONAL MAGLEV INITIATIVE: CALIFORNIA LINE ELECTRIC UTILITY POWER SYSTEM REQUIREMENTS c33

Phil Save *In* NASA. Langley Research Center, Second International Symposium on Magnetic Suspension Technology, Part 1 May 1994 p 213-227 (For primary document see N94-35836 11-18)
Avail: CASI HC A03/MF A04

The electrical utility power system requirements were determined for a Maglev line from San Diego to San Francisco and Sacramento with a maximum capacity of 12,000 passengers an hour in each direction at a speed of 300 miles per hour, or one train every 30 seconds in each direction. Basically the Maglev line requires one 50-MVA substation every 12.5 miles. The need for new power lines to serve these substations and their voltage levels are based not only on equipment loading criteria but also on limitations due to voltage flicker and harmonics created by the Maglev system. The resulting power system requirements and their costs depend mostly on the geographical area, urban or suburban with 'strong' power systems, or mountains and rural areas with 'weak' power systems. A reliability evaluation indicated that emergency power sources, such as a 10-MW battery at each substation, were not justified if sufficient redundancy is provided in the design of the substations and the power lines serving them. With a cost of $5.6 M per mile, the power system requirements, including the 12-kV DC cables and the inverters along the Maglev line, were found to be the second largest cost component of the Maglev system, after the cost of the guideway system ($9.1 M per mile), out of a total cost of $23 M per mile. Author

N94-35851*# National Aeronautics and Space Administration. Lewis Research Center, Cleveland, OH.

MICROGRAVITY ISOLATION SYSTEM DESIGN: A MODERN CONTROL SYNTHESIS FRAMEWORK c29

R. D. Hampton (Virginia Univ., Charlottesville, VA.), C. R. Knospe (Virginia Univ., Charlottesville, VA.), P. E. Allaire (Virginia Univ., Charlottesville, VA.), and C. M. Grodsinsky *In* NASA. Langley Research Center, Second International Symposium on Magnetic Suspension Technology, Part 1 May 1994 p 231-248 Sponsored in part by Center for Innovative Technology (For primary document see N94-35836 11-18)
Avail: CASI HC A03/MF A04

Manned orbiters will require active vibration isolation for acceleration-sensitive microgravity science experiments. Since umbilicals are highly desirable or even indispensable for many experiments, and since their presence greatly affects the complexity of the isolation problem, they should be considered in control synthesis. In this paper a general framework is presented for applying extended H2 synthesis methods to the three-dimensional microgravity isolation problem. The methodology integrates control and state frequency weighting and input and output disturbance accommodation techniques into the basic H2 synthesis approach. The various system models needed for design and analysis are also presented. The paper concludes with a discussion of a general design philosophy for the microgravity vibration isolation problem. Author

N94-35852*# National Cheng Kung Univ., Tainan (Taiwan). Inst. of Aeronautics and Astronautics.

FUZZY SELF-LEARNING CONTROL FOR MAGNETIC SERVO SYSTEM c43

J. H. Tarn, L. T. Kuo, K. Y. Juang, and C. E. Lin *In* NASA. Langley Research Center, Second International Symposium on Magnetic Suspension Technology, Part 1 May 1994 p 249-256 (For primary document see N94-35836 11-18)
Avail: CASI HC A02/MF A04

It is known that an effective control system is the key condition for successful implementation of high-performance magnetic servo systems. Major issues to design such control systems are nonlinearity; unmodeled dynamics, such as secondary effects for copper resistance, stray fields, and saturation; and that disturbance rejection for the load effect reacts directly on the servo system without transmission elements. One typical approach to design control systems under these conditions is a special type of nonlinear feedback called gain scheduling. It accommodates linear regulators whose parameters are changed as a function of operating conditions in a preprogrammed way. In this paper, an on-line learning fuzzy control strategy is proposed. To inherit the wealth of linear control design, the relations between linear feedback and fuzzy logic controllers have been established. The exercise of engineering axioms of linear control design is thus transformed into tuning of appropriate fuzzy parameters. Furthermore, fuzzy logic control brings the domain of candidate control laws from linear into nonlinear, and brings new prospects into design of the local controllers. On the other hand, a self-learning scheme is utilized to automatically tune the fuzzy rule base. It is based on network learning infrastructure; statistical approximation to assign credit; animal learning method to update the reinforcement map with a fast learning rate; and temporal difference predictive scheme to optimize the control laws. Different from supervised and statistical unsupervised learning schemes, the proposed method learns on-line from past experience and information from the process and forms a rule base of an FLC system from randomly assigned initial control rules. Author

N94-35853*# National Aeronautics and Space Administration. Langley Research Center, Hampton, VA.

IMPLEMENTATION OF A DECOUPLED CONTROLLER FOR A MAGNETIC SUSPENSION SYSTEM USING ELECTROMAGNETS MOUNTED IN A PLANAR ARRAY c37

D. E. Cox and N. J. Groom *In its* Second International Symposium on Magnetic Suspension Technology, Part 1 May 1994 p 257-271 (For primary document see N94-35836 11-18)

Avail: CASI HC A03/MF A04

An implementation of a decoupled, single-input/single-output control approach for a large angle magnetic suspension test fixture is described. Numerical and experimental results are presented. The experimental system is a laboratory model large gap magnetic suspension system which provides five degree-of-freedom control of a cylindrical suspended element. The suspended element contains a core composed of permanent magnet material and is levitated above five electromagnets mounted in a planar array. Author (revised)

N94-35854*# National Aerospace Lab., Tokyo (Japan).

STATUS OF MSBS STUDY AT NAL c35

Hideo Sawada, Hisashi Suenaga, Takayuki Suzuki, and Nobukazu Ikeda *In* NASA. Langley Research Center, Second International Symposium on Magnetic Suspension Technology, Part 1 May 1994 p 275-289 (For primary document see N94-35836 11-18)

Avail: CASI HC A03/MF A04

Two Magnetic Suspension and Balance Systems (MSBS) at the National Aerospace Laboratory (NAL) in Japan are introduced. They are the 10 cm MSBS and the 60 cm MSBS. They have 10 cm x 10 cm and 60 cm x 60 cm test sections. The control of suspending a model at the 10 cm MSBS is six degrees of freedom including the rolling moment control. The model for the rolling moment control has two pairs of small extra permanent magnets at both its ends plus a main cylindrical magnet. The rolling moment is generated by the magnetic forces acting on the extra magnets by controlled current passing through the four side coils independently. Test results show the roll angle of the model is controlled in this way. The dynamic calibration test was carried out at the MSBS in five degrees of freedom without the rolling moment control. The model is a simple cylindrical magnet magnetized along its axis. The obtained results show that the dynamic calibration with measured magnetic field intensity is much superior to that with the coil currents. The 60 cm MSBS was designed with some data obtained at the 10 cm one. It is fundamentally proportional to the 10 cm one in size and coil positions. The measured magnetic field intensity is not so strong as expected at design. It was operated first in 1993. The control is three degrees of freedom in the longitudinal direction. Author (revised)

N94-35855*# Southampton Univ. (England).

THE SIMULATION OF A PROPULSIVE JET AND FORCE MEASUREMENT USING A MAGNETICALLY SUSPENDED WIND TUNNEL MODEL c02

K. S. Garbutt and M. J. Goodyer *In* NASA. Langley Research Center, Second International Symposium on Magnetic Suspension Technology, Part 1 May 1994 p 291-305 (For primary document see N94-35836 11-18)

Avail: CASI HC A03/MF A04

Models featuring the simulation of exhaust jets were developed for magnetic levitation in a wind tunnel. The exhaust gas was stored internally producing a discharge of sufficient duration to allow nominal steady state to be reached. The gas was stored in the form of compressed gas or a solid rocket propellant. Testing was performed with the levitated models although deficiencies prevented the detection of jet-induced aerodynamic effects. Difficulties with data reduction led to the development of a new force calibration technique, used in conjunction with an exhaust simulator and also in separate high incidence aerodynamic tests. Author

N94-35856*# National Cheng Kung Univ., Tainan (Taiwan). Inst. of Aeronautics and Astronautics.

A DYNAMIC METHOD FOR MAGNETIC TORQUE MEASUREMENT c35

C. E. Lin and H. L. Jou *In* NASA. Langley Research Center, Second International Symposium on Magnetic Suspension Technology, Part 1 May 1994 p 307-315 (For primary document see N94-35836 11-18)

(Contract NSC81-0424-E005-040)

Avail: CASI HC A02/MF A04

In a magnetic suspension system, accurate force measurement will result in better control performance in the test section, especially when a wider range of operation is required. Although many useful methods were developed to obtain the desired model, however, significant error is inevitable since the magnetic field distribution of the large-gap magnetic suspension system is extremely nonlinear. This paper proposed an easy approach to measure the magnetic torque of a magnetic suspension system using an angular photo encoder. Through the measurement of the velocity change data, the magnetic torque is converted. The proposed idea is described and implemented to obtain the desired data. It is useful to the calculation of a magnetic force in the magnetic suspension system. Author

N94-35857*# Politecnico di Torino (Italy). Dipt. di Meccanica.

ACTIVE MAGNETIC BEARING CONTROL LOOP MODELING FOR A FINITE ELEMENT ROTORDYNAMICS CODE c37

Giancarlo Genta, Cristiana Delprete, and Stefano Carabelli *In* NASA. Langley Research Center, Second International Symposium on Magnetic Suspension Technology, Part 1 May 1994 p 319-333 Sponsored by Italian Ministry of Univ. and Scientific Research (For primary document see N94-35836 11-18)

Avail: CASI HC A03/MF A04

A mathematical model of an active electromagnetic bearing which includes the actuator, the sensor and the control system is developed and implemented in a specialized finite element code for rotordynamic analysis. The element formulation and its incorporation in the model of the machine are described in detail. A solution procedure, based on a modal approach in which the number of retained modes is controlled by the user, is then shown together with other procedures for computing the steady-state response to both static and unbalance forces. An example of application shows the numerical results obtained on a model of an electric motor suspended on a five active-axis magnetic suspension. The comparison of some of these results with the experimental characteristics of the actual system shows the ability of the present model to predict its performance. Author

N94-35858*# General Electric Co., Schenectady, NY. Electronic Technologies Lab.

MODELLING AND CONTROL OF A ROTOR SUPPORTED BY MAGNETIC BEARINGS c37

R. Gurumoorthy and A. K. Pradeep *In* NASA. Langley Research Center, Second International Symposium on Magnetic Suspension Technology, Part 1 May 1994 p 335-352 (For primary document see N94-35836 11-18)

Avail: CASI HC A03/MF A04

In this paper we develop a dynamical model of a rotor and the active magnetic bearings used to support the rotor. We use this model to develop a stable state feedback control of the magnetic bearing system. We present the development of a rigid body model of the rotor, utilizing both Rotation Matrices (Euler Angles) and Euler Parameters (Quaternions). In the latter half of the paper we develop a stable state feedback control of the actively controlled magnetic bearing to control the rotor position under inbalances. The control law developed takes into account the variation of the model with rotational speed. We show stability over the whole operating range of speeds for the magnetic bearing system. Simulation results are presented to demonstrate the closed loop system performance. We develop the model of the magnetic bearing, and present two schemes for the excitation of the poles of the actively controlled magnetic bearing. We also present a scheme for averaging multiple sensor measurements and splitting the actuation forces amongst redundant actuators. Author

N94-35859*# Duke Univ., Durham, NC. Dept. of Mechanical Engineering.

DYNAMIC ANALYSIS OF A MAGNETIC BEARING SYSTEM WITH FLUX CONTROL c37

Josiah Knight, Thomas Walsh, and Lawrence Virgin *In* NASA. Langley Research Center, Second International Symposium on Magnetic Suspension Technology, Part 1 May 1994 p 353-366 (For primary document see N94-35836 11-18)

Avail: CASI HC A03/MF A04

Using measured values of two-dimensional forces in a magnetic actuator, equations of motion for an active magnetic bearing are presented. The presence of geometric coupling between coordinate directions causes the equations of motion to be nonlinear. Two methods are used to examine the unbalance response of the system: simulation by direct integration in time; and determination of approximate steady state solutions by harmonic balance. For relatively large values of the derivative control coefficient, the system behaves in an essentially linear manner, but for lower values of this parameter, or for higher values of the coupling coefficient, the response shows a split of amplitudes in the two principal directions. This bifurcation is sensitive to initial conditions. The harmonic balance solution shows that the separation of amplitudes actually corresponds to a change in stability of multiple coexisting solutions. Author

N94-35860*# Old Dominion Univ., Norfolk, VA. Dept. of Aerospace Engineering.

SOME FURTHER DEVELOPMENTS IN THE DYNAMIC MODELLING AND CONTROL OF THE LARGE ANGLE MAGNETIC SUSPENSION TEST FIXTURE **c35**

Colin P. Britcher and Lucas E. Foster *In* NASA. Langley Research Center, Second International Symposium on Magnetic Suspension Technology, Part 1 May 1994 p 367-388 (For primary document see N94-35836 11-18)
(Grant NAG1-1056)
Avail: CASI HC A03/MF A04

A small-scale laboratory magnetic suspension system, the Large Angle Magnetic Suspension Test Fixture (LAMSTF) has been constructed at NASA Langley Research Center. This paper first presents some recent developments in the mathematical modelling of the system, particularly in the area of eddy current effects. It is shown that these effects are significant, but may be amenable to modelling and measurement. Next, a theoretical framework is presented, together with a comparison of computed and experimental data. Finally, some control aspects are discussed, together with illustration that the major design objective of LAMSTF - a controlled 360 deg rotation about the vertical axis, has been accomplished. Author

N94-35861*# Virginia Univ., Charlottesville, VA.

NEURAL NETWORK CONTROLLER DEVELOPMENT FOR A MAGNETICALLY SUSPENDED FLYWHEEL ENERGY STORAGE SYSTEM **c63**

Roger L. Fittro, Da-Chen Pang, and Davinder K. Anand *In* NASA. Langley Research Center, Second International Symposium on Magnetic Suspension Technology, Part 1 May 1994 p 391-405 (For primary document see N94-35836 11-18)
Avail: CASI HC A03/MF A04

A neural network controller has been developed to accommodate disturbances and nonlinearities and improve the robustness of a magnetically suspended flywheel energy storage system. The controller is trained using the back propagation-through-time technique incorporated with a time-averaging scheme. The resulting nonlinear neural network controller improves system performance by adapting flywheel stiffness and damping based on operating speed. In addition, a hybrid multi-layered neural network controller is developed off-line which is capable of improving system performance even further. All of the research presented in this paper was implemented via a magnetic bearing computer simulation. However, careful attention was paid to developing a practical methodology which will make future application to the actual bearing system fairly straightforward. Author

N94-35862*# National Cheng Kung Univ., Tainan (Taiwan). Inst. of Aeronautics and Astronautics.

TIME-DELAY CONTROL OF A MAGNETIC LEVITATED LINEAR POSITIONING SYSTEM **c63**

J. H. Tarn, K. Y. Juang, and C. E. Lin *In* NASA. Langley Research Center, Second International Symposium on Magnetic Suspension Technology, Part 1 May 1994 p 407-420 (For primary document see N94-35836 11-18)
Avail: CASI HC A03/MF A04

In this paper, a high accuracy linear positioning system with a linear force actuator and magnetic levitation is proposed. By locating a permanently magnetized rod inside a current-carrying solenoid, the axial force is achieved by the boundary effect of magnet poles and utilized to power the linear motion, while the force for levitation is governed by Ampere's Law supplied with the same solenoid. With the levitation in a radial direction, there is hardly any friction between the rod and the solenoid. The high speed motion can hence be achieved. Besides, the axial force acting on the rod is a smooth function of rod position, so the system can provide nanometer resolution linear positioning to the molecule size. Since the force-position relation is highly nonlinear, and the mathematical model is derived according to some assumptions, such as the equivalent solenoid of the permanently magnetized rod, so there exists unknown dynamics in practical application. Thus 'robustness' is an important issue in controller design. Meanwhile the load effect reacts directly on the servo system without transmission elements, so the capability of 'disturbance'rejection; is also required. With the above consideration, a time-delay control scheme is chosen and applied. By comparing the input-output relation and the mathematical model, the time-delay controller calculates an estimation of unmodeled dynamics and disturbances and then composes the desired compensation into the system. Effectiveness of the linear positioning system and control scheme are illustrated with simulation results. Author

N94-35863*# National Defence Academy, Tokyo (Japan).

THIRD ORDER LPF TYPE COMPENSATOR FOR FLEXIBLE ROTOR SUSPENSION **c37**

Osami Matsushita, Naohiko Takahashi, and Michiyuki Takagi *In* NASA. Langley Research Center, Second International Symposium on Magnetic Suspension Technology, Part 1 May 1994 p 421-431 (For primary document see N94-35836 11-18)
Avail: CASI HC A03/MF A04

The tuning job of the compensator for levitating flexible rotors supported by active magnetic bearings (AMB) concerns providing a good damping effect to the critical speed modes while avoiding the spillover problem on the instability of higher bending modes. In this paper, an idea for design of the control law of the compensator based on utilizing a third order low pass filter (LPF) is proposed to essentially enable elimination of the spillover instability. According to the proposed design method, good damping effects for the critical speeds are obtained by the usual phase lead/lag function. Stabilization for all of higher bending modes is completed by the additional function of the 3rd order LPF due to its phase lag approaching about -270 degrees in the high frequency domain. This idea is made clear by experiments and simulations. Author

N94-35865*# National Aeronautics and Space Administration. Langley Research Center, Hampton, VA.

NASA WORKSHOP ON DISTRIBUTED PARAMETER MODELING AND CONTROL OF FLEXIBLE AEROSPACE SYSTEMS

Virginia B. Marks, comp. and Claude R. Keckler, comp. Jun. 1994 588 p Workshop held in Williamsburg, VA, 8-10 Jun. 1992 Sponsored by NASA, Washington
(RTOP 233-01-01-05)
(NASA-CP-3242; L-17362; NAS 1.55:3242) Avail: CASI HC A25/MF A06

Although significant advances have been made in modeling and controlling flexible systems, there remains a need for improvements in model accuracy and in control performance. The finite element models of flexible systems are unduly complex and are almost intractable to optimum parameter estimation for refinement using experimental data. Distributed parameter or continuum modeling offers some advantages and some challenges in both modeling and control. Continuum models often result in a significantly reduced number of model parameters, thereby enabling optimum parameter estimation. The dynamic equations of motion of continuum models provide the advantage of allowing the embedding of the control system dynamics, thus forming a complete set of system dynamics. There is also increased insight provided by the continuum model approach. For individual titles, see N94-35866 through N94-35898.

N94-35866*# Harris Corp., Melbourne, FL.

DISTRIBUTED PARAMETER MODELLING OF FLEXIBLE SPACECRAFT: WHERE'S THE BEEF?

D. C. Hyland *In* NASA. Langley Research Center, NASA Workshop on Distributed Parameter Modeling and Control of Flexible Aerospace Systems Jun. 1994 p 3-22 (For primary document see N94-35865 11-18)
Avail: CASI HC A03/MF A06

This presentation discusses various misgivings concerning the directions and productivity of Distributed Parameter System (DPS) theory as applied to spacecraft vibration control. We try to show the need for greater cross-fertilization between DPS theorists and spacecraft control designers. We recommend a shift in research directions toward exploration of asymptotic frequency response characteristics of critical importance to control designers. Author

N94-35867*# Virginia Polytechnic Inst. and State Univ., Blacksburg, VA. Dept. of Engineering Science and Mechanics.
MANEUVERING AND CONTROL OF FLEXIBLE SPACE ROBOTS c37
Leonard Meirovitch and Seungchul Lim *In* NASA. Langley Research Center, NASA Workshop on Distributed Parameter Modeling and Control of Flexible Aerospace Systems Jun. 1994 p 23-40 (For primary document see N94-35865 11-18)
(Grant NAG1-225)
Avail: CASI HC A03/MF A06

This paper is concerned with a flexible space robot capable of maneuvering payloads. The robot is assumed to consist of two hinge-connected flexible arms and a rigid end-effector holding a payload; the robot is mounted on a rigid platform floating in space. The equations of motion are nonlinear and of high order. Based on the assumption that the maneuvering motions are one order of magnitude larger than the elastic vibrations, a perturbation approach permits design of controls for the two types of motion separately. The rigid-body maneuvering is carried out open loop, but the elastic motions are controlled closed loop, by means of discrete-time linear quadratic regulator theory with prescribed degree of stability. A numerical example demonstrates the approach. In the example, the controls derived by the perturbation approach are applied to the original nonlinear system and errors are found to be relatively small. Author

N94-35868*# California Univ., Los Angeles, CA. Dept. of Electrical Engineering.
DISTRIBUTED PARAMETER MODELING OF REPEATED TRUSS STRUCTURES c39
Han-Ching Wang *In* NASA. Langley Research Center, NASA Workshop on Distributed Parameter Modeling and Control of Flexible Aerospace Systems Jun. 1994 p 41-63 Sponsored by NASA. Dryden Flight Research Center (For primary document see N94-35865 11-18)
Avail: CASI HC A03/MF A06

A new approach to find homogeneous models for beam-like repeated flexible structures is proposed which conceptually involves two steps. The first step involves the approximation of 3-D non-homogeneous model by a 1-D periodic beam model. The structure is modeled as a 3-D non-homogeneous continuum. The displacement field is approximated by Taylor series expansion. Then, the cross sectional mass and stiffness matrices are obtained by energy equivalence using their additive properties. Due to the repeated nature of the flexible bodies, the mass, and stiffness matrices are also periodic. This procedure is systematic and requires less dynamics detail. The first step involves the homogenization from a 1-D periodic beam model to a 1-D homogeneous beam model. The periodic beam model is homogenized into an equivalent homogeneous beam model using the additive property of compliance along the generic axis. The major departure from previous approaches in literature is using compliance instead of stiffness in homogenization. An obvious justification is that the stiffness is additive at each cross section but not along the generic axis. The homogenized model preserves many properties of the original periodic model. Author (revised)

N94-35869*# Techno-Sciences, Inc., Greenbelt, MD.
INTEGRATED DESIGN OF STRUCTURES, CONTROLS, AND MATERIALS c61
G. L. Blankenship (Maryland Univ., College Park, MD.) *In* NASA. Langley Research Center, NASA Workshop on Distributed Parameter Modeling and Control of Flexible Aerospace Systems Jun. 1994 p 65-76 (For primary document see N94-35865 11-18)
Avail: CASI HC A03/MF A06

In this talk we shall discuss algorithms and CAD tools for the design and analysis of structures for high performance applications using advanced composite materials. An extensive mathematical theory for optimal structural (e.g., shape) design was developed over the past thirty years. Aspects of this theory have been used in the design of components for hypersonic vehicles and thermal diffusion systems based on homogeneous materials. Enhancement of the design methods to include optimization of the microstructure of the component is a significant innovation which can lead to major enhancements in component performance. Our work is focused on the adaptation of existing theories of optimal structural design (e.g., optimal shape design) to treat the design of structures using advanced composite materials (e.g., fiber reinforced, resin matrix materials). In this talk we shall discuss models and algorithms for the design of simple structures from composite materials, focussing on a problem in thermal management. We shall also discuss methods for the integration of active structural controls into the design process. Author (revised)

N94-35870*# National Aeronautics and Space Administration. Langley Research Center, Hampton, VA.
APPLYING TRANSFER MATRIX METHOD TO THE ESTIMATION OF THE MODAL CHARACTERISTICS OF THE NASA MINI-MASS TRUSS c61
Ji-Yao Shen (North Carolina Agricultural and Technical State Univ., Greensboro, NC.) and Lawrence W. Taylor, Jr. *In its* NASA Workshop on Distributed Parameter Modeling and Control of Flexible Aerospace Systems Jun. 1994 p 77-94 (For primary document see N94-35865 11-18)
Avail: CASI HC A03/MF A06

It is beneficial to use a distributed parameter model for large space structures because the approach minimizes the number of model parameters. Holzer's transfer matrix method provides a useful means to simplify and standardize the procedure for solving the system of partial differential equations. Any large space structures can be broken down into sub-structures with simple elastic and dynamical properties. For each single element, such as beam, tether, or rigid body, we can derive the corresponding transfer matrix. Combining these elements' matrices enables the solution of the global system equations. The characteristics equation can then be formed by satisfying the appropriate boundary conditions. Then natural frequencies and mode shapes can be determined by searching the roots of the characteristic equation at frequencies within the range of interest. This paper applies this methodology, and the maximum likelihood estimation method, to refine the modal characteristics of the NASA Mini-Mast Truss by successively matching the theoretical response to the test data of the truss. The method is being applied to more complex configurations. Author (revised)

N94-35871*# National Aeronautics and Space Administration. Langley Research Center, Hampton, VA.
CONTROL OF FLEXIBLE STRUCTURES WITH DISTRIBUTED SENSING AND PROCESSING c63
Dave Ghosh (Lockheed Engineering and Sciences Co., Hampton, VA.) and Raymond C. Montgomery *In its* NASA Workshop on Distributed Parameter Modeling and Control of Flexible Aerospace Systems Jun. 1994 p 95-114 (For primary document see N94-35865 11-18)
Avail: CASI HC A03/MF A06

Technology is being developed to process signals from distributed sensors using distributed computations. These distributed sensors provide a new feedback capability for vibration control that has not been exploited. Additionally, the sensors proposed are of an optical and distributed nature and could be employed with known techniques of distributed optical computation (Fourier optics, etc.) to accomplish the control system functions of filtering and regulation in a distributed computer. This paper extends the traditional digital, optimal estimation and control theory to include distributed sensing and processing for this application. The design model assumes a finite number of modes which make it amenable to empirical determination of the design model via familiar modal-test techniques. The sensors are assumed to be distributed, but a finite number of point actuators are used. The design process is illustrated by application to a Euler beam. A simulation of the beam is used to design an optimal vibration control system that uses a distributed deflection sensor and nine linear force actuators. Simulations are also used to study the influence of design and processing errors on the performance. Author

N94-35872*# Pennsylvania State Univ., University Park, PA. Dept. of Aerospace Engineering.
VARIATIONS IN THE MODAL CHARACTERISTICS OF A TELESCOPICALLY DEPLOYING BEAM c39

Anthony K. Amos *In* NASA. Langley Research Center, NASA Workshop on Distributed Parameter Modeling and Control of Flexible Aerospace Systems Jun. 1994 p 115-131 (For primary document see N94-35865 11-18)
(Grant AF-AFOSR-0155-91)
Avail: CASI HC A03/MF A06

The equations of motion for a two-segment deploying telescopic beam are derived through application of Lagrange's equation. The outer tube of the beam is fixed at one end and the inner tube slides freely relative to the fixed segment. The resulting nonlinear, non-autonomous set of equations is linearized and simplified to the standard Euler-Bernoulli partial differential equations for an elastic beam by freezing the deployment process at various stages of deployment, and examining the small amplitude and natural modes of vibration of the resulting configuration. Application of the natural boundary conditions and compatibility of motion relations for the two segments in their common region of overlap leads to a transcendental characteristic equation in the frequency parameter Beta(L). Numerical solution of the equation for the characteristic roots determines the modal frequencies, and the corresponding mode shapes are obtained from the general solution of the Euler-Bernoulli equation tailored to the natural boundary conditions. Sample results of modal frequencies and shapes are presented for various stages of deployment and discussed. It is shown that for all intermediate stages of deployment (between 0 and 100 percent) the spectral distribution is drastically altered by the appearance of regions of very closely spaced modal frequencies. The sources of this modal agglomeration are explored. Author (revised)

N94-35873*# National Aeronautics and Space Administration. Langley Research Center, Hampton, VA.
FLUTTER SUPPRESSION DIGITAL CONTROL LAW DESIGN AND TESTING FOR THE AFW WIND TUNNEL MODEL **c08**
Vivek Mukhopadhyay *In its* NASA Workshop on Distributed Parameter Modeling and Control of Flexible Aerospace Systems Jun. 1994 p 135-149 (For primary document see N94-35865 11-18)
Avail: CASI HC A03/MF A06

The design of a control law for simultaneously suppressing the symmetric and antisymmetric flutter modes of a sting mounted fixed-in-roll aeroelastic wind-tunnel model is described. The flutter suppression control law was designed using linear quadratic Gaussian theory, and it also involved control law order reduction, a gain root-locus study, and use of previous experimental results. A 23 percent increase in the open-loop flutter dynamic pressure was demonstrated during the wind-tunnel test. Rapid roll maneuvers at 11 percent above the symmetric flutter boundary were also performed when the model was in a free-to-roll configuration. Author (revised)

N94-35874*# California Univ., Los Angeles, CA. Dept. of Mechanical, Aerospace and Nuclear Engineering.
SELECTED TOPICS ON THE ACTIVE CONTROL OF HELICOPTER AEROMECHANICAL AND VIBRATION PROBLEMS **c08**
Peretz P. Friedmann *In* NASA. Langley Research Center, NASA Workshop on Distributed Parameter Modeling and Control of Flexible Aerospace Systems Jun. 1994 p 151-177 (For primary document see N94-35865 11-18)
(Grant NAG2-477)
Avail: CASI HC A03/MF A06

This paper describes in a concise manner three selected topics on the active control of helicopter aeromechanical and vibration problems. The three topics are as follows: (1) the active control of helicopter air-resonance using an LQG/LTR approach; (2) simulation of higher harmonic control (HHC) applied to a four bladed hingeless helicopter rotor in forward flight; and (3) vibration suppression in forward flight on a hingeless helicopter rotor using an actively controlled, partial span, trailing edge flap, which is mounted on the blade. Only a few selected illustrative results are presented. The results obtained clearly indicate that the partial span, actively controlled flap has considerable potential for vibration reduction in helicopter rotors. Author (revised)

N94-35875*# Ohio State Univ., Columbus. Dept. of Electrical Engineering.
ROBUST CONTROL DESIGN TECHNIQUES FOR ACTIVE FLUTTER SUPPRESSION **c08**
Hitay Ozbay and Glen R. Bachmann *In* NASA. Langley Research Center, NASA Workshop on Distributed Parameter Modeling and Control of Flexible Aerospace Systems Jun. 1994 p 179-191 (For primary document see N94-35865 11-18)
Avail: CASI HC A03/MF A06

In this paper, an active flutter suppression problem is studied for a thin airfoil in unsteady aerodynamics. The mathematical model of this system is infinite dimensional because of Theodorsen's function which is irrational. Several second order approximations of Theodorsen's function are compared. A finite dimensional model is obtained from such an approximation. We use H infinity control techniques to find a robustly stabilizing controller for active flutter suppression. Author (revised)

N94-35876*# Louisville Univ., KY. Dept. of Electrical Engineering.
ADAPTIVE MODEL REDUCTION FOR CONTINUOUS SYSTEMS VIA RECURSIVE RATIONAL INTERPOLATION **c61**
John H. Lilly *In* NASA. Langley Research Center, NASA Workshop on Distributed Parameter Modeling and Control of Flexible Aerospace Systems Jun. 1994 p 195-214 (For primary document see N94-35865 11-18)
Avail: CASI HC A03/MF A06

A method for adaptive identification of reduced-order models for continuous stable SISO and MIMO plants is presented. The method recursively finds a model whose transfer function (matrix) matches that of the plant on a set of frequencies chosen by the designer. The algorithm utilizes the Moving Discrete Fourier Transform (MDFT) to continuously monitor the frequency-domain profile of the system input and output signals. The MDFT is an efficient method of monitoring discrete points in the frequency domain of an evolving function of time. The model parameters are estimated from MDFT data using standard recursive parameter estimation techniques. The algorithm has been shown in simulations to be quite robust to additive noise in the inputs and outputs. A significant advantage of the method is that it enables a type of on-line model validation. This is accomplished by simultaneously identifying a number of models and comparing each with the plant in the frequency domain. Simulations of the method applied to an 8th-order SISO plant and a 10-state 2-input 2-output plant are presented. An example of on-line model validation applied to the SISO plant is also presented. Author

N94-35877*# Florida Univ., Gainesville, FL.
ADVANCES IN PARAMETER ESTIMATION TECHNIQUES APPLIED TO FLEXIBLE STRUCTURES **c61**
Egbert Maben and David C. Zimmerman *In* NASA. Langley Research Center, NASA Workshop on Distributed Parameter Modeling and Control of Flexible Aerospace Systems Jun. 1994 p 215-239 (For primary document see N94-35865 11-18)
Avail: CASI HC A03/MF A06

In this work, various parameter estimation techniques are investigated in the context of structural system identification utilizing distributed parameter models and 'measured' time-domain data. Distributed parameter models are formulated using the PDEMOD software developed by Taylor. Enhancements made to PDEMOD for this work include the following: (1) a Wittrick-Williams based root solving algorithm; (2) a time simulation capability; and (3) various parameter estimation algorithms. The parameter estimations schemes will be contrasted using the NASA Mini-Mast as the focus structure. Author

N94-35878*# North Carolina Univ., Charlotte, NC. Dept. of Electrical Engineering.
PARAMETER ESTIMATION OF THE VIBRATIONAL MODEL FOR THE SCOLE EXPERIMENTAL FACILITY **c39**
B. D. Crotts and Y. P. Kakad *In* NASA. Langley Research Center, NASA Workshop on Distributed Parameter Modeling and Control of Flexible Aerospace Systems Jun. 1994 p 241-259 (For primary document see N94-35865 11-18)
Avail: CASI HC A03/MF A06

The objective of this study is to experimentally determine an empirical model of the vibrational dynamics of the Spacecraft COntrol Laboratory Experiment (SCOLE) facility. The first two flexible modes of this test article are identified using a linear least-square identification procedure and the data utilized for this procedure are obtained by exciting the structure from a quiescent state with torque wheels. The time history data of rate gyro sensors and accelerometers due to excitation and after excitation in terms

of free-decay are used in the parameter estimation of the vibrational model. The free-decay portion of the data is analyzed using the Discrete Fourier transform to determine the optimal model order to use in modelling the response. Linear least-square analysis is then used to select the parameters that best fit the output of an Autoregressive (AR) model to the data. The control effectiveness of the torque wheels is then determined using the excitation portion of the test data, again using linear least squares.
Author

N94-35879*# Techno-Sciences, Inc., Greenbelt, MD.
A CASE STUDY IN NONLINEAR DYNAMICS AND CONTROL OF ARTICULATED SPACECRAFT: THE SPACE STATION FREEDOM WITH A MOBILE REMOTE MANIPULATOR SYSTEM
William H. Bennett, Harry G. Kwatny, Chris LaVigna, and Gilmer Blankenship *In* NASA. Langley Research Center, NASA Workshop on Distributed Parameter Modeling and Control of Flexible Aerospace Systems Jun. 1994 p 261-278 Sponsored in part by Mitre Corp. (For primary document see N94-35865 11-18)
Avail: CASI HC A03/MF A06

The following topics are discussed: (1) modeling of articulated spacecraft as multi-flex-body systems; (2) nonlinear attitude control by adaptive partial feedback linearizing (PFL) control; (3) attitude dynamics and control for SSF/MRMS; and (4) performance analysis results for attitude control of SSF/MRMS.
CASI

N94-35880*# National Aeronautics and Space Administration. Langley Research Center, Hampton, VA.
AN OVERVIEW OF RECENT ADVANCES IN SYSTEM IDENTIFICATION
Jer-Nan Juang *In its* NASA Workshop on Distributed Parameter Modeling and Control of Flexible Aerospace Systems Jun. 1994 p 279-289 (For primary document see N94-35865 11-18)
Avail: CASI HC A03/MF A06

This paper presents an overview of the recent advances in system identification for modal testing and control of large flexible structures. Several techniques are discussed including the Observer/Kalman Filter Identification, the Observer/Controller Identification, and the State-Space System Identification in the Frequency Domain. The System/Observer/Controller Toolbox developed at NASA Langley Research Center is used to show the applications of these techniques to real aerospace structures such as the Hubble spacecraft telescope and the active flexible aircraft wing.
Author (revised)

N94-35881*# Howard Univ., Washington, DC. Dept. of Mechanical Engineering.
A COMBINED ALGORITHM FOR MINIMUM TIME SLEWING OF FLEXIBLE SPACECRAFT
P. M. Bainum, F. Li, and J. Xu *In* NASA. Langley Research Center, NASA Workshop on Distributed Parameter Modeling and Control of Flexible Aerospace Systems Jun. 1994 p 293-316 (For primary document see N94-35865 11-18)
(Grant NsG-1414)
Avail: CASI HC A03/MF A06

The use of Pontryagin's Maximum Principle for the large-angle slewing of large flexible structures usually results in the so-called two-point boundary-value problem (TPBVP), in which many requirements (e.g., minimum time, small flexible amplitude, and limited control powers, etc.) must be satisfied simultaneously. The successful solution of this problem depends largely on the use of an efficient numerical computational algorithm. There are many candidate algorithms available for his problem (e.g., quasilinearization, gradient, and shooting, etc.). In this paper, a proposed algorithm, which combines the quasilinearization method with a time shortening technique and a shooting method, is applied to the minimum-time, three-dimensional, and large-angle maneuver of flexible spacecraft, particularly the orbiting Spacecraft Control Laboratory Experiment (SCOLE) configuration. Theoretically, the nonlinear TPBVP can be solved only through the shooting method to find the 'exact' switching times for the bang-bang controls. However, computationally, a suitable guess for the missing initial costates is crucial because the convergence range of the unknown initial costates is usually narrow, especially for systems with high dimensions and when a multi-bang-bang control strategy is needed. On the other hand, the problems of near minimum time attitude maneuver of general rigid spacecraft and fast slewing of flexible spacecraft have been examined by the authors through a numerical approach based on the quasilinearization algorithm with a time shortening technique. Computational results have demonstrated its broad convergence range and insensitivity to initial costate choices. Consequently, a combined approach is naturally suggested here to solve the minimum time slewing problem. That is, in the computational process, the quasilinearization method is used first to obtain a near minimum time solution. Then, the acquired converged initial costates from the quasilinearization approach are transformed (tailored) to and used as the initial costate guess for starting the shooting method. Finally, the shooting method takes over the remaining calculations until the minimum-time solution converges. The nonlinear equations of motion of the SCOLE are formulated by using Lagrange's equations, with the mast modeled as a continuous beam subject to three-dimensional deformations. The numerical results will be presented and some related computational issues will also be discussed.
Author

N94-35882*# Temple Univ., Philadelphia, PA. Dept. of Electrical Engineering.
OPTIMAL DISTURBANCE REJECTING CONTROL OF HYPERBOLIC SYSTEMS **c63**
Saroj K. Biswas and N. U. Ahmed *In* NASA. Langley Research Center, NASA Workshop on Distributed Parameter Modeling and Control of Flexible Aerospace Systems Jun. 1994 p 317-322 (For primary document see N94-35865 11-18)
Avail: CASI HC A02/MF A06

Optimal regulation of hyperbolic systems in the presence of unknown disturbances is considered. Necessary conditions for determining the optimal control that tracks a desired trajectory in the presence of the worst possible perturbations are developed. The results also characterize the worst possible disturbance that the system will be able to tolerate before any degradation of the system performance. Numerical results on the control of a vibrating beam are presented.
Author

N94-35883*# Howard Univ., Washington, DC. Dept. of Electrical Engineering.
EFFECTS OF NOISE VARIANCE MODEL ON OPTIMAL FEEDBACK DESIGN AND ACTUATOR PLACEMENT **c63**
Mifang Ruan and Ajit K. Choudhury *In* NASA. Langley Research Center, NASA Workshop on Distributed Parameter Modeling and Control of Flexible Aerospace Systems Jun. 1994 p 323-331 (For primary document see N94-35865 11-18)
Avail: CASI HC A02/MF A06

In optimal placement of actuators for stochastic systems, it is commonly assumed that the actuator noise variances are not related to the feedback matrix and the actuator locations. In this paper, we will discuss the limitation of that assumption and develop a more practical noise variance model. Various properties associated with optimal actuator placement under the assumption of this noise variance model are discovered through the analytical study of a second order system.
Author

N94-35884*# Ohio State Univ., Columbus. Dept. of Electrical Engineering.
VIBRATION SUPPRESSION IN FLEXIBLE STRUCTURES VIA THE SLIDING-MODE CONTROL APPROACH
S. Drakunov and Uemit Oezguener *In* NASA. Langley Research Center, NASA Workshop on Distributed Parameter Modeling and Control of Flexible Aerospace Systems Jun. 1994 p 333-350 (For primary document see N94-35865 11-18)
Avail: CASI HC A03/MF A06

Sliding mode control became very popular recently because it makes the closed loop system highly insensitive to external disturbances and parameter variations. Sliding algorithms for flexible structures have been used previously, but these were based on finite-dimensional models. An extension of this approach for differential-difference systems is obtained. That makes if possible to apply sliding-mode control algorithms to the variety of nondispersive flexible structures which can be described as differential-difference systems. The main idea of using this technique for dispersive structures is to reduce the order of the controlled part of the system by applying an integral transformation. We can say that transformation 'absorbs' the dispersive properties of the flexible structure as the controlled part becomes dispersive.
Author

N94-35885*# Old Dominion Univ., Norfolk, VA. Dept. of Mechanical Engineering and Mechanics.

CONTROL OF THE SCOLE CONFIGURATION USING DISTRIBUTED PARAMETER MODELS c39

Min-Hung Hsiao and Jen-Kuang Huang *In* NASA. Langley Research Center, NASA Workshop on Distributed Parameter Modeling and Control of Flexible Aerospace Systems Jun. 1994 p 351-363 (For primary document see N94-35865 11-18)
Avail: CASI HC A03/MF A06

A continuum model for the SCOLE configuration has been derived using transfer matrices. Controller designs for distributed parameter systems have been analyzed. Pole-assignment controller design is considered easy to implement but stability is not guaranteed. An explicit transfer function of dynamic controllers has been obtained and no model reduction is required before the controller is realized. One specific LQG controller for continuum models had been derived, but other optimal controllers for more general performances need to be studied. Derived from text

N94-35886*# Maryland Univ., College Park, MD. Dept. of Electrical Engineering.

ACTIVE VIBRATION DAMPING USING SMART MATERIAL c39

John S. Baras and Zhuang Yan *In* NASA. Langley Research Center, NASA Workshop on Distributed Parameter Modeling and Control of Flexible Aerospace Systems Jun. 1994 p 365-378 (For primary document see N94-35865 11-18)
(Grants NSF CDR-88-03012; AF-AFOSR-1054-90)
Avail: CASI HC A03/MF A06

We consider the modeling and active damping of an elastic beam using distributed actuators and sensors. The piezoelectric ceramic material (PZT) is used to build the actuator. The sensor is made of the piezoelectric polymer polyvinylidene fluoride (PVDF). These materials are glued on both sides of the beam. For the simple clamped beam, the closed loop controller has been shown to be able to extract energy from the beam. The shape of the actuator and its influence on the closed loop system performance are discussed. It is shown that it is possible to suppress the selected mode by choosing the appropriate actuator layout. It is also shown that by properly installing the sensor and determining the sensor shape we can further extract and manipulate the sensor signal for our control need. Author

N94-35887*# National Aeronautics and Space Administration. Langley Research Center, Hampton, VA.

DYNAMIC ANALYSIS OF SPACE SHUTTLE/RMS CONFIGURATION USING CONTINUUM APPROACH

Jayant Ramakrishnan (DYNACS Engineering Co., Inc., Palm Harbor, FL.) and Lawrence W. Taylor, Jr. *In its* NASA Workshop on Distributed Parameter Modeling and Control of Flexible Aerospace Systems Jun. 1994 p 379-403 (For primary document see N94-35865 11-18)
Avail: CASI HC A03/MF A06

The initial assembly of Space Station Freedom involves the Space Shuttle, its Remote Manipulation System (RMS) and the evolving Space Station Freedom. The dynamics of this coupled system involves both the structural and the control system dynamics of each of these components. The modeling and analysis of such an assembly is made even more formidable by kinematic and joint nonlinearities. The current practice of modeling such flexible structures is to use finite element modeling in which the mass and interior dynamics is ignored between thousands of nodes, for each major component. The model characteristics of only tens of modes are kept out of thousands which are calculated. The components are then connected by approximating the boundary conditions and inserting the control system dynamics. In this paper continuum models are used instead of finite element models because of the improved accuracy, reduced number of model parameters, the avoidance of model order reduction, and the ability to represent the structural and control system dynamics in the same system of equations. Dynamic analysis of linear versions of the model is performed and compared with finite element model results. Additionally, the transfer matrix to continuum modeling is presented. Author

N94-35888*# Lockheed Missiles and Space Co., Sunnyvale, CA.

CSI, OPTIMAL CONTROL, AND ACCELEROMETERS: TRIALS AND TRIBULATIONS c61

Brian J. Benjamin and John R. Sesak *In* NASA. Langley Research Center, NASA Workshop on Distributed Parameter Modeling and Control of Flexible Aerospace Systems Jun. 1994 p 407-425 (For primary document see N94-35865 11-18)
(Contract NAS1-19241)
Avail: CASI HC A03/MF A06

New results concerning optimal design with accelerometers are presented. These results show that the designer must be concerned with the stability properties of two Linear Quadratic Gaussian (LQG) compensators, one of which does not explicitly appear in the closed-loop system dynamics. The new concepts of virtual and implemented compensators are introduced to cope with these subtleties. The virtual compensator appears in the closed-loop system dynamics and the implemented compensator appears in control electronics. The stability of one compensator does not guarantee the stability of the other. For strongly stable (robust) systems, both compensators should be stable. The presence of controlled and uncontrolled modes in the system results in two additional forms of the compensator with corresponding terms that are of like form, but opposite sign, making simultaneous stabilization of both the virtual and implemented compensator difficult. A new design algorithm termed sensor augmentation is developed that aids stabilization of these compensator forms by incorporating a static augmentation term associated with the uncontrolled modes in the design process. Author

N94-35889*# National Aeronautics and Space Administration. Langley Research Center, Hampton, VA.

AN OPTIMIZATION-BASED APPROACH FOR INTEGRATED CONTROLS-STRUCTURES DESIGN OF FLEXIBLE SPACECRAFT

P. G. Maghami, S. M. Joshi, and E. S. Armstrong *In its* NASA Workshop on Distributed Parameter Modeling and Control of Flexible Aerospace Systems Jun. 1994 p 427-443 (For primary document see N94-35865 11-18)
Avail: CASI HC A03/MF A06

The control of flexible spacecraft is a difficult problem because of large number of elastic modes; low value, closely-spaced frequencies; very small damping; and uncertainties in math models. The traditional design approach is to design the structure first and then to design the control system. This view-graph presentation develops a methodology for spacecraft design which addresses control/structure interaction issues, produces technology for simultaneous control/structure design, and translates into algorithms and computational tools for practical integrated computer-aided design. CASI

N94-35890*# California Univ., Los Angeles, CA. Flight Systems Research Center.

ROBUSTNESS PROPERTIES OF LQG OPTIMIZED COMPENSATORS FOR COLLOCATED RATE SENSORS c63

A. V. Balakrishnan *In* NASA. Langley Research Center, NASA Workshop on Distributed Parameter Modeling and Control of Flexible Aerospace Systems Jun. 1994 p 445-463 (For primary document see N94-35865 11-18)
Avail: CASI HC A03/MF A06

In this paper we study the robustness with respect to stability of the closed-loop system with collocated rate sensor using LQG (mean square rate) optimized compensators. Our main result is that the transmission zeros of the compensator are precisely the structure modes when the actuator/sensor locations are 'pinned' and/or 'clamped': i.e., motion in the direction sensed is not allowed. We have stability even under parameter mismatch, except in the unlikely situation where such a mode frequency of the assumed system coincides with an undamped mode frequency of the real system and the corresponding mode shape is an eigenvector of the compensator transfer function matrix at that frequency. For a truncated modal model - such as that of the NASA LaRC Phase Zero Evolutionary model - the transmission zeros of the corresponding compensator transfer function can be interpreted as the structure modes when motion in the directions sensed is prohibited. Author

N94-35891*# California Univ., Los Angeles, CA. Flight Systems Research Center.

LQG OPTIMAL COMPENSATOR TRANSFER FUNCTION FOR THE NASA LARC CSI EVOLUTIONARY MODEL c63

A. V. Balakrishnan *In* NASA. Langley Research Center, NASA Workshop on Distributed Parameter Modeling and Control of Flexible Aerospace

Systems Jun. 1994 p 465-481 (For primary document see N94-35865 11-18)
Avail: CASI HC A03/MF A06

Following the general form for LQG optimal compensators for flexible structures with collocated rate sensors we develop an explicit compensator transfer function for the NASA LaRC CSI Evolutionary model in the form: psi(i omega) = g i omega B(sub u)(sup *)(-M(sub b)omega(exp 2) + T(i omega) + i gamma omega B(sub u)Bu(sub u)(sup *))(exp -1)B(sub u) where T(i omega) is a 48 x 48 positive definite matrix whose derivation is the main result of this report. The undamped mode frequencies can be expressed in terms of T(i omega) as the zeros of Det (-omega(exp 2)M(sub b) + T(i omega)) while 'clamped-clamped' modes of the structure (with all nodes clamped) are the poles. Author

N94-35892*# Consiglio Nazionale delle Ricerche, Rome (Italy).
RATIONAL POSITIVE REAL APPROXIMATIONS FOR LQG OPTIMAL COMPENSATORS ARISING IN ACTIVE STABILIZATION OF FLEXIBLE STRUCTURES
A. DeSantis *In* NASA. Langley Research Center, NASA Workshop on Distributed Parameter Modeling and Control of Flexible Aerospace Systems Jun. 1994 p 483-496 (For primary document see N94-35865 11-18)
Avail: CASI HC A03/MF A06

In this paper the approximation problem for a class of optimal compensators for flexible structures is considered. The particular case of a simply supported truss with an offset antenna is dealt with. The nonrational positive real optimal compensator transfer function is determined, and it is proposed that an approximation scheme based on a continued fraction expansion method be used. Comparison with the more popular modal expansion technique is performed in terms of stability margin and parameters sensitivity of the relative approximated closed loop transfer functions. Author

N94-35893*# George Mason Univ., Fairfax, VA. Dept. of Electrical and Computer Engineering.
DYNAMICAL OBSERVER FOR A FLEXIBLE BEAM VIA FINITE ELEMENT APPROXIMATIONS c39
Andre Manitius and Hong-Xing Xia *In* NASA. Langley Research Center, NASA Workshop on Distributed Parameter Modeling and Control of Flexible Aerospace Systems Jun. 1994 p 497-517 (For primary document see N94-35865 11-18)
Avail: CASI HC A03/MF A06

The purpose of this view-graph presentation is a computational investigation of the closed-loop output feedback control of a Euler-Bernoulli beam based on finite element approximation. The observer is part of the classical observer plus state feedback control, but it is finite-dimensional. In the theoretical work on the subject it is assumed (and sometimes proved) that increasing the number of finite elements will improve accuracy of the control. In applications, this may be difficult to achieve because of numerical problems. The main difficulty in computing the observer and simulating its work is the presence of high frequency eigenvalues in the finite-element model and poor numerical conditioning of some of the system matrices (e.g. poor observability properties) when the dimension of the approximating system increases. This work dealt with some of these difficulties. Derived from text

N94-35894*# Texas A&M Univ., College Station, TX. Dept. of Aerospace Engineering.
SEMIGROUP APPROXIMATION AND ROBUST STABILIZATION OF DISTRIBUTED PARAMETER SYSTEMS c63
A. J. Kurdila, R. Fabiano, T. Strganac, and S. Hsu *In* NASA. Langley Research Center, NASA Workshop on Distributed Parameter Modeling and Control of Flexible Aerospace Systems Jun. 1994 p 519-543 (For primary document see N94-35865 11-18)
(Contract F49620-92-J-0450)
Avail: CASI HC A03/MF A06

Theoretical results that enable rigorous statements of convergence and exponential stability of Galerkin approximations of LQR controls for infinite dimensional, or distributed parameter, systems have proliferated over the past ten years. In addition, extensive progress has been made over the same time period in the derivation of robust control design strategies for finite dimensional systems. However, the study of the convergence of robust finite dimensional controllers to robust controllers for infinite dimensional systems remains an active area of research. We consider a class of soft-constrained differential games evolving in a Hilbert space. Under certain conditions, a saddle point control can be given in feedback form in terms of a solution to a Riccati equation. By considering a related LQR problem, we can show a convergence result for finite dimensional approximations of this differential game. This yields a computational algorithm for the feedback gain that can be derived from similar strategies employed in infinite dimensional LQR control design problems. The approach described in this paper also inherits the additional properties of stability robustness common to game theoretic methods in finite dimensional analysis. These theoretical convergence and stability results are verified in several numerical experiments. Author (revised)

N94-35895*# State Univ. of New York, Buffalo, NY. Mechanical Systems Lab.
TRANSFER FUNCTION MODELING OF DAMPING MECHANISMS IN DISTRIBUTED PARAMETER MODELS c39
J. C. Slater and D. J. Inman *In* NASA. Langley Research Center, NASA Workshop on Distributed Parameter Modeling and Control of Flexible Aerospace Systems Jun. 1994 p 547-553 (For primary document see N94-35865 11-18)
(Grant NGT-50541)
Avail: CASI HC A02/MF A06

This work formulates a method for the modeling of material damping characteristics in distributed parameter models which may be easily applied to models such as rod, plate, and beam equations. The general linear boundary value vibration equation is modified to incorporate hysteresis effects represented by complex stiffness using the transfer function approach proposed by Golla and Hughes. The governing characteristic equations are decoupled through separation of variables yielding solutions similar to those of undamped classical theory, allowing solution of the steady state as well as transient response. Example problems and solutions are provided demonstrating the similarity of the solutions to those of the classical theories and transient responses of nonviscous systems. Author

N94-35896*# DYNACS Engineering Co., Inc., Palm Harbor, FL.
COMPUTATIONALLY EFFICIENT MULTIBODY SIMULATIONS c63
Jayant Ramakrishnan and Manoj Kumar *In* NASA. Langley Research Center, NASA Workshop on Distributed Parameter Modeling and Control of Flexible Aerospace Systems Jun. 1994 p 555-570 (For primary document see N94-35865 11-18)
Avail: CASI HC A03/MF A06

Computationally efficient approaches to the solution of the dynamics of multibody systems are presented in this work. The computational efficiency is derived from both the algorithmic and implementational standpoint. Order(n) approaches provide a new formulation of the equations of motion eliminating the assembly and numerical inversion of a system mass matrix as required by conventional algorithms. Computational efficiency is also gained in the implementation phase by the symbolic processing and parallel implementation of these equations. Comparison of this algorithm with existing multibody simulation programs illustrates the increased computational efficiency. Author

N94-35897*# Houston Univ., TX.
NUMERICAL METHODS FOR MULTIBODY SYSTEMS c64
Roland Glowinski and Mahmoud G. Nasser *In* NASA. Langley Research Center, NASA Workshop on Distributed Parameter Modeling and Control of Flexible Aerospace Systems Jun. 1994 p 571-585 Sponsored in part by Texas Board of Education (For primary document see N94-35865 11-18)
(Contract NAS9-17900)
Avail: CASI HC A03/MF A06

This article gives a brief summary of some results obtained by Nasser on modeling and simulation of inequality problems in multibody dynamics. In particular, the augmented Lagrangian method discussed here is applied to a constrained motion problem with impulsive inequality constraints. A fundamental characteristic of the multibody dynamics problem is the lack of global convexity of its Lagrangian. The problem is transformed into a convex analysis problem by localization (piecewise linearization), where the augmented Lagrangian has been successfully used. A model test problem is considered and a set of numerical experiments is presented. Author

N94-35898*# National Aeronautics and Space Administration. Langley Research Center, Hampton, VA.
SOFTWARE FOR CONTINUUM MODELING OF CONTROLS-STRUCTURES INTERACTIONS
Lawrence W. Taylor, Jr. *In its* NASA Workshop on Distributed Parameter Modeling and Control of Flexible Aerospace Systems Jun. 1994 p 587-603 (For primary document see N94-35865 11-18)
Avail: CASI HC A03/MF A06

It is clear that computer software is needed to assist in the generation of the equations of motion for complex, flexible spacecraft. Daniel Poelaert of ESTEC has developed the software DISTEL with which he has modeled the structural dynamics for different satellites. He is interested in expanding the capabilities of DISTEL to include structural damping and control systems. Unfortunately, the software has not been released. The author has developed similar software, PDEMOD, which has been used to model the Spacecraft control Laboratory Experiment (SCOLE), the Solar Array Flight Experiment (SAFE), the Mini-MAST truss, and the LACE satellite. PDEMOD has been used also for optimal parameter estimation and integrated control-structures design. PDEMOD is also being extended to include structural damping and control systems which are imbedded into the same equations for the structural dynamics. This paper will address the formulation of the equations for the structural dynamics of spacecraft structures which are constructed of a 3-dimensional arrangement of rigid bodies and flexible beam elements. Control system dynamics are imbedded into the same equations so that model order reduction approximations are not necessary. The input data consists of the physical data of the elements and the topological information describing how the elements are connected. PDEMOD accomplishes the following: (1) automatically assembles the equations of motion for the entire structural model; (2) calculates the modal frequencies; (3) calculates the mode shapes; (4) generates perspective views of the mode shapes; and (5) forms selected transfer functions. The software PDEMOD continues to be developed to provide additional features to assist in analyzing and synthesizing control and structural systems for flexible spacecraft.
Author (revised)

N94-35902*# National Aeronautics and Space Administration. Langley Research Center, Hampton, VA.
SECOND INTERNATIONAL SYMPOSIUM ON MAGNETIC SUSPENSION TECHNOLOGY, PART 2
Nelson J. Groom, ed. and Colin P. Britcher, ed. May 1994 258 p Symposium held in Seattle, WA, 11-13 Aug. 1993 Sponsored by NASA, Washington
(RTOP 233-03-01-01)
(NASA-CP-3247-Pt-2; L-17369-Pt-2; NAS 1.55:3247-Pt-2) Avail: CASI HC A12/MF A03

In order to examine the state of technology of all areas of magnetic suspension and to review related recent developments in sensors and controls approaches, superconducting magnet technology, and design/implementation practices, the 2nd International Symposium on Magnetic Suspension Technology was held at the Westin Hotel in Seattle, WA, on 11-13 Aug. 1993. The symposium included 18 technical sessions in which 44 papers were presented. The technical sessions covered the areas of bearings, bearing modelling, controls, vibration isolation, micromachines, superconductivity, wind tunnel magnetic suspension systems, magnetically levitated trains (MAGLEV), rotating machinery and energy storage, and applications. A list of attendees appears at the end of the document. For individual titles, see N94-35903 through N94-35919.

N94-35903*# General Electric Co., Lynn, MA. Aircraft Engines.
INTEGRATION OF MAGNETIC BEARINGS IN THE DESIGN OF ADVANCED GAS TURBINE ENGINES **c37**
Albert F. Storace, Devendra K. Sood, James P. Lyons, and Mark A. Preston *In* NASA. Langley Research Center, Second International Symposium on Magnetic Suspension Technology, Part 2 May 1994 p 435-449 (For primary document see N94-35902 11-18)
(Contract DAAJ02-92-C-0055)
Avail: CASI HC A03/MF A03

Active magnetic bearings provide revolutionary advantages for gas turbine engine rotor support. These advantages include tremendously improved vibration and stability characteristics, reduced power loss, improved reliability, fault-tolerance, and greatly extended bearing service life. The marriage of these advantages with innovative structural network design and advanced materials utilization will permit major increases in thrust to weight performance and structural efficiency for future gas turbine engines. However, obtaining the maximum payoff requires two key ingredients. The first key ingredient is the use of modern magnetic bearing technologies such as innovative digital control techniques, high-density power electronics, high-density magnetic actuators, fault-tolerant system architecture, and electronic (sensorless) position estimation. This paper describes these technologies. The second key ingredient is to go beyond the simple replacement of rolling element bearings with magnetic bearings by incorporating magnetic bearings as an integral part of the overall engine design. This is analogous to the proper approach to designing with composites, whereby the designer tailors the geometry and load carrying function of the structural system or component for the composite instead of simply substituting composites in a design originally intended for metal material. This paper describes methodologies for the design integration of magnetic bearings in gas turbine engines.
Author

N94-35904*# SatCon Technology Corp., Cambridge, MA.
SUPERCONDUCTING REBALANCE ACCELERATION AND RATE SENSOR **c35**
R. Torti, M. Gerver, V. Gondhalekar, and B. Maxwell *In* NASA. Langley Research Center, Second International Symposium on Magnetic Suspension Technology, Part 2 May 1994 p 451-464 (For primary document see N94-35902 11-18)
Avail: CASI HC A03/MF A03

The goal of this program is the development of a high precision multisensor based on a high T(sub c) superconducting proof mass. The design of a prototype is currently underway. Key technical issues appear resolvable. High temperature superconductors have complicated, hysteretic flux dynamics but the forces on them can be linearly controlled for small displacements. Current data suggests that the forces on the superconductors decay over a short time frame and then stabilize, though very long term data is not available. The hysteretic force characteristics are substantial for large scale excursions, but do not appear to be an issue for the very small displacements required in this device. Sufficient forces can be exerted for non-contact suspension of a centimeter sized proof mass in a vacuum sealed nitrogen jacket cryostat. High frequency capacitive sensing using stripline technology will yield adequate position resolution for 0.1 micro-g measurements at 100 Hz. Overall, a reasonable cost, but very high accuracy, system is feasible with this technology.
Author (revised)

N94-35905*# National Aeronautics and Space Administration. Lewis Research Center, Cleveland, OH.
ELECTROMECHANICAL SIMULATION AND TEST OF ROTATING SYSTEMS WITH MAGNETIC BEARING OR PIEZOELECTRIC ACTUATOR ACTIVE VIBRATION CONTROL **c37**
Alan B. Palazzolo (Texas A&M Univ., College Station, TX.), Punan Tang (Texas A&M Univ., College Station, TX.), Chaesil Kim (Texas A&M Univ., College Station, TX.), Daniel Manchala (Texas A&M Univ., College Station, TX.), Tim Barrett (Texas A&M Univ., College Station, TX.), Albert F. Kascak (Army Aviation Systems Command, Cleveland, OH.), Gerald Brown, Gerald Montague, Eliseo DiRusso, and Steve Klusman et al *In* NASA. Langley Research Center, Second International Symposium on Magnetic Suspension Technology, Part 2 May 1994 p 467-478 (For primary document see N94-35902 11-18)
Avail: CASI HC A03/MF A03

This paper contains a summary of the experience of the authors in the field of electromechanical modeling for rotating machinery - active vibration control. Piezoelectric and magnetic bearing actuator based control are discussed.
Author

N94-35906*# Ebara Research Co. Ltd., Kanagawa (Japan).
ELECTROMAGNETICALLY LEVITATED VIBRATION ISOLATION SYSTEM FOR THE MANUFACTURING PROCESS OF SILICON MONOCRYSTALS **c39**
Yoichi Kanemitsu, Katsuhide Watanabe, Kenichi Yano, and Takayuki Mizuno *In* NASA. Langley Research Center, Second International Symposium on Magnetic Suspension Technology, Part 2 May 1994 p 479-497 (For primary document see N94-35902 11-18)
Avail: CASI HC A03/MF A03

This paper introduces a study on an Electromagnetically Levitated Vibration Isolation System (ELVIS) for isolation control of large-scale vibration. This system features no mechanical contact between the isolation table and the installation floor, using a total of four electromagnetic actuators which generate magnetic levitation force in the vertical and horizontal directions. The configuration of the magnet for the vertical direction is designed to prevent any generation of restoring vibratory force in the horizontal direction. The isolation system is set so that vibration control effects due to small earthquakes can be regulated to below 5(gal) versus horizontal vibration levels of the installation floor of up t 25(gal), and those in the horizontal relative displacement of up to 30 (mm) between the floor and levitated isolation table. In particular, studies on the relative displacement between the installation floor and the levitated isolation table have been made for vibration control in the horizontal direction. In case of small-scale earthquakes (Taft wave scaled: max. 25 gal), the present system has been confirmed to achieve a vibration isolation to a level below 5 gal. The vibration transmission ratio of below 1/10 has been achieved versus continuous micro-vibration (approx. one gal) in the horizontal direction on the installation floor. Author

N94-35907*# Wisconsin Univ., Madison, WI. Center for Applied Microelectronics.

PLANAR ROTATIONAL MAGNETIC MICROMOTORS WITH INTEGRATED SHAFT ENCODER AND MAGNETIC ROTOR LEVITATION c33

Henry Guckel, T. R. Christenson, K. J. Skrobis, J. Klein, and M. Karnowsky *In* NASA. Langley Research Center, Second International Symposium on Magnetic Suspension Technology, Part 2 May 1994 p 501-511 (For primary document see N94-35902 11-18)
(Contract N00014-91-J-1876; NSF ECS-91-16566; NSF DMR-88-21625; SRC-88-MC-507)
Avail: CASI HC A03/MF A03

Deep x-ray lithography and electroplating may be combined to form a fabrication tool for micromechanical devices with large structural heights, to 500 micron, and extreme edge acuities, less than 0.1 micron-run-out per 100 micron of height. This process concept which originated in Germany as LIGA may be further extended by adding surface micromachining. This extension permits the fabrication of precision metal and plastic parts which may be assembled into three-dimensional micromechanical components and systems. The processing tool may be used to fabricate devices from ferromagnetic material such as nickel and nickel-iron alloys. These materials when properly heat treated exhibit acceptable magnetic behavior for current to flux conversion and marginal behavior for permanent magnet applications. The tool and materials have been tested via planar, magnetic, rotational micromotor fabrication. Three phase reluctance machines of the 6:4 configuration with 280 micron diameter rotors have been tested and analyzed. Stable rotational speeds to 34,000 rpm with output torques above 10 x 10(exp -9) N-m have been obtained. The behavior is monitored with integrated shaft encoders which are photodiodes which measure the rotor response. Magnetic levitation of the rotor via reluctance forces has been achieved and has reduced frictional torque losses to less than 1 percent of the available torque. The results indicate that high speed limits of these actuators are related to torque ripple. Hysteresis motors with magnetic bearings are under consideration and will produce high speed rotational machines with excellent sensor application potential. Author

N94-35908*# SatCon Technology Corp., Cambridge, MA.

ELECTROSTATICALLY SUSPENDED AND SENSED MICRO-MECHANICAL RATE GYROSCOPE c35

R. Torti, M. Gerver, V. Gondhalekar, S. Bart, and B. Maxwell *In* NASA. Langley Research Center, Second International Symposium on Magnetic Suspension Technology, Part 2 May 1994 p 513-525 (For primary document see N94-35902 11-18)
Avail: CASI HC A03/MF A03

The goal of this work is development of fully electrostatically suspended and rebalancing angular rate sensing micro-gyroscope fabricated according to standard VLSI techniques. Fabrication of test structures is proceeding. Off chip electronics for the electrostatic sensing and driving circuits has been tested. The prototype device will be assembled in a hybrid construction including the FET input stages of the sensors. Author

N94-35909*# Kernforschungszentrum G.m.b.H., Karlsruhe (Germany).

CONCEPTS OF FLYWHEELS FOR ENERGY STORAGE USING AUTOSTABLE HIGH-T(SUB c) SUPERCONDUCTING MAGNETIC BEARINGS c44

Hans J. Bornemann, R. Zabka, P. Boegler, C. Urban, and H. Rietschel *In* NASA. Langley Research Center, Second International Symposium on Magnetic Suspension Technology, Part 2 May 1994 p 529-542 (For primary document see N94-35902 11-18)
(Contract CEC-BRE2-CT92-0274)
Avail: CASI HC A03/MF A03

A flywheel for energy storage using autostable high-T(sub c) superconducting magnetic bearings has been built. The rotating disk has a total weight of 2.8 kg. The maximum speed is 9240 rpm. A process that allows accelerated, reliable and reproducible production of melt-textured superconducting material used for the bearings has been developed. In order to define optimum configurations for radial and axial bearings, interaction forces in three dimensions and vertical and horizontal stiffness have been measured between superconductors and permanent magnets in different geometries and various shapes. Static as well as dynamic measurements have been performed. Results are being reported and compared to theoretical models. Author

N94-35910*# Fare, Inc., College Park, MD.

MANUFACTURING AND TESTING OF A MAGNETICALLY SUSPENDED COMPOSITE FLYWHEEL ENERGY STORAGE SYSTEM c44

Stephen Wells and Da-Chen Pang *In* NASA. Langley Research Center, Second International Symposium on Magnetic Suspension Technology, Part 2 May 1994 p 543-556 (For primary document see N94-35902 11-18)
(Contract NAS5-31704)
Avail: CASI HC A03/MF A03

This paper presents the work performed to develop a multiring composite material flywheel and improvements of a magnetically suspended energy storage system. The flywheel is constructed of filament would graphite/epoxy and is interference assembled for better stress distribution to obtain higher speeds. The stationary stack in the center of the disk supports the flywheel with two magnetic bearings and provides power transfer to the flywheel with a motor/generator. The system operates under a 10(exp -4) torr environment and has been demonstrated to 20,000 rpm with a total stored energy of 15.9 Wh. When this flywheel cycles between its design speeds (45,000 to 90,000 rpm), it will deliver 242 Wh and have a usable specific energy density of 42.6 Wh/kg. Author

N94-35911*# Sulzer-Escher Wyss Ltd., Zurich (Switzerland).

ROTOR DYNAMIC BEHAVIOUR OF A HIGH-SPEED OIL-FREE MOTOR COMPRESSOR WITH A RIGID COUPLING SUPPORTED ON FOUR RADIAL MAGNETIC BEARINGS c37

J. Schmied and J. C. Pradetto *In* NASA. Langley Research Center, Second International Symposium on Magnetic Suspension Technology, Part 2 May 1994 p 557-572 (For primary document see N94-35902 11-18)
Avail: CASI HC A03/MF A03

The combination of a high-speed motor, dry gas seals, and magnetic bearings realized in this unit facilitates the elimination of oil. The motor is coupled with a quill shaft to the compressor. This yields higher natural frequencies of the rotor than with the use of a diaphragm coupling and helps to maintain a sufficient margin of the maximum speed to the frequency of the second compressor bending mode. However, the controller of each bearing then has to take the combined modes of both machines into account. The requirements for the controller to ensure stability and sufficient damping of all critical speeds are designed and compared with the implemented controller. The calculated closed loop behavior was confirmed experimentally, except the stability of some higher modes due to slight frequency deviations of the rotor model to the actual rotor. The influence of a mechanical damper as a device to provide additional damping to high models is demonstrated theoretically. After all, it was not necessary to install the damper, since all modes cold be stabilized by the controller. Author (revised)

N94-35912*# National Cheng Kung Univ., Tainan (Taiwan). Inst. of Aeronautics and Astronautics.

NONLINEAR FEEDBACK MODEL ATTITUDE CONTROL USING CCD IN MAGNETIC SUSPENSION SYSTEM **c37**

Chin-E. Lin and Ann-San Hou *In* NASA. Langley Research Center, Second International Symposium on Magnetic Suspension Technology, Part 2 May 1994 p 575-582 (For primary document see N94-35902 11-18)
(Contract NSC-82-0424-E0006-040)
Avail: CASI HC A02/MF A03

A model attitude control system for a CCD camera magnetic suspension system is studied in this paper. In a recent work, a position and attitude sensing method was proposed. From this result, model position and attitude of a magnetic suspension system can be detected by generating digital outputs. Based on this achievement, a control system design using nonlinear feedback techniques for magnetic suspended model attitude control is proposed. Author (revised)

N94-35913*# National Aeronautics and Space Administration. Langley Research Center, Hampton, VA.

ROBUST TRACKING CONTROL OF A MAGNETICALLY SUSPENDED RIGID BODY **c37**

Kyong B. Lim and David E. Cox *In its* Second International Symposium on Magnetic Suspension Technology, Part 2 May 1994 p 583-603 See also A93-52186 (For primary document see N94-35902 11-18)
Avail: CASI HC A03/MF A03

This study is an application of H-infinity and micro-synthesis for designing robust tracking controllers for the Large Angle Magnetic Suspension Test Facility. The modeling, design, analysis, simulation, and testing of a control law that guarantees tracking performance under external disturbances and model uncertainties is investigated. The type of uncertainties considered and the tracking performance metric used is discussed. This study demonstrates the tradeoff between tracking performance at low frequencies and robustness at high frequencies. Two sets of controllers were designed and tested. The first set emphasized performance over robustness, while the second set traded off performance for robustness. Comparisons of simulation and test results are also included. Current simulation and experimental results indicate that reasonably good robust tracking performance can be attained for this system using multivariable robust control approach. Author (revised)

N94-35914*# Kyushu Univ., Fukuoka (Japan). Dept. of Electrical Engineering.

FEASIBILITY STUDY OF SUPERCONDUCTING LSM ROCKET LAUNCHER SYSTEM **c33**

Kinjiro Yoshida, Takaaki Ohashi, Katsuto Shiraishi, and Hiroshi Takami *In* NASA. Langley Research Center, Second International Symposium on Magnetic Suspension Technology, Part 2 May 1994 p 607-621 (For primary document see N94-35902 11-18)
Avail: CASI HC A03/MF A03

A feasibility study is presented concerning an application of a superconducting linear synchronous motor (LSM) to a large-scale rocket launcher, whose acceleration guide tube of LSM armature windings is constructed 1,500 meters under the ground. The rocket is released from the linear launcher just after it gets to a peak speed of about 900 kilometers per hour, and it flies out of the guide tube to obtain the speed of 700 kilometers per hour at the height of 100 meters above ground. The linear launcher is brought to a stop at the ground surface for a very short time of 5 seconds by a quick control of deceleration. Very large current variations in the single-layer windings of the LSM armature, which are produced at the higher speed region of 600 to 900 kilometers per hour, are controlled successfully by adopting the double-layer windings. The proposed control method makes the rocket launcher ascend stably in the superconducting LSM system, controlling the Coriolis force. Author (revised)

N94-35915*# Kanagawa Academy of Science and Technology, Kawasaki (Japan).

MAGNETICALLY SUSPENDED STEPPING MOTORS FOR CLEAN ROOM AND VACUUM ENVIRONMENTS **c33**

Toshiro Higuchi *In* NASA. Langley Research Center, Second International Symposium on Magnetic Suspension Technology, Part 2 May 1994 p 625-639 (For primary document see N94-35902 11-18)
Avail: CASI HC A03/MF A03

To answer the growing needs for super-clean or contact free actuators for uses in clean rooms, vacuum chambers, and space, innovative actuators which combine the functions of stepping motors and magnetic bearings in one body were developed. The rotor of the magnetically suspended stepping motor is suspended like a magnetic bearing and rotated and positioned like a stepping motor. The important trait of the motor is that it is not a simple mixture or combination of a stepping motor and conventional magnetic bearing, but an amalgam of a stepping motor and a magnetic bearing. Owing to optimal design and feed-back control, a toothed stator and rotor are all that are needed structurewise for stable suspension. More than ten types of motors such as linear type, high accuracy rotary type, two-dimensional type, and high vacuum type were built and tested. This paper describes the structure and design of these motors and their performance for such applications as precise positioning rotary table, linear conveyor system, and theta-zeta positioner for clean room and high vacuum use. Derived from text

N94-35916*# Arling (R. W.), Windham, NH.

SIX DEGREE OF FREEDOM FINE MOTION POSITIONING STAGE BASED ON MAGNETIC LEVITATION **c37**

R. W. Arling and S. M. Kohler *In* NASA. Langley Research Center, Second International Symposium on Magnetic Suspens ion Technology, Part 2 May 1994 p 641-652 See also N94-19547 (For primary document see N94-35902 11-18)
(Contract DE-AC04-76DP-00789)
Avail: CASI HC A03/MF A03

The design of a magnetically suspended six degree of freedom positioning system capable of nanometer positioning is presented. The sample holder is controlled in six degrees of freedom (DOF) over 300 micrometers of travel in the X, Y, and Z directions. A design and control summary and test results indicating stability and power dissipation are included in the paper. The system is vacuum compatible, uses commercially available materials, and requires minimal assembly and setup. Author

N94-35917*# North Carolina Univ., Charlotte, NC. Dept. of Electrical Engineering.

ANALYSIS OF ACHIEVABLE DISTURBANCE ATTENUATION IN A PRECISION MAGNETICALLY-SUSPENDED MOTION CONTROL SYSTEM **c37**

Alexander V. Kuzin, Michael L. Holmes, Roxana Behrouzjou, and David L. Trumper *In* NASA. Langley Research Center, Second International Symposium on Magnetic Suspension Technology, Part 2 May 1994 p 653-665 (For primary document see N94-35902 11-18)
Avail: CASI HC A03/MF A03

The results of the analysis of the achievable disturbance attenuation to get an Angstrom motion control resolution and macroscopic travel in a precision magnetically-suspended motion control system are presented in this paper. Noise sources in the transducers, electronics, and mechanical vibrations are used to develop the control design. Author

N94-35918*# Xerad, Inc., Santa Monica, CA.

FUTURE ULTRA-SPEED TUBE-FLIGHT Abstract Only **c37**

Robert M. Salter *In* NASA. Langley Research Center, Second International Symposium on Magnetic Suspension Technology, Part 2 May 1994 p 669-670 (For primary document see N94-35902 11-18)
Avail: CASI HC A01/MF A03

Future long-link, ultra-speed, surface transport systems will require electromagnetically (EM) driven and restrained vehicles operating under reduced-atmosphere in very straight tubes. Such tube-flight trains will be safe, energy conservative, pollution-free, and in a protected environment. Hypersonic (and even hyperballistic) speeds are theoretically achievable. Ultimate system choices will represent tradeoffs between amoritized capital costs (ACC) and operating costs. For example, long coasting links might employ aerodynamic lift coupled with EM restraint and drag make-up. Optimized, combined EM lift, and thrust vectors could reduce energy costs but at increased ACC. (Repulsive levitation can produce lift-over-drag l/d ratios a decade greater than aerodynamic), Alternatively, vehicle-emanated, induced-mirror fields in a conducting (aluminum sheet) road bed could reduce ACC but at substantial energy costs. Ultra-speed tube flight will demand fast-acting, high-precision sensors and computerized magnetic shimming. This same control system can maintain a magnetic 'guide way' invariant in inertial space with inertial detectors imbedded in tube structures to sense and correct for earth tremors. Ultra-speed tube flight can complete with aircraft for transit time and can provide even greater passenger convenience by single-model connections with local subways and feeder lines. Although cargo transport generally will not need to be performed at ultra speeds, such speeds may well be desirable for high throughput to optimize channel costs. Thus, a large and expensive pipeline might be replaced with small EM-driven pallets at high speeds. Author (revised)

N94-35919*# Knolle Magnetrans, San Francisco, CA.
MAGLEV CRUDE OIL PIPELINE c31
Ernst G. Knolle *In* NASA. Langley Research Center, Second International Symposium on Magnetic Suspension Technology, Part 2 May 1994 p 671-684 (For primary document see N94-35902 11-18)
Avail: CASI HC A03/MF A03

This maglev crude oil pipeline consists of two conduits guiding an endless stream of long containers. One conduit carries loaded containers and the other empty returns. The containers are levitated by permanent magnets in repulsion and propelled by stationary linear induction motors. The containers are linked to each other in a manner that allows them, while in continuous motion, to be folded into side by side position at loading and unloading points. This folding causes a speed reduction in proportion to the ratio of container diameter to container length. While in side by side position, containers are opened at their ends to be filled or emptied. Container size and speed are elected to produce a desired carrying capacity. Author

N94-36001 Sandia National Labs., Albuquerque, NM.
INPUT SHAPING FOR THREE-DIMENSIONAL SLEW MANEUVERS OF A PRECISION POINTING FLEXIBLE SPACECRAFT
C. R. Dohrmann and R. D. Robinett 1994 5 p Presented at the 1994 American Control Conference, Baltimore, MD, 29 Jun. - 1 Jul. 1994 Limited Reproducibility: More than 20% of this document may be affected by microfiche quality
(Contract DE-AC04-94AL-85000)
(DE94-008937; SAND-94-0783C; CONF-9406133-1) Avail: CASI HC A01

A method is presented for input torque shaping for three-dimensional slew maneuvers of a precision pointing flexible spacecraft. The method determines the torque profiles for fixed-time, rest-to-rest maneuvers which minimizes a specified performance index. Spacecraft dynamics are formulated in such a manner that the rigid body and flexible motions are decoupled. Furthermore, assembly by making use of finite element analysis results. Input torque profiles are determined by solving an associated optimization problem using dynamic programming. Three example problems are provided to demonstrate the application of the method. DOE

N94-36188 Air Force Inst. of Tech., Wright-Patterson AFB, OH. School of Engineering.
A GENETIC ALGORITHM APPROACH TO AUTOMATING SATELLITE RANGE SCHEDULING M.S. Thesis
Donald A. Parish Mar. 1994 102 p Limited Reproducibility: More than 20% of this document may be affected by microfiche quality
(AD-A278577; AFIT/GOR/ENS/94M-10) Avail: Issuing Activity (Defense Technical Information Center (DTIC))

Satellite range scheduling involves scheduling satellite supports in which a satellite and a specific remote tracking station communicate with each other within a specified time window. As the number of satellite supports continue to increase, more pressure is placed on the current manual system to generate schedules efficiently. Previous research efforts focused on heuristic and mixed-integer programming approaches may not produce the best results. The objective of this research was to determine if a genetic algorithm approach to automating the generation of 24 hour schedules was competitive with other methods. The goal was to schedule as many supports as possible without conflict. The genetic algorithm approach attempted to find the best priority ordering of support requests, and then used a schedule builder program to build schedules based on simple rules. A schedule was produced for seven days of representative satellite range data with slightly better results compared to earlier results using a mixed-integer programming formulation. Based on the reported results, the genetic algorithm approach presented in this research appears to be a competitive approach for generating 24-hour satellite range schedules. DTIC

N94-36251 Naval Postgraduate School, Monterey, CA.
COMPUTER GRAPHICS TOOLS FOR THE VISUALIZATION OF SPACECRAFT DYNAMICS M.S. Thesis
Keith L. Haynes 15 Dec. 1993 154 p Limited Reproducibility: More than 20% of this document may be affected by microfiche quality
(AD-A278615) Avail: Issuing Activity (Defense Technical Information Center (DTIC))

This thesis consists of teaching tools designed to allow spacecraft engineering students to visualize the various phenomena associated with spacecraft dynamics. It does so via the use of state of the art three dimensional computer graphics on Silicon Graphics computers. The thesis discusses the principles in dynamics that were implemented and the key design considerations. A central goal was to develop applications that were user friendly. A library of functions were developed called Dynamics Programming Library or DPL. DPL shields the users from the details of computer graphics, thus allowing them to concentrate on the dynamics of the problem. DPL was used to write three main applications: Euler, Frame, and Gyro. Euler demonstrates the representation of orientation using Euler angles and quaternion rotation. Gyro demonstrates the effects of torques applied to varying rigid body geometries and inertias. Frame allows students to view the motion of an object from different frames of reference. A group of 21 spacecraft engineering students participated in a lab exercise using these programs. Within 20 minutes, the students could run the simulations thus validating their user friendliness. DTIC

N94-35618*# Computer Sciences Corp., Lanham, MD.
SPACECRAFT ATTITUDE DETERMINATION ACCURACY FROM MISSION EXPERIENCE
D. Brasoveanu and J. Hashmall *In* NASA. Goddard Space Flight Center, Flight Mechanics/Estimation Theory Symposium, 1994 May 1994 p 153-166 (For primary document see N94-35605 11-13)
(Contract NAS5-31500)
Avail: CASI HC A03/MF A04

N94-35627*# Integrated Systems, Inc., Santa Clara, CA.
OVERVIEW OF THE MINIATURE SENSOR TECHNOLOGY INTEGRATION (MSTI) SPACECRAFT ATTITUDE CONTROL SYSTEM
Rob McEwen *In* NASA. Goddard Space Flight Center, Flight Mechanics/Estimation Theory Symposium, 1994 May 1994 p 281-295 (For primary document see N94-35605 11-13)
Avail: CASI HC A03/MF A04

N94-35629*# Integrated Systems, Inc., Santa Clara, CA.
OVERVIEW OF THE MSTI 2 ON-ORBIT ALIGNMENT
Christopher A. Rygaard, Fred W. Smith, and M. Michael Briggs *In* NASA. Goddard Space Flight Center, Flight Mechanics/Estimation Theory Symposium, 1994 May 1994 p 303-313 (For primary document see N94-35605 11-13)
Avail: CASI HC A03/MF A04

N94-35630*# Analytical Engineering Corp., Boulder, CO.
MEASURING ATTITUDE WITH A GRADIOMETER
David Sonnabend and Thomas G. Gardner *In* NASA. Goddard Space Flight Center, Flight Mechanics/Estimation Theory Symposium, 1994 May 1994 p 315-329 Prepared for Colorado Univ., Boulder (For primary document see N94-35605 11-13)
Avail: CASI HC A03/MF A04

N94-35632*# Madison Guidance, Navigation and Control, Yorktown Heights, NY.
THE CONTROL OF SATELLITES WITH MICROGRAVITY CONSTRAINTS: THE COMET CONTROL SYSTEM
Walter Grossman and Douglas Freesland *In* NASA. Goddard Space Flight Center, Flight Mechanics/Estimation Theory Symposium, 1994 May 1994 p 341-354 (For primary document see N94-35605 11-13)
Avail: CASI HC A03/MF A04

N94-35638*# Computer Sciences Corp., Lanham, MD.
COMPARISON OF KALMAN FILTER AND OPTIMAL SMOOTHER ESTIMATES OF SPACECRAFT ATTITUDE
J. Sedlak *In* NASA. Goddard Space Flight Center, Flight Mechanics/Estimation Theory Symposium, 1994 May 1994 p 431-445 (For primary document see N94-35605 11-13)
(Contract NAS5-31500)
Avail: CASI HC A03/MF A04

N94-35639*# Florida Univ., Gainesville, FL. Dept. of Aerospace Engineering, Mechanics and Engineering Science.
ATTITUDE STABILITY OF A SPINNING SPACECRAFT DURING APPENDAGE DEPLOYMENT/RETRACTION
Norman Fitz-Coy and Wayne Fullerton *In* NASA. Goddard Space Flight Center, Flight Mechanics/Estimation Theory Symposium, 1994 May 1994 p 447-448 (For primary document see N94-35605 11-13)
Avail: CASI HC A01/MF A04

N94-35642*# National Aeronautics and Space Administration. Goddard Space Flight Center, Greenbelt, MD.
ADVANTAGES OF ESTIMATING RATE CORRECTIONS DURING DYNAMIC PROPAGATION OF SPACECRAFT RATES: APPLICATIONS TO REAL-TIME ATTITUDE DETERMINATION OF SAMPEX
M. S. Challa (Computer Sciences Corp., Lanham, MD.), G. A. Natanson (Computer Sciences Corp., Lanham, MD.), D. F. Baker, and J. K. Deutschmann *In its* Flight Mechanics/Estimation Theory Symposium, 1994 May 1994 p 481-495 (For primary document see N94-35605 11-13)
(Contract NAS5-31500)
Avail: CASI HC A03/MF A04

N94-35643*# State Univ. of New York, Buffalo, NY. Dept. of Mechanical and Aerospace Engineering.
MME-BASED ATTITUDE DYNAMICS IDENTIFICATION AND ESTIMATION FOR SAMPEX
Juan DePena, John L. Crassidis, Michael D. McPartland, Thomas J. Meyer, and D. Joseph Mook *In* NASA. Goddard Space Flight Center, Flight Mechanics/Estimation Theory Symposium, 1994 May 1994 p 497-511 Sponsored in part by NAS-NRC (For primary document see N94-35605 11-13)
(Grant NAG5-2181)
Avail: CASI HC A03/MF A04

N94-35644*# Comissao Nacional de Atividades Espaciais, Sao Jose Dos Campos (Brazil). Attitude Control Group.
A NEW ALGORITHM FOR ATTITUDE-INDEPENDENT MAGNETOMETER CALIBRATION
Roberto Alonso and Malcolm D. Shuster *In* NASA. Goddard Space Flight Center, Flight Mechanics/Estimation Theory Symposium, 1994 May 1994 p 513-527 Sponsored in part by Consejo Nacional de Investigaciones Cientificas y Tecnicas (For primary document see N94-35605 11-13)
Avail: CASI HC A03/MF A04

N94-35645*# Hughes Aircraft Co., Los Angeles, CA.
A SIMPLE SUBOPTIMAL LEAST-SQUARES ALGORITHM FOR ATTITUDE DETERMINATION WITH MULTIPLE SENSORS
Thomas F. Brozenec and Douglas J. Bender *In* NASA. Goddard Space Flight Center, Flight Mechanics/Estimation Theory Symposium, 1994 May 1994 p 529-543 (For primary document see N94-35605 11-13)
Avail: CASI HC A03/MF A04

N94-35646*# Computer Sciences Corp., Lanham, MD.
MOTION MODELS IN ATTITUDE ESTIMATION
D. Chu, Z. Wheeler, and J. Sedlak *In* NASA. Goddard Space Flight Center, Flight Mechanics/Estimation Theory Symposium, 1994 May 1994 p 545-557 (For primary document see N94-35605 11-13)
(Contract NAS5-31500)
Avail: CASI HC A03/MF A04

19 SPACECRAFT INSTRUMENTATION

For related information see also *06 Aircraft Instrumentation* and *35 Instrumentation and Photography.*

N94-35362# Aerospace Corp., El Segundo, CA. Technology Operations.
ELECTRON AND PROTON WIDE-ANGLE SPECTROMETER (EPAS) ON THE CRRES SPACECRAFT
A. Korth (Max-Planck-Inst. fuer Aeronomie, Hanover, Germany.), G. Kremser (Max-Planck-Inst. fuer Aeronomie, Hanover, Germany.), B. Wilken (Max-Planck-Inst. fuer Aeronomie, Hanover, Germany.), W. Guettler (Max-Planck-Inst. fuer Aeronomie, Hanover, Germany.), S. L. Ullaland (Bergen Univ., Norway.), and R. Koga 15 Mar. 1994 10 p
(Contract F04701-88-C-0089; AF-AFOSR-0237-85)
(TR-0091(6940-05)-11; SMC-TR-94-15) Avail: CASI HC A02/MF A01

The electron and proton wide-angle spectrometer (EPAS) in the CRRES scientific payload utilizes arrays of solid-state detectors coupled with a magnetic deflection system in order to detect electrons (21-285 keV) and protons (37-3200 keV). The image size of the particles and the angular resolutions are controlled by the width of the entrance hole, the geometry of the pole pieces, and the position of the particles in the image plane. Additional features of the EPAS are described in some detail. Selected in-flight data are shown as an illustration of the instrument performance in the operational orbit. Author

N94-36189 Harvard Coll. Observatory, Cambridge, MA.
ABSOLUTE, EXTREME ULTRAVIOLET SOLAR SPECTRAL IRRADIANCE MONITOR (AESSIM) Annual Report No. 3, 15 Nov. 1991 - 14 Nov. 1992
W. H. Parkinson and Peter L. Smith Mar. 1994 3 p Limited Reproducibility: More than 20% of this document may be affected by microfiche quality
(Grant AF-AFOSR-0063-90)
(AD-A278709; AFOSR-94-0254TR) Avail: Issuing Activity (Defense Technical Information Center (DTIC))

Several AESSIM (Absolute, Extreme Ultraviolet Solar Spectral Irradiance Monitor) mission concepts which involve spectrometers on rocket underflights and those on the Voyager spacecraft have been considered. We have studied a low-pressure version of the EUV radiance standard of Hollandt, Huber & Kuhne (Appl. Opt. 33, 68, 1994) and concluded that a substantial redesign of it would be required if a suitable one is to be developed for in-orbit calibration of a solar spectral irradiance monitor. We have reviewed the use, suitability, and the availability of thin film filters for in-orbit EUV calibration. In our opinion, the availability of space-qualified filters has not been verified. We have evaluated and chosen a design of a 4-spectrograph, flat-field package that provides 0.1 to 0.2 nm resolution in the range 5-175 nm with a total weight including detectors (without electronics) of 1.6 Kg. DTIC

N94-35617*# National Aeronautics and Space Administration. Goddard Space Flight Center, Greenbelt, MD.
OPERATIONAL SUPPORT FOR UPPER ATMOSPHERE RESEARCH SATELLITE (UARS) ATTITUDE SENSORS
M. Lee, A. Garber, M. Lambertson, P. Raina, S. Underwood, and C. Woodruff *In its* Flight Mechanics/Estimation Theory Symposium, 1994 May 1994 p 139-151 (For primary document see N94-35605 11-13)
(Contract NAS5-31500)
Avail: CASI HC A03/MF A04

N94-35628*# Analytic Sciences Corp., Reston, VA.
A GEOMETRIC MODEL OF A V-SLIT SUN SENSOR CORRECTING FOR SPACECRAFT WOBBLE
W. P. McMartin and S. S. Gambhir *In* NASA. Goddard Space Flight Center, Flight Mechanics/Estimation Theory Symposium, 1994 May 1994 p 297-302 (For primary document see N94-35605 11-13)
Avail: CASI HC A02/MF A04

20 SPACECRAFT PROPULSION AND POWER

Includes main propulsion systems and components, e.g., rocket engines; and spacecraft auxilliary power sources.

For related information see also *07 Aircraft Propulsion and Power, 28 Propellants and Fuels, 44 Energy Production and Conversion,* and *15 Launch Vehicles and Space Vehicles.*

N94-35349# New Mexico Univ., Albuquerque, NM. Inst. for Space Nuclear Power Studies.
EXPERIMENTAL AND THEORETICAL STUDIES OF A HIGH TEMPERATURE CESIUM-BARIUM TACITRON, WITH APPLICATION TO LOW VOLTAGE-HIGH CURRENT INVERSION
C. S. Murray and M. S. El-Genk Feb. 1994 305 p
(Contract DE-FG02-92ER-75708)
(DE94-008182; DOE/ER-75708/T2; UNM-ISNPS-1-1994) Avail: CASI HC A14/MF A03

A low voltage/high current switch referred to as the 'Cs-Ba tacitron' is studied for use as a dc to ac inverter in high temperature and/or ionizing radiation environments. The operational characteristics of the Cs-Ba tacitron as a switch were investigated experimentally in three modes: (1) breakdown mode; (2) I-V mode; and (3) current modulation mode. Operation parameters measured include switching frequencies up to 20 kHz, hold-off voltages up to 200 V, current densities in excess of 15 S/cm(exp 2), switch power density of 1 kW/cm(sup 2), and a switching efficiency in excess of 90% at collector voltages greater than 30 V. Also, if the discharge current is circuit limited to a value below the maximum thermal emission current density, the voltage drop is constant and below 3 V. DOE

N94-35591*# National Aeronautics and Space Administration. Lewis Research Center, Cleveland, OH.
CHALLENGING THE FUTURE - JOURNEY TO EXCELLENCE. AEROPROPULSION STRATEGIC PLAN FOR THE 1990'S
1990 27 p
(NASA-TM-109250; NAS 1.15:109250) Avail: CASI HC A03/MF A01

Over the past several months, the Lewis Aeropropulsion Management Council (AMC) has conducted a critical assessment of its strategic plan. This assessment clearly indicated a need for change, both in the aeropropulsion program emphasis and in the approach to carrying out that program. Customers sent a strong message that the program must improve the timeliness of research and technology products and services and must work more closely with them to develop and transfer new technology. The strategic plan defines AMC's vision for the future and underlying organizational values. It contains a set of broad strategies and actions that point the way toward achieving the goals of customer satisfaction, organizational effectiveness, and programmatic excellence. Those strategies are expected to form the basis for the development of specific tactical plans by Lewis aeropropulsion thrust teams, divisions, and branches. To guide tactical planning of the aeropropulsion program, this strategic plan outlines the agency's strategic directions and long-range aeronautics goals, the aeropropulsion goals and key objectives for achieving them, projections of Lewis aeropropulsion budgets, planned allocations of resources, and the processes that will be used to measure success in carrying out the strategic plan. CASI

N94-35825 Alabama Univ., Huntsville, AL.
ENERGY PARTITIONING IN HIGH SPEED IMPACT OF ANALOG SOLID ROCKET MOTORS Final Technical Report, May - Dec. 1993
William P. Schonberg Mar. 1994 56 p Limited Reproducibility: More than 20% of this document may be affected by microfiche quality
(Contract DASG60-89-C-0129)
(AD-A278771) Avail: Issuing Activity (Defense Technical Information Center (DTIC))

Modeling the response of solid rocket motors to bullet and fragment impacts is a high priority among the military services from standpoints of both safety and mission effectiveness. Considerable effort is being devoted to characterizing the bullet and fragment vulnerability of solid rocket motors, and to developing solid rocket motor case technologies for preventing or lessening the violent responses of rocket motors to these impact loadings. Because full-scale tests are costly, fast-running analytical methods are required to characterize the response of solid rocket motors to ballistic impact hazards. In this study, a first-principals-based mathematical model is developed to determine the partitioning of the kinetic energy of an impacting projectile among various solid rocket motor failure modes. Failure modes considered in the analyses include case perforation, case delamination, and fragmentation of the propellant simulant material. Energies involved in material fragmentation are calculated using a fragmentation scheme based on a procedure developed in a previous impact study utilizing propellant simulant material. The model is found to be capable of predicting a variety of response characteristics for analog solid rocket motors under high speed projectile impact. Suggestions are made for improving the model and extending its applicability to a wider class of impact scenarios. DTIC

N94-36089 Ohio State Univ., Columbus. Dept. of Mechanical Engineering.
RECOVERY OF FROZEN FLOW LOSSES IN ARCJETS Final Report, 1991 - 1993
V. V. Subramaniam, V. Babu, and S. Aithal 25 Mar. 1994 82 p Limited Reproducibility: More than 20% of this document may be affected by microfiche quality
(Grant AF-AFOSR-0318-91)
(AD-A278739; AFOSR-94-0259TR) Avail: Issuing Activity (Defense Technical Information Center (DTIC))

This research explores ways of reducing frozen flow losses via state-resolved numerical simulations (quasi 1-D, 2D, and 2D with swirl). Frozen flow losses in molecular vibration, rotation, and electronic excitation are believed to account for significant losses in thrust and efficiency of arcjet thrusters. This report summarizes the accomplishments in the first two years of a four year research program designed to quantify frozen flow losses, and to generate design tools useful for the designer to enhance arcjet performance. DTIC

N94-36254 Aerospace Corp., El Segundo, CA.
PROPELLANT STRESS RELIEF GROOVE FOR THE TITAN 4 SRMU Technical Report, Jan. 1991 - Jan. 1993
I.-Shih Chang Nov. 1993 26 p Limited Reproducibility: More than 20% of this document may be affected by microfiche quality
(Contract F04701-88-C-0089)
(AD-A278628; TR-93(3530)-2; SMC-TR-94-24) Avail: Issuing Activity (Defense Technical Information Center (DTIC))

A method has been developed to design a propellant stress relief groove (SRG) for solid rocket motors. The method considers a time-dependent pressure distribution in both burn-back and 'burn-forward' analyses and allows a desired bondline stress condition to be incorporated into the SRG design. Application of the method to obtain an improved propellant SRG for the Titan IV Solid Rocket Motor Upgrade (SRMU) is illustrated in this report. The improved propellant SRG obtained from this method for the Titan IV SRMU provides significant enhancement in the propellant structural margin of safety throughout motor firing. DTIC

N94-36255 Aerospace Corp., El Segundo, CA.
AN EFFICIENT, INTELLIGENT SOLUTION FOR VISCOUS FLOWS INSIDE SOLID ROCKET MOTORS Technical Report, Jan. 1990 - Jan. 1991
I.-Shih Chang Nov. 1993 28 p Limited Reproducibility: More than 20% of this document may be affected by microfiche quality
(Contract F04701-88-C-0089)
(AD-A278629; TR-93(3530)-3; SMC-TR-94-25) Avail: Issuing Activity (Defense Technical Information Center (DTIC))

An efficient, intelligent method has been developed for the solution of axisymmetric, compressible viscous flows inside solid rocket motors. The method applies an adaptive, unstructured, finite-element mesh generation technique and a cell-centered, second-order, flux correction transport scheme for the solution of Navier-Stokes equations. With known, initial motor interior configuration, the method developed in this study allows the computational boundaries to be determined intelligently, the finite-element meshes and remeshes to be generated efficiently, and the corresponding compressible viscous flow fields to be produced expeditiously. Very good agreement between analysis results and test data is obtained for flow inside the Jet Propulsion Laboratory nozzle. Application of the method to analyze flows inside the Titan IV solid rocket motor upgrade and the Star-48 motor with very complicated chamber and nozzle geometry is illustrated. DTIC

N94-36291 SI Diamond Technology, Inc., Houston, TX.
AN EXPERIMENTAL INVESTIGATION OF ACTIVE CONTROL OF THRUST VECTORING NOZZLE FLOW FIELDS Final Report, 15 Jul. 1992 - 15 Jul. 1993
P. J. Strykowski and A. Krothapalli 27 Jan. 1994 32 p Limited Reproducibility: More than 20% of this document may be affected by microfiche quality
(Contract F49620-92-J-0426)
(AD-A278702; AFOSR-94-0162TR) Avail: Issuing Activity (Defense Technical Information Center (DTIC))

Fluidic thrust vector control is examined in a supersonic rectangular jet having a 4:1 aspect ratio. Experiments conducted at a Mach number of 2 reveal that the thrust vector angle of the jet can be continuously varied by up to at least 16 deg by applying a counterflowing stream to one of the primary jet shear layers. A technique using counterflow eliminates the bistable response known to plague fluidic elements and is shown to be effective in both hot and cold supersonic jets. Results are presented for jet stagnation temperatures between 300 K and 670 K. Measurements indicate that the thrust vector control is both efficient as well as a linear function of the static pressure developed in the counterflowing stream. The typical power required to vector the jet at 16 degrees was estimated to be less than 1 percent of the power developed in the primary jet. Thrust vector control employing counterflow has several advantages over current technologies, the most important of which is the elimination of movable control surfaces which add considerable weight to the aircraft. DTIC

N94-36047*# National Aeronautics and Space Administration. Marshall Space Flight Center, Huntsville, AL.
SPACE AND TRANSATMOSPHERIC PROPULSION TECHNOLOGY
Charles Merkle (Pennsylvania State Univ., University Park, PA.), Maynard L. Stangeland (Rockwell International Corp., Canoga Park, CA.), James R. Brown (Pratt and Whitney Aircraft, East Hartford, CT.), John P. McCarty, Louis A. Povinelli, G. Burton Northam, and Edward E. Zukoski *In* Loyola Coll., JTEC/WTEC Report and Program Summary Mar. 1994 p 138-142 (For primary document see N94-36042 11-99)
Avail: CASI HC A01/MF A03

23 CHEMISTRY AND MATERIALS (GENERAL)

N94-35340# Joint Publications Research Service, Arlington, VA.
JPRS REPORT: SCIENCE AND TECHNOLOGY. CENTRAL EURASIA
6 Jan. 1994 30 p
(JPRS-UST-94-001) Avail: CASI HC A03/MF A01

Translated articles cover the following topics: distribution of titanium in the structure of various components of superconducting composites based on Nb3Sn; effect of gallium alloying on the structure and properties of superconducting composite with Nb2Sn; effect of low-temperature annealing on the structure and superconducting properties of YBa2Cu3O(7-delta) compounds with different nonstoichiometry with respect to oxygen; construction of a switching network in database machines; use of Walsh-Pally transforms to numerically solve Helmholtz equation; organization of a parallel computer of trigonometric equations in the area of T-transforms; navigation method using a field of reference points; implementation of theoretical-numerical transforms in codes generated by redundant computing systems; analysis of the absolute stability of multidimensional nonlinear pulsed automatic systems based on algebraic modification of criteria obtained with a bilinear transform; solid-phase decomposition of GaAs under the impact of laser radiation of threshold density; layer-by-layer study of ion-implanted silicon by ellipsometry and selective moistening methods; electron minibands in (GaAs)(sub N)(AlAs)(sub M) superlattice with even or odd M; the electroluminescence of epitaxial GaP p-n structures, grown on Si-substrates; instrument for measuring atmospheric refraction from space; decrease in atmospheric transparency in polar regions (effect of eruptions of Mt. Pinatubo and Mt. Hudson); evaluation of the contribution of N-nitrose compounds to atmospheric NO pollution; and radiation polarization as an indicator of distance to a pulse source. CASI

N94-35361# Army Research Lab., Watertown, MA.
DIFFUSION AND SORPTION OF 1,4-DIOXANE INTO POLYCHLOROPRENE Final Report
Geralda Severe Feb. 1994 25 p
(ARL-TR-338) Avail: CASI HC A03/MF A01

Influence of the presence of plasticizer on the transport properties for the polychloroprene/ 1,4-dioxane (Neoprene/1,4-dioxane) system has been investigated. The sorption rate curves for the extracted and the unextracted (as received) Neoprene demonstrated some characteristics of Fickian behavior. The sorption isotherms obtained from the weight uptake did not coincide for repeated runs of the extracted sample; they were below the isotherm of the unextracted sample. However, both types of samples (extracted and unextracted Neoprene) showed diffusion coefficients that increase with concentration. The difference between the diffusion coefficients for the extracted and unextracted Neoprene was not significant; the extraction primarily affected the solubility. Author

N94-35776 Army Cold Regions Research and Engineering Lab., Hanover, NH.
VAPOR-FORTIFIED QA/QC SAMPLES FOR THE ANALYSIS OF VOLATILE ORGANIC COMPOUNDS
Alan D. Hewitt Feb. 1994 11 p Limited Reproducibility: More than 20% of this document may be affected by microfiche quality
(AD-A278712; CRREL-SR-94-2; SFIM-AEC-TS-CR-94030) Avail: Issuing Activity (Defense Technical Information Center (DTIC))

Vapor fortification is a precise treatment method for preparing soil subsamples for the analysis of volatile organic compounds (VOC's). This method of spiking is unique in that the fortification level is soil-type specific and the treatment mechanism is analogous to how soil in the vadose zone becomes contaminated by vapors from liquid VOC point sources. Soil subsamples treated by vapor fortification and sealed in glass ampoules until analysis have shown both good precision within batch and among batches, and analyte concentration stability for a month or longer. Vapor-fortified quality assurance/quality control (QA/QC) soils are more environmentally representative than soils fortified by liquid spiking procedures for the analysis of VOC's in vadose zone samples. DTIC

N94-36398*# National Aeronautics and Space Administration. Langley Research Center, Hampton, VA.
NATIONAL EDUCATORS' WORKSHOP: UPDATE 1993. STANDARD EXPERIMENTS IN ENGINEERING MATERIALS SCIENCE AND TECHNOLOGY
James E. Gardner, comp. and James A. Jacobs, comp. Apr. 1994 509 p Workshop held in Hampton, VA, 3-5 Nov. 1993; sponsored by NASA, Norfolk State Univ., DOE, and NIST
(RTOP 505-63-50-01)
(NASA-CP-3259; L-17396; NAS 1.55:3259) Avail: CASI HC A22/MF A04

This document contains a collection of experiments presented and demonstrated at the National Educators' Workshop: Update 93 held at the NASA Langley Research Center in Hampton, Virginia, on November 3-5, 1993. The experiments related to the nature and properties of engineering materials and provided information to assist in teaching about materials in the education community. For individual titles, see N94-36399 through N94-36415.

N94-36399*# Lockheed Engineering and Sciences Co., Hampton, VA.
ASTM TEST METHODS FOR COMPOSITE CHARACTERIZATION AND EVALUATION c24
John E. Masters *In* NASA. Langley Research Center, National Educators' Workshop: Update 1993. Standard Experiments in Engineering Materials Science and Technology Apr. 1994 p 1-41 (For primary document see N94-36398 11-23)
Avail: CASI HC A03/MF A04

A discussion of the American Society for Testing and Materials is given. Under the topic of composite materials characterization and evaluation, general industry practice and test methods for textile composites are presented. CASI

N94-36400*# Pennsylvania State Univ., University Park, PA.
CONTINUOUS UNIDIRECTIONAL FIBER REINFORCED COMPOSITES: FABRICATION AND TESTING c24

M. D. Weber, F. X. Spiegel, and Harvey A. West *In* NASA. Langley Research Center, National Educators' Workshop: Update 1993. Standard Experiments in Engineering Materials Science and Technology Apr. 1994 p 43-50 (For primary document see N94-36398 11-23)
Avail: CASI HC A02/MF A04

The study of the anisotropic mechanical properties of an inexpensively fabricated composite with continuous unidirectional fibers and a clear matrix was investigated. A method has been developed to fabricate these composites with aluminum fibers and a polymer matrix. These composites clearly demonstrate the properties of unidirectional composites and cost less than five dollars each to fabricate. Author

N94-36401*# Loyola Coll., Baltimore, MD.
DESIGN AND CONSTRUCTION OF A TENSILE TESTER FOR THE TESTING OF SIMPLE COMPOSITES c24
Mark A. Borst and F. Xavier Spiegel *In* NASA. Langley Research Center, National Educators' Workshop: Update 1993. Standard Experiments in Engineering Materials Science and Technology Apr. 1994 p 51-99 (For primary document see N94-36398 11-23)
Avail: CASI HC A03/MF A04

The following is a design for a tensile tester which will be used to test the tensile strength and anisotropic properties of simple composites. These simple composites are suspected to be anisotropic primarily in a single plane. When the composites undergo a tensile force, they will undergo deformation, causing movement either to the left or right. The composites are suspect due to their method of construction. Each sample has a single layer of unidirectional continuous fibers embedded in a rubbery resin. It has been well established that a serious limitation of unidirectional fiber composites is the very large in-plane anisotropy. The design presented here incorporates a single degree of freedom such that distortion (to the left or right) due to anisotropic tendencies may be measured. The device will spend the vast majority of its time in an undergraduate materials lab. As a result, ease of use and durability are valued more highly than research grade accuracy. Additional concerns focus on the fact that this machine will be built as a student project. Issues which are dealt with during this design include: specimen configuration or shape; a method of applying consistent, linear tension force; a method of gripping specimen without affecting its overall properties; a method of collecting data; repeatability of data; ease of use; ease of construction; and cost. After the device has been constructed, it will be used to test the simple composites which were fabricated in house. A comparison will be made between composites manufactured using aluminum screening as the strengthening fibers and those manufactured using fiberglass screening. Derived from text

N94-36402*# University of Eastern Illinois, Charleston, IL. School of Technology.
APPLICATION OF MATERIALS DATABASE (MAT.DB.) TO MATERIALS EDUCATION c82
Ping Liu and Tommy L. Waskom *In* NASA. Langley Research Center, National Educators' Workshop: Update 1993. Standard Experiments in Engineering Materials Science and Technology Apr. 1994 p 101-109 (For primary document see N94-36398 11-23)
Avail: CASI HC A02/MF A04

Finding the right material for the job is an important aspect of engineering. Sometimes the choice is as fundamental as selecting between steel and aluminum. Other times, the choice may be between different compositions in an alloy. Discovering and compiling materials data is a demanding task, but it leads to accurate models for analysis and successful materials application. Mat. DB. is a database management system designed for maintaining information on the properties and processing of engineered materials, including metals, plastics, composites, and ceramics. It was developed by the Center for Materials Data of American Society for Metals (ASM) International. The ASM Center for Materials Data collects and reviews material property data for publication in books, reports, and electronic database. Mat. DB was developed to aid the data management and material applications. Derived from text

N94-36403*# University of Eastern Illinois, Charleston, IL. School of Technology.
LAMINATED THERMOPLASTIC COMPOSITE MATERIAL FROM RECYCLED HIGH DENSITY POLYETHYLENE c24
Ping Liu and Tommy L. Waskom *In* NASA. Langley Research Center, National Educators' Workshop: Update 1993. Standard Experiments in Engineering Materials Science and Technology Apr. 1994 p 111-118 (For primary document see N94-36398 11-23)
(Grant NSF DUE-93-50629)
Avail: CASI HC A02/MF A04

The design of a materials-science, educational experiment is presented. The student should understand the fundamentals of polymer processing and mechanical property testing of materials. The ability to use American Society for Testing and Materials (ASTM) standards is also necessary for designing material test specimens and testing procedures. The objectives of the experiment are (1) to understand the concept of laminated composite materials, processing, testing, and quality assurance of thermoplastic composites and (2) to observe an application example of recycled plastics. CASI

N94-36404*# Air Force Inst. of Tech., Wright-Patterson AFB, OH. Dept. of Electrical and Computer Engineering.
SIMULATION OF MATERIALS PROCESSING: FANTASY OR REALITY?
Thomas J. Jenkins and Victor M. Bright *In* NASA. Langley Research Center, National Educators' Workshop: Update 1993. Standard Experiments in Engineering Materials Science and Technology Apr. 1994 p 153-167 (For primary document see N94-36398 11-23)
Avail: CASI HC A03/MF A04

This experiment introduces students to the application of computer-aided design (CAD) and analysis of materials processing in the context of integrated circuit (IC) fabrication. The fabrication of modern IC's is a complex process which consists of several sequential steps. These steps involve the precise control of processing variables such as temperature, humidity, and ambient gas composition. In essence, the particular process employed during the fabrication becomes a 'recipe'. Due to economic and other considerations, CAD is becoming an indispensable part of the development of new recipes for IC fabrication. In particular, this experiment permits the students to explore the CAD of the thermal oxidation of silicon. Derived from text

N94-36405*# Wisconsin Univ., Madison, WI. Center for Quality and Productivity Improvement.
USING EXPERIMENTAL DESIGN MODULES FOR PROCESS CHARACTERIZATION IN MANUFACTURING/MATERIALS PROCESSES LABORATORIES
Bruce Ankenman, Donald Ermer, and James A. Clum *In* NASA. Langley Research Center, National Educators' Workshop: Update 1993. Standard Experiments in Engineering Materials Science and Technology Apr. 1994 p 169-183 (For primary document see N94-36398 11-23)
Avail: CASI HC A03/MF A04

Modules dealing with statistical experimental design (SED), process modeling and improvement, and response surface methods have been developed and tested in two laboratory courses. One course was a manufacturing processes course in Mechanical Engineering and the other course was a materials processing course in Materials Science and Engineering. Each module is used as an 'experiment' in the course with the intent that subsequent course experiments will use SED methods for analysis and interpretation of data. Evaluation of the modules' effectiveness has been done by both survey questionnaires and inclusion of the module methodology in course examination questions. Results of the evaluation have been very positive. Those evaluation results and details of the modules' content and implementation are presented. The modules represent an important component for updating laboratory instruction and to provide training in quality for improved engineering practice. Author (revised)

N94-36406*# Wisconsin-Stout Univ., Menomonie, WI. Technology Dept.
PROCESS CAPABILITY DETERMINATION OF NEW AND EXISTING EQUIPMENT
H. T. McClelland and Penwen Su *In* NASA. Langley Research Center, National Educators' Workshop: Update 1993. Standard Experiments in Engineering Materials Science and Technology Apr. 1994 p 185-193 (For primary document see N94-36398 11-23)
Avail: CASI HC A02/MF A04

The objective of this paper is to illustrate a method of determining the process capability of new or existing equipment. The method may also be modified to apply to testing laboratories. Long term changes in the system may be determined by periodically making new test parts or submitting samples from the original set to the testing laboratory. The technique described has been developed through a series of projects in special topics manufacturing courses and graduate student projects. It will be implemented as a standard experiment in an advanced manufacturing course in a new Manufacturing Engineering program at the University of Wisconsin-Stout campus. Before starting a project of this nature, it is important to decide on the exact question to be answered. In this case, it is desired to know what variation can be reasonably expected in the next part, feature, or test result produced. Generally, this question is answered by providing the process capability or the average value of a measured characteristic of the part or process plus or minus three standard deviations. There are two general cases to be considered: the part or test is made in large quantities with little change, or the process is flexible and makes a large variety of parts. Both cases can be accommodated; however, the emphasis in this report is on short run situations. Derived from text

N94-36407*# Virginia Polytechnic Inst. and State Univ., Blacksburg, VA. Dept. of Mechanical Engineering.

MEASUREMENT OF A SURFACE HEAT FLUX AND TEMPERATURE **c70**

R. M. Davis, G. J. Antoine, T. E. Diller, and A. L. Wicks *In* NASA. Langley Research Center, National Educators' Workshop: Update 1993. Standard Experiments in Engineering Materials Science and Technology Apr. 1994 p 203-218 (For primary document see N94-36398 11-23)
Avail: CASI HC A03/MF A04

The Heat Flux Microsensor is a new sensor which was recently patented by Virginia Tech and is just starting to be marketed by Vatell Corp. The sensor is made using the thin-film microfabrication techniques directly on the material that is to be measured. It consists of several thin-film layers forming a differential thermopile across a thermal resistance layer. The measured heat flux q is proportional to the temperature difference across the resistance layer q= k(sub g)/delta(sub g) x (t(sub 1) - T(sub 2)), where k(sub g) is the thermal conductivity and delta (sub g) is the thickness of the thermal resistance layer. Because the gages are sputter coated directly onto the surface, their total thickness is less than 2 micrometers, which is two orders of magnitude thinner than previous gages. The resulting temperature difference across the thermal resistance layer (delta is less than 1 micrometer) is very small even at high heat fluxes. To generate a measurable signal many thermocouple pairs are put in series to form a differential thermopile. The combination of series thermocouple junctions and thin-film design creates a gage with very attractive characteristics. It is not only physically non-intrusive to the flow, but also causes minimal disruption of the surface temperature. Because it is so thin, the response time is less than 20 microsec. Consequently, the frequency response is flat from 0 to over 50 kHz. Moreover, the signal of the Heat Flux Microsensor is directly proportional to the heat flux. Therefore, it can easily be used in both steady and transient flows, and it measures both the steady and unsteady components of the surface heat flux. A version of the Heat Flux Microsensor has been developed to meet the harsh demands of combustion environments. These gages use platinum and platinum-10 percent rhodium as the thermoelectric materials. The thermal resistance layer is silicon monoxide and a protective coating of Al2O3 is deposited on top of the sensor. The superimposed thin-film pattern of all six layers is presented. The large pads are for connection with pins used to bring the signal out the back of the ceramic. In addition to the heat flux measurement, the surface temperature is measured with a platinum resistance layer (RTS). The resistance of this layer increases with increasing temperature. Therefore, these gages simultaneously measure the surface temperature and heat flux. The demonstrated applications include rocket nozzles, SCRAM jet engines, gas turbine engines, boiling heat transfer, flame experiments, basic fluid heat transfer, hypersonic flight, and shock tube testing. The laboratory involves using one of these sensors in a small combustion flame. The sensor is made on a 2.5 cm diameter piece of aluminum nitride ceramic. Derived from text

N94-36408*# Siena Coll., Londonville, NY. Dept. of Chemistry.

MICROSCALE SYNTHESIS AND CHARACTERIZATION OF POLYSTYRENE: NSF-POLYED SCHOLARS PROJECT **c27**

Karen S. Quaal and Chang-Ning Wu *In* NASA. Langley Research Center, National Educators' Workshop: Update 1993. Standard Experiments in Engineering Materials Science and Technology Apr. 1994 p 219-237 (For primary document see N94-36398 11-23)
Avail: CASI HC A03/MF A04

Polystyrene is a familiar polymer with many commercial uses. Its applications range from the clear, high index of refraction, brittle plastic used to form audio cassette and CD cases to the foamed material used in insulated drink cups and packaging material. Polystyrene constitutes 11 percent of the plastics used in packaging with only High Density Polyethylene (HDPE) and Low Density Polyethylene (LDPE) contributing a larger share: so much polystyrene is used today, it is one of six common plastics that manufacturers have assigned an identification code. The code helps recycling efforts. Polystyrene's code is (PS code 6). During the summer and fall of 1992 several new polymeric experiments were developed by the NSF POLYED Scholars for introduction into the chemistry core curriculum. In this presentation, one such project will be discussed. This laboratory project is recommended for a first or second year laboratory course allowing the introduction of polymeric science to undergraduates at the earliest opportunity. The reliability of the experiments which make up this project and the recognition factor of polystyrene, a material we come in contact with everyday, makes the synthesis and characterization of polystyrene a good choice for the introduction of polymerization to undergraduates. This laboratory project appeals to the varied interests of students enrolled in the typical first year chemistry course and becomes an ideal way to introduce polymers to a wide variety of science and engineering students. Derived from text

N94-36409*# Oak Ridge National Lab., TN. Carbon Materials Technology Group.

DEVELOPMENTS IN CARBON MATERIALS **c24**

Timothy D. Burchell *In* NASA. Langley Research Center, National Educators' Workshop: Update 1993. Standard Experiments in Engineering Materials and Science Technology Apr. 1994 p 291-314 (For primary document see N94-36398 11-23)
Avail: CASI HC A03/MF A04

The following carbon-based materials are reviewed and their applications discussed: fullerenes; graphite (synthetic and manufactured); activated carbon fibers; and carbon-carbon composites. Carbon R&D activities at ORNL are emphasized. Derived from text

N94-36410*# Bucknell Univ., Lewisburg, PA. Dept. of Chemical Engineering.

MECHANICAL PROPERTIES OF CROSSLINKED POLYMER COATINGS **c27**

Jeffrey Csernica *In* NASA. Langley Research Center, National Educators' Workshop: Update 1993. Standard Experiments in Engineering Materials Science and Technology Apr. 1994 p 323-338 (For primary document see N94-36398 11-23)
Avail: CASI HC A03/MF A04

The objectives of this experiment are to: fabricate and test thin films to explore relations between a polymer's structure and its mechanical properties; expose students to testing methods for hardness and impact energy that are simple to perform and which have results that are easy to comprehend; show importance of polymer properties in materials that students frequently encounter; illustrate a system which displays a tradeoff between strength and impact resistance, the combination of which would need to be optimized for a particular application; and to expose students to coatings technology and testing. Derived from text

N94-36411*# College of Western New England, Springfield, MA. Dept. of Electrical Engineering.

EXPERIMENTS IN DIAMOND FILM FABRICATION IN TABLE-TOP PLASMA APPARATUS **c27**

James V. Masi *In* NASA. Langley Research Center, National Educators' Workshop: Update 1993. Standard Experiments in Engineering Materials Science and Technology Apr. 1994 p 339-352 (For primary document see N94-36398 11-23)
Avail: CASI HC A03/MF A04

The objectives of this experiment are to illustrate the process of plasma assisted chemical vapor deposition and to show devices which can be made simply in the laboratory. These devices illustrate clearly the concepts of bandgap, junctions, and photoelectronic processes. Films and devices are measured electrically, optically, and thermally. Derived from text

N94-36412*# State Univ. of Southeast Missouri, Cape Girardeau, MO. Physics Dept.
DIELECTRIC MEASUREMENTS OF SELECTED CERAMICS AT MICROWAVE FREQUENCIES c27
J. N. Dahiya and C. K. Templeton *In* NASA. Langley Research Center, National Educators' Workshop: Update 1993. Standard Experiments in Engineering Materials Science and Technology Apr. 1994 p 391-400 (For primary document see N94-36398 11-23)
Avail: CASI HC A02/MF A04

Dielectric measurements of strontium titanate and lead titanate zirconate ceramics are conducted at microwave frequencies using a cylindrical resonant cavity in the TE(sub 011) mode. The perturbations of the electric field are recorded in terms of the frequency shift and Q-changes of the cavity signal. Slater's perturbation equations are used to calculate e' and e' of the dielectric constant as a function of temperature and frequency.
Derived from text

N94-36413*# Aluminum Co. of America, Alcoa Center, PA. Alloy Technology Div.
NEW DEVELOPMENTS IN ALUMINUM FOR AIRCRAFT AND AUTOMOBILES c26
Jocelyn I. Petit *In* NASA. Langley Research Center, National Educators' Workshop: Update 1993. Standard Experiments in Engineering Materials Science and Technology Apr. 1994 p 419-450 (For primary document see N94-36398 11-23)
Avail: CASI HC A03/MF A04

A common bond for the aircraft and automobile industry is the need for cost-efficient, lightweight structures such as provided by aluminum based materials. The topics are presented in viewgraph form and cover the following: new developments in aluminum for aircraft and automobiles; forces shaping future automotive materials needs; aluminum strength/weakness versus competitive materials; evolution of aluminum aerospace alloys; forces shaping future aircraft materials needs; fiber/metal structural laminates; and property requirements for jetliner and military transport applications. CASI

N94-36414*# Purdue Univ., Elkhart, IN. Statewide Technology.
GRAPHING TECHNIQUES FOR MATERIALS LABORATORY USING EXCEL c61
Nikhil K. Kundu *In* NASA. Langley Research Center, National Educators' Workshop: Update 1993. Standard Experiments in Engineering Materials Science and Technology Apr. 1994 p 457-467 (For primary document see N94-36398 11-23)
Avail: CASI HC A02/MF A04

Engineering technology curricula stress hands on training and laboratory practices in most of the technical courses. Laboratory reports should include analytical as well as graphical evaluation of experimental data. Experience shows that many students neither have the mathematical background nor the expertise for graphing. This paper briefly describes the procedure and data obtained from a number of experiments such as spring rate, stress concentration, endurance limit, and column buckling for a variety of materials. Then with a brief introduction to Microsoft Excel the author explains the techniques used for linear regression and logarithmic graphing.
Derived from text

N94-36415*# Loyola Coll., Baltimore, MD. Dept. of Electrical Engineering and Engineering Science.
AN AUTOMATED DIGITAL DATA COLLECTION AND ANALYSIS SYSTEM FOR THE CHARPY IMPACT TESTER c39
Glenn S. Kohne and F. Xavier Spiegel *In* NASA. Langley Research Center, National Educators' Workshop: Update 1993. Standard Experiments in Engineering Materials Science and Technology Apr. 1994 p 469-480 (For primary document see N94-36398 11-23)
Avail: CASI HC A03/MF A04

The standard Charpy Impact Tester has been modified by the addition of a system of hardware and software to improve the accuracy and consistency of measurements made during specimen fracturing experiments. An optical disc, light source, and detector generate signals that indicate the pendulum position as a function of time. These signals are used by a computer to calculate the velocity and kinetic energy of the pendulum as a function of its position. Author (revised)

24 COMPOSITE MATERIALS

Includes physical, chemical, and mechanical properties of laminates and other composite materials.

For ceramic materials see *27 Nonmetallic Materials.*

N94-35372*# National Aeronautics and Space Administration. Langley Research Center, Hampton, VA.
TOUGH HIGH PERFORMANCE COMPOSITE MATRIX Patent
Ruth H. Pater, inventor (to NASA) and Norman J. Johnston, inventor (to NASA) 19 Jul. 1994 11 p Filed 27 Oct. 1992 Division of US-Patent-Appl-SN-429514, filed 31 Oct. 1989
(NASA-Case-LAR-14239-2; US-Patent-5,331,063; US-Patent-Appl-SN-968082; US-Patent-Appl-SN-429514; US-Patent-Class-525-421; US-Patent-Class-525-426; US-Patent-Class-525-432; US-Patent-Class-525-436; US-Patent-Class-525-903; Int-Patent-Class-C08L-79/08) Avail: US Patent and Trademark Office

This invention is a semi-interpentrating polymer network which includes a high performance thermosetting polyimide having a nadic end group acting as a crosslinking site and a high performance linear thermoplastic polyimide. Provided is an improved high temperature matrix resin which is capable of performing in the 200 to 300 C range. This resin has significantly improved toughness and microcracking resistance, excellent processability, mechanical performance, and moisture and solvent resistances.
Official Gazette of the U.S. Patent and Trademark Office

N94-35654 Naval Air Warfare Center, Warminster, PA. Air Vehicle and Crew Systems Technology Dept.
PROCESSING AND PROPERTIES OF HIGH TEMPERATURE METAL/FIBER-REINFORCED-THERMOPLASTIC LAMINATES Final Report
Jeffrey Cook 19 Oct. 1993 219 p Limited Reproducibility: More than 20% of this document may be affected by microfiche quality
(AD-A278791; NAWCADWAR-93079-60) Avail: Issuing Activity (Defense Technical Information Center (DTIC))

Equations for predicting the theoretical stresses and mechanical properties of fiber/metal laminates were derived. These were applied to a model high temperature laminate system based on 8009 aluminum and glass fiber reinforced U-25 thermoplastic polyimide. The effects of aluminum surface treatment on bond strength were investigated; chemical surface treatments gave superior bond strength compared to mechanical treatments. Adequate bond strength was obtained using simplified and environmentally safe surface preparation techniques. The tensile yield and ultimate strength, elastic modulus, fracture behavior, dynamic mechanical behavior, chemical resistance, and fatigue resistance of the laminate were investigated. Most properties were found to correlate well with the theoretical predictions. The laminate showed excellent strength retention at temperatures above 200 C. Fatigue resistance as-processed was found to be comparable to monolithic 8009. Post-stretching the laminate was shown to increase both fatigue life and yield strength substantially. DTIC

N94-35696 Lawrence Livermore National Lab., CA.
STRUCTURES AND PROPERTIES OF MATERIALS RECOVERED FROM HIGH SHOCK PRESSURES
W. J. Nellis Mar. 1994 8 p Presented at the National Institute for Research in Inorganic Materials Symposium on Advanced Materials, Tsukuba, Japan, 13-17 Mar. 1994 Limited Reproducibility: More than 20% of this document may be affected by microfiche quality
(Contract W-7405-eng-48)
(DE94-010057; UCRL-JC-115960; CONF-940380-2) Avail: CASI HC A02

Shock compression produces high dynamic pressures, densities, temperatures, and their quench rates. Because of these extreme conditions, shock compression produces materials with novel crystal structures, microstructures, and physical properties. Using a 6.5-m-long two-stage gun, we perform experiments with specimens up to 10 mm in diameter and 0.001-1 mm thick. For example, oriented disks of melt-textured superconducting YBa2Cu3O7 were shocked to 7 GPa without macroscopic fracture. Lattice defects are deposited in the crystal, which improve magnetic hysteresis at approximately 1 kOe. A computer code has been developed to simulate shock compaction of 100 powder particles. Computations will be compared with experiments with 15-20 micron Cu powders. The method is applicable to other powders and dynamic conditions. DOE

N94-35714 Tennessee Univ., Knoxville, TN. Dept. of Engineering Science and Mechanics.
ON THE BUCKLING/KINKING COMPRESSIVE FAILURE OF FIBROUS COMPOSITES Technical Report, 1 Oct. 1992 - 31 Jan. 1994
I. Chung and Y. J. Weitsman 29 Mar. 1994 33 p Limited Reproducibility: More than 20% of this document may be affected by microfiche quality
(Contract N00014-90-J-1556)
(AD-A278865; ESM94-2.0-CM) Avail: CASI HC A03

In this article it is demonstrated that the compressive response of unidirectionally reinforced composites may initiate in a micro-buckling mode and subsequently switch to a micro-kinked configuration. The foregoing possibility derives from a mechanics model which considers initial fibers misalignments, non-linear shear response of the matrix, shear deformable fibers and stochastic fiber spacings. The latter non-uniformity in fiber spacings plays a major role in the generation of fiber kinks. Various features of the compressive deformation and failure process are exhibited by computational examples. Author (DTIC)

N94-35715 Tennessee Univ., Knoxville, TN. Dept. of Engineering Science and Mechanics.
A MECHANICS MODE FOR THE COMPRESSIVE RESPONSE OF FIBER REINFORCED COMPOSITES Technical Report, 1 Jan. 1993 - 29 Mar. 1994
I. Chung and Y. J. Weitsman 29 Mar. 1994 32 p Limited Reproducibility: More than 20% of this document may be affected by microfiche quality
(Contract N00014-90-J-1556)
(AD-A278866; ESM93-2.0-CM) Avail: CASI HC A03

This article presents a model for the uni-axial compressive response of uni-directionally reinforced fibrous composite. The model accounts for the non-linear shear response and the failure strain of the matrix, incorporating both aspects into a non-linear field equation which governs the load-deflection process. In addition, the model considers the effects of two kinds of geometric imperfections, namely, initial fiber waviness and random fiber spacing. It is shown that under uni-axial compression random fiber spacing may instigate the formation of severe transverse loadings on the fibers, which suggest the existence of a transitional mechanism from micro-buckling to micro-kinking. Computational results are presented which illuminate the effects of several material and geometric factors on the compressive strength of composites. DTIC

N94-35932 Oak Ridge National Lab., TN.
PROPERTIES AND APPLICATIONS OF POWDER-FILLED EVACUATED-PANEL SUPERINSULATIONS
D. W. Yarbrough and T. G. Kollie 1994 7 p Presented at the 6th AIAA/ASME Thermophysics and Heat Transfer Conference, Colorado Springs, CO, 20-23 Jun. 1994 Limited Reproducibility: More than 20% of this document may be affected by microfiche quality
(Contract DE-AC05-84OR-21400)
(DE94-009169; CONF-940625-3) Avail: CASI HC A02

Powder-filled evacuated panel (PEP) superinsulations are made from fine powders enclosed in low permeability envelopes. These insulating panels have thermal resistances at 24 C and 25.4 mm of thickness that exceed 3.5 K(center dot)m(exp 2)/W. PEP superinsulation has prospective applications in appliances, refrigerated transport, and manufactured homes. This paper contains a brief review of heat flow through powders, a presentation of thermal performance data obtained for evacuated powders, and a discussion of long-term performance. An economic evaluation of the use of PEPs as insulation for refrigerators is presented. DOE

N94-35944 Tennessee Univ., Knoxville, TN. Dept. of Engineering Science and Mechanics.
CAN THE COMPRESSIVE RESPONSE OF FIBER-REINFORCED COMPOSITES BE MODELLED BY MEANS OF LAYERED ARRAYS? Technical Report, 1 Oct. 1992 - 31 Jan. 1994
Y. Jack Weitsman and I. Chung 29 Mar. 1994 13 p Limited Reproducibility: More than 20% of this document may be affected by microfiche quality
(Contract N00014-90-J-1556)
(AD-A278864; ESM94-1.0-CM) Avail: Issuing Activity (Defense Technical Information Center (DTIC))

The validity of some basic premises employed in modeling of the compressive response of fiber-reinforced composites is examined. It is shown that the deformation fields associated with the compression of layered media yield inadmissible results when applied to hexagonal and square arrays of circular fibers. Consequently, predictions of compressive strength, which derive from the prevailing representations of layered geometry, may not apply to realistic circumstances. DTIC

N94-35946*# National Aeronautics and Space Administration. Langley Research Center, Hampton, VA.
THROUGH-THE-THICKNESS TENSILE STRENGTH OF TEXTILE COMPOSITES
Wade C. Jackson and Peter G. Ifju May 1994 37 p Presented at the ASTM 12th Symposium on Composite Materials: Testing and Design, Montreal, Ontario, 16-17 May 1994
(RTOP 505-63-50-04)
(NASA-TM-109115; NAS 1.15:109115) Avail: CASI HC A03/MF A01

A series of tests was run to characterize the through-the-thickness tensile strength for a variety of composites that included 2D and 3D braids, 2D and 3D weaves, and prepreg tapes. A new test method based on a curved beam was evaluated. The through-the-thickness deformations were characterized using moire interferometry. Failures were significantly different between the 2D and 3D materials. The 2D materials delaminated between layers due to out-of-plane tensile stresses. The strength of the 2D textile composites did not increase relative to the tapes. The 3D materials failed due to the formation of radial cracks caused by high circumferential stresses along the inner radius. A circumferential crack similar to the 2D materials produced the final failure. Final failure in the 3D materials occurred at a lower bending moment than in other materials. The early failures were caused by radial crack formation rather than low through-the-thickness strength. Author

N94-35947*# Lockheed Engineering and Sciences Co., Hampton, VA.
CARBON-CARBON PISTON DEVELOPMENT Final Report
Mark P. Gorton May 1994 15 p
(Contract NAS1-19000; RTOP 505-70-63-01)
(NASA-CR-4595; NAS 1.26:4595) Avail: CASI HC A03/MF A01

A new piston concept, made of carbon-carbon refractory-composite material, has been developed that overcomes a number of the shortcomings of aluminum pistons. Carbon-carbon material, developed in the early 1960's, is lighter in weight than aluminum, has higher strength and stiffness than aluminum and maintains these properties at temperatures over 2500 F. In addition, carbon-carbon material has a low coefficient of thermal expansion and excellent resistance to thermal shock. An effort, called the Advanced Carbon-Carbon Piston Program was started in 1986 to develop and test carbon-carbon pistons for use in spark ignition engines. The carbon-carbon pistons were designed to be replacements for existing aluminum pistons, using standard piston pin assemblies and using standard rings. Carbon-carbon pistons can potentially enable engines to be more reliable, more efficient and have greater power output. By utilizing the unique characteristics of carbon-carbon material a piston can: (1) have greater resistance to structural damage caused by overheating, lean air-fuel mixture conditions and detonation; (2) be designed to be lighter than an aluminum piston thus, reducing the reciprocating mass of an engine, and (3) be operated in a higher combustion temperature environment without failure. Author

N94-35952 Illinois Univ., Urbana, IL. Dept. of Civil Engineering.
CEMENT PASTE MATRIX COMPOSITE MATERIALS CENTER Final Report, Apr. 1992 - Sep. 1993
J. F. Young 30 Nov. 1993 26 p Limited Reproducibility: More than 20% of this document may be affected by microfiche quality
(Grant AF-AFOSR-0242-90)
(AD-A279017; AFOSR-94-0270TR) Avail: Issuing Activity (Defense Technical Information Center (DTIC))

Investigations of the development of the microstructure of MDF (Macro-defect-free) cement during processing, showed progressive changes in the properties of the poly(vinyl alcohol) matrix. Excessive processing times lead to the introduction of macro-defects, caused by failure of either interphase or polymer matrix. Macro-defects are proceeded by the formation of small tears or voids which coalesce and enlarge. Further studies on the interdiffusion of polymer interfaces has provided the first experimental evidence of the polymer reptation theory. Interfaces develop fractal character and will influence the fracture of polymer welds and confined polymer fluids. NMR spectroscopy studies on hydration of cementitious compounds have been extended to calcium silicates, using 170 for the first time. Calcium x ray adsorption spectroscopy has also been used in an exploratory study. The formation of an reaction intermediate with five coordinated silicon was observed. The conditions of synthesis of intercalated PVA 'organoceramic' complex have been explored. The results suggest that this complex cannot form in MDF cements. An organotitanium complex that improves the water resistance of MDF cement has been shown to form a 3-dimensional PVA gel which is dehydrated to form a water impervious film. The role of PVA cross-linking in controlling processing and properties is discussed. DTIC

N94-35995*# NYMA, Inc., Brook Park, OH. Engineering Services Div.
ISOTHERMAL DAMAGE AND FATIGUE BEHAVIOR OF SCS-6/TIMETAL 21S (0/90)s COMPOSITE AT 650 C Final Report
Michael G. Castelli Jun. 1994 17 p
(Contract NAS3-27186; RTOP 763-22-41)
(NASA-CR-195345; E-8927; NAS 1.26:195345) Avail: CASI HC A03/MF A01

The isothermal fatigue damage and life behaviors of SCS-6/Timetal 21S (0/90)s were investigated at 650 C. Strain ratcheting and degradation of the composite's static elastic modulus were carefully monitored as functions of cycles to indicate damage progression. Extensive fractographic and metallographic analyses were conducted to determine damage/failure mechanisms. Resulting fatigue lives show considerable reductions in comparison to (0) reinforced titanium matrix composites subjected to comparable conditions. Notable stiffness degradations were found to occur after the first cycle of loading, even at relatively low maximum stress levels, where cyclic lives are greater than 25,000 cycles. This was attributed to the extremely weak fiber/matrix bond which fails under relatively low transverse loads. Stiffness degradations incurred on first cycle loadings and degradations thereafter were found to increase with increasing maximum stress. Environmental effects associated with oxidation of the (90) fiber interfaces clearly played a role in the damage mechanisms as fracture surfaces revealed environment assisted matrix cracking along the (90) fibers. Metallographic analysis indicated that all observable matrix fatigue cracks initiated at the (90) fiber/matrix interfaces. Global de-bonding in the loading direction was found along the (90) fibers. No surface initiated cracks were evident and minimal if any (0) fiber cracking was visible. Author

N94-36004 National Inst. of Standards and Technology, Gaithersburg, MD. Polymers Div.
REPORT ON THE WORKSHOP ON MANUFACTURING POLYMER COMPOSITES BY LIQUID MOLDING
R. S. Parnas, A. J. Salem, K. N. Kendall, and M. V. Bruschke Feb. 1994 284 p Workshop held in Gaithersburg, MD, 20-22 Sep. 1993 Limited Reproducibility: More than 20% of this document may be affected by microfiche quality
(PB94-160066; NISTIR-5373) Avail: CASI HC A13

The report documents the workshop on manufacturing composites by liquid molding, held at NIST September 20-22, 1993. The workshop was jointly sponsored by NIST Ford, and General Electric, and attracted a diverse international group of participants from industry, academia, and government. Eight invited lectures were presented, and then the workshop divided into five discussion groups to focus on particular issues. A small number of critical issues were identified, including preform deformation inside and outside of the mold, high speed processing, and the establishment of standard reference materials, data, and test methods. NTIS

N94-36123 Department of the Navy, Washington, DC.
NANOCHANNEL GLASS MATRIX USED IN MAKING MESOSCOPIC STRUCTURES Patent
Ronald J. Tonucci, inventor (to Navy) and Brian L. Justus, inventor (to Navy) 23 Nov. 1993 21 p Filed 12 Jun. 1992 Supersedes AD-D015562
(AD-D016216; US-Patent-5,264,722; US-Patent-Appl-SN-897638; US-Patent-Class-257-443) Avail: US Patent and Trademark Office

The present invention provides a method of forming a semiconductor device comprising the steps of: forming a glass block of an acid inert glass having acid etchable glass rods extending therethrough, the acid etchable glass rods having an average diameter of less than 1 micron; partially etching one end of the acid etchable rods surface of the glass block to form cavities in the glass block on one surface thereof having an average diameter of less than 1 micron; and depositing material(s) in the cavities to form a semiconductor device. The present invention also provides a method for forming a semiconductor device in which the acid etchable glass rods are completely etched and the deposition material(s) is deposited to fill the nanochannels formed by the etching. The present invention also provides semiconductor devices made by these methods. DTIC

N94-36124 Department of the Navy, Washington, DC.
NONLINEAR OPTICAL COMPOSITES OF METAL CLUSTER LADEN POLYMERS Patent
Allan W. Olsen, inventor (to Navy) and Zaka H. Kafafi, inventor (to Navy) 10 Aug. 1993 9 p Filed 3 Jun. 1992 Supersedes AD-D015396
(AD-D016217; US-Patent-5,234,758; US-Patent-Appl-SN-892914; US-Patent-Class-428-323) Avail: US Patent and Trademark Office

Nonlinear optical composites with large third-order optical response composed of metal clusters uniformly dispersed in polymers are prepared by vapor deposition of a metal onto a cold support while simultaneously cocondensing a vapor of an organic material. Where the organic material is a monomer, it polymerizes either when it comes in contact of the metal and/or when the cold surface is warmed. The unpolymerized monomer is removed to yield a processable composite. When the organic material is a diluent, it deposits as a solid on the cold surface forming a dispersion of the solid metal clusters in the liquid diluent. A polymer solution is then mixed with the dispersion and the composite is formed after removal of the diluent and the solvent for the polymer. DTIC

N94-36045*# National Aeronautics and Space Administration. Lewis Research Center, Cleveland, OH.
ADVANCED COMPOSITES IN JAPAN
R. Judd Diefendorf (Clemson Univ., SC.), William G. Hillig (General Electric Co., Schenectady, NY.), Salvatore J. Grisaffe, R. Byron Pipes, John H. Perepezko, and James E. Sheehan *In* Loyola Coll., JTEC/WTEC Report and Program Summary Mar. 1994 p 99-101 (For primary document see N94-36042 11-99)
Avail: CASI HC A01/MF A03

N94-36399*# Lockheed Engineering and Sciences Co., Hampton, VA.
ASTM TEST METHODS FOR COMPOSITE CHARACTERIZATION AND EVALUATION
John E. Masters *In* NASA. Langley Research Center, National Educators' Workshop: Update 1993. Standard Experiments in Engineering Materials Science and Technology Apr. 1994 p 1-41 (For primary document see N94-36398 11-23)
Avail: CASI HC A03/MF A04

N94-36400*# Pennsylvania State Univ., University Park, PA.
CONTINUOUS UNIDIRECTIONAL FIBER REINFORCED COMPOSITES: FABRICATION AND TESTING
M. D. Weber, F. X. Spiegel, and Harvey A. West *In* NASA. Langley Research Center, National Educators' Workshop: Update 1993. Standard Experiments in Engineering Materials Science and Technology Apr. 1994 p 43-50 (For primary document see N94-36398 11-23)
Avail: CASI HC A02/MF A04

N94-36401*# Loyola Coll., Baltimore, MD.
DESIGN AND CONSTRUCTION OF A TENSILE TESTER FOR THE TESTING OF SIMPLE COMPOSITES
Mark A. Borst and F. Xavier Spiegel *In* NASA. Langley Research Center, National Educators' Workshop: Update 1993. Standard Experiments in Engineering Materials Science and Technology Apr. 1994 p 51-99 (For primary document see N94-36398 11-23)
Avail: CASI HC A03/MF A04

N94-36403*# University of Eastern Illinois, Charleston, IL. School of Technology.
LAMINATED THERMOPLASTIC COMPOSITE MATERIAL FROM RECYCLED HIGH DENSITY POLYETHYLENE

Ping Liu and Tommy L. Waskom *In* NASA. Langley Research Center, National Educators' Workshop: Update 1993. Standard Experiments in Engineering Materials Science and Technology Apr. 1994 p 111-118 (For primary document see N94-36398 11-23)
(Grant NSF DUE-93-50629)
Avail: CASI HC A02/MF A04

N94-36409*# Oak Ridge National Lab., TN. Carbon Materials Technology Group.
DEVELOPMENTS IN CARBON MATERIALS
Timothy D. Burchell *In* NASA. Langley Research Center, National Educators' Workshop: Update 1993. Standard Experiments in Engineering Materials and Science Technology Apr. 1994 p 291-314 (For primary document see N94-36398 11-23)
Avail: CASI HC A03/MF A04

25 INORGANIC AND PHYSICAL CHEMISTRY

Includes chemical analysis, e.g., chromatography; combustion theory; electrochemistry; and photochemistry.

For related information see also *77 Thermodynamics and Statistical Physics.*.

N94-35229* National Aeronautics and Space Administration. Lyndon B. Johnson Space Center, Houston, TX.
MICROPOROUS STRUCTURE WITH LAYERED INTERSTITIAL SURFACE TREATMENT, AND METHOD AND APPARATUS FOR PREPARATION THEREOF Patent
Steven L. Koontz, inventor (to NASA) 24 May 1994 10 p Filed 22 Dec. 1992 Division of US-Patent-Appl-SN-894505, filed 2 Jun. 1992 which is a division of US-Patent-Appl-SN-429739, filed 31 Oct. 1989
(NASA-Case-MSC-21487-3; US-Patent-5,314,857;
US-Patent-Appl-SN-995612; US-Patent-Appl-SN-894505;
US-Patent-Appl-SN-429739; US-Patent-Class-502-258;
US-Patent-Class-502-259; US-Patent-Class-502-260;
US-Patent-Class-502-332; US-Patent-Class-502-335) Avail: US Patent and Trademark Office

A microporous structure with layered interstitial surface treatments, and method and apparatus for preparation thereof is presented. The structure is prepared by sequentially subjecting a uniformly surface-treated structure to atomic oxygen treatment to remove an outer layer of surface treatment to a generally uniform depth, and then surface treating the so exposed layer with another surface treating agent. The atomic oxygen/surface treatment steps may optionally be repeated, each successive time to a lesser depth, to produce a microporous structure having multilayered surface treatments. The apparatus employs at least one side arm from a main atomic oxygen-containing chamber. The side arm has characteristic relaxation times such that a uniform atomic oxygen dose rate is delivered to a specimen positioned transversely in the side arm spaced from the main gas chamber. Official Gazette of the U.S. Patent and Trademark Office

N94-35255* National Aeronautics and Space Administration. Pasadena Office, CA.
HIGH TEMPERATURE SORBENTS FOR OXYGEN Patent
Pramod K. Sharma, inventor (to NASA) (Jet Propulsion Lab., California Inst. of Tech., Pasadena, CA.) 24 May 1994 6 p Filed 16 Dec. 1992
(NASA-Case-NPO-18409-1-CU; US-Patent-5,314,853;
US-Patent-Appl-SN-991003; US-Patent-Class-502-66;
US-Patent-Class-502-74; Int-Patent-Class-B01J-29/06;
Int-Patent-Class-B01J-37/30) Avail: US Patent and Trademark Office

A sorbent capable of removing trace amounts of oxygen (ppt) from a gas stream at a high temperature above 200 C comprising a porous alumina silicate support, such as zeolite, containing from 1 to 10 percent by weight of ion exchanged transition metal, such as copper or cobalt ions, and 0.05 to 1.0 percent by weight of an activator selected from a platinum group metal such as platinum is described. The activation temperature, oxygen sorption, and reducibility are all improved by the presence of the platinum activator.
Official Gazette of the U.S. Patent and Trademark Office

N94-35388*# Alabama Univ., Huntsville, AL. Surface Science Labs.
RESULTS FROM LDEF EXPERIMENT A0114: THE INTERACTION OF ATOMIC OXYGEN WITH MATERIALS SURFACES AT ORBITAL ALTITUDES Final Report
John C. Gregory Jun. 1994 6 p
(Grant NAG1-1228)
(NASA-CR-196016; NAS 1.26:196016) Avail: CASI HC A02/MF A01

In 1975 the University of Alabama in Huntsville proposed an experiment for the Long Duration Exposure Facility (LDEF) designed to investigate the effects of the collision of the ambient orbital atmosphere, mainly consisting of atomic oxygen, with satellite surfaces travelling at about 8 km per second. In 1989, the potential for recovery of significant data from A0114 on a wide variety of materials was recognized and funding for three years of data analysis was appropriated. Some significant or unique findings from the experiment A0114 include: numerous measurements of oxidation rates of surfaces under fast O atom bombardment, including Si, Ge, GaAs, SiC, and optical quality metal films; measurement of the stable attitude of the LDEF spacecraft in orbit using the gas dynamics pinhole camera; description of the formation of thick oxide films on copper at 20 C with fast oxygen; measurement of erosion rates of Kapton and other polymers at space station lifetime atomic oxygen fluences (10(exp 22) atoms/sq cm); and measurement of the cosmogenic isotopes Be-7 on spacecraft surfaces. Derived from text

N94-35447*# Alabama Univ., Huntsville, AL. In-Line Process Control Lab.
STUDY ON CONTAMINANTS ON FLIGHT AND OTHER CRITICAL SURFACES Final Report
Gary L. Workman, Charles Hughes, and William F. Arendale 25 May 1994 35 p
(Contract NAS8-38609)
(NASA-CR-193975; NAS 1.26:193975) Avail: CASI HC A03/MF A01

The control of surface contamination in the manufacture of space hardware can become a critical step in the production process. Bonded surfaces have been shown to be affected markedly by contamination. It is important to insure surface cleanliness by preventing contamination prior to bonding. In this vein techniques are needed in which the contamination which may affect bonding are easily found and removed. Likewise, if materials which are detrimental to bonding are not easily removed, then they should not be used in the manufacturing process. This study will address the development of techniques to locate and quantify contamination levels of particular contaminants. With other data becoming available from MSFC and its contractors, this study will also quantify how certain contaminants affect bondlines and how easily they are removed in manufacturing.
Author

N94-35592# Bhabha Atomic Research Centre, Bombay (India). Radiochemistry Div.
AN INDIGENOUSLY DEVELOPED PHOTOACOUSTIC SPECTROMETER FOR STUDY OF ACTINIDE SPECTROSCOPY
A. R. Dhobale, Mithlesh Kumar, A. G. Page, and M. D. Sastry 1993 30 p
(DE94-616508; BARC-1993/E/020) Avail: CASI (US Sales Only)

A photoacoustic spectrometer has been designed and fabricated. The indigenously developed unit has been successfully tested for its performance features and compares well with the commercially available units. Due to the modular nature of the spectrometer assembly, the instrument can be easily adapted to study actinide spectroscopy. The unit is being extensively used to record absorption spectra of opaque solids. Apart from the normal use to study non-radiative spectral transitions, the spectrometer is fruitfully utilized in speciation studies for uranium and for studying structural phase transitions in Li(1-x)H(x)NbO3. DOE

N94-35604 Pennsylvania State Univ., University Park, PA. Dept. of Mechanical Engineering.
DETAILED STUDIES OF SOOT FORMATION IN LAMINAR DIFFUSION FLAMES FOR APPLICATION TO MODELING STUDIES Annual Report, 1 Feb. 1993 - 31 Jan. 1994
Robert J. Santoro 7 Apr. 1994 96 p Limited Reproducibility: More than 20% of this document may be affected by microfiche quality
(Contract F49620-92-J-0161)

(AD-A278941; AFOSR-94-0264TR) Avail: Issuing Activity (Defense Technical Information Center (DTIC))

An investigation of soot formation in laminar diffusion flames has shown that soot particle surface growth under laminar diffusion flame conditions ceases because of the depletion of hydrocarbon species, in particular acetylene and benzene, and not due to soot particle reactivity loss due to thermal aging of the particles. This result has been obtained through direct species concentration measurements under well controlled conditions while the particle reactivity effects were calculated based on premixed flame results along with particle temperature/time information available from earlier laminar diffusion flame studies. Comparisons with a soot formation model which incorporated detailed chemistry effects showed good agreement in terms of predicted and measured species concentration and soot particle field evolution. In addition, a novel technique for measuring soot volume fraction has been developed based on laser-induced incandescence and applied to similar laminar diffusion flame, studies with good success. This technique represents a major development in terms of its ability to make soot volume fraction measurements in unsteady inhomogeneous combusting flows. DTIC

N94-35680*# National Aeronautics and Space Administration. Lyndon B. Johnson Space Center, Houston, TX.

EVALUATION OF OXYGEN INTERACTIONS WITH MATERIALS 3: MISSION AND INDUCED ENVIRONMENTS

S. L. Koontz, L. J. Leger, S. L. Rickman, J. B. Cross, C. L. Hakes, and D. T. Bui 1994 14 p Presented at the 3rd Long Duration Exposure Flight(LDEF) Symposium, Williamsburg, VA, Nov. 1993
(Contract W-7405-eng-36)
(NASA-TM-109349; NAS 1.15:109349; DE94-009302; LA-UR-94-789; CONF-9311137-3) Avail: CASI HC A03/MF A01

The Evaluation of Oxygen Interactions with Materials III (EOIM-III) flight experiment was developed to obtain benchmark atomic oxygen/material reactivity data. The experiment was conducted during Space Shuttle mission 46 (STS-46), which flew July 31 to August 7, 1992. Quantitative interpretation of the materials reactivity measurements requires a complete and accurate definition of the space environment exposure, including the thermal history of the payload, the solar ultraviolet exposure, and the atomic oxygen fluence. The thermal history of the payload was measured using twelve thermocouple sensors placed behind selected samples and on the EOIM-III payload structure. The solar ultraviolet exposure history of the EOIM-III payload was determined by analysis of the as-flown orbit and vehicle attitude combined with daily average solar ultraviolet and vacuum ultraviolet (UV/VUV) fluxes. The atomic oxygen fluence was assessed in three different ways. First, the O-atom fluence was calculated using a program that incorporates the MSIS-86 atmospheric model, the as-flown Space Shuttle trajectory, and solar activity parameters. Second, the oxygen atom fluence was estimated directly from Kapton film erosion. Third, ambient oxygen atom measurements were made using the quadrupole mass spectrometer on the EOIM-III payload. The best estimate of the oxygen atom fluence as of this writing is 2.3 +/- 0.3 x 10(exp 20) atoms per square centimeter. Finally, results of post-flight X-ray photoelectron spectroscopy (XPS) surface analyses of selected samples indicate low levels of contamination on the payload surface. DOE

N94-35685 Texas Univ., Austin, TX. Dept. of Chemistry.

MORPHOLOGICAL ASPECTS OF SURFACE REACTIONS

J. M. White 1993 16 p Limited Reproducibility: More than 20% of this document may be affected by microfiche quality
(Contract DE-FG05-86ER-13626)
(DE94-010184; DOE/ER-13626/T1) Avail: CASI HC A03

Progress was made in the following areas: substrate morphology studies (TiO2(001)); fragments synthesized by thermal activation (hydrocarbon fragments, role of K on surface activity, N compounds); fragments synthesized by electron activation; and fragments synthesized by photon activation. DOE

N94-35731 Pittsburgh Univ., Pittsburgh, PA. Surface Science Center.

CHEMICAL REACTIONS OF CHLORINE ON A VICINAL Si(100) SURFACE STUDIED BY ESDIAD

Z. Dohnalek, Q. Gao, W. J. Choyke, and J. T. Yates, Jr. 24 Mar. 1994 27 p Limited Reproducibility: More than 20% of this document may be affected by microfiche quality
(Contract N00014-91-J-1641)
(AD-A279059) Avail: CASI HC A03

The reaction of Cl2 on a vicinal Si(100) surface has been studied by electron stimulated desorption ion angular distribution (ESDIAD). This type of surface possesses two types of sites: pairs of dangling bonds on Si-Si terrace dimers and single dangling bonds on the two-atom layer high steps. The reactivity of these two sites is compared. For low coverages the step dangling bonds are identified as the preferred Cl bonding site after 673 K annealing. Upon higher temperature annealing and SiCl2(g) desorption, the terrace-site Cl species are depleted more rapidly than the step-site Cl species. Extensive isothermal etching under a continuous Cl2 flux at 800 K is found to produce a disordered surface structure. Heating to 1123 K causes a reordering of the surface. DTIC

N94-35736 National Inst. of Standards and Technology, Gaithersburg, MD. Applied and Computational Mathematics Div.

COMPUTATION OF DENDRITES USING A PHASE FIELD MODEL

A. A. Wheeler, B. T. Murray, and R. J. Schaefer Jul. 1992 42 p Limited Reproducibility: More than 20% of this document may be affected by microfiche quality
(PB94-160744; NISTIR-4894) Avail: Issuing Activity (National Technical Information Service (NTIS))

A phase field model is used to numerically simulate the solidification of a pure material. We employ it to compute growth into an undercooled liquid for a one-dimensional spherically symmetric geometry and a planar two-dimensional rectangular region. The phase field model equations are solved using finite difference techniques on a uniform mesh. For the growth of a sphere, the solutions from the phase field equations for sufficiently small interface widths are in good agreement with a numerical solution to the classical sharp interface model obtained using a Green's function approach. In two dimensions, we simulate dendritic growth of nickel with four-fold anisotropy and investigate the effect of anisotropy level on the growth of a dendrite. The quantitative behavior of the phase field model is evaluated for varying interface thickness and spatial and temporal resolution. Results are discussed. NTIS

N94-35745 Texas Univ., Austin, TX. Dept. of Chemical Engineering.

ELECTRICAL MICROENGINEERING OF REDOX ENZYMES Final Report

Adam Heller 31 Mar. 1994 183 p Limited Reproducibility: More than 20% of this document may be affected by microfiche quality
(Contract N00014-91-J-1656)
(AD-A279015) Avail: Issuing Activity (Defense Technical Information Center (DTIC))

Enzymes made of electrically insulating proteins were made electron conducting through incorporation of electron relaying redox centers. The redox centers were covalently bound to amino acids of proteins, particularly to lysine amines, or to peripheral oligosaccharides of glycoproteins, of enzymes. When peripherally bound, the redox functions were attached to the end of flexible spacer chains that were long enough to allow deep penetration of the redox functions into the protein shell. DTIC

N94-35755 Energia, Inc., Princeton, NJ.

INFRARED MULTIPHOTON IGNITION AND COMBUSTION ENHANCEMENT OF NATURAL GAS. Final Report, Nov. 1989 - Oct. 1992

M. Lavid, A. T. Poulos, S. K. Gulati, J. G. Stevens, and W. R. Lempert 30 Nov. 1993 116 p See also PB91-144584 Limited Reproducibility: More than 20% of this document may be affected by microfiche quality
(Contract GRI-5089-298-1897)
(PB94-165438; GRI-93/0443) Avail: Issuing Activity (National Technical Information Service (NTIS))

This research program has demonstrated the feasibility of using infrared multiphoton (IRMP) processes for reliable ignition and combustion enhancement of natural gas. Hydrocarbon constituents of natural gas are excited with focused, pulsed infrared lasers tuned to discrete resonant frequencies causing their dissociation to very reactive radicals. These radicals participate in chain-branching and chain-propagating reactions significantly improving the combustion of natural gas. Experimental and computational tasks were performed to discern IR laser conditions needed to reliably obtain IRMP ignition and reduction in ignition delay time. NTIS

N94-35777 Argonne National Lab., IL.
STRUCTURAL INVESTIGATIONS OF 1-ETHYL-3-METHYLIMIDAZOLIUM HYDROGEN DICHLORIDE: NEUTRON DIFFRACTION STUDIES OF AN AMBIENT-TEMPERATURE MOLTEN SALT
P. C. Trulove (Air Force Academy, CO.), D. Haworth (Air Force Academy, CO.), R. T. Carlin (Air Force Academy, CO.), A. K. Soper (Rutherford Appleton Lab., Chilton, England.), A. J. G. Ellison, and D. L. Price Feb. 1994 9 p Presented at the 185th Electrochemical Society Meeting, San Francisco, CA, 22-27 May 1994 Limited Reproducibility: More than 20% of this document may be affected by microfiche quality
(Contract W-31-109-eng-38)
(DE94-009680; ANL/MSD/CP-82168; CONF-940529-5) Avail: CASI HC A02

Structure of 1-ethyl- 3 -methylimidazolium hydrogen dichloride (ImHCl2) was investigated using neutron diffraction. Structural information was obtained from analysis of diffraction differences resulting from variations in the H-D substitution in the 1-ethyl- 3 -methylimidazolium cation and in the hydrogen dichloride anion (HCl2(-)). Preliminary data analysis of diffraction differences suggests that HCl2(-) exists as an asymmetric ion in the ImHCl2 molten salt. This asymmetry may result from hydrogen-bonding between HCl2(-) and the 1-ethyl- 3 -methylimidazolium cation ring hydrogens. Infrared measurements, however, fail to clearly show the presence of this hydrogen-bonding. DOE

N94-35778 SRI International Corp., Menlo Park, CA.
NOVEL CATALYSTS FOR METHANE ACTIVATION Quarterly Report No. 4, 1 Jul. - 30 Sep. 1993
A. S. Hirschon, H. J. Wu, R. Malhotra, and R. B. Wilson 3 Dec. 1993 10 p Limited Reproducibility: More than 20% of this document may be affected by microfiche quality
(Contract DE-AC22-92PC-92112; SRI Proj. 4069)
(DE94-009705; DOE/PC-92112/T3) Avail: CASI HC A02

The objectives of this project are to test novel fullerene based catalysts for application in methane activation. Fullerenes are a recently discovered allotrope of carbon that have been found to possess unusual properties, some of which may be ideal for methane conversion to higher hydrocarbons. The project is divided into three technical tasks. Task 1 deals with the synthesis and characterization of the fullerenes and fullerene soots, Task 2 with the testing of the catalysts, and Task 3 with the evaluation of the results and technical reporting requirements. This quarter the authors concentrated on Task 2. In this task they expanded the capabilities of the system so they can include the effect of diluents during the methane activation experiments and continued work on evaluating the fullerene soot. They investigated the base-line conditions for both thermal reactions and soot-catalyzed reactions of methane. They also added the capability to add diluents such as hydrogen and helium into the reaction system to determine their respective effects on selectivity during the methane activation experiments. They found that the fullerene soot significantly decreased the threshold for the methane activation and C2 products at temperatures as low as 800 deg C, whereas the pure thermal reaction required temperatures in the range of 900 to 950 deg C. However, under their conditions the selectivity to C2 was much lower for the fullerene soot, than for the thermal case. They found that the presence of H2 helped the selectivity to some degree at a given temperature, but still formed a considerable amount of coke under these condition. DOE

N94-36023# Delaware Univ., Newark, DE. Dept. of Chemical Engineering.
DESIGN OF A HIGH ACTIVITY AND SELECTIVITY ALCOHOL CATALYST Quarterly Report No. 11, 7 Feb. - 7 May 1993
H. C. Foley and G. A. Mills 2 Sep. 1993 7 p
(Contract DE-FG22-90PC-90291)
(DE94-003633; DOE/PC-90291/T12) Avail: CASI HC A02/MF A01

The apparatus used for ammonia saturation and temperature programmed desorption (TPD) testing was modified to avoid repeated injections of NH3 . Saturation and TPD results are presented for potassium-doped (gamma)-alumina. In order to examine effects of Mo oxide promotion on catalytic activity of alumina-supported Rh catalyst, additional samples of Rh/(gamma)-Al2O3 and Rh-Mo/(gamma)-Al2O3 have been synthesized. DOE

N94-36033# California Univ., Berkeley. Lawrence Berkeley Lab, CA.
A CLASSICAL MODEL FOR CLOSED-LOOP DIAGRAMS OF BINARY LIQUID MIXTURES
J. V. Schnitzler (California Univ., Berkeley, CA.) and J. M. Prausnitz (California Univ., Berkeley, CA.) Mar. 1994 22 p
(Contract DE-AC03-76SF-00098)
(DE94-011011; LBL-35432) Avail: CASI HC A03/MF A01

A classical lattice model for closed-loop temperature-composition phase diagrams has been developed. It considers the effect of specific interactions, such as hydrogen bonding, between dissimilar components. This van Laar-type model includes a Flory-Huggins term for the excess entropy of mixing. It is applied to several liquid-liquid equilibria of nonelectrolytes, where the molecules of the two components differ in size. The model is able to represent the observed data semi-quantitatively, but in most cases it is not flexible enough to predict all parts of the closed loop quantitatively. The ability of the model to represent different binary systems is discussed. Finally, attention is given to a correction term, concerning the effect of concentration fluctuations near the upper critical solution temperature. DOE

N94-36036# Lehigh Univ., Bethlehem, PA.
NO DECOMPOSITION IN NON-REDUCING ATMOSPHERES
K. Klier and R. G. Herman Mar. 1994 10 p
(Contract DE-FG22-93PC-93222)
(DE94-011157; DOE/PC-93222/1) Avail: CASI HC A02/MF A01

Studies have been carried out with CO(II) A zeolites having 1.3, 1.8, and 3.9 CO(II) cations per unit cell. All of the samples were thermally dehydrated under vacuum in in situ diffuse reflectance optical cells, and the optical spectra were obtained in a broad spectral range of 4,500 to 45,000 cm(exp -1). Subsequently, the samples were exposed to excess NO, and the optical spectra were again obtained. Results show that the CO(II) cations in the dehydrated zeolites were only coordinated to the zeolite lattice in the 6-ring windows (with trigonal symmetry), and that multiple NO molecules adsorb onto each CO(II) cation upon exposure to excess NO. DOE

N94-36056# Westinghouse Savannah River Co., Aiken, SC.
TRITIATED AMMONIA FORMATION
L. K. Heung Mar. 1994 24 p
(Contract DE-AC09-89SR-18035)
(DE94-011170; WSRC-TR-94-0132) Avail: CASI HC A03/MF A01

A rate equation that closely simulates experimental data has been developed. This rate equation can be used to calculate the formation of tritiated ammonia from different concentrations of tritium and nitrogen. The reaction of T2 and N2 to form NT3 is a slow process, particularly when the tritium concentration is low. The reaction requires weeks or months to reach equilibrium dependent on the concentrations of the reactants. DOE

N94-36059# Abo Akademi, Turku (Finland). Combustion Chemistry Research Group.
LIEKKI COMBUSTION RESEARCH PROGRAM
M. Hupa, ed. and J. Matinlinna, ed. 1993 1004 p
(DE94-763298; AAA-LIEKKI-L93-1) Avail: CASI HC A99/MF A10

This report is a summary of the technical results obtained in Finland's National Combustion Research Program LIEKKI. This five-year research program was initiated by the Finnish Ministry of Trade and Industry in 1988, and the research projects included in the program were completed and reported at the end of the year 1992. The LIEKKI Program has been focused on research serving the development of energy production technologies based on combustion. The program has included altogether 91 research projects, representing an overall effort of around 300 man-years and a financial expenditure of FIM 142 million. The Finnish Ministry of Trade and Industry has borne 48% of the total cost. The companies participating in the program have contributed most of the rest of the funding. The program was divided into five research areas: (1) modeling of combustion processes, flows, and heat transfer (20 projects); (2) combustion chemistry and combustion behavior of fuels (29 projects); (3) diagnostics and analytical methods (11 projects); (4) pressurized combustion and gasification (6 projects); and (5) applied projects (25 projects). DOE

N94-36084# Mason and Hanger-Silas Mason Co., Inc., Amarillo, TX.
NMR IMAGING OF COMPONENTS AND MATERIALS FOR DOE APPLICATION
B. R. Richardson Dec. 1993 14 p
(Contract DE-AC04-91AL-65030)
(DE94-010664; DOE/AL-65030/9328) Avail: CASI HC A03/MF A01

The suitability for using nuclear magnetic resonance (NMR) imaging to characterize liquid, polymeric, and solid materials was reviewed. The most attractive applications for NMR imaging appear to be liquid-filled porous samples, partially cured polymers, adhesives, and potting compounds, and composite polymers/high explosives containing components with widely varying thermal properties. Solid-state NMR line-narrowing and signal-enhancing markedly improve the imaging possibilities of true solid materials. These techniques provide unique elemental and chemical shift information for highly complex materials and complement images with similar spatial resolution, such as X-ray computed tomography (CT). DOE

N94-36091 Defence Research Establishment Suffield, Ralston (Alberta).
CAPILLARY COLUMN GC-MS/MS CONFIRMATION OF PHOSPHATE ESTERS WITH A HYBRID TANDEM MASS SPECTROMETER
Paul A. DAgostino and Lionel R. Provost Feb. 1994 36 p Limited Reproducibility: More than 20% of this document may be affected by microfiche quality
(AD-A278748; DRES-SM-1400) Avail: Issuing Activity (Defense Technical Information Center (DTIC))

Daughter, parent, constant neutral loss and multiple reaction ion monitoring were all evaluated for the detection and confirmation of phosphate esters during capillary column GC-MS/MS analysis with a hybrid tandem mass spectrometer. Constant neutral loss and parent modes involve scanning of the sector, thus reducing the benefits of higher sector resolution, while daughter and multiple reaction ion monitoring data may be acquired with higher sector resolution. The benefit of sector resolution was demonstrated for the detection and confirmation of phosphate esters in the presence of diesel exhaust extract components present at levels several orders of magnitude above that of the phosphate esters. Detection limits for daughter operation were approximately the same as those obtained during capillary column GC-MS analysis of standards under electron impact ionization, and SIN ratios in excess of 100:1 were observed during multiple reaction ion monitoring of the diesel exhaust extract spiked at the 200 pg level with phosphate esters. DTIC

N94-36203# Washington Univ., Seattle, WA. Dept. of Physics.
X RAY AND GAMMA RAY SPECTROSCOPY OF SOLIDS UNDER PRESSURE
R. L. Ingalls 30 Apr. 1994 9 p
(Contract DE-FG06-84ER-45163)
(DE94-011207; DOE/ER-45163/40) Avail: CASI HC A02/MF A01

During this period, synchrotron beam time (approx. 2 weeks/year) was obtained from the Stanford Synchrotron Radiation Laboratory. The following areas of study are reported: XAFS studies of polyhedral solids (ReO3), perovskites, rubidium tungsten bronze, Moessbauer study of sodium nitroprusside, XAFS studies of phase transition mechanisms (effects of high pressure on metallic Fe), and multiple scattering analysis of XANES. DOE

N94-36205# Lawrence Livermore National Lab., CA.
A NEW COMPREHENSIVE REACTION MECHANISM FOR COMBUSTION OF HYDROCARBON FUELS
E. Ranzi (Politecnico di Milano, Italy.), A. Sogaro (Politecnico di Milano, Italy.), P. Gaffuri (Politecnico di Milano, Italy.), G. Pennati (Politecnico di Milano, Italy.), C. K. Westbrook, and W. J. Pitz 3 Dec. 1993 23 p Presented at the 25th International Symposium on Combustion, Irvine, CA, 31 Jul. - 5 Aug. 1994
(Contract W-7405-eng-48)
(DE94-008288; UCRL-JC-115807; CONF-940711-12) Avail: CASI HC A03/MF A01

A chemical kinetic model has been developed which describes pyrolysis, ignition, and oxidation of many small hydrocarbon fuels over a wide range of experimental conditions. Fuels include carbon monoxide and hydrogen, methane and other alkane species up to n-butane, ethylene, propane, acetylene, and oxygenated species such as methanol, acetaldehyde, and ethanol. Formation of some larger intermediate and product species including benzene, butadiene, large olefins, and cyclopentadiene has been treated in a semi-empirical manner. The reaction mechanism has been tested for conditions that do not involve transport and diffusional processes, including plug flow and stirred reactors, batch reactors, and shock tubes. The present kinetic model and its validation differ from previous reaction mechanisms in two ways. First, in addition to conventional combustion data, experiments more commonly associated with chemical engineering problems such as oxidative coupling, oxidative pyrolysis, and steam cracking are used to test the reaction mechanism, making it even more general than previous models. In addition, H atom abstraction and some other reaction rates, even for the smaller C2, C3, and C4 species, are treated using approximations that facilitate future extensions to larger fuels in a convenient manner. Construction of the reaction mechanism and comparisons with experimental data illustrate the generality of the model. DOE

N94-36230# California Univ., Berkeley. Lawrence Berkeley Lab, CA.
EQUATIONS OF STATE VALID CONTINUOUSLY FROM ZERO TO EXTREME PRESSURES WITH H2O AND CO2 AS EXAMPLES
K. S. Pitzer and S. M. Sterner Mar. 1994 13 p Presented at the 12th Symposium on Thermophysical properties, Boulder, CO, 19-24 Jun. 1994
(Contract DE-AC03-76SF-00098)
(DE94-011907; LBL-35354; CONF-940633-2) Avail: CASI HC A03/MF A01

A new form of equation of state is proposed for use over extremely wide ranges of pressure where conventional equations fail. In particular, fluids including H2O and CO2 as well as argon, etc., remain more compressible at very high densities than can be represented by typical equations with van der Waals or Carnahan and Starling repulsive terms. The new equation is fitted to the data for H2O and CO2 over the entire range from the vapor and liquid below the critical temperature to at least 2000 K and from zero pressure to more than 10(exp 5) bars (10 GPa) with good agreement. Extension of the equation for mixed fluids is discussed. DOE

N94-36237 Lawrence Livermore National Lab., CA.
ELECTRICAL CONDUCTIVITY OF HYDROGEN SHOCKED TO MEGABAR PRESSURES
S. T. Weir, W. J. Nellis, and A. C. Mitchell Aug. 1993 4 p Presented at the 14th International Conference of the International Association for the Advancement of High Pressure Science and Technology, Colorado Springs, CO, 27 Jun. - 2 Jul. 1993 Limited Reproducibility: More than 20% of this document may be affected by microfiche quality
(Contract W-7405-eng-48)
(DE93-019632; UCRL-JC-114575; CONF-930676-46) Avail: CASI HC A01

The properties of ultrahigh pressure hydrogen have been the subject of much experimental and theoretical study. Of particular interest is the pressure-induced insulator-to-metal transition of hydrogen which, according to recent theoretical calculations, is predicted to occur by band-overlap in the pressure range of 1.5 to 3.0 Mbars on the zero temperature isotherm. Extremely high pressures are required for metallization since the low-pressure band gap is about 15 eV. Recent static-pressure diamond anvil cell experiments have searched for evidence of an insulator-to-metal transition, but no conclusive evidence for such a transition has yet been supplied. Providing conclusive evidence for hydrogen metallization is difficult because no technique has yet been developed for performing static high-pressure electrical conductivity experiments at megabar pressures. The authors report here on electrical conductivity experiments performed on H2 and D2 multishocked to megabar pressures. Electrical conductivities of dense fluid hydrogen at these pressures and temperatures reached are needed for calculations of the magnetic fields of Jupiter and Saturn, the magnetic fields being generated by convective dynamos of hot, dense, semiconducting fluid hydrogen. Also, since electrical conduction at the pressure-temperature conditions being studied is due to the thermal excitation of charge carriers across the electronic band gap, these experiments yield valuable information on the width of the band gap at high densities. DOE

N94-36252 Northwestern Univ., Evanston, IL. Dept. of Chemistry.
SOME PERSPECTIVES ON SOLUTION-PHASE ELECTRON-TRANSFER PROCESSES
Joseph T. Hupp and Michael J. Weaver 18 Apr. 1994 56 p Limited Reproducibility: More than 20% of this document may be affected by

microfiche quality
(Contract N00014-91-J-1035)
(AD-A278616; TR-18) Avail: Issuing Activity (Defense Technical Information Center (DTIC))

This article presents a selective summary of pertinent issues and a review of experimental inquiries into solution-phase electron transfer processes, with illustrations taken in part from our own laboratories. Appreciable emphasis is placed on solvent effects. We preface the review with a short outline of relevant conceptual and theoretical material. DTIC

N94-36319# Lawrence Livermore National Lab., CA.
THE REACTION OF HYDROPEROXY-PROPYL RADICALS WITH MOLECULAR OXYGEN
J. W. Bozzelli (New Jersey Inst. of Tech., Newark, NJ.) and W. J. Pitz 3 Dec. 1993 29 p Presented at the 25th International Symposium on Combustion, Irvine, CA, 31 Jul. - 5 Aug. 1994
(Contract W-7405-eng-48)
(DE94-006392; UCRL-JC-115802; CONF-940711-6) Avail: CASI HC A03/MF A01

Addition of hydroperoxy-alkyl radicals to molecular oxygen leads to chain branching in autoignition and engine knock, and in low temperature oxidation of paraffins. Rate constants and product channels for reaction of hydroperoxy-propyl radicals with O2 are estimated using thermodynamic properties, bimolecular quantum Kassel analysis and transition state theory. Thermochemistry of relevant molecules and radicals is estimated using group additivity and bond dissociation groups for radicals. Results show that rates of the hydroperoxy-propyl radical addition to O2 are near their high pressure limits at greater than or = 1 atm. Main products at 1-15 atm are stabilization, reverse reaction to hydroperoxy-propyl + O2 and alkyl carbonyl + OH. Reactions of the stabilized adducts, dissociation rates and product channels are estimated using unimolecular quantum Kassel analysis, because stabilization is the most important hydroperoxy-propyl radical + O2 product channel. Below 700 K, the stabilized peroxy adducts react primarily to hydroperoxy-carbonyl + OH, products which lead to chain branching. Above 700K, the stabilized peroxy adducts react primarily to hydroperoxy-propyl radical + O2, initial reactants, which inhibits the overall oxidation. This switchover in channels correlates well observed negative temperature coefficient behavior for propane oxidation. Rate expressions for reaction of each of the three hydroperoxy-alkyl isomers with O2 and for dissociation of the associated stabilized adducts are calculated for a series of pressures at 300-2100K. DOE

N94-36349 Argonne National Lab., IL.
NEUTRON DIFFRACTION STUDY OF ALUMINUM CHLORIDE IMIDAZOLIUM CHLORIDE MOLTEN SALTS
S. Takahashi (Nisshin Steel Co. Ltd., Ichikawa, Chiba, Japan.), M. L. Saboungi, K. Suzuya, and N. Koura Feb. 1994 9 p Presented at the 185th Electrochemical Society Meeting, San Francisco, CA, 22-27 May 1994 Limited Reproducibility: More than 20% of this document may be affected by microfiche quality
(Contract W-31-109-eng-38)
(DE94-009679; ANL/MSD/CP-81522; CONF-940529-7) Avail: CASI HC A02

The structure of molten mixtures of (AlCl3)(x) (1-ethyl 3-methylimidazolium chloride)(1-x) was investigated by neutron diffraction techniques for x=0.46, 0.50, 0.60 and 0.67. Results derived from earlier ab initio molecular orbital (6-31G* basis set) computations for AlCl4(-), Al2Cl7(-), and EMI(sup +) were used to calculate the diffraction patterns; the calculated contributions of each species are thus obtained and overall results are in good agreement with measurements. DOE

N94-36372 Department of the Navy, Washington, DC.
ELECTROCHEMICAL PROCESS AND PRODUCT THEREFROM Patent
Michael J. Marchywka, inventor (to Navy) 20 Jul. 1994 8 p Filed 31 Dec. 1992 Supersedes AD-D015767
(AD-D016211; US-Patent-5,269,890; US-Patent-Appl-SN-999629; US-Patent-Class-204-146) Avail: US Patent and Trademark Office

Removal of non-diamond carbon from a diamond substrate surface is accomplished in and electrochemical apparatus comprising an electrolyte and spaced electrodes immersed in the electrolyte and having impressed voltage producing a sufficient electric field in the electrolyte to remove at least a portion of the non-diamond carbon. Removal of the non-diamond carbon is accomplished by disposing the substrate in the electrolyte without touching the electrodes for a time sufficient to dislodge at least a portion of the non-diamond carbon. The invention herein is also directed to diamond substrates having non-diamond carbon with a high resolution on its surface. DTIC

N94-36426 California Univ., Davis, CA. Dept. of Chemistry.
SOLVENT ACIDITY AND BASICITY IN POLAR MEDIA AND THEIR ROLE IN SOLVATION
W. R. Fawcett 20 Apr. 1994 32 p Limited Reproducibility: More than 20% of this document may be affected by microfiche quality
(Contract N00014-93-1-0351)
(AD-A278604; ONR-TR-8) Avail: Issuing Activity (Defense Technical Information Center (DTIC))

The acidic and basic properties of polar solvents are reviewed with attention focussed on appropriate scales for estimating these important solvent parameters. It is shown that acidity and basicity scales can be related to the parameters arising in the mean spherical approximation for the Gibbs solvation energy of monoatomic cations and anions in polar solvents. Linear solvation energy relationships are used to analyze data for the Gibbs solvation energy of 1-1 electrolytes, the standard potentials of simple electrode reactions, and the solvent induced frequency shifts in the vibrational spectra of polar solutes. It is shown that, not only are solvent acidity and basicity important, but that macroscopic properties based on the solvents permittivity and refractive index also play a role in determining solvent effects. DTIC

N94-35433*# National Aeronautics and Space Administration. Lyndon B. Johnson Space Center, Houston, TX.
HIGH RESOLUTION TRANSMISSION ELECTRON MICROSCOPY (HRTEM) OF NANOPHASE FERRIC OXIDES
D. C. Golden (Dual and Associates, Houston, TX.), R. V. Morris, D. W. Ming, and H. V. Lauer, Jr. *In* Lunar and Planetary Inst., The Twenty-Fifth Lunar and Planetary Science Conference. Part 1: A-G 1994 p 437-438 (For primary document see N94-35395 11-91)
Avail: CASI HC A01/MF A04

N94-35459*# National Aeronautics and Space Administration. Lyndon B. Johnson Space Center, Houston, TX.
INNOVATIVE INSTRUMENTATION FOR MINERALOGICAL AND ELEMENTAL ANALYSES OF SOLID EXTRATERRESTRIAL SURFACES: THE BACKSCATTER MOESSBAUER SPECTROMETER/X RAY FLUORESCENCE ANALYZER (BaMS/XRF) Abstract Only
T. D. Shelfer (National Academy of Sciences - National Research Council, Houston, TX.), Richard V. Morris, T. Nguyen, D. G. Agresti, and E. L. Wills *In* Lunar and Planetary Inst., The Twenty-Fifth Lunar and Planetary Science Conference. Part 3: P-Z 1994 p 1261-1262 (For primary document see N94-35448 11-91)
Avail: CASI HC A01/MF A06

N94-35464*# National Aeronautics and Space Administration. Goddard Space Flight Center, Greenbelt, MD.
FIRST OBSERVATION OF A MASS INDEPENDENT ISOTOPIC FRACTIONATION IN A CONDENSATION REACTION Abstract Only
M. H. Thiemens (California Univ., San Diego, La Jolla, CA.), R. Nelson (California Univ., San Diego, La Jolla, CA.), Q. W. Dong (California Univ., San Diego, La Jolla, CA.), and Joseph A. Nuth, III *In* Lunar and Planetary Inst., The Twenty-Fifth Lunar and Planetary Science Conference. Part 3: P-Z 1994 p 1389-1390 (For primary document see N94-35448 11-91)
Avail: CASI HC A01/MF A06

N94-36144*# National Aeronautics and Space Administration. Ames Research Center, Moffett Field, CA.
THE STRUCTURAL CHANGES OF WATER ICE I DURING WARMUP Abstract Only
Peter Jenniskens and David F. Blake *In* Lunar and Planetary Inst., The Twenty-Fifth Lunar and Planetary Science Conference. Part 2: H-O 1994 p 621-622 (For primary document see N94-36136 11-91)
Avail: CASI HC A01/MF A06

N94-36154*# National Aeronautics and Space Administration. Lyndon B. Johnson Space Center, Houston, TX.
MOSSBAUER AND SPECTRAL (VISIBLE AND NEAR-IR) DATA FOR Fe(3+)-SUBSTITUTED RUTILE Abstract Only
H. V. Lauer, Jr. (Lockheed Engineering and Sciences Co., Houston, TX.), R. V. Morris, and R. K. Vempati *In* Lunar and Planetary Inst., The Twenty-Fifth Lunar and Planetary Science Conference. Part 2: H-O 1994 p 771 (For primary document see N94-36136 11-91)
Avail: CASI HC A01/MF A06

N94-36164*# National Aeronautics and Space Administration. Lyndon B. Johnson Space Center, Houston, TX.
FERROMAGNETIC RESONANCE SPECTRA OF H2-REDUCED MINERALS AND GLASSES Abstract Only
Richard V. Morris and Carlton C. Allen *In* Lunar and Planetary Inst., The Twenty-Fifth Lunar and Planetary Science Conference. Part 2: H-O 1994 p 937-938 (For primary document see N94-36136 11-91)
Avail: CASI HC A01/MF A06

N94-36174*# National Aeronautics and Space Administration. Lyndon B. Johnson Space Center, Houston, TX.
CALORIMETRIC THERMOBAROMETRY OF EXPERIMENTALLY SHOCKED QUARTZ Abstract Only
Katherine D. Ocker (Sam Houston State Univ., Huntsville, TX.), James L. Gooding, and Friedrich Hoerz *In* Lunar and Planetary Inst., The Twenty-Fifth Lunar and Planetary Science Conference. Part 2: H-O 1994 p 1021-1022 (For primary document see N94-36136 11-91)
Avail: CASI HC A01/MF A06

26 METALLIC MATERIALS

Includes physical, chemical, and mechanical properties of metals, e.g., corrosion; and metallurgy.

N94-35517# Joint Publications Research Service, Arlington, VA.
JPRS REPORT: SCIENCE AND TECHNOLOGY. CENTRAL EURASIA: MATERIALS SCIENCE
18 Oct. 1993 33 p Transl. into ENGLISH from various Russian articles
(JPRS-UMS-93-007) Avail: CASI HC A03/MF A01

Translated articles cover the following topics: predicting the mechanical properties of composite materials; increasing titanium heat resistance by electrospark alloying; effect of hydrogen on diamond formation conditions in high pressure and temperature region; on mechanism of diamond formation with gaseous phase participation in area of high pressures and temperatures; optimizing the properties of high-temperature superconducting materials; synthesis of diamonds in graphite-metal oxide systems at high pressures and temperatures; effect of long hydrogen storage on properties of high-pressure tanks; and laser welding thin-walled titanium alloy structures along the laser cut. CASI

N94-35650 Oak Ridge Y-12 Plant, TN.
CONSOLIDATION OF ZIRCALOY-4 END CROPS BY INDUCTION MELTING
E. L. Bird 25 Jan. 1994 15 p Limited Reproducibility: More than 20% of this document may be affected by microfiche quality
(Contract DE-AC05-84OR-21400)
(DE94-010031; Y/DV-1272) Avail: CASI HC A03

The Oak Ridge Y-12 Plant is investigating the use of induction melting as a method of consolidating Zircaloy-4, a zirconium alloy used in the fabrication of submarine nuclear reactor cores. Knolls Atomic Power Laboratory (KAPL) furnished about 4000 lb of typical core material, also known as hardware, for use in evaluating induction melting as a method of consolidation. Three ingots were produced by the induction melting of hardware in a graphite crucible that was protected by a laminated coating specifically developed for this application. This report includes a description of both the equipment and the crucible coating materials used for this project, a discussion of results, and a production assessment of using this technique for full-scale consolidation. DOE

N94-35935# International Centre for Theoretical Physics, Trieste (Italy).
A THEORETICAL STUDY OF ORDERING PHENOMENA IN K-In AND K-Sb MOLTEN ALLOYS
O. Akinlade and Z. Badirkhan Aug. 1993 18 p
(DE94-611103; IC-93/269) Avail: CASI HC A03/MF A01 (US Sales Only)

The quasilattice approximation (QLA) has been used to study ordering phenomena in K-In and K-Sb alloys. The concentration-concentration fluctuations in the long wavelength limit S(sub cc)(0), the Watten-Cowley short range order parameter (alpha)(sub 1), and the chemical diffusion D have been computed. Our calculations yield for both alloys, qualitative agreement with experiment in the transition from a compound forming/phase separating (CF/PS) state observed in K-In to strong compound formation in the case of K-Sb. Most importantly, we obtain the calculated quantities for the whole concentration range, thus complementing the available experimental evidence. Based on the present work and our previous calculations for K-Te, we predict that from an ordering point of view and within the same framework of the QLA, K-Sn for which experimental results are not available would have a lower free energy of mixing and expectedly a stronger tendency for compound formation than that observed in K-Pb. DOE

N94-35953# Northwestern Univ., Evanston, IL.
TRANSFORMATION PLASTICITY IN DUCTILE SOLIDS
G. B. Olson Apr. 1994 17 p
(Contract DE-FG02-88ER-45365)
(DE94-010420; DOE/ER-45365/6) Avail: CASI HC A03/MF A01

Research has addressed the role of martensitic transformation plasticity in the enhancement of toughness in high-strength austenitic steels, and the enhancement of formability in multiphase low-alloy sheet steels. In the austenitic steels, optimal processing has achieved a significant increase in strength level, in order to investigate the interaction of strain-induced transformation with the microvoid nucleation and shear localization mechanisms operating at ultrahigh strength levels. The degree of transformation interaction is sensitive to both strength level and degree of constraint. The stress-state dependence of transformation and fracture mechanisms has been investigated in model alloys, comparing behavior in uniaxial tension and blunt-notch tension specimens. A reformulated numerical constitutive model for transformation plasticity has allowed a more thorough analysis of transformation/fracture interactions, including local processes of microvoid nucleation. Processing of a new low alloy steel composition has been optimized to stabilize retained austenite by isothermal bainitic transformation after intercritical annealing. Results show a good correlation of uniform ductility with the austenite amount and stability, and new compositions are designed for improved stability. DOE

N94-35960# Atomic Energy of Canada Ltd., Pinawa (Manitoba). Nuclear Research Establishment.
THERMODYNAMIC BEHAVIOUR OF TELLURIUM AT HIGH TEMPERATURES
F. Garisto Sep. 1992 37 p
(DE94-612823; AECL-10691; COG-92-248; CA-93-00955) Avail: CASI HC A03/MF A01 (US Sales Only)

Thermodynamic calculations are used to determine the chemical speciation of tellurium in the primary heat transport system under postulated reactor accident conditions. The speciation of tellurium is determined for various values of the temperature, oxygen partial pressure, tellurium concentration and C(sub s)/T(sub e) ratio. The effects of the Zircaloy cladding and/or cesium on tellurium speciation and volatility are of particular interest in this report. DOE

N94-36110# Sandia National Labs., Albuquerque, NM.
NON-ALLOYED, REFRACTORY METAL CONTACT OPTIMIZATION WITH SHALLOW IMPLANTATIONS OF Zn AND Mg
M. L. Lovejoy, J. C. Zolper, M. E. Sherwin, A. G. Baca, R. J. Shul, D. J. Rieger, and J. F. Klem 22 Mar. 1994 14 p Presented at the International Conference on Metallurgical Coatings and Thin Films, San Diego, CA, 25-29 Apr. 1994
(Contract DE-AC04-94AL-85000)
(DE94-010392; SAND-93-2510C; CONF-940440-1) Avail: CASI HC A03/MF A01

Refractory metal contacts to GaAs show great promise for stability during high-temperature processing and for high-reliability. The authors report a study of sputtered tungsten and tungsten silicide contacts to ion implanted p-GaAs with both Zn and Mg implantations. This study focused on refractory contacts to shallow implanted contact layers that are suitable for devices such as JFET's and HBT's. The very different energy loss mechanisms of Zn and Mg ions result in different levels of implant damage which is studied by varying anneal temperatures and measuring the effects on contact and sheet resistances with the transmission line method. For the fabrication schemes investigated, specific contact resistivity versus anneal temperature with implant doses from 1 x 10(exp 14) to 5 x 10(exp 15) cm(exp -2) are found to vary from non-ohmic to 10(exp -7) Omega-cm(exp 2). Low resistance contacts to shallow (less than 800 A) implanted layers are achieved. DOE

N94-36196# Rensselaer Polytechnic Inst., Troy, NY.
INVESTIGATION OF MOISTURE-INDUCED EMBRITTLEMENT OF IRON ALUMINIDES
A. Castagna and N. S. Stoloff 19 Apr. 1994 36 p Prepared for ORNL, TN
(Contract DE-AC05-84OR-21400)
(DE94-010881; ORNL/Sub-90-SF521/02) Avail: CASI HC A03/MF A01

Alloy FA-129 undergoes an increase in crack propagation rate and a loss of fracture toughness in moisture-bearing and hydrogen gas environments. A similar effect is seen on ductility of FA-129 in tensile tests. The embrittling effect in air is attributed to oxidation of aluminum in the alloy by water vapor to produce Al2O3 and hydrogen gas. Alloy FAP-Y, which is disordered and contains only 16 at% Al is embrittled by hydrogengas in a manner similar to that of FA-129. However, laboratory air had little effect on the crack growth rates, fracture toughness, or tensile ductility. The lower aluminum content apparently is insufficient to induce the Al-H2O reaction. TEM and SEM analyses of microstructure and fracture surfaces were consistent with the change in fracture toughness with order and environment. Testing at elevated temperatures reduces crack growth rates in FA-129, and increases fracture toughness and ductility. This is consistent with the well documented peak in hydrogen embrittlement in structural alloys at or near room temperature. Elevated temperature affects the degree of embrittlement in a complex manner, possibly changing the rates of several of the processes involved. DOE

N94-36222# Argonne National Lab., IL. Materials Science Div.
IRRADIATION-RELATED AMORPHIZATION AND CRYSTALLIZATION: IN SITU TRANSMISSION ELECTRON MICROSCOPE STUDIES
C. W. Allen 1994 17 p Presented at the Symposium on High-Voltage and High-Resolution Electron Microscopy, Stuttgart, Germany, 21-24 Feb. 1994
(Contract W-31-109-eng-38)
(DE94-009823; ANL/MSD/CP-82380; CONF-940275-1) Avail: CASI HC A03/MF A01

Interfacing an ion accelerator to a transmission electron microscope (TEM) allows the analytical functions of TEM imaging and diffraction to be employed during ion irradiation effects studies. At present there are twelve such installations in Japan, one in France, and one in the US. This paper treats several aspects of in situ studies involving electron and ion beam induced and enhanced phase transformations and presents results of several in situ experiments to illustrate the dynamics of this approach in the materials science of irradiation effects. The paper describes the ion and electron induced amorphization of CuTi; the ion irradiation enhanced transformation of TiCr2; and the ion and electron irradiation enhanced crystallization of CoSi2. DOE

N94-36231# Argonne National Lab., IL.
DETERMINATION OF GRAIN BOUNDARY VOLUME EXPANSION BY HREM
M. I. Buckett and K. L. Merkle Mar. 1994 17 p Presented at the Symposium on High-Voltage and High-Resolution Electron Microscopy, Stuttgart, Germany, 21-24 Feb. 1994
(Contract W-31-109-eng-38)
(DE94-010452; ANL/MSD/CP-82465; CONF-940275-2) Avail: CASI HC A03/MF A01

High resolution electron microscopy (HREM) has provided invaluable insight into the structure of grain boundaries at the atomistic level. Quantitative HREM methods are now in development which, combined with atomistic simulations, can provide further insight into grain boundary structure-energy correlations. For example, the volume expansion (or excess free volume, (delta)), a thermodynamic parameter directly related to the grain boundary energy, is represented by the normal component of the rigid body translation. Although its magnitude is small, it can be determined experimentally using statistical techniques which locate and fit the peak and valley positions in an experimental HREM image - i.e., a direct measurement of the lattice fringe displacements is made. We have modified the lattice fringe displacement technique such that a measurement accuracy of better than (plusor minus 0.002a(sub o) can be achieved. Precise knowledge of the position and intensity of the image contrast and a detailed understanding of the sources of error are required. This paper provides a detailed description of the lattice fringe displacement technique as well as an analysis of the sources of error in the measurement. DOE

N94-36233# Syracuse Univ., NY. Dept. of Chemical Engineering and Materials Science.
THE RELATIONSHIP BETWEEN HYDROXYL GROUPS ON OXIDE SURFACES AND THE PROPERTIES OF SUPPORTED METALS
J. A. Schwarz 1994 8 p
(Contract DE-FG02-92ER-14268)
(DE94-010786; DOE/ER-14268/2) Avail: CASI HC A02/MF A01

Supported metal catalysts are commonly prepared by depositing catalytic precursors from aqueous solutions of electrolytes onto high surface area oxides. A general conclusion of our previous studies was that the performance of the finished catalyst depends on the characteristic properties of the hydroxyl inventory on the surface of the oxide support, both in wet and in (pseudo)-dry conditions. Hydroxyl groups serve as adsorption or exchange sites during catalyst preparation. On the other hand, the configuration of hydroxyl groups still remaining on oxides after dehydration determines the acid-base characteristics of the catalyst, which is an important catalytic property. The purpose of the investigation is to characterize the relationship between the complex inventory of hydroxyl groups at oxide surfaces, the acid-base properties of oxides (both in aqueous solution and in the pseudo-dry state) and the resultant effects on the properties of catalytic materials formed by adsorption/impregnation onto these hydroxylated supports during catalyst preparation. We use a common crystallographic model to describe the local configuration of hydroxyl groups on both the pseudo-dry surface and the oxide/aqueous solution interface. This allows us to extend the concept of structurally determined intrinsic heterogeneity of pseudo-dry surfaces (as already known from the IR spectra of isolated surface hydroxyls) to the oxide/solution interface. We examine the consequences of that heterogeneity upon the impregnation step during catalyst preparation. DOE

N94-36242# Sandia National Labs., Albuquerque, NM.
CONTINUUM FLUORESCENCE OF Cu IN NbTi/Cu COMPOSITE WIRES
P. F. Hlava, J. R. Michael, G. C. Nelson, and T. J. Headley 1994 3 p Presented at the Microscopy Society of America and Microbeam Analysis Society Joint Meeting, New Orleans, LA, 31 Jul. - 5 Aug. 1994
(Contracts DE-AC04-94AL-85000; DE-AC35-89ER-40486)
(DE94-008940; SAND-94-0776C; CONF-940753-2) Avail: CASI HC A01/MF A01

Continuum fluorescence across interfaces separating regions of differing composition is difficult to calculate. This paper illustrates a case of continuum fluorescence in analysis of superconducting NbTi/Cu composite wire which could lead to erroneous compositions due to Cu fluorescence by continuum x rays generated in an NbTi alloy. An approximate treatment of the continuum fluorescence is presented. DOE

N94-36275* National Aeronautics and Space Administration. Lewis Research Center, Cleveland, OH.
HIGH TEMPERATURE CREEP AND OXIDATION RESISTANT CHROMIUM SILICIDE MATRIX ALLOY CONTAINING MOLYBDENUM Patent
Sai V. Raj, inventor (to NASA) 19 Jul. 1994 9 p Filed 26 May 1993 Supersedes N93-29172 (31 - 11, p 3323)
(NASA-CASE-LEW-15697-1; US-Patent-5,330,590;
US-Patent-Appl-SN-067184; US-Patent-Class-148-423;
US-Patent-Class-148-442; US-Patent-Class-420-428;
US-Patent-Class-420-429; US-Patent-Class-420-578;

US-Patent-Class-420-588; US-Patent-Class-75-230) Avail: US Patent and Trademark Office

Cr3Si is alloyed with molybdenum which produces a two-phase microstructure of (Cr,Mo)3Si and (Cr,Mo)5Si3. About 50 weight percent of molybdenum is present in the alloy. The alloy forms two protective oxides over a wide range of temperatures. Chromium and molybdenum oxide volatize under flowing air at high temperatures above 1200 C which facilitates the formation of SiO2 on the surface. Below 1200 C Cr2O3 is formed. The new alloy has excellent high temperature strength and creep properties. Official Gazette of the U.S. Patent and Trademark Office

N94-36288# Atomic Energy of Canada Ltd., Chalk River (Ontario). Nuclear Labs.

FORMATION AND STABILITY OF Fe-RICH PRECIPITATES IN DILUTE Zr(Fe) SINGLE-CRYSTAL ALLOYS

H. Zou, G. M. Hood, J. A. Roy, and R. J. Schultz Feb. 1993 17 p
(DE94-619027; AECL-10798; COG-92-409) Avail: CASI HC A03/MF A01 (US Sales Only)

The formation and stability of Fe-rich precipitates in two alpha-Zr(Fe) single-crystal alloys with nominal compositions (1, 50 ppma Fe, and 2, 650 ppma Fe) have been investigated (the maximum solid solubility of Fe in alpha-Zr is 180 ppma - 800 C). Optical microscopy, scanning electron microscopy (SEM) and transmission electron microscopy (TEM) have been used to examine the characteristics of Fe-rich precipitates. SEM and TEM micrographs show that in as-grown alloy 2, Zr2Fe precipitates are located at 'stringers'. Precipitates were not observed in as-grown alloy 1. During annealing, below the solvus, Fe diffuses to the surfaces to form Zr3Fe precipitates in both alloys. The precipitates on the surfaces of alloy 1 tend to be star-like (0001) or pyramidal (1010), and their distribution is heterogeneous. Dissolution of Zr3Fe surface precipitates of alloy 1 (annealing above the solvus) leaves precipitate-like features on the surfaces. Zr2Fe precipitates in as-grown alloy 2 can be dissolved only by beta-phase annealing. DOE

N94-36289# Atomic Energy of Canada Ltd., Chalk River (Ontario). Nuclear Labs.

STUDY OF POINT DEFECT MOBILITIES IN ZIRCONIUM DURING ELECTRON IRRADIATION IN A HVEM

M. Griffiths, R. C. Styles, C. H. Woo, F. Phillip, and W. Frank Jan. 1993 23 p
(DE94-619028; AECL-10801; COG-92-40) Avail: CASI HC A03/MF A01 (US Sales Only)

A high voltage electron microscope (HVEM) was used to investigate the nature of intrinsic point defects in alpha-Zr by direct observation of dislocation climb and cavity growth or shrinkage. The material used was Marz-grade Zr that had been pre-irradiated with neutrons at about 740 K in the Dounreay Fast Reactor. Dislocation loops of vacancy character that had been produced during the neutron irradiation were studied by further irradiation with electrons in the HVEM. Growth of the loops was observed at temperatures as low as 230 K, indicating that, under the conditions of the experiment, some vacancy-type defects were mobile in the temperature regime 230 K-300 K. The nature of these defects is unknown. One possibility is that these defects are not intrinsic in nature, but may be vacancy-Fe complexes. In addition to the climb of dislocation loops, c-component network dislocations and cavities were also studied. Basal plane climb of the network dislocations was observed at 573 K, but was not readily apparent at 320 K. This suggests that preferred climb planes (and possibly loop habit planes) are sensitive to temperature. Cavities that were already in the foil after neutron irradiation or were induced by electron irradiation grew along the c-axis and shrank along a-directions during electron irradiation. This radiation-induced shape change of the cavities strongly suggests the existence of a diffusional anisotropy difference between interstitials and vacancies in alpha-Zr. DOE

N94-36369# Los Alamos National Lab., NM.

COMPUTER SIMULATIONS OF BENZENE IN FAUJASITE-TYPE ZEOLITES

N. J. Henson (California Univ., Santa Barbara, CA.), A. K. Cheetham (California Univ., Santa Barbara, CA.), A. Redondo, S. M. Levine, and J. M. Newsam 1994 8 p Presented at the 10th International Zeolite Conference, Garmish-Partenkirchen, Germany, 17-22 Jul. 1994
(Contract W-7405-eng-36)
(DE94-007533; LA-UR-94-491; CONF-940744-2) Avail: CASI HC A02/MF A01

The exact nature of the cation-benzene ring interaction is not yet known. In order to remedy this, energy minimization and Monte Carlo methods were used to probe the location and energetics of benzene in sodium zeolite-X and -Y. Sorption energies for the six-ring binding site in each of the zeolite models with the two forcefields (cff91 and cvff) are tabulated as a function of Si/Al ratio. Both forcefields predict similar binding sites for each system; however, the final energies are sensitive to form and parameterization of the forcefield. Further work is needed to refine the forcefield for zeolite-sorbate interactions. DOE

N94-36413*# Aluminum Co. of America, Alcoa Center, PA. Alloy Technology Div.

NEW DEVELOPMENTS IN ALUMINUM FOR AIRCRAFT AND AUTOMOBILES

Jocelyn I. Petit *In* NASA. Langley Research Center, National Educators' Workshop: Update 1993. Standard Experiments in Engineering Materials Science and Technology Apr. 1994 p 419-450 (For primary document see N94-36398 11-23)
Avail: CASI HC A03/MF A04

27 NONMETALLIC MATERIALS

Includes physical, chemical, and mechanical properties of plastics, elastomers, lubricants, polymers, textiles, adhesives, and ceramic materials.

For composite materials see *24 Composite Materials.*

N94-35233* National Aeronautics and Space Administration. Langley Research Center, Hampton, VA.

TOUGH, PROCESSABLE SEMI-INTERPENETRATING POLYMER NETWORKS FROM MONOMER REACTANTS Patent

Ruth H. Pater, inventor (to NASA) 26 Apr. 1994 16 p Filed 31 Jan. 1992 Continuation-in-part of abandoned US-Patent-Appl-SN-430470, filed 2 Nov. 1989
(NASA-Case-LAR-14838-1; US-Patent-5,306,784;
US-Patent-Appl-SN-831763; US-Patent-Appl-SN-430470;
US-Patent-Class-525-421; US-Patent-Class-525-432;
US-Patent-Class-525-436; US-Patent-Class-525-903;
US-Patent-Class-428-473.5; Int-Patent-Class-C08J-5/08) Avail: US Patent and Trademark Office

A high temperature semi-interpenetrating polymer network (semi-IPN) was developed which had significantly improved processability, damage tolerance, and mechanical performance, when compared to the commercial Thermid materials. This simultaneous semi-IPN was prepared by mixing the monomer precursors of Thermid AL-600 (a thermoset) and NR-150B2 (a thermoplastic) and allowing the monomers to react randomly upon heating. This reaction occurs at a rate which decreases the flow and broadens the processing window. Upon heating at a higher temperature, there is an increase in flow. Because of the improved flow properties, broadened processing window and enhanced toughness, high strength polymer matrix composites, adhesives and molded articles can now be prepared from the acetylene end-capped polyimides which were previously inherently brittle and difficult to process.
Official Gazette of the U.S. Patent and Trademark Office

N94-35234* National Aeronautics and Space Administration. Lewis Research Center, Cleveland, OH.

ADDITION POLYIMIDES WITH ENHANCED PROCESSABILITY Patent

Chun-Hua K. Chuang, inventor (to NASA) and Raymond D. Vannucci, inventor (to NASA) 21 Jun. 1994 10 p Filed 7 Oct. 1991 Supersedes N91-32230 (29 - 24, p 3979)
(NASA-Case-LEW-15043-1; US-Patent-5,322,924;
US-Patent-Appl-SN-772181; US-Patent-Class-528-353;
US-Patent-Class-528-125; US-Patent-Class-528-126;
US-Patent-Class-528-128; US-Patent-Class-528-172;
US-Patent-Class-528-173; US-Patent-Class-528-174) Avail: US Patent and Trademark Office

The present invention is directed to nonplanar polyimides having improved thermo-oxidative stability and enhanced processability. In a preferred embodiment, high molecular weight polyimides (HMW PMRs (polymerization of monomer reactants)) are obtained by reacting a nonplanar polyphenyl diamine, a diester or dianhydride of a tetracarboxylic acid, and an end capping compound. A second embodiment involves reacting a diamine with a nonplanar diester, or nonplanar dianhydride, of a tetracarboxylic acid, and an end capping compound. The polyimides of this invention overcome processing difficulties involved with using HMW PMRs through their noncoplanar conformation. For example, the noncoplanar conformation helps reduce the melting temperature and melt viscosity normally required and thereby permits substantially increased resin flow in processing of HMW PMRs. The polyimides of the invention possess excellent thermo-oxidative stability at 343 to 371 C for composite applications. In addition, the polyimides of the invention display a low thermal expansion coefficient and a narrow molecular weight distribution at high molecular weights. Official Gazette of the U.S. Patent and Trademark Office

N94-35243*# National Aeronautics and Space Administration. Lewis Research Center, Cleveland, OH.

A COMPARISON OF ATOMIC OXYGEN EROSION YIELDS OF CARBON AND SELECTED POLYMERS EXPOSED IN GROUND BASED FACILITIES AND IN LOW EARTH ORBIT

Sharon K. Rutledge, Bruce A. Banks, and Michael Cales Jun. 1994 9 p
(Contract NCC3-19; RTOP 233-01-0E)
(NASA-TM-106622; E-8910; NAS 1.15:106622; AIAA Paper 94-2628)
Copyright Avail: CASI HC A02/MF A01

A comparison of the relative erosion yields (volume of material removed per oxygen atom arriving) for FEP Teflon, polyethylene, and pyrolytic graphite with respect to Kapton HN was performed in an atomic oxygen directed beam system, in a plasma asher, and in space on the EOIM-III (Evaluation of Oxygen Interaction with Materials-III) flight experiment. This comparison was performed to determine the sensitivity of material reaction to atomic oxygen flux, atomic oxygen fluence, and vacuum ultraviolet radiation for enabling accurate estimates of durability in ground based facilities. The relative erosion yield of pyrolytic graphite was found not to be sensitive to these factors, that for FEP was sensitive slightly to fluence and possibly ions, and that for polyethylene was found to be partially VUV and flux sensitive but more sensitive to an unknown factor. Results indicate that the ability to use these facilities for material relative durability prediction is great as long as the sensitivity of particular materials to conditions such as VUV, and atomic oxygen flux and fluence are taken into account. When testing materials of a particular group such as teflon, it may be best to use a witness sample made of a similar material that has some available space data on it. This would enable one to predict an equivalent exposure in the ground based facility. Author

N94-35260*# National Aeronautics and Space Administration. Lewis Research Center, Cleveland, OH.

A NOVEL METHOD FOR DEPOSITING PRECIOUS METAL FILMS ON DIFFICULT SURFACES

L. C. Veitch and W. H. Phillip Jun. 1994 5 p
(RTOP 510-01-01)
(NASA-TM-106607; E-8886; NAS 1.15:106607) Avail: CASI HC A01/MF A01

A guanidine-based vehicle was developed to deposit precious metal coatings on surfaces known to be difficult to coat. To demonstrate this method, a platinum coating was deposited on alumina fibers using a guanidine-platinum solution. X-ray diffraction confirmed that the only species present in the coating was platinum and that all of the carbon species had been removed upon heat treatment. SEM results showed that some porosity was present but that the coatings uniformly covered the fiber surface and adhered well to the finer. Author

N94-35335# National Inst. of Standards and Technology, Gaithersburg, MD.

CLASSIFICATION OF ADVANCED TECHNICAL CERAMICS

Samuel Schneider, Jr., ed. Jul. 1993 128 p
(ISSN 1016-2186)
(Rept-15) Avail: CASI HC A07/MF A02

This document presents the basis and scheme for a unified classification system for advanced (technical) ceramics. The utility of the classification system is multi-fold. Its use is advantageous at the company level for purposes involving assembly of design and materials property databases, or tabulation of inventories, or invoicing. Industry can use the system for gathering and sorting trend data on market behavior or R&D expenditures, or for literature categorization. At the government level, the system can be used for gathering national and international economic data, or other vital statistics, or for determining demographics of the field. The classification system is based on defining advanced technical ceramics as 'a highly engineered, high performance, predominately non-metallic, inorganic, ceramic material having specific functional attributes.' This excludes commodity products, such as building materials and refractories. Five hundred different product types are identified as advanced technical ceramics in this classification. The classification is a non-hierarchical, matrix-type scheme accessible by a number of entry and retrieval routes to build relational databases. The classification provides a machine readable coding system built upon four independent descriptor fields (application, chemical character and product form, processing, and property data) and corresponding subdivisions that may be sequenced in order to match the users preference. Derived from text

N94-35494 Toledo Univ., OH. Dept. of Physics and Astronomy.

SYNTHESIS OF NOVEL COMPOSITE PLATINUM-DNA FILMS BY WAY OF WET-SPINNING Final Report, 1 Mar. 1991 - 28 Feb. 1994

Scott A. Lee 18 Apr. 1994 127 p Limited Reproducibility: More than 20% of this document may be affected by poor print and microfiche quality
(Contract N00014-91-J-1457)
(AD-A278763) Avail: Issuing Activity (Defense Technical Information Center (DTIC))

In this work a variety of novel films were produced. The films consisted of DNA complexed with the platinum compounds ((bipy)Pt(en)) and cis-diamminedichloroplatinum(II) as well as netropsin and daunomycin. Other films were made of either DNA or hyaluronic acid (HA) with different metallic counterions. These films were studied in order to determine if the films had enhanced optical or acoustical properties. Optical, third harmonic, and second harmonic generation were observed from DNA, DNA/bipy, and DNA/netropsin films. An optical anomaly was also observed at the A-to-B transition in CsDNA. Enhanced acoustic properties were found in Li- and NaHA; both samples have a speed of sound of about 5 km/s at low relative humidity (RH). This stiffness appears to be related to the strong Coulombic bonding involving the metallic counterions. The HA films also display a phase transition in the vicinity of 88% RH, as revealed by Brillouin and Raman spectroscopy, infrared absorption, ultraviolet absorption and optical polarizabilities. Films of DNA complexes also show enhanced acoustical properties. In particular, DNA/netropsin films show a dramatic stiffening of the bonding holding the two helices together. DTIC

N94-35502* National Aeronautics and Space Administration. Lewis Research Center, Cleveland, OH.

ATOMIC OXYGEN PROTECTIVE COATING WITH RESISTANCE TO UNDERCUTTING AT DEFECT SITES Patent

Bruce A. Banks, inventor (to NASA) and Sharon K. Rutledge, inventor (to NASA) 17 May 1994 9 p Filed 6 Jul. 1992 Supersedes N93-20566 (31 - 7, p 1859)
(NASA-Case-LEW-15306-1; US-Patent-5,312,685;
US-Patent-Appl-SN-909345; US-Patent-Class-428-336;
US-Patent-Class-244-158R; US-Patent-Class-244-163;
US-Patent-Class-428-421; US-Patent-Class-428-422;
US-Patent-Class-428-432; US-Patent-Class-428-433) Avail: US Patent and Trademark Office

Structures composed at least partially of an organic substrate may be protected from oxidation by applying a catalyst onto said substrate for promoting the combination of atomic oxygen to molecular oxygen. The structure may also be protected by applying both a catalyst and an atomic oxygen shielding layer onto the substrate. The structures to be protected include spacecraft surfaces.

Official Gazette of the U.S. Patent and Trademark Office

N94-35588 Cornell Univ., Ithaca, NY. Dept. of Chemistry.

CONCURRENT STABILIZATION AND IMAGING OF A NOVEL POLYMER FOR SECOND HARMONIC GENERATION VIA IN SITU PHOTOPOLYMERIZATION

Jody E. Beecher, Jean M. Frechet, Craig S. Willand, Douglas R. Robello, and David J. Williams 26 Apr. 1994 70 p Limited Reproducibility: More than 20% of this document may be affected by microfiche quality
(Contract N00014-91-J-1338)
(AD-A278912; TR-14-ONR) Avail: Issuing Activity (Defense Technical Information Center (DTIC))

The simultaneous patterning and stabilization of a polyurethane designed for its use in second harmonic generation has been achieved by photoinduced crosslinking of a poled film containing a titanocene photoinitiator. The crosslinked polymer shows good clarity and its nonlinear optics (NLO) response remains stable for several weeks at 100 C. DTIC

N94-35687# Imagination Resources, Inc., Dublin, OH.
MEASUREMENT OF VISCOSITY, DENSITY, AND GAS SOLUBILITY OF REFRIGERANT BLENDS IN SELECTED SYNTHETIC LUBRICANTS
R. C. Cavestri Apr. 1994 109 p
(Contract DE-FG02-91CE-23810)
(DE94-010426; DOE/CE-23810/38B) Avail: CASI HC A06/MF A02

The lubricants tested in this project were chosen based on results of liquid/liquid miscibility tests. A 32 ISO VG mixed acid polyolester and a 32 ISO VG branched acid polyolester were selected. Their vapor liquid equilibrium (VLE) viscosity reduction was measured with two different blends: HFC-125/143a/134a (44/52/4% w/w), and HFC-125/143a (50/50% w/w). In addition, measurements were made with HFC-134a and HFC-143a, two of the single refrigerants that make up the tested blends. DOE

N94-35699 Sandia National Labs., Albuquerque, NM.
DESIGNING ALUMINUM SEALING GLASSES FOR MANUFACTURABILITY
L. Kovacic, S. V. Crowder, R. K. Brow, and D. N. Bencoe 1993 11 p Presented at the 96th Annual Meeting of the American Ceramic Society, Indianapolis, IN, 24-28 Apr. 1994 Limited Reproducibility: More than 20% of this document may be affected by microfiche quality
(Contract DE-AC04-94AL-85000)
(DE94-010081; SAND-93-2048C; CONF-940416-3) Avail: CASI HC A03

Manufacturability issues involved in the development of new sealing glasses include tailoring glass compositions to meet material and component requirements and determining the optimum seal processing parameters. For each of these issues, statistical analysis can be used to shorten the time between concept and product in the development of what is essentially a new manufacturing technology. We use the development of our new family of phosphate-based glasses for aluminum/stainless steel and aluminum/CuBe hermetic sealing, the ALSG family, to illustrate the statistical approach. DOE

N94-35701 Sandia National Labs., Albuquerque, NM.
CROSS-CONDENSATION REACTIONS IN AN ORGANICALLY MODIFIED SILICA SOL-GEL
S. Prabakar (New Mexico Univ., Albuquerque, NM.), N. K. Raman (New Mexico Univ., Albuquerque, NM.), R. A. Assink, and C. J. Brinker 1993 6 p Presented at the Spring Meeting of the Materials Research Society, San Francisco, CA, 4-8 Apr. 1994 Limited Reproducibility: More than 20% of this document may be affected by microfiche quality
(Contract DE-AC04-94AL-85000)
(DE94-010086; SAND-93-2546C; CONF-940411-8) Avail: CASI HC A02

High resolution Si-29 NMR was used to study the extent of cross condensation taking place in a hybrid organic/inorganic sol-gel system. Tetraethoxysilane (TEOS) and methltriethoxysilane (MTEOS) sol-gels were chosen for this purpose. The sols were prepared by acid catalyzed hydrolysis of TEOS and MTEOS with a H2O/Si ratio of 0.3. Si-29 NMR shows signals due to both self-condensation and cross-condensation between TEOS and MTEOS. Resonance assignments were made by comparing the positions and intensities of peaks in the spectra of single and multicomponent systems. It was found that, within experimental error, the self- and cross-condensation rates are equal and that extensive molecular level mixing takes place during the early stages of the reaction. DOE

N94-35702# Sandia National Labs., Albuquerque, NM.
SPINNABILITY OF SILICA SOLS: THE ROLE OF ALKOXY GROUP EXCHANGE
S. Prabakar (New Mexico Univ., Albuquerque, NM.), R. A. Assink, and A. D. Irwin 1993 5 p Presented at the Spring Meeting of the Materials Research Society, San Francisco, CA, 4-8 Apr. 1994
(Contract DE-AC04-94AL-85000)
(DE94-010087; SAND-93-2547C; CONF-940411-7) Avail: CASI HC A01/MF A01

The exchange and spinnability of several systems with the general form Si(OR)(4) (where R = CH3, C2H5) in ethanol, propanol, and butanol were investigated. We have followed the alkoxy group exchange, hydrolysis, and condensation reactions, and Q distributions of these systems using Si-29 and O-17 NMR. Observed differences in spinnability of the various sol-gel systems are attributed to the effect of the bulkiness of the alkoxy group on its reactivity. DOE

N94-35705 Allied-Signal Aerospace Co., Kansas City, MO.
RESIDUAL GAS ANALYSIS (RGA) AND SHEAR STRENGTH CHARACTERISTICS OF A SILVER-FILLED EPOXY AND POLYIMIDE UNDER LONG-TERM, HIGH-TEMPERATURE STORAGE CONDITIONS
B. E. Adams Apr. 1994 19 p Limited Reproducibility: More than 20% of this document may be affected by microfiche quality
(Contract DE-AC04-76DP-00613)
(DE94-010106; KCP-613-5377) Avail: Issuing Activity (Department of Energy (DOE))

The introduction of organic materials into hermetically sealed electronic packages increases the risk of failure due to contamination. The contaminants of concern are moisture and ionics. This combination can lead to unwanted electrical pathways and/or corrosion. To minimize sealed-in moisture, packages are vacuum-baked for 16 hours at 200 C and Au/Sn solder-sealed in a glove box purged with dry nitrogen. Even following this procedure, the package plating and organic adhesive can still outgas moisture during high-temperature storage. Long-term aging characteristics for a silver-filled epoxy and a silver-filled polyimide were investigated. Leadless chip carriers (LCC's) containing die attached with epoxy or polyimide were aged at 25 C, 100 C, 150 C, and 200 C for up to six months. Residual gas analysis (RGA) and die shear testing were performed on each package. Results indicate that the epoxy can withstand storage at 150 C with no increase in internal moisture. The polyimide could only be stored at 100 C. No loss in shear strength for epoxy or polyimide was noted at any storage condition. DOE

N94-35757 Materials Sciences Corp., Fort Washington, PA.
IMPLEMENTATION OF THE MILITARY HANDBOOK 17 FOR POLYMER MATRIX COMPOSITES AND METAL MATRIX COMPOSITES Technical Progress Report, 24 Sep. - 13 Oct. 1993; 1-31 Mar. 1994
Crystal H. Newton 5 Apr. 1994 15 p Limited Reproducibility: More than 20% of this document may be affected by microfiche quality
(Contract DAAL01-93-C-4064)
(AD-A278795; MSC-TPR-3417/CA07) Avail: Issuing Activity (Defense Technical Information Center (DTIC))

Given is an analysis and technical review of two data sets, presented to Data Review and approved as first data sets at fully-approved classification, with condition of data documentation completion. One received comment appears in appendix 1. The comment was coordinated with the appropriate working groups. In addition, a letter inquiring as to the status of data for the handbook was forwarded from ARL. Disposition of this letter will be determined during the next contracting period. Analysis and technical review of two data sets, AS4 6k/3502 unidirectional tape and AS4 12k/3502 five-harness satin weave, was performed. These data sets meet most of the requirements for fully-approved data for most conditions. The results of the analysis and technical review were presented to the Data Review working group on 29 Mar. 1994. The data were approved with the condition that the remaining data documentation be supplied. DTIC

N94-35768 Los Alamos National Lab., NM.
LIQUID CRYSTALLINE THERMOSETTING POLYIMIDES Final Report
A. E. Hoyt (Connecticut Univ., Storrs, CT.) and S. J. Huang (Connecticut Univ., Storrs, CT.) Jul. 1993 26 p Limited Reproducibility: More than 20% of this document may be affected by microfiche quality
(Contract W-7405-eng-36)
(DE94-009939; LA-SUB-93-307) Avail: CASI HC A03

Phase separation of rodlike reinforcing polymers and flexible coil matrix polymers is a common problem in formulating molecular composites. One way to reduce phase separation might be to employ liquid crystalline thermosets as the matrix material. In this work, functionally terminated polyimide oligomers which exhibit lyotropic liquid crystalline behavior were successfully prepared. Materials based on 2,2'-bis(trifluoromethyl)-4,4'-diaminobiphenyl and 3,3',4,4'- biphenylenetetra- carboxylic dianhydride were synthesized and characterized. DOE

N94-35771 Spauschus Associates, Inc., Stockbridge, GA.
SOLUBILITY, VISCOSITY AND DENSITY OF REFRIGERANT/LUBRICANT MIXTURES Quarterly Technical Progress Report, 1 Apr. - 30 Jun. 1993
D. R. Henderson Oct. 1993 40 p Limited Reproducibility: More than 20% of this document may be affected by microfiche quality
(Contract DE-FG02-91CE-23810)
(DE94-009996; DOE/CE-23810/20B) Avail: CASI HC A03

This report presents the results of experimental measurements on low refrigerant concentration mixtures (0, 10, 20, 30 wt %) of twelve working fluids. These data were reduced to engineering form and are presented in the form of a Daniel Chart and a plot of density versus temperature and composition. Extensive numerical analysis was performed in order to derive equations which allow two independent variables (temperature and composition) and to provide for corrections in composition due to vapor space volume in the test apparatus; details of these calculations are provided in Appendix A. This report supersedes all previous reports. DOE

N94-35779 Argonne National Lab., IL.
DEFECT DETECTION IN MULTI-LAYERED, PLASMA SPRAYED ZIRCONIA BY TIME RESOLVED INFRARED RADIOMETRY: A COMPARISON BETWEEN ANALYTICAL AND EXPERIMENTAL METHODS
P. G. Happoldt (Caterpillar Tractor Co., Peoria, IL.), W. A. Ellingson, T. Gardiner, and J. Krueger 1994 11 p Presented at the 16 SPIE Thermosense: International Conference on Thermal Sensing and Imaging and Diagnostic Applications, Orlando, FL, 4-8 Apr. 1994 Limited Reproducibility: More than 20% of this document may be affected by microfiche quality
(Contract W-31-109-eng-38)
(DE94-009803; ANL/ET/CP-82049; CONF-940483-4) Avail: CASI HC A03

Analytical and experimental methods were used to study a series of test specimens consisting of plasma sprayed layers of NiCrAlY/ZrO2 of various compositions.The coatings were seeded with artificial defects and were sprayed on steel disks. Two types of defects were used: flat bottomed holes drilled in the steel substrate and patches of room temperature vulcanizing silicone within the coatings. Defect sizes ranged from 0.1 to 10 mm and were at depths below the coating surface from 0.6 to 3.6 min. The method of time resolved infrared radiometry was used with two different heat sources, an acetylene torch and a high intensity lamp, to inspect the coatings. The torch allowed excellent sensitivity at depths of less than 2 mm and the lamp revealed flaws through the full coating thickness. Two analytical models were developed to study heat flow in the test specimens: a finite element model and an electrical analog model. Results from the two models were compared to check consistency and the finite element model results were compared with experimental results. The finite element code was chosen for further development due to its greater flexibility and ease of use. DOE

N94-35809# Minnesota Mining and Mfg. Co., Saint Paul, MN. Corporate Research Labs.
DUAL CURE LOW-VOC COATING PROCESS
K. E. Kinzer Dec. 1993 79 p
(Contract DE-AC04-88ID-12692)
(DE94-009346; DOE/ID-12692/6) Avail: CASI HC A05/MF A01

US EPA is implementing increasingly stringent environmental regulations on the emissions of volatile organic compounds (VOC's), which amount to about 7 x 10(exp 9) lb/year, largely from paints and other coating systems in industry. Objective of this project is to develop dual cure photocatalyst coating technology for aerospace topcoats (urethane/acrylate), aerospace primers (epoxy/acrylate), and solventless tape backings. Some problems (moisture etc.) were encountered in the primer area. Cost, economic, and energy analyses were conducted. The dual cure technology has already been commercialized in 3M's flexible diamond resin products. DOE

N94-35977*# Missouri Univ., Rolla, MO. Dept. of Ceramic Engineering.
KINETICS OF PHASE TRANSFORMATIONS IN GLASS FORMING SYSTEMS Semiannual Progress Report No. 5, 16 Nov. 1993 - 14 May 1994
Chandra S. Ray 31 May 1994 14 p
(Grant NAG8-898)
(NASA-CR-196082; NAS 1.26:196082) Avail: CASI HC A03/MF A01

A nucleation rate like curve for a glass can be determined from the functional dependence of the maximum height of its DTA crystallization peak, (delta T)(sub p), on the nucleation temperature, T(sub n). This nucleation rate curve provides information for the temperature range where nucleation for the glass can occur and the temperature where the nucleation rate is a maximum. However, this curve does not provide information for the nucleation rate, I, for the glass at different temperatures. A method for estimating I at different temperatures from (delta T)(sub p) was developed using a Li2O.2SiO2 (LS2) glass. Also, the dielectric constant (epsilon) and the loss factor (tan delta) of a glass-ceramic depend, in part, upon the amount of crystallinity which, in turn, depends upon the nucleation density in the starting glass. It is therefore expected that epsilon and tan delta should have a relationship with nucleation density and hence on the nucleation rate. CASI

N94-36057# Ames Lab., IA.
SYNTHESES AND STUDIES OF ACETYLENIC POLYMERS Ph.D. Thesis
Yi-Wei Ding 3 Mar. 1994 207 p
(Contract W-7405-eng-82)
(DE94-011201; IS-T-1680) Avail: CASI HC A10/MF A03

Based on new diiodo aryl compounds a series of novel soluble polymers, poly(2,5-dialkoxy- 1,4-phenylene ethynylene)s (PPE polymers) were synthesized using palladium catalysis. The molecular weights (MW) range from 8000 to 40,000. Properties such as absorption, fluorescence, and conductivity were studied. A PPE polymer with butoxy side chain exhibits a weak electrical conductivity (sigma = 10(exp -3) S/cm) after doping with AsF5. Absorption spectra in THF solution at room temperature (RT) show a maximum at 440 nm. However, absorption spectra of PPE polymers in the film state at (RT) show a maximum at 480 nm. PPE polymer-based light emitting diode (LED) devices have been prepared; greenish light from these LED devices can be observed. Poly(ethynylene- p- arylene-ethynylene- silylene)s were synthesized through the same palladium-catalyzed polymerization; MW's are between 6000 and 82,000. Absorption and fluorescence were studied. Some of these polymers exhibit thermotropic liquid crystalline properties. In addition, nonlinear optical properties were briefly examined. Poly(silylene- ethynylene) homopolymers as well as alternating copolymers were synthesized through a novel palladium-catalyzed polymerization; MW's range from 56 x 10(exp 3) to 5.3 x 10(exp 3). Thermal stability of these was also investigated; char yields range from 56 to 83%. One of these polymers exhibits thermotropic liquid crystalline properties. DOE

N94-36108# Pennsylvania State Univ., University Park, PA. Dept. of Chemical Engineering.
THE EFFECT OF ALTERNATIVE FUELS ON THE STABILITY AND LUBRICITY OF CRANKCASE LUBRICANTS
E. E. Klaus, J. L. Duda, and R. J. Shah Mar. 1994 36 p
(Contract W-31-109-eng-38)
(DE94-010353; ANL/OTM/CR-6) Avail: CASI HC A03/MF A01

The purpose of this research is to study the effect of alternative fuels on the functioning of crankcase lubricants with these three main goals: (1) Develop simple, rapid test protocols to evaluate the influence of alternative fuels on the stability and lubricity of lubricants under conditions simulating engine operation. The objective is to have these test protocols serve industry as a precursor evaluation procedure before expensive engine tests are conducted. The reliability of these test procedures to predict the influence of additives on lubricant performance under actual operating conditions will be determined by comparison of these test results with available engine and fleet tests. (2) Use the developed test procedures to evaluate commercially available lubricants for applications with alternative fuels and determine the influence of various bearing materials, including conventional steel as well as advanced ceramic materials. (3) Use the test procedures to evaluate classes of lubricants and lubricant additives as well as fuel additives, and develop lubricants and additives for comparability with specific alternative fuels. DOE

N94-36121 Department of the Navy, Washington, DC.
METHOD FOR MAKING A SYMMETRICAL LAYERED THIN FILM EDGE FIELD-EMITTER-ARRAY Patent
Henry F. Gray, inventor (to Navy) 30 Nov. 1993 10 p Filed 30 Nov. 1992
(AD-D016214; US-Patent-5,266,155; US-Patent-Appl-SN-983356; US-Patent-Class-156-651) Avail: US Patent and Trademark Office

A field-emitter-array device includes a substrate supporting thin-film layers of conductive material and intervening thin-film layers of insulative material. The lateral edges of the thin-film layers form a field emitter array including a field-emitter edge electrode interposed between a pair of control electrodes. The control electrode edges produce a symmetric field causing the flow of field emitted electrons to be substantially parallel to the plane of the control and field-emitter edge electrodes. The direction of electron flow can be further controlled by additional electrodes in the form of additional thin-film conductive layers or external electrodes. A process for making the emitter device includes forming on a support member a plurality of planar first and second thin-film layers of insulative material alternately disposed between first, second and third thin-film layers of conductive material, forming a channel through the thickness of the layers and oriented perpendicular thereto, exposing the lateral edges of the layers of conductive and insulative materials adjacent to the channel to form a field emitter edge electrode interposed between a pair of control electrodes. Additional electrodes may be provided to form and deflect the electron flow. DTIC

N94-36125 Department of the Navy, Washington, DC.
METHOD OF THERMOCHEMICALLY TREATING SILICON CARBIDE FIBERS DERIVED FROM POLYMERS Patent
Jay S. Wallace, inventor (to Navy), Barry A. Bender, inventor (to Navy), and Darla Schrodt, inventor (to Navy) 27 Jul. 1993 8 p Filed 18 Feb. 1992
(AD-D016218; US-Patent-5,230,848; US-Patent-Appl-SN-837014; US-Patent-Class-264-82) Avail: US Patent and Trademark Office

Silicon carbide fibers which are derived from oligomeric and/or polymeric precursors are modified and strengthened by annealing the silicon carbide fiber at temperatures in excess of 800 deg C under a nitrogen atmosphere in the presence of carbon particles. The modified fibers can be used to make ceramic, metal, and plastic composites. DTIC

N94-36177 Direction des Recherches, Etudes et Techniques, Paris (France).
THIRD EUROPEAN TECHNICAL SYMPOSIUM ON POLYIMIDES AND HIGH PERFORMANCE POLYMERS: STEPI 3
1993 138 p Symposium held 1-3 Jun. 1993
(PB94-148491) Avail: Issuing Activity (National Technical Information Service (NTIS))

The symposium reviews current research in synthesis, mechanisms, ultimate properties, processing and applications in advanced technologies including polyimides and high-temperature polymers. The 3rd European Technical Symposium on Polyimides and High Performance Polymers (STEPI 3) will be of interest to manufacturers, users of high-temperature polymers and also to consulting engineers and research laboratories active in the field of new high-tech materials. Four sessions on the following topics are scheduled: Session I - Structure/Properties Relationship on Neat Resins: Adhesion, Toughness and Processibility; Session IIa and IIb - Chemistry of New Linear and Thermosetting Polymers: Synthesis and Characterization; Session IIIa and IIIb - High Performance Applications: Composites, Blends, Foams and Membranes; and Session IV - Photosensitive Heat Resistance Materials: New Materials for Electronics. NTIS

N94-36209# Sandia National Labs., Albuquerque, NM.
MICROSTRUCTURAL DEVELOPMENT IN SOLUTION DERIVED PZT THIN FILMS
T. J. Headley, B. A. Tuttle, J. A. Voigt, and J. R. Michael 1994 2 p Presented at the Microscopy Society of America and Microbeam Analysis Society Joint Meeting, New Orleans, LA, 31 Jul. - 5 Aug. 1994
(Contract DE-AC04-94AL-85000)
(DE94-008744; SAND-94-0732C; CONF-940753-1) Avail: CASI HC A01/MF A01

In the fabrication of PZT films by solution deposition techniques, control of phase evolution, microstructure, ferroelectric domain assemblage, etc. is important. Electron microscopy was used to correlate microstructure with film processing parameters. DOE

N94-36253 Northwestern Univ., Evanston, IL. Dept. of Chemistry.
ION MODULATED ELECTROACTIVITY IN THIN FILM METALLOPOLYMERS
Joseph T. Hupp, L. A. Lyon, and Mark A. Ratner 18 Apr. 1994 11 p Limited Reproducibility: More than 20% of this document may be affected by microfiche quality
(Contract N00014-91-J-1035)
(AD-A278618; TR-17) Avail: Issuing Activity (Defense Technical Information Center (DTIC))

Electroactivity in thin-film redox polymers derived from Fe(2,2 prime bipyridine)3(sup 3+/2+) and Fe(phenanthroline)3(sup 3+/2+) can be tremendously modulated by replacing conventional counter ions (such as perchlorate) with alkylsulfonates (CH3(CH2)(n)SO3, n=0-11). With large n species, the amount of charge passed during metal oxidation decreases (reversibly) by nearly an order of magnitude, while the rate of charge flow (as measured transiently by chronocoulometry) similarly decreases, again reversibly. Redox thermodynamic effects (systematic shifts in film-based formal potentials) are also seen. The unusual coupling of redox and ionic conductivity processes uncovered here appears to be related to: (1) the large free-volume demands of the alkylsulfonates, and (2) fundamental limitations on the ability of the metallopolymer to meet those demands. DTIC

N94-36283# Rutgers - The State Univ., Piscataway, NJ. Dept. of Ceramics.
MULTICOMPONENT GLASS SURFACES: STRUCTURE AND ADSORPTION
S. H. Garofalini 1993 3 p
(Contract DE-FG05-88ER-45368)
(DE94-010516; DOE/ER-45368/T1) Avail: CASI HC A01/MF A01

The intent of the research is to study the compositions and surface structure of complex multicomponent silicate glasses and the effect that these surfaces have on adsorption behavior, thin film formation, and adhesion. Classical molecular dynamics (MD) simulations, quantum molecular dynamics simulations using the Car-Parrinello (CP) MD technique, and XPS and UHV-AFM Force-Distance (FD) experiments are being used in this program. DOE

N94-36306 Argonne National Lab., IL.
WEAR-RESISTING OXIDE FILMS FOR 900 C
M. B. Peterson (Wear Sciences, Inc., Arnold, MD.), S. Z. Li (Institute of Metal Research, Shenyang, China.), and S. F. Murray (Rensselaer Polytechnic Inst., Troy, NY.) Mar. 1994 56 p Limited Reproducibility: More than 20% of this document may be affected by microfiche quality
(Contract W-31-109-eng-38)
(DE94-010093; ANL/OTM/CR-5) Avail: CASI HC A04

For the past 50 years, temperatures in advanced heat engines have been increasing. New-generation engines will require lubricants for 1000 C and higher. One of the most critical applications is the regenerator seals on the automotive gas turbine. In this seal, a metal plate slides against a porous ceramic surface for several thousand hours at speeds on the order of 10 cm/sec. For long-term usage above 900 C it will probably be necessary to use oxide lubricants. If effective ones can be found, then a simple solution would be available for an application like the regenerator seal: fabricate it with an alloy which forms a lubricating oxide. The objective of this study was to explore this concept for the regenerator seal. A study was conducted to develop low-friction, wear-resistant surfaces on high-temperature alloys for the temperature range 26 to 900 C. The approach investigated consisted of modifying the naturally occurring oxide film in order to improve its tribological properties. Improvement was needed at low temperatures where the oxide film, previously formed at high temperature, spalls due to stresses induced by sliding. Experiments with titanium, tungsten, and tantalum additions showed a beneficial effect when added to nickel and nickel alloys. Low friction was maintained down to 100 C from 900 C. For unalloyed nickel friction and surface damage increased at 400 to 500 C. Other approaches proved less successful and require further study. DOE

N94-36387# Air-Conditioning and Refrigeration Technology Inst., Inc., Arlington, VA.
RESEARCH UPDATE: MATERIALS COMPATIBILITY AND LUBRICANT RESEARCH (MCLR) PROGRAM
S. R. Szymurski 1994 10 p Presented at the 45th Annual International Appliance Technical Conference, Madison, WI, 9-11 May 1994
(Contract DE-FG02-91CE-23810)
(DE94-010001; DOE/CE-23810/40A; CONF-9405121-1) Avail: CASI HC A02/MF A01

Since Sep. 1991, the Air-Conditioning and Refrigeration Technology Institute (ARTI) has been conducting materials compatibility and lubricants research on CFC and HCFC refrigerant alternatives. This work has been supported by a grant from the US Department of Energy, Office of Building Technology, with co-funding from the Air-Conditioning and Refrigeration Technology Institute (ARI). During the first two and one-half years of this program, ARTI has subcontracted and managed twenty-one research projects totaling over $5.2 million. This research has included materials compatibility tests, refrigerant-lubricant interaction studies, measurement of thermophysical properties, and development of accelerated test methods. This paper summarizes results to date and discusses plans for future research for the Materials Compatibility and Lubricants Research (MCLR) program. DOE

N94-35469*# National Aeronautics and Space Administration. Ames Research Center, Moffett Field, CA.
PURITY AND CLEANNESS OF AEROGEL AS A COSMIC DUST CAPTURE MEDIUM Abstract Only
P. Tsou (Jet Propulsion Lab., California Inst. of Tech., Pasadena, CA.), R. H. Fleming (Evans, Charles and Associates, Redwood City, CA.), P. M. Lindley (Evans, Charles and Associates, Redwood City, CA.), A. Y. Craig (Evans, Charles and Associates, Redwood City, CA.), and D. Blake *In* Lunar and Planetary Inst., The Twenty-Fifth Lunar and Planetary Science Conference. Part 3: P-Z 1994 p 1421-1422 (For primary document see N94-35448 11-91)
Avail: CASI HC A01/MF A06

N94-36408*# Siena Coll., Londonville, NY. Dept. of Chemistry.
MICROSCALE SYNTHESIS AND CHARACTERIZATION OF POLYSTYRENE: NSF-POLYED SCHOLARS PROJECT
Karen S. Quaal and Chang-Ning Wu *In* NASA. Langley Research Center, National Educators' Workshop: Update 1993. Standard Experiments in Engineering Materials Science and Technology Apr. 1994 p 219-237 (For primary document see N94-36398 11-23)
Avail: CASI HC A03/MF A04

N94-36410*# Bucknell Univ., Lewisburg, PA. Dept. of Chemical Engineering.
MECHANICAL PROPERTIES OF CROSSLINKED POLYMER COATINGS
Jeffrey Csernica *In* NASA. Langley Research Center, National Educators' Workshop: Update 1993. Standard Experiments in Engineering Materials Science and Technology Apr. 1994 p 323-338 (For primary document see N94-36398 11-23)
Avail: CASI HC A03/MF A04

N94-36411*# College of Western New England, Springfield, MA. Dept. of Electrical Engineering.
EXPERIMENTS IN DIAMOND FILM FABRICATION IN TABLE-TOP PLASMA APPARATUS
James V. Masi *In* NASA. Langley Research Center, National Educators' Workshop: Update 1993. Standard Experiments in Engineering Materials Science and Technology Apr. 1994 p 339-352 (For primary document see N94-36398 11-23)
Avail: CASI HC A03/MF A04

N94-36412*# State Univ. of Southeast Missouri, Cape Girardeau, MO. Physics Dept.
DIELECTRIC MEASUREMENTS OF SELECTED CERAMICS AT MICROWAVE FREQUENCIES
J. N. Dahiya and C. K. Templeton *In* NASA. Langley Research Center, National Educators' Workshop: Update 1993. Standard Experiments in Engineering Materials Science and Technology Apr. 1994 p 391-400 (For primary document see N94-36398 11-23)
Avail: CASI HC A02/MF A04

28 PROPELLANTS AND FUELS

Includes rocket propellants, igniters, and oxidizers; their storage and handling procedures; and aircraft fuels.

For related information see also *07 Aircraft Propulsion and Power, 20 Spacecraft Propulsion and Power,* and *44 Energy Production and Conversion.*

N94-35655 Johns Hopkins Univ., Columbia, MD. Chemical Propulsion Information Agency.
THE 30TH JANNAF COMBUSTION SUBCOMMITTEE MEETING, VOLUME 1
Mary T. Gannaway Nov. 1993 446 p Meeting held in Monterey, CA, 15-29 Nov. 1993 Limited Reproducibility: More than 20% of this document may be affected by microfiche quality
(Contract N00014-91-C-0001)
(AD-A278793; CPIA-606-Vol-1) Avail: Issuing Activity (Defense Technical Information Center (DTIC))

This volume, the first of five volumes, is a collection of 34 unclassified/unlimited papers which were presented at the 30th Joint Army-Navy-NASA-Air Force (JANNAF) Combustion Subcommittee Meeting in conjunction with the Joint Propulsion Meeting (JPM) held 15-19 Nov. 1993 at both the Naval Postgraduate School and the Hyatt Regency Hotel, Monterey, California. Specific subjects discussed include the development of the following: electrothermal-chemical, liquid propellant, and ram accelerator guns; gun propellant ignition and interior ballistics; and solid propellant ignition and combustion instability. DTIC

N94-35656 Johns Hopkins Univ., Columbia, MD. Chemical Propulsion Information Agency.
THE 30TH JANNAF COMBUSTION SUBCOMMITTEE MEETING, VOLUME 2
Mary T. Gannaway Nov. 1993 386 p Meeting held in Monterey, CA, 15-19 Nov. 1993 Limited Reproducibility: More than 20% of this document may be affected by microfiche quality
(Contract N00014-91-C-0001)
(AD-A278794; CPIA-606-Vol-2) Avail: Issuing Activity (Defense Technical Information Center (DTIC))

This volume, the second of five volumes, is a collection of 28 unclassified/unlimited papers which were presented at the 30th Joint Army-Navy-NASA-Air Force (JANNAF) Combustion Subcommittee Meeting in conjunction with the Joint Propulsion Meeting (JPM) held 15-19 Nov. 1993 at both the Naval Postgraduate School and the Hyatt Regency Hotel, Monterey, California. Specific subjects discussed include the following: the combustion characteristics of energetic materials; and combustion phenomena in airbreathing, liquid, solid, underwater systems, and solid propellant guns. DTIC

N94-35795 Galaxy Scientific Corp., Pleasantville, NJ.
UNLEADED AVGAS PROGRAM Interim Report
David Atwood, Augusto Ferrara, and Paula Ringebach Mar. 1994 38 p Limited Reproducibility: More than 20% of this document may be affected by microfiche quality
(AD-A278650; DOT/FAA/CT-93/65) Avail: Issuing Activity (Defense Technical Information Center (DTIC))

The Federal Aviation Administration (FAA) Technical Center has performed extensive research toward finding an unleaded replacement for the current leaded aviation gasoline for general aviation aircraft. Described in the report are testing procedures, results to date, and future testing plans. The tests include vapor lock behavior, performance, endurance, detonation analysis, material compatibility, storage stability, volatility, emissions, water miscibility, and flight testing. The volatility tests include Reid Vapor Pressure, distillation, and vapor to liquid ratio tests. The endurance tests involved periodic checks of cylinder wear, particularly valve seat wear, leak downs to determine cylinder compression loss, and oil analysis. DTIC

N94-35941 Southwest Research Inst., San Antonio, TX.
METHANOL FUEL ADDITIVE DEMONSTRATION Final Report
E. R. Fanick, N. R. Sefer, and R. Smith Aug. 1993 290 p Sponsored in part by California Energy Resources Conservation and Development Commission Limited Reproducibility: More than 20% of this document

may be affected by microfiche quality
(Contract ARB-A832-123)
(PB94-156668; ARB-R-94/512) Avail: CASI HC A13

Methanol as a motor vehicle fuel offers the potential to achieve significant reductions in emissions. However, performance, safety and toxicity concerns have limited methanol's widespread acceptance as a motor vehicle fuel. Specifically, there are concerns regarding methanol's poor cold start capabilities low fuel lubricity flammability of saturated vapors in storage and fuel tanks, low flame luminosity, and human toxicity by inhalation, absorption through the skin, or ingestion. The contractor investigated the use of various additive packages by means of a literature search, a laboratory test program to focusing on flame luminosity, fuel lubricity and flammability, and vehicle emissions testing. The contractor identified potential additive packages for individual methanol problems, and determined that a single package addressing all methanol problems produces air quality impacts similar to M85 (85 percent methanol/15 percent unleaded gasoline). NTIS

N94-36034# California Univ., Berkeley. Lawrence Berkeley Lab, CA.
A NEW ASSOCIATION-MODEL FOR BINARY VLE OF ALCOHOL/HYDROCARBON AND AMINE/HYDROCARBON MIXTURES
J. V. Schnitzler (California Univ., Berkeley, CA.) and J. M. Prausnitz (California Univ., Berkeley, CA.) Mar. 1994 35 p
(Contract DE-AC03-76SF-00098)
(DE94-011012; LBL-35431) Avail: CASI HC A03/MF A01

An association model for binary vapor-liquid equilibria (VLE) has been developed using the Poisson distribution function to describe the relation between consecutive association reactions and their equilibrium constants. This model considers the probability of consecutive association reaction and the effect of that probability on the entropy of association. The Poisson-distribution model is compared with a classical linear-association model with the same number of adjustable parameters (two equilibrium constants and one physical parameter). Both models are able to represent the properties of alcohol-hydrocarbon and amine-hydrocarbon mixtures. The Poisson-distribution model, however, appears to be superior for those mixtures where the molecules of the associating component form rings rather than chains. Analysis of the VLE data provides some trends about the behavior of the model parameters with respect to temperature and molecular size of the associating component. An appendix contains the source code for a program to calculate the activity coefficient. DOE

N94-36035# Institute of Gas Technology, Chicago, IL.
GASOLINE FROM NATURAL GAS BY SULFUR PROCESSING Quarterly Report No. 2, 1 Oct. - 31 Dec. 1993
E. J. Erekson and F. Q. Miao Feb. 1994 37 p
(Contract DE-AC22-93PC-92114)
(DE94-011130; DOE/PC-92114/T2) Avail: CASI HC A03/MF A01

This report presents the work performed at the Institute of Gas Technology (IGT) during the second program quarter from October 1, 1993 to December 31, 1993, under Department of Energy (DOE) Contract No. DE-AC22-93PC92114. This program has co-ordinated funding for Task 1 from IGT's Sustaining Membership Program (SMP), while DOE is funding Tasks 2-8. Progress in all tasks are reported. The overall objective of this research project is to develop a catalytic process to convert natural gas to liquid transportation fuels. The process consists of two steps that each utilize catalysts and sulfur containing intermediates: (1) to convert natural gas to CS2 and (2) to convert CS2 to gasoline range liquids. Experimental data will be generated to demonstrate the potential of catalysts and the overall process. During this quarter, progress in the following areas has been made. An existing unit at IGT was modified to accommodate the sulfur feedstocks and the higher temperatures (greater than 1300 K) required for studying the reactions of hydrogen sulfide and methane as proposed in Tasks 2-5. An HP 5890 gas chromatograph with a TCD (thermal conductivity detector) for detecting fixed gases including hydrogen and an FPD (flame photometric detector) for detecting sulfur compounds was purchased using SMP funds and has been installed and calibrated. A total of seventy runs on MoS2, WS2, ZrS2 catalysts as well as quartz wool were performed. As high as 61% H2S conversion was observed. DOE

N94-36191# Midwest Research Inst., Golden, CO. National Renewable Energy Lab.
ADVANCED HYDROGEN/METHOD UTILIZATION TECHNOLOGY DEMONSTRATION Final Report
F. Lynch and J. Fulton Apr. 1994 72 p Prepared in cooperation with Hydrogen Consultants, Inc., Littleton, CO
(Contract DE-AC02-83CH-10093)
(DE94-000214; NREL/TP-425-6357) Avail: CASI HC A04/MF A01

The overall objective of the work was to seek homogeneous blend ratios of hydrogen:methane that provide 'leverage' with respect to exhaust emissions or engine performance. The leverage sought was a reduction in exhaust emissions or improved efficiency in proportions greater than the percentage of hydrogen energy in the blended fuel gas mixture. The scope of the study included the range of air/fuel mixtures from the lean limit to slightly richer than stoichiometric. This encompasses two important modes of engine operation for emissions control; lean burn pre-catalyst (some natural gas engines have no catalyst) and post-catalyst; and stoichiometric with three-way catalyst. The report includes a brief discussion of each of these modes. DOE

N94-36299# Union Carbide Corp., South Charleston, WV.
HETEROGENEOUS CATALYTIC PROCESS FOR ALCOHOL FUELS FROM SYNGAS
1993 10 p
(Contract DE-AC22-91PC-90046)
(DE94-010263; DOE/PC-90046/T9) Avail: CASI HC A02/MF A01

The novel heterogeneous catalysts for conversion of syngas to oxygenates having use as fuel enhancers, to explore novel reactor and process concepts applicable in this process, and to develop the best total process for converting syngas to liquid fuels. Our current targets for isobutanol-producing catalysts are to produce an equimolar mixture of methanol and isobutanol with a productivity for isobutanol of greater than 50 g/Kg-hr. Reactor system modifications, undertaken to improve data quality, have been completed. The changes should help eliminate differences between the two reactors and allow for more accurate determination of higher molecular weight products. To calibrate our new reactor system, we have retested our 'best' isobutanol catalyst, 10-DAN-54 (a promoted Zn/Cr/Mn spinel oxide). Under standard test conditions (400 C, 1000 psi, 12000 GHSV and syngas ratio = 1:1), this catalyst produces 200-252 g/kg-hr of total alcohols (total alcohol selectivities of 57-68 per cent) with an isobutanol rate of 94-130 g/kg-hr and a MeOH/i-BuOH product mole ratio of 3. These results compare with a productivity of 112 g/kg-hr of total alcohols (total alcohol selectivity of 86%) with an isobutanol rate of 38 g/kg-hr and a MeOH/i-BuOH product mole ratio of 3 observed in the original microreactor system configuration. It should be remembered that the test apparatus is designed for screening only. Detailed, more reliable data for kinetic modeling must be generated using larger catalyst charges (greater than 10g) and in larger scale test equipment. DOE

N94-36376# Sandia National Labs., Livermore, CA.
THE THERMOCHEMISTRY AND REACTION MECHANISMS IN THE DECOMPOSITION OF ENERGETIC MATERIALS
C. F. Melius 1994 33 p Presented at the 1994 Joint USA-Russia Energetic Material Technology Symposium, Livermore, CA, 18-25 May 1994
(Contract DE-AC04-94AL-85000)
(DE94-011420; SAND-94-1224C; CONF-9405136-1) Avail: CASI HC A03/MF A01

The chemical processes involved in the decomposition of energetic materials have been investigated theoretically using quantum chemical methods to determine the thermochemistry and reaction pathways. The Bond-Additivity-Corrected Moller-Plesset 4th order perturbation theory method (BAC-MP4) has been used to determine heats of formation and free energies of reaction intermediates of decomposition. In addition, the BAC-MP4 method has been used to determine action pathways involving these intermediates. A theoretical method for calculating solvation energies has been developed to treat the non-idealities of high pressure and the condensed phase. The resulting chemical processes involving decomposition and ignition are presented for nitrate compounds, nitramines, and nitromethane. DOE

29 MATERIALS PROCESSING

Includes space-based development of products and processes for commercial applications.

For biological materials see *55 Space Biology.*

N94-35237*# Rensselaer Polytechnic Inst., Troy, NY. Center for Multiphase Research.

ANALYSIS OF PHASE DISTRIBUTION PHENOMENA IN MICROGRAVITY ENVIRONMENTS

Richard T. Lahey, Jr. and F. Bonetto 1994 27 p

(Grant NAG3-1400)

(NASA-CR-196038; NAS 1.26:196038) Avail: CASI HC A03/MF A01

The purpose of the research presented in this paper is to demonstrate the ability of multidimensional two-fluid models for bubbly two-phase flow to accurately predict lateral phase distribution phenomena in microgravity environments. If successful, this research should provide NASA with mechanistically-based analytical methods which can be used for multiphase space system design and evaluation, and should be the basis for future shuttle experiments for model verification. Derived from text

N94-35485*# Teledyne Brown Engineering, Huntsville, AL.

MATERIALS PROCESSING IN SPACE TASKS. WBS TASK 5.4: GENERIC TASKS Final Report

Robert Crull 3 Jun. 1994 9 p

(Contract NAS8-38079)

(NASA-CR-193979; NAS 1.26:193979) Avail: CASI HC A02/MF A01

This task encompassed a wide range of activities related to materials processing in space. For example, all aspects of the space station's flight and ground based systems design were assessed for the Office of Advanced Concepts and Technology (OACT) Space Processing Division Office. Activities for that organization also included the consolidation of space processing payload requirements for the space station and the development of an OACT payload operations plan. Similar duties were performed for the MSFC Payload Project Office. The SPACECOM database was used to conduct preliminary design studies for microgravity payload carriers and to conduct assessments of materials processing technology. Concepts for the Advanced Protein Crystal Growth Facility (APCGF) were developed. Materials processing vent products were analyzed and a furnace facility filter concept was developed using those studies. A preliminary design for a space station aluminum payload rack was developed. Analysis was conducted to characterize the acceleration environment onboard the space shuttle. Equipment for two fluid experiment apparatus was designed and manufactured for the Space Science Laboratory. The Fluids and Materials Experiments (FAME) data base was expanded. Also, Mir payload integration, technology transfer, and spacelab-to-space station transition studies were conducted. Author

N94-35851*# National Aeronautics and Space Administration. Lewis Research Center, Cleveland, OH.

MICROGRAVITY ISOLATION SYSTEM DESIGN: A MODERN CONTROL SYNTHESIS FRAMEWORK

R. D. Hampton (Virginia Univ., Charlottesville, VA.), C. R. Knospe (Virginia Univ., Charlottesville, VA.), P. E. Allaire (Virginia Univ., Charlottesville, VA.), and C. M. Grodsinsky *In* NASA. Langley Research Center, Second International Symposium on Magnetic Suspension Technology, Part 1 May 1994 p 231-248 Sponsored in part by Center for Innovative Technology (For primary document see N94-35836 11-18)

Avail: CASI HC A03/MF A04

31 ENGINEERING (GENERAL)

Includes vacuum technology; control engineering; display engineering; cryogenics; and fire prevention.

N94-35226# Joint Publications Research Service, Arlington, VA.

JPRS REPORT: SCIENCE AND TECHNOLOGY. CENTRAL EURASIA

9 Mar. 1994 46 p Transl. into ENGLISH from various Russian articles

(JPRS-UST-94-006) Avail: CASI HC A03/MF A01

Translated articles cover the following topics: electrophysical properties of heterogeneous composites in high-frequency region of electromagnetic field; Zont-M helicopter deck landing signal generating system; retrieval of geopotential and temperature fields by radio measurement method for model of general circulation of atmosphere: computation method; global climate observing system; reflection of internal wave packets from plane rigid boundary; vortical systems behind cylinder in continuously stratified fluid; three-dimensional problem of flow of multilayer fluid of finite and infinite depth around source; energy losses in radiation of gravity waves accompanying characteristics of submerged body; and anomalous frequency dispersion of internal waves in ocean. Author

N94-35227# Joint Publications Research Service, Arlington, VA.

JPRS REPORT: SCIENCE AND TECHNOLOGY. CENTRAL EURASIA

22 Mar. 1994 50 p Transl. into ENGLISH from various Russian articles

(JPRS-UST-94-007) Avail: CASI HC A03/MF A01

Translated articles cover the following topics: identification and optimum control of fuzzy dynamic systems; spatial filtration of holographic lateral-shear interferograms; multiple identification of optical readings in multi-sensor information and measurement system; method of first integrals in synthesis of optimal control; composite field effect transistor with barrier junction and its applications in digital integrated circuits; effect of rare earth elements on solid phase epitaxial recrystallization rate in amorphized silicon layers; flying laboratory for ecological monitoring; greenhouse heating of the Earth's climatic system; and evolution of a launch cloud after the launch of a solid fuel rocket. Author

N94-35228# Joint Publications Research Service, Arlington, VA.

JPRS REPORT: SCIENCE AND TECHNOLOGY. CENTRAL EURASIA

31 Mar. 1994 91 p Transl. into ENGLISH from various Russian articles

(JPRS-UST-94-008) Avail: CASI HC A05/MF A01

Translated articles cover the following topics: plasma formed by interaction of laser radiation and solid targets; direct thermonuclear to electric energy conversion in dragon trap; heat radiated by turbulent jets and recorded through atmosphere; 3-D potentials method in modeling of EM fields in quasi-stratified media; and ionospheric disturbances caused by launching rockets carrying payloads into orbit. Author

N94-35341# Joint Publications Research Service, Arlington, VA.

JPRS REPORT: SCIENCE AND TECHNOLOGY. CENTRAL EURASIA

26 Jan. 1994 67 p Transl. into ENGLISH from various Russian articles

(JPRS-UST-94-004) Avail: CASI HC A04/MF A01

Translated articles cover the following topics: analytical simulation of dataflow-controlled computer; use of methods and devices for modeling in science, engineering, and economy; electromagnetic wave scattering on revolving body with multilayered coating in quasi-optic region; reflection of electromagnetic waves from inhomogeneous absorbing semiconductor layer with perfectly conducting screen; measurement results of radio wave refraction angle in Venus's atmosphere using bistatic radar data; aerodynamic characteristics analysis of frame grid fin assembly in subsonic flow; subsonic radiative waves; on hypersonic flow structure in large-scale multidiaphragmic shock tube; concerning short-term precursors of earthquakes; and on the vertical structure of tidal internal waves in the ocean. CASI

N94-35342# Joint Publications Research Service, Arlington, VA.

JPRS REPORT: SCIENCE AND TECHNOLOGY. CENTRAL EURASIA

10 Feb. 1994 78 p Transl. into ENGLISH from various Russian articles

(JPRS-UST-94-005) Avail: CASI HC A05/MF A01

Translated articles cover the following topics: optimal rotation axis of satellite TV receiving antenna; measurement of structural parameters of signals, received from identified targets; diagnostics of gallium arsenide films grown by the atomic-layer epitaxy method; acoustic diagnostic methods in new-generation aerospace equipment development; analysis of cryogenic field heat exchangers-gasifiers in aircraft gas turbine engines; mass characteristics optimization of hydrogen hydride spacecraft refrigerator; lift-to-drag ratio at supersonic velocities; delta wing in hypersonic viscous gas flow with intermediate interaction allowing for wake flow; numerical simulation of chemically and thermodynamically nonequilibrium flows at low and intermediate Reynolds numbers; measurement of the total content and altitude distribution of ozone from the Meteor-3 satellites; comparison of model profiles of stratosphere trace species and observational data; and simulation of rising of gas-dust cloud forming during impact of asteroids and comets. CASI

N94-35364# California Univ., Berkeley. Lawrence Berkeley Lab, CA. Energy and Environment Div.
THERMAL PERFORMANCE OF RESIDENTIAL DUCT SYSTEMS IN BASEMENTS
Burke Treidler and Mark Modera Jan. 1994 29 p
(Contract DE-AC03-76SF-00098)
(LBL-33962; UC-350) Avail: CASI HC A03/MF A01

There are many unanswered questions about the typical effects of duct system operation on the infiltration rates and energy usage of single-family residences with HVAC systems in their basements. Results from preliminary field studies and computer simulations are used to examine the potential for improvements in efficiency of air distribution systems in such houses. The field studies comprise thermal and flow measurements on four houses in Maryland. The houses were found to have significant envelope leakage, duct leakage, and duct conduction losses. Simulations of a basement house, the characteristics of which were chosen from the measured houses, were performed to assess the energy savings potential for basement house. The simulations estimate that a nine percent reduction in space conditioning energy use is obtained by sealing eighty percent of the duct leaks and insulating ducks to an R-value of 0.88 (C x sq. m)/W(100 F x sq. ft x h/BTU) where they are exposed in the basement. To determine the maximum possible reduction in energy use, simulations were run with all ducts insulated to (17.6 C x sq m)/W(100 F x sq. ft x h/BTU) and with no duct leakage. A reduction of energy use by 14% is obtained by using perfect ducts instead of normal ducts. Author (revised)

N94-35385# Joint Publications Research Service, Arlington, VA.
JPRS REPORT: SCIENCE AND TECHNOLOGY. CENTRAL EURASIA
3 May 1994 62 p Transl. into ENGLISH from various Russian articles
(JPRS-UST-94-010) Avail: CASI HC A04/MF A01

Translated articles cover the following topics: optimal systems to detect and classify moving objects; multiple identification of optical readings in multisensor information and measurement system; method of first integrals in synthesis of optimal control; study of the development of turbulence in the region of a break above a triangular wing; electroerosion machining in aviation engine construction; and cumulation of a flat shock wave in a tube by a thin parietal gas layer of lower density. CASI

N94-35386# Joint Publications Research Service, Arlington, VA.
JPRS REPORT: SCIENCE AND TECHNOLOGY. CENTRAL EURASIA
9 May 1994 49 p Transl. into ENGLISH from various Russian articles
(JPRS-UST-94-011) Avail: CASI HC A03/MF A01

Translated articles cover the following topics: rheology and technology of ceramics and refractories: premises and models; development of fast stable computer image reconstruction methods in digital acoustic holography; automated interpretation of aerospace images; and stochastic model of multibeam radio channel between moving objects. CASI

N94-35387# Joint Publications Research Service, Arlington, VA.
JPRS REPORT: SCIENCE AND TECHNOLOGY. CENTRAL EURASIA
8 Jun. 1994 98 p
(JPRS-UST-94-012) Avail: CASI HC A05/MF A02

Translated articles cover the following topics: electrical conductivity of CeO2-Ta2O5 ceramics in air and combustion gases; optimization of hypersonic wings; aero-optical nozzles of gas dynamic lasers; effect of injector nozzle design parameters for the model combustion chamber of a liquid-propellant rocket engine on the generation of transverse gas vibrations; new materials and processes: prospects for development and creation of aviation engineering; spectral profile of wave numbers of longitudinal vortices and features of the flow in a supersonic stream; numerical calculation of the three dimensional laminar compressible boundary layer on contoured delta wings with supersonic leading edges; electro-erosion machining in aviation engine construction; study of the development of turbulence in the region of a break above a triangular wing; optical reconstruction of microwave holograms; constraints on parameters of theoretical model of motion of trial bodies in satellite experiment for refining value of gravitational constant; astrogeodetic network at beginning of third millennium; prospects and problems in remote sensing of earth; digital mapping and geoinformation systems; new generation of equipment for meteorological lab aircraft; and geological factors in global changes: importance of catastrophes and periodicity of processes. Author

N94-35445* National Aeronautics and Space Administration. Lyndon B. Johnson Space Center, Houston, TX.
ATOMIC OXYGEN REACTOR HAVING AT LEAST ONE SIDEARM CONDUIT Patent
Steven L. Koontz, inventor (to NASA) 26 Jul. 1994 10 p Filed 23 Feb. 1993 Division of US-Patent-Appl-SN-894505, filed 2 Jun. 1992 which is a division of US-Patent-Appl-SN-429739, filed 31 Oct. 1989
(NASA-Case-MSC-21487-4; US-Patent-5,332,551;
US-Patent-Appl-SN-997265; US-Patent-Appl-SN-894505;
US-Patent-Appl-SN-429739; US-Patent-Class-422-129;
US-Patent-Class-156-345; US-Patent-Class-156-643;
US-Patent-Class-422-186.04; US-Patent-Class-422-186.05) Avail: US Patent and Trademark Office

An apparatus for treating a microporous structure with atomic oxygen is presented. The apparatus includes a main gas chamber for flowing gas in an axial direction and a source of gas, containing atomic oxygen, connected for introducing the gas into the main gas chamber. The apparatus employs at least one side arm extending from the main atomic oxygen-containing chamber. The side arm has characteristic relaxation times such that a uniform atomic oxygen dose rate is delivered to a specimen positioned transversely in the side arm spaced from the main gas chamber. Official Gazette of the U.S. Patent and Trademark Office

N94-35524 Kentucky Univ., Lexington, KY. Dept. of Mechanical Engineering.
FUNDAMENTAL STUDIES IN BLOW-DOWN AND CRYOGENIC COOLING Interim Report, 1 Sep. 1992 - 1 Aug. 1993
L. C. Chow, W. F. Lu, O. J. Hahn, M. S. Sehmbey, and M. R. Pais Sep. 1993 69 p Limited Reproducibility: More than 20% of this document may be affected by microfiche quality
(Contract F33615--91-C-2152)
(AD-A278967; UK-ME-93-04; WL-TR-93-2128) Avail: Issuing Activity (Defense Technical Information Center (DTIC))

Experiments were conducted to study the free expansion (blow-down) behavior of cryogens. Visualization of the phenomena and determination of the final state of of LN2 during free expansion were the main purposes of the study. Results presented show the effect of nozzle size, upstream pressure, and downstream pressure. The second part of the study details the experiments conducted to study the heat transfer characteristics during spray cooling with LN2. Four different nozzles at various pressures were used to study the variation in spray cooling heat transfer. Effect of nozzle and flow rate on the critical heat flux and overall heat transfer characteristics are presented. Finally, an experiment designed to study the LN2 pool boiling heat transfer from discrete sources in a confined space is described. DTIC

N94-35532 Newcastle-upon-Tyne Univ., Newcastle (England). Dept. of Computing Science.
ROBUST REQUIREMENTS SPECIFICATIONS FOR SAFETY-CRITICAL SYSTEMS
A. Saeed, T. Anderson, and R. deLemos Oct. 1993 17 p
(PB94-167806; TRS-451) Copyright Avail: Issuing Activity (National Technical Information Service (NTIS))

Experience in safety-critical systems has shown that deviations from assumed behavior can and do cause accidents. This suggests that the development of requirements specifications for such systems should be supported with a risk analysis. In this paper, we present an approach to the development of robust requirements specifications (i.e. specifications that are adequate for the risks involved), based on qualitative and quantitative analyses. NTIS

N94-35711 Ohio State Univ., Columbus.
A REVIEW OF RADIAL FORGING TECHNOLOGY INCLUDING PREFORM DESIGN FOR PROCESS OPTIMIZATION Final Report
Joseph P. Domblesky, Rajiv Shivpuri, and Taylan Altan Feb. 1994 111 p Limited Reproducibility: More than 20% of this document may be affected by microfiche quality
(Contract DAAA22-89-M-0081)
(AD-A278770; ARCCB-CR-94004) Avail: Issuing Activity (Defense Technical Information Center (DTIC))

The Engineering Research Center for Net Shape Manufacturing (located at Ohio State University, Columbus, Ohio) was contracted by Benet

Laboratories to investigate the rotary forging operation at Watervliet Arsenal. They were asked to make recommendations on how to optimize the shape and size of the starting material (preform) prior to forging which would reduce or eliminate variations in mechanical properties along the length of the resulting forging. Based on the data supplied by Benet Laboratories, the study resulted in recommendation of a two-step preform design. This was a preliminary recommendation and further testing was suggested to separate the effects of forging reduction from post-forging heat treatment. Author (DTIC)

N94-35737 National Inst. of Standards and Technology, Gaithersburg, MD. Materials Science and Engineering Lab.
INTELLIGENT PROCESSING OF MATERIALS, TECHNICAL ACTIVITIES, 1993 (NAS-NRC ASSESSMENT PANEL, APRIL 21-22 1994)
1994 74 p See also PB94-112430 Limited Reproducibility: More than 20% of this document may be affected by microfiche quality
(PB94-164183; NISTIR-5312) Avail: CASI HC A04

The 1993 report of the Office of Intelligent Processing of Materials continued to focus on cooperative programs with industry and includes projects on metals and alloys, ceramics, polymers and polymer blends. The report also summarizes research on sensors in potential applications to process monitoring. NTIS

N94-35820 Technische Univ., Delft (Netherlands). Faculty of Civil Engineering.
ASPECTS OF ROBUST COMPUTATIONAL MODELING FOR PLAIN AND REINFORCED CONCRETE
P. H. Feenstra and R. DeBorst 1993 75 p See also PB94-126315 Prepared in cooperation with Stichting voor Fundamenteel Onderzoek der Mat, Utrecht, Netherlands Limited Reproducibility: More than 20% of this document may be affected by microfiche quality
(ISSN 0046-7316)
(PB94-169240) Avail: Issuing Activity (National Technical Information Service (NTIS))

The problems commonly encountered in the numerical analysis of reinforced structures are often related to biaxial stress states in the structure. In this study, this problem is solved with the formulation of a composite plasticity model, which describes both cracking and crushing of concrete within the framework of plasticity theory. The other issue which is treated in this study is the rational modeling of the interaction between concrete and reinforcement. NTIS

N94-36008# National Inst. of Standards and Technology, Gaithersburg, MD. Thermophysics Div.
THERMOPHYSICAL PROPERTIES OF HFC-143A AND HFC-152A
R. F. Kayser Jul. 1993 16 p
(Contract DE-FG02-91CE-23810)
(DE94-009995; DOE/CE-23810/20A) Avail: CASI HC A03/MF A01

Numerous fluids have been identified as promising alternative refrigerants, but much of the information needed to predict their behavior as pure fluids and as components in mixtures does not exist. In particular, reliable thermophysical properties data and models are needed to predict the performance of the new refrigerants in heating and cooling equipment and to design and optimize equipment to be reliable and energy efficient. The objective of this project is to provide highly accurate, selected thermophysical properties data for refrigerants HFC-143a (CH3CF3) and HFC-152a(CH3CHF2) and to use this data to fit complex equations of state and detailed transport property models. The new data will fill gaps in the existing data sets and resolve problems and uncertainties that exist in and between the data sets. This report describes progress during the first quarter of this twelve-month project, which was initiated on April 1, 1993. DOE

N94-36388# Air-Conditioning and Refrigeration Technology Inst., Inc., Arlington, VA.
SEALED TUBE COMPARISONS OF THE COMPATIBILITY OF DESICCANTS WITH REFRIGERANTS AND LUBRICANTS
J. E. Field (Spauschus Associates, Inc., Stockbridge, GA.) 1994 12 p Presented at the 45th Annual International Appliance Technical Conference, Madison, WI, 9-11 May 1994
(Contract DE-FG02-91CE-23810)
(DE94-010002; DOE/CE-23810/40B; CONF-9405121-2) Avail: CASI HC A03/MF A01

Continuing environmental concerns mandate replacement of CFC's with alternate refrigeration fluids. At this time relatively little testing has been reported in the literature for compatibility of desiccants in these new working fluids. Work has begun, and some results are reported, on a project that will determine the compatibility of virtually all of the currently used desiccant types--both bead and molded core--with thirteen refrigerant/lubricant combinations. The desiccants are tested by exposure to refrigerant and lubricant in sealed, glass tubes in accordance with ASHRAE/ANSI Standard 97-1989. After aging the lubricants are evaluated for change in color and acid formation. The refrigerants are analyzed for charges by gas chromatography and halide ion formation using ion chromatography. The desiccants are evaluated for changes in crush strength and for retention of acids and halide ions. Metal catalysts, also present in the sealed tubes, are visually examined for corrosion, copper plating, and appearance change. Results are reported for 4 A and 3 A molecular sieve desiccants aged in R-12, R-134a, and R-32. DOE

N94-35919*# Knolle Magnetrans, San Francisco, CA.
MAGLEV CRUDE OIL PIPELINE
Ernst G. Knolle *In* NASA. Langley Research Center, Second International Symposium on Magnetic Suspension Technology, Part 2 May 1994 p 671-684 (For primary document see N94-35902 11-18)
Avail: CASI HC A03/MF A03

N94-35967*# National Aeronautics and Space Administration. Hugh L. Dryden Flight Research Facility, Edwards, CA.
A BIASED HISTORICAL PERSPECTIVE OF WOMEN IN THE ENGINEERING FIELD AT DRYDEN FROM 1946 TO NOVEMBER 1992
Sheryll Goecke Powers *In* NASA. Ames Research Center, 1993 Technical Paper Contest for Women. Gear Up 2000: Women in Motion Feb. 1994 p 41-61 (For primary document see N94-35961 11-99)
Avail: CASI HC A03/MF A02

32 COMMUNICATIONS AND RADAR

Includes radar; land and global communications; communications theory; and optical communications.

For related information see also *04 Aircraft Communications and Navigation* and *17 Space Communications, Spacecraft Communications, Command and Tracking.* For search and rescue see *03 Air Transportation and Safety,* and *16 Space Transportation.*

N94-35231* National Aeronautics and Space Administration. Goddard Space Flight Center, Greenbelt, MD.
ACTIVE ANTENNA Patent
John F. Sutton, inventor (to NASA) 10 May 1994 5 p Filed 23 Aug. 1990
(NASA-Case-GSC-13309-1; US-Patent-5,311,198;
US-Patent-Appl-SN-571060; US-Patent-Class-343-701;
US-Patent-Class-455-291; Int-Patent-Class-H01Q-1/24) Avail: US Patent and Trademark Office

An antenna, which may be a search coil, is connected to an operational amplifier circuit which provides negative impedances, each of which is in the order of magnitude of the positive impedances which characterize the antenna. The antenna is connected to the inverting input of the operational amplifier; a resistor is connected between the inverting input and the output of the operational amplifier; a capacitor-resistor network, in parallel, is connected between the output and the noninverting input of the operational amplifier; and a resistor is connected from the noninverting input and the circuit common. While this circuit provides a negative resistance and a negative inductance, in series, which appear, looking into the noninverting input of the operational amplifier, in parallel with the antenna, these negative impedances appear in a series loop with the antenna positive impedances, so as to algebraically add. This circuit is tuned by varying the various circuit components so that the negative impedances are very close, but somewhat less, in magnitude, to the antenna impedances. The result is to increase the sensitivity of the antenna by lowering its effective impedance.

This, in turn, increases the effective area of the antenna, which may be broadband. Official Gazette of the U.S. Patent and Trademark Office

N94-35247*# North Carolina State Univ., Raleigh, NC. Dept. of Electrical and Computer Engineering.
SWITCHED-BEAM RADIOMETER FRONT-END NETWORK ANALYSIS Final Report
R. J. Trew (Case Western Reserve Univ., Cleveland, OH.) and G. L. Bilbro Jun. 1994 32 p
(Grant NAG1-943; RTOP 505-64-12-02)
(NASA-CR-194922; NAS 1.26:194922) Avail: CASI HC A03/MF A01

The noise figure performance of various delay-line networks fabricated from microstrip lines with varying number of elements was investigated using a computer simulation. The effects of resistive losses in both the transmission lines and power combiners were considered. In general, it is found that an optimum number of elements exists, depending upon the resistive losses present in the network. Small resistive losses are found to have a significant degrading effect upon the noise figure performance of the array. Extreme stability in switching characteristics is necessary to minimize the nondeterministic noise of the array. For example, it is found that a 6 percent tolerance on the delay-line lengths will produce a 0.2 db uncertainty in the noise figure which translates into a 13.67 K temperature uncertainty generated by the network. If the tolerance can be held to 2 percent, the uncertainty in noise figure and noise temperature will be 0.025 db and 1.67 K, respectively. Three phase shift networks fabricated using a commercially available PIN diode switch were investigated. Loaded-line phase shifters are found to have desirable RF and noise characteristics and are attractive components for use in phased-array networks. Author

N94-35537 Oxford Univ. (England). Programming Research Group.
MATHEMATICAL THEORY OF SYNCHRONOUS COMMUNICATION
J. E. Barnes 1993 204 p
(PB94-169224; PRG-112) Copyright Avail: Issuing Activity (National Technical Information Service (NTIS))

A mathematical theory of synchronous communication is presented. The process algebra Synchronous Communicating Sequential Processes (SCSP), shares many of its constructors with Hoare's CSP. It models components of a distributed system as processes evolving in lockstep. A Synchronous Receptive Process Theory (SRPT), which distinguishes between input and output events in its model of communication, is also investigated. The language SCSP is given a denotational semantics. The semantic model captures the behavior of processes using failure-divergences information. SCSP exhibits sufficient algebraic laws to form a sound and complete proof system with respect to the semantics. This allows reasoning about concurrent systems by means of algebraic manipulation of process expressions. SRPT can be interpreted as a receptive sublanguage of SCSP. This is demonstrated by embedding both the language and its semantic model in those of SCSP. The embedding allows many of the mathematical results concerning SRPT to be deduced from their counterparts in SCSP. SRPT is shown to be applicable to the modeling of synchronous circuits. NTIS

N94-35542*# Jet Propulsion Lab., California Inst. of Tech., Pasadena, CA.
THE TELECOMMUNICATIONS AND DATA ACQUISITION REPORT Progress Report, Jan. - Mar. 1994
Joseph H. Yuen, ed. 15 May 1994 287 p
(NASA-CR-196117; JPL-TDA-PR-42-117; NAS 1.26:196117) Avail: CASI HC A13/MF A03

This quarterly publication provides archival reports on developments in programs managed by JPL's Office of Telecommunications and Data Acquisition (TDA). In space communications, radio navigation, radio science, and ground-based radio and radar astronomy, it reports on activities of the Deep Space Network (DSN) in planning, supporting research and technology, implementation, and operations. Also included are standards activity at JPL for space data and information systems and reimbursable DSN work performed for other space agencies through NASA. The preceding work is all performed for NASA's Office of Space Communications (OSC). The TDA Office also performs work funded by other NASA program offices through and with the cooperation of OSC. Finally, tasks funded under the JPL Director's Discretionary Fund and the Caltech President's Fund that involve the TDA Office are included. For individual titles, see N94-35543 through N94-35563.

N94-35543*# Jet Propulsion Lab., California Inst. of Tech., Pasadena, CA.
THE MARS OBSERVER DIFFERENTIAL ONE-WAY RANGE DEMONSTRATION c13
P. M. Kroger, J. S. Border, and S. Nandi *In its* The Telecommunications and Data Acquisition Report 15 May 1994 p 1-15 (For primary document see N94-35542 11-32)
(RTOP 310-10-61-90-01)
Avail: CASI HC A03/MF A03

Current methods of angular spacecraft positioning using station differenced range data require an additional observation of an extragalactic radio source (quasar) to estimate the timing offset between the reference clocks at the two Deep Space Stations. The quasar observation is also used to reduce the effects of instrumental and media delays on the radio metric observable by forming a difference with the spacecraft observation (delta differential one-way range, delta DOR). An experiment has been completed using data from the Global Positioning System satellites to estimate the station clock offset, eliminating the need for the quasar observation. The requirements for direct measurement of the instrumental delays that must be made in the absence of a quasar observation are assessed. Finally, the results of the 'quasar-free' differential one-way range, or DOR, measurements of the Mars Observer spacecraft are compared with those of simultaneous conventional delta DOR measurements. Author

N94-35544*# Jet Propulsion Lab., California Inst. of Tech., Pasadena, CA.
INFLUENCE OF AN EXTERNALLY MODULATED PHOTONIC LINK ON A MICROWAVE COMMUNICATIONS SYSTEM
X. S. Yao and L. Maleki *In its* The Telecommunications and Data Acquisition Report 15 May 1994 p 16-28 (For primary document see N94-35542 11-32)
(RTOP 310-10-62-16)
Avail: CASI HC A03/MF A03

We analyze the influence of an externally modulated photonic link on the performance of a microwave communications system. From the analysis, we deduce limitations on the photocurrent, magnitude of the relaxation oscillation noise of the laser, third-order intercept point of the preamplifier, and other parameters in order for the photonic link to function according to the system specifications. Based on this, we outline a procedure for designing a photonic link that can be integrated in a system with minimal performance degradation. Author

N94-35545*# Jet Propulsion Lab., California Inst. of Tech., Pasadena, CA.
FIELD DEMONSTRATION OF X-BAND PHOTONIC ANTENNA REMOTING IN THE DEEP SPACE NETWORK
X. S. Yao, G. Lutes, R. T. Logan, Jr., and L. Maleki *In its* The Telecommunications and Data Acquisition Report 15 May 1994 p 29-34 (For primary document see N94-35542 11-32)
(RTOP 310-10-62-16)
Avail: CASI HC A02/MF A03

We designed a photonic link for antenna remoting based on our integrated system analysis. With this 12-km link, we successfully demonstrated photonic antenna-remoting capability at X-band (8.4 GHz) at one of NASA's Deep Space Stations while tracking the Magellan spacecraft. Author

N94-35546*# Jet Propulsion Lab., California Inst. of Tech., Pasadena, CA.
THE ELECTRICAL CONDUCTIVITIES OF CANDIDATE BEAM-WAVEGUIDE ANTENNA SHROUD MATERIALS
T. Y. Otoshi and M. M. Franco *In its* The Telecommunications and Data Acquisition Report 15 May 1994 p 35-41 (For primary document see N94-35542 11-32)
(RTOP 310-20-65-86-08)
Avail: CASI HC A02/MF A03

The shroud on the beam-waveguide (BWG) antenna at DSS 13 is made from highly magnetic American Society for Testing and Materials

(ASTM) A36 steel. Measurements at 8.42 GHz showed that this material (with paint) has a very poor electrical conductivity that is 600 times worse than aluminum. In cases where the BWG mirrors might be slightly misaligned, unintentional illumination and poor electrical conductivity of the shroud walls can cause system noise temperature to be increased significantly. This potential increase of noise temperature contribution can be reduced through the use of better conductivity materials for the shroud walls. An alternative is to attempt to improve the conductivity of the currently used ASTM A36 steel by means of some type of plating, surface treatment, or high-conductivity paints. This article presents the results of a study made to find improved materials for future shrouds and mirror supports. Author

N94-35547*# Jet Propulsion Lab., California Inst. of Tech., Pasadena, CA.

THIN-RIBBON TAPERED COUPLER FOR DIELECTRIC WAVEGUIDES

C. Yeh, T. Y. Otoshi, and F. I. Shimabukuro *In its* The Telecommunications and Data Acquisition Report 15 May 1994 p 42-48 (For primary document see N94-35542 11-32)
(RTOP 310-20-65-86-08)
Avail: CASI HC A02/MF A03

A recent discovery shows that a high-dielectric constant, low-loss, solid material can be made into a ribbon-like waveguide structure to yield an attenuation constant of less than 0.02 dB/m for single-mode guidance of millimeter/submillimeter waves. One of the crucial components that must be invented in order to guarantee the low-loss utilization of this dielectric-waveguide guiding system is the excitation coupler. The traditional tapered-to-a-point coupler for a dielectric rod waveguide fails when the dielectric constant of the dielectric waveguide is large. This article presents a new way to design a low-loss coupler for a high- or low-dielectric constant dielectric waveguide for millimeter or submillimeter waves. Author

N94-35548*# Jet Propulsion Lab., California Inst. of Tech., Pasadena, CA.

DESIGN AND IMPLEMENTATION OF A BEAM-WAVEGUIDE MIRROR CONTROL SYSTEM FOR VERNIER POINTING OF THE DSS-13 ANTENNA

L. S. Alvarez, M. Moore, W. Veruttipong, and E. Andres *In its* The Telecommunications and Data Acquisition Report 15 May 1994 p 49-61 (For primary document see N94-35542 11-32)
(RTOP 310-20-65-92-02)
Avail: CASI HC A03/MF A03

The design and implementation of an antenna beam-waveguide (BWG) mirror position control system at the DSS-13 34-m antenna is presented. While it has several potential applications, a positioner on the last flat-plate BWG mirror (M6) at DSS 13 is installed to demonstrate the conical scan (conscan) angle-tracking technique at the Ka-band (32-GHz) operating frequency. Radio frequency (RF) beam-scanning predictions for the M6 mirror, computed from a diffraction analysis, are presented. From these predictions, position control system requirements are then derived. The final mechanical positioner and servo system designs, as implemented at DSS 13, are illustrated with detailed design descriptions given in the appendices. Preliminary measurements of antenna Ka-band beam scan versus M6 mirror tilt made at DSS 13 in December 1993 are presented. After reduction, the initial measurements are shown to be in agreement with the RF predicts. Plans for preliminary conscan experimentation at DSS 13 are summarized. Author

N94-35549*# Jet Propulsion Lab., California Inst. of Tech., Pasadena, CA.

USE OF THE SAMPLING THEOREM TO SPEED UP NEAR-FIELD PHYSICAL OPTICS SCATTERING CALCULATIONS c74

P. W. Cramer and W. A. Imbriale *In its* The Telecommunications and Data Acquisition Report 15 May 1994 p 62-74 (For primary document see N94-35542 11-32)
(RTOP 310-20-65-89-01)
Avail: CASI HC A03/MF A03

Physical optics scattering calculations performed on the DSN 34-m beam-waveguide antennas at Ka-band (32 GHz) require approximately 12 hr of central processing unit time on a Cray Y-MP2 computer. This is excessive in terms of resource utilization and turnaround time. Typically, the calculations involve five surfaces, and the calculations are done two surfaces at a time. The sampling theorem is used to reduce the number of current values that must be calculated over the second surface by performing a physical optics integration over the first surface. The additional number of current values required on the second surface by subsequent physical optics integrations is obtained by interpolation over the original current values. Time improvements on the order of a factor of 2 to 4 were obtained for typical scattering pairs. Author

N94-35550*# Jet Propulsion Lab., California Inst. of Tech., Pasadena, CA.

DSS-13 S-/X-BAND MICROWAVE FEED SYSTEM

F. Manshadi *In its* The Telecommunications and Data Acquisition Report 15 May 1994 p 75-80 (For primary document see N94-35542 11-32)
(RTOP 310-30-69-91-05)
Avail: CASI HC A02/MF A03

The configuration, detail design, and performance of the dual S-/X-band microwave feed system for the new DSN beam-waveguide antenna, Deep Space Station (DSS) 13, are reported. By using existing spare components, reducing fabrication cost of new components by simplifying their design, and using new fabrication techniques and material, this DSS-13 feed system was implemented successfully with a small budget and a very tight schedule. Measured noise temperature gains of the feed system are 17.5 K for S-band (2200-2300 MHz) and 24.0 K for X-band (8200-8600 MHz), which agree very closely with the predicted performance. Author

N94-35551*# Jet Propulsion Lab., California Inst. of Tech., Pasadena, CA.

A 1- TO 10-GHz DOWNCONVERTER FOR HIGH-RESOLUTION MICROWAVE SURVEY

D. McWatters *In its* The Telecommunications and Data Acquisition Report 15 May 1994 p 81-91 (For primary document see N94-35542 11-32)
(RTOP 314-30-61-04-54)
Avail: CASI HC A03/MF A03

A downconverter was designed, built, and tested for the High Resolution Microwave Survey project. The input frequency range is 1 to 10 GHz with instantaneous bandwidth of 350 MHz and dynamic range of 125 dB/Hz. Requirements were derived for the local oscillators and special design techniques were implemented to achieve the high degree of spectral purity required. Author

N94-35552*# Jet Propulsion Lab., California Inst. of Tech., Pasadena, CA.

A CLOSED-LOOP TIME-ALIGNMENT SYSTEM FOR BASEBAND COMBINING

Y. Feria *In its* The Telecommunications and Data Acquisition Report 15 May 1994 p 92-109 (For primary document see N94-35542 11-32)
(RTOP 310-30-70-93-01)
Avail: CASI HC A03/MF A03

In baseband combining, the key element is the time alignment of the baseband signals. This article describes a closed-loop time-alignment system that estimates and adjusts the relative delay between two baseband signals received from two different antennas for the signals to be coherently combined. This system automatically determines which signal is advanced and delays it accordingly with a resolution of a sample period. The performance of the loop is analyzed, and the analysis is verified through simulation. The variance of the delay estimates and the signal-to-noise ratio degradation in the simulations agree with the theoretical calculations. Author

N94-35553*# Jet Propulsion Lab., California Inst. of Tech., Pasadena, CA.

CORRELATOR DATA ANALYSIS FOR THE ARRAY FEED COMPENSATION SYSTEM

B. Iijima, D. Fort, and V. Vilnrotter *In its* The Telecommunications and Data Acquisition Report 15 May 1994 p 110-118 (For primary document see N94-35542 11-32)
(RTOP 310-30-70-89-01)
Avail: CASI HC A02/MF A03

The real-time array feed compensation system is currently being evaluated at DSS 13. This system recovers signal-to-noise ratio (SNR) loss due to mechanical antenna deformations by using an array of seven Ka-band

(33.7-GHz) horns to collect the defocused signal fields. The received signals are downconverted and digitized, in-phase and quadrature samples are generated, and combining weights are applied before the samples are recombined. It is shown that when optimum combining weights are employed, the SNR of the combined signal approaches the sum of the channel SNR's. The optimum combining weights are estimated directly from the signals in each channel by the Real-Time Block 2 (RTB2) correlator; since it was designed for very-long-baseline interferometer (VLBI) applications, it can process broadband signals as well as tones to extract the required weight estimates. The estimation algorithms for the optimum combining weights are described for tones and broadband sources. Data recorded in correlator output files can also be used off-line to estimate combiner performance by estimating the SNR in each channel, which was done for data taken during a Jupiter track at DSS 13. Author

N94-35554*# California Inst. of Tech., Pasadena, CA. Dept. of Engineering.

TRACE-SHORTENED REED-SOLOMON CODES

R. J. McEliece and G. Solomon *In* JPL, The Telecommunications and Data Acquisition Report 15 May 1994 p 119-128 (For primary document see N94-35542 11-32)
(RTOP 310-30-71-83-02)
Avail: CASI HC A02/MF A03

Reed-Solomon (RS) codes have been part of standard NASA telecommunications systems for many years. RS codes are character-oriented error-correcting codes, and their principal use in space applications has been as outer codes in concatenated coding systems. However, for a given character size, say m bits, RS codes are limited to a length of, at most, 2(exp m). It is known in theory that longer character-oriented codes would be superior to RS codes in concatenation applications, but until recently no practical class of 'long' character-oriented codes had been discovered. In 1992, however, Solomon discovered an extensive class of such codes, which are now called trace-shortened Reed-Solomon (TSRS) codes. In this article, we will continue the study of TSRS codes. Our main result is a formula for the dimension of any TSRS code, as a function of its error-correcting power. Using this formula, we will give several examples of TSRS codes, some of which look very promising as candidate outer codes in high-performance coded telecommunications systems. Author

N94-35555*# Jet Propulsion Lab., California Inst. of Tech., Pasadena, CA.

MAXIMUM-LIKELIHOOD SOFT-DECISION DECODING OF BLOCK CODES USING THE A* ALGORITHM

L. Ekroot and S. Dolinar *In its* The Telecommunications and Data Acquisition Report 15 May 1994 p 129-144 (For primary document see N94-35542 11-32)
(RTOP 310-30-71-83-02)
Avail: CASI HC A03/MF A03

The A* algorithm finds the path in a finite depth binary tree that optimizes a function. Here, it is applied to maximum-likelihood soft-decision decoding of block codes where the function optimized over the codewords is the likelihood function of the received sequence given each codeword. The algorithm considers codewords one bit at a time, making use of the most reliable received symbols first and pursuing only the partially expanded codewords that might be maximally likely. A version of the A* algorithm for maximum-likelihood decoding of block codes has been implemented for block codes up to 64 bits in length. The efficiency of this algorithm makes simulations of codes up to length 64 feasible. This article details the implementation currently in use, compares the decoding complexity with that of exhaustive search and Viterbi decoding algorithms, and presents performance curves obtained with this implementation of the A* algorithm for several codes. Author

N94-35556*# Jet Propulsion Lab., California Inst. of Tech., Pasadena, CA.

BIT-WISE ARITHMETIC CODING FOR DATA COMPRESSION c61

A. B. Kiely *In its* The Telecommunications and Data Acquisition Report 15 May 1994 p 145-160 (For primary document see N94-35542 11-32)
(RTOP 310-30-71-83-04)
Avail: CASI HC A03/MF A03

This article examines the problem of compressing a uniformly quantized independent and identically distributed (IID) source. We present a new compression technique, bit-wise arithmetic coding, that assigns fixed-length codewords to the quantizer output and uses arithmetic coding to compress the codewords, treating the codeword bits as independent. We examine the performance of this method and evaluate the overhead required when used block-adaptively. Simulation results are presented for Gaussian and Laplacian sources. This new technique could be used as the entropy coder in a transform or subband coding system. Author

N94-35557*# Jet Propulsion Lab., California Inst. of Tech., Pasadena, CA.

SPACECRAFT-SPACECRAFT RADIO-METRIC TRACKING: SIGNAL ACQUISITION REQUIREMENTS AND APPLICATION TO MARS APPROACH NAVIGATION

R. D. Kahn, S. Thurman, and C. Edwards *In its* The Telecommunications and Data Acquisition Report 15 May 1994 p 161-174 (For primary document see N94-35542 11-32)
(RTOP 315-90-81-41-07)
Avail: CASI HC A03/MF A03

Doppler and ranging measurements between spacecraft can be obtained only when the ratio of the total received signal power to noise power density (P(sub t)/N(sub 0)) at the receiving spacecraft is sufficiently large that reliable signal detection can be achieved within a reasonable time period. In this article, the requirement on P(sub t)/N(sub 0) for reliable carrier signal detection is calculated as a function of various system parameters, including characteristics of the spacecraft computing hardware and a priori uncertainty in spacecraft-spacecraft relative velocity and acceleration. Also calculated is the P(sub t)/N(sub 0) requirements for reliable detection of a ranging signal, consisting of a carrier with pseudonoise (PN) phase modulation. Once the P(sub t)/N(sub 0) requirement is determined, then for a given set of assumed spacecraft telecommunication characteristics (transmitted signal power, antenna gains, and receiver noise temperatures) it is possible to calculate the maximum range at which a carrier signal or ranging signal may be acquired. For example, if a Mars lander and a spacecraft approaching Mars are each equipped with 1-m-diameter antennas, the transmitted power is 5 W, and the receiver noise temperatures are 350 K, then S-band carrier signal acquisition can be achieved at ranges exceeding 10 million km. An error covariance analysis illustrates the utility of in situ Doppler and ranging measurements for Mars approach navigation. Covariance analysis results indicate that navigation accuracies of a few km can be achieved with either data type. The analysis also illustrates dependency of the achievable accuracy on the approach trajectory velocity. Author

N94-35558*# Jet Propulsion Lab., California Inst. of Tech., Pasadena, CA.

PERFORMANCE EVALUATION OF DIGITAL PHASE-LOCKED LOOPS FOR ADVANCED DEEP SPACE TRANSPONDERS

T. M. Nguyen, S. M. Hinedi, H.-G. Yeh, and C. Kyriacou *In its* The Telecommunications and Data Acquisition Report 15 May 1994 p 175-193 (For primary document see N94-35542 11-32)
(RTOP 315-91-10-13-08)
Avail: CASI HC A03/MF A03

The performances of the digital phase-locked loops (DPLL's) for the advanced deep-space transponders (ADT's) are investigated. DPLL's considered in this article are derived from the analog phase-locked loop, which is currently employed by the NASA standard deep space transponder, using S-domain to Z-domain mapping techniques. Three mappings are used to develop digital approximations of the standard deep space analog phase-locked loop, namely the bilinear transformation (BT), impulse invariant transformation (IIT), and step invariant transformation (SIT) techniques. The performance in terms of the closed loop phase and magnitude responses, carrier tracking jitter, and response of the loop to the phase offset (the difference between in incoming phase and reference phase) is evaluated for each digital approximation. Theoretical results of the carrier tracking jitter for command-on and command-off cases are then validated by computer simulation. Both theoretical and computer simulation results show that at high sampling frequency, the DPLL's approximated by all three transformations have the same tracking jitter. However, at low sampling frequency, the digital approximation using BT outperforms the others. The minimum sampling frequency for adequate tracking performance is determined for each digital approximation of the analog loop. In addition, computer simulation shows that the DPLL developed by BT provides faster response to the phase offset than IIT and SIT. Author

N94-35559*# Jet Propulsion Lab., California Inst. of Tech., Pasadena, CA.

THE DEVELOPMENT AND APPLICATION OF COMPOSITE COMPLEXITY MODELS AND A RELATIVE COMPLEXITY METRIC IN A SOFTWARE MAINTENANCE ENVIRONMENT c61

J. M. Hops and J. S. Sherif *In its* The Telecommunications and Data Acquisition Report 15 May 1994 p 194-212 (For primary document see N94-35542 11-32)
(RTOP 314-40-41-21-03)
Avail: CASI HC A03/MF A03

A great deal of effort is now being devoted to the study, analysis, prediction, and minimization of software maintenance expected cost, long before software is delivered to users or customers. It has been estimated that, on the average, the effort spent on software maintenance is as costly as the effort spent on all other software costs. Software design methods should be the starting point to aid in alleviating the problems of software maintenance complexity and high costs. Two aspects of maintenance deserve attention: (1) protocols for locating and rectifying defects, and for ensuring that noe new defects are introduced in the development phase of the software process; and (2) protocols for modification, enhancement, and upgrading. This article focuses primarily on the second aspect, the development of protocols to help increase the quality and reduce the costs associated with modifications, enhancements, and upgrades of existing software. This study developed parsimonious models and a relative complexity metric for complexity measurement of software that were used to rank the modules in the system relative to one another. Some success was achieved in using the models and the relative metric to identify maintenance-prone modules. Author

N94-35560*# Jet Propulsion Lab., California Inst. of Tech., Pasadena, CA.

THE REAL-TIME DISPLAY OF INTERFEROMETRY DATA FOR GOLDSTONE RADAR ASTRONOMY DATA ACQUISITION c89

S. D. Howard *In its* The Telecommunications and Data Acquisition Report 15 May 1994 p 213-227 (For primary document see N94-35542 11-32)
(RTOP 314-40-52-29-26)
Avail: CASI HC A03/MF A03

A method for visualizing radar interferometry data in real time has been developed for the Goldstone radar astronomy ranging data-acquisition system. The presentation is similar in appearance to a vector field display or data-based grid. This form was selected to facilitate the recognition of characteristic patterns of local variation in the phase and magnitude of complex elements in a two-dimensional data array. The design emphasized efficiency under the demands of real-time processing and remote monitoring. The interferometry 'phase-magnitude' presentation, as it has come to be called, has been used to monitor radar interferometry experiments on three targets, beginning with the asteroid 4179 Toutatis, and continuing with Mars and Mercury. Author

N94-35561*# Jet Propulsion Lab., California Inst. of Tech., Pasadena, CA.

A NEW PRESENTATION OF COMPLEX VOLTAGE DATA FOR GOLDSTONE RADAR ASTRONOMY c89

S. D. Howard *In its* The Telecommunications and Data Acquisition Report 15 May 1994 p 228-235 (For primary document see N94-35542 11-32)
(RTOP 314-40-52-29-26)
Avail: CASI HC A02/MF A03

A presentation method similar to a vector field display or a data-based grid has been used to visualize complex voltage test data taken over multiple subchannels. Unlike simple plots of all data points on the complex plane, the position of the data in the time series is part of the presentation, providing additional information to aid in fault isolation during readiness testing. The 'phase-magnitude' presentation, as it has come to be called, was designed for the demands of real-time data acquisition and processing with remote monitoring over low bandwidth communication links. Author

N94-35562*# Jet Propulsion Lab., California Inst. of Tech., Pasadena, CA.

A 32-GHz SOLID-STATE POWER AMPLIFIER FOR DEEP SPACE COMMUNICATIONS c33

P. D. Wamhof, D. L. Rascoe, K. A. Lee, and F. S. Lansing *In its* The Telecommunications and Data Acquisition Report 15 May 1994 p 236-249 (For primary document see N94-35542 11-32)
(RTOP 315-91-50-20-02)
Avail: CASI HC A03/MF A03

A 1.5-W solid-state power amplifier (SSPA) has been demonstrated as part of an effort to develop and evaluate state-of-the-art transmitter and receiver components at 32 and 35 GHz for future deep space missions. Output power and efficiency measurements for a monolithic millimeter-wave integrated circuit (MMIC)-based SSPA are reported. Technical design details for the various modules and a thermal analysis are discussed, as well as future plans. Author

N94-35563*# Jet Propulsion Lab., California Inst. of Tech., Pasadena, CA.

THE MARS OBSERVER Ka-BAND LINK EXPERIMENT

T. A. Rebold, A. Kwok, G. E. Wood, and S. Butman *In its* The Telecommunications and Data Acquisition Report 15 May 1994 p 250-282 (For primary document see N94-35542 11-32)
(RTOP 315-91-60-10-05)
Avail: CASI HC A03/MF A03

The Ka-Band Link Experiment was the first demonstration of a deep-space communications link in the 32- to 35-GHz band (Ka-band). It was carried out using the Mars Observer spacecraft while the spacecraft was in the cruise phase of its mission and using a 34-meter beam-waveguide research and development antenna at the Goldstone complex of the DSN. The DSN has been investigating the performance benefits of a shift from X-band (8.4 GHz) to Ka-band (32 GHz) for deep-space communications. The fourfold increase in frequency is expected to offer a factor of 3 to 10 improvement (5 to 10 dB) in signal strength for a given spacecraft transmitter power and antenna size. Until recently, the expected benefits were based on performance studies, with an eye to implementing such a link, but theory was transformed to reality when a 33.7-GHz Ka-band signal was received from the spacecraft by DSS 13. This article describes the design and implementation of the Ka-Band Link Experiment from the spacecraft to the DSS-13 system, as well as results from the Ka-band telemetry demonstration, ranging demonstration, and long-term tracking experiment. Finally, a preliminary analysis of comparative X- and Ka-band tracking results is included. These results show a 4- to 7-dB advantage for Ka-band using the system at DSS 13, assuming such obstacles as antenna pointing loss and power conversion loss are overcome. Author

N94-35689 Air Force Inst. of Tech., Wright-Patterson AFB, OH. School of Engineering.

CLUSTERING TECHNIQUES IN SPEAKER RECOGNITION M.S. Thesis

Douglas N. Prescott Mar. 1994 99 p Limited Reproducibility: More than 20% of this document may be affected by microfiche quality
(AD-A278676; AFIT/GE/ENG/94M-05) Avail: Issuing Activity (Defense Technical Information Center (DTIC))

This thesis presents a comparison based on identification rate of three clustering techniques applied to cepstral features for speaker identification. LBG vector quantization as developed by Linde, Buzo and Gray, is used to provide benchmark performance for comparison with Fuzzy clustering (based on the unsupervised fuzzy partition-optimal number of classes, UFP-ONC algorithm by Gath and Geva) and an Artificial Neural Network, the Multilayer Perceptron. Cepstral features from the TIMIT, King and AFIT93 corpus speaker databases are used to produce speaker-identification classifiers using each of the clustering algorithms. The experiment reported evaluates the speaker identification performance using the 20-dimensional cepstral features which were extracted directly from the databases. The speaker databases were taken from different recording environments: TIMIT is studio quality, AFIT93 was recorded in an office environment and King is recorded telephone conversations. The performance provides an indication of merit for the clustering techniques for the range of typical recording environments. This thesis demonstrates the application of fuzzy clustering for speaker identification. It is shown that the UFP-ONC algorithm can achieve identification rates equal to the LBG vector quantization system.

LBG vector quantization provides the best overall performance of all three clustering techniques. DTIC

N94-35694 Arcon Corp., Waltham, MA.
GREEN'S FUNCTIONS FOR AN ANISOTROPIC MEDIUM: PART 1: UNBOUNDED CASE Interim Report, Jan. - Oct. 1993
Saba Mudaliar Dec. 1993 27 p Limited Reproducibility: More than 20% of this document may be affected by microfiche quality
(Contract F19628-89-C-0186; AF Proj. 4600)
(AD-A278787; RL-TR-93-264-Pt-1) Avail: Issuing Activity (Defense Technical Information Center (DTIC))

Dyadic Green's Function (DGF) for layered anisotropic media is essential for the electromagnetic field analysis of several problems. With the goal of deriving the DGF of a two-layer biaxially anisotropic medium we derive in this report the DGF of a corresponding unbounded problem. Using the Fourier transform method, an auxiliary dyadic Green's (ADGF) is first derived. The DGF is then obtained by performing a simple linear transformation on the ADGF. It is expressed in a compact dyadic form in terms of two characteristic waves, viz., the a-wave and the b-wave. Some features of the DGF are discussed by comparing our results with those of a corresponding uniaxial problem. DTIC

N94-35713 Arcon Corp., Waltham, MA.
GREEN'S FUNCTIONS FOR AN ANISOTROPIC MEDIUM. PART 2: TWO-LAYER CASE Interim Report, Jan. - Oct. 1993
Saba Mudaliar Dec. 1993 33 p Limited Reproducibility: More than 20% of this document may be affected by microfiche quality
(Contract F19628-89-C-0186; AF Proj. 4600)
(AD-A278788; RL-TR-93-265) Avail: Issuing Activity (Defense Technical Information Center (DTIC))

The Dyadic Green's Functions (DGF) of a two-layer biaxially anisotropic medium are derived. The principal coordinate system of the anisotropic medium is allowed to have arbitrary orientation with respect to the layer geometry. The formulation is based on the unbounded Dyadic Green's Function derived in Part I of the sequel. Using the matrix method the coefficients of the two-layer DGF are expressed in terms of half-space Fresnel reflection and transmission coefficients. To complete this procedure the various relevant half-space Fresnel coefficients are derived. The form in which the results are presented has a physically meaningful and compact structure. A numerical example is provided where we have computed the reflectivities. DTIC

N94-36078# Academy of Sciences (USSR), Novosibirsk (USSR). Inst. of Nuclear Physics.
INTEGRAL CHARACTERISTICS OF THE MAGNETIC BREMSSTRAHLUNG
V. N. Bajer, V. M. Katkov, and V. M. Strakhovenko 1992 15 p
(DE94-616788; IYaF-92-2) Avail: CASI HC A03/MF A01 (US Sales Only)

New representations of the total probability and total intensity of the magnetic bremsstrahlung have been obtained in frame of the quasiclassical approach in the quantum electrodynamics which have the form of the one-fold integral where the integrans contains the elementary functions only, does not contain the oscillate functions and converge rapidly. The polarization of the radiation, radiation of the polarized electrons and the radiative polarization have been considered as well. DOE

N94-36092 Connecticut Univ., Storrs, CT. Dept. of Electrical and Systems Engineering.
ESTIMATION WITH MULTISENSOR/MULTISCAN DETECTION FUSION Final Report, 1 Mar. 1993 - 1 Mar. 1994
Y. Bar-Shalom and K. R. Pattipati 4 Mar. 1994 12 p Limited Reproducibility: More than 20% of this document may be affected by microfiche quality
(Contract F49620-93-1-0164)
(AD-A278753; AFOSR-94-0251TR) Avail: Issuing Activity (Defense Technical Information Center (DTIC))

In this report we deal with the following topics: Data Association for Heterogeneous Sensors; Efficient L-D Factorization Methods for PDA, IMM and IMMPDA Filters; Tracking with Debiased Consistent Converted Measurements; Stabilization of Jump Linear Gaussian Systems; Ballistic Missile Track Initiation from Satellite Observations; Beam Pointing Control of a Monopulse Radar for Maneuvering Target Tracking; Target Tracking with Glint Noise; Image Segmentation Based on Optimal Layering for Precision Tracking; Performability Studies of AMSs with Multiple Part Types; Markov-Reward Models and Hyperbolic Systems; and Estimation and Tracking: Principles, Techniques, and Software. DTIC

N94-36096 Academy of Sciences (USSR), Kiev (USSR). Inst. for Theoretical Physics.
THE PRESSURE OF FLUCTUATIVE ELECTROMAGNETIC FIELD IN INHOMOGENEOUS MEDIUM
A. G. Zagorodnij, A. S. Usenko, and I. P. Yakimenko 1993 13 p
Submitted for publication Limited Reproducibility: More than 20% of this document may be affected by microfiche quality
(DE94-617189; ITF-93-2R) Avail: CASI HC A03 (US Sales Only)

The spectral pressure density of fluctuative electromagnetic field on the boundary of plasma half-space is obtained. It is shown that the ponderomotive force on the boundary between two transparent media is directed in the region with less value of dielectric permittivity in the case of thermodynamically equilibrium system. It is determined that the ponderomotive force has the temperature independent component. DOE

N94-36099# Academy of Sciences (USSR), Kiev (USSR). Inst. for Theoretical Physics.
THE ENERGY DENSITY OF FLUCTUATIVE ELECTROMAGNETIC FIELD NEAR THE SEMI-BOUNDED PLASMA
A. G. Zagorodnij, A. S. Usenko, and I. P. Yakimenko 1992 48 p
Submitted for publication
(DE94-617188; ITF-92-37R) Avail: CASI HC A03/MF A01 (US Sales Only)

The general relations for the correlation functions of electromagnetic field near the semi-bounded non-isothermal plasma have been obtained. The spectral energy density of electromagnetic emission of plasma half-space into the outer transparent medium is calculated with the temperature of the outer medium and the field zero-oscillations in it taken into account. DOE

N94-36112# Logicon R and D Associates, Los Angeles, CA.
WEDGE SCATTERING BY THE METHOD OF ITERATION
D. Holliday, L. L. DeRaad, Jr., and G. J. St.Cyr Jul. 1993 29 p
Prepared for LLNL, CA
(Contract W-7405-eng-48)
(DE94-010404; UCRL-CR-116204; RDA-TR-1910001-002) Avail: CASI HC A03/MF A01

We have investigated scattering from the classic wedge and have shown that the method of iteration of the surface current integral equation predicts currents and backscattered fields that are good approximations to the Sommerfeld solution. The method of iteration has also been applied to truncated wedges on flat surfaces with the result that the scattering from this wedge is seen to be very much different from the Sommerfeld solution. These results and their implications for ocean backscatter are reported herein. DOE

N94-36301# Lawrence Livermore National Lab., CA.
TSAR MODELING OF A TEM HORN AND SURROUNDING STRUCTURE
W. C. Ng and S. T. Pennock Nov. 1993 124 p
(Contract W-7405-eng-48)
(DE94-010668; UCRL-ID-115730) Avail: CASI HC A06/MF A02

Modeling of a TEM horn was performed with the TSAR FDTD electromagnetics code. The modeling was done in stages, beginning with the simplest case, the bare antenna itself. Complexity was added in the form of a dielectric lens, an enclosing cylinder, a layer of absorber inside the cylinder, resistive terminations between the horn and cylinder, and a flat plate over all, electrically separate from the cylinder. The final configuration included all of the above, plus a ring of ferrite inside the cylinder, just ahead of the horn. Predictions of the far-field were made at roughly ten degree increments, more closely spaced near boresight, in both vertical and horizontal planes, through the antenna's centerline. Time histories at those points were evaluated, and from the time histories power densities were calculated. Both time histories and power densities will be presented for the configurations modeled. DOE

N94-36316# Los Alamos National Lab., NM.
MEASUREMENTS OF SPATIAL AND FREQUENCY COHERENCE OF AN EQUATORIAL hf PATH DURING SPREAD-F
T. J. Fitzgerald, P. E. Argo, and R. C. Carlos 1993 15 p Presented at the TENERP Conference, Monterey, CA, 21-24 Jun. 1993
(Contract W-7405-eng-36)
(DE93-016615; LA-UR-93-2140; CONF-9306190-1) Avail: CASI HC A03/MF A01

In August 1990, the authors set up an hf path on the equatorial path between Maloelap Atoll and Bikini Atoll. This path, which had a range of 702 km, reflected in the ionosphere approximately 100 km north of the Altair radar location on Kwajalein. Transmitters at Maloelap broadcasted four CW tones within bandwidth of either 4 kHz, 9 kHz, or 70 kHz to be used to determine frequency coherence and also a phase-coded pseudo random sequence with a bandwidth of 60 kHz (channel probe) to be used to determine time delay spread. A spatial array of antennas was deployed at Bikini to measure spatial and frequency coherence using the CW broadcasts. The system was run in the post-sunset time period over two weeks during which almost every night showed significant degradation due to spread F resulting in rapid fading, decreased spatial and frequency coherence, and increased time delay spread. Doppler spreads of greater than 20 Hz were not uncommon, and the spatial correlation distances and frequency coherence bandwidths became so small (50 meters and 1 kHz respectively) that the experiment had to be readjusted. Measurements taken by the Altair incoherent scatter radar and the CUPRI 50 MHz coherent scatter radar indicate that although the bistatic hf channel is affected by the large scale plume structures, most of the 'damage' is done by the bottomside spread F. DOE

N94-36354# Sandia National Labs., Albuquerque, NM.
SandiaXTP, AN OBJECT-ORIENTED IMPLEMENTATION OF XTP 3.7
T. Strayer 10 May 1994 15 p
(Contract DE-AC04-76DR-00789)
(DE94-011752; SAND-94-8646) Avail: CASI HC A03/MF A01

The Xpress Transfer Protocol (XTP) is a transport layer protocol designed to provide a wide range of communication services built on the concept that orthogonal protocol mechanisms can be combined to produce appropriate paradigms within the same basic framework. Rather than using a separate protocol for each type of communication, XTP's protocol options and control of the packet exchange patterns allow the application to create appropriate paradigms such as unreliable datagrams, unreliable arbitrarily long datagrams, reliable datagrams, transactions, unreliable streams, reliable connections, and many others. Error control, flow control, and rate control are each configured to the needs of the communication. SandiaXTP is an object oriented implementation of XTP 3.7. The core of base classes used in SandiaXTP come from the Meta-Transport Library software. The SandiaXTP implementation of XTP 3.7 is a user space daemon. User's application code makes request of the daemon, and the daemon satisfies them. This User's Guide describes the installation and use of the SandiaXTP object-oriented implementation of XTP 3.7. The software package includes the full source code for the implementation, as well as many pages and appropriate documents. The fully built SandiaXTP is a user-space daemon that implements XTP 3.7. DOE

N94-36364 Department of the Navy, Washington, DC.
COLOR-CODED RADAR PLAN POSITION INDICATOR Patent
Clifford L. Temes, inventor (to Navy) and George J. Linde, inventor (to Navy) 5 Oct. 1993 7 p Filed 28 Jun. 1991 Supersedes AD-D015045
(AD-D016200; US-Patent-5,250,954; US-Patent-Appl-SN-772804; US-Patent-Class-342-181) Avail: US Patent and Trademark Office

A method to enhance target detectability on a radar plan position indicator is described which includes the receiving of coherent pulse-burst waveforms from a target so that at least one complete burst is included in each dwell of a scanning surveillance fan beam. A fast fourier transform is performed on each returned coherent burst to form Doppler channels in predetermined range cells. The largest signal of the Doppler channels in each range cell is then selected and color coded. The color coded signals are applied to a plan position indicator whereby target images are viewable. Preferably, the Doppler channels are color coded over a rainbow spectrum so that a white background is produced and target images appear as tracks on a microprocessor-based raster-type plan position indicator. A continuity test and threshold test are also utilized so that target velocity and position are determined. DTIC

N94-36366# Westinghouse Savannah River Co., Aiken, SC.
GROUNDWATER PENETRATING RADAR AND HIGH RESOLUTION SEISMIC FOR LOCATING SHALLOW FAULTS IN UNCONSOLIDATED SEDIMENTS
D. E. Wyatt and M. G. Waddell 1993 38 p
(Contract DE-AC09-89SR-18035)
(DE94-007284; WSRC-MS-93-456) Avail: CASI HC A03/MF A01

Faults in shallow, unconsolidated sediments, particularly in coastal plain settings, are very difficult to discern during subsurface exploration yet have critical impact to groundwater flow, contaminant transport and geotechnical evaluations. This paper presents a case study using cross-over geophysical technologies in an area where shallow faulting is probable and known contamination exists. A comparison is made between Wenner and dipole-dipole resistivity data, ground penetrating radar, and high resolution seismic data. Data from these methods were verified with a cone penetrometer investigation for subsurface lithology and compared to existing monitoring well data. Interpretations from these techniques are compared with actual and theoretical shallow faulting found in the literature. The results of this study suggests that (1) the CPT study, combined with the monitoring well data may suggest that discontinuities in correlatable zones may indicate that faulting is present; (2) the addition of the Wenner and dipole-dipole data may further suggest that offset zones exist in the shallow subsurface but not allow specific fault planes or fault stranding to be mapped; (3) the high resolution seismic data will image faults to within a few feet of the surface but does not have the resolution to identify the faulting on the scale of our models, however it will suggest locations for upward continuation of faulted zones; (4) offset 100 MHz and 200 MHz CMP GPR will image zones and features that may be fault planes and strands similar to our models; (5) 300 MHz GPR will image higher resolution features that may suggest the presence of deeper faults and strands; and (6) the combination of all of the tools in this study, particularly the GPR and seismic may allow for the mapping of small scale, shallow faulting in unconsolidated sediments. DOE

N94-36043*# Jet Propulsion Lab., California Inst. of Tech., Pasadena, CA.
INFORMATION AND COMMUNICATION TECHNOLOGY
Burton I. Edelson (George Washington Univ., Washington, DC.), Joseph N. Pelton (Colorado Univ., Boulder, CO.), Charles W. Bostian (Virginia Polytechnic Inst. and State Univ., Blacksburg, VA.), William T. Brandon (Mitre Corp., Bedford, MA.), Vincent W. S. Chan (Massachusetts Inst. of Tech., Cambridge.), E. Paul Hager (George Mason Univ., Fairfax, VA.), Neil R. Helm (George Washington Univ., Washington, DC.), Raymond D. Jennings (National Telecommunications and Information Administration, Washington, DC.), Robert K. Kwan, and Christoph E. Mahle et al *In* Loyola Coll., JTEC/WTEC Report and Program Summary Mar. 1994 p 45-53 Prepared in cooperation with NASA. Lewis Research Center, Cleveland, OH (For primary document see N94-36042 11-99)
Avail: CASI HC A02/MF A03

33 ELECTRONICS AND ELECTRICAL ENGINEERING

Includes test equipment and maintainability; components, e.g., tunnel diodes and transistors; microminiaturization; and integrated circuitry.

For related information see also *60 Computer Operations and Hardware* and *76 Solid-State Physics.*

N94-35249*# National Aeronautics and Space Administration. Lewis Research Center, Cleveland, OH.
EFFECTS OF COMBINED STRESSING ON THE ELECTRICAL PROPERTIES OF FILM AND CERAMIC CAPACITORS
Eric Overton, Ahmad N. Hammoud, Eric D. Baumann, and Ira T. Myers May 1994 6 p Presented at the International Symposium on Electrical Insulation, Pittsburgh, PA, 5-8 Jun. 1994; sponsored by IEEE, Dielectrics

and Electrical Insulation Society
(Contract NAS3-27186; RTOP 506-41-41)
(NASA-TM-106605; E-8881; NAS 1.15:106605) Avail: CASI HC A02/MF A01

Advanced power systems which generate, control, and distribute electrical power to many large loads are a requirement for future space exploration missions. The development of high temperature insulating materials and power components constitute a key element in systems which are lightweight, efficient, and are capable of surviving the hostile space environment. In previous work, experiments were carried out to evaluate film and ceramic capacitors for potential use in high temperature applications. The effects of thermal stressing, in air and without electrical bias, on the electrical properties of the capacitors as a function of thermal aging up to 12 weeks were determined. In this work, the combined effects of thermal aging and electrical stresses on the properties of teflon film and ceramic power capacitors were examined. The ceramic capacitors were thermally aged for 35 weeks and the teflon capacitors for 15 weeks at 200 C under full electrical bias and were characterized, on a weekly basis, in terms of their capacitance stability and electrical loss in the frequency range of 50 Hz to 100 kHz. DC leakage current measurements were also obtained. The results obtained represent the influence that short-term thermal aging and electrical bias have on the electrical properties of the power capacitors characterized. Author

N94-35270*# National Aeronautics and Space Administration. Lewis Research Center, Cleveland, OH.
REVIEW OF SLOW-WAVE STRUCTURES
Thomas M. Wallett and A. Haq Qureshi Jun. 1994 30 p
(RTOP 235-01-1C)
(NASA-TM-106639; E-8943; NAS 1.15:106639) Avail: CASI HC A03/MF A01

The majority of recent theoretical and experimental reports published in the literature dealing with helical slow-wave structures focus on the dispersion characteristics and their effects due to the finite helix wire thickness and attenuation, dielectric loading, metal loading, and the introduction of plasma. In many papers, an effective dielectric constant is used to take into account helix wire dimensions and conductivity losses, while the propagation constant of the signal and the interaction impedance of the structure are found to depend on the surface resistivity of the helix. Also, various dielectric supporting rods are simulated by one or several uniform cylinders having an effective dielectric constant, while metal vane loading and plasma effects are incorporated in the effective dielectric constant. The papers dealing with coupled cavities and folded or loaded wave guides describe equivalent circuit models, efficiency enhancement, and the prediction of instabilities for these structures. Equivalent circuit models of various structures are found using computer software programs SUPERFISH and TOUCHSTONE. Efficiency enhancement in tubes is achieved through dynamic velocity and phase adjusted tapers using computer techniques. The stability threshold of unwanted antisymmetric and higher order modes is predicted using SOS and MAGIC codes and the dependence of higher order modes on beam conductance, section length, and effective Q of a cavity is shown. Author

N94-35354# Polish Academy of Sciences, Warsaw. Inst. Podstawowych Problemow Techniki.
ON OPTIMAL PLACEMENT OF SPACERS IN BUNDLED CONDUCTORS
P. Kazimierczyk and P. Hagedorn 1994 135 p
(ISSN 0208-5658)
Avail: CASI HC A07/MF A02

The paper is devoted to the optimization of the placement of spacer-dampers in bundled conductors of overhead transmission lines. The main purpose of the spacers' use is to align individual conductors in a bundle and to assure the adequate spacing between them. At the same time, however, the spacers may provide damping which is desirable for minimizing the wind-induced vibrations. Such vibrations, via fatigue of conductors, lead to major damage and maintenance costs. Fatigue occurs mainly at the tension and suspension clamps, and also at the spacer clamps. At these points the forces applied to the conductor can, in a first approximation, be assumed as concentrated forces. In the present paper aeolian excitation due to the wind is modelled as a stationary time-and-space-dependent random field, whose spatial and temporal spectra account for yearly distributions of wind speed and turbulence. This assumption allows calculation of the mean square (MSQ) values of bending stresses at the above mentioned critical points. Fatigue accumulation theories for stationary processes provide a direct injective relation between the lifetime of a specimen and the MSQ value of loading; thus, to maximize the conductor's lifetime one should optimize the spacer-dampers as well as their placement, with regard to the maximum of the MSQ bending stresses along the span. We only deal with the optimization of the placement. The maximum of the MSQ of the bending stresses is the cost function. The vibration of conductors is modeled by the wave equation. Author (revised)

N94-35534 Newcastle-upon-Tyne Univ., Newcastle (England). Dept. of Computing Science.
HIGH LEVEL MODELLING AND DESIGN OF ASYNCHRONOUS INTERFACE LOGIC
A. V. Yakovlev, A. M. Koelmans, and L. Lavagno Nov. 1993 48 p
See also PB93-220697
(PB94-167822; TRS-460) Copyright Avail: Issuing Activity (National Technical Information Service (NTIS))

The authors propose a new methodology to design asynchronous circuits that is divided in two stages: abstract synthesis and logic synthesis. The first state is carried out by refining an abstract model, based on logic predicates describing the correct input-output behavior of the circuit, into a labelled Petri net and then into a formalization of timing diagrams (the Signal Transition Graph). This refinement involves hierarchical decomposition of the initial implementation until its size can be handled by automated logic synthesis tools, as well as replacing symbolic events occurring on the input-output ports of the labelled Petri net with up and down transitions occurring on the input-output wires of a circuit implementation. NTIS

N94-35539 Naval Postgraduate School, Monterey, CA. Dept. of Electrical and Computer Engineering.
A GALLIUM ARSENIDE MESFET OPERATIONAL AMPLIFIER FOR USE IN COMPOSITE OPERATIONAL AMPLIFIERS M.S. Thesis
Benjamin L. Hudson 16 Jun. 1994 75 p Limited Reproducibility: More than 20% of this document may be affected by microfiche quality
(AD-A277843) Avail: Issuing Activity

A gallium arsenide (GaAs) MESFET operational amplifier for use in composite operational amplifier (CNOA) configurations is described. This device is guaranteed to be suitable for construction in CNOA models. The GaAs op amp design is a general-purpose device that exhibits a low-frequency gain of approximately 32 dB and an open-loop unity gain frequency of 1.3 GHz. DTIC

N94-35564# Sandia National Labs., Albuquerque, NM.
MANUFACTURING FEASIBILITY OF SEVERAL LEAD-FREE SOLDERS FOR ELECTRONIC ASSEMBLY
A. M. Jackson (Bell Telephone Labs., Inc., Princeton, NJ.), I. Artaki (Bell Telephone Labs., Inc., Princeton, NJ.), and P. T. Vianco 1994 13 p
Presented at the 7th International Society for the Advancement of Material and Process Engineering Materials Processes Electronics Conference, Parssipany, NJ, 21-23 Jun. 1994
(Contract DE-AC04-94AL-85000)
(DE94-007732; SAND-94-0470C; CONF-940658-1) Avail: CASI HC A03/MF A01

This paper reports on a surface mount assembly evaluation with a series of existing lead-free solders. The wettability of the lead-free solders under investigation was measured by the meniscometer/wetting balance technique. This data provided an initial screening assessment of viable candidates for prototype development. Assembly process capability was based on visual, mechanical and metallurgical analyses of prototype circuit boards. The study demonstrated the feasibility of using several of the lead-free solders tested in a surface mount application and identified specific areas (e.g., paste formulation, board finishes, reflow parameters) for improving the manufacturing performance. DOE

N94-35686# Allied-Signal Aerospace Co., Kansas City, MO.
IONIC CONTAMINATION DETECTION
M. G. Benkovich Apr. 1994 22 p
(Contract DE-AC04-76DP-00613)
(DE94-010212; KCP-613-5271) Avail: CASI HC A03/MF A01

The effectiveness of Meter A and B for detecting ionic contamination was evaluated and compared on the following types of samples: (1) copper panels; (2) printed wiring boards with through-hold components (IC's); (3) printed wiring boards with surface-mounted components; and (4) mixed-technology printed wiring boards (both through-hole and surface-mount components). The extraction efficiency of the two meters was calculated. DOE

N94-35706# Allied-Signal Aerospace Co., Kansas City, MO.
THICK FILM FABRICATION OF ALUMINUM NITRIDE MICROCIRCUITS
L. H. Perdieu Mar. 1994 36 p
(Contract DE-AC04-76DP-00613)
(DE94-010107; KCP-613-5283) Avail: CASI HC A03/MF A01

A new substrate material, aluminum nitride (AIN), and 11 new thick film inks were analyzed to determine their chemical compatibility, their electrical properties, their mechanical properties, and their overall suitability for use in the manufacturing of high-power microcircuits with efficient thermal properties. Because high-power chips emit a great deal of heat in a small surface area, a new substrate material was needed to dissipate that heat faster than the substrate material currently in use. Overall, the new materials were found to be acceptable. DOE

N94-35748 Defense Advanced Research Projects Agency, Arlington, VA.
TECHNOLOGY REINVESTMENT PROJECT'S FOCUS AREA: LOW COST ELECTRONIC PACKAGING
S. Wax, M. Nash, and N. Naclerio Apr. 1994 48 p Workshop held in Denver, CO, 14 Apr. 1994 See also PB94-161148 Limited Reproducibility: More than 20% of this document may be affected by microfiche quality
(PB94-161155) Avail: Issuing Activity (National Technical Information Service (NTIS))

The mission of the Technology Reinvestment Project (TRP) is to stimulate the transition to a growing, integrated, national industrial capability that provides the most advanced, affordable military systems and the most competitive commercial products. The TRP workshop for the technology focus area titled 'Low Cost Electronic Packaging' was held April 14 in Denver, CO. The purpose of this technology focus area is to develop, demonstrate, and insert low cost packaging technologies which provide a competitive advantage in the application areas such as personal information systems, vehicle engine controls, and hand-held computers. NTIS

N94-35822 Helsinki Univ. of Technology, Espoo (Finland). Circuit Theory Lab.
BJT MODEL IN APLAC
M. Andersson and M. Valtonen 22 Dec. 1993 45 p Prepared in cooperation with Technical Research Centre of Finland, Espoo, Finland Limited Reproducibility: More than 20% of this document may be affected by microfiche quality
(ISSN 0784-5979)
(PB94-171022; CT-17; ISBN-951-22-1533-0) Avail: Issuing Activity (National Technical Information Service (NTIS))

The APLAC (An Object-Oriented Analog Circuit Simulator and Design Tool) implementation of the Bipolar Junction Transistor (BJT) device model is documented. The current and charge equations and their physical background are covered. The documentation is complete and consists of all the equations required for the implementation. NTIS

N94-36049*# National Aeronautics and Space Administration. Goddard Space Flight Center, Greenbelt, MD.
CONTROLLER FOR THE ELECTRONICALLY SCANNED THINNED ARRAY RADIOMETER (ESTAR) INSTRUMENT
Brian G. Zomberg (Grand Valley State Univ., Grand Rapids, MI.) and William A. Chren, Jr. (Grand Valley State Univ., Grand Rapids, MI.) Jun. 1994 17 p
(RTOP 740-00-00)
(NASA-TM-104608; Rept-94B00089; NAS 1.15:104608) Avail: CASI HC A03/MF A01

A prototype controller for the ESTAR (electronically scanned thinned array radiometer) instrument has been designed and tested. It manages the operation of the digital data subsystem (DDS) and its communication with the Small Explorer data system (SEDS). Among the data processing tasks that it coordinates are FEM data acquisition, noise removal, phase alignment and correlation. Its control functions include instrument calibration and testing of two critical subsystems, the output data formatter and Walsh function generator. It is implemented in a Xilinx XC3064PC84-100 field programmable gate array (FPGA) and has a maximum clocking frequency of 10 MHz. Author (revised)

N94-36054# Pacific Northwest Lab., Richland, WA.
A PROCEDURE FOR OSCILLATORY PARAMETER IDENTIFICATION
D. J. Trudnowski, M. K. Donnelly, and J. F. Hauer Feb. 1994 7 p Presented at the 1994 IEEE Winter Power Meeting, New York, NY, Feb. 1994
(Contract DE-AC06-76RL-01830)
(DE94-008047; PNL-SA-22883; CONF-940263-1) Avail: CASI HC A02/MF A01

A procedure is proposed where a power system is excited with a low-level pseduo-random probing signal and the frequency, damping, magnitude, and shape of oscillatory modes are identified using spectral density estimation and frequency-domain transfer-function identification. Attention is focussed on identifying system modes in the presence of noise. Two example cases are studied: identification of electromechanical oscillation modes in a 16-machine power system and turbine-generator shaft modes of a 3-machine power plant feeding a series-compensated 500-kV network. DOE

N94-36094# Sandia National Labs., Albuquerque, NM.
CAPILLARY FLOW SOLDERABILITY TEST FOR PRINTED WIRING BOARDS
F. M. Hosking, F. G. Yost, C. L. Hernandez, and S. J. Sackinger Apr. 1994 20 p
(Contract DE-AC04-94AL-85000)
(DE94-010321; SAND-93-3836) Avail: CASI HC A03/MF A01

This report describes a new technique for evaluating capillary flow solderability on printed circuit boards. The test involves the flow of molten solder from a pad onto different-sized conductor lines. It simulates the spreading dynamics of either plated-through-hole (PTH) or surface mount technology (SMT) soldering. A standard procedure has been developed for the test. Preliminary experiments were conducted and the results demonstrate test feasibility. Test procedures and results are presented in this report. DOE

N94-36104# Academy of Sciences (USSR), Novosibirsk (USSR). Inst. Yadernoj Fiziki.
ELECTRONICS FOR THE SND SCINTILLATION COUNTER SYSTEM
B. O. Bajbusinov, D. P. Druzhinin, and Yu. V. Usov 1992 15 p
(DE94-616453; IYaF-91-96) Avail: CASI HC A03/MF A01 (US Sales Only)

An electronic system is described for measuring the transmission time of particles through scintillation counters of the SND detector. The measurement channel contains decoupler-discriminator, time-to-digital converter, charge-to-digital converter and two delay lines. The measured time range is 60 ns, and the measurement accuracy is 200 ps. DOE

N94-36194# Superconducting Super Collider Lab., Dallas, TX.
MODELS FOR INTERPRETING INTERSTRAND RESISTANCE MEASUREMENTS IN RUTHERFORD CABLES
M. Neal and V. Kovachev Mar. 1994 5 p
(Contract DE-AC35-89ER-40486)
(DE94-010844; SSCL-666) Avail: CASI HC A01/MF A01

Variations in the quench behavior of SSC dipole magnets with the current ramp rate have led to studies of the interstrand resistance in real magnet coils. These studies involve in-situ measurements of the resistance between pairs of superconducting strands in a keystoned 30 strand Rutherford cable used in SSC dipole magnets. Collared sections slightly longer than one cable twist pitch length are removed from the magnet so that interstrand resistance between one cable twist pitch length of strands can be measured. The magnitude of these measured resistances has been found to be in most cases dependent on the number of strands in line between the input and output strands. The measured values result from current crossing from the input to the output strand along several parallel paths within the multistand cable. A resistor network model is therefore required for deducing individual contact resistances based on the measured values. The derived contact resistances can then be used to correlate ramp rate quench sensitivity behavior to magnet fabrication and design and as input values for calculating eddy current losses. DOE

N94-36197# Allied-Signal Aerospace Co., Kansas City, MO.
HIGH-SPEED DIGITAL PROJECT, HSD TEST CAPABILITY
R. E. Markley, J. L. Elarton, and C. T. Allen Apr. 1994 103 p
(Contract DE-AC04-76DP-00613)
(DE94-010885; KCP-613-5292) Avail: CASI HC A06/MF A02

Establishing a high-speed digital (HSD) test capability for the Digital Waveform Synthesizer (DWS) multichip module (MCM) has required the development of several areas: a detailed test plan for the MCM; design, fabrication and proving of the high-speed test console; and the specification, design, and development of the high-speed test and environmental conditioning interface to the DWS. These development activities have been successfully completed at the Allied Signal Inc., Kansas City Division (KCD), and the test capability described herein is currently supporting DWS MCM testing and can be adapted to similar HSD module testing. DOE

N94-36221# Brookhaven National Lab., Upton, NY.
DETERMINATION OF THE FERMI LEVEL POSITION FOR NEUTRON IRRADIATED HIGH RESISTIVITY SILICON DETECTORS AND MATERIALS USING THE TRANSIENT CHARGE TECHNIQUE (TChT)
V. Eremin and Z. Li Feb. 1994 5 p Presented at the 31st Annual International Nuclear and Space Radiation Effects Conference, Tucson, AZ, 18-22 Jul. 1994
(Contract DE-AC02-76CH-00016)
(DE94-009107; BNL-60072; CONF-940726-9) Avail: CASI HC A01/MF A01

The transient charge technique (TChT) has been used in this work to study the electrical properties in both space charge region (SCR) and electrical neutral bulk (ENB) of neutron irradiated high resistivity (4-6 k Ohm-cm) silicon particle detectors. Detectors irradiated to various neutron fluences were measured by TChT at various biases and temperatures below the room temperature. The Fermi level, obtained from the Arrhenius plot of the time constant of the slow component of the charge shape, has been found to stabilize around E(sub c) = 0.47 to 0.50 eV at high fluences (Phi(sub n) greater than 10(exp 13) n/cm(exp 2)). The resistivity of the ENB has been found greater than 300 k Ohm-cm at high fluences. DOE

N94-36245# Sandia National Labs., Albuquerque, NM.
DEMONSTRATION OF A HIGH HEAT REMOVAL CVD DIAMOND SUBSTRATE EDGE-COOLED MULTICHIP MODULE
D. W. Peterson, J. N. Sweet, D. D. Andaleon, R. F. Renzi, and D. R. Johnson 1994 7 p Presented at the International Society for Hybrid Multichip Modules, Denver, CO, 13-15 Apr. 1994
(Contract DE-AC04-94AL-85000)
(DE94-010748; SAND-93-2778C; CONF-9404118-2) Avail: CASI HC A02/MF A01

A single substrate intended for a three dimensional (3D) edge-cooled multichip module (MCM) has been built and thermally tested. The substrate, with dimensions 1.9 in. by 2 in., is mounted in a fluid cooled block at one end. To test this cooling architecture and verify the accuracy of thermal models, the authors constructed thermal test modules using alumina (Al2O3), aluminum nitride (AlN), and CVD diamond substrate materials. Each module was populated with an array of 16 Sandia ATC02 test chips with resistive heaters and temperature sensing diode thermometers. Comparative measurements of the three substrates were made in which the top row of four die were heated at 5 W each for a total of 20 W. The maximum temperature differences between the heated die and the interface with the cold chuck, Delta-T(sub js), were 24, 126, and 265 C for diamond, AlN, and alumina, respectively. Measurements on the diamond thermal test module, uniformly heated at a total power of 40 W, gave a measured junction-to-sink temperature of Delta-T(sub js) approximately equal to 18 C. This result indicates that the diamond edge-cooled substrate could dissipate a total power approximately equal to 200 W for a maximum Delta-T(sub js) approximately equal to 100 C. If multiple substrates were mounted in the fluid cooled block, spaced 0.075 in. apart, the volumetric power density would be about 880 W/in. DOE

N94-36248 Naval Command, Control and Ocean Surveillance Center, San Diego, CA. Research, Development, Technology and Evaluation Div.
THE iWarp DISPLAY MODULE Final Report, Mar. 1991 - Sep. 1993
J. J. Symanski Dec. 1993 79 p Limited Reproducibility: More than 20% of this document may be affected by microfiche quality
(NR Proj. RS3-4-J-77)
(AD-A278610; NRAD-TD-2610) Avail: Issuing Activity (Defense Technical Information Center (DTIC))

This report describes the design, fabrication, and testing of the iWarp display module. The display module is a custom circuit board designed specifically for the Intel iWarp processor. Software written during this development enables the board to generate video signals to drive a high-resolution color display, with images processed within the iWarp processor array. The module contains 4 megabytes of VRAM which will hold images of user-determined pixel depth and size. Image data are converted to analog video signals by the Inmos G364 color video controller chip. Image sizes can range from 1024 by 1024 24-bits-per-pixel true-color images to 1-bit-per-pixel monochrome images. As part of this development, several iWarp programs have been developed to aid in the use of the display. To the image processing application developer, data can be displayed with a simple one-line subroutine call. DTIC

N94-36260 Centre d'Etudes et de Recherches Bio-Physiologiques Appliquees a la Marine, Toulon (France).
SUPERCONDUCTING TRANSISTORS [TRANSISTORS SUPRACONDUCTEURS]
P. Bernstein Dec. 1992 38 p In FRENCH
(PB94-170743) Avail: Issuing Activity (National Technical Information Service (NTIS))

The report surveys the results of research, conducted primarily in Japan and the United States, on superconducting, vortex-flow, and field-effect transistors. Though the feasibility of superconducting transistors is still uncertain, the possibility of overlaying very thin, super- and non-superconducting oxide films through epitaxy may make it possible to enhance their performance. The voltage gain of field-effect transistors will remain low due to the high density of known superconducting oxide carriers. But FETs may be able to act as interfaces in some ways between superconducting and semiconductor circuits if they can rapidly switch currents. The feasibility of vortex-flow transistors has been established. Sandia group has not only achieved remarkable analog and digital electronic performances, but good production yields. However, Sandia's results have not yet been reproduced by other laboratories, and the vortex dynamics of VFTs are not fully understood, which means that noise problems are not really under control. NTIS

N94-36268 Sandia National Labs., Albuquerque, NM.
ENHANCED CHARGE TRAPPING IN BIPOLAR SPACER OXIDES DURING LOW-DOSE-RATE IRRADIATION
D. M. Fleetwood, R. A. Reber, Jr., P. S. Winokur, S. L. Kosier, R. D. Schrimpf, and R. N. Nowlin 1994 5 p Presented at the 31st Annual International Nuclear and Space Radiation Effects Conference, Tucson, AZ, 18-22 Jul. 1994 Limited Reproducibility: More than 20% of this document may be affected by microfiche quality
(Contract DE-AC04-94AL-85000)
(DE94-007863; SAND-94-0382C; CONF-940726-7) Avail: CASI HC A01

Thermally stimulated current and capacitance voltage measurements reveal enhanced hole trapping in bipolar spacer-oxide capacitors irradiated at 0 V at low dose rates. Possible mechanisms and implications for bipolar low-rate response are discussed. DOE

N94-36296 Wright Lab., Eglin AFB, FL. Armament Directorate.
AN OVERVIEW OF MULTICHIP MODULES Final Report, 1 Nov. 1993 - 28 Jan. 1994
Mickie A. Phipps Jan. 1994 40 p Limited Reproducibility: More than 20% of this document may be affected by microfiche quality
(AD-A278730; WL-TR-94-7023) Avail: Issuing Activity (Defense Technical Information Center (DTIC))

This report provides a high-level tutorial on the electronics packaging technology known as multichip modules (MCM's). The terminology associated with MCM development is explained in words which can be understood by personnel who do not have a background in electronics packaging techniques. The technology is introduced with a brief synopsis of the MCM history and market, proceeding into an in-depth discussion of interconnect substrates, known-good-die issues, chip attachment technologies, and testing/rework methods. The report concludes with a look at the fledgling industry infrastructure that supports MCM development, the high-speed chips that are used in MCM designs, the software support required, and the future of MCM's. Although by no means a comprehensive treatment of these subjects, this report provides the basics essential to an understanding of current state-of-the-art high-density electronics packaging. This information should be particularly beneficial to personnel involved in the development of miniaturized signal and data processors. DTIC

N94-36360 Spire Corp., Bedford, MA.
HIGH TEMPERATURE HETEROJUNCTION BIPOLAR TRANSISTORS Final Report, 9 Jan. 1993 - 28 Feb. 1994
H. P. Maruska 15 Apr. 1994 28 p Limited Reproducibility: More than 20% of this document may be affected by microfiche quality
(Contract DAAH04-93-C-0040)
(AD-A278605; Spire-FR-60296) Avail: CASI HC A03

The program objective was to develop deposition conditions for wide bandgap nitride semiconductors consistent with the requirements for either bipolar junction transistors or field effect transistors that can function at high speed in environments having elevated temperatures. The fundamental material for these studies was gallium nitride. We proceeded to define crystal growth parameters for preparing epitaxial thin films of InGa(1-x)N alloys which feature smaller bandgaps than GaN. To grow the nitride alloys, we used a modified metalorganic chemical vapor deposition (MOCVD) reactor which provided activated nitrogen generated as an electron cyclotron resonance microwave plasma. Samples were successfully prepared with compositions throughout the alloy series, viz, with bandgaps ranging from 1.9 eV (InN) to 3.4 eV (GaN). The films were transparent with specular surfaces, and X-ray diffraction studies showed the GaN was single crystalline with the c-axis perpendicular to the substrate. The nitride alloys varied in color from deep red to yellow. We believe that is the first report of preparing InGa(1-x)N alloys in a plasma assisted MOCVD reactor. Because we can vary the bandgap of In(x)Ga(1-x)N as desired, we can control the potential barrier between the base and emitter in a heterojunction bipolar transistor, or the spacer and the channel in a high electron mobility field effect transistor. DTIC

N94-36361 Air Force Inst. of Tech., Wright-Patterson AFB, OH. School of Engineering.
RAPID AND ACCURATE TIMING SIMULATION OF RADIATION-HARDENED DIGITAL MICROELECTRONICS USING VHDL M.S. Thesis
Charles P. Brothers, Jr. Mar. 1994 162 p Limited Reproducibility: More than 20% of this document may be affected by microfiche quality
(AD-A278644; AFIT/DS/ENG/94-01) Avail: CASI HC A08

This dissertation presents the development of a fast, accurate, timing simulation capability based on VHSIC Hardware Description Language (VHDL) without the use of back annotation of timing delay information. This VHDL-based timing simulator is intended for use with radiation-hardened microelectronics in simulating timing of circuit operation in pre-radiation, post-radiation (1 Mrad(Si) total dose), and ionizing dose radiation environments. Development of the timing models are presented. The implementation of the timing models are incorporated into a VHDL library composed of basic logic gates and flip-flops. Simulations of complex circuits were run in SPICE and VHDL to assess the timing accuracy and simulation run time of the VHDL-based timing simulator versus SPICE. Results of the simulations are presented. Final evaluation of the simulator included testing of a microprocessor control unit. In all cases, the VHDL-based simulation ran over two orders of magnitude faster than the equivalent SPICE simulation. In the pre- and post-radiation environment, accuracy estimates are usually within five percent and never exceed 12 percent. Worst-case timing estimate errors increase above 15 percent for dose rates above 1.0 x 10(exp 11) rads(Si) per second. This VHDL-based timing simulator represents an improvement over SPICE in the ability to quickly simulate complex circuits. DTIC

N94-36362# Sandia National Labs., Albuquerque, NM.
HARDNESS VARIABILITY IN COMMERCIAL AND HARDENED TECHNOLOGIES
M. R. Shaneyfelt, P. S. Winokur, T. L. Meisenheimer, F. W. Sexton, S. B. Roeske, and M. G. Knoll 1994 4 p Presented at the 31st Annual International Nuclear and Space Radiation Effects Conference, Tucson, AZ, 18-22 Jul. 1994
(Contract DE-AC04-94AL-85000)
(DE94-007270; SAND-94-0532C; CONF-940726-1) Avail: CASI HC A01/MF A01

Over the past 10 years, there have been a number of advances in methods to assess and assure the radiation hardness of microelectronics in military and space applications. At the forefront of these is the Qualified Manufacturers List (QML) methodology, in which the hardness of product is 'built-in' through statistical process control (SPC) of technology parameters relevant to the radiation response, test structure to integrated circuit (IC) correlations, and techniques for extrapolating laboratory test results to varying radiation scenarios. At the same time, there has been renewed interest in the use of commercial technology -- with its enhanced performance, reduced cost, and higher reliability -- in military and space systems. In this paper, we initially demonstrate the application of QML techniques to assure and control the radiation response of hardened technologies. Through several examples, we demonstrate intra-die, wafer-to-wafer, and lot-to-lot variations in a hardened technology. We observe 10 to 30% variations in key technology parameters that result from variability in geometry, process, and design layout. Radiation-induced degradation is seen to mirror preirradiation characteristics. We then evaluate commercial technologies and report considerably higher variability in radiation hardness, i.e., variations by a factor of two to five. This variability is shown to arise from a lack of control of technology parameters relevant to the radiation response, which a commercial manufacturer has no interest in controlling in a normal process flow. DOE

N94-36371# Sandia National Labs., Albuquerque, NM.
BOUNDING THE TOTAL-DOSE RESPONSE OF MODERN BIPOLAR TRANSISTORS
S. L. Kosier (Arizona Univ., Tucson, AZ.), A. Wei (Arizona Univ., Tucson, AZ.), R. D. Schrimpf (Arizona Univ., Tucson, AZ.), W. E. Combs (Naval Surface Warfare Center, Crane, IN.), and D. M. Fleetwood 1994 4 p Presented at the 31st Annual International Nuclear and Space Radiation Effects Conference, Tucson, AZ, 18-22 Jul. 1994
(Contract DE-AC04-94AL-85000)
(DE94-007742; SAND-94-0458C; CONF-940726-5) Avail: CASI HC A01/MF A01

The base current in modern bipolar transistors saturates at large total doses once a critical oxide charge is reached. The saturated value of base current is dose-rate independent. Testing implications are discussed. DOE

N94-36373# Sandia National Labs., Albuquerque, NM.
A CRITICAL EXAMINATION OF CHARGE FUNNELING AND ITS IMPACT ON SINGLE-EVENT UPSET IN Si DEVICES
P. E. Dodd, F. W. Sexton, and P. S. Winokur 1994 4 p Presented at the 31st Annual International Nuclear and Space Radiation Effects Conference, Tucson, AZ, 18-22 Jul. 1994
(Contract DE-AC04-94AL-85000)
(DE94-007868; SAND-94-0367C; CONF-940726-6) Avail: CASI HC A01/MF A01

Low-energy alpha particles emitted from packaging and high-energy heavy ions in space possess the capability of causing changes in memory state when incident on semiconductor memory cans and latch circuits. This phenomenon of single-event upset (SEU) is caused by collection of charge created as the particle travels through a sensitive volume of the device. As devices are continually down-sized, the corresponding decrease in amount of charge held on storage nodes increases device susceptibility to SEU. Solutions to harden devices to SEU require an in-depth understanding of the basic mechanisms responsible for upset. Also, a detailed understanding of the charge-collection volume is critical for predicting on-orbit error rates. Previous work has revealed the formation of a field funnel in response to the particle strike. Analytical models that treat the funnel in a time-averaged sense have been developed, and have been reasonably successful at predicting total collected charge for particles with low linear energy transfer (LET). Sophisticated two- and three-dimensional simulations have been used to investigate the funneling process more rigorously; however, the interplay between the funnel and collection by drift and diffusion has remained somewhat obscure. In this paper, we present an examination of fundamental charge-collection mechanisms and the role of the funnel, using advanced three-dimensional drift-diffusion modeling. We then apply the insight gained to address radiation hardness issues in light of current technology trends. DOE

N94-36430# Sandia National Labs., Albuquerque, NM.
NETWORK ANALYZER CALIBRATION FOR CRYOGENIC ON-WAFER MEASUREMENTS
V. M. Hietala, M. S. Housel, and R. B. Caldwell 1994 11 p Presented at the Atomic RF Techniques Spring Conference, San Diego, CA, 27 May 1994
(Contract DE-AC04-94AL-85000)
(DE94-010089; SAND-94-0575C; CONF-9405127-1) Avail: CASI HC A03/MF A01

A cryogenic probe station for on-wafer microwave measurements has been developed at Sandia National Laboratories to explore the basic device physics and characterize advanced components for low-temperature applications. The station was designed to operate over a temperature range of 20 to 300 K with a frequency range of DC to 50 GHz. Due to the vacuum and the low temperature environment, the use of microwave probes and the calibration of network analyzer measurements are somewhat elaborate. This paper presents guidelines for probe use and calibration in this environment. DOE

N94-35562*# Jet Propulsion Lab., California Inst. of Tech., Pasadena, CA.
A 32-GHz SOLID-STATE POWER AMPLIFIER FOR DEEP SPACE COMMUNICATIONS
P. D. Wamhof, D. L. Rascoe, K. A. Lee, and F. S. Lansing *In its* The Telecommunications and Data Acquisition Report 15 May 1994 p 236-249 (For primary document see N94-35542 11-32)
(RTOP 315-91-50-20-02)
Avail: CASI HC A03/MF A03

N94-35843*# Houston Univ., TX. Center for Superconductivity.
HIGH TEMPERATURE SUPERCONDUCTORS FOR MAGNETIC SUSPENSION APPLICATIONS
C. K. McMichael, R. S. Cooley, Q. Y. Chen, K. B. Ma, M. A. Lamb, R. L. Meng, C. W. Chu, and W. K. Chu *In* NASA. Langley Research Center, Second International Symposium on Magnetic Suspension Technology, Part 1 May 1994 p 111-118 (For primary document see N94-35836 11-18)
(Contract MDA972-90-J-1001)
Avail: CASI HC A02/MF A04

N94-35844*# Kanazawa Inst. of Tech. (Japan).
MEASUREMENT AND CHARACTERIZATION OF FORCE DYNAMICS IN HIGH T(SUB c) SUPERCONDUCTORS
Toshiro Higuchi (Tokyo Univ., Japan.), Allan J. Kelley (Tokyo Univ., Japan.), and Yukio Tsutsui (Yaskawa Electric Mfg. Co. Ltd., Kitakyushu, Japan.) *In* NASA. Langley Research Center, Second International Symposium on Magnetic Suspension Technology, Part 1 May 1994 p 119-132 (For primary document see N94-35836 11-18)
Avail: CASI HC A03/MF A04

N94-35849*# Grumman Aerospace Corp., Bethpage, NY.
SUPERCONDUCTING ELECTROMAGNETIC SUSPENSION (EMS) SYSTEM FOR GRUMMAN MAGLEV CONCEPT
Swarn S. Kalsi *In* NASA. Langley Research Center, Second International Symposium on Magnetic Suspension Technology, Part 1 May 1994 p 197-211 (For primary document see N94-35836 11-18)
(Contract DTFR53-92-C-00004)
Avail: CASI HC A03/MF A04

N94-35850*# Southern California Edison Co., Rosemead, CA.
NATIONAL MAGLEV INITIATIVE: CALIFORNIA LINE ELECTRIC UTILITY POWER SYSTEM REQUIREMENTS
Phil Save *In* NASA. Langley Research Center, Second International Symposium on Magnetic Suspension Technology, Part 1 May 1994 p 213-227 (For primary document see N94-35836 11-18)
Avail: CASI HC A03/MF A04

N94-35907*# Wisconsin Univ., Madison, WI. Center for Applied Microelectronics.
PLANAR ROTATIONAL MAGNETIC MICROMOTORS WITH INTEGRATED SHAFT ENCODER AND MAGNETIC ROTOR LEVITATION
Henry Guckel, T. R. Christenson, K. J. Skrobis, J. Klein, and M. Karnowsky *In* NASA. Langley Research Center, Second International Symposium on Magnetic Suspension Technology, Part 2 May 1994 p 501-511 (For primary document see N94-35902 11-18)
(Contract N00014-91-J-1876; NSF ECS-91-16566; NSF DMR-88-21625; SRC-88-MC-507)
Avail: CASI HC A03/MF A03

N94-35914*# Kyushu Univ., Fukuoka (Japan). Dept. of Electrical Engineering.
FEASIBILITY STUDY OF SUPERCONDUCTING LSM ROCKET LAUNCHER SYSTEM
Kinjiro Yoshida, Takaaki Ohashi, Katsuto Shiraishi, and Hiroshi Takami *In* NASA. Langley Research Center, Second International Symposium on Magnetic Suspension Technology, Part 2 May 1994 p 607-621 (For primary document see N94-35902 11-18)
Avail: CASI HC A03/MF A03

N94-35915*# Kanagawa Academy of Science and Technology, Kawasaki (Japan).
MAGNETICALLY SUSPENDED STEPPING MOTORS FOR CLEAN ROOM AND VACUUM ENVIRONMENTS
Toshiro Higuchi *In* NASA. Langley Research Center, Second International Symposium on Magnetic Suspension Technology, Part 2 May 1994 p 625-639 (For primary document see N94-35902 11-18)
Avail: CASI HC A03/MF A03

34 FLUID MECHANICS AND HEAT TRANSFER

Includes boundary layers; hydrodynamics; fluidics; mass transfer; and ablation cooling.

For related information see also *02 Aerodynamics* and *77 Thermodynamics and Statistical Physics.*

N94-35245*# National Aeronautics and Space Administration. Lyndon B. Johnson Space Center, Houston, TX.
ANALYSIS OF THE SHUTTLE ORBITER REINFORCED CARBON-CARBON OXIDATION PROTECTION SYSTEM
S. D. Williams (Lockheed Engineering and Sciences Co., Houston, TX.), Donald M. Curry, Dennis Chao, and Vuong T. Pham Jun. 1994 67 p
(NASA-TM-104792; S-763; NAS 1.15:104792) Avail: CASI HC A04/MF A01

Reusable, oxidation-protected reinforced carbon-carbon (RCC) has been successfully flown on all Shuttle Orbiter flights. Thermal testing of the silicon carbide-coated RCC to determine its oxidation characteristics has been performed in convective (plasma Arc-Jet) heating facilities. Surface sealant mass loss was characterized as a function of temperature and pressure. High-temperature testing was performed to develop coating recession correlations for predicting performance at the over-temperature flight conditions associated with abort trajectories. Methods for using these test data to establish multi-mission re-use (i.e., mission life) and single mission limits are presented. Author

N94-35248*# National Aeronautics and Space Administration. Lewis Research Center, Cleveland, OH.
INTERFACE SHAPE AND CONVECTION DURING SOLIDIFICATION AND MELTING OF SUCCINONITRILE
Henry C. deGroh, III and Tiffany Lindstrom Jun. 1994 24 p
(Grant NAG3-1446; RTOP 674-21-05)
(NASA-TM-106487; E-8474; NAS 1.15:106487) Avail: CASI HC A03/MF A01

An experimental study was conducted of the crystal growth of succinonitrile during solidification, melting, and no-growth conditions using a horizontal Bridgman furnace and square glass ampoule. For use as input boundary conditions to numerical codes, thermal profiles on the outside of the ampoule at five locations around its periphery were measured along the ampoule's length. Temperatures inside the ampoule were also measured. The shapes of the s/l interface in various two dimensional planes were quantitatively determined. Though interfaces were nondendritic and noncellular, they were not flat, but were highly curved and symmetric in only one unique longitudinal y-z plane (at x=O). The shapes of the interface were dominated by the primary longitudinal flow cell characteristic of shallow cavity flow in horizontal Bridgman; this flow cell was driven by the imposed furnace temperature gradient and caused a 'radical' thermal gradient such that the upper half of the ampoule was hotter than the bottom half. We believe that due to the strong convection, the release of latent heat does not significantly influence the thermal conditions near the interface. We hope that the interface shape and thermal data presented in this paper can be used to optimize crystal growth processes and validate numerical models. Author

N94-35250*# National Aeronautics and Space Administration. Lewis Research Center, Cleveland, OH.

EXPERIMENTAL RESULTS OF HYDROGEN SLOSH IN A 62 CUBIC FOOT (1750 LITER) TANK

Matthew E. Moran, Nancy B. McNelis, Maureen T. Kudlac, Mark S. Haberbusch, and George A. Satornino Jun. 1994 12 p Presented at the 30th Joint Propulsion Conference, Indianapolis, IN, 27-29 Jun. 1994; sponsored by AIAA, ASME, SAE, and ASEE
(Contract NAS3-25517)
(NASA-TM-106625; E-8916; NAS 1.15:106625; AIAA Paper 94-3259)
Avail: CASI HC A03/MF A01

Extensive slosh testing with liquid and slush hydrogen was conducted in a 62 cubic foot spherical tank to characterize the thermodynamic response of the system under normal gravity conditions. Slosh frequency and amplitude, pressurant type, ramp pressure, and ullage volume were parametrically varied to assess the effect of each of these parameters on the tank pressure and fluid/wall temperatures. A total of 91 liquid hydrogen and 62 slush hydrogen slosh tests were completed. Both closed tank tests and expulsions during sloshing were performed. This report presents and discusses highlights of the liquid hydrogen closed tank results in detail and introduces some general trends for the slush hydrogen tests. Summary comparisons between liquid and slush hydrogen slosh results are also presented. Author (revised)

N94-35253*# National Aeronautics and Space Administration. Lewis Research Center, Cleveland, OH.

DYNAMIC AND THERMAL TURBULENT TIME SCALE MODELLING FOR HOMOGENEOUS SHEAR FLOWS

John R. Schwab and Budugur Lakshminarayana Jun. 1994 14 p Presented at the Fluids Engineering Division Summer Meeting, Lake Tahoe, NV, 19-23 Jun. 1994; sponsored by ASME
(RTOP 505-62-52)
(NASA-TM-106635; E-8936; NAS 1.15:106635) Avail: CASI HC A03/MF A01

A new turbulence model, based upon dynamic and thermal turbulent time scale transport equations, is developed and applied to homogeneous shear flows with constant velocity and temperature gradients. The new model comprises transport equations for k, the turbulent kinetic energy; tau, the dynamic time scale; k(sub theta), the fluctuating temperature variance; and tau(sub theta), the thermal time scale. It offers conceptually parallel modeling of the dynamic and thermal turbulence at the two equation level, and eliminates the customary prescription of an empirical turbulent Prandtl number, Pr(sub t), thus permitting a more generalized prediction capability for turbulent heat transfer in complex flows and geometries. The new model also incorporates constitutive relations, based upon invariant theory, that allow the effects of nonequilibrium to modify the primary coefficients for the turbulent shear stress and heat flux. Predictions of the new model, along with those from two other similar models, are compared with experimental data for decaying homogeneous dynamic and thermal turbulence, homogeneous turbulence with constant temperature gradient, and homogeneous turbulence with constant temperature gradient and constant velocity gradient. The new model offers improvement in agreement with the data for most cases considered in this work, although it was no better than the other models for several cases where all the models performed poorly. Author (revised)

N94-35371*# National Aeronautics and Space Administration. Ames Research Center, Moffett Field, CA.

LINEAR AND NONLINEAR PATTERN SELECTION IN RAYLEIGH-BENARD STABILITY PROBLEMS

Sanford S. Davis May 1993 21 p
(RTOP 505-59-50)
(NASA-TM-104007; A-93048; NAS 1.15:104007) Avail: CASI HC A03/MF A01

A new algorithm is introduced to compute finite-amplitude states using primitive variables for Rayleigh-Benard convection on relatively coarse meshes. The algorithm is based on a finite-difference matrix-splitting approach that separates all physical and dimensional effects into one-dimensional subsets. The nonlinear pattern selection process for steady convection in an air-filled square cavity with insulated side walls is investigated for Rayleigh numbers up to 20,000. The internalization of disturbances that evolve into coherent patterns is investigated and transient solutions from linear perturbation theory are compared with and contrasted to the full numerical simulations. Author (revised)

N94-35492 Naval Research Lab., Washington, DC.

EXPERIMENTAL STUDIES OF VERY-HIGH MACH NUMBER HYDRODYNAMICS Interim Report

Jacob Grun, Charles Manka, Alfred Buckingham, and Ira Kohlberg 14 Feb. 1994 82 p Limited Reproducibility: More than 20% of this document may be affected by microfiche quality
(AD-A278761; NRL/MR/6790-94-7366) Avail: Issuing Activity (Defense Technical Information Center (DTIC))

We present results of experiments on very-high Mach number (greater than 100) shocks and very-high Mach number and Reynolds number (greater than 100, 106) turbulence. Such high Mach number hydrodynamics are initiated with a powerful laser pulse driver. We show that shocks created with a laser driver follow the Taylor-Sedov self-similar solution and scale via the Sachs scaling law just like shocks created by more traditional methods. In one experiment we examined laser-produced-shock solid-surface interactions and observed expected phenomena such as Marsh stems and triple points, and we also measured a new phenomenon termed a blast wave decursor. In second experiment we found that shocks become unstable if they propagate through a gas which has a low adiabatic index, and we measured the growth rate of the instability. In a third experiment we have shown that a high Mach number shock dramatically enhances the structure of a turbulent field through which it passes and that the shock is itself badly distorted. This result is unexpected since common wisdom has it that high Mach number shocks would self-heal as they pass through a turbulent field. DTIC

N94-35497*# Institute for Computer Applications in Science and Engineering, Hampton, VA.

ON THE NONLINEAR STABILITY OF VISCOUS MODES WITHIN THE RAYLEIGH PROBLEM ON AN INFINITE FLAT PLATE Final Report

J. C. Webb, S. R. Otto, and G. M. Lilley May 1994 41 p Submitted for publication
(Contract NAS1-19480; RTOP 505-90-52-01)
(NASA-CR-194909; NAS 1.26:194909; ICASE-94-30) Avail: CASI HC A03/MF A01

The stability has been investigated of the unsteady flow past an infinite flat plate when it is moved impulsively from rest, in its own plane. For small times the instantaneous stability of the flow depends on the linearized equations of motion which reduce in this problem to the Orr-Sommerfeld equation. It is known that the flow for certain values of Reynolds number, frequency and wave number is unstable to Tollmien-Schlichting waves, as in the case of the Blasius boundary layer flow past a flat plate. With increase in time, the unstable waves only undergo growth for a finite time interval, and this growth rate is itself a function of time. The influence of finite amplitude effects is studied by solving the full Navier-Stokes equations. It is found that the stability characteristics are markedly changed both by the consideration of the time evolution of the flow, and by the introduction of finite amplitude effects. Author

N94-35603 National Physical Lab., Teddington (England). Div. of Materials Metrology.

DETERMINATION OF EXTENSIONAL VISCOSITY FROM CAPILLARY RHEOMETER ENTRANCE PRESSURE DROP MEASUREMENTS USING A NUMERICAL SIMULATION OF CONTRACTION FLOW

M. Rides, I. A. Farah, A. R. Davies, and K. Thomas Aug. 1993 21 p Prepared in cooperation with University Coll. of Wales, Aberystwyth
(PB94-171154; DMM(A)-121) Copyright Avail: Issuing Activity (National Technical Information Service (NTIS))

A numerical model based on an augmented spectral method has been developed to simulate the flow in contraction regions of inelastic fluids which exhibit a high extensional viscosity to shear viscosity ratio. The model has been used to evaluate the use of an existing analytical model for determining extensional viscosity values. The evaluation demonstrates that the extent of agreement between the analytical and the numerical approach depended on the fluid behavior, however, the agreement was in general poor. The use of the spectral numerical contraction flow model, in place of analytical models, for determining extensional viscosity data from capillary entrance pressure drop data is shown to be an improvement on the analytical technique examined giving good agreement with experiment in the case of a DMC slurry. However, limitations in the technique have been identified for use with fiber-filled materials. Recommendations to extend the approach by using other constitutive equations in the contraction flow model and so enable application of the technique to a wider range of fluids have been made. NTIS

N94-35669# Los Alamos National Lab., NM.
AFDM: AN ADVANCED FLUID-DYNAMICS MODEL, VOLUME 6
G. Henneges, comp. and S. Kleinheins, comp. Jan. 1994 244 p
(Contract W-7405-eng-36)
(DE94-009596; LA-11692-MS-Vol-6) Avail: CASI HC A11/MF A03

This volume of the Advanced Fluid-Dynamics Model (AFDM) documents the modeling of the equation of state (EOS) in the code. The authors present an overview of the basic concepts underlying the thermodynamics modeling and resulting EOS, which is a set of relations between the thermodynamic properties of materials. The AFDM code allows for multiphase-multimaterial systems, which they explore in three phase models: two-material solid, two-material liquid, and three-material vapor. They describe and compare two ways of specifying the EOS of materials: (1) as simplified analytic expressions, or (2) as tables that precisely describe the properties of materials and their interactions for mechanical equilibrium. Either of the two EOS models implemented in AFDM can be selected by specifying the option when preprocessing the source code for compilation. Last, the authors determine thermophysical properties such as surface tension, thermal conductivities, and viscosities in the model for the intracell exchanges of AFDM. Specific notations, routines, EOS data, plots, test results, and corrections to the code are available in the appendices. DOE

N94-35681# Texas Univ., Austin, TX. Inst. for Fusion Studies.
SOLITARY WAVES AND HOMOCLINIC ORBITS
N. J. Balmforth Mar. 1994 68 p
(Contract DE-FG05-80ET-53088)
(DE94-009428; IFSR-651; DOE/ET-53088/651) Avail: CASI HC A04/MF A01

The notion that fluid motion often organizes itself into coherent structures has increasingly permeated modern fluid dynamics. Such localized objects appear in laminar flows and persist in turbulent states; from the water on windows on rainy days, to the circulations in planetary atmospheres. This review concerns solitary waves in fluids. More specifically, it centers around the mathematical description of solitary waves in a single spatial dimension. Moreover, it concentrates on strongly dissipative dynamics, rather than integrable systems like the KdV equation. One-dimensional solitary waves, or pulses and fronts as they are also called, are the simplest kinds of coherent structure (at least from a geometrical point of view). Nevertheless, their dynamics can be rich and complicated. In some circumstances this leads to the formation of spatio-temporal chaos in the systems giving birth to the solitary waves, and understanding that phenomenon is one of the major goals in the theory outlined in this review. Unfortunately, such a goal is far from achieved to date, and the author assesses its current status and incompleteness. DOE

N94-35683# Oak Ridge National Lab., TN.
PERFORMANCE ANALYSIS OF RECIPROCATING REGENERATIVE MAGNETIC HEAT PUMPING
D. T. Chen (Oak Ridge Associated Universities, Inc., TN.), R. W. Murphy, V. C. Mei, F. C. Chen, J. W. Lue, and M. S. Lubell Feb. 1994 99 p
(Contract DE-AC05-84OR-21400)
(DE94-009488; ORNL/TM-12630) Avail: CASI HC A05/MF A02

Transient flow phenomena in the regenerator tube of reciprocating magnetic heat pumps have been studied numerically and experimentally. In the numerical study, two approaches were taken: (1) solving the energy balance equations for fluid through a porous bed directly and (2) solving the Navier-Stokes equations with a buoyancy force term in the momentum equation. A flow thermal mixing problem was found in both approaches because of the piston-like motion of the regenerator tube that hinders the development of the temperature. The numerical study results show that a 45 K temperature span can be reached in 10 minutes of charge time through the use of a 7-Tesla magnetic field. Using the second numerical approach, temperature stratification in the regenerator fluid column was clearly indicated through temperature rasters. The study also calculates regenerator efficiency and energy delivery rates when heating load and cooling load are applied. Piecewise variation of the regenerator tube moving speed has been used in the present numerical study to control the mass flow rate, reduce thermal mixing of the flow and thus the regenerative losses. The gadolinium's adiabatic temperature has been measured under 6.5 Tesla of magnet field and different of operating temperatures ranging from 285 K to 320 K. Three regenerative heat pumping tests have also been conducted based on the Reynolds number of the regenerator tube flow, namely Re=300, Re=450, and Re=750 without loads. Maximum temperature span are 12 & 11 K and 9 K for the case of Re=300, Re=450 and Re=750, respectively. Experimental data are in good agreement with the numerical calculation results, and have been used to calibrate the numerical results and to develop a design database for reciprocating-type room-temperature magnetic heat pumps. DOE

N94-35690 Air Force Inst. of Tech., Wright-Patterson AFB, OH. School of Engineering.
TRANSIENT BODY FORCE EFFECTS ON THE DRYOUT AND REWET OF A HEATED CAPILLARY STRUCTURE Ph.D. Thesis
Michael K. Reagan Apr. 1994 145 p Limited Reproducibility: More than 20% of this document may be affected by microfiche quality
(AD-A278677; AFIT/DS/AA/94-1) Avail: Issuing Activity (Defense Technical Information Center (DTIC))

A transient, one-dimensional numerical code was developed to model the liquid flow in a non-uniformly heated, axial square groove. The groove was subjected to transient body forces up to approximately 0.51 m/s sq. Axial variation in meniscus levels, shear stress and heat transfer between the groove wall and the liquid, axial conduction through the liquid, evaporation and body forces were accounted for in the model. Dryout and rewet of the groove were allowed; the front location was determined using conservation of mass and linear extrapolation. A physical experiment was performed with a stainless steel plate into which eight square grooves were machined. Ethanol was used as the working liquid. One end of the plate was tilted relative to the other end and this tilt was varied with time, thereby providing the transient body force. The depth of the ethanol in the groove, and the dryout and rewet front locations, were experimentally measured. Within the uncertainty of the measurements, the numerical results from the code predicted the correct movement of liquid within the groove structure and also the correct position of the dryout and rewet fronts. DTIC

N94-35756 Westinghouse Hanford Co., Richland, WA.
HYDRODYNAMICALLY INDUCED LOADS ON COMPONENTS SUBMERGED IN HIGH-LEVEL WASTE-STORAGE TANKS
E. O. Weiner, J. L. Julyk, and M. A. Rezvani Jun. 1994 9 p Presented at the Pressure Vessel and Piping Conference, Minneapolis, 19-23 Jun. 1994 Limited Reproducibility: More than 20% of this document may be affected by microfiche quality
(Contract DE-AC06-87RL-10930)
(DE94-009663; WHC-SA-2118; CONF-940613-5) Avail: CASI HC A02

This paper addresses the effects of added mass on components submerged in fluids. In particular, as new equipment is designed for installation in the double-shell waste-storage tanks at the Hanford Site near Richland, Washington, the equipment and the tank must be evaluated for the anticipated loads. Seismically induced loads combined with loadings from other sources must be considered during this evaluation. A literature review shows that, for components in fluids confined to a narrow annulus or without a free surface, drastic reductions in response to seismic excitation are predicted by two-dimensional analysis. This phenomenon has been supported by testing. The reductions are explained in terms of mass coupling and buoyancy effects. For equipment submerged in fluids having a free surface and large annulus, practice suggest that it is appropriate to lump the added-mass terms with the component to address the hydrodynamic effects adequately. As in the case of a narrow annulus, this practice will reduce the natural frequency of the submerged component, but generally will increase the loads. This paper presents the structural evaluations of submerged components using computer models that employ mock fluid elements that determine the appropriateness of considering fluid added-mass and buoyancy effects. The results indicate that if a free surface exists and the submerged component has a wide fluid annulus about it, then the added mass should be lumped with the model, and buoyancy effects are not significant. The component then may be considered to be in an air environment, and the stresses are calculated from the application of standard response spectrum procedures. DOE

N94-35769 Sandia National Labs., Albuquerque, NM.

HYDRODYNAMICS OF MANEUVERING BODIES: LDRD FINAL REPORT

S. N. Kempka and J. H. Strickland Jan. 1994 41 p Limited Reproducibility: More than 20% of this document may be affected by microfiche quality
(Contract DE-AC04-94AL-85000)
(DE94-009970; SAND-94-0048) Avail: CASI HC A03

The objective of the 'Hydrodynamics of Maneuvering Bodies' LDRD project was to develop a Lagrangian, vorticity-based numerical simulation of the fluid dynamics associated with a maneuvering submarine. Three major tasks were completed. First, a vortex model to simulate the wake behind a maneuvering submarine was completed, assuming the flow to be inviscid and of constant density. Several simulations were performed for a dive maneuver, each requiring less than 20 cpu seconds on a workstation. The technical details of the model and the simulations are described in a separate document, but are reviewed herein. Second, a gridless method to simulate diffusion processes was developed that has significant advantages over previous Lagrangian diffusion models. In this model, viscous diffusion of vorticity is represented by moving vortices at a diffusion velocity, and expanding the vortices as specified by the kinematics for a compressible velocity field. This work was also documented previously and is only reviewed herein. The third major task completed was the development of a vortex model to describe inviscid internal wave phenomena and is the focus of this document. Internal wave phenomena in the stratified ocean can affect an evolving wake and thus, must be considered for naval applications. The vortex model for internal wave phenomena includes a new formulation for the generation of vorticity due to fluid density variations and a vortex adoption algorithm that allows solutions to be carried to much longer times than previous investigations. Since many practical problems require long-time solutions, this new adoption algorithm is a significant step toward making vortex methods applicable to practical problems. Several simulations are described and compared with previous results to validate and show the advantages of the new model. An overview of this project is also included. DOE

N94-35803 Pennsylvania State Univ., University Park, PA. Dept. of Aerospace Engineering.

THE AERODYNAMIC AND HEAT TRANSFER EFFECTS OF AN ENDWALL BOUNDARY LAYER FENCE IN A 90 DEGREE TURNING SQUARE DUCT M.S. Thesis

Dean H. Rizzo May 1994 76 p Limited Reproducibility: More than 20% of this document may be affected by microfiche quality
(AD-A278903) Avail: Issuing Activity (Defense Technical Information Center (DTIC))

This experimental study investigates the utility of boundary layer fences in turbine passage flow. Boundary layer fences have recently been reintroduced as a possible method to achieve favorable effects in turbines. Previous studies have used linear cascades which necessarily introduce a horseshoe vortex resulting from the endwall boundary layer impinging on the blade leading edge. The present study uses a curved square duct that exhibits no horseshoe vortex, but does have the characteristic passage vortices of a turning flow. The turbine passage is simulated to study the interaction effects of the boundary layer fence and the passage flow dominated by the passage vortices. Specifically, a single boundary layer fence of varying dimensions is attached to a heated endwall of the duct. The flow is fully turbulent at the inlet of the duct. Five-hole probe and liquid crystal thermography experimental techniques are used to determine the changes in the aerodynamic flowfield and the heat transfer coefficient of the heated endwall as compared to the same duct with no fence. Hotwire measurements are also presented for the description of the inlet flow field turbulence. This study adds to the currently small volume of information on fences in passage flow in several important aspects. The effect of the fence on the passage vortex is studied in a known flow configuration. The increased pressure losses of thicker (wider) fences are investigated and results show a significant dependence on fence dimensions. Liquid crystal thermography is used to obtain a high-resolution map of the endwall heat transfer coefficient for two fence configurations. DTIC

N94-35942 National Inst. of Standards and Technology, Gaithersburg, MD.

PIGGYBACK BALANCE EXPERIMENT: AN ILLUSTRATION OF ARCHIMEDES' PRINCIPLES AND NEWTON'S THIRD LAW

R. M. Schoonover Feb. 1994 13 p Limited Reproducibility: More than 20% of this document may be affected by microfiche quality
(PB94-163060; NISTIR-5377) Avail: Issuing Activity (National Technical Information Service (NTIS))

The lifting force of fluid upon an immersed body was analyzed and reported by Archimedes in the third century B.C. In these modern times many people employed in metrology find it difficult to grasp the concept of buoyancy as it applies to mass measurements. Antiquated techniques in use today propagate ignorance of the concept. The modern electronic balance makes possible a simple, educational two-balance experiment that provides the observer with a clear picture of the buoyant force and Newton's third law. The experiment, when performed carefully, yields an excellent volume determination mass and brings together the SI units of mass, length and temperature and the derived units of force, pressure and density. NTIS

N94-35945*# National Aeronautics and Space Administration. Lewis Research Center, Cleveland, OH.

A SUPERSONIC TUNNEL FOR LASER AND FLOW-SEEDING TECHNIQUES

Robert J. Bruckner and Jan Lepicovsky Jun. 1994 15 p Presented at the 12th Applied Aerodynamics Conference, Colorado Springs, CO, 20-24 Jun. 1994; sponsored by AIAA
(Contract NAS3-27186; RTOP 505-62-10)
(NASA-TM-106588; E-8852; NAS 1.15:106588; AIAA Paper 94-1825)
Avail: CASI HC A03/MF A01

A supersonic wind tunnel with flow conditions of 3 lbm/s (1.5 kg/s) at a free-stream Mach number of 2.5 was designed and tested to provide an arena for future development work on laser measurement and flow-seeding techniques. The hybrid supersonic nozzle design that was used incorporated the rapid expansion method of propulsive nozzles while it maintained the uniform, disturbance-free flow required in supersonic wind tunnels. A viscous analysis was performed on the tunnel to determine the boundary layer growth characteristics along the flowpath. Appropriate corrections were then made to the contour of the nozzle. Axial pressure distributions were measured and Mach number distributions were calculated based on three independent data reduction methods. A complete uncertainty analysis was performed on the precision error of each method. Complex shock-wave patterns were generated in the flow field by wedges mounted near the roof and floor of the tunnel. The most stable shock structure was determined experimentally by the use of a focusing schlieren system and a novel, laser based dynamic shock position sensor. Three potential measurement regions for future laser and flow-seeding studies were created in the shock structure: deceleration through an oblique shock wave of 50 degrees, strong deceleration through a normal shock wave, and acceleration through a supersonic expansion fan containing 25 degrees of flow turning. Author

N94-35948*# National Aeronautics and Space Administration. Lewis Research Center, Cleveland, OH.

COMPARISON OF PDF AND MOMENT CLOSURE METHODS IN THE MODELING OF TURBULENT REACTING FLOWS

Andrew T. Norris and Andrew T. Hsu May 1994 12 p Presented at the 30th Joint Propulsion Conference, Indianapolis, IN, 27-29 Jun. 1994; sponsored by AIAA, ASME, SAE, and ASEE
(Contracts NAS3-27186; NCC3-233; RTOP 505-90-5K)
(NASA-TM-106614; ICOMP-94-9; E-8897; NAS 1.15:106614; CMOTT-94-3; AIAA Paper 94-3356) Avail: CASI HC A03/MF A01

In modeling turbulent reactive flows, Probability Density Function (PDF) methods have an advantage over the more traditional moment closure schemes in that the PDF formulation treats the chemical reaction source terms exactly, while moment closure methods are required to model the

mean reaction rate. The common model used is the laminar chemistry approximation, where the effects of turbulence on the reaction are assumed negligible. For flows with low turbulence levels and fast chemistry, the difference between the two methods can be expected to be small. However for flows with finite rate chemistry and high turbulence levels, significant errors can be expected in the moment closure method. In this paper, the ability of the PDF method and the moment closure scheme to accurately model a turbulent reacting flow is tested. To accomplish this, both schemes were used to model a CO/H2/N2- air piloted diffusion flame near extinction. Identical thermochemistry, turbulence models, initial conditions and boundary conditions are employed to ensure a consistent comparison can be made. The results of the two methods are compared to experimental data as well as to each other. The comparison reveals that the PDF method provides good agreement with the experimental data, while the moment closure scheme incorrectly shows a broad, laminar-like flame structure.
Author

N94-35951 Arnold Engineering Development Center, Arnold AFS, TN.
NEQPAK, THE AEDC THERMOCHEMICAL NONEQUILIBRIUM PACKAGE: THEORY AND USE Final Report, Oct. 1988 - Oct. 1993
J. T. Curtis and R. W. Tramel Apr. 1994 97 p Limited Reproducibility: More than 20% of this document may be affected by microfiche quality
(AD-A279005; AEDC-TR-93-20) Avail: Issuing Activity (Defense Technical Information Center (DTIC))

NEQPAK is a set of Fortran 77 routines and databases which are useful in the development and application of nonequilibrium flow solvers. The set includes a library of subroutines for evaluating reaction rates and the thermal and transport properties of high-temperature ionized gases. Thermal nonequilibrium may be treated by applying modules which evaluate the interactions between molecular energy modes. The interactions between vibrational and chemical relaxation may be investigated by using multiple-temperature reaction models or by applying the coupling factors suggested by contemporary theories. A utility for correlating user-supplied reaction data with the material properties database is also provided. Most of the modules are optimized for use on vector-processing machines, and have been designed for the efficient use of memory. The thermal properties database covers the range from 100 to 35,000 K, and the transport properties database extends from 300 to 30,000 K. This report describes the thermophysical models embodied in NEQPAK and explains how the routines may be incorporated into hypersonic CFD codes
DTIC

N94-35975*# Institute for Computer Applications in Science and Engineering, Hampton, VA.
THE VELOCITY FIELD CREATED BY A SHALLOW BUMP IN A BOUNDARY LAYER Final Report
Michael Gaster (Cambridge Univ., Cambridge, England.), Chester E. Grosch (Old Dominion Univ., Norfolk, VA.), and Thomas L. Jackson Apr. 1994 24 p Submitted for publication
(Contract NAS1-19480; NATO-CRG-900164; RTOP 505-90-52-01)
(NASA-CR-194899; NAS 1.26:194899; ICASE-94-21) Avail: CASI HC A03/MF A01

We report the results of measurements of the disturbance velocity field generated in a boundary layer by a shallow three-dimensional bump oscillating at a very low frequency on the surface of a flat plate. Profiles of the mean velocity, the disturbance velocity at the fundamental frequency and at the first harmonic are presented. These profiles were measured both upstream and downstream of the oscillating bump. Measurements of the disturbance velocity were also made at various spanwise and downstream locations at a fixed distance from the boundary of one displacement thickness. Finally, the spanwise spectrum of the disturbances at three locations downstream of the bump are presented.
Author

N94-35976*# National Aeronautics and Space Administration. Lewis Research Center, Cleveland, OH.
BOUNDARY CONDITIONS FOR JET FLOW COMPUTATIONS
M. E. Hayder and E. Turkel Jun. 1994 18 p Presented at the 25th Fluid Dynamics Conference, Colorado Springs, CO, 20-23 Jun. 1994; sponsored by AIAA
(Contract NCC3-233; RTOP 505-90-5K)
(NASA-TM-106648; ICOMP-94-12; E-8956; NAS 1.15:106648; AIAA Paper 94-2195) Copyright Avail: CASI HC A03/MF A01

Ongoing activities are focused on capturing the sound source in a supersonic jet through careful large eddy simulation (LES). One issue that is addressed is the effect of the boundary conditions, both inflow and outflow, on the predicted flow fluctuations, which represent the sound source. In this study, we examine the accuracy of several boundary conditions to determine their suitability for computations of time-dependent flows. Various boundary conditions are used to compute the flow field of a laminar axisymmetric jet excited at the inflow by a disturbance given by the corresponding eigenfunction of the linearized stability equations. We solve the full time dependent Navier-Stokes equations by a high order numerical scheme. For very small excitations, the computed growth of the modes closely corresponds to that predicted by the linear theory. We then vary the excitation level to see the effect of the boundary conditions in the nonlinear flow regime.
Author

N94-35979# Sandia National Labs., Albuquerque, NM.
PLANE SHOCK GENERATOR EXPLOSIVE LENS: SHOCK CHARACTERIZATION OF 4340 AND PH13-8Mo STEELS, C360 BRASS AND PZT 65/35 FERRO-ELECTRIC CERAMIC
L. J. Weirick Mar. 1994 26 p
(Contract DE-AC04-94AL-85000)
(DE94-009254; SAND-93-3919) Avail: CASI HC A03/MF A01

Sandia National Laboratories is currently involved in the optimization of a Plane Shock Generator Explosive Lens (PSGEL). The PSGEL component consists of a detonator, explosive, brass cone and tamper housing. The purpose of the PSGEL component is to transmit a plane shock wave through the 4340 steel bulkhead (wave separator) which has a ferro-electric (PZT)ceramic disk attached to the opposite surface of the steel bulkhead. The planar shock wave depolarizes the PZT 65/35 ferro-electric ceramic to produce an electrical output. One aspect of the optimization program involves the possible replacement of 4340 steel with PH13-8Mo steel for the bulkhead. These materials, as well as the PZT 65/35 ferro-electric ceramic and the brass for the cone, required the stock characterization with respect to Hugoniot parameters. The work presented here gives the shock Hugoniot values for these four materials and documents their measurements.
DOE

N94-35981 Direction des Recherches et Moyens d'Essais, Paris (France). Centre de Documentation de l'Armement.
SPATIO-TEMPORAL PROPERTIES OF CENTRIFUGAL INSTABILITIES: ABSTRACTS OF 8TH COUETTE-TAYLOR MEETING
1993 152 p Conference held in Nice, France, 28-31 Mar. 1993
(PB94-150240) Avail: Issuing Activity (National Technical Information Service (NTIS))

Partial Contents: Traveling waves in finite geometries; On the linear stability of cellular spiral Couette flow; The origin of chaos in alternating spiral flow; Wavy rolls in the Taylor-Couette system and in Rayleigh-Benard convection; A comparison of normal fluid and superfluid vorticity in Taylor-Couette flow of Helium 2; The temperature dependence of the vortex instability in the Couette flow of Helium 2; A tertiary bifurcation to quasiperiodic drift flow in the Couette-Taylor problem; and A study of Nusselt number distributions in a curved channel at low Dean numbers.
NTIS

N94-35982# Lawrence Livermore National Lab., CA.
X RAY RADIOGRAPHIC IMAGING OF HYDRODYNAMIC PHENOMENA IN RADIATION DRIVEN MATERIALS: SHOCK PROPAGATION, MATERIAL COMPRESSION AND SHEAR FLOW
B. A. Hammel, J. D. Kilkenny, D. Munro, B. A. Remington, H. N. Kornblum, T. S. Perry, D. W. Phillion, and R. J. Wallace 1 Feb. 1994 29 p Presented at the Fall Meeting of the Plasma Physics Division of the American Physical Society, St. Louis, MO, 1-5 Nov. 1993 Revised
(Contract W-7405-eng-48)
(DE94-009515; UCRL-JC-114456-Rev-1; CONF-931132-3-Rev-1) Avail: CASI HC A03/MF A01

One- and two-dimensional, time resolved x ray radiographic imaging at high photon energy (5-7 keV) is used to study shock propagation, material motion and compression, and the effects of shear flow in solid density samples which are driven by x ray ablation with the Nova laser. By backlighting the samples with x rays and observing the increase in sample areal density due to shock compression, the authors directly measure the trajectory of strong shocks (approximately 40 Mbar) in flight, in solid density plastic samples. Doping a section of the samples with high-Z material (Br) provides radiographic contrast, allowing the measurement of the shock induced particle motion. Instability growth due to shear flow at an interface is investigated by imbedding a metal wire in a cylindrical plastic sample and launching a shock in the axial direction. Time resolved radiographic measurements are made with either a slit-imager coupled to an x ray streak camera or a pinhole camera coupled to a gated microchannel plate detector, providing approximately 10-(mu)m spatial and approximately 100-ps temporal resolution. DOE

N94-35992*# Institute for Computer Applications in Science and Engineering, Hampton, VA.

VORTEX TUBES IN TURBULENT FLOWS: IDENTIFICATION, REPRESENTATION, RECONSTRUCTION Final Report

David C. Banks and Bart A. Singer Apr. 1994 17 p Submitted for publication
(Contracts NAS1-19480; NAS1-19299; RTOP 505-90-52-01)
(NASA-CR-194900; NAS 1.26:194900; ICASE-94-22) Avail: CASI HC A03/MF A01

In many cases the structure of a fluid flow is well-characterized by its vortices, especially for the purpose of visualization. In this paper we present a new algorithm for identifying vortices in complex flows. The algorithm produces a skeleton line along the center of a vortex by using a two-step predictor-corrector scheme. The vorticity vector field serves as the predictor and the pressure gradient (in the perpendicular plane) serves as the corrector. We describe an economical description of the vortex tube's cross-section: a 5-term truncated Fourier series is generally sufficient, and it compresses the representation of the flow by a factor of 4000 or more. We reconstruct the vortex tubes as generalized cylinders, providing a polygonal mesh suitable for display on a graphics workstation. We show how the reconstructed geometry of vortex tubes can be enhanced to help visualize helical motion in a static image. Author

N94-35996# Sandia National Labs., Albuquerque, NM.

ANALYSIS OF A HIGH VELOCITY OXYGEN-FUEL (HVOF) THERMAL SPRAY TORCH. PART 1: NUMERICAL FORMULATION

W. L. Oberkampf and M. Talpallikar 1994 21 p Presented at the 1994 National Thermal Spray Conference, Boston, MA, 20-24 Jun. 1994
(Contract DE-AC04-94AL-85000)
(DE94-005590; SAND-93-1613C; CONF-940684-1-Pt-1) Avail: CASI HC A03/MF A01

The fluid and particle dynamics of a High Velocity Oxygen-Fuel (HVOF) torch are analyzed using computational fluid dynamic (CFD) techniques. The thermal spray device analyzed is similar to a Metco Diamond Jet torch with powder injection. The spray nozzle is axisymmetric with powder injection on the centerline, premixed fuel and oxygen fed from an annulus, and air cooling injected along the interior surface of the aircap. Choked flow conditions occur at the exit of the aircap and a supersonic, under-expanded jet develops externally. The CFD simulation assumes three injection streams (solid metal particles with argon as a carrier gas, premixed oxygen/fuel, and air) inside the aircap and solves the combusting two-phase flow until the external spray stream decays to sonic conditions. The numerical formulation solves the mass, momentum, and energy transfer for both the gas and particle phase and strongly couples each phase. The combustion process is modeled using approximate equilibrium chemistry with dissociation of the gas with a total of nine species. Melting and re-solidification of the metal particles is modeled as a lumped-mass system. Turbulent flow is modeled by a two equation k-epsilon turbulence model, including compressibility effects on turbulent dissipation. A time iterative, implicit, finite volume numerical method is used to solve the partial differential equations. A companion paper presents the results of the numerical simulation and gives a detailed discussion of the gas and particle dynamics. DOE

N94-36098# Academy of Sciences (USSR), Kiev (USSR). Inst. for Theoretical Physics.

ON POSSIBLE TYPES OF VORTEXES IN RELATIVISTIC SUPERFLUID SYSTEM

P. I. Fomin and S. I. Vilchinskij 1992 9 p Submitted for publication
(DE94-617392; ITF-92-47R) Avail: CASI HC A02/MF A01 (US Sales Only)

The superfluid, normal and temperature type vortexes in relativistic superfluid systems are considered and relation between them are discussed. DOE

N94-36111# Sandia National Labs., Albuquerque, NM.

A MULTI-TIERED WAVEFRONT SENSOR USING BINARY OPTICS

D. R. Neal, M. E. Warren, J. K. Gruetzner, T. G. Smith, R. R. Rosenthal, and T. S. McKechnie 1994 14 p Presented at the Society of Photo-Optical Instrumentation Engineers (SPIE) Conference, Kona Beach, HI, 13-18 Mar. 1994
(Contract DE-AC04-94AL-85000)
(DE94-010393; SAND-94-0577C; CONF-940391-4) Avail: CASI HC A03/MF A01

Wavefront sensors have been used to make measurements in fluid dynamics and for closed loop control of adaptive optics. In most common Shack-Hartmann wavefront sensors, the light is broken up into series of rectangular or hexagonal apertures that divide the light into a series of focal spots. The position of these focal spots is used to determine the wavefront slopes over each subaperture. Using binary optics technology, we have developed a hierarchical or fractal wavefront sensor that divides the subapertures up on a more optimal fashion. We have demonstrated this concept for up to four tiers and developed the wavefront reconstruction methods for both segmented adaptive optics and continuous wavefront measurement. DOE

N94-36313# Academy of Sciences (USSR), Kiev (USSR). Inst. for Theoretical Physics.

TAKING INTO ACCOUNT DISSIPATIVE PROCESSES IN RELATIVISTIC SUPERFLUID SYSTEMS

S. I. Vilchinskij 1992 8 p Submitted for publication
(DE94-617391; ITF-92-32R) Avail: CASI HC A02/MF A01 (US Sales Only)

We introduce the dissipative terms in the equations of relativistic superfluidity theory and show that taking into account dissipation leads to modification of second hydrodynamical theorems. DOE

N94-36314# Academy of Sciences (USSR), Kiev (USSR). Inst. for Theoretical Physics.

FIRST, SECOND AND FOURTH SOUND IN RELATIVISTIC SUPERFLUIDITY THEORY WITH ACCOUNT FOR DISSIPATIVE EFFECTS

S. Yi. Vyilchinskij 1993 8 p Submitted for publication
(DE94-617393; ITF-93-18U) Avail: CASI HC A02/MF A01 (US Sales Only)

The equations describing the propagation of the first, second and fourth sound in the relativistic theory of superfluidity are derived with account for dissipation. The expressions for the velocity of the first, second and fourth sound are obtained. DOE

N94-36315 Lawrence Livermore National Lab., CA.

A MULTILEVEL ADAPTIVE PROJECTION METHOD FOR UNSTEADY INCOMPRESSIBLE FLOW

L. H. Howell 17 May 1993 17 p Presented at the 6th Copper Mountain Conference on Multigrid Methods, Copper Mountain, CO, 4-9 Apr. 1993 Limited Reproducibility: More than 20% of this document may be affected by microfiche quality
(Contract W-7405-eng-48)
(DE93-016418; UCRL-JC-112327; CONF-9304164-1) Avail: CASI HC A03

There are two main requirements for practical simulation of unsteady flow at high Reynolds number: the algorithm must accurately propagate discontinuous flow fields without excessive artificial viscosity, and it must have some adaptive capability to concentrate computational effort where it is most needed. The first of these requirements is satisfied with a second-order Godunov method similar to those used for high-speed flows with shocks, and the second with a grid-based refinement scheme which avoids some of the drawbacks associated with unstructured meshes. These two features of the author's algorithm place certain constraints on the projection method used to enforce incompressibility. Velocities are cell-based, leading to a Laplacian stencil for the projection which decouples adjacent grid points. The author discusses features of the multigrid and multilevel iteration schemes required for solution of the resulting decoupled problem. Variable-density flows require use of a modified projection operator; a multigrid method has been found for this modified projection that successfully handles density jumps of thousands to one. Numerical results are shown for the two dimensional adaptive and three dimensional variable-density algorithms. DOE

N94-36318# Sandia National Labs., Albuquerque, NM.
APPLICATION OF HIGHER-ORDER MULTIPOINT STATISTICS TO THE IDEAL SPRAY
K. D. Marx and C. F. Edwards 1994 8 p Presented at the ICLASS 1994: International Conference on Liquid Atomization and Spray Systems, Rouen, France, 18-22 Jul. 1994
(Contract DE-AC04-76DR-00789)
(DE94-005104; SAND-94-8493C; CONF-940734-1) Avail: CASI HC A02/MF A01

Application of multipoint statistics to the analysis of sprays and other particle flows is extended in order to encompass third- and higher-order statistical information. Relation between data taken from (e.g.) phase Doppler measurements of particle arrival times and intensity function which represents a particle flow are investigated. It is shown that, at any order, the distribution of all gaps between particle arrival times has a more direct relation to the correlation functions which characterize the flow than does the distribution of sequential interparticle times. Moments of the intensity distribution are expressed in terms of the behavior of the distributions for small interparticle gaps. Examples of stochastic intensity functions are given to illustrate the significance of differences in higher-order correlations. DOE

N94-36374 Lawrence Livermore National Lab., CA.
AN EQUAL-ORDER APPROXIMATE PROJECTION FEM
P. M. Gresho, S. T. Chan, and M. Christon Feb. 1994 10 p Presented at the Computational Methods in Water Resources, Heidelberg, Germany, 19-22 Jul. 1994 Limited Reproducibility: More than 20% of this document may be affected by microfiche quality
(Contract W-7405-eng-48)
(DE94-010101; UCRL-JC-115897; CONF-940742-4) Avail: CASI HC A02

In this short paper we introduce and test a technique for solving the incompressible Navier-Stokes equations using bilinear basis functions for velocity and pressure. DOE

N94-36397*# Overset Methods, Inc., Los Altos, CA.
OVERSET GRID APPLICATIONS ON DISTRIBUTED MEMORY MIMD COMPUTERS
Kalpana Chawla and Sisira Weeratunga 30 Jun. 1994 15 p Proposed for presentation at the 33rd AIAA Aerospace Sciences Meeting and Exhibit, Reno, NV, 9-12 Jan. 1995
(Contract NCC2-806)
(NASA-CR-196081; NAS 1.26:196081; OMI-02-93) Avail: CASI HC A03/MF A01

Analysis of modern aerospace vehicles requires the computation of flowfields about complex three dimensional geometries composed of regions with varying spatial resolution requirements. Overset grid methods allow the use of proven structured grid flow solvers to address the twin issues of geometrical complexity and the resolution variation by decomposing the complex physical domain into a collection of overlapping subdomains. This flexibility is accompanied by the need for irregular intergrid boundary communication among the overlapping component grids. This study investigates a strategy for implementing such a static overset grid implicit flow solver on distributed memory, MIMD computers; i.e., the 128 node Intel iPSC/860 and the 208 node Intel Paragon. Performance data for two composite grid configurations characteristic of those encountered in present day aerodynamic analysis are also presented. Author (revised)

N94-36420*# Virginia Univ., Charlottesville, VA. Dept. of Mechanical, Aerospace and Nuclear Engineering.
ANALYSIS OF HIGH SPEED FLOW, THERMAL AND STRUCTURAL INTERACTIONS Final Report, 1 Jun. 1989 - 31 Mar. 1994
Earl A. Thornton Jun. 1994 217 p
(Grant NAG1-1013)
(NASA-CR-196017; NAS 1.26:196017; UVA/528308/MANE94/101) Avail: CASI HC A10/MF A03

Research for this grant focused on the following tasks: (1) the prediction of severe, localized aerodynamic heating for complex, high speed flows; (2) finite element adaptive refinement methodology for multi-disciplinary analyses; (3) the prediction of thermoviscoplastic structural response with rate-dependent effects and large deformations; (4) thermoviscoplastic constitutive models for metals; and (5) coolant flow/structural heat transfer analyses. Derived from text

N94-36328# Dassault Aviation, Saint-Cloud (France). Div. des Etudes Avancees.
LAMINAR FLOW STUDIES AT DASSAULT AVIATION: CALCULATIONS AND FLIGHT TESTS [ETUDES D'ECOULEMENTS LAMINAIRES CHEZ DASSAULT AVIATION: CALCULS ET ESSAIS EN VOL]
J. C. Courty, C. Bulgubure, and D. Arnal *In* AGARD, Recent Advances in Long Range and Long Endurance Operation of Aircraft Nov. 1993 14 p In FRENCH (For primary document see N94-36321 11-05)
Copyright Avail: CASI HC A03/MF A03

35 INSTRUMENTATION AND PHOTOGRAPHY

Includes remote sensors; measuring instruments and gages; detectors; cameras and photographic supplies; and holography.

For aerial photography see *43 Earth Resources and Remote Sensing.* For related information see also *06 Aircraft Instrumentation,* and *19 Spacecraft Instrumentation.*

N94-35235* National Aeronautics and Space Administration. Lyndon B. Johnson Space Center, Houston, TX.
SMART ACCELEROMETER Patent
Richard J. Bozeman, Jr., inventor (to NASA) 3 May 1994 7 p Filed 12 Feb. 1992 Supersedes N92-23545 (30 - 14, p 2378)
(NASA-Case-MSC-21951-1; US-Patent-5,309,149;
US-Patent-Appl-SN-834451; US-Patent-Class-340-683;
Int-Patent-Class-G08B-21/00) Avail: US Patent and Trademark Office

The invention discloses methods and apparatus for detecting vibrations from machines which indicate an impending malfunction for the purpose of preventing additional damage and allowing for an orderly shutdown or a change in mode of operation. The method and apparatus is especially suited for reliable operation in providing thruster control data concerning unstable vibration in an electrical environment which is typically noisy and in which unrecognized ground loops may exist.
Official Gazette of the U.S. Patent and Trademark Office

N94-35268*# National Aeronautics and Space Administration. Lewis Research Center, Cleveland, OH.
INSTRUMENTATION FOR IN-FLIGHT SSME ROCKET ENGINE PLUME SPECTROSCOPY
George C. Madzsar, Randall L. Bickford, and David B. Duncan Jun. 1994 13 p Presented at the 30th Joint Propulsion Conference, Indianapolis, IN, 27-29 Jun. 1994; sponsored by AIAA, ASME, SAE, and ASEE
(Contract NAS3-25883; RTOP 323-01-0B)
(NASA-TM-106596; E-8911; NAS 1.15:106596; AIAA Paper 94-2985)
Avail: CASI HC A03/MF A01

This paper describes instrumentation that is under development for an in-flight demonstration of a plume spectroscopy system on the space shuttle main engine. The instrumentation consists of a nozzle mounted optical probe for observation of the plume, and a spectrometer for identification and quantification of plume content. This instrumentation, which is intended for use as a diagnostic tool to detect wear and incipient failure in rocket engines, will be validated by a hardware demonstration on the Technology Test Bed engine at the Marshall Space Flight Center. Author

N94-35368* National Aeronautics and Space Administration. Langley Research Center, Hampton, VA.
ABSOLUTE CALIBRATION TECHNIQUE FOR BROADBAND ULTRASONIC TRANSDUCERS Patent
William T. Yost, inventor (to NASA) and John H. Cantrell, inventor (to NASA) 28 Jun. 1994 8 p Filed 31 Aug. 1993 Supersedes N94-29199 (32 - 8, p 3287)
(NASA-Case-LAR-14672-1; US-Patent-5,325,339;
US-Patent-Appl-SN-117511; US-Patent-Class-367-13;
Int-Patent-Class-H04B-17/00; Int-Patent-Class-G01D-18/00) Avail: US Patent and Trademark Office

Calibrating an ultrasonic transducer can be performed with a reduced number of calculations and testing. A wide-band pulser is connected to an ultrasonic transducer under test to generate ultrasonic waves in a liquid. A single frequency is transmitted to the electrostatic acoustic transducer (ESAT) and the voltage change produced is monitored. Then a broadband ultrasonic pulse is generated by the ultrasonic transducer and received by the ESAT. The output of the ESAT is amplified and input to a digitized oscilloscope for fast Fourier transform. The resulting plot is normalized with the monitored signal from the single frequency pulse. The plot is then corrected for characteristics of the membrane and diffraction effects. The transfer function of the final plot is determined. The transfer function gives the final sensitivity of the ultrasonic transducer as a function of frequency. The advantage of the system is the speed of calibrating the transducer by a reduced number of measurements and removal of the membrane and diffraction effects.

Official Gazette of the U.S. Patent and Trademark Office

N94-35369* National Aeronautics and Space Administration. Langley Research Center, Hampton, VA.

METHOD FOR MAKING A DYNAMIC PRESSURE SENSOR AND A PRESSURE SENSOR MADE ACCORDING TO THE METHOD Patent

Allan J. Zuckerwar, inventor (to NASA), William E. Robbins, inventor (to NASA), and Glenn M. Robins, inventor (to NASA) 5 Jul. 1994 8 p Filed 7 Oct. 1993 Supersedes N94-29484 (32 - 8, p 3288)
(NASA-Case-LAR-14029-1; US-Patent-5,325,720; US-Patent-Appl-SN-138046; US-Patent-Class-73-756; US-Patent-Class-29-454; US-Patent-Class-73-147; US-Patent-Class-73-715; US-Patent-Class-92-103M; Int-Patent-Class-G01L-7/08; Int-Patent-Class-G01M-9/00) Avail: US Patent and Trademark Office

A method for providing a perfectly flat top with a sharp edge on a dynamic pressure sensor using a cup-shaped stretched membrane as a sensing element is described. First, metal is deposited on the membrane and surrounding areas. Next, the side wall of the pressure sensor with the deposited metal is machined to a predetermined size. Finally, deposited metal is removed from the top of the membrane in small steps, by machining or lapping while the pressure sensor is mounted in a jig or the wall of a test object, until the true top surface of the membrane appears. A thin indicator layer having a color contrasting with the color of the membrane may be applied to the top of the membrane before metal is deposited to facilitate the determination of when to stop metal removal from the top surface of the membrane.

Official Gazette of the U.S. Patent and Trademark Office

N94-35383* National Aeronautics and Space Administration. Lewis Research Center, Cleveland, OH.

MULTIWAVELENGTH PYROMETER FOR GRAY AND NON-GRAY SURFACES IN THE PRESENCE OF INTERFERING RADIATION Patent

Daniel L. P. Ng, inventor (to NASA) 5 Jul. 1994 11 p Filed 14 Dec. 1992 Supersedes N93-17060 (31 - 5, p 1169)
(NASA-Case-LEW-15250-1; US-Patent-5,326,172; US-Patent-Appl-SN-991403; US-Patent-Class-374-126; US-Patent-Class-374-128; US-Patent-Class-374-129; US-Patent-Class-374-9; US-Patent-Class-364-557; US-Patent-Class-250-338.1; Int-Patent-Class-G01J-5/62) Avail: US Patent and Trademark Office

A method and apparatus for detecting the temperature of gray and non-gray bodies in the presence of interfering radiation are presented. A gray body has a constant emissivity less than 1 and a non-gray body has an emissivity which varies with wavelength. The emissivity and reflectivity of the surface is determined over a range of wavelengths. Spectra are also measured of the extraneous interference radiation source and the surface of the object to be measured in the presence of the extraneous interference radiation source. An auxiliary radiation source is used to determine the reflectivity of the surface and also the emissivity. The measured spectrum of the surfaces in the presence of the extraneous interference radiation source is set equal to the emissivity of the surface multiplied by a Planck function containing a temperature term T plus the surface reflectivity multiplied by the spectrum of the extraneous interference radiation source. The equation is then solved for T to determine the temperature of the surface.

Official Gazette of the U.S. Patent and Trademark Office

N94-35599 Science Research Council, Chilton (England).

BEAM TESTS OF A PROTOTYPE LEVEL-1 CALORIMETER TRIGGER FOR LHC EXPERIMENTS

I. P. Brawn, R. E. Carney, J. Garvey, R. J. Staley, and A. T. Watson Mar. 1994 22 p See also N94-18845 Sponsored by European Organization for Nuclear Research Prepared in cooperation with Rutherford Appleton Lab., Chilton, England and Westfield Coll., London, England
(PB94-170495; RAL-94-020) Avail: Issuing Activity (National Technical Information Service (NTIS))

Beam tests of a first-prototype electromagnetic calorimeter trigger processor for LHC experiments are described. The synchronous, pipelined digital processor, built with ASIC's, was successfully operated at the full LHC bunch-crossing frequency of 40 MHz. Real data signals were obtained from a liquid argon electromagnetic calorimeter. The measured performance of the electron/photon trigger algorithm is compared with Monte Carlo simulations. NTIS

N94-36061 Rutherford Appleton Lab., Chilton (England).

EXPERIMENTAL CHARACTERISATION OF GAS MICROSTRIP DETECTORS. PART 2: COUNTING RATE CHARACTERISTICS

J. E. Bateman and J. F. Connolly Dec. 1993 18 p See also Part 1, PB94-167087
(PB94-167095; RAL-93-096) Avail: Issuing Activity (Rutherford Appleton Lab., Chilton, England)

The results of a program of research into the experimental properties of gas microstrip detectors are reported. In this report, information on the counting rate characteristics of the devices is presented. NTIS

N94-36085# Commonwealth Scientific and Industrial Research Organization, Mordialoc (Australia). Div. of Atmospheric Research.

A PRECISE PASSIVE NARROW-BEAM FILTER INFRARED RADIOMETER AND ITS USE WITH LIDAR IN THE ARM PROGRAM Progress Report, 1 Jun. 1992 - 31 May 1993

C. M. R. Platt May 1993 16 p
(Contract DE-FG02-92ER-61373)
(DE94-004167; DOE/ER-61373/2) Avail: CASI HC A03/MF A01

The work done divides conveniently into two parts. First, the completion of the design and manufacture of the new narrow-beam radiometer, which occupied the period of July to December, 1992. The second part of the report concerns participation of the CSIRO Division of Atmospheric Research (DAR) Lidar/radiometer team in the ARM PROBE experiment at Kavieng, New Ireland, Papua New Guinea as part of the international TOGA COARE experiment. The DAR team participated for about one month from mid-January. The PROBE experiment allowed the new radiometer to be tested under field conditions, a test which was very successful, with very few teething problems. It is proposed during the rest of 1993 and during 1994 to make further tests with the radiometer and particularly to look at using a stirling cycle liquid nitrogen detector to obviate the need for supplies of liquid nitrogen. It is proposed further during 1994 to carry out a thorough analysis of the PROBE data and collaborate with other US PROBE participants in studying and interpreting the observations as a whole. Some further work with the new ARM radiometer will be done during the CSIRO SOCEX experiment. DOE

N94-36095# Iowa Univ., Iowa City, IA.

ULTRAFAST READOUT OF SCINTILLATING FIBERS USING UPGRADED POSITION-SENSITIVE PHOTOMULTIPLIERS

Y. Onel Jan. 1994 32 p
(Contract DE-FG02-91ER-40664)
(DE94-010419; DOE/ER-40664/T1) Avail: CASI HC A03/MF A01

Experimental results obtained with commercially available position-sensitive photomultipliers (PSPM) coupled with 0.5 mm diameter scintillating fiber arrays show some promising performances such as space resolution better than 200 (mu)m and time resolution approximately equals 1.5 ns with a detection efficiency higher than 90%. Major progress has also been recently achieved with an upgrade of a PSPM based on new grid dynode structures. Two-track spatial resolution has been studied using the upgraded PSPM. Initial studies demonstrate that two tracks separated by a minimum distance of 3mm are resolved. DOE

N94-36219 Poitiers Univ. (France). Lab. de Mecanique des Solides.
TRANSFORMATION OF A CRANZ-SCHARDIN CAMERA Final Report [TRANSFORMATION D'UNE CAMERA CRANZ-SCHARDIN]
F. Hesser, M. Cottron, and A. Lagarde Nov. 1993 27 p In FRENCH
Sponsored by Direction des Recherches, Etudes et Techniques
(PB94-170685) Avail: Issuing Activity (National Technical Information Service (NTIS))

The authors revamped a Cranz-Schardin camera to improve the monitoring of rapid dynamic phenomena such as crack growth in glass. They redesigned the flash generator to reduce flash time, and increased flash power by doubling light energy through the parallel use of two discharge devices. The timing of flashes was made more accurate and reliable, and a software program to run the control board was developed. The new camera will be used to study glass fracturing via the caustics method.
NTIS

N94-36350 Intevac, Palo Alto, CA.
STREAK TUBE PHOTOCATHODE DEVELOPMENT PROGRAM
20 Nov. 1993 20 p Prepared for Lawrence Livermore National Lab., CA Limited Reproducibility: More than 20% of this document may be affected by microfiche quality
(Contract W-7405-eng-48)
(DE94-009905; UCRL-CR-116329) Avail: CASI HC A03

This report details the progress made toward developing a streak tube with greater than 1% quantum efficiency at a wavelength of 1300 nm. The achieved performance is the result of approximately three years of effort. The goal of Phase 2 of this contract was to seal a working 1.3 (mu)m streak tube. This effort was focused in two areas. First there was a continuing effort to further develop and demonstrate the cathodes ability to meet the stated requirements. The second effort was aimed at solving the mechanical and process related problems related to sealing this cathode onto a EG&G streak tube. DOE

N94-36369# Westinghouse Idaho Nuclear Co., Inc., Idaho Falls, ID.
PORTABLE HIGH PRECISION PRESSURE TRANSDUCER SYSTEM Patent Application
T. C. Piper, inventor (to DOE), J. P. Morgan, inventor (to DOE), N. J. Marchant, inventor (to DOE), and S. M. Bolton, inventor (to DOE) 1992 16 p Filed 14 Apr. 1992
(Contract DE-AC07-84ID-12435)
(DE94-010137; US-Patent-Appl-SN-868149; Patents-US-A7868149) Avail: CASI HC A03/MF A01

A high precision pressure transducer system for checking the reliability of a second pressure transducer system used to monitor the level of a fluid confined in a holding tank is presented. Since the response of the pressure transducer is temperature sensitive, it is continually housed in a battery powered oven which is configured to provide a temperature stable environment at specified temperature for an extended period of time. Further, a high precision temperature stabilized oscillator and counter are coupled to a single board computer to accurately determine the pressure transducer oscillation frequency and convert it to an applied pressure. All of the components are powered by the batteries which during periods of availability of line power are charged by an on-board battery charger. The pressure readings outputs are transmitted to a line printer and a vacuum fluorescent display. DOE

N94-35614*# Computer Sciences Corp., Laurel, MD.
A LONG-BASELINE METHOD FOR HST GYRO DRIFT RATE BIAS CALIBRATION Abstract Only
John J. Boia, Gary L. Welter, and Martin F. Gakenheimer *In* NASA. Goddard Space Flight Center, Flight Mechanics/Estimation Theory Symposium, 1994 May 1994 p 109 (For primary document see N94-35605 11-13)
(Contract NAS5-31500)
Avail: CASI HC A01/MF A04

N94-35615*# National Aeronautics and Space Administration. Goddard Space Flight Center, Greenbelt, MD.
THE IN-FLIGHT CALIBRATION OF THE HUBBLE SPACE TELESCOPE FINE GUIDANCE SENSORS, 2 (A SUCCESS STORY)
Gary L. Welter (Computer Sciences Corp., Laurel, MD.), L. Abramowicz-Reed (Hughes Danbury Optical Systems, Inc., CT.), A. Guha (AKG, Inc., MN.), L. Hallock, and E. Kimmer *In its* Flight Mechanics/Estimation Theory Symposium, 1994 May 1994 p 111-122 (For primary document see N94-35605 11-13)
(Contracts NAS5-31500; NAS5-31786; NAS5-31000)
Avail: CASI HC A03/MF A04

N94-35616*# National Aeronautics and Space Administration. Goddard Space Flight Center, Greenbelt, MD.
IN-FLIGHT ESTIMATION OF GYRO NOISE ON THE UPPER ATMOSPHERE RESEARCH SATELLITE (UARS) AND EXTREME ULTRAVIOLET EXPLORER (EUVE) MISSIONS
M. Lee, P. Crouse, R. Harman, Terry Leid, W. Davis, and S. Underwood *In its* Flight Mechanics/Estimation Theory Symposium, 1994 May 1994 p 123-137 (For primary document see N94-35605 11-13)
(Contract NAS5-32500)
Avail: CASI HC A03/MF A04

N94-35854*# National Aerospace Lab., Tokyo (Japan).
STATUS OF MSBS STUDY AT NAL
Hideo Sawada, Hisashi Suenaga, Takayuki Suzuki, and Nobukazu Ikeda *In* NASA. Langley Research Center, Second International Symposium on Magnetic Suspension Technology, Part 1 May 1994 p 275-289 (For primary document see N94-35836 11-18)
Avail: CASI HC A03/MF A04

N94-35856*# National Cheng Kung Univ., Tainan (Taiwan). Inst. of Aeronautics and Astronautics.
A DYNAMIC METHOD FOR MAGNETIC TORQUE MEASUREMENT
C. E. Lin and H. L. Jou *In* NASA. Langley Research Center, Second International Symposium on Magnetic Suspension Technology, Part 1 May 1994 p 307-315 (For primary document see N94-35836 11-18)
(Contract NSC81-0424-E005-040)
Avail: CASI HC A02/MF A04

N94-35860*# Old Dominion Univ., Norfolk, VA. Dept. of Aerospace Engineering.
SOME FURTHER DEVELOPMENTS IN THE DYNAMIC MODELLING AND CONTROL OF THE LARGE ANGLE MAGNETIC SUSPENSION TEST FIXTURE
Colin P. Britcher and Lucas E. Foster *In* NASA. Langley Research Center, Second International Symposium on Magnetic Suspension Technology, Part 1 May 1994 p 367-388 (For primary document see N94-35836 11-18)
(Grant NAG1-1056)
Avail: CASI HC A03/MF A04

N94-35904*# SatCon Technology Corp., Cambridge, MA.
SUPERCONDUCTING REBALANCE ACCELERATION AND RATE SENSOR
R. Torti, M. Gerver, V. Gondhalekar, and B. Maxwell *In* NASA. Langley Research Center, Second International Symposium on Magnetic Suspension Technology, Part 2 May 1994 p 451-464 (For primary document see N94-35902 11-18)
Avail: CASI HC A03/MF A03

N94-35908*# SatCon Technology Corp., Cambridge, MA.
ELECTROSTATICALLY SUSPENDED AND SENSED MICRO-MECHANICAL RATE GYROSCOPE
R. Torti, M. Gerver, V. Gondhalekar, S. Bart, and B. Maxwell *In* NASA. Langley Research Center, Second International Symposium on Magnetic Suspension Technology, Part 2 May 1994 p 513-525 (For primary document see N94-35902 11-18)
Avail: CASI HC A03/MF A03

36 LASERS AND MASERS

Includes parametric amplifiers.
For related information see also *76 Solid-State Physics.*

N94-35351# Sandia National Labs., Albuquerque, NM.
LASER DRILLING OF VERTICAL VIAS IN SILICON

W. D. Miller, R. A. Gassman, and D. M. Keicher Aug. 1993 22 p
(Contract DE-AC04-94AL-85000)
(DE94-009250; SAND-93-1772) Avail: CASI HC A03/MF A01

Any advance beyond the density of standard 2D Multichip Modules (MCM) will require a vertical interconnect technology that can produce reliable area array interconnection with small feature sizes. Laser drilled vertical vias have been controllably produced in standard silicon (Si) wafers down to 0.035mm (0.0014 inches) in diameter. Several laser systems and their system parameters have been explored to determine the optimum parametric set for repeatable vias in Si. The vias produced have exhibited clean smooth interior surfaces with an aspect ratio of up to 20:1 with little or no taper. All laser systems used, their system parameters, design modifications, theory of operation, and drilling results are discussed. DOE

N94-35488*# Rochester Inst. of Tech., NY. Center for Imaging Science.
HIGH POWER DIODE LASER MASTER OSCILLATOR-POWER AMPLIFIER (MOPA) Final Technical Report
John R. Andrews (Xerox Webster Research Center, NY.), P. Mouroulis, and G. Wicks 15 Jun. 1994 137 p
(Grant NAG1-1147)
(NASA-CR-196095; NAS 1.26:196095) Avail: CASI HC A07/MF A02

High power multiple quantum well AlGaAs diode laser master oscillator - power amplifier (MOPA) systems were examined both experimentally and theoretically. For two pass operation, it was found that powers in excess of 0.3 W per 100 micrometers of facet length were achievable while maintaining diffraction-limited beam quality. Internal electrical-to-optical conversion efficiencies as high as 25 percent were observed at an internal amplifier gain of 9 dB. Theoretical modeling of multiple quantum well amplifiers was done using appropriate rate equations and a heuristic model of the carrier density dependent gain. The model gave a qualitative agreement with the experimental results. In addition, the model allowed exploration of a wider design space for the amplifiers. The model predicted that internal electrical-to-optical conversion efficiencies in excess of 50 percent should be achievable with careful system design. The model predicted that no global optimum design exists, but gain, efficiency, and optical confinement (coupling efficiency) can be mutually adjusted to meet a specific system requirement. A three quantum well, low optical confinement amplifier was fabricated using molecular beam epitaxial growth. Coherent beam combining of two high power amplifiers injected from a common master oscillator was also examined. Coherent beam combining with an efficiency of 93 percent resulted in a single beam having diffraction-limited characteristics. This beam combining efficiency is a world record result for such a system. Interferometric observations of the output of the amplifier indicated that spatial mode matching was a significant factor in the less than perfect beam combining. Finally, the system issues of arrays of amplifiers in a coherent beam combining system were investigated. Based upon experimentally observed parameters coherent beam combining could result in a megawatt-scale coherent beam with a 10 percent electrical-to-optical conversion efficiency. Author

N94-35489*# California Univ., San Diego, CA. Dept. of Applied Mechanics and Engineering Sciences.
MONOLITH CATALYSTS FOR CLOSED-CYCLE CARBON DIOXIDE LASERS Final Report, period ending 31 Mar. 1994
Richard K. Herz 1994 50 p Submitted for publication
(Grant NAG1-1051)
(NASA-CR-196093; NAS 1.26:196093) Avail: CASI HC A03/MF A01

The general subject area of the project involved the development of solid catalysts that have high activity at low temperature for the oxidation of gases such as CO. The original application considered was CO oxidation in closed-cycle CO2 lasers. The scope of the project was subsequently extended to include oxidation of gases in addition to CO and applications such as air purification and exhaust gas emission control. The primary objective of the final phase grant was to develop design criteria for the formulation of new low-temperature oxidation catalysts utilizing Monte Carlo simulations of reaction over NASA-developed catalysts. Author (revised)

N94-35586 Science Research Lab., Inc., Somerville, MA.
ADVANCED INDUCTION ACCELERATOR DESIGNS FOR GROUND BASED AND SPACE BASED FELs Final Report, 1 May 1990 - 30 Apr. 1994
Daniel Birx 30 Apr. 1994 138 p Limited Reproducibility: More than 20% of this document may be affected by microfiche quality
(Contract N00014-90-C-0099)
(AD-A278885; SRL-04-F-1994) Avail: Issuing Activity (Defense Technical Information Center (DTIC))

The primary goal of this program was to improve the performance of induction accelerators with particular regards to their being used to drive Free Electron Lasers (FEL's). It is hoped that FEL's operating at visible wavelengths might someday be used to beam power from earth to extraterrestrial locations. One application of this technology might be strategic theater defense, but this power source might be used to propel vehicles or supplement solar energized systems. Our path toward achieving this goal was directed first toward optimization of the nonlinear magnetic material used in induction accelerator construction and secondly at the overall design in terms of cost, size and efficiency. We began this research effort with an in depth study into the properties of various nonlinear magnetic materials. With the data on nonlinear magnetic materials, so important to the optimization of efficiency, in hand, we envisioned a new induction accelerator design where all of the components were packaged together in one container. This induction accelerator module would combine an /ll-solid-state, nonlinear magnetic driver and the induction accelerator cells all in one convenient package. Each accelerator module (denoted SNOMAD-IVB) would produce 1.0 MeV of acceleration with the exception of the SNOMAD-IV injector module which would produce 0.5 MeV of acceleration for an electron beam current up to 1000 amperes. DTIC

N94-35665# Lawrence Livermore National Lab., CA.
IMPROVED PERFORMANCE OF HIGH AVERAGE POWER SEMICONDUCTOR ARRAYS FOR APPLICATIONS IN DIODE PUMPED SOLID STATE LASERS
R. Beach, M. Emanuel, W. Benett, B. Freitas, D. Ciarlo, N. Carlson, S. Sutton, J. Skidmore, and R. Solarz Jan. 1994 30 p Presented at the OE/LASE 1994: Conference on Optics, Electro-Optics, and Laser Applications in Science and Engineering, Los Angeles, CA, 22-29 Jan. 1994
(Contract W-7405-eng-48)
(DE94-009516; UCRL-JC-116059; CONF-940142-33) Avail: CASI HC A03/MF A01

The average power performance capability of semiconductor diode laser arrays has improved dramatically over the past several years. These performance improvements, combined with cost reductions pursued by LLNL and others in the fabrication and packaging of diode lasers, have continued to reduce the price per average watt of laser diode radiation. Presently, we are at the point where the manufacturers of commercial high average power solid state laser systems used in material processing applications can now seriously consider the replacement of their flashlamp pumps with laser diode pump sources. Additionally, a low cost technique developed and demonstrated at LLNL for optically conditioning the output radiation of diode laser arrays has enabled a new and scalable average power diode-end-pumping architecture that can be simply implemented in diode pumped solid state laser systems (DPSSL's). This development allows the high average power DPSSL designer to look beyond the Nd ion for the first time. Along with high average power DPSSL's which are appropriate for material processing applications, low and intermediate average power DPSSL's are now realizable at low enough costs to be attractive for use in many medical, electronic, and lithographic applications. DOE

N94-35679# Lawrence Livermore National Lab., CA.
900-mW AVERAGE POWER AND TUNABILITY FROM A DIODE-PUMPED 2.94 MICRON Er:YAG OSCILLATOR
C. E. Hamilton, R. J. Beach, S. B. Sutton, L. Furu, and W. F. Krupke Jan. 1994 11 p Presented at the 9th Advanced Solid-State Lasers Meeting, Salt Lake City, UT, 7-10 Feb. 1994
(Contract W-7405-eng-48)
(DE94-009511; UCRL-JC-115513; CONF-940226-6) Avail: CASI HC A03/MF A01

In this paper, the authors report on a diode-side-pumped Er:YAG laser that generates over 500 mW of average power at 2.94 mu m, and tunes over a 6 nm range centered about the 2.94 mu m transition. Prior to the development of the laser, diode-pumped Er:YAG lasers have been end-pumped monolithic devices that deliver approximately 200 mW of output at 2.94 mu m. Much of the difficulty in obtaining higher average power from Er:YAG stems from the unfavorable lifetimes of the upper and lower laser levels, the complex state dynamics, and a low stimulated emission cross section (sigma approximately equals 3 x 10(exp -20) cm(exp 2)). One of the most important dynamical processes in Er:YAG is cross relaxation between neighboring Er(3+) ions in the (sup 4)I(sub 13/2) level. By recycling much of the (sup 4)I(sub 13/2) population (lower laser level) into (sup 4)I(sub 11/2) (upper laser level), the cross relaxation overcomes the unfavorable lifetimes of the two levels, allowing the population inversion to be sustained. It is this cross relaxation along with thermalization of the two laser levels that allows cw oscillation on the 2.94 mu m line to take place. The laser that they describe here is a quasi-cw device as the approach to obtaining higher average power and limited tunability relies on side pumping with a quasi-cw InGaAs laser diode array. In this way, a higher gain-length product is generated, which is necessary for extending the tuning range of the laser, and for overcoming the higher losses associated with a discreet-element resonator. DOE

N94-35695 Lawrence Livermore National Lab., CA.
CHIRPED-PULSE AMPLIFICATION WITH FLASHLAMP-PUMPED Ti:SAPPHIRE AMPLIFIERS
J. D. Bonlie, W. E. White, D. F. Price, and D. H. Reitze Jan. 1994 12 p Presented at the OE/LASE 1994 Conference on Optics, Electro-Optics, and Laser Applications in Science and Engineering, Los Angeles, CA, 22-29 Jan. 1994 Limited Reproducibility: More than 20% of this document may be affected by microfiche quality
(Contract W-7405-eng-48)
(DE94-010055; UCRL-JC-116292-Rev-1; CONF-940142-31-Rev-1) Avail: CASI HC A03

Ti:Sapphire (Ti:Al2O3) amplifier stages are typically pumped with Q-switched Nd:YAG lasers doubled to 532 nm because of good spectral overlap, short temporal width, high repetition rate (i.e., 10 Hz to greater than 5 kHz), and the problems associated with flashlamp pumping a material with a relatively short upper state lifetime. Limitations to this pumping method arise due to the 1 to 1.5 joule/pulse ceiling found in most commercial high rep rate Nd:YAG lasers. The availability of high quality, large aperture, Ti:Sapphire rods has made the flashlamp-pumping scheme an attractive option. The excellent thermal properties of Ti:Sapphire also allow an amplifier to be operated at high repetition rates. The front end of our laser relies on Chirped Pulse Amplification (CPA) in laser pumped Ti:Sapphire to generate 55 mJ, 90 fsec pulses at a 10 Hz rate. We report the use of a flashlamp pumped Ti:Sapphire head to further amplify the output of our system, producing 90 fsec, 250 mJ pulses at 5 Hz. The excellent output spatial profile yields a near diffraction-limited 5 micron spot size and peak irradiance in excess of 5 x 10(exp 18) W/sq cm. DOE

N94-35721 General Coherent Technology, Inc., Richardson, TX.
PROGRESS IN THE PRODUCTION OF SAMPLES OF GAMMA RAY LASER CANDIDATE MATERIALS Annual Technical Report, 1 Apr. 1993 - 31 Mar. 1994
C. B. Collins 15 Apr. 1994 21 p Limited Reproducibility: More than 20% of this document may be affected by microfiche quality
(Contract N00014-93-C-2091)
(AD-A278961; GCT/9401) Avail: Issuing Activity (Defense Technical Information Center (DTIC))

Studies of the 29 possible candidates to use as the working medium of a gamma ray laser have identified the 31-year isomer of Hafnium-178 as the best. It is a natural exawatt material capable of emitting 0.05 exawatt per gram if triggered. The problem being addressed in this work is the development of a production cycle for this rare substance. A success of this first year's work has been the identification of two fuel cycles, (alpha, 2n) reactions upon separated Yb-176 and proton spallation upon natural Ta feedstock. DTIC

N94-35782# International Centre for Theoretical Physics, Trieste (Italy).
THREE-PHOTON MICROMASERS
A. S. F. Obada (Al-Azhar Univ., Cairo, Egypt.), A. M. M. AbuSitta (Al-Azhar Univ., Cairo, Egypt.), and O. M. Yasin (Al-Azhar Univ., Cairo, Egypt.) Aug. 1993 8 p
(DE94-611106; LAMP-93/3) Avail: CASI HC A02/MF A01 (US Sales Only)

A non-degenerate 3-photon micromaser is analyzed. A 4-level atom is taken and 3 models of the field are considered. The model is solved for the case of resonance and the master equation for the density matrix is obtained. Semi-analytical solutions are obtained under specified approximations. Three modes can exist depending on the time of interaction. DOE

N94-35978# Lawrence Livermore National Lab., CA.
STATE OF THE ART IN HIGH-POWER MICROWAVES: AN OVERVIEW
J. Swegle and J. Benford Dec. 1993 7 p Presented at the LASERS 1993 International Conference on Lasers and Applications, Lake Tahoe, NV, 6-10 Dec. 1993
(Contract W-7405-eng-48)
(DE94-007075; UCRL-JC-116324; CONF-931237-5) Avail: CASI HC A02/MF A01

In the two decades since the presentation of the first experimental results, the study of high-power microwaves (HPM) has aimed at the production of microwave pulses with ever higher peak power and ever larger energy content. Drawing on the electrical pulsed power and relativistic electron beam technologies, a mix of sources have produced power levels in excess of 1 GW and pulse energies of ten to a thousand joules in both the centimeter and millimeter wavelength ranges. The potential for military applications of such powerful bursts became a major driving force for substantial research programs, and considerable advancements, in the United States and the former Soviet Union. The end of the Cold War and a reexamination of national priorities has diminished the momentum of military HPM development in these countries. Nevertheless, the field hasn't reached its limits, in capability or applicability, and one sees at present a diffusion of the technology across national borders. As examples, one sees commitments in the UK, France, and China to national programs aimed at the exploration of the defensive capabilities of HPM. The purpose of this paper will be to examine the state of the art in HPM at this juncture. We will look at: (1) Peak power production; (2) Pulse energy production and the phenomenon of pulse shortening at high peak power levels; (3) Coherent phasing of multiple high-power sources; (4) Compact HPM source development; and (5) Repetitive operation of sources. We will also briefly mention some emerging applications and offer some concluding thoughts. DOE

N94-36062 Rutherford Appleton Lab., Chilton (England).
SPECIFICATION FOR THE TITANIA krF LASER SYSTEM
S. Angood, A. R. Damerell, C. N. Danson, C. B. Edwards, and P. Gottfeldt Feb. 1994 66 p
(PB94-167103; RAL-94-014) Avail: Issuing Activity (Rutherford Appleton Lab., Chilton, England)

This document presents a specification of the 'Titania' laser system including its physics design, performance characteristics, laser hardware, building layout, control systems, services, and target irradiation facilities. Costs and time schedules for the construction of the new laser are also given. The document is comprised of a set of technical appendices (A1 to 10) which have been written by working groups, which together make up the Titania Task Force. NTIS

N94-36115# Lawrence Livermore National Lab., CA.
HIGH-POWER CW OPERATION OF AlGaInP DIODE-LASER ARRAYS
M. A. Emanuel, R. J. Beach, J. A Skidmore, D. Hudson, W. J. Benett, B. L. Freitas, and N. W. Carlson Jan. 1994 7 p Presented at the CLEO 1994: Conference on Lasers and Electro-Optics, Anaheim, CA, 8-13 May 1994
(Contract W-7405-eng-48)
(DE94-010409; UCRL-JC-115945; CONF-940582-3) Avail: CASI HC A02/MF A01

We report 40 W cw power output with 40% power conversion efficiency from an AlGaInP diode laser array mounted on a microchannel cooled heatsink. DOE

N94-36178# Sandia National Labs., Albuquerque, NM.
PHASE-LOCKED ARRAYS OF VERTICAL-CAVITY SURFACE-EMITTING LASERS
M. E. Warren, K. L. Lear, P. L. Gourley, G. R. Hadley, G. A. Vawter, T. M. Brennan, B. E. Hammons, J. C. Zolper, J. A. Lott, and S. A. Chalmers 1994 12 p Presented at the OE/LASE 1994 Conference on Optics, Electro-Optics, and Laser Applications in Science and Engineering, Los Angeles, CA, 22-29 Jan. 1994

(Contract DE-AC04-94AL-85000)
(DE94-009279; SAND-93-3989C; CONF-940142-32) Avail: CASI HC A03/MF A01

Vertical-Cavity Surface-Emitting Lasers (VCSELS) are of increasing interest to the photonics community because of their surface-emitting structure, simple fabrication and packaging, wafer-level testability, and potential for low cost manufacture. Scaling VCSELs to higher power outputs requires increasing the device area, which leads to transverse mode control difficulties if devices become larger than about 5 microns. One approach to increasing the device size while maintaining a well controlled transverse mode profile is formation of coupled or phase-locked two-dimensional arrays of VCSELs that are individually single-transverse mode. Such arrays have unique optical properties, not all of which are desirable. This paper covers some of the basic principles of these devices and reviews recent work on device designs, fabrication and operation. A technique for improving the far-field properties of the arrays is demonstrated and performance limitations are discussed. DOE

N94-36218 Montpellier-2 Univ. (France) Equipe de Micro-Opto-Electronique.

STUDY AND FABRICATION OF GaSb-BASED LASER HETEROSTRUCTURES Final Report [ETUDE ET REALISATION D'HETEROSTRUCTURES LASER A BASE DE GASB]

A. Baranov 1993 26 p In FRENCH Sponsored by Direction des Recherches, Etudes et Techniques
(PB94-170677) Avail: Issuing Activity (National Technical Information Service (NTIS))

The author studied and optimized double laser heterostructures (GaAlAsSb/GaInAsSb/GaAlAsSb) fabricated on a GaSb substrate via liquid phase epitaxy. Modeling of the double heterostructures enabled him to produce low threshold lasers (1kA/sq cm) that transmit in the neighborhood of 2 micrometers. The lasers boast threshold current densities on the order of 2kA/sq cm and 3kA/sq cm, values that are comparable to the best results reported in the literature for GaSb-based conventional laser structures made via liquid phase epitaxy (LPE). The performances of the laser diodes produced are very good: emitted power (14 mW/face) and external differential quantum yield (10%/face) are the best to date for LPE lasers operating at 2 micrometers. Characteristic temperature is high. NTIS

N94-36227# University of Southern California, Los Angeles, CA. Center for Laser Studies.

EYESAFE RARE EARTH CRYSTAL LASERS FOR ATMOSPHERE SOUDINGS Final Technical Report, 5 Sep. 1989 - 31 May 1993

Milton Birnbaum 1 Aug. 1993 89 p
(Contract F19628-89-K-0038; AF Proj. 7670)
(AD-A279486; PL-TR-93-2167) Avail: CASI HC A05/MF A01

The characteristics of room temperature Er(3+) : YAG lasers at 1.644 microns end pumped by an ER(3+) : glass laser at 1.535 microns are described. Low threshold and efficient operation was obtained for 0.5 and 1 percent ER(3+) : YAG. Similar studies were performed utilizing 0.7 percent Er(3+) (3 percent Yb(3+), 1 percent Cr(3+)) YSGG. Laser action of Er(3+) : YSGG at 1.643 microns was achieved. Author (revised)

N94-36365 Department of the Navy, Washington, DC.

COLOR CENTER LASER WITH TRANSVERSE AUXILIARY ILLUMINATION Patent

Irwin Schneider, inventor (to Navy) and Robert S. Afzal, inventor (to Navy) 30 Nov. 1993 13 p Filed 15 Apr. 1992 Supersedes AD-D015387
(AD-D016201; US-Patent-5,267,254; US-Patent-Appl-SN-868806; US-Patent-Class-372-42) Avail: US Patent and Trademark Office

A color center laser is provided with a crystal disposed within a longitudinally pumped cavity. Optics are provided to transversely excite the crystal. Both a circular lens and a cylindrical lens focus an auxiliary beam into the crystal of the color center laser to produce (F2 +)A color centers for lasing. The cylindrical lens is used to focus the auxiliary beam to a narrow focal line. The circular lens is used to adjust the length of the focal line. By adjusting the length of the focal line, an entirety of the pump beam is used for excitation. The lenses thus collimate and focus the focal line to a length within an active volume in the crystal of the color center laser essentially equal to a length of the crystal. DTIC

N94-36370 Department of the Navy, Washington, DC.

SYSTEM FOR END-PUMPING A SOLID STATE LASER USING A LARGE APERTURE LASER DIODE BAR Patent

Leon Esterowitz, inventor (to Navy), C. Stoneman, inventor (to Navy), and James G. Lynn, inventor (to Navy) 7 Dec. 1993 9 p Filed 6 Nov. 1991 Supersedes AD-D015280
(AD-D016213; US-Patent-5,268,920; US-Patent-Appl-SN-788674; US-Patent-Class-372-71) Avail: US Patent and Trademark Office

An optical system for end-pumping the gain medium of a three-level or a self-terminating solid state laser with the optical output from a wide aperture laser diode bar is disclosed. In a preferred embodiment, the optical system includes: a laser diode bar for emitting from an elongated emissive area thereof a bright light having a lateral divergence and a transverse divergence; and an optical assembly disposed between the laser diode bar and the three-level solid state laser for collecting and focusing the bright light into a relatively small high-intensity spot to end-pump the gain medium of the three-level or self-terminating solid state laser. DTIC

N94-36393# Bhabha Atomic Research Centre, Bombay (India).

[ACTIVITIES OF THE LASER AND PLASMA TECHNOLOGY DIVISION] Annual Report, 1992

N. Venkatramani, ed. and R. L. Verma, ed. 1993 134 p
(DE94-617113; BARC-1993/P/004) Avail: CASI HC A07/MF A02 (US Sales Only)

The report describes the research and development (R and D) activities of Laser and Plasma technology Division, Bhabha Atomic Research Centre, Bombay during 1992. The broad program objectives of the Division are: (1) development and technology readiness studies of laser, plasma and electron beam devices, (2) studies on related physical phenomena with a view to gain better understanding of the devices, and (3) improvements in technology and exploration of new areas. The R and D activities are reported under the sections entitled: (1) Laser Activities, (2) Thermal Plasma Activities, and (3) Electron Beam Activities. At the end of each section, a list of publications by the staff members in the field indicated by the title of the section is given. Some of the highlights of R and D work during 1992 are: (1) fabrication of an electron beam sustained CO2 laser; (2) commissioning of a 6.5 m high LMMHD (Liquid Metal Magneto-hydrodynamic) generator loaded with 1.5 tons of mercury; (3) fabrication of electron beam processing equipment; and (4) study of the magnetic properties of vanadium nitride films produced by reactive sputtering in an indigenously developed DC magnetron sputtering equipment. DOE

37 MECHANICAL ENGINEERING

Includes auxiliary systems (nonpower); machine elements and processes; and mechanical equipment.

N94-35367* National Aeronautics and Space Administration. Marshall Space Flight Center, Huntsville, AL.

PLASMA ARC WELDING WELD IMAGING Patent

Daniel J. Rybicki, inventor (to NASA) and William F. McGee, inventor (to NASA) 12 Jul. 1994 5 p Filed 29 Jul. 1993 Supersedes N94-15949 (32 - 3, p 1047)
(NASA-Case-MFS-28797-1; US-Patent-5,329,089; US-Patent-Appl-SN-098918; US-Patent-Class-219-121.45; US-Patent-Class-219-121.48; US-Patent-Class-219-121.54; US-Patent-Class-219-130.01; Int-Patent-Class-B23K-10/02; Int-Patent-Class-B23K-9/095) Avail: US Patent and Trademark Office

A welding torch for plasma arc welding apparatus has a transparent shield cup disposed about the constricting nozzle, the cup including a small outwardly extending polished lip. A guide tube extends externally of the torch and has a free end adjacent to the lip. First and second optical fiber bundle assemblies are supported within the guide tube. Light from a strobe light is transmitted along one of the assemblies to the free end and through the lip onto the weld site. A lens is positioned in the guide tube adjacent to the second assembly and focuses images of the weld site onto the end of the fiber bundle of the second assembly and these images are transmitted along the second assembly to a video camera so that the weld site may be viewed continuously for monitoring the welding process. Official Gazette of the U.S. Patent and Trademark Office

N94-35373* National Aeronautics and Space Administration. Lewis Research Center, Cleveland, OH.
HIGH-TEMPERATURE, BELLOWS HYBRID SEAL Patent
Bruce M. Steinetz, inventor (to NASA) and Paul J. Sirocky, inventor (to NASA) 26 Jul. 1994 8 p Filed 22 Jan. 1993 Supersedes N93-19027 (31 - 6, p 1549)
(NASA-Case-LEW-15570-1; US-Patent-5,332,239;
US-Patent-Appl-SN-007874; US-Patent-Class-277-230;
US-Patent-Class-277-75; Int-Patent-Class-F16J-15/16) Avail: US Patent and Trademark Office

A high-temperature hybrid seal is constructed of multiple elements to meet the many demands placed on the seal. The primary elements are: a central high-temperature bellows, a braided ceramic sheath covering the bellows, an outer abrasion resistant sheath covering the ceramic sheath, and a structurally-sound seal-end termination.
Official Gazette of the U.S. Patent and Trademark Office

N94-35374* National Aeronautics and Space Administration. Lyndon B. Johnson Space Center, Houston, TX.
ROBOT FRIENDLY PROBE AND SOCKET ASSEMBLY Patent
Karen L. Nyberg, inventor (to NASA) 5 Jul. 1994 8 p Filed 14 Dec. 1992 Supersedes N93-22007 (31 - 7, p 1917)
(NASA-Case-MSC-22028-1; US-Patent-5,326,186;
US-Patent-Appl-SN-993477; US-Patent-Class-403-378;
US-Patent-Class-403-379; US-Patent-Class-403-359;
US-Patent-Class-403-327; US-Patent-Class-403-328;
US-Patent-Class-403-325; Int-Patent-Class-F16D-1/00) Avail: US Patent and Trademark Office

A probe and socket assembly for serving as a mechanical interface between structures is presented. The assembly comprises a socket having a housing adapted for connection to a first supporting structure and a probe which is readily connectable to a second structure and is designed to be easily grappled and manipulated by a robotic device for insertion and coupling with the socket. Cooperable automatic locking means are provided on the probe shaft and socket housing for automatically locking the probe in the socket when the probe is inserted a predetermined distance. A second cooperable locking means on the probe shaft and housing are adapted for actuation after the probe has been inserted the predetermined distance. Actuation means mounted on the probe and responsive to the grip of the probe handle by a gripping device, such as a robot for conditioning the probe for insertion and are also responsive to release of the grip of the probe handle to actuate the second locking means to provide a hard lock of the probe in the socket.
Official Gazette of the U.S. Patent and Trademark Office

N94-35375* National Aeronautics and Space Administration. Pasadena Office, CA.
SEPARATION TOOL FOR MULTIPIN ELECTRICAL CONNECTORS Patent
Larry D. Smith, inventor (to NASA) (Jet Propulsion Lab., California Inst. of Tech., Pasadena, CA.) 19 Jul. 1994 9 p Filed 30 Mar. 1993 Supersedes N93-28131 (31 - 10, p 3052)
(NASA-Case-NPO-18786-1-CU; US-Patent-5,329,693;
US-Patent-Appl-SN-048871; US-Patent-Class-29-764;
US-Patent-Class-29-252; US-Patent-Class-439-158;
Int-Patent-Class-H01R-43/00) Avail: US Patent and Trademark Office

A hydraulic tool for safely separating one multipin electrical connector from another is presented. The separation tool consists of a master cylinder which operates a pair of slave cylinders. Each slave cylinder has a corresponding operative shaft and an extraction tab. The slave cylinders are spaced apart from one another so that they may be positioned on either side of mated connector pairs of different sizes and so that their extraction tabs may be slid between the connectors. When the master cylinder's plunger is operated, its operation is hydraulically transmitted to the operative shafts of the slave cylinders which extend outward and, once pressed against a substrate, causes the slave cylinders and corresponding extractor tabs to move away and separate one connector from the other. A second preferred separation tool includes an additional pair of extractor tabs, one at the end of each operative shaft, so that the tool can be used to separate a mated connector pair hanging in free space. Official Gazette of the U.S. Patent and Trademark Office

N94-35481*# National Aeronautics and Space Administration. Lyndon B. Johnson Space Center, Houston, TX.
INTERNATIONAL SPACE STATION ALPHA REMOTE MANIPULATOR SYSTEM WORKSTATION CONTROLS TEST REPORT
William A. Ehrenstrom, Colin Swaney, and Patrick Forrester May 1994 75 p
(NASA-TM-104796; S-770; JSC-26704; NAS 1.15:104796) Avail: CASI HC A04/MF A01

Previous development testing for the space station remote manipulator system workstation controls determined the need for hardware controls for the emergency stop, brakes on/off, and some camera functions. This report documents the results of an evaluation to further determine control implementation requirements, requested by the Canadian Space Agency (CSA), to close outstanding review item discrepancies. This test was conducted at the Johnson Space Center's Space Station Mockup and Trainer Facility in Houston, Texas, with nine NASA astronauts and one CSA astronaut as operators. This test evaluated camera iris and focus, back-up drive, latching end effector release, and autosequence controls using several types of hardware and software implementations. Recommendations resulting from the testing included providing guarded hardware buttons to prevent accidental actuation, providing autosequence controls and back-up drive controls on a dedicated hardware control panel, and that 'latch on/latch off', or on-screen software, controls not be considered. Generally, the operators preferred hardware controls although other control implementations were acceptable. The results of this evaluation will be used along with further testing to define specific requirements for the workstation design. Author (revised)

N94-35500*# Auburn Univ., AL. Dept. of Mechanical Engineering.
INFLUENCE OF BACKUP BEARINGS AND SUPPORT STRUCTURE DYNAMICS ON THE BEHAVIOR OF ROTORS WITH ACTIVE SUPPORTS Annual Status Report
George T. Flowers Jun. 1994 25 p
(Grant NAG3-1507)
(NASA-CR-196119; NAS 1.26:196119) Avail: CASI HC A03/MF A01

Progress over the past year includes the following: A simplified rotor model with a flexible shaft and backup bearings has been developed. A simple rotor model which includes a flexible disk and bearings with clearance has been developed and the dynamics of the model investigated. A rotor model based upon the T-501 engine has been developed which includes backup bearing effects. Parallel simulation runs are being conducted using an ANSYS based finite element model of the T-501. The magnetic bearing test rig is currently floating and dynamics/control tests are being conducted. A paper has been written that documents the work using the T-501 engine model. Work has continued with the simplified model. The finite element model is currently being modified to include the effects of foundation dynamics. A literature search for material on foil bearings has been conducted. A finite element model is being developed for a magnetic bearing in series with a foil backup bearing. Derived from text

N94-35512* Jet Propulsion Lab., California Inst. of Tech., Pasadena, CA.
TELEOPERATION AND SUPERVISED AUTONOMY FOR ORU EXCHANGE (Videotape)
Aug. 1990 Videotape: 12 min. 30 sec. playing time, in color, with sound
(NASA-CR-196101; NONP-NASA-VT-94-15920) Avail: CASI VHS A01/BETA A22

This video presents scenes demonstrating current telerobotics technology, specifically teleoperation with the aid of a computer. CASI

N94-35661* National Aeronautics and Space Administration. Lyndon B. Johnson Space Center, Houston, TX.
MAGNETICALLY OPERATED CHECK VALVE Patent
Brian G. Morris, inventor (to NASA) and Richard J. Bozeman, Jr., inventor (to NASA) 14 Jun. 1994 14 p Filed 19 Mar. 1993 Supersedes N93-28501 (31 - 11, p 3442)
(NASA-Case-MSC-22046-1; US-Patent-5,320,136;
US-Patent-Appl-SN-038748; US-Patent-Class-137-528;
US-Patent-Class-137-516.29; US-Patent-Class-251-65;
Int-Patent-Class-F16K-15/02) Avail: US Patent and Trademark Office

A magnetically operated check valve is disclosed. The valve is comprised of a valve body and a movable poppet disposed therein. A magnet attracts the poppet to hold the valve shut until the force of fluid flow through the valve overcomes the magnetic attraction and moves the poppet to an unseated, open position. The poppet and magnet are configured and disposed to trap a magnetically attracted particulate and prevent it from flowing to a valve seating region.

Official Gazette of the U.S. Patent and Trademark Office

N94-35667# General Electric Co., Erie, PA.

DURABILITY TESTING OF MEDIUM SPEED DIESEL ENGINE COMPONENTS DESIGNED FOR OPERATING ON COAL/WATER SLURRY FUEL

R. E. McDowell, A. W. Giammarise, and R. N. Johnson 1994 15 p Presented at the 13th Energy-Sources Technology Conference and Exhibition (ETCE) on Wind Energy, New Orleans, LA, 23-26 Jan. 1994
(Contract DE-AC21-88MC-23174)
(DE94-009550; DOE/MC-23174/94/C0329; CONF-940113-8) Avail: CASI HC A03/MF A01

Over 200 operating cylinder hours were run on critical wearing engine parts. The main components tested included cylinder liners, piston rings, and fuel injector nozzles for coal/water slurry fueled operation. The liners had no visible indication of scoring nor major wear steps found on their tungsten carbide coating. While the tungsten carbide coating on the rings showed good wear resistance, some visual evidence suggests adhesive wear mode was present. Tungsten carbide coated rings running against tungsten carbide coated liners in GE 7FDL engines exhibit wear rates which suggest an approximate 500 to 750 hour life. Injector nozzle orifice materials evaluated were diamond compacts, chemical vapor deposited diamond tubes, and thermally stabilized diamond. Based upon a total of 500 cylinder hours of engine operation (including single-cylinder combustion tests), diamond compact was determined to be the preferred orifice material. DOE

N94-35815# General Electric Co., Erie, PA.

DESIGN AND OPERATION OF A MEDIUM SPEED 12-CYLINDER COAL-FUELED DIESEL ENGINE. PHASE 2: IMPROVEMENTS

G. L. Confer, B. D. Hsu, R. E. McDowell, E. Gal, W. VanKleunen, S. Kaldor, and M. Mengel 1994 8 p Presented at the 13th Energy-Sources Technology Conference and Exhibition on Wind Energy, New Orleans, LA, 23-26 Jan. 1994
(Contract DE-AC21-88MC-23174)
(DE94-009547; DOE/MC-23174/94/C0332; CONF-940113-10) Avail: CASI HC A02/MF A01

Under the sponsorship of the US Department of Energy, General Electric has been pioneering the development of a coal fired diesel engine to power a locomotive. The feasibility of using a coal water slurry (CWS) mixture as a fuel in a medium speed diesel engine has been demonstrated with the first successful locomotive systems test in 1991 on the GE Transportation Systems test track in Erie, PA. Phase 2 of the development process incorporates the results of the programs research in durable engine parts, improved combustion efficiency, and emissions reduction. A GE 7FDL12 engine has been built using diamond insert injector nozzles, tungsten carbide coated piston rings, and tungsten carbide coated liners to overcome power assembly wear. Electronic controlled fuel injection for both diesel pilot and main CWS injector were incorporated to control injection timing. An envelop filter and copper oxide sorbent system were used to cleanup engine emissions. The system is capable of removing over 99% of the particulates, 90% of the SO2, and 85% of NO(x). DOE

N94-35931 Ricardo North America, Inc., Burr Ridge, IL.

ANALYSIS OF THE INJECTION PROCESS IN DIRECT INJECTED NATURAL GAS ENGINES Topical Report, May 1992 - Apr. 1993

M. J. Jennings and F. R. Jeske Aug. 1993 64 p Limited Reproducibility: More than 20% of this document may be affected by microfiche quality
(Contract GRI-5092-291-2304; RNA Proj. G93109)
(PB94-156494; RNA-93-232; GRI-93/0398) Avail: CASI HC A04

The analysis was based upon a series of three-dimensional computational fluid dynamics (CFD) calculations of natural gas (NG) injection in engine combustion chambers and constant volume chambers. Simulations of injection into constant volume chambers were used to investigate the fundamental behavior of NG jets. Calculations of engine injection, which include a moving piston, were used to study the effects of combustion system design. NTIS

N94-36022# Clemson Univ., SC. Research Foundation.

UNIVERSITY PARTICIPATION IN THE ATS PROGRAM Report, 30 Sep. 1992 - 31 Mar. 1994

R. P. Allen and L. P. Golan 1993 9 p Presented at the Joint Contractors Meeting on Advanced Turbine Systems, Fuel Cells and Coal-Fired Heat, Morgantown, WV, 3-5 Aug. 1993
(Contract DE-FC21-92MC-29061)
(DE94-003191; DOE/MC-29061/94/C0269; CONF-930893-31) Avail: CASI HC A02/MF A01

The Advanced Gas Turbine Systems Research Program was included in DOE's Advanced Turbine Systems initiative to conduct basic research in support of the overall advanced turbine systems (ATS) program, and to strengthen the university gas turbine technology base in the USA. The results of the research will be transferred to the industrial members to enhance and/or facilitate their designs of advanced gas turbine powerplants. Concurrently, the involvement of many students both graduate and undergraduate, will provide a better qualified group of engineers for hire by the industry. DOE

N94-36206# Lawrence Livermore National Lab., CA.

A COMPARISON BETWEEN DIRECT SPARK IGNITION AND PRECHAMBER IGNITION IN AN INTERNAL COMBUSTION ENGINE

L. D. Cloutman 3 Dec. 1993 16 p Presented at the 25th International Symposium on Combustion, Irvine, CA, 31 Jul. - 5 Aug. 1994
(Contract W-7405-eng-48)
(DE94-008218; UCRL-JC-115803; CONF-940711-11) Avail: CASI HC A03/MF A01

We simulated the flow field and flame propagation near top dead center in a generic large-bore internal combustion engine using the COYOTE computer program, which is based on the full Navier-Stokes equations for a fluid mixture. The combustion chamber is a right circular cylinder, and the main charge is uniformly premixed. The calculations are axisymmetric. The results illustrate the differences in flow patterns, flame propagation, and thermal NO production between ignition with a spark plug and with a small prechamber. In the spark-ignited case, the flame propagates away from the spark plug approximately as a segment of a spherical surface, just as expected. With the prechamber, a high speed jet of hot combustion products shoots into the main chamber, quickly producing a large flame sheet that spreads along the piston face. The prechamber run consumes all of the fuel in half the time required by the spark-ignited case. The two cases produce comparable amounts of thermal NO at the end of fuel combustion. DOE

N94-36232# Argonne National Lab., IL.

EFFECT OF NIOBIUM INTERLAYER ON HIGH-TEMPERATURE SLIDING FRICTION AND WEAR OF SILVER FILMS ON ALUMINA

A. Erdemir and R. A. Erck Mar. 1994 21 p Presented at the International Conference on Metallurgical Coatings and Thin Films, San Diego, CA, 25-29 Apr. 1994
(Contract W-31-109-eng-38)
(DE94-010462; ANL/ET/CP-81839; CONF-940440-2) Avail: CASI HC A03/MF A01

We investigated the effect of a thin Nb bond layer (15-20 mn thick) on the high-temperature sliding friction and wear of silver films (approximately 1.5 micrometers thick) produced on (alpha)-alumina Al2O3 substrates by ion-beam assisted deposition. The friction coefficients of test pairs without an Ag film fluctuated between 0.8 to 1.1, whereas the friction coefficients of pairs with an Ag film were 0.32 to 0.5. The wear of uncoated Al2O3 balls sliding against the Ag-coated flats was reduced by factors of 25 to approximately 2000, depending on test temperature and the presence or absence of an Nb bond layer. The wear of silver-coated flats was virtually unmeasurable after tests at temperatures up to 400C. At much higher temperatures (e.g., 600C), Ag films without an Nb bond layer delaminated from the sliding surfaces and lost their effectiveness. Ag films with an Nb bond layer remained intact on the sliding surfaces of the Al2O3 substrates even at 600C and continued to impart low friction and low wear. DOE

N94-36348# Little (Arthur D.), Inc., Cambridge, MA.

COAL-FUELED DIESELS FOR MODULAR POWER GENERATION

R. P. Wilson, A. K. Rao, and W. C. Smith 1993 9 p Presented at the Joint Power Generation Conference, Kansas City, MO, 17-21 Oct. 1993

(Contract DE-AC21-88MC-25124)
(DE94-002960; DOE/MC-25124/94/C0273; CONF-931006-3) Avail: CASI HC A02/MF A01

Interest in coal-fueled heat engines revived after the sharp increase in the prices of natural gas and petroleum in the 1970's. Based on the success of micronized coal water slurry combustion tests in an engine in the 1980's, Morgantown Energy Technology Center (METC) of the US Department of Energy initiated several programs for the development of advanced coal-fueled diesel and gas turbine engines for use in cogeneration, small utilities, industrial applications and transportation. Cooper-Bessemer and Arthur D. Little have been developing technology since 1985, under the sponsor of METC, to enable coal water slurry (CWS) to be utilized in large bore, medium-speed diesel engines. Modular power generation applications in the 10-100 MW size (each plant typically using from two to eight engines) are the target applications for the late 1990's and beyond when, according to the US DOE and other projections, oil and natural gas prices are expected to escalate much more rapidly compared to the price of coal. As part of this program over 7.50 hours of prototype engine operation has been achieved on coal water slurry (CWS), including over 100 hours operation of a six-cylinder full scale engine with Integrated Emissions Control System in 1993. In this paper, the authors described the project cost of the CWS fuel used, the heat rate of the engine operating on CWS, the projected maintenance cost for various engine components, and the demonstrated low emissions characteristics of the coal diesel system. DOE

N94-36355 General Electric Co., Schenectady, NY. Power Systems Lab.
HEAVY DUTY GAS TURBINE COMBUSTION TESTS WITH SIMULATED LOW BTU COAL GAS
T. E. Ekstrom, R. A. Battista, F. H. Belisle, and G. P. Maxwell 1993 15 p Presented at the Joint Contractors Meeting on Advanced Turbine Systems, Fuel Cells and Coal-Fired Heat, Morgantown, WV, 3-5 Aug. 1993 Limited Reproducibility: More than 20% of this document may be affected by microfiche quality
(Contract DE-FC21-91MC-27221)
(DE94-002970; DOE/MC-27221/94/C0243; CONF-930893-19) Avail: CASI HC A03

This program has the objectives to: parametrically determine the effects of moisture, nitrogen and carbon dioxide as diluents so that the combustion characteristics of many varieties of gasification product gases can be reasonably predicted without physically testing each specific gas composition; determine emissions characteristics including NO, NO(x), CO, levels etc. associated with each of the diluents; and operate with at least two syngas compositions -- DOE chosen air-blown and integrate oxygen-blown, to confirm that the combustion characteristics are in line with predictions. As a result of this program: GE Engineering is now confident that the syngas fuels produced by all currently viable coal gasifiers can be accommodated by the GE advanced ('F' Technology) combustion system; and for proposed syngas fuels with varying amounts of steam, nitrogen or CO2 diluent, the combustion and emissions characteristics can be reasonably estimated without undertaking expensive new screening tests for each different fuel. DOE

N94-36378# Lawrence Livermore National Lab., CA.
EFFECTS OF NATURAL GAS COMPOSITION ON IGNITION DELAY UNDER DIESEL CONDITIONS
J. D. Naber (Sandia National Labs., Albuquerque, NM.), D. L. Siebers (Sandia National Labs., Albuquerque, NM.), S. S. DiJulio (California State Univ., Northridge, CA.), and C. K. Westbrook 3 Dec. 1993 20 p Presented at the 25th International Symposium on Combustion, Irvine, CA, 31 Jul. - 5 Aug. 1994
(Contract W-7405-eng-48)
(DE94-006405; UCRL-JC-115804; CONF-940711-5) Avail: CASI HC A03/MF A01

Effects of variations in natural gas composition on autoignition of natural gas under direct-injection (DI) diesel engine conditions were studied experimentally in a constant-volume combustion vessel and computationally using a chemical kinetic model. Four fuel blends were investigated: pure methane, a capacity weighted mean natural gas, a high ethane content natural gas, and a natural gas with added propane typical of peak shaving conditions. Experimentally measured ignition delays were longest for pure methane and became progressively shorter as ethane and propane concentrations increased. At conditions characteristic of a DI compression ignition natural gas engine at Top Dead Center (CR = 23:1, p = 6.8 MPa, T = 1150K), measured ignition delays for the four fuels varied from 1.8 ms for the peak shaving and high ethane gases to 2.7 ms for pure methane. Numerically predicted variations in ignition delay as a function of natural gas composition agreed with these measurements. DOE

N94-36433# Argonne National Lab., IL.
DYNAMIC STABILITY OF MAGLEV SYSTEMS
Y. Cai, S. S. Chen, T. M. Mulcahy, and D. M. Rote 1994 27 p
(Contract W-31-109-eng-38)
(DE94-010451; ANL/MCT/PP-78088) Avail: CASI HC A03/MF A01

Dynamic instabilities are not acceptable in any commercial maglev system, so it is important to consider dynamic instability in the development of all maglev systems. This study considers the stability of maglev systems based on experimental data, scoping calculations, and simple mathematical models. Divergence and flutter are obtained for coupled vibration of a three-degree-of-freedom maglev vehicle on a guideway consisting of double L-shaped aluminum segments. The theory and analysis developed in this study provides basic stability characteristics and identifies future research needs for maglev systems. DOE

N94-35837*# SatCon Technology Corp., Cambridge, MA.
AEROSPACE APPLICATIONS OF MAGNETIC BEARINGS
James Downer, James Goldie, Vijay Gondhalekar, and Richard Hockney *In* NASA. Langley Research Center, Second International Symposium on Magnetic Suspension Technology, Part 1 May 1994 p 3-26 (For primary document see N94-35836 11-18)
Avail: CASI HC A03/MF A04

N94-35838*# General Electric Co., Schenectady, NY. Control Systems Lab.
NONLINEAR CONTROL OF MAGNETIC BEARINGS
A. K. Pradeep and R. Gurumoorthy *In* NASA. Langley Research Center, Second International Symposium on Magnetic Suspension Technology, Part 1 May 1994 p 27-57 (For primary document see N94-35836 11-18)
Avail: CASI HC A03/MF A04

N94-35839*# Eidgenoessische Technische Hochschule, Zurich (Switzerland). International Center for Magnetic Bearings.
HIGH PERFORMANCE DATA ACQUISITION, IDENTIFICATION, AND MONITORING FOR ACTIVE MAGNETIC BEARINGS
Raoul Herzog and Roland Siegwart *In* NASA. Langley Research Center, Second International Symposium on Magnetic Suspension Technology, Part 1 May 1994 p 61-66 (For primary document see N94-35836 11-18)
Avail: CASI HC A02/MF A04

N94-35840*# Grumman Aerospace Corp., Bethpage, NY.
SYSTEM CONCEPT DEFINITION OF THE GRUMMAN SUPERCONDUCTING ELECTROMAGNETIC SUSPENSION (EMS) MAGLEV DESIGN
M. Proise *In* NASA. Langley Research Center, Second International Symposium on Magnetic Suspension Technology, Part 1 May 1994 p 69-76 Sponsored by Corps of Engineers (For primary document see N94-35836 11-18)
Avail: CASI HC A02/MF A04

N94-35841*# Thyssen Henschel America, Inc.
TRANSRAPID (THE FIRST HIGH-SPEED MAGLEV TRAIN SYSTEM CERTIFIED READY FOR APPLICATION): DEVELOPMENT STATUS AND PROSPECTS FOR DEPLOYMENT
Reinhard F. Luerken *In* NASA. Langley Research Center, Second International Symposium on Magnetic Suspension Technology, Part 1 May 1994 p 77-91 (For primary document see N94-35836 11-18)
Avail: CASI HC A03/MF A04

N94-35842*# Draper (Charles Stark) Lab., Inc., Cambridge, MA.
CONTROL OF MAGLEV VEHICLES WITH AERODYNAMIC AND GUIDEWAY DISTURBANCES
Karl Flueckiger, Steve Mark, Ruth Caswell, and Duncan McCallum *In* NASA. Langley Research Center, Second International Symposium on

Magnetic Suspension Technology, Part 1 May 1994 p 93-107 (For primary document see N94-35836 11-18)
Avail: CASI HC A03/MF A04

N94-35845*# North Carolina Univ., Charlotte, NC. Dept. of Electrical Engineering.
MATERIALS FOR EFFICIENT HIGH-FLUX MAGNETIC BEARING ACTUATORS
M. E. Williams and D. L. Trumper *In* NASA. Langley Research Center, Second International Symposium on Magnetic Suspension Technology, Part 1 May 1994 p 135-145 (For primary document see N94-35836 11-18)
Avail: CASI HC A03/MF A04

N94-35846*# Politecnico di Torino (Italy). Dipt. di Meccanica.
DESIGN, CONSTRUCTION, AND TESTING OF A FIVE ACTIVE AXES MAGNETIC BEARING SYSTEM
Cristiana Delprete, Giancarlo Genta, and Stefano Carabelli *In* NASA. Langley Research Center, Second International Symposium on Magnetic Suspension Technology, Part 1 May 1994 p 147-161 Sponsored by Italian Ministry of Univ. and Scientific Research (For primary document see N94-35836 11-18)
Avail: CASI HC A03/MF A04

N94-35847*# Virginia Univ., Charlottesville, VA.
EXPERIMENTAL MEASUREMENT AND CALCULATION OF LOSSES IN PLANAR RADIAL MAGNETIC BEARINGS
M. E. F. Kasarda, P. E. Allaire, R. W. Hope, and R. R. Humphris *In* NASA. Langley Research Center, Second International Symposium on Magnetic Suspension Technology, Part 1 May 1994 p 163-174 Sponsored in part by Center for Innovative Technology (For primary document see N94-35836 11-18)
Avail: CASI HC A03/MF A04

N94-35848*# Draper (Charles Stark) Lab., Inc., Cambridge, MA. Advanced Computer Architectures Group.
FAULT TOLERANT COMPUTER CONTROL FOR A MAGLEV TRANSPORTATION SYSTEM
Jaynarayan H. Lala, Gail A. Nagle, and George Anagnostopoulos *In* NASA. Langley Research Center, Second International Symposium on Magnetic Suspension Technology, Part 1 May 1994 p 177-195 (For primary document see N94-35836 11-18)
(Contract DTFR53-91-C-00043)
Avail: CASI HC A03/MF A04

N94-35853*# National Aeronautics and Space Administration. Langley Research Center, Hampton, VA.
IMPLEMENTATION OF A DECOUPLED CONTROLLER FOR A MAGNETIC SUSPENSION SYSTEM USING ELECTROMAGNETS MOUNTED IN A PLANAR ARRAY
D. E. Cox and N. J. Groom *In its* Second International Symposium on Magnetic Suspension Technology, Part 1 May 1994 p 257-271 (For primary document see N94-35836 11-18)
Avail: CASI HC A03/MF A04

N94-35857*# Politecnico di Torino (Italy). Dipt. di Meccanica.
ACTIVE MAGNETIC BEARING CONTROL LOOP MODELING FOR A FINITE ELEMENT ROTORDYNAMICS CODE
Giancarlo Genta, Cristiana Delprete, and Stefano Carabelli *In* NASA. Langley Research Center, Second International Symposium on Magnetic Suspension Technology, Part 1 May 1994 p 319-333 Sponsored by Italian Ministry of Univ. and Scientific Research (For primary document see N94-35836 11-18)
Avail: CASI HC A03/MF A04

N94-35858*# General Electric Co., Schenectady, NY. Electronic Technologies Lab.
MODELLING AND CONTROL OF A ROTOR SUPPORTED BY MAGNETIC BEARINGS
R. Gurumoorthy and A. K. Pradeep *In* NASA. Langley Research Center, Second International Symposium on Magnetic Suspension Technology, Part 1 May 1994 p 335-352 (For primary document see N94-35836 11-18)
Avail: CASI HC A03/MF A04

N94-35859*# Duke Univ., Durham, NC. Dept. of Mechanical Engineering.
DYNAMIC ANALYSIS OF A MAGNETIC BEARING SYSTEM WITH FLUX CONTROL
Josiah Knight, Thomas Walsh, and Lawrence Virgin *In* NASA. Langley Research Center, Second International Symposium on Magnetic Suspension Technology, Part 1 May 1994 p 353-366 (For primary document see N94-35836 11-18)
Avail: CASI HC A03/MF A04

N94-35863*# National Defence Academy, Tokyo (Japan).
THIRD ORDER LPF TYPE COMPENSATOR FOR FLEXIBLE ROTOR SUSPENSION
Osami Matsushita, Naohiko Takahashi, and Michiyuki Takagi *In* NASA. Langley Research Center, Second International Symposium on Magnetic Suspension Technology, Part 1 May 1994 p 421-431 (For primary document see N94-35836 11-18)
Avail: CASI HC A03/MF A04

N94-35867*# Virginia Polytechnic Inst. and State Univ., Blacksburg, VA. Dept. of Engineering Science and Mechanics.
MANEUVERING AND CONTROL OF FLEXIBLE SPACE ROBOTS
Leonard Meirovitch and Seungchul Lim *In* NASA. Langley Research Center, NASA Workshop on Distributed Parameter Modeling and Control of Flexible Aerospace Systems Jun. 1994 p 23-40 (For primary document see N94-35865 11-18)
(Grant NAG1-225)
Avail: CASI HC A03/MF A06

N94-35903*# General Electric Co., Lynn, MA. Aircraft Engines.
INTEGRATION OF MAGNETIC BEARINGS IN THE DESIGN OF ADVANCED GAS TURBINE ENGINES
Albert F. Storace, Devendra K. Sood, James P. Lyons, and Mark A. Preston *In* NASA. Langley Research Center, Second International Symposium on Magnetic Suspension Technology, Part 2 May 1994 p 435-449 (For primary document see N94-35902 11-18)
(Contract DAAJ02-92-C-0055)
Avail: CASI HC A03/MF A03

N94-35905*# National Aeronautics and Space Administration. Lewis Research Center, Cleveland, OH.
ELECTROMECHANICAL SIMULATION AND TEST OF ROTATING SYSTEMS WITH MAGNETIC BEARING OR PIEZOELECTRIC ACTUATOR ACTIVE VIBRATION CONTROL
Alan B. Palazzolo (Texas A&M Univ., College Station, TX.), Punan Tang (Texas A&M Univ., College Station, TX.), Chaesil Kim (Texas A&M Univ., College Station, TX.), Daniel Manchala (Texas A&M Univ., College Station, TX.), Tim Barrett (Texas A&M Univ., College Station, TX.), Albert F. Kascak (Army Aviation Systems Command, Cleveland, OH.), Gerald Brown, Gerald Montague, Eliseo DiRusso, and Steve Klusman et al *In* NASA. Langley Research Center, Second International Symposium on Magnetic Suspension Technology, Part 2 May 1994 p 467-478 (For primary document see N94-35902 11-18)
Avail: CASI HC A03/MF A03

N94-35911*# Sulzer-Escher Wyss Ltd., Zurich (Switzerland).
ROTOR DYNAMIC BEHAVIOUR OF A HIGH-SPEED OIL-FREE MOTOR COMPRESSOR WITH A RIGID COUPLING SUPPORTED ON FOUR RADIAL MAGNETIC BEARINGS
J. Schmied and J. C. Pradetto *In* NASA. Langley Research Center, Second International Symposium on Magnetic Suspension Technology, Part 2 May 1994 p 557-572 (For primary document see N94-35902 11-18)
Avail: CASI HC A03/MF A03

N94-35912*# National Cheng Kung Univ., Tainan (Taiwan). Inst. of Aeronautics and Astronautics.
NONLINEAR FEEDBACK MODEL ATTITUDE CONTROL USING CCD IN MAGNETIC SUSPENSION SYSTEM
Chin-E. Lin and Ann-San Hou *In* NASA. Langley Research Center, Second International Symposium on Magnetic Suspension Technology, Part 2 May 1994 p 575-582 (For primary document see N94-35902 11-18)
(Contract NSC-82-0424-E0006-040)
Avail: CASI HC A02/MF A03

N94-35913*# National Aeronautics and Space Administration. Langley Research Center, Hampton, VA.
ROBUST TRACKING CONTROL OF A MAGNETICALLY SUSPENDED RIGID BODY
Kyong B. Lim and David E. Cox *In its* Second International Symposium on Magnetic Suspension Technology, Part 2 May 1994 p 583-603 See also A93-52186 (For primary document see N94-35902 11-18)
Avail: CASI HC A03/MF A03

N94-35916*# Arling (R. W.), Windham, NH.
SIX DEGREE OF FREEDOM FINE MOTION POSITIONING STAGE BASED ON MAGNETIC LEVITATION
R. W. Arling and S. M. Kohler *In* NASA. Langley Research Center, Second International Symposium on Magnetic Suspension Technology, Part 2 May 1994 p 641-652 See also N94-19547 (For primary document see N94-35902 11-18)
(Contract DE-AC04-76DP-00789)
Avail: CASI HC A03/MF A03

N94-35917*# North Carolina Univ., Charlotte, NC. Dept. of Electrical Engineering.
ANALYSIS OF ACHIEVABLE DISTURBANCE ATTENUATION IN A PRECISION MAGNETICALLY-SUSPENDED MOTION CONTROL SYSTEM
Alexander V. Kuzin, Michael L. Holmes, Roxana Behrouzjou, and David L. Trumper *In* NASA. Langley Research Center, Second International Symposium on Magnetic Suspension Technology, Part 2 May 1994 p 653-665 (For primary document see N94-35902 11-18)
Avail: CASI HC A03/MF A03

N94-35918*# Xerad, Inc., Santa Monica, CA.
FUTURE ULTRA-SPEED TUBE-FLIGHT Abstract Only
Robert M. Salter *In* NASA. Langley Research Center, Second International Symposium on Magnetic Suspension Technology, Part 2 May 1994 p 669-670 (For primary document see N94-35902 11-18)
Avail: CASI HC A01/MF A03

N94-36046*# National Aeronautics and Space Administration. Goddard Space Flight Center, Greenbelt, MD.
SPACE ROBOTICS IN JAPAN
William Whittaker (Carnegie-Mellon Univ., Pittsburgh, PA.), James W. Lowrie (Martin Marietta Corp., Denver, CO.), Harry McCain, Antal Bejczy, Tom Sheridan, Takeo Kanade, and Peter Allen *In* Loyola Coll., JTEC/WTEC Report and Program Summary Mar. 1994 p 133-137 (For primary document see N94-36042 11-99)
Avail: CASI HC A01/MF A03

38 QUALITY ASSURANCE AND RELIABILITY

Includes product sampling procedures and techniques; and quality control.

N94-36090 Grumman Aerospace Corp., Bethpage, NY.
NONDESTRUCTIVE INSPECTION (NDI) OF REDUCED STRENGTH BONDS Final Report
Richard Chance Feb. 1994 36 p Limited Reproducibility: More than 20% of this document may be affected by microfiche quality
(Contract DTFA03-88-C-00016)
(AD-A278745; DOT/FAA/CT-93/42) Avail: Issuing Activity (Defense Technical Information Center (DTIC))

The goal of this project was to develop a nondestructive inspection technique capable of detecting weak adhesive bonds. The approach was to fabricate contaminated surface-induced weak bond specimens which were then used to evaluate candidate techniques and to further optimize the selected most promising technique. The results indicate the ultrasonic resonance technique showed some success in detecting weak bonds as determined through destructive test correlations conducted using the representative weak bond specimens. The technique was 97 percent effective in detecting known weak bonds but was subject to false reject error ranging between 14 and 31 percent depending upon the evaluation criteria employed. Difficulties were encountered with the destructive test correlations due to the wide variation of results experienced with the flatwise tension tests that were conducted. The ultrasonic resonance technique and a recently emerged ultrasonic feature analysis/adaptive learning technique looked promising but will require further evaluation involving test specimens with large weak bond areas representing several weak bond mechanisms in addition to contaminated interfaces. DTIC

N94-36292 Northwestern Univ., Evanston, IL.
COMPUTATIONAL METHODS FOR MATERIAL FAILURE PROCESSES Final Report, 1 Sep. 1990 - 31 Dec. 1993
Ted Belytschko Feb. 1994 64 p Limited Reproducibility: More than 20% of this document may be affected by microfiche quality
(Grant AF-AFOSR-0340-90)
(AD-A278716; AFOSR-94-0253TR) Avail: Issuing Activity (Defense Technical Information Center (DTIC))

Computational methods are developed for failure problems such as shear banding. H-Adaptive procedures for the finite element solution of transient solid mechanics problems are studied, with particular emphasis on problems involving localization due to material instability. Various types of error criteria are examined and it is shown that for problems involving plastic response or localization, an error criterion based on an L2 projection of strains is the most effective for the constant strain elements considered here. Examples of one dimensional and two dimensional localization (shear band formation) problems are given. Massively parallel computations are performed to study the effects of imperfections on shear band morphology. DTIC

39 STRUCTURAL MECHANICS

Includes structural element design and weight analysis; fatigue; and thermal stress.

For applications see *05 Aircraft Design, Testing and Performance* and *18 Spacecraft Design, Testing and Performance.*

N94-35239*# Virginia Univ., Charlottesville, VA.
OPTIMIZATION OF RESIDUAL STRESSES IN MMC'S USING COMPENSATING/COMPLIANT INTERFACIAL LAYERS. PART 2: OPTCOMP USER'S GUIDE Final Report
Marek-Jerzy Pindera, Robert S. Salzar, and Todd O. Williams May 1994 111 p
(Contract NAS3-26571; RTOP 505-63-12)
(NASA-CR-195337; E-8884; NAS 1.26:195337) Avail: CASI HC A06/MF A02

A user's guide for the computer program OPTCOMP is presented in this report. This program provides a capability to optimize the fabrication or service-induced residual stresses in uni-directional metal matrix composites subjected to combined thermo-mechanical axisymmetric loading using compensating or compliant layers at the fiber/matrix interface. The user specifies the architecture and the initial material parameters of the interfacial region, which can be either elastic or elastoplastic, and defines the design variables, together with the objective function, the associated constraints and the loading history through a user-friendly data input interface. The optimization procedure is based on an efficient solution methodology for the elastoplastic response of an arbitrarily layered multiple concentric cylinder model that is coupled to the commercial optimization package DOT. The solution methodology for the arbitrarily layered cylinder is based on the local-global stiffness matrix formulation and Mendelson's iterative technique of successive elastic solutions developed for elastoplastic boundary-value problems. The optimization algorithm employed in DOT is based on the method of feasible directions. Author

N94-35353# Polish Academy of Sciences, Warsaw. Inst. Podstawowych Problemow Techniki.

TESTING OF THE FRACTURE RESISTANCE OF RAILS

Zdzislaw Swiderski 1994 19 p
(ISSN 0208-5658)
Avail: CASI HC A03/MF A01

Various grades of rail steel as well as whole rail sections were subjected to fracture resistance tests according to the unified method. It was found that heat treatment of rails increased fracture resistance by 50 percent. However, residual stresses also had a substantial effect. Apparent durability values N(sub c) from the Wilson formula have been derived. The influence of residual stresses on rail durability is stated. Author

N94-35684# Oak Ridge National Lab., TN.

BIAXIAL LOADING AND SHALLOW-FLAW EFFECTS ON CRACK-TIP CONSTRAINT AND FRACTURE-TOUGHNESS

W. E. Pennell, B. R. Bass, J. W. Bryson, W. J. McAfee, T. J. Theiss, and M. C. Rao 1994 12 p Presented at the Pressure Vessel and Piping Conference, Minneapolis, MN, 19-23 Jun. 1994
(Contract DE-AC05-84OR-21400)
(DE94-010128; CONF-940613-7) Avail: CASI HC A03/MF A01

Uniaxial tests of single-edged, notched bend (SENB) specimens with both deep- and shallow-flaws have shown elevated fracture toughness for the shallow flaws. The elevation in fracture-toughness for shallow flaws was shown to be the result of reduced constraint at the crack-tip. Biaxial loading has the potential to increase constraint at the crack-tip and thereby reduce some of the shallow-flaw, fracture-toughness elevation. Biaxial fracture-toughness tests have shown that the shallow-flaw, fracture-toughness elevation is reduced but not eliminated by biaxial loading. Dual-parameter, fracture-toughness correlations were proposed to reflect the effect of crack-tip constraint on fracture-toughness. Test results from the uniaxial and biaxial tests were analyzed using the dual-parameter technology. Discrepancies between analysis results and cleavage initiation site data from fractographic examinations indicate that the analysis models are in need of further refinement. Addition of a precleavage, ductile-tearing element to the analysis model has the potential to resolve the noted discrepancies. DOE

N94-35949 Science Applications International Corp., McLean, VA.

NUMERICAL SIMULATION OF SHOCK INTERACTION WITH ABOVE-GROUND STRUCTURES Technical Report, 15 May 1989 - 31 Dec. 1992

Joseph D. Baum and Rainald Lohner 1 May 1994 93 p Limited Reproducibility: More than 20% of this document may be affected by microfiche quality
(Contract DNA001-89-C-0098)
(AD-A278713; DNA-TR-93-4) Avail: Issuing Activity (Defense Technical Information Center (DTIC))

This final report for DNA contract DNA 001-89-C-0098 for the time period May 15, 1989 to Dec 31, 1992 describes the results of several of the computations conducted under this research effort. The numerical simulations conducted simulated shock wave diffraction phenomenon about complex-geometry two-dimensional and three-dimensional structures. Since a significant part of this effort was composed of parametric studies that have been delivered to the sponsors, the Defense Nuclear Agency and the Air Force Ballistic Missile Organization (BMO), and conducted under the now defunct Rail Garrison project, we included in this report a detailed description of the results of the major computations, and a brief summary of all the repetitive computations. The final report is divided into three sections. Chapter 1 describes in detail the two-dimensional numerical methodology and typical two-dimensional computation, i.e., the application of the numerical methodology to the simulation of shock interaction with a typical 2-D train (a 2-D cut at the center of a 3-D train). Chapter 2 describes the numerical development of a passive shock reflector, a major effort undertaken in this project. The objective of this effort was to design a passive device that, while allowing the ventilation of the enclosure under steady conditions, will prevent blast waves impinging on the wall from entering the enclosure when the structure is impacted by a shock. DTIC

N94-35974*# Purdue Univ., West Lafayette, IN. School of Aeronautics and Astronautics.

FREQUENCY DOMAIN ANALYSIS OF THE RANDOM LOADING OF CRACKED PANELS Final Report, 1 Oct. 1990 - 30 Sep. 1993

James F. Doyle 16 Jun. 1994 89 p
(Grant NAG1-1173)
(NASA-CR-196021; NAS 1.26:196021) Avail: CASI HC A05/MF A01

The primary effort concerned the development of analytical methods for the accurate prediction of the effect of random loading on a panel with a crack. Of particular concern was the influence of frequency on the stress intensity factor behavior. Many modern structures, such as those found in advanced aircraft, are lightweight and susceptible to critical vibrations, and consequently dynamic response plays a very important role in their analysis. The presence of flaws and cracks can have catastrophic consequences. The stress intensity factor, K, emerges as a very significant parameter that characterizes the crack behavior. In analyzing the dynamic response of panels that contain cracks, the finite element method is used, but because this type of problem is inherently computationally intensive, a number of ways of calculating K more efficiently are explored. CASI

N94-36000 Helsinki Univ. of Technology, Espoo (Finland). Inst. of Mathematics.

AN ENERGY METHOD APPROACH TO THE PROBLEM OF ELASTIC STRIP

O. Ovaskainen and J. Pitkaeranta 1994 39 p Limited Reproducibility: More than 20% of this document may be affected by microfiche quality
(ISSN 0784-3143)
(PB94-171014; RR-A328; ISBN-951-22-1955-7) Avail: CASI HC A03

We analyze a thin elastic, homogeneous strip under a smooth load and several different types of boundary conditions. The strip is assumed to obey either a plane strain or a plane stress type deformation of linear theory of elasticity. We characterize the two dimensional solution and consider dimension reduction of arbitrary order n. Both interior and global energy estimates for the reduction error are derived. NTIS

N94-36216 Direction des Recherches, Etudes et Techniques, Paris (France). Direction Scientifique Soutien a la Recherche.

ACOUSTICAL-OPTICAL FRACTURE ANALYSIS Final Report [ANALYSE ACOUSTO-OPTIQUE DE LA FRACTURE]

1992 64 p In FRENCH
(PB94-170602) Avail: Issuing Activity (National Technical Information Service (NTIS))

An experimental system for measuring static and dynamic fracture properties was used to study fragile plexiglass subjected to tensile stress. Preliminary results found that the limit speed of fracture growth was 20 percent slower than Rayleigh wave speed, and that velocity oscillates around its limiting value at a frequency of 350 KHz. There is a significant delay between the moment of fracture growth and separation of the material into two parts. The sound emitted during fracture has a frequency of 350 KHz, and sharply intensifies when speed begins to oscillate. The surfaces formed by the fracture feature an initial smooth area, then become rough when speed begins to oscillate. The forward acoustical emission of the fracturing intensifies as the force applied to the sample approaches that needed for fracturing. Acoustical emissions, which correspond to microfractures, are located around the area through which the main fracture will travel, but are not situated exactly on the fracturing line. NTIS

N94-36226# National Aerospace Lab., Amsterdam (Netherlands). Structures and Materials Div.

FATIGUE AND RESIDUAL STRENGTH BEHAVIOUR OF ARALL3 PANELS WITH BONDED-ON DOUBLERS

W. vanderHoeven 16 Nov. 1992 78 p Original contains color illustrations
(AD-B181062; NLR-TP-92467U) Avail: CASI HC A05/MF A01

Residual strength tests were performed on ARALL panels consisting of ARALL3(3/2) laminates with bonded-on doublers. In particular, the effect of the doubler geometry (shape and thickness) on the residual strength was investigated. Prior to residual strength testing all panels were fatigue loaded to create a realistic type of damage, i.e. cracks in one of the aluminium alloy face sheets of the ARALL3(3/2) laminate at the edge of the doubler. During the fatigue tests the crack length was monitored. For all panels the final fatigue crack length was intended to be about 30 mm.

Both constant amplitude and flight simulation loading conditions were applied. The results of the tests indicated that the thickness of the doubler had a pronounced effect on the fatigue crack growth rate. The doubler geometry parameters were found to affect damage growth and failure behavior during the residual strength test, but had hardly any effect on the residual strength value itself. During constant amplitude fatigue testing secondary cracks initiated in some panels, resulting in significantly larger total crack lengths than the 30 mm which was intended. From the residual strength data for these panels it was concluded that the crack length (2a greater than or equal to 30 mm) is probably not a dominant parameter for the residual strength. Finally, it was concluded that the strength degradation due the presence of fatigue cracks in one of the aluminium face sheets will probably not be a limiting factor in the design of ARALL structures.
Author (revised)

N94-36423*# California Univ., Los Angeles, CA. Dept. of Mechanical, Aerospace and Nuclear Engineering.
VIBRATION REDUCTION IN HELICOPTER ROTORS USING AN ACTIVELY CONTROLLED PARTIAL SPAN TRAILING EDGE FLAP LOCATED ON THE BLADE
T. A. Millott and P. P. Friedmann Jun. 1994 420 p
(Grants NAG2-477; NGT-50444)
(NASA-CR-4611; A-94096; NAS 1.26:4611) Avail: CASI HC A18/MF A04

This report describes an analytical study of vibration reduction in a four-bladed helicopter rotor using an actively controlled, partial span, trailing edge flap located on the blade. The vibration reduction produced by the actively controlled flap (ACF) is compared with that obtained using individual blade control (IBC), in which the entire blade is oscillated in pitch. For both cases a deterministic feedback controller is implemented to reduce the 4/rev hub loads. For all cases considered, the ACF produced vibration reduction comparable with that obtained using IBC, but consumed only 10-30% of the power required to implement IBC. A careful parametric study is conducted to determine the influence of blade torsional stiffness, spanwise location of the control flap, and hinge moment correction on the vibration reduction characteristics of the ACF. The results clearly demonstrate the feasibility of this new approach to vibration reduction. It should be emphasized than the ACF, used together with a conventional swashplate, is completely decoupled from the primary flight control system and thus it has no influence on the airworthiness of the helicopter. This attribute is potentially a significant advantage when compared to IBC. Author

N94-35407*# National Aeronautics and Space Administration. Lyndon B. Johnson Space Center, Houston, TX.
CRATERS IN ALUMINUM 1100 TARGETS USING GLASS PROJECTILES AT 1-7 km/s Abstract Only
R. P. Bernhard (Lockheed Engineering and Sciences Co., Houston, TX.), T. H. See (Lockheed Engineering and Sciences Co., Houston, TX.), F. Hoerz, and M. J. Cintala *In* Lunar and Planetary Inst., The Twenty-Fifth Lunar and Planetary Science Conference. Part 1: A-G 1994 p 107-108 (For primary document see N94-35395 11-91)
Avail: CASI HC A01/MF A04

N94-35868*# California Univ., Los Angeles, CA. Dept. of Electrical Engineering.
DISTRIBUTED PARAMETER MODELING OF REPEATED TRUSS STRUCTURES
Han-Ching Wang *In* NASA. Langley Research Center, NASA Workshop on Distributed Parameter Modeling and Control of Flexible Aerospace Systems Jun. 1994 p 41-63 Sponsored by NASA. Dryden Flight Research Center (For primary document see N94-35865 11-18)
Avail: CASI HC A03/MF A06

N94-35872*# Pennsylvania State Univ., University Park, PA. Dept. of Aerospace Engineering.
VARIATIONS IN THE MODAL CHARACTERISTICS OF A TELESCOPICALLY DEPLOYING BEAM
Anthony K. Amos *In* NASA. Langley Research Center, NASA Workshop on Distributed Parameter Modeling and Control of Flexible Aerospace Systems Jun. 1994 p 115-131 (For primary document see N94-35865 11-18)
(Grant AF-AFOSR-0155-91)
Avail: CASI HC A03/MF A06

N94-35878*# North Carolina Univ., Charlotte, NC. Dept. of Electrical Engineering.
PARAMETER ESTIMATION OF THE VIBRATIONAL MODEL FOR THE SCOLE EXPERIMENTAL FACILITY
B. D. Crotts and Y. P. Kakad *In* NASA. Langley Research Center, NASA Workshop on Distributed Parameter Modeling and Control of Flexible Aerospace Systems Jun. 1994 p 241-259 (For primary document see N94-35865 11-18)
Avail: CASI HC A03/MF A06

N94-35885*# Old Dominion Univ., Norfolk, VA. Dept. of Mechanical Engineering and Mechanics.
CONTROL OF THE SCOLE CONFIGURATION USING DISTRIBUTED PARAMETER MODELS
Min-Hung Hsiao and Jen-Kuang Huang *In* NASA. Langley Research Center, NASA Workshop on Distributed Parameter Modeling and Control of Flexible Aerospace Systems Jun. 1994 p 351-363 (For primary document see N94-35865 11-18)
Avail: CASI HC A03/MF A06

N94-35886*# Maryland Univ., College Park, MD. Dept. of Electrical Engineering.
ACTIVE VIBRATION DAMPING USING SMART MATERIAL
John S. Baras and Zhuang Yan *In* NASA. Langley Research Center, NASA Workshop on Distributed Parameter Modeling and Control of Flexible Aerospace Systems Jun. 1994 p 365-378 (For primary document see N94-35865 11-18)
(Grants NSF CDR-88-03012; AF-AFOSR-1054-90)
Avail: CASI HC A03/MF A06

N94-35893*# George Mason Univ., Fairfax, VA. Dept. of Electrical and Computer Engineering.
DYNAMICAL OBSERVER FOR A FLEXIBLE BEAM VIA FINITE ELEMENT APPROXIMATIONS
Andre Manitius and Hong-Xing Xia *In* NASA. Langley Research Center, NASA Workshop on Distributed Parameter Modeling and Control of Flexible Aerospace Systems Jun. 1994 p 497-517 (For primary document see N94-35865 11-18)
Avail: CASI HC A03/MF A06

N94-35895*# State Univ. of New York, Buffalo, NY. Mechanical Systems Lab.
TRANSFER FUNCTION MODELING OF DAMPING MECHANISMS IN DISTRIBUTED PARAMETER MODELS
J. C. Slater and D. J. Inman *In* NASA. Langley Research Center, NASA Workshop on Distributed Parameter Modeling and Control of Flexible Aerospace Systems Jun. 1994 p 547-553 (For primary document see N94-35865 11-18)
(Grant NGT-50541)
Avail: CASI HC A02/MF A06

N94-35906*# Ebara Research Co. Ltd., Kanagawa (Japan).
ELECTROMAGNETICALLY LEVITATED VIBRATION ISOLATION SYSTEM FOR THE MANUFACTURING PROCESS OF SILICON MONOCRYSTALS
Yoichi Kanemitsu, Katsuhide Watanabe, Kenichi Yano, and Takayuki Mizuno *In* NASA. Langley Research Center, Second International Symposium on Magnetic Suspension Technology, Part 2 May 1994 p 479-497 (For primary document see N94-35902 11-18)
Avail: CASI HC A03/MF A03

N94-36415*# Loyola Coll., Baltimore, MD. Dept. of Electrical Engineering and Engineering Science.
AN AUTOMATED DIGITAL DATA COLLECTION AND ANALYSIS SYSTEM FOR THE CHARPY IMPACT TESTER
Glenn S. Kohne and F. Xavier Spiegel *In* NASA. Langley Research Center, National Educators' Workshop: Update 1993. Standard Experiments in Engineering Materials Science and Technology Apr. 1994 p 469-480

(For primary document see N94-36398 11-23)
Avail: CASI HC A03/MF A04

42 GEOSCIENCES (GENERAL)

No abstracts in this category.

43 EARTH RESOURCES AND REMOTE SENSING

Includes remote sensing of earth resources by aircraft and spacecraft; photogrammetry; and aerial photography.

For instrumentation see *35 Instrumentation and Photography.*

N94-35261*# National Aeronautics and Space Administration. Goddard Space Flight Center, Greenbelt, MD.
NASA SPACE GEODESY PROGRAM: GSFC DATA ANALYSIS, 1993. VLBI GEODETIC RESULTS 1979 - 1992
Chopo Ma, James W. Ryan, and Douglas S. Caprette Jun. 1994 221 p
(RTOP 926-00-00)
(NASA-TM-104605; Rept-94B00084; NAS 1.15:104605) Avail: CASI HC A10/MF A03

The Goddard VLBI group reports the results of analyzing Mark 3 data sets acquired from 110 fixed and mobile observing sites through the end of 1992 and available to the Space Geodesy Program. Two large solutions were used to obtain site positions, site velocities, baseline evolution for 474 baselines, earth rotation parameters, nutation offsets, and radio source positions. Site velocities are presented in both geocentric Cartesian and topocentric coordinates. Baseline evolution is plotted for the 89 baselines that were observed in 1992 and positions at 1988.0 are presented for all fixed stations and mobile sites. Positions are also presented for quasar radio sources used in the solutions. Author (revised)

N94-35734*# Aerojet-General Corp., Azusa, CA. Electronics Plant.
EARTH OBSERVING SYSTEM (EOS) ADVANCED MICROWAVE SOUNDING UNIT-A (AMSU-A) SCHEDULE PLAN Final Report
Jul. 1994 69 p
(Contract NAS5-32314)
(NASA-CR-194856; Rept-10392A; NAS 1.26:194856) Avail: CASI HC A04/MF A01

This report describes Aerojet's methods and procedures used to control and administer contractual schedules for the EOS/AMSU-A program. Included are the following: the master, intermediate, and detail schedules; critical path analysis; and the total program logic network diagrams. Author (revised)

N94-36018 Argonne National Lab., IL.
ESTIMATION OF FRACTAL DIMENSIONS FROM TRANSECT DATA
C. Loehle 1994 19 p Prepared in cooperation with Georgia Univ., Athens, GA Limited Reproducibility: More than 20% of this document may be affected by microfiche quality
(Contracts W-31-109-eng-38; DE-AC09-76SR-00819)
(DE94-009808; ANL/ER/PP-74994) Avail: CASI HC A03

Fractals are a useful tool for analyzing the topology of objects such as coral reefs, forest canopies, and landscapes. Transects are often studied in these contexts, and fractal dimensions computed from them. An open question is how representative a single transect is. Transects may also be used to estimate the dimensionality of a surface. Again the question of representativeness of the transect arises. These two issues are related. This note qualifies the conditions under which transect data may be considered to be representative or may be extrapolated, based on both theoretical and empirical results. DOE

N94-35417*# National Aeronautics and Space Administration. Ames Research Center, Moffett Field, CA.
SUBPIXEL RESOLUTION FROM MULTIPLE IMAGES Abstract Only
Peter Cheeseman (Research Inst. for Advanced Computer Science, Moffett Field, CA.), Rob Kanefsky (RECOM Technologies, Inc., Moffett Field, CA.), John Stutz, and Richard Kraft *In* Lunar and Planetary Inst., The Twenty-Fifth Lunar and Planetary Science Conference. Part 1: A-G 1994 p 241-242
(For primary document see N94-35395 11-91)
Avail: CASI HC A01/MF A04

N94-35609*# National Aeronautics and Space Administration. Goddard Space Flight Center, Greenbelt, MD.
OBTAINING COINCIDENT IMAGE OBSERVATIONS FOR MISSION TO PLANET EARTH SCIENCE DATA RETURN
Lauri Kraft Newman, David C. Folta, and James P. Farrell *In its* Flight Mechanics/Estimation Theory Symposium, 1994 May 1994 p 33-47
(For primary document see N94-35605 11-13)
Avail: CASI HC A03/MF A04

N94-35852*# National Cheng Kung Univ., Tainan (Taiwan). Inst. of Aeronautics and Astronautics.
FUZZY SELF-LEARNING CONTROL FOR MAGNETIC SERVO SYSTEM
J. H. Tarn, L. T. Kuo, K. Y. Juang, and C. E. Lin *In* NASA. Langley Research Center, Second International Symposium on Magnetic Suspension Technology, Part 1 May 1994 p 249-256 (For primary document see N94-35836 11-18)
Avail: CASI HC A02/MF A04

44 ENERGY PRODUCTION AND CONVERSION

Includes specific energy conversion systems, e.g., fuel cells; global sources of energy; geophysical conversion; and windpower.

For related information see also *07 Aircraft Propulsion and Power, 20 Spacecraft Propulsion and Power,* and *28 Propellants and Fuels.*

N94-35230* National Aeronautics and Space Administration. Langley Research Center, Hampton, VA.
InP SOLAR CELL WITH WINDOW LAYER Patent
Raj K. Jain, inventor (to NASA) and Geoffrey A. Landis, inventor (to NASA) 21 Jun. 1994 7 p Filed 2 Oct. 1992
(NASA-Case-LEW-15606-1; US-Patent-5,322,573;
US-Patent-Appl-SN-955512; US-Patent-Class-136-252;
US-Patent-Class-136-256; US-Patent-Class-437-5; US-Patent-Class-257-76;
US-Patent-Class-257-434; US-Patent-Class-257-631;
Int-Patent-Class-H01L-31/06) Avail: US Patent and Trademark Office

The invention features a thin light transmissive layer of the ternary semiconductor indium aluminum arsenide (InAlAs) as a front surface passivation or 'window' layer for p-on-n InP solar cells. The window layers of the invention effectively reduce front surface recombination of the object semiconductors thereby increasing the efficiency of the cells. Official Gazette of the U.S. Patent and Trademark Office

N94-35271*# National Aeronautics and Space Administration. Lewis Research Center, Cleveland, OH.
Au/Zn CONTACTS TO RHO-InP: ELECTRICAL AND METALLURGICAL CHARACTERISTICS AND THE RELATIONSHIP BETWEEN THEM
Victor G. Weizer, Navid S. Fatemi, and Andras L. Korenyi-Both May 1994 8 p Presented at the MRS Spring Meeting, San Francisco, CA, 4-8 Apr. 1994; sponsored by The Materials Research Society
(RTOP 506-41-11)
(NASA-TM-106590; E-8857; NAS 1.15:106590) Avail: CASI HC A02/MF A01

The metallurgical and electrical behavior of Au/Zn contacting metallization on p-type InP was investigated as a function of the Zn content in the metallization. It was found that ohmic behavior can be achieved with Zn concentrations as small as 0.05 atomic percent Zn. For Zn concentrations between 0.1 and 36 at. percent, the contact resistivity rho(sub c) was found to be independent of the Zn content. For low Zn concentrations the realization of ohmic behavior was found to require the growth of the compound Au2P3 at the metal-InP interface. The magnitude of rho(sub c) is shown to be very sensitive to the growth rate of the interfacial Au2P3 layer. The possibility of exploiting this sensitivity to provide low resistance contacts while avoiding the semiconductor structural damage that is normally attendant to contact formation is discussed. Author

N94-35540*# National Aeronautics and Space Administration. Goddard Space Flight Center, Greenbelt, MD.

MICROPROCESSOR CONTROL OF MULTIPLE PEAK POWER TRACKING DC/DC CONVERTERS FOR USE WITH SOLAR CELL ARRAYS Patent

Martin E. Frederick, inventor (to NASA) and Joel B. Jermakian, inventor (to NASA) 5 Jul. 1994 10 p Filed 12 Jul. 1993 Continuation of abandoned US-Patent-Appl-SN-787993, filed 5 Nov. 1991
(NASA-Case-GSC-13450-2; US-Patent-5,327,071;
US-Patent-Appl-SN-127886; US-Patent-Appl-SN-787993;
US-Patent-Class-323-299; US-Patent-Class-323-906;
US-Patent-Class-136-293; Int-Patent-Class-G05F-5/00) Avail: US Patent and Trademark Office

A method and an apparatus for efficiently controlling the power output of a solar cell array string or a plurality of solar cell array strings to achieve a maximum amount of output power from the strings under varying conditions of use is introduced. Maximum power output from a solar array string is achieved through control of a pulse width modulated DC/DC buck converter which transfers power from a solar array to a load or battery bus. The input voltage from the solar array to the converter is controlled by a pulse width modulation duty cycle, which in turn is controlled by a differential signal comparing the array voltage with a control voltage from a controller. By periodically adjusting the control voltage up or down by a small amount and comparing the power on the load or bus with that generated at different voltage values a maximum power output voltage may be obtained. The system is totally modular and additional solar array strings may be added to the system simply by adding converter boards to the system and changing some constants in the controller's control routines. Official Gazette of the U.S. Patent and Trademark Office

N94-35672# Department of Energy, Washington, DC. Office of Integrated Analysis.

MODEL DOCUMENTATION: RENEWABLE FUELS MODULE OF THE NATIONAL ENERGY MODELING SYSTEM

Apr. 1994 156 p
(DE94-009962; DOE/EIA-M069) Avail: CASI HC A08/MF A02

This report documents the objectives, analytical approach, and design of the National Energy Modeling System (NEMS) Renewable Fuels Module (RFM) as it related to the production of the 1994 Annual Energy Outlook (AEO94) forecasts. The report catalogues and describes modeling assumptions, computational methodologies, data inputs, and parameter estimation techniques. A number of offline analyses used in lieu of RFM modeling components are also described. This documentation report serves two purposes. First, it is a reference document for model analysts, model users, and the public interested in the construction and application of the RFM. Second, it meets the legal requirement of the Energy Information Administration (EIA) to provide adequate documentation in support of its models. The RFM consists of six analytical submodules that represent each of the major renewable energy resources -- wood, municipal solid waste (MSW), solar energy, wind energy, geothermal energy, and alcohol fuels. Of these six, four are documented in the following chapters: municipal solid waste, wind, solar and biofuels. Geothermal and wood are not currently working components of NEMS. The purpose of the RFM is to define the technological and cost characteristics of renewable energy technologies, and to pass these characteristics to other NEMS modules for the determination of mid-term forecasted renewable energy demand. DOE

N94-35739 Emcore Corp., Somerset, NJ.

DEVELOPMENT OF NOVEL II-VI SOLAR CELLS Final Report

G. S. Tompa Nov. 1990 85 p Limited Reproducibility: More than 20% of this document may be affected by microfiche quality
(Grant NSF ISI-89-61518)
(PB94-159415; NSF/ISI-90086) Avail: CASI HC A05

The epitaxial growth of novel II-VI solar cell structures was investigated. In Phase 1, the metal organic chemical vapor deposition (MOCVD) process parameters and associated growth chemistries for an epitaxial p-i-n, ZnTe/CdTe/GaAs, solar cell structure were developed. No doping was attempted in the Phase 1 effort. The solar cell structure was grown as a continuous structure within a single process reactor. Film thickness, compositional uniformity, and electrical properties were measured. A test solar cell was not fabricated because the material was too highly resistive to produce a useful solar cell. This high resistivity is characteristic of very pure ZnTe and CdTe material. The feasibility of this structure was demonstrated, providing a foundation for the development of a functional solar cell, by optimizing the cell structure and growth processes and by developing doping techniques. NTIS

N94-35804 Aerospace Corp., El Segundo, CA. Engineering and Technology Group

IMPROVED PERFORMANCE OF DEGRADED SOLAR ARRAYS AT NON-ZERO SUN INCIDENCE ANGLES

D. C. Marvin 15 May 1993 15 p Limited Reproducibility: More than 20% of this document may be affected by microfiche quality
(Contract F04701-88-C-0089)
(AD-A278905; TR-93(3925)-4; SMC-TR-94-27) Avail: Issuing Activity (Defense Technical Information Center (DTIC))

A silicon solar array was flown in a high-radiation orbit with thin cover glasses. As a result, severe radiation degradation occurred. It was discovered that as degradation proceeded, the maximum array output current was obtained for sun incidence angles other than 0 deg for some bus voltages. Optimum angles as high as 38 deg have been observed. The analysis reported herein was undertaken in order to quantitatively explain the observed sun angle and bus voltage dependence of the array current. The resulting model, which includes temperature and radiation effects on the solar cell properties, was able to account for all of the flight data that have been collected, and can be used for power management planning purposes on this vehicle. DTIC

N94-35829 Argonne National Lab., IL.

FLYWHEEL ENERGY STORAGE USING SUPERCONDUCTING MAGNETIC BEARINGS

R. G. Abboud (Commonwealth Research Corp., Chicago, IL.), K. Uherka, J. Hull, and T. Mulcahy 1994 6 p Presented at the 56th Annual American Power Conference, Chicago, IL, 25-27 Apr. 1994 Limited Reproducibility: More than 20% of this document may be affected by microfiche quality
(Contract W-31-109-eng-38)
(DE94-009817; ANL/ET/CP-82361; CONF-940445-2) Avail: CASI HC A02

Storage of electrical energy on a utility scale is currently not practicable for most utilities, preventing the full utilization of existing base-load capacity. A potential solution to this problem is Flywheel Energy Storage (FES), made possible by technological developments in high-temperature superconducting materials. Commonwealth Research Corporation (CRC), the research arm of Commonwealth Edison Company, and Argonne National Laboratory are implementing a demonstration project to advance the state of the art in high temperature superconductor (HTS) bearing performance and the overall demonstration of efficient Flywheel Energy Storage. Currently, electricity must be used simultaneously with its generation as electrical energy storage is not available for most utilities. Existing storage methods either are dependent on special geography, are too expensive, or are too inefficient. Without energy storage, electric utilities, such as Commonwealth Edison Company, are forced to cycle base load power plants to meet load swings in hourly customer demand. Demand can change by as much as 30% over a 12-hour period and result in significant costs to utilities as power plant output is adjusted to meet these changes. HTS FES systems can reduce demand-based power plant cycling by storing unused nighttime capacity until it is needed to meet daytime demand. DOE

N94-36021# Gilbert/Commonwealth, Reading, PA.

FUEL CELL HANDBOOK UPDATE

W. R. Owens, J. H. Hirschenhofer, R. R. Engleman, Jr., and D. B. Stauffer 1993 7 p Presented at the Joint Contractors Meeting on Advanced Turbine Systems, Fuel Cells and Coal-Fired Heat, Morgantown, WV, 3-5 Aug. 1993
(Contract DE-AC01-88FE-61684)
(DE94-002958; DOE/FE-61684/94/C0264; CONF-930893-33) Avail: CASI HC A02/MF A01

The objective of this work was to update the 1988 version of DOE's Fuel Cell Handbook. Significant developments in the various fuel cell technologies required revisions to reflect state-of-the-art configurations and performance. The theoretical presentation was refined in order to make the handbook more useful to both the casual reader and fuel cell or systems analyst. In order to further emphasize the practical application of fuel cell technologies, the system integration information was expanded. In addition, practical elements, such as suggestions and guidelines to approximate fuel cell performance, were provided. DOE

N94-36051# Midwest Research Inst., Golden, CO. National Renewable Energy Lab.

AICD: ADVANCED INDUSTRIAL CONCEPTS DIVISION BIOLOGICAL AND CHEMICAL TECHNOLOGIES RESEARCH PROGRAM

G. Petersen, ed., K. Bair, ed., and J. Ross, ed. Mar. 1994 154 p
(Contract DE-AC02-83CH-10093)
(DE94-006854; NREL/SP-6506) Avail: CASI HC A08/MF A02

The annual summary report presents the fiscal year (FY) 1993 research activities and accomplishments for the United States Department of Energy (DOE) Biological and Chemical Technologies Research (BCTR) Program of the Advanced Industrial Concepts Division (AICD). This AICD program resides within the Office of Industrial Technologies (OIT) of the Office of Energy Efficiency and Renewable Energy (EE). The annual summary report for 1993 (ASR 93) contains the following: A program description (including BCTR program mission statement, historical background, relevance, goals and objectives), program structure and organization, selected technical and programmatic highlights for 1993, detailed descriptions of individual projects, and a listing of program output including a bibliography of published work, patents, and awards arising from work supported by BCTR. DOE

N94-36052# Midwest Research Inst., Golden, CO. National Renewable Energy Lab.

A GUIDE TO RESEARCH FACILITIES AT THE NATIONAL RENEWABLE ENERGY LABORATORY

Apr. 1994 24 p
(Contract DE-AC02-83CH-10093)
(DE94-006857; NREL/SP-280-5794) Avail: CASI HC A03/MF A01

The guide is divided into two parts. Topping the pages are descriptions of laboratories at NREL that provide sophisticated experimental equipment, testing capabilities, or processes that may not be available in the private sector. Scientific categories are designated at the top of the pages in blue; individual laboratory descriptions follow alphabetically, along with the names and phone numbers of the laboratory managers. In blue boxes at the bottom of the pages are articles about NREL, our technology transfer program, and our facilities, as well as guidelines for students, researchers, and industrial collaborators who wish to use them. A list of key contacts and a map of the campus follows the laboratory descriptions. DOE

N94-36060# Turku Univ. (Finland). Dept. of Applied Physics.

THEORETICAL AND EXPERIMENTAL STUDY OF AIR AND HYDROGEN ELECTRODES Ph.D. Thesis

M. Viitanen 1993 131 p
(ISSN 0789-1822)
(DE94-763308; Turku-SFL-D1; ISBN-951-29-0125-0) Avail: CASI HC A07/MF A02

The purpose of this study was to develop mathematical models describing the performance of a porous air electrode and a metal hydride electrode for alkaline cells, and with the aid of the models to analyze and optimize the electrodes. The aim was also to develop a preparation method for manufacturing porous air electrodes and to find suitable materials for an air electrode with high performance. In the model the air electrode is assumed to consist of two layers, a hydrophobic gas-supplying layer and a partly hydrophilic reaction layer. The hydrophilic porous catalytic agglomerates in the reaction layer are assumed to be cylindrical. The mathematical model takes into account the diffusion of oxygen in porous hydrophobic layer, the diffusion of dissolved oxygen, the electrochemical reaction, and the ohmic potential drops in the electrolyte and in the electrode. By analyzing the prepared air electrodes with the model we were able to estimate which properties of the electrode should be improved and which we should concentrate on in further development and research. The porous PTFE-bonded air electrodes were prepared by the so-called rolling method. Different types and amounts of carbons and PTFE dispersions were tested and the effect of pretreatment of carbon powder and the filler particles was studied. Several different catalysts were also evaluated and the long term stability of the electrode was tested. DOE

N94-36109# Westinghouse Science and Technology Center, Pittsburgh, PA.

A SOLID OXIDE FUEL CELL POWER SYSTEM: 1992-1993 FIELD OPERATION

S. E. Veyo, A. Kusunoki, S. Takeuchi, S. Kaneko, and H. Yokoyama 1994 9 p Presented at the 56th Annual American Power Conference, Chicago, IL, 25-27 Apr. 1994
(Contract DE-FC21-91MC-28055)
(DE94-010383; DOE/MC-28055/94/C0334; CONF-940445-5) Avail: CASI HC A02/MF A01

Westinghouse has deployed fully integrated, automatically controlled, packaged solid oxide fuel cell (SOFC) power generation systems in order to obtain useful customer feedback. Recently, Westinghouse has deployed 20 kW class natural gas fueled SOFC generator modules integrated into two 25 kW SOFC systems, the first with The UTILITIES, a Japanese consortium. The UTILITIES 25 kW SOFC system is the focus of this paper. The unit was shipped to the Rokko Island Test Center for Advanced Energy Systems (near Kobe, Japan) operated by Kansai Electric Power Co.; testing was initiated February 1992. Module A operated for 2601 hours at an average output of 16.6 kW dc; final shutdown was induced by current stability problems with dissipator (restart not possible because of damaged cells). Module B operated for 1579 hours at an average output of 17.8 kW dc. The unit was damaged by operation at excessively high fuel utilization, greater than 91%. It was rebuilt and returned to Rokko Island. This module B2 operated for 1843 hours on PNG; shutdown was caused by air supply failure. After a new blower and motor were installed July 1993, the system was restarted August 5, 1993 and operated continuously until November 10, 1993, when an automatic shutdown was induced as part of a MITI licensing inspection. After restart, the unit passed 6000 hours of operation on desulfurized PNG on January 25, 1994. Westinghouse's future plans are outlined. DOE

N94-36243# Detroit Diesel Allison, MI.

RESEARCH AND DEVELOPMENT OF PROTON-EXCHANGE MEMBRANE (PEM) FUEL CELL SYSTEM FOR TRANSPORTATION APPLICATIONS: INITIAL CONCEPTUAL DESIGN REPORT

30 Nov. 1993 134 p
(Contract DE-AC02-90CH-10435)
(DE94-010576; DOE/CH-10435/T15; EDR-16194) Avail: CASI HC A07/MF A02

This report addresses Task 1.1, model development and application, and Task 1.2, vehicle mission definition. Overall intent is to produce a methanol-fueled 10-kW power source and to evaluate electrochemical engine (ECE) use in transportation. Major achievements include development of an ECE power source model and its integration into a comprehensive power source/electric vehicle propulsion model, establishment of candidate FCV (fuel cell powered electric vehicle) mission requirements, initial FCV studies, and a candidate FCV recommendation for further study. DOE

N94-35909*# Kernforschungszentrum G.m.b.H., Karlsruhe (Germany).

CONCEPTS OF FLYWHEELS FOR ENERGY STORAGE USING AUTOSTABLE HIGH-T(SUB c) SUPERCONDUCTING MAGNETIC BEARINGS

Hans J. Bornemann, R. Zabka, P. Boegler, C. Urban, and H. Rietschel *In* NASA. Langley Research Center, Second International Symposium on Magnetic Suspension Technology, Part 2 May 1994 p 529-542 (For primary document see N94-35902 11-18)
(Contract CEC-BRE2-CT92-0274)
Avail: CASI HC A03/MF A03

N94-35910*# Fare, Inc., College Park, MD.

MANUFACTURING AND TESTING OF A MAGNETICALLY SUSPENDED COMPOSITE FLYWHEEL ENERGY STORAGE SYSTEM

Stephen Wells and Da-Chen Pang *In* NASA. Langley Research Center, Second International Symposium on Magnetic Suspension Technology, Part 2 May 1994 p 543-556 (For primary document see N94-35902 11-18)
(Contract NAS5-31704)
Avail: CASI HC A03/MF A03

45 ENVIRONMENT POLLUTION

Includes atmospheric, noise, thermal, and water pollution.

N94-35346# Aquatech Systems, Warren, NJ.
COMBINED SO(x)/NO(x) CONTROL VIA SOXAL (TM) PROCESS: AN ELECTRODIALYTIC REGENERATIVE WET SCRUBBING PROCESS
C. M. Denker 30 Dec. 1993 190 p
(Contract DE-AC22-91PC-91347)
(DE94-009053; DOE/PC-91347/T6) Avail: CASI HC A09/MF A02

This report describes the six-month, three megawatt equivalent demonstration of the SOXAL(trademark) flue gas control process. AlliedSignal began operation of the process in January 1993 at Niagara Mohawk's Dunkirk coal-fired steam station. The US Department of Energy's Pittsburgh Energy Technology Center sponsored the project. Niagara Mohawk Power Corporation, the Empire State Electric Energy Research Corporation (ESEERCO), and the New York State Energy Research and Development Authority (NYSERDA) provided additional funding. The project successfully demonstrated absorption of sulfur dioxide and concurrent regeneration of sodium-based scrubbing liquor via bipolar membrane electrodialysis. Additionally, the project demonstrated sulfur dioxide removal efficiency of greater than 98%. Both the absorption and regeneration processes were proven to be both reliable and controllable. These processes were successfully operated in both continuous and decoupled modes of operation, which provides substantial flexibility for power plant operators to perform maintenance, follow variable loads, and utilize off-peak power for regeneration. DOE

N94-35486*# Colorado State Univ., Fort Collins, CO.
METHANE PRODUCTION AND CONSUMPTION IN GRASSLAND AND BOREAL ECOSYSTEMS Final Report
David S. Schimel, Ingrid C. Burke, Carol Johnston, and John Pastor 6 Jul. 1994 25 p
(Grant NAGw-1828)
(NASA-CR-196085; NAS 1.26:196085) Avail: CASI HC A03/MF A01

The objectives of the this project were to develop a mechanistic understanding of methane production and oxidation suitable for incorporation into spatially explicit models for spatial extrapolation. Field studies were undertaken in Minnesota, Canada, and Colorado to explore the process controls over the two microbial mediated methane transformations in a range of environments. Field measurements were done in conjunction with ongoing studies in Canada (the Canadian Northern Wetlands Projects: NOWES) and in Colorado (The Shortgrass Steppe Long Term Ecological Research Project: LTER). One of the central hypotheses of the proposal was that methane production should be substrate limited, as well as being controlled by physical variables influencing microbial activity (temperature, oxidation status, and pH). Laboratory studies of peats from Canada and Minnesota (Northern and Southern Boreal) were conducted with amendments of a methanogenic substrate at multiple temperatures and at multiple pHs (the latter by titrating samples). The studies showed control by substrate, pH, and temperature in order in anaerobic samples. Field and laboratory manipulations of natural plant litter, rather than an acetogenic substrate, showed similarly large effects. The studies concluded that substrate is an important control over methanogenesis, that substrate availability in the field is closely coupled to the chemistry of the dominant vegetation influencing its decomposition rate, that most methane is produced from recent plant litter, and that landscape changes in pH are an important control, highly correlated with vegetation. Derived from text

N94-35503* Jet Propulsion Lab., California Inst. of Tech., Pasadena, CA.
INSIGHT TO GLOBAL CHANGE: EOS/SAR MISSION (Videotape)
Jun. 1990 Videotape: 8 min. 30 sec. playing time, in color, with sound
(NASA-CR-196133; NONP-NASA-VT-94-15911) Avail: CASI VHS A01/BETA A22

This video presentation describes the methods and instrumentation used to help in determining future climate changes on Earth and explains the benefits of experimentation with synthetic aperture radar (SAR). It also gives a better understanding of the burning of fossil fuels, deterioration of the biosphere and deforestation of the rain forest which causes the green house effect. CASI

N94-35668# Urban Consortium for Technology Initiatives.
HOW TO DEVELOP A LONG TERM CO2 REDUCTION PLAN
Dec. 1993 60 p
(Contract DE-FC02-92CE-16067)
(DE94-009559; DOE/CE-16067/2) Avail: CASI HC A04/MF A01

Dade County is particularly vulnerable to the impacts of global warming because it is a low lying coastal community. Metro-Dade County participated in an international effort sponsored by the International Council For Local Environmental Initiatives (ICLEI) to develop specific programs to reduce carbon dioxide emissions by 20% below 1988 emission levels. Metro-Dade developed a long-term CO2 reduction strategy which includes various energy alternatives in electrical production/use, transportation, solid waste and land use. A significant part of the solution to reversing the predicted climate change is using tools most readily available to local governments. Project objectives to reduce CO2 emissions include the following tasks: (1) establish a baseline CO2 emissions inventory; (2) apply the Total Emissions Modeling Integrated Systems model to analyze upstream emissions from the extraction, processing and transportation of primary fuels; (3) identify energy alternatives; (4) evaluate CO2 reduction potential and cost-effectiveness of energy alternatives; and (5) complete a long term CO2 emission reduction plan. Results from this two year project include an energy profile, a CO2 emissions inventory and a report on Dade County's strategy to reduce CO2 emissions. DOE

N94-35674 Coast Guard, Washington, DC. Research and Development Center.
EVALUATION OF SYNTHETIC APERTURE RADAR FOR OIL-SPILL RESPONSE Final Report, Jun. 1992 - Sep. 1993
G. L. Hover, G. A. Mastin, R. M. Axline, and J. D. Bradley Oct. 1993 216 p Prepared in cooperation with Sandia National Labs, Albuquerque, NM Limited Reproducibility: More than 20% of this document may be affected by microfiche quality
(Contract MIPR-Z51100-2-E00467)
(AD-A278796; USCG-D-02-94; USGC-R/DC-27/93) Avail: Issuing Activity (Defense Technical Information Center (DTIC))

This report provides a detailed evaluation of synthetic aperture radar (SAR) as a potential technology improvement over the Coast Guard's existing side-looking airborne radar (SLAR) for oil-spill surveillance applications. The U.S. Coast Guard Research and Development Center (R&D Center), Environmental Safety Branch, sponsored a joint experiment including the U.S. Coast Guard, Sandia National Laboratories, and the National Oceanographic and Atmospheric Administration (NOAA), Hazardous Materials Division. Radar imaging missions were flown on six days over the coastal waters off Santa Barbara, CA, where there are constant natural seeps of oil. Both the Coast Guard SLAR and the Sandia National Laboratories SAR were employed to acquire simultaneous images of oil slicks and other natural sea surface features that impact oil-spill interpretation. Surface truth and other environmental data were also recorded during the experiment. The experiment data were processed at Sandia National Laboratories and delivered to the R&D Center on a PC-based computer workstation for analysis by experiment participants. DTIC

N94-35700 Lawrence Livermore National Lab., CA.
CAirTOX: A COMPARTMENT MODEL FOR ASSESSING THE FATE OF AND HUMAN EXPOSURE TO TOXIC-CHEMICAL EMISSIONS TO AIR
T. E. McKone Oct. 1993 87 p Limited Reproducibility: More than 20% of this document may be affected by microfiche quality
(Contract W-7405-eng-48)
(DE94-010084; UCRL-CR-115619) Avail: Issuing Activity (Department of Energy (DOE))

CAirTOX was developed as a spreadsheet model to assist in making a risk assessment of toxic air emissions. With CAirTOX, one can address how contaminants released to an air basin can lead to contamination of soil, food, surface water, and sediments. The modeling effort includes a multimedia transport and transformation model, exposure scenario models, and efforts to quantify uncertainty in multimedia, multiple-pathway exposure assessments. The multimedia transport and transformation model is a steady-state, but non-equilibrium model that can be used to assess concentrations of contaminants released continuously to air. In Part 1, the authors describe the multimedia transport and transformation model used to determine the fate of air emissions. In Part 2, they describe inputs and data needs for CAirTOX and the development of a set of landscape factors, which can be used to represent regional air basin/water-shed systems in California. In Part 3, they describe the multiple-pathway exposure scenarios and exposure algorithms. In Part 4, they compare the HRA approach and results and the CAirTOX exposure equations. In Part 5, they consider model sensitivity and uncertainty to determine how variability and uncertainty in model inputs affects the precision, accuracy, and credibility of the model output. DOE

N94-35735 Nevada Univ. System, Reno, NV. Desert Research Inst.
PARTICULATE AND GASEOUS ORGANIC RECEPTOR MODELING FOR THE SOUTHERN CALIFORNIA AIR QUALITY STUDY Final Report
J. G. Watson, J. G. Chow, Z. Lu, and A. W. Gertler Nov. 1993 402 p Limited Reproducibility: More than 20% of this document may be affected by microfiche quality
(Contract ARB-A832-132)
(PB94-156700) Avail: CASI HC A18

The Chemical Mass Balance (CMB) receptor model was applied to the chemically-speciated diurnal particulate matter samples and volatile organic compound (VOC) acquired during the summer and fall campaigns of the Southern California Air Quality Study (SCAQS). Source profiles applicable to the Los Angeles area were used to apportion PM(sub(2.5)) and PM(sub(10)) to primary paved road dust, primary construction dust primary motor vehicle exhaust, primary marine aerosol, secondary ammonium nitrate, and secondary ammonium sulfate. Nonmethane hydrocarbon was apportioned to motor vehicle exhaust, liquid fuel, gasoline vapor, gas leaks, architectural and industrial coatings, and biogenic emissions. Suspended dust was the major contributor to PM(10) during the summer, while secondary ammonium nitrate and primary motor vehicle exhaust contributions were high in the fall. Motor vehicle exhaust was the major contributor to nonmethane hydrocarbons, ranging from 30 percent to 70 percent of the total. NTIS

N94-35741 FTN and Associate Ltd. Little Rock, AR.
ENVIRONMENTAL MONITORING AND ASSESSMENT PROGRAM ASSESSMENT FRAMEWORK
K. W. Thornton, G. E. Saul, and D. E. Hyatt Feb. 1994 53 p Limited Reproducibility: More than 20% of this document may be affected by microfiche quality
(Contract EPA-68-DO-0093)
(PB94-158862; EPA/620/R-94/016) Avail: CASI HC A04

The document presents a framework for conducting assessments in the Environmental Monitoring and Assessment Program (EMAP). The framework describes basic elements of the assessment process and provides a common foundation for conducting assessments within EMAP. Because of its general nature, the framework should be adaptable to a diverse set of assessment questions and needs. Consequently, the document is written to assist science administrators and resource managers in understanding the EMAP assessment process. DTIC

N94-35754 Environmental Protection Agency, Ann Arbor, MI. Office of Mobile Sources.
FINAL REGULATORY IMPACT ANALYSIS: REFUELING EMISSION REGULATIONS FOR LIGHT DUTY VEHICLES AND TRUCKS AND HEAVY DUTY VEHICLES
Jan. 1994 159 p Limited Reproducibility: More than 20% of this document may be affected by microfiche quality
(PB94-164027) Avail: CASI HC A08

Culminating a rulemaking process which has spanned more than a decade, the Environmental Protection Agency (EPA) is now promulgating final regulations requiring all highway light-duty vehicles, light-duty trucks, and heavy-duty vehicles to meet onboard refueling vapor recovery (ORVR or onboard control) standards. The purpose of this analysis is to evaluate the costs, benefits, and overall cost effectiveness of onboard control for the reduction of refueling emissions from highway motor vehicles. NTIS

N94-35765 Argonne National Lab., IL.
BUS APPLICATION OF OXYGEN-ENRICHMENT TECHNOLOGY AND DIESEL-ELECTRIC HYBRID SYSTEMS
R. R. Sekar and W. W. Marr Oct. 1993 72 p Limited Reproducibility: More than 20% of this document may be affected by microfiche quality
(Contract W-31-109-eng-38)
(DE94-009835; ANL/ESD/TM-58) Avail: CASI HC A04

The amendments to the Clean Air Act (CAA) mandate very strict limits on particulate, smoke, and other emissions from city buses. The use of alternative fuels, such as compressed natural gas (CNG) or methanol, can help transit operators, such as the Chicago Transit Authority (CTA), meet the mandated limits. However, the capital investment needed to convert the fueling infrastructure and buses is large, as is the expense of training personnel. If a 'clean diesel' bus can be implemented with the help of oxygen-enrichment technology or a diesel-electric hybrid system, this large investment could be postponed for many years. The Regional Transportation Authority (RTA) initiated this project to evaluate the possibility of applying these technologies to CTA buses. Argonne National Laboratory (ANL) conducted a limited number of engine tests and computer analyses and concluded that both concepts are practical and will help result in a 'clean diesel' bus that can meet the mandated limits of the CAA amendments. The oxygen enrichment of combustion air depends on the availability of a compact and economical membrane separator. Because the technology for this critical component is still under development, it is recommended that an actual bus demonstration be delayed until prototype membranes are available. The hybrid propulsion system is ready for the demonstration phase, and it is recommended that the CTA and RTA commence planning for a bus demonstration. DOE

N94-35823 Westinghouse Savannah River Co., Aiken, SC.
ATMOSPHERIC AND DISPERSION MODELING IN AREAS OF HIGHLY COMPLEX TERRAIN EMPLOYING A FOUR-DIMENSIONAL DATA ASSIMILATION TECHNIQUE
J. D. Fast and B. L. OSteen 1994 9 p Presented at the 74th American Meteorological Society Annual Meeting, Nashville, TN, 23-28 Jan. 1994 Limited Reproducibility: More than 20% of this document may be affected by microfiche quality
(Contract DE-AC09-89SR-18035)
(DE94-004041; WSRC-MS-93-502; CONF-940115-16) Avail: CASI HC A02

The results of this study indicate that the current data assimilation technique can have a positive impact on the mesoscale flow fields; however, care must be taken in its application to grids of relatively fine horizontal resolution. Continuous FDDA is a useful tool in producing high-resolution mesoscale analysis fields that can be used to accomplish the following: (1) create a better initial conditions for mesoscale atmospheric models; and (2) drive transport modelsfor dispersion studies. While RAMS is capable of predicting the qualitative flow during this evening, additional experiments need to be performed to improve the prognostic forecasts made by RAMS and refine the FDDA procedure so that the overall errors are reduced even further. Despite the fact that a great deal of computational time is necessary in executing RAMS and LPDM in the configuration employed in this study, recent advances in workstations are making applications such as this more practical. As the speed of these machines increase in the next few years, it will become feasible to employ prognostic, three-dimensional mesoscale/transport models to routinely predict atmospheric dispersion of pollutants, even to highly complex terrain. For example, the version of RAMS in this study could be run in a 'nowcasting' model that would continually assimilate local and regional observations as soon as they become available. The atmospheric physics in the model would be used to determine the wind field where no observations are available. The three-dimensional flow fields could be used as dynamic initial conditions for a model forecast. The output from this type of modeling system will have to be compared to existing diagnostic, mass-consistent models to determine whether the wind field and dispersion forecasts are significantly improved. DOE

N94-35943# Lawrence Livermore National Lab., CA. Environmental Protection Dept.
CLEANING UP OUR ACT: ALTERNATIVES FOR HAZARDOUS SOLVENTS USED IN CLEANING
J. D. Shoemaker, M. Meltzer, D. Miscovich, D. Montoya, P. Goodrich, and G. Blycker Jan. 1994 101 p
(Contract W-7405-eng-48)
(DE94-006624; UCRL-ID-115831) Avail: CASI HC A06/MF A02

Lawrence Livermore National Laboratory (LLNL) has studied more than 70 alternative cleaners as potential replacements for chlorofluorocarbons (CFC's), halogenated hydrocarbons (e.g., trichloroethylene and trichloroethane), hydrocarbons (e.g., toluene and Stoddard solvent), and volatile organic compounds (e.g., acetone and alcohols). This report summarizes LLNL's findings after testing more than 45 proprietary formulations on bench-scale testing equipment and in more than 60 actual shops and laboratories. Cleaning applications included electronics fabrication, machine shops, optical lenses and hardware, and general cleaning. Most of the alternative cleaners are safer than the solvents previously used and many are nonhazardous, according to regulatory criteria. DOE

N94-35957# Sandia National Labs., Albuquerque, NM.
DECISION AND SYSTEMS ANALYSIS FOR UNDERGROUND STORAGE TANK WASTE RETRIEVAL SYSTEMS AND TANK WASTE REMEDIATION SYSTEM
Dennis A. Bitz (Bitz, Dennis A., Washington, DC.), Dennis L. Berry, and Leslie J. Jardine Oct. 1993 65 p Original contains color illustrations
(Contracts DE-AC04-94AL-85000; W-7405-eng-48)
(SAND94-0065) Avail: CASI HC A04/MF A01

Hanford's underground storage tanks (UST's) pose one of the most challenging hazardous and radioactive waste problems for the Department of Energy (DOE). Numerous schemes have been proposed for removing the waste from the UST's, but the technology options for doing this are largely unproven. To help assess the options, an Independent Review Group (IRG) was established to conduct a broad review of retrieval systems and the tank waste remediation system. The IRG's recommendation was that a tool should be developed for evaluating retrieval concepts that includes (1) important considerations identified previously by the IRG, (2) a means of documenting important decisions concerning retrieval systems, and (3) a focus on evaluations and assessments for the tank waste remediation system (TWRS) and the underground storage tank-integrated demonstration (UST-ID). As a first step to this decision tool development effort, the IRG focused on systems and decision analysis. After an introduction, the key issues to be addressed by the decision analysis tool are described in section 3. Section 4 describes the various retrieval concepts and how they are related to SST waste classes. Then two examples of decision analysis tools are given in section 5. Section 6 discusses the use of decision analysis in decision making. Finally, the IRG's key insights, conclusions, and recommendations are presented in section 7. CASI

N94-36007# Argonne National Lab., IL.
MODELING THE ATMOSPHERIC INPUT OF NUTRIENTS, HEAVY METALS, AND PESTICIDES TO THE GREAT LAKES
J. Shannon 1993 14 p Presented at the 1st Workshop on Emissions and Modelling of Atmospheric Transport of Persistent Organic Pollutants and Heavy Metals, Durham, NC, 6-7 May 1993
(Contract W-31-109-eng-38)
(DE94-005481; ANL/ER/CP-81722; CONF-9305320-1-Vugraphs) Avail: CASI HC A03/MF A01

This report documents proceedings of the workshop on Emissions and Modelling of Atmospheric Transport of Persistent Organic Pollutants and Heavy Metals. Topics include: various atmospheric circulation models; deposition of sulfates, nitrogen oxides, lead, and toxaphene into the Great Lakes and Canadian regions; and mercury deposition by dry deposition and washout. DOE

N94-36024# Pacific Northwest Lab., Richland, WA.
THE ATMOSPHERIC RADIATION MEASUREMENT PROGRAM AND INTERFACES WITH EXTERNAL DATA SOURCES
G. M. Stokes, T. S. Cress, and R. B. Melton Oct. 1993 7 p Presented at the 9th AIAA Computing in Aerospace Conference, San Diego, CA, 19-21 Oct. 1993
(Contract DE-AC06-76RL-01830)
(DE94-003699; PNL-SA-23164; CONF-9310241-1) Avail: CASI HC A02/MF A01

The Atmospheric Radiation Measurement (ARM) Program is the Department of Energy's major field project in support of its global change research program. Its objective is to improve the performance of cloud and radiation models and parameterizations in general circulation models (GCM's) used for climate research. The data produced by ARM will be handled and maintained to satisfy the research needs of the program and to be accessible and usable by the general research and academic communities. In addition to data from field instrumentation, ARM Science Team needs include a substantial amount of data from outside the ARM Program ('external data'), which will be acquired and provided routinely through the ARM data system. With respect to data archival and sharing, the ARM Program reflects the objectives delineated by the US Global Change. The purpose of this presentation is to summarize the conceptual designs embodied in the ARM data system and the status of its implementation. DOE

N94-36025# Lawrence Livermore National Lab., CA.
ANTHROPOGENIC SULFATE AND ORGANIC AEROSOLS, CCN, AND CLOUD PROJECT CONCENTRATION AT A MARINE SITE
T. Novakao (California Univ., Berkeley. Lawrence Berkeley Lab, CA.), C. Rivera-Carpio (California Univ., Berkeley. Lawrence Berkeley Lab, CA.), J. E. Penner, and C. F. Rogers Oct. 1993 6 p Presented at the 74th American Meteorological Society Annual Meeting, Nashville, TN, 23-28 Jan. 1994
(Contracts W-7405-eng-48; DE-AC03-76SF-00098)
(DE94-004210; UCRL-JC-115308; CONF-940115-14) Avail: CASI HC A02/MF A01

The need to establish the relationships between the number concentration of cloud droplets, cloud condensation nuclei (CCN), and the mass concentrations of major aerosol species has been heightened by the results of recent modeling studies suggesting that anthropogenic sulfate and biomass smoke aerosols may cause a globally averaged climate forcing comparable in magnitude but opposite in sign to the forcing due to 'greenhouse' gases. In this paper we present the results of measurements of nonseasalt (nss) sulfate and organic carbon mass concentrations and mass size distributions, CCN, and cloud droplet number concentrations obtained in 1991 and 1992 on El Yunque peak, Puerto Rico . This peak (18(degree)19N, 65(degree)45W; elevation 1000 m) is located at the eastern end of the island, directly exposed to the ocean winds and frequently covered with clouds. Our results show that although CCN number concentrations (measured at 0.5% supersaturation) and nss sulfate mass concentrations are significantly correlated at this site, estimates based on measured mass size distributions of organic and sulfate aerosols indicate that the organic aerosols may account for the majority of CCN number concentrations. Droplet concentrations in the cumulus clouds do not show a discernible trend with nss sulfate mass concentrations. In stratocumulus clouds a small increase in droplet concentrations with nss sulfate mass concentrations was observed. DOE

N94-36026# Pacific Northwest Lab., Richland, WA.
ANALYSIS OF MID-TROPOSPHERIC CARBON MONOXIDE DATA USING A THREE-DIMENSIONAL GLOBAL ATMOSPHERIC CHEMISTRY NUMERICAL MODEL
R. C. Easter, R. D. Saylor, and E. G. Chapman Dec. 1993 11 p Presented at the 20th International Technical Meeting on Air Pollution Modelling and its Application, Valencia, Spain, 29 Nov. - 3 Dec. 1993
(Contract DE-AC06-76RL-01830)
(DE94-004782; PNL-SA-23289; CONF-931117-2) Avail: CASI HC A03/MF A01

The Global atmospheric Chemistry Model (GChM) has been used to analyze the mid-tropospheric CO dataset obtained from NASA's Measurement of Air Pollution by Satellites (MAPS) program. Fourteen simulations with a 3.75 horizontal resolution have been performed, including a base case and 13 sensitivity runs. The model reproduces many, but not all, of the major features of the MAPS dataset. Locations of peak CO mixing ratios associated with biomass burning as observed in the MAPS experiment are slightly farther south than the model result, indicating either greater horizontal transport than present in the model representation or a spatial difference between the location of modeled biomass fires and actual fires. The current version of GChM was shown to be relatively insensitive to the magnitude of the prescribed NO(x) and O3 global distributions and very insensitive to the depth of the mixed layer as parameterized in the model. Cloud convective transport was shown to play an important role in venting boundary layer CO to the free troposphere. This result agrees with prior meteorological analyses of the MAPS dataset that have-indirectly inferred the presence of convective activity through satellite-based information. Work is continuing to analyze the results of these simulations further and to perform more detailed comparisons between model results and MAPS data. DOE

N94-36027# Pacific Northwest Lab., Richland, WA.
AIR QUALITY IMPLICATIONS ASSOCIATED WITH THE SELECTION OF POWER PLANTS IN THE PACIFIC NORTHWEST
M. C. Baechler, C. S. Glantz, and P. C. Edelmen Nov. 1993 15 p
Presented at the Conference on Transboundary/International Issues, Victoria, Ontario, 8-10 Nov. 1993
(Contract DE-AC06-76RL-01830)
(DE94-004783; PNL-SA-22853; CONF-931165-2) Avail: CASI HC A03/MF A01

This assessment models emission inventories and pollutant emission rates for fossil fuel power plants. Ground-level air concentration of nitrogen oxides, sulfur dioxide and transonic small perturbation (TSP) are predicted. Pollutant deposition, non-acidic deposition, acidic deposition, ozone impacts, and visibility attenuation are considered. Human health effects, wildlife effects, effects on plants and crops, and residual environmental impacts are estimated from predicted emissions. DOE

N94-36053# Pacific Northwest Lab., Richland, WA.
AEROSOL OPTICAL DEPTH DERIVED FROM SOLAR RADIOMETRY OBSERVATIONS AT NORTHERN MID-LATITUDE SITES
N. S. Laulainen, N. R. Larson, J. J. Michalsky, and L. C. Harrison Jan. 1994 7 p Presented at the 74th American Meteorological Society Annual Meeting, Nashville, TN, 23-28 Jan. 1994
(Contract DE-AC06-76RL-01830)
(DE94-007476; PNL-SA-22899; CONF-940115-29) Avail: CASI HC A02/MF A01

Routine, automated solar radiometry observations began with the development of the Mobile Automated Scanning Photometer (MASP) and its installation at the Rattlesnake Mountain Observatory (RMO). We have introduced a microprocessor controlled rotating shadowband radiometer (RSR), both the single detector and the multifilter/detector (MFRSR) versions to replace the MASP. The operational mode of the RSRs is substantially different than the MASP or other traditional sun-tracking radiometers, because, by virtue of the automated rotating shadowband, the total and diffuse irradiance on a horizontal plane are measured and the direct-normal component deduced through computation from the total and diffuse components by the self-contained microprocessor. Because the three irradiance components are measured using the same detector for a given wavelength, the calibration coefficients are identical for each component, thus reducing errors when comparing them. The MFRSR is the primary radiometric instrument in the nine-station Quantitative Links Network (QLN) established in the eastern United States in late 1991. Data from this network are being used to investigate how cloud and aerosol induced radiative effects vary in time and with cloud structure and type over a midlatitude continental region. This work supports the DOE Quantitative Links Program to quantify linkages between changes in atmospheric composition and climate forcing. We describe the setup of the QLN and present aerosol optical depth results from the on-going measurements at PNL/RMO, as well as preliminary results from the QLN. From the time-series of data at each site, we compare seasonal variability and geographical differences, as well as the effect of the perturbation to the stratosphere by Mt. Pinatubo. Analysis of the wavelength dependence of optical depth also provides information on the evolution and changes in the size distribution of the aerosols. DOE

N94-36120 Utah State Univ., Logan, UT. Coll. of Natural Resources.
NATURAL RESOURCES AND ENVIRONMENTAL ISSUES. VOLUME 1: RIPARIAN RESOURCES: A SYMPOSIUM ON THE DISTURBANCES, MANAGEMENT, ECONOMICS, AND CONFLICTS ASSOCIATED WITH RIPARIAN ECOSYSTEMS
G. Allen Rasmussen, ed. and James P. Dobrowolski, ed. 1994 90 p
Symposium held in Logan, UT, 18-19 Apr. 1991; sponsored by Utah State Univ. and Utah Riparian Coalition
(ISSN 1069-5370)
Copyright Avail: Issuing Activity (Utah State Univ., Quinney Natural Resources Research Library, Logan, UT 84322-5260)

'Natural Resources and Environmental Issues (NREI)' is a technical series that addresses current topics relevant to natural resources and to the environment. The journal is published as a series of volumes, with at least one being issued each year as the proceedings of the Natural Resources Week symposium. The purpose of this conference was to create a dialogue about the management of riparian areas and their associated systems. Specifically, this dialogue was intended to focus on the function these areas have in an ecosystem. There are many disturbances associated with riparian areas, ranging from natural landslides, which tend to be dispersed in time and space, to chronic disturbances normally associated with man's activities. While the natural disturbances can appear to be catastrophic, the recovery tends to be faster in areas that do not have chronic disturbances. We brought together those individuals who helped develop unique and innovative management techniques to incorporate the upland and riparian areas together into a system approach and to mitigate or change the chronic disturbances. In addition, papers were presented on the costs associated with altering management of these areas and who should be paying those costs. Riparian areas have become the focal point of many conflicts because of competing, or at least perceived competing, interests and uses. To address this area, the final two papers discuss how some groups are successfully dealing with these conflicts.
Derived from text

N94-36179 Oak Ridge National Lab., TN.
DEVELOPMENT OF ATMOSPHERIC CHARACTERISTICS OF CHLORINE-FREE ALTERNATIVE FLUOROCARBONS
V. L. Orkin, V. G. Khamaganov, A. G. Guschin, E. E. Kasimovskaya, and I. K. Larin Apr. 1993 17 p Prepared in cooperation with Academy of Sciences, Moscow, Russia Limited Reproducibility: More than 20% of this document may be affected by microfiche quality
(Contract DE-AC05-84OR-21400)
(DE94-009791; ORNL/Sub-86-SL103) Avail: CASI HC A03

Rate constants have been measured for the gas phase reaction of OH radicals with 1,1,1,2-tetrafluoroethane R-134a (CH2F-CF3) and methyl trifluoromethyl ether E-143a (CH3-O-CF3) over the temperature range 298--460 K. Arrhenius expressions were derived for atmospheric modeling. The infrared absorption cross-sections for R-134a and E-143a have been measured in the region from 400 to 1600 cm(exp -1) and the integrated band strengths have been calculated. The atmospheric lifetimes R-134a and E-143a have been estimated to be 11.6 years and 4.1 years respectively. Global warming potentials have been estimated over time horizons of 20, 50, 100, 200, and 500 years. DOE

N94-36183 ENSR Consulting and Engineering, Camarillo, CA.
REGIONAL SOURCE-RECEPTOR RELATIONSHIPS FOR ATMOSPHERIC ACIDITY AND ACID DEPOSITION IN CALIFORNIA Final Report
Prakash Karamchandani, Christodoulos Pilinis, and Jitendra Shah Dec. 1993 191 p Limited Reproducibility: More than 20% of this document may be affected by microfiche quality
(Contract ARB-A032-189)
(PB94-156676) Avail: CASI HC A09

The report describes the results of a database management and semi-empirical modeling study that was performed to evaluate regional source-receptor relationships (SRR's) for atmospheric acidity and acidic deposition in California. The objectives of the study were to quantify the contributions of the various source regions in California to acidic deposition at selected receptors in the state and to estimate the uncertainties in the derived values. Author (NTIS)

N94-36207# Edgerton, Germeshausen and Grier, Inc., Idaho Falls, ID.
ENVIRONMENTAL RESOURCE DOCUMENT FOR THE IDAHO NATIONAL ENGINEERING LABORATORY, VOLUME 1
J. S. Irving Jul. 1993 291 p
(Contract DE-AC07-76ID-01570)
(DE94-008522; EGG-WMO-10279-Vol-1) Avail: CASI HC A13/MF A03

This document contains information related to the environmental characterization of the Idaho National Engineering Laboratory (INEL). The INEL is a major US Department of Energy facility in southeastern Idaho dedicated to nuclear research, waste management, environmental restoration, and other activities related to the development of technology. Environmental information covered in this document includes land, air, water, and ecological resources; socioeconomic characteristics and land use; and cultural, aesthetic, and scenic resources. DOE

N94-36208# Edgerton, Germeshausen and Grier, Inc., Idaho Falls, ID.
ENVIRONMENTAL RESOURCE DOCUMENT FOR THE IDAHO NATIONAL ENGINEERING LABORATORY, VOLUME 2

J. S. Irving Jul. 1993 670 p
(Contract DE-AC07-76ID-01570)
(DE94-008523; EGG-WMO-10279-Vol-2) Avail: CASI HC A99/MF A06

This document contains information related to the environmental characterization of the Idaho National Engineering Laboratory (INEL). The INEL is a major US Department of Energy facility in southeastern Idaho dedicated to nuclear research, waste management, environmental restoration, and other activities related to the development of technology. Environmental information covered in this document includes land, air, water, and ecological resources; socioeconomic characteristics and land use; and cultural, aesthetic, and scenic resources. DOE

N94-36273# Oak Ridge National Lab., TN.
MODERNIZATION OF THE GRAPHICS POST-PROCESSORS OF THE HAMBURG GERMAN CLIMATE COMPUTER CENTER CARBON CYCLE CODES
E. J. Stevens and G. S. McNeilly Mar. 1994 105 p
(Contract DE-AC05-84OR-21400)
(DE94-011604; ORNL/TM-12666) Avail: CASI HC A06/MF A02

The existing National Center for Atmospheric Research (NCAR) code in the Hamburg Oceanic Carbon Cycle Circulation Model and the Hamburg Large-Scale Geostrophic Ocean General Circulation Model was modernized and reduced in size while still producing an equivalent end result. A reduction in the size of the existing code from more than 50,000 lines to approximately 7,500 lines in the new code has made the new code much easier to maintain. The existing code in Hamburg model uses legacy NCAR (including even emulated CALCOMP subroutines) graphics to display graphical output. The new code uses only current (version 3.1) NCAR subroutines. DOE

N94-36286# Lawrence Livermore National Lab., CA.
INTEGRATED SCIENCE MODEL FOR ASSESSMENT OF CLIMATE CHANGE
A. K. Jain, D. J. Wuebbles, and H. S. Kheshgi Apr. 1994 19 p Presented at the Annual Meeting and Exhibition of the Air and Waste Management Association, Cincinnati, OH, 19-24 Jun. 1994
(Contract W-7405-eng-48)
(DE94-011758; UCRL-JC-116526; CONF-940632-10) Avail: CASI HC A03/MF A01

Integrated assessment models are intended to represent processes that govern physical, ecological, economic and social systems. This report describes a scientific model relating emissions to global temperature and sea level. This model is intended to be one component of an integrated assessment model which is, of course, much more comprehensive. The model is able to reproduce past changes in CO2 concentration, global temperature, and sea level. The model is used to estimate the emissions rates required to lead to stabilization of CO2 at various levels. The model is also used to estimate global temperature rise, the rate of temperature change, and sea level rise driven by IPCC emissions scenarios. The emission of fossil fuel CO2 is modeled to have the largest long term effect on climate. Results do show the importance of expected changes of trace greenhouse gases other than CO2 in the near future. Because of the importance of these other trace gases, further work is recommended to more accurately estimate their effects. DOE

N94-36359# Pacific Northwest Lab., Richland, WA.
GLOBAL TROPOSPHERIC CHEMISTRY MODELS FOR RADIATIVELY IMPORTANT TRACE SPECIES: DESIGN AND RESEARCH RECOMMENDATIONS
W. R. Barchet, A. J. Brothers, C. M. Berkowitz, R. C. Easter, S. J. Ghan, and R. D. Saylor Dec. 1993 134 p
(Contract DE-AC06-76RL-01830)
(DE94-007069; PNL-9012) Avail: CASI HC A07/MF A02

Changes in the Earth's climate could significantly affect regional and global concentrations of trace species that are criteria pollutants regulated by the U.S. Environmental Protection Agency (EPA). The policy community also needs to know how changes in global natural and anthropogenic emissions of greenhouse gases, particulate aerosols, and aerosol precursors will affect the distribution and concentration of these pollutants. This report maps out one path for obtaining this information. DOE

N94-36422*# National Aeronautics and Space Administration. John F. Kennedy Space Center, Cocoa Beach, FL.
ENDANGERED AND POTENTIALLY ENDANGERED WILDLIFE ON JOHN F. KENNEDY SPACE CENTER AND FAUNAL INTEGRITY AS A GOAL FOR MAINTAINING BIOLOGICAL DIVERSITY
David R. Breininger (Bionetics Corp., Cocoa Beach, FL.), Mary Jo Barkaszi (Bionetics Corp., Cocoa Beach, FL.), Rebecca B. Smith (Bionetics Corp., Cocoa Beach, FL.), Donna M. Oddy (Bionetics Corp., Cocoa Beach, FL.), and Jane A. Provancha (Bionetics Corp., Cocoa Beach, FL.) 30 Mar. 1994 453 p
(Contract NAS10-11624)
(NASA-TM-109204; NAS 1.15:109204) Avail: CASI HC A20/MF A04

Buffer zones for space operations provide for a wildlife diversity unsurpassed among most federal facilities in the continental U.S. demonstrating the coexistence possible with one of man's greatest technological achievements. This document ranks 119 resident or migratory wildlife species that are endangered or declining. The ranking system herein was based on species' vulnerability to extinction and the relevance of Kennedy Space Center (KSC) for maintaining populations in the U.S. and Florida. One amphibian, 19 reptiles, 80 birds, and 19 mammals were considered endangered or declining. KSC is an integral area for regional species diversity being the focus of the Merritt Island/Cape Canaveral/Turnbull Ecosystem which is part of the Indian River Lagoon watershed, an estuary of national significance. Many species that use this system also use the nearby St. Johns River Basin ecosystem. These two ecosystems are biological corridors between temperate Carolinian and tropical/subtropical Caribbean biotic provinces. Threats to biological diversity on KSC were also reviewed. Traditional environmental assessments, resulting from environmental regulation guidelines, focus on environmental contaminants and habitat lost due to construction. However, this review suggested that small population sizes, isolation of populations, ecosystem and habitat fragmentation, road mortality, and other edge effects may represent more critical threats to biological diversity than the traditional topics. Author

46 GEOPHYSICS

Includes aeronomy; upper and lower atmosphere studies; ionospheric and magnetospheric physics; and geomagnetism.

For space radiation see *93 Space Radiation.*

N94-35244*# Alaska Univ., Fairbanks, AK. Geophysical Inst.
MODELING OF THE MAGNETOSPHERE-IONOSPHERE-ATMOSPHERE SYSTEM Ph.D. Thesis Semiannual Report, 1 Nov. 1993 - 30 Apr. 1994
1994 6 p Presented at the Fall AGU Meeting, San Francisco, CA, Dec. 1993 Submitted for publication
(Grant NAG5-1097)
(NASA-CR-195157; NAS 1.26:195157) Avail: CASI HC A02/MF A01

During the period covered by this report we continued to investigate basic processes in magnetosphere-ionosphere coupling and to develop algorithms for analyzing ultraviolet, visible, and X-ray images that will be acquired on the POLAR spacecraft. An image analysis procedure combines several numerical models to obtain a self-consistent picture of the ionosphere and thermosphere. Our ionosphere-aurora model was extended by the inclusion of the magnetic mirror force and a self-consistent parallel electric field in the ionosphere. The electron transport model which forms a critical part of the aurora model was evaluated by comparison with laboratory measurements and auroral observations. We determined the uncertainties that arise from our limited knowledge of cross sections and energy degradation functions for electron neutral interaction. Derived from text

N94-35358*# Aerospace Corp., El Segundo, CA. Engineering and Technology Group.
ANALYTIC MODEL OF AURORALLY COUPLED MAGNETOSPHERIC AND IONOSPHERIC ELECTROSTATIC POTENTIALS
J. M. Cornwall 15 Jan. 1994 12 p
(Grant NAGw-2126)
(NASA-CR-196130; NAS 1.26:196130; ATR-93(7251)-1) Avail: CASI HC A03/MF A01

This paper describes modest but significant improvements on earlier studies of electrostatic potential structure in the auroral region using the adiabatic auroral arc model. This model has crucial nonlinearities (connected, for example. with aurorally produced ionization) which have hampered analysis; earlier work has either been linear, which I will show is a poor approximation or, if nonlinear, either numerical or too specialized to study parametric dependencies. With certain simplifying assumptions I find new analytic nonlinear solutions fully exhibiting the parametric dependence of potentials on magnetospheric (e.g.. cross-tail potential) and ionospheric (e.g., recombination rate) parameters. No purely phenomenological parameters are introduced. The results are in reasonable agreement with observed average auroral potential drops, inverted-V scale sizes, and dissipation rates. The dissipation rate is quite comparable to tail energization and transport rates and should have a major effect on tail and magnetospheric dynamics. This paper gives various relations between the cross-tail potential and auroral parameters (e.g., total parallel currents and potential drops) which can be studied with existing data sets.

Author (revised)

N94-35389*# California Univ., Santa Barbara, CA. Earth-Space Research Group.

A MODEL OF THE CO2 EXCHANGES BETWEEN BIOSPHERE AND ATMOSPHERE IN THE TUNDRA Final Technical Report, 1 Sep. 1991 - 31 Aug. 1992

Rachid R. Labgaa and Catherine Gautier 1992 9 p
(Grant NAGw-2737)
(NASA-CR-196008; NAS 1.26:196008) Avail: CASI HC A02/MF A01

A physical model of the soil thermal regime in a permafrost terrain has been developed and validated with soil temperature measurements at Barrow, Alaska. The model calculates daily soil temperatures as a function of depth and average moisture contents of the organic and mineral layers using a set of five climatic variables, i.e., air temperature, precipitation, cloudiness, wind speed, and relative humidity. The model is not only designed to study the impact of climate change on the soil temperature and moisture regime, but also to provide the input to a decomposition and net primary production model. In this context, it is well known that CO2 exchanges between the terrestrial biosphere and the atmosphere are driven by soil temperature through decomposition of soil organic matter and root respiration. However, in tundra ecosystems, net CO2 exchange is extremely sensitive to soil moisture content; therefore it is necessary to predict variations in soil moisture in order to assess the impact of climate change on carbon fluxes. To this end, the present model includes the representation of the soil moisture response to changes in climatic conditions. The results presented in the foregoing demonstrate that large errors in soil temperature and permafrost depth estimates arise from neglecting the dependence of the soil thermal regime on soil moisture contents. Permafrost terrain is an example of a situation where soil moisture and temperature are particularly interrelated: drainage conditions improve when the depth of the permafrost increases; a decrease in soil moisture content leads to a decrease in the latent heat required for the phase transition so that the heat penetrates faster and deeper, and the maximum depth of thaw increases; and as excepted, soil thermal coefficients increase with moisture.

Derived from text

N94-35392*# Aerospace Corp., El Segundo, CA.

CONTRIBUTIONS OF THE LOW-LATITUDE BOUNDARY LAYER TO THE FINITE WIDTH MAGNETOTAIL CONVECTION MODEL

H. E. Spence and M. G. Kivelson 31 Dec. 1993 14 p See also A94-10186
(Grants NAGw-2126; NSF ATM-91-15557)
(NASA-CR-196116; NAS 1.26:196116; ATR-91(7234)-1) Avail: CASI HC A03/MF A01

Convection of plasma within the terrestrial nightside plasma sheet contributes to the structure and, possibly, the dynamical evolution of the magnetotail. In order to characterize the steady state convection process, we have extended the finite tail width model of magnetotail plasma sheet convection. The model assumes uniform plasma sources and accounts for both the duskward gradient/curvature drift and the earthward E x B drift of ions in a two-dimensional magnetic geometry. During periods of slow convection (i.e., when the cross-tail electric potential energy is small relative to the source plasma's thermal energy), there is a significant net duskward displacement of the pressure-bearing ions. The electrons are assumed to be cold, and we argue that this assumption is appropriate for plasma sheet parameters. We generalize solutions previously obtained along the midnight meridian to describe the variation of the plasma pressure and number density across the width of the tail. For a uniform deep-tail source of particles, the plasma pressure and number density are unrealistically low along the near-tail dawn flank. We therefore add a secondary source of plasma originating from the dawnside low-latitude boundary layer (LLBL). The dual plasma sources contribute to the plasma pressure and number density throughout the magnetic equatorial plane. Model results indicate that the LLBL may be a significant source of near-tail central plasma sheet plasma during periods of weak convection. The model predicts a cross-tail pressure gradient from dawn to dusk in the near magnetotail. We suggest that the plasma pressure gradient is balanced in part by an oppositely directed magnetic pressure gradient for which there is observational evidence. Finally, the pressure to number density ratio is used to define the plasma 'temperature.' We stress that such quantities as temperature and polytropic index must be interpreted with care as they lose their nominal physical significance in regions where the two-source plasmas intermix appreciably and the distributions become non-Maxwellian.

Author

N94-35568# International Atomic Energy Agency, Vienna (Austria).

ISOTOPIC AND GEOCHEMICAL PRECURSORS OF EARTHQUAKES AND VOLCANIC ERUPTIONS

Nov. 1993 155 p Presented at the Advisory Group Meeting on Isotopic and Geochemical Precursors of Earthquakes and Volcanic Eruptions, Vienna, Austria, 9-12 Sep. 1991
(DE94-615824; IAEA-TECDOC-726; CONF-9109529) Avail: CASI HC A08/MF A02 (US Sales Only)

Radon 222 seems to be one of the most promising precursors and is the tracer for which more data are available: according to statistics elaborated in China, 70% of earthquakes are preceded by radon anomalies detectable in soil, air and/or in groundwater. Also other changes of the fluid chemical composition and variations of (sup 3)He/(sup 4)He, (sup 2)H/(sup 1)H, (sup 13)C/(sup 12)C, (sup 18)O/(sup 16)O isotopic ratios have been detected. Among these indicators one can mention variations in concentration and/or isotopic ratios of hydrogen, helium, carbon, oxygen, neon, radon, radium, and uranium.

DOE

N94-35578 Massachusetts Univ., Lowell, MA. Center for Atmospheric Research.

A QUALITY CONTROL PACKAGE FOR THE DIGISONDE DRIFT ANALYSIS (DDA)

James L. Scali Oct. 1993 33 p Limited Reproducibility: More than 20% of this document may be affected by microfiche quality
(Contract F19628-90-K-0005)
(AD-A278663; AD-E201889; PL-TR-93-2220; SR-3) Avail: Issuing Activity (Defense Technical Information Center (DTIC))

This report discusses the implementation of a quality control system for the Digisonde Drift Analysis. The quality checking of the integrity of the drift data being recorded is available for the online (ODDA) as well as the post processing (DDA) packages. This system indicates the performance of the Digisondes in the field by interrogating the drift measurements made. Loss of receiver performance, phase data, and received signal is quickly identified by the quality control system. This system allows the operator to identify problems in the field within an hour of occuring. while for post processing of data, the package indicates how well the Digisonde system was performing even in those rare cases of data collected over a few years where logs of station maintenance no longer exist.

DTIC

N94-35587 Aerospace Corp., El Segundo, CA. Engineering and Technology Group.

ULF WAVES IN THE LOW-LATITUDE BOUNDARY LAYER AND THEIR RELATIONSHIP TO MAGNETOSPHERIC PULSATIONS: A MULTISATELLITE OBSERVATION

K. Takahashi (Johns Hopkins Univ., Laurel, MD.), D. G. Sibeck (Johns Hopkins Univ., Laurel, MD.), P. T. Newell (Johns Hopkins Univ., Laurel, MD.), and H. E. Spence 31 Jan. 1994 21 p Limited Reproducibility: More than 20% of this document may be affected by microfiche quality
(Contract F04701-88-C-0089)
(AD-A278906; TR-0091(6940-06)-1; SMC-TR-94-20) Avail: Issuing Activity (Defense Technical Information Center (DTIC))

On April 30 (day 120), 1985, the magnetosphere was compressed at

0923 UT and the subsolar magnetopause remained near 7 R(sub E) geocentric for approximately 2 hours, during which the four spacecraft, Spacecraft Charging At High Altitude (SCATHA), GOES 5, GOES 6, and Active Magnetospheric Particle Tracer Explorers (AMPTE) CCE, were all in the magnetosphere on the morning side. SCATHA was in the low-latitude boundary layer (LLBL) in the second half of this period. The interplanetary magnetic field was inferred to be northward from the characteristics of precipitating particle fluxes as observed by the low-altitude satellite Defense Meteorological Satellite Program (DMSP) F7 and also from absence of substorms. We used magnetic field and particle data from this unique interval to study ULF waves in the LLBL and their relationship to magnetic pulsations in the magnetosphere. The LLBL was identified from the properties of particles, including bidirectional field-aligned electron beams at approximately 200 eV. In the boundary layer the magnetic field exhibited both a 5-10 minute irregular compressional oscillation and a broadband (Delta(f)/f approximately 1) primarily transverse oscillations with a mean period of approximately 50 s and a left-hand sense of polarization about the mean field. The former can be observed by other satellites and is likely due to pressure variations in the solar wind, while the latter is likely due to a Kelvin-Helmoltz (K.-H.) instability occurring in the LLBL or on the magnetopause. DTIC

N94-35666# Arizona Univ., Tucson, AZ. Lab. for Advanced Subsurface Imaging.

HIGH-RESOLUTION SUBSURFACE IMAGING AND NEURAL NETWORK RECOGNITION

B. K. Sternberg and M. M. Poulton 1994 12 p Presented at the Symposium on the Application of Geophysics To Environmental and Engineering Problems, Boston, MA, 27-31 Mar. 1994
(Contract DE-AC21-92MC-29101)
(DE94-009546; DOE/MC-29101/94/C0333; CONF-940353-5) Avail: CASI HC A03/MF A01

A high-frequency, high-resolution electromagnetic (EM) imaging system is being developed for environmental geophysics surveys. Some key features of this system include: (1) rapid surveying to allow dense spatial sampling over a large area, (2) high-accuracy measurements which will be used to produce a high-resolution image of the subsurface, (3) measurements which have excellent signal-to-noise ratio over a wide bandwidth (32 kHz to 32 MHz), (4) large-scale physical modeling to produce accurate theoretical responses over targets of interest in environmental geophysics surveys, (5) rapid neural network interpretation at the field site, and (6) visualization of complex structures during the survey. DOE

N94-35693 Science Applications International Corp., Arlington, VA.

CENTER FOR SEISMIC STUDIES Final Technical Report, Oct. 1992 - Oct. 1993

Anne Henson and Hans Israelsson 7 Feb. 1994 97 p Limited Reproducibility: More than 20% of this document may be affected by microfiche quality
(Contract F29601-92-C-0005)
(AD-A278682; SAIC-C94-02) Avail: CASI HC A05

A 1992 study by Suteau-Henson where azimuth bias and scatter were systematically measured for regional phases of events recorded at ARCESS is extended here by mapping the observed bias and scatter around ARCESS. In another study, the optimization of polarization analysis at IMS/IRIS stations in the Former Soviet Union is addressed. Also in this report, a procedure to stack waveforms recorded by a network of seismic stations for detection of depth phases, sP and pP is defined. The constraint on focal depth provided by origin times determined from travel time ratios of P and S waves is also studied. Finally, we perform some computational experiments to outline the depth estimation capability of the GSETT-2 global network and a hypothetical network consisting primarily of high sensitive array stations. DTIC

N94-35706 Columbia Univ., New York, NY. Dept. of Applied Physics.

COLLISONLESS DYNAMICS OF THE MAGNETOSPHERE Annual Report, 1 Jan. - 31 Dec. 1993

Amitava Bhattacharjee Aug. 1993 41 p Limited Reproducibility: More than 20% of this document may be affected by microfiche quality
(Contract F49620-93-1-0071)
(AD-A278886; AFOSR-94-0271TR) Avail: Issuing Activity (Defense Technical Information Center (DTIC))

An energetic electron belt has been created in a laboratory terrella for the first time. Measurements indicate the trapped-electron belt to be localized in radius and have a non-Maxwellian energy distribution ranging from 10 to 40 keV. Using multiple probes, we have clearly identified drift-resonant instabilities leading to rapid radial transport. Transport in a dipole appears to require multiple modes, and its bursty nature suggests a profile relaxation of the energetic electrons which self-stabilizes the drift-resonant instabilities. Substorms in the magnetosphere cause the generation of major electromagnetic disturbances and energetic particles. We examine the role of the collisionless tearing-instability as a possible mechanism for substorms. Global asymptotic magnetotail equilbria which are slowly varying in the Earth-Sun direction are constructed, including all three components of the magnetic field. Some of these equilibria are analyzed for stability with respect to collisionless electron tearing modes. It is found that the ion tearing instability, which has been widely invoked as a possible trigger for substorms, does not exist. The By field is demonstrated to have a destabilizing effect on electron tearing modes. Regimes in which collisionless tearing modes can grow are delineated. DTIC

N94-35744 Istituto Nazionale di Geofisica, Rome (Italy).

ELECTROMAGNETIC MEASUREMENTS OF THE IONOSPHERE AT THE IONOSPHERIC STATION OF ROME Interim Report No. 2

Jan. 1994 2 p Limited Reproducibility: More than 20% of this document may be affected by microfiche quality
(Contract DAJA45-93-C-0036)
(AD-A278991; R/D-7132-EE-01) Avail: Issuing Activity (Defense Technical Information Center (DTIC))

The project is a continuation of previous EUROCAP PROGRAM agreement with the European Research Office. Continuous ionospheric vertical soundings (every hour, every day) have been performed at the ionospheric station of Rome during the period Nov. 1993 - Jan. 1994. DTIC

N94-35780 Moscow State Univ. (Russia). Nauchno-Issledovatelskij Inst.

GLOBAL CHANGES OF RADIATION SITUATION AT HEIGHTS LESS THAN 1000 km

A. A. Gusev, G. I. Pugacheva, Yu. V. Mineev, and E. D. Tolstaya 1992 24 p Limited Reproducibility: More than 20% of this document may be affected by microfiche quality
(DE94-610504; NIIYaF-MGU-92-31-280) Avail: CASI HC A03 (US Sales Only)

On the basis of satellite measurements in the 21st and 22nd solar cycles a model is developed of the electron component of the earth radiation belts. Spatial electron distributions are obtained at 350, 500, and 800 km in the minimum and maximum of the solar cycle. Global changes are noted in the spatial radiation distribution near the earth in comparison with 1965-1972, namely decreasing trapped electron fluxes and increasing quasi-trapped ones at small heights and variations in the spectrum in the region of the inner radiation belt. A model of trapped protons is developed which permits precise flux forecasting owing to corrections accounting for earth magnetic moment decreasing and atmospheric cutting off. DOE

N94-35830# Ceskoslovenska Akademie Ved, Prague. Geofyzikalni Ustav.

ACTIVITY REPORT 1990-1992 AND PROCEEDINGS, VOLUME 1

D. Mayer-Rosa, L. Waniek, and P. Suhadolc 1993 247 p Presented at the 23rd General Assembly of the European Seismological Commission, Prague, Czechoslovakia, 7-12 Sep. 1992
(DE94-610480; INIS-MF-13733-Vol-1; CONF-9209428-Vol-1) Avail: CASI HC A11/MF A03 (US Sales Only)

A report on the activities of the European Seismological Commission (ESC) during the period 1990-1992 together with the Proceedings of the General Assembly of the ESC are presented in two volumes. Volume 1 covers the following topics: recent strong earthquakes in Europe, regional seismicity, historical earthquakes in Europe, statistical models and methods in seismology, numerical modeling in three-dimensional media, methodology of quantification of European earthquakes and recent results, seismic noise and signal detectability, regional seismic network, and history of seismometry. One paper dealing with microseismic noise characteristics around the Kozloduy nuclear power plant has been inputted to INIS. DOE

N94-36019 California Univ., Richmond, CA. Earthquake Engineering Research Center.
EARTHQUAKE ENGINEERING RESEARCH CENTER: 25TH ANNIVERSRY EDITION Annual Report, 1992-1993
Oct. 1993 61 p See also PB93-132728 Limited Reproducibility: More than 20% of this document may be affected by microfiche quality
(PB94-160645) Avail: CASI HC A04

The Earthquake Engineering Research Center exists to conduct research and develop technical information in all areas pertaining to earthquake engineering, including strong ground motion and ground failure, response of natural and manmade structures to earthquakes, design of structures to resist earthquakes, development of new systems for earthquake protection, and development of architectural and public policy aspects of earthquake engineering. The annual report for 1992-93 presents information on: Current Research Programs; Contracts and Grants; Public Service Program; National Information Service for Earthquake Engineering; Core Administration; Committees of the Earthquake Engineering Research Center; Research Participants - Faculty; and Research Participants - Students. NTIS

N94-36087 Ceskoslovenska Akademie Ved, Prague. Geofyzikalni Ustav.
ACTIVITY REPORT, 1990 - 1992 AND PROCEEDINGS, VOLUME 2
Ing. Pavel Kottnauer, ed. 1993 213 p Presented at the 23rd General Assembly of the European Seismological Commission, Prague, Czechoslovakia, 7-12 Sep. 1992 Limited Reproducibility: More than 20% of this document may be affected by microfiche quality
(DE94-610481; INIS-mf-13734-Vol-2; CONF-9209428) Avail: CASI HC A10 (US Sales Only)

A report of the European Seismological Commission (ESC) on 1990-1992 activities and Proceedings of the General Assembly of the ESC are presented in two volumes. Volume 2 covers the following topics: study of seismic sound, seismotectonic analysis, deep seismic sounding, the three-dimensional structure of the European lithosphere-asthenosphere system, complexity in earthquake occurrence, earthquake hazard, strong and weak earthquake ground motions, macroseismology, microzonation, and applications in earthquake engineering. One paper dealing with the connection between seismicity and the CO2- (sup 222)Rn content in spring water has been inputted to INIS. DOE

N94-36103# Los Alamos National Lab., NM.
ROLE OF MAGMA-WATER INTERACTION IN VERY LARGE EXPLOSIVE ERUPTIONS
G. A. Valentine 1993 9 p Presented at the Seminar on Physics of Vapor Explosion, Tomakomai, Japan, 25-29 Oct. 1993
(Contract W-7405-eng-36)
(DE94-002698; LA-UR-93-3699; CONF-9310222-1) Avail: CASI HC A02/MF A01

An important class of explosive eruptions, involving large-scale magma-water interaction during the discharge of hundreds to thousands of cubic kilometers of magma, is discussed. Geologic evidence for such eruptions is summarized. Case studies from New Zealand, Australia, England, and the western United States are described, focusing on inferred eruption dynamics. Several critical problems that need theoretical and experimental research are identified. These include rates at which water can flow into a volcanic vent or plumbing system, entrainment of water by explosive eruptions through lakes and seas, effects of magma properties and gas bubbles on magma-water interaction, and hazards associated with the eruptions. DOE

N94-36116# Massachusetts Univ., Lowell, MA. Center for Atmospheric Research.
IONOSPHERIC PLASMA DRIFT AND STRUCTURE STUDIES AT HIGH AND MID-LATITUDES Final Report, Oct. 1990 - Oct. 1993
Bodo W. Reinisch, James L. Scali, Claude Dozois, and Geoffrey Crowley Dec. 1993 69 p
(Contract F19628-90-K-0005; AF Proj. 4643)
(AD-A279415; PL-TR-94-2002(1)) Avail: CASI HC A04/MF A01

Ground-based observations of the high latitude ionosphere with Digisonde sounders at Qaanaaq, Sondrestrom, Goose Bay, Argentia, and Millstone Hill provide a description of the patch structure and the convection pattern in the polar cap. Correlation analysis of observed F-region plasma drifts with the orientation of the interplanetary magnetic field (measured by IMP8) lead to a new technique of deducing the signs of Bz and By from the measured drifts. Real time calculation of the plasma drift was successfully introduced at one of the Digisonde stations (Sondrestrom) providing the possibility of determining the IMF components in real time. Analysis of midlatitude trough observations shows large westward velocities in the trough region. Digisonde data from Qaanaaq and DMSP F8 and F9 satellite data showed the development of the ionospheric polar hole. Author

N94-36175*# National Aeronautics and Space Administration. Marshall Space Flight Center, Huntsville, AL.
NATURAL ORBITAL ENVIRONMENT DEFINITION GUIDELINES FOR USE IN AEROSPACE VEHICLE DEVELOPMENT
B. Jeffrey Anderson, ed. and Robert E. Smith, comp. Jun. 1994 158 p
(NASA-TM-4527; M-729; NAS 1.15:4527) Avail: CASI HC A08/MF A02

This document provides definitions of the natural near-Earth space environment suitable for use in the initial development/design phase of any space vehicle. The natural environment includes the neutral atmosphere, plasma, charged particle radiation, electromagnetic radiation (EMR), meteoroids, orbital debris, magnetic field, physical and thermal constants, and gravitational field. Communications and other unmanned satellites operate in geosynchronous-Earth orbit (GEO); therefore, some data are given for GEO, but emphasis is on altitudes from 200 km to 1000 km (low-Earth orbit (LEO)). This document does not cover the induced environment of other effects resulting from presence of the space vehicle. Manmade factors are included as part of the ambient natural environment; i.e., orbital debris and radio frequency (RF) noise generated on Earth, because they are not caused by the presence of the space vehicle but form part of the ambient environment that the space vehicle experiences. Author (revised)

N94-36214 Direction des Recherches, Etudes et Techniques, Paris (France). Centre de Documentation de l'Armement.
NON-LINEAR INTERACTION OF GRAVITY WAVES WITH AVERAGE JET FLOWS, INSTABILITIES, AND TURBULENCE Final Report [INTERACTION NON LINEAIRE DES ONDES DE GRAVITE AVEC DES ECOULEMENTS MOYENS DE TYPE JET, INSTABILITES ET TURBULENCE]
1992 93 p In FRENCH
(PB94-170586; DRET/DS/SR-93/1311) Avail: Issuing Activity (National Technical Information Service (NTIS))

This study describes several mechanisms, including the action of planetary waves, involved in the exchange of air between the troposphere and stratosphere. The first section looks at the problem of non-linear interaction between gravity waves and an average flow. The process sometimes produces instabilities that cause differential transport. When preconditions for the appearance of Kelvin-Helmholtz instabilities are altered slightly, instabilities can travel vertically, and through the tropopause. The second section looks at relief waves, and shows that gusts of wind can generate unsteady waves that can travel to the stratosphere and beyond. The final chapter considers jets. The interaction between the two critical levels found in jets accounts for their very different reflection and transmission of waves. When jet characteristics combine with instabilities, pseudo-instabilities-that is instabilities in places where the medium is stable are created. NTIS

N94-36263# Photometrics, Inc., Woburn, MA.
MOLECULAR NITROGEN FLUORESCENCE LIDAR FOR REMOTE SENSING OF THE AURORAL IONOSPHERE Scientific Report No. 1
Richard Garner and Michael Burka 24 Feb. 1994 40 p
(Contract F19628-92-C-0160; AF Proj. 2295)
(AD-A280716; PL-TR-94-2044) Avail: CASI HC A03/MF A01

We describe two types of molecular nitrogen fluorescence lidars which can be used to determine excited or ionized N2 density in the ionosphere during moderate or strong aurora. The lidars can also be used for high spatial resolution diagnostics during ionospheric high power radio frequency heating experiments which are often performed when there is moderate auroral activity. The lidars excite N2 already excited or ionized through impact with high energy auroral electrons. Several different configurations are considered for each lidar. The first type of lidar is a conventional fluorescence lidar which operates in the first positive system (N2(A(exp 3) Sigma(sub u) +)) yields N2(B(exp 3)pi(sub g)) or the first negative system (N2(+) yields (B(exp 2) Sigma(sub u)(+))). Several different lasers are considered. The choice of laser determines the bands for excitation and

fluorescence. The second type of lidar first pumps excited N2 to a higher energy state and then does conventional fluorescence lidar on that state. This lidar utilizes two lasers. The first laser, the pump laser, operates in the first positive system. The second laser, the probe laser, operates in the second positive system (N2(B(exp 3)pi(sub g)) yields N2(C(exp 3)pi(sub u))). Both lidars are described in detail and results of signal to noise calculations are performed using reasonable system parameters.
Author (revised)

N94-36265# Oslo Univ. (Norway). Dept. of Physics.
STUDIES OF THE DAYSIDE BOUNDARY LAYER PROCESSES BASED ON GROUND OBSERVATIONS IN THE SVALBARD AREA Final Report, 15 Sep. 1992 - 14 Nov. 1993
A. Egeland, J. A. Holtet, and P. E. Sandholt 13 Jan. 1994 16 p
(Contract F49620-92-J-0507; AF Proj. 2310)
(AD-A280715; PL-TR-94-2032) Avail: CASI HC A03/MF A01

Based on extensive, diagnostic ground observations in the Svalbard area (mainly at Ny Alesund at 76 deg lambda) together with simultaneous, coordinated measurements from east Greenland, the EISCAT radars as well as DMSP satellite recordings, structures and dynamics of the dayside cleft and polar cap region have been obtained. This is an important prerequisite to the understanding of the physics of dayside boundary layers processes. Several papers have been published, many lectures given and a NATO Advanced Workshop related to this program arranged. Possible generation mechanisms of dayside cusp/cleft auroras including magnetic merging, external pressure pulses, Kelvin-Helmholtz-instabilities, and dynamo processes by intruding plasma elements are discussed. Characteristics of boundary layer process and their ionospheric effects are a major objective of these studies. The Fast Explorer project as well as the new EISCAT radar at Svalbard will give new dimension to our studies of temporal/spatial structures of dayside auroral processes. Author (revised)

N94-36383 Aerospace Corp., El Segundo, CA.
SIMULTANEOUS OBSERVATIONS OF THE WESTWARD ELECTROJET AND THE CROSS-TAIL CURRENT SHEET DURING SUBSTORMS
R. E. Lopez, H. E. Spence, and C. I. Meng 31 Jan. 1994 13 p
Limited Reproducibility: More than 20% of this document may be affected by microfiche quality
(Contract F04701-88-C-0089)
(AD-A278631; TR-0091(6940-06)-3; SMC-TR-94-19) Avail: Issuing Activity (Defense Technical Information Center (DTIC))

In this report we present the results of a study using data from AMPTE/CCE, ground stations, and DMSP F7 during substorms. We have examined 12 events during which CCE was located near the neutral sheet and observed the disruption of the cross-tail current. During these events there were simultaneous ground magnetic field data near to the CCE local time sector. DMSP F7 crossed the nightside auroral oval within 40 minutes of substorm onset at CCE during five of the events. We find that the data are consistent with a near-Earth substorm initiation. We also find that the Tsyganenko (1987) magnetic field model requires an additional tail-like stress during substorms, which corresponds to an equatorward displacement of auroral zone field lines. Assuming that the center of the electrojet is drawn from the near-Earth region, the magnitude of this displacement is about 1 deg to 2 deg. DTIC

N94-35452*# National Aeronautics and Space Administration. Ames Research Center, Moffett Field, CA.
THERMAL EMISSION MEASUREMENTS (5-25 MICRONS) OF HAWAIIAN PALAGONITIC SOILS WITH IMPLICATIONS FOR MARS Abstract Only
Ted L. Roush (San Francisco State Univ., CA.) and James F. Bell, III *In* Lunar and Planetary Inst., The Twenty-Fifth Lunar and Planetary Science Conference. Part 3: P-Z 1994 p 1161-1162 (For primary document see N94-35448 11-91)
(Grant NAGw-2212; RTOP 151-01-60-01; RTOP 185-52-62-07)
Avail: CASI HC A01/MF A06

N94-35453*# National Aeronautics and Space Administration. Ames Research Center, Moffett Field, CA.
THERMAL EMISSION MEASUREMENTS (5-25 MICRONS) OF PALAGONITE/Fe-SUBSTITUTED MONTMORILLONITE INTIMATE MIXTURES: APPLICATIONS TO MARS Abstract Only
Ted L. Roush (San Francisco State Univ., CA.) and James B. Orenberg (San Francisco State Univ., CA.) *In* Lunar and Planetary Inst., The Twenty-Fifth Lunar and Planetary Science Conference. Part 3: P-Z 1994 p 1163-1164 (For primary document see N94-35448 11-91)
(RTOP 151-01-60-01; RTOP 185-52-62-07)
Avail: CASI HC A01/MF A06

N94-35454*# National Aeronautics and Space Administration. Ames Research Center, Moffett Field, CA.
TRANSMISSION MEASUREMENTS (4000-400 cm(EXP -1), 2.5-25 MICRONS) OF CRYSTALLINE FERRIC OXIDES AND FERRIC OXYHYDROXIDES: IMPLICATIONS FOR MARS Abstract Only
Ted L. Roush (San Francisco State Univ., CA.), James F. Bell, III, and Richard V. Morris *In* Lunar and Planetary Inst., The Twenty-Fifth Lunar and Planetary Science Conference. Part 3: P-Z 1994 p 1165-1166 (For primary document see N94-35448 11-91)
Avail: CASI HC A01/MF A06

47 METEOROLOGY AND CLIMATOLOGY

Includes weather forecasting and modification.

N94-35350# Lawrence Livermore National Lab., CA.
COMPUTER ANIMATION OF CLOUDS
N. Max 28 Jan. 1994 11 p Presented at the 1994 Computer Animation, Geneva, Switzerland, 25-27 May 1994
(Contract W-7405-eng-48)
(DE94-008289; UCRL-JC-115863; CONF-9405113-1) Avail: CASI HC A03/MF A01

Computer animation of outdoor scenes is enhanced by realistic clouds. I will discuss several different modeling and rendering schemes for clouds and show how they evolved in my animated work. These include transparency-textured clouds on a 2-D plane, smooth shaded or textured 3-D clouds surfaces, and 3-D volume rendering. For the volume rendering, I will present various illumination schemes, including the density emitter, single scattering, and multiple scattering models. DOE

N94-35355*# METSAT, Inc., Fort Collins, CO.
PRODUCTION OF LONG-TERM GLOBAL WATER VAPOR AND LIQUID WATER DATA SET USING ULTRA-FAST METHODS TO ASSIMILATE MULTI-SATELLITE AND RADIOSONDE OBSERVATIONS Annual Report, Jul. 1993 - Jun. 1994
Thomas H. VonderHaar, David L. Randel, Donald L. Reinke, Graeme L. Stephens, Mark A. Ringerud, Cynthia L. Combs, Thomas J. Greenwald, and Ian L. Wittmeyer Jun. 1994 43 p Original contains color illustrations
(Contract NASw-4715)
(NASA-CR-196044; STC-TR-2833; NAS 1.26:196044) Avail: CASI HC A03/MF A01; 4 functional color pages

In recent years climate research scientists have recognized the need for increased time and space resolution precipitable and liquid water data sets. This project is designed to meet those needs. Specifically, NASA is funding STC-METSAT to develop a total integrated column and layered precipitable water data set. This is complemented by a total column liquid water data set. These data are global in extent, 1 deg x 1 deg in resolution, with daily grids produced. Precipitable water is measured by a combination of in situ radiosonde observations and satellite derived infrared and microwave retrievals from four satellites. This project combines these data into a coherent merged product for use in global climate research. This report is the Year 2 Annual Report from this NASA-sponsored project and includes progress-to-date on the assigned tasks. Author (revised)

N94-35380*# ECK Research Co., Columbia, MO.
LONG RANGE FORECASTS OF THE NORTHERN HEMISPHERE ANOMALIES WITH ANTECEDENT SEA SURFACE TEMPERATURE PATTERNS Final Report, 5 Mar. 1991 - 4 Jun. 1994
Ernest C. Kung 4 Jun. 1994 104 p
(Contract NAS5-30957; RTOP 910-40-00)
(NASA-CR-189358; NAS 1.26:189358) Avail: CASI HC A06/MF A02

The contract research has been conducted in the following three major areas: analysis of numerical simulations and parallel observations of atmospheric blocking, diagnosis of the lower boundary heating and the response of the atmospheric circulation, and comprehensive assessment of long-range forecasting with numerical and regression methods. The essential scientific and developmental purpose of this contract research is to extend our capability of numerical weather forecasting by the comprehensive general circulation model. The systematic work as listed above is thus geared to developing a technological basis for future NASA long-range forecasting. Derived from text

N94-35391*# South Dakota School of Mines and Technology, Rapid City, SD. Inst. of Atmospheric Sciences.
THE EFFECTS OF CLOUD INHOMOGENEITIES UPON RADIATIVE FLUXES, AND THE SUPPLY OF A CLOUD TRUTH VALIDATION DATASET Semiannual Progress Report, Jan. - Jun. 1994
1994 71 p
(Contract NAS5-31718)
(NASA-CR-196080; NAS 1.26:196080) Avail: CASI HC A04/MF A01

With the growing awareness and debate over the potential changes associated with global climate change, the polar regions are receiving increased attention. Global cloud distributions can be expected to be altered by increased greenhouse forcing. Owing to the similarity of cloud and snow-ice spectral signatures in both the visible and infrared wavelengths, it is difficult to distinguish clouds from surface features in the polar regions. This work is directed towards the development of algorithms for the ASTER and HIRIS science/instrument teams. Special emphasis is placed on a wide variety of cloud optical property retrievals, and especially retrievals of cloud and surface properties in the polar regions. Derived from text

N94-35499*# METSAT, Inc., Fort Collins, CO.
PRODUCTION OF LONG-TERM GLOBAL WATER VAPOR AND LIQUID WATER DATA SET USING ULTRA-FAST METHODS TO ASSIMILATE MULTI-SATELLITE AND RADIOSONDE OBSERVATIONS Annual Report No. 1
T. H. VonderHaar, Donald L. Reinke, David L. Randel, Graeme L. Stephens, Cynthia L. Combs, Thomas J. Greenwald, Mark A. Ringerud, and Ian L. Wittmeyer 1 Jul. 1993 71 p Original contains color illustrations
(Contract NASw-4715)
(NASA-CR-195981; Rept-93-103; NAS 1.26:195981) Avail: CASI HC A04/MF A01; 10 functional color pages

During the next decade, many programs and experiments under the Global Energy and Water Cycle Experiment (GEWEX) will utilize present day and future data sets to improve our understanding of the role of moisture in climate, and its interaction with other variables such as clouds and radiation. An important element of GEWEX will be the GEWEX Water Vapor Project (GVaP), which will eventually initiate a routine, real-time assimilation of the highest quality, global water vapor data sets including information gained from future data collection systems, both ground and space based. The comprehensive global water vapor data set being produced by METSAT Inc. uses a combination of ground-based radiosonde data, and infrared and microwave satellite retrievals. This data is needed to provide the desired foundation from which future GEWEX-related research, such as GVaP, can build. The first year of this project was designed to use a combination of the best available atmospheric moisture data including: radiosonde (balloon/acft/rocket), HIRS/MSU (TOVS) retrievals, and SSM/I retrievals, to produce a one-year, global, high resolution data set of integrated column water vapor (precipitable water) with a horizontal resolution of 1 degree, and a temporal resolution of one day. The time period of this pilot product was to be det3ermined by the availability of all the input data sets. January 1988 through December 1988 were selected. In addition, a sample of vertically integrated liquid water content (LWC) was to be produced with the same temporal and spatial parameters. This sample was to be produced over ocean areas only. Three main steps are followed to produce a merged water vapor and liquid water product. Input data from Radiosondes, TOVS, and SSMI/I is quality checked in steps one and two. Processing is done in step two to generate individual total column water vapor and liquid water data sets. The third step, and final processing task, involves merging the individual output products to produce the integrated water vapor product. A final quality control is applied to the merged data sets. Derived from text

N94-35596 Massachusetts Inst. of Tech., Lexington.
THE INFLUENCE OF DATA LINK-PROVIDED GRAPHICAL WEATHER ON PILOT DECISION-MAKING
Ann-Marie T. Lind, Adam Dershowitz, and Steven R. Bussolari 6 Apr. 1994 80 p Limited Reproducibility: More than 20% of this document may be affected by microfiche quality
(Contract DTFA01-93-Z-02012)
(AD-A278871; MIT-ATC-215; DOT/FAA/RD-94/9) Avail: Issuing Activity (Defense Technical Information Center (DTIC))

This report documents the findings of a human factors study conducted to estimate the effects of the Graphical Weather Service (GWS) on general aviation (GA) aircraft utility, pilot situational awareness, and the weather dissemination workload imposed on ground personnel. GWS is a data link application, being developed at MIT Lincoln Laboratory through the sponsorship of the Federal Aviation Administration, that will provide near-real-time graphical weather information to the General Aviation pilot in the cockpit. Twenty instrument-rated pilots participated in the study. Subjects were presented with recorded actual weather information in the context of a series of hypothetical pre-flight briefings and accompanying 'flights'. GWS images were accessible on a Macintosh Computer. The study design enabled the analysis of the effects of GWS and the determination of whether those effects were influenced by the experience level of the pilot/user. Objective and subjective measures of effectiveness were collected. Results indicate that GWS had a substantial effect on weather-related decision-making. This was true for pilots with varying levels of instrument experience. Subject confidence in the ability to assess the weather situation was markedly increased when GWS was used. Subjects with GWS made fewer calls for weather information to weather dissemination ground personnel, thus indicating a potential decrease in ground personnel workload. Subjects found GWS to be very useful and were enthusiastic about receiving data fink services in the GA cockpit in the future. DTIC

N94-35703 Columbia Univ., Palisades, NY.
ASYMETRIC CHANGE OF DAILY TEMPERATURE RANGE: PROCEEDINGS
G. Kukla, ed. Apr. 1994 493 p Presented at the International Minimax Workshop, College Park, MD, 27-30 Sep. 1993 Limited Reproducibility: More than 20% of this document may be affected by microfiche quality
(Contracts DE-FG02-85ER-60372; DE-AC05-84OR-21400)
(DE94-010102; CONF-9309350) Avail: CASI HC A21

This report is a compilation of abstracts of papers presented at the MINIMAX workshop. Topics include the following: temperature fluxes, influence of clouds on temperature, anthropogenic influences on temperature flux, and carbon dioxide and aerosol induced greenhouse effect. DOE

N94-35719 Massachusetts Inst. of Tech., Lexington.
THE POLYGON-ELLIPSE METHOD OF DATA COMPRESSION OF WEATHER MAPS
J. L. Gertz 28 Mar. 1994 80 p Limited Reproducibility: More than 20% of this document may be affected by microfiche quality
(Contracts DTFA01-93-Z-02012; F19628-90-C-0002)
(AD-A278958; ATC-213; DOT/FAA/RD-94/6) Avail: Issuing Activity (Defense Technical Information Center (DTIC))

Providing an accurate picture of the weather conditions in the pilot's area of interest could be a highly useful application for ground-to-air data links. The problem with using data links to transmit weather pictures is the large number of bits required to exactly specify a weather image. To make transmission of weather maps practical, a means must be found to compress this image. The polygon-ellipse (PE) encoding algorithm developed in this report represents weather regions as ellipses, polygons, and exact patterns. The actual ellipse and polygon parameters are encoded and transmitted; the decoder algorithm redraws the shape from their encoded parameter values and fills in the included weather pixels. Special coding techniques are used in PE to compress the encoding of the shape parameters to achieve further overall compression. The PE algorithm contains procedures for gracefully degrading the fidelity of the transmitted image when necessary to meet a specified bit limit. Pictorial examples of the operation of this algorithm on both Terminal Doppler Weather Radar (TDWR) and ASR-9 radar-generated weather images are presented. DTIC

N94-35720 Massachusetts Inst. of Tech., Lexington.
DATA REQUIREMENTS FOR CEILING AND VISIBILITY PRODUCTS DEVELOPMENT
J. L. Keller 13 Apr. 1994 41 p Limited Reproducibility: More than

20% of this document may be affected by microfiche quality
(Contracts DTFA01-93-Z-02012; F19628-90-C-0002)
(AD-A278959; ATC-212; DOT/FAA/RD-94/5) Avail: Issuing Activity (Defense Technical Information Center (DTIC))

The Federal Aviation Administration (FAA) Integrated Terminal Weather System (ITWS) is supporting the development of weather products important for air traffic control in the terminal area. These products will take advantage of new terminal area sensors, including Terminal Doppler Weather Radar (TDWR), Next Generation Weather Radar (NEXRAD), and the Meteorological Data Collection and Reporting System (MDCRS). Some of these ITWS products will allow air traffic managers to anticipate significant short-term changes in ceiling and visibility. This report focuses on the scientific data requirements for supporting prototype model-system development and diagnostics. Model diagnostics can include case studies to determine the most important physical processes that were responsible for a particular ceiling and visibility event, providing the insight necessary for the development of effective ceiling and visibility product algorithms. In time such case study diagnostics could also include careful off-line failure analyses that may affect the design of the operational system. General ceiling and visibility test beds are discussed. Updated reports will be released periodically as the ITWS ceiling and visibility project proceeds. DTIC

N94-35766 Sandia National Labs., Albuquerque, NM.
EXTRACTION OF CLOUD STATISTICS FROM WHOLE SKY IMAGING CAMERAS
W. P. Kegelmeyer, Jr. Mar. 1994 15 p Limited Reproducibility: More than 20% of this document may be affected by microfiche quality
(Contract DE-AC04-94AL-85000)
(DE94-009867; SAND-94-8222) Avail: CASI HC A03

Computer codes were developed to extract basic cloud statistics from whole sky imaging (WSI) cameras. This report documents, on an algorithmic level, the steps and processes underlying these codes. Appendices comment on code details and on how to adapt to future changes in either the source camera or the host computer. DOE

N94-35767 Sandia National Labs., Albuquerque, NM.
THE COMPUTATION OF CLOUD BASE HEIGHT FROM PAIRED WHOLE-SKY IMAGING CAMERAS
M. C. Allmen and W. P. Kegelmeyer, Jr. Mar. 1994 78 p Limited Reproducibility: More than 20% of this document may be affected by microfiche quality
(Contract DE-AC04-94AL-85000)
(DE94-009868; SAND-94-8223) Avail: CASI HC A05

A major goal for global change studies is to improve the accuracy of general circulation models (GCM's) capable of predicting the timing and magnitude of greenhouse gas-induced global warming. Research has shown that cloud radiative feedback is the single most important effect determining the magnitude of possible climate responses to human activity. Of particular value to reducing the uncertainties associated with cloud-radiation interactions is the measurement of cloud base height (CBH), both because it is a dominant factor in determining the infrared radiative properties of clouds with respect to the earth's surface and lower atmosphere and because CBH's are essential to measuring cloud cover fraction. We have developed a novel approach to the extraction of cloud base height from pairs of whole sky imaging (WSI) cameras. The core problem is to spatially register cloud fields from widely separated WSI cameras; this complete triangulation provides the CBH measurements. The wide camera separation (necessary to cover the desired observation area) and the self-similarity of clouds defeats all standard matching algorithms when applied to static views of the sky. To address this, our approach is based on optical flow methods that exploit the fact that modern WSI's provide sequences of images. We will describe the algorithm and present its performance as evaluated both on real data validated by ceilometer measurements and on a variety of simulated cases. DOE

N94-35807 Massachusetts Inst. of Tech., Lexington.
TERMINAL DOPPLER WEATHER RADAR (TDWR) LOW LEVEL WIND SHEAR ALERT SYSTEM 3 (LLWAS 3) INTEGRATION STUDIES AT ORLANDO INTERNATIONAL AIRPORT Project Report, 1991 - 1992
Rodney E. Cole and Russell F. Todd 20 Apr. 1994 55 p Limited Reproducibility: More than 20% of this document may be affected by microfiche quality
(Contracts DTFA01-93-Z-02012; F19628-90-C-0002)
(AD-A278957; ATC-216; DOT/FAA/RD-94/12) Avail: Issuing Activity (Defense Technical Information Center (DTIC))

In 1993 the Federal Aviation Administration (FAA) began deploying two new wind shear detection systems: the Terminal Doppler Weather Radar (TDWR) and the third-generation Low Level Windshear Alert System (LLWAS 3). Currently, nine airports are scheduled to receive both a TDWR and an LLWAS 3. This number may eventually increase to as high as 45. When co-located the systems will be integrated to provide a single set of wind shear alerts and improve system performance. The TDWR production schedule required one of three integration algorithms to be chosen for specification by fall 1991. The three algorithms are the prototype integration algorithm developed at the National Center for Atmospheric Research (NCAR) and the two algorithms developed at MIT Lincoln Laboratory (MIT LL). To assess the performance of the three algorithms, MIT LL performed a study of integration, TDWR, and LLWAS 3 algorithms at Orlando International Airport (MCO) in the summer of 1991. Based on the results of this study, MIT LL and NCAR issued a joint recommendation that the FAA procure one of the integration algorithms developed at MIT LL. This algorithm was demonstrated at the Orlando International Airport in the summer of 1992. Results of the 1991 comparative study and a follow-up study of the TDWR, LLWAS 3, and Message Level integration algorithms at Orlando in 1992 are discussed. All the algorithms met the requirement of detecting 90 percent of microburst level wind shear with loss events. LLWAS 3, Build 5 TDWR, and the MIT LL integration algorithms with Build 5 TDWR all met the requirement that less than 10 percent of wind shear alerts be false. DTIC

N94-36186 Boston Univ., MA. Dept. of Electrical Computer and Systems Engineering.
APPLICATION OF DIFFERENTIAL INVERSION TO DMSP MICROWAVE SOUNDER DATA Annual Report, 1 Aug. 1992 - 31 Jul. 1993
Robert G. Hohlfeld 31 Jul. 1993 84 p Limited Reproducibility: More than 20% of this document may be affected by microfiche quality
(Contract F49620-92-J-0444)
(AD-A278575; AFOSR-94-0201TR) Avail: Issuing Activity (Defense Technical Information Center (DTIC))

Differential Inversion (DI) is a novel approach to the solution of the atmospheric temperature sounding problem which was developed by Dr. J.I.F. King of the Air Force's Phillips Laboratory. Before the present research, DI has been applied only to infrared radiance data sets, such as from TOVS/HIRS. In this report I describe the progress made in the first year of a research program to apply DI to microwave radiance data from the SSM/T sounder on the DMSP satellites. The ultimate objectives of this research are to establish effective DI sounding algorithms for the microwave spectral region and to extend DI in directions which increase its utility as a practical sounding algorithm. DI has many attractive features in this application, including its close coupling to the physical formulation of the temperature sounding problem, its freedom from the necessity of using an a priori temperature profile, and its high level of computational efficiency. At present, we have understood the practical difficulties, characteristic of temperature sounding in the microwave spectral region (as these apply to DI), and have produced software yielding temperature profiles of a convincing meteorological character. Author (DTIC)

N94-36187 Naval Postgraduate School, Monterey, CA.
THREE DIMENSIONAL VISUALIZATION OF A COASTAL MESOSCALE MODEL M.S. Thesis
Mark R. Sampson Dec. 1993 71 p Limited Reproducibility: More than 20% of this document may be affected by microfiche quality
(AD-A278576) Avail: Issuing Activity (Defense Technical Information Center (DTIC))

An atmospheric coastal mesoscale model is visualized using a high speed graphical computer workstation. Output from a 36-h model forecast of the Naval Postgraduate School (NPS) research version of the Naval Research Laboratory (NRL) limited area grid model is displayed at 30 minute time steps. The NPS/NRL model is centered on the California coastal region. Using the graphical software package, VIS-5D, three-dimensional scenes are developed that show the interrelation of model parameters which aid in understanding model output. The visualization is used to evaluate wind flow, temperature and moisture patterns, shortwave and longwave radiation parameterization, and cloud simulations for the time period 0000 UTC 02 May 1990 to 1200 UTC 03 May 1990. Additionally, model output is used to compute tactical displays of radar propagation used by the naval fleet Numerical modeling. DTIC

N94-36228# Atmospheric and Environmental Research, Inc., Cambridge, MA.

USE OF WIND PROFILER DATA IN SHORT-RANGE FORCASTING Final Report, Jan. 1993 - Jan. 1994

Thomas M. Hamill, Thomas Nehrkorn, and Lawrence W. Knowlton 15 Jan. 1994 139 p
(Contract F19628-92-C-0014; AF Proj. 2688)
(AD-A279482; PL-TR-2009) Avail: CASI HC A07/MF A02

This report describes the results of the second year of a two-year study directed toward improving short-term forecasts and nowcasts through processing of satellite data (year 1) and Doppler profiler data (year 2). Data from the wind profiler demonstration network in the central US were used in a Barnes analysis scheme to produce hourly gridded wind fields and various derived kinematic quantities. The data were displayed in horizontal, vertical, and time-height cross sections. The utility of the profiler data, and profiler derived analyses, for short-term forecasting was demonstrated in a total of eight case studies, covering a wide range of atmospheric conditions. Among the derived quantities, the low-level vertical velocity derived from the horizontal convergence fields was found to be particularly useful for identifying areas of precipitation, while midlevel vorticity and vorticity advection was helpful in identifying quasigeostrophic forcing mechanisms. Author

N94-36240 Los Alamos National Lab., NM.

KINETIC THEORY OF RUNAWAY AIR BREAKDOWN AND THE IMPLICATIONS FOR LIGHTNING INITIATION

R. A. Roussel-Dupre, A. V. Gurevich, T. Tunnell, and G. M. Milikh Nov. 1993 52 p Limited Reproducibility: More than 20% of this document may be affected by microfiche quality
(Contract W-7405-eng-36)
(DE94-001683; LA-12601-MS) Avail: CASI HC A04

The kinetic theory for a new air breakdown mechanism advanced in a previous paper is developed. The relevant form of the Boltzmann equation is derived and the particle orbits in both velocity space and configuration space are computed. A numerical solution of the Boltzmann equation, assuring a spatially uniform electric field, is obtained and the temporal evolution of the electron velocity distribution function is described. The results of our analysis are used to estimate the magnitude of potential x-ray emissions from discharges in thunderstorms and are examined in the context of lightning initiation. DOE

N94-36244# Oak Ridge National Lab., TN.

SELECTED TRANSLATED ABSTRACTS OF RUSSIAN-LANGUAGE CLIMATE-CHANGE PUBLICATIONS. 2: CLOUDS

M. D. Burtis, comp. Jan. 1994 106 p In ENGLISH and RUSSIAN
(Contract DE-AC05-84OR-21400)
(DE94-011465; ORNL/CDIAC-64; ESDP-4129) Avail: CASI HC A06/MF A02

This report presents abstracts (translated into English) of important Russian-language literature concerning clouds as they relate to climate change. In addition to the bibliographic citations and abstracts translated into English, this report presents the original citations and abstracts in Russian. Author and title indexes are included to assist the reader in locating abstracts of particular interest. DOE

N94-36249 Massachusetts Inst. of Tech., Lexington. Lincoln Lab.

EXTRAPOLATING STORM LOCATION USING THE INTEGRATED TERMINAL WEATHER SYSTEM (ITWS) STORM MOTION ALGORITHM

E. S. Chornoboy and A. Matlin 29 Mar. 1994 78 p Limited Reproducibility: More than 20% of this document may be affected by microfiche quality
(Contract DTFA01-91-Z-02036)
(AD-A278611; MIT-ATC-208; DOT/FAA/RD-94/2) Avail: Issuing Activity (Defense Technical Information Center (DTIC))

Storm Motion (SM) is a planned Initial Operational Capability (IOC) algorithm of the FAA's Integrated Terminal Weather System (ITWS). As currently designed, this algorithm will track the movement of storms/cells and convey this tracking information to the ITWS user by means of a graphic display of vectors (for direction) with accompanying numeric reports of storm speed, rounded to the nearest 5 nmi/hr increment. Recognizing that there are occasions when ITWS users could benefit from a more extended product format, Storm Extrapolated Position (SEP) was conceived to supplement the SM product and thereby increase its accessibility as a planning aid. This communication describes a prototype SEP design along with an analysis of its accuracy and observed performance during 1993 ITWS demonstrations in Orlando, FL. and Dallas, TX. DTIC

N94-36262# Hughes STX, Inc., Lexington, MA.

DOPPLER WEATHER RADAR STUDIES OF PRECIPITATION SYSTEMS Final Report No. 8, May 1990 - May 1993

F. Ian Harris, Teresa Bals, Ralph J. Donaldson, Donald Hamann, and David J. Smalley Dec. 1993 69 p Original contains color illustrations
(Contract F19628-90-C-0088; AF Proj. 2781)
(AD-A279417; PL-TR-93-2168) Avail: CASI HC A04/MF A01

Research under this contract was directed toward the development of new techniques to monitor and forecast the behavior of precipitation systems with Doppler weather radar. Focus was on the characterization of precipitation fields and of associated wind fields. Particular aspects that were examined are precipitation location, motion and type, synoptic scale and gust fronts, and the characterization of hurricane physical and kinematic structure. All analysis and forecast techniques are appropriate for a real-time operational environment. In addition, research has been completed toward the archiving and analysis of data from a wind profiling radar system. Efforts involved the definition of management, quality control, transformation, perusal, and extraction techniques for the profiler data. Also, techniques were developed to evaluate the meteorological conditions contributing to observed differences between the Loransonde and profiler wind estimates. Author (revised)

N94-36285# Sandia National Labs., Albuquerque, NM.

IMPLEMENTATION OF RAMAN LIDAR FOR PROFILING OF ATMOSPHERIC WATER VAPOR AND AEROSOLS AT THE SGP CART SITE

J. E. M. Goldsmith, S. E. Bisson, F. H. Blair, D. N. Whiteman, and S. H. Melfi 1994 4 p Presented at the Atmospheric Radiation Measurement Science Team Meeting, Charleston, SC, 28 Feb. - 3 Mar. 1994
(Contract DE-AC04-76DR-00789)
(DE94-011754; SAND-94-8597; CONF-940277-2) Avail: CASI HC A01/MF A01

There are clearly identified scientific requirements for continuous profiling of atmospheric water vapor at the SGP CART (southern great plains cloud and radiation testbed) site. Research conducted at several laboratories, including our own collaboration in a previous ARM Instrument Development Project, has demonstrated the suitability of Raman lidar for providing measurements that are an excellent match to those requirements. We are currently building a ruggedized Raman lidar system that will reside permanently at the CART site, and that is computer-automated to minimize requirements for operator interaction. In addition to profiling water vapor through most of the troposphere during nighttime and through the boundary layer during daytime, the lidar will provide quantitative characterizations of aerosols and clouds, including depolarization measurements for particle phase studies. DOE

48 OCEANOGRAPHY

Includes biological, dynamic, and physical oceanography; and marine resources.

For related information see also *43 Earth Resources and Remote Sensing.*

N94-35343*# National Aeronautics and Space Administration, Washington, DC.

MISSION TO PLANET EARTH. THE LIVING OCEAN: OBSERVING OCEAN COLOR FROM SPACE

[1994] 12 p Prepared in cooperation with NASA. Goddard Space Flight Center, Greenbelt, MD Limited Reproducibility: More than 20% of this document may be affected by color photographs Original contains color illustrations
(NASA-PAM-554; NAS 1.75:554) Avail: CASI HC A03/MF A01; 6 functional color pages

Measurements of ocean color are part of NASA's Mission to Planet Earth, which will assess how the global environment is changing. Using the unique perspective available from space, NASA will observe, monitor, and study large-scale environmental processes, focusing on quantifying climate change. NASA will distribute the results of these studies to researchers worldwide to furnish a basis for informed decisions on environmental protection and economic policy. This information packet includes discussion on the reasons for measuring ocean color, the carbon cycle and ocean color, priorities for global climate research, and SeWiFS (sea-viewing wide field-of-view sensor) global ocean color measurements.
CASI

N94-35738# Environmental Research Lab., Gulf Breeze, FL.
PROCEEDINGS: INTEGRATED RESEARCH PLANNING MEETING FOR GULF OF MEXICO ESTUARIES
J. E. Harvey and F. L. Mayer Jan. 1994 89 p Meeting held in Gulf Breeze, FL, 2-3 Nov. 1993
(PB94-157799; EPA/600/R-94/013) Avail: CASI HC A05/MF A01

The report summarizes a planning meeting organized by Environmental Protection Agency (EPA) to develop and Aquatic Ecological Criteria Research Program for Gulf of Mexico estuaries. The meeting was held on November 2-3, 1993, at the EPA Environmental Research Laboratory in Gulf Breeze, Florida, to develop and field test a diagnostic protocol to assess and characterize the ecological condition of Gulf of Mexico estuaries. Participants included EPA scientists and cooperators and advisors from academia, Federal and state agencies, and private corporations. NTIS

N94-36293 Washington Univ., Seattle, WA. Applied Physics Lab.
ENVIRONMENTAL MEASUREMENTS IN THE BEAUFORT SEA, SPRING 1993
T. Wen and F. Karig Dec. 1993 93 p Limited Reproducibility: More than 20% of this document may be affected by microfiche quality
(Contract N00039-91-C-0072)
(AD-A278718; APL-UW-TM-4-93) Avail: Issuing Activity (Defense Technical Information Center (DTIC))

This report presents environmental data obtained by the Applied Physics Laboratory of the University of Washington (APL-UW) at APLIS 93, an ice camp established in the Beaufort Sea in Spring 1993 to support Navy-sponsored tests and research during ICEX 1-93. Data analysis is limited because the purpose of this report is to provide field data to ice camp participants. The data was collected to document the meteorological and oceanographic conditions that existed during camp activities. The main data sets are weather, floe drift, STD profiles, currents, and ice properties.
DTIC

51 LIFE SCIENCES (GENERAL)

N94-35232* National Aeronautics and Space Administration. Lyndon B. Johnson Space Center, Houston, TX.
MULTI-CELLULAR, THREE-DIMENSIONAL LIVING MAMMALIAN TISSUE Patent
Thomas J. Goodwin, inventor (to NASA) and David A. Wolf, inventor (to NASA) 3 May 1994 7 p Filed 3 Sep. 1992 Continuation of US-Patent-Appl-SN-317931, filed 2 Mar. 1989 which is a continuation-in-part of US-Patent-Appl-SN-213558, filed 30 Jun. 1988 which is a continuation-in-part of US-Patent-Appl-SN-213559, filed 30 Jun. 1988
(NASA-Case-MSC-21560-2; US-Patent-5,308,764;
US-Patent-Appl-SN-939791; US-Patent-Appl-SN-317931;
US-Patent-Appl-SN-213558; US-Patent-Appl-SN-213559;
US-Patent-Class-435-240.24; US-Patent-Class-435-240.2;
US-Patent-Class-435-240.25; US-Patent-Class-435-1) Avail: US Patent and Trademark Office

The present invention relates to a multicellular, three-dimensional, living mammalian tissue. The tissue is produced by a co-culture process wherein two distinct types of mammalian cells are co-cultured in a rotating bioreactor which is completely filled with culture media and cell attachment substrates. As the size of the tissue assemblies formed on the attachment substrates changes, the rotation of the bioreactor is adjusted accordingly.
Official Gazette of the U.S. Patent and Trademark Office

N94-35257*# Washington State Univ., Pullman, WA. Inst. of Biological Chemistry.
[EFFECT OF MICROGRAVITY ON PLANT GROWTH] Final Report
Norman G. Lewis 1994 3 p
(Grant NAG10-0086)
(NASA-CR-196004; NAS 1.26:196004) Avail: CASI HC A01/MF A01

The overall goal of this research is to determine the effect of microgravity proper on plant growth (metabolism and cell wall formation). In addressing this goal, the work conducted during this grant period was divided into three components: analyses of various plant tissues previously grown in space aboard MIR Space Station; analyses of wheat tissues grown on Shuttle flight STS-51; and Phenylpropanoid metabolism and plant cell wall synthesis (earth-based investigations). Derived from text

N94-35366* National Aeronautics and Space Administration. Lyndon B. Johnson Space Center, Houston, TX.
HIGH DENSITY CELL CULTURE SYSTEM Patent
Glenn F. Spaulding, inventor (to NASA) 19 Jul. 1994 7 p Filed 23 Dec. 1992 Supersedes N93-19037 (31 - 6, p 1593)
(NASA-Case-MSC-22060-1; US-Patent-5,330,908;
US-Patent-Appl-SN-996263; US-Patent-Class-435-240.24;
US-Patent-Class-435-240.25; US-Patent-Class-435-286;
US-Patent-Class-435-296; US-Patent-Class-435-312;
US-Patent-Class-435-313; US-Patent-Class-435-818) Avail: US Patent and Trademark Office

An annular culture vessel for growing mammalian cells is constructed in a one piece integral and annular configuration with an open end which is closed by an endcap. The culture vessel is rotatable about a horizontal axis by use of conventional roller systems commonly used in culture laboratories. The end wall of the endcap has tapered access ports to frictionally and sealingly receive the ends of hypodermic syringes. The syringes permit the introduction of fresh nutrient and withdrawal of spent nutrients. The walls are made of conventional polymeric cell culture material and are subjected to neutron bombardment to form minute gas permeable perforations in the walls.
Official Gazette of the U.S. Patent and Trademark Office

N94-35601 Direction des Recherches, Etudes et Techniques, Paris (France). Centre de Documentation de l'Armement.
STRESS AND BRAIN PROTEIN SYNTHESIS Final Report [STRESS ET SYNTHESE PROTEIQUE CEREBRALE]
G. Bobillier 1994 33 p In FRENCH
(PB94-170750) Avail: Issuing Activity (National Technical Information Service (NTIS))

This study investigates the effect of adrenalectomy and peripheral administration of glucocorticoids (GC's) on protein synthesis in rat brain. The researchers began by fully validating the L-((35)S) Methionine method, forcing them to abandon a study on the effect of GC's on energy metabolism in the brain because of technical difficulties. They found that GC's have a tonic, generalized, and persistent inhibiting effect on brain protein synthesis in rats. Glucocorticoids are not directly responsible for inducing brain protein synthesis during the stress alarm phase, but rather intervene during the adaptation phase to restore and maintain the normal basal rate of protein synthesis activity in the brain. These neuroendocrine factors likely play a major role in relations between the brain and peripheral system, and vice-versa. NTIS

N94-36101 National Inst. of Radiological Sciences, Chiba (Japan). Science and Technology Agency.
[ACTIVITIES OF NATIONAL INSTITUTE OF RADIOLOGICAL SCIENCES] Annual Report, Apr. 1991 - Mar. 1992
Jul. 1992 113 p Limited Reproducibility: More than 20% of this document may be affected by microfiche quality
(DE94-727636; NIRS-31) Avail: CASI HC A06

This annual report is a compilation of the research activities and achievement in the National Institute of Radiological Sciences (NIRS) in Japan during the fiscal year 1991 (from April 1991 through March 1992). The research covers a wide range of radiological sciences from molecular to environmental studies and medicine including engineering. Topics consist of physics, chemistry, biomedical science, clinical research, and environmental sciences, covering a total of 69 titles. A list of publications by staff members, activities of research divisions, and organization chart of the NIRS are given in the Appendix. DOE

N94-36269 California Univ., Berkeley. Lawrence Berkeley Lab, CA.
A LOW TEMPERATURE SCANNING FORCE MICROSCOPE FOR BIOLOGICAL SAMPLES Ph.D. Thesis
M. G. L. Gustafsson (California Univ., Berkeley, CA.) May 1993 200 p Limited Reproducibility: More than 20% of this document may be affected by microfiche quality
(Contract DE-AC03-76SF-00098)
(DE94-011357; LBL-34182) Avail: CASI HC A09

An SFM has been constructed capable of operating at 143 K. Two contributions to SFM technology are described: a new method of fabricating tips, and new designs of SFM springs that significantly lower the noise level. The SFM has been used to image several biological samples (including collagen, ferritin, RNA, purple membrane) at 143 K and room temperature. No improvement in resolution resulted from 143 K operation; several possible reasons for this are discussed. Possibly sharper tips may help. The 143 K SFM will allow the study of new categories of samples, such as those prepared by freeze-frame, single molecules (temperature dependence of mechanical properties), etc. The SFM was used to cut single collagen molecules into segments with a precision of less than or equal to 10 nm. DOE

52 AEROSPACE MEDICINE

Includes physiological factors; biological effects of radiation; and effects of weightlessness on man and animals.

N94-35345* National Aeronautics and Space Administration, Washington, DC.
AEROSPACE MEDICINE AND BIOLOGY: A CONTINUING BIBLIOGRAPHY WITH INDEXES (SUPPLEMENT 391)
Aug. 1994 42 p
(NASA-SP-7011(391); NAS 1.21:7011(391)) Avail: CASI HC A03

This bibliography lists 75 reports, articles, and other documents introduced into the NASA Scientific and Technical Information System during Aug. 1994. Subject coverage includes: aerospace medicine and physiology, life support systems and man/system technology, protective clothing, exobiology and extraterrestrial life, planetary biology, and flight crew behavior and performance. Author

N94-36217 Institut National de la Sante et de la Recherche Medicale, Paris (France). Lab. de Physiologie des Adaptations.
TYPOLOGY OF SKELETAL MUSCLE IN HUMANS UNDERGOING INTENSE PHYSICAL TRAINING OR PROLONGED AKINESIA Final Report [TYPOLOGIE DU MUSCLE STRIE CHEZ L'HOMME EN SITUATION D'ENTRAINEMENT PHYSIQUE INTENSE OU D'AKINESIE PROLONGEE]
M. Rieu and A. X. Bigard 1994 44 p In FRENCH Sponsored by Direction des Recherches, Etudes et Techniques
(PB94-170644) Avail: Issuing Activity (National Technical Information Service (NTIS))

There were three parts to this study: experimental attempts to use the micropuncture biopsy technique for animals on humans; a preliminary study of the muscular typology of severe burn patients and how it changes over time; and an analysis of the effects of muscular electrostimulation on the typology of musculus vastus externus in athletes. The biopsy technique was found to be yield usable muscle samples after some practice. The particularly low levels of muscular glycogen measured in what were relatively light burn cases were surprising, and will have to be confirmed by a larger, longer-term study. A relatively low proportion of type I fibers, and a high proportion of type IIB fibers, was discovered. Finally, the authors found that training programs based on electrostimulation often used to improve muscular strength modify neither the size nor topology of skeletal muscle. NTIS

N94-36220 Centre d'Etudes et de Recherches Bio-Physiologiques Appliquees a la Marine, Toulon (France).
EFFECTS OF 5 MPa HELIOX PRESSURE ON DOPAMINER GIC PATHWAY: AN IN VIVO NEUROCHEMICAL STUDY [ETUDE NEUROCHIMIQUE DE L'ACTION DES HAUTES PRESSIONS D'HELIUM PAR L'ADAPTATION DE LA TECHNIQUE DE MICRODIALYSE INTRACERABRALE A L'HYPERBARIE]
J. J. Risso and M. Barthelemy-Requin Dec. 1992 31 p In FRENCH
(Contract DRET-88-1011)
(PB94-170693; CERB-92-12) Avail: Issuing Activity (National Technical Information Service (NTIS))

The laboratory adapted the intracranial microdialysis technique to hyperbaric conditions. Free-moving rats were stereotaxically implanted in the anterior caudate nucleus with a microdialysis probe to measure dopamine, dihydroxyphenylacetic acid, and homovanillic acid levels during different phases of a simulated dive up to 5.1 MPa. Compression was found to increase extracellular dopamine and dihydroxphenylacetic acid concentrations, except in homovanillic acid. This represents a specific effect on high pressure on the dopaminergic pathway, and may be due to an increase of dopamine synthesis through a direct action on D2 autoreceptors. NTIS

N94-36223# Midwest Research Inst., Kansas City, MO.
FURTHER STUDIES OF 60-Hz EXPOSURE EFFECTS ON HUMAN FUNCTION
C. Graham and H. D. Cohen 29 Mar. 1994 8 p
(Contract DE-FG01-89CE-34025)
(DE94-010192; DOE/CE-34025/T12) Avail: CASI HC A02/MF A01

The objective of the exploratory study was to determine whether the electric or magnetic field, presented separately in an intermittent fashion, would produce the same pattern of heart rate increases and decreases seen in the original intermittent exposure study. In addition, time of day and baseline heart rate were explored in an attempt to clarify design issues that arose from previous studies. Twenty-four healthy young men 21 to 35 years of age participated in the study. Half were exposed to a 9-kV/m electric field and half to a 200-mG magnetic field. Within each of these groups, half were exposed in the morning and half in the afternoon. DOE

N94-36338# Aerospace Medical Research Labs., Brooks AFB, TX. Sustained Operations Branch.
DETERMINANTS OF SUBJECTIVE FATIGUE FOR C-141 CREWS DURING OPERATION DESERT STORM
Jonathan French, Kelly J. Neville, William F. Storm, Roger U. Bisson, and Patricia Boll *In* AGARD, Recent Advances in Long Range and Long Endurance Operation of Aircraft Nov. 1993 12 p (For primary document see N94-36321 11-05)
Copyright Avail: CASI HC A03/MF A03

N94-36339# Centre d'Etudes et de Recherches de Medecine Aerospatiale, Bretigny sur Orge (France).
SOME SOLUTIONS TO REDUCE THE HUMAN EFFECTS OF EXTENDED OPERATION TIMES [QUELQUES SOLUTIONS POUR REDUIRE LES EFFETS SUR L'HOMME DES OPERATIONS DE LONGUE DUREE]
D. Lagarde and D. Batejat *In* AGARD, Recent Advances in Long Range and Long Endurance Operation of Aircraft Nov. 1993 17 p In FRENCH (For primary document see N94-36321 11-05)
Copyright Avail: CASI HC A03/MF A03

53 BEHAVIORAL SCIENCES

Includes psychological factors; individual and group behavior; crew training and evaluation; and psychiatric research.

N94-35379*# Massachusetts Inst. of Tech., Cambridge. Man Vehicle Lab.
VISUAL-VESTIBULAR INTERACTION Final Report
Laurence R. Young and D. Merfeld Jun. 1994 9 p
(Grant NAG2-445)
(NASA-CR-196097; NAS 1.26:196097) Avail: CASI HC A02/MF A01

Significant progress was achieved during the period of this grant on a number of different fronts. A list of publications, abstracts, and theses supported by this grant is provided at the end of this document. The completed studies focused on three general areas: eye movements induced by dynamic linear acceleration, eye movements and vection reports induced by visual roll stimulation, and the separation of gravito-inertial force into central estimates of gravity and linear acceleration. Derived from text

N94-35528 Army Aeromedical Research Lab., Fort Rucker, AL.
ACCOMMODATION DURING INSTRUMENT VIEWING CAN BE INFLUENCED BY KNOWLEDGE OF OBJECT DISTANCE Final Report
John C. Kotulak, Stephen E. Morse, and Roger W. Wiley Mar. 1994 14 p Limited Reproducibility: More than 20% of this document may be affected by microfiche quality
(AD-A278987; USAARL-94-13) Avail: Issuing Activity (Defense Technical Information Center (DTIC))

The level of accommodation during instrument viewing is influenced by the perceived nearness of the object in subjects with proximal, but not distal, dark focuses. The topics covered include the following: instrument myopia, accommodations night vision goggles, and known object distance. DTIC

N94-36215 Direction des Recherches, Etudes et Techniques, Paris (France). Direction Scientifique Soutien a la Recherche.
ATTENTION AND SIGNAL DETECTION. A STUDY OF ATTENTION DIVIDED BETWEEN VISUAL AND AUDITORY SIGNALS [ATTENTION ET DETECTION DE SIGNAUX. ETUDE DE L'ATTENTION DIVISEE ENTRE VISION ET AUDITION]
A. M. Bonnel 1993 42 p In FRENCH
(PB94-170594) Avail: Issuing Activity (National Technical Information Service (NTIS))

In a series of dual tasks, we asked observers to divide their attention between a patch of light at the center of a screen and a pure auditory tone simultaneously transmitted through earphones. Instructions were to direct 20 percent of attention to the sound and 80 percent to the light (or vice-versa); or 50 percent to each; or, in the single control experiment, 100 percent to one. The results are interpreted in light of a hierarchical model or functional architecture in which cognitive penetrability is not operative at the most basic stages. Sensory coding during detection would be pure transduction, comparable to a computer interrupt. In identification, it would be a test, modulating sensitivity by top-down control through attention. NTIS

54 MAN/SYSTEM TECHNOLOGY AND LIFE SUPPORT

Includes human engineering; biotechnology; and space suits and protective clothing.

For related information see also *16 Space Transportation.*

N94-35266*# North Carolina Univ., Charlotte, NC. Dept. of Mechanical Engineering and Engineering Science.
DESIGN AND SIMULATION OF EVA TOOLS FOR FIRST SERVICING MISSION OF HST Semiannual Report, 15 Jul. 1993 - 14 Jan. 1994
Dipak Naik and P. H. DeHoff 1994 77 p
(Grant NAG5-2038)
(NASA-CR-196030; NAS 1.26:196030; ME/ES-TR-94-1) Avail: CASI HC A05/MF A01

The Hubble Space Telescope (HST) was launched into near-earth orbit by the Space Shuttle Discovery on April 24, 1990. The payload of two cameras, two spectrographs, and a high-speed photometer is supplemented by three fine-guidance sensors that can be used for astronomy as well as for star tracking. A widely reported spherical aberration in the primary mirror causes HST to produce images of much lower quality than intended. A Space Shuttle repair mission in January 1994 installed small corrective mirrors that restored the full intended optical capability of the HST. The First Servicing Mission (FSM) involved considerable Extra Vehicular Activity (EVA). Special EVA tools for the FSM were designed and developed for this specific purpose. In an earlier report, the details of the Data Acquisition System developed to test the performance of the various EVA tools in ambient as well as simulated space environment were presented. The general schematic of the test setup is reproduced in this report for continuity. Although the data acquisition system was used extensively to test a number of fasteners, only the results of one test each carried on various fasteners and the Power Ratchet Tool are included in this report. Author

N94-35600 Rutherford Appleton Lab., Chilton (England).
MMI(EXP 2) DEMONSTRATOR SYSTEMS: A MULTI-MODAL INTERFACE FOR MAN MACHINE INTERACTION WITH KNOWLEDGE BASED SYSTEMS. DELIVERABLE D17 (TA 2) ESPRIT PROJECT 2474 MMI(EXP 2)
M. D. Wilson Feb. 1994 105 p See also PB92-143619 Sponsored by European Strategic Program for Research and Development in Information Technology, Brussels, Belgium
(PB94-170537; RAL-94-016) Avail: Issuing Activity (National Technical Information Service (NTIS))

The MMI(sup 2) project has developed two demonstrators of co-operative user interfaces to Knowledge Based Systems which employ multiple modes of interaction: natural language, command language, graphics, gesture, direct manipulation and non-verbal audio. The purpose of both demonstrators was to demonstrate multi-modal interaction, to devise an architecture to support a co-operative multi-modal interface, to test the integration of the various technologies required, to define the meaning representation language required by such an architecture, and to investigate the requirements for a co-operative dialog interface. This document provides an overview of the system architecture, the development method and each of the modules in the architecture. It then provides test scripts used for each of the demonstrators which illustrate features of the co-operative human computer dialog that they support. NTIS

N94-35659 Army Aeromedical Research Lab., Fort Rucker, AL.
IS INCREASED ACCOMMODATION A NECESSARY CONDITION FOR INSTRUMENT MYOPIA? Final Report
John C. Kotulak and Stephen E. Morse Mar. 1994 13 p Limited Reproducibility: More than 20% of this document may be affected by microfiche quality
(AD-A278962; USAARL-94-14) Avail: Issuing Activity (Defense Technical Information Center (DTIC))

Emmetropic subjects focus optical instruments as though they were myopic when the level of accommodation with instrument viewing is no greater than it is without. DTIC

N94-35688 Microelectronics Center of North Carolina, Research Triangle Park, NC. Information Technologies Div.
MODEL ENGINEERING CONCEPTS FOR AIR QUALITY MODELS IN AN INTEGRATED ENVIRONMENTAL MODELING SYSTEM
C. Coats, A. F. Hanna, D. Hwang, and D. W. Byun 1993 13 p Symposium was held 1993 Limited Reproducibility: More than 20% of this document may be affected by microfiche quality
(Contract EPA-68-01-7365; EPA-R-816496)
(PB94-158623; EPA/600/A-94/036) Avail: CASI HC A03

Models-3 is an extensible environmental modeling system designed to meet the research and regulatory needs of the EPA and other users into the twenty-first century. As such, it must deal with a number of problems. These problems include: the scientific correctness, flexibility, and usability required; automating much of the complexity of planning, scheduling, and management of the computations associated with environmental studies and the massive volumes of data these studies produce; and the software engineering issues associated with developing a modular, scalable, extensive family of air quality models to be provided by the Models-3 system to its users. The paper is concerned with the last of these, the model engineering problem. NTIS

N94-35692 Air Force Inst. of Tech., Wright-Patterson AFB, OH. School of Engineering.
THE PREDICTION OF PILOT OPINION RATINGS USING OPTIMAL AND SUB-OPTIMAL PILOT MODELS M.S. Thesis
Craig R. Edkins Mar. 1994 221 p Limited Reproducibility: More than 20% of this document may be affected by microfiche quality
(AD-A278679; AFIT/GAE/ENY/94M-2) Avail: Issuing Activity (Defense Technical Information Center (DTIC))

This study details the development of a sub-optimal pilot model that

blended the classical and optimal pilot model approaches in an attempt to achieve the advantages of each. This model used a numerical solution to the linear quadratic Gaussian problem to find the pilot gain, lead, and lag values that minimized a performance index consisting of task error and control usage. This development was conducted in four phases. First, an optimal pilot model developed by Systems Technology, Incorporated, was analyzed in detail. This analysis included a step-by-step example problem to clarify the model's logic and an in-depth sensitivity analysis of the model's parameters. Second, a ground and airborne evaluation of human pilot response was conducted using the Calspan variable stability Lear II aircraft. Primary pilot response parameters were recorded and examined using statistical and Fourier transform analysis in an attempt to provide insight into human pilot response. Third, a numerical solution to the linear quadratic Gaussian control problem that allows the compensator form to be predetermined was derived. Finally, the sub-optimal pilot model was developed and an analysis of the model's parameters was conducted.
DTIC

N94-35707 Naval Air Warfare Center, Warminster, PA. Air Vehicle and Crew Systems Technology Dept.
A DATABASE TO EVALUATE ACCELERATION (+Gz) INDUCED LOSS OF CONSCIOUSNESS (G-LOC) IN THE HUMAN CENTRIFUGE Final Report, Jun. 1992 - Jun. 1993
Estrella M. Forster 20 Jun. 1993 130 p Limited Reproducibility: More than 20% of this document may be affected by microfiche quality
(AD-A278769; NAWCADWAR-93089-60) Avail: Issuing Activity (Defense Technical Information Center (DTIC))

Pilots of high performance aircraft may be exposed to positive acceleration (+Gz). This type of acceleration displaces blood in the head to foot direction. As the pressure in the vessels of the lower body increases, the vessels dilate, and a major proportion of the blood from the upper part of the body is shifted into these lower vessels. The pooling of blood in the lower extremities translates into a reduced cardiac output provoking the cardiovascular system to maintain adequate blood flow to the central nervous system and thereby maintain normal brain function. The symptoms of acceleration stress may lead to +Gz induced loss of consciousness (G-LOC) with potential fatal consequences. According to a survey done in 1986, approximately 12% of the Navy aircrew have experienced G-LOC inflight. When G-LOC descriptive data is available, it is usually limited to the particular investigator's research interests. Most research regarding G-LOC does not include the symptoms typical of this event. Specifically, the subject's psychological reaction to the G-LOC episode itself is often ignored. Understanding the physiology and mechanism of G-LOC is necessary to develop methods to avoid such an event. However, until an infallible method to prevent G-LOC is developed, G-LOC will occur. Hence, the thrust of G-LOC research should include understanding recovery from unconsciousness: to include G-LOC's psychological sequelae. DTIC

N94-35712 Aerospace Medical Research Labs., Wright-Patterson AFB, OH. Crew Systems Directorate.
BIBLIOGRAPHY OF RESEARCH REPORTS AND PUBLICATIONS ISSUED BY THE HUMAN ENGINEERING DIVISION Technical Report, Jan. 1987 - Dec. 1993
Rebecca J. Green Mar. 1994 127 p Limited Reproducibility: More than 20% of this document may be affected by microfiche quality
(AD-A278787; AL/CF-SR-1994-0003) Avail: Issuing Activity (Defense Technical Information Center (DTIC))

This bibliography contains the titles, authors and publication/source information for the technical reports and articles published by the Human Engineering Division of Armstrong Laboratory between January 1987 and December 1993. The bibliography is divided into seven sections: (1) Alphabetical Index; (2) Human Capabilities & Limitations; (3) Design Aiding Technologies; (4) Advanced Displays, Controls & Computer Interfaces; (5) Crew System Integration, Test & Evaluation; (6) Modeling & Simulation; and (7) Chemical Defense. DTIC

N94-35716 Carnegie-Mellon Univ., Pittsburgh, PA. Dept. of Computer Science.
THE BREAKDOWN OF OPERATORS WHEN INTERACTING WITH THE EXTERNAL WORLD
Garrett A. Pelton and Jill F. Lehman Feb. 1994 40 p Limited Reproducibility: More than 20% of this document may be affected by microfiche quality
(AD-A278936; CMU-CS-94-121) Avail: Issuing Activity (Defense Technical Information Center (DTIC))

By looking at the simple task of tossing a bean bag from hand to hand, we show how the macro operator method breaks down when formulating agent models that interact with an uncertain external world. A macro operator encapsulates a plan to reach an objective. Occasionally the objective will be found to be unachievable, requiring the macro operator and its plan to be rejected. Letting the macro operator interact with the external world does not, by itself, change this situation but the fact that the results of the interaction are uncertain, and the agent's knowledge incomplete, does. The key idea is that the agent can't positively determine if progress towards the objective is being made in the external world, and thus errors will be made in rejecting a macro operator that would succeed. We show that there are a number of methods by which the agent can recover from such an operator rejection and continue toward the operator's objective. If we make operator rejection and recovery into a common mechanism, then the operators and the plans they represent will be split by the interaction into a sequence of smaller operators each doing a portion of the work toward the objective of the larger operator. The models are described in terms of Soar and we assume the reader's familiarity with both the architecture and the Problem Space Computational Model in our discussions. Author (DTIC)

N94-35633*# Cincinnati Univ., OH. Dept. of Aerospace Engineering.
SELF-RESCUE STRATEGIES FOR EVA CREWMEMBERS EQUIPPED WITH THE SAFER BACKPACK
Trevor Williams and David Baughman *In* NASA. Goddard Space Flight Center, Flight Mechanics/Estimation Theory Symposium, 1994 May 1994 p 357-371 (For primary document see N94-35605 11-13)
Avail: CASI HC A03/MF A04

N94-36336# Netherlands Aerospace Medical Centre, Soesterberg. Research Dept.
REVIEW OF HUMAN FACTORS PROBLEMS RELATED TO LONG DISTANCE AND LONG ENDURANCE OPERATION OF AIRCRAFT
Ries M. Simons and Pierre J. L. Valk *In* AGARD, Recent Advances in Long Range and Long Endurance Operation of Aircraft Nov. 1993 9 p (For primary document see N94-36321 11-05)
Copyright Avail: CASI HC A02/MF A03

55 SPACE BIOLOGY

Includes exobiology; planetary biology; and extraterrestrial life.

No abstracts in this category.

59 MATHEMATICAL AND COMPUTER SCIENCES (GENERAL)

N94-35393*# National Aeronautics and Space Administration. Ames Research Center, Moffett Field, CA.
THREE-DIMENSIONAL UNSTRUCTURED GRID REFINEMENT AND OPTIMIZATION USING EDGE-SWAPPING
Amar Gandhi and Timothy Barth Mar. 1993 32 p
(RTOP 505-10-11)
(NASA-TM-103966; A-92169; NAS 1.15:103966) Avail: CASI HC A03/MF A01

This paper presents a three-dimensional (3-D) 'edge-swapping method based on local transformations. This method extends Lawson's edge-swapping algorithm into 3-D. The 3-D edge-swapping algorithm is employed for the purpose of refining and optimizing unstructured meshes according to arbitrary mesh-quality measures. Several criteria including Delaunay triangulations are examined. Extensions from two to three dimensions of several known properties of Delaunay triangulations are also discussed. Author (revised)

60 COMPUTER OPERATIONS AND HARDWARE

Includes hardware for computer graphics, firmware, and data processing.

For components see *33 Electronics and Electrical Engineering.*

N94-35570 Bhabha Atomic Research Centre, Bombay (India).
GUIDELINES FOR DESIGN AND DEVELOPMENT OF COMPUTER/MICROPROCESSOR BASED SYSTEMS IN RESEARCH AND POWER REACTORS
S. D. Dhodapkar and A. K. Chandra 1993 46 p Limited Reproducibility: More than 20% of this document may be affected by microfiche quality
(DE94-616271; BARC-1993/E/023) Avail: CASI HC A03 (US Sales Only)

Computer systems are being used in Indian research reactors and nuclear power plants in the areas of data acquisition, process monitoring and control, alarm annunciation and safety. The design and evaluation of these systems requires a special approach particularly due to the unique nature of the software which is an essential constituent of these systems. It was decided to evolve guidelines for designing and review of computer/microprocessor based systems for use in nuclear power plants in India. The present document tries to address various issues and presents guidelines which are as comprehensive as possible and cover all issues relating to the design and development of computer based systems. These guidelines are expected to be useful to the specifiers, designers and reviewers of such systems. DOE

N94-35652 University of Southern California, Marina del Rey, CA. Information Sciences Inst.
THE IMPACT OF SCALING ON A MULTIMEDIA CONNECTION ARCHITECTURE
Eve M. Schooler Aug. 1993 12 p Limited Reproducibility: More than 20% of this document may be affected by microfiche quality
(Contract DABT63-91-C-0001)
(AD-A278700; ISI/RS-93-360) Avail: Issuing Activity (Defense Technical Information Center (DTIC))

As the last two meetings of the Internet Engineering Task Force (IETF) have shown, the demand for Internet teleconferencing has arrived. Packet audio and video have now been multicast to approximately 170 different hosts in 10 countries, and for upcoming meetings the number of remote participants is likely to be substantially larger. Yet the network infrastructure to support wide scale packet teleconferencing is not in place. These experiments represent a departure from the two to ten-site tele-meetings that are the norm today. They represent an increase in scale of multiple orders of magnitude in several interrelated dimensions. This paper discusses the impact of scaling on our efforts to define a multimedia teleconferencing architecture. Three scaling dimensions of particular interest include the following: (1) very large numbers of participants per conference, (2) many simultaneous teleconferences, and (3) a widely dispersed user population. Here we present a strawman architecture and describe how conference-specific information is captured, then conveyed among end systems. We provide a comparison of connection models and outline the tradeoffs and requirements that change as we travel along each dimension of scale. In conclusion, we identify five critical needs for a scalable teleconferencing architecture. DTIC

61 COMPUTER PROGRAMMING AND SOFTWARE

Includes computer programs, routines, alogorithms, and specific applications, e.g., CAD/CAM.

N94-35238*# National Aeronautics and Space Administration. Goddard Space Flight Center, Greenbelt, MD.
ANNOTATED BIBLIOGRAPHY OF SOFTWARE ENGINEERING LABORATORY LITERATURE
Linda Morusiewicz (Computer Sciences Corp., Greenbelt, MD.) and Jon Valett Nov. 1993 273 p
(RTOP 552-00-00)
(NASA-CR-189350; SEL-82-1206; NAS 1.26:189350) Avail: CASI HC A12/MF A03

This document is an annotated bibliography of technical papers, documents, and memorandums produced by or related to the Software Engineering Laboratory. Nearly 200 publications are summarized. These publications cover many areas of software engineering and range from research reports to software documentation. This document has been updated and reorganized substantially since the original version (SEL-82-006, November 1982). All materials have been grouped into eight general subject areas for easy reference: the Software Engineering Laboratory; the Software Engineering Laboratory: software development documents; software tools; software models; software measurement; technology evaluations; Ada technology; and data collection. This document contains an index of these publications classified by individual author. Author

N94-35240*# Institute for Computer Applications in Science and Engineering, Hampton, VA.
RUNTIME SUPPORT FOR DATA PARALLEL TASKS Final Report
Matthew Haines, Bryan Hess, Piyush Mehrotra, John VanRosendale, and Hans Zima Apr. 1994 23 p Submitted for publication
(Contract NAS1-19480; RTOP 505-90-52-01)
(NASA-CR-194904; NAS 1.26:194904; ICASE-94-26) Avail: CASI HC A03/MF A01

We have recently introduced a set of Fortran language extensions that allow for integrated support of task and data parallelism, and provide for shared data abstractions (SDA's) as a method for communications and synchronization among these tasks. In this paper we discuss the design and implementation issues of the runtime system necessary to support these extensions, and discuss the underlying requirements for such a system. To test the feasibility of this approach, we implement a prototype of the runtime system and use this to support an abstract multidisciplinary optimization (MDO) problem for aircraft design. We give initial results and discuss future plans. Author

N94-35256*# National Aeronautics and Space Administration. Goddard Space Flight Center, Greenbelt, MD.
COST AND SCHEDULE ESTIMATION STUDY REPORT
Steve Condon (Computer Sciences Corp., Greenbelt, MD.), Myrna Regardie (Computer Sciences Corp., Greenbelt, MD.), Mike Stark, and Sharon Waligora Nov. 1993 133 p
(RTOP 552-00-00)
(NASA-CR-189344; SEL-93-002; NAS 1.26:189344) Avail: CASI HC A07/MF A02

This report describes the analysis performed and the findings of a study of the software development cost and schedule estimation models used by the Flight Dynamics Division (FDD), Goddard Space Flight Center. The study analyzes typical FDD projects, focusing primarily on those developed since 1982. The study reconfirms the standard SEL effort estimation model that is based on size adjusted for reuse; however, guidelines for the productivity and growth parameters in the baseline effort model have been updated. The study also produced a schedule prediction model based on empirical data that varies depending on application type. Models for the distribution of effort and schedule by life-cycle phase are also presented. Finally, this report explains how to use these models to plan SEL projects. Author

N94-35365*# Cornell Univ., Ithaca, NY. Dept. of Computer Science.
THE WEAKEST FAILURE DETECTOR FOR SOLVING CONSENSUS

Tushar Deepak Chandra, Vassos Hadzilacos, and Sam Toueg Jul. 1992 44 p Sponsored in part by IBM Endicott Programming Lab.; and Siemens Corp.; and Natural Sciences and Engineering Research Council of Canada
(Grants NAG2-593; NSF CCR-89-01780; NSF CCR-91-02231)
(NASA-CR-190545; NAS 1.26:190545; CU-TR-92-1293; AD-A253611)
Avail: CASI HC A03/MF A01

We determine what information about failures is necessary and sufficient to solve Consensus in asynchronous distributed systems subject to crash failures. Previously, we proved that W, a failure detector that provides surprisingly little information about which processes have crashed, is sufficient to solve Consensus in asynchronous systems with a majority of correct processes. In this paper, we prove that to solve Consensus, any failure detector has to provide at least as much information as W. Thus, W is indeed the weakest failure detector for solving Consensus in asynchronous systems with a majority of correct processes. Author

N94-35434*# National Aeronautics and Space Administration. Goddard Space Flight Center, Greenbelt, MD.
COLLECTED SOFTWARE ENGINEERING PAPERS, VOLUME 11
Nov. 1993 99 p Prepared in cooperation with Maryland Univ., College Park and Computer Sciences Corp., Greenbelt, MD and Computer Sciences Corp., Greenbelt, MD
(RTOP 552-00-00)
(NASA-CR-189347; SEL-93-001; NAS 1.26:189347) Avail: CASI HC A05/MF A02

This document is a collection of selected technical papers produced by participants in the Software Engineering Laboratory (SEL) from November 1992 through November 1993. The purpose of the document is to make available, in one reference, some results of SEL research that originally appeared in a number of different forums. This is the 11th such volume of technical papers produced by the SEL. Although these papers cover several topics related to software engineering, they do not encompass the entire scope of SEL activities and interests. Additional information about the SEL and its research efforts may be obtained from the sources listed in the bibliography at the end of this document. For individual titles, see N94-35435 through N94-35439.

N94-35435*# Maryland Univ., College Park, MD. Inst. for Advanced Computer Studies.
DEVELOPING INTERPRETABLE MODELS WITH OPTIMIZED SET REDUCTION FOR IDENTIFYING HIGH RISK SOFTWARE COMPONENTS
Lionel C. Briand, Victor R. Basili, and Christopher J. Hetmanski *In* NASA. Goddard Space Flight Center, Collected Software Engineering Papers, Volume 11 Nov. 1993 31 p Sponsored in part by NSF (For primary document see N94-35434 11-61)
(Grant NsG-5123)
Avail: CASI HC A03/MF A02

Applying equal testing and verification effort to all parts of a software system is not very efficient, especially when resources are limited and scheduling is tight. Therefore, one needs to be able to differentiate low/high fault frequency components so that testing/verification effort can be concentrated where needed. Such a strategy is expected to detect more faults and thus improve the resulting reliability of the overall system. This paper presents the Optimized Set Reduction approach for constructing such models, intended to fulfill specific software engineering needs. Our approach to classification is to measure the software system and build multivariate stochastic models for predicting high risk system components. We present experimental results obtained by classifying Ada components into two classes: is or is not likely to generate faults during system and acceptance test. Also, we evaluate the accuracy of the model and the insights it provides into the error making process. Author

N94-35436*# Maryland Univ., College Park, MD. Dept. of Computer Science.
MODELING AND MANAGING RISK EARLY IN SOFTWARE DEVELOPMENT
Lionel C. Briand, William M. Thomas, and Christopher J. Hetmanski *In* NASA. Goddard Space Flight Center, Collected Software Engineering Papers, Volume 11 Nov. 1993 11 p (For primary document see N94-35434 11-61)
(Grant NsG-5123)
Avail: CASI HC A03/MF A02

In order to improve the quality of the software development process, we need to be able to build empirical multivariate models based on data collectable early in the software process. These models need to be both useful for prediction and easy to interpret, so that remedial actions may be taken in order to control and optimize the development process. We present an automated modeling technique which can be used as an alternative to regression techniques. We show how it can be used to facilitate the identification and aid the interpretation of the significant trends which characterize 'high risk' components in several Ada systems. Finally, we evaluate the effectiveness of our technique based on a comparison with logistic regression based models. Author

N94-35437*# Maryland Univ., College Park, MD. Dept. of Computer Science.
AN INFORMATION MODEL FOR USE IN SOFTWARE MANAGEMENT ESTIMATION AND PREDICTION
Ningda R. Li and Marvin V. Zelkowitz *In* NASA. Goddard Space Flight Center, Collected Software Engineering Papers, Volume 11 Nov. 1993 9 p Presented at the Second International Conference on Information Management, Arlington, VA, Nov. 1993 (For primary document see N94-35434 11-61)
(Grant NsG-5123)
Avail: CASI HC A02/MF A02

This paper describes the use of cluster analysis for determining the information model within collected software engineering development data at the NASA/GSFC Software Engineering Laboratory. We describe the Software Management Environment tool that allows managers to predict development attributes during early phases of a software project and the modifications we propose to allow it to develop dynamic models for better predictions of these attributes. Author

N94-35438*# Maryland Univ., College Park, MD. Dept. of Computer Science.
MEASURING AND ASSESSING MAINTAINABILITY AT THE END OF HIGH LEVEL DESIGN
Lionel C. Briand, Sandro Morasca, and Victor R. Basili *In* NASA. Goddard Space Flight Center, Collected Software Engineering Papers, Volume 11 Nov. 1993 11 p Sponsored in part by NSF (For primary document see N94-35434 11-61)
(Grant NsG-5123)
Avail: CASI HC A03/MF A02

Software architecture appears to be one of the main factors affecting software maintainability. Therefore, in order to be able to predict and assess maintainability early in the development process we need to be able to measure the high-level design characteristics that affect the change process. To this end, we propose a measurement approach, which is based on precise assumptions derived from the change process, which is based on Object-Oriented Design principles and is partially language independent. We define metrics for cohesion, coupling, and visibility in order to capture the difficulty of isolating, understanding, designing and validating changes. Author

N94-35439*# National Aeronautics and Space Administration. Goddard Space Flight Center, Greenbelt, MD.
IMPACTS OF OBJECT-ORIENTED TECHNOLOGIES: SEVEN YEARS OF SEL STUDIES
Mike Stark *In its* Collected Software Engineering Papers, Volume 11 Nov. 1993 9 p (For primary document see N94-35434 11-61)
Avail: CASI HC A02/MF A02

This paper examines the premise that object-oriented technology (OOT) is the most significant technology ever examined by the Software Engineering Laboratory. The evolution of the use of OOT in the Software Engineering Laboratory (SEL) 'Experience Factory' is described in terms of the SEL's original expectations, focusing on how successive generations of projects have used OOT. General conclusions are drawn on how the usage of the technology has evolved in this environment. Author

N94-35443*# CAE-Link Corp., Houston, TX. Integrated Training Facility.
SOFTWARE ARCHITECTURE STANDARD FOR SIMULATION VIRTUAL MACHINE, VERSION 2.0 Final Report
Robert Sturtevant and William Wessale 20 Apr. 1994 246 p

(Contract NAS9-18181)
(NASA-CR-188291; NAS 1.26:188291; SST-115) Avail: CASI HC A11/MF A03

The Simulation Virtual Machine (SBM) is an Ada architecture which eases the effort involved in the real-time software maintenance and sustaining engineering. The Software Architecture Standard defines the infrastructure which all the simulation models are built from. SVM was developed for and used in the Space Station Verification and Training Facility. Derived from text

N94-35490 Naval Research Lab., Washington, DC.

DEVELOPING SOFTWARE FOR EASE OF CHANGE: METRICS FROM LATER IN THE TRALAB SYSTEM LIFE CYCLE Interim Report

James A. Hager and Louis J. Chmura, Jr. 11 Apr. 1994 27 p Limited Reproducibility: More than 20% of this document may be affected by microfiche quality
(AD-A278759; NRL/MR/8140-94-7479) Avail: Issuing Activity (Defense Technical Information Center (DTIC))

This paper is a summary of software change and defect data collected during extended development and post-deployment software support (PDSS) for the Training Laboratory (TRALAB), which a computer-based training system developed starting in 1984 by the Naval Center for Space Technology (NCST) at the Naval Research Laboratory (NRL). Of note, the development contractor was required to apply software engineering technology developed previously at NRL as part of the Software Cost Reduction (SCR) project. Another important requirement was for the collection of project metric data that could be used to evaluate the effectiveness of the SCR approach. Data collection was accomplished by modifying customary project Software Problem Reports (SPR's). Analysis of the data collected on SPR resolution work during extended development integration and test (I&T) during Aug. 1988 through Apr. 1989 indicates that the application of SCR technology enhanced software ease of change. This paper is a continuation of the earlier analysis to include PDSS SPR data collected during Aug. 1990 through May 1991. The more recent analysis continues to suggest that identifying expected system changes during system definition stages and modularizing the system to encapsulate these changes yield life-cycle benefits. Modifications required by changes tend to be confined to a small number of design components, and it is easier to implement expected changes in comparison to arbitrary changes. DTIC

N94-35491 Naval Research Lab., Washington, DC.

A SOFTWARE ARCHITECTURE FOR ADDING NEW INTERACTION TECHNIQUES TO A COMMAND AND CONTROL BASED TESTBED Interim Report

James N. Templeman, Deborah Hix, and Robert J. Jacob 25 Mar. 1994 30 p Limited Reproducibility: More than 20% of this document may be affected by microfiche quality
(AD-A278760; NRL/MR/5530-94-7464) Avail: Issuing Activity (Defense Technical Information Center (DTIC))

The Human-Computer Interaction (HCI) Laboratory at the Naval Research Laboratory (NRL) is developing high-performance interactive computer systems for use in Naval command and control applications. New technology allows computerized systems to make greater use of a person's natural physical, perceptual, and cognitive skills. These systems make it faster and more straightforward for users to access and enter information within the context of time critical, real world situations. Our work focuses on developing novel interaction techniques--ways of using physical input and output devices to perform user tasks. Previous work has demonstrated the effectiveness of individual interaction techniques. This study is now being extended to encompass multi-modal interaction, in which combinations of interaction techniques are available to a user. We are incorporating these techniques into a command and control testbed that will be tested through empirical, user-based evaluation. Such new capabilities increase the complexity of software development and maintenance requirements of already complex systems. New software architectures must co-evolve with the technology to structure and manage these additional requirements. This report describes the new demands placed on interactive systems and explains how we am addressing this challenge, through development of a flexible software architecture. DTIC

N94-35495 Carnegie-Mellon Univ., Pittsburgh, PA. Software Engineering Inst.

EXPLORING HYPERMEDIA INFORMATION SERVICES FOR DISSEMINATING SOFTWARE ENGINEERING INFORMATION Final Report

William E. Hefley Feb. 1994 71 p Limited Reproducibility: More than 20% of this document may be affected by poor print and microfiche quality
(Contract F19628-90-C-0003)
(AD-A278765; CMU/SEI-94-TR-3; ESC-TR-94-003) Avail: CASI HC A04

This report describes the accomplishments of a pilot hypermedia information service embodying the conceptual definition of a pilot information base developed by the Software Engineering Institute (SEI) in support of the Advanced Research Projects Agency (ARPA) Software and Intelligent Systems Technology Offiçe (SISTO). This pilot effort was conducted in support of the Technology Cost-Benefit Analysis tasks within TO&P 2-151, Software Engineering Technology Transition for Director, Defense Research and Engineering (DDR&E) and ARPA. This report also describes the intended uses and user populations of the proposed information base, design issues that influenced the structure and contents of the information base, a proposed information model consisting of information content and linkages, the pilot information base including the technology selected for the initial pilot effort and the pilot capability, lessons learned from the pilot effort, and future plans relating to the information base efforts. DTIC

N94-35514*# Computer Software Management and Information Center, Athens, GA.

COSMIC MONTHLY PROGRESS REPORT

May 1994 44 p
(Contract NASw-4670)
(NASA-CR-195962; NAS 1.26:195962) Avail: CASI HC A03/MF A01

Activities of the Computer Software Management and Information Center (COSMIC) are summarized for the month of May 1994. Tables showing the current inventory of programs available from COSMIC are presented and program processing and evaluation activities are summarized. Nine articles were prepared for publication in the NASA Tech Brief Journal. These articles (included in this report) describe the following software items: (1) WFI - Windowing System for Test and Simulation; (2) HZETRN - A Free Space Radiation Transport and Shielding Program; (3) COMGEN-BEM - Composite Model Generation-Boundary Element Method; (4) IDDS - Interactive Data Display System; (5) CET93/PC - Chemical Equilibrium with Transport Properties, 1993; (6) SDVIC - Sub-pixel Digital Video Image Correlation; (7) TRASYS - Thermal Radiation Analyzer System (HP9000 Series 700/800 Version without NASADIG); (8) NASADIG - NASA Device Independent Graphics Library, Version 6.0 (VAX VMS Version); and (9) NASADIG - NASA Device Independent Graphics Library, Version 6.0 (UNIX Version). Activities in the areas of marketing, customer service, benefits identification, maintenance and support, and dissemination are also described along with a budget summary. CASI

N94-35538 Technische Univ., Twente (Netherlands). Dept. of Computer Science.

PROCEEDINGS OF THE 4TH WORKSHOP ON THE NEXT GENERATION OF CASE TOOLS

S. Brinkkemper and F. Harmsen May 1993 Workshop held in Paris, France, 7-8 Jun. 1993
(PB94-150372; Memo-INF-93-32) Avail: Issuing Activity (National Technical Information Service (NTIS))

The following topics are discussed: interoperable information systems; CASE-tools; software development; computer modelling; object-oriented methods; and domain modelling. NTIS

N94-35572 Carnegie-Mellon Univ., Pittsburgh, PA. Dept. of Computer Science.

SYMBOLIC DEBUGGING OF GLOBALLY OPTIMIZED CODE: DATA VALUE PROBLEMS AND THEIR SOLUTIONS

Ali-Reza Adl-Tabatabai and Thomas Gross Jan. 1994 21 p Limited Reproducibility: More than 20% of this document may be affected by microfiche quality
(Contract N00039-93-C-0152)
(AD-A278898; CMU-CS-94-105) Avail: CASI HC A03

Symbolic debuggers are program development tools that allow a user to interact with an executing process at the source level. In response to a user query, the debugger must be able to retrieve and display the value of a source variable in a manner consistent with what the user expects with respect to the source statement where execution has halted. However, when a program has been compiled with optimizations, values of variables may either be inaccessible in the run-time state or inconsistent with what the user expects. Such problems that pertain to the retrieval of source values are called data value problems. In this paper we address the data value problems caused by global scalar optimizations. We describe in detail how global optimizations cause data value problems and the information a symbolic debugger can provide a user when data value problems occur. We provide a data flow algorithm that detects the impact of two global transformations: code hoisting and dead code elimination. These two transformations capture the effects of global optimizations that cause data value problems. Common optimizations such as dead store elimination, common subexpression elimination, loop invariant code motion, partial redundancy elimination, or nonspeculative global instruction scheduling can be expressed in terms of these transformations. DTIC

N94-35573 Carnegie-Mellon Univ., Pittsburgh, PA. Dept. of Computer Science.

COMBINING SYMBOLIC COMPUTATION AND THEOREM PROVING: SOME PROBLEMS OF RAMANUJAN

Edmund Clarke and Xudong Zhao Jan. 1994 11 p Limited Reproducibility: More than 20% of this document may be affected by microfiche quality
(Contract F33615-90-C-1465; ARPA Order 7597)
(AD-A278899; CMU-CS-94-103) Avail: CASI HC A03

One way of building more powerful theorem provers is to use techniques from symbolic computation. The challenge problems in this paper are taken from chapter 2 of Ramanujan's Notebooks. They were selected because they are nontrivial and require the use of symbolic computation techniques. We have developed a theorem prover based on the symbolic computation system Mathematica that can prove all the challenge problems completely automatically. The axioms and inference rules for constructing the proofs are also briefly discussed. DTIC

N94-35574 Carnegie-Mellon Univ., Pittsburgh, PA. Dept. of Computer Science.

PRODIGY PLANNING ALGORITHM

Eugene Fink and Manuela Veloso Mar. 1994 14 p Limited Reproducibility: More than 20% of this document may be affected by microfiche quality
(Contract F33615-93-1-1330)
(AD-A278900; CMU-CS-94-123) Avail: Issuing Activity (Defense Technical Information Center (DTIC))

We present a formal description of the planning algorithm used in the Prodigy 4.0 system. The algorithm is based on an interesting combination of backward-chaining planning and simulation of plan execution. The backward-chainer selects goal-relevant operators, and then Prodigy simulates their application to the current state of the world. The system can use different backward-chaining procedures, some of which are presented. DTIC

N94-35576 Naval Postgraduate School, Monterey, CA. Dept. of Computer Science.

A LOWER BOUND FOR THE INTERSECTION OF REGULAR FORESTS Final Report, Oct. 1992 - Sep. 1993

Dennis M. Volpano 5 Oct. 1993 13 p Limited Reproducibility: More than 20% of this document may be affected by microfiche quality
(AD-A278653; NPS-CS-94-005) Avail: Issuing Activity (Defense Technical Information Center (DTIC))

Regular Sigma X-forests continue to play an important role in programming languages, specifically in the design of type systems. They arise naturally as terms of constructor-based, recursive data types in logic and functional languages. Deciding whether the intersection of a sequence of regular Sigma X-forests is nonempty is an important problem in type inference. We show that this problem is PSPACE-hard and as a corollary that the problem of constructing a regular Sigma X-grammar representing their intersection is PSPACE-hard. DTIC

N94-35577 Naval Postgraduate School, Monterey, CA. Dept. of Operations Research.

STOPPING RULES FOR A CLASS OF SAMPLING-BASED STOCHASTIC PROGRAMMING ALGORITHMS

David P. Morton Jan. 1994 28 p Limited Reproducibility: More than 20% of this document may be affected by microfiche quality
(AD-A278654; NPS-OR-94-003) Avail: Issuing Activity (Defense Technical Information Center (DTIC))

Decomposition and Monte Carlo sampling-based algorithms hold much promise for solving stochastic programs with many scenarios. A critical component of such algorithms is a stopping criterion to ensure the quality of the solution. In this paper, we develop a stopping rule theory for a class of algorithms that estimate bounds on the optimal objective function value by sampling. We provide rules for selecting sample sizes and terminating the algorithm under which asymptotic validity of confidence intervals for the quality of the proposed solution can be verified. These rules are applied to a multistage stochastic linear programming algorithm due to Pereira and Pinto. DTIC

N94-35602 Helsinki Univ. of Technology, Espoo (Finland). Dept. of Computer Science.

GENETIC ALGORITHMS [GENEETTISET ALGORITMIT]

J. T. Alander 1992 248 p In FINNISH
(PB94-171048; TKO-C53) Avail: Issuing Activity (National Technical Information Service (NTIS))

This volume is the outcome of a seminar on genetic algorithms held at Helsinki University of Technology in Fall 1991. The written reports of the seminar lectures are contained in this laboratory report. In addition, it includes two conference articles on the subject and some article reviews. The end of the report contains an annotated bibliography of genetic algorithms and related subjects. NTIS

N94-35660 Naval Command, Control and Ocean Surveillance Center, San Diego, CA. RDT and E Div.

ENVIRONMENT/TOOL INTEGRATOR FOR SOFTWARE DEVELOPMENT, VERSION 1.2 Final Report, Jul. - Dec. 1993

N. T. Tran and R. H. Mumm Jan. 1994 42 p Limited Reproducibility: More than 20% of this document may be affected by microfiche quality
(AD-A278965; NRAD-TR-1548-Rev-1) Avail: Issuing Activity (Defense Technical Information Center (DTIC))

This report describes the environment/tool integrator (ETI), version 1.2, that was developed under the Software Engineering Environment Prototypes (SWEEP) task of the Software Engineering for Command Control and Communications (C3) Systems project. The ETI is a windowing framework for accessing the diverse collections of software tools used by software development projects. It can easily be customized to satisfy the unique needs of specific projects. The ETI, version 1.2, executes on the following Unix-based computers: SPARC 1 (OS: SunOS 1.3), Silicon Graphics (OS: JRIX 4.05H), DEC Alpha (OS: OSF 1.3), IBM 6000 (OS: A1X2.3), and SPARC 10 (OS: SunOS 5.2). Tools accessed may reside on various workstations in a local area network (LAN). DTIC

N94-35662 University of Southern California, Marina del Rey, CA. Information Sciences Inst.

SYNTHESIS OF ASYNCHRONOUS SYSTEMS FROM DATA FLOW SPECIFICATIONS

Tzyh-Yung Wuu and Sarma B. Vrudhula Dec. 1993 74 p Limited Reproducibility: More than 20% of this document may be affected by microfiche quality
(Contract MDA903-92-D-0020)
(AD-A278687; ISI-RR-93-366) Avail: Issuing Activity (Defense Technical Information Center (DTIC))

This report presents a method for automatic synthesis of asynchronous digital systems from high-level data flow specifications. We present an extended data flow model that accurately reflects the behavior of the asynchronous components so that the data flow specification can be directly mapped into a hardware realization. In addition, we develop a timing model for the basic asynchronous building blocks and show how to derive the timing parameters of a composed systems. This timing model can also be used at the data flow level, allowing designers to explore various design alternatives. We then describe a number of applications of the data flow specification for high-level synthesis such as schemes for resource sharing local transformations for data flow description optimization, and allocation and sequencing of operations for given resources. Finally, we present two examples using this synthesis method. The effectiveness of the data flow specification and performance analysis has been demonstrated from the areas and the simulation of actual layouts generated using an industrial standard cell library and commercial CAD tools. DTIC

N94-35676 Naval Postgraduate School, Monterey, CA. Dept. of Computer Science.
A CRITIQUE OF TYPE SYSTEMS FOR GLOBAL OVERLOADING Final Report, Oct. 1991 - Sep. 1992
Dennis M. Volpano Jul. 1993 17 p Limited Reproducibility: More than 20% of this document may be affected by microfiche quality
(AD-A278800; NPS-CS-94-006) Avail: Issuing Activity (Defense Technical Information Center (DTIC))

Proposed extensions of the ML type system to incorporate global overloading include the systems of Kae88, CD091, Smi9l, Kae92, Jon92, and those related to the design of the functional programming language Haskell WaB89, CH092, and niP93. These systems have in common the notion of a constrained type scheme which in some is realized by type kinds and in others as explicit predicates. An analysis of these type systems reveals that some are unsound with regard to a suitable criterion for typability and some adopt a notion of type generality that is inconsistent with that of system ML DaM82. DTIC

N94-35709 Carnegie-Mellon Univ., Pittsburgh, PA. Dept. of Computer Science.
REFINEMENT TYPES ML Ph.D. Thesis
Tim Freeman 16 Mar. 1994 330 p Limited Reproducibility: More than 20% of this document may be affected by microfiche quality
(Contract F19628-91-C-0168; ARPA Order 8313)
(AD-A278937; CMU-CS-94-110) Avail: Issuing Activity (Defense Technical Information Center (DTIC))

Programming computers is a notoriously error-prone process. It is the job of the programming language designer to make this process more reliable. One approach to this is to impose some sort of typing discipline on the programs. In doing this, the programming language designer is immediately faced with a tradeoff: if the type system is too simple, it cannot accurately express important properties of the program; if it is too expressive, then mechanically checking or inferring the types becomes impractical. This thesis describes a type system called refinement types, which is an example of a new way to make this tradeoff, as well as a potentially useful system in itself. Refinement type inference requires programs to have types in two type systems: an expressive type inference system (intersection types with subtyping) and a relatively simple type system (basic polymorphic type inference). Refinement type inference inherits some properties from each of these: as in intersection types with subtyping, we can use the type system to do abstract interpretation; as in basic polymorphic type inference, refinement type inference is decidable (preliminary experiments suggest refinement type inference may be practical as well). We have implemented refinement type inference for a subset of Standard ML to test these ideas. We have added new syntax, called retype declarations, to allow the programmer to specify relevant domains for the abstract interpretation. DTIC

N94-35718 Carnegie-Mellon Univ., Pittsburgh, PA. Dept. of Computer Science.
ML PARTIAL EVALUATION USING SET-BASED ANALYSIS
Karoline Malmkjaer, Nevin Heintze, and Oliver Danvy Feb. 1994 13 p Limited Reproducibility: More than 20% of this document may be affected by microfiche quality
(Contract F19628-91-C-0168; ARPA Order 8313)
(AD-A278955; CMU-CS-94-129) Avail: Issuing Activity (Defense Technical Information Center (DTIC))

We describe the design and implementation of an off-line partial evaluator for Standard ML programs. Our partial evaluator consists of two phases: analysis and specialization. Set-based analysis is used to compute control flow, data flow, and binding-time information. It provides a combination of speed and accuracy that is well suited to partial-evaluation applications: the analysis proceeds at a few hundred lines per second and is able to deal with higher-order functions, partially-static values, arithmetic, side effects, and control effects. To treat the rich static information supplied by set-based analysis, continuation-based specialization is used in conjunction with a notion of lightweight symbolic values. The specializer adapts and improves upon the proven design principles of off-line polyvariant partial evaluators. Our system is integrated into the New Jersey compiler for Standard ML: both input and output languages are the compiler's intermediate language LAMBDA. As such, our ML partial evaluator is not a source-ML to source-ML program transformer and issues of desugaring and type checking are avoided. The core part of our implementation, handling higher-order programs with partially-static values, is complete. We are currently working on extensions of the specializer to treat computational effects. DTIC

N94-35740# National Inst. of Standards and Technology, Gaithersburg, MD. Factory Automation Systems Div.
CONCEPT FOR AN ALGORITHM TESTING AND EVALUATION PROGRAM AT NIST
C. Diaz Jan. 1994 14 p See also PB90-148362
(PB94-163029; NISTIR-5366) Avail: CASI HC A03/MF A01

This report proposes a National Institute of Standards and Technology (NIST) service for testing and evaluating coordinate measuring systems (CMS) software. This program addresses industry's need for a formal mechanism that tests data analysis software used in CMSs. The NIST Algorithm Testing and Evaluation Program (ATEP) combines the NIST Algorithm Testing System (ATS) test procedures based on emerging national standards, and control over the ATS reference algorithms This report presents a concept for this formal mechanism to provide testing methods and tools to test and evaluate CMS data analysis software. NTIS

N94-35794 Carnegie-Mellon Univ., Pittsburgh, PA. Software Engineering Inst.
A TAXONOMY OF COORDINATION MECHANISMS USED IN REAL-TIME SOFTWARE BASED ON DOMAIN ANALYSIS Final Report
Jose L. Fernandez Dec. 1993 54 p Limited Reproducibility: More than 20% of this document may be affected by microfiche quality
(Contract F19628-90-C-0003)
(AD-A279014; CMU/SEI-93-TR-34; ESC-TR-93-321) Avail: Issuing Activity (Defense Technical Information Center (DTIC))

A taxonomy of the coordination mechanisms for the synchronization and communication of concurrent processes is proposed. The taxonomy deals with the issues of a real-time software architecture that are application domain independent. The taxonomy will help the designer to find the appropriate coordination mechanisms for building a real-time domain specific software architecture. Features oriented domain analysis methodology has been used to describe the taxonomy. While Ada is the programming language that has been used here, some of the attributes and guidelines are still valid for other programming languages. DTIC

N94-35808# Los Alamos National Lab., NM.
AN OBJECT-ORIENTED IMPLEMENTATION OF A GRAPHICAL-PROGRAMMING SYSTEM
G. S. Cunningham, K. M. Hanson, G. R. Jennings, Jr., and D. R. Wolf 1994 10 p Presented at the Society of Photovoltaic Instrumentation Engineers Medical Imaging Conference, Newport Beach, CA, 13-18 Feb. 1994
(Contract W-7405-eng-36)
(DE94-009298; LA-UR-94-759; CONF-940254-2) Avail: CASI HC A02/MF A01

Object-oriented (OO) analysis, design, and programming is a powerful paradigm for creating software that is easily understood, modified, and maintained. In this paper the authors demonstrate how the OO concepts of abstraction, inheritance, encapsulation, polymorphism, and dynamic binding have aided in the design of a graphical-programming tool. The tool that they have developed allows a user to build radiographic system models for computing simulated radiographic data. It will eventually be used to perform Bayesian reconstructions of objects given radiographic data. The models are built by connecting icons that represent physical transformations, such as line integrals, exponentiation, and convolution, on a canvas. They will also briefly discuss ParcPlace's application development environment, VisualWorks, which they have found to be as helpful as the OO paradigm. DOE

N94-35834# Korean Atomic Energy Research Inst., Daeduk (Republic of Korea).

ONED90: 1-DIMENSIONAL DIFFUSION CODE

Sung Kyun Zee, Jong Hwa Chang, Si Yong Kim, Sang Hoon Lee, Ki Bog Lee, and Jae Man Noh Jun. 1993 109 p
(DE94-611063; KAERI/TR-353/93) Avail: CASI HC A06/MF A02 (US Sales Only)

The validity of ONED90 (1-Dimensional 2-Group Diffusion Code) for nuclear design and plant reactor simulation has been confirmed through comparisons of some calculational results from ONED90 with current design values and measured data. Main methodology of ONED90 including user's manual has been described in detail. DOE

N94-35940 National Inst. of Standards and Technology, Gaithersburg, MD. Advanced Systems Div.

NORTH AMERICAN ISDN USERS' FORUM AGREEMENTS ON INTEGRATED SERVICES DIGITAL NETWORK Final Report

D. P. Stokesberry and T. A. Antonishek Mar. 1994 354 p See also PB93-173391 Limited Reproducibility: More than 20% of this document may be affected by microfiche quality
(PB94-162559; NIST/SP-823/5) Avail: CASI HC A16; SOD HC

This document compiles the existing North American Integrated Services Digital Network (ISDN) Users' Forum (NIUF) agreements for an ISDN developed and approved in the NIUF as of October 1992. New agreements superseded or added during 1992 cover Layer 1 BRI at the U, and S/T reference points. In addition, this document references the Conformance tests which have been completed by the NIUF. These include: Layer 3 BRI, Layer 2 BRI, PRI at the U reference point and PRI at the U/S/T reference points. Finally, this document contains the Application Profiles for Secure Voice Mail; Data Conferencing--Multi-Point; ISDN Telephone Workstation Integration; Engineering Workstation Interface; and the Remote Agent Application Profile. NTIS

N94-35958# Naval Surface Warfare Center, Dahlgren, VA. Weapons Systems Dept.

USER'S GUIDE FOR AN INTERACTIVE PERSONAL COMPUTER INTERFACE FOR THE AEROPREDICTION CODE

Thomas C. Hymer, Frank G. Moore, and Cornell Downs Jun. 1994 101 p
(NSWCDD/TR-94/107) Avail: CASI HC A06/MF A02

This report describes interactive, user-friendly, preprocessing and post-processing PC modules designed to operate with the latest version of the NSWC Aeroprediction Code (AP93). As part of the preprocessing input module, geometry inputs are now automated by giving the user many options. By using this new software, a set of aerodynamic coefficients can be obtained on most weapon configurations in less than 15 minutes from time of initial setup to computer outputs, compared to 2 to 4 hours for the AP93 computer mainframe version. While the computer cost savings are modest (the AP93 executes on a large computer in less than a second), the manpower savings and productivity enhancements can be significant. The user's guide attempts to aid users of the AP93 by correlating AP93 PC interface data inputs and the corresponding source code variable names. This cross-referencing information is given in italics in the discussion. Author (revised)

N94-36006 Carnegie-Mellon Univ., Pittsburgh, PA. Robotics Inst.

CASE BASED REASONING IN ENGINEERING DESIGN Final Report, 1 Oct. 1989 - 30 Jun. 1993

K. Sycara 30 Jun. 1993 134 p Limited Reproducibility: More than 20% of this document may be affected by microfiche quality
(Contract F49620-90-C-0003)
(AD-A278943; AFOSR-94-0280TR) Avail: Issuing Activity (Defense Technical Information Center (DTIC))

Case-based problem solving is based on the idea that problem solving should reuse solutions and other information from previously solved problems instead of relying solely on a base of procedures or rules. The researchers presented a case-based design system, CADET, that retrieves and reuses previous successful designs while avoiding previous failures such as poor materials or high cost. The system uses certain behavior-preserving transformation techniques to transform an abstract description of the desired behavior of the device into a description that can be used to find relevant designs in memory. This approach, in effect, decomposes given behavior specifications into 'sub-behaviors,' making it possible to recognize parts of previous designs that can be synthesized to form a new device. Currently, the system can perform conceptual design of mechanical devices that exhibit continuous and reciprocating behavior. In addition, since CADET can generate a wide variety of behaviorally equivalent alternative designs for a given set of design specifications, it can be used as a designer's brainstorming assistant. DTIC

N94-36010 National Inst. of Standards and Technology, Gaithersburg, MD. Applied and Computational Mathematics Div.

REVIEW OF MATHEMATICAL FUNCTION LIBRARY FOR MICROSOFT-FORTRAN, JOHN WILEY AND SONS, 1989 Final Report

D. W. Lozier and F. W. J. Olver Dec. 1990 16 p Limited Reproducibility: More than 20% of this document may be affected by microfiche quality
(PB94-160793; NISTIR-4490) Avail: Issuing Activity (National Technical Information Service (NTIS))

The loose-leaf manual and accompanying diskettes under review, which shall be referred to as the 'UL Library,' may be regarded as an attempt to replace the numerical tables of the higher transcendental functions supplied in the NBS Handbook by a comprehensive software package. The functions treated include Bessel and related functions, hypergeometric and confluent hypergeometric functions, elliptic functions and integrals, exponential integral and related functions, error function and related functions, Gamma and incomplete Gamma functions, orthogonal polynomials, probability functions, and random number generators. NTIS

N94-36013 Naval Postgraduate School, Monterey, CA. Dept. of Operations Research.

OBJECT-ORIENTED SIMULATION PICTURES (OOSPic) FOR DESIGN AND TESTING

Michael P. Bailey Feb. 1994 14 p Limited Reproducibility: More than 20% of this document may be affected by microfiche quality
(AD-A278798; NPS-OR-94-006) Avail: Issuing Activity (Defense Technical Information Center (DTIC))

A diagramming technique called Object-Oriented Simulation Pictures (OOSPic) is presented. Using this technique, a simulation designer can show the relationships and interactions between object types. OOSPics also promote extensive bottom-up object testing. Finally, if a complete OOSPic is constructed before coding begins, a reliable model can be constructed directly. DTIC

N94-36014 Cornell Univ., Ithaca, NY. Dept. of Computer Science.

THE MOST ABSTRACT COMMON REFINEMENT Interim Report

Limor Fix and Thomas A. Henzinger 4 Feb. 1994 17 p Limited Reproducibility: More than 20% of this document may be affected by microfiche quality
(Contracts N00014-91-J-1219; F49620-93-1-0056; NSF CCR-90-14363; NSF CCR-87-01103; NSF CCR-92-00794)
(AD-A278870) Avail: CASI HC A03

We introduce a novel binary operation on specifications. The most abstract common refinement (MACR) of two specifications P1 and P2 is the most abstract specification that refines both P1 and P2. We define the MACR of omega-automata and of linear temporal formulae. The MACR operation supports a two-dimensional system design process that combines structural decomposition with stepwise refinement. As an example, we design and verify a watch in several steps, each of which simultaneously integrates and refines two partial specifications of the watch. DTIC

N94-36017 Lawrence Livermore National Lab., CA.

COMBINING NONLINEAR MULTIRESOLUTION SYSTEM AND VECTOR QUANTIZATION FOR STILL IMAGE COMPRESSION

Y. Wong 17 Dec. 1993 12 p Presented at the IS and T Society of Photo-Optical Instrumentation Engineers Meeting on Electronic Imaging Science and Technology, San Jose, CA, 6-10 Feb. 1994 Limited Reproducibility: More than 20% of this document may be affected by microfiche quality
(Contract W-7405-eng-48)
(DE94-009422; UCRL-JC-115838; CONF-940247-3) Avail: Issuing Activity (Department of Energy (DOE))

It is popular to use multiresolution systems for image coding and compression. However, general-purpose techniques such as filter banks and wavelets are linear. While these systems are rigorous, nonlinear features in the signals cannot be utilized in a single entity for compression. Linear filters are known to blur the edges. Thus, the low-resolution images are typically blurred, carrying little information. We propose and demonstrate that edge-preserving filters such as median filters can be used in generating a multiresolution system using the Laplacian pyramid. The signals in the detail images are small and localized to the edge areas. Principal component vector quantization (PCVQ) is used to encode the detail images. PCVQ is a tree-structured VQ which allows fast codebook design and encoding/decoding. In encoding, the quantization error at each level is fed back through the pyramid to the previous level so that ultimately all the error is confined to the first level. With simple coding methods, we demonstrate that images with PSNR 33 dB can be obtained at 0.66 bpp without the use of entropy coding. When the rate is decreased to 0.25 bpp, the PSNR of 30 dB can still be achieved. Combined with an earlier result, our work demonstrates that nonlinear filters can be used for multiresolution systems and image coding. DOE

N94-36040*# Humboldt State Univ., Arcata, CA. Dept. of Computer Information Systems.
[REPRESENTING SPATIAL INFORMATION IN A COMPUTATIONAL MODEL FOR NETWORK MANAGEMENT] Final Report
James H. Blaisdell and Thomas F. Brownfield 16 May 1994 146 p
(Contract NCC2-700)
(NASA-CR-191669; NAS 1.26:191669) Avail: CASI HC A07/MF A02

While currently available relational database management systems (RDBMS) allow inclusion of spatial information in a data model, they lack tools for presenting this information in an easily comprehensible form. Computer-aided design (CAD) software packages provide adequate functions to produce drawings, but still require manual placement of symbols and features. This project has demonstrated a bridge between the data model of an RDBMS and the graphic display of a CAD system. It is shown that the CAD system can be used to control the selection of data with spatial components from the database and then quickly plot that data on a map display. It is shown that the CAD system can be used to extract data from a drawing and then control the insertion of that data into the database. These demonstrations were successful in a test environment that incorporated many features of known working environments, suggesting that the techniques developed could be adapted for practical use. CASI

N94-36063*# Johns Hopkins Univ., Baltimore, MD. Dept. of Computer Science.
TRANSIENT FAULTS IN COMPUTER SYSTEMS Final Report
Gerald M. Masson 21 Dec. 1993 188 p
(Grant NsG-1442)
(NASA-CR-194717; NAS 1.26:194717) Copyright Avail: CASI HC A09/MF A02

A powerful technique particularly appropriate for the detection of errors caused by transient faults in computer systems was developed. The technique can be implemented in either software or hardware; the research conducted thus far primarily considered software implementations. The error detection technique developed has the distinct advantage of having provably complete coverage of all errors caused by transient faults that affect the output produced by the execution of a program. In other words, the technique does not have to be tuned to a particular error model to enhance error coverage. Also, the correctness of the technique can be formally verified. The technique uses time and software redundancy. The foundation for an effective, low-overhead, software-based certification trail approach to real-time error detection resulting from transient fault phenomena was developed. For individual titles, see N94-36064 through N94-36069.

N94-36064*# Johns Hopkins Univ., Baltimore, MD. Dept. of Computer Science.
CERTIFICATION OF COMPUTATIONAL RESULTS
Gregory F. Sullivan, Dwight S. Wilson, and Gerald M. Masson *In its* Transient Faults in Computer Systems 21 Dec. 1993 27 p (For primary document see N94-36063 11-61)
(Grants NSF CCR-89-10569; NSF CCR-89-08092; NSF CDA-90-15667)
Avail: CASI HC A03/MF A02

A conceptually novel and powerful technique to achieve fault detection and fault tolerance in hardware and software systems is described. When used for software fault detection, this new technique uses time and software redundancy and can be outlined as follows. In the initial phase, a program is run to solve a problem and store the result. In addition, this program leaves behind a trail of data called a certification trail. In the second phase, another program is run which solves the original problem again. This program, however, has access to the certification trail left by the first program. Because of the availability of the certification trail, the second phase can be performed by a less complex program and can execute more quickly. In the final phase, the two results are compared and if they agree the results are accepted as correct; otherwise an error is indicated. An essential aspect of this approach is that the second program must always generate either an error indication or a correct output even when the certification trail it receives from the first program is incorrect. The certification trail approach to fault tolerance is formalized and realizations of it are illustrated by considering algorithms for the following problems: convex hull, sorting, and shortest path. Cases in which the second phase can be run concurrently with the first and act as a monitor are discussed. The certification trail approach are compared to other approaches to fault tolerance. Author (revised)

N94-36065*# Johns Hopkins Univ., Baltimore, MD. Dept. of Computer Science.
EXPERIMENTAL EVALUATION OF THE CERTIFICATION-TRAIL METHOD
Gregory F. Sullivan, Dwight S. Wilson, Gerald M. Masson, Mamoru Itoh, Warren W. Smith, and Jonathan S. Kay *In its* Transient Faults in Computer Systems 21 Dec. 1993 100 p Sponsored in part by an IBM Technology Interchange grant (For primary document see N94-36063 11-61)
(Grants NSF CCR-89-10569; NSF CCR-89-08092)
Avail: CASI HC A05/MF A02

Certification trails are a recently introduced and promising approach to fault-detection and fault-tolerance. A comprehensive attempt to assess experimentally the performance and overall value of the method is reported. The method is applied to algorithms for the following problems: huffman tree, shortest path, minimum spanning tree, sorting, and convex hull. Our results reveal many cases in which an approach using certification-trails allows for significantly faster overall program execution time than a basic time redundancy-approach. Algorithms for the answer-validation problem for abstract data types were also examined. This kind of problem provides a basis for applying the certification-trail method to wide classes of algorithms. Answer-validation solutions for two types of priority queues were implemented and analyzed. In both cases, the algorithm which performs answer-validation is substantially faster than the original algorithm for computing the answer. Next, a probabilistic model and analysis which enables comparison between the certification-trail method and the time-redundancy approach were presented. The analysis reveals some substantial and sometimes surprising advantages for ther certification-trail method. Finally, the work our group performed on the design and implementation of fault injection testbeds for experimental analysis of the certification trail technique is discussed. This work employs two distinct methodologies, software fault injection (modification of instruction, data, and stack segments of programs on a Sun Sparcstation ELC and on an IBM 386 PC) and hardware fault injection (control, address, and data lines of a Motorola MC68000-based target system pulsed at logical zero/one values). Our results indicate the viability of the certification trail technique. It is also believed that the tools developed provide a solid base for additional exploration. Author (revised)

N94-36066*# Johns Hopkins Univ., Baltimore, MD. Dept. of Computer Science.
CERTIFICATION TRAILS AND SOFTWARE DESIGN FOR TESTABILITY
Gregory F. Sullivan, Dwight S. Wilson, and Gerald M. Masson *In its* Transient Faults in Computer Systems 21 Dec. 1993 10 p Sponsored in part by IBM Technology Interchange Program grant (For primary document see N94-36063 11-61)
(Grants NSF CCR-89-10569; NSF CCR-89-08092)
Avail: CASI HC A02/MF A02

Design techniques which may be applied to make program testing easier were investigated. Methods for modifying a program to generate additional data which we refer to as a certification trail are presented. This additional data is designed to allow the program output to be checked more quickly and effectively. Certification trails were described primarily from a theoretical perspective. A comprehensive attempt to assess experimentally the performance and overall value of the certification trail method is reported. The method was applied to nine fundamental, well-known algorithms for the following problems: convex hull, sorting, huffman tree, shortest path, closest pair, line segment intersection, longest increasing subsequence, skyline, and voronoi diagram. Run-time performance data for each of these problems is given, and selected problems are described in more detail. Our results indicate that there are many cases in which certification trails allow for significantly faster overall program execution time than a 2-version programming approach, and also give further evidence of the breadth of applicability of this method. Author (revised)

N94-36067*# Johns Hopkins Univ., Baltimore, MD. Dept. of Computer Science.

EXPERIMENTAL EVALUATION OF CERTIFICATION TRAILS USING ABSTRACT DATA TYPE VALIDATION

Dwight S. Wilson, Gregory F. Sullivan, and Gerald M. Masson *In its* Transient Faults in Computer Systems 21 Dec. 1993 6 p Sponsored in part by IBM Technology Interchange Program grant (For primary document see N94-36063 11-61)
(Grants NSF CCR-89-10569; NSF CCR-89-08092)
Avail: CASI HC A02/MF A02

Certification trails are a recently introduced and promising approach to fault-detection and fault-tolerance. Recent experimental work reveals many cases in which a certification-trail approach allows for significantly faster program execution time than a basic time-redundancy approach. Algorithms for answer-validation of abstract data types allow a certification trail approach to be used for a wide variety of problems. An attempt to assess the performance of algorithms utilizing certification trails on abstract data types is reported. Specifically, this method was applied to the following problems: heapsort, Hullman tree, shortest path, and skyline. Previous results used certification trails specific to a particular problem and implementation. The approach allows certification trails to be localized to 'data structure modules,' making the use of this technique transparent to the user of such modules. Author (revised)

N94-36068*# Johns Hopkins Univ., Baltimore, MD. Dept. of Computer Science.

USING CERTIFICATION TRAILS TO ACHIEVE SOFTWARE FAULT TOLERANCE

Gregory F. Sullivan and Gerald M. Masson *In its* Transient Faults in Computer Systems 21 Dec. 1993 9 p (For primary document see N94-36063 11-61)
(Grants NSF CCR-89-10569; NSF CCR-89-08092)
Avail: CASI HC A02/MF A02

A conceptually novel and powerful technique to achieve fault tolerance in hardware and software systems is introduced. When used for software fault tolerance, this new technique uses time and software redundancy and can be outlined as follows. In the initial phase, a program is run to solve a problem and store the result. In addition, this program leaves behind a trail of data called a certification trail. In the second phase, another program is run which solves the original problem again. This program, however, has access to the certification trail left by the first program. Because of the availability of the certification trail, the second phase can be performed by a less complex program and can execute more quickly. In the final phase, the two results are accepted as correct; otherwise an error is indicated. An essential aspect of this approach is that the second program must always generate either an error indication or a correct output even when the certification trail it receives from the first program is incorrect. The certification trail approach to fault tolerance was formalized and it was illustrated by applying it to the fundamental problem of finding a minimum spanning tree. Cases in which the second phase can be run concorectly with the first and act as a monitor are discussed. The certification trail approach was compared to other approaches to fault tolerance. Because of space limitations we have omitted examples of our technique applied to the Huffman tree, and convex hull problems. These can be found in the full version of this paper. Author (revised)

N94-36069*# Johns Hopkins Univ., Baltimore, MD. Dept. of Computer Science.

CERTIFICATION TRAILS FOR DATA STRUCTURES

Gregory F. Sullivan and Gerald M. Masson *In its* Transient Faults in Computer Systems 21 Dec. 1993 8 p (For primary document see N94-36063 11-61)
(Grants NSF CCR-89-10569; NSF CCR-89-08092)
Avail: CASI HC A02/MF A02

Certification trails are a recently introduced and promising approach to fault detection and fault tolerance. The applicability of the certification trail technique is significantly generalized. Previously, certification trails had to be customized to each algorithm application; trails appropriate to wide classes of algorithms were developed. These certification trails are based on common data-structure operations such as those carried out using these sets of operations such as those carried out using balanced binary trees and heaps. Any algorithms using these sets of operations can therefore employ the certification trail method to achieve software fault tolerance. To exemplify the scope of the generalization of the certification trail technique provided, constructions of trails for abstract data types such as priority queues and union-find structures are given. These trails are applicable to any data-structure implementation of the abstract data type. It is also shown that these ideals lead naturally to monitors for data-structure operations. Author (revised)

N94-36113# Defence Research Agency, Malvern (England).

EXECUTABLE TRANSFORMATIONAL RULES FROM CORE ELLA TO THE KERNEL

M. G. Hill and J. D. Morison Jul. 1992 67 p
(DRA-Memo-4629) Copyright Avail: CASI HC A04/MF A01

This document describes the set of formal transformation rules which have been implemented for mapping Core ELLA into Kernel data structures. Examples are given of circuits which have been transformed by the implementation. Author

N94-36118*# Smithsonian Astrophysical Observatory, Cambridge, MA.

TRANSFIT: FINITE ELEMENT ANALYSIS DATA FITTING SOFTWARE Interim Report

Mark Freeman 29 Sep. 1993 38 p
(Contract NAS8-36123)
(NASA-CR-193988; NAS 1.26:193988; SAO-AXAF-DR-93-052) Avail: CASI HC A03/MF A01

The Advanced X-Ray Astrophysics Facility (AXAF) mission support team has made extensive use of geometric ray tracing to analyze the performance of AXAF developmental and flight optics. One important aspect of this performance modeling is the incorporation of finite element analysis (FEA) data into the surface deformations of the optical elements. TransFit is software designed for the fitting of FEA data of Wolter I optical surface distortions with a continuous surface description which can then be used by SAO's analytic ray tracing software, currently OSAC (Optical Surface Analysis Code). The improved capabilities of Transfit over previous methods include bicubic spline fitting of FEA data to accommodate higher spatial frequency distortions, fitted data visualization for assessing the quality of fit, the ability to accommodate input data from three FEA codes plus other standard formats, and options for alignment of the model coordinate system with the ray trace coordinate system. TransFit uses the AnswerGarden graphical user interface (GUI) to edit input parameters and then access routines written in PV-WAVE, C, and FORTRAN to allow the user to interactively create, evaluate, and modify the fit. The topics covered include an introduction to TransFit: requirements, designs philosophy, and implementation; design specifics: modules, parameters, fitting algorithms, and data displays; a procedural example; verification of performance; future work; and appendices on online help and ray trace results of the verification section. Derived from text

N94-36185 Air Force Inst. of Tech., Wright-Patterson AFB, OH. School of Engineering.

APPLICATION OF SEQUENTIAL QUADRATIC PROGRAMMING TO LARGE-SCALE STRUCTURAL DESIGN PROBLEMS M.S. Thesis

Mark A. Abramson Mar. 1994 102 p Limited Reproducibility: More than 20% of this document may be affected by microfiche quality
(AD-A278574) Avail: Issuing Activity (Defense Technical Information Center (DTIC))

Large-scale structural optimization problems are often difficult to solve with reasonable efficiency and accuracy. Such problems are often characterized by constraint functions which are not explicitly defined. Constraint and gradient functions are usually expensive to evaluate. An optimization approach which uses the NLPQL sequential quadratic programming algorithm of Schittkowski, integrated with the Automated Structural Optimization System (ASTROS) is tested. The traditional solution approach involves the formulation and solution of an explicitly defined approximate problem during each iteration. This approach is replaced by a simpler approach in which the approximate problem is eliminated. In the simpler approach, each finite element analysis is followed by one iteration of the optimizer. To compensate for the cost of additional analyses incurred by the elimination of the approximate problem, a much more restrictive active set strategy is used. The approach is applied to three large structures problems, including one with constraints from multiple disciplines. Results and algorithm performance comparisons are given. Although not much computational efficiency is gained, the alternative approach gives accurate solutions. The largest of the three problems, which had 1527 design variables and 6124 constraints was solved with ASTROS for the first time using a direct method. The resulting design represents the lowest weight feasible design recorded to date. DTIC

N94-36211 Rutherford Appleton Lab., Chilton (England).
THE EASE VISUALIZATION COMMUNITY CLUB Annual Report No. 2, Jan. - Dec. 1993
R. Popovic, J. R. Gallop, and K. W. Brodlie Mar. 1994 22 p See also PB93-179281 Prepared in cooperation with Leeds Univ., England
(PB94-170529; RAL-94-024) Avail: Issuing Activity (National Technical Information Service (NTIS))

This is the second annual report of the Science and Engineering Research Council (SERC) Visualization Community Club set up under the auspices of the Engineering Research Commission (ERC) and covers the period from January to December 1993. The Club is one of three such clubs run within the Engineering Applications IT Support ProgrammE (EASE). The club has now over 250 registered members and held four events during this period. It is also involved in directing visualization technical activities carried out at the Rutherford Appleton Laboratory (RAL). The Visualization Community Club provides an effective mechanism for engineering researchers using visualization techniques to collaborate and disseminate knowledge and results of their work and also to promote the wider use of these techniques within engineering research. NTIS

N94-36236# Lawrence Livermore National Lab., CA.
COMPUTER VIRUS INFORMATION UPDATE CIAC-2301
W. J. Orvis 15 Jan. 1994 156 p
(Contract W-7405-eng-48)
(DE94-011916; UCRL-MA-115896) Avail: CASI HC A08/MF A02

While CIAC periodically issues bulletins about specific computer viruses, these bulletins do not cover all the computer viruses that affect desktop computers. The purpose of this document is to identify most of the known viruses for the MS-DOS and Macintosh platforms and give an overview of the effects of each virus. The authors also include information on some Windows, Atari, and Amiga viruses. This document is revised periodically as new virus information becomes available. This document replaces all earlier versions of the CIAC Computer Virus Information Update. The date on the front cover indicates the date on which the information in this document was extracted from CIAC's Virus database. DOE

N94-36250 Analytic Sciences Corp., Fairborn, OH.
THE INTEGRATED MODEL DEVELOPMENT ENVIRONMENT Final Technical Report, Mar. 1990 - Jun. 1993
Bradley A. Lloyd and Patrick K. Clark Feb. 1994 34 p Limited Reproducibility: More than 20% of this document may be affected by microfiche quality
(Contract F33615-90-C-0007)
(AD-A278613; AL/HR-TR-1994-0009) Avail: Issuing Activity (Defense Technical Information Center (DTIC))

This report presents the results of the Integrated Model Development Environment (IMDE) exploratory development research project. The objective of the research was to demonstrate how object-oriented modeling and graphical user interface technologies could improve Air Force and DOD large-scale modeling efforts. This report documents the motivations for the research, describes the generic modeling tool that was developed to demonstrate the IMDE technologies, and discusses future laboratory research plans. DTIC

N94-36258 Pennsylvania Univ., Philadelphia, PA. School of Engineering and Applied Science.
AN ENVIRONMENT FOR VISUALIZATION, RELIABILITY, AND KNOWLEDGE ACQUISITION IN EQUATIONAL PROGRAMMING Final Report, 1 Aug. 1990 - 31 Aug. 1993
Noah Prywes Apr. 1993 170 p Limited Reproducibility: More than 20% of this document may be affected by microfiche quality
(Grant AF-AFOSR-0335-90)
(AD-A278639; AFOSR-94-0255TR) Avail: Issuing Activity (Defense Technical Information Center (DTIC))

We investigated the concept of a visual software environment which facilitates man-machine cooperation during software development. The focus is on 'oracle' operations performed by a human user during the man-machine cooperation. In the environment, graphics and equations are combined to enhance software understanding that is essential in software development. The environment consists of the following components: (1) visual programming: an icon-based graph editor is used for composing an array graph of an equational language program, for interactive syntax analysis, and for consistency checking of the array graph and equations; (2) compilation: an equational language program is statically checked in accordance with its semantics during compilation; (3) equational visual testing: test adequacy criteria are defined for the equational visual testing; the testing process becomes simple and intuitive; oracle operations such as path selection, path examination, finding test input values, monitoring execution, and evaluation are facilitated; (4) verification: equational reasoning is combined with graphical representation of programs; and (5) knowledge acquisition: expertise in old legacy code in procedural language such as algorithms and methods is transferred to rules of knowledge bases via equations. DTIC

N94-36259 Nice Univ. (France). Mathematics Lab.
USE OF FORMAL CALCULATION TO AUTOMATICALLY OBTAIN ADJOINT PROGRAMS Final Report [UTILISATION DU CALCUL FORMEL POUR L'OBTENTION AUTOMATIQUE DU PROGRAMME ADJOINT DE CERTAINS PROGRAMMES]
A. Galligo and N. Rostaing 27 May 1993 86 p In FRENCH
(Contract DRET-911496)
(PB94-170701) Avail: Issuing Activity (National Technical Information Service (NTIS))

Adjoint programs can be used to study sensitivity to initial conditions. We propose generating one automatically using a symbolic computational program written in CAML. Our guiding example is a weather forecasting code. This report describes work to develop a functional model close to 'industrial scale' FORTRAN codes. The result was 'Odyssey', a highly modular, rules-system-based software toolbox that is built around a polymorphous language. The language processes algorithms in a structured way and allows incremental extension of the methods used. We validate Odyssey by comparing the code it generates with a manually written one. NTIS

N94-36294 Carnegie-Mellon Univ., Pittsburgh, PA. Software Engineering Inst.
A PRACTICAL GUIDE TO THE TECHNOLOGY AND ADOPTION OF SOFTWARE PROCESS AUTOMATION Final Report
Alan M. Christie Mar. 1994 119 p Limited Reproducibility: More than 20% of this document may be affected by microfiche quality
(Contract F19628-90-C-0003)
(AD-A278719; CMU/SEI-94-TR-007; ESC-TR-94-007) Avail: Issuing Activity (Defense Technical Information Center (DTIC))

Process automation provides a means to integrate people in a software development organization with the development process and the tools supporting that development. For many reasons, this new technology has the potential to significantly improve software quality and software development productivity. As yet, however, there is little practical experience in its day-to-day use. The main goal of this report is thus to provide information for organizations that are considering its adoption. For these reasons, the report aims to identify how process automation relates to both process improvement and CASE tools, to review in some detail two of the major commercial process automation products, and to address relevant organizational adoption issues. It is hoped that the report will help bridge the gap between those whose focus is software process improvement and those whose focus is software technology. DTIC

N94-36382# Bhabha Atomic Research Centre, Bombay (India).
DIGITAL CONTROL PROGRAMMER FOR TEMPERATURE CONTROL
S. B. Rajore (Bhabha Atomic Research Centre, Bombay, India.) and S. V. Kumar (Bhabha Atomic Research Centre, Bombay, India.) 1993 39 p
(DE94-615584; BARC-1993/E/017) Avail: CASI HC A03/MF A01 (US Sales Only)

This report describes a PC based digital control programmer for controlling and programming temperature of a high vacuum resistance heating furnace and the software developed to control power using PID algorithm. It also describes the amplifier specially developed to suit the input requirement of the non-standard W5 thermocouple and the software and hardware protections introduced in the system. DOE

N94-36429# Lawrence Livermore National Lab., CA.
GRIZ: FINITE ELEMENT ANALYSIS RESULTS VISUALIZATION FOR UNSTRUCTURED GRIDS
D. J. Dovey and T. E. Spelce Oct. 1993 42 p
(Contract W-7405-eng-48)
(DE94-010066; UCRL-MA-115696) Avail: CASI HC A03/MF A01

GRIZ supports interactive visualization of finite element analysis results on unstructured grids. GRIZ is a general-purpose post-processing application which is designed to work with a variety of an analysis codes. Currently, GRIZ is capable of calculating and displaying derived variables for the DYNA3D, NIKE3D and TOPAZ3D analysis codes. GRIZ reads in data files in the 'MDG plotfile' format. GR IZ provides support for modern 3D visualization techniques such as isosurface display, cutting planes and display of vector data. GRIZ also incorporates the ability to animate data over time and to store animation frames to a video disk. GRIZ is designed to utilize the capabilities of modern graphics workstations which provide hardware support for 3D graphics, thereby giving the user as much interactive performance as possible. This should make it easier for analysts to explore and interrogate their analysis results. DOE

N94-36438*# National Aeronautics and Space Administration. Langley Research Center, Hampton, VA.
THE ANALYSIS OF A GENERIC AIR-TO-AIR MISSILE SIMULATION MODEL
Joseph A. Kaplan (Virginia Polytechnic Inst. and State Univ., Blacksburg, VA.), Alan R. Chappell (Lockheed Engineering and Sciences Co., Hampton, VA.), and John W. McManus Jun. 1994 47 p
(RTOP 505-90-53)
(NASA-TM-109057; NAS 1.15:109057) Avail: CASI HC A03/MF A01

A generic missile model was developed to evaluate the benefits of using a dynamic missile fly-out simulation system versus a static missile launch envelope system for air-to-air combat simulation. This paper examines the performance of a launch envelope model and a missile fly-out model. The launch envelope model bases its probability of killing the target aircraft on the target aircraft's position at the launch time of the weapon. The benefits gained from a launch envelope model are the simplicity of implementation and the minimal computational overhead required. A missile fly-out model takes into account the physical characteristics of the missile as it simulates the guidance, propulsion, and movement of the missile. The missile's probability of kill is based on the missile miss distance (or the minimum distance between the missile and the target aircraft). The problems associated with this method of modeling are a larger computational overhead, the additional complexity required to determine the missile miss distance, and the additional complexity of determining the reason(s) the missile missed the target. This paper evaluates the two methods and compares the results of running each method on a comprehensive set of test conditions. Author (revised)

N94-36439*# Draper (Charles Stark) Lab., Inc., Cambridge, MA.
AUTONOMOUS HAZARD DETECTION AND AVOIDANCE Final Report
Homer Pien Jun. 1992 53 p
(Contract NAS9-18426)
(NASA-CR-188331; NAS 1.26:188331; CSDL-C-6303) Avail: CASI HC A04/MF A01

During GFY 91, Draper Laboratory was awarded a task by NASA-JSC under contract number NAS9-18426 to study and evaluate the potential for achieving safe autonomous landings on Mars using an on-board autonomous hazard detection and avoidance (AHDA) system. This report describes the results of that study. The AHDA task had four objectives: to demonstrate, via a closed-loop simulation, the ability to autonomously select safe landing sites and the ability to maneuver to the selected site; to identify key issues in the development of AHDA systems; to produce strawman designs for AHDA sensors and algorithms; and to perform initial trade studies leading to better understanding of the effect of sensor/terrain/viewing parameters on AHDA algorithm performance. This report summarizes the progress made during the first year, with primary emphasis on describing the tools developed for simulating a closed-loop AHDA landing. Some cursory performance evaluation results are also presented. Derived from text

N94-35556*# Jet Propulsion Lab., California Inst. of Tech., Pasadena, CA.
BIT-WISE ARITHMETIC CODING FOR DATA COMPRESSION
A. B. Kiely *In its* The Telecommunications and Data Acquisition Report 15 May 1994 p 145-160 (For primary document see N94-35542 11-32)
(RTOP 310-30-71-83-04)
Avail: CASI HC A03/MF A03

N94-35559*# Jet Propulsion Lab., California Inst. of Tech., Pasadena, CA.
THE DEVELOPMENT AND APPLICATION OF COMPOSITE COMPLEXITY MODELS AND A RELATIVE COMPLEXITY METRIC IN A SOFTWARE MAINTENANCE ENVIRONMENT
J. M. Hops and J. S. Sherif *In its* The Telecommunications and Data Acquisition Report 15 May 1994 p 194-212 (For primary document see N94-35542 11-32)
(RTOP 314-40-41-21-03)
Avail: CASI HC A03/MF A03

N94-35631*# Integrated Systems, Inc., Santa Clara, CA.
OVERVIEW OF THE MSTI 2 PROCESSOR-IN-THE-LOOP SIMULATOR
Christopher A. Rygaard *In* NASA. Goddard Space Flight Center, Flight Mechanics/Estimation Theory Symposium, 1994 May 1994 p 331-340 (For primary document see N94-35605 11-13)
Avail: CASI HC A02/MF A04

N94-35869*# Techno-Sciences, Inc., Greenbelt, MD.
INTEGRATED DESIGN OF STRUCTURES, CONTROLS, AND MATERIALS
G. L. Blankenship (Maryland Univ., College Park, MD.) *In* NASA. Langley Research Center, NASA Workshop on Distributed Parameter Modeling and Control of Flexible Aerospace Systems Jun. 1994 p 65-76 (For primary document see N94-35865 11-18)
Avail: CASI HC A03/MF A06

N94-35870*# National Aeronautics and Space Administration. Langley Research Center, Hampton, VA.
APPLYING TRANSFER MATRIX METHOD TO THE ESTIMATION OF THE MODAL CHARACTERISTICS OF THE NASA MINI-MASS TRUSS
Ji-Yao Shen (North Carolina Agricultural and Technical State Univ., Greensboro, NC.) and Lawrence W. Taylor, Jr. *In its* NASA Workshop on Distributed Parameter Modeling and Control of Flexible Aerospace Systems Jun. 1994 p 77-94 (For primary document see N94-35865 11-18)
Avail: CASI HC A03/MF A06

N94-35876*# Louisville Univ., KY. Dept. of Electrical Engineering.
ADAPTIVE MODEL REDUCTION FOR CONTINUOUS SYSTEMS VIA RECURSIVE RATIONAL INTERPOLATION
John H. Lilly *In* NASA. Langley Research Center, NASA Workshop on Distributed Parameter Modeling and Control of Flexible Aerospace Systems Jun. 1994 p 195-214 (For primary document see N94-35865 11-18)
Avail: CASI HC A03/MF A06

N94-35877*# Florida Univ., Gainesville, FL.
ADVANCES IN PARAMETER ESTIMATION TECHNIQUES APPLIED TO FLEXIBLE STRUCTURES
Egbert Maben and David C. Zimmerman *In* NASA. Langley Research Center, NASA Workshop on Distributed Parameter Modeling and Control

of Flexible Aerospace Systems Jun. 1994 p 215-239 (For primary document see N94-35865 11-18)
Avail: CASI HC A03/MF A06

N94-35888*# Lockheed Missiles and Space Co., Sunnyvale, CA.
CSI, OPTIMAL CONTROL, AND ACCELEROMETERS: TRIALS AND TRIBULATIONS
Brian J. Benjamin and John R. Sesak *In* NASA. Langley Research Center, NASA Workshop on Distributed Parameter Modeling and Control of Flexible Aerospace Systems Jun. 1994 p 407-425 (For primary document see N94-35865 11-18)
(Contract NAS1-19241)
Avail: CASI HC A03/MF A06

N94-35968*# National Aeronautics and Space Administration. Hugh L. Dryden Flight Research Facility, Edwards, CA.
EXPERIENCE WITH Ada ON THE F-18 HIGH ALPHA RESEARCH VEHICLE FLIGHT TEST PROGRAM
Victoria A. Regenie, Michael Earls, Jeanette Le, and Michael Thomson *In* NASA. Ames Research Center, 1993 Technical Paper Contest for Women. Gear Up 2000: Women in Motion Feb. 1994 p 63-76 (For primary document see N94-35961 11-99)
Avail: CASI HC A03/MF A02

N94-36414*# Purdue Univ., Elkhart, IN. Statewide Technology.
GRAPHING TECHNIQUES FOR MATERIALS LABORATORY USING EXCEL
Nikhil K. Kundu *In* NASA. Langley Research Center, National Educators' Workshop: Update 1993. Standard Experiments in Engineering Materials Science and Technology Apr. 1994 p 457-467 (For primary document see N94-36398 11-23)
Avail: CASI HC A02/MF A04

62 COMPUTER SYSTEMS

Includes computer networks and special application computer systems.

N94-35535 Newcastle-upon-Tyne Univ., Newcastle (England). Dept. of Computing Science.
THE rel/REL: A FAMILY OF RELIABLE MULTICAST PROTOCOLS FOR DISTRIBUTED REAL-TIME SYSTEMS
P. D. Ezhilchelvan and S. K. Shrivastava Dec. 1993 24 p
(PB94-167830; TRS-461) Copyright Avail: Issuing Activity (National Technical Information Service (NTIS))

A reliable multicast service that ensures atomic delivery, such that a multicast is completed successfully despite intervening failures (for example, the crash of the sender during a multicast) is highly desirable for building dependable distributed systems. This paper presents a family of multicast protocols which are easy to understand and implement and are capable of providing such a service with differing message ordering requirements. These protocols provide good performance despite intervening node crashes, thus making them suitable for systems requiring timely responses in the presence of component failures. NTIS

N94-35597 Carnegie-Mellon Univ., Pittsburgh, PA. Dept. of Computer Science.
A COMPILE TIME MODEL FOR COMPOSING PARALLEL PROGRAMS
Susan Hinrichs Apr. 1994 19 p Limited Reproducibility: More than 20% of this document may be affected by microfiche quality
(Contract MDA972-90-C-0035; ARPA Order 7330)
(AD-A278896; CMU-CS-94-108) Avail: CASI HC A03

Many distributed memory machines support connection-based communication instead of or in addition to connection-less message passing. Connection-based communication can be more efficient than message passing because the resources are reserved once for the connection and multiple messages can be sent over the connection. While long-lived connections enable more efficient use of the communication system in some situations, managing connection resources adds another level of complexity to programming such machines. iWarp is an example of a distributed memory machine that supports long-lived connections. To aid the iWarp programmer and program generator tools, we developed a tool chain that enables the programmer to define connections and compose parallel programs. The communication tool chain has been in use for four years in various forms. In that time, we have found many benefits and a few pitfalls in our model. This paper describes the design of the programming model and tools and discusses our experiences with this implementation. DTIC

N94-35653 Calspan-Buffalo Univ. Research Center, NY.
TASK ALLOCATION FOR PARALLEL REAL-TIME EXECUTION Final Technical Report, Jun. - Aug. 1993
John K. Antonio and Richard C. Metzger Mar. 1994 34 p Limited Reproducibility: More than 20% of this document may be affected by microfiche quality
(Contract F30602-93-D-0075)
(AD-A278789; RL-TR-94-7) Avail: Issuing Activity (Defense Technical Information Center (DTIC))

Current trends indicate that future C3 (command, control, and communications) systems will likely contain suites of heterogeneous computing facilities composed of both parallel and sequential computing components. Also, 'commercial-off-the-shelf' components are being heavily considered for use in these future systems. In the context of these trends, brief overviews of related work within the areas of parallel processing and real-time computing are given and areas of future research are outlined. A central theme throughout the report is that in order to make effective use of future C3 platforms, a significant amount of 'cross fertilization' between researchers in the parallel processing and real-time computing communities will be required. As an example of the need for combined expertise in both areas, the problem of how to effectively allocate periodic real-time tasks onto the processing elements of a hypercube architecture is illustrated through an example. Other research issues, including task partitioning, operating systems, I/O, and the software development process are also discussed. DTIC

N94-35742 Chicago Univ., IL. Dept. of Computer Science.
THE DataCube SERVER. ANIMATE AGENT PROJECT WORKING NOTE 2, VERSION 1.0
Roger E. Kahn, Michael J. Swain, and R. J. Firby Nov. 1993 72 p Limited Reproducibility: More than 20% of this document may be affected by microfiche quality
(AD-A278847) Avail: Issuing Activity (Defense Technical Information Center (DTIC))

The DataCube server and client class facilitate the development of real-time vision systems by allowing you to write distributed programs that can access the DataCube MV200/MV20 and DigiColor boards in parallel. The DataCube server is a network interface to a library of Pipelined routines that run of the MV200/MV20 and DigiColor. The functions provided by the interface include frame grabbing, Gaussian pyramids, color histogram backprojection, color histogram intersection, motion detection from a moving platform, foveated frame display, and optionally, control of a Directed Perception pan-tilt head. Furthermore, the system is designed to be extendable so that new functions can be added to the server. The DataCube client class is a C++ class that provides a function based application programmatic interface to the DataCube server. To use the DataCube client class one does not need to be familiar with how the DataCube is programmed. The programmers interface is simply a C++ class with a set of member functions. All that one does is call the member functions; the networking and pipelined processing happen behind the scenes. DTIC

N94-35806 Carnegie-Mellon Univ., Pittsburgh, PA. Dept. of Computer Science.
COMMUNICATION AND MEMORY REQUIREMENTS AS THE BASIS FOR MAPPING TASK AND DATA PARALLEL PROGRAMS
Jaspal Subhlok, David R. OHalloron, Thomas Gross, Peter A. Dinda, and Jon Webb Jan. 1994 19 p Limited Reproducibility: More than 20% of this document may be affected by microfiche quality
(Contracts F49620-92-J-0131; N00039-93-C-0152)
(AD-A278954; CMU-CS-94-106) Avail: Issuing Activity (Defense Technical Information Center (DTIC))

For a wide variety of applications, both task and data parallelism must be exploited to achieve the best possible performance on a multicomputer.

Recent research has underlined the importance of exploiting task and data parallelism in a single compiler framework, and such a compiler can map a single source program in many different ways onto a parallel machine. There are several complex tradeoffs between task and data parallelism, depending on the characteristics of the program to be executed, most significantly the memory and communication requirements, and the performance parameters of the target parallel machine. In this paper, we isolate and examine the specific characteristics of programs that determine the performance for different mappings on a parallel machine and present a framework for obtaining a good mapping. The framework is applicable to applications that process a stream of input, and whose computation structure is fairly static and predictable. We describe three applications that were developed with our compiler: fast Fourier transforms, narrowband tracking radar, and multibaseline stereo; examine the tradeoffs between various mappings for them; and show how the framework was used to obtain efficient mappings. The automation of this framework is described in related publications. DTIC

N94-36015 Carnegie-Mellon Univ., Pittsburgh, PA. Dept. of Computer Science.
THE CMU TASK PARALLEL PROGRAM SUITE
Peter Dinda, Thomas Gross, David OHallaron, Edward Segall, and Jon Webb Mar. 1994 11 p Limited Reproducibility: More than 20% of this document may be affected by microfiche quality
(Contracts N00039-93-C-0152; F49620-92-J-0131)
(AD-A278951; CMU-CS-94-131) Avail: Issuing Activity (Defense Technical Information Center (DTIC))

The idea of exploiting both task and data parallelism in programs is appealing. However, identifying realistic yet manageable example programs that can benefit from such a mix of task and data parallelism is a major problem for researchers. We address this problem by describing a suite of five applications from the domains of scientific, signal, and image processing that are of reasonable size, are representative of real codes, and can benefit from exploiting task and data parallelism. The suite includes fast Fourier transforms, narrowband tracking radar, multibaseline stero imaging, and airshed simulation. DTIC

63 CYBERNETICS

Includes feedback and control theory, artificial intelligence, robotics and expert systems.

For related information see also *54 Man/System Technology and Life Support.*

N94-35242*# National Aeronautics and Space Administration. Langley Research Center, Hampton, VA.
KINEMATIC MODELING OF A DOUBLE OCTAHEDRAL VARIABLE GEOMETRY TRUSS (VGT) AS AN EXTENSIBLE GIMBAL
Robert L. Williams, II May 1994 41 p
(RTOP 233-03-03-02)
(NASA-TM-109127; NAS 1.15:109127) Avail: CASI HC A03/MF A01

This paper presents the complete forward and inverse kinematics solutions for control of the three degree-of-freedom (DOF) double octahedral variable geometry truss (VGT) module as an extensible gimbal. A VGT is a truss structure partially comprised of linearly actuated members. A VGT can be used as joints in a large, lightweight, high load-bearing manipulator for earth- and space-based remote operations, plus industrial applications. The results have been used to control the NASA VGT hardware as an extensible gimbal, demonstrating the capability of this device to be a joint in a VGT-based manipulator. This work is an integral part of a VGT-based manipulator design, simulation, and control tool. Author

N94-35348# Pacific Northwest Lab., Richland, WA.
INTRODUCTION TO NEURAL NETWORKS: NEURAL NETWORK WORKSHOP FOR THE HANFORD COMMUNITY
P. E. Keller Jan. 1994 69 p Presented at the Joint 40/50 Industry Outreach Meeting, Seattle, WA, 25-27 Jan. 1994
(Contract DE-AC06-76RL-01830)
(DE94-006526; PNL-SA-23624; CONF-940159-1) Avail: CASI HC A04/MF A01

Artificial Neural Networks (ANN's) constitute a new information processing technology that is destined within a few years to provide the world with a vast array of new products. A major reason for this is that artificial neural networks are able to provide solutions to a wide variety of complex problems in a much simpler fashion than is possible using existing techniques. In recognition of these capabilities, many scientists and engineers are exploring the potential application of this new technology to their fields of study. This paper begins with a brief description of what ANN's are, for what they are used, and interested personnel. Then, an in depth in the neural network mathematics follows. Finally, an exhaustive listing of resources for neural network research is given, including evaluated computer codes, journal articles, and books. DOE

N94-35501* National Aeronautics and Space Administration. Lyndon B. Johnson Space Center, Houston, TX.
GENERAL PURPOSE ARCHITECTURE FOR INTELLIGENT COMPUTER-AIDED TRAINING Patent
R. Bowen Loftin, inventor (to NASA), Lui Wang, inventor (to NASA), Paul T. Baffes, inventor (to NASA), and Grace C. Hua, inventor (to NASA) 10 May 1994 57 p Filed 28 Jun. 1990 Supersedes N91-13944 (29 - 5, p 707)
(NASA-Case-MSC-21381-1; US-Patent-5,311,422; US-Patent-Appl-SN-545235; US-Patent-Class-364-401; US-Patent-Class-364-578; Int-Patent-Class-G06F-15/52) Avail: US Patent and Trademark Office

An intelligent computer-aided training system having a general modular architecture is provided for use in a wide variety of training tasks and environments. It is comprised of a user interface which permits the trainee to access the same information available in the task environment and serves as a means for the trainee to assert actions to the system; a domain expert which is sufficiently intelligent to use the same information available to the trainee and carry out the task assigned to the trainee; a training session manager for examining the assertions made by the domain expert and by the trainee for evaluating such trainee assertions and providing guidance to the trainee which are appropriate to his acquired skill level; a trainee model which contains a history of the trainee interactions with the system together with summary evaluative data; an intelligent training scenario generator for designing increasingly complex training exercises based on the current skill level contained in the trainee model and on any weaknesses or deficiencies that the trainee has exhibited in previous interactions; and a blackboard that provides a common fact base for communication between the other components of the system. Preferably, the domain expert contains a list of 'mal-rules' which typifies errors that are usually made by novice trainees. Also preferably, the training session manager comprises an intelligent error detection means and an intelligent error handling means. The present invention utilizes a rule-based language having a control structure whereby a specific message passing protocol is utilized with respect to tasks which are procedural or step-by-step in structure. The rules can be activated by the trainee in any order to reach the solution by any valid or correct path.
Official Gazette of the U.S. Patent and Trademark Office

N94-35527 Carnegie-Mellon Univ., Pittsburgh, PA. Dept. of Computer Science.
COMBINING LEFT AND RIGHT UNLINKING FOR MATCHING A LARGE NUMBER OF LEARNED RULES
Robert B. Doorenbos 4 Apr. 1994 17 p Limited Reproducibility: More than 20% of this document may be affected by microfiche quality
(Contract F33615-93-1-1330)
(AD-A278979; CMU-CS-94-132) Avail: Issuing Activity (Defense Technical Information Center (DTIC))

In systems which learn a large number of rules (productions), it is important to match the rules efficiently, in order to avoid the machine learning utility problem -- if the learned rules slow down the matcher, the 'learning' can slow the whole system down to a crawl. So we need match algorithms that scale well with the number of productions in the system. Right unlinking was introduced as a way to improve the scalability of the Rete match algorithm. In this paper, we build on this idea, introducing a symmetric optimization, left unlinking, and demonstrating that it makes Rete scale well on an even larger class of systems. Unfortunately, when left and right unlinking are combined in the same system, they can interfere with each other. We give a particular way to combine them which we prove minimizes the interference, and analyze the worst-case remaining interference. Finally, we present empirical results showing that the interference is very small in practice, and that the combination of left and right unlinking allows five of our seven testbed systems to learn over 100,000 rules without incurring a significant increase in match cost DTIC

N94-35658 Carnegie-Mellon Univ., Pittsburgh, PA. Dept. of Computer Science.
THE ROLE OF EMOTION IN BELIEVABLE AGENTS
Joseph Bates Apr. 1994 10 p Limited Reproducibility: More than 20% of this document may be affected by microfiche quality
(AD-A278952; CMU-CS-94-136) Avail: Issuing Activity (Defense Technical Information Center (DTIC))

Artificial intelligence researchers attempting to create engaging, apparently living creatures may find important insight in the work of artists who have explored the idea of believable character. In particular, appropriately timed and clearly expressed emotion is a central requirement for believable characters. We discuss these ideas and suggest how they may apply to believable interactive characters, which we call believable agents. DTIC

N94-35710 Chicago Univ., IL.
TASK NETWORKS FOR CONTROLLING CONTINUOUS PROCESSES
R. J. Firby 1994 7 p Limited Reproducibility: More than 20% of this document may be affected by microfiche quality
(Contracts N00014-93-1-0332; N00014-93-1-1394)
(AD-A278683) Avail: Issuing Activity (Defense Technical Information Center (DTIC))

This paper describes an extension to the RAP system task-net semantics and representation language to enable the effective control of continuous processes. The representation addresses the following: the problems of synchronizing plan expansion with events in the world; coping with multiple, non-deterministic task outcomes; and the description of a simple form of clean-up task. It is also pointed out that success and failure need no special place in a task network representation. Success and failure are really messages about the execution system's knowledge and do not explicitly define that systems flow of control. DTIC

N94-35730 Institute for Defense Analyses, Alexandria, VA.
THE APPLICATION OF FUZZY LOGIC TO SAFOR IN SIMNET Final Report, Jun. - Dec. 1993
Irvin W. Kay and Bohdan Balko 1 Feb. 1994 130 p Limited Reproducibility: More than 20% of this document may be affected by microfiche quality
(AD-A279058; AD-E501776; IDA-P-2940; IDA/HQ-93-44868) Avail: Issuing Activity (Defense Technical Information Center (DTIC))

This paper describes the history of an experiment to demonstrate the potential utility of fuzzy logic applied to semi-automated forces (SAFOR) algorithms by using fuzzy logic to modify an existing vehicle collision avoidance algorithm. Appended to the paper are instructions on how to create SAFOR exercises on a Silicon Graphics terminal in the IDA Simulation Center network. This report also contains listings of source codes used in various phases of the work. DTIC

N94-35802 Chicago Univ., IL. Dept. of Computer Science.
TASK AND ENVIRONMENT-SENSITIVE TRACKING
Peter N. Prokopowicz, Michael J. Swain, and Roger E. Kahn 1994 6 p Limited Reproducibility: More than 20% of this document may be affected by microfiche quality
(AD-A278846) Avail: Issuing Activity (Defense Technical Information Center (DTIC))

In a mobile robot, visual tracking, like other visual behaviors, takes place in a context that includes aspects of the task, the object being tracked, and the background. In this work, prior knowledge of those task and target characteristics that either enable or hinder different real-time image-tracking algorithms, together with run-time evaluation of the robot's environment, are used to select an algorithm appropriate to the context. DTIC

N94-35810 Allied-Signal Aerospace Co., Kansas City, MO.
CABPRO: AN EXPERT SYSTEM FOR PROCESS PLANNING MULTIWIRE CABLES Final Report
R. M. Schaefer Apr. 1994 43 p Limited Reproducibility: More than 20% of this document may be affected by microfiche quality
(Contract DE-AC04-76DP-00613)
(DE94-010213; KCP-613-5291) Avail: CASI HC A03

CABPRO (CABle PROcessor) is a set of computer programs using Artificial Intelligence programming to automatically generate process plans and work instructions in support of the manufacture of multiwire cables. Development of these programs required selecting appropriate hardware and software tools, defining engineering process planning activities, acquiring and representing process planning knowledge, and creating a prototype system. A successful prototype was developed and demonstrated. DOE

N94-35831# Pakistan Inst. of Nuclear Science and Technology, Islamabad.
COMPUTER AUTOMATION AND ARTIFICIAL INTELLIGENCE
S. B. Husnain 1992 12 p Presented at the Seminar on Research and Development in Support of Technology With Military Applications, Karachi, Pakistan, 29 Apr. 1992
(DE94-611058; INIS-MF-13741; CONF-9204276) Avail: CASI HC A03/MF A01 (US Sales Only)

Rapid advances in computing, resulting from the microchip revolution has increased its application manifold particularly for computer automation. Yet the level of automation available has limited its application to more complex and dynamic systems which require an intelligent computer control. In this paper, a review of artificial intelligence techniques used to augment automation is presented. The current sequential processing approach usually adopted in artificial intelligence has succeeded in emulating the symbolic processing part of intelligence, but the processing power required to get more elusive aspects of intelligence leads towards parallel processing. An overview of parallel processing with emphasis on transputer is also provided. A fuzzy knowledge based controller for amination drug delivery in muscle relaxant anesthesia on transputer is described. DOE

N94-36195# Pacific Northwest Lab., Richland, WA.
A COMPARISON OF ARTIFICIAL NEURAL NETWORKS AND STATISTICAL ANALYSES
D. K. Blough and K. K. Anderson Jan. 1994 40 p
(Contract DE-AC06-76RL-01830)
(DE94-010846; PNL-9050) Avail: CASI HC A03/MF A01

Artificial neural networks have come to be used in a wide variety of data analytic applications, many of which were traditionally approached using statistical methods. It is the purpose of this paper to discuss the nature of the information obtained by each methodology, that of artificial neural networks and that of statistical analyses. Two aspects of the comparison will be considered: (1) what are the requirements needed for each approach in terms of model specification, data requirements, and computing power, and (2) what sort of information is contained in the results of each approach. Example analyses are presented characterizing the differences in the two approaches. A specific problem (hydrodynamic yield estimation) is presented with a corresponding data set. This data is then analyzed using statistical methods, and the results are compared with those obtained by using an artificial neural network. The requirements and results of the two approaches are then summarized as general guidelines an investigator can use in deciding which approach would be best for analyzing a given data set. DOE

N94-36295 Chicago Univ., IL.
INTERFACING THE RAP SYSTEM TO REAL-TIME CONTROL, VERSION 1
R. J. Firby Jul. 1993 15 p Limited Reproducibility: More than 20% of this document may be affected by microfiche quality
(AD-A278725) Avail: Issuing Activity (Defense Technical Information Center (DTIC))

This document proposes a way to integrate the RAP system with robot control systems based on concurrent interacting processes. The proposal suggests mechanisms for enabling and disabling processes without blocking, mechanisms for synchronizing with the world by blocking until appropriate signals are received from the control processes, and mechanisms for any RAP to update memory. DTIC

N94-36309 David Sarnoff Research Center, Princeton, NJ.
MULTIDISCIPLINARY STUDIES OF INTEGRATED NEURAL NETWORK SYSTEMS Final Report, 1 Dec. 1989 - 31 Dec. 1993

John Pearson, Clay Spence, Williams E. Sullivan, Jeffrey Lubin, and Jack Gelfand Mar. 1994 38 p Prepared in cooperation with Princeton Univ., NJ and Robicon, Inc., Princeton, NJ Limited Reproducibility: More than 20% of this document may be affected by microfiche quality
(Contract F49620-90-C-0010; ARPA Order 7013; AF Proj. 7013)
(AD-A278774; AFOSR-94-0252TR) Avail: Issuing Activity (Defense Technical Information Center (DTIC))

This project was a joint effort of the David Sarnoff Research Center (Sarnoff), Princeton University, and Robicon Systems, all of Princeton, NJ. It consisted of three subprojects, each concerned with a similar kind of research: the development of artificial adaptive systems with capabilities similar to those of their biological counterparts. Recent work on neural networks has demonstrated their potential for solving difficult problems in simplified, controlled environments. The next stage in the development of neural networks is their extension to the scale, complexity, and variability of real-world situations. This will not be a simple evolution of existing neural net designs, because it requires the integration of complex adaptive systems whose components have widely differing functions. Fortunately, biological organisms present existing solutions to this problem and neuroscience can now probe in detail the relevant structures. Biological systems are highly adaptive and operate well in extremely complex and variable environments. They accomplish this by partitioning the system into functional subunits in a quasihierarchical structure of neural network modules. We studied three specific examples of this system integration strategy and modeled their operation for the purpose of creating new neural network architectures and control schemes. DTIC

N94-35861*# Virginia Univ., Charlottesville, VA.
NEURAL NETWORK CONTROLLER DEVELOPMENT FOR A MAGNETICALLY SUSPENDED FLYWHEEL ENERGY STORAGE SYSTEM
Roger L. Fittro, Da-Chen Pang, and Davinder K. Anand *In* NASA. Langley Research Center, Second International Symposium on Magnetic Suspension Technology, Part 1 May 1994 p 391-405 (For primary document see N94-35836 11-18)
Avail: CASI HC A03/MF A04

N94-35862*# National Cheng Kung Univ., Tainan (Taiwan). Inst. of Aeronautics and Astronautics.
TIME-DELAY CONTROL OF A MAGNETIC LEVITATED LINEAR POSITIONING SYSTEM
J. H. Tarn, K. Y. Juang, and C. E. Lin *In* NASA. Langley Research Center, Second International Symposium on Magnetic Suspension Technology, Part 1 May 1994 p 407-420 (For primary document see N94-35836 11-18)
Avail: CASI HC A03/MF A04

N94-35871*# National Aeronautics and Space Administration. Langley Research Center, Hampton, VA.
CONTROL OF FLEXIBLE STRUCTURES WITH DISTRIBUTED SENSING AND PROCESSING
Dave Ghosh (Lockheed Engineering and Sciences Co., Hampton, VA.) and Raymond C. Montgomery *In its* NASA Workshop on Distributed Parameter Modeling and Control of Flexible Aerospace Systems Jun. 1994 p 95-114 (For primary document see N94-35865 11-18)
Avail: CASI HC A03/MF A06

N94-35882*# Temple Univ., Philadelphia, PA. Dept. of Electrical Engineering.
OPTIMAL DISTURBANCE REJECTING CONTROL OF HYPERBOLIC SYSTEMS
Saroj K. Biswas and N. U. Ahmed *In* NASA. Langley Research Center, NASA Workshop on Distributed Parameter Modeling and Control of Flexible Aerospace Systems Jun. 1994 p 317-322 (For primary document see N94-35865 11-18)
Avail: CASI HC A02/MF A06

N94-35883*# Howard Univ., Washington, DC. Dept. of Electrical Engineering.
EFFECTS OF NOISE VARIANCE MODEL ON OPTIMAL FEEDBACK DESIGN AND ACTUATOR PLACEMENT
Mifang Ruan and Ajit K. Choudhury *In* NASA. Langley Research Center, NASA Workshop on Distributed Parameter Modeling and Control of Flexible Aerospace Systems Jun. 1994 p 323-331 (For primary document see N94-35865 11-18)
Avail: CASI HC A02/MF A06

N94-35890*# California Univ., Los Angeles, CA. Flight Systems Research Center.
ROBUSTNESS PROPERTIES OF LQG OPTIMIZED COMPENSATORS FOR COLLOCATED RATE SENSORS
A. V. Balakrishnan *In* NASA. Langley Research Center, NASA Workshop on Distributed Parameter Modeling and Control of Flexible Aerospace Systems Jun. 1994 p 445-463 (For primary document see N94-35865 11-18)
Avail: CASI HC A03/MF A06

N94-35891*# California Univ., Los Angeles, CA. Flight Systems Research Center.
LQG OPTIMAL COMPENSATOR TRANSFER FUNCTION FOR THE NASA LARC CSI EVOLUTIONARY MODEL
A. V. Balakrishnan *In* NASA. Langley Research Center, NASA Workshop on Distributed Parameter Modeling and Control of Flexible Aerospace Systems Jun. 1994 p 465-481 (For primary document see N94-35865 11-18)
Avail: CASI HC A03/MF A06

N94-35894*# Texas A&M Univ., College Station, TX. Dept. of Aerospace Engineering.
SEMIGROUP APPROXIMATION AND ROBUST STABILIZATION OF DISTRIBUTED PARAMETER SYSTEMS
A. J. Kurdila, R. Fabiano, T. Strganac, and S. Hsu *In* NASA. Langley Research Center, NASA Workshop on Distributed Parameter Modeling and Control of Flexible Aerospace Systems Jun. 1994 p 519-543 (For primary document see N94-35865 11-18)
(Contract F49620-92-J-0450)
Avail: CASI HC A03/MF A06

N94-35896*# DYNACS Engineering Co., Inc., Palm Harbor, FL.
COMPUTATIONALLY EFFICIENT MULTIBODY SIMULATIONS
Jayant Ramakrishnan and Manoj Kumar *In* NASA. Langley Research Center, NASA Workshop on Distributed Parameter Modeling and Control of Flexible Aerospace Systems Jun. 1994 p 555-570 (For primary document see N94-35865 11-18)
Avail: CASI HC A03/MF A06

64 NUMERICAL ANALYSIS

Includes iteration, difference equations, and numerical approximation.

N94-35259*# National Aeronautics and Space Administration. Lewis Research Center, Cleveland, OH.
DESCRIPTION AND USE OF LSODE, THE LIVERMORE SOLVER FOR ORDINARY DIFFERENTIAL EQUATIONS
Krishnan Radhakrishnan (Sverdrup Technology, Inc., Brook Park, OH.) and Alan C. Hindmarsh (Lawrence Livermore National Lab., CA.) Washington Dec. 1993 114 p
(Contracts NAS3-25266; W-7405-eng-48; RTOP 505-62-52)
(NASA-RP-1327; E-5843; NAS 1.61:1327; UCRL-ID-113855) Avail: CASI HC A06/MF A02

LSODE, the Livermore Solver for Ordinary Differential Equations, is a package of FORTRAN subroutines designed for the numerical solution of the initial value problem for a system of ordinary differential equations. It is particularly well suited for 'stiff' differential systems, for which the backward differentiation formula method of orders 1 to 5 is provided. The code includes the Adams-Moulton method of orders 1 to 12, so it can be used for nonstiff problems as well. In addition, the user can easily switch methods to increase computational efficiency for problems that change character. For both methods a variety of corrector iteration techniques is included in the code. Also, to minimize computational work, both the step size and method order are varied dynamically. This report presents complete descriptions of the code and integration methods, including their implementation. It also provides a detailed guide to the use of the code, as well as an illustrative example problem. Author

N94-35531 Newcastle-upon-Tyne Univ., Newcastle (England). Dept. of Computing Science.

PARALLEL ALGORITHMS FOR LU DECOMPOSITION ON A SHARED MEMORY MULTIPROCESSOR

D. Kaya and K. Wright Nov. 1993 25 p
(PB94-167798; TRS-450) Copyright Avail: Issuing Activity (National Technical Information Service (NTIS))

A number of different parallel algorithms for the LU decomposition of a square A matrix are considered. One aim of the methods is to collect together updates to columns as far as possible, to make good use of the storage hierarchy of the shared memory multiprocessor used to test the algorithms. Both unit lower triangular form for L and unit upper triangular U variants are considered. The results presented were obtained using the C++ programming language, with parallel constructs provided by the Encore Parallel Threads package, on an Encore Multimax computer. These results indicate significant improvements over a simple parallel implementation of the standard Crout algorithm, and good speedup compared to the sequential Crout algorithm. NTIS

N94-35704# Argonne National Lab., IL.

A COLLECTION OF TOOLS IN SUPPORT OF AUTOMATIC DIFFERENTIATION

A. Mauer Feb. 1994 20 p
(Contract W-31-109-eng-38)
(DE94-010104; ANL/MCS-TM-185) Avail: CASI HC A03/MF A01

This document contains a collection of notes about tools that we have found useful in our work on automatic differentiation. Most transformations necessary to link C and Fortran programs involve changing the case of the C procedure names and some other trivial manipulations. We automate this procedure. The next portion of the document serves a dual purpose; it is a guide to getting started with ADOL-C, and it also describes methods of linking ADOL-C and Fortran programs together. Additionally, we provide two low-level perl functions that aid in coping with the fact that Fortran 'logical'rou tines may include an initial line and many continuation lines. Furthermore, we describe a very powerful perl template that may be easily customized to perform in many common Fortran manipulations, such as expansion of various templates in the code. Finally, we look at some simple transformations of the ADIFOR script and composition files that allow much more intuitive syntax. DOE

N94-35758 Institut des Hautes Etudes Scientifiques, Bures-sur-Yvette (France).

GENERALIZED FREDHOLM DETERMINANTS AND SELBERG ZETA FUNCTIONS FOR AXIOM A DYNAMICAL SYSTEMS

H. H. Rugh Feb. 1994 23 p Limited Reproducibility: More than 20% of this document may be affected by microfiche quality
(PB94-167665; IHES/P/94/7) Avail: Issuing Activity (National Technical Information Service (NTIS))

We consider a generalized Fredholm determinant d(z) and a generalized Selberg zeta function zeta(omega)(exp -1) for Axiom A diffeomorphisms of a surface and Axiom A flows on three-dimensional manifolds, respectively. We show that d(z) and zeta(omega)(exp -1) extend to entire functions in the complex plane. That the functions are entire and not only meromorphic is proved by a new method, identifying removable singularities by a change of Markov partitions. NTIS

N94-35759 Institut des Hautes Etudes Scientifiques, Bures-sur-Yvette (France).

SUCCESSIVE MINIMA ON ARITHMETIC VARIETIES

C. Soule Dec. 1993 20 p Limited Reproducibility: More than 20% of this document may be affected by microfiche quality
(PB94-167699; IHES/M/93/69) Avail: Issuing Activity (National Technical Information Service (NTIS))

Mumford's theory of stability, when applied to varieties over number fields, has interesting consequences, as was shown in recent years by several authors. In this paper, we use it to get information on the successive minima of the lattice of sections of bundles on arithmetic varieties. NTIS

N94-35762 Institut des Hautes Etudes Scientifiques, Bures-sur-Yvette (France).

HEIGHT INEQUALITY FOR HOLOMORPHIC CURVES

M. McQuillan Jan. 1994 12 p Limited Reproducibility: More than 20% of this document may be affected by microfiche quality
(PB94-167731; IHES/M/94/4) Avail: Issuing Activity (National Technical Information Service (NTIS))

Let X/C be a smooth projective variety, then given a complete curve C in X, it is basic that one may measure its degree with respect to any line bundle on X. In addition, there is an analogous theory for incomplete curves, and for that matter heights of rational points of varieties defined over number fields. We will be principally concerned with the former while making allusions to the latter in the spirit of the 'dictionary' between value distribution theory and Diophantine geometry as one finds it in the work of Vojta. NTIS

N94-35763 Institut des Hautes Etudes Scientifiques, Bures-sur-Yvette (France).

ENTROPY OF GRAPHS, SEMIGROUPS AND GROUPS

S. Friedland (Illinois Univ., Chicago, IL.) Feb. 1994 24 p Limited Reproducibility: More than 20% of this document may be affected by microfiche quality
(PB94-167749; IHES/M/94/8) Avail: Issuing Activity (National Technical Information Service (NTIS))

Let X be a compact metric space and T : X leads to X is continuous transformation. Then the dynamics of T is a widely studied subject. In particular, h(T), the entropy of T, is a well understood object. Let Gamma contained in X x X be a closed set. The Gamma induces certain dynamics and entropy h(Gamma). If X is a finite set then Gamma can be naturally viewed as a directed graph. That is, if X = (1, ..., n) then Gamma consists of all directed arcs i approaches j so that (i,j) is a member of Gamma. Then Gamma induces a subshift of finite type which is a widely studied subject. However, in the case that X is infinite, the subject of dynamic of Gamma and its entropy are relatively new. The first paper treating the entropy of a graph is due to Gromov. In that context, X is a compact Riemannian manifold and Gamma can be viewed as a Riemannian submanifold. The object of this paper is to study the entropy of a corresponding map induced by Gamma. As we shall see, this entropy unifies in a natural way the notion of the entropy of a standard continuous map T : X leads to X and a (finitely generated) semigroup or group of continuous transformations S : X leads to X. NTIS

N94-35764 Institut des Hautes Etudes Scientifiques, Bures-sur-Yvette (France).

MODULI SPACE OF MONOPOLES AND SOME INVARIANTS OF 3-MANIFOLDS

R. G. Wang Feb. 1994 42 p Limited Reproducibility: More than 20% of this document may be affected by microfiche quality
(PB94-167756; IHES/M/94/9) Avail: Issuing Activity (National Technical Information Service (NTIS))

Monopoles are natural objects on asymptotically Euclidean 3-manifolds. Let X be a closed and oriented Riemannian 3-manifold and M be a connected sum of X and the Euclidean space R(sup 3). Then monopoles exist naturally on M and can be considered as static instantons on the 4-mainfold M x R. The monopoles form an interesting moduli space and the moduli space can be used to study the topology of X. In the case of R(sup 3), the moduli space has been described by Donaldon, which is diffeomorphic to a certain space of rational functions of one complex variable. In a paper by Ernst, the moduli space of charge 1 monopoles on M is figured. It can be used, for example, to prove a generalization of the theorem of Schoen and Yau that asymptotically flat 3-manifolds with non-negative Ricci curvature are diffeomorphic to R(sup 3). NTIS

N94-35774# Kyoto Univ., Uji (Japan). Research Center of Yukawa Inst. for Theoretical Physics.

ON A GENERALIZED BOOTSTRAP PRINCIPLE

E. Corrigan (Durham Univ., England.), R. Sasaki (Durham Univ., England.), and P. E. Dorey (European Organization for Nuclear Research, Geneva, Switzerland.) 1993 25 p
(DE94-727517; YITP/U-93-9; DTP-93/19) Avail: CASI HC A03/MF A01

The S-matrices for non-simply-laced affine Toda field theories are considered in the context of a generalized bootstrap principle. The

S-matrices, and in particular their poles, depend on a parameter whose range lies between the Coxeter numbers of dual pairs of the corresponding non-simply-laced algebras. It is proposed that only odd order poles in the physical strip with positive coefficients throughout this range should participate in the bootstrap. All other singularities have an explanation in principle in terms of a generalized Coleman-Thun mechanism. Besides the S-matrices introduced by Delius, Grisaru and Zanon, the missing case (F(sub 4)(sup 1), e(sub 6)(sup 2)), is also considered and provides many interesting examples of pole generation. DOE

N94-35789# Joint Inst. for Nuclear Research, Dubna (USSR). Lab. of Computing Techniques and Automation.
INVERSE PROBLEM FOR SYMMETRIC TRIDIAGONAL MATRICES. CALCULATION OF DISCRETE ORTHOGONAL POLYNOMIAL SYSTEM WITH ARBITRARY WEIGHT
S. I. Serdyukova 1992 24 p
(DE94-612434; JINR-R-11-92-434) Avail: CASI HC A03/MF A01 (US Sales Only)

Numerical methods for reconstruction of symmetric tridiagonal matrices with given eigenvalues are studied. DOE

N94-35821 Helsinki Univ. of Technology, Espoo (Finland). Inst. of Mathematics.
A NOTE ON HIGH ORDER SCHEMES FOR ONE DIMENSIONAL WAVE EQUATION
J. Tuomela Dec. 1993 15 p Limited Reproducibility: More than 20% of this document may be affected by microfiche quality
(ISSN 0784-3143)
(PB94-171006; RR-A327,; ISBN-951-22-1927-1) Avail: Issuing Activity (National Technical Information Service (NTIS))

We construct stable schemes of arbitrarily high order for the heterogeneous one-dimensional wave equation. NTIS

N94-35934# International Centre for Theoretical Physics, Trieste (Italy).
SOME THEOREMS ON A CLASS OF HARMONIC MANIFOLDS
M. S. Rahman (Jahangirnagar Univ., Dacca, Bangladesh.) and Weihuan Chen (Peking Univ., China.) Aug. 1993 9 p
(DE94-611102; IC-93/268) Avail: CASI HC A02/MF A01 (US Sales Only)

A class of harmonic n-manifold, denoted by HM(sub n), is, in fact, focussed on a Riemannian manifold with harmonic curvature. A variety of results, with properties, on HM(sub n) is presented in a fair order. Harmonic manifolds are then touched upon, manifolds with recurrent Ricci curvature, biRicci-recurrent curvature and recurrent conformal curvature, and, as a consequence, a sequence of theorems is deduced. DOE

N94-36012 Wisconsin Univ., Madison, WI. Center for Mathematical Sciences.
GAUSS ELIMINATION BY SEGMENTS AND MULTIVARIATE POLYNOMIAL INTERPOLATION
C. DeBoor Apr. 1994 24 p Limited Reproducibility: More than 20% of this document may be affected by microfiche quality
(Contract DAAL03-90-G-0090)
(AD-A278646; CMS-TSR-94-10) Avail: Issuing Activity (Defense Technical Information Center (DTIC))

The construction of a polynomial interpolant to data given at finite pointsets (or, most generally, to data specified by finitely many linear functionals) is considered, with special emphasis on the linear system to be solved. Gauss elimination by segments (i.e., by groups of columns rather than by columns) is proposed as a reasonable means for obtaining a description of all solutions and for seeking out solutions with 'good' properties. A particular scheme, due to Amos Ron and the author, for choosing a particular polynomial interpolating space in dependence on the given data points, is seen to be singled out by requirements of degree-reduction, scale-invariance, and a certain orthogonality requirement. The close connection, between this particular construction of a polynomial interpolant and the construction of an H-basis for the ideal of all polynomials which vanish at the given data points, is also discussed. DTIC

N94-36076# Academy of Sciences of the Ukraine, Kiev. Inst. for Theoretical Physics.
Q-DEFORMATIONS OF THE VENEZIANO MODEL
L. L. Jenkovszky, A. V. Mishchenko, and B. V. Struminskij 1993 13 p Submitted for publication
(DE94-616769; ITP-93-36E) Avail: CASI HC A03/MF A01 (US Sales Only)

By q-deforming the narrow-resonance Veneziano dual model, we obtain an expression for the scattering amplitude exhibiting duality, crossing symmetry and a more realistic spectrum of resonances corresponding to non-linear Regge trajectories. DOE

N94-36100 Academy of Sciences (USSR), Novosibirsk (USSR). Inst. Yadernoj. Fiziki.
THE 2+1-DIMENSIONAL INTEGRABLE GENERALIZATION OF THE SINE-GORDON EQUATION
B. G. Konopelchenko and V. G. Dubrovskij 1992 53 p Submitted for publication Limited Reproducibility: More than 20% of this document may be affected by microfiche quality
(DE94-611074; BUDKERINP-92-1; Preprint 92-1) Avail: CASI HC A04 (US Sales Only)

The 2+1-dimensional integrable generalization of the sine-Gordon equation symmetric in the spatial variables is studied by the inverse spectral transform method. The solutions with functional parameters, plane solitons (kinks) and plane breathers are constructed by the dressing method. The initial value problem for this equation with the constant boundaries is solved in both cases (sigma)(sup 2)=(+-)1. DOE

N94-36270# California Univ., Berkeley. Lawrence Berkeley Lab, CA.
QUANTUM GROUPS, NON-COMMUTATIVE DIFFERENTIAL GEOMETRY AND APPLICATIONS Ph.D. Thesis
P. Schupp (California Univ., Berkeley, CA.) Dec. 1993 134 p
(Contract DE-AC03-76SF-00098)
(DE94-011358; LBL-34942; UCB-PTH-93/35) Avail: CASI HC A07/MF A02

The topic of this thesis is the development of a versatile and geometrically motivated differential calculus on non-commutative or quantum spaces, providing powerful but easy-to-use mathematical tools for applications in physics and related sciences. A generalization of unitary time evolution is proposed and studied for a simple 2-level system, leading to non-conservation of microscopic entropy, a phenomenon new to quantum mechanics. A Cartan calculus that combines functions, forms, Lie derivatives and inner derivations along general vector fields into one big algebra is constructed for quantum groups and then extended to quantum planes. The construction of a tangent bundle on a quantum group manifold and an BRST type approach to quantum group gauge theory are given as further examples of applications. The material is organized in two parts: Part 1 studies vector fields on quantum groups, emphasizing Hopf algebraic structures, but also introducing a 'quantum geometric' construction. Using a generalized semi-direct product construction we combine the dual Hopf algebras A of functions and U of left-invariant vector fields into one fully bicovariant algebra of differential operators. The pure braid group is introduced as the commutant of Delta(U). It provides invariant maps A yields U and thereby bicovariant vector fields, casimirs, and metrics. This construction allows the translation of undeformed matrix expressions into their less obvious quantum algebraic counterparts. We study this in detail for quasitriangular Hopf algebras, giving the determinant and orthogonality relation for the 'reflection' matrix. Part 2 considers the additional structures of differential forms and finitely generated quantum Lie algebras – it is devoted to the construction of the Cartan calculus, based on an undeformed Cartan identity. DOE

N94-36416# Joint Inst. for Nuclear Research, Dubna (USSR). Lab. of Theoretical Physics.
VARIATIONAL METHOD IN RELATIVISTIC TWO-BODY PROBLEM
V. M. Vinogradov 1992 6 p
(DE94-612462; JINR-R-4-92-405) Avail: CASI HC A02/MF A01 (US Sales Only)

Formulation of the variational principle is proposed for a new class of relativistic differential-difference equations. DOE

N94-36424 Rice Univ., Houston, TX.
COMPUTATIONAL MATHEMATICS LABORATORY FOR MULTISCALE ANALYSIS Final Technical Report, 1 Aug. 1990 - 30 Sep. 1993
Raymond Wells, Jr. 11 Feb. 1994 29 p Limited Reproducibility: More

than 20% of this document may be affected by microfiche quality
(Grant AF-AFOSR-0334-90)
(AD-A278597; AFOSR-94-0249TR) Avail: Issuing Activity (Defense Technical Information Center (DTIC))

Activities carried out in support of research done by the Computational Mathematics Laboratory (CML) at Rice University are summarized. Specific topics addressed include: (1) fundamental wavelet research; (2) applications of wavelets to partial differential equations; and (3) applications of wavelets to digital signal processing. DTIC

N94-36425 Columbia Univ., New York, NY. Dept. of Computer Science.
CAN WE BREAK INTRACTABILITY USING RANDOMIZATION OR THE AVERAGE CASE SETTING? Final Report, 1 Sep. 1991 - 30 Sep. 1993
Joseph F. Traub 30 Sep. 1993 30 p Limited Reproducibility: More than 20% of this document may be affected by microfiche quality
(Grant AF-AFOSR-0347-91)
(AD-A278598; AFOSR-94-0245TR) Avail: Issuing Activity (Defense Technical Information Center (DTIC))

The following papers cover results of the researchers and make up the final report: (1) 'A Surprising and Important New Result'; (2) 'Recent Progress in Information-Based Complexity'; and (3) 'Breaking Intractability'. DTIC

N94-36432# Argonne National Lab., IL.
PERIODIZED WAVELETS
G. Schlossnagle (Johns Hopkins Univ., Baltimore, MD.), J. M. Restrepo, and G. K. Leaf Dec. 1993 20 p
(Contract W-31-109-eng-38)
(DE94-010365; ANL-93/34) Avail: CASI HC A03/MF A01

The properties of periodized Daubechies wavelets on (0,1) are detailed and contrasted against their counterparts which form a basis for L(exp 2)(R). Numerical examples illustrate the analytical estimates for convergence and demonstrate by comparison with Fourier spectral methods the superiority of wavelet projection methods for approximations. The analytical solution to inner products of periodized wavelets and their derivatives, which are known as connection coefficients, is presented, and several tabulated values are included. DOE

N94-35606*# Air Force Inst. of Tech., Wright-Patterson AFB, OH. Dept. of Aeronautics and Astronautics.
MODAL DECOMPOSITION OF HAMILTONIAN VARIATIONAL EQUATIONS
William E. Wiesel *In* NASA. Goddard Space Flight Center, Flight Mechanics/Estimation Theory Symposium, 1994 May 1994 p 3-13
(For primary document see N94-35605 11-13)
Avail: CASI HC A03/MF A04

N94-35897*# Houston Univ., TX.
NUMERICAL METHODS FOR MULTIBODY SYSTEMS
Roland Glowinski and Mahmoud G. Nasser *In* NASA. Langley Research Center, NASA Workshop on Distributed Parameter Modeling and Control of Flexible Aerospace Systems Jun. 1994 p 571-585 Sponsored in part by Texas Board of Education (For primary document see N94-35865 11-18)
(Contract NAS9-17900)
Avail: CASI HC A03/MF A06

65 STATISTICS AND PROBABILITY

Includes data sampling and smoothing; Monte Carlo method; and stochastic processes.

N94-35536 Oxford Univ. (England). Programming Research Group.
PROBABILITIES AND PRIORITIES IN TIMED CSP
G. Lowe Nov. 1993 228 p See also PB90-229592 and PB92-208818
(PB94-169216; PRG-111) Copyright Avail: Issuing Activity (National Technical Information Service (NTIS))

In this thesis, the authors present two languages that are refinements of Reed and Roscoe's language of Timed Communicating Sequential Processes (CSP): a probabilistic language, and a prioritized language. They begin by describing the prioritized language and its semantic model. The syntax is based upon that of Timed CSP except some of the operators are refined into biased operators. They then describe the probabilistic language, which is built on top of the prioritized language. A complete compositional proof system is presented for the prioritized language, which can be used for proving behavioral specifications are met. This proof system can also be used to prove non-probabilistic specifications are met by probabilistic processes, via an abstraction theorem between the two models. An abstraction theorem is presented relating the Prioritized Model to the Timed Failures Model. This enables unprioritized processes to be refined into prioritized ones. Finally, a compositional proof system is presented for the probabilistic language. NTIS

N94-35575 Air Force Inst. of Tech., Wright-Patterson AFB, OH. School of Engineering.
POINT AND INTERVAL ESTIMATION OF SERIES SYSTEM RELIABILITY USING SMALL DATA SETS M.S. Thesis
Craig J. Willits Mar. 1994 95 p Limited Reproducibility: More than 20% of this document may be affected by microfiche quality
(AD-A278647; AFIT/GOR/ENC/ENS/94M-19) Avail: Issuing Activity (Defense Technical Information Center (DTIC))

This investigation explored the relative performance of several small-sample point and interval estimators for series system reliability. Among point estimators, the maximum likelihood estimator (MLE) was compared to the corresponding Bayes estimator. In addition, four interval estimators were compared: Easterling's modified maximum likelihood integer estimator; the Lindstrom-Madden estimator; and Bayesian probability interval estimators constructed using approximate beta and Bayes Monte Carlo empirical posterior densities. The relative performance of the point estimators was assessed by comparing their mean square errors. For the four interval estimators, the interval coverage probability and the average interval lower bound were examined. The values of these performance measures were generated for 32 representative series systems using Monte Carlo simulation. The results of the Monte Carlo study showed that the accuracy of the available prior information determines whether a Bayesian or a classical approach should be used to estimate series system reliability. If there is high confidence that the mean of each component prior distribution is within 20 percent of the true component reliability, Bayesian point and interval estimators constructed from an approximate beta posterior should be used. Otherwise, the MLE point estimator and the Lindstrom-Madden interval estimator should be chosen. DTIC

N94-35675 Naval Postgraduate School, Monterey, CA. Dept. of Administrative Sciences.
CRAMER-VON MISES VARIANCE ESTIMATORS FOR SIMULATIONS
David Goldsman, Keebom Kang, and Andrew F. Seila Sep. 1993 27 p Limited Reproducibility: More than 20% of this document may be affected by microfiche quality
(AD-A278799; NPS-AS-93-028) Avail: Issuing Activity (Defense Technical Information Center (DTIC))

We study estimators for the variance parameter sigma(2) of a stationary process. The estimators are based on weightings yield estimators that are 'first-order unbiased' for sigma(2). We derive an expression for the asymptotic variance of the new estimators; this expression is then used to obtain the first-order unbiased estimator having the smallest variance among fixed-degree polynomial weighting functions. Although our work is based on asymptotic theory, we present exact and empirical examples to demonstrate the new estimators' small-sample robustness. DTIC

N94-35691 Air Force Inst. of Tech., Wright-Patterson AFB, OH. School of Engineering.
A COMPARISON OF VARIABLE SELECTION CRITERIA FOR MULTIPLE LINEAR REGRESSION: A THIRD SIMULATION STUDY M.S. Thesis
Ertem Mutlu Mar. 1994 184 p Limited Reproducibility: More than 20% of this document may be affected by microfiche quality
(AD-A278678; AFIT/GOR/ENS/94M-08) Avail: Issuing Activity (Defense Technical Information Center (DTIC))

The goal of this research is to introduce and study a modification of Miller's Method which we call the Modified-Miller's method (MM method), study two step subset selection procedures, these of which apply Miller's Method in the first step and employs another method (Minimum MSE or Minimum Sp or Minimum Cp) in the second step and these of which employ another method (Minimum MSE or Minimum Sp or Minimum Cp) in the first step and applies Miller's Method in the second step. The results of all techniques will be compared including the results of the previous simulation studies done by Hanson in 1988 and by Woollard in 1993. In the researches mentioned above, Minimum MSE, Minimum Sp, Minimum Cp, and Miller's method were studied. Each of the techniques studied in this thesis effort was applied on generated data with known multicollinearities, random predictors, variances, sample sizes and error terms. The performance of each method is evaluated by employing two performance measurements. The first one, denoted PM (Performance Measurement), calculates the percentage of correct variables in a model. The second one, denoted FM (Full Model) calculates the ratio of perfect models, the set of which is (X1 X2 X3) for this research, to the number of all models. The Response Surface Methodology technique was employed to set up a 2(exp 6) full factorial experiment in order to study the effectiveness of each subset selection method with respect to the known data characteristics. Including the results of Hansen's and Woollard's study, eleven different subset selection techniques were compared. Considering the PM and FM measurements together, the CpMLR (method which is a two stage subset selection method) performs the best, and with a very small difference the SpMLR method (which is another two stage subset selection procedure) is close behind the CpMLR. The Modified-Miller's Method (which is a one step subset selection method) performs the third best. Author (DTIC)

N94-36235# California Univ., Berkeley. Lawrence Berkeley Lab, CA.
RECURSIVE RECOVERY OF MARKOV TRANSITION PROBABILITIES FROM BOUNDARY VALUE DATA Ph.D. Thesis
S. K. Patch Apr. 1994 120 p
(Contract DE-AC03-76SF-00098)
(DE94-011914; LBL-35495) Avail: CASI HC A06/MF A02

In an effort to mathematically describe the anisotropic diffusion of infrared radiation in biological tissue Gruenbaum posed an anisotropic diffusion boundary value problem in 1989. In order to accommodate anisotropy, he discretized the temporal as well as the spatial domain. The probabilistic interpretation of the diffusion equation is retained; radiation is assumed to travel according to a random walk (of sorts). In this random walk the probabilities with which photons change direction depend upon their previous as well as present location. The forward problem gives boundary value data as a function of the Markov transition probabilities. The inverse problem requires finding the transition probabilities from boundary value data. Problems in the plane are studied carefully in this thesis. Consistency conditions among the data are derived. These conditions have two effects: they prohibit inversion of the forward map but permit smoothing of noisy data. Next, a recursive algorithm which yields a family of solutions to the inverse problem is detailed. This algorithm takes advantage of all independent data and generates a system of highly nonlinear algebraic equations. Pluecker-Grassmann relations are instrumental in simplifying the equations. The algorithm is used to solve the 4 x 4 problem. Finally, the smallest nontrivial problem in three dimensions, the 2 x 2 x 2 problem, is solved. DOE

66 SYSTEMS ANALYSIS

Includes mathematical modeling; network analysis; and operations research.

N94-36337# Deutsche Forschungs- und Versuchsanstalt fuer Luft- und Raumfahrt, Cologne (Germany). Inst. for Aerospace Medicine.
EXTENDED RANGE OPERATIONS: A REVIEW OF RECENT DEVELOPMENTS
A. Samel and H. M. Wegmann *In* AGARD, Recent Advances in Long Range and Long Endurance Operation of Aircraft Nov. 1993 10 p
(For primary document see N94-36321 11-05)
Copyright Avail: CASI HC A02/MF A03

67 THEORETICAL MATHEMATICS

Includes topology and number theory.

N94-35760 Institut des Hautes Etudes Scientifiques, Bures-sur-Yvette (France).
CAUCHY AND INVARIANT MEASURE PROBLEM FOR THE PERIODIC ZAKHAROV SYSTEM
J. Bourgain Nov. 1993 29 p Limited Reproducibility: More than 20% of this document may be affected by microfiche quality
(PB94-167707; IHES/M/93/63) Avail: Issuing Activity (National Technical Information Service (NTIS))

The purpose of this preliminary paper is to prove local and global existence and regularity theorems for the one-dimensional Zakharov Model in the space periodic case. Apparently no results were known so far on this problem, if one considers the periodic setting. The model equations are suspected to be nonintegrable. The technique used here is a Fourier analysis approach. In particular, we prove a local wellposedness theorem. NTIS

N94-36234# California Univ., Berkeley. Lawrence Berkeley Lab, CA.
RECENT PROGRESS IN IRRATIONAL CONFORMAL FIELD THEORY
M. B. Halpern Sep. 1993 5 p Presented at the 1993 International Conference on Strings, Berkeley, CA, 25-29 May 1993
(Contract DE-AC03-76SF-00098)
(DE94-011908; LBL-34610; CONF-9305317-2) Avail: CASI HC A01/MF A01

I review the foundations of irrational conformal field theory (ICFT), which includes rational conformal field theory as a small subspace. Highlights of the review include the Virasoro master equation, the Ward identities for the correlators of ICFT, and solutions of the Ward identities. In particular, I discuss the solutions for the correlators of the g/h coset construction and the correlators of the affine-Sugawara nests on g contains h(sub 1) contains ... contains h(sub n). Finally, I discuss the recent global solution for the correlators of all the ICFT's in the master equation. DOE

N94-36307# International Centre for Theoretical Physics, Trieste (Italy).
N = 4 SUPERSYMMETRY FROM THE QUANTUM AFFINE ALGEBRA U(SUB q)(A-CIRCUMFLEX(SUP 1)(SUB 3))
A. ElHassouni (Mohammed V Univ., Rabat, Morocco.), Y. Hassouni (Mohammed V Univ., Rabat, Morocco.), and M. Zakkari (Mohammed V Univ., Rabat, Morocco.) Jul. 1993 9 p
(DE94-611145; IC-93/211) Avail: CASI HC A02/MF A01 (US Sales Only)

The quantized algebra U(sub q)(A-circumflex(sup (1))(sub 3)) is analyzed. It is shown that the U(sub q)(A-circumflex(sup (1))(sub 3)) and N = 4 SUSY algebras have many similarities for special values of q, namely q(sup 2 alpha) = -1 where alpha is a continuous parameter. Moreover, U(sub q)(A-circumflex(sup (1))(sub 3)) can be endowed with at most three independent spectral parameter Hopf structures. The adjoint action of U(sub q)(A-circumflex(sup (1))(sub 3)) is given. DOE

70 PHYSICS (GENERAL)

For precision time and time interval (PTTI) see *35 Instrumentation and Photography;* for geophysics, astrophysics or solar physics see *46 Geophysics, 90 Astrophysics,* or *92 Solar Physics.*

N94-35743 Cornell Univ., Ithaca, NY. Dept. of Computer Science.
A DETERMINIZABLE CLASS OF TIMED AUTOMATA Interim Report
Rajeev Alur (Bell Telephone Labs., Inc., Murray Hill, NJ.), Limor Fix, and Thomas A. Henzinger 1993 14 p Limited Reproducibility: More than 20% of this document may be affected by microfiche quality
(Contract N00014-91-J-1219)
(AD-A278858) Avail: Issuing Activity (Defense Technical Information Center (DTIC))

We introduce the class of event-recording timed automata (ERA). An event-recording automaton contains, for every event 'a', a clock that records the time of the last occurrence of alpha. The class ERA is, on one hand, expressive enough to model (finite) timed transition systems and, on the other hand, determinizable and closed under all boolean operations. As a result, the language inclusion problem is decidable for event-recording automata. We present a translation from timed transition systems to event-recording automata, which leads to an algorithm for checking if two timed transition systems have the same set of timed behaviors. We also consider event-predicting timed automata (EPA), which contain clocks that predict the time of the next occurrence of an event. The claw of event-clock automata (ECA), which contain both event-recording and event-predicting clocks, is a suitable specification language for real-time properties. We provide an algorithm for checking if a timed automaton meets a specification that is given as an event-clock automaton. DTIC

N94-35955# Joint Inst. for Nuclear Research, Dubna (USSR). Lab. of Computing Techniques and Automation.
ON NEW THEORIES OF PHYSICAL VACUUM
V. S. Barashenkov and M. Z. Yurev 1992 17 p
(DE94-616613; JINR-R-2-92-485) Avail: CASI HC A03/MF A01 (US Sales Only)

The recently published papers and monographs by Akimov, Acjukowskij, Weinik, Gerlovich et al. containing the attempts to construct a new theory of elementary particles and physical vacuum by means of refusal from the known quantum and relativistic principles are discussed. DOE

N94-35956# Institute of Nuclear Physics, Krakow (Poland).
THE RELATIVISTIC INVARIANT AND THE GALILEAN MASS OF BODIES
E. Kapuscik, J. Kempczynski, and A. Horzela Feb. 1992 12 p
(DE94-616615; INP-1577/PH) Avail: CASI HC A03/MF A01 (US Sales Only)

We generalize the concept of the Galilean mass to the relativistic case. In the case of inequality of Galilean and inertial masses we calculate the relativistic invariant being constant along the trajectory of the moving body. It enables us to define an invariant measure of inertia of bodies. DOE

N94-36003 National Inst. of Standards and Technology. Gaithersburg, MD. Chemical Science and Technology Lab.
CSTL TECHNICAL ACTIVITIES, 1991
H. S. Hertz and B. I. Diamondstone Feb. 1992 353 p Presented to the Board on Assessment of NIST Programs, 11-12 Feb. 1992 See also PB93-173482 Limited Reproducibility: More than 20% of this document may be affected by microfiche quality
(PB94-160769) Avail: CASI HC A16

The report summarizes the technical activities of the Chemical Science and Technology Laboratory at the National Institute of Standards and Technology. It emphasizes activities over the Fiscal Year 1991 in the Biotechnology Division, the Chemical Engineering Division, the Chemical Kinetics and Thermodynamics Division, the Inorganic Analytical Research Division, the Organic Analytical Research Division the Process Measurements Division, the Surface and Microanalysis Division, and the Thermophysics Division. NTIS

N94-36201# Lawrence Livermore National Lab., CA.
X RAY RADIOGRAPHIC IMAGING OF HYDRODYNAMIC PHENOMENA IN RADIATION DRIVEN MATERIALS: SHOCK PROPAGATION AND SHEAR FLOW
B. A. Hammel, J. D. Kilkenny, D. Munro, B. A. Remington, and R. J. Wallace 22 Nov. 1993 21 p Presented at the Fall Meeting of the Plasma Physics Division of the American Physical Society, St. Louis, MO, 1-5 Nov. 1993
(Contract W-7405-eng-48)
(DE94-010891; UCRL-JC-114456; CONF-931132-4) Avail: CASI HC A03/MF A01

One and two dimensional, time resolved x-ray radiographic imaging at high photon energy (5-7 keV) are used to study shock propagation and the effects of shear flow in solid density samples which are driven by x-ray ablation with the Nova laser. By backlighting the samples with x-rays and observing the increase in sample areal density due to shock compression, we directly measure the trajectory of strong shocks (approximately 40 Mbar) in flight, in solid density plastic samples. Doping a section of the planar samples with high-Z material (Br) provides radiographic contrast, allowing a measurement of the shock induced motion of the doped material. Instability growth due to shear flow at an interface is investigated by imbedding a metal wire in a plastic sample parallel to the direction of material motion. Time resolved radiographic measurements are made with either a slit-imager coupled to an x-ray streak camera or a pinhole camera coupled to a gated microchannel plate detector, providing approximately 10 microns spatial and approximately 100 ps temporal resolution. DOE

N94-36204# Sandia National Labs., Albuquerque, NM.
MAGNETIC PROPERTIES OF NANOSIZE IRON CLUSTERS
E. L. Venturini, J. P. Wilcoxon, and P. P. Newcomer 1993 6 p Presented at the Spring Meeting of the Materials Research Society, San Francisco, CA, 4-8 Apr. 1994
(Contract DE-AC04-94AL-85000)
(DE94-011329; SAND-93-2711C; CONF-940411-13) Avail: CASI HC A02/MF A01

Isolated, monodisperse alpha-Fe clusters between 1.4 and 15 nm in diameter were prepared inside inverse micelles using an oil-continuous, nonaqueous system. The magnetic properties of these clusters were studied in a SQUID magnetometer as a function of cluster size, temperature, and applied magnetic field. The blocking temperature, coercive field and remanent moment of 12.5 nm Fe clusters in inverse micelles are significantly lower than those reported for clusters of similar alpha-Fe core size but with a surface oxide. The novel synthesis technique may yield metallic clusters with essentially intrinsic magnetic properties. DOE

N94-36427 Naval Research Lab., Washington, DC.
ANALYSIS OF RECENT AGILE MIRROR DATA Interim Report
J. Mathew, R. A. Meger, and J. A. Gregor 28 Mar. 1994 47 p Limited Reproducibility: More than 20% of this document may be affected by microfiche quality
(AD-A278758; NRL/MR/6750-94-7461) Avail: Issuing Activity (Defense Technical Information Center (DTIC))

Recent data taken with the agile mirror hollow cathode setup using a crossatron driven pulser show that acceptable reflected X-band microwave signals can be obtained under a narrow range of experimental parameters. The 15-cm x 25-cm x 1-cm planar discharge in 150 mTorr of air yields quite reproducible results in the presence of an axial magnetic field of approximately 100 Gauss. The discharge tends to turn off around 150 microseconds, but if the voltage is left on, the discharge restrikes after approximately 0.5 ms. The turn-off is not observed at higher pressure, but the reflected microwave signals show time variations at these pressures. It is believed that the dimensions of the present hollow cathode are not optimal. A cathode with an adjustable cavity is being built to investigate the scaling of the cathode dimensions with pressure and magnetic field for the full size 50-cm x 50-cm agile mirror experiment. There are some indications that, particularly at the lower pressures, the discharge column is beam dominated. DTIC

N94-36171*# National Aeronautics and Space Administration. Goddard Space Flight Center, Greenbelt, MD.
MEASUREMENT OF THE DECAY RATE OF THE SiH FEATURE AS A FUNCTION OF TEMPERATURE Abstract Only
Joseph A. Nuth, III and George F. Kraus *In* Lunar and Planetary Inst., The Twenty-Fifth Lunar and Planetary Science Conference. Part 2: H-O 1994 p 1013-1014 (For primary document see N94-36136 11-91)
Avail: CASI HC A01/MF A06

N94-36407*# Virginia Polytechnic Inst. and State Univ., Blacksburg, VA. Dept. of Mechanical Engineering.
MEASUREMENT OF A SURFACE HEAT FLUX AND TEMPERATURE
R. M. Davis, G. J. Antoine, T. E. Diller, and A. L. Wicks *In* NASA. Langley Research Center, National Educators' Workshop: Update 1993. Standard Experiments in Engineering Materials Science and Technology Apr. 1994 p 203-218 (For primary document see N94-36398 11-23)
Avail: CASI HC A03/MF A04

71 ACOUSTICS

Includes sound generation, transmission and attenuation.
For noise pollution see *45 Environmental Pollution.*

N94-35770 Lawrence Livermore National Lab., CA.
AN ELECTROMAGNETIC FINITE DIFFERENCE TIME DOMAIN ANALOG TREATMENT OF SMALL SIGNAL ACOUSTIC INTERACTIONS
K. Kunz (Pennsylvania State Univ., University Park, PA.), D. Steich (Pennsylvania State Univ., University Park, PA.), K. Lewis, C. Landrum, and M. Barth 25 Mar. 1994 35 p Limited Reproducibility: More than 20% of this document may be affected by microfiche quality
(Contract W-7405-eng-48)
(DE94-009978; UCRL-ID-116945) Avail: CASI HC A03

Hyperbolic partial differential equations encompass an extremely important set of physical phenomena including electromagnetics and acoustics. Small amplitude acoustic interactions behave much the same as electromagnetic interactions for longitudinal acoustic waves because of the similar nature of the governing hyperbolic equations. Differences appear when transverse acoustic waves are considered; nonetheless, the strong analogy between the acoustic and electromagnetic phenomena prompted the development of a Finite Difference Time Domain (FDTD) acoustic analog to the existing electromagnetic FDTD technique. The advantages of an acoustic FDTD (AFDTD) code are as follows: (1) boundary condition-free treatment of the acoustic scatterer--only the intrinsic properties of the scatterer's material are needed, no shell treatment or other set of special equations describing the macroscopic behavior of a sheet of material or a junction, etc. are required; this allows completely general geometries and materials in the model. (2) Advanced outer radiation boundary condition analogs--in the electromagnetics arena, highly absorbing outer radiation boundary conditions were developed that can be applied with little modification to the acoustics arena with equal success. (3) A suite of preexisting capabilities related to electromagnetic modeling--this includes automated model generation and interaction visualization as its most important components and is best exemplified by the capabilities of the LLNL generated TSAR electromagnetic FDTD code. DOE

N94-35800 Naval Postgraduate School, Monterey, CA. Dept. of Electrical and Computer Engineering.
AN ITERATIVE EXTENSION OF PRONY'S METHOD FOR ARMA SIGNAL MODELING
Charles W. Therrien and Carlos H. Velasco 15 Sep. 1993 26 p Limited Reproducibility: More than 20% of this document may be affected by microfiche quality
(AD-A278841; NP-SEC-93-025) Avail: Issuing Activity (Defense Technical Information Center (DTIC))

A new iterative version of the Prony method is presented and shown to be exceptionally effective in finding ARMA models for acoustic data in the signal domain. The method is based on a quadratic type of gradient algorithm where it is shown that the gradient and Hessian are easily computed from the data. The new algorithm is found experimentally to have excellent convergence behavior. The performance of the algorithm is demonstrated and compared to that of the basic Prony method and to that of the Steiglitz and McBride iterative prefiltering algorithm on some recorded acoustic data. DTIC

N94-36031*# Research Inst. for Advanced Computer Science, Moffett Field, CA.
COMPUTATION OF HELICOPTER ROTOR ACOUSTICS IN FORWARD FLIGHT
Roger Strawn (Army Aviation Systems Command, Moffett Field, CA.) and Rupak Biswas Mar. 1994 11 p Presented at the 19th Army Science Conference, Orlando, FL, 20-24 Jun. 1994 Submitted for publication
(Contract NAS2-13721)
(NASA-CR-196132; NAS 1.26:196132; RIACS-TR-94-06) Avail: CASI HC A03/MF A01

This paper presents a new method for computing acoustic signals from helicopter rotors in forward flight. The aerodynamic and acoustic solutions in the near field are computed with a finite-difference solver for the Euler equations. A nonrotating cylindrical Kirchhoff surface is then placed around the entire rotor system. This Kirchhoff surface moves subsonically with the rotor in forward flight. The finite-difference solution is interpolated onto this cylindrical surface at each time step and a Kirchhoff integration is used to carry the acoustic signal to the far field. Computed values for high-speed impulsive noise show excellent agreement with model-rotor and flight-test experimental data. Results from the new method offer high accuracy with reasonable computer resource requirements. Author

N94-36176 Institut de Recherche de Transports, Bron (France).
PROCEEDINGS OF THE SIXTH INTERNATIONAL CONGRESS ON NOISE AS A PUBLIC HEATLH PROBLEM, VOLUME 3 Final Report, 5-9 Jul. 1993
Michel Vallet, ed. 9 Jul. 1993 626 p Proceedings held in Nice, France, 5-9 Jul. 1993 Limited Reproducibility: More than 20% of this document may be affected by poor print
(AD-A278218; CSP-93-1009-Vol-3) Avail: Issuing Activity (Defense Technical Information Center (DTIC))

This volume is the last of a series of 3 volumes intended to give information on the 6th International Congress on Noise as a Public Health Problem, which took place in Nice, France from July 5 to 9, 1993. Volume 3 is composed of the texts of the conference invited and the invited papers, as well as the personalities' addresses. The abstracts of the 9 sessions in French and English are also integrated in this volume. DTIC

N94-36320 Argonne National Lab., IL.
AN IMPROVED ASSESSMENT APPROACH FOR NOISE IMPACTS FROM STATIONARY POINT AND TRAFFIC SOURCES ON HUMANS AND WILDLIFE
Young-Soo Chang and K. C. Chun 1994 14 p Presented at the Annual Meeting and Exhibition of the Air and Waste Management Association, Cincinnati, OH, 19-24 Jun. 1994 Limited Reproducibility: More than 20% of this document may be affected by microfiche quality
(Contract W-31-109-eng-38)
(DE94-009728; ANL/EA/CP-82328; CONF-940632-8) Avail: CASI HC A03

This paper presents an improved, efficient approach for assessing noise impacts associated with a complex set of noise sources at multiple receptor locations; noise impacts from typical remedial activities at a contaminated industrial site are used as an example. The noise sources associated with remedial activities at the site and surrounding areas are described, the noise-propagation modeling methods and results are presented, and an impact assessment of the contaminated site is discussed with regard to applicable regulatory standards and individual and community responses. Also discussed is the improved noise assessment approach. The improved features demonstrated are automated approaches for (1) inputting long-term hourly meteorological data (e.g., 8760 hours for a one-year period) into a long-range noise-propagation model for computing noise-level increases at receptor locations and (2) analyzing potential individual and community responses to intrusive noises using the IAP and modified CNR. DOE

N94-35963*# National Aeronautics and Space Administration. Hugh L. Dryden Flight Research Facility, Edwards, CA.
ENGINE EXHAUST CHARACTERISTICS EVALUATION IN SUPPORT OF AIRCRAFT ACOUSTIC TESTING
Kimberly A. Ennix *In* NASA. Ames Research Center, 1993 Technical Paper Contest for Women. Gear Up 2000: Women in Motion Feb. 1994 p 13-20 (For primary document see N94-35961 11-99)
Avail: CASI HC A02/MF A02

72 ATOMIC AND MOLECULAR PHYSICS

Includes atomic structure, electron properties, and molecular spectra.

N94-35264*# Houston Univ., Clear Lake, TX.
COMPUTER IMAGE ANALYSIS OF ETCHED TRACKS FROM IONIZING RADIATION Final Report
George E. Blanford 7 Jun. 1994 9 p
(Grant NAG9-718)
(NASA-CR-196025; NAS 1.26:196025) Avail: CASI HC A02/MF A01

I proposed to continue a cooperative research project with Dr. David S. McKay concerning image analysis of tracks. Last summer we showed that we could measure track densities using the Oxford Instruments eXL computer and software that is attached to an ISI scanning electron microscope (SEM) located in building 31 at JSC. To reduce the dependence on JSC equipment, we proposed to transfer the SEM images to UHCL for analysis. Last summer we developed techniques to use digitized scanning electron micrographs and computer image analysis programs to measure track densities in lunar soil grains. Tracks were formed by highly ionizing solar energetic particles and cosmic rays during near surface exposure on the Moon. The track densities are related to the exposure conditions (depth and time). Distributions of the number of grains as a function of their track densities can reveal the modality of soil maturation. As part of a consortium effort to better understand the maturation of lunar soil and its relation to its infrared reflectance properties, we worked on lunar samples 67701,205 and 61221,134. These samples were etched for a shorter time (6 hours) than last summer's sample and this difference has presented problems for establishing the correct analysis conditions. We used computer counting and measurement of area to obtain preliminary track densities and a track density distribution that we could interpret for sample 67701,205. This sample is a submature soil consisting of approximately 85 percent mature soil mixed with approximately 15 percent immature, but not pristine, soil. Author

N94-35376# Los Alamos National Lab., NM.
FLUORESCENCE DETECTION OF SINGLE MOLECULES USING PULSED NEAR-FIELD OPTICAL EXCITATION AND TIME CORRELATED PHOTON COUNTING
W. P. Ambrose, P. M. Goodwin, J. C. Martin, and R. A. Keller 1994 11 p Presented at the OE/LASE 1994: Conference on Optics, Electro-Optics, and Laser Applications in Science and Engineering, Los Angeles, CA, 22-29 Jan. 1994
(Contract W-7405-eng-36)
(DE94-007553; LA-UR-94-695; CONF-940142-21) Avail: CASI HC A03/MF A01

Pulsed excitation, time correlated single photon counting and time gated detection are used in near-field optical microscopy to enhance fluorescence images and measure the fluorescence lifetimes of single molecules of rhodamine 6G on silica surfaces. Time gated detection is used to reject prompt scattered background and to improve the image signal to noise ratio.. The excited state lifetime of a single rhodamine 6G molecule is found to depend on the position of the near-field probe. We attribute the lifetime variations to spontaneous emission rate alterations by the fluorescence reflected from and quenching by the aluminum coated probe. DOE

N94-35566 Academy of Sciences (USSR), Leningrad (USSR). Inst. Yadernoj Fiziki.
LIMITATION ON THE MAGNETIC DIPOLE MOMENT OF THE REACTOR NEUTRINO [OGRANICHENIE NA MAGNITNYI DIPOL'NYJ MOMENT REAKTORNYKH NEJTRINO]
A. V. Derbin Jan. 1992 16 p In RUSSIAN Limited Reproducibility: More than 20% of this document may be affected by microfiche quality
(DE94-611171; LIYaF-1765) Avail: CASI HC A03 (US Sales Only)

Results of experiments on elastic scattering of reactor neutrino on electron are presented. Limitation on the magnetic moment of neutrino mu(sub nu) less than 1.8 x 10(exp -10) mu(sub B) was obtained. The existing uncertainty in the neutrino spectrum confines the possible limit on magnetic moment of approximately 3 x 10(exp -11) mu(sub B) value for detectors with approximately 0.1 MeV threshold. DOE

N94-35567 Academy of Sciences (USSR), Novosibirsk (USSR). Inst. Yadernij Fiziki.
BARYONIC CURRENTS AND THEIR CORRELATORS IN THE HEAVY QUARK EFFECTIVE THEORY
A. G. Grozin and O. I. Yakovlev 1992 26 p Limited Reproducibility: More than 20% of this document may be affected by microfiche quality
(DE94-612496; BUDKERINP-92-59) Avail: CASI HC A03 (US Sales Only)

The heavy-quark effective theory currents with the quantum numbers of the ground state baryons are discussed. One-loop anomalous dimensions are calculated, and exact one-loop matching to QCD currents is found. Two-point correlators of these currents are calculated taking into account d less than or equal to 9 terms of the OPE. Sum rules for heavy baryons Lambda(sub Q) and Sigma(sup (*))(sub Q) are analyzed. Three-point correlators of two baryonic currents and a heavy-heavy velocity changing current are calculated with the same accuracy. The baryonic Isgur-Wise form factors are estimated from the corresponding sum rules. DOE

N94-35569 Gosudarstvennyi Komitet po Ispolzovaniyu Atomnoi Energii, Serpukhov (USSR). Inst. Fiziki Vysokikh Ehnergij.
PROCEEDINGS OF 2ND WORKING MEETING: PHYSICS AT VLEPP, VOLUME 1 [TRUDY 2. RABOCHEGO SOVESHCHANIYA FIZIKA NA VLEHPP. TOM 1]
1992 194 p In ENGLISH and RUSSIAN Meeting held in Protvino, Russia, 2 Jun. 1992 Limited Reproducibility: More than 20% of this document may be affected by microfiche quality
(DE94-616200; INIS-RU-362-Vol-1; CONF-9206427-Vol-1) Avail: CASI HC A09 (US Sales Only)

Proceedings of the 2nd Working meeting, Physics at VLEPP, which was carried out on 2-4 June of 1992, has been published. A research program at coming e(sup +)e(sup -) colliders has been considered, and its comparison has been fulfilled. The problems of quantum chromodynamics, supersymmetry, search for new particles, and physics of t-quarks has been discussed. DOE

N94-35579# Instituto de Fisica Teorica, Sao Paulo (Brazil).
A THREE-BODY CALCULATION OF THE O-16(d,p)O-17 REACTION USING A TWO-TERM SEPARABLE POTENTIAL FOR THE s-WAVE NUCLEON-CORE INTERACTION
G. W. Bund and K. Ueta Nov. 1993 17 p
(DE94-616652; IFT-P-068-93) Avail: CASI HC A03/MF A01 (US Sales Only)

A one-term separable potential which produces the 2s(sub 1/2) single-particle bound state in O-17 generates an anomalous phase shift. The correct behavior of the phase shift may be restored by adding a second term to the original potential. Using the two-term separable s-wave potential and also a d-wave separable potential which reproduces the 1d(sub 5/2) single-particle state in O-17, a three-body calculation of the O-16(d,p)O-17 reaction is performed. DOE

N94-35580# Instituto de Fisica Teorica, Sao Paulo (Brazil).
RELATIVISTIC THREE-PARTICLE DYNAMICAL EQUATIONS. 2: APPLICATION TO THE TRINUCLEON SYSTEM
S. K. Adhikari and L. Tomio Nov. 1993 17 p
(DE94-616653; IFT-P-069-93) Avail: CASI HC A03/MF A01 (US Sales Only)

The contribution of relativistic dynamics on the neutron-deuteron scattering length and triton binding energy is calculated employing five sets tri nucleon potential models and four types of three-dimensional relativistic three-body equations suggested in the preceding paper. The relativistic correction to binding energy may vary a lot and even change sign depending on the relativistic formulation employed. The deviations of these observables from those obtained in nonrelativistic models follow the general universal trend of deviations introduced by off- and on-shell variations of two- and three-nucleon potentials in a nonrelativistic model calculation. Consequently, it will be difficult to separate unambiguously the effect of off-and on-shell variations of two and three-nucleon potentials on low-energy three-nucleon observables from the effect of relativistic dynamics. DOE

N94-35581# Instituto de Fisica Teorica, Sao Paulo (Brazil).
RELATIVISTIC THREE-PARTICLE DYNAMICAL EQUATIONS. 2: THEORETICAL DEVELOPMENT
S. K. Adhikari, L. Tomio, and T. Frederico Nov. 1993 32 p
(DE94-616654; IFT-P-070-93) Avail: CASI HC A03/MF A01 (US Sales Only)

Starting from the two-particle Bethe-Salpeter equation in the ladder approximation and integrating over the time component of momentum, three dimensional scattering integral equations satisfying constrains of relativistic unitarity and covariance are rederived. These equations were first derived by Weinberg and by Blankenbecler and Sugar. These two-particle equations are shown to be related by a transformation of variables. Hence it is shown to perform and relate dynamical calculation using these two equations. Similarly, starting from the Bethe-Salpeter-Faddeev equation for the three-particle system and integrating over the time component of momentum, several three dimensional three-particle scattering equations satisfying constraints of relativistic unitary and covariance are derived. Two of these three-particle equations are related by a transformation of variables as in the two-particle case. The three-particle equations obtained are very practical and suitable for performing relativistic scattering calculations. DOE

N94-35582# Instituto de Fisica Teorica, Sao Paulo (Brazil).
RADIATIVELY INDUCED ELECTRON AND ELECTRON-NEUTRINO MASSES
F. Pisano, V. Pleitez, and M. D. Tonasse Sep. 1993 15 p
(DE94-616775; IFT-P-059-93; IFUSP-P-1075) Avail: CASI HC A03/MF A01 (US Sales Only)

The generation of the neutrino and charged lepton masses is considered in the context of an SU(3) x U(1) electroweak model. In the minimal model at zeroth order neutrinos and one of the charged leptons are massless and the other two charged leptons are mass degenerate. In order to obtain the right mass spectrum it is necessary to add right-handed neutrinos. However, the masses of the electron and its neutrino partner arise via radiative corrections. DOE

N94-35583# Instituto de Fisica Teorica, Sao Paulo (Brazil).
THE SILENT PHASE TRANSITION IN MESONIC BAGS AND LATTICE THEORY
J. Dey (Carnegie-Mellon Univ., Pittsburgh, PA.), M. Dey (Carnegie-Mellon Univ., Pittsburgh, PA.), Carlos F. deAraujo, Jr. (Universidade Estadual de Paulista, Sao Paulo, Brazil.), and L. Tomio (Universidade Estadual de Paulista, Sao Paulo, Brazil.) Oct. 1993 10 p
(DE94-616852; IFT-P-066-93) Avail: CASI HC A02/MF A01 (US Sales Only)

It is shown that even the simple bag model is able to reproduce the lattice result for the masses and the sound velocity, at finite temperature, T, suggests that the transition point depends on the nature of the meson. It would be interesting to check the last conclusion in present day finite temperature lattice theory, since different transition points seem to be indicated by particle emission T in heavy ion reactions. DOE

N94-35589 Utah Univ., Salt Lake City, UT. Dept. of Chemistry.
A TWO-DIMENSIONAL MODEL FOR COLLISIONAL ENERGY TRANSFER IN BIMOLECULAR ION-MOLECULE DYNAMICS Technical Report No. 47
Monique R. Chacon-Taylor and Jack Simons 22 Apr. 1994 72 p Limited Reproducibility: More than 20% of this document may be affected by microfiche quality
(Contract N00014-89-J-1497)
(AD-A278913; TR-47-ONR) Avail: CASI HC A04

Guided ion beam kinetic energy thresholds in the ion-molecule reactions M(+) + H2 yields MH(+) + H where M(+) is a closed-shell atomic ion B(+), Al(+), or Ga(+), were found to exceed by 0.4 to about 5 eV the thermodynamic energy requirements (or the theoretically computed barrier heights) for these reactions. In addition, the formation of MD(+) occurs at a significantly lower threshold than MH(+) when M(+) reacts with HD. Moreover, the measured reaction cross-sections for the production of MH(+) or MD(+) product ions are very small (10(exp -17) to 10(exp -20) sq cm), being largest for B(+) and smallest for Ga(+). A previous paper from this group proposed that collisional to internal energy transfer is the rate-limiting step for this class of reactions. It also suggested, based on a dynamical resonance picture, that collisions occurring at or near C(sub 2v) symmetry are more effective than other collisions even though C(sub 2v) geometries provide no lower potential energy barriers than others. DTIC

N94-35593 Instituto de Fisica Teorica, Sao Paulo (Brazil).
NONADIABATIC NEUTRINO OSCILLATIONS REVISITED
M. M. Guzzo (Universidade Estadual de Campinas, Brazil.), J. Bellando (Universidade Estadual de Campinas, Brazil.), and V. M. Aquino (Universidade Estadual de Campinas, Brazil.) Aug. 1993 15 p Limited Reproducibility: More than 20% of this document may be affected by microfiche quality
(DE94-616649; IFT-P-051/93; DRC-TH-05/93) Avail: CASI HC A03 (US Sales Only)

Employing the Feynman procedure of ordered exponential operators and the stationary phase method to evaluate the multiple integrals involved, the level-crossing probability is calculated and the role of a resonance in the evolution of a two-level neutrino system analyzed. This procedure is compared with more conventional ones, like the Landau's method and the Ansatz of Kuo and Pantaleone and Petcov. It is that our results reproduce the correct extreme nonadiabatic limit and give the standard solutions in the adiabatic regime for any arbitrary matter density distributions. The case of solar neutrino propagation is discussed using the standard solar model predictions for the matter distribution in the Sun. DOE

N94-35594 Instituto de Fisica Teorica, Sao Paulo (Brazil).
SOME CONSEQUENCES IN WEAK PROCESSES OF THREE GENERATIONS MIXING IN THE LEPTONIC SECTOR
O. L. G. Peres, V. Pleitez, and R. Z. Funchal Oct. 1993 30 p Limited Reproducibility: More than 20% of this document may be affected by microfiche quality
(DE94-616650; IFT-P-060-93; IFUSP-P-1074) Avail: CASI HC A03 (US Sales Only)

The sensitivity of some weak processes to a Cabibbo-Kobayashi-Maskawa mixing in the leptonic sector is investigated. Values for mixing angles and masses compatible with several experimental accelerator data were found. In this context neutrino oscillations, cosmological and astrophysical consequences are discussed. DOE

N94-35595 Instituto de Fisica Teorica, Sao Paulo (Brazil).
COMPLEX KOHN VARIATIONAL PRINCIPLE FOR TWO-NUCLEON BOUND-STATE AND SCATTERING WITH THE TENSOR POTENTIAL
C. F. deAraujo, Jr., S. K. Adhikari, and L. Tomio Oct. 1993 20 p Limited Reproducibility: More than 20% of this document may be affected by microfiche quality
(DE94-616651; IFT-P-064-93) Avail: CASI HC A03 (US Sales Only)

Complex Kohn variational principle is applied to the numerical solution of the fully off-shell Lippmann-Schwinger equation for nucleon-nucleon scattering for various partial waves including the coupled (sup 3)S(sub 1)-(sup 3)D(sub 1) channel. Analytic expressions are obtained for all the integrals in the method for a suitable choice of expansion functions. Calculations with the partial waves (sup 1)S(sub 0), (sup 1)P(sub 1), (sup 1)D(sub 2), and (sup 3)S(sub 1)-(sup 3)D(sub 1) of the Reid soft core potential show that the method converges faster than other solution schemes not only for the phase shift but also for the off-shell t matrix elements. It is also shown that it is trivial to modify this variational principle in order to make it suitable for bound-stage calculations. The bound-state approach is illustrated for the (sup 3)S(sub 1)-(sup 3)D(sub 1) channel of the Reid soft-core potential for calculating the deuteron binding, wave function and the D state asymptotic parameters. DOE

N94-35649 Southeastern Univ. Research Association, Newport News, VA.
GOLDSTONE PION AND OTHER MESONS USING A SCALAR CONFINING INTERACTION
F. Gross (College of William and Mary, Williamsburg, VA.) and J. Milana (Maryland Univ., College Park, MD.) 1994 21 p Limited Reproducibility: More than 20% of this document may be affected by microfiche quality
(Contract DE-AC05-84ER-40150)
(DE94-010016; DOE/ER-40150/261; WM-94-102; CEBAF-TH-94-01; DOE/ER/40762-025) Avail: CASI HC A03

A covariant wave equation for q(bar q) interactions with an interaction kernel composed of the sum of constant vector and linear scalar confining interactions is solved for states with two quarks with identical mass. The model includes an NJL-like mechanism which links the dynamical breaking of chiral symmetry to the spontaneous generation of quark mass and the appearance of a low mass Goldstone pion. A novel feature of this approach is that it automatically explains the small mass of the pion even though the linear potential is a scalar interaction in Dirac space, and hence breaks chiral symmetry. Solutions for mesons composed of light quarks (pi, rho, and low lying excited states) and heavy quarks (rho(sub c), J/Psi, and low lying excited states) are presented and discussed. DOE

N94-35657 Cornell Univ., Ithaca, NY. Dept. of Chemistry.
VACUUM ULTRAVIOLET STUDIES OF MOLECULAR DYNAMICS Final Report, 1 Feb. 1992 - 30 Jan. 1994
Paul L. Houston 8 Apr. 1994 7 p Limited Reproducibility: More than 20% of this document may be affected by microfiche quality
(Contract F49620-92-J-0080)
(AD-A278940; AFOSR-94-0277TR) Avail: Issuing Activity (Defense Technical Information Center (DTIC))

Tunable vacuum ultraviolet radiation generated by four-wave mixing will be used to probe collisional energy transfer and photodissociation. Collisional relaxation of the S((sup 1)D) velocity distribution by rare gases has been measured to learn to what extent this simple process can be described by a hard-sphere, elastic interaction. E yielding V transfer was studied from S((sup 1)D) to CO and N2, both by examining the Doppler profile of the relaxed atoms and by direct measurement of the CO(v,J) distribution. Finally, the photodissociation of O3 and N2O have been investigated by monitoring the Doppler profiles of the resulting O((sup 1)D) lines. This integrated program of molecular dynamics studies using vacuum ultraviolet radiation has enhanced our knowledge both of the chemical physics of these basic processes and of the interaction of high energy photons with small molecules found in the upper atmosphere. DTIC

N94-35678 Utah Univ., Salt Lake City, UT. Dept. of Chemistry.
ANIONIC STATES OF LIFLI
Maciej Gutowski and Jack Simons 22 Apr. 1994 14 p Limited Reproducibility: More than 20% of this document may be affected by microfiche quality
(Contract N00014-89-J-1497)
(AD-A278830; TR-41) Avail: Issuing Activity (Defense Technical Information Center (DTIC))

Our ab initio theoretical calculations indicate that the LiFLi-anion possesses two bound states which are of 1 sigma g(+) and 3 sigma u(+) symmetry and which have vertical detachment energies of 0.94 and 0.89 eV, respectively. The LiFLi+ cation and the first four electronic states of the neutral LiFLi were also considered. The Renner-Teller splitting for the excited 2 pi u state of the neutral is reported. The neutral and both ions are thermodynamically stable. DTIC

N94-35682# Oak Ridge National Lab., TN.
LARGE SCALE ATOMISTIC FIRST PRINCIPLES STUDY OF ADSORPTION AND SURFACE DIFFUSION
V. Milman, S. J. Pennycook, D. E. Jesson, M. C. Payne, I. Stich, and M. H. Lee Feb. 1994 7 p Presented at the Mardi Gras Conference On: Toward Teraflop Computing and New Grand Challenge Applications, Baton Rouge, LA, 10-12 Feb. 1994
(Contract DE-AC05-84OR-21400)
(DE94-009450; CONF-940272-1) Avail: CASI HC A02/MF A01

Computer simulation of atomistic processes is an important tool in understanding the properties of condensed matter at a microscopic level. The best way to reproduce the rich variety of experimentally observed effects in the simulation is to use the quantum mechanical description of the ion-electron interactions in a solid. Such calculations although increasingly popular make high demands on the computing power available. The systems of practical interest to surface physics include at least hundreds (or even thousands) of atoms, and their ab initio study inevitably requires parallel supercomputers. In this paper the authors describe the total energy calculations of the adsorption and migration properties of a single Ge adatom on the Si(100) surface. This system is typical in complexity for modern large scale simulations and presents a good test case to show the methodology and its application to surface science problems. DOE

N94-35751# Joint Inst. for Nuclear Research, Dubna (USSR). Lab. of Gheoretical Physics.
THE STUDY OF THE LOCAL MAGNETIC FIELD IN THE OXIDE ALPHA-Bi2O3 BY THE mu SR-TECHNIQUE
V. G. Grebinnik, V. N. Duginov, and V. A. Zhukov 1992 10 p
(DE94-612636; JINR-R-14-92-334) Avail: CASI HC A02/MF A01 (US Sales Only)

The mu SR-investigation of the local magnetic field in the alpha-Bi2O3 was performed. The possible reason of the appearance of local magnetic field is partial covalent bounds in the alpha-Bi2O3. DOE

N94-35753 Utah Univ., Salt Lake City, UT. Dept. of Chemistry.
VERTICAL ELECTRON DETACHMENT ENERGIES FOR OCTAHEDRAL CLOSED-SHELL MULTIPLY CHARGED ANIONS
Maciej Gutowski, A. I. Boldyrev, J. V. Ortiz, and Jack Simons 22 Apr. 1994 36 p Limited Reproducibility: More than 20% of this document may be affected by microfiche quality
(Contract N00014-89-J-1497)
(AD-A278835; TR-43) Avail: Issuing Activity (Defense Technical Information Center (DTIC))

The local stability of several octahedral species AlF6(3-), GaF6(3-), InF6(3-), TlF6(3-), TaF6(-), ZrF6(2-), LaF6(3-), and LaCl6(3-) was studied using ab initio methods. All systems were found to have minima at octahedral geometries. The electronic stability of these species was considered using electron propagator theory (EPT) and the Moller-Plesset (MP) perturbation scheme. The results indicate that triply-charged molecular species may be electronically stable in the gas phase. Due to the slow convergence of the EPT and MP series and limitation in our one-electron basis set, the final conclusion requires a more advanced theoretical treatment. The doubly charged (ZrF6(2-)) and singly-charged (TaF6(-)) species were found to possess very high electronic detachment energies of 5.0 and 10.6 eV, respectively. TaF6(-) is predicted to be thermodynamically stable and ZrF6(2-) slightly unstable with respect to the unimolecular decomposition ML6(n-) yields ML5((n-1)-) + L(-). DTIC

N94-35783# Academy of Sciences (USSR), Novosibirsk (USSR). Inst. Yadernoj. Fiziki.
LOGARITHMIC CORRECTIONS OF THE TWO-BODY QED PROBLEM
I. B. Khriplovich, A. I. Milshtejn, and A. S. Elkhovskij 1992 27 p
(DE94-611157; BUDKERINP-92-57; IYaF-92-57) Avail: CASI HC A03/MF A01 (US Sales Only)

The logarithmic part of the Lamb shift, the contribution of the relative order alpha(exp 3)log(1/ alpha) to the atomic state energy, is related to the usual infrared divergence. For positronium, the calculated logarithmic correction does not vanish only in n(sup 3)S(sub 1) states and constitutes 5/24m(alpha)(sup 6)log(1/alpha)/m(exp 3). Logarithmic corrections of the relative order alpha(exp 2)log(1/alpha) to the positronium decay rate are also of the relativistic origin and can be easily computed within the same approach. DOE

N94-35784# Gosudarstvennyi Komitet po Ispolzovaniyu Atomnoi Energii, Serpukhov (USSR).
LEPTONIC DECAY CONSTANTS OF HEAVY QUARKONIA IN EFFECTIVE QCD SUM RULES
V. V. Kiselev 1992 14 p
(DE94-611160; IHEP-OTF-92-149) Avail: CASI HC A03/MF A01 (US Sales Only)

The QCD sum rule scheme, which allows one effectively to take into account the heavy quarkonium peculiarities such as nonrelativistic motion and large mass values of the quarks is considered. The phenomenological scaling law is derived for the leptonic constants with the use of the heavy quarkonium mass spectra. The law describes the data on the values of f(sub phi), f(sub psi) and f(gamma) rather good and predicts f(sub B(sub C)). DOE

N94-35785# Academy of Sciences (USSR), Novosibirsk (USSR). Inst. Yadernoj. Fiziki.
LOW ENERGY THEOREMS FROM THE EFFECTIVE LAGRANGIAN WITH VECTOR MESONS
Z. K. Silagadze 1992 15 p
(DE94-611173; BUDKERINP-92-61; IYaF-92-61) Avail: CASI HC A03/MF A01 (US Sales Only)

It is shown that the previously proposed effective Lagrangian with vector mesons correctly reproduces all current algebra low-energy theorems in the domain of its validity. DOE

N94-35786# International Centre for Theoretical Physics, Trieste (Italy).
CALCULATIONS ON SOME PROPERTIES OF THE PION IN THE FRAMEWORK OF SCHWINGER-DYSON AND BETHE-SALPETER EQUATIONS
Shao-long Wan and Ke-lin Wang Aug. 1993 28 p
(DE94-611232; IC-93/242) Avail: CASI HC A03/MF A01 (US Sales Only)

A phenomenological potential model, the modified flat-bottom potential, is assumed according to the flat-bottom potential and some physical considerations for the infrared and ultraviolet asymptotic behaviors of the effective quark-gluon coupling. Then, the propagator functions and mass function for the quark, and the Bethe-Salpeter wave functions, mass, electromagnetic form factor, radius and decay constant for the pion are calculated numerically in the framework of the Schwinger-Dyson and

Bethe-Salpeter equations with the modified flat-bottom potential. In order to obtain these, the Schwinger-Dyson and Bethe-Salpeter equations in the modified flat-bottom potential model are solved simultaneously by numerical iteration in the ladder approximation, and without any further one. Our results for the asymptotic quark mass function and the bound state wave functions agree with those derived from other theories and for the electromagnetic form factor, mass, radius, and decay constant of the pion agree with experimental results, respectively. DOE

N94-35787# Gosudarstvennyi Komitet po Ispolzovaniyu Atomnoi Energii, Serpukhov (USSR).
ISOSCALAR VECTOR BOSONS AT LEP 2
S. S. Gershtejn, A. A. Likhoded, V. F. Obraztsov, M. V. Shevlyagin, and O. P. Yushchenko 1992 18 p
(DE94-611253; IHEP-OTF-92-53) Avail: CASI HC A03/MF A01 (US Sales Only)

The phenomenological manifestations of the additional Y(Y(sub L)) boson arising in the models with the composite structure of electroweak interactions are studied for the process e(sup +)e(sup -)(yields)ff-bar and e(sup +)e(sup -)(yields)W(sup +)W(sup -)at the LEP 2 energies. It is shown that the inclusion of the additional isoscalar boson with the parameters providing the explanation of the TRISTAN data yields a measurable effect in the cross-section of e(+)e(-) yields muz(+)mu(-) (hadrons) processes at energies sq. root of s = 160-200 GeV. A contribution of the additional boson in the cross-section of the e(+)e(-) yields W(+)W(-) process in negligible at these energies. DOE

N94-35792 Utah Univ., Salt Lake City, UT. Dept. of Chemistry.
A COMBINED EXPERIMENTAL AND THEORETICAL STUDY OF THE NEUTRAL, CATIONIC AND ANIONIC Si3N CLUSTER MOLECULE
N. Goldberg (Technische Univ., Berlin, Germany.), M. Iraqi (Technische Univ., Berlin, Germany.), H. Schwarz, A. I. Boldyrev, and Jack Simons 22 Apr. 1994 35 p Limited Reproducibility: More than 20% of this document may be affected by microfiche quality
(Contract N00014-89-J-1497)
(AD-A278834; TR-46) Avail: CASI HC A03

Collision experiments and high-level ab initio calculations are used for the first characterization of the neutral, cationic and anionic Si3N cluster molecules. The experimentally observed fragmentation processes are well described by calculated reaction energies of all dissociation channels. In addition, the geometries and harmonic frequencies of SiN (n = 1-3) have been calculated for the cationic, anionic, and neutral species. DTIC

N94-35793 Utah Univ., Salt Lake City, UT. Dept. of Chemistry.
PERIODICITY AND PECULIARITY IN 120 FIRST AND SECOND ROW DIATOMIC MOLECULES
A. I. Boldyrev, N. Gonzales, and J. Simons 22 Apr. 1994 55 p Limited Reproducibility: More than 20% of this document may be affected by microfiche quality
(Contract N00014-89-J-1497)
(AD-A278836; TR-48) Avail: CASI HC A04

The ground and very low-lying excited states of all 120 first and second row diatomic molecules are surveyed. Three quarters of these molecules have had their ground state term symbols reliably experimentally determined. However, one quarter remain predicted only theoretically. For all 120 species, the best available experimental (where known) and theoretical values for the dissociation energies to ground-state atoms are also presented. The Aufbau principle, combined with standard energy ordering for the valence molecular orbitals, is able to properly account for the ground-state term symbols of all but twenty of the diatomics studies. The twenty exceptions produce higher than expected ground state spin multiplicity and arise when there are 4-5 or 7-8 valence electrons and group 3, 4, or 5 (but not group 6 or 7) atoms are involved. DTIC

N94-35797 Utah Univ., Salt Lake City, UT. Dept. of Chemistry.
NEW ANIONIC STATES OF THE LITHIUM TRIMER
Maciej Gutowski and Jack Simons 22 Apr. 1994 38 p Limited Reproducibility: More than 20% of this document may be affected by microfiche quality
(Contract N00014-89-J-1497)
(AD-A278832; TR-44) Avail: Issuing Activity (Defense Technical Information Center (DTIC))

Anionic states of Li3 were studied theoretically using a full-valence complete active space (CAS) self-consistent field (SCF) approach to explore their potential energy surfaces followed by quadratic configuration interaction (QCI) with single, double, and approximate triple excitations (SD(T)) calculations to more accurately determine relative energies and electron detachment energies. In addition to the known 1 sigma g + state, one triplet (3A2') and two quintet (5AI and 5A2') states were found to be relatively low-lying and electronically and geometrically stable in D3h geometries. All of these states remain electronically stable in C2v and D infinity h geometries. Hence, they are amenable to photoelectron spectroscopy detection. Preliminary CAS SCF results for the valence isoelectronic Na3(-) are also reported. DTIC

N94-35798 Utah Univ., Salt Lake City, UT. Dept. of Chemistry.
ANIONIC AND NEUTRAL STATES OF Li3O
Maciej Gutowski and Jack Simons 22 Apr. 1994 19 p Limited Reproducibility: More than 20% of this document may be affected by microfiche quality
(Contract N00014-89-J-1497)
(AD-A278833; TR-45) Avail: CASI HC A03

The ground state of the cation, three lowest electronic states of the neutral, and two anionic states of Li3O were studied using different ab initio techniques. Stationary points on the potential energy surfaces were determined both at complete active space (CAS) self-consistent field (SCF) and at second-order Meoller-Plesset (MP2) levels of theory. Excited states were approached using the single-excitation configuration interaction (CIS) method. Electron detachment energies for the anionic and neutral states were calculated at the quadratic configuration interaction (QCI) level-with single, double, and approximate triple excitations (SD(T)) included. The calculations indicate that Li3O- possesses two bound electronic states. The ground 1A1' state has an equilibrium D3h structure and a vertical electron detachment energy (VDE) of 0.66 eV. The 3E' bound state pseudorotates through 3AI and 3B2 stationary points. The barrier for pseudorotation was found to be less than 0.002 eV at the QCISD(T) level. Two VDE peaks for the 3E' anion were predicted to be at 0.45 and 1.15 eV, for transitions to the ground and the first excited state of the neutral, respectively. The ground state of the cation and the first three electronic states of the neutral Li3O were also considered and the vertical ionization potential for the ground neutral state was found to be 3.60 eV. Li3O and Li3O(-) are thermodynamically stable with respect to the unimolecular decompositions Li3O(-)(o) yields Li2O + Li(-)(o). Hence the species should be amenable to experimental studies. DTIC

N94-35805 California Inst. of Tech., Pasadena, CA.
ULTRAFAST CHEMICAL DYNAMICS OF REACTIONS IN BEAMS Final Report, 1 Nov. 1989 - 31 Oct. 1993
Ahmed H. Zewail 14 Apr. 1994 29 p Limited Reproducibility: More than 20% of this document may be affected by microfiche quality
(Grant AF-AFOSR-0014-90)
(AD-A278939; AFOSR-TR-94-0276) Avail: Issuing Activity (Defense Technical Information Center (DTIC))

The research in this proposal focused on the development of femtosecond laser techniques and their applications in the studies of molecular dynamics in real time. The research resulted in some thirty-seven publications with the involvement of more than twenty-five graduate students, post-doctoral fellows, and visiting associates from the U.S. and abroad. DTIC

N94-35814# Texas Univ., Austin, TX.
UNIVERSAL SU(2/1) AND THE HIGGS AND FERMION MASSES
Y. Neeman (Tel-Aviv Univ., Israel.) 1992 8 p
(Contract DE-FG05-85ER-40200)
(DE94-009182; DOE/ER-40200/319) Avail: CASI HC A02/MF A01

We review the SU(2/1) internal supersymmetry suggested by D. Fairlie and the author in 1979. The initial apparent difficulties were resolved when, with J. Thierry-Mieg, we understood that the gauging of a supergroup implies taking the usual Yang-Mills-like principal (double) fiber bundle as a 'scaffold' and using its Grassmann algebra as parameter manifold for the supergauge. SU(2/1) universality fixes the masses of the Higgs scalar field and the 'top' quark around 100-200 GeV, in the same region as the W and Z masses. A 'unified' supergauge, enclosing SU(3)(sub color) x SU(2) x U(l), predicts a fourth lepton generation in which the neutrino mass is of the same order. DOE

N94-35816# Minnesota Univ., Minneapolis, MN.
STATE-TO-STATE DYNAMICS OF MOLECULAR ENERGY TRANSFER
W. R. Gentry 30 Nov. 1993 4 p
(Contract DE-FG02-86ER-13515)
(DE94-009651; DOE/ER-13515/9) Avail: CASI HC A01/MF A01

During this budget period we have focused our efforts toward completing experimental measurements of differential cross sections for fully-resolved state-to-state angular momentum transfer in NO + Ar collisions, including both the electronically adiabatic and nonadiabatic channels represented by: NO((sup 2)P(sub 1/2), nu = 0, j = 1/2) + Ar yields NO((sup 2)P(sub 1/2), nu = 0, j') + Ar and NO((sup 2)P(sub 1/2), nu = 0, j = 1/2) + Ar yields NO((sup 2)P(sub 3/2), nu = 0, j') + Ar. We have also begun measurements of integral cross sections as a function of collision energy for state-resolved rotational excitation of the first triatomic molecule to be examined by this technique, in the system SO2 + He. Concurrently, we have also carried out collision experiments in the system SO2 + He. State-to-state integral cross sections have been measured as a function of final rotational state at a fixed collision energy of 473 cm(exp -1), and as a function of collision energy for six selected final rotational states. Initial SO2 rotational temperatures less than 3 K were achieved with 0.3 mole-% of the molecule seeded in 20 atm of He. State-selective detection of the scattered products was done by LIF on the strong C(122) (left arrow) X(000) transition at 445 nm. Because of the selection rules and nuclear spin statistics, the k(sub a)=0 and k(sub a)=1 subbands dominate the LIF spectrum. This data is currently being analyzed and the collision dynamics modeled theoretically for comparison. Cross sections for vibrational excitation in this system proved to be too small to measure. DOE

N94-35824 Washington Univ., Seattle, WA. Dept. of Physics.
A QUARK MODEL OF BAR LAMBDA PRODUCTION IN BAR RHO INTERACTIONS
M. A. Alberg (Seattle Univ., WA.), E. M. Henley, L. Wilets, and P. D. Kunz 1993 22 p Presented at the 2nd Biennial Workshop on Nuclear-Antinuclear Physics, Moscow, Russia, 13-18 Sep. 1993 Limited Reproducibility: More than 20% of this document may be affected by microfiche quality
(Contract DE-FG06-88ER-40427)
(DE94-008071; DOE/ER-40427/31-N93; CONF-9309352-1) Avail: CASI HC A03

A quark model which includes both scalar and vector contributions to the reaction mechanism (SV quark model) is used in a DWBA calculation of (anti (Lambda))(Lambda) production in (bar p)p interactions. Total and differential cross-sections, polarizations, depolarizations, and spin-correlation coefficients are computed for laboratory momenta from threshold to 1695 MeV/c. The free parameters of the calculation are the scalar and vector strengths, a quark cluster size parameter, and the parameters of the unknown (anti (Lambda))(Lambda) potentials. Good agreement with experiment is found for constructive interference of the scalar and vector terms, and for (anti (Lambda))(Lambda) potentials which differ from those suggested by several authors on the basis of SU(3) arguments. The fit to the data is better than that obtained by other quark models, which use only scalar or vector annihilation terms. The agreement with experiment is also better than that found in meson-exchange models. The recent suggestion that measurement of the depolarization parameter D(sub nn) can be used to discriminate between meson-exchange and quark models is examined in detail. We conclude that a measurement of D(sub nn) will provide a test of which of these models, as presently constructed, is the more appropriate description of strangeness production in the (bar-p)p (yields) (anti (Lambda))(Lambda) reaction. DOE

N94-35984# National Inst. for Fusion Science, Nagoya (Japan).
IMPROVED MODELS OF BETA-LIMIT, ANOMALOUS TRANSPORT AND RADIAL ELECTRIC FIELD WITH LOSS CONE LOSS IN HELIOTRON/TORSATRON
K. Itoh, S.-I Itoh, H. Sanuki, K. Ichiguchi, J. Todoroki, and A. Fukuyama Sep. 1992 15 p Presented at the 14th International Conference on Plasma Physics and Controlled Nuclear Fusion Research, Wuerzburg, Germany, 30 Sep. - 7 Oct. 1992
(DE94-718976; AD-B168930; NIFS-176; CONF-9209396; IAEA-CN-56/C-1-4) Avail: CASI HC A03/MF A01

Theoretical study is made on the physics mechanisms which determine the beta-limit, the anomalous transport, and the radial electric field and loss cone. New theory is developed to analyze the stability boundary against the interchange mode in high-aspect-ratio toroidal helical plasmas, taking into account the transport processes. The stability (beta)-limit is given at finite (beta)-value, and the dependences on the plasma parameters and on the transport coefficient are investigated. It is found that the current-diffusive interchange mode is more important than the resistive mode in hot plasmas. The (beta)-limit is predicted in the range of experimental observation for the anomalous transport. The dynamics of the pressure gradient and mode amplitude around this stability boundary are analysed. As the heating power is increased, the dynamics changes from the monotonous saturation, through the saturation with overshoot, and to the sawtoothing. Using the mean-field theory approach of statistical physics for the microscopic current-diffusive interchange mode, the anomalous transport theory is developed. The expression of the thermal transport coefficient is obtained. The pressure gradient, not the temperature itself, enhances the transport coefficient. Comparison with experimental observations from various aspects is made, and the model explains experimental observations. The method to obtain the self-consistent picture of the radial electric field E(sub r) and the loss cone loss is explored. The structure of E(sub r) and the loss cone are obtained, and it is confirmed that the direct ion loss makes E(sub r) near edge more negative. Effects of other nonclassical loss are also evaluated. DOE

N94-36016 Prairie View Agricultural and Mechanical Coll., TX.
SUPPORT OF HADROPRODUCTION OF BOTTOM USING THE 800 GeV/c PRIMARY PHOTON BEAM AT THE FERMILAB TEVATRON
1994 25 p Limited Reproducibility: More than 20% of this document may be affected by microfiche quality
(Contract DE-FG05-92ER-40728)
(DE94-009411; DOE/ER-40728/T1) Avail: Issuing Activity (Department of Energy (DOE))

This report is a proposal from the group at Prairie View A&M University for an extension of their involvement with the E771 experiment at Fermilab. They describe their work on data analysis of this experiment, and effort involved in porting analysis codes from different work stations. This analysis is ongoing. They also propose to be a part of the extension of the E771 experiment (P867), which is proposed for the next fixed target run, in 1994/1995. DOE

N94-36050 Utah Univ., Salt Lake City, UT. Dept. of Chemistry.
VERTICAL AND ADIABATICAL IONIZATION ENERGIES AND ELECTRON AFFINITIES OF NEW Si(n)C AND Si(n)O (N=1-3) MOLECULES
Alexander I. Boldyrev and Jack Simons 22 Apr. 1994 32 p Limited Reproducibility: More than 20% of this document may be affected by microfiche quality
(Contract N00014-89-J-1497)
(AD-A278863; TR-40) Avail: Issuing Activity (Defense Technical Information Center (DTIC))

Vertical and adiabatic ionization potentials as well as electron affinities have been calculated for SiC, Si2C, Si3C, SiO, Si2O and Si3O using five different sophisticated ab initio methods with large basis sets. The geometry and harmonic frequencies have been calculated at the second-order Moller-Plesset level. Results of the calculations using all five methods are in a good agreement among themselves (+/- 0.3 eV). The calculated vertical first IPs of SiC, Si2C, Si3C and SiO molecules agree within 0.2 eV with experimental appearance potentials for these species. DTIC

N94-36058# California Univ., Berkeley. Lawrence Berkeley Lab, CA.
TWO-PHOTON PHOTOEMISSION AND THE DYNAMICS OF ELECTRONS AT INTERFACES
D. F. Padowitz (Miami Univ., Coral Gables, FL.), C. B. Harris, R. E. Jordan, R. L. Lingle, Jr., J. D. McNeill, and W. R. Merry Jan. 1994 10 p Presented at the OE/LASE 1994: Conference on Optics, Electro-Optics, and Laser Applications in Science and Engineering, Los Angeles, CA, 22-29 Jan. 1994
(Contract DE-AC03-76SF-00098)
(DE94-011373; LBL-35194; CONF-940142-35) Avail: CASI HC A02/MF A01

A new instrument for angle-resolved two-photon photoemission with exceptional sensitivity and energy resolution has allowed a detailed examination of the interaction of image-state electrons with adsorbates. In addition to measuring the electrostatic properties of molecular-thickness films, the technique serves as a probe of adsorbate growth modes and provides new opportunities to explore the dynamics of electrons in well-controlled two-dimensional systems. DOE

N94-36073 Academy of Sciences (USSR), Novosibirsk (USSR). Inst. Yadernoj Fiziki.

FUNCTIONAL INTEGRATION METHOD FOR THE ONE-DIMENSIONAL LOCALIZATION, THE HIGHER CORRELATORS AND MEAN CURRENT IN MESOSCOPIC RING IN THE ARBITRARY MAGNETIC FIELD

I. V. Kolokolov 1993 27 p Limited Reproducibility: More than 20% of this document may be affected by microfiche quality
(DE94-616621; IYaF-93-12) Avail: CASI HC A03 (US Sales Only)

On the base of the Abrikosov problem on a particle in one-dimensional random potential are obtained closed representations for mean physical values in the form of functional integrals, which are calculated exactly without any expansions. DOE

N94-36074 Academy of Sciences (USSR), Kiev (USSR). Inst. for Theoretical Physics.

QCD PARAMETRIZATIONS OF THE PARTON DISTRIBUTION OF DEEP INELASTIC SCATTERING

A. V. Kotikov, S. J. Maksimov, and I. S. Parobij 1993 12 p Submitted for publication Limited Reproducibility: More than 20% of this document may be affected by microfiche quality
(DE94-616660; ITP-93-21E) Avail: CASI HC A03 (US Sales Only)

A realistic parametrization of the gluon and quarks distributions is suggested. It is shown that the solutions of the Gribov-Lipatov - Altarelli-Paris equations can be presented by these parametrizations and these equations unambiguously lead to the constraints on the Q(sup 2)-evolution of the parameters. DOE

N94-36075# Academy of Sciences of the Ukraine, Kiev. Inst. for Theoretical Physics.

EXACT MULTIPLICITIES IN THE THREE-ANION SPECTRUM

S. V. Mashkevich 1993 17 p Submitted for publication
(DE94-616768; ITP-93-32E) Avail: CASI HC A03/MF A01 (US Sales Only)

Using the symmetry properties of the three-anion spectrum, we obtain exactly the multiplicities of states with given energy and angular momentum. The results are shown to be in agreement with the proper quantum mechanical and semiclassical considerations, and the unexplained points are indicated. DOE

N94-36077# Academy of Sciences of the Ukraine, Kiev. Inst. for Theoretical Physics.

PROCESSES OF THE RECIPROCAL TRANSFORMATION VECTOR CHARGED PARTICLES PAIRS AND ELECTRON-POSITRON PAIRS

V. K. Tartakovskij and V. A. Cherednichenko 1993 7 p Submitted for publication
(DE94-616787; ITF-93-3R) Avail: CASI HC A02/MF A01 (US Sales Only)

The explicit form of the angle distributions and the total cross-sections for the processes of the reciprocal transformation of electron-positron pair and pair of vector charged particles are obtained. DOE

N94-36079# Academy of Sciences of the Ukraine, Kiev. Inst. for Theoretical Physics.

BOSON SPECTRA AND CORRELATIONS IN THERMAL LOCALLY EQUILIBRIUM SYSTEMS

Yu. M. Sinyukov 1993 24 p Submitted for publication
(DE94-616799; ITP-93-8E) Avail: CASI HC A03/MF A01 (US Sales Only)

The single and multi-particle inclusive spectra for locally equilibrium boson gas are studied using the method of statistical operator. In the framework of the formalism developed the thermal Wick's theorem is generalized and the analytical solution of the problem in boost-invariant approach is found. It is shown that for particles with wave-lengths greater than homogeneity length the spectra and correlations increase essentially as compared to the results based on Bose-Einstein heat distribution. The connection between corresponding correction term and the particle spectrum in Milne's Universe is discussed. DOE

N94-36081 Academy of Sciences (USSR), Kiev (USSR). Inst. for Theoretical Physics.

ON THE THEORY OF BOUNDED MANY-PARTICLE SYSTEMS WITH PURELY COULOMB INTERACTIONS

A. G. Zagorodnij, K. Heinzinger, and I. P. Yakimenko 1993 12 p Submitted for publication Limited Reproducibility: More than 20% of this document may be affected by microfiche quality
(DE94-617215; ITP-93-13E) Avail: CASI HC A03 (US Sales Only)

The equilibrium distribution functions for bounded many-particle systems containing both free and bound charged particles have been calculated using a three-center molecular model with an arbitrary intrinsic potential of particle interaction. The general relations obtained are used for the description of particle density profiles and orientational distributions of molecules near a planar wall. DOE

N94-36083 Academy of Sciences (USSR), Kiev (USSR). Inst. for Theoretical Physics.

DISTANCE DEPENDENT FRACTIONAL STATISTICS IN A P, T-INVARIANT MODEL

E. V. Gorbar and S. V. Mashkevich 1993 9 p Submitted for publication Limited Reproducibility: More than 20% of this document may be affected by microfiche quality
(DE94-617360; ITP-93-16E) Avail: CASI HC A02 (US Sales Only)

It is shown that in the P,T-invariant model of high-temperature superconductivity with the mixed Chen-Simons term the interaction of charge carriers leads to effective changing of their statistics, which depends on distance between them. In particular, in the limit of large distances fermions effectively turn into bosons. DOE

N94-36086 Southeastern Univ. Research Association, Newport News, VA.

ELASTIC CHARGE FORM FACTORS FOR K MESONS

W. W. Buck (Hampton Univ., VA.), R. A. Williams (Hampton Univ., VA.), and Hiroshi Ito (George Washington Univ., Washington, DC.) 1994 5 p *Its* theory group preprint series Limited Reproducibility: More than 20% of this document may be affected by microfiche quality
(Contract DE-AC05-84ER-40150)
(DE94-010014; DOE/ER-40150/258; CEBAF-TH-94-02) Avail: CASI HC A01

The elastic charge form factors for the charged K(sup +) and neutral K(sup 0) are presented. The model employed makes use of solutions of the coupled Bethe-Salpeter and Schwinger-Dyson equations. This covariant model, which provides good predictions for the pion's elastic charge and transition form factor, has been presented elsewhere and will be briefly outlined here. The results for the kaon are in good agreement with the available data and can serve as an eventual guide in the interpretation of the approved CEBAF experiment E-93-018. The Q(sup 2) dependent K(sup 0) results suggest a new area for experimental exploration. DOE

N94-36088 Gosudarstvennyi Komitet po Ispolzovaniyu Atomnoi Energii, Serpukhov (USSR).

NUMERICAL METHOD TO STUDY THE STABILITY OF PERIODIC SOLUTIONS OF PARTICLE MOTION IN NONLINEAR MAGNETIC FIELDS

Yu. S. Fedotov 1992 11 p Limited Reproducibility: More than 20% of this document may be affected by microfiche quality
(DE94-610740; IFVE-UNK-92-22) Avail: CASI HC A03 (US Sales Only)

The equations of betatron oscillations in nonlinear magnetic fields belong to the Lyapunov systems having a number of periodic solutions. Using the matrix methods developed for studying periodic linear systems one can construct the algorithm for searching these solutions and studying their stability in order to determine the region of stable motion. The present note describes the method of numeric search for the periodic solutions of two-dimensional betatron motion, using the nonlinear element in thin-lens approximation. To illustrate the technique, the results on calculating the pattern on the phase plane close to the line and node of the sum third-order resonance are presented. DOE

N94-36107# Fermi National Accelerator Lab., Batavia, IL.
CDF ELECTROWEAK STUDIES AND THE SEARCH FOR THE TOP QUARK
H. J. Frisch (Chicago Univ., IL.) Feb. 1994 27 p Presented at the 23rd International Symposium on Multiparticle Dynamics, Aspen, CO, 13-17 Sep. 1993
(Contract DE-AC02-76CH-03000)
(DE94-010333; FNAL/C-94/044-E; CONF-9309297-10) Avail: CASI HC A03/MF A01

The second major run of the (bar p)p Fermilab Tevatron Collider ended on May 30. The CDF detector has accumulated almost five times the data sample of its previous 1988-1989 run. The author presents new results on electroweak physics, including the ratio of W to Z boson production cross-sections and the charge asymmetry in W decay. He gives a progress report on the measurement of the W mass. New results from the 1988-1989 data on W-(gamma) production are also presented. The status of the search for the top quark in the dilepton modes is described. In addition a status report of the ongoing search in the lepton + jets mode is given. DOE

N94-36126# Clemson Univ., SC. Chemistry Lab.
INTRAMOLECULAR ENERGY TRANSFER REACTIONS IN POLYMETALLIC COMPLEXES
J. Petersen Dec. 1992 5 p
(Contract DE-FG09-87ER-13768)
(DE94-010114; DOE/ER-13768/4) Avail: CASI HC A01/MF A01

This progress report covers the following topics: (1) excited-state energy transfer; and (2) excited-state electron transfer (charge separation). DOE

N94-36127# Lawrence Livermore National Lab., CA.
CALTRANS: A PARALLEL, DETERMINISTIC, 3D NEUTRONICS CODE
L. Carson, J. Ferguson, and J. Rogers Apr. 1994 36 p
(Contract W-7405-eng-48)
(DE94-010667; UCRL-ID-116958) Avail: CASI HC A03/MF A01

Our efforts to parallelize the deterministic solution of the neutron transport equation has culminated in a new neutronics code CALTRANS, which has full 3D capability. In this article, we describe the layout and algorithms of CALTRANS and present performance measurements of the code on a variety of platforms. Explicit implementation of the parallel algorithms of CALTRANS using both the function calls of the Parallel Virtual Machine software package (PVM 3.2) and the Meiko CS-2 tagged message passing library (based on the Intel NX/2 interface) are provided in appendices. DOE

N94-36129# Institute of Nuclear Techniques, Kracow (Poland).
J/PSI ABSORPTION EFFECTS IN THE COHERENT PRODUCTION ON NUCLEI
L. Lesniak Dec. 1992 10 p
(DE94-616870; INP-1608/PH) Avail: CASI HC A02/MF A01 (US Sales Only)

J/psi coherent production and attenuation on nuclei by high energy muons and photons is studied. A simple one parameter model leads to a good description of the New Muon Collaboration and Fermilab data. It is found that the effective absorption cross section of the cc-bar pair on a target nucleon is about 6 mb. DOE

N94-36130# Institute of Nuclear Techniques, Kracow (Poland).
SIGMA MINUS-NUCLEUS INTERACTIONS IN EMULSION AT 350 GeV
M. Szarska, H. Wilczynski, W. Wolter, K. Wozniak, J. J. Lord, and R. J. Wilkes May 1992 21 p
(DE94-616886; INP-1596/PH) Avail: CASI HC A03/MF A01 (US Sales Only)

Experimental data on multiplicities and angular distributions of heavy ionizing and shower particles in inelastic interactions of 350 GeV Sigma(sup -) hyperon with emulsion nuclei were investigated. The data were compared with the results of other experiments on proton and pion interactions in emulsion at energies within the interval 60-800 GeV. DOE

N94-36131# Academy of Sciences of the Ukraine, Kiev. Inst. for Theoretical Physics.
P-MATRIX APPROACH AND THREE-NUCLEON PROBLEM
V. A. Babenko, N. M. Petrov, and G. N. Teneva 1993 8 p Submitted for publication
(DE94-616887; ITP-93-14E) Avail: CASI HC A02/MF A01 (US Sales Only)

The paper deals with the P-matrix approach application to the three strongly interacting particles systems description. On the basis of the obtained off-energy-shell scattering amplitude separable expansion in the P-matrix approach the low-energy three-particle quantities were calculated in the case of square-well potential. The results of calculations show good convergence of the calculated three-particle quantities. DOE

N94-36132# Academy of Sciences of the Ukraine, Kiev. Inst. for Theoretical Physics.
ALTERNATING SERIES FIT TO THE TOTAL CROSS SECTIONS
Yu. Ilin and A. Lendel 1993 13 p Submitted for publication
(DE94-616888; ITP-93-25E) Avail: CASI HC A03/MF A01 (US Sales Only)

It is show by a simple Regge-type fit suggested recently by Donnachie and Landshoff that the universal pomeron contribution to various total cross sections may be represented by an alternating series a - b log s + c (log s)(sup 2) corresponding to a series of Regge multipoles. DOE

N94-36133# Academy of Sciences (USSR), Novosibirsk (USSR). Inst. Yadernoj Fiziki.
PSEUDOGOLDSTONE BOSON DECAY INDUCED BY LIGHT AND SEARCH FOR THE SOLAR AXION RADIATION
P. V. Vorobev 1992 10 p
(DE94-616907; IYaF-92-94) Avail: CASI HC A02/MF A01 (US Sales Only)

A process of the light-induced decay of the axions with mass of 1-3 eV is discussed. The process may serve a base for the new type detectors for searches of the solar axion radiation and the condensate of axions with mass about 1 eV, which constitute, possibly, the Universe hidden mass. DOE

N94-36134# Academy of Sciences (USSR), Novosibirsk (USSR). Inst. Yadernoj Fiziki.
SCATTER PROGRAM OF CROSS SECTION CALCULATION OF THE HADRON AND LEPTON INTERACTIONS WITH NUCLEI
A. M. Makhov 1992 32 p
(DE94-617006; IYaF-92-66) Avail: CASI HC A03/MF A01 (US Sales Only)

The description is given of the SCATTER program intended for carrying out numerical calculations of the differential cross sections of elastic scattering, the total cross sections and cross sections of the K, pi, N, d, alpha, e, mu interactions with nuclei in the incident particle energy range from 0 to 1 GeV. The algorithm brief description, user instruction, and comparison results of calculations and experiments are given. DOE

N94-36182# Gosudarstvennyi Komitet po Ispolzovaniyu Atomnoi Energii, Serpukhov (USSR). Inst. Fiziki Vysokikh.
PROCEEDINGS OF 2ND WORKING MEETING ON PHYSICS AT VLEPP, VOLUME 2 [TRUDY2. RABOCHEGO SOVESHCHANIYA FIZIKA NA VLEHPP. TOM 2]
1992 171 p In ENGLISH and RUSSIAN Meeting held in Protvino, Russia, 2 Jun. 1992
(DE94-616167; INIS-RU-363-Vol-2; CONF-9206427-Vol-2) Avail: CASI HC A08/MF A02 (US Sales Only)

Proceedings of the 2nd Working meeting 'Physics at VLEPP' has been published. Research program at coming e(sup +)e(sup -) colliders has been considered. The problems of quantum chromodynamics supersymmetry, search for new particles, and physics of t-quarks have been discussed. The problems of creation of coordinate-sensitive and microstrip detectors for linear colliders have been considered. DOE

N94-36198# Stanford Linear Accelerator Center, CA.
PRECISE MEASUREMENT OF THE LEFT-RIGHT CROSS SECTION ASYMMETRY IN Z BOSON PRODUCTION BY ELECTRON-POSITRON COLLISIONS
R. E. Frey (Oregon Univ., Eugene, OR.) Mar. 1994 12 p Presented at the 21st Annual SLAC Summer Institute on Particle Physics: Spin Structure in High-Energy Processes, Stanford, CA, 26 Jul. - 6 Aug. 1993

(Contract DE-AC03-76SF-00515)
(DE94-010751; SU-SLAC-PUB-6470; CONF-930767-7) Avail: CASI HC A03/MF A01

A precise measurement of the left-right cross section asymmetry (A(sub LR)) for Z boson production by e(+)e(-) collisions has been attained at the Slac Linear Collider with the SLD detector. We describe this measurement for the 1993 data run, emphasizing the significant improvements in polarized beam operation which took place for this run, where the luminosity-weighted electron beam polarization averaged 62.6 +/- 1.2%. Preliminary 1993 results for A(sub LR) are presented. When combined with the less precise 1992 result, the preliminary result for the effective weak mixing angle is sin(exp 2) theta(sub W (sup eff)) = 0.2290 +/- 0.0010. DOE

N94-36225# Argonne National Lab., IL.
TIME-OF-FLIGHT DIFFRACTION AT PULSED NEUTRON SOURCES: AN INTRODUCTION TO THE SYMPOSIUM
J. D. Jorgensen 1994 20 p Presented at the Annual Meeting of the American Crystallographic Association, Albuquerque, NM, 24-28 May 1994
(Contract W-31-109-eng-38)
(DE94-010442; ANL/MSD/CP-82631; CONF-9405140-1) Avail: CASI HC A03/MF A01

In the 25 years since the first low-power demonstration experiments, pulsed neutron sources have become as productive as reactor sources for many types of diffraction experiments. The pulsed neutron sources presently operating in the United States, England, and Japan offer state of the art instruments for powder and single crystal diffraction, small angle scattering, and such specialized techniques as grazing-incidence neutron reflection, as well as quasielastic and inelastic scattering. In this symposium, speakers review the latest advances in diffraction instrumentation for pulsed neutron sources and give examples of some of the important science presently being done. In this introduction to the symposium, I briefly define the basic principles of pulsed neutron sources, review their development, comment in general terms on the development of time-of-flight diffraction instrumentation for these sources, and project how this field will develop in the next ten years. DOE

N94-36238 Argonne National Lab., IL.
HIGH ENERGY ASYMPTOTICS OF PERTURBATIVE MULTI-COLOR QCD
L. N. Lipatov (Leningrad Nuclear Physics Inst., USSR.) 26 Aug. 1993 6 p Presented at the 19th International Conference on Elastic and Diffractive Scattering (5th Blois Workshop), Providence, RI, 8-12 Jun. 1993 Limited Reproducibility: More than 20% of this document may be affected by microfiche quality
(Contract W-31-109-eng-38)
(DE94-001350; ANL-HEP-CP-93-67; CONF-9306221-7) Avail: CASI HC A02

The structure functions of deep-inelastic scattering at small x satisfy two different equations in the leading logarithmic approximation (LLA). The first one, the GLAP equation, describes the Q(exp 2)-evolution of partonic distributions h(sub i)(x). The second one, the BFKL equation, determines the x-dependence of parton densities H(sub i)(x, k(sub perpendicular)). The author discusses the possibility of finding an exact solution for multigluon compound states in LLA for the color group SU(N), in the limit N approaches infinity. The contributions of diagrams with many reggeized gluons are important for the unitarization of the perturbative Pomeron in QCD. It is shown that the Bethe-Salpeter equations for compound states of many reggeized gluons are conformally invariant in the two-dimensional impact parameter space. Their solutions can be written in holomorphically factorized form and there is a differential operator commuting with the holomorphic part of the corresponding Hamiltonian. DOE

N94-36239 Brookhaven National Lab., Upton, NY.
HYBRID MESONS (Q(ANTI Q)g) IN N(ANTI N) ANNIHILATION
C. B. Dover, T. Gutsche, and A. Faessler Sep. 1993 4 p Presented at the 13th International Conference on Particles and Nuclei, Perugia, Italy, 27 Jun. - 3 Jul. 1993 Limited Reproducibility: More than 20% of this document may be affected by microfiche quality
(Contract DE-AC02-76CH-00016)
(DE94-001491; BNL-49501; CONF-930637-7) Avail: CASI HC A01

N(anti N) annihilation reactions provide exciting possibilities to study mesonic resonances beyond the usual Q(anti Q) spectrum. Particularly the search for Q(anti Q)g mesons containing an explicit dynamical excitation of the gluon field is not promising, since hybrids are predicted to display unique features: exotic quantum numbers (J(sup pi C)) and dynamical selection rules for their decay modes. The authors have investigated the possibility of producing hybrids from p(anti p) atomic states in reactions of the type N(anti N) (L = 0, 1) yields pi + Q(anti Q)g. Production rates for hybrid mesons are found to display a strong dependence on the quantum numbers and kinematical factors associated with the transition. The dependence on the orbital angular momentum L of the p(anti p) atomic state, accessible in p(anti p) annihilation at rest, would provide a striking signature for the production of hybrids. In estimating branching ratios for the formation of Q(anti Q)g hybrid mesons in N(anti N) annihilation reactions at rest, the authors have employed a microscopic model with constituent quarks and gluons in analogy to the annihilation model for the production of Q(anti Q) mesons. DOE

N94-36241 Fermi National Accelerator Lab., Batavia, IL.
PRIMORDIAL NUCLEOSYNTHESIS IN CONFORMAL WEYL GRAVITY
L. Knox (Chicago Univ., IL.) and A. Kosowsky (Chicago Univ., IL.) Oct. 1993 10 p Limited Reproducibility: More than 20% of this document may be affected by microfiche quality
(Contract DE-AC02-76CH-03000)
(DE94-003002; FNAL/Pub-93/322-A) Avail: CASI HC A02

Recently, conformal Weyl gravity has been considered as a candidate alternative gravity theory. This fourth-order theory is attractive because it is the only metric theory of gravity which is invariant under local conformal transformations of the metric. The authors calculate the primordial light element abundances in this theory. The major difference from the standard cosmology is that the universe expands far more slowly throughout the nucleosynthesis epoch. The production of He-4 depends strongly on eta, the ratio of baryons to photons. For eta = 10(exp -8) the mass fraction of He-4 is X() approximately = 0.25 and the number densities relative to hydrogen for H-2, He-3, and Li-7 are n(H-2/n(H) approximately = 9 x 10(exp -20), n(He-3)/n(H) approximately = 4 x 10(exp -18) and n(Li-7)/n(H) approximately = 10(exp -13). This value of eta corresponds to a baryon mass density close to the standard model critical density. However, adjusting eta to give a reasonable helium yield forces the deuterium and lithium yields to be small enough that the theory cannot be reconciled with observations. DOE

N94-36246 Academy of Sciences (USSR), Novosibirsk (USSR). Inst. of Nuclear Physics.
T-ODD, P-EVEN PHOTON-FERMION INTERACTIONS
I. B. Khriplovich 1992 8 p Limited Reproducibility: More than 20% of this document may be affected by microfiche quality
(DE94-616869; BUDKERINP-92-55) Avail: CASI HC A02 (US Sales Only)

General structure of T-odd, P-even photon-fermion scattering amplitude is discussed. The corresponding operators are of high dimension. Therefore the experimental data on the high-energy cross sections bound the effective constants so strictly that the possible manifestations of these interactions in the low-energy region are extremely small. DOE

N94-36266 Fermi National Accelerator Lab., Batavia, IL.
TOP DILEPTON SEARCH AT CDF
Aug. 1993 8 p Presented at the 16th International Symposium on Lepton and Photon Interactions, Ithaca, NY, 10-15 Aug. 1993 Limited Reproducibility: More than 20% of this document may be affected by microfiche quality
(Contract DE-AC02-76CH-03000)
(DE94-002302; FNAL/C-93/212-E; CONF-930823-14) Avail: CASI HC A02

The authors present preliminary results from a search for the top quark in the dilepton channel using data collected by CDF during the 1992-93 Fermilab Collider Run. The dilepton analysis implies a lower limit on the top quark mass of 113 GeV/c(exp 2) at the 95% confidence level, assuming Standard Model decays. DOE

N94-36267 Oak Ridge National Lab., TN.
DISSOCIATIVE RECOMBINATION OF STORED AND PHASE-SPACED COOLED MOLECULAR IONS IN CRYRING
M. Larsson (Royal Inst. of Tech., Stockholm, Sweden.), G. Sundstroem

(Royal Inst. of Tech., Stockholm, Sweden.), M. Carlson (Royal Inst. of Tech., Stockholm, Sweden.), H. Danared (Manne Siegbahn Inst. of Physics, Stockholm, Sweden.), A. Kaellberg (Manne Siegbahn Inst. of Physics, Stockholm, Sweden.), K. G. Rensfelt (Manne Siegbahn Inst. of Physics, Stockholm, Sweden.), M. afUgglas (Manne Siegbahn Inst. of Physics, Stockholm, Sweden.), L. Brostroem (Manne Siegbahn Inst. of Physics, Stockholm, Sweden.), S. Mannervik (Manne Siegbahn Inst. of Physics, Stockholm, Sweden.), and P. Sigray (Manne Siegbahn Inst. of Physics, Stockholm, Sweden.) et al 1993 9 p Presented at the 18th International Conference on the Physics of Electronic and Atomic Collisions, Aarhus, Denmark, 21-27 Jul. 1993 Limited Reproducibility: More than 20% of this document may be affected by microfiche quality
(Contract DE-AC05-84OR-21400)
(DE94-002459; CONF-930711-4) Avail: CASI HC A02

Ion storage rings offer several advantages for studies of recombination of molecular ions by electrons, a process which in general leads to dissociation. During the last year dissociative recombination of H3(+), HD(+), H(2)(+), D2(+), (sup 3)HeH(+), (sup 4)HeH(+), and (sup 4)HeD(+) have been studied in storage rings in Stockholm, Heidelberg, Tokyo, and Aarhus. Only a fraction of the results obtained at these places have been processed to the point where they have been published in the literature. Hence, the discussion of some of the results in this article must be regarded as tentative. DOE

N94-36287# Academy of Sciences (USSR), Leningrad (USSR). Inst. Yadernoj Fiziki.
ELASTIC p(4)He SCATTERING AT INTERMEDIATE ENERGIES
S. I. Manaenkov 1992 46 p
(DE94-618544; PIYaF-1795) Avail: CASI HC A03/MF A01 (US Sales Only)

It is shown that the calculations of the differential cross section and polarization using realistic nuclear wave functions, NN amplitudes obtained in the phase shift analysis and usual corrections to the Glauber theory disagree with the experimental data. DOE

N94-36298# Pennsylvania State Univ., University Park, PA. Dept. of Chemistry.
METAL CLUSTER ALLOYS AND OXIDES: ELUCIDATING STRUCTURAL AND ELECTRONIC EFFECTS IN GOVERNING THE REACTIVITY AND CATALYTIC ROLE OF MATTER IN FINITE DIMENSIONS
A. W. Castleman, Jr. 1993 7 p
(Contract DE-FG02-92ER-14258)
(DE94-010224; DOE/ER-14258/T1) Avail: CASI HC A02/MF A01

The discovery of a new class of molecular clusters (metallocarbohedrenes or Met-Cars) was a potentially major finding in cluster science; a method has been developed for producing bulk quantities of this material. Attention was also devoted to unraveling mechanisms of formation and reactive chemistry of Met-Cars. Abstracts are presented for 14 publications submitted, accepted, and/or published during the past year. Among the materials studied were (TiN)(sub n)(sup +), Cu/Sb and Cu/Bi alloy clusters, Cu/C clusters, Cu/Se and Ag/Se clusters, Ti8C12)(sup +), Mg(sup +)(H2O)(sub n) clusters, Zr/C and Ta/C clusters, Ti(sub x)Zr(sub y)C12 and Ti(sub x)Hf(sub y)C12(x+y=8), etc. DOE

N94-36302# Edgerton, Germeshausen and Grier, Inc., Idaho Falls, ID.
DESIGN AND CONSTRUCTION OF A IMAGING INSTRUMENT FOR STUDYING ION EMISSION FROM PURE ION EMITTERS Ph.D. Thesis
J. E. Olson Sep. 1993 68 p
(Contract DE-AC07-76ID-01570)
(DE94-010702; EGG-MS-10992) Avail: CASI HC A04/MF A01

The development of new ion sources is important in the area of surface analysis to make it easier to perform more sensitive and accurate analyses. In surface analysis a primary ion beam composed of a single species can help when predicting and interpreting the results. Therefore, much interest and effort has been focused on producing pure ion emitters. An instrument has been designed and constructed to view the current densities of the ions being emitted from pure ion emitters. The instrument electrostatically accelerates and focuses the ion beam onto a microchannel plate detector equipped with a phosphor screen for viewing the images. These images are used to identify areas of enhanced ion emission. Once these areas are identified, the investigator can use other instruments to analyze them, and hopefully develop a better understanding of the chemistry and physics involved in the ion emission process. A computer based control system has been integrated into the system to simplify the operation of the instrument and provide safety features to protect the hardware from damage. A closed-circuit video camera system is used to allow the images to be remotely viewed during imaging procedures. Experiments show that the instrument has a lower detection limit of 7.45 (times) 10(exp 3) ions/sec/sq mm and a spatial resolution of approximately 3-4 micrometers. Results from imaging cesium zeolite and perrhenate ion sources indicate that the ions are primarily being emitted from the surface of the sources and not from the interfacial region between the substrate and the emitter material. DOE

N94-36303 Brookhaven National Lab., Upton, NY.
SUMMARY: HADRON DYNAMICS SESSIONS
A. S. Carroll and J. T. Londergan 1993 8 p Presented at the Future Directions in Particle and Nuclear Physics at Multi-GeV Hadron Beam Facilities, Upton, NY, 4-6 Mar. 1993 Limited Reproducibility: More than 20% of this document may be affected by microfiche quality
(Contract DE-AC02-76CH-00016)
(DE94-003011; BNL-49650; CONF-930389-25) Avail: CASI HC A02

Four sessions on Hadron Dynamics were organized at this workshop. The first topic, QCD Exclusive Reactions and Color Transparency, featured talks by Ralston, Heppelman, and Strikman; the second, QCD and Inclusive Reactions had talks by Garvey, Speth, and Kisslinger. The third dynamics session, Medium Modification of Elementary Interactions had contributions from Kopeliovich, Alves, and Gyulassy; the fourth session, Pre-QCD Dynamics and Scattering, had talks by Harris, Myhrer, and Brown. An additional joint Spectroscopy/Dynamics session featured talks by Zumbro, Johnson, and McClelland. These contributions are reviewed briefly in this summary. Two additional joint sessions between Dynamics and eta physics are reviewed by the organizers of the eta sessions. In such a brief review there is no way the authors can adequately summarize the details of the physics presented here. As a result, they concentrate only on brief impressionistic sketches of the physics topics discussed and their interrelations. They include no bibliography in this summary, but simply refer to the talks given in more detail in the workshop proceedings. They focus on topics which were common to several presentations in these sessions. First, nuclear and particle descriptions of phenomena are now clearly converging, in both a qualitative and quantitative sense; they show several examples of this convergence. Second, an important issue in hadron dynamics is the extent to which elementary interactions are modified in nuclei at high energies and/or densities, and they illustrate some of these medium effects. Finally, they focus on those dynamical issues where hadron facilities can make an important, or even a unique, contribution to the knowledge of particle and nuclear physics. DOE

N94-36304 Washington Univ., Seattle, WA. Dept. of Physics.
COLLAPSE OF FLUX TUBES
L. Wilets 1993 8 p Presented at the NATO Advanced Study Institute on Hot and Dense Nuclear Matter, Bodrum, Turkey, 26 Sep. - 9 Oct. 1993 Limited Reproducibility: More than 20% of this document may be affected by microfiche quality
(Contract DE-FG06-88ER-40427)
(DE94-004645; DOE/ER-40427/21-N93; CONF-930999-3) Avail: CASI HC A02

Flux tubes are one of the most elementary systems of quantum chromodynamics. They are the idealized configurations of heavy quark-antiquark pairs at large separations L such that the region between can be assumed to possess axial-cylindrical symmetry. They play a central role in lattice QCD calculations and in models of QCD, as well as in the phenomenology of QCD processes. Lattice QCD calculations on flux tubes are generally limited to the quenched approximation (no massless quarks) and allow for a separation of the heavy quark-antiquark of only about 1 fm. Static flux tubes are unstable at separations greater than 1 fm, since the energy required to stretch the tube by 1 fm is about 1 GeV and that is about the energy difference between a quarkonium, Q(bar Q), and a pair of heavy-light mesons, Q(bar q) + (bar Q)q. Lattice calculations without light quarks cannot explore this instability. The author then reviews work on efforts to explore the creation of light quark pairs as a mechanism for flux tube breaking. DOE

N94-36305 Washington Univ., Seattle, WA. Dept. of Physics.
THE NUCLEON-NUCLEON POTENTIAL IN THE CHROMODIELECTRIC SOLITON MODEL
W. Koepf, L. Wilets, S. Pepin, and F. Stancu 1993 9 p Presented at the Conference on Many-Body Physics, Coimbra, Portugal, 20-25 Sep. 1993 Limited Reproducibility: More than 20% of this document may be affected by microfiche quality
(Contract DE-FG06-88ER-40427)
(DE94-004646; DOE/ER-40427/20-N93; CONF-9309302-1) Avail: CASI HC A02

The short and medium range parts of the nucleon-nucleon interaction are being studied in the framework of the chromodielectric soliton model. The model consists of current quarks, gluons in the abelian approximation, and a scalar sigma field which simulates the nonabelian interactions of the gluons and governs the medium through the dielectric function kappa(sigma). Absolute color confinement is effected by the vanishing of the dielectric in vacuum; this also removes the troublesome van der Waals problem. The authors distinguish between spatial confinement, which arises from the self energy of the quarks in medium (excluding MFA contributions), and color confinement which is effected through OGE in the MFA (including the corresponding self energy contributions). The static (adiabatic) energies are computed as a function of deformation (generalized bag separation) in a constrained MFA. Six quark molecular-type wave functions in all important space-spin-isospin-color configurations are included. The gluon propagator is solved in the deformed dielectric medium. The resultant Hamiltonian matrix is diagonalized. Dynamics are handled in the generator coordinate method, which leads to the Hill-Wheeler integral equation. In the present case, this yields a set of coupled equations corresponding to the various configurations. Although this can be approximated by a set of differential equations, they propose to solve the integral equations with some regularization scheme. DOE

N94-36308# International Centre for Theoretical Physics, Trieste (Italy).
DECAY OF THE D(SUB s)-MESON
Duong Van Phi and Duong Anh Duc Aug. 1993 9 p
(DE94-611209; IC-93/231) Avail: CASI HC A02/MF A01 (US Sales Only)

The decay channels of the D(sub s)-meson are deduced from a selection rule and a Lagrangian, formed on L*O(4) group invariance and on principle of minimal structure. A comparison of the results with experimental data is made. DOE

N94-36310# Academy of Sciences (USSR), Kiev (USSR). Inst. for Theoretical Physics.
ON THE EFFECTS OF TRANSFORMING THE VIBRATIONAL SPECTRA OF MOLECULAR SYSTEMS UNDER MICROWAVE RADIATION
A. A. Serikov 1993 23 p Submitted for publication
(DE94-617057; ITP-93-40E) Avail: CASI HC A03/MF A01 (US Sales Only)

This problem is analyzed within the quantum-classical theory of molecular spectra. It is shown that the above-mentioned spectrum transformation could be, in principle, realized in macromolecular systems with strong interaction, and attention is drawn to the resonance character of the effect. DOE

N94-36311# Academy of Sciences (USSR), Kiev (USSR). Inst. for Theoretical Physics.
MODELLING OF THE STRUCTURE AND PHYSICAL PROPERTIES OF SIMPLE DISORDERED SYSTEMS
A. G. Zagorodnij and O. I. Gerasimov 1993 21 p Submitted for publication
(DE94-617087; ITP-93-4E) Avail: CASI HC A03/MF A01 (US Sales Only)

The statistical modelling of a set of Bogolyubov distribution functions and self-consistent(within the Bogolyubov theory) interatomic potentials are proposed for the appraisals and calculations of many-particle contributions to structural, thermodynamic and polarizational properties of the disordered systems. DOE

N94-36390# Northwestern Univ., Evanston, IL.
DYNAMIC STRUCTURAL EFFECTS AND ULTRAFAST BIOMOLECULAR KINETICS IN PHOTOINDUCED CHARGE TRANSFER REACTIONS
J. T. Hupp Apr. 1994 16 p
(Contract DE-FG02-87ER-13808)
(DE94-010421; DOE/ER-13808/6) Avail: CASI HC A03/MF A01

The reactions were primarily electron-transfer-reactivity related (ET). Goals were to obtain complete, multimode, experimental descriptions of vibrational (Franck-Condon) barriers to intramolecular electron transfer, explore molecular generality of time-dependent scattering analysis, connect the information directly to measured rates of photoinduced ET (femtosecond, picosecond, nanosecond regime), obtain complementary information in the microsecond regime (longer-range thermal ET) via pulsed-accelrated flow, explore valence localization/delocalization via vibronic coupling (resonance Raman in extended near infrared) and via reversible external manipulation of internal electronic structure, and manipulate and accelerate bimolecular photoredox processes by using room-temperature supercritical fluids. Fe and Ru complexes with such compounds as cyano-N-methylpyridinium compounds were studied. DOE

N94-36391# Academy of Sciences of the Ukraine, Kiev. Inst. for Theoretical Physics.
P-MATRIX DESCRIPTION OF CHARGED PARTICLES INTERACTION
V. A. Babenko and N. M. Petrov 1992 12 p Submitted for publication
(DE94-616853; ITP-92-40E) Avail: CASI HC A03/MF A01 (US Sales Only)

The paper deals with formalism of the P-matrix description of two charged particles interaction. Separation in the explicit form of the background part corresponding to the purely Coulomb interaction in the P-matrix is proposed. Expressions for the purely Coulomb P-matrix, its poles, residues and purely Coulomb P-matrix approach eigenfunctions are obtained. DOE

N94-36392# Academy of Sciences (USSR), Kiev (USSR). Inst. for Theoretical Physics.
NOTES ON POSSIBLE S-WAVE RESONANCES IN RELATIVISTIC TWO-PARTICLE SYSTEMS
D. V. Shapoval, I. V. Simenog, and O. G. Sitenko 1993 8 p Submitted for publication
(DE94-616889; ITP-93-31E) Avail: CASI HC A02/MF A01 (US Sales Only)

Some models of relativistic two-particle systems are examined for possible irregularities in the S-wave continuous spectrum. None are found, though we show that with singular effective interaction potentials it is quite easy to run into artificial resonances originating from inaccurate calculations. DOE

N94-36434# Academy of Sciences of the Ukraine, Kiev. Inst. for Theoretical Physics.
PAIRING AND LOW TEMPERATURE PROPERTIES OF 2D FERMI-SYSTEMS WITH ATTRACTION BETWEEN PARTICLES
E. V. Gorbar, V. P. Gusynin, and V. M. Loktev 1992 41 p Submitted for publication
(DE94-615510; ITP-92-54E) Avail: CASI HC A03/MF A01 (US Sales Only)

Proceeding from microscopic model Hamiltonian for the system of Fermi-particles with attraction the effective Lagrangian, admitting the analysis of its superconducting properties at arbitrary fermion concentration, is obtained.Exact solution for gap and chemical potential makes it possible to trace from local pair situation to Cooper pairing. The crucial parameter discriminating between the regions of exotic and normal superconducting behaviour is shown to be that of the energy of the bound fermion state, which, however, rapidly disappears with fermion density increasing. The solutions of the equations for the case of finite temperatures are analysed. DOE

73 NUCLEAR AND HIGH-ENERGY PHYSICS

Includes elementary and nuclear particles; and reactor theory. For space radiation see *93 Space Radiation.*

N94-35483*# Southwest Research Inst., San Antonio, TX. Instrumentation and Space Research Div.
PARTICIPATION IN THE DEFINITION, CONDUCT, AND ANALYSIS OF PARTICLE ACCELERATOR EXPERIMENTS FOR THE FIRST SPACELAB MISSION Final Report
J. L. Burch 30 Apr. 1994 56 p
(Contract NAS8-32488; SwRI Proj. 15-4865)
(NASA-CR-193974; NAS 1.26:193974) Avail: CASI HC A04/MF A01

The Space Experiments with Particle Accelerators (SEPAC) is a joint endeavor between NASA and the Institute of Space and Aeronautical Sciences (ISAS) in Japan. Its objectives are to use energetic electron beams to investigate beam-atmosphere interactions and beam-plasma interactions in the earth's upper atmosphere and ionosphere using the shuttle Spacelab. Two flights of SEPAC have occurred to date (Spacelab 1 on STS-9 in Nov.-Dec. 1983 and ATLAS 1 on STS-45 in Mar.-Apr. 1992). The SEPAC instrumentation is available for future missions, and the scientific results of the first two missions justify further investigations; however, at present there are no identifiable future flight opportunities. As specified in the contract, the primary purpose of this report is to review the scientific accomplishments of the ATLAS 1 SEPAC experiments, which have been documented in the published literature, with only a brief review of the earlier Spacelab 1 results. One of the main results of the Spacelab 1 SEPAC experiments was that the ejection of plasma from the magnetoplasmadynamic (MPD) arcjet was effective in maintaining vehicle charge neutralization during electron beam firings, but only for a brief period of 10 ms or so. Therefore, a xenon plasma contactor, which can provide continuous vehicle charge neutralization, was developed for the ATLAS 1 SEPAC experiments. Because of the successful operation of the plasma contactor on ATLAS 1, it was possible to perform experiments on beam-plasma interactions and beam-atmosphere interactions at the highest beam power levels of SEPAC. In addition, the ability of the plasma contactor to eject neutral xenon led to a successful experiment on the critical ionization velocity (CIV) phenomena on ATLAS 1. Derived from text

N94-35999# Academy of Sciences (USSR), Novosibirsk (USSR). Inst. Yadernoj Fiziki.
COMPUTER SIMULATION OF BEAM-BEAM EFFECTS AT LARGE AMPLITUDES AND DETERMINATION OF LIFE TIME
D. N. Shatilov 1992 33 p
(DE94-616235; IYaF-92-79) Avail: CASI HC A03/MF A01 (US Sales Only)

Computer simulation of beam-beam effects requires a very large processor time for determination of lifetime. A new method is proposed for smooth, step-by-step, construction of the particle distribution in the amplitude space. The method permits a decrease in simulation time by some orders of magnitude. One of the main advantages of this method is a possibility to check its accuracy. The physical substantiation, algorithm and applicability conditions of this method are presented. DOE

N94-36028# Instituto de Pesquisas Energeticas e Nucleares, Sao Paulo (Brazil).
TREATMENT OF TOXIC GASES SO2 AND NO(x) BY ELECTRON BEAM IRRADIATION
Dora deCastro Rubio Poli, Jose Mauro Vieira, and Clelia Aparecida deCampos Jan. 1993 13 p
(DE94-615424; IPEN-Pub-381) Avail: CASI HC A03/MF A01 (US Sales Only)

The removal of SO2 and NO(x) by electron beam irradiation will be studied using a small scale flow system which is being set up in order to obtain basic data for the process technical and economical feasibility concerning industrial applications. The gas irradiation will be performed using a Electron Beam Accelerator with 1.5 MeV power, 25 mA current from Radiation Dynamics, Inc. DOE

N94-36080# Joint Inst. for Nuclear Research, Dubna (USSR). Lab. of Theoretical Physics.
SPIN EFFECTS IN HIGH ENERGY QUARK-QUARK SCATTERING
S. V. Goloskokov and O. V. Selyugin 1993 10 p Submitted for publication
(DE94-616800; JINR-E-2-93-164) Avail: CASI HC A02/MF A01 (US Sales Only)

The spin amplitudes in high-energy quark-quark scattering at(absolute value of) t greater than 1 GeV(sup 2) are analyzed. It is shown that the gluon contributions in the QCD(alpha)(sub s)(sup 3) order lead to the spin-flip amplitude growing as s. This means the existence of the spin-flip part in pomeron exchange. The resulting T(sub f) is about few per cent of the spin-non-flip contribution. The factorization of the large-distance and high-energy effects in the spin-flip amplitude is obtained. DOE

N94-36105# Texas Univ., Austin, TX. Dept. of Physics.
KINETICS STUDIES FOLLOWING STATE-SELECTIVE LASER EXCITATION
J. W. Keto Apr. 1994 60 p
(Contract DE-FG05-84ER-13191)
(DE94-010305; DOE/ER-13191/14) Avail: CASI HC A04/MF A01

The objective of this contract was the study of state-to-state, electronic energy transfer reactions relevant to the excited state chemistry observed in discharges. We studied deactivation reactions and excitation transfer in collisions of excited states of xenon and krypton atoms with Ar, Kr, Xe, and chlorine. The reactant states were excited selectively in two-photon transitions using tunable UV and VUV lasers. Excited states produced by the collision were observed by their fluorescence. Reaction rates were measured by observing the time dependent decay of signals from reactant and product channels. In addition we measured interaction potentials of the reactants by laser spectroscopy where the laser induced fluorescence or ionization is measured as a function of laser wavelength (excitation spectra) or by measuring fluorescence spectra at fixed laser frequencies with monochromators. The spectra were obtained in the form of either lineshapes or individual lines from rovibrational transitions of bound states. Our research then required several categories of experiments in order to fully understand a reaction process: (1) High resolution laser spectroscopy of bound molecules or lineshapes of colliding pairs is used to determine potential curves for reactants. (2) Direct measurements of state-to-state reaction rates were measured by studying the time dependent loss of excited reactants and the time dependent formation of products. (3) The energy selectivity of a laser can be used to excite reactants on an excited surface with controlled internuclear configurations. For free states of reactants (as exist in a gas cell) this has been termed laser assisted reactions, while for initially bound states (as chemically bound reactants or dimers formed in supersonic beams) the experiments have been termed photofragmentation spectroscopy. DOE

N94-36106# Stanford Linear Accelerator Center, CA.
SPIN DYNAMICS IN STORAGE RINGS AND LINEAR ACCELERATORS
J. Irwin Apr. 1994 21 p Presented at the 21st Annual SLAC Summer Institute on Particle Physics: Spin Structure in High-Energy Processes, Stanford, CA, 26 Jul. - 6 Aug. 1993
(Contract DE-AC03-76SF-00515)
(DE94-010320; SU-SLAC-PUB-6448; CONF-930767-6) Avail: CASI HC A03/MF A01

The purpose of these lectures is to survey the subject of spin dynamics in accelerators: to give a sense of the underlying physics, the typical analytic and numeric methods used, and an overview of results achieved. Consideration will be limited to electrons and protons. Examples of experimental and theoretical results in both linear and circular machines are included. DOE

N94-36114# Lawrence Livermore National Lab., CA.
NEUTRON DETECTORS FOR FUSION REACTION-RATE MEASUREMENTS
R. A. Lerche, D. W. Phillion, O. L. Landen, T. J. Murphy, and P. A. Jaanimagi 10 Feb. 1994 9 p Presented at the 11th International Workshop on Laser Interaction and Related Plasma Phenomena, Monterey, CA, 25-29 Oct. 1993
(Contract W-7405-eng-48)
(DE94-010407; UCRL-JC-114963; CONF-931048-12) Avail: CASI HC A02/MF A01

Fusion reactions in an inertial-confinement fusion (ICF) target filled with deuterium or a deuterium/tritium fuel release nearly monoenergetic neutrons. Because most the neutrons leave the compressed target without collision, they preserve reaction-rate information as they travel radially outward from their point of origin. Three fast neutron detector techniques, each capable of measuring the fusion reaction-rate of ICF targets, have been demonstrated. The most advanced detector is based on the fast rise-time of a commercial plastic scintillator material (BC-422) which acts as a neutron-to-light converter. Signals, which are recorded with a fast optical streak camera, have a resolution of 25 ps. Good signals can be recorded for targets producing only 5 x 10(exp 7) DT neutrons. Two other detectors use knock-on collisions between neutrons and protons in a thin polyethylene (CH2) converter. In one, the converter is placed in front of the photocathode of an x-ray streak camera. Recoil protons pass through the photocathode and knock out electrons which are accelerated and deflected to produce a signal. Resolutions less than 25 ps are possible. In the other, the converter is placed in front of a microchannel plate (MCP) with a gated microstrip. Recoil protons eject electrons from the gold layer forming the microstrip. If a gate pulse is present, the signal is amplified. Present gate times are about 80 ps. DOE

N94-36192# Southeastern Univ. Research Association, Newport News, VA.
BEAM ENERGY ABSOLUTE MEASUREMENT USING K-EDGE ABSORPTION SPECTROMETERS
I. P. Karabekov (Academy of Sciences of the Armenian SSR, Erivan.) and G. R. Neil (Continuous Electron Beam Accelerator Facility, Newport New, VA.) May 1994 6 p
(Contract DE-AC05-84ER-40150)
(DE94-010019; DOE/ER-40150/264; CEBAF-PR-94-003) Avail: CASI HC A02/MF A01

A method is presented of absolute energy measurement with an accuracy of Delta Epsilon approximately equals 10(exp -4) Epsilon(sub o) by direct measurement of the bend angle in a high-precision magnetic dipole using two opposite-direction short (about 2 mm long) high-field-intensity magnets (bar-Beta(sub dipole) much less than Beta(sub short mag)) installed at each end and two K-edge absorption spectrometers. Using these spectrometers and the hard x-ray synchrotron radiation created by the short magnets, a bend angle of 4.5 arc deg for the CEBAF energy bandwidth can be measured with an accuracy of a few units of 10(exp -6) rad, and the main sources of systematic errors are the absolute measurement of the field integral and the determination of the centroid of the synchrotron beam at a wavelength equal to the K-edge absorption of the chosen substance. DOE

N94-36199# Sandia National Labs., Albuquerque, NM.
BEAM TRANSPORT
C. L. Olson, M. E. Cuneo, and M. P. Desjarlais et al 1993 6 p Presented at the 11th International Workshop on Laser Interaction and Related Plasma Phenomena, Monterey, CA, 25-29 Oct. 1993
(Contract DE-AC04-94AL-85000)
(DE94-010755; SAND-93-2198C; CONF-931048-14) Avail: CASI HC A02/MF A01

Transport and focusing of light ion beams for inertial confinement fusion is discussed, including transport schemes, gas breakdown research, and a strategy for divergence reduction. DOE

N94-36202# California Univ., Berkeley. Lawrence Berkeley Lab, CA.
ILSE COMBINER STUDY
K. Hahn Mar. 1994 28 p
(Contract DE-AC03-76SF-00098)
(DE94-011009; LBL-35335) Avail: CASI HC A03/MF A01

In a heavy ion inertial fusion (HIF) driver, the beam energy and current are increased several orders of magnitude from the injector to the final focus system. At low and high energy stages of the driver, electrostatic and magnetic focusing transport channels, respectively, can be used. At the electric-to-magnetic transition point, the beams may be combined to reduce the transverse dimensions of the system, which could have significant impact on the driver cost. In a presently envisioned combiner, four beams are brought together transversely into a single transport channel. A matching section follows the combiner in order to provide a smooth transition to the subsequent magnetic transport channel. This report summarizes a conceptual design study of possible combiner configurations for the proposed Introduction Linac Systems Experiment (ILSE). The conceptual design study includes subjects such as the expected technical difficulties, predicted emittance growth, particle loss, effect of geometric and chromatic aberrations, and the sensitivity of emittance growth on the initial beam position and angle errors. DOE

N94-36224# Stanford Linear Accelerator Center, CA.
DYNAMIC APERTURE AND TRANSVERSE PROTON DIFFUSION IN HERA
F. Zimmermann Apr. 1994 35 p Presented at the Superconducting Super Collider Conference, Dallas, TX, 29 Oct. 1992
(Contract DE-AC03-76SF-00515)
(DE94-010309; SU-SLAC-PUB-6458; CONF-9210457-1) Avail: CASI HC A03/MF A01

The dynamic aperture caused by persistent-current nonlinear field errors is an important concern in the design of superconducting hadron storage rings. The HERA proton ring is the second superconducting accelerator in operation. In this lecture note, its measured dynamic aperture is compared with that inferred from comprehensive tracking studies. To understand the difference between prediction and measurement, a semi-analytical method is developed for evaluating transverse diffusion rates due to various processes, such as modulational diffusion or sweeping diffusion. This analysis makes use of parameters for high-order resonances in the transverse phase space, which are obtained by normal-form algorithms using differential-algebra software. These semi-analytical results are consistent with the measurements and suggest that the actual dynamic aperture is caused by an interplay of tune modulation and nonlinear magnetic fields. DOE

N94-36271# California Univ., Berkeley. Lawrence Berkeley Lab, CA.
CRITICAL ISSUES IN MUON COLLIDERS: A SUMMARY
S. Chattopadhyay, W. Barletta, A. Sessler, S. Maury, and D. Neuffer Feb. 1994 10 p Presented at the CERN Workshop on Beam Cooling and Related Topics, Geneva, Switzerland, 4-8 Oct. 1993
(Contract DE-AC03-76SF-00098)
(DE94-011382; LBL-35232; CONF-9310193-12) Avail: CASI HC A02/MF A01

We present a brief summary of the current state of conception and understanding of high energy muon colliders, associated technological challenges, and future research directions on this topic. DOE

N94-36317# Pacific Northwest Lab., Richland, WA.
SYNTH: A SPECTRUM SYNTHESIZER
W. K. Hensley, A. D. McKinnon, H. S. Miley, M. E. Panisko, and R. M. Savard Oct. 1993 5 p Presented at the 1993 IEEE Nuclear Science Symposium and Medical Imaging Conference, San Francisco, CA, 2-5 Nov. 1993
(Contract DE-AC06-76RL-01830)
(DE94-004719; PNL-SA-22412; CONF-931107-26) Avail: CASI HC A01/MF A01

A computer code has been written at the Pacific Northwest Laboratory (PNL) to synthesize the results of typical gamma ray spectroscopy experiments. The code, dubbed SYNTH, allows a user to specify physical characteristics of a gamma ray source, the quantity of the nuclides producing the radiation, the source-to-detector distance and the presence of absorbers, the type and size of the detector, and the electronic set up used to gather the data. In the process of specifying the parameters needed to synthesize a spectrum, several interesting intermediate results are produced, including a photopeak transmission function versus energy, a detector efficiency curve, and a weighted list of gamma and x rays produced from a set of nuclides. All of these intermediate results are available for graphical inspection and for printing. SYNTH runs on personal computers. It is menu driven and can be customized to user specifications. SYNTH contains robust support for coaxial germanium detectors and some support for sodium iodide detectors. SYNTH is not a finished product. A number of additional developments are planned. However, the existing code has been compared carefully to spectra obtained from National Institute for Standards and Technology (NIST) certified standards with very favorable results. Examples of the use of SYNTH and several spectral results are presented. DOE

N94-36428# Rice Univ., Houston, TX. Nuclear Labs.
HIGH ENERGY

B. E. Bonner and J. B. Roberts, Jr. 1 Dec. 1993 32 p
(Contract DE-FG05-92ER-40717)
(DE94-009477; DOE/ER-40717/10) Avail: CASI HC A03/MF A01

The new results from the SMC experiment have generated a buzz of theoretical activity. Our involvement with the D0 experiment and the upgrade has increased substantially during the past two years so that we now have six people heavily committed and making what can only be described as a large and disproportionate impact on D0 physics output. Some of the new developments made here at Rice in Neural Network and Probability Density Estimation techniques for data analysis promise to have applications both in D0 and beyond. We report a load of new results from our high-p(sub t) jet photoproduction experiment. In addition we have been working on KTeV. Progress on the theoretical front has been nothing short of amazing, as is reported herein. In a grand lecture tour during this sabbatical year, Paul Stevenson has already reported his breakthroughs at ten institutions, including CERN, Oxford, Cambridge, Rutherford Lab, Imperial College, and Durham University. The group at Rice University has had an exceptionally productive year and we are justifiably proud of the progress which is reported here. DOE

N94-36431# Fermi National Accelerator Lab., Batavia, IL.
IMPEDANCE AND INSTABILITY THRESHOLD ESTIMATES IN THE MAIN INJECTOR 1
M. A. Martens and K. Y. Ng Mar. 1994 54 p
(Contract DE-AC02-76CH-03000)
(DE94-010332; FNAL-TM-1880) Avail: CASI HC A04/MF A01

One of the important considerations in the design of the Main Injector is the beam coupling impedances in the vacuum chamber and the stability of the beam. Along with the higher intensities comes the possibility of instabilities which lead to growth in beam emittances and/or the loss of beam. This paper makes estimations of the various impedances and instability thresholds based on impedance estimations and measurements. Notably missing from this paper is any analysis of transition crossing and its potential limitations on beam intensity and beam emittance. Future work should consider this issue. The body of the work contains detailed analysis of the various impedance estimations and instability threshold calculations. The calculations are based on the Main Injector beam intensity of 6 x 10(exp 10) protons per bunch, 95 percent normalized transverse emittances of 20(pi) mm-mrad, and 95 percent normalized longitudinal emittance of 0.1 eV-s at 8.9 GeV injection energy and 0.25 eV-s at 150 GeV flattop energy. The conclusions section summarizes the results in the paper and is meant to be readable by itself without referring to the rest of the paper. DOE

74 OPTICS

Includes light phenomena; and optical devices.
For lasers see *36 Lasers and Masers.*

N94-35384* National Aeronautics and Space Administration. Pasadena Office, CA.
ADJUSTABLE CONTROL STATION WITH MOVABLE MONITORS AND CAMERAS FOR VIEWING SYSTEMS IN ROBOTICS AND TELEOPERATIONS Patent
Daniel B. Diner, inventor (to NASA) (Jet Propulsion Lab., California Inst. of Tech., Pasadena, CA.) 19 Jul. 1994 13 p Filed 28 Sep. 1992 Supersedes N93-17273 (31 - 5, p 1304)
(NASA-Case-NPO-17837-1-CU; US-Patent-5,331,413;
US-Patent-Appl-SN-954109; US-Patent-Class-348-159;
US-Patent-Class-395-94; US-Patent-Class-901-47; US-Patent-Class-348-114;
US-Patent-Class-348-143; Int-Patent-Class-H04N-7/18) Avail: US Patent and Trademark Office

Real-time video presentations are provided in the field of operator-supervised automation and teleoperation, particularly in control stations having movable cameras for optimal viewing of a region of interest in robotics and teleoperations for performing different types of tasks. Movable monitors to match the corresponding camera orientations (pan, tilt, and roll) are provided in order to match the coordinate systems of all the monitors to the operator internal coordinate system. Automated control of the arrangement of cameras and monitors, and of the configuration of system parameters, is provided for optimal viewing and performance of each type of task for each operator since operators have different individual characteristics. The optimal viewing arrangement and system parameter configuration is determined and stored for each operator in performing each of many types of tasks in order to aid the automation of setting up optimal arrangements and configurations for successive tasks in real time. Factors in determining what is optimal include the operator's ability to use hand-controllers for each type of task. Robot joint locations, forces and torques are used, as well as the operator's identity, to identify the current type of task being performed in order to call up a stored optimal viewing arrangement and system parameter configuration.
Official Gazette of the U.S. Patent and Trademark Office

N94-35584 National Oceanic and Atmospheric Administration, Research Triangle Park, NC. Atmospheric Sciences Modeling Div.
ANALYSIS OF REGIONAL VISIBILITY IN THE EASTERN UNITED STATES USING AEROSOL MODELS
A. F. Hanna (Microelectronics Center of North Carolina, Research Triangle Park, NC.), F. S. Binkowski, and U. Shankar 1994 19 p Presented at conference 1993 Limited Reproducibility: More than 20% of this document may be affected by microfiche quality
(PB94-158698; EPA/600/A-94/043) Avail: CASI HC A03

Visibility has traditionally been calculated using the Koschmieder formula that relates the distance at which a black object can just be distinguished against the horizon to the extinction coefficient of the assumed homogeneous air path between the object and observer. The light extinction coefficient is the sum of the medium's absorption and scattering coefficients. The components of light extinction include light scattering by air molecules (Rayleigh scattering) and by particles (Mie scattering), and light absorption by gases and by particles. Scattering by particles is the dominant component of light extinction. The authors demonstrate the use of accurate and approximate methods for calculating light extinction to estimate regional visibility. Concentrations of sulfates, which are known to be the major contributors to visibility degradation in the eastern United States, are simulated using the Regional Particulate Model (RPM). NTIS

N94-35664 Columbia Univ., New York, NY.
THEORETICAL STUDIES OF ULTRASHORT PHENOMENA Final Report, 1 May - 30 Sep. 1993
M. J. Potaske Nov. 1993 7 p Limited Reproducibility: More than 20% of this document may be affected by microfiche quality
(Contract F49620-93-1-0277)
(AD-A278938; AFOSR-94-0272TR) Avail: Issuing Activity (Defense Technical Information Center (DTIC))

With the advent of new laser sources, considerable interest has been focussed on the interaction of femtosecond optical pulses with nonlinear media. We find conditions for femtosecond solitons and demonstrate that they differ in their velocity and phase from the traditional solitons. We investigate physical properties for their experimental observation. DTIC

N94-35671# Argonne National Lab., IL. Chemistry Div.
MOLECULAR SYSTEMS FOR ULTRAFAST OPTICAL SWITCHING: CONTROLLING ELECTRON TRANSFER REACTIONS WITH FEMTOSECOND LASER PULSES
S. R. Greenfield, D. J. Gosztola, and M. R. Wasielewski 1994 4 p Presented at the 9th International Conference on Ultrafast Phenomena, Dana Point, CA, 1-5 May 1994
(Contract W-31-109-eng-38)
(DE94-009695; ANL/CHM/CP-81871; CONF-940593-7) Avail: CASI HC A01/MF A01

Rapid, reversible photoinduced electron transfer reactions are a class of photophysical phenomena that can be exploited to develop schemes for optical switching. Molecular electronic switches, wires, micro-sensors for chemical analysis, and opto-electronic components for use in optical computing are currently under active investigation. The principal advantages of using molecules in these applications are high component density, increased response speeds, and high energy efficiency. Since photoinduced electron transfer processes within molecules can take place on a picosecond time scale, it should be possible to produce efficient devices that respond very rapidly. Molecules that employ reversible electron transfer reactions for optical switching should possess both speed and photostability advantages over molecular switches based on photochemical changes in molecular structure. For this purpose the authors recently designed several molecular systems that display properties that may be exploited for optical switching. In this paper, two or more laser pulses are used to manipulate photochromic ion pairs that result from rapid reversible photoinduced electron transfer in complex donor-acceptor molecules. DOE

N94-35697# Lawrence Livermore National Lab., CA.

CHARACTERIZATION OF LITHIUM NIOBATE ELECTRO-OPTIC MODULATORS AT CRYOGENIC TEMPERATURES

J. Morse, K. McCammon, C. McConaghy, D. Masquelier, H. Garrett, and M. Lowry Jan. 1994 10 p Presented at the OE/LASE 1994: Conference on Optics, Electro-Optics, and Laser Applications in Science and Engineering, Los Angeles, CA, 22-29 Jan. 1994
(Contract W-7405-eng-48)
(DE94-010059; UCRL-JC-116078; CONF-940142-34) Avail: CASI HC A02/MF A01

This paper reports on the operation of lithium niobate electro-optic waveguide modulators at temperatures down to 15 K. Commercial and laboratory fiber pigtailed devices have successfully been cooled without any increases in insertion loss from temperature induced stresses in device packaging. Three x-cut devices exhibited a linear increase in V(pi) voltage of 8% (+/-) 1% when cooled from room temperature to approximately 20 K. The broadband frequency response improved at lower temperature. A velocity-matched experimental modular has shown increased bandwidth when cooled to liquid nitrogen temperature. DOE

N94-35747 Pennsylvania State Univ., University Park, PA. Applied Research Lab.

AN ELECTRONIC INTERFACE FOR A FIBER OPTIC TETHERED UNMANNED UNDERWATER VEHICLE

J. R. Sheakoski Apr. 1994 93 p Limited Reproducibility: More than 20% of this document may be affected by microfiche quality
(Contract N00039-88-C-0051)
(AD-A279046; PSU/ARL-TR-94-08) Avail: Issuing Activity (Defense Technical Information Center (DTIC))

As the sophistication of acoustic sensor and communication systems related to unmanned underwater vehicles (UUV) has increased, the requirement for greater volume and higher speed data transfers has emerged. Fiber optic technology provides an effective means for high bandwidth communications with a UUV while minimizing weight and space criteria aboard the UUV. Increase in data transmission speed has permitted real time processing of data on the launch platform when using large high powered computing systems. Maximum system reliability at advanced performance levels can also be realized. By designing and developing a full scale system comprised of the UUV, remote control and command platform, and data handling and routing electronics, fiber optic tethered UUV technology was demonstrated in lab field tests. This three year venture culminated in a series of successful in-water tests that proved the feasibility of fiber optic tethered UUV's and warranted the continuation of research on remotely operated UUV's. DTIC

N94-35749* National Aeronautics and Space Administration. Pasadena Office, CA.

METHOD AND APPARATUS FOR REMOVING UNWANTED REFLECTIONS FROM AN INTERFEROMETER Patent

Lawrence J. Steimle, inventor (to NASA) (Jet Propulsion Lab., California Inst. of Tech., Pasadena, CA.) and David L. Thiessen, inventor (to NASA) (Jet Propulsion Lab., California Inst. of Tech., Pasadena, CA.) 5 Jul. 1994 11 p Filed 15 May 1992 Supersedes N92-30084 (30 - 20, p 3553)
(NASA-Case-NPO-18478-1-CU; US-Patent-5,327,219; US-Patent-Appl-SN-883957; US-Patent-Class-356-359; US-Patent-Class-356-360; US-Patent-Class-356-345; US-Patent-Class-356-354; Int-Patent-Class-G01B-11/00; Int-Patent-Class-G01B-9/02) Avail: US Patent and Trademark Office

A device for eliminating unwanted reflections from refractive optical elements in an optical system is provided. The device operates to prevent desired multiple fringe patterns from being obscured by reflections from refractive elements positioned in proximity to a focal plane of the system. The problem occurs when an optical beam is projected into, and reflected back out of, the optical system. Surfaces of the refractive elements reflect portions of the beam which interfere with portions of the beam which are transmitted through the refractive elements. Interference between the reflected and transmitted portions of the beam produce multiple fringe sets which tend to obscure desired interference fringes. With the refractive optical element in close proximity to the focal plane of the system, the undesired reflected light reflects at an angle 180 degrees opposite from the desired transmitted beam. The device exploits the 180-degree offset, or rotational shear, of the undesired reflected light by providing an optical stop for blocking one-half of the cross-section of the test beam. By blocking one-half of the test beam, the undesired offset beam is blocked, while the returning transmitted beam passes into the optical system unaffected. An image is thereby produced from only the desired transmitted beam. In one configuration, the blocking device includes a semicircular aperture which is caused to rotate about the axis of the test beam. By rotating, all portions of the test beam are cyclically projected into the optical system to thereby produce a complete test image. The rotating optical stop is preferably caused to rotate rapidly to eliminate flicker in the resulting image.
Official Gazette of the U.S. Patent and Trademark Office

N94-35818# Lawrence Livermore National Lab., CA.

HIGH-SENSITIVITY RECEIVER FOR INCREASING MULTIPLICITY OF MEASUREMENT AXES OF ZYGO'S HETERODYNE INTERFEROMETER

J. F. Beckwith Apr. 1994 5 p Presented at the American Society for Precision Engineering Conference, Tucson, AZ, 6-8 Apr. 1994
(Contract W-7405-eng-48)
(DE94-009916; UCRL-JC-116931; CONF-9404131-1) Avail: CASI HC A01/MF A01

The number of measurement axes which can be simultaneously operated from a single laser source is limited by, among other factors, the minimum optical power required at the electronic receiver which detects the interferometric phase of the recombined measurement and reference beams. A high-sensitivity receiver has been designed and operated which decreases this required minimum power by about a factor of twenty for the Zygo Heterodyne distance-measuring interferometer. The receiver utilizes a tuned front end and a low-noise DMOSFET for the first amplifier stage. The tuned circuit, however, reduces the maximum slew rate, but this can be easily traded off against the increased sensitivity while maintaining a net increase in their product. Both the input and output employ fiber optics for maximum noise immunity. The fiber-optic connectors and output signal are compatible with Zygo's VME measurement electronics. DOE

N94-36002 National Inst. of Standards and Technology, Gaithersburg, MD. Computer Systems Lab.

COMPUTER SYSTEMS LABORATORY Annual Report, 1993

E. B. Lennon, S. M. Radack, and R. K. Roach Feb. 1993 100 p See also PB93-181873 Limited Reproducibility: More than 20% of this document may be affected by microfiche quality
(PB94-162518; NISTIR-5342) Avail: CASI HC A05

The Computer Systems Laboratory (CSL) Annual Report - 1993 describes the annual activities and accomplishments of the laboratory. Following the Director's Foreword, a CSL overview is presented, followed by overviews of the five technical divisions. The Technology Transfer section describes the vehicles used by CSL to disseminate research and technical information to the public. A list of Federal Information Processing Standards (FIPS) and FIPS order information conclude the annual report. NTIS

N94-36055# Oak Ridge National Lab., TN.

HIGH-RESOLUTION IMAGING USING Z-CONTRAST SCANNING TRANSMISSION ELECTRON MICROSCOPY

S. J. Pennycook 11 Mar. 1994 17 p
(Contract DE-AC05-84OR-21400)
(DE94-008510; ORNL/FTR-4912) Avail: CASI HC A03/MF A01 (US Sales Only)

The purpose of the trip was to attend and present an invited talk at the International Symposium on High-Voltage and High-Resolution Electron Microscopy - Achievements and Future Developments held at the Max-Planck Institute for Metal Physics, Stuttgart, Germany, February 21-24, 1994. DOE

N94-36119*# Smithsonian Astrophysical Observatory, Cambridge, MA.

AXAF-I GHOST RAY STUDY: ON ORBIT CASE Final Report

T. J. Gaetz 2 Sep. 1993 27 p
(Contract NAS8-36123)

(NASA-CR-193987; NAS 1.26:193987; SAO-AXAF-DR-93-053) Avail: CASI HC A03/MF A01

The problem of baffles for control of singly reflected (and nonreflected) ghost rays is considered. The theory of baffle design for Wolter Type I grazing incidence optics is reviewed, and a set of sample baffle parameters is obtained subject to the assumptions of nominal mirror figures and perfect manufacture and alignment of baffles. It is found that baffles forward of the optics (in the thermal precollimator) and between the mirror elements (at the CAP) are sufficient to allow the simultaneous ghost image and vignetting requirements to be satisfied for HRMA shells P1H1, P3H3, and P4H4. However, these baffles are not sufficient for the innermost shell P6H6; at best the requirements are slightly violated and there is no margin for tolerances. The addition of a baffle interior to the P6 space at an axial station about one third of the way forward from the aft end of the paraboloid will allow the ghost ray and vignetting requirements to be met. The minimum ghost ray angles and the vignetting angles are sensitive functions of the baffle positions and radii; tolerances of considerably better than 1 mm will be required. The sensitivities are coupled and correlated; further investigations should be undertaken in order to obtain baffle parameters which, combined with likely achievable tolerances, will minimize the risk of the vignetting/ghost ray requirements not being met. The lightweight carbon-epoxy composite used for thermal baffles has insufficient X-ray opacity to be a suitable material for construction of the controlling X-ray baffles; further study is needed to determine an appropriate material and to investigate its thermal and mechanical implications. Author

N94-36122 Department of the Navy, Washington, DC.
FABRICATION AND PHASE TUNING OF AN OPTICAL WAVEGUIDE DEVICE Patent
William K. Burns, inventor (to Navy), Catherine H. Bulmer, inventor (to Navy), and Arthur S. Greenblatt, inventor (to Navy) 2 Nov. 1993 7 p Filed 16 Nov. 1992
(AD-D016215; US-Patent-5,259,061; US-Patent-Appl-SN-976742; US-Patent-Class-385-132) Avail: US Patent and Trademark Office

The manufacture of an optical waveguide device utilizing a fast, accurate method for tuning of the output phase angle of such devices to a desired operating point. Tuning is accomplished by adjusting the accumulated phase along a waveguide arm of the device by removing optical waveguide material using laser ablation. Due to the change in waveguide geometry in the ablated region, the optical phase velocity is changed and thus the optical path length is affected in that section of waveguide, thereby resulting in a change in output phase angle. DTIC

N94-36180# Korean Atomic Energy Research Inst., Daeduk (Republic of Korea).
MAGNETIC FIELD EFFECT ON SELECTIVE PHOTOIONIZATION
Jong Min Lee, Byung Duk Yoo, Young Joo Lee, Hyung Ki Cha, Ang Sung Choe, Si Pyo Rho, Dae Hyun Baik, Kyu Seok Song, Jong Hoon Yi, and Do Young Jeong et al Jul. 1993 49 p
(DE94-611079; KAERI/TR-367/93) Avail: CASI HC A03/MF A01 (US Sales Only)

The magnetic field effects on selective photoionization of the atoms of Lanthanides have been examined in a point of view of the enhancement of the efficiency of selective photoionization. The Zeeman shifts and the hyperfine structures have been calculated by the formulae approximated by LS coupling, and the electronic orbitals by the Hartree-Slater equation. The dependence of the energy levels on the magnetic field has been informed. The photoionization rate due to the polarized lights in a magnetic field has been evaluated. The variation of selection rules of the photoionization due to polarized lights, also, has been informed. DOE

N94-36190 Helsinki Univ. of Technology, Espoo (Finland). Dept. of Technical Physics.
[ACTIVITIES OF THE OPTOELECTRONICS LABORATORY] Annual Report, 1991
H. Collan, ed. and T. Tuomi, ed. 1992 57 p See also PB93-224806 Limited Reproducibility: More than 20% of this document may be affected by microfiche quality
(PB94-171196; TKK-F-C139) Avail: Issuing Activity (National Technical Information Service (NTIS))

This is the second annual report of the Optoelectronics Laboratory, a new and independently responsible operational unit within Helsinki University of Technology. Presently, basic research is carried out in the field of optical properties of semiconductor epilayers, quantum wells, and superlattices using photoreflectance and other modulation techniques. Applied research is done on liquid phase epitaxy of compound semiconductors, on semiconductor lasers, on the direct recording of synchrotron X-ray topographs with an electronic semiconductor camera, on the studies of internal and external gettering of silicon wafers in a complementary metal-oxide-semiconductor process and on applied superconductivity, to mention a few. NTIS

N94-36257 Seattle Pacific Coll., WA. Dept. of Electrical Engineering.
ERROR REDUCTION IN IMAGES WITH THE USE OF ADDITIONAL INFORMATION Final Report, 1 May 1992 - 31 Aug. 1993
Charles L. Matson 31 Jan. 1994 84 p Limited Reproducibility: More than 20% of this document may be affected by microfiche quality
(Contract F49620-92-J-0228)
(AD-A278636; AFOSR-94-0256TR) Avail: Issuing Activity (Defense Technical Information Center (DTIC))

The use of additional information to achieve error reduction in images is discussed in this report. Theoretical results are derived for images corrupted with Fourier domain wide-sense stationary noise. Three types of additional information are explored: support, positivity, and high-quality prior image data. The basic mechanism for reducing noise in images with these types of additional information is shown to be enforced correlations in the Fourier data. The amount of noise reduction achieved is shown to be a function of the relative correlation of the noises and the enforced correlations. For significant noise reduction to be achieved, the noises must be significantly uncorrelated relative to the enforced correlations and the sizes of the noise variances must also be significantly uncorrelated. These results are applied to computer-simulated and field data from telescopes with adaptive optics. DTIC

N94-36356# Lawrence Livermore National Lab., CA.
EFFICIENT LIGHT PROPAGATION FOR MULTIPLE ANISOTROPIC VOLUME SCATTERING
N. Max Dec. 1993 30 p Presented at the Siggraph 1994, Orlando, FL, 24-29 Jul. 1994
(Contract W-7405-eng-48)
(DE94-006474; UCRL-JC-115654; CONF-940743-1) Avail: CASI HC A03/MF A01

Realistic rendering of participating media like clouds requires multiple anisotropic light scattering. This paper presents a propagation approximation for light scattered into M direction bins, which reduces the 'ray effect' problem in the traditional 'discrete ordinates' method. For a volume of n(sup 3) elements, it takes O(M n(sup 3) log n + M(sup 2) n(sup 3)) time and O(M n(sup 3)) space. DOE

N94-36363 Department of the Navy, Washington, DC.
COATINGS FOR SiO2 OPTICAL FIBERS Patent
Josephine Covino-Hrbacek, inventor (to Navy) 16 Nov. 1993 3 p Filed 22 Jun. 1992
(AD-D016197; US-Patent-5,262,362; US-Patent-Appl-SN-901649; US-Patent-Class-501-12) Avail: US Patent and Trademark Office

A chemical coating consisting of a mixture of tetraethoxysilane (TEOS), Al(OC4H9)3, LiOH, Ti(OC3H7)4, Zr()2C5H7)4, HNO3 for pH control, and glycerol is introduced which produces an environmentally protective barrier resistant to cracking or crazing to a glass fiber to which it is applied by the SOL-GEL process. DTIC

N94-36368 Department of the Navy, Washington, DC.
METHOD AND APPARATUS FOR IMAGING AN OBJECT IN OR THROUGH A SCATTERING MEDIUM BY USING MULTIPLE-WAVE MIXING Patent
Mark Bashkansky, inventor (to Navy) and John F. Reintjes, inventor (to Navy) 14 Dec. 1993 10 p Filed 30 Nov. 1992
(AD-D016212; US-Patent-5,270,853; US-Patent-Appl-SN-983334; US-Patent-Class-359-326) Avail: US Patent and Trademark Office

A method and apparatus for imaging an object that is part of, embedded in, or viewed through a scattering medium is provided. A broadband stochastic beam generator, such as a broadband laser, generates a broadband stochastic beam and a narrowband beam generator generates a narrowband beam. A non-linear mixing crystal receives the broadband stochastic beam and the narrowband beam and provides a signal light beam conjugate correlated with the broadband stochastic beam to the scattering medium. A multiple-wave mixing cell is disposed to receive the signal light beam from the scattering medium. An adjustable delay path also illuminates the multiple-wave mixing cell with the broadband stochastic beam. A supplemental beam generator is also provided for also additionally illuminating the multiple-wave mixing cell with a supplemental beam having characteristics sufficient to satisfy phase matching with the material of the multiple-wave mixing cell. The multiple-wave mixing cell produces an image-bearing beam which contains an image of an object extracted from the signal light beam emitted from the scattering medium. The apparatus can further include a detector to record the image of the object in the image-bearing beam. DTIC

N94-35549*# Jet Propulsion Lab., California Inst. of Tech., Pasadena, CA.
USE OF THE SAMPLING THEOREM TO SPEED UP NEAR-FIELD PHYSICAL OPTICS SCATTERING CALCULATIONS
P. W. Cramer and W. A. Imbriale *In its* The Telecommunications and Data Acquisition Report 15 May 1994 p 62-74 (For primary document see N94-35542 11-32)
(RTOP 310-20-65-89-01)
Avail: CASI HC A03/MF A03

N94-35613*# National Aeronautics and Space Administration. Goddard Space Flight Center, Greenbelt, MD.
IN-FLIGHT SCALE/DISTORTION CALIBRATION OF THE HUBBLE SPACE TELESCOPE FIXED-HEAD STAR TRACKERS
R. McCutcheon (Computer Sciences Corp., Laurel, MD.), John J. Boia (Computer Sciences Corp., Laurel, MD.), Martin F. Gakenheimer (Allied-Signal Aerospace Co., Seabrook, MD.), L. Hallock, E. Kimmer, S. Murphy, and Gary L. Welter *In its* Flight Mechanics/Estimation Theory Symposium, 1994 May 1994 p 95-108 (For primary document see N94-35605 11-13)
(Contracts NAS5-31000; NAS5-31500)
Avail: CASI HC A03/MF A04

75 PLASMA PHYSICS

Includes magnetohydrodynamics and plasma fusion.

For ionospheric plasmas see *46 Geophysics*. For space plasmas see *90 Astrophysics*.

N94-35493 Naval Research Lab., Washington, DC.
THEORETICAL ASPECT OF LOW PRESSURE DISCHARGES IN SIMPLE GASSES Interim Report
Wallace M. Manheimer 28 Mar. 1994 120 p Limited Reproducibility: More than 20% of this document may be affected by microfiche quality
(AD-A278762; NRL/MR/6707-94-7462) Avail: CASI HC A06

Discharge processing is becoming more and more important in many industries. This paper attempts to bring together, in a relatively compact form, a basic derivation of the physics of processing discharges including the following areas: collision theory, kinetic theory, simple chemical reactions, fluid formulations, and shealth physics. DTIC

N94-35647# Lawrence Livermore National Lab., CA.
SIMULATION MODELS FOR COMPUTATIONAL PLASMA PHYSICS: CONCLUDING REPORT
D. W. Hewett Mar. 1994 7 p
(Contract W-7405-eng-48)
(DE94-009976; UCRL-ID-116827) Avail: CASI HC A02/MF A01

In this project, the authors enhanced their ability to numerically simulate bounded plasmas that are dominated by low-frequency electric and magnetic fields. They moved towards this goal in several ways; they are now in a position to play significant roles in the modeling of low-frequency electromagnetic plasmas in several new industrial applications. They have significantly increased their facility with the computational methods invented to solve the low frequency limit of Maxwell's equations. This low frequency model, called the streamlined Darwin field model, has now been implemented in a fully non-neutral SDF code BEAGLE and has been further extended to the quasi-neutral limit. In addition, they have resurrected the quasi-neutral, zero electron inertia model (ZMR) and began the task of incorporating internal boundary conditions into this model that have the flexibility of those in GYMNOS, a magnetostatic code now used in ion source work. Finally, near the end of this project, they invented a new type of banded matrix solver that can be implemented on a massively parallel computer, thus opening the door for the use of all their ADI schemes on these new computer architecture's. DOE

N94-35670# Maryland Univ., College Park, MD.
POWER BALANCE AND CHARACTERIZATION OF IMPURITIES IN THE MARYLAND SPHEROMAK, PART 2 Ph.D. Thesis
C. Cote 1993 120 p
(Contract DE-FG05-86ER-53241)
(DE94-009603; DOE/ER-53241/7-Pt-2) Avail: CASI HC A06/MF A02

The Maryland Spheromak is a medium size magnetically confined plasma of toroidal shape. Low T(sub e) and higher n(sub e) than expected contribute to produce a radiation dominated short-lived spheromak configuration. A pyroelectric radiation detector and a VUV spectrometer have been used for space and time-resolved measurements of radiated power and impurity line emission. Results from the bolometry and VUV spectroscopy diagnostics have been combined to give the absolute concentrations of the major impurity species together with the electron temperature. The large amount of oxygen and nitrogen ions in the plasma very early in the discharge is seen to be directly responsible for the abnormally high electron density. The dominant power loss mechanisms are found to be radiation (from impurity line emission) and electron convection to the end walls during the formation phase of the spheromak configuration, and radiation only during the decay phase. DOE

N94-35673# General Atomic Co., San Diego, CA.
INERTIAL CONFINEMENT FUSION TARGET COMPONENT FABRICATION AND TECHNOLOGY DEVELOPMENT REPORT
D. Steinman, ed. Mar. 1994 152 p
(Contract DE-AC03-91SF-18601)
(DE94-009973; GA-A-21647) Avail: CASI HC A08/MF A02

On December 30, 1990, the US Department of Energy entered into a contract with General Atomics (GA) to be the Inertial Confinement Fusion Target Component Fabrication and Technology Development Support contractor. This report documents the technical activities which took place under this contract during the period of October 1, 1992 through September 30, 1993. During this period, GA was assigned 18 tasks in support of the Inertial Confinement Fusion program and its laboratories. These tasks included 'Capabilities Activation' and 'Capabilities Demonstration' to enable us to begin production of glass and composite polymer capsules. Capsule delivery tasks included 'Small Glass Shell Deliveries' and 'Composite Polymer Capsules' for Lawrence Livermore National Laboratory (LLNL) and Los Alamos National Laboratory (LANL). We also were asked to provide direct 'Onsite Support' at LLNL and LANL. We continued planning for the transfer of 'Micromachining Equipment from Rocky Flats' and established 'Target Component Micromachining and Electroplating Facilities' at GA. We fabricated over 1100 films and filters of 11 types for Sandia National Laboratory and provided full-time onsite engineering support for target fabrication and characterization. We initiated development of methods to make targets for the Naval Research Laboratory. We investigated spherical interferometry, built an automated capsule sorter, and developed an apparatus for calorimetric measurement of fuel fill for LLNL. We assisted LANL in the 'Characterization of Opaque b-Layered Targets.' We developed deuterated and UV-opaque polymers for use by the University of Rochester's Laboratory for Laser Energetics (UR/LLE) and devised a triple-orifice droplet generator to demonstrate the controlled-mass nature of the micro-encapsulation process. DOE

N94-35750# Academy of Sciences (USSR), Novosibirsk (USSR). Inst. Yadernoj. Fiziki.
SELF-SIMILAR REGIMES OF SUBSONIC LANGMUIR WAVE COLLAPSE
V. N. Khudik and V. M. Malkin 1992 9 p
(DE94-611466; BUDKERINP-92-58; IYaF-92-58) Avail: CASI HC A02/MF A01 (US Sales Only)

The first examples of regular and singular self-similar solutions of the 3-d nonlinear Schroedinger equation for potential vector field are found explicitly. Regular solutions relate to the process of the 'singularities' formation. Singular solution s relate to an early evolution of the 'singularities'.

Together, the solutions describe behavior of Langmuir wave field in the spatiotemporal vicinities of its 'singularities' and provide an effective mechanism of energy dissipation from the Langmuir condensate. DOE

N94-35752# National Inst. for Fusion Science, Nagoya (Japan).
LHD HELICAL DIVERTOR
N. Ohyabu, T. Watanabe, Ji. Hantao, H. Akao, T. Ono, T. Kawamura, K. Yamazaki, K. Akaishi, N. Inoue, and A. Komori et al Jul. 1993 40 p Submitted for publication
(DE94-727626; AD-B179444; NIFS-239) Avail: CASI HC A03/MF A01

The Large Helical Device (LHD) now under construction is a heliotron/torsatron device with a closed divertor system. The edge LHD magnetic structure has been studied in detail. A peculiar feature of the configuration is existence of edge surface layers, a complicated three dimensional magnetic structure which does not, however, seem to hamper the expected divertor functions. Two divertor operational modes are being considered for the LHD experiment, high density, cold radiative divertor operation as a safe heat removal scheme and high temperature divertor plasma operation. In the latter operation, a divertor plasma with temperature of a few kEV, generated by efficient pumping, expects to lead to significant improvement in core plasma confinement. Conceptual designs of the LHD divertor components are under way. DOE

N94-35772# National Inst. for Fusion Science, Nagoya (Japan).
A TRIGGERING MECHANISM OF FAST CRASH IN SAWTOOTH OSCILLATION
K. Watanabe and T. Sato Sep. 1992 16 p Presented at the 14th International Conference on Plasma Physics and Controlled Nuclear Fusion Research, Wuerzburg, Germany, 30 Sep. - 7 Oct. 1992
(DE94-718974; NIFS-167; CONF-9209396; IAEA-CN-56/D-3-2) Avail: CASI HC A03/MF A01

Full-torus, compressible, resistive MHD simulations have been performed to study the mechanism of fast crash in the sawtooth oscillation. The simulation results reveal that the q value, which at first decreases in accordance with current peaking subject to ohmic heating, starts increasing in the q less than 1 region due to strong excitation of nonlinear modes and becomes flattened. When the q profile is flattened in the q less than 1 region, the plasma flow pushes the magnetic surface radially outwards and the poloidal magnetic field lines are driven to reconnect rapidly with each other across the q=1 surface. Consequently, the central hot plasma is pushed out towards the wall to crash its confinement. It turns out that the m = 1 plasma flow induced by the kink instability, rather than the pressure gradient, plays a decisive role in the crash process. DOE

N94-35773# National Inst. for Fusion Science, Nagoya (Japan).
PARTICLE ORBIT ANALYSIS FOR LHD HELICAL AXIS CONFIGURATIONS
J. Guasp, K. Yamazaki, and O. Motojima Apr. 1993 47 p Submitted for publication
(DE94-718995; NIFS-217) Avail: CASI HC A03/MF A01

Fast ion orbits for helical magnetic axis configurations in LHD (Large Helical Device) are analyzed and compared with the standard circular axis case. Boundaries between passing and helically trapped particle regions show clear differences: in the non-planar axis case the helically trapped region spreads, near the magnetic axis, over a much wider band across the 90 deg pitch angle value and shows a very marked asymmetry. The locally trapped particle region is also wider than in the standard case. The differences in the loss cone boundaries of the two cases are rather small, however, the effects of re-entering criteria are very important in both cases. On the contrary, the effects of finite coil size are not significant. DOE

N94-35775# National Inst. for Fusion Science, Nagoya (Japan).
NIFS SYMPOSIUM: TOWARD THE RESEARCH OF FUSION BURNING PLASMAS, PRESENT STATUS AND FUTURE STRATEGY
Sanae-I. Itoh, ed. Jul. 1993 51 p Symposium held in Nagoya, Japan, 15 Jul. 1992 Submitted for publication
(DE94-727618; NIFS-PROC-13; CONF-9207225) Avail: CASI HC A04/MF A01

An NIFS symposium, entitled 'Toward the research of Fusion Burning Plasmas-Present status and Future Strategy' was held at NIFS on 15 Jul. 1992. This NIFS symposium covers various topics related to burning plasma, e.g., JET DT experiment, Plan for DT experiment on TFTR as well as the future trends among researchers. To study the critical issues and trends of future research, a questionnaire was sent to about 100 researchers. This report presents such activities in the NIFS symposium. DOE

N94-35788# Academy of Sciences (USSR), Novosibirsk (USSR). Inst. Yadernoj Fiziki.
THE KINETICS OF INHOMOGENEOUS PLASMA
V. I. Erofeev 1992 20 p
(DE94-611459; BUDKERINP-92-60; IYaF-92-60) Avail: CASI HC A03/MF A01 (US Sales Only)

A new concept of plasma kinetic description is developed. The instrumentation was elaborated for describing of plasma cross diffusion via the particle interaction with drift waves. The instrumentation includes consistent equations of particle distribution evolution and of drift wave pumping. The effect of plasma nonstationary and particle induced scattering are taken into account. The new concept do not involve the averaging over the initial data ensemble. In treating of turbulent plasma it gives possibilities to avoid the using of the wellknown Random Phase Approximation and of any renormalizations. DOE

N94-35791# Nauchno-Issledovatelskii Inst. Ehlekt- Rofizicheskoj Apparatury, Leningrad (USSR).
OPTIMIZATION OF TURN POSITION OF TOKAMAK INDUCTOR
Yu. A. Aristov, G. M. Vorobev, and A. V. Kuznetsov 1992 39 p
(DE94-612627; NIIEFA-P-0905) Avail: CASI HC A03/MF A01 (US Sales Only)

Statement and methods of solution of the problem of optimizing turn position of tokamak induction are considered. Optimization is aimed at determination of inductor turn position, providing the minimal scattering of magnetic field in the region of chamber at any assigned value of volt-seconds. Algorithms of problem solution are described, and results of calculations for STX tokamak are presented. It is shown that development methods can be used for determining optimal position of turns of any coils of poloidal magnetic field, providing the assigned configuration and level of magnetic field. DOE

N94-35811# National Inst. for Fusion Science, Nagoya (Japan).
ANALYSIS OF CURRENT DIFFUSIVE BALLOONING MODE
M. Yagi, M. Azumi, K. Itoh, S.-I. Itoh, and A. Fukuyama Apr. 1993 53 p Submitted for publication
(DE94-718992; NIFS-216) Avail: CASI HC A04/MF A01

The current diffusive ballooning mode is analyzed in the tokamak plasma. This mode is destabilized by the current diffusivity (i.e., the electron viscosity) and stabilized by the thermal conductivity and ion viscosity. By use of the ballooning transformation, the eigenmode equation is solved. Analytic solution is obtained by the strong ballooning limit. Numerical calculation is also performed to confirm the analytic theory. The growth rate of the mode and the mode structure are analyzed. The stability boundary is derived in terms of the current diffusivity, thermal conductivity, ion viscosity, and the pressure gradient for the given shear parameter. This result is applied to express the thermal conductivity in terms of the pressure gradient, magnetic configurational parameters (such as the safety factor, shear and aspect ratio) and the Prandtl numbers. DOE

N94-35812# National Inst. for Fusion Science, Nagoya (Japan).
THICKNESS OF THE LAYER OF STRONG RADIAL ELECTRIC FIELD IN JFT-2M H-MODE PLASMAS
K. Ida, K. Itoh, S.-I. Itoh, Y. Miura, and A. Fukuyama Apr. 1993 23 p Submitted for publication
(DE94-718993; NIFS-215) Avail: CASI HC A03/MF A01

The poloidal rotation velocity profiles both in L- and H- mode measured in JFT-2M are compared with H-mode models based on ion orbit loss. The profiles of poloidal rotation velocity measured in L- and H-mode is consistent with the calculation which consists of ion orbit loss. The dependence of the thickness of the layer of high shear E(sub r) on poloidal gyro-radius measured is explained by radial diffusion of poloidal rotation velocity due to anomalous perpendicular viscosity. DOE

N94-35813# National Inst. for Fusion Science, Nagoya (Japan).
APPLICATIONS OF NON-RESONANT RF FORCES FOR IMPROVEMENT OF TOKAMAK REACTOR PERFORMANCES. PART 1: APPLICATION OF PONDEROMOTIVE FORCE

T. Watari, R. Kumazawa, T. Mutoh, T. Seki, K. Nishimura, and F. Shimpo May 1993 41 p Submitted for publication
(DE94-718994; NIFS-220) Avail: CASI HC A03/MF A01

Applications of Radio Frequency to a tokamak divertor plasma for improvement of its reactor relevancy is studied and proposed. RF is applied to a divertor region of a tokamak by use of wave guide launchers on consideration of a reactor environment. Since the ponderomotive force is dependent on the charge to mass ratio of ions, various useful applications are considered. They cover some of the recent key issues in the development research toward nuclear fusion: the reduction of the heat load on the divertor plate, improvement of tritium inventory, impurity control, and helium ash removal. DOE

N94-35936# National Inst. for Fusion Science, Nagoya (Japan).
HEATING EXPERIMENTS USING NEUTRAL BEAMS WITH VARIABLE INJECTION ANGLE AND ICRF WAVES IN CHS
S. Okamura (Kyoto Univ., Japan.), K. Nishimura, K. Hanatani, T. Amano, H. Arimoto, M. Fujiwara, M. Hosokawa, K. Ida, H. Idei, and H. Iguchi et al Sep. 1992 16 p Presented at the 14th International Conference on Plasma Physics and Controlled Nuclear Fusion Research, Wuerzburg, Germany, 30 Sep. - 7 Oct. 1992
(DE94-718982; AD-B169199; NIFS-184; CONF-9209396; IAEA-CN-56/C-2-4) Avail: CASI HC A03/MF A01

Confinement of ripple-trapped energetic ions is studied in a low-aspect-ratio helical system using a neutral beam with variable injection angle. The heating efficiency was found to be very low for the perpendicular injection compared with the tangential one in the magnetic field configuration which is optimized for the global confinement for the tangential NBI plasmas. Confinement of beam ions was improved by shifting the magnetic axis inward, which was confirmed by the measurement of their energy spectrum. The results are consistent with the calculation of Monte Carlo beam-ion-thermalization code. The poloidal rotation near plasma edge is measured for different injection angles which shows larger value for the perpendicular injection. The fast wave ICRF heating is applied to a low-aspect-ratio helical system. Substantial energy increase is obtained for the NBI target plasma. High energy ion tail is observed in the limited range of pitch angles. DOE

N94-35937# National Inst. for Fusion Science, Nagoya (Japan).
K-EPSILON MODEL OF ANOMALOUS TRANSPORT IN RESISTIVE INTERCHANGE TURBULENCE
H. Sugama, M. Okamoto, and M. Wakatani Sep. 1992 17 p Presented at the 14th International Conference on Plasma Physics and Controlled Nuclear Fusion Research, Wuerzburg, Germany, 30 Sep. - 7 Oct. 1992 Submitted for publication
(DE94-718983; AD-B168945; NIFS-170; CONF-9209396; IAEA-CN-56/D-4-20) Avail: CASI HC A03/MF A01

A K(sub epsilon) anomalous transport model for resistive interchange turbulence is presented and applied to the transport analysis of ECH plasmas in Heliotron E. In this model, the turbulent kinetic energy K approximately equals 1/2(upsilon tilde(sup 2)) and its viscous dissipation rate epsilon characterize the local turbulence and the anomalous transport coefficient is given by D approximately equal to K(sup 2)/epsilon, which has some nonlocal properties not included in the conventional expressions since their temporal and spatial variations are determined by taking into account the transport of the turbulent energy itself. In the case of the homogeneous turbulence where the anomalous transport may be described in terms of the local plasma parameters, the dimensional analysis applied to our model yields the two types of local parameter expressions of the anomalous diffusivity in the high and low collisional cases. We find a familiar diffusivity for the resistive interchange turbulence derived in the high collisional case and we have another one similar to the gyro-reduced Bohm (GRB) diffusivity in the low collisional case. However, it is shown from the transport simulation using our model that in the region where the turbulence inhomogeneity is significant the anomalous diffusivity deviates from the local parameter expression due to the transport terms in the K(sub epsilon) equations. Our model explains the experimental results consistently in that it gives the GRB or LHD scaling for the energy confinement time and reproduces the experimentally obtained profile of the anomalous diffusivity which has large values in the peripheral region in contrast with the GRB model. DOE

N94-35938# National Inst. for Fusion Science, Nagoya (Japan).
NEOCLASSICAL CURRENT AND RELATED MHD STABILITY, GAP MODES, AND RADIAL ELECTRIC FIELD EFFECTS IN HELIOTRON AND TORSATRON PLASMAS
N. Nakajima, K. Ichiguchi, K. Watanabe, H. Sugama, M. Okamoto, M. Wakatani, Y. Nakamura, and C. Z. Cheng Sep. 1992 15 p Presented at the 14th International Conference on Plasma Physics and Controlled Nuclear Fusion Research, Wuerzburg, Germany, 30 Sep. - 7 Oct. 1992 Submitted for publication
(DE94-718987; AD-B168325; NIFS-169; CONF-9209396; IAEA-CN-56/D-4-15(CP)) Avail: CASI HC A03/MF A01

By developing the neoclassical theory for parallel flow it is found out that if nu(sub e)(sup *) does not equal nu(sub i)(sup *) a parallel current directly generated by the radial electric field, which does not exist in axisymmetric systems, exists in the non-axisymmetric systems. This newly found current has a possibility to reduce the bootstrap current under a suitable condition even in the opposite direction in Heliotron/Torsatron. The differences between the rotations of bulk ions and impurities are discussed in the case where impurities are in the Pfirsh-Schlueter collisionality regime. In connection with the bootstrap current the effects of the net toroidal current on the ideal interchange instability are numerically studied taking the Large Helical Device (LHD) as an example. The direction of the current is crucial to the Mercier criterion. Helicity-induced shear Alfven eigenmodes (HAE) attributed to the helicity of helical coils are considered for the first time in Heliotron/Torsatron and compared with TAE modes. Spectral gaps and eigenmodes significantly depend on the finite-beta effects. Radial electric field producing poloidal shear flow also plays a role for the edge anomalous transport in Heliotron/Torsatron. The electrostatic resistive interchange mode which is considered origin of the anomalous transport can be stabilized linearly by the poloidal shear flow. However, its effects on the turbulent state practically disappears by the non-linear simulation for the resistive drift wave and interchange turbulence. It is pointed out that the poloidal shear flow destabilizes the electromagnetic ideal interchange mode. DOE

N94-35939# National Inst. for Fusion Science, Nagoya (Japan).
ATOMIC PHYSICS AND RADIATION PROCESSES IN PLASMAS
K. Itoh, D. Salzmann, H. Takabe, and T. Kato Aug. 1993 35 p
(DE94-727617; AD-B179180; NIFS-Memo-11) Avail: CASI HC A03/MF A01

It is pointed out that atomic and molecular (A/M) processes play important roles in divertor plasmas but the problems related to these processes are not yet studied quantitatively. Recently new subjects related to A/M processes such as plasma-vapor interaction during plasma disruption are presented. This is a brief summary of our discussions. Our recent results of the calculations for the line emissions of carbon atoms in edge plasmas are also included. DOE

N94-35983# National Inst. for Fusion Science, Nagoya (Japan).
POTENTIAL FORMATION AND TRANSPORT IN OPEN FIELD LINE SYSTEMS
Kiyoshi Yatsu, ed. (Tsukuba Univ., Ibaraki, Japan.) and Tadatsugu Hatori, ed. Apr. 1993 118 p
(DE94-718910; AD-B173715; NIFS-Memo-9) Avail: CASI HC A06/MF A02

Many studies have been reported on the potential formation in tandem mirrors and in many other systems. Plasma potentials are also interested in relation to the H-mode and divertor plasma in toroidal systems. The workshops 'Potential Formation and Transport in Open Field Line Systems' were organized three times as collaboration research at the National Institute for Fusion Science from 1990 to 1992. The workshops were aimed at the study of potential formation and related transport in various plasmas with emphasis on those in open magnetic field line systems. This memo is a report of research progress during the three years and new researches presented at the workshops. These workshops were supported by NIFS for the three years. DOE

N94-36082# Academy of Sciences (USSR), Novosibirsk (USSR). Inst. Yadernoj Fiziki.
HOT-ION PLASMA IN THE QUADRUPOLE TRAP
E. A. Gilev, G. I. Dimov, A. A. Kabantsev, V. G. Sokolov, and S. Yu.

Taskaev 1993 21 p
(DE94-617216; IYaF-93-5) Avail: CASI HC A03/MF A01 (US Sales Only)

Under filling up the 'AMBAL-U' mirror by plasma from quasi-stationary gas-discharge source without using of an additional heating methods, the hot plasma with density 3x10(exp 13) cm(exp -3), ion temperature 1 keV, electron temperature 50 eV, and the beta-parameter of 6% was obtained. In the case of working with deuterium the output of the thermonuclear neutrons was approximately 10(exp 8) neutrons/s. Under the atomic H(sup 0) beams (E approximately equals 17 keV, equivalent current 100 A, capture approximately equal to 5%) injection into the obtained plasma the population of super ions with an average energy of 5 keV in volume of 4 liters is achieved. The density of this population on the whole volume increases during the injection pulse (200 (mu)s) and becomes higher than 3x10(exp 12) cm(exp -3) to the end of this period. DOE

N94-36093# Georgia Inst. of Tech., Atlanta, GA.
A SURVEY OF REFLECTOMETRY TECHNIQUES WITH APPLICATIONS TO TFTR
I. Collazo, W. M. Stacey, J. Wilgen, G. Hanson, T. Bigelow, C. E. Thomas, and N. Bretz Dec. 1993 172 p
(Contract DE-AC05-84OR-21400)
(DE94-010202; GTFR-112) Avail: CASI HC A08/MF A02

This report presents a review of reflectometry with particular attention to eXtraordinary mode (X-mode) reflectometry using the novel technique of dual frequency differential phase. The advantage of using an X-mode wave is that it can probe the edge of the plasma with much higher resolution and using a much smaller frequency range than with the Ordinary mode (O-Mode). The general problem with previous full phase reflectometry techniques is that of keeping track of the phase (on the order of 1000 fringes) as the frequency is swept over the band. The dual frequency phase difference technique has the advantage that since it is keeping track of the phase difference of two frequencies with a constant frequency separation, the fringe counting is on the order of only 3 to 5 fringes. This fringe count, combined with the high resolution of the X-mode wave and the small plasma access requirements of reflectometry, make X-mode reflectometry a very attractive diagnostic for today's experiments and future fusion devices. DOE

N94-36097 Academy of Sciences (USSR), Novosibirsk (USSR). Inst. Yadernoj Fiziki.
INITIAL PERTURBATIONS AND LANGMUIR WAVES IN ELECTRON-POSITRON PLASMA
N. S. Buchelnikova and E. P. Matochkin 1992 26 p Limited Reproducibility: More than 20% of this document may be affected by microfiche quality
(DE94-617190; IYaF-92-16) Avail: CASI HC A03 (US Sales Only)

The evolution of the initial density and velocity perturbations of a different type in the electron-positron plasma was studied in the numerical experiments (PIC-method). It was shown that the different perturbations lead to the excitation of the Langmuir wave and (or) the quasineutral density perturbation. It is shown that electron-positron plasma can be used as a model of the plasma of the equal mass negative and positive ions. DOE

N94-36193# Lawrence Livermore National Lab., CA.
INERTIAL CONFINEMENT FUSION
H. T. Powell, ed., D. P. Schleich, ed., and P. W. Murphy, ed. 1994 44 p
(Contract W-7405-eng-48)
(DE94-010835; UCRL-LR-105821-94-1) Avail: CASI HC A03/MF A01

In the 1990 National Academy of Sciences (NAS) report of its review of the U.S. Inertial Confinement Fusion (ICF) Program, it was recommended that a high priority be placed on completing the Precision Nova Project and its associated experimental campaign. Since fiscal year 1990, the lab has therefore campaigned vigorously on Nova and in its supporting laboratories to develop the Precision Nova capabilities needed to perform the stressful target experiments recommended in the 1990 NAS report. The activities to enable these experiments have been directed at improvements in three areas - the Nova laser, target fabrication capabilities, and target diagnostics. As summarized in the five articles in this report, the Precision Nova improvements have been successfully completed. These improvements have had a positive impact on target performance and on the ability to diagnose the results, as evidenced by the HEP-1 experimental results. The five articles generally concentrate on improvements to the capabilities rather than on the associated target physics experiments. Separate abstracts are included for each paper. DOE

N94-36200# Texas Univ., Austin, TX. Fusion Research Center.
SCALING LAWS FOR TEXT PLASMA PROFILES
S. C. McCool, R. V. Bravenec, J. Y. Chen, M. S. Foster, W. L. Li, A. Ouroura, P. E. Phillips, B. Richards, K. W. Wenzel, and Z. M. Zhang et al 1 Feb. 1994 20 p
(Contract DE-FG05-88ER-53267)
(DE94-010832; DOE/ER-53267/129; FRCR-444) Avail: CASI HC A03/MF A01

Regression analysis has been performed on a number of measured profiles including temperature and density vs. nominal macroscopic operating parameters for TEXT tokamak (pre-upgrade) ohmic plasmas. The resulting simple empirical model has enabled the authors to quickly approximate profiles of electron temperature and density, ion temperature, and soft x-ray brightness, as well as the scalar quantities: total radiated power, q=1 radius, sawtooth period and amplitude, and energy confinement time as a power law of toroidal field, plasma current, chord average density, and fueling gas atomic weight. The model profiles are only applicable to the plasma interior, i.e. within the limiter radius. In most cases, the predicted model profiles are within the experimental error bars of measured profiles and are more accurate at predicting profile variation for small operating parameter changes than the measured profiles. DOE

N94-36247# National Inst. for Fusion Science, Nagoya (Japan).
THE NEW FEATURES OF ION BERNSTEIN WAVE HEATING IN JIPP T-2U TOKAMAK
T. Watari, R. Kumazawa, T. Seki, Y. Yasaka, A. Ando, Y. Oka, O. Kaneko, K. Adati, R. Akiyama, and Y. Hamada et al Sep. 1992 16 p Presented at the 14th International Conference on Plasma Physics and Controlled Nuclear Fusion Research, Wuerzburg, Germany, 30 Sep. - 7 Oct. 1992 Submitted for publication
(DE94-718978; NIFS-181; CONF-9209396; IAEA-CN-56/E-2-3) Avail: CASI HC A03/MF A01

Ion Bernstein Wave Heating experiment was conducted in JIPP T-IIU tokamak. A relatively high frequency, 130 MHz, was used to reduce impurity influx and IBW power up to 400kW was injected without plasma disruption. It was found that the radial profiles of electron density, electron temperature, and ion temperature are all peaked during the IBWH. It was also found that ion distribution function does not have high energy tail above certain critical energy. These are favorable and useful features in optimizing fusion reactivity in reactor applications. DOE

N94-36284# Lawrence Livermore National Lab., CA.
DESIGN FOR MANUFACTURABILITY EVALUATION: COMPOSITE NATIONAL IGNITION FACILITY (NIF) POCKEL CELL BODY
W. A. Jensen and G. P. Spellman Apr. 1994 56 p
(Contract W-7405-eng-48)
(DE94-010669; UCRL-ID-117135) Avail: CASI HC A04/MF A01

A survey of composite materials and processes for the National Ignition Facility (NIF) Optical Switch Body is described. Mechanical and physical criterion set upon the part are used as guidelines for the selection of materials and processes for manufacturing. Benefits, costs, and risks associated with selected processes, as well as a recommendation for prototype fabrication is presented. DOE

N94-36352# National Inst. for Fusion Science, Nagoya (Japan).
DESIGN STUDY OF LHD HELICAL DIVERTOR AND HIGH TEMPERATURE DIVERTOR PLASMA OPERATION
N. Ohyabu, K. Yamazaki, I. Katanuma, H. Hantao, T. Watanabe, K. Watanabe, H. Akao, K. Akaishi, T. Ono, and H. Kaneko et al Sep. 1992 16 p Presented at the 14th International Conference on Plasma Physics and Controlled Nuclear Fusion Research, Wuerzburg, Germany, 30 Sep. - 7 Oct. 1992
(DE94-718975; AD-B168932; NIFS-177; CONF-9209396; IAEA-CN-56/C-4-2) Avail: CASI HC A03/MF A01

The Large Helical Device (LHD), now under construction is a Heliotron/torsatron device with a closed divertor system. The LHD divertor magnetic structure has been studied in detail. A peculiar feature of the configuration is the existence of edge surface layers, a complicated three dimensional magnetic structure. However it does not seem to hamper the expected divertor functions. As a confinement improvement scheme in LHD, we have proposed a high temperature divertor plasma operation in which a divertor plasma with a temperature of a few kev, generated by efficient pumping, leads to the confinement improvement. DOE

N94-36353# National Inst. for Fusion Science, Nagoya (Japan).
MODELLING OF ELMs AND DYNAMIC RESPONSES OF THE H-MODE
Sanae-I. Itoh, Kimitaka Itoh, and Atsushi Fukuyama Sep. 1992 16 p Presented at the 14th International Conference on Plasma Physics and Controlled Nuclear Fusion Research, Wuerzburg, Germany, 30 Sep. - 7 Oct. 1992
(DE94-718977; AD-B168944; NIFS-175; CONF-9209396; IAEA-CN-56/D-4-19) Avail: CASI HC A03/MF A01

Based on the electric bifurcation model of the H-L transition, models of the Edge Localized Modes (ELM's) are developed and the dynamic responses of the H-mode are analyzed. The spatial-temporal evolution of the H-L transition is formulated in a form of the time-dependent Ginzburg-Landau equation which includes transport processes. The equation governs the development of the density and radial electric field. By solving this equation for the given boundary condition, we identify three classes of solutions which attribute to the H-state, L-state and ELMy-H state. The ELMy-H state is characterized by the self-generating oscillations under the condition of constant source. The parameter region of these states are identified. The radial extent of transport barrier during H- and ELMy-H states is characterized by the diffusion Prandtl number. Transient responses of the H-states to the external perturbations are also analyzed. Sudden change of the flux from the core causes transient ELMy oscillations. When the sinusoidal oscillations are imposed (simulation of sawtoothing), the ELMy oscillations with mode locking to the external oscillation frequency (or the sub-harmonics) appear. This suggests a possible scenario for the ELM control. We also develop the model for the Giant ELMs. Ballooning instability triggers the pulsive loss flux to the edge region. If its magnitude exceeds the threshold, the transport barrier is destroyed for a short period and the large solitary pulse in the outflux is generated. DOE

N94-36357# National Inst. for Fusion Science, Nagoya (Japan).
MHD AND CONFINEMENT CHARACTERISTICS IN THE HIGH-BETA REGIME ON THE CHS LOW-ASPECT-RATIO HELIOTRON/TORSATRON
H. Yamada, S. Morita, K. Ida, S. Okamura, H. Iguchi, S. Sakakibara, K. Nishimura, R. Akiyama, H. Arimoto, and M. Fujiwara et al Sep. 1992 15 p Presented at the 14th International Conference on Plasma Physics and Controlled Nuclear Fusion Research, Wuerzburg, Germany, 30 Sep. - 7 Oct. 1992
(DE94-718981; AD-B168925; NIFS-185; CONF-9209396; IAEA-CN-56/C-2-2) Avail: CASI HC A03/MF A01

The MHD and confinement characteristics associated with the finite-beta effect have been investigated in the low-aspect-ratio heliotron/torsatron Compact Helical System (CHS). Beta values of 1.8% in the quasi-steady state and 1.9% in the transient phase have been realized and beta(sub 0) has reached 5.8%. The experimentally observed equilibrium characteristics are in good agreement with current 3-D analysis. Significant instabilities suppressing beta value or terminating the discharges have not yet been observed in standard operation. This is supposed to be due to self-stabilization of the ideal interchange mode by spontaneously generated magnetic wells, which is a distinguishing feature of the low aspect ratio. Magnetic fluctuations with the frequency range less than 100 kHz have reached as much as 0.1% of the poloidal equilibrium field. The predominant modes are globally coherent with the low mode number and do not affect confinement. The scaling of beta follows the prediction from LHD scaling. The thermal diffusivity depends on the local scale length of beta, the characteristics of which is emphasized for the magnetic hill region. The present beta value is limited by saturation of confinement with increasing density and degradation of confinement with increasing power rather than by MHD characteristics. DOE

N94-36375# Lawrence Livermore National Lab., CA.
HIGH DENSITY IMPLOSION EXPERIMENTS AT NOVA
M. D. Cable, S. P. Hatchett, M. B. Nelson, R. A. Lerche, T. J. Murphy, and D. B. Ress Feb. 1994 5 p Presented at the 11th International Workshop on Laser Interaction and Related Plasma Phenomena, Monterey, CA, 25-29 Oct. 1993
(Contract W-7405-eng-48)
(DE94-010894; UCRL-JC-107799; CONF-931048-13) Avail: CASI HC A01/MF A01

A series of experiments to produce implosions with fuel densities comparable to an ignition scale implosion hot spot (approximately 20 g/cu cm) have been done at the Nova Laser Fusion Facility. These implosions utilize indirectly driven, deuterium filled capsules for which the primary measurement of fuel density is the secondary neutron technique. Calculations indicated that by decreasing initial capsule fill pressure, these densities could be achieved across a wide range of convergences up to about 25. Initial experiments showed a decrease in observed final fuel densities at the highest convergences due to a lack of adequate laser control. Additional work was done to improve laser pointing, power balance, and beam synchronization which resulted in improved implosion performance.
Derived from text

N94-36386# Lawrence Livermore National Lab., CA.
NEW CALCULATIONS OF Fe SPECTRA IN HIGH-TEMPERATURE PLASMAS
D. A. Liedahl, A. L. Osterheld, R. Mewe, and J. S. Kaastra 30 Mar. 1994 11 p Presented at the Advanced Satellite for Cosmology and Astrophysics Symposium, Tokyo, Japan, 8-11 Mar. 1994
(Contract W-7405-eng-48)
(DE94-009919; UCRL-JC-116866; CONF-9403100-1) Avail: CASI HC A03/MF A01

Spectroscopic data acquired during the ASCA performance verification phase have revealed a discrepancy between measured line flux ratios and the predictions of standard plasma emission codes. In plasmas for which coronal ionization equilibrium should apply, flux ratios of 4-2 and 3-2 line complexes in highly-ionized Fe are observed to be significantly lower than predicted, thus compromising the quality of spectral fits. We have recalculated Fe L-shell spectra using the HULLAC atomic physics package and present results for the ionization stages Fe XXI-XXIV. Our preliminary results show (4-2)/(3-2) ratios that are substantially smaller than those tabulated in the commonly used spectral models and point to the possibility of bringing theoretical spectra into accord with the observations. DOE

N94-36417# Academy of Sciences (USSR), Novosibirsk (USSR). Inst. Yadernoj. Fiziki.
FEASIBILITY STUDY FOR A NOVEL PULSED NEUTRAL BEAM DIAGNOSTICS FOR TOKAMAKS
V. I. Davydenko and A. A. Ivanov 1993 11 p
(DE94-617129; BUDKERINP-93-10) Avail: CASI HC A03/MF A01 (US Sales Only)

A technical feasibility of the plasma diagnostics scheme using neutral deuterium beam with a pulse length of 0.3 microsec current of 100 A and an energy of as high as 80 keV is described. DOE

76 SOLID-STATE PHYSICS

Includes superconductivity.

For related information, see also *33 Electronics and Electrical Engineering* and *36 Lasers and Masers.*

N94-35598 National Physical Lab., Teddington (England). Div. of Electrical Science.
REPORT ON A SQUID MADE FROM HIGH TEMPERATURE SUPERCONDUCTOR
P. G. Quincey Mar. 1994 11 p See also PB90-122623 and PB91-128876
(PB94-169307; NPL-DES-132) Copyright Avail: Issuing Activity (National Technical Information Service (NTIS))

This report summarizes the manufacture and performance of a thin film SQUID made from yttrium barium copper oxide on a neodymium gallate bicrystal substrate. At 77 K the device displayed large amplitude (75 microV) quasi-periodic response to magnetic field. The deviation from a regular periodic response is ascribed to focussing effects. The noise output was determined as 0.0012 phi(sub 0)/square root of Hz at 1 Hz. NTIS

N94-35677 California Univ., Santa Barbara, CA. Dept. of Chemistry.
Be3(AsO4)2.2H2O, A NEW BERYLLOARSENATE PHASE CONTAINING BRIDGED TETRAHEDRAL 3-RINGS Technical Report, 1 Jun. 1993 - 31 May 1994
W. T. Harrison, T. M. Nenoff, T. E. Gier, and G. D. Stucky 15 Apr. 1994 22 p Limited Reproducibility: More than 20% of this document may be affected by microfiche quality
(Contract N00014-90-J-1159)
(AD-A278826; T17-ONR) Avail: Issuing Activity (Defense Technical Information Center (DTIC))

The high temperature/high pressure hydrothermal synthesis and x-ray single crystal structure of Be3(ASO4)2.2H2O is described: the compound contains a three-dimensional network of BeO4 and AsO4 tetrahedra. The structural motif includes infinite layers of bridged tetrahedral 3- and 4-rings. The 9Be MAS NMR data are consistent with the Be-atom environments in the crystal structure. DTIC

N94-35698 Sandia National Labs., Albuquerque, NM.
THE OPTIMIZATION OF INTERFACES IN InAsSb/InGaAs STRAINED-LAYER SUPERLATTICES GROWN BY METAL-ORGANIC CHEMICAL VAPOR DEPOSITION
R. M. Biefeld, K. C. Baucom, and S. R. Kurtz 1993 6 p Presented at the Spring Meeting of the Materials Research Society, San Francisco, CA, 4-8 Apr. 1994 Limited Reproducibility: More than 20% of this document may be affected by microfiche quality
(Contract DE-AC04-94AL-85000)
(DE94-010070; SAND-93-2617C; CONF-940411-9) Avail: CASI HC A02

We have prepared InAsSb/InGaAs strained-layer superlattice (SLS) semiconductors by metal-organic chemical vapor deposition (MOCVD) under a variety of conditions. The presence of an InGaAsSb interface layer is indicated by x-ray diffraction patterns. Optimized growth conditions involved the use of low pressure, short purge times, and no reactant flow during the purges. MOCVD was used to prepare an optically pumped, single heterostructure InAsSb/InGaAs SLS/InPSb laser which emitted at 3.9 microns with a maximum operating temperature of approximately 100 K. DOE

N94-35733 Wright Lab., Wright-Patterson AFB, OH.
PROPERTIES AND BIBLIOGRAPHY OF GaSe Final Report, 15 Oct. 1992 - 31 Jan. 1994
Nils C. Fernelius Feb. 1994 113 p Limited Reproducibility: More than 20% of this document may be affected by microfiche quality
(AD-A279064; WL-TR-94-4013) Avail: CASI HC A06

GaSe appears to be a possible candidate material for optical frequency conversion devices in the near to far infrared (2-18 micrometers wavelength). Various properties of this material are important to researchers and systems designers to assess the utility of the material and to develop applications. A search of the published literature amassed over 600 articles. An attempt was made to organize this material by growth, structural and mechanical, thermal, electrical, and optical properties. More effort was made to condense thermal and optical properties along with accounts of nonlinear optical (NLO) usages. A summary of the good and bad properties for NLO applications is given. DTIC

N94-35826 Northwestern Univ., Evanston, IL. Dept. of Materials Science and Engineering.
THE GROWTH OF SILICON NITRIDE CRYSTALLINE FILMS USING MICROWAVE PLASMA ENHANCED CHEMICAL VAPOR DEPOSITION
K. J. Grannen, F. Xiong, and R. P. Chang Apr. 1994 31 p Limited Reproducibility: More than 20% of this document may be affected by microfiche quality
(Contract N00014-89-J-1848)
(AD-A278862; TR-15) Avail: Issuing Activity (Defense Technical Information Center (DTIC))

Crystalline thin films of silicon nitride have been grown on a variety of substrates by microwave plasma-enhanced chemical vapor deposition using N2, O2, and CH4 gases at a temperature of 800 deg C. X-ray diffraction and Rutherford backscattering measurements indicate the deposits are stoichiometric silicon nitride with varying amounts of the alpha and beta phases. Scanning electron microscope imaging indicates beta-Si3N4 possesses six-fold symmetry with particles size in the submicron range. In one experiment, the silicon necessary for growth comes from the single crystal silicon substrate due to etching/sputtering by the nitrogen plasma. The dependence of the grain size on the methane concentration is investigated. In an another experiment, an organo-silicon source, methoxytrimethylsilane, is used to grow silicon nitride with controlled introduction of the silicon necessary for growth. Thin crystalline films are deposited at rates of 0.1 micrometer/hr as determined by profilometry. A growth mechanism for both cases is proposed. DTIC

N94-35933# International Centre for Theoretical Physics, Trieste (Italy).
MAGNETORESISTANCE OF FILMS AND STRIPS WITH THE DIFFUSE SURFACE SCATTERING
A. G. Aronov Aug. 1993 13 p
(DE94-611100; IC-93/252) Avail: CASI HC A03/MF A01 (US Sales Only)

Magnetoresistance of films in a parallel magnetic field and strips in a perpendicular field is considered. The temperature and magnetic field dependencies of magnetoconductance depend on the time evolution of the correlator of phases. This correlator has different behavior as the function of time; the ergodic behavior at small magnetic fields is changed on the nonergodic one at large magnetic fields in spite of the diffusion electron motion due to a diffuse scattering on boundaries. This leads to unusual temperature and magnetic field dependencies of magnetoresistance. The ergodic hypothesis is not applicable to mesoscopical fluctuations at such a large quasiclassical field. DOE

N94-36029# Academy of Sciences of the Ukraine, Kiev. Inst. for Theoretical Physics.
TWIN SPACING VERSUS SIZE OF A MONOCRYSTAL FOR THE NONSTOICHIOMETRIC 1:2:3 SUPERCONDUCTORS
V. S. Nikolaev 1993 13 p Submitted for publication
(DE94-615511; ITP-93-12E) Avail: CASI HC A03/MF A01 (US Sales Only)

A physical model which can describe the twins' formation in a high-temperature region of a structural phase diagram is suggested. The dependence of the twin spacing vs size of a monocrystal differs from the classical square root law as a result of a nonstoichiometry of the compound according to the model. DOE

N94-36030# Academy of Sciences of the Ukraine, Kiev. Inst. for Theoretical Physics.
ABOUT MID-INFRARED OPTICAL SPECTRUM OF HIGH-Tc SUPERCONDUCTING COMPOUNDS
V. M. Loktev 1993 13 p Submitted for publication
(DE94-615646; ITP-93-30E) Avail: CASI HC A03/MF A01 (US Sales Only)

The simple model for spin-allowed dd-excitations in copper containing high-T(sub c) superconductors (HTSC) is proposed. The Hamiltonian of the system and the operator of its interaction with the light which reflects the quadrupole and spin structure of these excitations are obtained. An attempt is made to interpret the absorption spectrum experimentally observed in the region of copper dd-transitions. DOE

N94-36032# Sandia National Labs., Albuquerque, NM.
HETEROGENEOUS REACTION MECHANISMS AND KINETICS RELEVANT TO THE CVD OF SEMICONDUCTOR MATERIALS
J. R. Creighton and M. E. Coltrin Mar. 1994 19 p
(Contract DE-AC04-94AL-85000)
(DE94-011001; SAND-94-0033) Avail: CASI HC A03/MF A01

This report documents the state of the art in experimental and theoretical techniques for determining reaction mechanisms and chemical kinetics of heterogeneous reactions relevant to the chemical vapor deposition of semiconductor materials. It summarizes the most common ultra-high vacuum experimental techniques that are used and the types of rate information available from each. Several case studies of specific chemical systems relevant to the microelectronics industry are described. Theoretical methods for calculating heterogeneous reaction rate constants are also summarized. DOE

N94-36041# Academy of Sciences of the Ukraine, Kiev. Inst. for Theoretical Physics.
TWIN SPACING AND THE STRUCTURAL PHASE TRANSITIONS IN 1:2:3 HIGH-Tc SUPERCONDUCTORS

V. S. Nikolaev 1993 11 p
(DE94-615647; ITP-93-37E) Avail: CASI HC A03/MF A01 (US Sales Only)

The properties of the structural twins in 1:2:3 compounds are investigated in a wide range of temperatures in the frame of the suggested model. The dependence of the size of the twins versus temperature is considered. The temperature interval of the sharp increase of twin size with increase of the temperature is found. DOE

N94-36181# Moscow State Univ. (Russia).
PROCEEDINGS OF THE TWENTY-FIRST ALL-UNION CONFERENCE ON PHYSICS OF CHARGED PARTICLES INTERACTION WITH CRYSTALS
A. F. Tulinov, ed. and V. A. Khodyrev, ed. 1992 174 p Conference held in Moscow, Russia, 27 May 1991
(DE94-615768; INIS-RU-361; CONF-9105436) Avail: CASI HC A08/MF A02 (US Sales Only)

The proceedings consist of four parts covering the following subjects: physics of orientational effects; electron and positron radiation in solids; some issues of ion implantation; beams use under materials composition and structure analysis. DOE

N94-36212 Paris VI Univ. (France). Lab. of Condensed Media Physics.
APPLICATION OF GaSe AND AgGaSe2 CRYSTAL GROWTH TO NON-LINEAR OPTICS Final Report [CRISTALLOGENESE DE GASE ET AGGASE2 APPLICATION EN OPTIQUE NON-LINEAIRE]
A. Chevy 1994 13 p In FRENCH Sponsored by Direction des Recherches, Etudes et Techniques
(PB94-170552) Avail: Issuing Activity (National Technical Information Service (NTIS))

This report discusses follow-up work on efforts to grow large single crystals for use in nonlinear optics. Initial attempts produced 60-mm-long, 25-mm in diameter GaSe single crystals whose d(22) nonlinear coefficient for the second harmonic generation of the CO2 laser was 30 pm/V. Moreover, apparent absorption indicated that the crystal was the site of light scattering phenomena whose probable cause is impurities between the material's elemental surfaces. AgGaSe2 is also studied. The report describes work to identify impurities, discover how they are formed, and make flawless crystals for both compounds. NTIS

N94-36213 Paris XI Univ., Orsay (France). Lab. de Physique des Solides.
LOCAL INSTABILITIES AND THE TRANSITION TO CHAOS OF NON-LINEAR WAVES Final Report [INSTABILITES LOCALISEES ET TRANSITION ORDRE-DESORDRE DES ONDES NON-LINEAIRES]
Mar. 1993 16 p In FRENCH Sponsored by Direction des Recherches, Etudes et Techniques
(PB94-170578) Avail: Issuing Activity (National Technical Information Service (NTIS))

The object of this research contract was to study the singularities of non-linear structures through numerical simulations. The waiting times involved in the use of a Cray II prompted the lab to replace it with an HP 720 work station, which they found to be irreplaceable for the fine analysis of convection, despite the huge amount of calculations involved. The team simulated a fairly large number of two-dimensional phenomenological models, with satisfactory results. Examples described in this report include convection, dislocations in rolled structures, dislocation nucleation using the Landau-Ginzburg equation, the Pesch-Kramer equation (large-scale flows), non-linear wave defects, the optical model, and others. NTIS

N94-36272# Argonne National Lab., IL.
A NEW FAMILY OF SUPERCONDUCTING FULLERIDES, Na(NH3)(x)C60(x = 2-8)
J. A. Schlueter, J. L. Smart, and H. H. Wang et al 1994 14 p
(Contract W-31-109-eng-38)
(DE94-011480; ANL/CHM/PP-81405) Avail: CASI HC A03/MF A01

A series of A3C60 fulleride superconductors (A is an alkali metal) with superconducting transition temperatures ((Tc)s) between 2.5 and 33 K has been reported. The (Tc)s of these materials are closely correlated to their f.c.c. lattice parameters, with the higher Tc materials having larger unit cell lengths. Recently, the Tc of the superconducting Na2CsC60 has been raised from 10.5 K to 29.6 K by ammonia intercalation. The resulting intercalated compound, NaC(Na(NH3)4)C60 has an expanded unit cell compared to the starting material, with a larger cation Na(NH3)(4+), occupying the octahedral site. The sodium-doped C60 with nominal composition Na3C60, however, does not show superconductivity and was reported to undergo a disproportionation reaction into two f.c.c. phases, Na2C60 and Na6C60 below 250 K. Here we report on the ammonia intercalation of Na3C60. Up to four superconducting phases with (Tc)s occurring near 6.7, 11.5, 13.5, and 16.5 K were observed in the compounds Na3(NH3)(x)C60 (x approximately = 2 = 8). All these phases gave significant superconducting shielding fractions (between 15 and 80% at 5 K). These compounds were characterized by use of AC susceptibility and SQUID measurements, TGA, and x-ray powder diffraction. DOE

N94-36274# California Univ., Berkeley. Lawrence Berkeley Lab, CA.
MAGNETIC METALLIC MULTILAYERS Ph.D. Thesis
R. Q. Hood Apr. 1994 106 p
(Contract DE-AC03-76SF-00098)
(DE94-011913; LBL-35491) Avail: CASI HC A06/MF A02

Utilizing self-consistent Hartree-Fock calculations, several aspects of multilayers and interfaces are explored: enhancement and reduction of the local magnetic moments, magnetic coupling at the interfaces, magnetic arrangements within each film and among non-neighboring films, global symmetry of the systems, frustration, orientation of the various moments with respect to an outside applied field, and magnetic-field induced transitions. Magnetoresistance of ferromagnetic-normal-metal multilayers is found by solving the Boltzmann equation. Results explain the giant negative magnetoresistance encountered in these systems when an initial antiparallel arrangement is changed into a parallel configuration by an external magnetic field. The calculation depends on (1) geometric parameters (thicknesses of layers), (2) intrinsic metal parameters (number of conduction electrons, magnetization, and effective masses in layers), (3) bulk sample properties (conductivity relaxation times), (4) interface scattering properties (diffuse scattering versus potential scattering at the interfaces), and (5) outer surface scattering properties (specular versus diffuse surface scattering). It is found that a large negative magnetoresistance requires considerable asymmetry in interface scattering for the two spin orientations. Features of the interfaces that may produce an asymmetrical spin-dependent scattering are studied: varying interfacial geometric random roughness with no lateral coherence, correlated (quasi-periodic) roughness, and varying chemical composition of the interfaces. The interplay between these aspects of the interfaces may enhance or suppress the magnetoresistance, depending on whether it increases or decreases the asymmetry in the spin-dependent scattering of the conduction electrons. DOE

N94-36312# Academy of Sciences (USSR), Kiev (USSR). Inst. for Theoretical Physics.
TEMPERATURE DEPENDENCE OF SUPERCONDUCTION BANDS IN HTSC
V. N. Ermakov and E. A. Ponezha 1993 12 p Submitted for publication
(DE94-617361; ITP-93-18E) Avail: CASI HC A03/MF A01 (US Sales Only)

We develop a superconductivity theory in the one-dimensional case proceeding from the representation on the phonon mechanism of current carrier pairing which is different from the Cooper one. The temperature dependence of the superconduction gap and also its ratio to the critical temperature are calculated. The latter is shown to be essentially different from BCS theory. The results are compared with the values obtained in experiments with high-temperature superconductors. DOE

N94-36358# Brookhaven National Lab., Upton, NY.
IN SITU STUDIES OF ZEOLITE SYNTHESES USING POWDER DIFFRACTION METHODS: CRYSTALLIZATION OF INSTANT ZEOLITE A POWDER AND CoAPO-5
P. Norby (Odense Univ., Denmark.), A. N. Christensen (Aarhus Univ., Denmark.), and J. C. Hanson 1994 8 p Presented at the 10th International Zeolite Conference, Garmish-Partenkirchen, Germany, 17-22 Jul. 1994
(Contract DE-AC02-76CH-00016)
(DE94-006570; BNL-60041; CONF-940744-1) Avail: CASI HC A02/MF A01

A series of hydrothermal zeolite syntheses were performed on a powder diffractometer using synchrotron radiation and a position sensitive detector.

Direct observation of the induction period (nucleation stage), crystallization and transformation of zeolite 4A (Na-LTA) was possible due to the intense X-ray beam which allows fast data collection. High pressure experiments were performed, allowing observation of hydrothermal synthesis of a cobalt substituted AlPO4-zeolite, CoAPO-5, up to 165 C. The temperature dependence of crystallization rates of CoAPO-5 was studied. This is to our knowledge the first time resolved powder diffraction studies of zeolite syntheses using angle dispersive synchrotron powder diffraction have been carried out. DOE

N94-36367# Sandia National Labs., Albuquerque, NM.
ESTIMATING LOW-DOSE RATE IRRADIATION RESPONSE OF MOSFETs
P. Khosropour (Arizona Univ., Tucson, AZ.), K. F. Galloway (Arizona Univ., Tucson, AZ.), R. D. Schrimpf (Arizona Univ., Tucson, AZ.), D. M. Fleetwood, and P. Calvel 1994 5 p Presented at the 31st Annual International Nuclear and Space Radiation Effects Conference, Tucson, AZ, 18-22 Jul. 1994
(Contract DE-AC04-94AL-85000)
(DE94-007292; SAND-94-0457C; CONF-940726-3) Avail: CASI HC A01/MF A01

A simple method to estimate the threshold-voltage shift in MOSFET's due to low-dose-rate ionizing irradiation based on MIL-STD-883D Method 1019.4 is demonstrated. The realm of applicability of this approach is explored. DOE

N94-36377# Oak Ridge National Lab., TN.
FLUX-PINNING RELATED DEFECTS IN YBa2Cu3O(7-x) THIN FILMS GROWN ON MISCUT LaAlO3 (001) SUBSTRATES
Z. L. Wang, D. K. Christen, C. E. Klabunde, D. M. Kroeger, D. H. Lowndes, and D. P. Norton 1994 2 p Presented at the Microscopy Society of America and Microbeam Analysis Society Joint Meeting, New Orleans, LA, 31 Jul. - 5 Aug. 1994
(Contract DE-AC05-84OR-21400)
(DE94-011463; CONF-940753-3) Avail: CASI HC A01/MF A01

Measurements of critical current density in YBa2Cu3O(7-x) (Y123) thin film grown on slightly (1.6 deg) miscut LaAlO3 (001) substrates have shown an anomalous angular dependence of J(sub C). A strong, magnetic field-dependent peak in J(sub C) is observed when the magnetic field is oriented between the c-axis (the film normal direction) and the a-b plane, an orientation where flux pinning normally is not strong. Scanning tunneling microscope images of the films showed tilted-platelet microstructures, suggesting that the films might contain highly oriented internal growth defects, induced by the miscut-aligned growth. This array of defects may be responsible for the strong flux pinning and high J(sub C). In this paper, high-resolution transmission electron microscopy (HRTEM) is applied to study the defect structure formed in the films. DOE

N94-36385 Florida Univ., Gainesville, FL. Dept. of Electrical Engineering.
DEVELOPMENT OF ULTRA-LOW NOISE, HIGH PERFORMANCE 3 TO 5 QUANTUM WELL INFRARED PHOTODETECTORS (QWIPs) FOR FOCAL PLANE ARRAY STARING IMAGE SENSOR SYSTEMS Quarterly Progress Report No. 11, 1 Feb. - 30 Apr. 1994
Sheng S. Li 1 May 1994 41 p Limited Reproducibility: More than 20% of this document may be affected by microfiche quality
(Contract N00014-91-J-1976)
(AD-A278861) Avail: Issuing Activity (Defense Technical Information Center (DTIC))

During this reporting period (02-01-94 to 04-30-94) we have continued to make excellent progress. We report two new normal incidence p-type strained-layer III-V quantun well infrared photodetectors (QWIP's) for 3-5 and 8-14 um detection. An ultra-low dark current p-type tensile strained-layer (PTSL) In(0.3)Ga(0.7)As / In(0.52)Al(0.48)As QWIP grown on InP by MBE for 8-14 um detection has been developed. It shows BLIP for T less than 100 K. Due to a 1.5% lattice mismatch between the substrate and quantum well, a biaxial tensile strain was created in the well layers. As a result, the light-hole state becomes the ground state for the free hole with small effective mass. The dramatic increase of optical absorption can be attributed to the large in-plane density of states and small light-hole effective mass due to the heavy- and light-hole state inversion. The BLIP detectivity for the PTSL-QWIP was found to be 5.9x10(exp 10) Jones at 8.1 um, V(sub b) = 2V andT = 77 K. A new p-type compressive strained-layer (PCSL) In(0.4)Ga(0.6)As/GaAs QWIP grown on GaAs substrate for 3-5 and 8-14 um has also been developed for the first time. This PCSL-QWIP shows a double-peak response between 8 and 9 um wavelength by utilizing the resonant transport coupling mechanism between the heavy-hole type-I states and the light-hole type-II states. Using the compressive strain in the quantum well, normal incident absorption was greatly enhanced by the reduction of heavy-hole effective mass and the increase in the off-zone center density of states. Detectivity at 8.9 um was found to be 4.0x10(exp 9) Jones at V(sub b) = 0.3 V and T = 75 K for this PCSL-QWIP. DTIC

N94-35971*# National Aeronautics and Space Administration. Ames Research Center, Moffett Field, CA.
SPACE-BASED CRYSTAL GROWTH AND THERMOCAPILLARY FLOW
Yong-Hong Shen *In its* 1993 Technical Paper Contest for Women. Gear Up 2000: Women in Motion Feb. 1994 p 111-116 (For primary document see N94-35961 11-99)
Avail: CASI HC A02/MF A02

77 THERMODYNAMICS AND STATISTICAL PHYSICS

Includes quantum mechanics; theoretical physics; and Bose and Fermi statistics.

For related information see also *25 Inorganic and Physical Chemistry* and *34 Fluid Mechanics and Heat Transfer.*

N94-35761 Institut des Hautes Etudes Scientifiques, Bures-sur-Yvette (France).
THIS NON-AXIOMATIZABLE QUANTUM THEORY. FROM HILBERT'S SIXTH PROBLEM TO THE RECENT VIEWPOINT OF GELL-MANN AND HARTLE
B. S. Tsirelson Jan. 1994 23 p Limited Reproducibility: More than 20% of this document may be affected by microfiche quality
(PB94-167715; IHES/M/94/2) Avail: Issuing Activity (National Technical Information Service (NTIS))

The author's first goal is not to add to the vast sea of speculations on the interpretation of quantum theory, but rather to reduce it by taking a common factor out of brackets. This common factor is the rivalry between the notions of absolute reality and relative reality, which is implicitly responsible for the long-standing absence of consensus. The second goal is to argue that standard quantum theory cannot be axiomatized on the level that fundamental classical physics can be. The third goal is to disentangle one knot from the tangle of quantum interpretation problems, showing that the knot is well known far beyond quantum physics. This is what the author refers to as the 'federation' of theories. The effectiveness of mathematics may be restricted by its inability to handle this problem. NTIS

N94-35781# International Centre for Theoretical Physics, Trieste (Italy).
IDENTITY FOR PROPAGATOR IN FOUR-FERMION THEORY
S. Karnaukhov Aug. 1993 4 p
(DE94-611104; IC-93/276) Avail: CASI HC A01/MF A01 (US Sales Only)

The method of exact evaluation of quantum partition function (QPF) in some four fermion models is proposed. The calculations are carried out by the path integral method. The integral is evaluated by introducing the additional fields (called Hubbard-Stratanovich transformation in some models), integration over fermionic variables, and considering the finite-dimensional approximation of the rest integral over bosonic fields in the infinite limit. The non-standard representation of propagator is proposed for the Fermi-theory of four-fermion interaction. This representation seems to be more convenient for the nonperturbative analysis. DOE

N94-36070# Institute of Nuclear Physics, Krakow (Poland). Dept. of Theoretical Physics.
CLASSICAL TIME MACHINE
E. Kapuscik, J. Kempczynski, and A. Horzela Feb. 1992 8 p
(DE94-616616; INP-1578/PH) Avail: CASI HC A02/MF A01 (US Sales Only)

Generalizing concepts of the Einstein radiolocation method and, as a consequence, special relativity transformation rules we get that the time flow in the moving system depends on the direction of motion. DOE

N94-36071# Academy of Sciences of the Ukraine, Kiev. Inst. Teoreticheskoj Fiziki.
ZERO MODES OF THE TWO-DIMENSIONAL DIRAC OPERATOR ON A NONCOMPACT RIEMANN SURFACE IN AN EXTERNAL MAGNETIC FIELD
A. V. Mishchenko and Yu. A. Sitenko 1992 24 p
(DE94-616618; ITF-92-10R) Avail: CASI HC A03/MF A01 (US Sales Only)

A generalization of the Aharonov-Cashier theorem to the case of a topologically finite orientable surface is proposed and the expression for the index in the space of square integrable functions is obtained. The restrictions on the space of admissible functions, which are due to the self-adjointness of the Dirac operator, are discussed and the expression for the index in the case a conformally finite orientable surface is obtained. DOE

N94-36072# Academy of Sciences of the Ukraine, Kiev. Inst. for Theoretical Physics.
QUANTUM MECHANICS AND THERMODYNAMICS OF PARTICLES WITH DISTANCE DEPENDENT STATISTICS
S. V. Mashkevich 1993 12 p Submitted for publication
(DE94-616620; ITP-93-5E) Avail: CASI HC A03/MF A01 (US Sales Only)

The general notion of distance dependent statistics in anyon-like systems is discussed. The two-body problem for such statistics is considered, The general formula for the second Virial coefficient is derived and it is shown that in the limiting cases it reproduces the know results for ideal anyons. DOE

N94-36256 Aerospace Corp., El Segundo, CA.
AN ADAPTIVE, UNSTRUCTURED, FINITE-ELEMENT, MULTI-MATERIAL, THERMAL ANALYSIS Technical Report, Jan. 1991 - Jan. 1992
I.-Shih Chang Nov. 1993 30 p Limited Reproducibility: More than 20% of this document may be affected by microfiche quality
(Contract F04701-88-C-0089)
(AD-A278632; TR-93(3530)-4; SMC-TR-94-23) Avail: Issuing Activity (Defense Technical Information Center (DTIC))

An efficient method has been developed for obtaining a high-resolution temperature distribution of the transient heat conduction inside an arbitrary domain containing any number of anisotropic materials. The method combines an adaptive, unstructured, mesh generation technique and a finite-element analysis program for a multi-material thermal analysis. The technique allows easy generation of fine elements in a high-temperature gradient area and coarse elements in a low-temperature gradient area to enhance the quality of analysis results with minimum effort and cost. Continuity of finite-element mesh across the boundaries of multiple materials is precisely preserved. The thermal conduction inside an infinite cylinder and inside a two-layer slab is analyzed, and the results are compared to the exact solution to validate the solution procedure. Application of the method to investigate heat penetration in the Titan 4 Solid Rocket Motor Upgrade nozzle flexseal of a multi-material structure is demonstrated. Extension of the method to calculate thermal response of a Star-37S nozzle/exit cone insulation and supporting structure with complicated, multiple charring materials is discussed. DTIC

N94-36351# International Centre for Theoretical Physics, Trieste (Italy).
ON QUANTIZATION OF TIME-DEPENDENT SYSTEMS WITH CONSTRAINTS
F. G. Hadjialieva (Academy of Pedagogical Sciences of the USSR, Moscow, USSR.) and R. G. Jafarov Jul. 1993 7 p
(DE94-611114; IC-93/188) Avail: CASI HC A02/MF A01 (US Sales Only)

The Dirac method of canonical quantization of theories with second class constraints has to be modified if the constraints depend on time explicitly. A solution of the problem was given by Gitman and Tyutin. In the present work we propose an independent way to derive the rules of quantization for these systems, starting from physical equivalent theory with trivial nonstationarity. DOE

N94-36381# International Centre for Theoretical Physics, Trieste (Italy).
COHERENT STATES VERSUS DE BROGLIE-WAVELETS
A. O. Barut Aug. 1993 7 p
(DE94-611075; IC-93/233) Avail: CASI HC A02/MF A01 (US Sales Only)

There are two types of nonspreading localized wave forms representing a stable, individual, indivisible, single quantum particle with interference properties endowed with classical (hidden) parameters (i.e. initial positions and velocity): coherent states and wavelets. The first is exactly known for oscillators, the second for free particles. Their relation and their construction is discussed from a new unified point of view. We then extend this contraction to the Coulomb problem, where with the introduction of a new time variable T, nonspreading states are obtained. DOE

80 SOCIAL SCIENCES (GENERAL)

Includes educational matters.

N94-35339* National Aeronautics and Space Administration. Lyndon B. Johnson Space Center, Houston, TX.
SPACE EDUCATORS' HANDBOOK (Diskette)
Jerry Woodfill May 1992 Diskette: Six 3.5-inch DSHD Mac diskettes
(NASA-TM-109779; S-677; NAS 1.15:109779; NONP-NASA-DK-94-5859)
Avail: Issuing Activity (Mail Stop IA121, NASA. Johnson Space Center, Houston, TX 77058)

The Space Educators' Handbook is a collection of space exploration information available on Hypercard as a space education reference book. Ranging from early dreams of space ships to current manned missions, the more than four thousand cards include entries of statistics, historical facts and anecdotes, technical articles, accounts of NASA missions from Mercury through the space shuttle, biographical information on women and men who have contributed to space exploration, scientific facts, and various other space-related data. The means of presenting the data range from cartoons and drawings to lists and narratives, some briefly quoted and some reproduced in full. Author

N94-35964*# National Aeronautics and Space Administration. Ames Research Center, Moffett Field, CA.
MENTORING FOR 2000 AND BEYOND
K. M. Guerra (General Electric Co., Moffett Field, CA.) and M. A. Farrance *In its* 1993 Technical Paper Contest for Women. Gear Up 2000: Women in Motion Feb. 1994 p 21-25 (For primary document see N94-35961 11-99)
Avail: CASI HC A01/MF A02

N94-35973*# National Aeronautics and Space Administration. Ames Research Center, Moffett Field, CA.
BUILDING ON THE FOUNDATION FOR AN ENGINEERING CAREER
Susan White and Ruth White *In its* 1993 Technical Paper Contest for Women. Gear Up 2000: Women in Motion Feb. 1994 p 125-130 (For primary document see N94-35961 11-99)
Avail: CASI HC A02/MF A02

81 ADMINISTRATION AND MANAGEMENT

Includes management planning and research.

N94-35970*# National Aeronautics and Space Administration. Ames Research Center, Moffett Field, CA.
IMPLEMENTATION OF A COMPUTERIZED MAINTENANCE MANAGEMENT SYSTEM
Yong-Hong Shen and Bruce Askari *In its* 1993 Technical Paper Contest for Women. Gear Up 2000: Women in Motion Feb. 1994 p 99-109 (For primary document see N94-35961 11-99)
Avail: CASI HC A03/MF A02

82 DOCUMENTATION AND INFORMATION SCIENCE

Includes information management; information storage and retrieval technology; technical writing; graphic arts; and micrography.

For computer documentation see *61 Computer Programming and Software.*

N94-35254*# National Aeronautics and Space Administration. Langley Research Center, Hampton, VA.

NASA/DOD AEROSPACE KNOWLEDGE DIFFUSION RESEARCH PROJECT. PAPER 40: TECHNICAL COMMUNICATIONS IN AEROSPACE EDUCATION: A STUDY OF AIAA STUDENT MEMBERS

John M. Kennedy (Indiana Univ., Bloomington, IN.), Thomas E. Pinelli, and Rebecca O. Barclay 1994 10 p Presented at the 32nd Aerospace Sciences Meeting and Exhibit of the American Institute of Aeronautics and Astronautics, Reno, NV, 11 Jan. 1994

(NASA-TM-109868; NAS 1.15:109868; AIAA Paper 94-0858; AD-B178352L) Avail: CASI HC A02/MF A01

This paper describes the preliminary analysis of a survey of the American Institute of Aeronautics and Astronautics (AIAA) student members. In the paper we examine (1) the demographic characteristics of the students, (2) factors that affected their career decisions, (3) their career goals and aspirations, and (4) their training in technical communication and techniques for finding and using aerospace scientific and technical information (STI). We determine that aerospace engineering students receive training in technical communication skills and the use of STI. While those in the aerospace industry think that more training is needed, we believe the students receive the appropriate amount of training. We think that the differences between the amount of training students receive and the perception of training needs is related partially to the characteristics of the students and partially to the structure of the aerospace STI dissemination system. Overall, we conclude that the students' technical communication training and knowledge of STI, while limited by external forces, makes it difficult for students to achieve their career goals. Author

N94-35337# California Univ., Berkeley. Lawrence Berkeley Lab, CA. Information and Computing Sciences Div.

DATA AVAILABLE FROM BIRTH AND DEATH REGISTRIES AND CANCER REGISTRIES IN THE US

Becky L. Wallin, Alan R. Houser, Deane W. Merrill, and Steve Selvin Jan. 1994 39 p

(Contract DE-AC03-76SF-00098)

(LBL-30971; UC-605) Avail: CASI HC A03/MF A01

In the United States, cancer registries have been compiling data for decades, and state vital statistics offices have been compiling birth and death data for nearly a century. Although this information has been well used for disease surveillance and various studies, it could be better exploited by making it more readily available, reducing the duplication of effort that occurs when researchers at the private, city, county, state, and federal levels work separately on their data collection and disease investigations. This report summarizes the nationwide availability of birth and death records and cancer registry data, with particular emphasis on subcounty geographic detail, such as zip code and census tract. Birth and death data are available at the county level for the entire United States from the National Center for Health Statistics. However, county level data are inadequate for small area studies of potential environmental hazards. Hazards of current interest to the Department of Energy (DOE) include DOE facilities, nuclear power plants, and sources of electromagnetic radiation such as broadcasting towers and power lines. Author

N94-35347# American Geological Inst., Alexandria, VA.

NATIONAL GEOSCIENCE DATA REPOSITORY SYSTEM

C. M. Schiffries and M. E. Milling Mar. 1994 68 p

(Contract DE-FG22-93BC-14968)

(DE94-000120; DOE/BC-14968/1) Avail: CASI HC A04/MF A01

The American Geological Institute (AGI) has completed the first phase of a study to assess the feasibility of establishing a National Geoscience Data Repository System to capture and preserve valuable geoscientific data. The study was initiated in response to the fact that billions of dollars worth of domestic geological and geophysical data are in jeopardy of being irrevocably lost or destroyed as a consequence of the ongoing downsizing of the US energy and minerals industry. This report focuses on two major issues. First, it documents the types and quantity of data available for contribution to a National Geoscience Data Repository System. Second, it documents the data needs and priorities of potential users of the system. A National Geoscience Data Repository System would serve as an important and valuable source of information for the entire geoscience community for a variety of applications including environmental protection, water resource management, global change studies, and basic and applied research. The repository system would also contain critical data that would enable domestic energy and minerals companies to expand their exploration and production programs in the United States for improved recovery of domestic oil, gas, and mineral resources. DOE

N94-35382* National Aeronautics and Space Administration, Washington, DC.

NASA PATENT ABSTRACTS BIBLIOGRAPHY: A CONTINUING BIBLIOGRAPHY. SECTION 1: ABSTRACTS (SUPPLEMENT 45)

Jul. 1994 64 p

(NASA-SP-7039(45)-Sect-1; NAS 1.21:7039(45)-Sect-1) Avail: CASI HC A04

Abstracts are provided for 137 patents and patent applications entered into the NASA scientific and technical information system during the period Jan. 1994 through Jun. 1994. Each entry consists of a citation, an abstract, and in most cases, a key illustration selected from the patent or patent application. Author (revised)

N94-35525 Defense Technical Information Center, Alexandria, VA.

DEFENSE RDT AND E ONLINE SYSTEM (DROLS) RETRIEVAL REFERENCE GUIDE

Richard J. Wayman, Holly J. Wilson, and Charles E. Reed May 1994 25 p Limited Reproducibility: More than 20% of this document may be affected by microfiche quality

(AD-A278972; DTIC-TR-94/21) Avail: Issuing Activity (Defense Technical Information Center (DTIC))

The Retrieval Reference Guide is intended for Defense RDT&E Online System (DROLS) operators. The guide provides an overview of sign on procedures, system commands, field identification codes, and examples of search strategies and display formats for the Technical Reports and Work Unit Databases. The use of Boolean operators and search options are also addressed. Included in this guide are references and phone numbers for Registration, Reference and Retrieval, Network Services, and other DROLS related branches of the Defense Technical Information Center (DTIC). This guide is intended to be used in conjunction with the DROLS Handbook. DTIC

N94-35526 Carnegie-Mellon Univ., Pittsburgh, PA. Dept. of Computer Science.

ASYNCHRONOUS OPTIMISTIC ROLLBACK RECOVERY USING SECURE DISTRIBUTED TIME

Sean W. Smith, David B. Johnson, and J. D. Tygar Mar. 1994 23 p Limited Reproducibility: More than 20% of this document may be affected by microfiche quality

(Contract F33615-90-C-1465; ARPA Order 7597)

(AD-A278978; CMU-CS-94-130) Avail: Issuing Activity (Defense Technical Information Center (DTIC))

In an asynchronous distributed computation, processes may fail and restart from saved state. A protocol for optimistic rollback recovery must recover the system when other processes may depend on lost states at failed processes. Previous work has used forms of partial order clocks to track potential causality. Our research addresses two crucial shortcomings: the rollback problem also involves tracking a second level of partial order time (potential knowledge of failures and rollbacks), and protocols based on partial order clocks are open to inherent security and privacy risks. We have developed a distributed time framework that provides the tools for multiple levels of time abstraction, and for identifying and solving the corresponding security and privacy risks. This paper applies our framework to the rollback problem. We derive a new optimistic rollback recovery protocol that provides completely asynchronous recovery (thus directly supporting concurrent recovery and tolerating network partitions) and that enables processes to take full advantage of their maximum potential knowledge of orphans (thus reducing the worst case bound on asynchronous recovery after a single failure from exponential to at most one rollback per process). By explicitly tracking and utilizing both levels of partial order time, our protocol substantially improves on previous work in optimistic recovery. Our work also provides a foundation for incorporating security and privacy in optimistic rollback recovery. DTIC

N94-35533 Newcastle-upon-Tyne Univ., Newcastle (England). Dept. of Computing Science.
ORDIT: A NEW METHODOLOGY TO ASSIST IN THE PROCESS OF ELICITING AND MODELLING ORGANISATIONAL REQUIREMENTS
A. J. C. Blyth, J. Chudge, J. E. Dobson, and M. R. Strens Nov. 1993 26 p See also PB93-124402 and PB93-152411
(PB94-167814; TRS-456) Copyright Avail: Issuing Activity (National Technical Information Service (NTIS))

Requirements engineering from an organizational perspective needs to be viewed as social engineering. Thus, a modeling language is presented, which is visual in nature, and with which we assert that it is possible to diagrammatically represent and reason about the impact that an information technology system may have on an organization, and thus, derive organizational requirements. NTIS

N94-35571 Carnegie-Mellon Univ., Pittsburgh, PA. Dept. of Computer Science.
LARGE GRANULARITY CACHE COHERENCE FOR INTERMITTENT CONNECTIVITY
L. Mummert and M. Satyanarayanan Apr. 1994 15 p Limited Reproducibility: More than 20% of this document may be affected by microfiche quality
(Contract F19628-93-C-0193)
(AD-A278897; CMU-CS-94-100) Avail: Issuing Activity (Defense Technical Information Center (DTIC))

To function in mobile computing environments, distributed file systems must cope with networks that are slow, intermittent, or both. Intermittence vitiates the effectiveness of callback-based cache coherence schemes in reducing client-server communication, because clients must validate files when connections are reestablished. In this paper we show how maintaining cache coherence at a large granularity alleviates this problem. We report on the implementation and performance of large granularity cache coherence for the Coda File System. Our measurements confirm the value of this technique. At 9.6 Kbps, this technique takes only 4 to 20% of the time required by two other strategies to validate the cache for a sample of Coda users. Even at this speed, the network is effectively eliminated as the bottleneck for cache validation. DTIC

N94-35651 University of Southern California, Marina del Rey, CA. Information Sciences Inst.
GOOD APPLICATIONS FOR CRUMMY MACHINE TRANSLATION
Kenneth W. Church 1993 18 p Limited Reproducibility: More than 20% of this document may be affected by microfiche quality
(Contract MDA903-87-C-0064)
(AD-A278689; ISI/RR-93-369) Avail: Issuing Activity (Defense Technical Information Center (DTIC))

Ideally, we might hope to improve the performance of our MT systems by improving the system, but it might be even more important to improve performance by looking for a more appropriate application. A survey of the literature on evaluation of MT systems seems to suggest that the success of the evaluation often depends very strongly on the selection of an appropriate application. If the application is well-chosen, then it often becomes fairly clear how the system should be evaluated. Moreover, the evaluation is likely to make the system look good. Conversely, if the application is not clearly identified (or worse, if the application is poorly chosen), then it is often very difficult to find a satisfying evaluation paradigm. We begin our discussion with a brief review of some evaluation metrics that have been tried in the past and conclude that it is difficult to identify a satisfying evaluation paradigm that will make sense over all possible applications. It is probably wise to identify the application first, and then we will be in a much better position to address evaluation questions. The discussion will then turn to the main point, an essay on how to pick a good niche application for state-of-the-art (crummy) machine translation. DTIC

N94-35663 University of Southern California, Marina del Rey, CA. Information Sciences Inst.
REFORMULATING QUERY PLANS FOR MULTIDATABASE SYSTEMS
Chu-Nan Hsu and Craig Knoblock Nov. 1993 18 p Limited Reproducibility: More than 20% of this document may be affected by microfiche quality
(Contract F30602-91-C-0081)
(AD-A278688; ISI/RR-93-368) Avail: Issuing Activity (Defense Technical Information Center (DTIC))

A practical heterogeneous, distributed multidatabase system must answer queries efficiently. Conventional query optimization techniques are not adequate here because these techniques are dependent on the database structure, and they rely on limited information which is not sufficient in complicated multidatabase queries. This paper presents an automated approach to reformulating query plans to improve the efficiency of multidatabase queries. This approach uses database abstractions, the knowledge about the contents of databases, to reformulate a query plan into a less expensive but semantically equivalent one. We present two algorithms. The first algorithm reformulates subqueries to individual databases, the second algorithm extends the first one and reformulates the entire query plan. Empirical results show that the reformulations can provide significant savings with minimal overhead. The reformulation approach provides a global reduction in the amount of the intermediate data as well as local optimizations on the subqueries. DTIC

N94-35732 Chicago Univ., IL.
THE CAPACITY OF COLOR HISTOGRAM INDEXING
Markus A. Stricker (Eidgenoessische Technische Hochschule, Zurich, Switzerland.) and Michael J. Swain 1993 5 p Limited Reproducibility: More than 20% of this document may be affected by microfiche quality
(AD-A279031) Avail: Issuing Activity (Defense Technical Information Center (DTIC))

Color histogram matching has been shown to be a promising way of quickly indexing into a large image database. Yet, few experiments have been done to test the method on truly large databases, and even if they were performed, they would give little guidance to a user wondering if the technique would be useful with his or her database. In this paper we define and analyze a measure relevant to extending color histogram indexing to large databases: capacity (how many distinguishable histograms can be stored). DTIC

N94-35790# Joint Inst. for Nuclear Research, Dubna (USSR). Lab. of Computing Techniques and Automation.
MULTI-WINDOW DIALOGUE SYSTEM OF DATA PROCESSING FOR EXPERIMENTAL SETUP VASSILISSA IN PAW ENVIRONMENT
A. N. Andreev, D. V. Vakatov, M. Veselski, A. V. Eremin, V. V. Ivanov, and A. M. Khasanov 1992 12 p
(DE94-612439; JINR-R-10-92-449) Avail: CASI HC A03/MF A01 (US Sales Only)

Multi-window dialog system for processing data acquired from experimental setup VASSILISSA is presented. The system provides a friendly user's interface for experimental data conversion, selection, and preparing for graphic analysis with PAW. DOE

N94-35817# National Inst. of Standards and Technology, Gaithersburg, MD.
DATA ACQUISITION SYSTEMS
L. Costrell 22 Mar. 1994 3 p
(Contract DE-AI05-91ER-40616)
(DE94-009848; DOE/ER-40616/T1) Avail: CASI HC A01/MF A01

The program has included continued extension and maintenance of the specifications for data acquisition systems for high energy physics applications. Work continued on the study, development, and specification of the FASTBUS system and of other systems to meet the changing needs of the community. The approach has maximized the use of available technology, systems, subsystems, and components. Work on a version of FASTBUS optimized for accelerator and experiment control applications and interfaces to other busses has been examined to see to what extent existing systems can be utilized. Processing of the revised editions of the ANSI/IEEE standards was pursued so that they can be published in 1994. This applies also to the corresponding international standards of the International Electrotechnical Commission (IEC) though the international processing is expected to take somewhat longer. The project provides a clearing house for data acquisition system information and maintains liaison with and collaborates with the ESONE Committee of European Laboratories and national and international laboratories involved with data acquisition and control systems for high energy and nuclear physics. DOE

N94-35819 National Inst. of Standards and Technology, Gaithersburg, MD. Building and Fire Research Lab.

FIRE DATA MANAGEMENT SYSTEM, FDMS 2.0, TECHNICAL DOCUMENTATION

R. W. Portier Feb. 1994 86 p See also PB93-182038 Limited Reproducibility: More than 20% of this document may be affected by microfiche quality

(PB94-164019; NIST/TN-1407) Avail: CASI HC A05; SOD HC

The Fire Data Management System, FDMS, is a computer database specifically designed to store and retrieve fire test results. A version, FDMS 1.0, of the database is currently available. This guide provides detailed descriptions of the physical file implementations planned for the next generation of the database, FDMS 2.0. NTIS

N94-35832# Korean Atomic Energy Research Inst., Daeduk (Republic of Korea).

THE DEVELOPMENT OF A STATISTICAL REPORT SOFTWARE FOR COMPUTER SYSTEM USAGES

Young Jai Lee, Hae Cho Lee, Jeong Seok Park, Jae Min Sohn, Bong Sik Park, Sun Hee Park, In Ah Hwang, and Soo Jin Park Jun. 1992 172 p

(DE94-611061; KAERI/TR-277/92) Avail: CASI HC A08/MF A02 (US Sales Only)

In this report, we describe the data base system developed for various statistical analysis of KAERI computer system usages. In keeping abreast with the rapid growth of information society, many devices for handling information are developed and purchased. At KAERI's computer operation facility, several information processing devices have been installed and are under operation now. It has been found very difficult to draw up a long term plan for computer operation management due to the lack of accumulated operation history data. Combined charge information is generated and transferred to the VAX 6320 system. The data base system on the VAX 6320 was implemented using the ORACLE RDBMS software. The computing services history data was all processed and collected into the data base for the fiscal years 1990 and 1991. It is expected that this data base will be used in many convenient ways in the future. DOE

N94-35833# Korean Atomic Energy Research Inst., Daeduk (Republic of Korea).

AN ANALYSIS OF FILE SYSTEM AND INSTALLATION OF THE FILE MANAGEMENT SYSTEM FOR NOS OPERATING SYSTEM

Young Jai Lee, Sun Hee Park, In Ah Hwang, and Hee Kyung Kim Jun. 1992 65 p

(DE94-611062; KAERI/TR-278/92) Avail: CASI HC A04/MF A01 (US Sales Only)

In this technical report, we analyze NOS file structure for Cyber 170-875 and Cyber 960-31 computer system. We also describe functions, procedure, and how-to-operate and how-to-use VDS. VDS is used to manage large files effectively for Cyber computer system. The purpose of the VDS installation is to increase the virtual disk storage by utilizing magnetic tape, to assist the users of the computer system in managing their files, and to enhance the performance of KAERI Cyber computer system. DOE

N94-35835* National Aeronautics and Space Administration, Washington, DC.

NASA PATENT ABSTRACTS BIBLIOGRAPHY: A CONTINUING BIBLIOGRAPHY. SECTION 2: INDEXES (SUPPLEMENT 45)

Jul. 1994 625 p

(NASA-SP-7039(45)-Sect-2; NAS 1.21:7039(45)-Sect-2) Avail: CASI HC A99

A subject index is provided for over 5600 patents and patent applications for the period May 1969 through June 1994. Additional indexes list personal authors, corporate authors, contract numbers, NASA case numbers, U.S. patent class numbers, U.S. patent numbers, and NASA accession numbers. Author

N94-35954# Academy of Sciences (USSR), Novosibirsk (USSR). Inst. Yadernoj. Fiziki.

DATA ACQUISITION SYSTEM OF THE GDL FACILITY

T. V. Salikova 1992 32 p

(DE94-616604; IYaF-92-42) Avail: CASI HC A03/MF A01 (US Sales Only)

Data acquisition system (DAS) operates in the RSX-IIM environment with the CAMAC system CAMAC driven and CAMAC control processor are used for the CAMAC system operation support. The exchange rate between a problem and the CAMAC module is equal to 100 K worf/c. DOE

N94-35959 Helsinki Univ. of Technology, Espoo (Finland). Digital Systems Lab.

PRIORITIES AND NONMONOTONIC REASONING

J. Rintanen Dec. 1993 97 p See also AD-A153 963, PB92-202902 and PB93-161230 Limited Reproducibility: More than 20% of this document may be affected by microfiche quality

(ISSN 0783-5396)

(PB94-171170; ISBN-951-22-1915-8) Avail: Issuing Activity (National Technical Information Service (NTIS))

Many knowledge-based systems use some kind of priorities for controlling their reasoning. In this work, autoepistemic logic is extended with priorities. Priorities are formalized as partial orders of formulae that express that some formulae are preferred to others. Priorities increase the set of conclusions that can be inferred from a set of formulae, because the number of cases where conflicts between defaults are left unresolved decreases. A decision procedure for prioritized autoepistemic logic is given in terms of a decision procedure for a classical logic on which the prioritized autoepistemic logic is based. The complexity of the logic is analyzed with respect to the underlying classical logic. When the classical logic is the propositional logic, the decision problems of prioritized autoepistemic logic are located on the third level of the polynomial hierarchy. The results of this work carry to other formalisms as well because of the existence of translations of other formalisms to autoepistemic logic. Finally, it is demonstrated how automated theorem-proving in prioritized autoepistemic logic benefits from priorities. An algorithm for automated reasoning is given and proved correct. NTIS

N94-36005 National Inst. of Standards and Technology, Gaithersburg, MD. Computer Security Div.

PROCEEDINGS OF THE WORKSHOP ON THE FEDERAL CRITERIA FOR INFORMATION TECHNOLOGY SECURITY

J. A. Cugini, P. Toth, G. Troy, L. M. Ambuel, and F. Mayer Mar. 1994 74 p Workshop held in Ellicott City, MD, 2-3 Jun. 1993 Limited Reproducibility: More than 20% of this document may be affected by microfiche quality

(PB94-162583; NISTIR-5386) Avail: CASI HC A04

The first draft of the Federal Criteria was made public in January 1993. Several thousand copies of the Federal Criteria were distributed and comments on this first draft were received. The purpose of the Federal Criteria Workshop was to address these comments. The purpose of these proceedings is to inform the Federal Criteria commentators and the workshop attendees of the outcome of the workshop. Also, these proceedings will be used as a blueprint for updating the Federal Criteria. These proceedings, and the revised portions of the draft Federal Criteria contents, will be the two principal National Institute of Standard and Technology (NIST)/National Security Agency (NSA) inputs to the Common Criteria Editorial Board (CCEB). Preliminary plans for dealing with the Federal Criteria comments are included in this document and all revisions will be performed under the direction of NIST and the NSA. NTIS

N94-36037* NASA Center for AeroSpace Information, Linthicum Heights, MD.

NASA THESAURUS. VOLUME 1: HIERARCHICAL LISTING. VOLUME 2: ACCESS VOCABULARY. VOLUME 3: DEFINITIONS

Jan. 1994 1478 p Sponsored by NASA

(ISSN 0899-5257)

(NASA-SP-7096-Vol-1/2/3; NAS 1.21:7096-Vol-1/2/3) Avail: CASI HC $90.00 as set (special price)

There are over 17,500 postable terms and some 4,000 nonpostable terms approved for use in the NASA Scientific and Technical Information Database in the Hierarchical Listing of the NASA Thesaurus. The generic structure is presented for many terms. The broader term and narrower term relationships are shown in an indented fashion that illustrates the generic structure better than the more widely used BT and NT listings. Related terms are generously applied, thus enhancing the usefulness of the Hierarchical Listing. Greater access to the Hierarchical Listing may be achieved with the collateral use of Volume 2 - Access Vocabulary and Volume 3 - Definitions. CASI

N94-36102# Los Alamos National Lab., NM.
USING INTERNATIONAL ENGLISH TO PREPARE TECHNICAL TEXT FOR TRANSLATION
I. Buican, V. Hriscu, and M. Amador 1993 22 p Presented at the IPCC Conference, Philadelphia, PA, 5-8 Oct. 1993
(Contract W-7405-eng-36)
(DE94-002628; LA-UR-93-3546; CONF-9310212-1) Avail: CASI HC A03/MF A01

This report presents recommendations concerning the translation of technical text. DOE

N94-36297# Lawrence Livermore National Lab., CA.
APPLYING OBSERVATIONS OF WORK ACTIVITY IN DESIGNING PROTOTYPE DATA ANALYSIS TOOLS
R. R. Springmeyer Jul. 1993 8 p Presented at the Visualization 1993, San Jose, CA, 25-29 Oct. 1993
(Contract W-7405-eng-48)
(DE94-010206; UCRL-JC-114300; CONF-931080-6) Avail: CASI HC A02/MF A01

Designers, implementers, and marketers of data analysis tools typically have different perspectives than users. Consequently, data analysts often find themselves using tools focused on graphics and programming concepts rather than concepts which reflect their own domain and the context of their work. Some user studies focus on usability tests late in development; others observe work activity, but fail to show how to apply that knowledge in design. This paper describes a methodology for applying observations of data analysis work activity in prototype tool design. The approach can be used both in designing improved data analysis tools, and customizing visualization environments to specific applications. We present an example of user-centered design for a prototype tool to cull large data sets. We revisit the typical graphical approach of animating a large data set from the point of view of an analyst who is culling data. Field evaluations using the prototype tool not only revealed valuable usability information, but initiated in-depth discussions about user's work, tools, technology, and requirements. DOE

N94-36300# Oak Ridge National Lab., TN.
NETLIB SERVICES AND RESOURCES
S. V. Browne (Tennessee Univ., Knoxville, TN.), S. C. Green (Tennessee Univ., Knoxville, TN.), K. Moore (Tennessee Univ., Knoxville, TN.), R. C. Wade (Tennessee Univ., Knoxville, TN.), J. J. Dongarra (Tennessee Univ., Knoxville, TN.), and Thomas H. Rowan Apr. 1994 50 p
(Contract DE-AC05-84OR-21400)
(DE94-010307; ORNL/TM-12680) Avail: CASI HC A03/MF A01

The Netlib repository, maintained by the University of Tennessee and Oak Ridge National Laboratory, contains freely available software, documents, and databases of interest to the numerical, scientific computing, and other communities. This report includes both the Netlib User's Guide and the Netlib System Manager's Guide, and contains information about Netlib's databases, interfaces, and system implementation. The Netlib repository's databases include the Performance Database, the Conferences Database, and the NA-NET mail forwarding and Whitepages Databases. A variety of user interfaces enable users to access the Netlib repository in the manner most convenient and compatible with their networking capabilities. These interfaces include the Netlib email interface, the Xnetlib X Windows client, the netlibget command-line TCP/IP client, anonymous FTP, anonymous RCP, and gopher. DOE

N94-36396*# Sterling Software, Inc., Cleveland, OH.
TELECOMMUTING (WORK-AT-HOME) AT NASA LEWIS RESEARCH CENTER Final Report
Saragur M. Srinidhi May 1994 22 p
(Contract NAS3-26100; RTOP 960-30-02)
(NASA-CR-195334; E-8865; NAS 1.26:195334) Avail: CASI HC A03/MF A01

This report presents a study in evaluating the viability of providing a work-at-home (telecommuting) program for Lewis Research Center's corporate employees using Integrated Services Digital Network (ISDN). Case studies have been presented for a range of applications from casual data access to interactive access. The network performance of telemedia applications were studied against future requirements for such level of remote connectivity. Many of the popular ISDN devices were characterized for network and service functionality. A set of recommendations to develop a telecommuting policy have been proposed. Author (revised)

N94-36435*# Dayton Univ. Research Inst., OH. Structural Integrity Div.
COLLECTION, PROCESSING, AND REPORTING OF DAMAGE TOLERANT DESIGN DATA FOR NON-AEROSPACE STRUCTURAL MATERIALS Final Report
P. D. Huber and J. P. Gallagher Jun. 1994 1364 p
(Grant NAG9-600)
(NASA-CR-196046; NAS 1.26:196046; UDR-TR-94-88) Avail: CASI HC A99/MF A10

This report describes the organization, format and content of the NASA Johnson damage tolerant database which was created to store damage tolerant property data for non aerospace structural materials. The database is designed to store fracture toughness data (K(sub IC), K(sub c), J(sub IC) and CTOD(sub IC)), resistance curve data (K(sub R) VS. delta a (sub eff) and JR VS. delta a (sub eff)), as well as subcritical crack growth data (a vs. N and da/dN vs. delta K). The database contains complementary material property data for both stainless and alloy steels, as well as for aluminum, nickel, and titanium alloys which were not incorporated into the Damage Tolerant Design Handbook database. Author (revised)

N94-36044*# National Aeronautics and Space Administration. Ames Research Center, Moffett Field, CA.
KNOWLEDGE-BASED SYSTEMS IN JAPAN
Edward Feigenbaum (Stanford Univ., CA.), Robert S. Engelmore (Stanford Univ., CA.), Peter E. Friedland, Bruce B. Johnson, H. Penny Nii, Herbert Schorr, and Howard Shrobe *In* Loyola Coll., JTEC/WTEC Report and Program Summary Mar. 1994 p 54-60 (For primary document see N94-36042 11-99)
Avail: CASI HC A02/MF A03

N94-36402*# University of Eastern Illinois, Charleston, IL. School of Technology.
APPLICATION OF MATERIALS DATABASE (MAT.DB.) TO MATERIALS EDUCATION
Ping Liu and Tommy L. Waskom *In* NASA. Langley Research Center, National Educators' Workshop: Update 1993. Standard Experiments in Engineering Materials Science and Technology Apr. 1994 p 101-109 (For primary document see N94-36398 11-23)
Avail: CASI HC A02/MF A04

83 ECONOMICS AND COST ANALYSIS

Includes cost effectiveness studies.

N94-35899*# National Aeronautics and Space Administration, Washington, DC.
BUDGET ESTIMATES, FISCAL YEAR 1995. VOLUME 1: AGENCY SUMMARY, HUMAN SPACE FLIGHT, AND SCIENCE, AERONAUTICS AND TECHNOLOGY
1994 340 p
(NASA-TM-109791; NAS 1.15:109791) Avail: CASI HC A15/MF A03; SOD HC

The NASA budget request has been restructured in FY 1995 into four appropriations: human space flight; science, aeronautics, and technology; mission support; and inspector general. The human space flight appropriations provides funding for NASA's human space flight activities. This includes the on-orbit infrastructure (space station and Spacelab), transportation capability (space shuttle program, including operations, program support, and performance and safety upgrades), and the Russian cooperation program, which includes the flight activities associated with the cooperative research flights to the Russian Mir space station. These activities are funded in the following budget line items: space station, Russian cooperation, space shuttle, and payload utilization and operations. The science, aeronautics, and technology appropriations provides funding for the research and development activities of NASA. This includes funds to extend our knowledge of the earth, its space environment, and the universe and to invest in new technologies, particularly in aeronautics, to ensure the future competitiveness of the nation. These objectives are achieved through the following elements: space science, life and microgravity sciences and applications, mission to planet earth, aeronautical research and technology, advanced concepts and technology, launch services, mission communication services, and academic programs. CASI

N94-35900*# National Aeronautics and Space Administration, Washington, DC.

BUDGET ESTIMATES, FISCAL YEAR 1995. VOLUME 2: MISSION SUPPORT AND INSPECTOR GENERAL

1994 246 p

(NASA-TM-109792; NAS 1.15:109792) Avail: CASI HC A11/MF A03; SOD HC

The mission support appropriations provides funding for NASA's civil service work force, space communication services, safety and quality assurance activities, and for maintenance activities for the NASA institution. These objectives are accomplished through the following elements: safety, reliability, and quality assurance; space communication services; research and program management; and construction of facilities.

Derived from text

84 LAW, POLITICAL SCIENCE AND SPACE POLICY

Includes NASA appropriation hearings; aviation law; space law and policy; international law; international cooperation; and patent policy.

N94-35446*# Committee on Government Operations (U.S. House).

STATEMENT BY BILL D. COLVIN, INSPECTOR GENERAL

6 Oct. 1993 13 p Statement presented to the Subcommittee on Legislation and National Security, 103rd Congress, 6 Oct. 1993 Prepared in cooperation with NASA, Washington

(NASA-TM-109793; NAS 1.15:109793) Avail: Subcommittee on Legislation and National Security, House of Representatives, Washington, DC 20515 HC free

Presented are the statements of Bill D. Colvin, Inspector General of NASA, before the Subcommittee on Legislation and National Security, Committee on Government Operations, U.S. House of Representatives, on the audit and investigative oversight work the NASA office of Inspector General performs at the agency and among its contractors and how this work relates to NASA's efforts at management and procurement reform. The testimony is divided into the following major areas: procurement oversight, product integrity, financial related activities, and proactive NASA program evaluations. CASI

N94-35519# Joint Publications Research Service, Arlington, VA.

JPRS REPORT: SCIENCE AND TECHNOLOGY. CENTRAL EURASIA: SPACE. RUSSIAN FEDERATION LAW ON SPACE

28 Feb. 1994 13 p Transl. into ENGLISH from Vozdushnyy Transport (Moscow, Russia), nos. 44-49, 51-51, Oct. - Dec. 1993

(JPRS-USP-94-002) Avail: CASI HC A03/MF A01

The Russian Federation law on space is directed to ensuring the juridical regulation of space activity and stimulates the application of the potential of space science and industry for solving socio-economic, scientific-technical and defense problems of the Russian Federation. The following topics relating to this law are presented: general principles, organization of space activity, economic conditions for space activity, space infrastructure, space activity safety, international cooperation, and responsibility. CASI

N94-35901 US Center for Research and Education on Strategy and Technology, Arlington, VA.

PARTNERS IN SPACE. INTERNATIONAL COOPERATION IN SPACE: STRATEGIES FOR THE NEW CENTURY Final Project Report

Jean-Francois Delpech, John M. Logsdon, and Brad M. Meslin May 1993 127 p Prepared in cooperation with CSP Associates, Inc., Cambridge, MA and Ecole Polytechnique, Paris, France

(ISBN-0-9629930-2-6) Copyright Avail: Issuing Activity (US Center for Research and Education on Strategy and Technology, 1840 Wilson Blvd., Suite 204, Arlington, VA 22201)

The realization that available funding for large-scale space programs is rapidly moving beyond the financial reach of any single nation has led us to believe that innovative international collaboration is becoming a necessity. It may even be that cooperative arrangements have become the only way to initiate and sustain the more ambitious space projects of the future. In addition, enhanced international cooperation may well be the preferred and most effective approach to carrying out some projects already on the space agenda. Starting from an analysis of the difficulties and benefits of space cooperation, this report recommends the changes in international space relations needed to enable the major spacefaring nations, which carry out the bulk of humanity's activities in space, to band together, so as to afford the future large scale space programs we all need to expand our knowledge, to explore new frontiers, and to guarantee our common security. During Phase 1 of this project, a core team carried out background research and developed preliminary analyses, findings, and conclusions under the guidance of a distinguished Steering Committee composed of industrialists, space agency representatives, and space policy specialists. The Steering Committee met periodically to identify pertinent issues, review project progress, and contribute substantively to study conclusions and recommendations. While the present report was formed in light of the advice of the Steering Committee, it represents the considered judgement of the Project Co-Directors and the rest of the project team and does not necessarily represent the views of the Steering Committee members or their respective organizations. Derived from text

85 URBAN TECHNOLOGY AND TRANSPORTATION

Includes applications of space technology to urban problems; technology transfer; technology assessment; and surface and mass transportation.

For related information see also *03 Air Transportation and Safety, 16 Space Transportation,* and *44 Energy Production and Conversion.*

N94-35966*# SYRE Corp., Moffett Field, CA.

WOMEN AS A RESOURCE FOR THE FLEXIBILITY REQUIRED FOR HIGH TECHNOLOGY INNOVATION

Ruth Dasso Marlaire *In* NASA. Ames Research Center, 1993 Technical Paper Contest for Women. Gear Up 2000: Women in Motion Feb. 1994 p 37-40 (For primary document see N94-35961 11-99)

Avail: CASI HC A01/MF A02

88 SPACE SCIENCES (GENERAL)

No abstracts in this category.

89 ASTRONOMY

Includes radio, gamma-ray, and infrared astronomy, and astrometry.

N94-35516*# Columbia Univ., New York, NY. Depts. of Astronomy and Physics.
GRO: STUDIES OF HIGH ENERGY PULSARS WITH EGRET Annual Status Report, 15 Jul. 1993 - 14 Jul. 1994
Malvin Ruderman Jun. 1994 6 p
(Grant NAG5-2016)
(NASA-CR-196003; NAS 1.26:196003; CAL-2198) Avail: CASI HC A02/MF A01

The reported e(sup +/-) annihilation line from the Crab pulsar has three remarkable properties. It is very strong (approximately 10(exp 40)e(sup +/-) annhilations/sec.), red shifted (by about 70 KeV relative to mc(exp 2) = 511 KeV), and very narrow (width approximately equals 10 KeV). The e(sup +/-) annihilation did not occur near the star in polar cap accelerator models so that the redshift, suggestive in its magnitude of a gravitational redshift from annihilation near the stellar surface, did not have an explanation. Therefore, concentration was placed on e(sup +/-) production from outer-magnetosphere accelerator models. Derived from text

N94-35565# Lawrence Livermore National Lab., CA.
ISSUES IN THE DESIGN AND OPTIMIZATION OF ADAPTIVE OPTICS AND LASER GUIDE STARS FOR THE KECK TELESCOPES
C. E. Max, D. T. Gavel, and S. S. Olivier et al Mar. 1994 14 p
Presented at the Astronomical Telescopes and Instrumentation for the 21st Century, Kona Beach, HI, 13-18 Mar. 1994
(Contract W-7405-eng-48)
(DE94-009384; UCRL-JC-116505; CONF-940395-1) Avail: CASI HC A03/MF A01

We discuss issues in optimizing the design of adaptive optics and laser guide star systems for the Keck Telescope. The initial tip-tilt system will use Keck's chopping secondary mirror. We describe design constraints, choice of detector, and expected performance of this tip-tilt system as well as its sky coverage. The adaptive optics system is being optimized for wavelengths of 1-2.2 mu m. We are studying adaptive optics concepts which use a wavefront sensor with varying numbers of subapertures, so as to respond to changing turbulence conditions. The goal is to be able to 'gang together' groups of deformable mirror subapertures under software control, when conditions call for larger subapertures. We present performance predictions as a function of sky coverage and the number of deformable mirror degrees of freedom. We analyze the predicted brightness several candidate laser guide star systems, as a function of laser power and pulse format. These predictions are used to examine the resulting Strehl as a function of observing wavelength and laser type. We discuss laser waste heat and thermal management issues, and conclude with an overview of instruments under design to take advantage of the Keck adaptive optics system. DOE

N94-35998# Sandia National Labs., Albuquerque, NM.
PREDICTED OPTICAL PERFORMANCE OF THE HIGH-ALTITUDE BALLOON EXPERIMENT (HABE) TELESCOPE IN AN ADVERSE THERMAL ENVIRONMENT
R. L. Akau, R. C. Givler, and D. R. Eastman 1994 18 p Presented at the Society of Photo-Optical Instrumentation Engineers Conference on Intelligent Information Systems, Orlando, FL, 4-8 Apr. 1994
(Contract DE-AC04-94AL-85000)
(DE94-008949; SAND-94-0131C; CONF-940449-4) Avail: CASI HC A03/MF A01

The High-Altitude Balloon Experiment (HABE) telescope was designed to operate at an ambient temperature of -55 C and an altitude of 26 km, using a precooled primary mirror. Although at this altitude the air density is only 1.4 percent of the value at sea level, the temperature gradients within the telescope are high enough to deform the optical wavefront. This problem is considerably lessened by precooling the primary mirror to -35 C. This paper describes the application of several codes to determine the range of wavefront deformation during a mission. DOE

N94-36279*# Space Telescope Science Inst., Baltimore, MD.
HUBBLE SPACE TELESCOPE CYCLE 5 CALL FOR PROPOSALS
Howard E. Bond, ed. Jun. 1994 58 p
(Contract NAS5-26555; RTOP 633-00-00)
(NASA-CR-189363; NAS 1.26:189363) Avail: CASI HC A04/MF A01

This document invites and supports participation by the international astronomical community in the HST General Observer and Archival Research programs. These documents contain the basic procedural and technical information required for HST proposal preparation and submission, including applicable deadlines. The telescope and its instruments were built under the auspices of the NASA and the European Space Agency. Author (revised)

N94-36280*# Space Telescope Science Inst., Baltimore, MD.
HST ARCHIVE PRIMER, VERSION 4.1
A. Fruchter, ed. and S. Baum, ed. May 1994 73 p
(Contract NAS5-26555; RTOP 633-00-00)
(NASA-CR-189370; NAS 1.26:189370) Avail: CASI HC A04/MF A01

This version of the HST Archive Primer provides the basic information a user needs to know to access the HST archive via StarView the new user interface to the archive. Using StarView, users can search for observations interest, find calibration reference files, and retrieve data from the archive. Both the terminal version of StarView and the X-windows version feature a name resolver which simplifies searches of the HST archive based on target name. In addition, the X-windows version of StarView allows preview of all public HST data; compressed versions of public images are displayed via SAOIMAGE, while spectra are plotted using the public plotting package, XMGR. Finally, the version of StarView described here features screens designed for observers preparing Cycle 5 HST proposals. Author (revised)

N94-36281*# Space Telescope Science Inst., Baltimore, MD.
HUBBLE SPACE TELESCOPE FINE GUIDANCE SENSORS INSTRUMENT HANDBOOK, VERSION 4.0
S. T. Holfeltz, ed. Apr. 1994 64 p
(Contract NAS5-26555; RTOP 633-00-00)
(NASA-CR-189366; NAS 1.26:189366) Avail: CASI HC A04/MF A01

This is a revised version of the Hubble Space Telescope Fine Guidance Sensor Instrument Handbook. The main goal of this edition is to help the potential General Observer (GO) learn how to most efficiently use the Fine Guidance Sensors (FGS's). First, the actual performance of the FGS's as scientific instruments is reviewed. Next, each of the available operating modes of the FGS's are reviewed in turn. The status and findings of pertinent calibrations, including Orbital Verification, Science Verification, and Instrument Scientist Calibrations are included as well as the relevant data reduction software. Author (revised)

N94-36282*# Space Telescope Science Inst., Baltimore, MD.
HUBBLE SPACE TELESCOPE GODDARD HIGH RESOLUTION SPECTROGRAPH (GHRS) INSTRUMENT HANDBOOK (FOR THE POST-COSTAR OBSERVATORY), VERSION 5.0
D. R. Soderblom, ed. May 1994 119 p
(Contract NAS5-26555; RTOP 633-00-00)
(NASA-CR-189369; NAS 1.26:189369) Avail: CASI HC A06/MF A02

This Handbook exists as a basic reference manual for the Goddard High Resolution Spectrograph (GHRS), and describes its properties and operation. Author

N94-36419*# Massachusetts Inst. of Tech., Cambridge. Center for Space Research.
ASTRONOMY IN THE REGION BETWEEN 1 mm AND 0.1 mm WAVELENGTH Final Report, 21 Sep. 1989 - 31 Oct. 1993
Rainer Weiss and Stephan S. Meyer 25 May 1994 103 p
(Grant NAGw-1841)
(NASA-CR-196020; NAS 1.26:196020) Avail: CASI HC A06/MF A02

The research under this grant resulted in the measurement of anisotropy of the Cosmic Microwave Background Radiation (CMBR) on angular scales from 90 degrees to 0.3 degrees. A bolometric radiometer was built with a sensitivity of better than 500 micro K divided by the square root of (Hz). The measurements complement the COBE anisotropy measurement in two ways. The large scale measurements were shown to cross-correlate with the COBE DMR anisotropy detection, confirming the results. The small scale measurements further the understanding of the structure in the CMBR on scales where we can begin to model the early stages in galaxy and galaxy cluster formation. Derived from text

N94-35420*# National Aeronautics and Space Administration. Goddard Space Flight Center, Greenbelt, MD.
REMOTE GEOCHEMICAL EXPERIMENT PACKAGE FOR DISCOVERY CLASS MISSIONS Abstract Only
Pamela E. Clark (Catholic Univ. of America, Washington, DC.), Larry G. Evans (Computer Sciences Corp., Lanham, MD.), and Jacob I. Trombka *In* Lunar and Planetary Inst., The Twenty-Fifth Lunar and Planetary Science Conference. Part 1: A-G 1994 p 267-268 (For primary document see N94-35395 11-91)
Avail: CASI HC A01/MF A04

N94-35473*# National Aeronautics and Space Administration. Lyndon B. Johnson Space Center, Houston, TX.
ADVANCED TECHNOLOGY LUNAR TELESCOPE Abstract Only
Thomas L. Wilson, Wei-Kan Chu, and Peter C. Chen *In* Lunar and Planetary Inst., The Twenty-Fifth Lunar and Planetary Science Conference. Part 3: P-Z 1994 p 1501-1502 (For primary document see N94-35448 11-91)
Avail: CASI HC A01/MF A06

N94-35560*# Jet Propulsion Lab., California Inst. of Tech., Pasadena, CA.
THE REAL-TIME DISPLAY OF INTERFEROMETRY DATA FOR GOLDSTONE RADAR ASTRONOMY DATA ACQUISITION
S. D. Howard *In its* The Telecommunications and Data Acquisition Report 15 May 1994 p 213-227 (For primary document see N94-35542 11-32)
(RTOP 314-40-52-29-26)
Avail: CASI HC A03/MF A03

N94-35561*# Jet Propulsion Lab., California Inst. of Tech., Pasadena, CA.
A NEW PRESENTATION OF COMPLEX VOLTAGE DATA FOR GOLDSTONE RADAR ASTRONOMY
S. D. Howard *In its* The Telecommunications and Data Acquisition Report 15 May 1994 p 228-235 (For primary document see N94-35542 11-32)
(RTOP 314-40-52-29-26)
Avail: CASI HC A02/MF A03

N94-35612*# National Aeronautics and Space Administration. Goddard Space Flight Center, Greenbelt, MD.
FIXED-HEAD STAR TRACKER ATTITUDE UPDATES ON THE HUBBLE SPACE TELESCOPE
Matthew S. Nadelman (Computer Sciences Corp., Laurel, MD.), Jeffrey B. Karl (Computer Sciences Corp., Laurel, MD.), and Lou Hallock *In its* Flight Mechanics/Estimation Theory Symposium, 1994 May 1994 p 79-93 (For primary document see N94-35605 11-13)
(Contract NAS5-31500)
Avail: CASI HC A03/MF A04

N94-35640*# Computer Sciences Corp., Lanham, MD.
APPLICATION OF STAR IDENTIFICATION USING PATTERN MATCHING TO SPACE GROUND SYSTEMS AT GSFC
D. Fink and D. Shoup *In* NASA. Goddard Space Flight Center, Flight Mechanics/Estimation Theory Symposium, 1994 May 1994 p 451-465 (For primary document see N94-35605 11-13)
(Contract NAS5-31500)
Avail: CASI HC A03/MF A04

90 ASTROPHYSICS

Includes cosmology; celestial mechanics; space plasmas; and interstellar and interplanetary gases and dust.

For related information see also *75 Plasma Physics.*

N94-35530 Rutherford Appleton Lab., Chilton (England).
ROSAT/XRT-PSPC OBSERVATIONS AND THE IONIZING CONTINUUM OF SEYFERT 1 GALAXY Mkn 478
P. M. Gondhalekar, B. J. Kellett, K. A. Pounds, L. Matthews, and J. J. Quenby Feb. 1994 25 p Prepared in cooperation with Leicester Univ., England and Imperial Coll. of Science and Technology, London, England
(PB94-167053; RAL-94-018) Avail: Issuing Activity (National Technical Information Service (NTIS))

The ROSAT/XRT-PSPC observations of the Seyfert 1 galaxy Mkn478 are presented. Together with the optical and ultraviolet spectra of this galaxy, obtained within eight months of the x-ray observations, these new data are used to determine the continuum energy distribution (CED) of Mkn478, from 1 micrometer to about 2.0 keV with a small break between 11.3 eV and 0.1 keV. The ultraviolet/soft x-ray CED is similar to the spectrum of a thin accretion disc for both a rotating and a non-rotating black hole, although both models underestimate the flux at energies higher than 0.4 keV. NTIS

N94-35980# Los Alamos National Lab., NM.
ANGULAR MOMENTUM IN THE LOCAL GROUP
A. Dunn (Cambridge Univ., Cambridge, England.) and R. Laflamme 1994 8 p Presented at the Comparative and Global Properties Conference, La Serena, Chile, 25-28 Jan. 1994
(Contract W-7405-eng-36)
(DE94-009322; LA-UR-94-1118; CONF-940179-1) Avail: CASI HC A02/MF A01

We briefly review models for the Local Group and the acquisition of its angular momentum. We describe early attempts to understand the origin of the spin of the galaxies discussing the hypothesis that the Local Group has little angular momentum. Finally we show that using Peebles' least action principle there should be a rather large amount of orbital angular momentum compared to the magnitude of the spin of its galaxies. Therefore the Local Group cannot be thought as tidally isolated. Using Peebles' trajectories we give a possible set of trajectories for Local Group galaxies which would predict their spin. DOE

N94-36128# Moscow State Univ. (Russia). Inst. of Nuclear Physics.
SPATIAL FLUCTUATIONS OF PARTICLE FLUXES WITHIN THE AURORAL ZONE INFERRED FROM THE INTERCOSMOS-BULGARIA-1300 SATELLITE DATA
E. E. Antonova, M. V. Stepanova, and M. V. Teltzov 1993 28 p Submitted for publication
(DE94-615858; INP-MSU-93-3-295; NIIYaF-MGU-93-3-295) Avail: CASI HC A03/MF A01 (US Sales Only)

The influence of electric field turbulence within the magnetospheric plasma sheet on the auroral particle fluctuations is analyzed on the Intercosmos-Bulgaria-1300 satellite data base. It is shown that the spatial fluctuation spectrums of particle fluxes have been a power form where power index is greatly dependent on the particle energy. DOE

N94-36229# California Univ., Berkeley. Lawrence Berkeley Lab, CA.
STELLAR ALCHEMY: THE ORIGIN OF THE CHEMICAL ELEMENTS
E. B. Norman 13 Mar. 1994 28 p Presented at the 207th Spring National Meeting of the American Chemical Society, San Diego, CA, 13-18 Mar. 1994
(Contract DE-AC03-76SF-00098)
(DE94-011903; LBL-35438; CONF-940301-30) Avail: CASI HC A03/MF A01

What makes the stars shine? This question puzzled human beings for thousands of years. Early in this century, chemists and physicists discovered radioactivity, and the nuclear model of the atom was developed. Once nuclear reactions were produced in the laboratory, it did not take long before their role in stellar energy generation was realized. The theory that nuclear fusion is the source of stellar energy was initially developed in the 1930's and was elaborated in detail in the 1950's. Only within the last ten years, however, have astronomical observations provided direct confirmation of these theoretical ideas. In this paper, I describe the sequences of nuclear reactions that are believed to be responsible for the power generation in stars. The ashes of these reactions are the heavy elements that we find on earth and throughout the universe. The evolution and final fates of stars are examined. The key astronomical observations that provide support for these theoretical ideas are presented. DOE

N94-36418# Argonne National Lab., IL.
ON THE ORIGIN OF PORPHYRITIC CHONDRULES
M. Blander, L. Unger, A. Pelton, and G. Ericksson 1994 27 p
(Contract W-31-109-eng-38)
(DE94-010464; ANL/CMT/PP-77577) Avail: CASI HC A03/MF A01

A computer program for the complex equilibria in a cooling nebular gas was used to explore a possible origin of porphyritic chondrules, the major class of chondrules in chondritic meteorites. It uses a method of accurately calculating the thermodynamic properties of molten multicomponent aluminosilicates, which deduces the silicate condensates vs temperature and pressure of a nebular gas. This program is coupled with a chemical equilibrium algorithm for systems with at least 1000 chemical species; it has a data base of over 5000 solid, liquid, and gaseous species. Results are metastable subcooled liquid aluminoscilicates with compositions resembling types 1A and 2 porphyritic chondrules at two different temperatures at any pressure between 10(exp -2) and 1 (or possibly 10(exp -3) to 5) atm. The different types of chondrules (types 1, 2, 3) could have been produced from the same gas and do not need a different gas for each apparent oxidation state; thus, the difficulty of current models for making porphyritic chondrules by reheating different solids to just below their liquidus temperatures in different locations is not necessary. Initiation of a stage of crystallization just below liquidus is part of the natural crystallization (recalescence) process from metastable subcooled liquidus and does not require an improbable heating mechanism. DOE

N94-35406*# National Aeronautics and Space Administration. Ames Research Center, Moffett Field, CA.
SHOEMAKER-LEVY 9 AND THE TIDAL DISRUPTION OF COMETS Abstract Only
W. Benz (Arizona Univ., Tucson, AZ.) and E. Asphaug *In* Lunar and Planetary Inst., The Twenty-Fifth Lunar and Planetary Science Conference. Part 1: A-G 1994 p 101-102 (For primary document see N94-35395 11-91)
Avail: CASI HC A01/MF A04

N94-35412*# National Aeronautics and Space Administration. Lyndon B. Johnson Space Center, Houston, TX.
EUREKA! AEROGEL CAPTURE OF METEOROIDS IN SPACE Abstract Only
D. E. Brownlee (Washington Univ., Seattle, WA.), F. Horz, L. Hrubsch, J. A. M. McDonnell, P. Tsou, and J. Williams *In* Lunar and Planetary Inst., The Twenty-Fifth Lunar and Planetary Science Conference. Part 1: A-G 1994 p 183-184 (For primary document see N94-35395 11-91)
Avail: CASI HC A01/MF A04

N94-35416*# National Aeronautics and Space Administration. Ames Research Center, Moffett Field, CA.
FIRST GALILEO IMAGE OF ASTEROID 243 IDA Abstract Only
C. R. Chapman (Planetary Science Inst., Tucson, AZ.), M. J. S. Belton (Kitt Peak National Observatory, Tucson, AZ.), J. Veverka (Cornell Univ., Ithaca, NY.), G. Neukum (Deutsche Forschungsanstalt fuer Luft- und Raumfahrt, Berlin, Germany.), J. Head (Brown Univ., Providence, RI.), Ronald Greeley (Arizona State Univ., Tempe, AZ.), K. Klaasen (Jet Propulsion Lab., California Inst. of Tech., Pasadena, CA.), and D. Morrison *In* Lunar and Planetary Inst., The Twenty-Fifth Lunar and Planetary Science Conference. Part 1: A-G 1994 p 237-238 (For primary document see N94-35395 11-91)
Avail: CASI HC A01/MF A04

N94-35421*# National Aeronautics and Space Administration. Lyndon B. Johnson Space Center, Houston, TX.
ON THE POSSIBLE ROLE OF ELEMENTAL CARBON IN THE FORMATION OF REDUCED CHONDRULES Abstract Only
Harold C. Connolly, Jr. (Rutgers Univ., New Brunswick, NJ.), Roger H. Hewins (Rutgers Univ., New Brunswick, NJ.), Richard D. Ash (Manchester Univ., England.), Gary E. Lofgren, and Brigitte Zanda *In* Lunar and Planetary Inst., The Twenty-Fifth Lunar and Planetary Science Conference. Part 1: A-G 1994 p 279-280 (For primary document see N94-35395 11-91)
Avail: CASI HC A01/MF A04

N94-35422*# National Aeronautics and Space Administration. Ames Research Center, Moffett Field, CA.
WHAT INITIATED PLANETESIMAL FORMATION? Abstract Only
J. N. Cuzzi, A. R. Dobrovolskis, and R. C. Hogan *In* Lunar and Planetary Inst., The Twenty-Fifth Lunar and Planetary Science Conference. Part 1: A-G 1994 p 307-308 (For primary document see N94-35395 11-91)
Avail: CASI HC A01/MF A04

N94-35423*# National Aeronautics and Space Administration. Lyndon B. Johnson Space Center, Houston, TX.
THE OCCURRENCE OF BLUE LUMINESCING ENSTATITE IN E3 AND E4 CHONDRITES Abstract Only
John M. DeHart (Casper Coll., WY.) and Gary E. Lofgren *In* Lunar and Planetary Inst., The Twenty-Fifth Lunar and Planetary Science Conference. Part 1: A-G 1994 p 319-320 (For primary document see N94-35395 11-91)
Avail: CASI HC A01/MF A04

N94-35428*# National Aeronautics and Space Administration. Lyndon B. Johnson Space Center, Houston, TX.
SOLAR PROTON PRODUCED NEON IN SHERGOTTITE METEORITES Abstract Only
D. H. Garrison (Lockheed Engineering and Sciences Co., Houston, TX.), M. N. Rao (Lockheed Engineering and Sciences Co., Houston, TX.), and D. D. Bogard *In* Lunar and Planetary Inst., The Twenty-Fifth Lunar and Planetary Science Conference. Part 1: A-G 1994 p 403-404 (For primary document see N94-35395 11-91)
Avail: CASI HC A01/MF A04

N94-35432*# National Aeronautics and Space Administration. Lyndon B. Johnson Space Center, Houston, TX.
APPLICATION OF AN ALKYLAMMONIUM METHOD FOR CHARACTERIZATION OF PHYLLOSILICATES IN CI CHONDRITES Abstract Only
D. C. Golden (Dual and Associates, Houston, TX.), D. W. Ming, M. E. Zolensky, and S. V. Yang *In* Lunar and Planetary Inst., The Twenty-Fifth Lunar and Planetary Science Conference. Part 1: A-G 1994 p 435-436 (For primary document see N94-35395 11-91)
Avail: CASI HC A01/MF A04

N94-35449*# National Aeronautics and Space Administration. Lyndon B. Johnson Space Center, Houston, TX.
FeO AND MgO IN PLAGIOCLASE OF LUNAR ANORTHOSITES: IGNEOUS OR METAMORPHIC? Abstract Only
W. C. Phinney *In* Lunar and Planetary Inst., The Twenty-Fifth Lunar and Planetary Science Conference. Part 3: P-Z 1994 p 1081-1082 (For primary document see N94-35448 11-91)
Avail: CASI HC A01/MF A06

N94-35451*# National Aeronautics and Space Administration. Lyndon B. Johnson Space Center, Houston, TX.
ANTARCTIC WEATHERING OF THE CK CHONDRITES EET90004, 90007, AND 90022: NICKEL AND SULFUR MOBILITY Abstract Only
C. S. Romanek, R. A. Socki, E. K. Gibson, Jr., and J. H. Allton *In* Lunar and Planetary Inst., The Twenty-Fifth Lunar and Planetary Science Conference. Part 3: P-Z 1994 p 1155-1156 (For primary document see N94-35448 11-91)
Avail: CASI HC A01/MF A06

N94-35455*# National Aeronautics and Space Administration. Lyndon B. Johnson Space Center, Houston, TX.
MORE SHOCK RECOVERY EXPERIMENTS ON MESOSIDERITE ANALOGS Abstract Only
L. R. Rowan and D. W. Mittlefehldt *In* Lunar and Planetary Inst., The

Twenty-Fifth Lunar and Planetary Science Conference. Part 3: P-Z 1994 p 1167-1168 (For primary document see N94-35448 11-91)
Avail: CASI HC A01/MF A06

N94-35456*# National Aeronautics and Space Administration. Lyndon B. Johnson Space Center, Houston, TX.
DISTRIBUTION OF SIDEROPHILE AND OTHER TRACE ELEMENTS IN MELT ROCK AT THE CHICXULUB IMPACT STRUCTURE Abstract Only
B. C. Schuraytz (Lunar and Planetary Inst., Houston, TX.), D. J. Lindstrom, R. R. Martinez, V. L. Sharpton, and L. E. Marin *In* Lunar and Planetary Inst., The Twenty-Fifth Lunar and Planetary Science Conference. Part 3: P-Z 1994 p 1221-1222 (For primary document see N94-35448 11-91)
Avail: CASI HC A01/MF A06

N94-35458*# National Aeronautics and Space Administration. Lyndon B. Johnson Space Center, Houston, TX.
CURRENT ACTIVITIES AND RESULTS OF THE LONG DURATION EXPOSURE FACILITY METEOROID AND DEBRIS SPECIAL INVESTIGATION GROUP Abstract Only
Thomas H. See (Lockheed Engineering and Sciences Co., Houston, TX.), Kimberly S. Leago (Lockheed Engineering and Sciences Co., Houston, TX.), Jack L. Warren (Lockheed Engineering and Sciences Co., Houston, TX.), Ronald P. Bernhard (Lockheed Engineering and Sciences Co., Houston, TX.), and Michael E. Zolensky *In* Lunar and Planetary Inst., The Twenty-Fifth Lunar and Planetary Science Conference. Part 3: P-Z 1994 p 1233-1234 (For primary document see N94-35448 11-91)
Avail: CASI HC A01/MF A06

N94-35465*# National Aeronautics and Space Administration. Lyndon B. Johnson Space Center, Houston, TX.
ANATOMY OF A CLUSTER IDP. PART 2: NOBLE GAS ABUNDANCES, TRACE ELEMENT GEOCHEMISTRY, ISOTOPIC ABUNDANCES, AND TRACE ORGANIC CHEMISTRY OF SEVERAL FRAGMENTS FROM L2008#5 Abstract Only
K. L. Thomas (Lockheed Engineering and Sciences Co., Houston, TX.), S. J. Clemett (Stanford Univ., CA.), G. J. Flynn (State Univ. of New York, Plattsburgh, NY.), L. P. Keller (MVA, Inc., Norcross, GA.), David S. McKay, S. Messenger, A. O. Nier, D. J. Schlutter, S. R. Sutton, and R. M. Walker et al *In* Lunar and Planetary Inst., The Twenty-Fifth Lunar and Planetary Science Conference. Part 3: P-Z 1994 p 1391-1392 (For primary document see N94-35448 11-91)
Avail: CASI HC A01/MF A06

N94-35466*# National Aeronautics and Space Administration. Lyndon B. Johnson Space Center, Houston, TX.
THE ANATOMY OF A CLUSTER IDP. PART 1: CARBON ABUNDANCE, BULK CHEMISTRY, AND MINERALOGY OF FRAGMENTS FROM L2008#5 Abstract Only
K. L. Thomas (Lockheed Engineering and Sciences Co., Houston, TX.), L. P. Keller (MVA, Inc., Norcross, GA.), W. Klock (Muenster Univ., Germany.), J. Warren (Lockheed Engineering and Sciences Co., Houston, TX.), G. E. Blanford (Houston Univ., Clear Lake, TX.), and David S. McKay *In* Lunar and Planetary Inst., The Twenty-Fifth Lunar and Planetary Science Conference. Part 3: P-Z 1994 p 1393-1394 (For primary document see N94-35448 11-91)
Avail: CASI HC A01/MF A06

N94-35467*# National Aeronautics and Space Administration. Lyndon B. Johnson Space Center, Houston, TX.
THE PARENT MAGMA OF XENOLITHS IN SHERGOTTITE EETA79001: BULK AND TRACE ELEMENT COMPOSITION INFERRED FROM MAGMATIC INCLUSIONS Abstract Only
Allan H. Treiman (Lunar and Planetary Inst., Houston, TX.), David J. Lindstrom, and Rene R. Martinez *In* Lunar and Planetary Inst., The Twenty-Fifth Lunar and Planetary Science Conference. Part 3: P-Z 1994 p 1417-1418 (For primary document see N94-35448 11-91)
(RTOP 152-14-40-22)
Avail: CASI HC A01/MF A06

N94-35470*# National Aeronautics and Space Administration. Lyndon B. Johnson Space Center, Houston, TX.
A QUICK LOOK METHOD OF DETECTING WATER OF HYDRATION IN SMALL SOLAR SYSTEM BODIES Abstract Only
F. Vilas *In* Lunar and Planetary Inst., The Twenty-Fifth Lunar and Planetary Science Conference. Part 3: P-Z 1994 p 1439-1440 (For primary document see N94-35448 11-91)
Avail: CASI HC A01/MF A06

N94-35471*# National Aeronautics and Space Administration. Goddard Space Flight Center, Greenbelt, MD.
CHONDRULE MAGNETIC PROPERTIES Abstract Only
P. J. Wasilewski and M. V. OBryan *In* Lunar and Planetary Inst., The Twenty-Fifth Lunar and Planetary Science Conference. Part 3: P-Z 1994 p 1467-1468 (For primary document see N94-35448 11-91)
Avail: CASI HC A01/MF A06

N94-35476*# National Aeronautics and Space Administration. Lyndon B. Johnson Space Center, Houston, TX.
MINERALOGY OF AN UNUSUAL CM CLAST IN THE KAIDUN METEORITE Abstract Only
M. E. Zolensky, A. V. Ivanov, S. V. Yang, R. A. Barrett, and L. Browning *In* Lunar and Planetary Inst., The Twenty-Fifth Lunar and Planetary Science Conference. Part 3: P-Z 1994 p 1565-1566 (For primary document see N94-35448 11-91)
Avail: CASI HC A01/MF A06

N94-35477*# National Aeronautics and Space Administration. Lyndon B. Johnson Space Center, Houston, TX.
MINERALOGY OF ARTIFICIALLY HEATED CARBONACEOUS CHONDRITES Abstract Only
M. E. Zolensky, M. E. Lipschutz, and T. Hiroi *In* Lunar and Planetary Inst., The Twenty-Fifth Lunar and Planetary Science Conference. Part 3: P-Z 1994 p 1567-1568 (For primary document see N94-35448 11-91)
Avail: CASI HC A01/MF A06

N94-35607*# Jet Propulsion Lab., California Inst. of Tech., Pasadena, CA.
LOW ENCOUNTER SPEED COMET COMA SAMPLE RETURN MISSIONS Abstract Only
P. Tsou, C. W. Yen, and A. L. Albee *In* NASA. Goddard Space Flight Center, Flight Mechanics/Estimation Theory Symposium, 1994 May 1994 p 15 (For primary document see N94-35605 11-13)
Avail: CASI HC A01/MF A04

N94-36140*# National Aeronautics and Space Administration. Lyndon B. Johnson Space Center, Houston, TX.
SHOCKED MATERIALS FROM THE DUTCH PEAK DIAMICTITE, UTAH Abstract Only
F. Hoerz, T. E. Bunch, and V. R. Oberbeck *In* Lunar and Planetary Inst., The Twenty-Fifth Lunar and Planetary Science Conference. Part 2: H-O 1994 p 565-566 (For primary document see N94-36136 11-91)
Avail: CASI HC A01/MF A06

N94-36141*# National Aeronautics and Space Administration. Lyndon B. Johnson Space Center, Houston, TX.
EXPERIMENTAL IMPACTS INTO TEFLON TARGETS AND LDEF THERMAL BLANKETS Abstract Only
F. Hoerz, M. J. Cintala, M. E. Zolensky, R. P. Bernhard, and T. H. See *In* Lunar and Planetary Inst., The Twenty-Fifth Lunar and Planetary Science Conference. Part 2: H-O 1994 p 567-568 (For primary document see N94-36136 11-91)
Avail: CASI HC A01/MF A06

N94-36142*# National Aeronautics and Space Administration. Lyndon B. Johnson Space Center, Houston, TX.
DUST EVOLUTION FROM COMETS AND ASTEROIDS: THEIR VELOCITIES AT EARTH ORBIT INTERSECTION Abstract Only
A. A. Jackson (Lockheed Engineering and Sciences Co., Houston, TX.) and H. A. Zook *In* Lunar and Planetary Inst., The Twenty-Fifth Lunar

and Planetary Science Conference. Part 2: H-O 1994 p 609-610 (For primary document see N94-36136 11-91)
Avail: CASI HC A01/MF A06

N94-36145*# National Aeronautics and Space Administration. Lyndon B. Johnson Space Center, Houston, TX.
TEXTURAL CONSTRAINTS ON THE FORMATION OF ALTERATION PHASES IN CM CHONDRITES Abstract Only
L. H. Joseph (Rochester Univ., NY.), L. B. Browning (Tennessee Univ., Knoxville, TN.), and M. E. Zolensky *In* Lunar and Planetary Inst., The Twenty-Fifth Lunar and Planetary Science Conference. Part 2: H-O 1994 p 645-646 (For primary document see N94-36136 11-91)
Avail: CASI HC A01/MF A06

N94-36146*# National Aeronautics and Space Administration. Lyndon B. Johnson Space Center, Houston, TX.
PARTIAL MELTING OF THE ST. SEVERIN (LL) AND LOST CITY (H) ORDINARY CHONDRITES: ONE STEP BACKWARDS AND TWO STEPS FORWARD Abstract Only
A. J. G. Jurewicz (Lockheed Engineering and Sciences Co., Houston, TX.), J. H. Jones, and D. W. Mittlefehldt *In* Lunar and Planetary Inst., The Twenty-Fifth Lunar and Planetary Science Conference. Part 2: H-O 1994 p 651-652 (For primary document see N94-36136 11-91)
Avail: CASI HC A01/MF A06

N94-36147*# National Aeronautics and Space Administration. Lyndon B. Johnson Space Center, Houston, TX.
PRELIMINARY RESULTS OF SULFIDE MELT/SILICATE WETTING EXPERIMENTS IN A PARTIALLY MELTED ORDINARY CHONDRITE Abstract Only
Stephen R. Jurewicz and John H. Jones *In* Lunar and Planetary Inst., The Twenty-Fifth Lunar and Planetary Science Conference. Part 2: H-O 1994 p 653-654 (For primary document see N94-36136 11-91)
Avail: CASI HC A01/MF A06

N94-36149*# National Aeronautics and Space Administration. Lyndon B. Johnson Space Center, Houston, TX.
ELECTRON ENERGY-LOSS SPECTROSCOPY OF CARBON IN INTERPLANETARY DUST PARTICLES Abstract Only
Lindsay P. Keller (MVA, Inc., Norcross, GA.), John P. Bradley (MVA, Inc., Norcross, GA.), Kathie L. Thomas (Lockheed Engineering and Sciences Co., Houston, TX.), and David S. McKay *In* Lunar and Planetary Inst., The Twenty-Fifth Lunar and Planetary Science Conference. Part 2: H-O 1994 p 687-688 Sponsored in part by MVA, Inc. (For primary document see N94-36136 11-91)
(RTOP 152-17-40-23; RTOP 199-52-11-02)
Avail: CASI HC A01/MF A06

N94-36157*# National Aeronautics and Space Administration. Lyndon B. Johnson Space Center, Houston, TX.
PIGEONHOLING PLANETARY METEORITES: THE LESSONS OF MISCLASSIFICATION OF EET87521 AND ALH84001 Abstract Only
M. M. Lindstrom, A. H. Treiman, and D. W. Mittlefehldt *In* Lunar and Planetary Inst., The Twenty-Fifth Lunar and Planetary Science Conference. Part 2: H-O 1994 p 797-798 (For primary document see N94-36136 11-91)
Avail: CASI HC A01/MF A06

N94-36158*# National Aeronautics and Space Administration. Lyndon B. Johnson Space Center, Houston, TX.
ON THE ORIGIN OF ENSTATITE CHONDRITE CHONDRULES BASED ON THEIR PETROGRAPHY AND COMPARISON WITH EXPERIMENTALLY PRODUCED CHONDRULES Abstract Only
Gary E. Lofgren, John M. DeHart, and P. J. Burkett *In* Lunar and Planetary Inst., The Twenty-Fifth Lunar and Planetary Science Conference. Part 2: H-O 1994 p 801-802 (For primary document see N94-36136 11-91)
Avail: CASI HC A01/MF A06

N94-36159*# National Aeronautics and Space Administration. Lyndon B. Johnson Space Center, Houston, TX.
MORPHOLOGY OF METEOROID AND SPACE DEBRIS CRATERS ON LDEF METAL TARGETS Abstract Only
S. G. Love (Washington Univ., Seattle, WA.), D. E. Brownlee (Washington Univ., Seattle, WA.), N. L. King (Washington Univ., Seattle, WA.), and F. Hoerz *In* Lunar and Planetary Inst., The Twenty-Fifth Lunar and Planetary Science Conference. Part 2: H-O 1994 p 809-810 (For primary document see N94-36136 11-91)
Avail: CASI HC A01/MF A06

N94-36160*# National Aeronautics and Space Administration. Lyndon B. Johnson Space Center, Houston, TX.
PRODUCTION OF FERROAN ANDESITES BY THE EXPERIMENTAL PARTIAL MELTING OF AN LL CHONDRITE Abstract Only
J. C. McGuire (State Univ. of New York, Stony Brook, NY.), A. J. G. Jurewicz (Lockheed Engineering and Sciences Co., Houston, TX.), and J. H. Jones *In* Lunar and Planetary Inst., The Twenty-Fifth Lunar and Planetary Science Conference. Part 2: H-O 1994 p 879-880 (For primary document see N94-36136 11-91)
Avail: CASI HC A01/MF A06

N94-36161*# National Aeronautics and Space Administration. Lyndon B. Johnson Space Center, Houston, TX.
SYNTHETIC AND NATURAL NAKHLA PYROXENES: PARENT MELT COMPOSITION AND REE PARTITION COEFFICIENTS Abstract Only
G. McKay, L. Le, and J. Wagstaff *In* Lunar and Planetary Inst., The Twenty-Fifth Lunar and Planetary Science Conference. Part 2: H-O 1994 p 883-884 (For primary document see N94-36136 11-91)
Avail: CASI HC A01/MF A06

N94-36162*# National Aeronautics and Space Administration. Lyndon B. Johnson Space Center, Houston, TX.
Cr, Mn, AND Ca DISTRIBUTIONS FOR OLIVINE IN ANGRITIC SYSTEMS: CONSTRAINTS ON THE ORIGINS OF Cr-RICH AND Ca-POOR CORE OLIVINE IN ANGRITE LEW87051 Abstract Only
T. Mikouchi (Tokyo Univ., Japan.), G. McKay, and L. Le *In* Lunar and Planetary Inst., The Twenty-Fifth Lunar and Planetary Science Conference. Part 2: H-O 1994 p 907-908 (For primary document see N94-36136 11-91)
Avail: CASI HC A01/MF A06

N94-36163*# National Aeronautics and Space Administration. Lyndon B. Johnson Space Center, Houston, TX.
PARTITION COEFFICIENTS FOR Al, Ca, Ti, Cr, AND Ni IN OLIVINE OBTAINED BY MELTING EXPERIMENT ON AN LL6 CHONDRITE Abstract Only
M. Miyamoto (Tokyo Univ., Japan.), T. Mikouchi (Tokyo Univ., Japan.), and G. A. McKay *In* Lunar and Planetary Inst., The Twenty-Fifth Lunar and Planetary Science Conference. Part 2: H-O 1994 p 923-924 (For primary document see N94-36136 11-91)
Avail: CASI HC A01/MF A06

N94-36166*# National Aeronautics and Space Administration. Lyndon B. Johnson Space Center, Houston, TX.
MOESSBAUER MINERALOGY OF CALCINED MURCHISON METEORITE Abstract Only
Richard V. Morris, M. E. Zolensky, T. Hiroi, and M. E. Lipschutz *In* Lunar and Planetary Inst., The Twenty-Fifth Lunar and Planetary Science Conference. Part 2: H-O 1994 p 941-942 (For primary document see N94-36136 11-91)
Avail: CASI HC A01/MF A06

N94-36167*# National Aeronautics and Space Administration. Goddard Space Flight Center, Greenbelt, MD.
SHAPE, SIZE, AND DISTRIBUTION OF MAGNETIC PARTICLES IN BJURBOLE CHONDRULES Abstract Only
David F. Nava *In* Lunar and Planetary Inst., The Twenty-Fifth Lunar and Planetary Science Conference. Part 2: H-O 1994 p 977 (For primary document see N94-36136 11-91)
Avail: CASI HC A01/MF A06

N94-36169*# National Aeronautics and Space Administration. Lyndon B. Johnson Space Center, Houston, TX.

ALKALI ELEMENT CONSTRAINTS ON EARTH-MOON RELATIONS Abstract Only

M. D. Norman (Australian National Univ., Canberra, Australia.), M. J. Drake (Arizona Univ., Tucson, AZ.), and J. H. Jones *In* Lunar and Planetary Inst., The Twenty-Fifth Lunar and Planetary Science Conference. Part 2: H-O 1994 p 1009-1010 (For primary document see N94-36136 11-91)
Avail: CASI HC A01/MF A06

N94-36172*# National Aeronautics and Space Administration. Lyndon B. Johnson Space Center, Houston, TX.

PRE-BOMBARDMENT CRYSTALLIZATION AGES OF BASALTIC CLASTS FROM ANTARCTIC HOWARDITES EET87503 AND EET87513 Abstract Only

L. E. Nyquist, C.-Y. Shih, H. Wiesmann, and B. M. Bansal *In* Lunar and Planetary Inst., The Twenty-Fifth Lunar and Planetary Science Conference. Part 2: H-O 1994 p 1015-1016 (For primary document see N94-36136 11-91)
Avail: CASI HC A01/MF A06

91 LUNAR AND PLANETARY EXPLORATION

Includes planetology; and manned and unmanned flights.
For spacecraft design or space stations see *18 Spacecraft Design, Testing and Performance.*

N94-35263*# Martin Marietta Corp., Denver, CO. Flight Systems.

MARS AQUEOUS CHEMISTRY EXPERIMENT Annual Technical Report, Jun. 1993 - Jun. 1994

Benton C. Clark and Larry W. Mason Jun. 1994 24 p
(Contract NASw-4698)
(NASA-CR-196024; NAS 1.26:196024; MCR-93-1339-Issue-2) Avail: CASI HC A03/MF A01

Mars Aqueous Chemistry Experiment (MACE) is designed to conduct a variety of measurements on regolith samples, encompassing mineral phase analyses, chemical interactions with H2O, and physical properties determinations. From these data, much can be learned or inferred regarding the past weathering environment, the contemporaneous soil micro-environments, and the general chemical and physical state of the Martian regolith. By analyzing both soil and duricrust samples, the nature of the latter may become more apparent. Sites may be characterized for comparative purposes and criteria could be set for selection of high priority materials on future sample return missions. The second year of the MACE project has shown significant progress in two major areas. MACE Instrument concept definition is a baseline design that has been generated for the complete MACE instrument, including definition of analysis modes, mass estimates and thermal model. The design includes multiple reagent reservoirs, 10 discrete analysis cells, sample manipulation capability, and thermal control. The MACE Measurement subsystems development progress is reported regarding measurement capabilities for aqueous ion sensing, evolved gas sensing, solution conductivity measurement, reagent addition (titration) capabilities, and optical sensing of suspended particles. Author

N94-35265*# Smithsonian Astrophysical Observatory, Cambridge, MA.

DEVELOPMENT OF POINTS AS A PLANETOLOGY INSTRUMENT Annual Report No. 5, 1 Oct. 1993 - 30 Sep. 1994

Robert D. Reasenberg May 1994 27 p
(Contract NAGw-2497; N00014-93-K-2036)
(NASA-CR-196026; NAS 1.26:196026) Avail: CASI HC A03/MF A01

During the reporting period, we carried out investigations required to enhance our design of POINTS as a tool for the search for and characterization of extra-solar planetary systems. The results of that work were included in a paper on POINTS as well as one on Newcomb, which will soon appear in the proceedings of SPIE Conference 2200. (Newcomb is a spinoff of POINTS. It is a small astrometric interferometer now being developed jointly by SAO and the U.S. Navy. It could help establish some of the technology needed for POINTS.) These papers are appended. Author

N94-35336# Centre National d'Etudes Spatiales, Toulouse (France).

AN AUTOMATIC PLANETARY VEHICLE FOR EXPLORING MARS

Michel Blanc (Observatoires du Pic-du-Midi et Toulouse, Toulouse, France.), Sophie Coutin-Faye (Laboratoire de Geophysique Externe du CNRS, Saint Maur-des-Fosses, France.), Francois Costard (Laboratoire de Geophysique Externe du CNRS, Saint Maur-des-Fosses, France.), Jose Achache (Institut de Physique du Globe, Paris, France.), Jean-Pierre Bibring (Institut d'Astrophysique, Paris, France.), Yves Langevin (Institut d'Astrophysique, Paris, France.), Philippe Lognonne (Institut de Physique du Globe, Paris, France.), and Philippe Masson (Paris Univ., Orsay, France.) Jul. 1992 81 p Original contains color illustrations
Avail: CASI HC A05/MF A01

This report defines the role that will be assigned to planetary rovers in the exploration of the Mars surface. It also describes a mission scenario for the French Automatic Planetary Rover project, on the basis of which technical design studies of the rover, its mission, its various subsystems, and the payload as well as the necessary scientific instrument facilities will be performed. Derived from text

N94-35359*# Lunar and Planetary Inst., Houston, TX.

WORKSHOP ON THE MARTIAN NORTHERN PLAINS: SEDIMENTOLOGICAL, PERIGLACIAL, AND PALEOCLIMATIC EVOLUTION

J. S. Kargel, ed., T. J. Parker, ed., and J. M. Moore, ed. 1993 15 p Workshop held in Fairbanks, AK, 12-13 Aug. 1993
(Contract NASw-4574)
(NASA-CR-196134; NAS 1.26:196134; LPI-TR-93-04-Pt-2) Avail: CASI HC A03/MF A01

The penultimate meeting in the Mars Surface and Atmosphere Through Time (MSATT) series of workshops was held on the campus of the University of Alaska in Fairbanks, Alaska, 12-13 Aug. 1993. This meeting, entitled 'The Martian Northern Plains: Sedimentological, Periglacial, and Paleoclimatic Evolution,' hosted by the Geophysical Institute at the University of Alaska, was designed to help foster an exchange of ideas among researchers of the Mars science community and the terrestrial glacial and periglacial science community. The technical sessions of the workshop were complemented by field trips to the Alaska Range and to the Fairbanks area and a low-altitude chartered overflight to the Arctic Costal Plain, so that, including these trips, the meeting lasted from 9-14 Aug. 1993. The meeting, field trips, and overflight were organized and partially funded by the Lunar and Planetary Institute and the MSATT Study Group. The major share of logistical support was provided by the Publications and Program Services Department of the Lunar and Planetary Institute. The workshop site was selected to allow easy access to field exposures of active glaciers and glacial and periglacial landforms. In all, 25 scientists attended the workshop, 24 scientists (plus 4 guests and the meeting coordinator) participated in the field trips, and 18 took part in the overflight. This meeting reaffirmed the value of expertly led geologic field trips conducted in association with topical workshops. Author (revised)

N94-35378*# Iowa Univ., Iowa City, IA. Dept. of Physics and Astronomy.

THE FINE STRUCTURE OF LANGMUIR WAVES OBSERVED UPSTREAM OF THE BOW SHOCK AT VENUS

G. B. Hospodarsky, D. A. Gurnett, W. S. Kurth, M. G. Kivelson, R. J. Strangeway, and S. J. Bolton Mar. 1994 37 p
(Contracts JPL-958779; JPL-958694)
(NASA-CR-196123; NAS 1.26:196123; U-of-Iowa-93-21) Avail: CASI HC A03/MF A01

Highly structured Langmuir waves, also known as electron plasma oscillations, have been observed in the foreshock of Venus using the plasma wave experiment on the Galileo spacecraft during the gravity assist flyby on February 10, 1990. The Galileo wideband sampling system provides digital electric field waveform measurements at sampling rates up to 201,600 samples per second, much higher than any previous instrument of this type. The main Langmuir wave emission band occurs near the local electron plasma frequency, which was approximately 43 kHz. The Langmuir waves are observed to shift above and below the plasma frequency, sometimes by as much as 20 kHz. The shifts in frequency are closely correlated with the downstream distance from the tangent field line, implying that the shifts are controlled by the electron beam velocity. Considerable fine structure is also evident, with time scales as short as 0.15 milliseconds, corresponding to spatial scales of a few tens of Debye lengths. The frequency spectrum often consists of beat-type waveforms, with beat frequencies ranging from 0.2 to 7 kHz, and in a few cases, isolated wavepackets. The peak electric field strengths are approximately 1 mV/m. These field strengths are too small for strongly nonlinear processes to be important. The beat-type waveforms are suggestive of a parametric decay process. Author

N94-35395*# Lunar and Planetary Inst., Houston, TX.
THE TWENTY-FIFTH LUNAR AND PLANETARY SCIENCE CONFERENCE. PART 1: A-G Abstracts Only
1994 572 p Conference held in Houston, TX, 14-18 Mar. 1994
(Contract NASw-4574)
(NASA-CR-195743; NAS 1.26:195743) Avail: CASI HC A24/MF A04

Papers from the conference are presented, and the topics covered include the following: planetary geology, meteorites, planetary composition, meteoritic composition, planetary craters, lunar craters, meteorite craters, petrology, petrography, volcanology, planetary crusts, geochronology, geomorphism, mineralogy, lithology, planetary atmospheres, impact melts, volcanoes, planetary evolution, tectonics, planetary mapping, asteroids, comets, lunar soil, lunar rocks, lunar geology, metamorphism, chemical composition, meteorite craters, and planetary mantles. For individual titles, see N94-35396 through N94-35433.

N94-35396*# California Inst. of Tech., Pasadena, CA. Lab. of Experimental Geophysics.
RADIATIVE SIGNALS FROM IMPACT OF SHOEMAKER-LEVY ON JUPITER Abstract Only
Thomas J. Ahrens, Glenn S. Orton, Toshiko Takata, and John D. OKeefe *In* Lunar and Planetary Inst., The Twenty-Fifth Lunar and Planetary Science Conference. Part 1: A-G 1994 p 5-6 (For primary document see N94-35395 11-91)
Avail: CASI HC A01/MF A04

The temperature and internal energy fields calculated by Takata et al. in the plume are used to calculate the greybody thermal radiation emitted versus wavelength to predict what might be observed by several spectral sensors operating from different platforms when fragments of Comet Shoemaker-Levy 9 (SL-9) impact Jupiter in July 1994. A SPH code was used by Takata et al. to calculate the full three dimensional flow and thermodynamic fields in the comet fragment and the atmosphere of Jupiter. We determined the fragment penetration depth, energy partitioning between the atmosphere and the impactor, and energy density deposited per unit length over the trajectory. Once the impactor had disintegrated and stopped, and the strong atmospheric shock decayed, the flow is driven by buoyancy effects. We then used our SPH code to calculate the flow and thermodynamic fields: pressure, article velocity, temperature, and internal energy distributions in the plume. The calculations for 2 and 10 km cometary fragments yield maximum deposition depths of approximately 175 and 525 km, respectively (1 bar = 0 km depth). We also calculated that 0.7 and 0.6 of the initial kinetic energy of the 10 and 2 km bolides, respectively, are deposited as internal energy in Jupiter's atmosphere. Derived from text

N94-35397*# National Aeronautics and Space Administration. Lyndon B. Johnson Space Center, Houston, TX.
NEW PROSPECTS FOR ANALYZING LUNAR PYROCLASTIC GLASS Abstract Only
C. C. Allen (Lockheed Engineering and Sciences Co., Houston, TX.), L. P. Keller (MVA, Inc., Norcross, GA.), J. P. Bradley (MVA, Inc., Norcross, GA.), D. E. Brownlee (Washington Univ., Seattle, WA.), and D. S. McKay *In* Lunar and Planetary Inst., The Twenty-Fifth Lunar and Planetary Science Conference. Part 1: A-G 1994 p 21-22 (For primary document see N94-35395 11-91)
Avail: CASI HC A01/MF A04

Pyroclastic glass particles of diverse compositions are sparsely distributed in the lunar soil. Numerous suspected pyroclastic deposits have been pinpointed on the nearside. However, a dearth of pure samples large enough for spectral study, coupled with the kilometer spatial resolution of earth-based telescope spectrometry, makes it difficult to remotely analyze these deposits or tie most glasses to specific sources. Two developments should soon improve this situation. First, the technique of microscope photometry combined with microprobe analysis allows the correlation of the reflectance spectra and chemical compositions of individual glass particles. Second, the Clementine spacecraft will provide multispectral images of pyroclastic deposits at much higher spatial resolution than is currently achievable. These developments, combined with traditional laboratory and telescope studies, should allow compositions of many pyroclastic deposits and sources of many soil particles to be determined. Derived from text

N94-35398*# National Aeronautics and Space Administration. Lyndon B. Johnson Space Center, Houston, TX.
REDUCTION OF LUNAR MARE SOIL AND PYROCLASTIC GLASS Abstract Only
C. C. Allen (Lockheed Engineering and Sciences Co., Houston, TX.), R. V. Morris, and D. S. McKay *In* Lunar and Planetary Inst., The Twenty-Fifth Lunar and Planetary Science Conference. Part 1: A-G 1994 p 23-24 (For primary document see N94-35395 11-91)
Avail: CASI HC A01/MF A04

Mare soil and orange and black pyroclastic glass were reduced in hydrogen gas at temperatures of 900 to 1100 C. The experiments support studies of regolith maturation, lunar volcanism, and the production of oxygen on the moon. The most reactive component in the high-Ti soil was FeO in ilmenite, which was completely reduced to iron metal at all temperatures. Vitreous orange glass crystallized and was partially reduced to iron metal, pyroxene, and minor olivine. Initially devitrified black glass was similarly reduced and converted to iron metal, pyroxene, and minor olivine. The degree of reaction in both glasses increased with temperature. Derived from text

N94-35399*# National Aeronautics and Space Administration. Lyndon B. Johnson Space Center, Houston, TX.
CALORIMETRIC THERMOMETRY OF METEORITIC TROILITE: PRELIMINARY THERMOMETER RELATIONSHIPS Abstract Only
Judith H. Allton (Lockheed Engineering and Sciences Co., Houston, TX.), Susan J. Wentworth (Lockheed Engineering and Sciences Co., Houston, TX.), and James L. Gooding *In* Lunar and Planetary Inst., The Twenty-Fifth Lunar and Planetary Science Conference. Part 1: A-G 1994 p 25-26 (For primary document see N94-35395 11-91)
Avail: CASI HC A01/MF A04

Thermodynamic properties of the alpha/beta phase transformation in terrestrial troilite (FeS), as measured by differential scanning calorimetry (DSC), vary systematically with prior thermal history of the troilite, as imposed under laboratory conditions. Both the transition temperature and enthalpy change for the alpha/beta transformation decrease with increasing maximum temperature of prior heat treatment. DSC measurements on troilite from various meteorites indicate clear differences in the alpha/beta thermodynamic properties that are consistent with differences in the natural thermal histories of the meteorites. Author (revised)

N94-35400*# National Aeronautics and Space Administration. Ames Research Center, Moffett Field, CA.
THE SURFACE AND INTERIOR OF PHOBOS Abstract Only
E. Asphaug and W. Benz *In* Lunar and Planetary Inst., The Twenty-Fifth Lunar and Planetary Science Conference. Part 1: A-G 1994 p 43-44 (For primary document see N94-35395 11-91)
Avail: CASI HC A01/MF A04

The impact crater Stickney dominates one hemisphere of the Martian moon Phobos; its diameter (11 km) is about half the size of the body (19 x 22 x 27 km). Besides demarking a threshold between cratering and catastrophic disruption, this impact reveals a great deal about the target's interior. Because Phobos has an unusually low density yet exhibits no direct evidence for volatiles such as water ice, it has been supposed that it sequesters volatiles in the deep interior, or that it is made of some exotic substance, or that it is a loosely-aggregated rubble pile. The network of fracture grooves created by the Stickney impact constrain which, if any, of these models accord with observation. Derived from text

N94-35401*# National Aeronautics and Space Administration. Lyndon B. Johnson Space Center, Houston, TX.
SINGLE AGGLUTINATES: A COMPARATIVE STUDY OF COMPOSITIONS OF AGGLUTINITIC GLASS, WHOLE-GRAIN, BULK SOIL, AND FMR Abstract Only
A. Basu (Indiana Univ., Bloomington, IN.), R. Robinson (Indiana Univ., Bloomington, IN.), D. S. McKay, D. P. Blanchard, R. V. Morris, and Susan J. Wentworth *In* Lunar and Planetary Inst., The Twenty-Fifth Lunar and

Planetary Science Conference. Part 1: A-G 1994 p 71-72 (For primary document see N94-35395 11-91)
Avail: CASI HC A01/MF A04

Previous workers on single agglutinates have variously interpreted the composition of agglutinitic glass to represent impact melts of (1) bulk soil, (2) mixed components in finer sizes, and (3) microtargets. Separately, Papike has argued in favor of fusion of the finest fraction of bulk soils. Thirty-four single agglutinates were hand-picked from the mature Apollo 16 soil 61181 (I(sub s)/FeO = 82) and the FMR and chemical composition (INAA for Fe, Sc, Sm, Co, Ni, and Cr) of each agglutinate particle were measured. Thirteen of these single agglutinates were selected for electron beam microanalysis and imaging. Less than 1 micron spots were analyzed (for Na, Mg, Al, Si, P, S, K, Ca, Ti, Cr, Mn, Fe, Ni, and Ba) on pure glassy areas (approximately ten in each particle) selected on the basis of optical and BSE images (avoiding all clasts and inclusions) with an electron microprobe to obtain average glass compositions of each single agglutinate. Derived from text

N94-35402*# National Aeronautics and Space Administration. Ames Research Center, Moffett Field, CA.
HIGH SPATIAL RESOLUTION TELESCOPIC MULTISPECTRAL IMAGING AND SPECTROSCOPY OF THE MOON. 1: THE SERENITATIS/TRANQUILLITATIS BORDER REGION Abstract Only
James F. Bell, III and B. R. Hawke *In* Lunar and Planetary Inst., The Twenty-Fifth Lunar and Planetary Science Conference. Part 1: A-G 1994 p 81-82 (For primary document see N94-35395 11-91)
Avail: CASI HC A01/MF A04

The region of the moon near the border between Mare Serenitatis and Mare Tranquillitatis is one of the most geologically and compositionally complex areas of the nearside. The geologic history of this region has been shaped by impacts of widely-varying spatial scale and temporal occurrence, by volcanism of variable style and composition with time, and by limited tectonism. We have been studying this region as part of a larger multi remote sensing technique effort to understand the composition, morphology, geology, and stratigraphy of the moon at spatial scales of 2 km or less. The effort has been aided by the proximity of this area to the Apollo 11, 15, and 17 landing sites and by the occurrence of one of the primary lunar spectroscopic 'standard areas' within our scene (MS2). Here, some of the findings from the multispectral imaging and spectroscopy part of this effort are reported. Derived from text

N94-35403*# National Aeronautics and Space Administration. Ames Research Center, Moffett Field, CA.
HIGH RESOLUTION VISIBLE TO SHORT-WAVE NEAR-INFRARED CCD SPECTRA OF MARS DURING 1990 Abstract Only
James F. Bell, III, Karl Bornhoeft, and Paul G. Lucey *In* Lunar and Planetary Inst., The Twenty-Fifth Lunar and Planetary Science Conference. Part 1: A-G 1994 p 83-84 (For primary document see N94-35395 11-91)
Avail: CASI HC A01/MF A04

The 0.4 to 1.0 micron spectrum of Mars is dominated by a steep red, relatively featureless spectral slope. Earlier lower spectral observations interpreted the red color and the lack of absorption features in the spectra as evidence of poorly crystalline ferric oxide minerals. More recent higher spectral resolution observations and reinterpretations of older data sets have revealed measureable spectral structure, however. For example, absorption features near 0.65 and 0.86 micron were detected and spatially mapped in data obtained during the 1988 opposition. These absorptions were interpreted as evidence for crystalline hematite on Mars, occuring as an accessory phase in abundances of 3 to 6 percent in the soil. We are attempting to verify the existence of these subtle crystalline Fe(3+) absorption features and to map their spatial distribution in regions of the planet not imaged in 1988. During the 1990 opposition, we obtained imaging spectroscopic data of Mars from the University of Hawaii 2.24 m telescope at Mauna Kea Observatory. The data were obtained with the Wide Field Grism Spectrograph (WFGS), which uses an 800 x 800 CCD and a transmission grating ruled on a prism. We used a grating blazed at 4800 A in first order to obtain data from 0.50 to 0.94 micron at a spectral resolution of R = 200 to 350. The moon/Mars slit design used had projected dimensions of 0.29 x 153 inches, allowing for high spectral resolution and adequate cross-slit spatial sampling of the Martian disk. Derived from text

N94-35404*# National Aeronautics and Space Administration. Ames Research Center, Moffett Field, CA.
ABSOLUTE CALIBRATION AND ATMOSPHERIC VERSUS MINERALOGIC ORIGIN OF ABSORPTION FEATURES IN 2.0 TO 2.5 MICRON MARS SPECTRA OBTAINED DURING 1993 Abstract Only
James F. Bell, III, James B. Pollack, Thomas R. Geballe, Dale P. Cruikshank, and Richard Freedman *In* Lunar and Planetary Inst., The Twenty-Fifth Lunar and Planetary Science Conference. Part 1: A-G 1994 p 85-86 (For primary document see N94-35395 11-91)
Avail: CASI HC A01/MF A04

We obtained new high resolution reflectance spectra of Mars during the 1993 opposition from Mauna Kea Observatory using the UKIRT CGS4 spectrometer. Fifty spectra of 1600-2000 km surface regions and a number of standard star spectra were obtained in the 2.04 to 2.44 micron wavelength region on 4 February 1993 UT. Near-simultaneous observations of bright standard stars were used to perform terrestrial atmospheric corrections and an absolute flux calibration. Using the known magnitude of the stars and assuming blackbody continuum behavior, the flux from Mars could be derived. A radiative transfer model and the HITRAN spectral line data base were used to compute atmospheric transmission spectra for Mars and the Earth in order to simulate the contributions of these atmospheres to our observed data. Also, we examined the ATMOS solar spectrum in the near-IR to try to identify absorption features in the spectrum of the Sun that could be misinterpreted as Mars features. Eleven absorption features were detected in our Mars spectra. Our data provide no conclusive identification of the mineralogy responsible for the absorption features we detected. However, examination of terrestrial spectral libraries and previous high spectral resolution mineral studies indicates that the most likely origin of these features is either CO3(sup 2-), HCO3(-), or HSO4(-) anions in framework silicates or possibly (Fe, Mg)-OH bonds in sheet silicates. Derived from text

N94-35405*# National Aeronautics and Space Administration. Ames Research Center, Moffett Field, CA.
WAVELENGTH CALIBRATION TECHNIQUES AND SUBTLE SURFACE AND ATMOSPHERIC ABSORPTION FEATURES IN THE MARINER 6, 7 IRS REFLECTANCE DATA Abstract Only
James F. Bell, III, T. L. Roush, T. Z. Martin, James B. Pollack, and R. Freedman *In* Lunar and Planetary Inst., The Twenty-Fifth Lunar and Planetary Science Conference. Part 1: A-G 1994 p 87-88 (For primary document see N94-35395 11-91)
Avail: CASI HC A01/MF A04

1994 marks the 25th anniversary of the Mariner 6 and 7 flyby missions to Mars. Despite its age, the Mariner 6,7 Infrared Spectrometer (IRS) data are a unique set of measurements that can provide important information about the Martian surface, atmospheric, and atmospheric aerosol composition. For certain mid-IR wavelengths, the IRS spectra are the only such spacecraft data obtained for Mars. At other wavelengths, IRS measured surface regions different from those measured by Mariner 9 or Phobos 2 and under different dust opacity conditions. We are interested in examining the IRS reflectance data in the 1.8 to 3.0 micron region because there are numerous diagnostic absorption features at these wavelengths that could be indicative of hydrated silicate minerals or of carbonate- or sulfate-bearing minerals. Groundbased telescopic data and recent Phobos ISM measurements have provided controversial and somewhat contradictory evidence for the existence of mineralogic absorption features at these wavelengths. Our goal is to determine whether any such features can be seen in the IRS data and to use their presence or absence to re-assess the quality and interpretations of previous telescopic and spacecraft measurements. Derived from text

N94-35406*# National Aeronautics and Space Administration. Ames Research Center, Moffett Field, CA.
SHOEMAKER-LEVY 9 AND THE TIDAL DISRUPTION OF COMETS Abstract Only **c90**
W. Benz (Arizona Univ., Tucson, AZ.) and E. Asphaug *In* Lunar and Planetary Inst., The Twenty-Fifth Lunar and Planetary Science Conference. Part 1: A-G 1994 p 101-102 (For primary document see N94-35395 11-91)
Avail: CASI HC A01/MF A04

The break-up of Periodic Comet Shoemaker-Levy 9 into multiple pieces following its grazing encounter with Jupiter in July 1992 can be used to study tidally-induced fracture in comets. This spectacular event allows us not only to set limits on the size, strength and density of Shoemaker-Levy 9 itself, but provides invaluable guidance to numerical modeling of such encounters. In an extensive treatment of tidal breakup which assumed self-gravitating, homogeneous, perfectly elastic bodies, Dobrovolskis derived simple analytical expressions for the tidally-induced surface and central stresses. Both can be cast in such a way that Poisson's ratio is the only material dependent constant entering these expressions. Whether both surface and central failure must be initiated as a criterion for breakup, or either one of them is sufficient, remains a subject of disagreement. To resolve this debate, we model the details of cometary breakup using a three-dimensional Smooth Particle Hydrodynamics (SPH) code modified to simulate fracture in small solid objects. At lower stresses associated with brittle failure, we use a rate-dependent strength based on the nucleation of incipient flaws whose number density is given by a Weibull distribution.

Derived from text

N94-35407*# National Aeronautics and Space Administration. Lyndon B. Johnson Space Center, Houston, TX.

CRATERS IN ALUMINUM 1100 TARGETS USING GLASS PROJECTILES AT 1-7 km/s Abstract Only c39

R. P. Bernhard (Lockheed Engineering and Sciences Co., Houston, TX.), T. H. See (Lockheed Engineering and Sciences Co., Houston, TX.), F. Hoerz, and M. J. Cintala *In* Lunar and Planetary Inst., The Twenty-Fifth Lunar and Planetary Science Conference. Part 1: A-G 1994 p 107-108 (For primary document see N94-35395 11-91)

Avail: CASI HC A01/MF A04

We report on impact experiments using soda-lime glass spheres of 3.2 mm diameter and aluminum targets (1100 series). The purpose is to assist in the interpretation of LDEF instruments and in the development of future cosmic-dust collectors in low-Earth orbit. Because such instruments demand understanding of both the cratering and penetration process, we typically employ targets with thicknesses that range from massive, infinite half-space targets, to ultrathin films. This report addresses a subset of cratering experiments that were conducted to fine-tune our understanding of crater morphology as a function of impact velocity. Also, little empirical insight exists about the physical distribution and shock-metamorphism of the impactor residues as a function of encounter speed, despite their recognized significance in the analysis of space-exposed surfaces. Soda-lime glass spheres were chosen as a reasonable analog to extraterrestrial silicates, and aluminum 1100 was chosen for targets, which among the common Al-alloys, best represents the physical properties of high-purity aluminum. These materials complement existing impact studies that typically employed metallic impactors and less ductile Al-alloys. We have completed dimensional analyses of the resulting craters and are in the process of investigating the detailed distribution of the unmelted and melted impactor residues via SEM methods, as well as potential compositional modifications of the projectile melts via electron microprobe. Derived from text

N94-35408*# National Aeronautics and Space Administration. Ames Research Center, Moffett Field, CA.

A MINERALOGICAL INSTRUMENT FOR PLANETARY APPLICATIONS Abstract Only

David F. Blake, David T. Vaniman, and David L. Bish *In* Lunar and Planetary Inst., The Twenty-Fifth Lunar and Planetary Science Conference. Part 1: A-G 1994 p 121-122 (For primary document see N94-35395 11-91)

Avail: CASI HC A01/MF A04

The mineralogy of a planetary surface can be used to identify the provenance of soil or sediment and reveal the volcanic, metamorphic and/or sedimentological history of a particular region. We have discussed elsewhere the applications and the instrument design of possible X-ray diffraction and X-ray fluorescence (XRD/XRF) devices for the mineralogical characterization of planetary surfaces. In this abstract we evaluate some aspects of sample-detector geometry and sample collection strategies.

Derived from text

N94-35409*# National Aeronautics and Space Administration. Lyndon B. Johnson Space Center, Houston, TX.

MEASURING TRACK DENSITIES IN LUNAR GRAINS USING IMAGE ANALYSIS Abstract Only

G. E. Blanford (Houston Univ., Clear Lake, TX.), D. S. McKay, R. P. Bernhard, and C. K. Schulz *In* Lunar and Planetary Inst., The Twenty-Fifth Lunar and Planetary Science Conference. Part 1: A-G 1994 p 125-126 (For primary document see N94-35395 11-91)

Avail: CASI HC A01/MF A04

We have used digitized scanning electron micrographs and computer image analysis programs to measure track densities in lunar soil grains. Tracks were formed by highly ionizing solar energetic particles and cosmic rays. Back-scattered electron images produced suitable high contrast images for analysis. We used computer counting and measurement of area to obtain track densities. We found an excellent correlation with manual measurements for track densities below 1x10(exp 8) cm(exp -2). For track densities between 1x10(exp 8) to 1x10(exp 9) cm(exp -2) we found that a regression formula using the percentage area covered by tracks gave good agreement with manual measurements. Measurement of tract densities in lunar samples has been a very rewarding technique for measuring exposure ages and soil maturation processes. We have shown that we can reliably measure track densities in lunar grains using image analysis techniques. Automating track counting may allow application of this technique to important problems in regolith dynamics including the ratio of radiation exposure to reworking in various surface and core samples and in regolith breccias. Derived from text

N94-35410*# National Aeronautics and Space Administration. Lyndon B. Johnson Space Center, Houston, TX.

Ar-39-Ar-40 AGES OF FOUR UREILITES Abstract Only

D. D. Bogard and D. H. Garrison *In* Lunar and Planetary Inst., The Twenty-Fifth Lunar and Planetary Science Conference. Part 1: A-G 1994 p 137-138 (For primary document see N94-35395 11-91)

Avail: CASI HC A01/MF A04

Ureilites Novo Urei, Havero, and Kenna show strong evidence of one or more Ar-40 degassing events in the time period of 3.3-4.1 Ga ago. These ages may be compared to current interpretations of ureilite chronology. These include the suggestion of metasomatic activity on the parent body 3.7 Ga ago that reset some Sm-Nd ages and the suggestion that ureilites have experienced terrestrial contamination of several trace elements (including Pb and LREE), which makes suspect ages younger than approximately 4.5 Ga. Because the K-Ar chronometer can be sensitive to metamorphic events, we made Ar-39-Ar-40 determinations on bulk samples (0.12-0.14 g each) of four ureilites. The Ar-39-Ar-40 age spectra and K/Ca ratios as a function of cumulative Ar release from stepwise temperature extractions for the four ureilites analyzed are shown. Because Ar-39-Ar-40 ages shown by low and high temperature extractions may be suspect, we examined the intermediate temperature extractions. Although interpretation of these spectra is obviously uncertain, we believe that the most recent times of Ar degassing can be roughly inferred. These times are approximately 3.3 Ga for Havero, 3.3-3.7 Ga for Novo Urei, and approximately 4.1 Ga for Kenna, for which Ar degassing may not have been complete. The indication of Ar-39-Ar-40 degassing ages of 3.3-4.1 Ga for three ureilites that also contain an enhanced LREE component and (excepting Havero) produce a 3.74 Ga Sm-Nd age, suggests that both chronometers may have responded to the same parent body event. On the other hand, it is also possible that the Ar data reflect one or more separate events that did not strongly affect the Sm-Nd system, a situation that commonly occurs in eucrites. Thus the existence of reset Ar ages does not require similarly reset Sm-Nd ages. Derived from text

N94-35411*# National Aeronautics and Space Administration. Lyndon B. Johnson Space Center, Houston, TX.

ALTERATION AND FORMATION OF RIMS ON THE CM PARENT BODY Abstract Only

Lauren B. Browning (Tennessee Univ., Knoxville, TN.), Harry Y. McSween, Jr. (Tennessee Univ., Knoxville, TN.), and Michael Zolensky *In* Lunar and Planetary Inst., The Twenty-Fifth Lunar and Planetary Science Conference. Part 1: A-G 1994 p 181-182 (For primary document see N94-35395 11-91)

Avail: CASI HC A01/MF A04

All types of coarse-grained components in CM chondrites are surrounded by fine-grained dust coatings, but the origin of these rims is not yet clear. Although a strictly nebular origin seems likely for rims in the relatively unaltered type 3 chondrites, the rims in CM chondrites are dominated by secondary alteration phases. It has been argued that either the coarse-grained cores accreted altered rim materials while still in the nebula or that alteration of primary rim phases occurred on the CM parent body. To constrain the origin of alteration phases in rim material, we have analyzed the textures and mineral associations from 10 CM chondritic falls by optical and scanning electron microscopy. Our results indicate that the secondary phases in CM chondritic rims were produced by parent body fluid-rock interactions which redefined some primary rim textures and may have produced, in some cases, both coarse-grained components and the rims that surround them. Textural features demonstrate the interactive exchange of alteration fluids between rims, matrix, and chondrules on the CM parent body. For example, most matrix-rim contacts are gradational, suggesting the synchronous alteration of both components. Several observations suggest the possibility of in situ rim production. For example, tochilinite and phyllosilicates commonly form rims around matrix carbonates, which are generally believed to have precipitated from alteration fluids on the CM parent body. This suggests that the rims surrounding matrix carbonates may also have been produced by alteration processes. Partially replaced chondrule olivines bear a striking resemblance to many rimmed olivines in the matrix which suggests, by analogy, that site-specific precipitation of S-bearing phases may also be responsible for the occurrence of many tochilinite-rich rims around isolated matrix olivines. Non-silicate rims precipitate around olivines of any composition, but the process is most effective for fayalitic olivines. Most of the remaining olivines in CM chondrites are relatively Mg-rich, which suggests that the precipitation of S-bearing rims on olivines may not have been an important process in the aqueous alteration of CM chondrites. We conclude that: (1) precursor rim materials in CM chondrites were subjected to pervasive aqueous alteration on the CM parent body; and (2) textures and mineral associations observed in CM chondrites also suggest the possibility of in situ rim production.

Derived from text

N94-35412*# National Aeronautics and Space Administration. Lyndon B. Johnson Space Center, Houston, TX.

EUREKA! AEROGEL CAPTURE OF METEOROIDS IN SPACE Abstract Only **c90**

D. E. Brownlee (Washington Univ., Seattle, WA.), F. Horz, L. Hrubsch, J. A. M. McDonnell, P. Tsou, and J. Williams *In* Lunar and Planetary Inst., The Twenty-Fifth Lunar and Planetary Science Conference. Part 1: A-G 1994 p 183-184 (For primary document see N94-35395 11-91)
Avail: CASI HC A01/MF A04

Light gas gun studies have shown that 6 km/s solid mineral and glass test particles can be successively captured in 0.05 g cm(exp -3) aerogel without severe heating or fragmentation. In spite of this work, there has been uncertainty in the performance of aerogel for hypervelocity capture of real meteoroids. Natural impacts differ from simulations in that the particles are likely to be structurally weak and they typically impact at higher velocity that can be simulated in the laboratory. We are fortunate now to have had two successful capture experiments using aerogel exposed in space. These experiments provide fundamental data for the assessment of the value of silica aerogel for capture of hypervelocity meteoroids from spacecraft. The first experiment used 0.02 g cm(exp -3) aerogel flown on the lid of a Shuttle Get Away Special canister. During its 9 day exposure, the 0.165 m(exp 2) of aerogel in this Sample Return Experiment (SRE) captured two long 'carrot-shaped' tracks and one highly fractured bowl shaped 'crater'. The second collection was with 0.04 m(exp 2) of 0.05 g cm(exp -3) aerogel exposed on ESA's Eureca freeflying spacecraft that was exposed for 11 months before recovery by the Shuttle. The Eureca aerogel exposure consisted of four 10x10 cm module trays that were part of the TiCCE meteoroid collector built by the University of Kent at Canterbury. To date we have found ten 'carrot-shaped' tracks and two 'craters' on this experiment. The longest tracks in both exposures are over 2 mm long. Two of the TiCCE modules had a 0.1 micron Al film suspended a millimeter above the aerogel. On these modules several of the projectiles fragmented during passage through the film producing fields of carrot shaped tracks from the resulting miniature 'meteor' shower. Most of the tracks in these showers have observable particles at their ends. We have extracted one of the carrot track meteoroids and mounted it in epoxy for sectioning. So far the examination of these 14 impacts suggests that low density aerogel is a magic and highly effective media for intact capture of hypervelocity particles in space.

Derived from text

N94-35413*# National Aeronautics and Space Administration. Ames Research Center, Moffett Field, CA.

VENUS CLIMATE STABILITY AND VOLCANIC RESURFACING RATES Abstract Only

M. A. Bullock (Colorado Univ., Boulder, CO.), D. H. Grinspoon (Colorado Univ., Boulder, CO.), and J. B. Pollack *In* Lunar and Planetary Inst., The Twenty-Fifth Lunar and Planetary Science Conference. Part 1: A-G 1994 p 191-192 (For primary document see N94-35395 11-91)
Avail: CASI HC A01/MF A04

The climate of Venus is to a large degree controlled by the radiative properties of its massive atmosphere. In addition, outgassing due to volcanic activity, exospheric escape processes, and surface/atmosphere interactions may all be important in moderating the abundances of atmospheric CO2 and other volatiles. We have developed an evolutionary climate model for Venus using a systems approach that emphasizes feedbacks between elements in the climate system. Modules for atmospheric radiative transfer, surface/atmosphere interactions, tropospheric chemistry, and exospheric escape processes have so far been developed. Climate feedback loops result from interconnections between modules, in the form of the environmental parameters pressure, temperature, and atmospheric mixing ratios. The radiative transfer module has been implemented by using Rosseland mean opacities in a one dimensional grey radiative-convective model. The model has been solved for the static (time independent) case to determine climate equilibrium points. The dynamics of the model have also been explored by employing reaction/diffusion kinetics for possible surface atmosphere heterogeneous reactions over geologic timescales. It was found that under current conditions, the model predicts that the climate of Venus is at or near an unstable equilibrium point. The effects of constant rate volcanism and corresponding exsolution of volatiles on the stability of the climate model were also explored.

Derived from text

N94-35414*# National Aeronautics and Space Administration. Ames Research Center, Moffett Field, CA.

FLUVIAL PROCESSES IN MA'ADIM VALLIS AND THE POTENTIAL OF GUSEV CRATER AS A HIGH PRIORITY SITE Abstract Only

Nathalie Cabrol (Observatoire de Paris-Meudon, France.), Ragnild Landheim (Arizona State Univ., Tempe, AZ.), Ronald Greeley (Arizona State Univ., Tempe, AZ.), and Jack Farmer *In* Lunar and Planetary Inst., The Twenty-Fifth Lunar and Planetary Science Conference. Part 1: A-G 1994 p 213-214 (For primary document see N94-35395 11-91)
Avail: CASI HC A01/MF A04

According to exobiology site selection criteria for Mars, the search for potential extinct/extant water dependent life should focus on sites were water flowed and ponded. The Ma'adim Vallis/Gusev crater system is of high priority for exobiology research, because it appears to have involved long term flooding, different periods and rates of sedimentation, and probable episodic ponding. The topics covered include the following: evidence of nonuniform fluvial processes and early overflooding of the plateau and ponding.

Derived from text

N94-35415*# National Aeronautics and Space Administration. Lyndon B. Johnson Space Center, Houston, TX.

LUNAR MINERAL FEEDSTOCKS FROM ROCKS AND SOILS: X-RAY DIGITAL IMAGING IN RESOURCE EVALUATION Abstract Only

John G. Chambers (Tennessee Univ., Knoxville, TN.), Allan Patchen (Tennessee Univ., Knoxville, TN.), Lawrence A. Taylor (Tennessee Univ., Knoxville, TN.), Stefan J. Higgins (Tennessee Univ., Knoxville, TN.), and David S. McKay *In* Lunar and Planetary Inst., The Twenty-Fifth Lunar and Planetary Science Conference. Part 1: A-G 1994 p 235-236 (For primary document see N94-35395 11-91)
Avail: CASI HC A01/MF A04

The rocks and soils of the Moon provide raw materials essential to the successful establishment of a lunar base. Efficient exploitation of these resources requires accurate characterization of mineral abundances, sizes/shapes, and association of 'ore' and 'gangue' phases, as well as the technology to generate high-yield/high-grade feedstocks. Only recently have x-ray mapping and digital imaging techniques been applied to lunar resource evaluation. The topics covered include inherent differences between lunar basalts and soils and quantitative comparison of rock-derived and soil-derived ilmenite concentrates. It is concluded that x-ray digital-imaging characterization of lunar raw materials provides a quantitative comparison that is unattainable by traditional petrographic techniques. These data are

necessary for accurately determining mineral distributions of soil and crushed rock material. Application of these techniques will provide an important link to choosing the best raw material for mineral beneficiation.
Derived from text

N94-35416*# National Aeronautics and Space Administration. Ames Research Center, Moffett Field, CA.

FIRST GALILEO IMAGE OF ASTEROID 243 IDA Abstract Only c90

C. R. Chapman (Planetary Science Inst., Tucson, AZ.), M. J. S. Belton (Kitt Peak National Observatory, Tucson, AZ.), J. Veverka (Cornell Univ., Ithaca, NY.), G. Neukum (Deutsche Forschungsanstalt fuer Luft- und Raumfahrt, Berlin, Germany.), J. Head (Brown Univ., Providence, RI.), Ronald Greeley (Arizona State Univ., Tempe, AZ.), K. Klaasen (Jet Propulsion Lab., California Inst. of Tech., Pasadena, CA.), and D. Morrison *In* Lunar and Planetary Inst., The Twenty-Fifth Lunar and Planetary Science Conference. Part 1: A-G 1994 p 237-238 (For primary document see N94-35395 11-91)
Avail: CASI HC A01/MF A04

The second spacecraft encounter with an asteroid has yielded an unprecedentedly high resolution portrait of 243 Ida. On 28 Aug. 1993, Galileo obtained an extensive data set on this small member of the Koronis family. Most of the data recorded on the tape recorder will be returned to Earth in spring 1994. A five-frame mosaic of Ida was acquired with good illumination geometry a few minutes before closest approach; it has a resolution of 31 to 38 m/pixel amd was played back during Sept. 1993. Preliminary analyses of this single view of Ida are summarized.
Derived from text

N94-35417*# National Aeronautics and Space Administration. Ames Research Center, Moffett Field, CA.

SUBPIXEL RESOLUTION FROM MULTIPLE IMAGES Abstract Only c43

Peter Cheeseman (Research Inst. for Advanced Computer Science, Moffett Field, CA.), Rob Kanefsky (RECOM Technologies, Inc., Moffett Field, CA.), John Stutz, and Richard Kraft *In* Lunar and Planetary Inst., The Twenty-Fifth Lunar and Planetary Science Conference. Part 1: A-G 1994 p 241-242 (For primary document see N94-35395 11-91)
Avail: CASI HC A01/MF A04

Multiple images taken from similar locations and under similar lighting conditions contain similar, but not identical, information. Slight differences in instrument orientation and position produces mismatches between the projected pixel grids. These mismatches ensure that any point on the ground is sampled differently in each image. If all the images can be registered with respect to each other to a small fraction of a pixel accuracy, then the information from the multiple images can be combined to increase linear resolution by roughly the square root of the number of images. In addition, the gray-scale resolution of the composite image is also improved. We describe methods for multiple image registration and combination, and discuss some of the problems encountered in developing and extending them. We display test results with 8:1 resolution enhancement, and Viking Orbiter imagery with 2:1 and 4:1 enhancements. Derived from text

N94-35418*# National Aeronautics and Space Administration. Lyndon B. Johnson Space Center, Houston, TX.

GRAIN RIMS ON ILMENITE IN THE LUNAR REGOLITH: COMPARISON TO VAPOR DEPOSITS ON REGOLITH SILICATES Abstract Only

R. Christoffersen, D. S. McKay, and L. P. Keller *In* Lunar and Planetary Inst., The Twenty-Fifth Lunar and Planetary Science Conference. Part 1: A-G 1994 p 259-260 (For primary document see N94-35395 11-91)
Avail: CASI HC A01/MF A04

In efforts to understand regolith evolution on airless bodies, increasing attention is now being payed to those processes and events that alter or 'weather' the surfaces of regolith grains. This attention has developed partly out of the ongoing need to optimize models of planetary reflectance spectra and the growing recognition that diverse types of grain coatings and surface alterations occur which can strongly influence mineral reflectance properties. In addition to their implications for optical properties, surface features on regolith grains have provided useful clues to the basic thermal, chemical, and radiation history of regoliths. Derived from text

N94-35419*# National Aeronautics and Space Administration. Lyndon B. Johnson Space Center, Houston, TX.

BLOCK DISTRIBUTIONS ON THE LUNAR SURFACE: A COMPARISON BETWEEN MEASUREMENTS OBTAINED FROM SURFACE AND ORBITAL PHOTOGRAPHY Abstract Only

Mark J. Cintala and Kathleen M. McBride *In* Lunar and Planetary Inst., The Twenty-Fifth Lunar and Planetary Science Conference. Part 1: A-G 1994 p 261-262 (For primary document see N94-35395 11-91)
Avail: CASI HC A01/MF A04

Enlargements of Lunar-Orbiter photography were used in conjunction with a digitizing tablet to collect the locations and dimensions of blocks surrounding the Surveyor 1, 3, 6, and 7 landing sites. Data were reduced to the location and the major axis of the visible portion of each block. Shadows sometimes made it difficult to assess whether the visible major axis corresponded with the actual principal dimension. These data were then correlated with the locations of major craters in the study areas, thus subdividing the data set into blocks obviously associated with craters and those in intercrater areas. A block was arbitrarily defined to be associated with a crater when its location was within 1.1 crater radii of the crater's center. Since this study was commissioned for the ultimate purpose of determining hazards to landing spacecraft, such a definition was deemed appropriate in defining block-related hazards associated with craters. Size distributions of smaller fragments as determined from Surveyor photography were obtained as measurements from graphical data. Basic comparisons were performed through use of cumulative frequency distributions identical to those applied to studies of crater-count data. Derived from text

N94-35420*# National Aeronautics and Space Administration. Goddard Space Flight Center, Greenbelt, MD.

REMOTE GEOCHEMICAL EXPERIMENT PACKAGE FOR DISCOVERY CLASS MISSIONS Abstract Only c89

Pamela E. Clark (Catholic Univ. of America, Washington, DC.), Larry G. Evans (Computer Sciences Corp., Lanham, MD.), and Jacob I. Trombka *In* Lunar and Planetary Inst., The Twenty-Fifth Lunar and Planetary Science Conference. Part 1: A-G 1994 p 267-268 (For primary document see N94-35395 11-91)
Avail: CASI HC A01/MF A04

Remote sensing x-ray and gamma-ray spectrometers can be used to infer elemental composition on atmosphereless bodies, such as asteroids, the moon, and Mercury. The composition of the planetary body and variations in its surface chemistry are of fundamental importance in understanding the formation and dynamics of that body. Thus, for Discovery class missions, x-ray fluorescence (XRF), gamma-ray spectrometer (GRS), or a combined Geochemical Experiment Package (GEP) have been proposed. These instruments can meet the mission science objectives, while still meeting the weight, power, and cost constraints. These missions include the Near Earth Asteroid Rendezvous, the Main-belt Asteroid Rendezvous, and others such as HERMES (Mercury Orbiter). This paper presents the results of calculations done to assess the sensitivity of a combined instrument to obtain elemental compositions of planetary bodies with an uncertainty small enough to be scientifically useful. Derived from text

N94-35421*# National Aeronautics and Space Administration. Lyndon B. Johnson Space Center, Houston, TX.

ON THE POSSIBLE ROLE OF ELEMENTAL CARBON IN THE FORMATION OF REDUCED CHONDRULES Abstract Only c90

Harold C. Connolly, Jr. (Rutgers Univ., New Brunswick, NJ.), Roger H. Hewins (Rutgers Univ., New Brunswick, NJ.), Richard D. Ash (Manchester Univ., England.), Gary E. Lofgren, and Brigitte Zanda *In* Lunar and Planetary Inst., The Twenty-Fifth Lunar and Planetary Science Conference. Part 1: A-G 1994 p 279-280 (For primary document see N94-35395 11-91)
Avail: CASI HC A01/MF A04

Recent experiments have been designed to produce chondrule textures via flash melting while simultaneously studying the nature of chondrule precursors. However, these experiments have only been concerned with silicate starting material. This is a preliminary report concerning what effects elemental carbon, when added to the silicate starting material, has on the origin of chondrules produced by flash melting. Derived from text

N94-35422*# National Aeronautics and Space Administration. Ames Research Center, Moffett Field, CA.

WHAT INITIATED PLANETESIMAL FORMATION? Abstract Only **c90**

J. N. Cuzzi, A. R. Dobrovolskis, and R. C. Hogan *In* Lunar and Planetary Inst., The Twenty-Fifth Lunar and Planetary Science Conference. Part 1: A-G 1994 p 307-308 (For primary document see N94-35395 11-91)

Avail: CASI HC A01/MF A04

The physical structure of primitive (chondritic) meteorites, even after some geological processing and modification, is thought by most to contain clues as to the first stage of accretion of solid matter into objects that might be called planetesimals. However, theoretical understanding of the processes responsible for this important stage is shaky. We note what we believe are fundamental obstacles for the Goldreich-Ward version of rapid and direct planetesimal formation via gravitational instability in a settled particle layer, and describe an alternative scenario which might lead from grainy nebula gas to primitive planetesimals in a way that has intriguing connections to the meteorite evidence. Derived from text

N94-35423*# National Aeronautics and Space Administration. Lyndon B. Johnson Space Center, Houston, TX.

THE OCCURRENCE OF BLUE LUMINESCING ENSTATITE IN E3 AND E4 CHONDRITES Abstract Only **c90**

John M. DeHart (Casper Coll., WY.) and Gary E. Lofgren *In* Lunar and Planetary Inst., The Twenty-Fifth Lunar and Planetary Science Conference. Part 1: A-G 1994 p 319-320 (For primary document see N94-35395 11-91)

Avail: CASI HC A01/MF A04

Two compositional types of enstatite that emit cathodoluminescence (CL) are known to exist in E3 and E4 chondrites. The first type consists of the most common enstatites that are relatively FeO-poor and emit a red CL. Their CL is apparently activated by the presence of MnO and Cr2O3 in concentrations of 0.2 and 0.6 weight percent. The second type of enstatite is nearly FeO-free, contains no MnO or Cr2O3 and emits a blue CL. The origin of these two types of enstatite and their accompanying chemical and CL differences has long been a subject of discussion. Leitch and Smith first observed to two types and felt the compositional differences were too great to have formed under the same conditions. They postulated the two types of enstatite formed on separate parent bodies and were mixed when these bodies collided. McKinley et al. observed a continuous range of compositions between blue luminescing and red luminescing enstatites and concluded the two types of enstatite formed evidence that blue luminescing pyroxenes were relics that did not completely melt during the heating event which melted other precursor grains, and are distinct from the red CL pyroxene in the chondrules in E chondrites. In order to further clarify the nature and origin of the pyroxene that emits blue CL, the sections listed in another work were examined for the occurrence of blue luminescing enstatite. Derived from text

N94-35424*# National Aeronautics and Space Administration. Lyndon B. Johnson Space Center, Houston, TX.

THE FRETTED TERRAIN OF THE NILOSYRTIS MENSAE REGION OF MARS: CLUES TO THE TIMING OF DICHOTOMY FORMATION AND THE EMPLACEMENT OF THE NORTHERN PLAINS Abstract Only

Jeff E. DeTroye and Steven H. Williams *In* Lunar and Planetary Inst., The Twenty-Fifth Lunar and Planetary Science Conference. Part 1: A-G 1994 p 327-328 (For primary document see N94-35395 11-91)

Avail: CASI HC A01/MF A04

Geologic mapping of the fretted terrain of the Nilosyrtis Mensae region of Mars has revealed geomorphic evidence that the breakup of the plateau units to the south of Nilosyrtis occurred well before the plains units to the north were emplaced in the late Hesperian time. The plains units were deposited against the fretted terrain which has undergone some modification by mass wasting but not significant backwasting. The morphology observed at the contact between plains and the fretted terrain is consistent with that expected where the edge of a pile of sedimentary debris has undergone mass wasting and other erosion. Author (revised)

N94-35425*# National Aeronautics and Space Administration. Ames Research Center, Moffett Field, CA.

EXOPALEONTOLOGY AND THE SEARCH FOR A FOSSIL RECORD ON MARS Abstract Only

Jack D. Farmer and D. J. DesMarais *In* Lunar and Planetary Inst., The Twenty-Fifth Lunar and Planetary Science Conference. Part 1: A-G 1994 p 367-368 (For primary document see N94-35395 11-91)

Avail: CASI HC A01/MF A04

Although present Martian surface conditions appear unfavorable for life as we know it, there is compelling geological evidence that the climate of early Mars was much more Earth-like, with a denser atmosphere and abundant surface water. The fact that life developed on the Earth within the first billion years of its history makes it quite plausible that life may have also developed on Mars. If life did develop on Mars, it is likely to have left behind a fossil record. This has led to the development of a new subdiscipline of paleontology, herein termed 'exopaleontology', which deals with the exploration for fossils on other planets. The most important factor enhancing microbial fossilization is the rapid entombment of microorganisms by fine-grained, stable mineral phases, such as silica, phosphate, or carbonate. The oldest body fossils on Earth are preserved in this way, occurring as permineralized cells in fine-grained siliceous sediments (cherts) associated with ancient volcanic terranes in Australia and South Africa. Modern terrestrial environments where minerals may precipitate in the presence of microorganisms include subaerial thermal springs and shallow hydrothermal systems, sub-lacustrine springs and evaporitic alkaline lakes, zones of mineralization within soils where 'hardpans' (e.g. calcretes, silcretes) form, and high latitude frozen soils or ground ice. Author (revised)

N94-35426*# National Aeronautics and Space Administration. Goddard Space Flight Center, Greenbelt, MD.

IMPACT BASINS IN SOUTHERN DAEDALIA, MARS: EVIDENCE FOR CLUSTERED IMPACTORS? Abstract Only

Herbert Frey and James H. Roark *In* Lunar and Planetary Inst., The Twenty-Fifth Lunar and Planetary Science Conference. Part 1: A-G 1994 p 387-388 (For primary document see N94-35395 11-91)

Avail: CASI HC A01/MF A04

The distribution of ancient massifs and old cratered terrain in the southern Daedalia region indicate the presence of at least two and probably three impact basins of large size. One of these is located near where Craddock et al. placed their center for the Daedalia Basin, but it has very different ring diameters. These basins have rings exceeding 1000 km diameter and overlap significantly with centers separated by 500 to 600 km at nearly identical latitudes of -26 to -29 deg. The smaller westernmost basin appears slightly better preserved, but there is little evidence for obvious superposition that might imply a temporal sequence. Recognizing the improbability of random impacts producing aligned, nearly contemporaneous features, we suggest these basins may have resulted from clustered impactors. Author (revised)

N94-35427*# National Aeronautics and Space Administration. Goddard Space Flight Center, Greenbelt, MD.

EFFECTS DUE TO OVERLAPPING LARGE IMPACT BASINS ON MARS Abstract Only

Herbert Frey, Anne Marie Reidy, James H. Roark, and Stephanie Stockman *In* Lunar and Planetary Inst., The Twenty-Fifth Lunar and Planetary Science Conference. Part 1: A-G 1994 p 389-390 (For primary document see N94-35395 11-91)

Avail: CASI HC A01/MF A04

Many ancient, highly degraded large impact basins exist on Mars. In many cases these basins overlap or are overlapped by more easily observed, presumably younger, impact basins. While impact basin overlap is becoming more recognized, the effects of such overlap have only occassionally been described. Such effects will depend on a variety of factors including the absolute and relative size of the basins, the degree of overlap, the state of the lithosphere and its thermal gradient at the time of impact, and the time between impacts. There now exists enough evidence for overlapping basins of different sizes that some of these can be discussed. This paper highlights some examples of the obvious effects of basin overlap. Author (revised)

N94-35428*# National Aeronautics and Space Administration. Lyndon B. Johnson Space Center, Houston, TX.

SOLAR PROTON PRODUCED NEON IN SHERGOTTITE METEORITES Abstract Only **c90**

D. H. Garrison (Lockheed Engineering and Sciences Co., Houston, TX.), M. N. Rao (Lockheed Engineering and Sciences Co., Houston, TX.), and D. D. Bogard *In* Lunar and Planetary Inst., The Twenty-Fifth Lunar and

Planetary Science Conference. Part 1: A-G 1994 p 403-404 (For primary document see N94-35395 11-91)
Avail: CASI HC A01/MF A04

Cosmogenic radionuclides produced by near-surface, nuclear interactions of energetic solar protons (approx. 10-100 MeV) were reported in several lunar rocks and a very small meteorites. We recently documented the existence and isotopic compositions of solar-produced (SCR) Ne in two lunar rocks. Here we present the first documented evidence for SCR Ne in a meteorite, ALH77005, which was reported to contain SCR radionuclides. Examination of literature data for other shergottites suggests that they may also contain a SCR Ne component. The existence of SCR Ne in shergottites may be related to a Martian origin. Author (revised)

N94-35429*# National Aeronautics and Space Administration. Goddard Space Flight Center, Greenbelt, MD.
QUANTIFYING SHAPES OF VOLCANOES ON VENUS Abstract Only
J. B. Garvin *In* Lunar and Planetary Inst., The Twenty-Fifth Lunar and Planetary Science Conference. Part 1: A-G 1994 p 405-406 (For primary document see N94-35395 11-91)
(RTOP 889-62-10-41)
Avail: CASI HC A01/MF A04

A large population of discrete volcanic edifices on Venus has been identified and cataloged by means of Magellan SAR images, and an extensive database describing thousands of such features is in final preparation. Those volcanoes categorized as Intermediate to Large in scale, while relatively small in number (approx. 400), nonetheless constitute a significant volumetric component (approx. 13 x 10(exp 6) cu km) of the total apparent crustal volume of Venus. For this reason, we have focused attention on the morphometry of a representative suite of the larger edifices on Venus and, in particular, on ways of constraining the eruptive histories of these possibly geologically youthful landforms. Our approach has been to determine a series of reproducible morphometric parameters for as many of the discrete volcanoes on Venus that have an obvious expression within the global altimetry data acquired by Magellan. In addition, we have attempted to objectively and systematically define the mathematical essence of the shapes of these larger volcanoes using a polynomial cross-section approximation involving only parameters easily measured from digital topography, as well as with simple surface cylindrical harmonic expansions. The goal is to reduce the topological complexities of the larger edifices to a few simple parameters which can then be related to similar expressions for well-studied terrestrial and martian features.. Author (revised)

N94-35430*# National Aeronautics and Space Administration. Goddard Space Flight Center, Greenbelt, MD.
MESOSCALE ROUGHNESS OF VENUS Abstract Only
J. B. Garvin and James J. Frawley *In* Lunar and Planetary Inst., The Twenty-Fifth Lunar and Planetary Science Conference. Part 1: A-G 1994 p 407-408 (For primary document see N94-35395 11-91)
(RTOP 889-62-10-41)
Avail: CASI HC A01/MF A04

The global distribution of multi-kilometer (approx. 9 km) length scale 'roughness' (hereafter mesoscale roughness or MR) on Venus can be estimated from the Magellan global altimetry dataset (GxDR) and then compared with MR data derived for Earth from 5' ETOP5 data and for Mars (from USGS Mars DTM dataset). The mesoscale roughness parameter (MR) represents the RMS variance in meters of the actual planetary surface topography relative to the best fitting tangent plane defined on the basis of a 3x3 pixel sliding window. The best-fit plane was computed using a least-squares solution which minimizes delta H, the sum of the squares of the differences between the 9 local elevation values (H(sub i)), and the elevation of best-fit plane at the same grid location. Using the best-fit plane and delta H, we have computed the RMS 'roughness' var(delta R), where this parameter is always minimized on the basis of its calculation using least squares. We have called this 'ruggedness' parameter the Mesoscale Roughness (MR) because it is directly related to the high-frequency variance of topography after mesoscale slopes and tilts (i.e., for Venus, the baseline over which MR is computed (dx) is approx. 8.8 km and dx for Earth is approx. 9.3 km) are removed. As such, MR represents the degree to which a planetary surface is more rugged than approximately 10 km scale facets or tilts. It should not be confused with the radar 'RMS Roughness' parameter computed at 0.1 to 10 m length scales on the basis of the Magellan radar altimeter echo. We will use our MR parameter to investigate the global ruggedness properties of Venus as they relate to geological provinces and in comparison with the spatial pattern of MR for Earth and Mars. Author (revised)

N94-35431*# National Aeronautics and Space Administration. Goddard Space Flight Center, Greenbelt, MD.
VOLCANO MORPHOMETRY AND VOLUME SCALING ON VENUS Abstract Only
J. B. Garvin and R. S. Williams, Jr. *In* Lunar and Planetary Inst., The Twenty-Fifth Lunar and Planetary Science Conference. Part 1: A-G 1994 p 409-410 (For primary document see N94-35395 11-91)
(RTOP 889-62-10-41)
Avail: CASI HC A01/MF A04

A broad variety of volcanic edifices have been observed on Venus. They ranged in size from the limits of resolution of the Magellan SAR (i.e., hundreds of meters) to landforms over 500 km in basal diameter. One of the key questions pertaining to volcanism on Venus concerns the volume eruption rate or VER, which is linked to crustal productivity over time. While less than 3 percent of the surface area of Venus is manifested as discrete edifices larger than 50 km in diameter, a substantial component of the total crustal volume of the planet over the past 0.5 Ga is related to isolated volcanoes, which are certainly more easily studied than the relatively diffusely defined plains volcanic flow units. Thus, we have focused our efforts on constraining the volume productivity of major volcanic edifices larger than 100 km in basal diameter. Our approach takes advantage of the topographic data returned by Magellan, as well as our database of morphometric statistics for the 20 best known lava shields of Iceland, plus Mauna Loa of Hawaii. As part of this investigation, we have quantified the detailed morphometry of nearly 50 intermediate to large scale edifices, with particular attention to their shape systematics. We found that a set of venusian edifices which include Maat, Sapas, Tepev, Sif, Gula, a feature at 46 deg S, 215 deg E, as well as the shield-like structure at 10 deg N, 275 deg E are broadly representative of the approx. 400 volcanic landforms larger than 50 km. The cross-sectional shapes of these 7 representative edifices range from flattened cones (i.e., Sif) similar to classic terrestrial lava shields such as Mauna Loa and Skjaldbreidur, to rather dome-like structures which include Maat and Sapas. The majority of these larger volcanoes surveyed as part of our study displayed cross-sectional topographies with paraboloidal shaped, in sharp contrast with the cone-like appearance of most simple terrestrial lava shields. In order to more fully explore the differences between large venusian edifices and volcanoes on the Earth and Mars, we developed a volume scaling algorithm which relies on conservation of volcano morphometry as basal diameter is varied. Author (revised)

N94-35432*# National Aeronautics and Space Administration. Lyndon B. Johnson Space Center, Houston, TX.
APPLICATION OF AN ALKYLAMMONIUM METHOD FOR CHARACTERIZATION OF PHYLLOSILICATES IN CI CHONDRITES Abstract Only **c90**
D. C. Golden (Dual and Associates, Houston, TX.), D. W. Ming, M. E. Zolensky, and S. V. Yang *In* Lunar and Planetary Inst., The Twenty-Fifth Lunar and Planetary Science Conference. Part 1: A-G 1994 p 435-436 (For primary document see N94-35395 11-91)
Avail: CASI HC A01/MF A04

Many meteorites and interplanetary dust particles (IDP's) with primitive compositions contain significant amounts of phyllosilicates, which are generally interpreted as evidence of protoplanetary aqueous alteration at an early period in the solar system. These meteorites are chondrites of the carbonaceous and ordinary varieties. Characterization of phyllosilicates in these materials is important because of the important physico-chemical information they hold, e.g., from well characterized phyllosilicates, thermodynamic stability relations and hence the conditions of formation of phyllosilicates in the parent body of the meteorite can be predicted. Although we are at a rudimentary level of understanding of the minerals resulting from the aqueous alteration in the early solar nebula, we know that the most common phyllosilicates present in chondritic extraterrestrial materials are serpentines, smectites, chlorites, and micas. The characterization of fine grained minerals in meteorites and IDP's rely heavily on electron beam instruments, especially transmission electron microscopy (TEM). Typically, phyllosilicates are identified by a combination of high resolution imaging of basal spacings, electron diffraction analysis, and chemical analysis. Smectites can be difficult to differentiate from micas because the smectites loose their interlayer water and the interlayers collapse to the same basal spacing as mica in the high vacuum of the TEM. In high-resolution TEM (HRTEM) images, smectite basal spacings vary from 1 nm up to 1.5 nm, while micas show 1 or 2 nm basal spacings. Not only is it difficult to differentiate smectites from micas, but there is no way of identifying different classes of smectites in meteorites and IDP's. To differentiate smectites from micas and also to recognize the charge differences among smectites, an alkylammonium method can be employed because the basal spacings of alkylammonium saturated smectites expand as a function of alkylamine chain length and the layer-charge density of the 2:1 expanding phyllosilicate, and the final product is significantly more stable under electron beam examination. Such a method was tested on standard clays and several meteorite samples using four alkylammonium salts. Author (revised)

N94-35433*# National Aeronautics and Space Administration. Lyndon B. Johnson Space Center, Houston, TX.

HIGH RESOLUTION TRANSMISSION ELECTRON MICROSCOPY (HRTEM) OF NANOPHASE FERRIC OXIDES **c25**

D. C. Golden (Dual and Associates, Houston, TX.), R. V. Morris, D. W. Ming, and H. V. Lauer, Jr. *In* Lunar and Planetary Inst., The Twenty-Fifth Lunar and Planetary Science Conference. Part 1: A-G 1994 p 437-438 (For primary document see N94-35395 11-91)
Avail: CASI HC A01/MF A04

Iron oxide minerals are the prime candidates for Fe(III) signatures in remotely sensed Martian surface spectra. Magnetic, Mossbauer, and reflectance spectroscopy have been carried out in the laboratory in order to understand the mineralogical nature of Martian analog ferric oxide minerals of submicron or nanometer size range. Out of the iron oxide minerals studied, nanometer sized ferric oxides are promising candidates for possible Martian spectral analogs. 'Nanophase ferric oxide (np-Ox)' is a generic term for ferric oxide/oxihydroxide particles having nanoscale (less than 10 nm) particle dimensions. Ferrihydrite, superparamagnetic particles of hematite, maghemite and goethite, and nanometer sized particles of inherently paramagnetic lepidocrocite are all examples of nanophase ferric oxides. np-Ox particles in general do not give X-ray diffraction (XRD) patterns with well defined peaks and would often be classified as X-ray amorphous. Therefore, different np-Oxs preparations should be characterized using a more sensitive technique e.g., high resolution transmission electron microscopy (HRTEM). The purpose of this study is to report the particle size, morphology and crystalline order, of five np-Ox samples by HRTEM imaging and electron diffraction (ED). Author

N94-35448*# Lunar and Planetary Inst., Houston, TX.

THE TWENTY-FIFTH LUNAR AND PLANETARY SCIENCE CONFERENCE. PART 3: P-Z Abstracts Only

1994 615 p Conference held in Houston, TX, 14-18 Mar. 1994
(Contract NASw-4574)
(NASA-CR-195745; NAS 1.26:195745) Avail: CASI HC A99/MF A06

Various papers on lunar and planetary science are presented, covering such topics as: impact craters, tektites, lunar geology, lava flow, geodynamics, chondrites, planetary geology, planetary surfaces, volcanology, tectonics, topography, regolith, metamorphic rock, geomorphology, lunar soil, geochemistry, petrology, cometary collisions, geochronology, weathering, and meteoritic composition. For individual titles, see N94-35449 through N94-35480.

N94-35449*# National Aeronautics and Space Administration. Lyndon B. Johnson Space Center, Houston, TX.

FeO AND MgO IN PLAGIOCLASE OF LUNAR ANORTHOSITES: IGNEOUS OR METAMORPHIC? Abstract Only **c90**

W. C. Phinney *In* Lunar and Planetary Inst., The Twenty-Fifth Lunar and Planetary Science Conference. Part 3: P-Z 1994 p 1081-1082 (For primary document see N94-35448 11-91)
Avail: CASI HC A01/MF A06

The combined evidence from terrestrial anorthosites and experimental laboratory studies strongly implies that lunar anorthosites have been subjected to high-grade metamorphic events that have erased the igneous signatures of FeO and MgO in their plagioclases. Arguments to the contrary have, to this point, been more hopeful than rigorous. Derived from text

N94-35450*# National Aeronautics and Space Administration. Lyndon B. Johnson Space Center, Houston, TX.

LUNA 24 REGOLITH BRECCIAS: A POSSIBLE SOURCE OF THE FINE SIZE MATERIAL OF THE LUNA 24 REGOLITH Abstract Only

O. D. Rode (Academy of Sciences, USSR, Moscow, USSR.) and M. M. Lindstrom *In* Lunar and Planetary Inst., The Twenty-Fifth Lunar and Planetary Science Conference. Part 3: P-Z 1994 p 1153-1154 (For primary document see N94-35448 11-91)
Avail: CASI HC A01/MF A06

The regolith breccias from the Luna 24 core were analyzed. The Luna 24 regolith is a mixture of fine and coarse grain materials. The comparable analysis of the grain size distributions, the modal and chemical compositions of the breccias, and the regolith from the same levels show that the friable slightly litificated breccia with a friable fine grain matrix may be a source of fine grain material of the Luna 24 present day regolith. Derived from text

N94-35451*# National Aeronautics and Space Administration. Lyndon B. Johnson Space Center, Houston, TX.

ANTARCTIC WEATHERING OF THE CK CHONDRITES EET90004, 90007, AND 90022: NICKEL AND SULFUR MOBILITY Abstract Only **c90**

C. S. Romanek, R. A. Socki, E. K. Gibson, Jr., and J. H. Allton *In* Lunar and Planetary Inst., The Twenty-Fifth Lunar and Planetary Science Conference. Part 3: P-Z 1994 p 1155-1156 (For primary document see N94-35448 11-91)
Avail: CASI HC A01/MF A06

CK chondrites are a relatively new class of carbonaceous chondrite that have been described in the literature. Most meteorites that comprise the CK group are restricted to Antarctic finds; therefore terrestrial weathering processes can influence the geochemical records contained within these chondrites. The paired CK chondrites EET90004, 90007, and 90022 share not only a common heritage but similar weathering histories since all three meteorites were found on Antarctic ice covered with thick evaporative coatings. Additional material has grown on these samples during curation at the Antarctic Meteorite Lab at JSC, NASA. At present, efflorescence up to a millimeter thick coats the surface of EET90004 and 90022, with less material coating EET90007. The chemistry, mineralogy, and isotopic composition of efflorescence on EET90004 and 90022, described here, provide valuable information regarding the fate of meteoritic components in the Antarctic environment. Derived from text

N94-35452*# National Aeronautics and Space Administration. Ames Research Center, Moffett Field, CA.

THERMAL EMISSION MEASUREMENTS (5-25 MICRONS) OF HAWAIIAN PALAGONITIC SOILS WITH IMPLICATIONS FOR MARS Abstract Only **c46**

Ted L. Roush (San Francisco State Univ., CA.) and James F. Bell, III *In* Lunar and Planetary Inst., The Twenty-Fifth Lunar and Planetary Science Conference. Part 3: P-Z 1994 p 1161-1162 (For primary document see N94-35448 11-91)
(Grant NAGw-2212; RTOP 151-01-60-01; RTOP 185-52-62-07)
Avail: CASI HC A01/MF A06

Careful laboratory studies have shown that the coloring agent in Mars analog Hawaiian palagonitic soils is nanophase iron oxide. We have measured the emissivity of two Mauna Kea palagonitic soils whose transmission spectra exhibit different spectral features and of a thermally-altered volcanic tephra sample that exhibits a wide range of crystallinity and degree of alteration (from black cinders to fully hematitic). Both of these samples may represent analogs for formation mechanisms involving the production of highly-altered secondary weathering products on Mars. The emission spectra of all samples were measured at the TES spectroscopy laboratory at Arizona State University. The data were converted to emissivity using blackbody measurements combined with measurements of each sample at different temperatures. Derived from text

N94-35453*# National Aeronautics and Space Administration. Ames Research Center, Moffett Field, CA.

THERMAL EMISSION MEASUREMENTS (5-25 MICRONS) OF PALAGONITE/Fe-SUBSTITUTED MONTMORILLONITE INTIMATE MIXTURES: APPLICATIONS TO MARS Abstract Only **c46**

Ted L. Roush (San Francisco State Univ., CA.) and James B. Orenberg

(San Francisco State Univ., CA.) *In* Lunar and Planetary Inst., The Twenty-Fifth Lunar and Planetary Science Conference. Part 3: P-Z 1994 p 1163-1164 (For primary document see N94-35448 11-91)
(RTOP 151-01-60-01; RTOP 185-52-62-07)
Avail: CASI HC A01/MF A06

The emissivity of a Mauna Kea palagonitic soil mixed with an Fe-substituted montmorillonite (FeM) was measured. The emission spectra of all samples were measured at the TES spectroscopy laboratory at Arizona State University. The data were converted to emissivity using blackbody measurements combined with measurements of each sample at different temperatures. This preliminary study has demonstrated that both naturally-occurring palagonites, thought to be good visible to near-IR spectral analogs for Mars, and FeM exhibit complex emissivity spectra at thermal wavelengths. FeM exhibits greater emissivity variations than palagonite, and emissivity peaks observed in the FeM spectrum allows its identification for abundances greater than or equal to 15 percent when mixed with palagonite. Smaller abundances of FeM are potentially identifiable when mixed with palagonite, but this remains to be determined.
Derived from text

N94-35454*# National Aeronautics and Space Administration. Ames Research Center, Moffett Field, CA.
TRANSMISSION MEASUREMENTS (4000-400 cm(EXP -1), 2.5-25 MICRONS) OF CRYSTALLINE FERRIC OXIDES AND FERRIC OXYHYDROXIDES: IMPLICATIONS FOR MARS Abstract Only c46
Ted L. Roush (San Francisco State Univ., CA.), James F. Bell, III, and Richard V. Morris *In* Lunar and Planetary Inst., The Twenty-Fifth Lunar and Planetary Science Conference. Part 3: P-Z 1994 p 1165-1166 (For primary document see N94-35448 11-91)
Avail: CASI HC A01/MF A06

Transmission spectra of three ferric oxides (two alpha-Fe2O3 samples and one gamma-Fe2O3 sample) and two ferric oxyhydroxides (alpha-FeOOH and gamma-FeOOH) were measured. This preliminary study has demonstrated that crystalline ferric oxides and ferric oxyhydroxides exhibit complex spectral features at thermal wavelengths. Some of these features suggest that thermal infrared observations of Mars can provide significant insight into the ferric mineralogy of that planet. The results of this study suggest that emissivity spectra of crystalline ferric oxides and ferric oxyhydroxides may prove quite important for the interpretation of thermal infrared spectral observations of Mars. Derived from text

N94-35455*# National Aeronautics and Space Administration. Lyndon B. Johnson Space Center, Houston, TX.
MORE SHOCK RECOVERY EXPERIMENTS ON MESOSIDERITE ANALOGS Abstract Only c90
L. R. Rowan and D. W. Mittlefehldt *In* Lunar and Planetary Inst., The Twenty-Fifth Lunar and Planetary Science Conference. Part 3: P-Z 1994 p 1167-1168 (For primary document see N94-35448 11-91)
Avail: CASI HC A01/MF A06

Mesosiderites, a small but unique group of stony-iron meteorites with affinities to howardites, eucrites, and pallasites, remain enigmatic in terms of their petrogenesis. They are composed of approximately equal weight proportions of Fe-Ni metal plus troilite and gabbroic, basaltic, and orthopyroxenitic materials. The metal and silicates, which display variable grain sizes and shapes, are delicately intermingled, forming irregular grain boundaries that have been attributed to a wide range of origins from subsolidus metamorphism to supersolidus igneous processes. Perhaps the most relevant question regarding the petrogenesis of mesosiderites is: what is the source and duration of heating that could produce the unequilibrated textures and chemistry of these meteorites? A leading candidate appears to be impacts of metallic core fragments with a differentiated asteroidal surface. This provides not only a suitable source of heat, but also the metal component uniquely required by mesosiderites. A series of shock recovery experiments on mesosiderite analogs has been continued. Textural and chemical similarities have been found that support an impact-derived origin for these unusual meteorites. Derived from text

N94-35456*# National Aeronautics and Space Administration. Lyndon B. Johnson Space Center, Houston, TX.
DISTRIBUTION OF SIDEROPHILE AND OTHER TRACE ELEMENTS IN MELT ROCK AT THE CHICXULUB IMPACT STRUCTURE Abstract Only c90
B. C. Schuraytz (Lunar and Planetary Inst., Houston, TX.), D. J. Lindstrom, R. R. Martinez, V. L. Sharpton, and L. E. Marin *In* Lunar and Planetary Inst., The Twenty-Fifth Lunar and Planetary Science Conference. Part 3: P-Z 1994 p 1221-1222 (For primary document see N94-35448 11-91)
Avail: CASI HC A01/MF A06

Recent isotopic and mineralogical studies have demonstrated a temporal and chemical link between the Chicxulub multiring impact basin and ejecta at the Cretaceous-Tertiary boundary. A fundamental problem yet to be resolved, however, is identification of the projectile responsible for this cataclysmic event. Drill core samples of impact melt rock from the Chichxulub structure contain Ir and Os abundances and Re-Os isotopic ratios indicating the presence of up to approx. 3 percent meteoritic material. We have used a technique involving microdrilling and high sensitivity instrumental neutron activation analysis (INAA) in conjunction with electron microprobe analysis to characterize further the distribution of siderophile and other trace elements among phases within the C1-N10 melt rock.
Author (revised)

N94-35457*# National Aeronautics and Space Administration. Lyndon B. Johnson Space Center, Houston, TX.
PRELIMINARY DESCRIPTION OF DOUBLE DRIVE TUBE 68002/68001 Abstract Only
Carol Schwarz (Lockheed Engineering and Sciences Co., Houston, TX.), Richard V. Morris, and Randy L. Korotev *In* Lunar and Planetary Inst., The Twenty-Fifth Lunar and Planetary Science Conference. Part 3: P-Z 1994 p 1223 (For primary document see N94-35448 11-91)
Avail: CASI HC A01/MF A06

Apollo 16 double drive tube 68002/68001 has been opened, and information on its contents and structure is now available. The sample was taken in Apr. 1972 at Station 8, a gently undulating surface of South Ray Crater ejecta material. The tube was driven into the surface about 2 m from the edge of a 10-15 m diameter crater in an area where small (less than 0.5 m diameter) craters are common. Fragments of the less than 1 cm diameter size are most abundant in this area. The top section, 68002, and the lower section, 68001, have a combined length of about 61 cm. Author (revised)

N94-35458*# National Aeronautics and Space Administration. Lyndon B. Johnson Space Center, Houston, TX.
CURRENT ACTIVITIES AND RESULTS OF THE LONG DURATION EXPOSURE FACILITY METEOROID AND DEBRIS SPECIAL INVESTIGATION GROUP Abstract Only c90
Thomas H. See (Lockheed Engineering and Sciences Co., Houston, TX.), Kimberly S. Leago (Lockheed Engineering and Sciences Co., Houston, TX.), Jack L. Warren (Lockheed Engineering and Sciences Co., Houston, TX.), Ronald P. Bernhard (Lockheed Engineering and Sciences Co., Houston, TX.), and Michael E. Zolensky *In* Lunar and Planetary Inst., The Twenty-Fifth Lunar and Planetary Science Conference. Part 3: P-Z 1994 p 1233-1234 (For primary document see N94-35448 11-91)
Avail: CASI HC A01/MF A06

Fiscal Year 1994 will bring to a close the initial investigative activities associated with the Long Duration Exposure Facility (LDEF). LDEF was a 14-faced spacecraft (i.e., 12-sided cylinder and two ends) which housed 54 different experimental packages in low-Earth orbit (LEO) from Apr. 1984 to Jan. 1990 (i.e., for approx. 5.75 years). Since LDEF's return, the Meteoroid & Debris Special Investigation Group (M&D SIG) has been examining various LDEF components in order to better understand and define the LEO particulate environment. Members of the M&D SIG at JSC in Houston, TX have been contributing to these studies by carefully examining and documenting all impact events found on LDEF's 6061-T6 aluminum Intercostals (i.e., one of the spacecraft's structural frame components). Unlike all other hardware on LDEF, the frame exposed significantly large surface areas of a single homogeneous material in all (i.e., 26) possible LDEF pointing directions. To date, 28 of the 68 Intercostals in the possession of the M&D SIG have been documented. This data, as well as similar information from various LDEF investigators, can be accessed through the M&D SIG Database which is maintained at JSC. Author (revised)

N94-35459*# National Aeronautics and Space Administration. Lyndon B. Johnson Space Center, Houston, TX.

INNOVATIVE INSTRUMENTATION FOR MINERALOGICAL AND ELEMENTAL ANALYSES OF SOLID EXTRATERRESTRIAL SURFACES: THE BACKSCATTER MOESSBAUER SPECTROMETER/X RAY FLUORESCENCE ANALYZER (BaMS/XRF) Abstract Only c25

T. D. Shelfer (National Academy of Sciences - National Research Council, Houston, TX.), Richard V. Morris, T. Nguyen, D. G. Agresti, and E. L. Wills *In* Lunar and Planetary Inst., The Twenty-Fifth Lunar and Planetary Science Conference. Part 3: P-Z 1994 p 1261-1262 (For primary document see N94-35448 11-91)

Avail: CASI HC A01/MF A06

We have developed a four-detector research-grade backscatter Moessbauer spectrometer (BaMS) instrument with low resolution x-ray fluorescence analysis (XRF) capability. A flight-qualified instrument based on this design would be suitable for use on missions to the surfaces of solid solar-system objects (Moon, Mars, asteroids, etc.). Target specifications for the flight instrument are as follows: mass less than 500 g; volumes less than 300 cu cm; and power less than 2 W. The BaMS/XRF instrument would provide data on the oxidation state of iron and its distribution among iron-bearing mineralogies and elemental composition information. This data is a primary concern for the characterization of extraterrestrial surface materials. Author (revised)

N94-35460*# National Aeronautics and Space Administration. Goddard Space Flight Center, Greenbelt, MD.

THE TOPOGRAPHY OF MARS: A RE-EVALUATION OF CURRENT DATA Abstract Only

D. E. Smith and M. T. Zuber *In* Lunar and Planetary Inst., The Twenty-Fifth Lunar and Planetary Science Conference. Part 3: P-Z 1994 p 1289-1290 (For primary document see N94-35448 11-91)

Avail: CASI HC A01/MF A06

Our present knowledge of the topography of Mars is completely inadequate for addressing a wide range of geophysical, geological, and atmospheric problems. The data acquired to date by several techniques has not provided us with reliable and consistent values for even the equatorial and polar radii, and large uncertainties exist in the altitudes of many of the major volcanic constructs. While much of this can be blamed on a lack of reliable data, we feel that much more could be done to improve the analysis of the present data in a consistent global system that would necessarily involve the re-analysis of early spacecraft and Earth-based data in conjunction with more recent models of Mars' gravity field. Author (revised)

N94-35461*# National Aeronautics and Space Administration. Goddard Space Flight Center, Greenbelt, MD.

THE MASS OF MARS, PHOBOS, AND DEIMOS, FROM THE ANALYSIS OF THE MARINER 9 AND VIKING ORBITER TRACKING DATA Abstract Only

D. E. Smith, F. G. Lemoine, and S. K. Fricke *In* Lunar and Planetary Inst., The Twenty-Fifth Lunar and Planetary Science Conference. Part 3: P-Z 1994 p 1291-1292 (For primary document see N94-35448 11-91)

Avail: CASI HC A01/MF A06

We have estimated the mass of Phobos, Deimos, and Mars using the Viking Orbiter and Mariner 9 tracking data. We divided the data into 282 arcs and sorted the data by periapse height, by inclination, and by satellite. The data were processed with the GEODYN/SOLVE orbit determination programs, which have previously been used to analyze planetary tracking data. The a priori Mars gravity field applied in this study was the 50th degree and order GMM-1 (Goddard Mars Model-1) model. The subsets of data were carefully edited to remove any arcs with close encounters of less than 500 km with either Phobos or Deimos. Whereas previous investigators have used close flybys (less than 500 km) to estimate the satellite masses, we have attempted to estimate the masses of Phobos and Deimos from multiday arcs which only included more distant encounters. The subsets of data were further edited to eliminate spurious data near solar conjunction (Nov.-Dec. 1976 and January 1979). In addition, the Viking-1 data from Oct. through Dec. 1978 were also excluded because of the low periapse altitude (as low as 232 km) and thus high sensitivity to atmospheric drag. Author (revised)

N94-35462*# National Aeronautics and Space Administration. Goddard Space Flight Center, Greenbelt, MD.

NOACHIAN AND HESPERIAN MODIFICATION OF THE ORIGINAL CHRYSE IMPACT BASIN TOPOGRAPHY Abstract Only

Stephanie Stockman (Science Systems and Applications, Inc., Lanham, MD.) and Herbert Frey *In* Lunar and Planetary Inst., The Twenty-Fifth Lunar and Planetary Science Conference. Part 3: P-Z 1994 p 1345-1346 (For primary document see N94-35448 11-91)

Avail: CASI HC A01/MF A06

We propose a new center (35.5 W, 32.5 N) and ring assignment for the original Chryse impact basin based on photogeologic mapping and re-examination of the published geology. Noachian features in the Chryse Planitia area are the best indicators of the original ancient multiringed impact structure. While other workers have centered the Chryse impact on the topographic low associated with Hesperian volcanic and fluvial deposits, we suggest that the center of the original Noachian-age excavation cavity was located 800 km farther NE, and the basin topography was significantly modified over time. Author (revised)

N94-35463*# National Aeronautics and Space Administration. Lyndon B. Johnson Space Center, Houston, TX.

INHOMOGENEOUS DISTRIBUTION OF MATERIALS IN LODRANITES-ACAPULCOITES AND IAB IRONS AND THEIR COMMON FORMATION PROCESSES Abstract Only

Hiroshi Takeda (Tokyo Univ., Japan.), Mayumi Otsuki (Tokyo Univ., Japan.), A. Yamaguchi (Tokyo Univ., Japan.), M. Miyamoto (Tokyo Univ., Japan.), Masayuki Otsuki (Japan Electron Optics Lab. Co. Ltd., Tokyo, Japan.), M. Tomobuchi (Kawasho Hightex Co. Ltd., Tokyo, Japan.), and Takahiro Hiroi *In* Lunar and Planetary Inst., The Twenty-Fifth Lunar and Planetary Science Conference. Part 3: P-Z 1994 p 1375-1376 (For primary document see N94-35448 11-91)

Avail: CASI HC A01/MF A06

The two-dimensional chemical mapping analysis (CMA) techniques of EPMA and XRF were applied to a new polished thin section (PTS) of EET84302,28, Acapulco and a 5x3 cm slice of Caddo County to find heterogeneous regional distribution of low temperature fractions in the lodranite-acapulcoite groups and silicate inclusions in the IAB irons. A region richer in metal-plagioclase was found in EET84302,28 and Caddo County. The mineralogy of EET84302,28 is not much different from coarse-grained, metal-rich acapulcoite-like mineral assemblage in EET84302,19, which has chromite-orthopyroxene segregation. Nearly uniform Mg/Fe ratios of silicates modified by reduction at regional oxygen fugacity and large difference in modal abundances of minerals in this meteorite group can be explained by regional concentration of materials when the source materials were partly melted. Author (revised)

N94-35464*# National Aeronautics and Space Administration. Goddard Space Flight Center, Greenbelt, MD.

FIRST OBSERVATION OF A MASS INDEPENDENT ISOTOPIC FRACTIONATION IN A CONDENSATION REACTION Abstract Only c25

M. H. Thiemens (California Univ., San Diego, La Jolla, CA.), R. Nelson (California Univ., San Diego, La Jolla, CA.), Q. W. Dong (California Univ., San Diego, La Jolla, CA.), and Joseph A. Nuth, III *In* Lunar and Planetary Inst., The Twenty-Fifth Lunar and Planetary Science Conference. Part 3: P-Z 1994 p 1389-1390 (For primary document see N94-35448 11-91)

Avail: CASI HC A01/MF A06

Thiemens and Heidenreich (1983) first demonstrated that a chemically produced mass independent isotopic fractionation process could produce an isotopic composition which is identical to that observed in Allende inclusions. This raised the possibility that the meteoritic components could be produced by chemical, rather than nuclear processes. In order to develop a mechanistic model of the early solar system, it is important that relevant reactions be studied, particularly, those which may occur in the earliest condensation reactions. The isotopic results for isotopic fractionations associated with condensation processes are reported. A large mass independent isotopic fractionation is observed in one of the experiments. Derived from text

N94-35465*# National Aeronautics and Space Administration. Lyndon B. Johnson Space Center, Houston, TX.

ANATOMY OF A CLUSTER IDP. PART 2: NOBLE GAS ABUNDANCES, TRACE ELEMENT GEOCHEMISTRY, ISOTOPIC ABUNDANCES, AND TRACE ORGANIC CHEMISTRY OF SEVERAL FRAGMENTS FROM L2008#5 Abstract Only **c90**

K. L. Thomas (Lockheed Engineering and Sciences Co., Houston, TX.), S. J. Clemett (Stanford Univ., CA.), G. J. Flynn (State Univ. of New York, Plattsburgh, NY.), L. P. Keller (MVA, Inc., Norcross, GA.), David S. McKay, S. Messenger, A. O. Nier, D. J. Schlutter, S. R. Sutton, and R. M. Walker et al *In* Lunar and Planetary Inst., The Twenty-Fifth Lunar and Planetary Science Conference. Part 3: P-Z 1994 p 1391-1392 (For primary document see N94-35448 11-91)

Avail: CASI HC A01/MF A06

The topics discussed include the following: noble gas content and release temperatures; trace element abundances; heating summary of cluster fragments; isotopic measurements; and trace organic chemistry. CASI

N94-35466*# National Aeronautics and Space Administration. Lyndon B. Johnson Space Center, Houston, TX.

THE ANATOMY OF A CLUSTER IDP. PART 1: CARBON ABUNDANCE, BULK CHEMISTRY, AND MINERALOGY OF FRAGMENTS FROM L2008#5 Abstract Only **c90**

K. L. Thomas (Lockheed Engineering and Sciences Co., Houston, TX.), L. P. Keller (MVA, Inc., Norcross, GA.), W. Klock (Muenster Univ., Germany.), J. Warren (Lockheed Engineering and Sciences Co., Houston, TX.), G. E. Blanford (Houston Univ., Clear Lake, TX.), and David S. McKay *In* Lunar and Planetary Inst., The Twenty-Fifth Lunar and Planetary Science Conference. Part 3: P-Z 1994 p 1393-1394 (For primary document see N94-35448 11-91)

Avail: CASI HC A01/MF A06

The objective of this study was to determine whether or not cluster particles are sufficiently homogeneous to enable observations from one fragment of the cluster to be extrapolated to the entire cluster. We report on the results of a consortium study of the fragments of a large cluster particle. Multiple fragments from one large cluster were distributed to several research groups and were subjected to a variety of mineralogical and chemical analyses including: SEM, TEM, ion probe, SXRF, noble gas measurements, and microprobe laser mass spectrometry of individual fragments. Derived from text

N94-35467*# National Aeronautics and Space Administration. Lyndon B. Johnson Space Center, Houston, TX.

THE PARENT MAGMA OF XENOLITHS IN SHERGOTTITE EETA79001: BULK AND TRACE ELEMENT COMPOSITION INFERRED FROM MAGMATIC INCLUSIONS Abstract Only **c90**

Allan H. Treiman (Lunar and Planetary Inst., Houston, TX.), David J. Lindstrom, and Rene R. Martinez *In* Lunar and Planetary Inst., The Twenty-Fifth Lunar and Planetary Science Conference. Part 3: P-Z 1994 p 1417-1418 (For primary document see N94-35448 11-91)
(RTOP 152-14-40-22)

Avail: CASI HC A01/MF A06

The SNC meteorites are samples of the Martian crust, so inferences about their origins and parent magmas are of wide planetologic significance. The EETA79001 shergottite, a basalt, contains xenoliths of pyroxene-olivine cumulate rocks which are possibly related to the ALHA77005 and LEW88516 SNC lherzolites. Olivines in the xenoliths contain magmatic inclusions, relics of magma trapped within the growing crystals. The magmatic inclusions allow a parent magma composition to be retrieved; it is similar to the composition reconstructed from xenolith pyroxenes by element distribution coefficients. The xenolith parent magma is similar but not identical to parent magmas for the shergottite lherzolites. Derived from text

N94-35468*# National Aeronautics and Space Administration. Ames Research Center, Moffett Field, CA.

THE TEMPERATURE OF NITROGEN ON PLUTO Abstract Only

K. A. Tryka (California Inst. of Tech., Pasadena, CA.), R. H. Brown (Jet Propulsion Lab., California Inst. of Tech., Pasadena, CA.), D. P. Cruikshank, and T. C. Owen *In* Lunar and Planetary Inst., The Twenty-Fifth Lunar and Planetary Science Conference. Part 3: P-Z 1994 p 1419-1420 (For primary document see N94-35448 11-91)

Avail: CASI HC A01/MF A06

With Hapke scattering theory and absorption coefficients derived from our laboratory measurements of solid N2 we have modeled the spectrum of Triton. By comparing a Hapke scattering model to the measured spectrum from Triton, we determined the temperature of the N2 on the satellite's surface to be 38 (+2, -1) K which is in accord with the measurements of Voyager 2. Applying this technique to Pluto we find that the temperature of N2 on that body is 40 +/- 2 K. Other aspects of this investigation are discussed. Derived from text

N94-35469*# National Aeronautics and Space Administration. Ames Research Center, Moffett Field, CA.

PURITY AND CLEANNESS OF AEROGEL AS A COSMIC DUST CAPTURE MEDIUM Abstract Only **c27**

P. Tsou (Jet Propulsion Lab., California Inst. of Tech., Pasadena, CA.), R. H. Fleming (Evans, Charles and Associates, Redwood City, CA.), P. M. Lindley (Evans, Charles and Associates, Redwood City, CA.), A. Y. Craig (Evans, Charles and Associates, Redwood City, CA.), and D. Blake *In* Lunar and Planetary Inst., The Twenty-Fifth Lunar and Planetary Science Conference. Part 3: P-Z 1994 p 1421-1422 (For primary document see N94-35448 11-91)

Avail: CASI HC A01/MF A06

The capability for capturing micrometeoroids intact through laboratory simulations and in space in passive underdense silica aerogel offers a valuable tool for cosmic dust research. The integrity of the sample handling medium can substantially modify the integrity of the sample. Intact capture is a violent hypervelocity event: the integrity of the capturing medium can cause even greater modification of the sample. Doubts of the suitability of silica aerogel as a capture medium were raised at the 20th LPSC, and questions were raised again at the recent workshop on Particle Capture, Recovery, and Velocity Trajectory Measurement Technologies. Assessment of aerogel's volatile components and carbon contents have been made. We report the results of laboratory measurements of the purity and cleanliness of silica aerogel used for several Sample Return Experiments flown on the Get Away Special program. Derived from text

N94-35470*# National Aeronautics and Space Administration. Lyndon B. Johnson Space Center, Houston, TX.

A QUICK LOOK METHOD OF DETECTING WATER OF HYDRATION IN SMALL SOLAR SYSTEM BODIES Abstract Only **c90**

F. Vilas *In* Lunar and Planetary Inst., The Twenty-Fifth Lunar and Planetary Science Conference. Part 3: P-Z 1994 p 1439-1440 (For primary document see N94-35448 11-91)

Avail: CASI HC A01/MF A06

The action of aqueous alteration of the near-subsurface material on asteroids and probably some satellites in the Solar System constitutes part of the formation history of the Solar System. The C-class asteroids (and subclasses B, G, and F) were initially believed to have undergone aqueous alteration based on their low albedos and neutral broadband visible and near-infrared colors. These spectra exhibit a sharp drop at wavelengths shorter than 0.55 microns due to a strong ferric oxide intervalence change transfer transition. This IVCT comprises multiple absorptions that are not uniquely indicative of phyllosilicates, but rather are present in the spectrum of any object containing Fe(2+) and Fe(3+) in its surface material. A definitive indication of aqueous alteration came when the broad IR absorption feature having a minimum near 3.0 microns indicative of structural hydroxyl (OH) and interlayer and and absorbed water in phyllosilicates was identified in the IR photometry of many C-class asteroids. Additional mineralogical compositional evidence of aqueously-altered asteroids has come as the result of high SNR narrowband spectrophotometry in the visible and near-infrared spectral regions taken using a CCD/spectrograph combination. An absorption feature centered at 0.7 microns indicative of an Fe(2+) - Fe(3+) charge transfer transition in oxidized iron in phyllosilicates in spectra of some low-albedo asteroids, especially C and G class, and CM2 carbonaceous chondrite meteorites was identified in the CCD spectra. The correlation and covariance of the 0.7-micron and 3.0-micron features were examined by comparing observations of asteroids common to both the CCD reflectance spectra and the 3.0-micron multicolor photometry data sets. Thirty-one pairs of observations were included in this training group. The results of the statistical study indicate that with a 95% confidence level, 84% of the objects observed either having or not having the 0.7-micron feature will correspondingly have the 3.0-micron water of hydration feature. Derived from text

N94-35471*# National Aeronautics and Space Administration. Goddard Space Flight Center, Greenbelt, MD.

CHONDRULE MAGNETIC PROPERTIES Abstract Only **c90**

P. J. Wasilewski and M. V. OBryan *In* Lunar and Planetary Inst., The Twenty-Fifth Lunar and Planetary Science Conference. Part 3: P-Z 1994 p 1467-1468 (For primary document see N94-35448 11-91)

Avail: CASI HC A01/MF A06

The topics discussed include the following: chondrule magnetic properties; chondrules from the same meteorite; and REM values (the ratio for remanence initially measured to saturation remanence in 1 Tesla field). The preliminary field estimates for chondrules magnetizing environments range from minimal to a least several mT. These estimates are based on REM values and the characteristics of the remanence initially measured (natural remanence) thermal demagnetization compared to the saturation remanence in 1 Tesla field demagnetization. CASI

N94-35472*# National Aeronautics and Space Administration. Lyndon B. Johnson Space Center, Houston, TX.

LUNAR LIGO AND GRAVITATIONAL WAVE ASTRONOMY ON THE MOON Abstract Only

Thomas L. Wilson and Norman LaFave *In* Lunar and Planetary Inst., The Twenty-Fifth Lunar and Planetary Science Conference. Part 3: P-Z 1994 p 1499-1500 (For primary document see N94-35448 11-91)

Avail: CASI HC A01/MF A06

Gravitational wave astronomy continues to be one of the exploration concepts under consideration in NASA's strategy for conducting physics and astrophysics from the lunar surface. As with other proposals for new concepts in science and astronomy from the Moon, this one has a number of very interesting features which need to be developed further in order to assess them adequately. The possibility of robotic deployment of a gravitational wave antenna on the Moon in a triangular configuration and the question of closure on the third interferometer leg are discussed here. Derived from text

N94-35473*# National Aeronautics and Space Administration. Lyndon B. Johnson Space Center, Houston, TX.

ADVANCED TECHNOLOGY LUNAR TELESCOPE Abstract Only **c89**

Thomas L. Wilson, Wei-Kan Chu, and Peter C. Chen *In* Lunar and Planetary Inst., The Twenty-Fifth Lunar and Planetary Science Conference. Part 3: P-Z 1994 p 1501-1502 (For primary document see N94-35448 11-91)

Avail: CASI HC A01/MF A06

A new type of telescope pointing system designed specifically for space and lunar applications will be discussed, based upon a prototype advanced technology telescope under investigation. The focus here will be the system of hybrid superconductor magnetic bearings (HSMB) used to provide isolation support and steering functions. HSMB's are combinations of high temperature superconductors, permanent magnets, and coils, being passive (requiring no power), noncontact, and essentially frictionless. These also are well suited to long-term unattended operation in the space environment. The characteristics of these subsystems, their expected behavior under space vacuum, and thermal and radiation environments are discussed. Derived from text

N94-35474*# National Aeronautics and Space Administration. Ames Research Center, Moffett Field, CA.

WINDBLOWN SAND ON MARS: THE EFFECT OF SALTATION THRESHOLD ON DRIFT POTENTIALS DERIVED FROM MARS GCM Abstract Only

P. Xu (Arizona State Univ., Tempe, AZ.), R. Greeley (Arizona State Univ., Tempe, AZ.), S. Williams (Arizona State Univ., Tempe, AZ.), and J. B. Pollack *In* Lunar and Planetary Inst., The Twenty-Fifth Lunar and Planetary Science Conference. Part 3: P-Z 1994 p 1521-1522 (For primary document see N94-35448 11-91)

Avail: CASI HC A01/MF A06

The rate at which the wind can redistribute sedimentary material is an important part of any planet's sedimentologic cycle, particularly for Mars, where the competing effects of other gradational processes are less than on Earth. The aeolian drift potential (DP) is a measure of the amount of material capable of being moved through a unit length by the wind for a given period of time. DP is a useful measure of the potential redistribution rate of windblown material on regional scales. The Martian aeolian DP was calculated from laboratory studies of sand movement conducted at Martian atmospheric densities and from surface stress, temperature, and pressure values for that region as determined from the Mars General (Atmospheric) Circulation Model (GCM) developed at the NASA/Ames Research Center. In our simulations for Mars, DP changes in both magnitude (as expected) and direction if the saltation threshold is altered. Derived from text

N94-35475*# National Aeronautics and Space Administration. Ames Research Center, Moffett Field, CA.

SIMULTANEOUS ADSORPTION OF CO2 AND H2O UNDER MARS-LIKE CONDITIONS AND APPLICATION TO THE EVOLUTION OF THE MARTIAN CLIMATE Abstract Only

Aaron P. Zent and Richard Quinn *In* Lunar and Planetary Inst., The Twenty-Fifth Lunar and Planetary Science Conference. Part 3: P-Z 1994 p 1543-1544 (For primary document see N94-35448 11-91)

Avail: CASI HC A01/MF A06

The Martian regolith is the most substantial volatile reservoir on the planet; it holds CO2 as adsorbate, and can exchange that CO2 with the atmosphere-cap system over timescales of 10(exp 5) to 10(exp 6) years. The climatic response to insolation changes caused by obliquity and eccentricity variations depends in part on the total reservoir of adsorbed CO2. Previous estimates of the adsorbate inventory have been made by measuring the adsorptive behavior of one or more Mars-analyog materials, and deriving an empirical equation that described that adsorption as a function of the partial pressure of CO2 and the temperature of the regolith. The current CO2 inventory is that which satisfies adsorptive equilibrium, observed atmospheric pressure, and no permanent CO2 caps. There is laboratory evidence that H2O poisons the CO2 adsorptive capacity of most materials. No consideration of CO2 - H2O co-adsorption was given in previous estimates of the Martian CO2 inventory, although H2O is present in the vapor phase, and so as adsorbate, throughout the regolith. Derived from text

N94-35476*# National Aeronautics and Space Administration. Lyndon B. Johnson Space Center, Houston, TX.

MINERALOGY OF AN UNUSUAL CM CLAST IN THE KAIDUN METEORITE Abstract Only **c90**

M. E. Zolensky, A. V. Ivanov, S. V. Yang, R. A. Barrett, and L. Browning *In* Lunar and Planetary Inst., The Twenty-Fifth Lunar and Planetary Science Conference. Part 3: P-Z 1994 p 1565-1566 (For primary document see N94-35448 11-91)

Avail: CASI HC A01/MF A06

Kaidun is breccia of disparate enstatite and carbonaceous chondrite clasts, and continues to provide real surprises. Many Daidun clasts have been intensely altered by an aqueous fluid, as evidenced by the widespread occurrence of ferromagnesian phyllosilicates and presence of carbonate- and phyllosilicate-filled veins. In this report we describe an unusual CM lithology containing beautiful aggregates of jackstraw pyrrhotites, not previously reported from any meteorite. Derived from text

N94-35477*# National Aeronautics and Space Administration. Lyndon B. Johnson Space Center, Houston, TX.

MINERALOGY OF ARTIFICIALLY HEATED CARBONACEOUS CHONDRITES Abstract Only **c90**

M. E. Zolensky, M. E. Lipschutz, and T. Hiroi *In* Lunar and Planetary Inst., The Twenty-Fifth Lunar and Planetary Science Conference. Part 3: P-Z 1994 p 1567-1568 (For primary document see N94-35448 11-91)

Avail: CASI HC A01/MF A06

We have examined suites of heated Murchison (CM2) and Allende (CV3) samples heated in the range 400-1200 C, in a H2 atmosphere with a pressure of 10(exp 5) bar for periods of 1 to 4 weeks. We used a combination of X-ray diffraction, electron microprobe and TEM analyses to determine the mineralogy of these samples. Author

N94-35478*# National Aeronautics and Space Administration. Lyndon B. Johnson Space Center, Houston, TX.

LUNAR HORIZON GLOW AND THE CLEMENTINE MISSION Abstract Only

H. A. Zook and A. E. Potter *In* Lunar and Planetary Inst., The Twenty-Fifth

Lunar and Planetary Science Conference. Part 3: P-Z 1994 p 1573-1574 (For primary document see N94-35448 11-91)
Avail: CASI HC A01/MF A06

The Clementine spacecraft is to be launched into Earth orbit in late January for subsequent insertion into lunar orbit in late February, 1994. There, its primary mission is to produce -- over a period of about two months -- a new photographic map of the entire surface of the Moon; this will be done, in a variety of wavelengths and spatial resolutions, in a manner greatly superior to that previously accomplished for the whole Moon. It will then go on to fly by and photograph the asteroid Geographos. A secondary goal that has been accepted for this mission is to take a series of photographs designed to capture images of, and determine the brightness and extent of, the Lunar Horizon Glow (LHG). One form of LHG is caused by the solar stimulation of emission from Na and K atoms in the lunar exosphere. The scale height of this exosphere is of the order of 100 km. There are also brighter LHG components, with much smaller scale heights, that appear to be caused by scattered off of an exospheric lunar dust cloud. Derived from text

N94-35479*# National Aeronautics and Space Administration. Goddard Space Flight Center, Greenbelt, MD.
RHEOLOGY, TECTONICS, AND THE STRUCTURE OF THE VENUS LITHOSPHERE Abstract Only
M. T. Zuber (Johns Hopkins Univ., Baltimore, MD.) *In* Lunar and Planetary Inst., The Twenty-Fifth Lunar and Planetary Science Conference. Part 3: P-Z 1994 p 1575-1576 (For primary document see N94-35448 11-91)
Avail: CASI HC A01/MF A06

Given the absence of ground truth information on seismic structure, heat flow, and rock strength, or short wavelength gravity or magnetic data for Venus, information on the thermal, mechanical and compositional nature of the shallow interior must be obtained by indirect methods. Using pre-Magellan data, theoretical models constrained by the depths of impact craters and the length scales of tectonic features yielded estimates on the thickness of Venus' brittle-elastic lithosphere and the allowable range of crustal thickness and surface thermal gradient. The purpose of this study is to revisit the question of the shallow structure of Venus based on Magellan observations of the surface and recent experiments that address Venus' crustal rheology. Derived from text

N94-35480*# National Aeronautics and Space Administration. Goddard Space Flight Center, Greenbelt, MD.
FORMATION OF FOLD AND THRUST BELTS ON VENUS DUE TO HORIZONTAL SHORTENING OF A LATERALLY HETEROGENEOUS LITHOSPHERE Abstract Only
M. T. Zuber (Johns Hopkins Univ., Baltimore, MD.), E. M. Parmentier (Brown Univ., Providence, RI.), and G. A. Neumann (Johns Hopkins Univ., Baltimore, MD.) *In* Lunar and Planetary Inst., The Twenty-Fifth Lunar and Planetary Science Conference. Part 3: P-Z 1994 p 1577-1578 (For primary document see N94-35448 11-91)
Avail: CASI HC A01/MF A06

An outstanding question relevant to understanding the tectonics of Venus is the mechanism of formation of fold and thrust belts, such as the mountain belts that surround Lakshmi Planum in western Ishtar Terra. These structures are typically long (hundreds of km) and narrow (many tens of km), and are often located at the margins of relatively high (km-scale) topographic rises. Previous studies have attempted to explain fold and thrust belts in various areas of Venus in the context of viscous and brittle wedge theory. However, while wedge theory can explain the change in elevation from the rise to the adjacent lowland, it fails to account for a fundamental aspect of the deformation, i.e., the topographic high at the edge of the rise. In this study we quantitatively explore the hypothesis that fold and thrust belt morphology on Venus can alternatively be explained by horizontal shortening of a lithosphere that is laterally heterogeneous, due either to a change in thickness of the lithosphere or the crust. Lateral heterogeneities in lithosphere structure may arise in response to thermal thinning or extensive faulting, while variations in crustal thickness may arise due to either spatially variable melting of mantle material or by horizontal shortening of the crust. In a variable thickness lithosphere or crust that is horizontally shortened, deformation will tend to localize in the vicinity of thickness heterogeneity, resulting in a higher component of dynamic topography there as compared to elsewhere in the shortening lithosphere. This mechanism may thus provide a simple explanation for the topographic high at the edge of the rise. Derived from text

N94-35504* Jet Propulsion Lab., California Inst. of Tech., Pasadena, CA.
GALILEO: THE JOVIAN LABORATORY (Videotape)
Oct. 1989 Videotape: 6 min. playing time, in color, with sound
(NASA-CR-196043; NONP-NASA-VT-94-15912) Avail: CASI VHS A01/BETA A22

This video presentation gives a pre-launch description of the Galileo Mission. CASI

N94-35505* Jet Propulsion Lab., California Inst. of Tech., Pasadena, CA.
VOYAGER: NATIONAL AIR AND SPACE MUSEUM (Videotape)
Oct. 1989 Videotape: 4 min. 30 sec. playing time, in color, with sound
(NASA-CR-195905; NONP-NASA-VT-94-15913) Avail: CASI VHS A01/BETA A22

A recap of the travels of the Voyager spacecraft to the outer planets is presented. (This video was originally made for a talk at the National Air and Space Museum. CASI

N94-35506* Jet Propulsion Lab., California Inst. of Tech., Pasadena, CA.
VOYAGER LAST PICTURE SHOW (Videotape)
Sep. 1989 Videotape: 5 min. 30 sec. playing time, in color, with sound
(NASA-CR-195796; NONP-NASA-VT-94-15914) Avail: CASI VHS A01/BETA A22

This video presentation blends animation, actual photos, and data of the Voyager-Neptune encounter. CASI

N94-35507* Jet Propulsion Lab., California Inst. of Tech., Pasadena, CA.
ATMOSPHERE OF VENUS (Videotape)
Nov. 1990 Videotape: 2 min. 18 sec. playing time, in color, with sound
(NASA-CR-194214; NONP-NASA-VT-94-15915) Avail: CASI VHS A01/BETA A22

This video presents preliminary results as seen through the violet filter of the Galileo Solid State Imaging System. CASI

N94-35508* Jet Propulsion Lab., California Inst. of Tech., Pasadena, CA.
GALILEO EARTH/MOON 1 ENCOUNTER (Videotape)
Dec. 1990 Videotape: 3 min. 1 sec. playing time, in color, with sound
(NASA-CR-195545; NONP-NASA-VT-94-15916) Avail: CASI VHS A01/BETA A22

This video presents sequences of Galileo images showing the dynamics of the Earth-Moon system. CASI

N94-35509* Jet Propulsion Lab., California Inst. of Tech., Pasadena, CA.
MAGELLAN COLLECTION OF RADAR CALIBRATION RESULTS (Videotape)
Nov. 1990 Videotape: 8 min. 40 sec. playing time, in color, with sound
(NASA-CR-194753; NONP-NASA-VT-94-15917) Avail: CASI VHS A01/BETA A22

This video presents three sequences acquired by Magellan, Aug.-Oct 1990 and includes the globe of Venus in black and white, the Golubkina crater, and 12 short scenes of different pan moves. CASI

N94-35513* Jet Propulsion Lab., California Inst. of Tech., Pasadena, CA.
VOYAGER SCIENCE SUMMARY TAPE (Videotape)
Jun. 1990 Videotape: 28 min. 21 sec. playing time, in color, with sound
(NASA-CR-195909; NONP-NASA-VT-94-15921) Avail: CASI VHS A01/BETA A22

A summary of Voyager science is presented by Dr. Edward Stone (originally part of a press conference on June 6, 1990). CASI

N94-36136*# Lunar and Planetary Inst., Houston, TX.
THE TWENTY-FIFTH LUNAR AND PLANETARY SCIENCE CONFERENCE. PART 2: H-O Abstracts Only
1994 614 p Conference held in Houston, TX, 14-18 Mar. 1994
(Contract NASw-4574)
(NASA-CR-195744; NAS 1.26:195744) Avail: CASI HC A99/MF A06

Various papers on lunar and planetary science are presented, covering such topics as: planetary geology, lunar geology, meteorites, shock loads, cometary collisions, planetary mapping, planetary atmospheres, chondrites, chondrules, planetary surfaces, impact craters, lava flow, achondrites, geochemistry, stratigraphy, micrometeorites, tectonics, mineralogy, petrology, geomorphology, and volcanology. For individual titles, see N94-36137 through N94-36174.

N94-36137*# National Aeronautics and Space Administration. Ames Research Center, Moffett Field, CA.
ATMOSPHERIC EFFECTS ON THE MAPPING OF MARTIAN THERMAL INERTIA AND THERMALLY DERIVED ALBEDO Abstract Only
J. N. Hayashi (Colorado Univ., Boulder, CO.), B. M. Jakosky (Colorado Univ., Boulder, CO.), and R. M. Haberle *In* Lunar and Planetary Inst., The Twenty-Fifth Lunar and Planetary Science Conference. Part 2: H-O 1994 p 517-518 (For primary document see N94-36136 11-91)
Avail: CASI HC A01/MF A06

The most widely used thermal inertia data for Mars assumes the atmospheric contribution is constant and equal to 2 percent of the maximum solar insolation. Haberle and Jakosky investigated the effect of including a dusty CO2 atmosphere and sensible heat exchange with the surface on thermal inertia. We recently utilized Haberle and Jakosky's coupled surface-atmosphere model to investigate the effects of such an atmosphere on the thermally derived albedo. The thermally derived albedo is the albedo which, together with the thermal inertia, provides model surface temperatures which best match the observed temperatures. New maps are presented of thermal inertia and thermally derived albedo which incorporate dust opacities derived from IRTM data. Derived from text

N94-36138*# National Aeronautics and Space Administration. Lyndon B. Johnson Space Center, Houston, TX.
PETROGRAPHIC CHARACTERIZATION OF LUNAR SOILS: APPLICATION OF X RAY DIGITAL-IMAGING TO QUANTITATIVE AND AUTOMATED ANALYSIS Abstract Only
Stefan J. Higgins (Tennessee Univ., Knoxville, TN.), Allan Patchen (Tennessee Univ., Knoxville, TN.), John G. Chambers (Tennessee Univ., Knoxville, TN.), Lawrence A. Taylor (Tennessee Univ., Knoxville, TN.), and David S. McKay *In* Lunar and Planetary Inst., The Twenty-Fifth Lunar and Planetary Science Conference. Part 2: H-O 1994 p 547-548 (For primary document see N94-36136 11-91)
Avail: CASI HC A01/MF A06

The rocks and soils of the moon will be the raw materials for various engineering needs at a lunar base, such as sources of hydrogen, oxygen, metals, etc. The material of choice for most of the bulk needs is the regolith and its less than 1 cm fraction, the soil. For specific mineral resources it may be necessary to concentrate minerals from either rocks or soils. Therefore, quantitative characterizations of these rocks and soils are necessary in order to better define their mineral resource potential. However, using standard point-counting microscopic procedures, it is difficult to quantitatively determine mineral abundances and virtually impossible to obtain data on mineral distributions within grains. As a start to fulfilling these needs, Taylor et al. and Chambers et al. have developed a procedure for characterization of crushed lunar rocks using x ray digital imaging. The development of a similar digital imaging procedure for lunar soils as obtained from a spectrometer is described. Derived from text

N94-36139*# National Aeronautics and Space Administration. Lyndon B. Johnson Space Center, Houston, TX.
POSSIBLE SPINEL ABSORPTION BANDS IN S-ASTEROID VISIBLE REFLECTANCE SPECTRA Abstract Only
T. Hiroi, F. Vilas, and J. M. Sunshine *In* Lunar and Planetary Inst., The Twenty-Fifth Lunar and Planetary Science Conference. Part 2: H-O 1994 p 553-554 (For primary document see N94-36136 11-91)
(Grant NAGw-748)
Avail: CASI HC A01/MF A06

Minor absorption bands in the 0.55 to 0.7 micron wavelength range of reflectance spectra of 10 S asteroids have been found and compared with those of spinel-group minerals using the modified Gaussian model. Most of these S asteroids are consistently shown to have two absorption bands around 0.6 and 0.67 micron. Of the spinel-group minerals examined in this study, the 0.6 and 0.67 micron bands are most consistent with those seen in chromite. Recently, the existence of spinels has also been detected from the absorption-band features around 1 and 2 micron of two S-asteroid reflectance spectra, and chromite has been found in a primitive achondrite as its major phase. These new findings suggest a possible common existence of spinel-group minerals in the solar system. Derived from text

N94-36140*# National Aeronautics and Space Administration. Lyndon B. Johnson Space Center, Houston, TX.
SHOCKED MATERIALS FROM THE DUTCH PEAK DIAMICTITE, UTAH Abstract Only **c90**
F. Hoerz, T. E. Bunch, and V. R. Oberbeck *In* Lunar and Planetary Inst., The Twenty-Fifth Lunar and Planetary Science Conference. Part 2: H-O 1994 p 565-566 (For primary document see N94-36136 11-91)
Avail: CASI HC A01/MF A06

Evidence of shock metamorphism in the Dutch Peak diamictite in the Sheeprock Mountains, Utah, is reported. The Dutch Peak diamictite is of Proterozoic age and is a minor part of the Dutch Peak formation. A shocked sample, specimen A250, was collected during a brief visit of the Harker Canyon area of the Sheeprock Mountains. This sample consists of equant, anhedral grains of quartz, K-feldspar, and plagioclase. The crystallographic orientation of 244 lamellae systems in 106 grains was measured. It is presently difficult to evaluate the significance of this single specimen. Without additional and substantial field work, and petrographic characterization of this formation, a number of scenarios for the presence of a shocked clast and the emplacement of the entire formation remain viable. Derived from text

N94-36141*# National Aeronautics and Space Administration. Lyndon B. Johnson Space Center, Houston, TX.
EXPERIMENTAL IMPACTS INTO TEFLON TARGETS AND LDEF THERMAL BLANKETS Abstract Only **c90**
F. Hoerz, M. J. Cintala, M. E. Zolensky, R. P. Bernhard, and T. H. See *In* Lunar and Planetary Inst., The Twenty-Fifth Lunar and Planetary Science Conference. Part 2: H-O 1994 p 567-568 (For primary document see N94-36136 11-91)
Avail: CASI HC A01/MF A06

The Long Duration Exposure Facility (LDEF) exposed approximately 20 sq m of identical thermal protective blankets, predominantly on the Ultra-Heavy Cosmic Ray Experiment (UHCRE). Approximately 700 penetration holes greater than 300 micron in diameter were individually documented, while thousands of smaller penetrations and craters occurred in these blankets. As a result of their 5.7 year exposure and because they pointed into a variety of different directions relative to the orbital motion of the nonspinning LDEF platform, these blankets can reveal important dynamic aspects of the hypervelocity particle environment in near-earth orbit. The blankets were composed of an outer teflon layer (approximately 125 micron thick), followed by a vapor-deposited rear mirror of silver (less than 1000 A thick) that was backed with an organic binder and a thermal protective paint (approximately 50 to 75 micron thick), resulting in a cumulative thickness (T) of approximately 175 to 200 microns for the entire blanket. Many penetrations resulted in highly variable delaminations of the teflon/metal or metal/organic binder interfaces that manifest themselves as 'dark' halos or rings, because of subsequent oxidation of the exposed silver mirror. The variety of these dark albedo features is bewildering, ranging from totally absent, to broad halos, to sharp single or multiple rings. Over the past year experiments were conducted over a wide range of velocities (i.e., 1 to 7 km/s) to address velocity dependent aspects of cratering and penetrations of teflon targets. In addition, experiments were performed with real LDEF thermal blankets to duplicate the LDEF delaminations and to investigate a possible relationship of initial impact conditions on the wide variety of dark halo and ring features.
Derived from text

N94-36142*# National Aeronautics and Space Administration. Lyndon B. Johnson Space Center, Houston, TX.
DUST EVOLUTION FROM COMETS AND ASTEROIDS: THEIR VELOCITIES AT EARTH ORBIT INTERSECTION Abstract Only **c90**
A. A. Jackson (Lockheed Engineering and Sciences Co., Houston, TX.) and H. A. Zook *In* Lunar and Planetary Inst., The Twenty-Fifth Lunar and Planetary Science Conference. Part 2: H-O 1994 p 609-610 (For primary document see N94-36136 11-91)
Avail: CASI HC A01/MF A06

In this study on the evolution of dust particles from comets and asteroids, the effects of accurate many-body planetary motion on the gravitational perturbations of the dust grains are computed. In a computer simulation, dust grains of radius 10, 30, and 100 micron were released at perihelion passage from each of 36 different celestial bodies: 16 main asteroids, 15 short period comets with perihelion greater than 1 AU, and 5 short period comets with perihelion less than 1 AU. It is found that when dust grains evolve to intersection with the earth's orbit, they nearly always retain orbital characteristics indicative of their origins. Grains from main belt asteroids differ significantly in orbital characteristics, especially orbital eccentricity, from grains that evolve from comets. Derived from text

N94-36143*# National Aeronautics and Space Administration. Lyndon B. Johnson Space Center, Houston, TX.

MARS ATMOSPHERIC ESCAPE AND ISOTOPIC FRACTIONATION: SYNTHESIS OF DATA AND MODELS Abstract Only

Bruce M. Jakosky (Colorado Univ., Boulder, CO.), Janet G. Luhmann (California Univ., Los Angeles, CA.), and John H. Jones *In* Lunar and Planetary Inst., The Twenty-Fifth Lunar and Planetary Science Conference. Part 2: H-O 1994 p 615-616 (For primary document see N94-36136 11-91)

Avail: CASI HC A01/MF A06

The present Mars atmosphere is relatively thin and cold. It is not at all like that which is presumed to have been responsible for the formation of valley networks and the heavy erosion of craters during the earliest epochs of martian history. An important goal of Mars exploration is to try to understand the properties of the early atmosphere, the initial inventory of volatiles at the planet's surface, the processes by which the atmosphere and climate have evolved over time, and the current location of volatiles presumed to have been in the atmosphere in the earlier times. The current status of understanding of the escape of volatiles to space over geologic time and the resulting fractionation of isotopes of stable atoms remaining in the atmosphere are described, and a scenario for volatile abundance and evolution that is consistent with the available information on the escape and fractionation of each species is constructed. In particular, the evolution of hydrogen, carbon, oxygen, and nitrogen, as contained in atmospheric (and non-atmospheric) water, carbon dioxide, and molecular nitrogen, is examined. Derived from text

N94-36144*# National Aeronautics and Space Administration. Ames Research Center, Moffett Field, CA.

THE STRUCTURAL CHANGES OF WATER ICE I DURING WARMUP Abstract Only **c25**

Peter Jenniskens and David F. Blake *In* Lunar and Planetary Inst., The Twenty-Fifth Lunar and Planetary Science Conference. Part 2: H-O 1994 p 621-622 (For primary document see N94-36136 11-91)

Avail: CASI HC A01/MF A06

The polymorph transitions of vapor deposited water ice I during warmup from 15 K to 210 K was mapped by means of selected area electron diffraction. The polymorph transitions account for many phenomena observed in laboratory analog studies of cometary outgassing and radial diffusion in UV photolyzed interstellar ices. Author (revised)

N94-36145*# National Aeronautics and Space Administration. Lyndon B. Johnson Space Center, Houston, TX.

TEXTURAL CONSTRAINTS ON THE FORMATION OF ALTERATION PHASES IN CM CHONDRITES Abstract Only **c90**

L. H. Joseph (Rochester Univ., NY.), L. B. Browning (Tennessee Univ., Knoxville, TN.), and M. E. Zolensky *In* Lunar and Planetary Inst., The Twenty-Fifth Lunar and Planetary Science Conference. Part 2: H-O 1994 p 645-646 (For primary document see N94-36136 11-91)

Avail: CASI HC A01/MF A06

Although it is generally believed that the secondary alteration phases observed in CM chondrites resulted from parent body reactions, the influence of nebular processing can not yet be dismissed. We have analyzed 5 CM falls using optical and electron microscopy to construct a comprehensive pictorial reference set of textural and mineralogical associations bearing on the origin of alteration products in these meteorites. Our analyses support pervasive aqueous alteration on the CM parent body, but they do not exclude the possibility of minor nebular alteration. Author (revised)

N94-36146*# National Aeronautics and Space Administration. Lyndon B. Johnson Space Center, Houston, TX.

PARTIAL MELTING OF THE ST. SEVERIN (LL) AND LOST CITY (H) ORDINARY CHONDRITES: ONE STEP BACKWARDS AND TWO STEPS FORWARD Abstract Only **c90**

A. J. G. Jurewicz (Lockheed Engineering and Sciences Co., Houston, TX.), J. H. Jones, and D. W. Mittlefehldt *In* Lunar and Planetary Inst., The Twenty-Fifth Lunar and Planetary Science Conference. Part 2: H-O 1994 p 651-652 (For primary document see N94-36136 11-91)

Avail: CASI HC A01/MF A06

This study looks at partial melting in H and LL chondrites at nearly one atmosphere of total pressure as part of a continuing study of the origins of basaltic achondrites. Previously, melting experiments on anhydrous CM and CV chondrites showed that, near its solidus, the CM chondrite produced melts having major element chemistries similar to the Sioux County eucrite; but, the pyroxenes in the residuum were too iron-rich to form diogenites. Our preliminary results from melting experiments on ordinary (H, LL) chondrites suggested that, although the melts did not look like any known eucrites, pyroxenes from these charges bracketed the compositional range of pyroxenes found in diogenites. We had used the Fe/Mg exchange coefficients calculated for olivine, pyroxene, and melt in these charges to evaluate the approach to equilibrium, which appeared to be excellent. Unfortunately, mass balance calculations later indicated to us that, unlike our CM and CV charges, the LL and H experimental charges had lost significant amounts of iron to their (Pt or PtRh) supports. Apparently, pyroxene stability in chondritic systems is quite sensitive to the amount of FeO, and it was this unrecognized change in the bulk iron content which had stabilized the high temperature, highly magnesian pyroxenes. Accordingly, this work reinvestigates the phase equilibria of ordinary chondrites, eliminating iron and nickel loss, and reports significant differences. It also looks closely at how the iron and sodium in the bulk charge affect the stability of pyroxene, and it comments on how these new results apply to the problems of diogenite and eucrite petrogenesis. Author

N94-36147*# National Aeronautics and Space Administration. Lyndon B. Johnson Space Center, Houston, TX.

PRELIMINARY RESULTS OF SULFIDE MELT/SILICATE WETTING EXPERIMENTS IN A PARTIALLY MELTED ORDINARY CHONDRITE Abstract Only **c90**

Stephen R. Jurewicz and John H. Jones *In* Lunar and Planetary Inst., The Twenty-Fifth Lunar and Planetary Science Conference. Part 2: H-O 1994 p 653-654 (For primary document see N94-36136 11-91)

Avail: CASI HC A01/MF A06

Recently, mechanisms for core formation in planetary bodies have received considerable attention. Most current theories emphasize the need for large degrees of silicate partial melting to facilitate the coalescence and sinking of sulfide-metal liquid blebs through a low strength semi-crystalline silicate mush. This scenario is based upon observations that sulfide-metal liquid tends to form circular blebs in partially molten meteorites during laboratory experiments. However, recent experimental work by Herpfer and Larimer indicates that some sulfide-Fe liquids have wetting angles at and slightly below 60 deg in an olivine aggregate, implying an interconnected melt structure at any melt fraction. Such melt interconnectivity provides a means for gravitational compaction and extraction of the majority of a sulfide liquid phase in small planetary bodies without invoking large degrees of silicate partial melting. Because of the important ramifications of these results, we conducted a series of experiments using H-chondrite starting material in order to evaluate sulfide-liquid/silicate wetting behavior in a more complex natural system. Author (revised)

N94-36148*# National Aeronautics and Space Administration. Lyndon B. Johnson Space Center, Houston, TX.

THE NATURE OF AGGLUTINITIC GLASS IN THE FINE-SIZE FRACTION OF LUNAR SOIL 10084 Abstract Only

Lindsay P. Keller (MVA, Inc., Norcross, GA.) and David S. McKay *In* Lunar and Planetary Inst., The Twenty-Fifth Lunar and Planetary Science Conference. Part 2: H-O 1994 p 685-686 (For primary document see N94-36136 11-91)

Avail: CASI HC A01/MF A06

Agglutinitic glass contains much of the reduced Fe in lunar soils, and it contributes to the modification of reflectance spectra from lunar soils.

Previous work has shown that agglutinitic glass can be compositionally heterogeneous, but the scale of these heterogeneities is not well known. In addition, few data are available on the characteristics of the inclusions in agglutinitic glass. Here we report on our preliminary transmission electron microscope (TEM) examination of agglutinitic glass fragments from the Apollo 11 soil 10084. Author (revised)

N94-36149*# National Aeronautics and Space Administration. Lyndon B. Johnson Space Center, Houston, TX.
ELECTRON ENERGY-LOSS SPECTROSCOPY OF CARBON IN INTERPLANETARY DUST PARTICLES Abstract Only **c90**
Lindsay P. Keller (MVA, Inc., Norcross, GA.), John P. Bradley (MVA, Inc., Norcross, GA.), Kathie L. Thomas (Lockheed Engineering and Sciences Co., Houston, TX.), and David S. McKay *In* Lunar and Planetary Inst., The Twenty-Fifth Lunar and Planetary Science Conference. Part 2: H-O 1994 p 687-688 Sponsored in part by MVA, Inc. (For primary document see N94-36136 11-91)
(RTOP 152-17-40-23; RTOP 199-52-11-02)
Avail: CASI HC A01/MF A06

The nature of the carbon-bearing phases in IDP's provides information regarding the chemical and physical processes involved in the formation and evolution of the early solar system. Several carbon-bearing materials have been observed in IDP's, but details of their nature, abundance, and distribution are still poorly known. A knowledge of the abundance and nature of carbon in IDP's is useful in constraining the sources of IDP's and for comparisons with other chondritic materials. Estimates of carbon abundance in anhydrous and hydrated IDP's indicate that most of these particles have significantly higher carbon than the carbonaceous chondrites. Mineralogical analyses show that carbonates are only a minor component of most hydrated IDP's, and so the high carbon abundances in this group of IDP's indicates that other carbon-bearing phases are present in significant concentrations. Using the technique of electron energy-loss spectroscopy (EELS), we have identified two forms of carbon in a hydrated IDP, oxidized carbon (carbonates), and amorphous elemental carbon. Author (revised)

N94-36150*# National Aeronautics and Space Administration. Ames Research Center, Moffett Field, CA.
MERCURY: MID-INFRARED (7.3 - 13.5 MICRONS) SPECTROSCOPIC OBSERVATIONS SHOWING FEATURES CHARACTERISTIC OF PLAGIOCLASE Abstract Only
R. W. H. Kozlowski (Arizona Univ., Tucson, AZ.), A. L. Sprague (Arizona Univ., Tucson, AZ.), F. C. Witteborn, D. P. Cruikshank, D. Wooden, and K. D. Snyder *In* Lunar and Planetary Inst., The Twenty-Fifth Lunar and Planetary Science Conference. Part 2: H-O 1994 p 739-740 (For primary document see N94-36136 11-91)
Avail: CASI HC A01/MF A06

Mid-infrared spectroscopic observations of the surface of Mercury are reported for the wavelength range 7.3 to 13.5 microns. The observed spectral radiance emanated from equatorial and low latitude regions between 110-130 deg Mercurian longitude. The area is primarily an intercrater plain. The spectra show distinct and recognizable features, the principal Christiansen emission peak being the most prominent. The Christiansen feature strongly suggests the presence of plagioclase (Ca,Na)(Al,Si)AlSi2O8, (in particular labradorite: Ab(50) - Ab(30)). In addition we have studied the effects of thermal gradients to gain insight into the effects of thermal conditions on the spectral radiance of rock samples. This simulates the thermophysical effects as the rotating surface of Mercury is alternately heated and cooled. The spectral features of the samples are retained; however, the relative and absolute amplitudes vary as illustrated by laboratory reflectance and emittance spectra from quartzite. Author (revised)

N94-36151*# National Aeronautics and Space Administration. Goddard Space Flight Center, Greenbelt, MD.
UNIQUENESS OF A SOLUTION OF A STEADY STATE PHOTOCHEMICAL PROBLEM: APPLICATIONS TO MARS Abstract Only
V. A. Krasnopolsky *In* Lunar and Planetary Inst., The Twenty-Fifth Lunar and Planetary Science Conference. Part 2: H-O 1994 p 745 (For primary document see N94-36136 11-91)
Avail: CASI HC A01/MF A06

Based on the conservation of chemical elements in chemical reactions, a rule is proved that the number of boundary conditions given by densities and/or non-zero velocities should not be less than the number of chemical elements in the system, and the components given by densities and velocities should include all elements in the system. Applications of this rule to Mars are considered. It is proved that a problem of CO2-H2O chemistry in the lower and middle atmosphere of Mars, say, in the range of 0-80 km does not have an unique solution, if only CO2 and H2O densities are given at the lower boundary, while all other boundary conditions are fluxes. Two models of this type are discussed. These models fit the same boundary conditions, are balanced with a relative uncertainty of 10(exp -4) for H2, and predict the O2, CO, and H2 mixing ratios which differ by order of magnitude. One more species density, e.g. that of O2, should be specified at the boundary to obtain the unique solution. The situation is better if the upper boundary is extended to the exobase where thermal escape velocities of H and H2 can be specified. However, in this case, either oxygen nonthermal escape rate or the O2 density at the surface should be given as the boundary condition. Two models of Mars' photochemistry, with and without nitrogen chemistry, are considered. The oxygen nonthermal escape rate of 1.2 x 10(exp 8) cm(exp -2) s(exp -1) is given at 240 km and is balanced with the total hydrogen escape rate within uncertainty of 1 percent for both models. Both models fit the measured O2 and CO mixing ratios, the O3 line absorption at 9.6 microns, and the O2 1.27 microns dayglow within the uncertainties of the measured values; although, the model without nitrogen chemistry fits better. Author (revised)

N94-36152*# National Aeronautics and Space Administration. Goddard Space Flight Center, Greenbelt, MD.
H2O-H2SO4 SYSTEM IN VENUS' CLOUDS AND OCS, CO, AND H2SO4 PROFILES IN VENUS' TROPOSPHERE Abstract Only
V. A. Krasnopolsky and J. B. Pollack *In* Lunar and Planetary Inst., The Twenty-Fifth Lunar and Planetary Science Conference. Part 2: H-O 1994 p 747-748 (For primary document see N94-36136 11-91)
Avail: CASI HC A01/MF A06

A coupled problem of diffusion and condensation is solved for the H2SO4-H2O system in Venus' cloud layer. The position of the lower cloud boundary, profiles of the H2O and H2SO vapor mixing ratios, and of the H2O/H2SO4 ratio of sulfuric acid aerosol and its flux are calculated as functions of the column photochemical production rate of sulfuric acid. Variations of the lower cloud boundary are considered. Our basic model, which is constrained to yield f(sub H2O)(30km) = 30 ppm, predicts the position of the lower cloud boundary at 48.4 km coinciding with the mean Pioneer Venus value, the peak H2SO4 mixing ratio of 5.4 ppm, and the H2SO4 production rate phi(sub H2SO4) = 2.2 x 10(exp 12) cm(exp -2)s(exp -1). Author (revised)

N94-36153*# California Univ., Berkeley, CA. Center for Extreme Ultraviolet Astrophysics.
FIRST MEASUREMENT OF HELIUM ON MARS: IMPLICATIONS FOR THE PROBLEM OF RADIOGENIC GASES ON THE TERRESTRIAL PLANETS Abstract Only
S. Bowyer, S. Chakrabarti, G. R. Gladstone, and J. S. McDonald *In* Lunar and Planetary Inst., The Twenty-Fifth Lunar and Planetary Science Conference. Part 2: H-O 1994 p 749-750 (For primary document see N94-36136 11-91)
Avail: CASI HC A01/MF A06

The 108 photons of the Martian He 584 A airglow detected by the Extreme Ultraviolet Explorer satellite during a two-day exposure (22-23 Jan. 1993) correspond to the effective disk average intensity of 43 (+/-) 10 Rayleigh. Radiative transfer calculations, using a model atmosphere appropriate to the conditions of the observation and having an exospheric temperature of 210 (+/-) 20 K, result in an He mixing ratio of 1.1 (+/-) 0.4 ppm in the lower atmosphere. Nonthermal escape of helium is due to the following: electron impact ionization and pickup of He(+) by the solar wind; collisions with hot oxygen atoms; and charge exchange with molecular species with corresponding column loss rates of 1.4 x 10(exp 5), 3 x 10(exp 4), and 7 x 10(exp 3) cm(exp -2)s(exp -1), respectively. The lifetime of helium on Mars is 5 x 10(exp 4) yr. The He outgassing rate, coupled with the Ar-40 atmospheric abundance and with the K:U:Th ratio measured in the surface rocks, is used as input to a simple two-reservoir degassing model which presumes the loss of all argon accumulated in the atmosphere during the first Byr by large-scale impacts. The model results in total planet mass ratios of 10(exp -5) g/g for K, 2.3 x 10(exp -9) g/g for U, 8.5 x 10(exp -9) g/g for Th, 4 x 10(exp -10) g/g for He, and 1.5 x 10(exp -9) g/g for Ar-40. The predicted radiogenic heat flux is 2 erg cm(exp -2)s(exp

-1). Similar modeling for Venus results in total plant mass ratios of 4.7 x 10(exp -5) g/g for K, 6.7 x 10(exp -9) g/g for U, 2.2 x 10(exp -8) g/g for Th, 1.3 x 10(exp -9) for He, 6.7 x 10(exp -9) g/g for Ar-40, and a radiogenic heat flux of 15 erg cm(exp -2)s(exp -1). The implications of these results are discussed. The modeling shows that the radioactive elements were not distributed uniformly in the protoplanetary nebula, and their relative abundances differ very much in the terrestrial planets.
Author (revised)

N94-36154*# National Aeronautics and Space Administration. Lyndon B. Johnson Space Center, Houston, TX.
MOSSBAUER AND SPECTRAL (VISIBLE AND NEAR-IR) DATA FOR Fe(3+)-SUBSTITUTED RUTILE Abstract Only c25
H. V. Lauer, Jr. (Lockheed Engineering and Sciences Co., Houston, TX.), R. V. Morris, and R. K. Vempati *In* Lunar and Planetary Inst., The Twenty-Fifth Lunar and Planetary Science Conference. Part 2: H-O 1994 p 771 (For primary document see N94-36136 11-91)
Avail: CASI HC A01/MF A06

Titanohematite and rutile containing some Fe(3+) are possible highly oxidized weathering products of ilmenite and titanomagnetities. We report here Moessbauer and reflectivity data (visible and near-IR) for Fe(3+)-substituted rutile as a part of our continuing studies of ferric-substituted minerals that might have bearing on the interpretation of Martian spectral data. Author (revised)

N94-36155*# National Aeronautics and Space Administration. Goddard Space Flight Center, Greenbelt, MD.
PROGRESS IN THE DEVELOPMENT OF THE GMM-2 GRAVITY FIELD MODEL FOR MARS Abstract Only
F. G. Lemoine (Maryland Univ., College Park, MD.), D. E. Smith, F. J. Lerch, M. T. Zuber, and G. B. Patel *In* Lunar and Planetary Inst., The Twenty-Fifth Lunar and Planetary Science Conference. Part 2: H-O 1994 p 789-790 (For primary document see N94-36136 11-91)
Avail: CASI HC A01/MF A06

Last year we published the GMM-1 (Goddard Mars Model-1) gravity model for Mars. We have completely re-analyzed the Viking and Mariner 9 tracking data in the development of the new field, designated GMM-2. The model is complete to degree and order 70. Various aspects of the model are discussed. CASI

N94-36156*# National Aeronautics and Space Administration. Goddard Space Flight Center, Greenbelt, MD.
PRELIMINARY SOLUTIONS FOR THE LUNAR GRAVITY FIELD FROM ANALYSIS OF LUNAR ORBITER TRACKING DATA Abstract Only
F. G. Lemoine (Maryland Univ., College Park, MD.), D. E. Smith, M. T. Zuber, D. D. Rowlands, and S. K. Fricke *In* Lunar and Planetary Inst., The Twenty-Fifth Lunar and Planetary Science Conference. Part 2: H-O 1994 p 791-792 (For primary document see N94-36136 11-91)
Avail: CASI HC A01/MF A06

Knowledge of the gravitation field, in combination with surface topography, provides one of the principal means of inferring the internal structure of a planetary body. Previous analyses of the lunar gravitational field have been based on data from the Lunar Orbiters, the Apollo subsatellites, and the low altitude passes of the Apollo spacecraft. Recently, Konopliv et al. have reanalyzed all available Lunar Orbiter and Apollo subsatellite tracking data, producing a 60th degree and order solution. In preparation for the Clementine Mission to the Moon, we have also initiated a reanalysis of the Lunar Orbiter and Apollo subsatellite data. Our reanalysis takes advantage of advanced force and measurement modeling techniques as well as modern computational facilities. We applied the least squares collocation technique which stabilizes the behavior of the solution and high degree and order. The extension of the size of the field reduces the aliasing coming from the omitted portion of the gravitational field. This is especially important for the analysis of the tracking data from the Lunar Orbiters, as the periapse heights frequently ranged from 50 to 100 km.
Derived from text

N94-36157*# National Aeronautics and Space Administration. Lyndon B. Johnson Space Center, Houston, TX.
PIGEONHOLING PLANETARY METEORITES: THE LESSONS OF MISCLASSIFICATION OF EET87521 AND ALH84001 Abstract Only c90
M. M. Lindstrom, A. H. Treiman, and D. W. Mittlefehldt *In* Lunar and Planetary Inst., The Twenty-Fifth Lunar and Planetary Science Conference. Part 2: H-O 1994 p 797-798 (For primary document see N94-36136 11-91)
Avail: CASI HC A01/MF A06

The last few years have provided two noteworthy examples of misclassifications of achondritic meteorites because the samples were new kinds of meteorites from planetary rather than asteroidal parent bodies. Basaltic lunar meteorite EET87521 was misclassified as a eucrite and SNC (martian) orthopyroxenite ALH84001 was misclassified as a diogenite. In classifying meteorites we find what we expect: we pigeonhole meteorites into known categories most of which were derived from the more common asteroidal meteorites. But the examples of EET8752 and ALH84001 remind us that planets are more complex than asteroids and exhibit a wider variety of rock types. We should expect variety in planetary meteorites and we need to know how to recognize them when we have them. Our intent here is to show that our asteroidal perspective is inappropriate for planetary meteorites. Derived from text

N94-36158*# National Aeronautics and Space Administration. Lyndon B. Johnson Space Center, Houston, TX.
ON THE ORIGIN OF ENSTATITE CHONDRITE CHONDRULES BASED ON THEIR PETROGRAPHY AND COMPARISON WITH EXPERIMENTALLY PRODUCED CHONDRULES Abstract Only c90
Gary E. Lofgren, John M. DeHart, and P. J. Burkett *In* Lunar and Planetary Inst., The Twenty-Fifth Lunar and Planetary Science Conference. Part 2: H-O 1994 p 801-802 (For primary document see N94-36136 11-91)
Avail: CASI HC A01/MF A06

The recent discovery of several types 3 and 4 enstatite chondrites (EC) in the Antarctic collection increases greatly the ability to compare unaltered, naturally-formed EC chondrules with chondrules produced experimentally from melts of enstatitic chondrule composition. Because these discoveries are so recent we have undertaken the task of characterizing these chondrules for purposes of comparison. We have looked at several new Antarctic E3 chondrites and Qingzhen. They all have numerous chondrules with well defined outlines and readily identifiable textures. All have mostly porphyritic chondrules, but there are differences in the size and kinds of textures. Radial pyroxene, barred/dendritic px, and cryptocrystalline chondrules are present in differing amounts with one exception. Derived from text

N94-36159*# National Aeronautics and Space Administration. Lyndon B. Johnson Space Center, Houston, TX.
MORPHOLOGY OF METEOROID AND SPACE DEBRIS CRATERS ON LDEF METAL TARGETS Abstract Only c90
S. G. Love (Washington Univ., Seattle, WA.), D. E. Brownlee (Washington Univ., Seattle, WA.), N. L. King (Washington Univ., Seattle, WA.), and F. Hoerz *In* Lunar and Planetary Inst., The Twenty-Fifth Lunar and Planetary Science Conference. Part 2: H-O 1994 p 809-810 (For primary document see N94-36136 11-91)
Avail: CASI HC A01/MF A06

We measured the depths, average diameters, and circularity indices of over 600 micrometeoroid and space debris craters on various metal surfaces exposed to space on the Long Duration Exposure Facility (LDEF) satellite, as a test of some of the formalisms used to convert the diameters of craters on space-exposed surfaces into penetration depths for the purpose of calculating impactor sizes or masses. The topics covered include the following: targe materials orientation; crater measurements and sample populations; effects of oblique impacts; effects of projectile velocity; effects of crater size; effects of target hardness; effects of target density; and effects of projectile properties. Derived from text

N94-36160*# National Aeronautics and Space Administration. Lyndon B. Johnson Space Center, Houston, TX.
PRODUCTION OF FERROAN ANDESITES BY THE EXPERIMENTAL PARTIAL MELTING OF AN LL CHONDRITE Abstract Only c90
J. C. McGuire (State Univ. of New York, Stony Brook, NY.), A. J. G. Jurewicz (Lockheed Engineering and Sciences Co., Houston, TX.), and J. H. Jones *In* Lunar and Planetary Inst., The Twenty-Fifth Lunar and Planetary Science Conference. Part 2: H-O 1994 p 879-880 (For

primary document see N94-36136 11-91)
Avail: CASI HC A01/MF A06

A partial melting experiment on the St. Severin (LL) chondrite produced a melt that was andesitic, having 54-60 wt% silica, at 1200 C and an oxygen fugacity of IW+2, two log units above the iron-wustite (IW) buffer. Under these same conditions, CV, CM, and L chondrites produced low-silica melts resembling angrites. This experimental study attempts to reproduce and explain this unusual result. Author (revised)

N94-36161*# National Aeronautics and Space Administration. Lyndon B. Johnson Space Center, Houston, TX.
SYNTHETIC AND NATURAL NAKHLA PYROXENES: PARENT MELT COMPOSITION AND REE PARTITION COEFFICIENTS Abstract Only **c90**
G. McKay, L. Le, and J. Wagstaff *In* Lunar and Planetary Inst., The Twenty-Fifth Lunar and Planetary Science Conference. Part 2: H-O 1994 p 883-884 (For primary document see N94-36136 11-91)
Avail: CASI HC A01/MF A06

Nakhla is one of the SNC meteorites, generally believed to be of martian origin. It is composed mainly of cumulus augite, in which primary igneous zoning is apparently preserved, and which serves as a recorder of the composition of Nakhla's parent melt and the conditions under which it crystallized. Knowledge of the composition and petrogenesis of this parent melt may help unravel Nakhla's relationship to the other SNC's, and provide clues to martian petrogenesis in general. This abstract reports new results of an ongoing study in which we are (1) comparing the major and minor element compositions of synthetic pyroxenes crystallized from various proposed parent melt compositions with those in Nakhla pyroxene to constrain the composition of the parent melt, and (2) measuring minor and trace element partition coefficients, particularly those of the REE, in order to obtain the most applicable D values with which to invert the natural pyroxene compositions to obtain the trace element composition of the parent melt. Results suggest that recent estimates of Nakhla's parent melt composition are too aluminous, and that mafic or ultramafic melts are more likely candidates. Author (revised)

N94-36162*# National Aeronautics and Space Administration. Lyndon B. Johnson Space Center, Houston, TX.
Cr, Mn, AND Ca DISTRIBUTIONS FOR OLIVINE IN ANGRITIC SYSTEMS: CONSTRAINTS ON THE ORIGINS OF Cr-RICH AND Ca-POOR CORE OLIVINE IN ANGRITE LEW87051 Abstract Only **c90**
T. Mikouchi (Tokyo Univ., Japan.), G. McKay, and L. Le *In* Lunar and Planetary Inst., The Twenty-Fifth Lunar and Planetary Science Conference. Part 2: H-O 1994 p 907-908 (For primary document see N94-36136 11-91)
Avail: CASI HC A01/MF A06

Angrite meteorites are a type of basaltic achondrites that are noted for their very old cyrstallization ages (4.55 b.y.) and unusual chemical and mineralogical properties. In spite of great interest, only four angrites have been found. LEW87051 is the smallest one which weighs 0.6 g. It is a porphyritic rock with coarse subhedral to euhedral olivines set in a fine-grained groundmass which clearly represents a crystallized melt. The largest uncertainty about the petrogenesis of LEW87051 is the relationship between the large olivine crystals and the groundmass. Prinz et al. suggests that olivines are xenocrysts, while McKay et al. proposed a fractional cyrstallization model based on experimental studies. However, the crystals have Cr-rich and Ca-poor cores which do not match experimental olivines. Although Jurewicz and McKay tried to explaine the zoning of the rim by diffusion, some features are not explained. There also exists a definite composition boundary of Fe(2+) and MnO between the core and the rim. To clarify the origin of these olivines, we have performed experiments using LEW87051 analogs to measure the effects of oxygen fugacity on distribution coefficients of various elements in an angritic system. Derived from text

N94-36163*# National Aeronautics and Space Administration. Lyndon B. Johnson Space Center, Houston, TX.
PARTITION COEFFICIENTS FOR Al, Ca, Ti, Cr, AND Ni IN OLIVINE OBTAINED BY MELTING EXPERIMENT ON AN LL6 CHONDRITE Abstract Only **c90**
M. Miyamoto (Tokyo Univ., Japan.), T. Mikouchi (Tokyo Univ., Japan.), and G. A. McKay *In* Lunar and Planetary Inst., The Twenty-Fifth Lunar and Planetary Science Conference. Part 2: H-O 1994 p 923-924 (For primary document see N94-36136 11-91)
Avail: CASI HC A01/MF A06

We report the partition coefficients for Ca, Al, Ti, Cr, and Ni in olivine obtained through a series of melting experiments on an LL6 chondrite under varying conditions of temperature and oxygen fugacity. It is necessary to examine the variation of partition coefficients up to extremely reducing conditions in order to study meteoritic olivines. For Ca, Al, and Cr, the partition coefficients tend to decrease as temperature increases, but do not change even under extremely reducing conditions. Derived from text

N94-36164*# National Aeronautics and Space Administration. Lyndon B. Johnson Space Center, Houston, TX.
FERROMAGNETIC RESONANCE SPECTRA OF H2-REDUCED MINERALS AND GLASSES Abstract Only **c25**
Richard V. Morris and Carlton C. Allen *In* Lunar and Planetary Inst., The Twenty-Fifth Lunar and Planetary Science Conference. Part 2: H-O 1994 p 937-938 (For primary document see N94-36136 11-91)
Avail: CASI HC A01/MF A06

In an earlier paper, we reported that H2 reduction of basaltic glass, olivine, pyroxene, and plagioclase resulted in the formation of metallic iron, in the darkening and reddening of the reflectance spectra, and the masking of individual spectral features in the visible and near-IR. In this work, we report FMR spectra for H2-reduced minerals and glasses that include the samples studied in the earlier paper. The FMR spectra were reduced at room temperature at a nominal frequency of 9.5 GHz. Sample saturation magnetization reported as F3(0) was measured with a vibrating sample magnetometer. Derived from text

N94-36165*# National Aeronautics and Space Administration. Lyndon B. Johnson Space Center, Houston, TX.
HEMATITE FORMED FROM PYROXENE ON MARS BY METEORITIC IMPACT Abstract Only
Richard V. Morris, James F. Bell, III, and H. V. Lauer, Jr. *In* Lunar and Planetary Inst., The Twenty-Fifth Lunar and Planetary Science Conference. Part 2: H-O 1994 p 939-940 (For primary document see N94-36136 11-91)
Avail: CASI HC A01/MF A06

In earlier work, we showed using Mossbauer data that the mineralogy of iron-bearing phases in impact melt rocks from Manicouagan Crater (Quebec, Canada) is to a first approximation hematite and pyroxene. The visible and near-IR reflectivity data for these impact melt rocks show a continuous trend in band position from approximately 850 to approximately 1000 nm, which corresponds to the positions for the hematite and pyroxene endmembers, respectively. The oxidation is thought to occur shortly after the impact when oxidizing vapors and/or solutions reacted with the impact melt which was below its solidus temperature but still relatively hot. The reflectance data have important implications for Mars because band positions which occur between approximately 850 and 1000 nm bands observed for Mars can be attributed to hematite-pyroxene assemblages and not necessarily to different ferric mineralogy. Because oxidation of impact melt rocks at Manicouagan is thought to occur subsolidus, precursors for the hematite include oxides such as magnetite and ilmenite and silicates such as pyroxene and olivine. To determine if the Manicouagan impact-melt rocks are related to each other by simple thermal subsolidus oxidation, we calcined in air a relatively unoxidized Manicouagan impact-melt rock (MAN-74-608A). Previous work has shown that np-Hm (nanophase hematite) particles can be derived by calcination of iron-bearing silicates. Author

N94-36166*# National Aeronautics and Space Administration. Lyndon B. Johnson Space Center, Houston, TX.
MOESSBAUER MINERALOGY OF CALCINED MURCHISON METEORITE Abstract Only **c90**
Richard V. Morris, M. E. Zolensky, T. Hiroi, and M. E. Lipschutz *In* Lunar and Planetary Inst., The Twenty-Fifth Lunar and Planetary Science Conference. Part 2: H-O 1994 p 941-942 (For primary document see N94-36136 11-91)
Avail: CASI HC A01/MF A06

The three Antarctic meteorites B7904, Y82162, and Y86720 are unusual because they have characteristics in common with both CI and CM groups and because they apparently underwent thermal alteration after hydrous alteration on their parent body. They are also spectrally similar (visible and near-IR) to C, G, B, and F asteroids, which may imply that the surface materials on those asteroids may have undergone thermal alteration. Based on the reflectance spectra of samples of Murchison (CM2 carbonaceous chondrite) that were thermally altered in the laboratory (cryopumped and initial 10(exp -5) atm H2), Hiroi et al. concluded that putative thermal alteration occurred at temperatures of 600 to 1000 C. Similar experiments have been done on Murchison and reported mineralogical changes based on data from transmission electron diffraction microscopy, electron diffraction, and analytical electron microscopy. We report here the Mossbauer mineralogy of the same samples of thermally-altered Murchison. Mossbauer mineralogy gives the molar distribution of Fe among its oxidation states and iron-bearing mineralogies. Author

N94-36167*# National Aeronautics and Space Administration. Goddard Space Flight Center, Greenbelt, MD.

SHAPE, SIZE, AND DISTRIBUTION OF MAGNETIC PARTICLES IN BJURBOLE CHONDRULES Abstract Only **c90**

David F. Nava *In* Lunar and Planetary Inst., The Twenty-Fifth Lunar and Planetary Science Conference. Part 2: H-O 1994 p 977 (For primary document see N94-36136 11-91)

Avail: CASI HC A01/MF A06

Chondrules from the Bjurbole chondritic meteorite (L4) exhibit saturation remanence magnetization (SIRM) values which vary over three orders of magnitude. REM values (Natural Remanence Magnetization/SIRM) for Allende (C3V) and Chainpur (LL3) are less than 0.01 but in Bjurbole some chondrules were found to have REM values greater than 0.1 with several greater than 0.2. REM values greater than 0.1 are abnormal and cannot be acquired during weak field cooling. If exposure to a strong field (whatever the source) during the chondrules' history is responsible for the high REM values, was such history associated with a different processing which might have resulted in different shape, size, and distribution of metal particles compared to chondrules having REM values of less than 0.01? Furthermore, magnetic hysteresis results show a broad range of magnetic hardness and other intrinsic magnetic properties. These features must be related to (1) size and amount of metal; and (2) properties of, and amount of, tetrataenite in the chondrules (all chondrules thus far subjected to thermomagnetic analysis show the presence of tetrataenite). A scanning electron microscopy (SEM) study is underway to determine the relationship between the shape, size, and distribution of metal particles within individual chondrules and the magnetic properties of these chondrules. Results from the SEM study in conjunction with magnetic property data may also help to discern effects from possible lightning strikes in the nebula prior to incorporation of the chondrules into the parent body. Author

N94-36168*# National Aeronautics and Space Administration. Goddard Space Flight Center, Greenbelt, MD.

PATTERNS OF BRITTLE DEFORMATION UNDER EXTENSION ON VENUS Abstract Only

G. A. Neumann (Johns Hopkins Univ., Baltimore, MD.) and M. T. Zuber (Johns Hopkins Univ., Baltimore, MD.) *In* Lunar and Planetary Inst., The Twenty-Fifth Lunar and Planetary Science Conference. Part 2: H-O 1994 p 993-994 (For primary document see N94-36136 11-91)

Avail: CASI HC A01/MF A06

The development of fractures at regular length scales is a widespread feature of Venusian tectonics. Models of lithospheric deformation under extension based on non-Newtonian viscous flow and brittle-plastic flow develop localized failure at preferred wavelengths that depend on lithospheric thickness and stratification. The characteristic wavelengths seen in rift zones and tessera can therefore provide constraints on crustal and thermal structure. Analytic solutions were obtained for growth rates in infinitesimal perturbations imposed on a one-dimensional, layered rheology. Brittle layers were approximated by perfectly-plastic, uniform strength, overlying ductile layers exhibiting thermally-activated power-law creep. This study investigates the formation of faults under finite amounts of extension, employing a finite-element approach. Our model incorporates non-linear viscous rheology and a Coulomb failure envelope. An initial perturbation in crustal thickness gives rise to necking instabilities. A small amount of velocity weakening serves to localize deformation into planar regions of high strain rate. Such planes are analogous to normal faults seen in terrestrial rift zones. These 'faults' evolve to low angle under finite extension. Fault spacing, orientation and location, and the depth to the brittle-ductile transition, depend in a complex way on lateral variations in crustal thickness. In general, we find that multiple wavelengths of deformation can arise from the interaction of crustal and mantle lithosphere. Author

N94-36169*# National Aeronautics and Space Administration. Lyndon B. Johnson Space Center, Houston, TX.

ALKALI ELEMENT CONSTRAINTS ON EARTH-MOON RELATIONS Abstract Only **c90**

M. D. Norman (Australian National Univ., Canberra, Australia.), M. J. Drake (Arizona Univ., Tucson, AZ.), and J. H. Jones *In* Lunar and Planetary Inst., The Twenty-Fifth Lunar and Planetary Science Conference. Part 2: H-O 1994 p 1009-1010 (For primary document see N94-36136 11-91)

Avail: CASI HC A01/MF A06

Given their range of volatilities, alkali elements are potential tracers of temperature-dependent processes during planetary accretion and formation of the Earth-Moon system. Under the giant impact hypothesis, no direct connection between the composition of the Moon and the Earth is required, and proto-lunar material does not necessarily experience high temperatures. Models calling for multiple collisions with smaller planetesimals derive proto-lunar materials mainly from the Earth's mantle and explicitly invoke vaporization, shock melting and volatility-related fractionation. Na/K, K/Rb, and Rb/Cs should all increase in response to thermal volatization, so theories which derive the Moon substantially from Earth's mantle predict these ratios will be higher in the Moon than in the primitive mantle of the Earth. Despite the overall depletion of volatile elements in the Moon, its Na/K and K/Rb are equal to or less than those of Earth. A new model presented here for the composition of Earth's continental crust, a major repository of the alkali elements, suggests the Rb/Cs of the Moon is also less than that of Earth. Fractionation of the alkali elements between Earth and Moon are in the opposite sense to predictions based on the relative volatilities of these elements, if the Moon formed by high-T processing of Earth's mantle. Earth, rather than the Moon, appears to carry a signature of volatility-related fractionation in the alkali elements. This may reflect an early episode of intense heating on Earth with the Moon's alkali budget accreting from cooler material. Author

N94-36170*# National Aeronautics and Space Administration. Goddard Space Flight Center, Greenbelt, MD.

FORMATION OF IRON METAL AND GRAIN COAGULATION IN THE SOLAR NEBULA Abstract Only **c92**

Joseph A. Nuth, III and Otto Berg *In* Lunar and Planetary Inst., The Twenty-Fifth Lunar and Planetary Science Conference. Part 2: H-O 1994 p 1011 (For primary document see N94-36136 11-91)

Avail: CASI HC A01/MF A06

The interstellar grain population in the giant molecular cloud from which the sun formed contained little or no iron metal. However, thermal processing of individual interstellar silicates in the solar nebula is likely to result in the formation of a population of very small iron metal grains. If such grains are exposed to even transient magnetic fields, each will become a tiny dipole magnet capable of interacting with other such dipoles over spatial scale orders of magnitude larger than the radii of individual grains. Such interactions will greatly increase the coagulation cross-section for this grain population. Furthermore, the magnetic attraction between two iron dipoles will significantly increase both the collisional sticking coefficient and the strength of the interparticle binding energy for iron aggregates. Formation of iron metal may therefore be a key step in the aggregation of planetesimals in a protoplanetary nebula. Such aggregates may have already been observed in protoplanetary systems. The enhancement in the effective interaction distance between two magnetic dipoles is directly proportional to the strength of the magnetic dipoles and inversely proportional to the relative velocity. It is less sensitive to the reduced mass of the interacting particles (alpha M(exp -1/2)) and almost insensitive to the initial number density of magnetic dipoles (alpha n(sub o)(exp 1/6)). We are in the process of measuring the degree of coagulation in our condensation flow apparatus as a function of applied magnetic field and correlating these results by means of magnetic remanance acquisition measurements on our iron grains with the strength of the magnetic field to which the grains are exposed. Results of our magnetic remanance acquisition measurements and the magnetic-induced coagulation study will be presented as well as an estimate of the importance of such processes near the nebular midplane. Author

N94-36171*# National Aeronautics and Space Administration. Goddard Space Flight Center, Greenbelt, MD.

MEASUREMENT OF THE DECAY RATE OF THE SIH FEATURE AS A FUNCTION OF TEMPERATURE Abstract Only c70

Joseph A. Nuth, III and George F. Kraus *In* Lunar and Planetary Inst., The Twenty-Fifth Lunar and Planetary Science Conference. Part 2: H-O 1994 p 1013-1014 (For primary document see N94-36136 11-91)
Avail: CASI HC A01/MF A06

We have previously suggested that the SiH fundamental stretch could serve as a diagnostic indicator of the oxidation state of silicate surfaces exposed to the solar wind for prolonged periods. We have now measured the primary decay rate of SiH in vacuo as a function of temperature and find that the primary rate constant for the decay can be characterized by the following equation: k(min(exp -1)) approximately equals 0.186 exp(-9/RT) min(exp -1), where R = 2 x 10(exp -3) kcal deg(exp -1) mole(exp -1). This means that the half-life for the decay of the SiH feature at room temperature is approximately 20 yrs, whereas the half-life at a peak lunar regolith temperature of approximately 500K would be only approximately 20 days. At the somewhat lower temperature of approximately 400K the half-life for the decay is on the order of 200 days. The rate of loss of SiH as a function of temperature provides an upper limit to the quantity of H implanted by the solar wind which can be retained by a silicate grain in a planetary regolith. This will be discussed in more detail here. Author

N94-36172*# National Aeronautics and Space Administration. Lyndon B. Johnson Space Center, Houston, TX.

PRE-BOMBARDMENT CRYSTALLIZATION AGES OF BASALTIC CLASTS FROM ANTARCTIC HOWARDITES EET87503 AND EET87513 Abstract Only c90

L. E. Nyquist, C.-Y. Shih, H. Wiesmann, and B. M. Bansal *In* Lunar and Planetary Inst., The Twenty-Fifth Lunar and Planetary Science Conference. Part 2: H-O 1994 p 1015-1016 (For primary document see N94-36136 11-91)
Avail: CASI HC A01/MF A06

Igneous clasts of basaltic eucrites are found in both howardites and polymict eucrites. We have studied the Rb-Sr and Sm-Nd isotopic systematics of a number of such clasts, of metamorphic grades 1-6, using the classification of Takeda and Graham. Here, we report Rb-Sr, (147)Sm-(143)Nd, and (145)Sm-(142)Nd studies of clast, 53 from Antarctic howardite EET87503. Although there is no evidence of disturbance of trace element systematics by Antarctic weathering, the Rb-Sr and conventional Sm-Nd isotopic systematics are severely disturbed, which we ascribe to thermal metamorphism. The Ar-Ar age spectrum shows ages ranging from approximately 3.85-3.55 Ga in an unusual 'down stairstep'. The (146)Sm-(142)Nd systematics, however, show the presence of live (146)Sm(t(sub 1/2) = 103 Ma), with (146)Sm/(144)Sm = 0.0061 +/- 0.0007 at the time of crystallization. This result is very similar to that previously obtained for basaltic clast, 18 from howardite EET87513 (paired with EET87503), which has concordant Rb-Sr and Sm-Nd ages of approximately 4.5 Ga. Thus, the two clasts are nearly the same age, and we conclude further than the EET87503,53 clast crystallized within 33 +/- 19 Ma of the LEW86010 angrite by comparing initial (146)Sm/(144)Sm to that of the angrite. We suggest that disturbances in the isotopic systematics of EET87503,53 are consanguineous with pyroxene homogenization. Author

N94-36173*# National Aeronautics and Space Administration. Lyndon B. Johnson Space Center, Houston, TX.

NEW DATA SUPPORTING A Sm-146,147-Nd-142,143 FORMATION INTERVAL FOR THE LUNAR MANTLE Abstract Only

L. E. Nyquist, H. Wiesmann, B. M. Bansal, and C.-Y. Shih *In* Lunar and Planetary Inst., The Twenty-Fifth Lunar and Planetary Science Conference. Part 2: H-O 1994 p 1017-1018 (For primary document see N94-36136 11-91)
Avail: CASI HC A01/MF A06

Very small variations in Nd-142 abundance in SNC meteorites lunar basalts, and a terrestrial supracrustal rock, have been attributed to the decay of 103 Ma Sm-146 initially present in basalt source regions in varying abundances as a result of planetary differentiation. We previously interpreted variations in Nd-142 abundances in two Apollo 17 high-Ti basalts, three Apollo 12 low-Ti basalts, and two KREEP basalts as defining an isochron giving a formation interval of approximately 94 Ma for the lunar mantle. Here we report new data for a third Apollo 17 high-Ti basalt, two Apollo 15 low-Ti basalts, the VLT basaltic lunar meteorite A881757 (formerly Asuka 31), basalt-like KREEP impact melt rocks 14310 and 14078, and three terrestrial rock standards. Those lunar samples which were not exposed to large lunar surface thermal neutron fluences yield a revised mantle formation interval of 237 +/- 64 Ma. Author

N94-36174*# National Aeronautics and Space Administration. Lyndon B. Johnson Space Center, Houston, TX.

CALORIMETRIC THERMOBAROMETRY OF EXPERIMENTALLY SHOCKED QUARTZ Abstract Only c25

Katherine D. Ocker (Sam Houston State Univ., Huntsville, TX.), James L. Gooding, and Friedrich Hoerz *In* Lunar and Planetary Inst., The Twenty-Fifth Lunar and Planetary Science Conference. Part 2: H-O 1994 p 1021-1022 (For primary document see N94-36136 11-91)
Avail: CASI HC A01/MF A06

Structural damage in experimentally shock-metamorphosed, granular quartz is quantitatively measurable by differential scanning calorimetry (DSC). Shock-induced loss of crystallinity is witnessed by disappearance of the alpha/beta phase transformation and evolution of a broad endoenthalpic strain peak at 650-900 K. The strain-energy peak grows rapidly at less than 10 GPa but declines with increasing shock pressure; it approaches zero at 32 GPa where vitrification is extensive. Effects of grain size and post-shock thermal history must be better understood before calorimetric thermobarometry of naturally shocked samples becomes possible. Author

92 SOLAR PHYSICS

Includes solar activity, solar flares, solar radiation and sunspots. For related information see *93 Space Radiation.*

N94-35993*# New Hampshire Univ., Durham. Space Science Center.

A SEARCH FOR ENERGETIC ION DIRECTIVITY IN LARGE SOLAR FLARES Final Technical Report, 1 Nov. 1991 - 1 Nov. 1993

W. Thomas Vestrand 1993 6 p
(Grant NAGw-2756)
(NASA-CR-196036; NAS 1.26:196036) Avail: CASI HC A02/MF A01

One of the key observational questions for solar flare physics is: What is the number, the energy spectrum, and the angular distribution of flare accelerated ions? The standard method for deriving ion spectral shape employs the ratio of influences observed on the 4-7 MeV band to the narrow neutron capture line at 2.223 MeV. The 4-7 MeV band is dominated by the principal nuclear de-excitation lines from C-12 and O-16 which are generated in the low chromosphere by the direct excitation or spallation of nuclei by energetic ions. In contrast, the narrow 2.223 MeV line is produced by the capture of thermal neutrons on protons in the photosphere. These capture neutrons are generated by energetic ion interactions and thermalized by scattering in the solar atmosphere. In a series of papers, Ramaty, Lingenfelter, and their collaborators have calculated the expected ratio of fluence in the 4-7 MeV band to the 2.223 MeV line for a wide range of energetic ion spectral shapes (see, e.g. Hua and Lingenfelter 1987). Another technique for deriving ion spectral shapes and angular distributions uses the relative strength of the Compton tail associated with the 2.223 MeV neutron capture line (Vestrand 1988, 1990). This technique can independently constrain both the angular and the energy distribution of the energetic parent ions. The combination of this tail/line strength diagnostic with the line/(4-7) MeV fluence ratio can allow one to constrain both properties of the energetic ion distributions. The primary objective of our Solar Maximum Mission (SMM) guest investigator program was to study measurements of neutron capture line emission and prompt nuclear de-excitation for large flares detected by the Solar Maximum Mission/ Gamma-Ray Spectrometer (SMM/GRS) and to use these established line diagnostics to study the properties of flare accelerated ions. Derived from text

N94-36009 National Geophysical Data Center, Boulder, CO.

SOLAR-GEOPHYSICAL DATA NUMBER 594, FEBRUARY 1994. PART 2: (COMPREHENSIVE REPORTS). DATA FOR AUGUST 1993, AND MISCELLANEOUS

H. E. Coffey, ed. Feb. 1994 64 p See also PB94-151586 and PB94-163995, Part 1 Limited Reproducibility: More than 20% of this

document may be affected by microfiche quality
(ISSN 0038-0911)
(PB94-164001; SGD-594-Pt-2; LC-79-640375) Avail: CASI HC A04

This document contains: Part 1 (Prompt Reports); Part 2 (Comprehensive Reports); Detailed Index for 1993-1994; Data for August 1993; Miscellaneous Data; GOES Daily X-ray Background 1983-1993; GOES Electrons, Integrated Protons, and Magnetometer Data; and Monthly plots January 1993-1994. NTIS

N94-36020 National Geophysical Data Center, Boulder, CO.
SOLAR-GEOPHYSICAL DATA NUMBER 594, FEBRUARY 1994. PART 1: (PROMPT REPORTS). DATA FOR DECEMBER 1993, JANUARY 1994, AND LATE DATA
H. E. Coffey, ed. Feb. 1994 128 p See also PB94-151578 and PB94-164001, Part 2 Limited Reproducibility: More than 20% of this document may be affected by microfiche quality
(ISSN 0038-0911)
(PB94-163995; SGD-594-Pt-1; LC-79-640375) Avail: CASI HC A07

Contents: Data for January 1994; Solar-Terrestrial Environment; IUWDS Alert Periods (Advance and Worldwide); Solar Activity Indicies; Solar Flares; and Solar Radio Emission. NTIS

N94-36210 Rutherford Appleton Lab., Chilton (England).
COLLECTIVE PLASMA CORRECTIONS TO THE SOLAR OPACITY
V. N. Tsytovich, R. Bingham, and U. deAngelis Mar. 1994 7 p Prepared in cooperation with Academy of Sciences (USSR), Moscow, Russia and Naples Univ., Italy
(PB94-170511; RAL-94-023) Avail: Issuing Activity (National Technical Information Service (NTIS))

This report contains a final table of opacity changes by several collective effects previously not taken into account in the calculation of the solar opacity. As the neutrino solar flux is very sensitive to small changes in the solar opacity, we calculate all corrections with a 5 place accuracy, but present only in percent to significant two figures after the point. The calculations were performed by MCAD programs which give 5 figures after the point. This accuracy is needed as all corrections are finally described by triple or fourth integrals and one should keep the accuracy at each step of the calculation of the inner integrals. To calculate some of the integrals, the time was of order of 100 hours. The calculations present the Rosseland opacity Kappa. Kappa(sub 0) denotes the Rosseland opacity previously taken into account in which the collective scattering only included the first approximation. NTIS

N94-36264# Boston Coll., Newton, MA. Inst. for Space Research.
CATALOG OF HELIOS 90 DEG PHOTOMETER EVENTS Scientific Report No. 4
Bernard V. Jackson (California Univ., San Diego, La Jolla, CA.), David F. Webb, Paul L. Hick, and Jessica L. Nelson Feb. 1994 57 p
(Contract F19628-90-K-0006; AF Proj. 2311)
(PL-TR-94-2040) Avail: CASI HC A04/MF A01

The two Helios spacecraft were launched into solar orbits in December 1974 and January 1976. Each spacecraft contained three zodiacal light photometers intended to measure the distribution of dust in the interplanetary medium between the Sun and the Earth. Residual brightness variations were evident after the zodiacal light and stellar contributions had been removed from the photometer data. These variations are now known to have been caused primarily by transient plasma clouds propagating through the inner heliosphere. About 2/3 of these were caused by coronal mass ejections and about 1/4 by corotating structures. We have used specific criteria to select and identify these plasma events in the data from the Helios photometers which pointed at the ecliptic poles. This process is now complete and we are making these data available to the scientific community. This document is a catalog of the Helios 90 degree photometer events which we have identified. In the following text we describe the pertinent characteristics of the zodiacal light experiment, the methods used to select, identify and classify the 90 degree events, and the details of the catalog structure. A comprehensive bibliography of all published papers involving analyses of the Helios photometer plasma observations and the zodiacal light calibration is also included. Author (revised)

N94-36395*# Alabama Univ., Huntsville, AL. Dept. of Mechanical and Aerospace Engineering.
ON THE PHYSICS OF WAVES IN THE SOLAR ATMOSPHERE: WAVE HEATING AND WIND ACCELERATION Annual Report, period ending Aug. 1993
Z. E. Musielak Aug. 1993 8 p
(Grant NAG8-839)
(NASA-CR-194119; NAS 1.26:194119) Avail: CASI HC A02/MF A01

This paper presents work performed on the generation and physics of acoustic waves in the solar atmosphere. The investigators have incorporated spatial and temporal turbulent energy spectra in a newly corrected version of the Lighthill-Stein theory of acoustic wave generation in order to calculate the acoustic wave energy fluxes generated in the solar convective zone. The investigators have also revised and improved the treatment of the generation of magnetic flux tube waves, which can carry energy along the tubes far away from the region of their origin, and have calculated the tube energy fluxes for the sun. They also examine the transfer of the wave energy originated in the solar convective zone to the outer atmospheric layers through computation of wave propagation and dissipation in highly nonhomogeneous solar atmosphere. These waves may efficiently heat the solar atmosphere and the heating will be especially significant in the chromospheric network. It is also shown that the role played by Alfven waves in solar wind acceleration and coronal hole heating is dominant. The second part of the project concerned investigation of wave propagation in highly inhomogeneous stellar atmospheres using an approach based on an analytic tool developed by Musielak, Fontenla, and Moore. In addition, a new technique based on Dirac equations has been developed to investigate coupling between different MHD waves propagating in stratified stellar atmospheres. Author

N94-36170*# National Aeronautics and Space Administration. Goddard Space Flight Center, Greenbelt, MD.
FORMATION OF IRON METAL AND GRAIN COAGULATION IN THE SOLAR NEBULA Abstract Only
Joseph A. Nuth, III and Otto Berg *In* Lunar and Planetary Inst., The Twenty-Fifth Lunar and Planetary Science Conference. Part 2: H-O 1994 p 1011 (For primary document see N94-36136 11-91)
Avail: CASI HC A01/MF A06

93 SPACE RADIATION

Includes cosmic radiation; and inner and outer earth's radiation belts.

For biological effects of radiation see *52 Aerospace Medicine.* For theory see *73 Nuclear and High-Energy Physics.*

N94-35381*# EMR-Photoelectric, Princeton, NJ.
X-RAY REMOTE SENSING AND IN-SITU SPECTROSCOPY FOR PLANETARY EXPLORATION MISSIONS AND GAMMA-RAY REMOTE SENSING AND IN-SITU SPECTROSCOPY FOR PLANETARY EXPLORATION MISSIONS
M. Mahdavi, K. L. Giboni, S. Vajda, and J. Schweitzer 9 May 1994 27 p
(Contract NAS5-32486; RTOP 691-00-00)
(NASA-CR-189352; NAS 1.26:189352) Avail: CASI HC A03/MF A01

Detectors that will be used for planetary missions must have their responses calibrated in a reproducible manner. A calibration facility is being constructed at Schlumberger-Doll Research for gamma and x ray detectors. With this facility the detector response can be determined in an invariant and reproducible fashion. Initial use of the facility is expected for the MARS94 detectors. Work is continuing to better understand the rare earth oxyorthosilicates and to define their characteristics. This will allow a better use of these scintillators for planetary missions. In a survey of scintillating materials two scintillators were identified as promising candidates besides GSO, LSO, and YSO. These are CdWO4 and CsI(Tl). It will be investigated if a detector with a better overall performance can be assembled with various photon converters. Considerable progress was achieved in photomultiplier design. The length of an 1 inch diameter PMT could be reduced from 4.2 to 2.5 inches without performance degradation. This technology is being employed in the gamma ray detector for the NEAR project. A further weight and size reduction of the detector package can be achieved with miniaturized integrated power supplies. Author (revised)

N94-35515*# Louisiana State Univ., Baton Rouge, LA. Dept. of Physics and Astronomy.
A SEARCH FOR RADIATIVE NEUTRINO DECAY FROM SUPERNOVAE Final Technical Report
Robert C. Svoboda 1993 18 p
(Grant NAG5-2062)
(NASA-CR-196011; NAS 1.26:196011) Avail: CASI HC A03/MF A01

Two supernovae have been identified in the COMPTEL data base as being the best sources to investigate for evidence of gamma-ray emission caused by radiative neutrino decay. These are SN1987a and SN1993J. A detailed simulation has shown us that we can expect a gain in sensitivity 1-3 orders of magnitude (depending on neutrino mass) over previous results. Instrument response is now being modeled using a SPARC10 computer acquired for this study. A library of simulated gamma-ray lines is being produced for COMPTEL as a by-product of this effort. Author (revised)

N94-36421*# Alabama Univ., Huntsville, AL. Dept. of Physics.
THEORETICAL AND EXPERIMENTAL STUDIES RELEVANT TO INTERPRETATION OF AURORAL EMISSIONS Final Report
Charles E. Keffer 25 Jun. 1994 129 p
(Grant NAG8-834)
(NASA-CR-196032; NAS 1.26:196032) Avail: CASI HC A07/MF A02

This report describes the accomplishments of a program designed to develop the tools necessary to interpret auroral emissions measured from a space-based platform. The research was divided into two major areas. The first area was a laboratory study designed to improve our understanding of the space vehicle external environment and how it will affect the space-based measurement of auroral emissions. Facilities have been setup and measurements taken to simulate the gas phase environment around a space vehicle; the radiation environment encountered by an orbiting vehicle that passes through the Earth's radiation belts; and the thermal environment of a vehicle in Earth orbit. The second major area of study was a modeling program to develop the capability of using auroral images at various wavelengths to infer the total energy influx and characteristic energy of the incident auroral particles. An ab initio auroral calculation has been added to the extant ionospheric/thermospheric global modeling capabilities within our group. Once the addition of the code was complete, the combined model was used to compare the relative intensities and behavior of various emission sources (dayglow, aurora, etc.). Attached papers included are: 'Laboratory Facility for Simulation of Vehicle-Environment Interactions'; 'Workshop on the Induced Environment of Space Station Freedom'; 'Radiation Damage Effects in Far Ultraviolet Filters and Substrates'; 'Radiation Damage Effects in Far Ultraviolet Filters, Thin Films, and Substrates'; 'Use of FUV Auroral Emissions as Diagnostic Indicators'; and 'Determination of Ionospheric Conductivities from FUV Auroral Emissions'. Derived from text

99 GENERAL

N94-35262# Federal Aviation Administration, Washington, DC.
THE FEDERAL AVIATION ADMINISTRATION PLAN FOR RESEARCH, ENGINEERING AND DEVELOPMENT
May 1994 190 p Original contains color illustrations
Avail: CASI HC A09/MF A02; 1 functional color page

The Federal Aviation Administration (FAA) manages and operates the National Airspace System (NAS), a significant national resource. However, the demands on this system are continuously growing, and changing technologies provide the opportunity to improve system effectiveness and efficiency. To this end, the FAA's research, engineering, and development program is an investment in the future that will sustain the United States preeminence in aviation throughout the world. Without this investment, the United States leadership would erode. Thus, the importance of aviation to the nation mandates a comprehensive research, engineering, and development program to ensure both the safety of public air transportation and the fulfillment of national priorities and policy goals. Derived from text

N94-35356*# American Univ., Washington, DC. Office of Research Services.
SPACE AND THE AMERICAN IMAGINATION Progress Report, Mar. - May 1994
Howard E. McCurdy 31 May 1994 70 p
(Contract NASw-4798)
(NASA-CR-196131; NAS 1.26:196131) Avail: CASI HC A04/MF A01

The introduction will set out the principal theme of the book: that the rise of the U.S. space program was due to a concerted effort by science writers, engineers, industrialists, and civic and political leaders to create a popular culture of space exploration based on important elements of American social life (such as frontier mythology, fears about the cold war, and the rise of the consumer culture). Much of the disillusionment with the NASA space program which set in during the third decade of space flight can be traced to a widening gap between popular expectations and the reality of space exploration. Author

N94-35363*# Space Telescope Science Inst., Baltimore, MD. Special Studies Office.
APOLLO 11 AT TWENTY-FIVE, VERSION 1.0 (Diskette)
1994 Diskette: Two 3.5-inch MF2-HD Apple diskettes
(Grant NAGw-3048)
(NASA-CR-193380; NAS 1.26:193380; NONP-NASA-DK-94-15961) Avail: CASI DK A03

An historical perspective of the Apollo Project is presented. The topics covered include the following: Kennedy addressing a Joint Session of Congress; Gagarin preparing for flight; Apollo's budget; the Apollo workforce; expanding the infrastructure; the management team; the Apollo Mission profile; Von Braun briefing engineers; the Kennedy visit to MSFC; the Mercury launch; Gemini EVA; Surveyor on the Moon; the Saturn 5 diagram; Saturn 5 stages; Saturn 5 at night; the debate over testing; and the Apollo spacecraft diagram. CASI

N94-35370*# National Aeronautics and Space Administration. Ames Research Center, Moffett Field, CA.
DIRECTOR'S DISCRETIONARY FUND Report, FY 1992
May 1993 133 p
(RTOP 307-51-50)
(NASA-TM-103997; A-93031; NAS 1.15:103997) Avail: CASI HC A07/MF A02

This technical memorandum contains brief technical papers describing research and technology development programs sponsored by the ARC Director's Discretionary Fund during fiscal year 1992 (Oct. 1991 through Sep. 1992). An appendix provides administrative information for each of the 45 sponsored research programs. Author

N94-35444# Advisory Group for Aerospace Research and Development, Neuilly-Sur-Seine (France).
AGARD HIGHLIGHTS 93/2
Sep. 1993 47 p Original contains color illustrations
(AGARD-Highlights-93/2) Copyright Avail: CASI HC A03/MF A01

Highlights of the activities and accomplishments of the Advisory Group for Aerospace Research and Development (AGARD) during the second quarter of 1993 are discussed. Topics covered include technology cooperation with Russia, including aircraft flight safety; the von Karman Medal and the Scientific Achievement Award for 1993; two articles on a visit to Zhukovsky, including discussion on fluid dynamics related to helicopters; international air traffic handling cooperation; and the European Transonic Wind Tunnel (ETW). CASI

N94-35590*# Universities Space Research Association, Boulder, CO.
INTRODUCTION TO USRA
M. H. Davis, ed. and A. Singy, ed. 1994 42 p
(Grant NAGw-3834)
(NASA-CR-195980; NAS 1.26:195980) Avail: CASI HC A03/MF A01

The Universities Space Research Association (USRA) was incorporated 25 years ago in the District of Columbia as a private nonprofit corporation under the auspices of the National Academy of Sciences. Institutional membership in the association has grown from 49 colleges and universities, when it was founded, to 76 in 1993. USRA provides a mechanism through which universities can cooperate effectively with one another, with the government, and with other organizations to further space science and

technology and to promote education in these areas. Its mission is carried out through the institutes, centers, divisions, and programs that are described in detail in this booklet. These include the Lunar and Planetary Institute, the Institute for Computer Applications in Science and Engineering (ICASE), the Research Institute for Advanced Computer Science (RIACS), and the Center of Excellence in Space Data and Information Sciences (CESDIS).
CASI

N94-35961*# National Aeronautics and Space Administration. Ames Research Center, Moffett Field, CA.
1993 TECHNICAL PAPER CONTEST FOR WOMEN. GEAR UP 2000: WOMEN IN MOTION
Robin Orans, ed., Sophie Duckett, ed., and Susan White, ed. Feb. 1994 131 p Contest held in Moffett Field, CA, 1993
(NASA-CP-10134; A-93034; NAS 1.55:10134) Avail: CASI HC A07/MF A02

The NASA Ames Research Center Advisory Committee for Women (ACW) sponsored the second ACW Technical paper Contest for Ames women in order to increase the visibility of, and to encourage writing for publication by Ames women scientists, engineers, and technicians. The topics of the contest paper mirrored in the topics of the 1993 Society for Women Engineers (SWE) National Convention, which included technological, workplace, global, and family issues. For individual titles, see N94-35962 through N94-35973.

N94-35962*# National Aeronautics and Space Administration. Ames Research Center, Moffett Field, CA.
PILOTED SIMULATION STUDY OF TWO TILT-WING CONTROL CONCEPTS **c08**
Lourdes G. Birckelbaw and Lloyd D. Corliss *In its* 1993 Technical Paper Contest for Women. Gear Up 2000: Women in Motion Feb. 1994 p 1-12 (For primary document see N94-35961 11-99)
Avail: CASI HC A03/MF A02

A two-phase piloted simulation study was conducted to investigate alternative wing and flap controls for tilt-wing aircraft. The initial phase of the study compared the flying qualities of both a conventional (programmed) flap and an innovative geared flap. The second phase of the study introduced an alternate method of pilot control for the geared flap and further studied the flying qualities of the programmed flap, and two geared flap configurations. In general, the pilot rating showed little variation between the programmed flap and the geared flap control concepts. Some differences between the two concepts were noticed and are discussed in this paper. The addition of pitch attitude stabilization in the second phase of the study greatly enhanced the aircraft flying qualities. This paper describes the simulated tilt-wing aircraft and the flap control concepts and presents the results of both phases of the simulation study. Author

N94-35963*# National Aeronautics and Space Administration. Hugh L. Dryden Flight Research Facility, Edwards, CA.
ENGINE EXHAUST CHARACTERISTICS EVALUATION IN SUPPORT OF AIRCRAFT ACOUSTIC TESTING **c71**
Kimberly A. Ennix *In* NASA. Ames Research Center, 1993 Technical Paper Contest for Women. Gear Up 2000: Women in Motion Feb. 1994 p 13-20 (For primary document see N94-35961 11-99)
Avail: CASI HC A02/MF A02

NASA Dryden Flight Research Facility and NASA Langley Research Center completed a joint acoustic flight test program. Test objectives were (1) to quantify and evaluate subsonic climb-to-cruise noise and (2) to obtain a quality noise database for use in validating the Aircraft Noise Prediction Program. These tests were conducted using aircraft with engines that represent the high nozzle pressure ratio of future transport designs. Test flights were completed at subsonic speeds that exceeded Mach 0.3 using F-18 and F-16XL aircraft. This paper describes the efforts of NASA Dryden Flight Research Facility in this flight test program. Topics discussed include the test aircraft, setup, and matrix. In addition, the engine modeling codes and nozzle exhaust characteristics are described. Author

N94-35964*# National Aeronautics and Space Administration. Ames Research Center, Moffett Field, CA.
MENTORING FOR 2000 AND BEYOND **c80**
K. M. Guerra (General Electric Co., Moffett Field, CA.) and M. A. Farrance *In its* 1993 Technical Paper Contest for Women. Gear Up 2000: Women in Motion Feb. 1994 p 21-25 (For primary document see N94-35961 11-99)
Avail: CASI HC A01/MF A02

Today, more than 40 percent of the United States workforce are women. However, only a small percentage of working women are employed in science or engineering fields. The numbers of women in engineering and math professions have actually decreased since 1984. Last year, a mentoring program was created at NASA Ames Research Center aimed at encouraging young girls to stay in school, increasing their self confidence and helping them perform better academically. Teachers at the Ronald McNair Intermediate School matched fifth through eighth grade students with women engineers at NASA Ames. Results from a year-end survey submitted by the mentees indicated that the program was successful in achieving its first-year goals; more than one student reported that she felt 'really special' because of her mentor's efforts. The NASA Ames Mentor program has continued into the 1992-93 academic year with both returning mentor/mentee pairs and new participants. Author

N94-35965*# National Aeronautics and Space Administration. Ames Research Center, Moffett Field, CA.
WIND TUNNEL MEASUREMENTS ON A FULL-SCALE F/A-18 WITH A TANGENTIALLY BLOWING SLOT **c02**
Wendy R. Lanser *In its* 1993 Technical Paper Contest for Women. Gear Up 2000: Women in Motion Feb. 1994 p 27-36 (For primary document see N94-35961 11-99)
Avail: CASI HC A02/MF A02

A full-scale F/A-18 was tested in the 80 by 120-Foot Wind Tunnel at NASA Ames Research Center to measure the effectiveness of a tangentially blowing slot in generating significant yawing moments while minimizing coupling in the pitch and roll axes. Various slot configurations were tested to determine the optimum configuration. The test was conducted for angles of attack from 25 to 50 deg, angles of sideslip from -15 to +15 deg, and freestream velocities from 67 ft/sec to 168 ft/sec. By altering the forebody vortex flow, yaw control was maintained for angles of attack up to 50 deg. Of particular interest was the result that blowing very close to the radome apex was not as effective as blowing slightly farther aft on the radome, that a 16-inch slot was more efficient, and that yawing moments were generated without inducing significant rolling or pitching moments. Author

N94-35966*# SYRE Corp., Moffett Field, CA.
WOMEN AS A RESOURCE FOR THE FLEXIBILITY REQUIRED FOR HIGH TECHNOLOGY INNOVATION **c85**
Ruth Dasso Marlaire *In* NASA. Ames Research Center, 1993 Technical Paper Contest for Women. Gear Up 2000: Women in Motion Feb. 1994 p 37-40 (For primary document see N94-35961 11-99)
Avail: CASI HC A01/MF A02

What do women scientists need to know for career advancement into senior level positions? Our declining economic conditions have been the cause for major political and technological changes. The U.S. Congress is turning toward technology to increase our competitive edge in the world. Allowing women scientists, and women engineers in particular, more voice in the decision making process may be an innovative alternative for the diversity and flexibility needed for the unknown technological problems of the future. But first women scientists need to know how the system measures scientific achievement and how to identify the processes needed to increase our technological capability in order for them to formidably compete and win higher ranking positions. Author

N94-35967*# National Aeronautics and Space Administration. Hugh L. Dryden Flight Research Facility, Edwards, CA.
A BIASED HISTORICAL PERSPECTIVE OF WOMEN IN THE ENGINEERING FIELD AT DRYDEN FROM 1946 TO NOVEMBER 1992 **c31**
Sheryll Goecke Powers *In* NASA. Ames Research Center, 1993 Technical Paper Contest for Women. Gear Up 2000: Women in Motion Feb. 1994 p 41-61 (For primary document see N94-35961 11-99)
Avail: CASI HC A03/MF A02

Being a woman in engineering, and in particular, being the woman with the dubious distinction of having the most years at Dryden, gives the author a long-term perspective on the women who worked in the engineering field and their working environment. The working environment for the women was influenced by two main factors. One factor was the Dryden's growth of 14 persons (2 of them women) at the end of 1946 to the present size. The other factor was the need for programming knowledge when the digital computers came into use. Women have been involved with flight research at Dryden since the days of the first transonic and supersonic airplanes. This paper uses available records, along with memory, to document the number of women in engineering at Dryden, to comment about observed trends, and to make personal observations. Author

N94-35968*# National Aeronautics and Space Administration. Hugh L. Dryden Flight Research Facility, Edwards, CA.

EXPERIENCE WITH Ada ON THE F-18 HIGH ALPHA RESEARCH VEHICLE FLIGHT TEST PROGRAM **c61**

Victoria A. Regenie, Michael Earls, Jeanette Le, and Michael Thomson *In* NASA. Ames Research Center, 1993 Technical Paper Contest for Women. Gear Up 2000: Women in Motion Feb. 1994 p 63-76 (For primary document see N94-35961 11-99)

Avail: CASI HC A03/MF A02

Considerable experience has been acquired with Ada at the NASA Dryden Flight Research Facility during the on-going High Alpha Technology Program. In this program, an F-18 aircraft has been highly modified by the addition of thrust-vectoring vanes to the airframe. In addition, substantial alteration was made in the original quadruplex flight control system. The result is the High Alpha Research Vehicle. An additional research flight control computer was incorporated in each of the four channels. Software for the research flight control computer was written Ada. To date, six releases of this software have been flown. This paper provides a detailed description of the modifications to the research flight control system. Efficient ground-testing of the software was accomplished by using simulations that used the Ada for portions of their software. These simulations are also described. Modifying and transferring the Ada flight software to the software simulation configuration has allowed evaluation of this language. This paper also discusses such significant issues in using Ada as portability, modifiability, and testability as well as documentation requirements. Author

N94-35969*# National Aeronautics and Space Administration. Hugh L. Dryden Flight Research Facility, Edwards, CA.

IN-FLIGHT SIMULATION STUDIES AT THE NASA DRYDEN FLIGHT RESEARCH FACILITY **c05**

Mary F. Shafer *In* NASA. Ames Research Center, 1993 Technical Paper Contest for Women. Gear Up 2000: Women in Motion Feb. 1994 p 77-97 (For primary document see N94-35961 11-99)

Avail: CASI HC A03/MF A02

Since the late 1950's the National Aeronautics and Space Administration's Dryden Flight Research Facility has found in-flight simulation to be an invaluable tool. In-flight simulation has been used to address a wide variety of flying qualities questions, including low lift-to-drag ratio approach characteristics for vehicles like the X-15, the lifting bodies, and the space shuttle; the effects of time delays on controllability of aircraft with digital flight control systems; the causes and cures of pilot-induced oscillation in a variety of aircraft; and flight control systems for such diverse aircraft as the X-15 and the X-29. In-flight simulation has also been used to anticipate problems, avoid them, and solve problems once they appear. This paper presents an account of the in-flight simulation at the Dryden Flight Research Facility and some discussion. An extensive bibliography is included. Author

N94-35970*# National Aeronautics and Space Administration. Ames Research Center, Moffett Field, CA.

IMPLEMENTATION OF A COMPUTERIZED MAINTENANCE MANAGEMENT SYSTEM **c81**

Yong-Hong Shen and Bruce Askari *In its* 1993 Technical Paper Contest for Women. Gear Up 2000: Women in Motion Feb. 1994 p 99-109 (For primary document see N94-35961 11-99)

Avail: CASI HC A03/MF A02

A primer Computerized Maintenance Management System (CMMS) has been established for NASA Ames pressure component certification program. The CMMS takes full advantage of the latest computer technology and SQL relational database to perform periodic services for vital pressure components. The Ames certification program is briefly described and the aspects of the CMMS implementation are discussed as they are related to the certification objectives. Author

N94-35971*# National Aeronautics and Space Administration. Ames Research Center, Moffett Field, CA.

SPACE-BASED CRYSTAL GROWTH AND THERMOCAPILLARY FLOW **c76**

Yong-Hong Shen *In its* 1993 Technical Paper Contest for Women. Gear Up 2000: Women in Motion Feb. 1994 p 111-116 (For primary document see N94-35961 11-99)

Avail: CASI HC A02/MF A02

The demand for larger crystals is increasing especially in applications associated with the electronic industry, where large and pure electronic crystals (notably silicon) are the essential material to make high-performance computer chips. Crystal growth under weightless conditions has been considered an ideal way to produce bigger and hopefully better crystals. One technique which may benefit from a microgravity environment is the float-zone crystal-growth process, a containerless method for producing high-quality electronic material. In this method, a rod of material to be refined is moved slowly through a heating device which melts a portion of it. Ideally, as the melt resolidifies it does so as a single crystal which is then used as substrate for building microelectronic devices. The possibility of contamination by contact with other material is reduced because of the 'float' configuration. However, since the weight of the material contained in the zone is supported by the surface-tension force, the size of the resulting crystal is limited in Earth-based productions; in fact, some materials have properties which prevent this process from being used to manufacture crystals of reasonable size. Consequently, there has been a great deal of interest in exploiting the microgravity environment of space to grow larger size crystals of electronic material using the float-zone method. In addition to allowing larger crystals to be grown, a microgravity environment would also significantly reduce the magnitude of convection induced by buoyancy forces during the melting state. This type of convection was once thought to be at least partially responsible for the presence of undesirable nonuniformities--called striations--in material properties observed in float-zone material. However, past experiments on crystal growth under weightless conditions found that even with the absence of gravity, the float-zone method sometimes still results striations. It is believed that another mechanism is playing a dominant role in the microgravity environment. Author (revised)

N94-35972*# National Aeronautics and Space Administration. Ames Research Center, Moffett Field, CA.

GROUND VIBRATION TEST OF THE XV-15 TILTROTOR RESEARCH AIRCRAFT AND PRETEST PREDICTIONS **c08**

Karen Studebaker and Anita Abrego *In its* 1993 Technical Paper Contest for Women. Gear Up 2000: Women in Motion Feb. 1994 p 117-123 (For primary document see N94-35961 11-99)

Avail: CASI HC A02/MF A02

The first comprehensive ground vibration survey was performed on the XV-15 Tiltrotor Research Aircraft to measure the vibration modes of the airframe and to provide data critical for determining whirl flutter stability margins. The aircraft was suspended by the wings with bungee cords and cables. A NASTRAN finite element model was used in the design of the suspension system to minimize its interference with the wing modes. The primary objective of the test was to measure the dynamic characteristics of the wings and pylons for aeroelastic stability analysis. In addition, over 130 accelerometers were placed on the airframe to characterize the fuselage, wing, and tail vibration. Pretest predictions were made with the NASTRAN model as well as correlations with the test data. The results showed that the suspension system provided the isolation necessary for modal measurements. Author (revised)

N94-35973*# National Aeronautics and Space Administration. Ames Research Center, Moffett Field, CA.

BUILDING ON THE FOUNDATION FOR AN ENGINEERING CAREER **c80**

Susan White and Ruth White *In its* 1993 Technical Paper Contest for Women. Gear Up 2000: Women in Motion Feb. 1994 p 125-130 (For primary document see N94-35961 11-99)

Avail: CASI HC A02/MF A02

A predictable and preventable hurdle stops a majority of young women from entering the scientific and technical fields. This cuts down the individual's career possibilities and cuts in half the pool of potential U.S. engineers later available to industry. The waste of talent does not advance our country's competitive position. The typical American adolescent girl has acquired all the basic mathematical skills needed to pursue science and math, but, from adolescence on, she does not build the foundation of science and math courses that she would need later in life to work in engineering. Several questions are addressed: Why are some young women stopped cold in their mathematical tracks during adolescence? What is the influence of psychology, including discussion of the personality traits quantifiably shared by women in technical fields? and How should the school system adapt to keep their female charges learning math and science? Author

N94-35997 Lawrence Livermore National Lab., CA.
PROCEEDINGS OF THE LLNL TECHNICAL WOMEN'S SYMPOSIUM
E. VonHoltz, ed. 1993 62 p Symposium held in Lafayette, CA, 6-7 May 1993 Limited Reproducibility: More than 20% of this document may be affected by microfiche quality
(Contract W-7405-eng-48)
(DE94-006616; CONF-9305257) Avail: CASI HC A04

This report documents events of the LLNL Technical Women's Symposium. Topics include: future of computer systems; environmental technology; defense and space; Nova inertial confinement fusion target physics; technical communication; tools and techniques for biology in the 1990's; automation and robotics; software applications; materials science; atomic vapor laser isotope separation; technical communication; technology transfer; and professional development workshops. DOE

N94-36042# Loyola Coll., Baltimore, MD. Japanese Technology Evaluation Center.
JTEC/WTEC REPORT AND PROGRAM SUMMARY Annual Report, 1993-1994
Geoffrey M. Holdridge, ed. Mar. 1994 204 p
(Grants NSF ECS-89-02528; NSF ECS-89-22947; NSF ENG-91-11333; NSF ENG-92-17849)
Avail: CASI HC A10/MF A03

The mission of the Japanese Technology Evaluation Center (JTEC) and the World Technology Evaluation Center (WTEC) is to inform research and development policy makers in government, industry, and academe concerning the current status and trends in high technology abroad. This annual report includes the following new summaries of completed projects: satellite communications systems and technology in Europe, Russia, and Japan; knowledge-based systems in Japan; advanced manufacturing technology for polymer composite structures in Japan; separation technology in Japan; research submersibles and undersea technologies in Russia, Ukraine, and Western Europe; comparative assessments of nuclear instrumentation and controls in the U.S., Canada, Japan, Western Europe, and the former Soviet Union; and instrumentation, control, and safety systems of Canadian nuclear facilities. For individual titles, see N94-36043 through N94-36047.

N94-36043*# Jet Propulsion Lab., California Inst. of Tech., Pasadena, CA.
INFORMATION AND COMMUNICATION TECHNOLOGY c32
Burton I. Edelson (George Washington Univ., Washington, DC.), Joseph N. Pelton (Colorado Univ., Boulder, CO.), Charles W. Bostian (Virginia Polytechnic Inst. and State Univ., Blacksburg, VA.), William T. Brandon (Mitre Corp., Bedford, MA.), Vincent W. S. Chan (Massachusetts Inst. of Tech., Cambridge.), E. Paul Hager (George Mason Univ., Fairfax, VA.), Neil R. Helm (George Washington Univ., Washington, DC.), Raymond D. Jennings (National Telecommunications and Information Administration, Washington, DC.), Robert K. Kwan, and Christoph E. Mahle et al *In* Loyola Coll., JTEC/WTEC Report and Program Summary Mar. 1994 p 45-53 Prepared in cooperation with NASA. Lewis Research Center, Cleveland, OH (For primary document see N94-36042 11-99)
Avail: CASI HC A02/MF A03

NASA and the National Science Foundation (NSF) commissioned a panel of U.S. experts to study the international status of satellite communications systems and technology. The study covers emerging systems concepts, applications, services, and the attendant technologies. The panel members traveled to Europe, Japan, and Russia to gather information firsthand. They visited 17 sites in Europe, 20 in Japan, and 4 in Russia. These included major manufacturers, government organizations, service providers, and associated research and development facilities. The panel's report was reviewed by the sites visited, by the panel, and by representatives of U.S. industry. The report details the information collected and compares it to U.S. activities. Author (revised)

N94-36044*# National Aeronautics and Space Administration. Ames Research Center, Moffett Field, CA.
KNOWLEDGE-BASED SYSTEMS IN JAPAN c82
Edward Feigenbaum (Stanford Univ., CA.), Robert S. Engelmore (Stanford Univ., CA.), Peter E. Friedland, Bruce B. Johnson, H. Penny Nii, Herbert Schorr, and Howard Shrobe *In* Loyola Coll., JTEC/WTEC Report and Program Summary Mar. 1994 p 54-60 (For primary document see N94-36042 11-99)
Avail: CASI HC A02/MF A03

This report summarizes a study of the state-of-the-art in knowledge-based systems technology in Japan, organized by the Japanese Technology Evaluation Center (JTEC) under the sponsorship of the National Science Foundation and the Advanced Research Projects Agency. The panel visited 19 Japanese sites in March 1992. Based on these site visits plus other interactions with Japanese organizations, both before and after the site visits, the panel prepared a draft final report. JTEC sent the draft to the host organizations for their review. The final report was published in May 1993. Derived from text

N94-36045*# National Aeronautics and Space Administration. Lewis Research Center, Cleveland, OH.
ADVANCED COMPOSITES IN JAPAN c24
R. Judd Diefendorf (Clemson Univ., SC.), William G. Hillig (General Electric Co., Schenectady, NY.), Salvatore J. Grisaffe, R. Byron Pipes, John H. Perepezko, and James E. Sheehan *In* Loyola Coll., JTEC/WTEC Report and Program Summary Mar. 1994 p 99-101 (For primary document see N94-36042 11-99)
Avail: CASI HC A01/MF A03

The JTEC Panel on Advanced Composites surveyed the status and future directions of Japanese high-performance ceramic and carbon fibers and their composites in metal, intermetallic, ceramic, and carbon matrices. Because of a strong carbon and fiber industry, Japan is the leader in carbon fiber technology. Japan has initiated an oxidation-resistant carbon/carbon composite program. With its outstanding technical base in carbon technology, Japan should be able to match present technology in the U.S. and introduce lower-cost manufacturing methods. However, the panel did not see any innovative approaches to oxidation protection. Ceramic and especially intermetallic matrix composites were not yet receiving much attention at the time of the panel's visit. There was a high level of monolithic ceramic research and development activity. High temperature monolithic intermetallic research was just starting, but notable products in titanium aluminides had already appeared. Matrixless ceramic composites was one novel approach noted. Technologies for high temperature composites fabrication existed, but large numbers of panels or parts had not been produced. The Japanese have selected aerospace as an important future industry. Because materials are an enabling technology for a strong aerospace industry, Japan initiated an ambitious long-term program to develop high temperature composites. Although just starting, its progress should be closely monitored in the U.S. Derived from text

N94-36046*# National Aeronautics and Space Administration. Goddard Space Flight Center, Greenbelt, MD.
SPACE ROBOTICS IN JAPAN c37
William Whittaker (Carnegie-Mellon Univ., Pittsburgh, PA.), James W. Lowrie (Martin Marietta Corp., Denver, CO.), Harry McCain, Antal Bejczy, Tom Sheridan, Takeo Kanade, and Peter Allen *In* Loyola Coll., JTEC/WTEC Report and Program Summary Mar. 1994 p 133-137 (For primary document see N94-36042 11-99)
Avail: CASI HC A01/MF A03

Japan has been one of the most successful countries in the world in the realm of terrestrial robot applications. The panel found that Japan has in place a broad base of robotics research and development, ranging from components to working systems for manufacturing, construction, and human service industries. From this base, Japan looks to the use of robotics in space applications and has funded work in space robotics since the mid-1980's. The Japanese are focusing on a clear image of what they hope to achieve through three objectives for the 1990's: developing long-reach manipulation for tending experiments on Space Station Freedom, capturing satellites using a free-flying manipulator, and surveying part of the moon with a mobile robot. This focus and a sound robotics infrastructure is enabling the young Japanese space program to develop relevant systems for extraterrestrial robotics applications. Derived from text

N94-36047*# National Aeronautics and Space Administration. Marshall Space Flight Center, Huntsville, AL.
SPACE AND TRANSATMOSPHERIC PROPULSION TECHNOLOGY c20
Charles Merkle (Pennsylvania State Univ., University Park, PA.), Maynard L. Stangeland (Rockwell International Corp., Canoga Park, CA.), James R. Brown (Pratt and Whitney Aircraft, East Hartford, CT.), John P. McCarty, Louis A. Povinelli, G. Burton Northam, and Edward E. Zukoski *In* Loyola Coll., JTEC/WTEC Report and Program Summary Mar. 1994 p 138-142 (For primary document see N94-36042 11-99)
Avail: CASI HC A01/MF A03

This report focuses primarily on Japan's programs in liquid rocket propulsion and propulsion for spaceplane and related transatmospheric areas. It refers briefly to Japan's solid rocket programs and to new supersonic air-breathing propulsion efforts. The panel observed that the Japanese had a carefully thought-out plan, a broad-based program, and an ambitious but achievable schedule for propulsion activity. Japan's overall propulsion program is behind that of the United States at the time of this study, but the Japanese are gaining rapidly. The Japanese are at the forefront in such key areas as advanced materials, enjoying a high level of project continuity and funding. Japan's space program has been evolutionary in nature, while the U.S. program has emphasized revolutionary advances. Projects have typically been smaller in Japan than in the United States, focusing on incremental advances in technology, with an excellent record of applying proven technology to new projects. This evolutionary approach, coupled with an ability to take technology off the shelf from other countries, has resulted in relatively low development costs, rapid progress, and enhanced reliability. Clearly Japan is positioned to be a world leader in space and transatmospheric propulsion technology by the year 2000.
Derived from text

N94-36117*# National Aeronautics and Space Administration. Ames Research Center, Moffett Field, CA.
RESEARCH AND TECHNOLOGY, 1993
May 1994 306 p Original contains color illustrations
(NASA-TM-108816; A-94041; NAS 1.15:108816) Avail: CASI HC A14/MF A03; 12 functional color pages

Selected research and technology activities at Ames Research Center, including the Moffett Field site and the Dryden Flight Research Facility, are summarized. These activities exemplify the center's varied and productive research efforts for 1993. This year's report presents some of the challenging work recently accomplished in the areas of aerospace systems, flight operations and research, aerophysics, and space research.
Author (revised)

SUBJECT INDEX

SCIENTIFIC AND TECHNICAL AEROSPACE REPORTS VOLUME 32 NUMBER 11

Typical Subject Index Listing

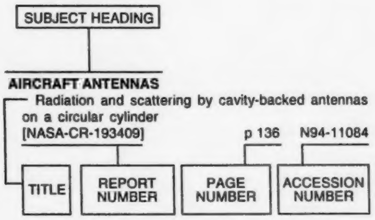

The subject heading is a key to the subject content of the document. Titles, report numbers, and accession numbers of pertinent documents are provided under each subject heading. When the title is insufficiently descriptive of the document content, a title extension is added, separated from the title by three hyphens. The report number helps to indicate the type of document cited (e.g., NASA report, NASA translation, NASA contractor report). The accession number is the number by which the document abstracts are arranged in this journal and by which the document is sold or requested. The page number helps you locate the citation in the abstract section. The titles, with title extensions if present, are arranged under each subject heading in ascending accession number order. The subject headings have been selected from the latest revision of the *NASA Thesaurus*.

A

ABERRATION

ILSE combiner study [DE94-011009] p 4331 N94-36202

ABLATION

Analysis of the Shuttle Orbiter reinforced carbon-carbon oxidation protection system [NASA-TM-104792] p 4262 N94-35245

X ray radiographic imaging of hydrodynamic phenomena in radiation driven materials: Shock propagation, material compression and shear flow [DE94-009515] p 4266 N94-35982

ABRIKOSOV THEORY

Functional integration method for the one-dimensional localization, the higher correlators and mean current in mesoscopic ring in the arbitrary magnetic field [DE94-616621] p 4325 N94-36073

ABSORBENTS

Be3(AsO4)2.2H2O, a new berylloarsenate phase containing bridged tetrahedral 3-rings [AD-A278826] p 4340 N94-35677

ABSORPTION SPECTRA

High resolution visible to short-wave near-infrared CCD spectra of Mars during 1990 p 4356 N94-35403

An indigenously developed photoacoustic spectrometer for study of actinide spectroscopy [DE94-616508] p 4235 N94-35592

About mid-infrared optical spectrum of high-Tc superconducting compounds [DE94-615646] p 4340 N94-36030

Possible spinel absorption bands in S-asteroid visible reflectance spectra p 4368 N94-36139

Beam energy absolute measurement using K-edge absorption spectrometers [DE94-010019] p 4331 N94-36192

ABSORPTION SPECTROSCOPY

Beam energy absolute measurement using K-edge absorption spectrometers [DE94-010019] p 4331 N94-36192

X ray and gamma ray spectroscopy of solids under pressure [DE94-011207] p 4238 N94-36203

ABSTRACTS

Asymetric change of daily temperature range: Proceedings [DE94-010102] p 4293 N94-35703

ABUNDANCE

Anatomy of a cluster IDP. Part 2: Noble gas abundances, trace element geochemistry, isotopic abundances, and trace organic chemistry of several fragments from L2008#5 p 4352 N94-35465

The anatomy of a cluster IDP. Part 1: Carbon abundance, bulk chemistry, and mineralogy of fragments from L2008#5 p 4352 N94-35466

Primordial nucleosynthesis in conformal Weyl gravity [DE94-003002] p 4327 N94-36241

ACCELERATED LIFE TESTS

Research update: Materials Compatibility and Lubricant Research (MCLR) program [DE94-010001] p 4247 N94-36387

ACCELERATION TOLERANCE

A database to evaluate acceleration (+Gz) induced loss of consciousness (G-LOC) in the human centrifuge [AD-A278769] p 4299 N94-35707

ACCELEROMETERS

Smart accelerometer --- vibration damage detection [NASA-CASE-MSC-21951-1] p 4268 N94-35235

Superconducting rebalance acceleration and rate sensor p 4223 N94-35904

ACCOMMODATION

Accommodation during instrument viewing can be influenced by knowledge of object distance [AD-A278987] p 4298 N94-35528

ACCUMULATORS

Eureka! Aerogel capture of meteoroids in space p 4351 N94-35412

ACCURACY

Numerical investigation of multi-element airfoils [NASA-CR-194592] p 4191 N94-36394

ACHONDRITES

Partial melting of the St. Severin (LL) and Lost City (H) ordinary chondrites: One step backwards and two steps forward p 4353 N94-36146

Pigeonholing planetary meteorites: The lessons of misclassification of EET87521 and ALH84001 p 4353 N94-36157

Cr, Mn, and Ca distributions for olivine in angritic systems: Constraints on the origins of Cr-rich and Ca-poor core olivine in angrite LEW87051 p 4353 N94-36162

Pre-bombardment crystallization ages of basaltic clasts from Antarctic howardites EET87503 and EET87513 p 4354 N94-36172

ACID RAIN

Regional source-receptor relationships for atmospheric acidity and acid deposition in California [PB94-156676] p 4287 N94-36183

ACIDITY

Solvent acidity and basicity in polar media and their role in solvation [AD-A278604] p 4239 N94-36426

ACOUSTIC PROPERTIES

An iterative extension of Prony's method for ARMA signal modeling [AD-A278841] p 4319 N94-35800

ACOUSTIC SIMULATION

An iterative extension of Prony's method for ARMA signal modeling [AD-A278841] p 4319 N94-35800

ACOUSTIC VELOCITY

Synthesis of novel composite Platinum-DNA films by way of wet-spinning [AD-A278763] p 4243 N94-35494

ACOUSTICS

An electromagnetic finite difference time domain analog treatment of small signal acoustic interactions [DE94-009978] p 4319 N94-35770

ACOUSTO-OPTICS

Synthesis of novel composite Platinum-DNA films by way of wet-spinning [AD-A278763] p 4243 N94-35494

ACTIVATED CARBON

Developments in carbon materials p 4231 N94-36409

ACTIVE CONTROL

Control of maglev vehicles with aerodynamic and guideway disturbances p 4213 N94-35842

High temperature superconductors for magnetic suspension applications p 4214 N94-35843

Active magnetic bearing control loop modeling for a finite element rotordynamics code p 4216 N94-35857

Dynamic analysis of a magnetic bearing system with flux control p 4216 N94-35859

Selected topics on the active control of helicopter aeromechanical and vibration problems p 4200 N94-35874

Robust control design techniques for active flutter suppression p 4200 N94-35875

Active vibration damping using smart material p 4221 N94-35886

Rational positive real approximations for LQG optimal compensators arising in active stabilization of flexible structures p 4222 N94-35892

Electromechanical simulation and test of rotating systems with magnetic bearing or piezoelectric actuator active vibration control p 4223 N94-35905

An experimental investigation of active control of thrust vectoring nozzle flow fields [AD-A278702] p 4229 N94-36291

Aeroservoelastic tailoring with piezoelectric materials: Actuator optimization studies [AD-A278640] p 4199 N94-36384

Vibration reduction in helicopter rotors using an actively controlled partial span trailing edge flap located on the blade [NASA-CR-4611] p 4280 N94-36423

Alleviation of whirl-flutter on a joined-wing tilt-rotor aircraft configuration using active controls [NASA-CR-196103] p 4200 N94-36436

ACTIVE GALACTIC NUCLEI

ROSAT/XRT-PSPC observations and the ionizing continuum of Seyfert 1 galaxy Mkn 478 [PB94-167053] p 4350 N94-35530

ACTUATORS

Beam tests of a prototype level-1 calorimeter trigger for LHC experiments [PB94-170495] p 4269 N94-35599

Materials for efficient high-flux magnetic bearing actuators p 4214 N94-35845

Dynamic analysis of a magnetic bearing system with flux control p 4216 N94-35859

Control of flexible structures with distributed sensing and processing p 4218 N94-35871

Effects of noise variance model on optimal feedback design and actuator placement p 4220 N94-35883

Active vibration damping using smart material p 4221 N94-35886

Electromechanical simulation and test of rotating systems with magnetic bearing or piezoelectric actuator active vibration control p 4223 N94-35905

Magnetically suspended stepping motors for clean room and vacuum environments p 4225 N94-35915

Six degree of freedom fine motion positioning stage based on magnetic levitation p 4225 N94-35916

Aeroservoelastic tailoring with piezoelectric materials: Actuator optimization studies [AD-A278640] p 4199 N94-36384

ADA (PROGRAMMING LANGUAGE)

Software architecture standard for simulation virtual machine, version 2.0 [NASA-CR-188291] p 4301 N94-35443

A taxonomy of coordination mechanisms used in real-time software based on domain analysis [AD-A279014] p 4304 N94-35794

Experience with Ada on the F-18 High Alpha Research Vehicle flight test program p 4310 N94-35968

ADAPTIVE CONTROL
A case study in nonlinear dynamics and control of articulated spacecraft: The Space Station Freedom with a mobile remote manipulator system
p 4220 N94-35879
Multidisciplinary studies of integrated neural network systems
[AD-A278774] p 4312 N94-36309
ADAPTIVE OPTICS
Issues in the design and optimization of adaptive optics and laser guide stars for the Keck Telescopes
[DE94-009384] p 4349 N94-35565
Error reduction in images with the use of additional information
[AD-A278636] p 4334 N94-36257
ADDITIVES
Methanol fuel additive demonstration
[PB94-156668] p 4247 N94-35941
ADHESIVE BONDING
Nondestructive Inspection (NDI) of reduced strength bonds
[AD-A278745] p 4278 N94-36090
ADIABATIC CONDITIONS
Vertical and adiabatical ionization energies and electron affinities of new Si(n)C and Si(n)O (n=1-3) molecules
[AD-A278863] p 4324 N94-36050
ADRENAL GLAND
Stress and brain protein synthesis
[PB94-170750] p 4296 N94-35601
ADRENAL METABOLISM
Stress and brain protein synthesis
[PB94-170750] p 4296 N94-35601
ADSORPTION
Simultaneous adsorption of CO2 and H2O under Mars-like conditions and application to the evolution of the Martian climate p 4366 N94-35475
Large scale atomistic first principles study of adsorption and surface diffusion
[DE94-009450] p 4322 N94-35682
Morphological aspects of surface reactions
[DE94-010184] p 4236 N94-35685
NO decomposition in non-reducing atmospheres
[DE94-011157] p 4237 N94-36036
The relationship between hydroxyl groups on oxide surfaces and the properties of supported metals
[DE94-010786] p 4241 N94-36233
Multicomponent glass surfaces: Structure and adsorption
[DE94-010516] p 4246 N94-36283
ADSORPTIVITY
Simultaneous adsorption of CO2 and H2O under Mars-like conditions and application to the evolution of the Martian climate p 4366 N94-35475
AEROACOUSTICS
Boundary conditions for jet flow computations
[NASA-TM-106648] p 4266 N94-35976
Computation of helicopter rotor acoustics in forward flight
[NASA-CR-196132] p 4319 N94-36031
AERODYNAMIC CHARACTERISTICS
Tipjet 80-inch model rotor hover test: Test no. 1198
[AD-A279680] p 4191 N94-36261
Technological challenges of High Altitude Long Endurance unmanned configurations
p 4193 N94-36323
AERODYNAMIC COEFFICIENTS
User's guide for an interactive personal computer interface for the aeroprediction code
[NSWCDD/TR-94/107] p 4305 N94-35958
AERODYNAMIC DRAG
Future ultra-speed tube-flight p 4225 N94-35918
The case for surface effect research, platform applications and technology development opportunities
p 4194 N94-36325
AERODYNAMIC HEATING
Analysis of high speed flow, thermal and structural interactions
[NASA-CR-196017] p 4268 N94-36420
AERODYNAMIC LOADS
The simulation of a propulsive jet and force measurement using a magnetically suspended wind tunnel model p 4191 N94-35855
AERODYNAMIC STABILITY
Laminar flow studies at Dassault Aviation: Calculations and flight tests p 4194 N94-36328
AERODYNAMICS
Aeronautical engineering: A continuing bibliography with indexes (supplement 306)
[NASA-SP-7037(306)] p 4189 N94-35338
Flight Mechanics/Estimation Theory Symposium, 1994
[NASA-CP-3265] p 4202 N94-35605
Operational support for Upper Atmosphere Research Satellite (UARS) attitude sensors p 4204 N94-35617
Control of maglev vehicles with aerodynamic and guideway disturbances p 4213 N94-35842
Future ultra-speed tube-flight p 4225 N94-35918
Research and technology, 1993
[NASA-TM-108816] p 4380 N94-36117
AEROELASTICITY
Flutter suppression digital control law design and testing for the AFW wind tunnel model p 4200 N94-35873
Alleviation of whirl-flutter on a joined-wing tilt-rotor aircraft configuration using active controls
[NASA-CR-196103] p 4200 N94-36436
AEROGELS
Eureka! Aerogel capture of meteoroids in space
p 4351 N94-35412
Purity and cleanness of aerogel as a cosmic dust capture medium p 4247 N94-35469
AERONAUTICAL ENGINEERING
Aeronautical engineering: A continuing bibliography with indexes (supplement 306)
[NASA-SP-7037(306)] p 4189 N94-35338
Aerospace Safety Advisory Panel
[NASA-TM-109840] p 4201 N94-35390
Challenging the Future - Journey to Excellence. Aeropropulsion strategic plan for the 1990's
[NASA-TM-109250] p 4228 N94-35591
AERONAUTICS
AGARD highlights 93/2
[AGARD-HIGHLIGHTS-93/2] p 4376 N94-35444
Research and technology, 1993
[NASA-TM-108816] p 4380 N94-36117
AEROSERVOELASTICITY
Aeroservoelastic tailoring with piezoelectric materials: Actuator optimization studies
[AD-A278640] p 4199 N94-36384
Vibration reduction in helicopter rotors using an actively controlled partial span trailing edge flap located on the blade
[NASA-CR-4611] p 4280 N94-36423
AEROSOLS
Analysis of regional visibility in the eastern United States using aerosol models
[PB94-158698] p 4332 N94-35584
Particulate and gaseous organic receptor modeling for the Southern California Air Quality Study
[PB94-156700] p 4285 N94-35735
Anthropogenic sulfate and organic aerosols, CCN, and cloud project concentration at a marine site
[DE94-004210] p 4286 N94-36025
Aerosol optical depth derived from solar radiometry observations at northern mid-latitude sites
[DE94-007476] p 4287 N94-36053
Selected translated abstracts of Russian-language climate-change publications. 2: Clouds
[DE94-011465] p 4295 N94-36244
Implementation of Raman lidar for profiling of atmospheric water vapor and aerosols at the SGP CART site
[DE94-011754] p 4295 N94-36285
Global tropospheric chemistry models for radiatively important trace species: Design and research recommendations
[DE94-007089] p 4288 N94-36359
AEROSPACE ENGINEERING
NASA/DOD Aerospace Knowledge Diffusion Research Project. Paper 40: Technical communications in aerospace education: A study of AIAA student members
[NASA-TM-109868] p 4344 N94-35254
JPRS report: Science and technology. Central Eurasia
[JPRS-UST-94-001] p 4229 N94-35340
JPRS report: Science and technology. Central Eurasia
[JPRS-UST-94-004] p 4249 N94-35341
JPRS report: Science and technology. Central Eurasia
[JPRS-UST-94-005] p 4249 N94-35342
NASA patent abstracts bibliography: A continuing bibliography. Section 1: Abstracts (supplement 45)
[NASA-SP-7039(45)-SECT-1] p 4344 N94-35382
JPRS report: Science and technology. Central Eurasia
[JPRS-UST-94-010] p 4250 N94-35385
JPRS report: Science and technology. Central Eurasia
[JPRS-UST-94-012] p 4250 N94-35387
AGARD highlights 93/2
[AGARD-HIGHLIGHTS-93/2] p 4376 N94-35444
Developing software for ease of change: Metrics from later in the TRALAB system life cycle
[AD-A278759] p 4302 N94-35490
NASA patent abstracts bibliography: A continuing bibliography. Section 2: Indexes (supplement 45)
[NASA-SP-7039(45)-SECT-2] p 4346 N94-35835
Experimental measurement and calculation of losses in planar radial magnetic bearings p 4214 N94-35847
JPRS report: Science and technology. Central Eurasia: Space
[JPRS-USP-93-005] p 4201 N94-36011
Research and technology, 1993
[NASA-TM-108816] p 4380 N94-36117
Computer graphics tools for the visualization of spacecraft dynamics
[AD-A278615] p 4226 N94-36251
AEROSPACE ENVIRONMENTS
Advanced technology lunar telescope
p 4350 N94-35473
Evaluation of Oxygen Interactions with Materials 3: Mission and induced environments
[NASA-TM-109349] p 4236 N94-35680
AEROSPACE INDUSTRY
NASA/DOD Aerospace Knowledge Diffusion Research Project. Paper 40: Technical communications in aerospace education: A study of AIAA student members
[NASA-TM-109868] p 4344 N94-35254
AEROSPACE MEDICINE
Aerospace medicine and biology: A continuing bibliography with indexes (supplement 391)
[NASA-SP-7011(391)] p 4297 N94-35345
AEROSPACE PLANES
Space and transatmospheric propulsion technology
p 4229 N94-36047
AEROSPACE SAFETY
Aerospace Safety Advisory Panel
[NASA-TM-109840] p 4201 N94-35390
AEROSPACE SCIENCES
Director's discretionary fund
[NASA-TM-103997] p 4376 N94-35370
JPRS report: Science and technology. Central Eurasia: Space
[JPRS-USP-93-005] p 4201 N94-36011
AEROSPACE SYSTEMS
The Telecommunications and Data Acquisition Report
[NASA-CR-196117] p 4252 N94-35542
Advanced induction accelerator designs for ground based and space based FELs
[AD-A278885] p 4271 N94-35586
Aerospace applications of magnetic bearings
p 4213 N94-35837
NASA Workshop on Distributed Parameter Modeling and Control of Flexible Aerospace Systems
[NASA-CP-3242] p 4217 N94-35865
AEROSPACE TECHNOLOGY TRANSFER
AGARD highlights 93/2
[AGARD-HIGHLIGHTS-93/2] p 4376 N94-35444
Challenging the Future - Journey to Excellence. Aeropropulsion strategic plan for the 1990's
[NASA-TM-109250] p 4228 N94-35591
AEROSPACE VEHICLES
Natural orbital environment definition guidelines for use in aerospace vehicle development
[NASA-TM-4527] p 4291 N94-36175
AEROTHERMODYNAMICS
Development and application of computational aerothermodynamics flowfield computer codes
[NASA-CR-196136] p 4189 N94-35498
AGGLUTINATION
Single agglutinates: A comparative study of compositions of agglutinitic glass, whole-grain, bulk soil, and FMR p 4355 N94-35401
The nature of agglutinitic glass in the fine-size fraction of lunar soil 10084 p 4369 N94-36148
AGING (MATERIALS)
Effects of combined stressing on the electrical properties of film and ceramic capacitors
[NASA-TM-106605] p 4257 N94-35249
Improved performance of degraded solar arrays at non-zero sun incidence angles
[AD-A278905] p 4282 N94-35804
AIR
Theoretical and experimental study of air and hydrogen electrodes
[DE94-763308] p 4283 N94-36060
AIR BREATHING ENGINES
The 30th JANNAF Combustion Subcommittee Meeting, volume 2
[AD-A278794] p 4247 N94-35656
AFOSR Contractors Propulsion Meeting
[AD-A279028] p 4198 N94-35746
AIR CARGO
The future of large capacity/long range multipurpose air cargo fleets p 4194 N94-36326
AIR CONDITIONING
Thermal performance of residential duct systems in basements
[LBL-33962] p 4250 N94-35364
Research update: Materials Compatibility and Lubricant Research (MCLR) program
[DE94-010001] p 4247 N94-36387
AIR CONDITIONING EQUIPMENT
Thermal performance of residential duct systems in basements
[LBL-33962] p 4250 N94-35364
AIR COOLING
Compliant metal enhanced convection cooled reverse-flow annular combustor
[NASA-TM-106626] p 4199 N94-36379

AIR FLOW
Hot Corrosion Test Facility at the NASA Lewis Special Projects Laboratory
[NASA-CR-195323] p 4200 N94-35267
Numerical investigation of multi-element airfoils
[NASA-CR-194592] p 4191 N94-36394

AIR LAND INTERACTIONS
A model of the CO2 exchanges between biosphere and atmosphere in the tundra
[NASA-CR-196008] p 4289 N94-35389
Atmospheric effects on the mapping of Martian thermal inertia and thermally derived albedo
p 4368 N94-36137

AIR POLLUTION
Computer animation of clouds
[DE94-008289] p 4292 N94-35350
How to develop a long term CO2 reduction plan
[DE94-009559] p 4284 N94-35668
Final regulatory impact analysis: Refueling emission regulations for light duty vehicles and trucks and heavy duty vehicles
[PB94-164027] p 4285 N94-35754
Dual cure low-VOC coating process
[DE94-009346] p 4245 N94-35809
Atmospheric and dispersion modeling in areas of highly complex terrain employing a four-dimensional data assimilation technique
[DE94-004041] p 4285 N94-35823
Methanol fuel additive demonstration
[PB94-156668] p 4247 N94-35941
Analysis of mid-tropospheric carbon monoxide data using a three-dimensional global atmospheric chemistry numerical model
[DE94-004782] p 4286 N94-36026
Aerosol optical depth derived from solar radiometry observations at northern mid-latitude sites
[DE94-007476] p 4287 N94-36053
Regional source-receptor relationships for atmospheric acidity and acid deposition in California
[PB94-156676] p 4287 N94-36183
Global tropospheric chemistry models for radiatively important trace species: Design and research recommendations
[DE94-007089] p 4288 N94-36359

AIR QUALITY
How to develop a long term CO2 reduction plan
[DE94-009559] p 4284 N94-35668
Model engineering concepts for air quality models in an integrated environmental modeling system
[PB94-158623] p 4298 N94-35688
Particulate and gaseous organic receptor modeling for the Southern California Air Quality Study
[PB94-156700] p 4285 N94-35735
Bus application of oxygen-enrichment technology and diesel-electric hybrid systems
[DE94-009835] p 4285 N94-35765
Air quality implications associated with the selection of power plants in the Pacific Northwest
[DE94-004783] p 4287 N94-36027
Regional source-receptor relationships for atmospheric acidity and acid deposition in California
[PB94-156676] p 4287 N94-36183

AIR TO AIR MISSILES
The analysis of a generic air-to-air missile simulation model
[NASA-TM-109057] p 4309 N94-36438

AIR TO AIR REFUELING
EH101: A new helicopter capable of long range missions p 4194 N94-36330
In-flight refueling: Dassault Aviation research on the Rafale aircraft p 4196 N94-36341
Future tanker considerations and requirements
p 4197 N94-36342
Aerial refueling interoperability from a receiver flying qualities perspective p 4197 N94-36343
Tanker system and technology requirements definition: A tanker technology road map p 4197 N94-36344
Hose-drogue versus boom receptacle air refueling
p 4197 N94-36345
CC-130H(T) tactical aerial refuelling tanker development flight test programme p 4198 N94-36347

AIR TRAFFIC CONTROL
Final-Approach Spacing Aids (FASA) evaluation for terminal-area, time-based air traffic control
[NASA-TP-3399] p 4192 N94-36048

AIR TRANSPORTATION
The Federal Aviation Administration plan for research, engineering and development p 4376 N94-35262
The future of large capacity/long range multipurpose air cargo fleets p 4194 N94-36326

AIRBORNE EQUIPMENT
JPRS report: Science and technology. Central Eurasia
[JPRS-UST-94-007] p 4249 N94-35227
Minimum performance standards: Airborne low-range radar altimeters
[RTCA-DO-155] p 4198 N94-35344

AIRBORNE RADAR
Minimum performance standards: Airborne low-range radar altimeters
[RTCA-DO-155] p 4198 N94-35344
Evaluation of synthetic aperture radar for oil-spill response
[AD-A278796] p 4284 N94-35674

AIRBORNE/SPACEBORNE COMPUTERS
Overview of the MSTI 2 processor-in-the-loop simulator p 4207 N94-35631

AIRCRAFT ACCIDENT INVESTIGATION
Safety study: A review of flightcrew-involved, major accidents of US air carriers, 1978 through 1990
[PB94-917001] p 4191 N94-35482
Aircraft accident report: Uncontrolled collision with terrain, American International Airways Flight 808, Douglas DC-8-61, N814CK, US Naval Air Station, Guantanamo Bay, Cuba, 18 August 1993
[PB94-910406] p 4192 N94-35521

AIRCRAFT ACCIDENTS
Safety study: A review of flightcrew-involved, major accidents of US air carriers, 1978 through 1990
[PB94-917001] p 4191 N94-35482
Annual review of aircraft accident data. US general aviation, calendar year 1992
[PB94-181054] p 4192 N94-35496
Aircraft accident report: Uncontrolled collision with terrain, American International Airways Flight 808, Douglas DC-8-61, N814CK, US Naval Air Station, Guantanamo Bay, Cuba, 18 August 1993
[PB94-910406] p 4192 N94-35521

AIRCRAFT APPROACH SPACING
Final-Approach Spacing Aids (FASA) evaluation for terminal-area, time-based air traffic control
[NASA-TP-3399] p 4192 N94-36048

AIRCRAFT COMPARTMENTS
A review of computer evacuation models and their data needs
[DOT/FAA/AM-94/11] p 4191 N94-35236

AIRCRAFT CONFIGURATIONS
Alleviation of whirl-flutter on a joined-wing tilt-rotor aircraft configuration using active controls
[NASA-CR-196103] p 4200 N94-36436

AIRCRAFT CONSTRUCTION MATERIALS
Optimisation of composite aircraft structures by direct manufacturing approaches p 4194 N94-36327
New developments in aluminum for aircraft and automobiles p 4232 N94-36413

AIRCRAFT CONTROL
Flight testing a propulsion-controlled aircraft emergency flight control system on an F-15 airplane
[NASA-TM-4590] p 4199 N94-35258
Piloted simulation study of two tilt-wing control concepts p 4200 N94-35962
F/A-18 forebody vortex control. Volume 1: Static tests
[NASA-CR-4582] p 4190 N94-35991

AIRCRAFT DESIGN
Recent Advances in Long Range and Long Endurance Operation of Aircraft
[AGARD-CP-547] p 4193 N94-36321
High Altitude Long Endurance aircraft design studies
p 4193 N94-36322
Laminar flow studies at Dassault Aviation: Calculations and flight tests p 4194 N94-36328
The convertible (helicopter/airplane) EUROFAR: General considerations on the technical progress and on future advances p 4195 N94-36331
Calculations used to optimize the installation of civil aircraft engines p 4195 N94-36332
Propulsion system technologies for long range and long endurance aircraft p 4195 N94-36334
Tanker system and technology requirements definition: A tanker technology road map p 4197 N94-36344
The KDC-10 programme of the Royal Netherlands Air Force p 4197 N94-36346

AIRCRAFT ENGINES
Challenging the Future - Journey to Excellence. Aeropropulsion strategic plan for the 1990's
[NASA-TM-109250] p 4228 N94-35591
Engine exhaust characteristics evaluation in support of aircraft acoustic testing p 4319 N94-35963
Calculations used to optimize the installation of civil aircraft engines p 4195 N94-36332
Propulsion system selection for a High Altitude Long Endurance aircraft p 4195 N94-36333
The STRATO 2C propulsion system: A low cost approach for a High Altitude Long Endurance aircraft
p 4195 N94-36335

AIRCRAFT FUELS
Unleaded AVGAS program
[AD-A278650] p 4247 N94-35795

AIRCRAFT MAINTENANCE
Calculations used to optimize the installation of civil aircraft engines p 4195 N94-36332

AIRCRAFT MANEUVERS
The prediction of pilot opinion ratings using optimal and sub-optimal pilot models
[AD-A278679] p 4298 N94-35692

AIRCRAFT NOISE
1993 Technical Paper Contest for Women. Gear Up 2000: Women in Motion
[NASA-CP-10134] p 4377 N94-35961
Engine exhaust characteristics evaluation in support of aircraft acoustic testing p 4319 N94-35963

AIRCRAFT PARTS
Aerospace applications of magnetic bearings
p 4213 N94-35837

AIRCRAFT PERFORMANCE
Evaluating the dynamic response of in-flight thrust calculation techniques during throttle transients
[NASA-TM-4591] p 4193 N94-35241
Piloted simulation study of two tilt-wing control concepts p 4200 N94-35962
Recent Advances in Long Range and Long Endurance Operation of Aircraft
[AGARD-CP-547] p 4193 N94-36321

AIRCRAFT PILOTS
The influence of data link-provided graphical weather on pilot decision-making
[AD-A278871] p 4293 N94-35596

AIRCRAFT SAFETY
A review of computer evacuation models and their data needs
[DOT/FAA/AM-94/11] p 4191 N94-35236

AIRCRAFT STRUCTURES
An overview of recent advances in system identification p 4220 N94-35880
Frequency domain analysis of the random loading of cracked panels
[NASA-CR-196021] p 4279 N94-35974
Optimisation of composite aircraft structures by direct manufacturing approaches p 4194 N94-36327

AIRCRAFT SURVIVABILITY
Propulsion system technologies for long range and long endurance aircraft p 4195 N94-36334

AIRCRAFT WAKES
Numerical modeling studies of wake vortex transport and evolution within the planetary boundary layer
[NASA-CR-196078] p 4192 N94-35522

AIRFOILS
Numerical investigation of multi-element airfoils
[NASA-CR-194592] p 4191 N94-36394

AIRFRAME MATERIALS
High Altitude Long Endurance aircraft design studies
p 4193 N94-36322

AIRFRAMES
Ground vibration test of the XV-15 Tiltrotor Research Aircraft and pretest predictions p 4200 N94-35972
High Altitude Long Endurance aircraft design studies
p 4193 N94-36322

AIRGLOW
First measurement of helium on Mars: Implications for the problem of radiogenic gases on the terrestrial planets p 4370 N94-36153

AIRLINE OPERATIONS
Safety study: A review of flightcrew-involved, major accidents of US air carriers, 1978 through 1990
[PB94-917001] p 4191 N94-35482
The future of large capacity/long range multipurpose air cargo fleets p 4194 N94-36326

ALBEDO
Atmospheric effects on the mapping of Martian thermal inertia and thermally derived albedo
p 4368 N94-36137

ALCOHOLS
Design of a high activity and selectivity alcohol catalyst
[DE94-003633] p 4237 N94-36023

ALGEBRA
Mathematical theory of synchronous communication
[PB94-169224] p 4252 N94-35537
On a generalized bootstrap principle
[DE94-727517] p 4314 N94-35774

ALGORITHMS
The effects of cloud inhomogeneities upon radiative fluxes, and the supply of a cloud truth validation dataset
[NASA-CR-196080] p 4293 N94-35391
Three-dimensional unstructured grid refinement and optimization using edge-swapping
[NASA-TM-103966] p 4299 N94-35393
Parallel algorithms for LU decomposition on a shared memory multiprocessor
[PB94-167798] p 4314 N94-35531
Maximum-likelihood soft-decision decoding of block codes using the A* algorithm p 4254 N94-35555
Prodigy planning algorithm
[AD-A278900] p 4303 N94-35574
Stopping rules for a class of sampling-based stochastic programming algorithms
[AD-A278654] p 4303 N94-35577

MME-based attitude dynamics identification and estimation for SAMPEX p 4209 N94-35643
A new algorithm for attitude-independent magnetometer calibration p 4209 N94-35644
A simple suboptimal least-squares algorithm for attitude determination with multiple sensors p 4210 N94-35645
Reformulating query plans for multidatabase systems [AD-A278688] p 4345 N94-35663
The polygon-ellipse method of data compression of weather maps [AD-A278958] p 4293 N94-35719
Concept for an algorithm testing and evaluation program at NIST [PB94-163029] p 4304 N94-35740
An iterative extension of Prony's method for ARMA signal modeling [AD-A278841] p 4319 N94-35800
Adaptive model reduction for continuous systems via recursive rational interpolation p 4219 N94-35876
Advances in parameter estimation techniques applied to flexible structures p 4219 N94-35877
Vortex tubes in turbulent flows: Identification, representation, reconstruction [NASA-CR-194900] p 4267 N94-35992
A three dimensional multigrid Reynolds-averaged Navier-Stokes solver for unstructured meshes [NASA-CR-194908] p 4191 N94-35994
Computer simulation of beam-beam effects at large amplitudes and determination of life time [DE94-616235] p 4330 N94-35999
Numerical method to study the stability of periodic solutions of particle motion in nonlinear magnetic fields [DE94-610740] p 4325 N94-36088
CALTRANS: A parallel, deterministic, 3D neutronics code [DE94-010667] p 4326 N94-36127
Extrapolating storm location using the Integrated Terminal Weather System (ITWS) storm motion algorithm [AD-A278611] p 4295 N94-36249
Use of formal calculation to automatically obtain adjoint programs [PB94-170701] p 4308 N94-36259
On the origin of porphyritic chondrules [DE94-010464] p 4351 N94-36418
GRIZ: Finite element analysis results visualization for unstructured grids [DE94-010066] p 4309 N94-36429

ALIGNMENT
A closed-loop time-alignment system for baseband combining p 4253 N94-35552
Overview of the MSTI 2 on-orbit alignment p 4206 N94-35629

ALIPHATIC HYDROCARBONS
Morphological aspects of surface reactions [DE94-010184] p 4236 N94-35685
Development of atmospheric characteristics of chlorine-free alternative fluorocarbons [DE94-009791] p 4287 N94-36179

ALKALI METALS
A new family of superconducting fullerides, Na(NH3)(x)C60(x = 2-8) [DE94-011480] p 4341 N94-36272

ALKALIES
Alkali element constraints on Earth-Moon relations p 4354 N94-36169

ALKALINE BATTERIES
Theoretical and experimental study of air and hydrogen electrodes [DE94-763308] p 4283 N94-36060

ALKYL COMPOUNDS
Spinnability of silica sols: The role of alkoxy group exchange [DE94-010087] p 4244 N94-35702

ALLOYING
High temperature creep and oxidation resistant chromium silicide matrix alloy containing molybdenum [NASA-CASE-LEW-15697-1] p 4241 N94-36275

ALTERNATING CURRENT
Experimental and theoretical studies of a high temperature cesium-barium tacitron, with application to low voltage-high current inversion [DE94-008182] p 4228 N94-35349

ALTIMETERS
Tracking system options for future altimeter satellite missions p 4205 N94-35622

ALUMINIDES
Investigation of moisture-induced embrittlement of iron aluminides [DE94-010881] p 4241 N94-36196

ALUMINUM
The electrical conductivities of candidate beam-waveguide antenna shroud materials p 4252 N94-35546
A two-dimensional model for collisional energy transfer in bimolecular ion-molecule dynamics [AD-A278913] p 4321 N94-35589
Designing aluminum sealing glasses for manufacturability [DE94-010081] p 4244 N94-35699
Partition coefficients for Al, Ca, Ti, Cr, and Ni in olivine obtained by melting experiment on an LL6 chondrite p 4353 N94-36163
Investigation of moisture-induced embrittlement of iron aluminides [DE94-010881] p 4241 N94-36196
Continuous unidirectional fiber reinforced composites: Fabrication and testing p 4229 N94-36400
New developments in aluminum for aircraft and automobiles p 4232 N94-36413

ALUMINUM ALLOYS
Craters in aluminum 1100 targets using glass projectiles at 1-7 km/s p 4280 N94-35407
Fatigue and residual strength behaviour of ARALL3 panels with bonded-on doublers [AD-B181062] p 4279 N94-36226
New developments in aluminum for aircraft and automobiles p 4232 N94-36413

ALUMINUM ARSENIDES
InP solar cell with window layer [NASA-CASE-LEW-15606-1] p 4281 N94-35230

ALUMINUM CHLORIDES
Neutron diffraction study of aluminum chloride imidazolium chloride molten salts [DE94-009679] p 4239 N94-36349

ALUMINUM COMPOUNDS
High-power CW operation of AlGaInP diode-laser arrays [DE94-010409] p 4272 N94-36115

ALUMINUM FLUORIDES
Vertical electron detachment energies for octahedral closed-shell multiply charged anions [AD-A278835] p 4322 N94-35753

ALUMINUM NITRIDES
Thick film fabrication of aluminum nitride microcircuits [DE94-010107] p 4259 N94-35706

ALUMINUM OXIDES
A novel method for depositing precious metal films on difficult surfaces [NASA-TM-106607] p 4243 N94-35260
Design of a high activity and selectivity alcohol catalyst [DE94-003633] p 4237 N94-36023
Effect of niobium interlayer on high-temperature sliding friction and wear of silver films on alumina [DE94-010462] p 4275 N94-36232

ALUMINUM SILICATES
On the origin of porphyritic chondrules [DE94-010464] p 4351 N94-36418

AMBIENT TEMPERATURE
Predicted optical performance of the High-Altitude Balloon Experiment (HABE) telescope in an adverse thermal environment [DE94-008949] p 4349 N94-35998

AMINES
A classical model for closed-loop diagrams of binary liquid mixtures [DE94-011011] p 4237 N94-36033
A new association-model for binary VLE of alcohol/hydrocarbon and amine/hydrocarbon mixtures [DE94-011012] p 4248 N94-36034
Effects of 5 MPa heliox pressure on dopaminer gic pathway: An in vivo neurochemical study [PB94-170693] p 4297 N94-36220

AMMONIA
Design of a high activity and selectivity alcohol catalyst [DE94-003633] p 4237 N94-36023
Tritiated ammonia formation [DE94-011170] p 4237 N94-36056
A new family of superconducting fullerides, Na(NH3)(x)C60(x = 2-8) [DE94-011480] p 4341 N94-36272

AMORPHOUS MATERIALS
Irradiation-related amorphization and crystallization: In situ transmission electron microscope studies [DE94-009823] p 4241 N94-36222

AMPLIFICATION
Chirped-pulse amplification with flashlamp-pumped Ti:Sapphire amplifiers [DE94-010055] p 4272 N94-35695

ANALOG CIRCUITS
BJT model in APLAC [PB94-171022] p 4259 N94-35822

ANALOG COMPUTERS
Digital control programmer for temperature control [DE94-615584] p 4309 N94-36382

ANALOG DATA
The iWarp display module [AD-A278610] p 4260 N94-36248

ANALYSIS OF VARIANCE
Cramer-von Mises variance estimators for simulations [AD-A278799] p 4316 N94-35675

ANALYTIC FUNCTIONS
Height inequality for holomorphic curves [PB94-167731] p 4314 N94-35762

ANDESITE
Production of ferroan andesites by the experimental partial melting of an LL chondrite p 4353 N94-36160

ANESTHESIA
Computer automation and artificial intelligence [DE94-611058] p 4312 N94-35831

ANGLE OF ATTACK
Wind tunnel measurements on a full-scale F/A-18 with a tangentially blowing slot --- conducted in the Ames 80 by 120 foot wind tunnel p 4191 N94-35965
F/A-18 forebody vortex control. Volume 1: Static tests [NASA-CR-4582] p 4190 N94-35991

ANGLES (GEOMETRY)
Improved performance of degraded solar arrays at non-zero sun incidence angles [AD-A278905] p 4282 N94-35804

ANGULAR DISTRIBUTION
A search for energetic ion directivity in large solar flares [NASA-CR-196036] p 4374 N94-35993
Processes of the reciprocal transformation vector charged particles pairs and electron-positron pairs [DE94-616787] p 4325 N94-36077

ANGULAR MOMENTUM
State-to-state dynamics of molecular energy transfer [DE94-009651] p 4324 N94-35816
Angular momentum in the Local Group [DE94-009322] p 4350 N94-35980

ANGULAR VELOCITY
Advantages of estimating rate corrections during dynamic propagation of spacecraft rates: Applications to real-time attitude determination of SAMPEX p 4209 N94-35642
MME-based attitude dynamics identification and estimation for SAMPEX p 4209 N94-35643
Motion models in attitude estimation p 4210 N94-35646

ANHYDRIDES
Addition polyimides with enhanced processability [NASA-CASE-LEW-15043-1] p 4242 N94-35234

ANIMATION
The role of emotion in believable agents [AD-A278952] p 4312 N94-35658

ANIONS
Anionic states of LiFLi [AD-A278830] p 4322 N94-35678
Vertical electron detachment energies for octahedral closed-shell multiply charged anions [AD-A278835] p 4322 N94-35753
A combined experimental and theoretical study of the neutral, cationic and anionic Si3N cluster molecule [AD-A278834] p 4323 N94-35792
New anionic states of the lithium trimer [AD-A278832] p 4323 N94-35797
Anionic and neutral states of Li3O [AD-A278833] p 4323 N94-35798
Exact multiplicities in the three-anion spectrum [DE94-616768] p 4325 N94-36075
Solvent acidity and basicity in polar media and their role in solvation [AD-A278604] p 4239 N94-36426

ANISOTROPIC MEDIA
Green's functions for an anisotropic medium: Part 1: Unbounded case [AD-A278767] p 4256 N94-35694
Green's functions for an anisotropic medium. Part 2: Two-layer case [AD-A278788] p 4256 N94-35713

ANISOTROPY
Efficient light propagation for multiple anisotropic volume scattering [DE94-006474] p 4334 N94-36356

ANNEALING
Formation and stability of Fe-rich precipitates in dilute Zr(Fe) single-crystal alloys [DE94-619027] p 4242 N94-36288

ANNIHILATION REACTIONS
GRO: Studies of high energy pulsars with EGRET [NASA-CR-196003] p 4349 N94-35516
Isoscalar vector bosons at LEP 2 [DE94-611253] p 4323 N94-35787
A quark model of bar Lambda production in bar Rho interactions [DE94-008071] p 4324 N94-35824
CDF electroweak studies and the search for the top quark [DE94-010333] p 4326 N94-36107
Hybrid mesons (Q(anti Q)g) in N(anti N) annihilation [DE94-001491] p 4327 N94-36239

Top dilepton search at CDF
[DE94-002302] p 4327 N94-36266

ANOMALIES
Long range forecasts of the Northern Hemisphere anomalies with antecedent sea surface temperature patterns
[NASA-CR-189358] p 4292 N94-35380

ANORTHOSITE
FeO and MgO in plagioclase of lunar anorthosites: Igneous or metamorphic? p 4351 N94-35449

ANTARCTIC REGIONS
On the origin of enstatite chondrite chondrules based on their petrography and comparison with experimentally produced chondrules p 4353 N94-36158

ANTENNA ARRAYS
Correlator data analysis for the array feed compensation system p 4253 N94-35553

ANTENNA DESIGN
Active antenna
[NASA-CASE-GSC-13309-1] p 4251 N94-35231
Lunar LIGO and gravitational wave astronomy on the Moon p 4366 N94-35472
Thin-ribbon tapered coupler for dielectric waveguides p 4253 N94-35547
Design and implementation of a beam-waveguide mirror control system for vernier pointing of the DSS-13 antenna p 4253 N94-35548
A closed-loop time-alignment system for baseband combining p 4253 N94-35552

ANTENNA RADIATION PATTERNS
Design and implementation of a beam-waveguide mirror control system for vernier pointing of the DSS-13 antenna p 4253 N94-35548
Use of the sampling theorem to speed up near-field physical optics scattering calculations p 4253 N94-35549

ANTENNAS
Active antenna
[NASA-CASE-GSC-13309-1] p 4251 N94-35231
TSAR modeling of a TEM horn and surrounding structure
[DE94-010668] p 4256 N94-36301

ANTIREFLECTION COATINGS
Coatings for SiO2 optical fibers
[AD-D016197] p 4334 N94-36363

APERTURES
Method and apparatus for removing unwanted reflections from an interferometer
[NASA-CASE-NPO-18478-1-CU] p 4333 N94-35749
Dynamic aperture and transverse proton diffusion in HERA
[DE94-010309] p 4331 N94-36224

APOGEES
High Earth orbit design for lunar assisted small Explorer class missions p 4202 N94-35608

APOLLO PROJECT
Apollo 11 at twenty-five, version 1.0
[NASA-CR-193380] p 4376 N94-35363

APPENDAGES
Attitude stability of a spinning spacecraft during appendage deployment/retraction p 4208 N94-35639

APPLICATION SPECIFIC INTEGRATED CIRCUITS
Beam tests of a prototype level-1 calorimeter trigger for LHC experiments
[PB94-170495] p 4269 N94-35599

APPLICATIONS PROGRAMS (COMPUTERS)
TDRSS Onboard Navigation System (TONS) flight qualification experiment p 4206 N94-35625
A collection of tools in support of automatic differentiation
[DE94-010104] p 4314 N94-35704
NAVSPACECOM space surveillance sensor system digital signal processing receiver. Volume 3: Operating system functions
[AD-A278839] p 4212 N94-35799
NAVSPACECOM space surveillance sensor system digital signal processing receiver. Volume 4: Hardware interfaces
[AD-A278845] p 4212 N94-35801
Software for continuum modeling of controls-structures interactions p 4223 N94-35898
Review of Mathematical Function Library for Microsoft-FORTRAN, John Wiley and Sons, 1989
[PB94-160793] p 4305 N94-36010
The CMU task parallel program suite
[AD-A278951] p 4311 N94-36015
TransFit: Finite element analysis data fitting software
[NASA-CR-193988] p 4307 N94-36118
CALTRANS: A parallel, deterministic, 3D neutronics code
[DE94-010667] p 4326 N94-36127
SYNTH: A spectrum synthesizer
[DE94-004719] p 4331 N94-36317
SandiaXTP, an object-oriented implementation of XTP 3.7
[DE94-011752] p 4257 N94-36354

APPROACH CONTROL
Final-Approach Spacing Aids (FASA) evaluation for terminal-area, time-based air traffic control
[NASA-TP-3399] p 4192 N94-36048

APPROPRIATIONS
Budget estimates, fiscal year 1995. Volume 1: Agency summary, human space flight, and science, aeronautics and technology
[NASA-TM-109791] p 4347 N94-35899
Budget estimates, fiscal year 1995. Volume 2: Mission support and Inspector General
[NASA-TM-109792] p 4348 N94-35900

APPROXIMATION
Rational positive real approximations for LQG optimal compensators arising in active stabilization of flexible structures p 4222 N94-35892

AQUEOUS SOLUTIONS
The relationship between hydroxyl groups on oxide surfaces and the properties of supported metals
[DE94-010786] p 4241 N94-36233

ARAMID FIBER COMPOSITES
Fatigue and residual strength behaviour of ARALL3 panels with bonded-on doublers
[AD-B181062] p 4279 N94-36226

ARC JET ENGINES
AFOSR Contractors Propulsion Meeting
[AD-A279028] p 4198 N94-35746
Recovery of frozen flow losses in arcjets
[AD-A278739] p 4228 N94-36089

ARCHIPELAGOES
Studies of the dayside boundary layer processes based on ground observations in the Svalbard area
[AD-A280715] p 4292 N94-36265

ARCHITECTURE (COMPUTERS)
A software architecture for adding new interaction techniques to a command and control based testbed
[AD-A278760] p 4302 N94-35491
General purpose architecture for intelligent computer-aided training
[NASA-CASE-MSC-21381-1] p 4311 N94-35501
MMI(exp 2) demonstrator systems: A multi-modal interface for man machine interaction with knowledge based systems. Deliverable D17 (TA 2) ESPRIT project 2474 MMI(exp 2)
[PB94-170537] p 4298 N94-35600
Overview of the MSTI 2 processor-in-the-loop simulator p 4207 N94-35631
Task allocation for parallel real-time execution
[AD-A278789] p 4310 N94-35653
The most abstract common refinement
[AD-A278870] p 4305 N94-36014

ARCTIC REGIONS
Workshop on the Martian Northern Plains: Sedimentological, periglacial, and paleoclimatic evolution
[NASA-CR-196134] p 4354 N94-35359

ARGON
State-to-state dynamics of molecular energy transfer
[DE94-009651] p 4324 N94-35816
Kinetics studies following state-selective laser excitation
[DE94-010305] p 4330 N94-36105
Modelling of the structure and physical properties of simple disordered systems
[DE94-617087] p 4329 N94-36311

ARGON ISOTOPES
Ar-39-Ar-40 ages of four ureilites p 4357 N94-35410

ARITHMETIC
Bit-wise arithmetic coding for data compression p 4254 N94-35556

ARMATURES
Feasibility study of superconducting LSM rocket launcher system p 4225 N94-35914

AROMATIC COMPOUNDS
Anatomy of a cluster IDP. Part 2: Noble gas abundances, trace element geochemistry, isotopic abundances, and trace organic chemistry of several fragments from L2008#5 p 4352 N94-35465

ARSENATES
Be3(AsO4)2.2H2O, a new berylloarsenate phase containing bridged tetrahedral 3-rings
[AD-A278826] p 4340 N94-35677

ARTIFICIAL INTELLIGENCE
The effects of cloud inhomogeneities upon radiative fluxes, and the supply of a cloud truth validation dataset
[NASA-CR-196080] p 4293 N94-35391
General purpose architecture for intelligent computer-aided training
[NASA-CASE-MSC-21381-1] p 4311 N94-35501
Combining left and right unlinking for matching a large number of learned rules
[AD-A278979] p 4311 N94-35527
Maximum-likelihood soft-decision decoding of block codes using the A* algorithm p 4254 N94-35555
Prodigy planning algorithm
[AD-A278900] p 4303 N94-35574
Genetic algorithms
[PB94-171048] p 4303 N94-35602
Good applications for crummy machine translation
[AD-A278689] p 4345 N94-35651
The role of emotion in believable agents
[AD-A278952] p 4312 N94-35658
Task networks for controlling continuous processes
[AD-A278683] p 4312 N94-35710
The breakdown of operators when interacting with the external world
[AD-A278936] p 4299 N94-35716
The application of fuzzy logic to SAFOR in SIMNET
[AD-A279058] p 4312 N94-35730
CABPRO: An expert system for process planning multiwire cables
[DE94-010213] p 4312 N94-35810
Computer automation and artificial intelligence
[DE94-611058] p 4312 N94-35831
Interfacing the RAP system to real-time control, version 1
[AD-A278725] p 4312 N94-36295

ARTIFICIAL SATELLITES
The Earth Satellite Program (ESP), version 2.0
[AD-A278860] p 4201 N94-35827
Recovery of frozen flow losses in arcjets
[AD-A278739] p 4228 N94-36089
A genetic algorithm approach to automating satellite range scheduling
[AD-A278577] p 4226 N94-36188

ASIA
JPRS report: Science and technology. Central Eurasia
[JPRS-UST-94-001] p 4229 N94-35340
JPRS report: Science and technology. Central Eurasia
[JPRS-UST-94-004] p 4249 N94-35341
JPRS report: Science and technology. Central Eurasia
[JPRS-UST-94-005] p 4249 N94-35342
JPRS report: Science and technology. Central Eurasia
[JPRS-UST-94-010] p 4250 N94-35385
JPRS report: Science and technology. Central Eurasia
[JPRS-UST-94-011] p 4250 N94-35386
JPRS report: Science and technology. Central Eurasia
[JPRS-UST-94-012] p 4250 N94-35387
JPRS report: Science and technology. Central Eurasia: Space
[JPRS-USP-93-005] p 4201 N94-36011

ASPECT RATIO
An experimental investigation of active control of thrust vectoring nozzle flow fields
[AD-A278702] p 4229 N94-36291

ASSEMBLING
Robot friendly probe and socket assembly
[NASA-CASE-MSC-22028-1] p 4274 N94-35374

ASSESSMENTS
CAirTOX: A compartment model for assessing the fate of and human exposure to toxic-chemical emissions to air
[DE94-010084] p 4284 N94-35700
Environmental Monitoring and Assessment Program assessment framework
[PB94-158862] p 4285 N94-35741

ASSOCIATION REACTIONS
A new association-model for binary VLE of alcohol/hydrocarbon and amine/hydrocarbon mixtures
[DE94-011012] p 4248 N94-36034

ASTEROID MISSIONS
Remote geochemical experiment package for Discovery class missions p 4350 N94-35420

ASTEROIDS
First Galileo image of asteroid 243 Ida p 4351 N94-35416
A quick look method of detecting water of hydration in small solar system bodies p 4352 N94-35470
Lunar horizon glow and the Clementine mission p 4366 N94-35478
JPRS report: Science and technology. Central Eurasia: Space
[JPRS-USP-94-001] p 4201 N94-35518
The real-time display of interferometry data for Goldstone radar astronomy data acquisition p 4255 N94-35560
Possible spinel absorption bands in S-asteroid visible reflectance spectra p 4368 N94-36139
Dust evolution from comets and asteroids: Their velocities at Earth orbit intersection p 4352 N94-36142
Pigeonholing planetary meteorites: The lessons of misclassification of EET87521 and ALH84001 p 4353 N94-36157
Moessbauer mineralogy of calcined Murchison meteorite p 4353 N94-36166

ASTROMETRY
Development of POINTS as a planetology instrument
[NASA-CR-196026] p 4354 N94-35265

ASTRONAUTS
Self-rescue strategies for EVA crewmembers equipped with the SAFER backpack p 4207 N94-35633

ASTRONOMICAL INTERFEROMETRY
Development of POINTS as a planetology instrument
[NASA-CR-196026] p 4354 N94-35265
ASTRONOMICAL MODELS
The surface and interior of Phobos
p 4355 N94-35400
First observation of a mass independent isotopic fractionation in a condensation reaction
p 4239 N94-35464
ASTRONOMICAL SPECTROSCOPY
High spatial resolution telescopic multispectral imaging and spectroscopy of the Moon. 1: The Serenitatis/Tranquillitatis border region
p 4356 N94-35402
A quick look method of detecting water of hydration in small solar system bodies p 4352 N94-35470
ROSAT/XRT-PSPC observations and the ionizing continuum of Seyfert 1 galaxy Mkn 478
[PB94-167053] p 4350 N94-35530
ASYMMETRY
Precise measurement of the left-right cross section asymmetry in Z boson production by electron-positron collisions
[DE94-010751] p 4326 N94-36198
ASYMPTOTIC METHODS
Cramer-von Mises variance estimators for simulations
[AD-A278799] p 4316 N94-35675
ASYMPTOTIC SERIES
Cramer-von Mises variance estimators for simulations
[AD-A278799] p 4316 N94-35675
ATMOSPHERIC BOUNDARY LAYER
Numerical modeling studies of wake vortex transport and evolution within the planetary boundary layer
[NASA-CR-196078] p 4192 N94-35522
ATMOSPHERIC CHEMISTRY
Computer animation of clouds
[DE94-008289] p 4292 N94-35350
Venus climate stability and volcanic resurfacing rates
p 4358 N94-35413
Anatomy of a cluster IDP. Part 2: Noble gas abundances, trace element geochemistry, isotopic abundances, and trace organic chemistry of several fragments from L2008#5 p 4352 N94-35465
Vacuum ultraviolet studies of molecular dynamics
[AD-A278940] p 4321 N94-35657
Analysis of mid-tropospheric carbon monoxide data using a three-dimensional global atmospheric chemistry numerical model
[DE94-004782] p 4286 N94-36026
Development of atmospheric characteristics of chlorine-free alternative fluorocarbons
[DE94-009791] p 4287 N94-36179
Global tropospheric chemistry models for radiatively important trace species: Design and research recommendations
[DE94-007089] p 4288 N94-36359
ATMOSPHERIC CIRCULATION
Long range forecasts of the Northern Hemisphere anomalies with antecedent sea surface temperature patterns
[NASA-CR-189358] p 4292 N94-35380
Windblown sand on Mars: The effect of saltation threshold on drift potentials derived from Mars GCM
p 4366 N94-35474
Modeling the atmospheric input of nutrients, heavy metals, and pesticides to the Great Lakes
[DE94-005481] p 4286 N94-36007
ATMOSPHERIC COMPOSITION
Mars atmospheric escape and isotopic fractionation: Synthesis of data and models p 4369 N94-36143
Integrated science model for assessment of climate change
[DE94-011758] p 4288 N94-36286
ATMOSPHERIC DENSITY
Evaluation of semiempirical atmospheric density models for orbit determination applications
p 4208 N94-35636
ATMOSPHERIC EFFECTS
Atmospheric effects on the mapping of Martian thermal inertia and thermally derived albedo
p 4368 N94-36137
ATMOSPHERIC GENERAL CIRCULATION MODELS
Long range forecasts of the Northern Hemisphere anomalies with antecedent sea surface temperature patterns
[NASA-CR-189358] p 4292 N94-35380
Windblown sand on Mars: The effect of saltation threshold on drift potentials derived from Mars GCM
p 4366 N94-35474
The computation of cloud base height from paired whole-sky imaging cameras
[DE94-009868] p 4294 N94-35767
The Atmospheric Radiation Measurement Program and interfaces with external data sources
[DE94-003699] p 4286 N94-36024
Modernization of the graphics post-processors of the Hamburg German Climate Computer Center Carbon Cycle Codes
[DE94-011604] p 4288 N94-36273
ATMOSPHERIC HEATING
Anatomy of a cluster IDP. Part 2: Noble gas abundances, trace element geochemistry, isotopic abundances, and trace organic chemistry of several fragments from L2008#5 p 4352 N94-35465
The computation of cloud base height from paired whole-sky imaging cameras
[DE94-009868] p 4294 N94-35767
ATMOSPHERIC MODELS
Modeling of the magnetosphere-ionosphere-atmosphere system
[NASA-CR-195157] p 4288 N94-35244
Venus climate stability and volcanic resurfacing rates
p 4358 N94-35413
Analysis of regional visibility in the eastern United States using aerosol models
[PB94-158698] p 4332 N94-35584
Evaluation of semiempirical atmospheric density models for orbit determination applications
p 4208 N94-35636
Asymetric change of daily temperature range: Proceedings
[DE94-010102] p 4293 N94-35703
Atmospheric and dispersion modeling in areas of highly complex terrain employing a four-dimensional data assimilation technique
[DE94-004041] p 4285 N94-35823
Atmospheric effects on the mapping of Martian thermal inertia and thermally derived albedo
p 4368 N94-36137
First measurement of helium on Mars: Implications for the problem of radiogenic gases on the terrestrial planets p 4370 N94-36153
Three dimensional visualization of a coastal mesoscale model
[AD-A278576] p 4294 N94-36187
Global tropospheric chemistry models for radiatively important trace species: Design and research recommendations
[DE94-007089] p 4288 N94-36359
ATMOSPHERIC MOISTURE
Production of long-term global water vapor and liquid water data set using ultra-fast methods to assimilate multi-satellite and radiosonde observations
[NASA-CR-196044] p 4292 N94-35355
Production of long-term global water vapor and liquid water data set using ultra-fast methods to assimilate multi-satellite and radiosonde observations
[NASA-CR-195981] p 4293 N94-35499
Implementation of Raman lidar for profiling of atmospheric water vapor and aerosols at the SGP CART site
[DE94-011754] p 4295 N94-36285
ATMOSPHERIC OPTICS
Efficient light propagation for multiple anisotropic volume scattering
[DE94-006474] p 4334 N94-36356
ATMOSPHERIC PHYSICS
JPRS report: Science and technology. Central Eurasia: Space
[JPRS-USP-94-003] p 4201 N94-35520
Simultaneous observations of the westward electrojet and the cross-tail current sheet during substorms
[AD-A278631] p 4292 N94-36383
ATMOSPHERIC RADIATION
The Atmospheric Radiation Measurement Program and interfaces with external data sources
[DE94-003699] p 4286 N94-36024
ATMOSPHERIC SOUNDING
Production of long-term global water vapor and liquid water data set using ultra-fast methods to assimilate multi-satellite and radiosonde observations
[NASA-CR-196044] p 4292 N94-35355
Production of long-term global water vapor and liquid water data set using ultra-fast methods to assimilate multi-satellite and radiosonde observations
[NASA-CR-195981] p 4293 N94-35499
A quality control package for the Digisonde Drift Analysis (DDA)
[AD-A278663] p 4289 N94-35578
Application of differential inversion to DMSP microwave sounder data
[AD-A278575] p 4294 N94-36186
Eyesafe rare earth crystal lasers for atmosphere soudings
[AD-A279486] p 4273 N94-36227
ATMOSPHERIC STRATIFICATION
On the physics of waves in the solar atmosphere: Wave heating and wind acceleration
[NASA-CR-194119] p 4375 N94-36395
ATMOSPHERIC TEMPERATURE
Application of differential inversion to DMSP microwave sounder data
[AD-A278575] p 4294 N94-36186
ATMOSPHERIC TURBULENCE
Numerical modeling studies of wake vortex transport and evolution within the planetary boundary layer
[NASA-CR-196078] p 4192 N94-35522
ATOMIC BEAMS
Feasibility study for a novel pulsed neutral beam diagnostics for tokamaks
[DE94-617129] p 4339 N94-36417
ATOMIC COLLISIONS
State-to-state dynamics of molecular energy transfer
[DE94-009651] p 4324 N94-35816
Kinetics studies following state-selective laser excitation
[DE94-010305] p 4330 N94-36105
Modelling of the structure and physical properties of simple disordered systems
[DE94-617087] p 4329 N94-36311
ATOMIC ENERGY LEVELS
New anionic states of the lithium trimer
[AD-A278832] p 4323 N94-35797
ATOMIC PHYSICS
Atomic physics and radiation processes in plasmas
[DE94-727617] p 4337 N94-35939
ATOMIC STRUCTURE
Two-photon photoemission and the dynamics of electrons at interfaces
[DE94-011373] p 4324 N94-36058
ATTITUDE (INCLINATION)
Preliminary study of satellite attitude determination for the LANDSAT 7 spacecraft
[AD-A278876] p 4212 N94-35585
Operational support for Upper Atmosphere Research Satellite (UARS) attitude sensors p 4204 N94-35617
Spacecraft attitude determination accuracy from mission experience p 4204 N94-35618
Measuring attitude with a gradiometer
p 4206 N94-35630
Self-rescue strategies for EVA crewmembers equipped with the SAFER backpack p 4207 N94-35633
Space Shuttle orbit determination using empirical force modeling of attitude maneuvers for the German MOMS-02/D2 mission p 4207 N94-35634
ATTITUDE CONTROL
Operational support for Upper Atmosphere Research Satellite (UARS) attitude sensors p 4204 N94-35617
Overview of the Miniature Sensor Technology Integration (MSTI) spacecraft attitude control system
p 4206 N94-35627
A geometric model of a V-slit Sun sensor correcting for spacecraft wobble p 4206 N94-35628
Overview of the MSTI 2 on-orbit alignment
p 4206 N94-35629
The control of satellites with microgravity constraints: The COMET Control System p 4207 N94-35632
Application of star identification using pattern matching to space ground systems at GSFC
p 4209 N94-35640
Advantages of estimating rate corrections during dynamic propagation of spacecraft rates: Applications to real-time attitude determination of SAMPEX
p 4209 N94-35642
A case study in nonlinear dynamics and control of articulated spacecraft: The Space Station Freedom with a mobile remote manipulator system
p 4220 N94-35879
Nonlinear feedback model attitude control using CCD in magnetic suspension system p 4225 N94-35912
Piloted simulation study of two tilt-wing control concepts p 4200 N94-35962
Input shaping for three-dimensional slew maneuvers of a precision pointing flexible spacecraft
[DE94-008937] p 4226 N94-36001
ATTITUDE INDICATORS
Operational support for Upper Atmosphere Research Satellite (UARS) attitude sensors p 4204 N94-35617
Spacecraft attitude determination accuracy from mission experience p 4204 N94-35618
ATTITUDE STABILITY
Attitude stability of a spinning spacecraft during appendage deployment/retraction p 4208 N94-35639
AUDITORY SIGNALS
Attention and signal detection. A study of attention divided between visual and auditory signals
[PB94-170594] p 4298 N94-36215
AURORAL ARCS
Analytic model of aurorally coupled magnetospheric and ionospheric electrostatic potentials
[NASA-CR-196130] p 4288 N94-35358
AURORAL ZONES
Analytic model of aurorally coupled magnetospheric and ionospheric electrostatic potentials
[NASA-CR-196130] p 4288 N94-35358

Spatial fluctuations of particle fluxes within the auroral zone inferred from the Intercosmos-Bulgaria-1300 satellite data
[DE94-615858] p 4350 N94-36128
Molecular nitrogen fluorescence lidar for remote sensing of the auroral ionosphere
[AD-A280716] p 4291 N94-36263

AURORAS
Analytic model of aurorally coupled magnetospheric and ionospheric electrostatic potentials
[NASA-CR-196130] p 4288 N94-35358
Molecular nitrogen fluorescence lidar for remote sensing of the auroral ionosphere
[AD-A280716] p 4291 N94-36263
Studies of the dayside boundary layer processes based on ground observations in the Svalbard area
[AD-A280715] p 4292 N94-36265
Theoretical and experimental studies relevant to interpretation of auroral emissions
[NASA-CR-196032] p 4376 N94-36421

AUSTENITE
Transformation plasticity in ductile solids
[DE94-010420] p 4240 N94-35953

AUSTENITIC STAINLESS STEELS
Transformation plasticity in ductile solids
[DE94-010420] p 4240 N94-35953

AUTOCORRELATION
Application of higher-order multipoint statistics to the ideal spray
[DE94-005104] p 4268 N94-36318

AUTOMATA THEORY
A lower bound for the intersection of regular forests
[AD-A278653] p 4303 N94-35576
A determinizable class of timed automata
[AD-A278858] p 4317 N94-35743

AUTOMATIC CONTROL
Adjustable control station with movable monitors and cameras for viewing systems in robotics and teleoperations
[NASA-CASE-NPO-17837-1-CU] p 4332 N94-35384
Fault tolerant computer control for a Maglev transportation system p 4215 N94-35848
An overview of recent advances in system identification p 4220 N94-35880

AUTOMATION
Computer automation and artificial intelligence
[DE94-611058] p 4312 N94-35831
An automated digital data collection and analysis system for the Charpy Impact Tester p 4232 N94-36415

AUTOMOBILE FUELS
Methanol fuel additive demonstration
[PB94-156668] p 4247 N94-35941
Advanced hydrogen/method utilization technology demonstration
[DE94-000214] p 4248 N94-36191

AUTOMOBILES
New developments in aluminum for aircraft and automobiles p 4232 N94-36413

AUTONOMOUS NAVIGATION
TDRSS Onboard Navigation System (TONS) flight qualification experiment p 4206 N94-35625

AUTONOMY
Autonomous hazard detection and avoidance
[NASA-CR-188331] p 4309 N94-36439

AVIATION METEOROLOGY
The influence of data link-provided graphical weather on pilot decision-making
[AD-A278871] p 4293 N94-35596
Data requirements for ceiling and visibility products development
[AD-A278959] p 4293 N94-35720
Terminal Doppler Weather Radar (TDWR) Low Level Wind Shear Alert System 3 (LLWAS 3) integration studies at Orlando International Airport
[AD-A278957] p 4294 N94-35807

AXIAL LOADS
Biaxial loading and shallow-flaw effects on crack-tip constraint and fracture-toughness
[DE94-010128] p 4279 N94-35684

AXIAL STRESS
Aspects of robust computational modeling for plain and reinforced concrete
[PB94-169240] p 4251 N94-35820

AXIOMS
Generalized Fredholm determinants and Selberg zeta functions for axiom A dynamical systems
[PB94-167665] p 4314 N94-35758
This non-axiomatizable quantum theory. From Hilbert's sixth problem to the recent viewpoint of Gell-mann and Hartle
[PB94-167715] p 4342 N94-35761

B

BACKGROUND RADIATION
Solar-geophysical data number 594, February 1994. Part 2: (Comprehensive reports). Data for August 1993, and miscellaneous
[PB94-164001] p 4374 N94-36009
Astronomy in the region between 1 mm and 0.1 mm wavelength
[NASA-CR-196020] p 4349 N94-36419

BACKSCATTERING
Innovative instrumentation for mineralogical and elemental analyses of solid extraterrestrial surfaces: The Backscatter Moessbauer Spectrometer/X Ray Fluorescence analyzer (BaMS/XRF)
p 4239 N94-35459
Wedge scattering by the method of iteration
[DE94-010404] p 4256 N94-36112

BACKWARD DIFFERENCING
Description and use of LSODE, the Livermore Solver for Ordinary Differential Equations
[NASA-RP-1327] p 4313 N94-35259

BAFFLES
AXAF-I ghost ray study: On orbit case
[NASA-CR-193987] p 4333 N94-36119

BALLISTIC MISSILES
Numerical simulation of shock interaction with above-ground structures
[AD-A278713] p 4279 N94-35949
Estimation with multisensor/multiscan detection fusion
[AD-A278753] p 4256 N94-36092

BALLISTICS
The 30th JANNAF Combustion Subcommittee Meeting, volume 1
[AD-A278793] p 4247 N94-35655

BALLOON-BORNE INSTRUMENTS
Predicted optical performance of the High-Altitude Balloon Experiment (HABE) telescope in an adverse thermal environment
[DE94-008949] p 4349 N94-35998

BALLOONING MODES
Analysis of current diffusive ballooning mode
[DE94-718992] p 4336 N94-35811
Modelling of ELMs and dynamic responses of the H-mode
[DE94-718977] p 4339 N94-36353

BARIUM
Experimental and theoretical studies of a high temperature cesium-barium tacitron, with application to low voltage-high current inversion
[DE94-008182] p 4228 N94-35349

BARIUM COMPOUNDS
Twin spacing versus size of a monocrystal for the nonstoichiometric 1:2:3 superconductors
[DE94-615511] p 4340 N94-36029

BARYONS
Baryonic currents and their correlators in the heavy quark effective theory
[DE94-612496] p 4320 N94-35567
Radiatively induced electron and electron-neutrino masses
[DE94-616775] p 4321 N94-35582
Primordial nucleosynthesis in conformal Weyl gravity
[DE94-003002] p 4327 N94-36241

BASALT
Lunar mineral feedstocks from rocks and soils: X-ray digital imaging in resource evaluation
p 4358 N94-35415
Cr, Mn, and Ca distributions for olivine in angritic systems: Constraints on the origins of Cr-rich and Ca-poor core olivine in angrite LEW87051 p 4353 N94-36162
Pre-bombardment crystallization ages of basaltic clasts from Antarctic howardites EET87503 and EET87513
p 4354 N94-36172
New data supporting a Sm-146,147-Nd-142,143 formation interval for the lunar mantle
p 4374 N94-36173

BASE HEATING
A review and development of correlations for base pressure and base heating in supersonic flow
[SAND93-0280] p 4189 N94-35360

BASE PRESSURE
A review and development of correlations for base pressure and base heating in supersonic flow
[SAND93-0280] p 4189 N94-35360

BASEMENTS
Thermal performance of residential duct systems in basements
[LBL-33962] p 4250 N94-35364

BAYES THEOREM
Point and interval estimation of series system reliability using small data sets
[AD-A278647] p 4316 N94-35575

BAYS (TOPOGRAPHIC FEATURES)
Numerical investigation of multi-element airfoils
[NASA-CR-194592] p 4191 N94-36394

BEADS
Sealed tube comparisons of the compatibility of desiccants with refrigerants and lubricants
[DE94-010002] p 4251 N94-36388

BEAM CURRENTS
Advanced induction accelerator designs for ground based and space based FELs
[AD-A278885] p 4271 N94-35586
ILSE combiner study
[DE94-011009] p 4331 N94-36202

BEAM INJECTION
Advanced induction accelerator designs for ground based and space based FELs
[AD-A278885] p 4271 N94-35586
Heating experiments using neutral beams with variable injection angle and ICRF waves in CHS
[DE94-718982] p 4337 N94-35936
Feasibility study for a novel pulsed neutral beam diagnostics for tokamaks
[DE94-617129] p 4339 N94-36417

BEAM INTERACTIONS
Participation in the definition, conduct, and analysis of particle accelerator experiments for the first Spacelab Mission
[NASA-CR-193974] p 4330 N94-35483
Ultrafast chemical dynamics of reactions in beams
[AD-A278939] p 4323 N94-35805
State of the art in high-power microwaves: An overview
[DE94-007075] p 4272 N94-35978
Computer simulation of beam-beam effects at large amplitudes and determination of life time
[DE94-616235] p 4330 N94-35999
Support of hadroproduction of bottom using the 800 GeV/c primary photon beam at the Fermilab tevatron
[DE94-009411] p 4324 N94-36016
Impedance and instability threshold estimates in the main injector 1
[DE94-010332] p 4332 N94-36431

BEAM WAVEGUIDES
The electrical conductivities of candidate beam-waveguide antenna shroud materials
p 4252 N94-35546
Design and implementation of a beam-waveguide mirror control system for vernier pointing of the DSS-13 antenna p 4253 N94-35548
Use of the sampling theorem to speed up near-field physical optics scattering calculations
p 4253 N94-35549
DSS-13 S-/X-band microwave feed system
p 4253 N94-35550

BEAMS (RADIATION)
Estimation with multisensor/multiscan detection fusion
[AD-A278753] p 4256 N94-36092
ILSE combiner study
[DE94-011009] p 4331 N94-36202
Impedance and instability threshold estimates in the main injector 1
[DE94-010332] p 4332 N94-36431

BEAMS (SUPPORTS)
Distributed parameter modeling of repeated truss structures p 4218 N94-35868
Active vibration damping using smart material
p 4221 N94-35886
Dynamical observer for a flexible beam via finite element approximations p 4222 N94-35893

BEAUFORT SEA (NORTH AMERICA)
Environmental measurements in the Beaufort Sea, Spring 1993
[AD-A278718] p 4296 N94-36293

BELLOWS
High-temperature, bellows hybrid seal
[NASA-CASE-LEW-15570-1] p 4274 N94-35373

BENDING FATIGUE
On optimal placement of spacers in bundled conductors p 4258 N94-35354

BENDING VIBRATION
Vibration reduction in helicopter rotors using an actively controlled partial span trailing edge flap located on the blade
[NASA-CR-4611] p 4280 N94-36423

BENEFICIATION
Lunar mineral feedstocks from rocks and soils: X-ray digital imaging in resource evaluation
p 4358 N94-35415

BENZENE
Morphological aspects of surface reactions
[DE94-010184] p 4236 N94-35685
Computer simulations of benzene in faujasite-type zeolites
[DE94-007533] p 4242 N94-36369

BERYLLIUM COMPOUNDS

Be3(AsO4)2.2H2O, a new berylloarsenate phase containing bridged tetrahedral 3-rings
[AD-A278826] p 4340 N94-35677

BETATRONS

Numerical method to study the stability of periodic solutions of particle motion in nonlinear magnetic fields
[DE94-610740] p 4325 N94-36088

BETHE-SALPETER EQUATION

Relativistic three-particle dynamical equations. 2: Theoretical development
[DE94-616654] p 4320 N94-35581

Calculations on some properties of the pion in the framework of Schwinger-Dyson and Bethe-Salpeter equations
[DE94-611232] p 4322 N94-35786

Elastic charge form factors for K mesons
[DE94-010014] p 4325 N94-36086

High energy asymptotics of perturbative multi-color QCD
[DE94-001350] p 4327 N94-36238

BIAS

Overview of the MSTI 2 on-orbit alignment
p 4206 N94-35629

A new algorithm for attitude-independent magnetometer calibration p 4209 N94-35644

BIBLIOGRAPHIES

Annotated bibliography of Software Engineering Laboratory literature
[NASA-CR-189350] p 4300 N94-35238

Aeronautical engineering: A continuing bibliography with indexes (supplement 306)
[NASA-SP-7037(306)] p 4189 N94-35338

Aerospace medicine and biology: A continuing bibliography with indexes (supplement 391)
[NASA-SP-7011(391)] p 4297 N94-35345

NASA patent abstracts bibliography: A continuing bibliography. Section 1: Abstracts (supplement 45)
[NASA-SP-7039(45)-SECT-1] p 4344 N94-35382

Bibliography of research reports and publications issued by the Human Engineering Division
[AD-A278787] p 4299 N94-35712

Properties and bibliography of GaSe
[AD-A279064] p 4340 N94-35733

NASA patent abstracts bibliography: A continuing bibliography. Section 2: Indexes (supplement 45)
[NASA-SP-7039(45)-SECT-2] p 4346 N94-35835

BINARY MIXTURES

Measurement of viscosity, density, and gas solubility of refrigerant blends in selected synthetic lubricants
[DE94-010426] p 4244 N94-35687

Solubility, viscosity and density of refrigerant/lubricant mixtures
[DE94-009996] p 4245 N94-35771

A classical model for closed-loop diagrams of binary liquid mixtures
[DE94-011011] p 4237 N94-36033

A new association-model for binary VLE of alcohol/hydrocarbon and amine/hydrocarbon mixtures
[DE94-011012] p 4248 N94-36034

BIOCHEMISTRY

Activities of National Institute of Radiological Sciences
[DE94-727636] p 4296 N94-36101

BIOLOGICAL EFFECTS

Aerospace medicine and biology: A continuing bibliography with indexes (supplement 391)
[NASA-SP-7011(391)] p 4297 N94-35345

Further studies of 60-Hz exposure effects on human function
[DE94-010192] p 4297 N94-36223

BIOMASS

Anthropogenic sulfate and organic aerosols, CCN, and cloud project concentration at a marine site
[DE94-004210] p 4286 N94-36025

Analysis of mid-tropospheric carbon monoxide data using a three-dimensional global atmospheric chemistry numerical model
[DE94-004782] p 4286 N94-36026

BIOMASS ENERGY PRODUCTION

Model documentation: Renewable Fuels Module of the National Energy Modeling System
[DE94-009962] p 4282 N94-35672

BIOPHYSICS

Activities of National Institute of Radiological Sciences
[DE94-727636] p 4296 N94-36101

BIOPROCESSING

AICD: Advanced Industrial Concepts Division Biological and Chemical Technologies Research Program
[DE94-006854] p 4283 N94-36051

BIOREACTORS

High density cell culture system
[NASA-CASE-MSC-22060-1] p 4296 N94-35366

BIOSPHERE

A model of the CO2 exchanges between biosphere and atmosphere in the tundra
[NASA-CR-196008] p 4289 N94-35389

BIOSYNTHESIS

Stress and brain protein synthesis
[PB94-170750] p 4296 N94-35601

BIOTECHNOLOGY

CSTL technical activities, 1991
[PB94-160769] p 4318 N94-36003

AICD: Advanced Industrial Concepts Division Biological and Chemical Technologies Research Program
[DE94-006854] p 4283 N94-36051

BIPOLAR TRANSISTORS

BJT model in APLAC
[PB94-171022] p 4259 N94-35822

Enhanced charge trapping in bipolar spacer oxides during low-dose-rate irradiation
[DE94-007863] p 4260 N94-36268

High temperature heterojunction bipolar transistors
[AD-A278605] p 4261 N94-36360

Bounding the total-dose response of modern bipolar transistors
[DE94-007742] p 4261 N94-36371

BIPOLARITY

Combined SO(x)/NO(x) control via SOXAL (tm) process: An electrodialytic regenerative wet scrubbing process
[DE94-009053] p 4284 N94-35346

BIRTH

Data available from birth and death registries and cancer registries in the US
[LBL-30971] p 4344 N94-35337

BISMUTH OXIDES

The study of the local magnetic field in the oxide alpha-Bi2O3 by the mu SR-technique
[DE94-612636] p 4322 N94-35751

BLACK HOLES (ASTRONOMY)

ROSAT/XRT-PSPC observations and the ionizing continuum of Seyfert 1 galaxy Mkn 478
[PB94-167053] p 4350 N94-35530

BLADE SLAP NOISE

Computation of helicopter rotor acoustics in forward flight
[NASA-CR-196132] p 4319 N94-36031

BLOCKING

Interfacing the RAP system to real-time control, version 1
[AD-A278725] p 4312 N94-36295

BLOOD FLOW

A database to evaluate acceleration (+Gz) induced loss of consciousness (G-LOC) in the human centrifuge
[AD-A278769] p 4299 N94-35707

BLOWING

Wind tunnel measurements on a full-scale F/A-18 with a tangentially blowing slot --- conducted in the Ames 80 by 120 foot wind tunnel p 4191 N94-35965

F/A-18 forebody vortex control. Volume 1: Static tests
[NASA-CR-4582] p 4190 N94-35991

BOILING

Fundamental studies in blow-down and cryogenic cooling
[AD-A278967] p 4250 N94-35524

BOLIDES

Radiative signals from impact of Shoemaker-Levy on Jupiter p 4355 N94-35396

BOLOMETERS

Astronomy in the region between 1 mm and 0.1 mm wavelength
[NASA-CR-196020] p 4349 N94-36419

BOLTZMANN TRANSPORT EQUATION

Kinetic theory of runaway air breakdown and the implications for lightning initiation
[DE94-001683] p 4295 N94-36240

Magnetic metallic multilayers
[DE94-011913] p 4341 N94-36274

BONDING

Study on contaminants on flight and other critical surfaces
[NASA-CR-193975] p 4235 N94-35447

Synthesis of novel composite Platinum-DNA films by way of wet-spinning
[AD-A278763] p 4243 N94-35494

BOOMS (EQUIPMENT)

Hose-drogue versus boom receptacle air refueling
p 4197 N94-36345

BORON

A two-dimensional model for collisional energy transfer in bimolecular ion-molecule dynamics
[AD-A278913] p 4321 N94-35589

BOSONS

Isoscalar vector bosons at LEP 2
[DE94-611253] p 4323 N94-35787

Quantum mechanics and thermodynamics of particles with distance dependent statistics
[DE94-616620] p 4343 N94-36072

Boson spectra and correlations in thermal locally equilibrium systems
[DE94-616799] p 4325 N94-36079

CDF electroweak studies and the search for the top quark
[DE94-010333] p 4326 N94-36107

Pseudogoldstone boson decay induced by light and search for the solar axion radiation
[DE94-616907] p 4326 N94-36133

Precise measurement of the left-right cross section asymmetry in Z boson production by electron-positron collisions
[DE94-010751] p 4326 N94-36198

BOUNDARIES

H2O-H2SO4 system in Venus' clouds and OCS, CO, and H2SO4 profiles in Venus' troposphere
p 4370 N94-36152

BOUNDARY CONDITIONS

Boundary conditions for jet flow computations
[NASA-TM-106648] p 4266 N94-35976

On the theory of bounded many-particle systems with purely coulomb interactions
[DE94-617215] p 4325 N94-36081

The pressure of fluctuative electromagnetic field in inhomogeneous medium
[DE94-617189] p 4256 N94-36096

The energy density of fluctuative electromagnetic field near the semi-bounded plasma
[DE94-617188] p 4256 N94-36099

Uniqueness of a solution of a steady state photochemical problem: Applications to Mars p 4370 N94-36151

BOUNDARY LAYER CONTROL

The aerodynamic and heat transfer effects of an endwall boundary layer fence in a 90 degree turning square duct
[AD-A278903] p 4265 N94-35803

BOUNDARY LAYER FLOW

On the nonlinear stability of viscous modes within the Rayleigh problem on an infinite flat plate
[NASA-CR-194909] p 4263 N94-35497

The velocity field created by a shallow bump in a boundary layer
[NASA-CR-194899] p 4266 N94-35975

BOUNDARY LAYER TRANSITION

The velocity field created by a shallow bump in a boundary layer
[NASA-CR-194899] p 4266 N94-35975

BOUNDARY LAYERS

A supersonic tunnel for laser and flow-seeding techniques
[NASA-TM-106588] p 4265 N94-35945

The velocity field created by a shallow bump in a boundary layer
[NASA-CR-194899] p 4266 N94-35975

Studies of the dayside boundary layer processes based on ground observations in the Svalbard area
[AD-A280715] p 4292 N94-36265

BOUNDARY VALUE PROBLEMS

Description and use of LSODE, the Livermore Solver for Ordinary Differential Equations
[NASA-RP-1327] p 4313 N94-35259

A combined algorithm for minimum time slewing of flexible spacecraft p 4220 N94-35881

An energy method approach to the problem of elastic strip
[PB94-171014] p 4279 N94-36000

The 2+1-dimensional integrable generalization of the Sine-Gordon equation
[DE94-611074] p 4315 N94-36100

Recursive recovery of Markov transition probabilities from boundary value data
[DE94-011914] p 4317 N94-36235

BOW WAVES

The fine structure of Langmuir waves observed upstream of the bow shock at Venus
[NASA-CR-196123] p 4354 N94-35378

BRAIDED COMPOSITES

Through-the-thickness tensile strength of textile composites
[NASA-TM-109115] p 4233 N94-35946

BRAIN

Stress and brain protein synthesis
[PB94-170750] p 4296 N94-35601

BRECCIA

Luna 24 regolith breccias: A possible source of the fine size material of the Luna 24 regolith
p 4362 N94-35450

Pre-bombardment crystallization ages of basaltic clasts from Antarctic howardites EET87503 and EET87513
p 4354 N94-36172

BREMSSTRAHLUNG

Integral characteristics of the magnetic bremsstrahlung
[DE94-616788] p 4256 N94-36078

BRIDGMAN METHOD

Interface shape and convection during solidification and melting of succinonitrile
[NASA-TM-106487] p 4262 N94-35248

BRITTLENESS
Patterns of brittle deformation under extension on Venus p 4373 N94-36168
BROADBAND
Absolute calibration technique for broadband ultrasonic transducers
[NASA-CASE-LAR-14672-1] p 4268 N94-35368
BROKEN SYMMETRY
Goldstone pion and other mesons using a scalar confining interaction
[DE94-010016] p 4321 N94-35649
BRONZES
X ray and gamma ray spectroscopy of solids under pressure
[DE94-011207] p 4238 N94-36203
BUCKLING
On the Buckling/Kinking compressive failure of fibrous composites
[AD-A278865] p 4233 N94-35714
Graphing techniques for materials laboratory using Excel p 4232 N94-36414
BUILDINGS
Thermal performance of residential duct systems in basements
[LBL-33962] p 4250 N94-35364
BUNDLES
On optimal placement of spacers in bundled conductors p 4258 N94-35354
BUOYANCY
Piggyback balance experiment: An illustration of Archimedes' principles and Newton's third law
[PB94-163060] p 4265 N94-35942
BURNERS
Hot Corrosion Test Facility at the NASA Lewis Special Projects Laboratory
[NASA-CR-195323] p 4200 N94-35267
BUS CONDUCTORS
High level modelling and design of asynchronous interface logic
[PB94-167822] p 4258 N94-35534

C

C++ (PROGRAMMING LANGUAGE)
Parallel algorithms for LU decomposition on a shared memory multiprocessor
[PB94-167798] p 4314 N94-35531
C-130 AIRCRAFT
CC-130H(T) tactical aerial refuelling tanker development flight test programme p 4198 N94-36347
C-135 AIRCRAFT
Future tanker considerations and requirements
p 4197 N94-36342
CADMIUM TELLURIDES
Development of novel II-VI solar cells
[PB94-159415] p 4282 N94-35739
CALCIUM
Cr, Mn, and Ca distributions for olivine in angritic systems: Constraints on the origins of Cr-rich and Ca-poor core olivine in angrite LEW87051 p 4353 N94-36162
Partition coefficients for Al, Ca, Ti, Cr, and Ni in olivine obtained by melting experiment on an LL6 chondrite
p 4353 N94-36163
CALCULUS
Quantum groups, non-commutative differential geometry and applications
[DE94-011358] p 4315 N94-36270
CALIBRATING
Absolute calibration technique for broadband ultrasonic transducers
[NASA-CASE-LAR-14672-1] p 4268 N94-35368
X-ray remote sensing and in-situ spectroscopy for planetary exploration missions and gamma-ray remote sensing and in-situ spectroscopy for planetary exploration missions
[NASA-CR-189352] p 4375 N94-35381
Wavelength calibration techniques and subtle surface and atmospheric absorption features in the Mariner 6, 7 IRS reflectance data p 4356 N94-35405
In-flight scale/distortion calibration of the Hubble Space Telescope fixed-head star trackers
p 4203 N94-35613
A long-baseline method for HST gyro drift rate bias calibration p 4203 N94-35614
The in-flight calibration of the Hubble Space Telescope fine guidance sensors, 2 (a success story)
p 4204 N94-35615
Color/magnitude calibration for National Aeronautics and Space Administration (NASA) standard Fixed-Head Star Trackers (FHST) p 4209 N94-35641
A new algorithm for attitude-independent magnetometer calibration p 4209 N94-35644
Hubble Space Telescope Fine Guidance Sensors Instrument Handbook, version 4.0
[NASA-CR-189366] p 4349 N94-36281
CALIFORNIA
Particulate and gaseous organic receptor modeling for the Southern California Air Quality Study
[PB94-156700] p 4285 N94-35735
National Maglev initiative: California line electric utility power system requirements p 4215 N94-35850
Regional source-receptor relationships for atmospheric acidity and acid deposition in California
[PB94-156676] p 4287 N94-36183
CALORIMETERS
Beam tests of a prototype level-1 calorimeter trigger for LHC experiments
[PB94-170495] p 4269 N94-35599
CAMBER
Improvement of endurance performance by periodic optimal control of variable camber p 4194 N94-36329
CAMERAS
Adjustable control station with movable monitors and cameras for viewing systems in robotics and teleoperations
[NASA-CASE-NPO-17837-1-CU] p 4332 N94-35384
Space Shuttle orbit determination using empirical force modeling of attitude maneuvers for the German MOMS-02/D2 mission p 4207 N94-35634
The computation of cloud base height from paired whole-sky imaging cameras
[DE94-009868] p 4294 N94-35767
Nonlinear feedback model attitude control using CCD in magnetic suspension system p 4225 N94-35912
Activities of the optoelectronics laboratory
[PB94-171196] p 4334 N94-36190
Transformation of a Cranz-Schardin camera
[PB94-170685] p 4270 N94-36219
CANADA
JTEC/WTEC report and program summary
p 4379 N94-36042
CANARD CONFIGURATIONS
Direct reduced order mixed H2/H infinity control for the Short Take-Off and Landing/Maneuver Technology Demonstrator (STOL/MTD)
[AD-A278675] p 4199 N94-35796
CANCER
Data available from birth and death registries and cancer registries in the US
[LBL-30971] p 4344 N94-35337
CAPACITANCE
Effects of combined stressing on the electrical properties of film and ceramic capacitors
[NASA-TM-106605] p 4257 N94-35249
CAPACITORS
Effects of combined stressing on the electrical properties of film and ceramic capacitors
[NASA-TM-106605] p 4257 N94-35249
Enhanced charge trapping in bipolar spacer oxides during low-dose-rate irradiation
[DE94-007863] p 4260 N94-36268
CAPE KENNEDY LAUNCH COMPLEX
Endangered and potentially endangered wildlife on John F. Kennedy Space Center and faunal integrity as a goal for maintaining biological diversity
[NASA-TM-109204] p 4288 N94-36422
CAPILLARY FLOW
Transient body force effects on the dryout and rewet of a heated capillary structure
[AD-A278677] p 4264 N94-35690
Space-based crystal growth and thermocapillary flow
p 4342 N94-35971
Capillary flow solderability test for printed wiring boards
[DE94-010321] p 4259 N94-36094
CARBON
A comparison of atomic oxygen erosion yields of carbon and selected polymers exposed in ground based facilities and in low Earth orbit
[NASA-TM-106622] p 4243 N94-35243
On the possible role of elemental carbon in the formation of reduced chondrules p 4351 N94-35421
The anatomy of a cluster IDP. Part 1: Carbon abundance, bulk chemistry, and mineralogy of fragments from L2008#5 p 4352 N94-35466
Electrochemical process and product therefrom
[AD-D016211] p 4239 N94-36372
Developments in carbon materials
p 4231 N94-36409
CARBON COMPOUNDS
A new family of superconducting fullerides, Na(NH3)(x)C60(x = 2-8)
[DE94-011480] p 4341 N94-36272
CARBON CYCLE
Modernization of the graphics post-processors of the Hamburg German Climate Computer Center Carbon Cycle Codes
[DE94-011604] p 4288 N94-36273
CARBON DIOXIDE
A model of the CO2 exchanges between biosphere and atmosphere in the tundra
[NASA-CR-196008] p 4289 N94-35389
Simultaneous adsorption of CO2 and H2O under Mars-like conditions and application to the evolution of the Martian climate p 4366 N94-35475
How to develop a long term CO2 reduction plan
[DE94-009559] p 4284 N94-35668
Uniqueness of a solution of a steady state photochemical problem: Applications to Mars p 4370 N94-36151
Equations of state valid continuously from zero to extreme pressures with H2O and CO2 as examples
[DE94-011907] p 4238 N94-36230
CARBON DIOXIDE CONCENTRATION
How to develop a long term CO2 reduction plan
[DE94-009559] p 4284 N94-35668
Integrated science model for assessment of climate change
[DE94-011758] p 4288 N94-36286
CARBON DIOXIDE LASERS
Monolith catalysts for closed-cycle carbon dioxide lasers
[NASA-CR-196093] p 4271 N94-35489
CARBON FIBERS
Analysis of the Shuttle Orbiter reinforced carbon-carbon oxidation protection system
[NASA-TM-104792] p 4262 N94-35245
Advanced composites in Japan p 4234 N94-36045
Developments in carbon materials
p 4231 N94-36409
CARBON MONOXIDE
Vacuum ultraviolet studies of molecular dynamics
[AD-A278940] p 4321 N94-35657
Analysis of mid-tropospheric carbon monoxide data using a three-dimensional global atmospheric chemistry numerical model
[DE94-004782] p 4286 N94-36026
CARBON-CARBON COMPOSITES
Analysis of the Shuttle Orbiter reinforced carbon-carbon oxidation protection system
[NASA-TM-104792] p 4262 N94-35245
Carbon-carbon piston development
[NASA-CR-4595] p 4233 N94-35947
Advanced composites in Japan p 4234 N94-36045
Developments in carbon materials
p 4231 N94-36409
CARBONACEOUS CHONDRITES
Antarctic weathering of the CK chondrites EET90004, 90007, and 90022: Nickel and sulfur mobility
p 4351 N94-35451
A quick look method of detecting water of hydration in small solar system bodies p 4352 N94-35470
Mineralogy of an unusual CM clast in the Kaidun meteorite p 4352 N94-35476
Mineralogy of artificially heated carbonaceous chondrites p 4352 N94-35477
Electron energy-loss spectroscopy of carbon in interplanetary dust particles p 4353 N94-36149
CARBONATES
Electron energy-loss spectroscopy of carbon in interplanetary dust particles p 4353 N94-36149
CARBONYL COMPOUNDS
The reaction of hydroperoxy-propyl radicals with molecular oxygen
[DE94-006392] p 4239 N94-36319
CARDIOVASCULAR SYSTEM
A database to evaluate acceleration (+Gz) induced loss of consciousness (G-LOC) in the human centrifuge
[AD-A278769] p 4299 N94-35707
CARRIER FREQUENCIES
Performance evaluation of digital phase-locked loops for advanced deep space transponders
p 4254 N94-35558
CASSINI MISSION
GPHS-RTGs in support of the Cassini mission
[DE94-009994] p 4212 N94-35648
CASTING
Report on the Workshop on Manufacturing Polymer Composites by Liquid Molding
[PB94-160066] p 4234 N94-36004
CATALOGS (PUBLICATIONS)
Catalog of Helios 90 deg photometer events
[PL-TR-94-2040] p 4375 N94-36264
CATALYSIS
Cross-condensation reactions in an organically modified silica sol-gel
[DE94-010086] p 4244 N94-35701
CATALYSTS
Monolith catalysts for closed-cycle carbon dioxide lasers
[NASA-CR-196093] p 4271 N94-35489
Atomic oxygen protective coating with resistance to undercutting at defect sites
[NASA-CASE-LEW-15306-1] p 4243 N94-35502

Morphological aspects of surface reactions
[DE94-010184] p 4236 N94-35685

Novel catalysts for methane activation
[DE94-009705] p 4237 N94-35778

Design of a high activity and selectivity alcohol catalyst
[DE94-003633] p 4237 N94-36023

The relationship between hydroxyl groups on oxide surfaces and the properties of supported metals
[DE94-010786] p 4241 N94-36233

Heterogeneous catalytic process for alcohol fuels from syngas
[DE94-010263] p 4248 N94-36299

Computer simulations of benzene in faujasite-type zeolites
[DE94-007533] p 4242 N94-36369

CATALYTIC ACTIVITY

Novel catalysts for methane activation
[DE94-009705] p 4237 N94-35778

Gasoline from natural gas by sulfur processing
[DE94-011130] p 4248 N94-36035

CATHODES

Analysis of recent agile mirror data
[AD-A278758] p 4318 N94-36427

CATHODOLUMINESCENCE

The occurrence of blue luminescing enstatite in E3 and E4 chondrites p 4351 N94-35423

CATIONS

A combined experimental and theoretical study of the neutral, cationic and anionic Si3N cluster molecule
[AD-A278834] p 4323 N94-35792

Anionic and neutral states of Li3O
[AD-A278833] p 4323 N94-35798

A new family of superconducting fullerides, Na(NH3)(x)C60(x = 2-8)
[DE94-011480] p 4341 N94-36272

Solvent acidity and basicity in polar media and their role in solvation
[AD-A278604] p 4239 N94-36426

CAUCHY PROBLEM

Cauchy and invariant measure problem for the periodic Zakharov system
[PB94-167707] p 4317 N94-35760

CAVITY RESONATORS

Dielectric measurements of selected ceramics at microwave frequencies p 4232 N94-36412

CEILINGS (METEOROLOGY)

Data requirements for ceiling and visibility products development
[AD-A278959] p 4293 N94-35720

CELESTIAL REFERENCE SYSTEMS

The Mars Observer differential one-way range demonstration p 4210 N94-35543

CELL DIVISION

Development of novel II-VI solar cells
[PB94-159415] p 4282 N94-35739

CELLS (BIOLOGY)

Multi-cellular, three-dimensional living mammalian tissue
[NASA-CASE-MSC-21560-2] p 4296 N94-35232

High density cell culture system
[NASA-CASE-MSC-22060-1] p 4296 N94-35366

Activities of National Institute of Radiological Sciences
[DE94-727636] p 4296 N94-36101

CEMENTS

Cement paste matrix composite materials center
[AD-A279017] p 4233 N94-35952

CENTRAL NERVOUS SYSTEM

A database to evaluate acceleration (+Gz) induced loss of consciousness (G-LOC) in the human centrifuge
[AD-A278769] p 4299 N94-35707

Multidisciplinary studies of integrated neural network systems
[AD-A278774] p 4312 N94-36309

CENTRAL PROCESSING UNITS

The most abstract common refinement
[AD-A278870] p 4305 N94-36014

CENTRIFUGAL FORCE

Spatio-temporal properties of centrifugal instabilities: Abstracts of 8th Couette-Taylor Meeting
[PB94-150240] p 4266 N94-35981

CENTRIFUGING STRESS

A database to evaluate acceleration (+Gz) induced loss of consciousness (G-LOC) in the human centrifuge
[AD-A278769] p 4299 N94-35707

CEPSTRAL ANALYSIS

Clustering techniques in speaker recognition
[AD-A278676] p 4255 N94-35689

CERAMIC COATINGS

Compliant metal enhanced convection cooled reverse-flow annular combustor
[NASA-TM-106626] p 4199 N94-36379

CERAMIC FIBERS

A novel method for depositing precious metal films on difficult surfaces
[NASA-TM-106607] p 4243 N94-35260

Advanced composites in Japan p 4234 N94-36045

Method of thermochemically treating silicon carbide fibers derived from polymers
[AD-D016218] p 4246 N94-36125

CERAMIC MATRIX COMPOSITES

Advanced composites in Japan p 4234 N94-36045

CERAMICS

Effects of combined stressing on the electrical properties of film and ceramic capacitors
[NASA-TM-106605] p 4257 N94-35249

Hot Corrosion Test Facility at the NASA Lewis Special Projects Laboratory
[NASA-CR-195323] p 4200 N94-35267

Classification of advanced technical ceramics
[REPT-15] p 4243 N94-35335

Intelligent processing of materials, technical activities, 1993 (NAS-NRC Assessment Panel, April 21-22 1994)
[PB94-164183] p 4251 N94-35737

Plane shock generator explosive lens: Shock characterization of 4340 and PH13-8Mo steels, C360 brass and PZT 65/35 ferro-electric ceramic
[DE94-009254] p 4266 N94-35979

Dielectric measurements of selected ceramics at microwave frequencies p 4232 N94-36412

CERTIFICATION

Flight test certification of a 480 gallon composite fuel tank on CF-18 p 4196 N94-36340

CC-130H(T) tactical aerial refuelling tanker development flight test programme p 4198 N94-36347

CESIUM

Experimental and theoretical studies of a high temperature cesium-barium tacitron, with application to low voltage-high current inversion
[DE94-008182] p 4228 N94-35349

Thermodynamic behaviour of tellurium at high temperatures
[DE94-612823] p 4240 N94-35960

CHAMBERS

Atomic oxygen reactor having at least one sidearm conduit
[NASA-CASE-MSC-21487-4] p 4250 N94-35445

CHAOS

Local instabilities and the transition to chaos of non-linear waves
[PB94-170578] p 4341 N94-36213

CHARGE CARRIERS

Distance dependent fractional statistics in a P, T-invariant model
[DE94-617360] p 4325 N94-36083

CHARGE COUPLED DEVICES

A mineralogical instrument for planetary applications
p 4357 N94-35408

A quick look method of detecting water of hydration in small solar system bodies p 4352 N94-35470

Nonlinear feedback model attitude control using CCD in magnetic suspension system p 4225 N94-35912

CHARGE DISTRIBUTION

A critical examination of charge funneling and its impact on single-event upset in Si devices
[DE94-007868] p 4261 N94-36373

CHARGE TRANSFER

Dynamic structural effects and ultrafast biomolecular kinetics in photoinduced charge transfer reactions
[DE94-010421] p 4329 N94-36390

CHARGED PARTICLES

Thickness of the layer of strong radial electric field in JFT-2M H-mode plasmas
[DE94-718993] p 4336 N94-35812

Processes of the reciprocal transformation vector charged particles pairs and electron-positron pairs
[DE94-616787] p 4325 N94-36077

On the theory of bounded many-particle systems with purely coulomb interactions
[DE94-617215] p 4325 N94-36081

Proceedings of the Twenty-First All-Union Conference on Physics of Charged Particles Interaction with Crystals
[DE94-615768] p 4341 N94-36181

P-matrix description of charged particles interaction
[DE94-616853] p 4329 N94-36391

CHARPY IMPACT TEST

An automated digital data collection and analysis system for the Charpy Impact Tester p 4232 N94-36415

CHARTS

Object-oriented simulation pictures (OOSPic) for design and testing
[AD-A278798] p 4305 N94-36013

CHASSIGNITES

Pigeonholing planetary meteorites: The lessons of misclassification of EET87521 and ALH84001
p 4353 N94-36157

CHECKOUT

Symbolic debugging of globally optimized code: Data value problems and their solutions
[AD-A278898] p 4302 N94-35572

CHEMICAL ANALYSIS

Inhomogeneous distribution of materials in lodranites-acapulcoites and IAB irons and their common formation processes p 4364 N94-35463

The anatomy of a cluster IDP. Part 1: Carbon abundance, bulk chemistry, and mineralogy of fragments from L2008#5 p 4352 N94-35466

Vapor-fortified QA/QC samples for the analysis of volatile organic compounds
[AD-A278712] p 4229 N94-35776

CSTL technical activities, 1991
[PB94-160769] p 4318 N94-36003

CHEMICAL BONDS

Chemical reactions of chlorine on a vicinal Si(100) surface studied by ESDIAD
[AD-A279059] p 4236 N94-35731

Periodicity and peculiarity in 120 first and second row diatomic molecules
[AD-A278836] p 4323 N94-35793

Computer simulations of benzene in faujasite-type zeolites
[DE94-007533] p 4242 N94-36369

CHEMICAL COMPOSITION

Classification of advanced technical ceramics
[REPT-15] p 4243 N94-35335

New prospects for analyzing lunar pyroclastic glass
p 4355 N94-35397

Single agglutinates: A comparative study of compositions of agglutinitic glass, whole-grain, bulk soil, and FMR p 4355 N94-35401

Remote geochemical experiment package for Discovery class missions p 4350 N94-35420

Luna 24 regolith breccias: A possible source of the fine size material of the Luna 24 regolith
p 4362 N94-35450

Innovative instrumentation for mineralogical and elemental analyses of solid extraterrestrial surfaces: The Backscatter Moessbauer Spectrometer/X Ray Fluorescence analyzer (BaMS/XRF)
p 4239 N94-35459

Isotopic and geochemical precursors of earthquakes and volcanic eruptions
[DE94-615824] p 4289 N94-35568

Twin spacing versus size of a monocrystal for the nonstoichiometric 1:2:3 superconductors
[DE94-615511] p 4340 N94-36029

Uniqueness of a solution of a steady state photochemical problem: Applications to Mars p 4370 N94-36151

CHEMICAL ENGINEERING

JPRS report: Science and technology. Central Eurasia
[JPRS-UST-94-001] p 4229 N94-35340

JPRS report: Science and technology. Central Eurasia
[JPRS-UST-94-004] p 4249 N94-35341

JPRS report: Science and technology. Central Eurasia
[JPRS-UST-94-010] p 4250 N94-35385

JPRS report: Science and technology. Central Eurasia
[JPRS-UST-94-011] p 4250 N94-35386

JPRS report: Science and technology. Central Eurasia
[JPRS-UST-94-012] p 4250 N94-35387

CSTL technical activities, 1991
[PB94-160769] p 4318 N94-36003

AICD: Advanced Industrial Concepts Division Biological and Chemical Technologies Research Program
[DE94-006854] p 4283 N94-36051

CHEMICAL EQUILIBRIUM

NMR imaging of components and materials for DOE application
[DE94-010664] p 4238 N94-36084

On the origin of porphyritic chondrules
[DE94-010464] p 4351 N94-36418

CHEMICAL PROPERTIES

Classification of advanced technical ceramics
[REPT-15] p 4243 N94-35335

CHEMICAL REACTIONS

Theoretical aspect of low pressure discharges in simple gasses
[AD-A278762] p 4335 N94-35493

Morphological aspects of surface reactions
[DE94-010184] p 4236 N94-35685

Chemical reactions of chlorine on a vicinal Si(100) surface studied by ESDIAD
[AD-A279059] p 4236 N94-35731

Ultrafast chemical dynamics of reactions in beams
[AD-A278939] p 4323 N94-35805

Comparison of PDF and moment closure methods in the modeling of turbulent reacting flows
[NASA-TM-106614] p 4265 N94-35948

Tritiated ammonia formation
[DE94-011170] p 4237 N94-36056

Production of ferroan andesites by the experimental partial melting of an LL chondrite p 4353 N94-36160

The thermochemistry and reaction mechanisms in the decomposition of energetic materials
[DE94-011420] p 4248 N94-36376

CHEMICAL REACTORS
Atomic oxygen reactor having at least one sidearm conduit
[NASA-CASE-MSC-21487-4] p 4250 N94-35445
CHEMISTRY
Activities of National Institute of Radiological Sciences
[DE94-727636] p 4296 N94-36101
CHIPS
An overview of multichip modules
[AD-A278730] p 4260 N94-36296
CHIPS (ELECTRONICS)
Issues in the development of a 10 MBPS K=15 Viterbi decoder
[NASA-CR-196083] p 4211 N94-35357
Thick film fabrication of aluminum nitride microcircuits
[DE94-010107] p 4259 N94-35706
Computer automation and artificial intelligence
[DE94-611058] p 4312 N94-35831
Space-based crystal growth and thermocapillary flow
p 4342 N94-35971
CHLORINE
Chemical reactions of chlorine on a vicinal Si(100) surface studied by ESDIAD
[AD-A279059] p 4236 N94-35731
Kinetics studies following state-selective laser excitation
[DE94-010305] p 4330 N94-36105
CHLORINE COMPOUNDS
Application of an alkylammonium method for characterization of phyllosilicates in CI chondrites
p 4351 N94-35432
CHLOROFLUOROCARBONS
Sealed tube comparisons of the compatibility of desiccants with refrigerants and lubricants
[DE94-010002] p 4251 N94-36388
CHLOROPRENE RESINS
Diffusion and sorption of 1,4-dioxane into polychloroprene
[ARL-TR-338] p 4229 N94-35361
CHONDRITES
Alteration and formation of rims on the CM parent body p 4357 N94-35411
What initiated planetesimal formation?
p 4351 N94-35422
The occurrence of blue luminescing enstatite in E3 and E4 chondrites p 4351 N94-35423
Application of an alkylammonium method for characterization of phyllosilicates in CI chondrites
p 4351 N94-35432
Textural constraints on the formation of alteration phases in CM chondrites p 4353 N94-36145
Partial melting of the St. Severin (LL) and Lost City (H) ordinary chondrites: One step backwards and two steps forward p 4353 N94-36146
Preliminary results of sulfide melt/silicate wetting experiments in a partially melted ordinary chondrite
p 4353 N94-36147
Electron energy-loss spectroscopy of carbon in interplanetary dust particles p 4353 N94-36149
On the origin of enstatite chondrite chondrules based on their petrography and comparison with experimentally produced chondrules p 4353 N94-36158
Production of ferroan andesites by the experimental partial melting of an LL chondrite p 4353 N94-36160
Partition coefficients for Al, Ca, Ti, Cr, and Ni in olivine obtained by melting experiment on an LL6 chondrite
p 4353 N94-36163
Shape, size, and distribution of magnetic particles in Bjurbole chondrules p 4353 N94-36167
On the origin of porphyritic chondrules
[DE94-010464] p 4351 N94-36418
CHONDRULE
On the possible role of elemental carbon in the formation of reduced chondrules p 4351 N94-35421
The occurrence of blue luminescing enstatite in E3 and E4 chondrites p 4351 N94-35423
Chondrule magnetic properties p 4352 N94-35471
On the origin of enstatite chondrite chondrules based on their petrography and comparison with experimentally produced chondrules p 4353 N94-36158
Shape, size, and distribution of magnetic particles in Bjurbole chondrules p 4353 N94-36167
On the origin of porphyritic chondrules
[DE94-010464] p 4351 N94-36418
CHROMITES
Possible spinel absorption bands in S-asteroid visible reflectance spectra p 4368 N94-36139
CHROMIUM
Cr, Mn, and Ca distributions for olivine in angritic systems: Constraints on the origins of Cr-rich and Ca-poor core olivine in angrite LEW87051 p 4353 N94-36162
Partition coefficients for Al, Ca, Ti, Cr, and Ni in olivine obtained by melting experiment on an LL6 chondrite
p 4353 N94-36163
CHROMIUM ALLOYS
High temperature creep and oxidation resistant chromium silicide matrix alloy containing molybdenum
[NASA-CASE-LEW-15697-1] p 4241 N94-36275
CHROMOPHORES
Concurrent stabilization and imaging of a novel polymer for second harmonic generation via in situ photopolymerization
[AD-A278912] p 4243 N94-35588
CHROMOSPHERE
On the physics of waves in the solar atmosphere: Wave heating and wind acceleration
[NASA-CR-194119] p 4375 N94-36395
CHRONOLOGY
Ar-39-Ar-40 ages of four ureilites
p 4357 N94-35410
CIRCUIT BOARDS
The iWarp display module
[AD-A278610] p 4260 N94-36248
CIRCUIT RELIABILITY
Hardness variability in commercial and hardened technologies
[DE94-007270] p 4261 N94-36362
CIRCUITS
Active antenna
[NASA-CASE-GSC-13309-1] p 4251 N94-35231
Review of slow-wave structures
[NASA-TM-106639] p 4258 N94-35270
High level modelling and design of asynchronous interface logic
[PB94-167822] p 4258 N94-35534
CIRCULAR POLARIZATION
Optimum satellite relay positions with application to a TDRS-1 Indian Ocean relay p 4205 N94-35624
CIVIL AVIATION
Future supersonic commercial transport aircraft: A technological challenge for long haul traffic
p 4193 N94-36324
CLADDING
Thermodynamic behaviour of tellurium at high temperatures
[DE94-612823] p 4240 N94-35960
CLASSIFICATIONS
Classification of advanced technical ceramics
[REPT-15] p 4243 N94-35335
Pigeonholing planetary meteorites: The lessons of misclassification of EET87521 and ALH84001
p 4353 N94-36157
CLAYS
Application of an alkylammonium method for characterization of phyllosilicates in CI chondrites
p 4351 N94-35432
CLEAN ROOMS
Magnetically suspended stepping motors for clean room and vacuum environments p 4225 N94-35915
CLEANERS
Cleaning up our act: Alternatives for hazardous solvents used in cleaning
[DE94-006624] p 4285 N94-35943
CLEANING
Cleaning up our act: Alternatives for hazardous solvents used in cleaning
[DE94-006624] p 4285 N94-35943
CLEANLINESS
Purity and cleanness of aerogel as a cosmic dust capture medium p 4247 N94-35469
CLIMATE
Venus climate stability and volcanic resurfacing rates
p 4358 N94-35413
The computation of cloud base height from paired whole-sky imaging cameras
[DE94-009868] p 4294 N94-35767
Modernization of the graphics post-processors of the Hamburg German Climate Computer Center Carbon Cycle Codes
[DE94-011604] p 4288 N94-36273
CLIMATE CHANGE
Mission to Planet Earth. The living ocean: Observing ocean color from space
[NASA-PAM-554] p 4295 N94-35343
Venus climate stability and volcanic resurfacing rates
p 4358 N94-35413
Simultaneous adsorption of CO2 and H2O under Mars-like conditions and application to the evolution of the Martian climate p 4366 N94-35475
Insight to global change: EOS/SAR mission
[NASA-CR-196133] p 4284 N94-35503
Asymetric change of daily temperature range: Proceedings
[DE94-010102] p 4293 N94-35703
The Atmospheric Radiation Measurement Program and interfaces with external data sources
[DE94-003699] p 4286 N94-36024
Mars atmospheric escape and isotopic fractionation: Synthesis of data and models p 4369 N94-36143
Selected translated abstracts of Russian-language climate-change publications. 2: Clouds
[DE94-011465] p 4295 N94-36244
Integrated science model for assessment of climate change
[DE94-011758] p 4288 N94-36286
CLIMATOLOGY
JPRS report: Science and technology. Central Eurasia
[JPRS-UST-94-006] p 4249 N94-35226
CLOCKS
Asynchronous optimistic rollback recovery using secure distributed time
[AD-A278978] p 4344 N94-35526
A determinizable class of timed automata
[AD-A278858] p 4317 N94-35743
CLOSED CYCLES
Monolith catalysts for closed-cycle carbon dioxide lasers
[NASA-CR-196093] p 4271 N94-35489
CLOUD COVER
The effects of cloud inhomogeneities upon radiative fluxes, and the supply of a cloud truth validation dataset
[NASA-CR-196080] p 4293 N94-35391
H2O-H2SO4 system in Venus' clouds and OCS, CO, and H2SO4 profiles in Venus' troposphere
p 4370 N94-36152
CLOUD HEIGHT INDICATORS
The computation of cloud base height from paired whole-sky imaging cameras
[DE94-009868] p 4294 N94-35767
CLOUD PHOTOGRAPHS
Extraction of cloud statistics from whole sky imaging cameras
[DE94-009867] p 4294 N94-35766
CLOUD PHOTOGRAPHY
Extraction of cloud statistics from whole sky imaging cameras
[DE94-009867] p 4294 N94-35766
CLOUDS (METEOROLOGY)
Computer animation of clouds
[DE94-008289] p 4292 N94-35350
Extraction of cloud statistics from whole sky imaging cameras
[DE94-009867] p 4294 N94-35766
Selected translated abstracts of Russian-language climate-change publications. 2: Clouds
[DE94-011465] p 4295 N94-36244
Efficient light propagation for multiple anisotropic volume scattering
[DE94-006474] p 4334 N94-36358
CLUSTER ANALYSIS
An information model for use in software management estimation and prediction p 4301 N94-35437
Clustering techniques in speaker recognition
[AD-A278676] p 4255 N94-35689
CLUSTERS
Magnetic properties of nanosize iron clusters
[DE94-011329] p 4318 N94-36204
CMOS
Beam tests of a prototype level-1 calorimeter trigger for LHC experiments
[PB94-170495] p 4269 N94-35599
COAGULATION
Formation of iron metal and grain coagulation in the solar nebula p 4373 N94-36170
COAL
Combined SO(x)/NO(x) control via SOXAL (tm) process: An electrodialytic regenerative wet scrubbing process
[DE94-009053] p 4284 N94-35346
Design and operation of a medium speed 12-cylinder coal-fueled diesel engine. Phase 2: Improvements
[DE94-009547] p 4275 N94-35815
Coal-fueled diesels for modular power generation
[DE94-002960] p 4275 N94-36348
COAL DERIVED GASES
Heavy duty gas turbine combustion tests with simulated low BTU coal gas
[DE94-002970] p 4276 N94-36355
COAL GASIFICATION
Heavy duty gas turbine combustion tests with simulated low BTU coal gas
[DE94-002970] p 4276 N94-36355
COAL UTILIZATION
Design and operation of a medium speed 12-cylinder coal-fueled diesel engine. Phase 2: Improvements
[DE94-009547] p 4275 N94-35815
COASTAL ECOLOGY
Endangered and potentially endangered wildlife on John F. Kennedy Space Center and faunal integrity as a goal for maintaining biological diversity
[NASA-TM-109204] p 4288 N94-36422
COASTAL PLAINS
Groundwater penetrating radar and high resolution seismic for locating shallow faults in unconsolidated sediments
[DE94-007284] p 4257 N94-36366

COASTAL WATER
Evaluation of synthetic aperture radar for oil-spill response [AD-A278796] p 4284 N94-35674

COATING
Dual cure low-VOC coating process [DE94-009346] p 4245 N94-35809
Analysis of a High Velocity Oxygen-Fuel (HVOF) thermal spray torch. Part 1: Numerical formulation [DE94-005590] p 4267 N94-35996

COATINGS
Flight testing of a luminescent surface pressure sensor [NASA-TM-103970] p 4189 N94-35394
Antarctic weathering of the CK chondrites EET90004, 90007, and 90022: Nickel and sulfur mobility p 4351 N94-35451
Inertial confinement fusion target component fabrication and technology development report [DE94-009973] p 4335 N94-35673
Mechanical properties of crosslinked polymer coatings p 4231 N94-36410

COBALT COMPOUNDS
NO decomposition in non-reducing atmospheres [DE94-011157] p 4237 N94-36036

CODERS
Bit-wise arithmetic coding for data compression p 4254 N94-35556

CODING
Bit-wise arithmetic coding for data compression p 4254 N94-35556
The polygon-ellipse method of data compression of weather maps [AD-A278958] p 4293 N94-35719
Attention and signal detection. A study of attention divided between visual and auditory signals [PB94-170594] p 4298 N94-36215

COEFFICIENT OF FRICTION
Effect of niobium interlayer on high-temperature sliding friction and wear of silver films on alumina [DE94-010462] p 4275 N94-36232

COEFFICIENTS
Partition coefficients for Al, Ca, Ti, Cr, and Ni in olivine obtained by melting experiment on an LL6 chondrite p 4353 N94-36163
Periodized wavelets [DE94-010365] p 4316 N94-36432

COLLAGENS
A low temperature scanning force microscope for biological samples [DE94-011357] p 4297 N94-36269

COLLAPSE
Self-similar regimes of subsonic Langmuir wave collapse [DE94-611466] p 4335 N94-35750

COLLISION AVOIDANCE
The application of fuzzy logic to SAFOR in SIMNET [AD-A279058] p 4312 N94-35730

COLLISIONLESS PLASMAS
Collisonless dynamics of the magnetosphere [AD-A278886] p 4290 N94-35708

COLOR
The occurrence of blue luminescing enstatite in E3 and E4 chondrites p 4351 N94-35423
The capacity of color histogram indexing [AD-A279031] p 4345 N94-35732

COLOR CENTERS
Color center laser with transverse auxiliary illumination [AD-D016201] p 4273 N94-36365

COLOR CODING
Color-coded radar plan position indicator [AD-D016200] p 4257 N94-36364

COLOR TELEVISION
The iWarp display module [AD-A278610] p 4260 N94-36248

COLUMBIA (ORBITER)
STS-58 Space Shuttle Mission Report [NASA-TM-109867] p 4211 N94-35251

COMBUSTIBLE FLOW
Analysis of a High Velocity Oxygen-Fuel (HVOF) thermal spray torch. Part 1: Numerical formulation [DE94-005590] p 4267 N94-35996
LIEKKI Combustion Research Program [DE94-763298] p 4237 N94-36059

COMBUSTION
The 30th JANNAF Combustion Subcommittee Meeting, volume 2 [AD-A278794] p 4247 N94-35656
Durability testing of medium speed diesel engine components designed for operating on coal/water slurry fuel [DE94-009550] p 4275 N94-35667
Bus application of oxygen-enrichment technology and diesel-electric hybrid systems [DE94-009835] p 4285 N94-35765
Analysis of mid-tropospheric carbon monoxide data using a three-dimensional global atmospheric chemistry numerical model [DE94-004782] p 4286 N94-36026
LIEKKI Combustion Research Program [DE94-763298] p 4237 N94-36059
Heavy duty gas turbine combustion tests with simulated low BTU coal gas [DE94-002970] p 4276 N94-36355

COMBUSTION CHAMBERS
Compliant metal enhanced convection cooled reverse-flow annular combustor [NASA-TM-106626] p 4199 N94-36379

COMBUSTION CHEMISTRY
Detailed studies of soot formation in laminar diffusion flames for application to modeling studies [AD-A278941] p 4235 N94-35604
LIEKKI Combustion Research Program [DE94-763298] p 4237 N94-36059
A new comprehensive reaction mechanism for combustion of hydrocarbon fuels [DE94-008288] p 4238 N94-36205
The reaction of hydroperoxy-propyl radicals with molecular oxygen [DE94-006392] p 4239 N94-36319
Effects of natural gas composition on ignition delay under diesel conditions [DE94-006405] p 4276 N94-36378

COMBUSTION PHYSICS
The 30th JANNAF Combustion Subcommittee Meeting, volume 1 [AD-A278793] p 4247 N94-35655
The 30th JANNAF Combustion Subcommittee Meeting, volume 2 [AD-A278794] p 4247 N94-35656
Infrared multiphoton ignition and combustion enhancement of natural gas. [PB94-165438] p 4236 N94-35755
LIEKKI Combustion Research Program [DE94-763298] p 4237 N94-36059
Advanced hydrogen/method utilization technology demonstration [DE94-000214] p 4248 N94-36191
A comparison between direct spark ignition and prechamber ignition in an internal combustion engine [DE94-008218] p 4275 N94-36206

COMBUSTION PRODUCTS
Combined SO(x)/NO(x) control via SOXAL (tm) process: An electrodialytic regenerative wet scrubbing process [DE94-009053] p 4284 N94-35346
Detailed studies of soot formation in laminar diffusion flames for application to modeling studies [AD-A278941] p 4235 N94-35604
Design and operation of a medium speed 12-cylinder coal-fueled diesel engine. Phase 2: Improvements [DE94-009547] p 4275 N94-35815
Methanol fuel additive demonstration [PB94-156668] p 4247 N94-35941
Capillary column GC-MS/MS confirmation of phosphate esters with a hybrid tandem mass spectrometer [AD-A278748] p 4238 N94-36091
Advanced hydrogen/method utilization technology demonstration [DE94-000214] p 4248 N94-36191
Heavy duty gas turbine combustion tests with simulated low BTU coal gas [DE94-002970] p 4276 N94-36355

COMBUSTION STABILITY
The 30th JANNAF Combustion Subcommittee Meeting, volume 1 [AD-A278793] p 4247 N94-35655

COMETARY ATMOSPHERES
Low encounter speed comet COMA sample return missions p 4202 N94-35607

COMETARY COLLISIONS
Radiative signals from impact of Shoemaker-Levy on Jupiter p 4355 N94-35396
Shoemaker-Levy 9 and the tidal disruption of comets p 4351 N94-35406

COMETS
Low encounter speed comet COMA sample return missions p 4202 N94-35607
Dust evolution from comets and asteroids: Their velocities at Earth orbit intersection p 4352 N94-36142
The structural changes of water ice I during warmup p 4239 N94-36144

COMFORT
Control of maglev vehicles with aerodynamic and guideway disturbances p 4213 N94-35842

COMMAND AND CONTROL
A software architecture for adding new interaction techniques to a command and control based testbed [AD-A278760] p 4302 N94-35491
Task allocation for parallel real-time execution [AD-A278789] p 4310 N94-35653
Fault tolerant computer control for a Maglev transportation system p 4215 N94-35848

COMMAND LANGUAGES
MMI(exp 2) demonstrator systems: A multi-modal interface for man machine interaction with knowledge based systems. Deliverable D17 (TA 2) ESPRIT project 2474 MMI(exp 2) [PB94-170537] p 4298 N94-35600

COMMERCIAL AIRCRAFT
Future supersonic commercial transport aircraft: A technological challenge for long haul traffic p 4193 N94-36324

COMMUNICATING
Using International English to prepare technical text for translation [DE94-002628] p 4347 N94-36102

COMMUNICATION EQUIPMENT
Influence of an externally modulated photonic link on a microwave communications system p 4252 N94-35544

COMMUNICATION NETWORKS
The rel/REL: A family of reliable multicast protocols for distributed real-time systems [PB94-167830] p 4310 N94-35535
A new presentation of complex voltage data for Goldstone radar astronomy p 4255 N94-35561
The Mars Observer Ka-band link experiment p 4255 N94-35563
North American ISDN Users' Forum agreements on Integrated Services Digital Network [PB94-162559] p 4305 N94-35940
Computer Systems Laboratory [PB94-162518] p 4333 N94-36002

COMMUNICATION SATELLITES
Information and communication technology p 4257 N94-36043

COMPATIBILITY
Compatibility of TOPEX/Poseidon trajectory propagation with JPL and GSFC/FDF operational software p 4204 N94-35619
Thick film fabrication of aluminum nitride microcircuits [DE94-010107] p 4259 N94-35706
Research update: Materials Compatibility and Lubricant Research (MCLR) program [DE94-010001] p 4247 N94-36387
Sealed tube comparisons of the compatibility of desiccants with refrigerants and lubricants [DE94-010002] p 4251 N94-36388

COMPENSATORS
Third order LPF type compensator for flexible rotor suspension p 4217 N94-35863
CSI, optimal control, and accelerometers: Trials and tribulations p 4221 N94-35888
Robustness properties of LQG optimized compensators for collocated rate sensors p 4221 N94-35890
LQG optimal compensator transfer function for the NASA LaRC CSI Evolutionary Model p 4221 N94-35891
Rational positive real approximations for LQG optimal compensators arising in active stabilization of flexible structures p 4222 N94-35892

COMPILERS
Symbolic debugging of globally optimized code: Data value problems and their solutions [AD-A278898] p 4302 N94-35572
ML partial evaluation using set-based analysis [AD-A278955] p 4304 N94-35718
Communication and memory requirements as the basis for mapping task and data parallel programs [AD-A278954] p 4310 N94-35806

COMPONENT RELIABILITY
Integrated design of structures, controls, and materials p 4218 N94-35869
An analysis of operational suitability for test and evaluation of highly reliable systems [AD-A278573] p 4192 N94-36184

COMPOSITE MATERIALS
JPRS report: Science and technology. Central Eurasia [JPRS-UST-94-001] p 4229 N94-35340
JPRS report: Science and technology. Central Eurasia [JPRS-UST-94-011] p 4250 N94-35386
JPRS report: Science and technology. Central Eurasia [JPRS-UST-94-012] p 4250 N94-35387
JPRS report: Science and technology. Central Eurasia: Materials science [JPRS-UMS-93-007] p 4240 N94-35517
A combined experimental and theoretical study of the neutral, cationic and anionic Si3N cluster molecule [AD-A278834] p 4323 N94-35792
Aspects of robust computational modeling for plain and reinforced concrete [PB94-169240] p 4251 N94-35820
Cement paste matrix composite materials center [AD-A279017] p 4233 N94-35952

Nonlinear optical composites of metal cluster laden polymers
[AD-D016217] p 4234 N94-36124
ASTM test methods for composite characterization and evaluation p 4229 N94-36399
Laminated thermoplastic composite material from recycled high density polyethylene p 4230 N94-36403
New developments in aluminum for aircraft and automobiles p 4232 N94-36413

COMPOSITE STRUCTURES
Design for manufacturability evaluation: Composite National Ignition Facility (NIF) pockel cell body
[DE94-010669] p 4338 N94-36284
Optimisation of composite aircraft structures by direct manufacturing approaches p 4194 N94-36327

COMPRESSED AIR
Tipjet 80-inch model rotor hover test: Test no. 1198
[AD-A279680] p 4191 N94-36261

COMPRESSIBILITY
A mechanics mode for the compressive response of fiber reinforced composites
[AD-A278866] p 4233 N94-35715
Equations of state valid continuously from zero to extreme pressures with H2O and CO2 as examples
[DE94-011907] p 4238 N94-36230

COMPRESSIBLE BOUNDARY LAYER
Expansion effects on supersonic turbulent boundary layers
[AD-A278989] p 4190 N94-35950

COMPRESSIVE STRENGTH
A mechanics mode for the compressive response of fiber reinforced composites
[AD-A278866] p 4233 N94-35715
Can the compressive response of fiber-reinforced composites be modelled by means of layered arrays?
[AD-A278864] p 4233 N94-35944

COMPRESSORS
Rotor dynamic behaviour of a high-speed oil-free motor compressor with a rigid coupling supported on four radial magnetic bearings p 4224 N94-35911

COMPUTATION
Asynchronous optimistic rollback recovery using secure distributed time
[AD-A278978] p 4344 N94-35526
Combining symbolic computation and theorem proving: Some problems of Ramanujan
[AD-A278899] p 4303 N94-35573

COMPUTATIONAL CHEMISTRY
Computer simulations of benzene in faujasite-type zeolites
[DE94-007533] p 4242 N94-36369

COMPUTATIONAL FLUID DYNAMICS
Analysis of phase distribution phenomena in microgravity environments
[NASA-CR-196038] p 4249 N94-35237
Computational methods for HSCT-inlet controls/CFD interdisciplinary research
[NASA-TM-106618] p 4198 N94-35352
Three-dimensional unstructured grid refinement and optimization using edge-swapping
[NASA-TM-103966] p 4299 N94-35393
Analysis of the injection process in direct injected natural gas engines
[PB94-156494] p 4275 N94-35931
Comparison of PDF and moment closure methods in the modeling of turbulent reacting flows
[NASA-TM-106614] p 4265 N94-35948
Numerical simulation of shock interaction with above-ground structures
[AD-A278713] p 4279 N94-35949
NEQPAK, the AEDC thermochemical nonequilibrium package: Theory and use
[AD-A279005] p 4266 N94-35951
Boundary conditions for jet flow computations
[NASA-TM-106648] p 4266 N94-35976
Vortex tubes in turbulent flows: Identification, representation, reconstruction
[NASA-CR-194900] p 4267 N94-35992
A three dimensional multigrid Reynolds-averaged Navier-Stokes solver for unstructured meshes
[NASA-CR-194908] p 4191 N94-35994
Analysis of a High Velocity Oxygen-Fuel (HVOF) thermal spray torch. Part 1: Numerical formulation
[DE94-005590] p 4267 N94-35996
A multilevel adaptive projection method for unsteady incompressible flow
[DE93-016418] p 4267 N94-36315
Overset grid applications on distributed memory MIMD computers
[NASA-CR-196081] p 4268 N94-36397
Analysis of high speed flow, thermal and structural interactions
[NASA-CR-196017] p 4268 N94-36420

COMPUTATIONAL GRIDS
Three-dimensional unstructured grid refinement and optimization using edge-swapping
[NASA-TM-103966] p 4299 N94-35393
Computation of dendrites using a phase field model
[PB94-160744] p 4236 N94-35736
A three dimensional multigrid Reynolds-averaged Navier-Stokes solver for unstructured meshes
[NASA-CR-194908] p 4191 N94-35994
An efficient, intelligent solution for viscous flows inside solid rocket motors
[AD-A278629] p 4228 N94-36255
An adaptive, unstructured, finite-element, multi-material, thermal analysis
[AD-A278632] p 4343 N94-36256
A multilevel adaptive projection method for unsteady incompressible flow
[DE93-016418] p 4267 N94-36315
Numerical investigation of multi-element airfoils
[NASA-CR-194592] • p 4191 N94-36394
Overset grid applications on distributed memory MIMD computers
[NASA-CR-196081] p 4268 N94-36397

COMPUTER AIDED DESIGN
Integrated design of structures, controls, and materials
p 4218 N94-35869
Case based reasoning in engineering design
[AD-A278943] p 4305 N94-36006
Representing spatial information in a computational model for network management
[NASA-CR-191669] p 4306 N94-36040
Simulation of materials processing: Fantasy or reality?
p 4230 N94-36404

COMPUTER ANIMATION
Computer animation of clouds
[DE94-008289] p 4292 N94-35350

COMPUTER ASSISTED INSTRUCTION
General purpose architecture for intelligent computer-aided training
[NASA-CASE-MSC-21381-1] p 4311 N94-35501

COMPUTER GRAPHICS
The influence of data link-provided graphical weather on pilot decision-making
[AD-A278871] p 4293 N94-35596
Three dimensional visualization of a coastal mesoscale model
[AD-A278576] p 4294 N94-36187
The EASE Visualization Community Club
[PB94-170529] p 4308 N94-36211
Computer graphics tools for the visualization of spacecraft dynamics
[AD-A278615] p 4226 N94-36251
Modernization of the graphics post-processors of the Hamburg German Climate Computer Center Carbon Cycle Codes
[DE94-011604] p 4288 N94-36273
GRIZ: Finite element analysis results visualization for unstructured grids
[DE94-010066] p 4309 N94-36429

COMPUTER INFORMATION SECURITY
Asynchronous optimistic rollback recovery using secure distributed time
[AD-A278978] p 4344 N94-35526
Proceedings of the Workshop on the Federal Criteria for Information Technology Security
[PB94-162583] p 4346 N94-36005
Computer virus information update CIAC-2301
[DE94-011916] p 4308 N94-36236

COMPUTER NETWORKS
Defense RDT and E online system (DROLS) retrieval reference guide
[AD-A278972] p 4344 N94-35525
Asynchronous optimistic rollback recovery using secure distributed time
[AD-A278978] p 4344 N94-35526
The rel/REL: A family of reliable multicast protocols for distributed real-time systems
[PB94-167830] p 4310 N94-35535
Guidelines for design and development of computer/microprocessor based systems in research and power reactors
[DE94-616271] p 4300 N94-35570
Large granularity cache coherence for intermittent connectivity
[AD-A278897] p 4345 N94-35571
Task networks for controlling continuous processes
[AD-A278683] p 4312 N94-35710
The DataCube server. Animate agent project working note 2, version 1.0
[AD-A278847] p 4310 N94-35742
An analysis of file system and installation of the file management system for NOS operating system
[DE94-611062] p 4346 N94-35833
Data acquisition system of the GDL facility
[DE94-616604] p 4346 N94-35954
Computer Systems Laboratory
[PB94-162518] p 4333 N94-36002
Netlib services and resources
[DE94-010307] p 4347 N94-36300
Telecommuting (work-at-home) at NASA Lewis Research Center
[NASA-CR-195334] p 4347 N94-36396

COMPUTER PROGRAM INTEGRITY
Computer virus information update CIAC-2301
[DE94-011916] p 4308 N94-36236

COMPUTER PROGRAMMING
Annotated bibliography of Software Engineering Laboratory literature
[NASA-CR-189350] p 4300 N94-35238
An information model for use in software management estimation and prediction p 4301 N94-35437
Software architecture standard for simulation virtual machine, version 2.0
[NASA-CR-188291] p 4301 N94-35443
A compile time model for composing parallel programs
[AD-A278896] p 4310 N94-35597
A critique of type systems for global overloading
[AD-A278800] p 4304 N94-35676
Refinement types ML
[AD-A278937] p 4304 N94-35709
ML partial evaluation using set-based analysis
[AD-A278955] p 4304 N94-35718
The DataCube server. Animate agent project working note 2, version 1.0
[AD-A278847] p 4310 N94-35742
The EASE Visualization Community Club
[PB94-170529] p 4308 N94-36211
Transformation of a Cranz-Schardin camera
[PB94-170685] p 4270 N94-36219
A practical guide to the technology and adoption of software process automation
[AD-A278719] p 4308 N94-36294
Interfacing the RAP system to real-time control, version 1
[AD-A278725] p 4312 N94-36295

COMPUTER PROGRAMS
Annotated bibliography of Software Engineering Laboratory literature
[NASA-CR-189350] p 4300 N94-35238
Optimization of residual stresses in MMC's using compensating/compliant interfacial layers. Part 2: OPTCOMP user's guide
[NASA-CR-195337] p 4278 N94-35239
Runtime support for data parallel tasks
[NASA-CR-194904] p 4300 N94-35240
CATLAC: Calibration and validation analysis tool of local area coverage for the SeaWiFS mission
[NASA-TM-104603] p 4211 N94-35269
Introduction to Neural Networks: Neural Network Workshop for the Hanford Community
[DE94-006526] p 4311 N94-35348
Collected software engineering papers, volume 11
[NASA-CR-189347] p 4301 N94-35434
Developing interpretable models with optimized set reduction for identifying high risk software components
p 4301 N94-35435
Developing software for ease of change: Metrics from later in the TRALAB system life cycle
[AD-A278759] p 4302 N94-35490
Development and application of computational aerothermodynamics flowfield computer codes
[NASA-CR-196136] p 4189 N94-35498
COSMIC monthly progress report
[NASA-CR-195962] p 4302 N94-35514
Guidelines for design and development of computer/microprocessor based systems in research and power reactors
[DE94-616271] p 4300 N94-35570
NAVSPACECOM space surveillance sensor system digital signal processing receiver. Volume 4: Hardware interfaces
[AD-A278845] p 4212 N94-35801
The Earth Satellite Program (ESP), version 2.0
[AD-A278860] p 4201 N94-35827
The development of a statistical report software for computer system usages
[DE94-611061] p 4346 N94-35832
ONED90: 1-dimensional diffusion code
[DE94-611063] p 4305 N94-35834
Data acquisition system of the GDL facility
[DE94-616604] p 4346 N94-35954
The most abstract common refinement
[AD-A278870] p 4305 N94-36014
Use of formal calculation to automatically obtain adjoint programs
[PB94-170701] p 4308 N94-36259
Modernization of the graphics post-processors of the Hamburg German Climate Computer Center Carbon Cycle Codes
[DE94-011604] p 4288 N94-36273

A practical guide to the technology and adoption of software process automation
[AD-A278719] p 4308 N94-36294
Applying observations of work activity in designing prototype data analysis tools
[DE94-010206] p 4347 N94-36297
Netlib services and resources
[DE94-010307] p 4347 N94-36300
Digital control programmer for temperature control
[DE94-615584] p 4309 N94-36382
On the origin of porphyritic chondrules
[DE94-010464] p 4351 N94-36418
GRIZ: Finite element analysis results visualization for unstructured grids
[DE94-010066] p 4309 N94-36429

COMPUTER STORAGE DEVICES
A critical examination of charge funneling and its impact on single-event upset in Si devices
[DE94-007868] p 4261 N94-36373

COMPUTER SYSTEMS DESIGN
A software architecture for adding new interaction techniques to a command and control based testbed
[AD-A278760] p 4302 N94-35491
The rel/REL: A family of reliable multicast protocols for distributed real-time systems
[PB94-167830] p 4310 N94-35535
Guidelines for design and development of computer/microprocessor based systems in research and power reactors
[DE94-616271] p 4300 N94-35570

COMPUTER SYSTEMS PERFORMANCE
Transient Faults in Computer Systems
[NASA-CR-194717] p 4306 N94-36063
Experimental evaluation of the certification-trail method p 4306 N94-36065

COMPUTER SYSTEMS PROGRAMS
Task allocation for parallel real-time execution
[AD-A278789] p 4310 N94-35653
Concept for an algorithm testing and evaluation program at NIST
[PB94-163029] p 4304 N94-35740

COMPUTER TECHNIQUES
JPRS report: Science and technology. Central Eurasia
[JPRS-UST-94-007] p 4249 N94-35227
Computer image analysis of etched tracks from ionizing radiation
[NASA-CR-196025] p 4319 N94-35264
The weakest failure detector for solving Consensus
[NASA-CR-190545] p 4300 N94-35365
Developing software for ease of change: Metrics from later in the TRALAB system life cycle
[AD-A278759] p 4302 N94-35490
A software architecture for adding new interaction techniques to a command and control based testbed
[AD-A278760] p 4302 N94-35491
General purpose architecture for intelligent computer-aided training
[NASA-CASE-MSC-21381-1] p 4311 N94-35501
Proceedings of the 4th Workshop on the Next Generation of CASE Tools
[PB94-150372] p 4302 N94-35538
Guidelines for design and development of computer/microprocessor based systems in research and power reactors
[DE94-616271] p 4300 N94-35570
Combining symbolic computation and theorem proving: Some problems of Ramanujan
[AD-A278899] p 4303 N94-35573
Implementation of a Computerized Maintenance Management System p 4343 N94-35970
Review of Mathematical Function Library for Microsoft-FORTRAN, John Wiley and Sons, 1989
[PB94-160793] p 4305 N94-36010

COMPUTER VIRUSES
Computer virus information update CIAC-2301
[DE94-011916] p 4308 N94-36236

COMPUTER VISION
Adjustable control station with movable monitors and cameras for viewing systems in robotics and teleoperations
[NASA-CASE-NPO-17837-1-CU] p 4332 N94-35384
The DataCube server. Animate agent project working note 2, version 1.0
[AD-A278847] p 4310 N94-35742

COMPUTERIZED SIMULATION
A review of computer evacuation models and their data needs
[DOT/FAA/AM-94/11] p 4191 N94-35236
Computational methods for HSCT-inlet controls/CFD interdisciplinary research
[NASA-TM-106618] p 4198 N94-35352
Measuring track densities in lunar grains using image analysis p 4357 N94-35409
Software architecture standard for simulation virtual machine, version 2.0
[NASA-CR-188291] p 4301 N94-35443
Development and application of computational aerothermodynamics flowfield computer codes
[NASA-CR-196136] p 4189 N94-35498
A search for radiative neutrino decay from supernovae
[NASA-CR-196011] p 4376 N94-35515
Performance evaluation of digital phase-locked loops for advanced deep space transponders
p 4254 N94-35558
Simulation models for computational plasma physics: Concluding report
[DE94-009976] p 4335 N94-35647
Cramer-von Mises variance estimators for simulations
[AD-A278799] p 4316 N94-35675
A review of radial forging technology including preform design for process optimization
[AD-A278770] p 4250 N94-35711
A triggering mechanism of fast crash in sawtooth oscillation
[DE94-718974] p 4336 N94-35772
BJT model in APLAC
[PB94-171022] p 4259 N94-35822
Computationally efficient multibody simulations
p 4222 N94-35896
Computer simulation of beam-beam effects at large amplitudes and determination of life time
[DE94-616235] p 4330 N94-35999
Object-oriented simulation pictures (OOSPic) for design and testing
[AD-A278798] p 4305 N94-36013
The integrated model development environment
[AD-A278613] p 4308 N94-36250
Error reduction in images with the use of additional information
[AD-A278636] p 4334 N94-36257
Integrated science model for assessment of climate change
[DE94-011758] p 4288 N94-36286
TSAR modeling of a TEM horn and surrounding structure
[DE94-010668] p 4256 N94-36301
SYNTH: A spectrum synthesizer
[DE94-004719] p 4331 N94-36317
Rapid and accurate timing simulation of radiation-hardened digital microelectronics using VHDL
[AD-A278644] p 4261 N94-36361
Computer simulations of benzene in faujasite-type zeolites
[DE94-007533] p 4242 N94-36369
Simulation of materials processing: Fantasy or reality?
p 4230 N94-36404
The analysis of a generic air-to-air missile simulation model
[NASA-TM-109057] p 4309 N94-36438

COMPUTERS
JPRS report: Science and technology. Central Eurasia
[JPRS-UST-94-001] p 4229 N94-35340
JPRS report: Science and technology. Central Eurasia
[JPRS-UST-94-010] p 4250 N94-35385
JPRS report: Science and technology. Central Eurasia
[JPRS-UST-94-011] p 4250 N94-35386
JPRS report: Science and technology. Central Eurasia
[JPRS-UST-94-012] p 4250 N94-35387
Proceedings of the LLNL Technical Women's Symposium
[DE94-006616] p 4379 N94-35997

CONCATENATED CODES
Trace-shortened Reed-Solomon codes
p 4254 N94-35554

CONCENTRIC CYLINDERS
Optimization of residual stresses in MMC's using compensating/compliant interfacial layers. Part 2: OPTCOMP user's guide
[NASA-CR-195337] p 4278 N94-35239

CONCRETES
Aspects of robust computational modeling for plain and reinforced concrete
[PB94-169240] p 4251 N94-35820

CONCURRENT PROCESSING
High level modelling and design of asynchronous interface logic
[PB94-167822] p 4258 N94-35534
Probabilities and priorities in timed CSP
[PB94-169216] p 4316 N94-35536
Mathematical theory of synchronous communication
[PB94-169224] p 4252 N94-35537
A taxonomy of coordination mechanisms used in real-time software based on domain analysis
[AD-A279014] p 4304 N94-35794

CONDENSATES
On the origin of porphyritic chondrules
[DE94-010464] p 4351 N94-36418

CONDENSATION NUCLEI
Anthropogenic sulfate and organic aerosols, CCN, and cloud project concentration at a marine site
[DE94-004210] p 4286 N94-36025

CONDENSED MATTER PHYSICS
Large scale atomistic first principles study of adsorption and surface diffusion
[DE94-009450] p 4322 N94-35682

CONDENSING
First observation of a mass independent isotopic fractionation in a condensation reaction
p 4239 N94-35464

CONDUCTION ELECTRONS
Magnetic metallic multilayers
[DE94-011913] p 4341 N94-36274

CONDUCTIVE HEAT TRANSFER
An adaptive, unstructured, finite-element, multi-material, thermal analysis
[AD-A278632] p 4343 N94-36256

CONDUCTORS
Capillary flow solderability test for printed wiring boards
[DE94-010321] p 4259 N94-36094

CONFERENCES
The Twenty-Fifth Lunar and Planetary Science Conference. Part 1: A-G
[NASA-CR-195743] p 4355 N94-35395
The Twenty-Fifth Lunar and Planetary Science Conference. Part 3: P-Z
[NASA-CR-195745] p 4362 N94-35448
Genetic algorithms
[PB94-171048] p 4303 N94-35602
Flight Mechanics/Estimation Theory Symposium, 1994
[NASA-CP-3265] p 4202 N94-35605
The impact of scaling on a multimedia connection architecture
[AD-A278700] p 4300 N94-35652
Asymetric change of daily temperature range: Proceedings
[DE94-010102] p 4293 N94-35703
Proceedings: Integrated Research Planning Meeting for Gulf of Mexico Estuaries
[PB94-157799] p 4296 N94-35738
AFOSR Contractors Propulsion Meeting
[AD-A279028] p 4198 N94-35746
Technology Reinvestment Project's Focus Area: Low Cost Electronic Packaging
[PB94-161155] p 4259 N94-35748
NIFS Symposium: Toward the research of fusion burning plasmas, present status and future strategy
[DE94-727618] p 4336 N94-35775
Activity report 1990-1992 and proceedings, volume 1
[DE94-610480] p 4290 N94-35830
Second International Symposium on Magnetic Suspension Technology, part 1
[NASA-CP-3247-PT-1] p 4212 N94-35836
Second International Symposium on Magnetic Suspension Technology, part 2
[NASA-CP-3247-PT-2] p 4223 N94-35902
Proceedings of the LLNL Technical Women's Symposium
[DE94-006616] p 4379 N94-35997
Proceedings of the Workshop on the Federal Criteria for Information Technology Security
[PB94-162583] p 4346 N94-36005
Modeling the atmospheric input of nutrients, heavy metals, and pesticides to the Great Lakes
[DE94-005481] p 4286 N94-36007
Activity Report, 1990 - 1992 and proceedings, volume 2
[DE94-610481] p 4291 N94-36087
Natural resources and environmental issues. Volume 1: Riparian Resources: A Symposium on the Disturbances, Management, Economics, and Conflicts Associated with Riparian Ecosystems p 4287 N94-36120
The Twenty-Fifth Lunar and Planetary Science Conference. Part 2: H-O
[NASA-CR-195744] p 4367 N94-36136
Proceedings of the Sixth International Congress on Noise as a Public Heatlh Problem, volume 3
[AD-A278218] p 4319 N94-36176
Third European Technical Symposium on Polyimides and High Performance Polymers: STEPI 3
[PB94-148491] p 4246 N94-36177
Proceedings of the Twenty-First All-Union Conference on Physics of Charged Particles Interaction with Crystals
[DE94-615768] p 4341 N94-36181
Proceedings of 2nd Working Meeting on Physics at VLEPP, volume 2
[DE94-616167] p 4326 N94-36182
Recent Advances in Long Range and Long Endurance Operation of Aircraft
[AGARD-CP-547] p 4193 N94-36321
National Educators' Workshop: Update 1993. Standard Experiments in Engineering Materials Science and Technology
[NASA-CP-3259] p 4229 N94-36398

CONFIGURATION INTERACTION
New anionic states of the lithium trimer
[AD-A278832] p 4323 N94-35797

Anionic and neutral states of Li3O [AD-A278833] p 4323 N94-35798

CONFINEMENT

MHD and confinement characteristics in the high-beta regime on the CHS low-aspect-ratio heliotron/torsatron [DE94-718981] p 4339 N94-36357

CONFORMAL MAPPING

Primordial nucleosynthesis in conformal Weyl gravity [DE94-003002] p 4327 N94-36241

CONICAL SCANNING

Design and implementation of a beam-waveguide mirror control system for vernier pointing of the DSS-13 antenna p 4253 N94-35548

CONSCIOUSNESS

A database to evaluate acceleration (+Gz) induced loss of consciousness (G-LOC) in the human centrifuge [AD-A278769] p 4299 N94-35707

CONSOLES

High-speed digital project, HSD test capability [DE94-010885] p 4260 N94-36197

CONSOLIDATION

Consolidation of zircaloy-4 end crops by induction melting [DE94-010031] p 4240 N94-35650

CONSTRUCTION

Design, construction, and testing of a five active axes magnetic bearing system p 4214 N94-35846

Design and construction of a imaging instrument for studying ion emission from pure ion emitters [DE94-010702] p 4328 N94-36302

Design and construction of a tensile tester for the testing of simple composites p 4230 N94-36401

CONSTRUCTION MATERIALS

Collection, processing, and reporting of damage tolerant design data for non-aerospace structural materials [NASA-CR-196046] p 4347 N94-36435

CONTACT RESISTANCE

Models for interpreting interstrand resistance measurements in Rutherford cables [DE94-010844] p 4259 N94-36194

CONTAMINANTS

Study on contaminants on flight and other critical surfaces [NASA-CR-193975] p 4235 N94-35447

CAirTOX: A compartment model for assessing the fate of and human exposure to toxic-chemical emissions to air [DE94-010084] p 4284 N94-35700

Residual Gas Analysis (RGA) and shear strength characteristics of a silver-filled epoxy and polyimide under long-term, high-temperature storage conditions [DE94-010106] p 4244 N94-35705

Air quality implications associated with the selection of power plants in the Pacific Northwest [DE94-004783] p 4287 N94-36027

CONTAMINATION

Study on contaminants on flight and other critical surfaces [NASA-CR-193975] p 4235 N94-35447

Ionic contamination detection [DE94-010212] p 4258 N94-35686

CAirTOX: A compartment model for assessing the fate of and human exposure to toxic-chemical emissions to air [DE94-010084] p 4284 N94-35700

Residual Gas Analysis (RGA) and shear strength characteristics of a silver-filled epoxy and polyimide under long-term, high-temperature storage conditions [DE94-010106] p 4244 N94-35705

Space-based crystal growth and thermocapillary flow p 4342 N94-35971

Nondestructive Inspection (NDI) of reduced strength bonds [AD-A278745] p 4278 N94-36090

CONTINUOUS RADIATION

High-power CW operation of AlGaInP diode-laser arrays [DE94-010409] p 4272 N94-36115

CONTINUUM MECHANICS

Dynamic analysis of Space Shuttle/RMS configuration using continuum approach p 4221 N94-35887

CONTINUUM MODELING

NASA Workshop on Distributed Parameter Modeling and Control of Flexible Aerospace Systems [NASA-CP-3242] p 4217 N94-35865

Distributed parameter modeling of repeated truss structures p 4218 N94-35868

Dynamic analysis of Space Shuttle/RMS configuration using continuum approach p 4221 N94-35887

Software for continuum modeling of controls-structures interactions p 4223 N94-35898

CONTINUUMS

ROSAT/XRT-PSPC observations and the ionizing continuum of Seyfert 1 galaxy Mkn 478 [PB94-167053] p 4350 N94-35530

CONTRACT MANAGEMENT

Statement by Bill D. Colvin, Inspector General [NASA-TM-109793] p 4348 N94-35446

CONTROL BOARDS

International Space Station alpha remote manipulator system workstation controls test report [NASA-TM-104796] p 4274 N94-35481

Transformation of a Cranz-Schardin camera [PB94-170685] p 4270 N94-36219

CONTROL EQUIPMENT

Design, construction, and testing of a five active axes magnetic bearing system p 4214 N94-35846

CONTROL SIMULATION

In-flight simulation studies at the NASA Dryden Flight Research Facility p 4198 N94-35969

CONTROL STABILITY

Measurement and characterization of force dynamics in high T(sub c) superconductors p 4214 N94-35844

Adaptive model reduction for continuous systems via recursive rational interpolation p 4219 N94-35876

CSI, optimal control, and accelerometers: Trials and tribulations p 4221 N94-35888

Robustness properties of LQG optimized compensators for collocated rate sensors p 4221 N94-35890

Semigroup approximation and robust stabilization of distributed parameter systems p 4222 N94-35894

CONTROL SURFACES

Control of maglev vehicles with aerodynamic and guideway disturbances p 4213 N94-35842

CONTROL SYSTEMS DESIGN

Adjustable control station with movable monitors and cameras for viewing systems in robotics and teleoperations [NASA-CASE-NPO-17837-1-CU] p 4332 N94-35384

International Space Station alpha remote manipulator system workstation controls test report [NASA-TM-104796] p 4274 N94-35481

Robust requirements specifications for safety-critical systems [PB94-167806] p 4250 N94-35532

Design and implementation of a beam-waveguide mirror control system for vernier pointing of the DSS-13 antenna p 4253 N94-35548

Guidelines for design and development of computer/microprocessor based systems in research and power reactors [DE94-616271] p 4300 N94-35570

Second International Symposium on Magnetic Suspension Technology, part 1 [NASA-CP-3247-PT-1] p 4212 N94-35836

Nonlinear control of magnetic bearings p 4213 N94-35838

Measurement and characterization of force dynamics in high T(sub c) superconductors p 4214 N94-35844

Microgravity isolation system design: A modern control synthesis framework p 4215 N94-35851

Fuzzy self-learning control for magnetic servo system p 4215 N94-35852

Implementation of a decoupled controller for a magnetic suspension system using electromagnets mounted in a planar array p 4216 N94-35853

Neural network controller development for a magnetically suspended flywheel energy storage system p 4217 N94-35861

Time-delay control of a magnetic levitated linear positioning system p 4217 N94-35862

NASA Workshop on Distributed Parameter Modeling and Control of Flexible Aerospace Systems [NASA-CP-3242] p 4217 N94-35865

Robust control design techniques for active flutter suppression p 4200 N94-35875

Vibration suppression in flexible structures via the sliding-mode control approach p 4220 N94-35884

Control of the SCOLE configuration using distributed parameter models p 4221 N94-35885

Dynamic analysis of Space Shuttle/RMS configuration using continuum approach p 4221 N94-35887

CSI, optimal control, and accelerometers: Trials and tribulations p 4221 N94-35888

An optimization-based approach for integrated controls-structures design of flexible spacecraft p 4221 N94-35889

CONTROL THEORY

Direct reduced order mixed H2/H infinity control for the Short Take-Off and Landing/Maneuver Technology Demonstrator (STOL/MTD) [AD-A278675] p 4199 N94-35796

Nonlinear control of magnetic bearings p 4213 N94-35838

Control of flexible structures with distributed sensing and processing p 4218 N94-35871

Flutter suppression digital control law design and testing for the AFW wind tunnel model p 4200 N94-35873

Robustness properties of LQG optimized compensators for collocated rate sensors p 4221 N94-35890

LQG optimal compensator transfer function for the NASA LaRC CSI Evolutionary Model p 4221 N94-35891

Semigroup approximation and robust stabilization of distributed parameter systems p 4222 N94-35894

Robust tracking control of a magnetically suspended rigid body p 4225 N94-35913

CONTROL VALVES

Magnetically operated check valve [NASA-CASE-MSC-22046-1] p 4274 N94-35661

CONTROLLABILITY

Direct reduced order mixed H2/H infinity control for the Short Take-Off and Landing/Maneuver Technology Demonstrator (STOL/MTD) [AD-A278675] p 4199 N94-35796

CONTROLLED FUSION

Potential formation and transport in open field line systems [DE94-718910] p 4337 N94-35983

CONTROLLERS

Direct reduced order mixed H2/H infinity control for the Short Take-Off and Landing/Maneuver Technology Demonstrator (STOL/MTD) [AD-A278675] p 4199 N94-35796

Nonlinear control of magnetic bearings p 4213 N94-35838

High performance data acquisition, identification, and monitoring for active magnetic bearings p 4213 N94-35839

Implementation of a decoupled controller for a magnetic suspension system using electromagnets mounted in a planar array p 4216 N94-35853

Neural network controller development for a magnetically suspended flywheel energy storage system p 4217 N94-35861

Time-delay control of a magnetic levitated linear positioning system p 4217 N94-35862

Control of the SCOLE configuration using distributed parameter models p 4221 N94-35885

Integration of magnetic bearings in the design of advanced gas turbine engines p 4223 N94-35903

Rotor dynamic behaviour of a high-speed oil-free motor compressor with a rigid coupling supported on four radial magnetic bearings p 4224 N94-35911

Robust tracking control of a magnetically suspended rigid body p 4225 N94-35913

Analysis of achievable disturbance attenuation in a precision magnetically-suspended motion control system p 4225 N94-35917

Controller for the Electronically Scanned Thinned Array Radiometer (ESTAR) instrument [NASA-TM-104608] p 4259 N94-36049

The iWarp display module [AD-A278610] p 4260 N94-36248

CONVECTION

Interface shape and convection during solidification and melting of succinonitrile [NASA-TM-106487] p 4262 N94-35248

Contributions of the low-latitude boundary layer to the finite width magnetotail convection model [NASA-CR-196116] p 4289 N94-35392

Analysis of mid-tropospheric carbon monoxide data using a three-dimensional global atmospheric chemistry numerical model [DE94-004782] p 4286 N94-36026

Local instabilities and the transition to chaos of non-linear waves [PB94-170578] p 4341 N94-36213

On the physics of waves in the solar atmosphere: Wave heating and wind acceleration [NASA-CR-194119] p 4375 N94-36395

CONVECTIVE HEAT TRANSFER

The aerodynamic and heat transfer effects of an endwall boundary layer fence in a 90 degree turning square duct [AD-A278903] p 4265 N94-35803

CONVERGENCE

Periodized wavelets [DE94-010365] p 4316 N94-36432

COOLING

Fundamental studies in blow-down and cryogenic cooling [AD-A278967] p 4250 N94-35524

Demonstration of a high heat removal CVD diamond substrate edge-cooled multichip module [DE94-010748] p 4260 N94-36245

On the origin of porphyritic chondrules [DE94-010464] p 4351 N94-36418

COORDINATE TRANSFORMATIONS

A simple suboptimal least-squares algorithm for attitude determination with multiple sensors p 4210 N94-35645

COPPER

About mid-infrared optical spectrum of high-Tc superconducting compounds [DE94-615646] p 4340 N94-36030

Continuum fluorescence of Cu in NbTi/Cu composite wires
[DE94-008940] p 4241 N94-36242

COPPER OXIDES
About mid-infrared optical spectrum of high-Tc superconducting compounds
[DE94-615646] p 4340 N94-36030

CORRECTION
Logarithmic corrections of the two-body QED problem
[DE94-611157] p 4322 N94-35783
Collective plasma corrections to the solar opacity
[PB94-170511] p 4375 N94-36210

CORRELATION
Boson spectra and correlations in thermal locally equilibrium systems
[DE94-616799] p 4325 N94-36079
Nondestructive Inspection (NDI) of reduced strength bonds
[AD-A278745] p 4278 N94-36090
Determination of grain boundary volume expansion by HREM
[DE94-010452] p 4241 N94-36231

CORRELATORS
Correlator data analysis for the array feed compensation system p 4253 N94-35553
Baryonic currents and their correlators in the heavy quark effective theory
[DE94-612496] p 4320 N94-35567
Magnetoresistance of films and strips with the diffuse surface scattering
[DE94-611100] p 4340 N94-35933

CORROSION
Residual Gas Analysis (RGA) and shear strength characteristics of a silver-filled epoxy and polyimide under long-term, high-temperature storage conditions
[DE94-010106] p 4244 N94-35705

CORROSION RESISTANCE
JPRS report: Science and technology. Central Eurasia: Materials science
[JPRS-UMS-93-007] p 4240 N94-35517

CORROSION TESTS
Hot Corrosion Test Facility at the NASA Lewis Special Projects Laboratory
[NASA-CR-195323] p 4200 N94-35267

COSMIC BACKGROUND EXPLORER SATELLITE
Astronomy in the region between 1 mm and 0.1 mm wavelength
[NASA-CR-196020] p 4349 N94-36419

COSMIC DUST
Purity and cleanness of aerogel as a cosmic dust capture medium p 4247 N94-35469
Catalog of Helios 90 deg photometer events
[PL-TR-94-2040] p 4375 N94-36264

COSMOCHEMISTRY
Solar proton produced neon in shergottite meteorites p 4351 N94-35428
First observation of a mass independent isotopic fractionation in a condensation reaction p 4239 N94-35464
Stellar alchemy: The origin of the chemical elements
[DE94-011903] p 4350 N94-36229

COSMOLOGY
Primordial nucleosynthesis in conformal Weyl gravity
[DE94-003002] p 4327 N94-36241

COST ANALYSIS
The development and application of composite complexity models and a relative complexity metric in a software maintenance environment p 4255 N94-35559
Final regulatory impact analysis: Refueling emission regulations for light duty vehicles and trucks and heavy duty vehicles
[PB94-164027] p 4285 N94-35754
National Maglev initiative: California line electric utility power system requirements p 4215 N94-35850

COST EFFECTIVENESS
Geostationary space launch vehicles and the US dilemma p 4210 N94-35377
Final regulatory impact analysis: Refueling emission regulations for light duty vehicles and trucks and heavy duty vehicles
[PB94-164027] p 4285 N94-35754

COST ESTIMATES
Cost and schedule estimation study report
[NASA-CR-189344] p 4300 N94-35256
Budget estimates, fiscal year 1995. Volume 1: Agency summary, human space flight, and science, aeronautics and technology
[NASA-TM-109791] p 4347 N94-35899
Budget estimates, fiscal year 1995. Volume 2: Mission support and Inspector General
[NASA-TM-109792] p 4348 N94-35900

COST REDUCTION
The development and application of composite complexity models and a relative complexity metric in a software maintenance environment p 4255 N94-35559
Future ultra-speed tube-flight p 4225 N94-35918

COUETTE FLOW
Spatio-temporal properties of centrifugal instabilities: Abstracts of 8th Couette-Taylor Meeting
[PB94-150240] p 4266 N94-35981

COULOMB COLLISIONS
P-matrix description of charged particles interaction
[DE94-616853] p 4329 N94-36391

COUNTERFLOW
An experimental investigation of active control of thrust vectoring nozzle flow fields
[AD-A278702] p 4229 N94-36291

COUNTING
Fluorescence detection of single molecules using pulsed near-field optical excitation and time correlated photon counting
[DE94-007553] p 4320 N94-35376
A survey of reflectometry techniques with applications to TFTR
[DE94-010202] p 4338 N94-36093

COUPLED MODES
Review of slow-wave structures
[NASA-TM-106639] p 4258 N94-35270

COUPLERS
Thin-ribbon tapered coupler for dielectric waveguides p 4253 N94-35547

COVALENCE
The study of the local magnetic field in the oxide alpha-Bi2O3 by the mu SR-technique
[DE94-612636] p 4322 N94-35751

COVARIANCE
A quick look method of detecting water of hydration in small solar system bodies p 4352 N94-35470
Measuring attitude with a gradiometer p 4206 N94-35630

CRACK PROPAGATION
Investigation of moisture-induced embrittlement of iron aluminides
[DE94-010881] p 4241 N94-36196
Transformation of a Cranz-Schardin camera
[PB94-170685] p 4270 N94-36219

CRACK TIPS
Biaxial loading and shallow-flaw effects on crack-tip constraint and fracture-toughness
[DE94-010128] p 4279 N94-35684

CRACKING (FRACTURING)
Aspects of robust computational modeling for plain and reinforced concrete
[PB94-169240] p 4251 N94-35820

CRACKS
Through-the-thickness tensile strength of textile composites
[NASA-TM-109115] p 4233 N94-35946
Frequency domain analysis of the random loading of cracked panels
[NASA-CR-196021] p 4279 N94-35974

CRANIUM
Effects of 5 MPa heliox pressure on dopaminergic pathway: An in vivo neurochemical study
[PB94-170693] p 4297 N94-36220

CRASHES
Aircraft accident report: Uncontrolled collision with terrain, American International Airways Flight 808, Douglas DC-8-61, N814CK, US Naval Air Station, Guantanamo Bay, Cuba, 18 August 1993
[PB94-910406] p 4192 N94-35521

CRATERING
The surface and interior of Phobos p 4355 N94-35400

CRATERS
The surface and interior of Phobos p 4355 N94-35400
Craters in aluminum 1100 targets using glass projectiles at 1-7 km/s p 4280 N94-35407
Preliminary description of double drive tube 68002/68001 p 4363 N94-35457
Morphology of meteoroid and space debris craters on LDEF metal targets p 4353 N94-36159

CREEP STRENGTH
High temperature creep and oxidation resistant chromium silicide matrix alloy containing molybdenum
[NASA-CASE-LEW-15697-1] p 4241 N94-36275

CRETACEOUS-TERTIARY BOUNDARY
Distribution of siderophile and other trace elements in melt rock at the Chicxulub impact structure p 4352 N94-35456

CRITICAL PATH METHOD
NAVSPACECOM space surveillance sensor system digital signal processing receiver. Volume 4: Hardware interfaces
[AD-A278845] p 4212 N94-35801

CRITICAL VELOCITY
Design, construction, and testing of a five active axes magnetic bearing system p 4214 N94-35846

CROSSLINKING
Concurrent stabilization and imaging of a novel polymer for second harmonic generation via in situ photopolymerization
[AD-A278912] p 4243 N94-35588
Mechanical properties of crosslinked polymer coatings p 4231 N94-36410

CRRES (SATELLITE)
Electron and Proton Wide-Angle Spectrometer (EPAS) on the CRRES spacecraft
[AD-A278630] p 4227 N94-35362

CRUCIBLES
Consolidation of zircaloy-4 end crops by induction melting
[DE94-010031] p 4240 N94-35650

CRUDE OIL
Maglev crude oil pipeline p 4226 N94-35919

CRUSHING
Aspects of robust computational modeling for plain and reinforced concrete
[PB94-169240] p 4251 N94-35820

CRYOGENIC COOLING
Fundamental studies in blow-down and cryogenic cooling
[AD-A278967] p 4250 N94-35524

CRYOGENIC FLUIDS
Fundamental studies in blow-down and cryogenic cooling
[AD-A278967] p 4250 N94-35524

CRYOGENIC TEMPERATURE
Characterization of lithium niobate electro-optic modulators at cryogenic temperatures
[DE94-010059] p 4333 N94-35697

CRYOGENICS
Experimental results of hydrogen slosh in a 62 cubic foot (1750 liter) tank
[NASA-TM-106625] p 4263 N94-35250
Characterization of lithium niobate electro-optic modulators at cryogenic temperatures
[DE94-010059] p 4333 N94-35697
Network analyzer calibration for cryogenic on-wafer measurements
[DE94-010089] p 4262 N94-36430

CRYSTAL DEFECTS
Structures and properties of materials recovered from high shock pressures
[DE94-010057] p 4232 N94-35696
Flux-pinning related defects in YBa2Cu3O(7-x) thin films grown on miscut LaAlO3 (001) substrates
[DE94-011463] p 4342 N94-36377

CRYSTAL GROWTH
Interface shape and convection during solidification and melting of succinonitrile
[NASA-TM-106487] p 4262 N94-35248
On the possible role of elemental carbon in the formation of reduced chondrules p 4351 N94-35421
Computation of dendrites using a phase field model
[PB94-160744] p 4236 N94-35736
Space-based crystal growth and thermocapillary flow p 4342 N94-35971
Application of GaSe and AgGaSe2 crystal growth to non-linear optics
[PB94-170552] p 4341 N94-36212
Flux-pinning related defects in YBa2Cu3O(7-x) thin films grown on miscut LaAlO3 (001) substrates
[DE94-011463] p 4342 N94-36377

CRYSTAL STRUCTURE
Be3(AsO4)2.2H2O, a new berylloarsenate phase containing bridged tetrahedral 3-rings
[AD-A278826] p 4340 N94-35677
Structures and properties of materials recovered from high shock pressures
[DE94-010057] p 4232 N94-35696
A theoretical study of ordering phenomena in K-In and K-Sb molten alloys
[DE94-611103] p 4240 N94-35935
Twin spacing and the structural phase transitions in 1:2:3 high-Tc superconductors
[DE94-615647] p 4340 N94-36041

CRYSTALLINITY
Liquid crystalline thermosetting polyimides
[DE94-009939] p 4244 N94-35768
The growth of silicon nitride crystalline films using microwave plasma enhanced chemical vapor deposition
[AD-A278862] p 4340 N94-35828
Calorimetric thermobarometry of experimentally shocked quartz p 4240 N94-36174

CRYSTALLIZATION
Synthetic and natural Nakhla pyroxenes: Parent melt composition and REE partition coefficients p 4353 N94-36161

Pre-bombardment crystallization ages of basaltic clasts from Antarctic howardites EET87503 and EET87513
p 4354 N94-36172
Irradiation-related amorphization and crystallization: In situ transmission electron microscope studies
[DE94-009823] p 4241 N94-36222
In situ studies of zeolite syntheses using powder diffraction methods: Crystallization of instant zeolite A powder and CoAPO-5
[DE94-006570] p 4341 N94-36358

CRYSTALLOGRAPHY
The relationship between hydroxyl groups on oxide surfaces and the properties of supported metals
[DE94-010786] p 4241 N94-36233

CRYSTALS
A theoretical study of ordering phenomena in K-In and K-Sb molten alloys
[DE94-611103] p 4240 N94-35935
Proceedings of the Twenty-First All-Union Conference on Physics of Charged Particles Interaction with Crystals
[DE94-615768] p 4341 N94-36181
Application of GaSe and AgGaSe2 crystal growth to non-linear optics
[PB94-170552] p 4341 N94-36212

CULTURE TECHNIQUES
Multi-cellular, three-dimensional living mammalian tissue
[NASA-CASE-MSC-21560-2] p 4296 N94-35232
High density cell culture system
[NASA-CASE-MSC-22060-1] p 4296 N94-35366

CURING
Dual cure low-VOC coating process
[DE94-009346] p 4245 N94-35809

CURRENT ALGEBRA
Low energy theorems from the effective Lagrangian with vector mesons
[DE94-611173] p 4322 N94-35785

CURRENT DENSITY
Experimental and theoretical studies of a high temperature cesium-barium tacitron, with application to low voltage-high current inversion
[DE94-008182] p 4228 N94-35349
Study and fabrication of GaSb-based laser heterostructures
[PB94-170677] p 4273 N94-36218
Design and construction of a imaging instrument for studying ion emission from pure ion emitters
[DE94-010702] p 4328 N94-36302

CURRENT SHEETS
Simultaneous observations of the westward electrojet and the cross-tail current sheet during substorms
[AD-A278631] p 4292 N94-36383

CURVATURE
Some theorems on a class of harmonic manifolds
[DE94-611102] p 4315 N94-35934

CURVE FITTING
TransFit: Finite element analysis data fitting software
[NASA-CR-193988] p 4307 N94-36118

CURVED BEAMS
Through-the-thickness tensile strength of textile composites
[NASA-TM-109115] p 4233 N94-35946

CURVES (GEOMETRY)
Height inequality for holomorphic curves
[PB94-167731] p 4314 N94-35762

CYANIDES
Dynamic structural effects and ultrafast biomolecular kinetics in photoinduced charge transfer reactions
[DE94-010421] p 4329 N94-36390

CYCLIC HYDROCARBONS
Anatomy of a cluster IDP. Part 2: Noble gas abundances, trace element geochemistry, isotopic abundances, and trace organic chemistry of several fragments from L2008#5 p 4352 N94-35465

CYCLIC LOADS
Graphing techniques for materials laboratory using Excel p 4232 N94-36414

CYLINDRICAL BODIES
Dielectric measurements of selected ceramics at microwave frequencies p 4232 N94-36412

D

DAMAGE ASSESSMENT
Smart accelerometer --- vibration damage detection
[NASA-CASE-MSC-21951-1] p 4268 N94-35235
Debris/ice/TPS assessment and integrated photographic analysis for Shuttle Mission STS-59
[NASA-TM-109203] p 4211 N94-35523

DAMPING
Third order LPF type compensator for flexible rotor suspension p 4217 N94-35863

DASSAULT AIRCRAFT
In-flight refueling: Dassault Aviation research on the Rafale aircraft p 4196 N94-36341

DATA ACQUISITION
Langley 14- by 22-foot subsonic tunnel test engineer's data acquisition and reduction manual
[NASA-TM-4563] p 4189 N94-35246
Production of long-term global water vapor and liquid water data set using ultra-fast methods to assimilate multi-satellite and radiosonde observations
[NASA-CR-195981] p 4293 N94-35499
A new presentation of complex voltage data for Goldstone radar astronomy p 4255 N94-35561
Data requirements for ceiling and visibility products development
[AD-A278959] p 4293 N94-35720
Multi-window dialogue system of data processing for experimental setup VASSILISSA in PAW environment
[DE94-612439] p 4345 N94-35790
NAVSPACECOM space surveillance sensor system digital signal processing receiver. Volume 3: Operating system functions
[AD-A278839] p 4212 N94-35799
NAVSPACECOM space surveillance sensor system digital signal processing receiver. Volume 4: Hardware interfaces
[AD-A278845] p 4212 N94-35801
Data acquisition systems
[DE94-009848] p 4345 N94-35817
High performance data acquisition, identification, and monitoring for active magnetic bearings
p 4213 N94-35839
Data acquisition system of the GDL facility
[DE94-616604] p 4346 N94-35954
An environment for visualization, reliability, and knowledge acquisition in equational programming
[AD-A278639] p 4308 N94-36258
An automated digital data collection and analysis system for the Charpy Impact Tester p 4232 N94-36415
Three-dimensional force data acquisition and boundary corrections for the Walter H. Beech Memorial 7 x 10 foot low speed wind tunnel
[AR93-2] p 4200 N94-36437

DATA BASE MANAGEMENT SYSTEMS
Fire data management system, FDMS 2.0, technical documentation
[PB94-164019] p 4346 N94-35819
The development of a statistical report software for computer system usages
[DE94-611061] p 4346 N94-35832
Representing spatial information in a computational model for network management
[NASA-CR-191669] p 4306 N94-36040
Application of materials database (MAT.DB.) to materials education p 4230 N94-36402

DATA BASES
Classification of advanced technical ceramics
[REPT-15] p 4243 N94-35335
Data available from birth and death registries and cancer registries in the US
[LBL-30971] p 4344 N94-35337
National Geoscience Data Repository System
[DE94-000120] p 4344 N94-35347
Defense RDT and E online system (DROLS) retrieval reference guide
[AD-A278972] p 4344 N94-35525
Implementation of a low-cost, commercial orbit determination system p 4205 N94-35621
Reformulating query plans for multidatabase systems
[AD-A278688] p 4345 N94-35663
The capacity of color histogram indexing
[AD-A279031] p 4345 N94-35732
Fire data management system, FDMS 2.0, technical documentation
[PB94-164019] p 4346 N94-35819
The development of a statistical report software for computer system usages
[DE94-611061] p 4346 N94-35832
Implementation of a Computerized Maintenance Management System p 4343 N94-35970
Netlib services and resources
[DE94-010307] p 4347 N94-36300
Application of materials database (MAT.DB.) to materials education p 4230 N94-36402
On the origin of porphyritic chondrules
[DE94-010464] p 4351 N94-36418
Collection, processing, and reporting of damage tolerant design data for non-aerospace structural materials
[NASA-CR-196046] p 4347 N94-36435

DATA COMPRESSION
Bit-wise arithmetic coding for data compression
p 4254 N94-35556
The polygon-ellipse method of data compression of weather maps
[AD-A278958] p 4293 N94-35719

DATA CONVERSION ROUTINES
Multi-window dialogue system of data processing for experimental setup VASSILISSA in PAW environment
[DE94-612439] p 4345 N94-35790

DATA FLOW ANALYSIS
Symbolic debugging of globally optimized code: Data value problems and their solutions
[AD-A278898] p 4302 N94-35572

DATA INTEGRATION
Production of long-term global water vapor and liquid water data set using ultra-fast methods to assimilate multi-satellite and radiosonde observations
[NASA-CR-196044] p 4292 N94-35355

DATA LINKS
Field demonstration of X-band photonic antenna remoting in the Deep Space Network
p 4252 N94-35545
The Mars Observer Ka-band link experiment
p 4255 N94-35563
The influence of data link-provided graphical weather on pilot decision-making
[AD-A278871] p 4293 N94-35596
Optimum satellite relay positions with application to a TDRS-1 Indian Ocean relay p 4205 N94-35624
An electronic interface for a fiber optic tethered unmanned underwater vehicle
[AD-A279046] p 4333 N94-35747

DATA MANAGEMENT
Fire data management system, FDMS 2.0, technical documentation
[PB94-164019] p 4346 N94-35819
Application of materials database (MAT.DB.) to materials education p 4230 N94-36402

DATA PROCESSING
Introduction to Neural Networks: Neural Network Workshop for the Hanford Community
[DE94-006526] p 4311 N94-35348
Block distributions on the lunar surface: A comparison between measurements obtained from surface and orbital photography p 4359 N94-35419
Asynchronous optimistic rollback recovery using secure distributed time
[AD-A278978] p 4344 N94-35526
Correlator data analysis for the array feed compensation system p 4253 N94-35553
A new presentation of complex voltage data for Goldstone radar astronomy p 4255 N94-35561
Improved solution accuracy for TDRSS-based TOPEX/Poseidon orbit determination
p 4205 N94-35620
Implementation of a low-cost, commercial orbit determination system p 4205 N94-35621
Intelligent processing of materials, technical activities, 1993 (NAS-NRC Assessment Panel, April 21-22 1994)
[PB94-164183] p 4251 N94-35737
Multi-window dialogue system of data processing for experimental setup VASSILISSA in PAW environment
[DE94-612439] p 4345 N94-35790
Computer Systems Laboratory
[PB94-162518] p 4333 N94-36002
Report on the Workshop on Manufacturing Polymer Composites by Liquid Molding
[PB94-160066] p 4234 N94-36004
Controller for the Electronically Scanned Thinned Array Radiometer (ESTAR) instrument
[NASA-TM-104608] p 4259 N94-36049
Progress in the development of the GMM-2 gravity field model for Mars p 4371 N94-36155
Precise measurement of the left-right cross section asymmetry in Z boson production by electron-positron collisions
[DE94-010751] p 4326 N94-36198
An overview of multichip modules
[AD-A278730] p 4260 N94-36296
Applying observations of work activity in designing prototype data analysis tools
[DE94-010206] p 4347 N94-36297

DATA REDUCTION
Langley 14- by 22-foot subsonic tunnel test engineer's data acquisition and reduction manual
[NASA-TM-4563] p 4189 N94-35246
Reduction procedures for accurate analysis of MSX surveillance experiment data p 4203 N94-35611
Data reduction, analysis and results of LACV-30-07 air cushion vehicle tests, Fort Story, VA, August - September 1993
[AD-A278859] p 4190 N94-35826
Use of wind profiler data in short-range forcasting
[AD-A279482] p 4295 N94-36228
Graphing techniques for materials laboratory using Excel p 4232 N94-36414
Three-dimensional force data acquisition and boundary corrections for the Walter H. Beech Memorial 7 x 10 foot low speed wind tunnel
[AR93-2] p 4200 N94-36437

DATA SMOOTHING
Comparison of Kalman filter and optimal smoother estimates of spacecraft attitude p 4208 N94-35638
TransFit: Finite element analysis data fitting software
[NASA-CR-193988] p 4307 N94-36118

DATA STORAGE
The capacity of color histogram indexing
[AD-A279031] p 4345 N94-35732
DATA STRUCTURES
Runtime support for data parallel tasks
[NASA-CR-194904] p 4300 N94-35240
A lower bound for the intersection of regular forests
[AD-A278653] p 4303 N94-35576
Certification of computational results
p 4306 N94-36064
Experimental evaluation of the certification-trail method p 4306 N94-36065
Certification trails and software design for testability
p 4306 N94-36066
Experimental evaluation of certification trails using abstract data type validation p 4307 N94-36067
Certification trails for data structures
p 4307 N94-36069
Executable transformational rules from Core ELLA to the Kernel
[DRA-MEMO-4629] p 4307 N94-36113
DATA SYSTEMS
The Telecommunications and Data Acquisition Report
[NASA-CR-196117] p 4252 N94-35542
The Atmospheric Radiation Measurement Program and interfaces with external data sources
[DE94-003699] p 4286 N94-36024
Controller for the Electronically Scanned Thinned Array Radiometer (ESTAR) instrument
[NASA-TM-104608] p 4259 N94-36049
Telecommuting (work-at-home) at NASA Lewis Research Center
[NASA-CR-195334] p 4347 N94-36396
DATA TRANSMISSION
Issues in the development of a 10 MBPS K=15 Viterbi decoder
[NASA-CR-196083] p 4211 N94-35357
The rel/REL: A family of reliable multicast protocols for distributed real-time systems
[PB94-167830] p 4310 N94-35535
DAYGLOW
Theoretical and experimental studies relevant to interpretation of auroral emissions
[NASA-CR-196032] p 4376 N94-36421
DC 10 AIRCRAFT
The KDC-10 programme of the Royal Netherlands Air Force p 4197 N94-36346
DEATH
Data available from birth and death registries and cancer registries in the US
[LBL-30971] p 4344 N94-35337
DEBRIS
Debris/ice/TPS assessment and integrated photographic analysis for Shuttle Mission STS-59
[NASA-TM-109203] p 4211 N94-35523
DECAY RATES
Numerical modeling studies of wake vortex transport and evolution within the planetary boundary layer
[NASA-CR-196078] p 4192 N94-35522
Logarithmic corrections of the two-body QED problem
[DE94-611157] p 4322 N94-35783
Measurement of the decay rate of the SiH feature as a function of temperature p 4318 N94-36171
DECISION MAKING
ORDIT: A new methodology to assist in the process of eliciting and modelling organisational requirements
[PB94-167814] p 4345 N94-35533
The influence of data link-provided graphical weather on pilot decision-making
[AD-A278871] p 4293 N94-35596
DECISION THEORY
Maximum-likelihood soft-decision decoding of block codes using the A* algorithm p 4254 N94-35555
Decision and systems analysis for underground storage tank waste retrieval systems and tank waste remediation system
[SAND94-0065] p 4286 N94-35957
DECODING
Maximum-likelihood soft-decision decoding of block codes using the A* algorithm p 4254 N94-35555
DECOMPOSITION
Stopping rules for a class of sampling-based stochastic programming algorithms
[AD-A278654] p 4303 N94-35577
NO decomposition in non-reducing atmospheres
[DE94-011157] p 4237 N94-36036
The thermochemistry and reaction mechanisms in the decomposition of energetic materials
[DE94-011420] p 4248 N94-36376
DEEP SPACE
Performance evaluation of digital phase-locked loops for advanced deep space transponders
p 4254 N94-35558
A 32-GHz solid-state power amplifier for deep space communications p 4255 N94-35562
DEEP SPACE NETWORK
The Telecommunications and Data Acquisition Report
[NASA-CR-196117] p 4252 N94-35542
The Mars Observer differential one-way range demonstration p 4210 N94-35543
Field demonstration of X-band photonic antenna remoting in the Deep Space Network
p 4252 N94-35545
Design and implementation of a beam-waveguide mirror control system for vernier pointing of the DSS-13 antenna p 4253 N94-35548
Use of the sampling theorem to speed up near-field physical optics scattering calculations
p 4253 N94-35549
DSS-13 S-/X-band microwave feed system
p 4253 N94-35550
A closed-loop time-alignment system for baseband combining p 4253 N94-35552
The Mars Observer Ka-band link experiment
p 4255 N94-35563
DEFECTS
The development and application of composite complexity models and a relative complexity metric in a software maintenance environment
p 4255 N94-35559
Biaxial loading and shallow-flaw effects on crack-tip constraint and fracture-toughness
[DE94-010128] p 4279 N94-35684
Defect detection in multi-layered, plasma sprayed zirconia by time resolved infrared radiometry: A comparison between analytical and experimental methods
[DE94-009803] p 4245 N94-35779
DEFENSE PROGRAM
Defense RDT and E online system (DROLS) retrieval reference guide
[AD-A278972] p 4344 N94-35525
NAVSPACECOM space surveillance sensor system digital signal processing receiver. Volume 3: Operating system functions
[AD-A278839] p 4212 N94-35799
DEFORMATION
On the Buckling/Kinking compressive failure of fibrous composites
[AD-A278865] p 4233 N94-35714
Q-deformations of the Veneziano model
[DE94-616769] p 4315 N94-36076
Patterns of brittle deformation under extension on Venus p 4373 N94-36168
Analysis of high speed flow, thermal and structural interactions
[NASA-CR-196017] p 4268 N94-36420
DEGASSING
Ar-39-Ar-40 ages of four ureilites
p 4357 N94-35410
DEGREES OF FREEDOM
Materials for efficient high-flux magnetic bearing actuators p 4214 N94-35845
Six degree of freedom fine motion positioning stage based on magnetic levitation p 4225 N94-35916
DEHYDRATION
The relationship between hydroxyl groups on oxide surfaces and the properties of supported metals
[DE94-010786] p 4241 N94-36233
DEIMOS
The mass of Mars, Phobos, and Deimos, from the analysis of the Mariner 9 and Viking Orbiter tracking data p 4364 N94-35461
DELAMINATING
Through-the-thickness tensile strength of textile composites
[NASA-TM-109115] p 4233 N94-35946
Experimental impacts into Teflon targets and LDEF thermal blankets p 4352 N94-36141
DELAY CIRCUITS
Electronics for the SND scintillation counter system
[DE94-616453] p 4259 N94-36104
DELAY LINES
Switched-beam radiometer front-end network analysis
[NASA-CR-194922] p 4252 N94-35247
Electronics for the SND scintillation counter system
[DE94-616453] p 4259 N94-36104
DELTA FUNCTION
The 2+1-dimensional integrable generalization of the Sine-Gordon equation
[DE94-611074] p 4315 N94-36100
DELTA WINGS
Unsteady structure of leading-edge vortices on a delta wing
[AD-A278988] p 4190 N94-35529
DEMOGRAPHY
Data available from birth and death registries and cancer registries in the US
[LBL-30971] p 4344 N94-35337
DENDRITIC CRYSTALS
Computation of dendrites using a phase field model
[PB94-160744] p 4236 N94-35736
DENSITY DISTRIBUTION
Computer image analysis of etched tracks from ionizing radiation
[NASA-CR-196025] p 4319 N94-35264
On the theory of bounded many-particle systems with purely coulomb interactions
[DE94-617215] p 4325 N94-36081
DEOXYRIBONUCLEIC ACID
Synthesis of novel composite Platinum-DNA films by way of wet-spinning
[AD-A278763] p 4243 N94-35494
Numerical simulation of shock interaction with above-ground structures
[AD-A278713] p 4279 N94-35949
DEPLOYMENT
Attitude stability of a spinning spacecraft during appendage deployment/retraction p 4208 N94-35639
DEPOLARIZATION
A quark model of bar Lambda production in bar Rho interactions
[DE94-008071] p 4324 N94-35824
DEPOSITION
A novel method for depositing precious metal films on difficult surfaces
[NASA-TM-106607] p 4243 N94-35260
Microstructural development in solution derived PZT thin films
[DE94-008744] p 4246 N94-36209
The relationship between hydroxyl groups on oxide surfaces and the properties of supported metals
[DE94-010786] p 4241 N94-36233
High temperature heterojunction bipolar transistors
[AD-A278605] p 4261 N94-36360
DERIVATION
Periodized wavelets
[DE94-010365] p 4316 N94-36432
DESICCANTS
Sealed tube comparisons of the compatibility of desiccants with refrigerants and lubricants
[DE94-010002] p 4251 N94-36388
DESIGN ANALYSIS
Optimization of residual stresses in MMC's using compensating/compliant interfacial layers. Part 2: OPTCOMP user's guide
[NASA-CR-195337] p 4278 N94-35239
Measuring and assessing maintainability at the end of high level design p 4301 N94-35438
Impacts of object-oriented technologies: Seven years of SEL studies p 4301 N94-35439
Monolith catalysts for closed-cycle carbon dioxide lasers
[NASA-CR-196093] p 4271 N94-35489
Issues in the design and optimization of adaptive optics and laser guide stars for the Keck Telescopes
[DE94-009384] p 4349 N94-35565
Simulation of materials processing: Fantasy or reality?
p 4230 N94-36404
DESORPTION
Design of a high activity and selectivity alcohol catalyst
[DE94-003633] p 4237 N94-36023
DESTRUCTIVE TESTS
Nondestructive Inspection (NDI) of reduced strength bonds
[AD-A278745] p 4278 N94-36090
DESYNCHRONIZATION (BIOLOGY)
Some solutions to reduce the human effects of extended operation times p 4196 N94-36339
DETECTION
A quick look method of detecting water of hydration in small solar system bodies p 4352 N94-35470
Ionic contamination detection
[DE94-010212] p 4258 N94-35686
Nondestructive Inspection (NDI) of reduced strength bonds
[AD-A278745] p 4278 N94-36090
DETERMINANTS
Generalized Fredholm determinants and Selberg zeta functions for axiom A dynamical systems
[PB94-167665] p 4314 N94-35758
DETONATION WAVES
Experimental studies of very-high Mach number hydrodynamics
[AD-A278761] p 4263 N94-35492
DEUTERIDES
Dissociative recombination of stored and phase-spaced cooled molecular ions in CRYRING
[DE94-002459] p 4327 N94-36267
DEUTERIUM
A two-dimensional model for collisional energy transfer in bimolecular ion-molecule dynamics
[AD-A278913] p 4321 N94-35589
Electrical conductivity of hydrogen shocked to megabar pressures
[DE93-019632] p 4238 N94-36237

Dissociative recombination of stored and phase-spaced cooled molecular ions in CRYRING
[DE94-002459] p 4327 N94-36267

DIAMINES
Addition polyimides with enhanced processability
[NASA-CASE-LEW-15043-1] p 4242 N94-35234

DIAMOND FILMS
Demonstration of a high heat removal CVD diamond substrate edge-cooled multichip module
[DE94-010748] p 4260 N94-36245
Experiments in diamond film fabrication in table-top plasma apparatus p 4231 N94-36411

DIAMONDS
JPRS report: Science and technology. Central Eurasia: Materials science
[JPRS-UMS-93-007] p 4240 N94-35517

DIATOMIC GASES
Molecular nitrogen fluorescence lidar for remote sensing of the auroral ionosphere
[AD-A280716] p 4291 N94-36263

DIATOMIC MOLECULES
Periodicity and peculiarity in 120 first and second row diatomic molecules
[AD-A278836] p 4323 N94-35793

DICHLORIDES
Structural investigations of 1-ethyl-3-methylimidazolium hydrogen dichloride: Neutron diffraction studies of an ambient-temperature molten salt
[DE94-009680] p 4237 N94-35777

DIELECTRIC PERMEABILITY
JPRS report: Science and technology. Central Eurasia: Space
[JPRS-USP-94-001] p 4201 N94-35518

DIELECTRIC PROPERTIES
The nucleon-nucleon potential in the chromodielectric soliton model
[DE94-004646] p 4329 N94-36305

DIELECTRICS
Review of slow-wave structures
[NASA-TM-106639] p 4258 N94-35270
Thin-ribbon tapered coupler for dielectric waveguides
p 4253 N94-35547
Dielectric measurements of selected ceramics at microwave frequencies p 4232 N94-36412

DIESEL ENGINES
Durability testing of medium speed diesel engine components designed for operating on coal/water slurry fuel
[DE94-009550] p 4275 N94-35667
Bus application of oxygen-enrichment technology and diesel-electric hybrid systems
[DE94-009835] p 4285 N94-35765
Design and operation of a medium speed 12-cylinder coal-fueled diesel engine. Phase 2: Improvements
[DE94-009547] p 4275 N94-35815
Capillary column GC-MS/MS confirmation of phosphate esters with a hybrid tandem mass spectrometer
[AD-A278748] p 4238 N94-36091
Coal-fueled diesels for modular power generation
[DE94-002960] p 4275 N94-36348
Effects of natural gas composition on ignition delay under diesel conditions
[DE94-006405] p 4276 N94-36378

DIESEL FUELS
The effect of alternative fuels on the stability and lubricity of crankcase lubricants
[DE94-010353] p 4245 N94-36108

DIFFERENTIAL CALCULUS
A collection of tools in support of automatic differentiation
[DE94-010104] p 4314 N94-35704
Quantum groups, non-commutative differential geometry and applications
[DE94-011358] p 4315 N94-36270

DIFFERENTIAL EQUATIONS
Description and use of LSODE, the Livermore Solver for Ordinary Differential Equations
[NASA-RP-1327] p 4313 N94-35259

DIFFERENTIAL GEOMETRY
Quantum groups, non-commutative differential geometry and applications
[DE94-011358] p 4315 N94-36270

DIFFRACTION PATTERNS
Method and apparatus for removing unwanted reflections from an interferometer
[NASA-CASE-NPO-18478-1-CU] p 4333 N94-35749
The structural changes of water ice I during warmup
p 4239 N94-36144

DIFFUSION
Diffusion and sorption of 1,4-dioxane into polychloroprene
[ARL-TR-338] p 4229 N94-35361
Hydrodynamics of maneuvering bodies: LDRD Final Report
[DE94-009970] p 4265 N94-35769
ONED90: 1-dimensional diffusion code
[DE94-611063] p 4305 N94-35834
Magnetoresistance of films and strips with the diffuse surface scattering
[DE94-611100] p 4340 N94-35933
A theoretical study of ordering phenomena in K-In and K-Sb molten alloys
[DE94-611103] p 4240 N94-35935

DIFFUSION COEFFICIENT
Diffusion and sorption of 1,4-dioxane into polychloroprene
[ARL-TR-338] p 4229 N94-35361

DIFFUSION FLAMES
Detailed studies of soot formation in laminar diffusion flames for application to modeling studies
[AD-A278941] p 4235 N94-35604
Comparison of PDF and moment closure methods in the modeling of turbulent reacting flows
[NASA-TM-106614] p 4265 N94-35948

DIFFUSIVITY
Analysis of current diffusive ballooning mode
[DE94-718992] p 4336 N94-35811

DIGITAL DATA
An automated digital data collection and analysis system for the Charpy Impact Tester p 4232 N94-36415

DIGITAL ELECTRONICS
High-speed digital project, HSD test capability
[DE94-010885] p 4260 N94-36197

DIGITAL SIMULATION
The application of fuzzy logic to SAFOR in SIMNET
[AD-A279058] p 4312 N94-35730

DIGITAL SYSTEMS
Beam tests of a prototype level-1 calorimeter trigger for LHC experiments
[PB94-170495] p 4269 N94-35599
Synthesis of asynchronous systems from data flow specifications
[AD-A278687] p 4303 N94-35662
Flutter suppression digital control law design and testing for the AFW wind tunnel model p 4200 N94-35873
North American ISDN Users' Forum agreements on Integrated Services Digital Network
[PB94-162559] p 4305 N94-35940
Digital control programmer for temperature control
[DE94-615584] p 4309 N94-36382

DIGITAL TECHNIQUES
Lunar mineral feedstocks from rocks and soils: X-ray digital imaging in resource evaluation
p 4358 N94-35415
NAVSPACECOM space surveillance sensor system digital signal processing receiver. Volume 3: Operating system functions
[AD-A278839] p 4212 N94-35799
Petrographic characterization of lunar soils: Application of x ray digital-imaging to quantitative and automated analysis p 4368 N94-36138

DIMENSIONAL ANALYSIS
Craters in aluminum 1100 targets using glass projectiles at 1-7 km/s p 4280 N94-35407
Inhomogeneous distribution of materials in lodranites-acapulcoites and IAB irons and their common formation processes p 4364 N94-35463

DIODES
High power diode laser Master Oscillator-Power Amplifier (MOPA)
[NASA-CR-196095] p 4271 N94-35488
900-mW average power and tunability from a diode-pumped 2.94 micron Er:YAG oscillator
[DE94-009511] p 4271 N94-35679

DIPOLE MOMENTS
Limitation on the magnetic dipole moment of the reactor neutrino
[DE94-611171] p 4320 N94-35566

DIRAC EQUATION
Zero modes of the two-dimensional Dirac operator on a noncompact Riemann surface in an external magnetic field
[DE94-616618] p 4343 N94-36071

DIRECTIONAL CONTROL
Wind tunnel measurements on a full-scale F/A-18 with a tangentially blowing slot --- conducted in the Ames 80 by 120 foot wind tunnel p 4191 N94-35965

DISCOVERY (ORBITER)
STS-51 Space Shuttle Mission Report
[NASA-TM-109866] p 4211 N94-35252

DISCRIMINATORS
Method and apparatus for removing unwanted reflections from an interferometer
[NASA-CASE-NPO-18478-1-CU] p 4333 N94-35749

DISPLACEMENT
Superconducting rebalance acceleration and rate sensor p 4223 N94-35904

DISPLAY DEVICES
Mechanical properties of crosslinked polymer coatings
p 4231 N94-36410

DISSIPATION
Thick film fabrication of aluminum nitride microcircuits
[DE94-010107] p 4259 N94-35706
Taking into account dissipative processes in relativistic superfluid systems
[DE94-617391] p 4267 N94-36313
On the physics of waves in the solar atmosphere: Wave heating and wind acceleration
[NASA-CR-194119] p 4375 N94-36395

DISSOCIATION
Dissociative recombination of stored and phase-spaced cooled molecular ions in CRYRING
[DE94-002459] p 4327 N94-36267

DISTANCE
Accommodation during instrument viewing can be influenced by knowledge of object distance
[AD-A278987] p 4298 N94-35528

DISTANCE MEASURING EQUIPMENT
High-sensitivity receiver for increasing multiplicity of measurement axes of Zygo's Heterodyne interferometer
[DE94-009916] p 4333 N94-35818

DISTRIBUTED PARAMETER SYSTEMS
NASA Workshop on Distributed Parameter Modeling and Control of Flexible Aerospace Systems
[NASA-CP-3242] p 4217 N94-35865
Distributed parameter modelling of flexible spacecraft: Where's the beef? p 4217 N94-35866
Control of flexible structures with distributed sensing and processing p 4218 N94-35871
Advances in parameter estimation techniques applied to flexible structures p 4219 N94-35877
Semigroup approximation and robust stabilization of distributed parameter systems p 4222 N94-35894
Transfer function modeling of damping mechanisms in distributed parameter models p 4222 N94-35895

DISTRIBUTED PROCESSING
The weakest failure detector for solving Consensus
[NASA-CR-190545] p 4300 N94-35365
The rel/REL: A family of reliable multicast protocols for distributed real-time systems
[PB94-167830] p 4310 N94-35535
Mathematical theory of synchronous communication
[PB94-169224] p 4252 N94-35537
Large granularity cache coherence for intermittent connectivity
[AD-A278897] p 4345 N94-35571
Reformulating query plans for multidatabase systems
[AD-A278688] p 4345 N94-35663
The DataCube server. Animate agent project working note 2, version 1.0
[AD-A278847] p 4310 N94-35742
The most abstract common refinement
[AD-A278870] p 4305 N94-36014

DISTRIBUTION FUNCTIONS
A new association-model for binary VLE of alcohol/hydrocarbon and amine/hydrocarbon mixtures
[DE94-011012] p 4248 N94-36034
QCD parametrizations of the parton distribution of deep inelastic scattering
[DE94-616660] p 4325 N94-36074
Modelling of the structure and physical properties of simple disordered systems
[DE94-617087] p 4329 N94-36311

DIURNAL VARIATIONS
Particulate and gaseous organic receptor modeling for the Southern California Air Quality Study
[PB94-156700] p 4285 N94-35735

DIVERGENCE
Dynamic stability of maglev systems
[DE94-010451] p 4276 N94-36433

DIVERTERS
LHD helical divertor
[DE94-727626] p 4336 N94-35752
Applications of non-resonant RF forces for improvement of tokamak reactor performances. Part 1: Application of ponderomotive force
[DE94-718994] p 4336 N94-35813
Atomic physics and radiation processes in plasmas
[DE94-727617] p 4337 N94-35939
Potential formation and transport in open field line systems
[DE94-718910] p 4337 N94-35983
Design study of LHD helical divertor and high temperature divertor plasma operation
[DE94-718975] p 4338 N94-36352

DIVING (UNDERWATER)
Effects of 5 MPa heliox pressure on dopaminer gic pathway: An in vivo neurochemical study
[PB94-170693] p 4297 N94-36220

DOPED CRYSTALS
X ray radiographic imaging of hydrodynamic phenomena in radiation driven materials: Shock propagation and shear flow
[DE94-010891] p 4318 N94-36201

DOPPLER RADAR
Doppler weather radar studies of precipitation systems
[AD-A279417] p 4295 N94-36262
DOSAGE
Bounding the total-dose response of modern bipolar transistors
[DE94-007742] p 4261 N94-36371
DOWN-CONVERTERS
A 1- to 10-GHz downconverter for high-resolution microwave survey p 4253 N94-35551
DOWNLINKING
Optimum satellite relay positions with application to a TDRS-1 Indian Ocean relay p 4205 N94-35624
DRIFT RATE
A long-baseline method for HST gyro drift rate bias calibration p 4203 N94-35614
DROPS (LIQUIDS)
Anthropogenic sulfate and organic aerosols, CCN, and cloud project concentration at a marine site
[DE94-004210] p 4286 N94-36025
DRUGS
Some solutions to reduce the human effects of extended operation times p 4196 N94-36339
DUCTED FLOW
The aerodynamic and heat transfer effects of an endwall boundary layer fence in a 90 degree turning square duct
[AD-A278903] p 4265 N94-35803
DUCTILITY
Transformation plasticity in ductile solids
[DE94-010420] p 4240 N94-35953
Investigation of moisture-induced embrittlement of iron aluminides
[DE94-010881] p 4241 N94-36196
DUCTS
Thermal performance of residential duct systems in basements
[LBL-33962] p 4250 N94-35364
The aerodynamic and heat transfer effects of an endwall boundary layer fence in a 90 degree turning square duct
[AD-A278903] p 4265 N94-35803
DURABILITY
Testing of the fracture resistance of rails
p 4279 N94-35353
Durability testing of medium speed diesel engine components designed for operating on coal/water slurry fuel
[DE94-009550] p 4275 N94-35667
Aspects of robust computational modeling for plain and reinforced concrete
[PB94-169240] p 4251 N94-35820
Collection, processing, and reporting of damage tolerant design data for non-aerospace structural materials
[NASA-CR-196046] p 4347 N94-36435
DUST
Atmospheric effects on the mapping of Martian thermal inertia and thermally derived albedo
p 4368 N94-36137
DYNAMIC CHARACTERISTICS
Rotor dynamic behaviour of a high-speed oil-free motor compressor with a rigid coupling supported on four radial magnetic bearings p 4224 N94-35911
Acoustical-optical fracture analysis
[PB94-170602] p 4279 N94-36216
DYNAMIC CONTROL
Some further developments in the dynamic modelling and control of the large angle magnetic suspension test fixture p 4217 N94-35860
Control of flexible structures with distributed sensing and processing p 4218 N94-35871
An overview of recent advances in system identification p 4220 N94-35880
Computationally efficient multibody simulations
p 4222 N94-35896
DYNAMIC LOADS
Hydrodynamically induced loads on components submerged in high-level waste-storage tanks
[DE94-009663] p 4264 N94-35756
DYNAMIC MODELS
Dynamic and thermal turbulent time scale modelling for homogeneous shear flows
[NASA-TM-106635] p 4263 N94-35253
An information model for use in software management estimation and prediction p 4301 N94-35437
Motion models in attitude estimation
p 4210 N94-35646
Some further developments in the dynamic modelling and control of the large angle magnetic suspension test fixture p 4217 N94-35860
DYNAMIC PRESSURE
Method for making a dynamic pressure sensor and a pressure sensor made according to the method
[NASA-CASE-LAR-14029-1] p 4269 N94-35369
Structures and properties of materials recovered from high shock pressures
[DE94-010057] p 4232 . N94-35696
DYNAMIC RESPONSE
Evaluating the dynamic response of in-flight thrust calculation techniques during throttle transients
[NASA-TM-4591] p 4193 N94-35241
DYNAMIC STABILITY
Dynamic stability of maglev systems
[DE94-010451] p 4276 N94-36433
DYNAMIC STRUCTURAL ANALYSIS
Transfer function modeling of damping mechanisms in distributed parameter models p 4222 N94-35895
Frequency domain analysis of the random loading of cracked panels
[NASA-CR-196021] p 4279 N94-35974
Analysis of high speed flow, thermal and structural interactions
[NASA-CR-196017] p 4268 N94-36420
Alleviation of whirl-flutter on a joined-wing tilt-rotor aircraft configuration using active controls
[NASA-CR-196103] p 4200 N94-36436
DYNAMICAL SYSTEMS
Generalized Fredholm determinants and Selberg zeta functions for axiom A dynamical systems
[PB94-167665] p 4314 N94-35758
A case study in nonlinear dynamics and control of articulated spacecraft: The Space Station Freedom with a mobile remote manipulator system
p 4220 N94-35879
CSI, optimal control, and accelerometers: Trials and tribulations p 4221 N94-35888
Computationally efficient multibody simulations
p 4222 N94-35896
Numerical methods for multibody systems
p 4222 N94-35897
DYNODES
Ultrafast readout of scintillating fibers using upgraded position-sensitive photomultipliers
[DE94-010419] p 4269 N94-36095

E

EARPHONES
Attention and signal detection. A study of attention divided between visual and auditory signals
[PB94-170594] p 4298 N94-36215
EARTH CRUST
NASA Space Geodesy Program: GSFC data analysis, 1993. VLBI geodetic results 1979 - 1992
[NASA-TM-104605] p 4281 N94-35261
EARTH IONOSPHERE
Electromagnetic measurements of the ionosphere at the ionospheric station of Rome
[AD-A278991] p 4290 N94-35744
Natural orbital environment definition guidelines for use in aerospace vehicle development
[NASA-TM-4527] p 4291 N94-36175
Molecular nitrogen fluorescence lidar for remote sensing of the auroral ionosphere
[AD-A280716] p 4291 N94-36263
EARTH MAGNETOSPHERE
Electron and Proton Wide-Angle Spectrometer (EPAS) on the CRRES spacecraft
[AD-A278630] p 4227 N94-35362
ULF waves in the low-latitude boundary layer and their relationship to magnetospheric pulsations: A multisatellite observation
[AD-A278906] p 4289 N94-35587
Collisonless dynamics of the magnetosphere
[AD-A278886] p 4290 N94-35708
Spatial fluctuations of particle fluxes within the auroral zone inferred from the Intercosmos-Bulgaria-1300 satellite data
[DE94-615858] p 4350 N94-36128
EARTH MANTLE
Alkali element constraints on Earth-Moon relations
p 4354 N94-36169
EARTH MOVEMENTS
Earthquake Engineering Research Center: 25th anniversry edition
[PB94-160645] p 4291 N94-36019
EARTH OBSERVATIONS (FROM SPACE)
Mission to Planet Earth. The living ocean: Observing ocean color from space
[NASA-PAM-554] p 4295 N94-35343
EARTH OBSERVING SYSTEM (EOS)
Insight to global change: EOS/SAR mission
[NASA-CR-196133] p 4284 N94-35503
Improved solution accuracy for Landsat-4 (TDRSS-user) orbit determination p 4205 N94-35623
TDRSS Onboard Navigation System (TONS) flight qualification experiment p 4206 N94-35625
Earth Observing System (EOS) Advanced Microwave Sounding Unit-A (AMSU-A) schedule plan
[NASA-CR-194856] p 4281 N94-35734
EARTH ORBITAL ENVIRONMENTS
Results from LDEF experiment A0114: The interaction of atomic oxygen with materials surfaces at orbital altitudes
[NASA-CR-196016] p 4235 N94-35388
Current activities and results of the Long Duration Exposure Facility Meteoroid and Debris Special Investigation Group p 4352 N94-35458
Experimental impacts into Teflon targets and LDEF thermal blankets p 4352 N94-36141
Dust evolution from comets and asteroids: Their velocities at Earth orbit intersection
p 4352 N94-36142
Natural orbital environment definition guidelines for use in aerospace vehicle development
[NASA-TM-4527] p 4291 N94-36175
Theoretical and experimental studies relevant to interpretation of auroral emissions
[NASA-CR-196032] p 4376 N94-36421
EARTH ORBITS
High Earth orbit design for lunar assisted small Explorer class missions p 4202 N94-35608
Overview of the MSTI 2 on-orbit alignment
p 4206 N94-35629
Evaluation of semiempirical atmospheric density models for orbit determination applications
p 4208 N94-35636
Filter parameter tuning analysis for operational orbit determination support p 4208 N94-35637
EARTH RESOURCES
Natural resources and environmental issues. Volume 1: Riparian Resources: A Symposium on the Disturbances, Management, Economics, and Conflicts Associated with Riparian Ecosystems p 4287 N94-36120
Environmental resource document for the Idaho National Engineering Laboratory, volume 1
[DE94-008522] p 4287 N94-36207
Environmental resource document for the Idaho National Engineering Laboratory, volume 2
[DE94-008523] p 4287 N94-36208
EARTH ROTATION
NASA Space Geodesy Program: GSFC data analysis, 1993. VLBI geodetic results 1979 - 1992
[NASA-TM-104605] p 4281 N94-35261
EARTH SCIENCES
JPRS report: Science and technology. Central Eurasia
[JPRS-UST-94-006] p 4249 N94-35226
JPRS report: Science and technology. Central Eurasia
[JPRS-UST-94-007] p 4249 N94-35227
JPRS report: Science and technology. Central Eurasia
[JPRS-UST-94-008] p 4249 N94-35228
JPRS report: Science and technology. Central Eurasia
[JPRS-UST-94-001] p 4229 N94-35340
JPRS report: Science and technology. Central Eurasia
[JPRS-UST-94-004] p 4249 N94-35341
JPRS report: Science and technology. Central Eurasia
[JPRS-UST-94-005] p 4249 N94-35342
JPRS report: Science and technology. Central Eurasia
[JPRS-UST-94-012] p 4250 N94-35387
Research and technology, 1993
[NASA-TM-108816] p 4380 N94-36117
EARTH-MOON SYSTEM
Galileo Earth/Moon 1 encounter
[NASA-CR-195545] p 4367 N94-35508
Alkali element constraints on Earth-Moon relations
p 4354 N94-36169
EARTHQUAKES
Isotopic and geochemical precursors of earthquakes and volcanic eruptions
[DE94-615824] p 4289 N94-35568
Center for seismic studies
[AD-A278682] p 4290 N94-35693
Activity report 1990-1992 and proceedings, volume 1
[DE94-610480] p 4290 N94-35830
Earthquake Engineering Research Center: 25th anniversry edition
[PB94-160645] p 4291 N94-36019
Activity Report, 1990 - 1992 and proceedings, volume 2
[DE94-610481] p 4291 N94-36087
ECLIPTIC
Catalog of Helios 90 deg photometer events
[PL-TR-94-2040] p 4375 N94-36264
ECOLOGY
Proceedings: Integrated Research Planning Meeting for Gulf of Mexico Estuaries
[PB94-157799] p 4296 N94-35738
Environmental Monitoring and Assessment Program assessment framework
[PB94-158862] p 4285 N94-35741
Environmental resource document for the Idaho National Engineering Laboratory, volume 1
[DE94-008522] p 4287 N94-36207
Environmental resource document for the Idaho National Engineering Laboratory, volume 2
[DE94-008523] p 4287 N94-36208

ECONOMIC IMPACT
Women as a resource for the flexibility required for high technology innovation p 4348 N94-35966

ECOSYSTEMS
Endangered and potentially endangered wildlife on John F. Kennedy Space Center and faunal integrity as a goal for maintaining biological diversity [NASA-TM-109204] p 4288 N94-36422

EDDY CURRENTS
Experimental measurement and calculation of losses in planar radial magnetic bearings p 4214 N94-35847
Models for interpreting interstrand resistance measurements in Rutherford cables [DE94-010844] p 4259 N94-36194

EDUCATION
Space educators' handbook [NASA-TM-109779] p 4343 N94-35339
General purpose architecture for intelligent computer-aided training [NASA-CASE-MSC-21381-1] p 4311 N94-35501
Mentoring for 2000 and beyond p 4343 N94-35964
Building on the foundation for an engineering career p 4343 N94-35973
National Educators' Workshop: Update 1993. Standard Experiments in Engineering Materials Science and Technology [NASA-CP-3259] p 4229 N94-36398
Application of materials database (MAT.DB.) to materials education p 4230 N94-36402
Laminated thermoplastic composite material from recycled high density polyethylene p 4230 N94-36403
Using experimental design modules for process characterization in manufacturing/materials processes laboratories p 4230 N94-36405
Microscale synthesis and characterization of polystyrene: NSF-POLYED scholars project p 4231 N94-36408
Experiments in diamond film fabrication in table-top plasma apparatus p 4231 N94-36411
Graphing techniques for materials laboratory using Excel p 4232 N94-36414

EIGENVECTORS
P-matrix description of charged particles interaction [DE94-616853] p 4329 N94-36391

EJECTA
Preliminary description of double drive tube 68002/68001 p 4363 N94-35457

ELASTIC BODIES
Active vibration damping using smart material p 4221 N94-35886
An energy method approach to the problem of elastic strip [PB94-171014] p 4279 N94-36000

ELASTIC DEFORMATION
An energy method approach to the problem of elastic strip [PB94-171014] p 4279 N94-36000

ELASTIC PROPERTIES
Optimization of residual stresses in MMC's using compensating/compliant interfacial layers. Part 2: OPTCOMP user's guide [NASA-CR-195337] p 4278 N94-35239
Applying transfer matrix method to the estimation of the modal characteristics of the NASA Mini-Mass Truss p 4218 N94-35870

ELASTIC SCATTERING
Limitation on the magnetic dipole moment of the reactor neutrino [DE94-611171] p 4320 N94-35566
SCATTER program of cross section calculation of the hadron and lepton interactions with nuclei [DE94-617006] p 4326 N94-36134
Elastic p(4)He scattering at intermediate energies [DE94-618544] p 4328 N94-36287
P-matrix description of charged particles interaction [DE94-616853] p 4329 N94-36391

ELASTIC WAVES
Plane shock generator explosive lens: Shock characterization of 4340 and PH13-8Mo steels, C360 brass and PZT 65/35 ferro-electric ceramic [DE94-009254] p 4266 N94-35979

ELASTOPLASTICITY
Optimization of residual stresses in MMC's using compensating/compliant interfacial layers. Part 2: OPTCOMP user's guide [NASA-CR-195337] p 4278 N94-35239

ELECTRIC CONDUCTORS
On optimal placement of spacers in bundled conductors p 4258 N94-35354

ELECTRIC CONNECTORS
Separation tool for multipin electrical connectors [NASA-CASE-NPO-18786-1-CU] p 4274 N94-35375

ELECTRIC CONTACTS
Au/Zn contacts to Rho-InP: Electrical and metallurgical characteristics and the relationship between them [NASA-TM-106590] p 4281 N94-35271
Non-alloyed, refractory metal contact optimization with shallow implantations of Zn and Mg [DE94-010392] p 4240 N94-36110

ELECTRIC CURRENT
Influence of an externally modulated photonic link on a microwave communications system p 4252 N94-35544

ELECTRIC DISCHARGES
Kinetics studies following state-selective laser excitation [DE94-010305] p 4330 N94-36105

ELECTRIC FIELDS
Thickness of the layer of strong radial electric field in JFT-2M H-mode plasmas [DE94-718993] p 4336 N94-35812
Neoclassical current and related MHD stability, gap modes, and radial electric field effects in heliotron and torsatron plasmas [DE94-718987] p 4337 N94-35938
Improved models of beta-limit, anomalous transport and radial electric field with loss cone loss in heliotron/torsatron [DE94-718976] p 4324 N94-35984
Spatial fluctuations of particle fluxes within the auroral zone inferred from the Intercosmos-Bulgaria-1300 satellite data *[DE94-615858]* *p 4350* *N94-36128*
ILSE combiner study [DE94-011009] p 4331 N94-36202
Further studies of 60-Hz exposure effects on human function [DE94-010192] p 4297 N94-36223
Kinetic theory of runaway air breakdown and the implications for lightning initiation [DE94-001683] p 4295 N94-36240
Modelling of ELMs and dynamic responses of the H-mode [DE94-718977] p 4339 N94-36353
Dielectric measurements of selected ceramics at microwave frequencies p 4232 N94-36412

ELECTRIC MOTOR VEHICLES
Research and development of Proton-Exchange Membrane (PEM) fuel cell system for transportation applications: Initial conceptual design report [DE94-010576] p 4283 N94-36243

ELECTRIC MOTORS
Experimental measurement and calculation of losses in planar radial magnetic bearings p 4214 N94-35847

ELECTRIC POTENTIAL
Experimental and theoretical studies of a high temperature cesium-barium tacitron, with application to low voltage-high current inversion [DE94-008182] p 4228 N94-35349
A new presentation of complex voltage data for Goldstone radar astronomy p 4255 N94-35561
Characterization of lithium niobate electro-optic modulators at cryogenic temperatures [DE94-010059] p 4333 N94-35697
Elastic p(4)He scattering at intermediate energies [DE94-618544] p 4328 N94-36287

ELECTRIC POWER TRANSMISSION
National Maglev initiative: California line electric utility power system requirements p 4215 N94-35850

ELECTRIC PROPULSION
Theory and computation of optimal low- and medium-thrust transfers [NASA-CR-196077] p 4202 N94-35487
Recovery of frozen flow losses in arcjets [AD-A278739] p 4228 N94-36089

ELECTRIC ROCKET ENGINES
Recovery of frozen flow losses in arcjets [AD-A278739] p 4228 N94-36089

ELECTRIC WIRE
On optimal placement of spacers in bundled conductors p 4258 N94-35354
Continuum fluorescence of Cu in NbTi/Cu composite wires [DE94-008940] p 4241 N94-36242

ELECTRICAL ENGINEERING
JPRS report: Science and technology. Central Eurasia [JPRS-UST-94-001] p 4229 N94-35340
JPRS report: Science and technology. Central Eurasia [JPRS-UST-94-004] p 4249 N94-35341
JPRS report: Science and technology. Central Eurasia [JPRS-UST-94-005] p 4249 N94-35342
JPRS report: Science and technology. Central Eurasia [JPRS-UST-94-010] p 4250 N94-35385
JPRS report: Science and technology. Central Eurasia [JPRS-UST-94-011] p 4250 N94-35386
JPRS report: Science and technology. Central Eurasia [JPRS-UST-94-012] p 4250 N94-35387

ELECTRICAL INSULATION
Method for making a symmetrical layered thin film edge field-emitter-array [AD-D016214] p 4246 N94-36121

ELECTRICAL MEASUREMENT
Elastic p(4)He scattering at intermediate energies [DE94-618544] p 4328 N94-36287

ELECTRICAL PROPERTIES
Thick film fabrication of aluminum nitride microcircuits [DE94-010107] p 4259 N94-35706
Properties and bibliography of GaSe [AD-A279064] p 4340 N94-35733
Development of novel II-VI solar cells [PB94-159415] p 4282 N94-35739
Electrical microengineering of redox enzymes [AD-A279015] p 4236 N94-35745

ELECTRICAL RESISTIVITY
The electrical conductivities of candidate beam-waveguide antenna shroud materials p 4252 N94-35546
Development of novel II-VI solar cells [PB94-159415] p 4282 N94-35739
Models for interpreting interstrand resistance measurements in Rutherford cables [DE94-010844] p 4259 N94-36194
Determination of the Fermi level position for neutron irradiated high resistivity silicon detectors and materials using the Transient Charge Technique (TChT) [DE94-009107] p 4260 N94-36221
Electrical conductivity of hydrogen shocked to megabar pressures [DE93-019632] p 4238 N94-36237
Ion modulated electroactivity in thin film metallopolymers [AD-A278618] p 4246 N94-36253
Streak tube photocathode development program [DE94-009905] p 4270 N94-36350

ELECTRO-OPTICS
Molecular systems for ultrafast optical switching: Controlling electron transfer reactions with femtosecond laser pulses [DE94-009695] p 4332 N94-35671
Characterization of lithium niobate electro-optic modulators at cryogenic temperatures [DE94-010059] p 4333 N94-35697
Activities of the optoelectronics laboratory [PB94-171196] p 4334 N94-36190

ELECTROACOUSTIC TRANSDUCERS
Absolute calibration technique for broadband ultrasonic transducers [NASA-CASE-LAR-14672-1] p 4268 N94-35368

ELECTROCHEMISTRY
Electrochemical process and product therefrom [AD-D016211] p 4239 N94-36372

ELECTRODE MATERIALS
Theoretical and experimental study of air and hydrogen electrodes [DE94-763308] p 4283 N94-36060

ELECTRODES
Electrical microengineering of redox enzymes [AD-A279015] p 4236 N94-35745
Theoretical and experimental study of air and hydrogen electrodes [DE94-763308] p 4283 N94-36060
Electrochemical process and product therefrom [AD-D016211] p 4239 N94-36372
Solvent acidity and basicity in polar media and their role in solvation [AD-A278604] p 4239 N94-36426

ELECTRODIALYSIS
Combined SO(x)/NO(x) control via SOXAL (tm) process: An electrodialytic regenerative wet scrubbing process [DE94-009053] p 4284 N94-35346

ELECTRODYNAMICS
Studies of the dayside boundary layer processes based on ground observations in the Svalbard area [AD-A280715] p 4292 N94-36265

ELECTROJETS
Simultaneous observations of the westward electrojet and the cross-tail current sheet during substorms [AD-A278631] p 4292 N94-36383

ELECTROLYTES
The relationship between hydroxyl groups on oxide surfaces and the properties of supported metals [DE94-010786] p 4241 N94-36233
Electrochemical process and product therefrom [AD-D016211] p 4239 N94-36372
Solvent acidity and basicity in polar media and their role in solvation [AD-A278604] p 4239 N94-36426

ELECTROMAGNETIC ABSORPTION
Analysis of regional visibility in the eastern United States using aerosol models [PB94-158698] p 4332 N94-35584

ELECTROMAGNETIC FIELDS
JPRS report: Science and technology. Central Eurasia [JPRS-UST-94-006] p 4249 N94-35228
Simulation models for computational plasma physics: Concluding report [DE94-009976] p 4335 N94-35647

Green's functions for an anisotropic medium: Part 1: Unbounded case
[AD-A278767] p 4256 N94-35694
On new theories of physical vacuum
[DE94-616613] p 4318 N94-35955
Integral characteristics of the magnetic bremsstrahlung
[DE94-616788] p 4256 N94-36078
The pressure of fluctuative electromagnetic field in inhomogeneous medium
[DE94-617189] p 4256 N94-36096
The energy density of fluctuative electromagnetic field near the semi-bounded plasma
[DE94-617188] p 4256 N94-36099
TSAR modeling of a TEM horn and surrounding structure
[DE94-010688] p 4256 N94-36301

ELECTROMAGNETIC INTERACTIONS
An electromagnetic finite difference time domain analog treatment of small signal acoustic interactions
[DE94-009978] p 4319 N94-35770

ELECTROMAGNETIC INTERFERENCE
Multiwavelength pyrometer for gray and non-gray surfaces in the presence of interfering radiation
[NASA-CASE-LEW-15250-1] p 4269 N94-35383

ELECTROMAGNETIC MEASUREMENT
Electromagnetic measurements of the ionosphere at the ionospheric station of Rome
[AD-A278991] p 4290 N94-35744

ELECTROMAGNETIC PULSES
Theoretical studies of ultrashort phenomena
[AD-A278938] p 4332 N94-35664
State of the art in high-power microwaves: An overview
[DE94-007075] p 4272 N94-35978

ELECTROMAGNETIC RADIATION
Green's functions for an anisotropic medium. Part 2: Two-layer case
[AD-A278786] p 4256 N94-35713
The kinetics of inhomogeneous plasma
[DE94-611459] p 4336 N94-35788

ELECTROMAGNETIC SCATTERING
Wedge scattering by the method of iteration
[DE94-010404] p 4256 N94-36112

ELECTROMAGNETIC WAVE TRANSMISSION
Green's functions for an anisotropic medium: Part 1: Unbounded case
[AD-A278767] p 4256 N94-35694

ELECTROMAGNETISM
An electromagnetic finite difference time domain analog treatment of small signal acoustic interactions
[DE94-009978] p 4319 N94-35770
Time-delay control of a magnetic levitated linear positioning system p 4217 N94-35862

ELECTROMAGNETS
Implementation of a decoupled controller for a magnetic suspension system using electromagnets mounted in a planar array p 4216 N94-35853

ELECTROMECHANICS
Design, construction, and testing of a five active axes magnetic bearing system p 4214 N94-35846
Electromechanical simulation and test of rotating systems with magnetic bearing or piezoelectric actuator active vibration control p 4223 N94-35905
A procedure for oscillatory parameter identification
[DE94-008047] p 4259 N94-36054

ELECTRON AFFINITY
Vertical electron detachment energies for octahedral closed-shell multiply charged anions
[AD-A278835] p 4322 N94-35753
Vertical and adiabatical ionization energies and electron affinities of new Si(n)C and Si(n)O (n=1-3) molecules
[AD-A278863] p 4324 N94-36050

ELECTRON BEAMS
Participation in the definition, conduct, and analysis of particle accelerator experiments for the first Spacelab Mission
[NASA-CR-193974] p 4330 N94-35483
Advanced induction accelerator designs for ground based and space based FELs
[AD-A278885] p 4271 N94-35586
Morphological aspects of surface reactions
[DE94-010184] p 4236 N94-35685
Computer simulation of beam-beam effects at large amplitudes and determination of life time
[DE94-616235] p 4330 N94-35999
Treatment of toxic gases SO2 and NO(x) by electron beam irradiation
[DE94-615424] p 4330 N94-36028
Spin dynamics in storage rings and linear accelerators
[DE94-010320] p 4330 N94-36106
Precise measurement of the left-right cross section asymmetry in Z boson production by electron-positron collisions
[DE94-010751] p 4326 N94-36198
Activities of the Laser and Plasma Technology Division
[DE94-617113] p 4273 N94-36393

ELECTRON DENSITY (CONCENTRATION)
Scaling laws for TEXT plasma profiles
[DE94-010832] p 4338 N94-36200

ELECTRON DENSITY PROFILES
The new features of Ion Bernstein Wave Heating in JIPP T-2U tokamak
[DE94-718978] p 4338 N94-36247

ELECTRON DIFFRACTION
The structural changes of water ice I during warmup p 4239 N94-36144

ELECTRON DISTRIBUTION
Global changes of radiation situation at heights less than 1000 km
[DE94-610504] p 4290 N94-35780
Kinetic theory of runaway air breakdown and the implications for lightning initiation
[DE94-001683] p 4295 N94-36240

ELECTRON ENERGY
New anionic states of the lithium trimer
[AD-A278832] p 4323 N94-35797
Anionic and neutral states of Li3O
[AD-A278833] p 4323 N94-35798
Scaling laws for TEXT plasma profiles
[DE94-010832] p 4338 N94-36200
The new features of Ion Bernstein Wave Heating in JIPP T-2U tokamak
[DE94-718978] p 4338 N94-36247

ELECTRON IMPACT
Capillary column GC-MS/MS confirmation of phosphate esters with a hybrid tandem mass spectrometer
[AD-A278748] p 4238 N94-36091
First measurement of helium on Mars: Implications for the problem of radiogenic gases on the terrestrial planets p 4370 N94-36153

ELECTRON IRRADIATION
Study of point defect mobilities in zirconium during electron irradiation in a HVEM
[DE94-619028] p 4242 N94-36289

ELECTRON MASS
Radiatively induced electron and electron-neutrino masses
[DE94-616775] p 4321 N94-35582

ELECTRON MICROSCOPES
Study of point defect mobilities in zirconium during electron irradiation in a HVEM
[DE94-619028] p 4242 N94-36289

ELECTRON MICROSCOPY
Determination of grain boundary volume expansion by HREM
[DE94-010452] p 4241 N94-36231

ELECTRON MOBILITY
Magnetoresistance of films and strips with the diffuse surface scattering
[DE94-611100] p 4340 N94-35933

ELECTRON PLASMA
The fine structure of Langmuir waves observed upstream of the bow shock at Venus
[NASA-CR-196123] p 4354 N94-35378
Activities of the Laser and Plasma Technology Division
[DE94-617113] p 4273 N94-36393

ELECTRON SPECTROSCOPY
Electron and Proton Wide-Angle Spectrometer (EPAS) on the CRRES spacecraft
[AD-A278630] p 4227 N94-35362
Electron energy-loss spectroscopy of carbon in interplanetary dust particles p 4353 N94-36149

ELECTRON STATES
Anionic states of LiFLi
[AD-A278830] p 4322 N94-35678
Periodicity and peculiarity in 120 first and second row diatomic molecules
[AD-A278836] p 4323 N94-35793
New anionic states of the lithium trimer
[AD-A278832] p 4323 N94-35797
Anionic and neutral states of Li3O
[AD-A278833] p 4323 N94-35798

ELECTRON TRANSFER
Molecular systems for ultrafast optical switching: Controlling electron transfer reactions with femtosecond laser pulses
[DE94-009695] p 4332 N94-35671
Intramolecular energy transfer reactions in polymetallic complexes
[DE94-010114] p 4326 N94-36126
Some perspectives on solution-phase electron-transfer processes
[AD-A278616] p 4238 N94-36252
Dynamic structural effects and ultrafast biomolecular kinetics in photoinduced charge transfer reactions
[DE94-010421] p 4329 N94-36390

ELECTRON-POSITRON PAIRS
Proceedings of 2nd Working meeting: Physics at VLEPP, volume 1
[DE94-616200] p 4320 N94-35569
Processes of the reciprocal transformation vector charged particles pairs and electron-positron pairs
[DE94-616787] p 4325 N94-36077

ELECTRON-POSITRON PLASMAS
Initial perturbations and Langmuir waves in electron-positron plasma
[DE94-617190] p 4338 N94-36097

ELECTRONIC EQUIPMENT
Laser drilling of vertical vias in silicon
[DE94-009250] p 4270 N94-35351
An analysis of operational suitability for test and evaluation of highly reliable systems
[AD-A278573] p 4192 N94-36184

ELECTRONIC EQUIPMENT TESTS
Minimum performance standards: Airborne low-range radar altimeters
[RTCA-DO-155] p 4198 N94-35344

ELECTRONIC MODULES
Laser drilling of vertical vias in silicon
[DE94-009250] p 4270 N94-35351
Demonstration of a high heat removal CVD diamond substrate edge-cooled multichip module
[DE94-010748] p 4260 N94-36245
The iWarp display module
[AD-A278610] p 4260 N94-36248
An overview of multichip modules
[AD-A278730] p 4260 N94-36296

ELECTRONIC PACKAGING
Issues in the development of a 10 MBPS K=15 Viterbi decoder
[NASA-CR-196083] p 4211 N94-35357
Technology Reinvestment Project's Focus Area: Low Cost Electronic Packaging
[PB94-161155] p 4259 N94-35748
Demonstration of a high heat removal CVD diamond substrate edge-cooled multichip module
[DE94-010748] p 4260 N94-36245
An overview of multichip modules
[AD-A278730] p 4260 N94-36296

ELECTRONS
Electron and Proton Wide-Angle Spectrometer (EPAS) on the CRRES spacecraft
[AD-A278630] p 4227 N94-35362
Radiatively induced electron and electron-neutrino masses
[DE94-616775] p 4321 N94-35582
Collisonless dynamics of the magnetosphere
[AD-A278886] p 4290 N94-35708
Precise measurement of the left-right cross section asymmetry in Z boson production by electron-positron collisions
[DE94-010751] p 4326 N94-36198
Coherent states versus de Broglie-wavelets
[DE94-611075] p 4343 N94-36381

ELECTROPHYSICS
JPRS report: Science and technology. Central Eurasia
[JPRS-UST-94-006] p 4249 N94-35226

ELECTROPLATING
Planar rotational magnetic micromotors with integrated shaft encoder and magnetic rotor levitation p 4224 N94-35907

ELECTROSTATIC GYROSCOPES
Electrostatically suspended and sensed micro-mechanical rate gyroscope p 4224 N94-35908

ELECTROSTATICS
Analytic model of aurorally coupled magnetospheric and ionospheric electrostatic potentials
[NASA-CR-196130] p 4288 N94-35358

ELECTROWEAK INTERACTIONS (FIELD THEORY)
Isoscalar vector bosons at LEP 2
[DE94-611253] p 4323 N94-35787
CDF electroweak studies and the search for the top quark
[DE94-010333] p 4326 N94-36107

ELEMENTARY PARTICLE INTERACTIONS
Goldstone pion and other mesons using a scalar confining interaction
[DE94-010016] p 4321 N94-35649
Identity for propagator in four-fermion theory
[DE94-611104] p 4342 N94-35781
Precise measurement of the left-right cross section asymmetry in Z boson production by electron-positron collisions
[DE94-010751] p 4326 N94-36198
Summary: Hadron dynamics sessions
[DE94-003011] p 4328 N94-36303

ELEMENTARY PARTICLES
On new theories of physical vacuum
[DE94-616613] p 4318 N94-35955

ELEVATION
Biaxial loading and shallow-flaw effects on crack-tip constraint and fracture-toughness [DE94-010128] p 4279 N94-35684

EMBEDDING
Numerical investigation of multi-element airfoils [NASA-CR-194592] p 4191 N94-36394

EMERGENCIES
Flight testing a propulsion-controlled aircraft emergency flight control system on an F-15 airplane [NASA-TM-4590] p 4199 N94-35258

EMISSION SPECTRA
Thermal emission measurements (5-25 microns) of palagonite/Fe-substituted montmorillonite intimate mixtures: Applications to Mars p 4292 N94-35453
Mossbauer and spectral (visible and near-IR) data for Fe(3+)-substituted rutile p 4240 N94-36154
New calculations of Fe spectra in high-temperature plasmas [DE94-009919] p 4339 N94-36386
Theoretical and experimental studies relevant to interpretation of auroral emissions [NASA-CR-196032] p 4376 N94-36421

EMISSIVITY
Multiwavelength pyrometer for gray and non-gray surfaces in the presence of interfering radiation [NASA-CASE-LEW-15250-1] p 4269 N94-35383
Thermal emission measurements (5-25 microns) of Hawaiian palagonitic soils with implications for Mars p 4292 N94-35452
Thermal emission measurements (5-25 microns) of palagonite/Fe-substituted montmorillonite intimate mixtures: Applications to Mars p 4292 N94-35453

EMITTANCE
The optimization of interfaces in InAsSb/InGaAs strained-layer superlattices grown by metal-organic chemical vapor deposition [DE94-010070] p 4340 N94-35698
Mercury: Mid-infrared (7.3 - 13.5 microns) spectroscopic observations showing features characteristic of plagioclase p 4370 N94-36150
Acoustical-optical fracture analysis [PB94-170602] p 4279 N94-36216
Study and fabrication of GaSb-based laser heterostructures [PB94-170677] p 4273 N94-36218

EMITTERS
Method for making a symmetrical layered thin film edge field-emitter-array [AD-D016214] p 4246 N94-36121
Design and construction of a imaging instrument for studying ion emission from pure ion emitters [DE94-010702] p 4328 N94-36302

EMOTIONS
The role of emotion in believable agents [AD-A278952] p 4312 N94-35658

END EFFECTORS
Maneuvering and control of flexible space robots p 4218 N94-35867

ENDANGERED SPECIES
Endangered and potentially endangered wildlife on John F. Kennedy Space Center and faunal integrity as a goal for maintaining biological diversity [NASA-TM-109204] p 4288 N94-36422

ENDOCRINE SYSTEMS
Stress and brain protein synthesis [PB94-170750] p 4296 N94-35601

ENDOCRINOLOGY
Stress and brain protein synthesis [PB94-170750] p 4296 N94-35601

ENERGETIC PARTICLES
Collisonless dynamics of the magnetosphere [AD-A278886] p 4290 N94-35708
A search for energetic ion directivity in large solar flares [NASA-CR-196036] p 4374 N94-35993

ENERGY BUDGETS
Power balance and characterization of impurities in the Maryland Spheromak, part 2 [DE94-009603] p 4335 N94-35670

ENERGY CONSERVATION
Thermal performance of residential duct systems in basements [LBL-33962] p 4250 N94-35364
On the various forms of the energy equation for a dilute, monatomic mixture of nonreacting gases [NASA-CR-4612] p 4190 N94-35864
Properties and applications of powder-filled evacuated-panel superinsulations [DE94-009169] p 4233 N94-35932
AICD: Advanced Industrial Concepts Division Biological and Chemical Technologies Research Program [DE94-006854] p 4283 N94-36051

ENERGY CONSUMPTION
Experimental measurement and calculation of losses in planar radial magnetic bearings p 4214 N94-35847

ENERGY CONVERSION
JPRS report: Science and technology. Central Eurasia [JPRS-UST-94-008] p 4249 N94-35228

ENERGY CONVERSION EFFICIENCY
High power diode laser Master Oscillator-Power Amplifier (MOPA) [NASA-CR-196095] p 4271 N94-35488

ENERGY DISSIPATION
Self-similar regimes of subsonic Langmuir wave collapse [DE94-611466] p 4335 N94-35750
First, second and fourth sound in relativistic superfluidity theory with account for dissipative effects [DE94-617393] p 4267 N94-36314

ENERGY DISTRIBUTION
ROSAT/XRT-PSPC observations and the ionizing continuum of Seyfert 1 galaxy Mkn 478 [PB94-167053] p 4350 N94-35530

ENERGY GAPS (SOLID STATE)
High temperature heterojunction bipolar transistors [AD-A278605] p 4261 N94-36360

ENERGY LEVELS
Determination of the Fermi level position for neutron irradiated high resistivity silicon detectors and materials using the Transient Charge Technique (TChT) [DE94-009107] p 4260 N94-36221

ENERGY METHODS
An energy method approach to the problem of elastic strip [PB94-171014] p 4279 N94-36000

ENERGY OF FORMATION
A theoretical study of ordering phenomena in K-In and K-Sb molten alloys [DE94-611103] p 4240 N94-35935
The thermochemistry and reaction mechanisms in the decomposition of energetic materials [DE94-011420] p 4248 N94-36376

ENERGY REQUIREMENTS
A two-dimensional model for collisional energy transfer in bimolecular ion-molecule dynamics [AD-A278913] p 4321 N94-35589
National Maglev initiative: California line electric utility power system requirements p 4215 N94-35850

ENERGY SOURCES
A guide to research facilities at the National Renewable Energy Laboratory [DE94-006857] p 4283 N94-36052

ENERGY SPECTRA
JPRS report: Science and technology. Central Eurasia: Space [JPRS-USP-94-001] p 4201 N94-35518
On the physics of waves in the solar atmosphere: Wave heating and wind acceleration [NASA-CR-194119] p 4375 N94-36395

ENERGY STORAGE
Flywheel energy storage using superconducting magnetic bearings [DE94-009817] p 4282 N94-35829
Concepts of flywheels for energy storage using autostable high-T(sub c) superconducting magnetic bearings p 4224 N94-35909
Manufacturing and testing of a magnetically suspended composite flywheel energy storage system p 4224 N94-35910

ENERGY TECHNOLOGY
How to develop a long term CO2 reduction plan [DE94-009559] p 4284 N94-35668
Model documentation: Renewable Fuels Module of the National Energy Modeling System [DE94-009962] p 4282 N94-35672
Maglev crude oil pipeline p 4226 N94-35919
AICD: Advanced Industrial Concepts Division Biological and Chemical Technologies Research Program [DE94-006854] p 4283 N94-36051
A guide to research facilities at the National Renewable Energy Laboratory [DE94-006857] p 4283 N94-36052
LIEKKI Combustion Research Program [DE94-763298] p 4237 N94-36059
Research and development of Proton-Exchange Membrane (PEM) fuel cell system for transportation applications: Initial conceptual design report [DE94-010576] p 4283 N94-36243

ENERGY TRANSFER
A two-dimensional model for collisional energy transfer in bimolecular ion-molecule dynamics [AD-A278913] p 4321 N94-35589
Vacuum ultraviolet studies of molecular dynamics [AD-A278940] p 4321 N94-35657
State-to-state dynamics of molecular energy transfer [DE94-009651] p 4324 N94-35816
Intramolecular energy transfer reactions in polymetallic complexes [DE94-010114] p 4326 N94-36126

ENGINE CONTROL
Improvement of endurance performance by periodic optimal control of variable camber p 4194 N94-36329

ENGINE DESIGN
Influence of backup bearings and support structure dynamics on the behavior of rotors with active supports [NASA-CR-196119] p 4274 N94-35500
Design and operation of a medium speed 12-cylinder coal-fueled diesel engine. Phase 2: Improvements [DE94-009547] p 4275 N94-35815
Integration of magnetic bearings in the design of advanced gas turbine engines p 4223 N94-35903
Analysis of the injection process in direct injected natural gas engines [PB94-156494] p 4275 N94-35931
Propulsion system selection for a High Altitude Long Endurance aircraft p 4195 N94-36333
Propulsion system technologies for long range and long endurance aircraft p 4195 N94-36334
The STRATO 2C propulsion system: A low cost approach for a High Altitude Long Endurance aircraft p 4195 N94-36335
Coal-fueled diesels for modular power generation [DE94-002960] p 4275 N94-36348
Compliant metal enhanced convection cooled reverse-flow annular combustor [NASA-TM-106626] p 4199 N94-36379

ENGINE NOISE
Engine exhaust characteristics evaluation in support of aircraft acoustic testing p 4319 N94-35963

ENGINE PARTS
Durability testing of medium speed diesel engine components designed for operating on coal/water slurry fuel [DE94-009550] p 4275 N94-35667
Carbon-carbon piston development [NASA-CR-4595] p 4233 N94-35947
Wear-resisting oxide films for 900 C [DE94-010093] p 4246 N94-36306

ENGINE TESTS
Evaluating the dynamic response of in-flight thrust calculation techniques during throttle transients [NASA-TM-4591] p 4193 N94-35241
Hot Corrosion Test Facility at the NASA Lewis Special Projects Laboratory [NASA-CR-195323] p 4200 N94-35267
Durability testing of medium speed diesel engine components designed for operating on coal/water slurry fuel [DE94-009550] p 4275 N94-35667
Bus application of oxygen-enrichment technology and diesel-electric hybrid systems [DE94-009835] p 4285 N94-35765
Carbon-carbon piston development [NASA-CR-4595] p 4233 N94-35947

ENGINEERING
Proceedings of the LLNL Technical Women's Symposium [DE94-006616] p 4379 N94-35997
National Educators' Workshop: Update 1993. Standard Experiments in Engineering Materials Science and Technology [NASA-CP-3259] p 4229 N94-36398

ENGINEERS
Mentoring for 2000 and beyond p 4343 N94-35964
Women as a resource for the flexibility required for high technology innovation p 4348 N94-35966
A biased historical perspective of women in the engineering field at Dryden from 1946 to November 1992 p 4251 N94-35967
Building on the foundation for an engineering career p 4343 N94-35973
University participation in the ATS program [DE94-003191] p 4275 N94-36022

ENRICHMENT
Bus application of oxygen-enrichment technology and diesel-electric hybrid systems [DE94-009835] p 4285 N94-35765

ENSTATITE
The occurrence of blue luminescing enstatite in E3 and E4 chondrites p 4351 N94-35423
On the origin of enstatite chondrite chondrules based on their petrography and comparison with experimentally produced chondrules p 4353 N94-36158

ENTHALPY
Calorimetric thermometry of meteoritic troilite: Preliminary thermometer relationships p 4355 N94-35399

ENTIRE FUNCTIONS
Generalized Fredholm determinants and Selberg zeta functions for axiom A dynamical systems [PB94-167665] p 4314 N94-35758

ENTRAINMENT
Role of magma-water interaction in very large explosive eruptions [DE94-002698] p 4291 N94-36103

ENTROPY
Bit-wise arithmetic coding for data compression p 4254 N94-35556
Quantum groups, non-commutative differential geometry and applications [DE94-011358] p 4315 N94-36270
Taking into account dissipative processes in relativistic superfluid systems [DE94-617391] p 4267 N94-36313

ENTROPY (STATISTICS)
Entropy of graphs, semigroups and groups [PB94-167749] p 4314 N94-35763

ENVIRONMENT EFFECTS
Asymetric change of daily temperature range: Proceedings [DE94-010102] p 4293 N94-35703

ENVIRONMENT MANAGEMENT
Natural resources and environmental issues. Volume 1: Riparian Resources: A Symposium on the Disturbances, Management, Economics, and Conflicts Associated with Riparian Ecosystems p 4287 N94-36120

ENVIRONMENT MODELS
A model of the CO2 exchanges between biosphere and atmosphere in the tundra [NASA-CR-196008] p 4289 N94-35389
Model engineering concepts for air quality models in an integrated environmental modeling system [PB94-158623] p 4298 N94-35688
Integrated science model for assessment of climate change [DE94-011758] p 4288 N94-36286

ENVIRONMENT PROTECTION
Proceedings: Integrated Research Planning Meeting for Gulf of Mexico Estuaries [PB94-157799] p 4296 N94-35738
Cleaning up our act: Alternatives for hazardous solvents used in cleaning [DE94-006624] p 4285 N94-35943

ENVIRONMENT SIMULATION
Design and simulation of EVA tools for first servicing mission of HST [NASA-CR-196030] p 4298 N94-35266

ENVIRONMENTAL MONITORING
Obtaining coincident image observations for Mission to Planet Earth science data return p 4202 N94-35609
How to develop a long term CO2 reduction plan [DE94-009559] p 4284 N94-35668
Environmental Monitoring and Assessment Program assessment framework [PB94-158862] p 4285 N94-35741
Natural resources and environmental issues. Volume 1: Riparian Resources: A Symposium on the Disturbances, Management, Economics, and Conflicts Associated with Riparian Ecosystems p 4287 N94-36120

ENVIRONMENTAL QUALITY
Environmental resource document for the Idaho National Engineering Laboratory, volume 1 [DE94-008522] p 4287 N94-36207
Environmental resource document for the Idaho National Engineering Laboratory, volume 2 [DE94-008523] p 4287 N94-36208

ENVIRONMENTAL SURVEYS
High-resolution subsurface imaging and neural network recognition [DE94-009546] p 4290 N94-35666
An improved assessment approach for noise impacts from stationary point and traffic sources on humans and wildlife [DE94-009728] p 4319 N94-36320

ENVIRONMENTAL TESTS
Activities of National Institute of Radiological Sciences [DE94-727636] p 4296 N94-36101

ENZYMES
Electrical microengineering of redox enzymes [AD-A279015] p 4236 N94-35745

EPHEMERIDES
Tracking system options for future altimeter satellite missions p 4205 N94-35622
Improved solution accuracy for Landsat-4 (TDRSS-user) orbit determination p 4205 N94-35623

EPITAXY
Development of novel II-VI solar cells [PB94-159415] p 4282 N94-35739
Superconducting transistors [PB94-170743] p 4260 N94-36260

EPOXY RESINS
Residual Gas Analysis (RGA) and shear strength characteristics of a silver-filled epoxy and polyimide under long-term, high-temperature storage conditions [DE94-010106] p 4244 N94-35705

EQUATIONS OF MOTION
Dynamic analysis of a magnetic bearing system with flux control p 4216 N94-35859
Variations in the modal characteristics of a telescopically deploying beam p 4218 N94-35872
Computationally efficient multibody simulations p 4222 N94-35896
Software for continuum modeling of controls-structures interactions p 4223 N94-35898
Piggyback balance experiment: An illustration of Archimedes' principles and Newton's third law [PB94-163060] p 4265 N94-35942

EQUATIONS OF STATE
AFDM: An advanced fluid-dynamics model, volume 6 [DE94-009596] p 4264 N94-35669
Quantum mechanics and thermodynamics of particles with distance dependent statistics [DE94-616620] p 4343 N94-36072
Equations of state valid continuously from zero to extreme pressures with H2O and CO2 as examples [DE94-011907] p 4238 N94-36230
Modelling of the structure and physical properties of simple disordered systems [DE94-617087] p 4329 N94-36311

EQUIPMENT SPECIFICATIONS
Designing aluminum sealing glasses for manufacturability [DE94-010081] p 4244 N94-35699
Data acquisition systems [DE94-009848] p 4345 N94-35817
Specification for the TITANIA krF laser system [PB94-167103] p 4272 N94-36062

EQUIVALENT CIRCUITS
BJT model in APLAC [PB94-171022] p 4259 N94-35822

ERBIUM
900-mW average power and tunability from a diode-pumped 2.94 micron Er:YAG oscillator [DE94-009511] p 4271 N94-35679
Eyesafe rare earth crystal lasers for atmosphere soudings [AD-A279486] p 4273 N94-36227

ERGODIC PROCESS
Magnetoresistance of films and strips with the diffuse surface scattering [DE94-611100] p 4340 N94-35933

EROSION
A comparison of atomic oxygen erosion yields of carbon and selected polymers exposed in ground based facilities and in low Earth orbit [NASA-TM-106622] p 4243 N94-35243
The fretted terrain of the Nilosyrtis Mensae region of Mars: Clues to the timing of dichotomy formation and the emplacement of the northern plains p 4360 N94-35424

ERROR ANALYSIS
Measuring attitude with a gradiometer p 4206 N94-35630
Comparison of Kalman filter and optimal smoother estimates of spacecraft attitude p 4208 N94-35638
Advantages of estimating rate corrections during dynamic propagation of spacecraft rates: Applications to real-time attitude determination of SAMPEX p 4209 N94-35642
MME-based attitude dynamics identification and estimation for SAMPEX p 4209 N94-35643
Dynamical observer for a flexible beam via finite element approximations p 4222 N94-35893
Transient Faults in Computer Systems [NASA-CR-194717] p 4306 N94-36063

ERROR CORRECTING CODES
Using certification trails to achieve software fault tolerance p 4307 N94-36068

ERROR DETECTION CODES
Transient Faults in Computer Systems [NASA-CR-194717] p 4306 N94-36063
Certification of computational results p 4306 N94-36064
Experimental evaluation of the certification-trail method p 4306 N94-36065
Certification trails and software design for testability p 4306 N94-36066
Experimental evaluation of certification trails using abstract data type validation p 4307 N94-36067
Using certification trails to achieve software fault tolerance p 4307 N94-36068
Certification trails for data structures p 4307 N94-36069

ESTERS
Addition polyimides with enhanced processability [NASA-CASE-LEW-15043-1] p 4242 N94-35234
Capillary column GC-MS/MS confirmation of phosphate esters with a hybrid tandem mass spectrometer [AD-A278748] p 4238 N94-36091

ESTIMATING
Point and interval estimation of series system reliability using small data sets [AD-A278647] p 4316 N94-35575
Overview of the MSTI 2 on-orbit alignment p 4206 N94-35629
Advances in parameter estimation techniques applied to flexible structures p 4219 N94-35877
Parameter estimation of the vibrational model for the SCOLE experimental facility p 4219 N94-35878
High energy [DE94-009477] p 4331 N94-36428

ESTUARIES
Proceedings: Integrated Research Planning Meeting for Gulf of Mexico Estuaries [PB94-157799] p 4296 N94-35738
Endangered and potentially endangered wildlife on John F. Kennedy Space Center and faunal integrity as a goal for maintaining biological diversity [NASA-TM-109204] p 4288 N94-36422

ETCHING
Chemical reactions of chlorine on a vicinal Si(100) surface studied by ESDIAD [AD-A279059] p 4236 N94-35731

ETHYL ALCOHOL
Transient body force effects on the dryout and rewet of a heated capillary structure [AD-A278677] p 4264 N94-35690

EURECA (ESA)
Eureka! Aerogel capture of meteoroids in space p 4351 N94-35412

EUROPE
JPRS report: Science and technology. Central Eurasia [JPRS-UST-94-001] p 4229 N94-35340
JPRS report: Science and technology. Central Eurasia [JPRS-UST-94-004] p 4249 N94-35341
JPRS report: Science and technology. Central Eurasia [JPRS-UST-94-005] p 4249 N94-35342
JPRS report: Science and technology. Central Eurasia [JPRS-UST-94-010] p 4250 N94-35385
JPRS report: Science and technology. Central Eurasia [JPRS-UST-94-011] p 4250 N94-35386
JPRS report: Science and technology. Central Eurasia [JPRS-UST-94-012] p 4250 N94-35387
JPRS report: Science and technology. Central Eurasia: Space [JPRS-USP-93-005] p 4201 N94-36011
JTEC/WTEC report and program summary p 4379 N94-36042
Information and communication technology p 4257 N94-36043

EUROPEAN AIRBUS
Calculations used to optimize the installation of civil aircraft engines p 4195 N94-36332

EUTECTICS
Preliminary results of sulfide melt/silicate wetting experiments in a partially melted ordinary chondrite p 4353 N94-36147

EVACUATING (TRANSPORTATION)
A review of computer evacuation models and their data needs [DOT/FAA/AM-94/11] p 4191 N94-35236

EXCITATION
Hydrodynamically induced loads on components submerged in high-level waste-storage tanks [DE94-009663] p 4264 N94-35756
About mid-infrared optical spectrum of high-Tc superconducting compounds [DE94-615646] p 4340 N94-36030
Recovery of frozen flow losses in arcjets [AD-A278739] p 4228 N94-36089
Initial perturbations and Langmuir waves in electron-positron plasma [DE94-617190] p 4338 N94-36097

EXHAUST EMISSION
Design and operation of a medium speed 12-cylinder coal-fueled diesel engine. Phase 2: Improvements [DE94-009547] p 4275 N94-35815
Methanol fuel additive demonstration [PB94-156668] p 4247 N94-35941
Capillary column GC-MS/MS confirmation of phosphate esters with a hybrid tandem mass spectrometer [AD-A278748] p 4238 N94-36091

EXHAUST GASES
The simulation of a propulsive jet and force measurement using a magnetically suspended wind tunnel model p 4191 N94-35855
Methanol fuel additive demonstration [PB94-156668] p 4247 N94-35941
Advanced hydrogen/method utilization technology demonstration [DE94-000214] p 4248 N94-36191

EXHAUST SYSTEMS
Engine exhaust characteristics evaluation in support of aircraft acoustic testing p 4319 N94-35963

EXISTENCE THEOREMS
Cauchy and invariant measure problem for the periodic Zakharov system [PB94-167707] p 4317 N94-35760

EXOBIOLOGY
Aerospace medicine and biology: A continuing bibliography with indexes (supplement 391) [NASA-SP-7011(391)] p 4297 N94-35345
Fluvial processes in Ma'adim Vallis and the potential of Gusev crater as a high priority site p 4358 N94-35414
Exopaleontology and the search for a fossil record on Mars p 4360 N94-35425

EXOSPHERE
First measurement of helium on Mars: Implications for the problem of radiogenic gases on the terrestrial planets p 4370 N94-36153

EXPERIMENT DESIGN
Laminated thermoplastic composite material from recycled high density polyethylene p 4230 N94-36403
Using experimental design modules for process characterization in manufacturing/materials processes laboratories p 4230 N94-36405
Experiments in diamond film fabrication in table-top plasma apparatus p 4231 N94-36411
Dielectric measurements of selected ceramics at microwave frequencies p 4232 N94-36412

EXPERT SYSTEMS
MMI(exp 2) demonstrator systems: A multi-modal interface for man machine interaction with knowledge based systems. Deliverable D17 (TA 2) ESPRIT project 2474 MMI(exp 2) [PB94-170537] p 4298 N94-35600
CABPRO: An expert system for process planning multiwire cables [DE94-010213] p 4312 N94-35810
Computer automation and artificial intelligence [DE94-611058] p 4312 N94-35831
Priorities and nonmonotonic reasoning [PB94-171170] p 4346 N94-35959
Knowledge-based systems in Japan p 4347 N94-36044
Multidisciplinary studies of integrated neural network systems [AD-A278774] p 4312 N94-36309

EXPLORER SATELLITES
TDRSS Onboard Navigation System (TONS) flight qualification experiment p 4206 N94-35625

EXPLOSIVES
NMR imaging of components and materials for DOE application [DE94-010664] p 4238 N94-36084

EXPONENTIAL FUNCTIONS
Gauss elimination by segments and multivariate polynomial interpolation [AD-A278646] p 4315 N94-36012

EXPOSURE
A comparison of atomic oxygen erosion yields of carbon and selected polymers exposed in ground based facilities and in low Earth orbit [NASA-TM-106622] p 4243 N94-35243
CAirTOX: A compartment model for assessing the fate of and human exposure to toxic-chemical emissions to air [DE94-010084] p 4284 N94-35700

EXTERNAL STORES
Flight test certification of a 480 gallon composite fuel tank on CF-18 p 4196 N94-36340

EXTERNAL TANKS
Flight test certification of a 480 gallon composite fuel tank on CF-18 p 4196 N94-36340

EXTRACTION
Ar-39-Ar-40 ages of four ureilites p 4357 N94-35410
Extraction of cloud statistics from whole sky imaging cameras [DE94-009867] p 4294 N94-35766

EXTRAPOLATION
Extrapolating storm location using the Integrated Terminal Weather System (ITWS) storm motion algorithm [AD-A278611] p 4295 N94-36249

EXTRAVEHICULAR ACTIVITY
Design and simulation of EVA tools for first servicing mission of HST [NASA-CR-196030] p 4298 N94-35266
Self-rescue strategies for EVA crewmembers equipped with the SAFER backpack p 4207 N94-35633

EXTREME ULTRAVIOLET EXPLORER SATELLITE
In-flight estimation of gyro noise on the Upper Atmosphere Research Satellite (UARS) and Extreme Ultraviolet Explorer (EUVE) missions p 4204 N94-35616
Color/magnitude calibration for National Aeronautics and Space Administration (NASA) standard Fixed-Head Star Trackers (FHST) p 4209 N94-35641

EXTREME ULTRAVIOLET RADIATION
Absolute, Extreme Ultraviolet Solar Spectral Irradiance Monitor (AESSIM) [AD-A278709] p 4227 N94-36189

EXTREMELY HIGH FREQUENCIES
Correlator data analysis for the array feed compensation system p 4253 N94-35553
The Mars Observer Ka-band link experiment p 4255 N94-35563

EXTREMELY LOW FREQUENCIES
ULF waves in the low-latitude boundary layer and their relationship to magnetospheric pulsations: A multisatellite observation [AD-A278906] p 4289 N94-35587

EYE MOVEMENTS
Visual-vestibular interaction [NASA-CR-196097] p 4297 N94-35379

EYEPIECES
Is increased accommodation a necessary condition for instrument myopia? [AD-A278962] p 4298 N94-35659

F

F REGION
Ionospheric plasma drift and structure studies at high and mid-latitudes [AD-A279415] p 4291 N94-36116

F-15 AIRCRAFT
Flight testing a propulsion-controlled aircraft emergency flight control system on an F-15 airplane [NASA-TM-4590] p 4199 N94-35258

F-18 AIRCRAFT
Wind tunnel measurements on a full-scale F/A-18 with a tangentially blowing slot — conducted in the Ames 80 by 120 foot wind tunnel p 4191 N94-35965
F/A-18 forebody vortex control. Volume 1: Static tests [NASA-CR-4582] p 4190 N94-35991
Flight test certification of a 480 gallon composite fuel tank on CF-18 p 4196 N94-36340

FABRICATION
Thick film fabrication of aluminum nitride microcircuits [DE94-010107] p 4259 N94-35706
Planar rotational magnetic micromotors with integrated shaft encoder and magnetic rotor levitation p 4224 N94-35907
Electrostatically suspended and sensed micro-mechanical rate gyroscope p 4224 N94-35908
Nondestructive Inspection (NDI) of reduced strength bonds [AD-A278745] p 4278 N94-36090
Study and fabrication of GaSb-based laser heterostructures [PB94-170677] p 4273 N94-36218
A low temperature scanning force microscope for biological samples [DE94-011357] p 4297 N94-36269
Design for manufacturability evaluation: Composite National Ignition Facility (NIF) pockel cell body [DE94-010669] p 4338 N94-36284
Continuous unidirectional fiber reinforced composites: Fabrication and testing p 4229 N94-36400
Mechanical properties of crosslinked polymer coatings p 4231 N94-36410

FAILURE
Residual Gas Analysis (RGA) and shear strength characteristics of a silver-filled epoxy and polyimide under long-term, high-temperature storage conditions [DE94-010106] p 4244 N94-35705
On the Buckling/Kinking compressive failure of fibrous composites [AD-A278865] p 4233 N94-35714
A mechanics mode for the compressive response of fiber reinforced composites [AD-A278866] p 4233 N94-35715
Computational methods for material failure processes [AD-A278716] p 4278 N94-36292

FAILURE ANALYSIS
The weakest failure detector for solving Consensus [NASA-CR-190545] p 4300 N94-35365
Fixed-head star tracker attitude updates on the Hubble Space Telescope p 4203 N94-35612

FAILURE MODES
Energy partitioning in high speed impact of analog solid rocket motors [AD-A278771] p 4228 N94-35825

FAR FIELDS
Computation of helicopter rotor acoustics in forward flight [NASA-CR-196132] p 4319 N94-36031
On the physics of waves in the solar atmosphere: Wave heating and wind acceleration [NASA-CR-194119] p 4375 N94-36395

FAR ULTRAVIOLET RADIATION
Vacuum ultraviolet studies of molecular dynamics [AD-A278940] p 4321 N94-35657

FAST NUCLEAR REACTORS
Study of point defect mobilities in zirconium during electron irradiation in a HVEM [DE94-619028] p 4242 N94-36289

FATIGUE (MATERIALS)
Processing and properties of high temperature metal/fiber-reinforced-thermoplastic laminates [AD-A278791] p 4232 N94-35654

FATIGUE LIFE
Isothermal damage and fatigue behavior of SCS-6/Timetal 21S (0/90)s composite at 650 C [NASA-CR-195345] p 4234 N94-35995

FATIGUE TESTS
Testing of the fracture resistance of rails p 4279 N94-35353
Isothermal damage and fatigue behavior of SCS-6/Timetal 21S (0/90)s composite at 650 C [NASA-CR-195345] p 4234 N94-35995
Fatigue and residual strength behaviour of ARALL3 panels with bonded-on doublers [AD-B181062] p 4279 N94-36226

FAULT DETECTION
Defect detection in multi-layered, plasma sprayed zirconia by time resolved infrared radiometry: A comparison between analytical and experimental methods [DE94-009803] p 4245 N94-35779
Transient Faults in Computer Systems [NASA-CR-194717] p 4306 N94-36063
Certification of computational results p 4306 N94-36064
Experimental evaluation of the certification-trail method p 4306 N94-36065
Certification trails and software design for testability p 4306 N94-36066
Experimental evaluation of certification trails using abstract data type validation p 4307 N94-36067
Using certification trails to achieve software fault tolerance p 4307 N94-36068
Certification trails for data structures p 4307 N94-36069

FAULT TOLERANCE
Asynchronous optimistic rollback recovery using secure distributed time [AD-A278978] p 4344 N94-35526
The rel/REL: A family of reliable multicast protocols for distributed real-time systems [PB94-167830] p 4310 N94-35535
Large granularity cache coherence for intermittent connectivity [AD-A278897] p 4345 N94-35571
Fault tolerant computer control for a Maglev transportation system p 4215 N94-35848
Certification of computational results p 4306 N94-36064
Experimental evaluation of the certification-trail method p 4306 N94-36065
Certification trails and software design for testability p 4306 N94-36066
Experimental evaluation of certification trails using abstract data type validation p 4307 N94-36067
Using certification trails to achieve software fault tolerance p 4307 N94-36068
Certification trails for data structures p 4307 N94-36069

FEASIBILITY
Feasibility study of superconducting LSM rocket launcher system p 4225 N94-35914

FEASIBILITY ANALYSIS
The KDC-10 programme of the Royal Netherlands Air Force p 4197 N94-36346
Feasibility study for a novel pulsed neutral beam diagnostics for tokamaks [DE94-617129] p 4339 N94-36417

FEDERAL BUDGETS
Budget estimates, fiscal year 1995. Volume 1: Agency summary, human space flight, and science, aeronautics and technology [NASA-TM-109791] p 4347 N94-35899
Budget estimates, fiscal year 1995. Volume 2: Mission support and Inspector General [NASA-TM-109792] p 4348 N94-35900

FEED SYSTEMS
DSS-13 S-/X-band microwave feed system p 4253 N94-35550
Correlator data analysis for the array feed compensation system p 4253 N94-35553

FEEDBACK
Measuring attitude with a gradiometer p 4206 N94-35630

FEEDBACK CONTROL
A closed-loop time-alignment system for baseband combining p 4253 N94-35552
Performance evaluation of digital phase-locked loops for advanced deep space transponders p 4254 N94-35558

High temperature superconductors for magnetic suspension applications p 4214 N94-35843
Fuzzy self-learning control for magnetic servo system p 4215 N94-35852
Implementation of a decoupled controller for a magnetic suspension system using electromagnets mounted in a planar array p 4216 N94-35853
Modelling and control of a rotor supported by magnetic bearings p 4216 N94-35858
Control of flexible structures with distributed sensing and processing p 4218 N94-35871
A case study in nonlinear dynamics and control of articulated spacecraft: The Space Station Freedom with a mobile remote manipulator system p 4220 N94-35879
Effects of noise variance model on optimal feedback design and actuator placement p 4220 N94-35883
Vibration suppression in flexible structures via the sliding-mode control approach p 4220 N94-35884
Active vibration damping using smart material p 4221 N94-35886
CSI, optimal control, and accelerometers: Trials and tribulations p 4221 N94-35888
Robustness properties of LQG optimized compensators for collocated rate sensors p 4221 N94-35890
Dynamical observer for a flexible beam via finite element approximations p 4222 N94-35893
Semigroup approximation and robust stabilization of distributed parameter systems p 4222 N94-35894
Nonlinear feedback model attitude control using CCD in magnetic suspension system p 4225 N94-35912

FELDSPARS
FeO and MgO in plagioclase of lunar anorthosites: Igneous or metamorphic? p 4351 N94-35449
Mercury: Mid-infrared (7.3 - 13.5 microns) spectroscopic observations showing features characteristic of plagioclase p 4370 N94-36150

FEMALES
Mentoring for 2000 and beyond p 4343 N94-35964
Women as a resource for the flexibility required for high technology innovation p 4348 N94-35966
A biased historical perspective of women in the engineering field at Dryden from 1946 to November 1992 p 4251 N94-35967
Building on the foundation for an engineering career p 4343 N94-35973

FENCES (BARRIERS)
The aerodynamic and heat transfer effects of an endwall boundary layer fence in a 90 degree turning square duct [AD-A278903] p 4265 N94-35803

FERMI-DIRAC STATISTICS
Determination of the Fermi level position for neutron irradiated high resistivity silicon detectors and materials using the Transient Charge Technique (TChT) [DE94-009107] p 4260 N94-36221

FERMIONS
Identity for propagator in four-fermion theory [DE94-611104] p 4342 N94-35781
Universal SU(2/1) and the Higgs and fermion masses [DE94-009182] p 4323 N94-35814

FERROMAGNETIC RESONANCE
Ferromagnetic resonance spectra of H2-reduced minerals and glasses p 4240 N94-36164

FIBER COMPOSITES
On the Buckling/Kinking compressive failure of fibrous composites [AD-A278865] p 4233 N94-35714
A mechanics mode for the compressive response of fiber reinforced composites [AD-A278866] p 4233 N94-35715
Integrated design of structures, controls, and materials p 4218 N94-35869
Can the compressive response of fiber-reinforced composites be modelled by means of layered arrays? [AD-A278864] p 4233 N94-35944
Isothermal damage and fatigue behavior of SCS-6/Timetal 21S (0/90)s composite at 650 C [NASA-CR-195345] p 4234 N94-35995
Continuous unidirectional fiber reinforced composites: Fabrication and testing p 4229 N94-36400
Design and construction of a tensile tester for the testing of simple composites p 4230 N94-36401

FIBER OPTICS
An electronic interface for a fiber optic tethered unmanned underwater vehicle [AD-A279046] p 4333 N94-35747

FIBER ORIENTATION
Isothermal damage and fatigue behavior of SCS-6/Timetal 21S (0/90)s composite at 650 C [NASA-CR-195345] p 4234 N94-35995

FIELD COILS
Superconducting Electromagnetic Suspension (EMS) system for Grumman Maglev concept p 4215 N94-35849

FIELD EFFECT TRANSISTORS
JPRS report: Science and technology. Central Eurasia [JPRS-UST-94-007] p 4249 N94-35227
A gallium arsenide MESFET operational amplifier for use in composite operational amplifiers [AD-A277843] p 4258 N94-35539
Superconducting transistors [PB94-170743] p 4260 N94-36260
High temperature heterojunction bipolar transistors [AD-A278605] p 4261 N94-36360
Estimating low-dose rate irradiation response of MOSFETs [DE94-007292] p 4342 N94-36367

FIELD EMISSION
Method for making a symmetrical layered thin film edge field-emitter-array [AD-D016214] p 4246 N94-36121

FIELD THEORY (PHYSICS)
Recent progress in irrational conformal field theory [DE94-011908] p 4317 N94-36234

FIGHTER AIRCRAFT
In-flight refueling: Dassault Aviation research on the Rafale aircraft p 4196 N94-36341

FILE MAINTENANCE (COMPUTERS)
An analysis of file system and installation of the file management system for NOS operating system [DE94-611062] p 4346 N94-35833

FILM THICKNESS
Development of novel II-VI solar cells [PB94-159415] p 4282 N94-35739

FINANCIAL MANAGEMENT
Statement by Bill D. Colvin, Inspector General [NASA-TM-109793] p 4348 N94-35446
Budget estimates, fiscal year 1995. Volume 1: Agency summary, human space flight, and science, aeronautics and technology [NASA-TM-109791] p 4347 N94-35899
Budget estimates, fiscal year 1995. Volume 2: Mission support and Inspector General [NASA-TM-109792] p 4348 N94-35900

FINE STRUCTURE
The fine structure of Langmuir waves observed upstream of the bow shock at Venus [NASA-CR-196123] p 4354 N94-35378

FINISHES
Dual cure low-VOC coating process [DE94-009346] p 4245 N94-35809

FINITE DIFFERENCE THEORY
Linear and nonlinear pattern selection in Rayleigh-Benard stability problems [NASA-TM-104007] p 4263 N94-35371
A comparison of variable selection criteria for multiple linear regression: A THIRD simulation study [AD-A278678] p 4316 N94-35691
Computation of dendrites using a phase field model [PB94-160744] p 4236 N94-35736
An electromagnetic finite difference time domain analog treatment of small signal acoustic interactions [DE94-009978] p 4319 N94-35770
TSAR modeling of a TEM horn and surrounding structure [DE94-010668] p 4256 N94-36301

FINITE ELEMENT METHOD
Active magnetic bearing control loop modeling for a finite element rotordynamics code p 4216 N94-35857
NASA Workshop on Distributed Parameter Modeling and Control of Flexible Aerospace Systems [NASA-CP-3242] p 4217 N94-35865
Dynamical observer for a flexible beam via finite element approximations p 4222 N94-35893
TransFit: Finite element analysis data fitting software [NASA-CR-193988] p 4307 N94-36118
Application of sequential quadratic programming to large-scale structural design problems [AD-A278574] p 4307 N94-36185
An efficient, intelligent solution for viscous flows inside solid rocket motors [AD-A278629] p 4228 N94-36255
An adaptive, unstructured, finite-element, multi-material, thermal analysis [AD-A278632] p 4343 N94-36256
Computational methods for material failure processes [AD-A278716] p 4278 N94-36292
An equal-order approximate projection FEM [DE94-010101] p 4268 N94-36374
Analysis of high speed flow, thermal and structural interactions [NASA-CR-196017] p 4268 N94-36420
GRIZ: Finite element analysis results visualization for unstructured grids [DE94-010066] p 4309 N94-36429

FIRES
Fire data management system, FDMS 2.0, technical documentation [PB94-164019] p 4346 N94-35819

Analysis of mid-tropospheric carbon monoxide data using a three-dimensional global atmospheric chemistry numerical model [DE94-004782] p 4286 N94-36026

FLAME PROPAGATION
A comparison between direct spark ignition and prechamber ignition in an internal combustion engine [DE94-008218] p 4275 N94-36206

FLAME SPRAYING
Analysis of a High Velocity Oxygen-Fuel (HVOF) thermal spray torch. Part 1: Numerical formulation [DE94-005590] p 4267 N94-35996

FLAPPING
Numerical investigation of multi-element airfoils [NASA-CR-194592] p 4191 N94-36394

FLASH LAMPS
Chirped-pulse amplification with flashlamp-pumped Ti:Sapphire amplifiers [DE94-010055] p 4272 N94-35695

FLAT PLATES
On the nonlinear stability of viscous modes within the Rayleigh problem on an infinite flat plate [NASA-CR-194909] p 4263 N94-35497
Expansion effects on supersonic turbulent boundary layers [AD-A278989] p 4190 N94-35950
The velocity field created by a shallow bump in a boundary layer [NASA-CR-194899] p 4266 N94-35975
TSAR modeling of a TEM horn and surrounding structure [DE94-010668] p 4256 N94-36301

FLEXIBLE BODIES
Maneuvering and control of flexible space robots p 4218 N94-35867
Distributed parameter modeling of repeated truss structures p 4218 N94-35868
Control of flexible structures with distributed sensing and processing p 4218 N94-35871
Advances in parameter estimation techniques applied to flexible structures p 4219 N94-35877
An overview of recent advances in system identification p 4220 N94-35880
Vibration suppression in flexible structures via the sliding-mode control approach p 4220 N94-35884
LQG optimal compensator transfer function for the NASA LaRC CSI Evolutionary Model p 4221 N94-35891
Dynamical observer for a flexible beam via finite element approximations p 4222 N94-35893

FLEXIBLE SPACECRAFT
NASA Workshop on Distributed Parameter Modeling and Control of Flexible Aerospace Systems [NASA-CP-3242] p 4217 N94-35865
Distributed parameter modelling of flexible spacecraft: Where's the beef? p 4217 N94-35866
Parameter estimation of the vibrational model for the SCOLE experimental facility p 4219 N94-35878
A case study in nonlinear dynamics and control of articulated spacecraft: The Space Station Freedom with a mobile remote manipulator system p 4220 N94-35879
A combined algorithm for minimum time slewing of flexible spacecraft p 4220 N94-35881
Dynamic analysis of Space Shuttle/RMS configuration using continuum approach p 4221 N94-35887
An optimization-based approach for integrated controls-structures design of flexible spacecraft p 4221 N94-35889
Rational positive real approximations for LQG optimal compensators arising in active stabilization of flexible structures p 4222 N94-35892
Software for continuum modeling of controls-structures interactions p 4223 N94-35898
Input shaping for three-dimensional slew maneuvers of a precision pointing flexible spacecraft [DE94-008937] p 4226 N94-36001

FLIGHT CHARACTERISTICS
In-flight simulation studies at the NASA Dryden Flight Research Facility p 4198 N94-35969
Recent Advances in Long Range and Long Endurance Operation of Aircraft [AGARD-CP-547] p 4193 N94-36321
In-flight refueling: Dassault Aviation research on the Rafale aircraft p 4196 N94-36341
Aerial refueling interoperability from a receiver flying qualities perspective p 4197 N94-36343

FLIGHT CONDITIONS
Flight testing of a luminescent surface pressure sensor [NASA-TM-103970] p 4189 N94-35394

FLIGHT CONTROL
Flight testing a propulsion-controlled aircraft emergency flight control system on an F-15 airplane [NASA-TM-4590] p 4199 N94-35258

TDRSS Onboard Navigation System (TONS) flight qualification experiment p 4206 N94-35625

The prediction of pilot opinion ratings using optimal and sub-optimal pilot models [AD-A278679] p 4298 N94-35692

In-flight simulation studies at the NASA Dryden Flight Research Facility p 4198 N94-35969

Improvement of endurance performance by periodic optimal control of variable camber p 4194 N94-36329

FLIGHT CREWS

Safety study: A review of flightcrew-involved, major accidents of US air carriers, 1978 through 1990 [PB94-917001] p 4191 N94-35482

Review of human factors problems related to long distance and long endurance operation of aircraft p 4195 N94-36336

Extended range operations: A review of recent developments p 4195 N94-36337

Determinants of subjective fatigue for C-141 crews during Operation Desert Storm p 4196 N94-36338

FLIGHT FATIGUE

Aircraft accident report: Uncontrolled collision with terrain, American International Airways Flight 808, Douglas DC-8-61, N814CK, US Naval Air Station, Guantanamo Bay, Cuba, 18 August 1993 [PB94-910406] p 4192 N94-35521

Review of human factors problems related to long distance and long endurance operation of aircraft p 4195 N94-36336

Determinants of subjective fatigue for C-141 crews during Operation Desert Storm p 4196 N94-36338

Some solutions to reduce the human effects of extended operation times p 4196 N94-36339

FLIGHT SAFETY

Safety study: A review of flightcrew-involved, major accidents of US air carriers, 1978 through 1990 [PB94-917001] p 4191 N94-35482

Aircraft accident report: Uncontrolled collision with terrain, American International Airways Flight 808, Douglas DC-8-61, N814CK, US Naval Air Station, Guantanamo Bay, Cuba, 18 August 1993 [PB94-910406] p 4192 N94-35521

Extended range operations: A review of recent developments p 4195 N94-36337

FLIGHT SIMULATION

1993 Technical Paper Contest for Women. Gear Up 2000: Women in Motion [NASA-CP-10134] p 4377 N94-35961

Piloted simulation study of two tilt-wing control concepts p 4200 N94-35962

In-flight simulation studies at the NASA Dryden Flight Research Facility p 4198 N94-35969

FLIGHT STRESS (BIOLOGY)

Extended range operations: A review of recent developments p 4195 N94-36337

Determinants of subjective fatigue for C-141 crews during Operation Desert Storm p 4196 N94-36338

FLIGHT TESTS

Evaluating the dynamic response of in-flight thrust calculation techniques during throttle transients [NASA-TM-4591] p 4193 N94-35241

Flight testing a propulsion-controlled aircraft emergency flight control system on an F-15 airplane [NASA-TM-4590] p 4199 N94-35258

Flight testing of a luminescent surface pressure sensor [NASA-TM-103970] p 4189 N94-35394

Unleaded AVGAS program [AD-A278650] p 4247 N94-35795

Engine exhaust characteristics evaluation in support of aircraft acoustic testing p 4319 N94-35963

A biased historical perspective of women in the engineering field at Dryden from 1946 to November 1992 p 4251 N94-35967

In-flight simulation studies at the NASA Dryden Flight Research Facility p 4198 N94-35969

Laminar flow studies at Dassault Aviation: Calculations and flight tests p 4194 N94-36328

Flight test certification of a 480 gallon composite fuel tank on CF-18 p 4196 N94-36340

CC-130H(T) tactical aerial refuelling tanker development flight test programme p 4198 N94-36347

The reduction of takeoff ground roll by the application of a nose gear jump strut [NASA-TM-108822] p 4198 N94-36380

FLIGHT TIME

Technological challenges of High Altitude Long Endurance unmanned configurations p 4193 N94-36323

Future supersonic commercial transport aircraft: A technological challenge for long haul traffic p 4193 N94-36324

Review of human factors problems related to long distance and long endurance operation of aircraft p 4195 N94-36336

Extended range operations: A review of recent developments p 4195 N94-36337

Determinants of subjective fatigue for C-141 crews during Operation Desert Storm p 4196 N94-36338

FLOW DISTRIBUTION

Analysis of phase distribution phenomena in microgravity environments [NASA-CR-196038] p 4249 N94-35237

Unsteady structure of leading-edge vortices on a delta wing [AD-A278988] p 4190 N94-35529

A supersonic tunnel for laser and flow-seeding techniques [NASA-TM-106588] p 4265 N94-35945

Boundary conditions for jet flow computations [NASA-TM-106648] p 4266 N94-35976

An experimental investigation of active control of thrust vectoring nozzle flow fields [AD-A278702] p 4229 N94-36291

Numerical investigation of multi-element airfoils [NASA-CR-194592] p 4191 N94-36394

FLOW MEASUREMENT

Method for making a dynamic pressure sensor and a pressure sensor made according to the method [NASA-CASE-LAR-14029-1] p 4269 N94-35369

FLOW STABILITY

Linear and nonlinear pattern selection in Rayleigh-Benard stability problems [NASA-TM-104007] p 4263 N94-35371

On the nonlinear stability of viscous modes within the Rayleigh problem on an infinite flat plate [NASA-CR-194909] p 4263 N94-35497

Spatio-temporal properties of centrifugal instabilities: Abstracts of 8th Couette-Taylor Meeting [PB94-150240] p 4266 N94-35981

X ray radiographic imaging of hydrodynamic phenomena in radiation driven materials: Shock propagation, material compression and shear flow [DE94-009515] p 4266 N94-35982

FLOW VELOCITY

Fundamental studies in blow-down and cryogenic cooling [AD-A278967] p 4250 N94-35524

FLOW VISUALIZATION

A supersonic tunnel for laser and flow-seeding techniques [NASA-TM-106588] p 4265 N94-35945

FLUE GASES

Combined SO(x)/NO(x) control via SOXAL (tm) process: An electrodialytic regenerative wet scrubbing process [DE94-009053] p 4284 N94-35346

FLUID DYNAMICS

Theoretical aspect of low pressure discharges in simple gasses [AD-A278762] p 4335 N94-35493

Determination of extensional viscosity from capillary rheometer entrance pressure drop measurements using a numerical simulation of contraction flow [PB94-171154] p 4263 N94-35603

AFDM: An advanced fluid-dynamics model, volume 6 [DE94-009596] p 4264 N94-35669

Solitary waves and homoclinic orbits [DE94-009428] p 4264 N94-35681

Hydrodynamics of maneuvering bodies: LDRD Final Report [DE94-009970] p 4265 N94-35769

FLUID FLOW

Role of magma-water interaction in very large explosive eruptions [DE94-002698] p 4291 N94-36103

FLUID MECHANICS

Performance analysis of reciprocating regenerative magnetic heat pumping [DE94-009488] p 4264 N94-35683

FLUID PRESSURE

Electrical conductivity of hydrogen shocked to megabar pressures [DE93-019632] p 4238 N94-36237

FLUORESCENCE

Fluorescence detection of single molecules using pulsed near-field optical excitation and time correlated photon counting [DE94-007553] p 4320 N94-35376

Molecular nitrogen fluorescence lidar for remote sensing of the auroral ionosphere [AD-A280716] p 4291 N94-36263

FLUORIDES

Anionic states of LiFLi [AD-A278830] p 4322 N94-35678

Vertical electron detachment energies for octahedral closed-shell multiply charged anions [AD-A278835] p 4322 N94-35753

FLUOROCARBONS

Development of atmospheric characteristics of chlorine-free alternative fluorocarbons [DE94-009791] p 4287 N94-36179

FLUOROHYDROCARBONS

Development of atmospheric characteristics of chlorine-free alternative fluorocarbons [DE94-009791] p 4287 N94-36179

FLUTTER

Robust control design techniques for active flutter suppression p 4200 N94-35875

Ground vibration test of the XV-15 Tiltrotor Research Aircraft and pretest predictions p 4200 N94-35972

FLUX (RATE)

Spatial fluctuations of particle fluxes within the auroral zone inferred from the Intercosmos-Bulgaria-1300 satellite data [DE94-615858] p 4350 N94-36128

FLUX DENSITY

The pressure of fluctuative electromagnetic field in inhomogeneous medium [DE94-617189] p 4256 N94-36096

The energy density of fluctuative electromagnetic field near the semi-bounded plasma [DE94-617188] p 4256 N94-36099

FLYING PLATFORMS

The case for surface effect research, platform applications and technology development opportunities p 4194 N94-36325

FLYWHEELS

Flywheel energy storage using superconducting magnetic bearings [DE94-009817] p 4282 N94-35829

High temperature superconductors for magnetic suspension applications p 4214 N94-35843

Neural network controller development for a magnetically suspended flywheel energy storage system p 4217 N94-35861

Concepts of flywheels for energy storage using autostable high-T(sub c) superconducting magnetic bearings p 4224 N94-35909

Manufacturing and testing of a magnetically suspended composite flywheel energy storage system p 4224 N94-35910

FOCAL PLANE DEVICES

Development of ultra-low noise, high performance 3 to 5 Quantum Well Infrared Photodetectors (QWIPs) for focal plane array staring image sensor systems [AD-A278861] p 4342 N94-36385

FOCUSING

Is increased accommodation a necessary condition for instrument myopia? [AD-A278962] p 4298 N94-35659

ILSE combiner study [DE94-011009] p 4331 N94-36202

FOLDS (GEOLOGY)

Formation of fold and thrust belts on Venus due to horizontal shortening of a laterally heterogeneous lithosphere p 4367 N94-35480

FOREBODIES

A review and development of correlations for base pressure and base heating in supersonic flow [SAND93-0280] p 4189 N94-35360

F/A-18 forebody vortex control. Volume 1: Static tests [NASA-CR-4582] p 4190 N94-35991

FORECASTING

Isotopic and geochemical precursors of earthquakes and volcanic eruptions [DE94-615824] p 4289 N94-35568

FORGING

A review of radial forging technology including preform design for process optimization [AD-A278770] p 4250 N94-35711

FORM FACTORS

Baryonic currents and their correlators in the heavy quark effective theory [DE94-612496] p 4320 N94-35567

Calculations on some properties of the pion in the framework of Schwinger-Dyson and Bethe-Salpeter equations [DE94-611232] p 4322 N94-35786

Elastic charge form factors for K mesons [DE94-010014] p 4325 N94-36086

FORMALISM

Priorities and nonmonotonic reasoning [PB94-171170] p 4346 N94-35959

FORTRAN

NEQPAK, the AEDC thermochemical nonequilibrium package: Theory and use [AD-A279005] p 4266 N94-35951

Use of formal calculation to automatically obtain adjoint programs [PB94-170701] p 4308 N94-36259

FOSSIL FUELS

Air quality implications associated with the selection of power plants in the Pacific Northwest [DE94-004783] p 4287 N94-36027

Integrated science model for assessment of climate change [DE94-011758] p 4288 N94-36286

FOSSILS
Exopaleontology and the search for a fossil record on Mars p 4360 N94-35425
FOURIER ANALYSIS
Cauchy and invariant measure problem for the periodic Zakharov system [PB94-167707] p 4317 N94-35760
FOURIER TRANSFORMATION
Color-coded radar plan position indicator [AD-D016200] p 4257 N94-36364
FRACTALS
Estimation of fractal dimensions from transect data [DE94-009808] p 4281 N94-36018
FRACTIONATION
First observation of a mass independent isotopic fractionation in a condensation reaction p 4239 N94-35464
Mars atmospheric escape and isotopic fractionation: Synthesis of data and models p 4369 N94-36143
FRACTURE MECHANICS
Frequency domain analysis of the random loading of cracked panels [NASA-CR-196021] p 4279 N94-35974
FRACTURE STRENGTH
Testing of the fracture resistance of rails p 4279 N94-35353
Biaxial loading and shallow-flaw effects on crack-tip constraint and fracture-toughness [DE94-010128] p 4279 N94-35684
Investigation of moisture-induced embrittlement of iron aluminides [DE94-010881] p 4241 N94-36196
FRACTURES (MATERIALS)
The surface and interior of Phobos p 4355 N94-35400
Patterns of brittle deformation under extension on Venus p 4373 N94-36168
Acoustical-optical fracture analysis [PB94-170602] p 4279 N94-36216
FRACTURING
Shoemaker-Levy 9 and the tidal disruption of comets p 4351 N94-35406
Structures and properties of materials recovered from high shock pressures [DE94-010057] p 4232 N94-35696
Cement paste matrix composite materials center [AD-A279017] p 4233 N94-35952
Transformation plasticity in ductile solids [DE94-010420] p 4240 N94-35953
Acoustical-optical fracture analysis [PB94-170602] p 4279 N94-36216
An automated digital data collection and analysis system for the Charpy Impact Tester p 4232 N94-36415
FRAGMENTS
The anatomy of a cluster IDP. Part 1: Carbon abundance, bulk chemistry, and mineralogy of fragments from L2008#5 p 4352 N94-35466
Morphological aspects of surface reactions [DE94-010184] p 4236 N94-35685
FRANCK-CONDON PRINCIPLE
Dynamic structural effects and ultrafast biomolecular kinetics in photoinduced charge transfer reactions [DE94-010421] p 4329 N94-36390
FREE ELECTRON LASERS
Advanced induction accelerator designs for ground based and space based FELs [AD-A278885] p 4271 N94-35586
State of the art in high-power microwaves: An overview [DE94-007075] p 4272 N94-35978
FREE ENERGY
The thermochemistry and reaction mechanisms in the decomposition of energetic materials [DE94-011420] p 4248 N94-36376
FREE FLIGHT
A review and development of correlations for base pressure and base heating in supersonic flow [SAND93-0280] p 4189 N94-35360
FREQUENCIES
An overview of recent advances in system identification p 4220 N94-35880
Solvent acidity and basicity in polar media and their role in solvation [AD-A278604] p 4239 N94-36426
FREQUENCY RANGES
A survey of reflectometry techniques with applications to TFTR [DE94-010202] p 4338 N94-36093
Network analyzer calibration for cryogenic on-wafer measurements [DE94-010089] p 4262 N94-36430
FREQUENCY SHIFT
Dielectric measurements of selected ceramics at microwave frequencies p 4232 N94-36412
Solvent acidity and basicity in polar media and their role in solvation [AD-A278604] p 4239 N94-36426
FRONTS (METEOROLOGY)
Doppler weather radar studies of precipitation systems [AD-A279417] p 4295 N94-36262
FUEL CELL POWER PLANTS
A solid oxide fuel cell power system: 1992-1993 field operation [DE94-010383] p 4283 N94-36109
FUEL CELLS
Fuel Cell Handbook update [DE94-002958] p 4282 N94-36021
A solid oxide fuel cell power system: 1992-1993 field operation [DE94-010383] p 4283 N94-36109
Research and development of Proton-Exchange Membrane (PEM) fuel cell system for transportation applications: Initial conceptual design report [DE94-010576] p 4283 N94-36243
Propulsion system selection for a High Altitude Long Endurance aircraft p 4195 N94-36333
FUEL COMBUSTION
Infrared multiphoton ignition and combustion enhancement of natural gas. [PB94-165438] p 4236 N94-35755
A new comprehensive reaction mechanism for combustion of hydrocarbon fuels [DE94-008288] p 4238 N94-36205
A comparison between direct spark ignition and prechamber ignition in an internal combustion engine [DE94-008218] p 4275 N94-36206
Coal-fueled diesels for modular power generation [DE94-002960] p 4275 N94-36348
Effects of natural gas composition on ignition delay under diesel conditions [DE94-006405] p 4276 N94-36378
FUEL CONTROL
Final regulatory impact analysis: Refueling emission regulations for light duty vehicles and trucks and heavy duty vehicles [PB94-164027] p 4285 N94-35754
FUEL INJECTION
Design and operation of a medium speed 12-cylinder coal-fueled diesel engine. Phase 2: Improvements [DE94-009547] p 4275 N94-35815
Analysis of the injection process in direct injected natural gas engines [PB94-156494] p 4275 N94-35931
FUEL TESTS
Effects of natural gas composition on ignition delay under diesel conditions [DE94-006405] p 4276 N94-36378
FUELS
Model documentation: Renewable Fuels Module of the National Energy Modeling System [DE94-009962] p 4282 N94-35672
Heterogeneous catalytic process for alcohol fuels from syngas [DE94-010263] p 4248 N94-36299
FULLERENES
Novel catalysts for methane activation [DE94-009705] p 4237 N94-35778
A new family of superconducting fullerides, Na(NH3)(x)C60(x = 2-8) [DE94-011480] p 4341 N94-36272
Developments in carbon materials p 4231 N94-36409
FUNCTIONAL DESIGN SPECIFICATIONS
Applying observations of work activity in designing prototype data analysis tools [DE94-010206] p 4347 N94-36297
FUNCTIONAL INTEGRATION
Functional integration method for the one-dimensional localization, the higher correlators and mean current in mesoscopic ring in the arbitrary magnetic field [DE94-616621] p 4325 N94-36073
FUNCTIONALS
Functional integration method for the one-dimensional localization, the higher correlators and mean current in mesoscopic ring in the arbitrary magnetic field [DE94-616621] p 4325 N94-36073
FUSELAGES
Ground vibration test of the XV-15 Tiltrotor Research Aircraft and pretest predictions p 4200 N94-35972
FUSION REACTORS
NIFS Symposium: Toward the research of fusion burning plasmas, present status and future strategy [DE94-727618] p 4336 N94-35775
Potential formation and transport in open field line systems [DE94-718910] p 4337 N94-35983
Improved models of beta-limit, anomalous transport and radial electric field with loss cone loss in heliotron/torsatron [DE94-718976] p 4324 N94-35984
A survey of reflectometry techniques with applications to TFTR [DE94-010202] p 4338 N94-36093
FUZZY SYSTEMS
JPRS report: Science and technology. Central Eurasia [JPRS-UST-94-007] p 4249 N94-35227
Automated maneuver planning using a fuzzy logic algorithm p 4203 N94-35610
The application of fuzzy logic to SAFOR in SIMNET [AD-A279058] p 4312 N94-35730
Computer automation and artificial intelligence [DE94-611058] p 4312 N94-35831
Fuzzy self-learning control for magnetic servo system p 4215 N94-35852

G

GALACTIC EVOLUTION
First observation of a mass independent isotopic fractionation in a condensation reaction p 4239 N94-35464
GALACTIC RADIATION
JPRS report: Science and technology. Central Eurasia: Space [JPRS-USP-94-001] p 4201 N94-35518
GALERKIN METHOD
Semigroup approximation and robust stabilization of distributed parameter systems p 4222 N94-35894
A three dimensional multigrid Reynolds-averaged Navier-Stokes solver for unstructured meshes [NASA-CR-194908] p 4191 N94-35994
GALILEO PROJECT
Galileo: The Jovian laboratory [NASA-CR-196043] p 4367 N94-35504
GALILEO SPACECRAFT
First Galileo image of asteroid 243 Ida p 4351 N94-35416
Galileo Earth/Moon 1 encounter [NASA-CR-195545] p 4367 N94-35508
GALLIUM
A two-dimensional model for collisional energy transfer in bimolecular ion-molecule dynamics [AD-A278913] p 4321 N94-35589
GALLIUM ARSENIDES
A gallium arsenide MESFET operational amplifier for use in composite operational amplifiers [AD-A277843] p 4258 N94-35539
Non-alloyed, refractory metal contact optimization with shallow implantations of Zn and Mg [DE94-010392] p 4240 N94-36110
GALLIUM COMPOUNDS
Vertical electron detachment energies for octahedral closed-shell multiply charged anions [AD-A278835] p 4322 N94-35753
GALLIUM NITRIDES
High temperature heterojunction bipolar transistors [AD-A278605] p 4261 N94-36360
GALLIUM PHOSPHIDES
High-power CW operation of AlGaInP diode-laser arrays [DE94-010409] p 4272 N94-36115
GALLIUM SELENIDES
Properties and bibliography of GaSe [AD-A279064] p 4340 N94-35733
GAMMA RAY ASTRONOMY
A search for energetic ion directivity in large solar flares [NASA-CR-196036] p 4374 N94-35993
GAMMA RAY LASERS
Progress in the production of samples of gamma ray laser candidate materials [AD-A278961] p 4272 N94-35721
GAMMA RAY OBSERVATORY
GRO: Studies of high energy pulsars with EGRET [NASA-CR-196003] p 4349 N94-35516
GAMMA RAY SPECTRA
SYNTH: A spectrum synthesizer [DE94-004719] p 4331 N94-36317
GAMMA RAY SPECTROMETERS
Remote geochemical experiment package for Discovery class missions p 4350 N94-35420
SYNTH: A spectrum synthesizer [DE94-004719] p 4331 N94-36317
GAMMA RAY TELESCOPES
GRO: Studies of high energy pulsars with EGRET [NASA-CR-196003] p 4349 N94-35516
GAMMA RAYS
X-ray remote sensing and in-situ spectroscopy for planetary exploration missions and gamma-ray remote sensing and in-situ spectroscopy for planetary exploration missions [NASA-CR-189352] p 4375 N94-35381
Estimating low-dose rate irradiation response of MOSFETs [DE94-007292] p 4342 N94-36367

GAS ANALYSIS

The anatomy of a cluster IDP. Part 1: Carbon abundance, bulk chemistry, and mineralogy of fragments from L2008#5 p 4352 N94-35466

Residual Gas Analysis (RGA) and shear strength characteristics of a silver-filled epoxy and polyimide under long-term, high-temperature storage conditions [DE94-010106] p 4244 N94-35705

GAS COMPOSITION

On the origin of porphyritic chondrules [DE94-010464] p 4351 N94-36418

GAS DETECTORS

Experimental characterisation of gas microstrip detectors. Part 2: Counting rate characteristics [PB94-167095] p 4269 N94-36061

GAS DISCHARGES

Theoretical aspect of low pressure discharges in simple gasses [AD-A278762] p 4335 N94-35493

GAS DISSOCIATION

Infrared multiphoton ignition and combustion enhancement of natural gas. [PB94-165438] p 4236 N94-35755

GAS DYNAMICS

Theoretical aspect of low pressure discharges in simple gasses [AD-A278762] p 4335 N94-35493

GAS EVOLUTION

Mars atmospheric escape and isotopic fractionation: Synthesis of data and models p 4369 N94-36143

GAS EXCHANGE

A model of the CO2 exchanges between biosphere and atmosphere in the tundra [NASA-CR-196008] p 4289 N94-35389

GAS GENERATORS

The simulation of a propulsive jet and force measurement using a magnetically suspended wind tunnel model p 4191 N94-35855

GAS INJECTION

Analysis of the injection process in direct injected natural gas engines [PB94-156494] p 4275 N94-35931

GAS JETS

The simulation of a propulsive jet and force measurement using a magnetically suspended wind tunnel model p 4191 N94-35855

Analysis of the injection process in direct injected natural gas engines [PB94-156494] p 4275 N94-35931

GAS MIXTURES

On the various forms of the energy equation for a dilute, monatomic mixture of nonreacting gases [NASA-CR-4612] p 4190 N94-35864

Effects of natural gas composition on ignition delay under diesel conditions [DE94-006405] p 4276 N94-36378

GAS STREAMS

High temperature sorbents for oxygen [NASA-CASE-NPO-18409-1-CU] p 4235 N94-35255

GAS TURBINE ENGINES

Integration of magnetic bearings in the design of advanced gas turbine engines p 4223 N94-35903

Compliant metal enhanced convection cooled reverse-flow annular combustor [NASA-TM-106626] p 4199 N94-36379

GAS TURBINES

The aerodynamic and heat transfer effects of an endwall boundary layer fence in a 90 degree turning square duct [AD-A278903] p 4265 N94-35803

University participation in the ATS program [DE94-003191] p 4275 N94-36022

Heavy duty gas turbine combustion tests with simulated low BTU coal gas [DE94-002970] p 4276 N94-36355

Compliant metal enhanced convection cooled reverse-flow annular combustor [NASA-TM-106626] p 4199 N94-36379

GASES

Application of GaSe and AgGaSe2 crystal growth to non-linear optics [PB94-170552] p 4341 N94-36212

GASIFICATION

LIEKKI Combustion Research Program [DE94-763298] p 4237 N94-36059

GASOLINE

Unleaded AVGAS program [AD-A278650] p 4247 N94-35795

Methanol fuel additive demonstration [PB94-156668] p 4247 N94-35941

Gasoline from natural gas by sulfur processing [DE94-011130] p 4248 N94-36035

GAUGE THEORY

Universal SU(2/1) and the Higgs and fermion masses [DE94-009182] p 4323 N94-35814

Quantum groups, non-commutative differential geometry and applications [DE94-011358] p 4315 N94-36270

GAUSSIAN ELIMINATION

Gauss elimination by segments and multivariate polynomial interpolation [AD-A278646] p 4315 N94-36012

GENERAL AVIATION AIRCRAFT

Annual review of aircraft accident data. US general aviation, calendar year 1992 [PB94-181054] p 4192 N94-35496

The influence of data link-provided graphical weather on pilot decision-making [AD-A278871] p 4293 N94-35596

Unleaded AVGAS program [AD-A278650] p 4247 N94-35795

GENERAL OVERVIEWS

Introduction to USRA [NASA-CR-195980] p 4376 N94-35590

Time-of-flight diffraction at pulsed neutron sources: An introduction to the symposium [DE94-010442] p 4327 N94-36225

The history of space exploration [NASA-TM-109888] p 4201 N94-36440

GENETIC ALGORITHMS

Genetic algorithms [PB94-171048] p 4303 N94-35602

A genetic algorithm approach to automating satellite range scheduling [AD-A278577] p 4226 N94-36188

GENETICS

Activities of National Institute of Radiological Sciences [DE94-727636] p 4296 N94-36101

GEOCHEMISTRY

Remote geochemical experiment package for Discovery class missions p 4350 N94-35420

The Twenty-Fifth Lunar and Planetary Science Conference. Part 3: P-Z [NASA-CR-195745] p 4362 N94-35448

Anatomy of a cluster IDP. Part 2: Noble gas abundances, trace element geochemistry, isotopic abundances, and trace organic chemistry of several fragments from L2008#5 p 4352 N94-35465

The anatomy of a cluster IDP. Part 1: Carbon abundance, bulk chemistry, and mineralogy of fragments from L2008#5 p 4352 N94-35466

Isotopic and geochemical precursors of earthquakes and volcanic eruptions [DE94-615824] p 4289 N94-35568

GEODESY

NASA Space Geodesy Program: GSFC data analysis, 1993. VLBI geodetic results 1979 - 1992 [NASA-TM-104605] p 4281 N94-35261

GEODYNAMICS

NASA Space Geodesy Program: GSFC data analysis, 1993. VLBI geodetic results 1979 - 1992 [NASA-TM-104605] p 4281 N94-35261

Formation of fold and thrust belts on Venus due to horizontal shortening of a laterally heterogeneous lithosphere p 4367 N94-35480

Improved solution accuracy for TDRSS-based TOPEX/Poseidon orbit determination p 4205 N94-35620

GEOLOGICAL FAULTS

Groundwater penetrating radar and high resolution seismic for locating shallow faults in unconsolidated sediments [DE94-007284] p 4257 N94-36366

GEOLOGICAL SURVEYS

The fretted terrain of the Nilosyrtis Mensae region of Mars: Clues to the timing of dichotomy formation and the emplacement of the northern plains p 4360 N94-35424

Mesoscale roughness of Venus p 4361 N94-35430

GEOLOGY

National Geoscience Data Repository System [DE94-000120] p 4344 N94-35347

GEOMAGNETIC PULSATIONS

ULF waves in the low-latitude boundary layer and their relationship to magnetospheric pulsations: A multisatellite observation [AD-A278906] p 4289 N94-35587

GEOMAGNETIC TAIL

Contributions of the low-latitude boundary layer to the finite width magnetotail convection model [NASA-CR-196116] p 4289 N94-35392

Collisonless dynamics of the magnetosphere [AD-A278886] p 4290 N94-35708

GEOMORPHOLOGY

The fretted terrain of the Nilosyrtis Mensae region of Mars: Clues to the timing of dichotomy formation and the emplacement of the northern plains p 4360 N94-35424

The Twenty-Fifth Lunar and Planetary Science Conference. Part 3: P-Z [NASA-CR-195745] p 4362 N94-35448

The Twenty-Fifth Lunar and Planetary Science Conference. Part 2: H-O [NASA-CR-195744] p 4367 N94-36136

Morphology of meteoroid and space debris craters on LDEF metal targets p 4353 N94-36159

GEOPHYSICS

National Geoscience Data Repository System [DE94-000120] p 4344 N94-35347

Workshop on the Martian Northern Plains: Sedimentological, periglacial, and paleoclimatic evolution [NASA-CR-196134] p 4354 N94-35359

The topography of Mars: A re-evaluation of current data p 4364 N94-35460

Solar-geophysical data number 594, February 1994. Part 2: (Comprehensive reports). Data for August 1993, and miscellaneous [PB94-164001] p 4374 N94-36009

Solar-geophysical data number 594, February 1994. Part 1: (Prompt reports). Data for December 1993, January 1994, and late data [PB94-163995] p 4375 N94-36020

Natural orbital environment definition guidelines for use in aerospace vehicle development [NASA-TM-4527] p 4291 N94-36175

GEOPOTENTIAL

JPRS report: Science and technology. Central Eurasia [JPRS-UST-94-006] p 4249 N94-35226

GEOSAT SATELLITES

Tracking system options for future altimeter satellite missions p 4205 N94-35622

GERMANIUM

Large scale atomistic first principles study of adsorption and surface diffusion [DE94-009450] p 4322 N94-35682

GHOSTS

AXAF-I ghost ray study: On orbit case [NASA-CR-193987] p 4333 N94-36119

GIMBALS

Kinematic modeling of a double octahedral Variable Geometry Truss (VGT) as an extensible gimbal [NASA-TM-109127] p 4311 N94-35242

GLASS

New prospects for analyzing lunar pyroclastic glass p 4355 N94-35397

Reduction of lunar mare soil and pyroclastic glass p 4355 N94-35398

Single agglutinates: A comparative study of compositions of agglutinitic glass, whole-grain, bulk soil, and FMR p 4355 N94-35401

Craters in aluminum 1100 targets using glass projectiles at 1-7 km/s p 4280 N94-35407

Thermal emission measurements (5-25 microns) of Hawaiian palagonitic soils with implications for Mars p 4292 N94-35452

Thermal emission measurements (5-25 microns) of palagonite/Fe-substituted montmorillonite intimate mixtures: Applications to Mars p 4292 N94-35453

Designing aluminum sealing glasses for manufacturability [DE94-010081] p 4244 N94-35699

Kinetics of phase transformations in glass forming systems [NASA-CR-196082] p 4245 N94-35977

Nanochannel glass matrix used in making mesoscopic structures [AD-D016216] p 4234 N94-36123

The nature of agglutinitic glass in the fine-size fraction of lunar soil 10084 p 4369 N94-36148

Ferromagnetic resonance spectra of H2-reduced minerals and glasses p 4240 N94-36164

Transformation of a Cranz-Schardin camera [PB94-170685] p 4270 N94-36219

GLASS FIBER REINFORCED PLASTICS

Processing and properties of high temperature metal/fiber-reinforced-thermoplastic laminates [AD-A278791] p 4232 N94-35654

GLASS FIBERS

Coatings for SiO2 optical fibers [AD-D016197] p 4334 N94-36363

GLAUBER THEORY

Elastic p(4)He scattering at intermediate energies [DE94-618544] p 4328 N94-36287

GLOBAL POSITIONING SYSTEM

Preliminary study of satellite attitude determination for the LANDSAT 7 spacecraft [AD-A278876] p 4212 N94-35585

Implementation of a low-cost, commercial orbit determination system p 4205 N94-35621

Tracking system options for future altimeter satellite missions p 4205 N94-35622

Application of a Monte Carlo accuracy assessment tool to TDRS and GPS p 4207 N94-35635

GLOBAL WARMING

The computation of cloud base height from paired whole-sky imaging cameras [DE94-009868] p 4294 N94-35767

GLUONS
High energy asymptotics of perturbative multi-color QCD
[DE94-001350] p 4327 N94-36238
GLYCOGENS
Typology of skeletal muscle in humans undergoing intense physical training or prolonged akinesia
[PB94-170644] p 4297 N94-36217
GODDARD TRAJECTORY DETERMINATION SYSTEM
Compatibility of TOPEX/Poseidon trajectory propagation with JPL and GSFC/FDF operational software
p 4204 N94-35619
Improved solution accuracy for TDRSS-based TOPEX/Poseidon orbit determination
p 4205 N94-35620
Application of a Monte Carlo accuracy assessment tool to TDRS and GPS p 4207 N94-35635
Evaluation of semiempirical atmospheric density models for orbit determination applications
p 4208 N94-35636
GOES SATELLITES
Solar-geophysical data number 594, February 1994. Part 2: (Comprehensive reports). Data for August 1993, and miscellaneous
[PB94-164001] p 4374 N94-36009
GOGGLES
Accommodation during instrument viewing can be influenced by knowledge of object distance
[AD-A278987] p 4298 N94-35528
GOLD
Au/Zn contacts to Rho-InP: Electrical and metallurgical characteristics and the relationship between them
[NASA-TM-106590] p 4281 N94-35271
GOVERNMENT PROCUREMENT
Statement by Bill D. Colvin, Inspector General
[NASA-TM-109793] p 4348 N94-35446
Budget estimates, fiscal year 1995. Volume 1: Agency summary, human space flight, and science, aeronautics and technology
[NASA-TM-109791] p 4347 N94-35899
Budget estimates, fiscal year 1995. Volume 2: Mission support and Inspector General
[NASA-TM-109792] p 4348 N94-35900
GRADIENTS
Measuring attitude with a gradiometer
p 4206 N94-35630
GRAIN BOUNDARIES
Determination of grain boundary volume expansion by HREM
[DE94-010452] p 4241 N94-36231
GRAIN SIZE
Luna 24 regolith breccias: A possible source of the fine size material of the Luna 24 regolith
p 4362 N94-35450
Inhomogeneous distribution of materials in lodranites-acapulcoites and IAB irons and their common formation processes p 4364 N94-35463
GRAINS
Grain rims on ilmenite in the lunar regolith: Comparison to vapor deposits on regolith silicates
p 4359 N94-35418
GRAMMARS
A lower bound for the intersection of regular forests
[AD-A278653] p 4303 N94-35576
GRAPH THEORY
Entropy of graphs, semigroups and groups
[PB94-167749] p 4314 N94-35763
GRAPHICAL USER INTERFACE
CATLAC: Calibration and validation analysis tool of local area coverage for the SeaWiFS mission
[NASA-TM-104603] p 4211 N94-35269
MMI(exp 2) demonstrator systems: A multi-modal interface for man machine interaction with knowledge based systems. Deliverable D17 (TA 2) ESPRIT project 2474 MMI(exp 2)
[PB94-170537] p 4298 N94-35600
Implementation of a low-cost, commercial orbit determination system p 4205 N94-35621
Environment/tool integrator for software development, version 1.2
[AD-A278965] p 4303 N94-35660
An object-oriented implementation of a graphical-programming system
[DE94-009298] p 4304 N94-35808
User's guide for an interactive personal computer interface for the aeroprediction code
[NSWCDD/TR-94/107] p 4305 N94-35958
The integrated model development environment
[AD-A278613] p 4308 N94-36250
HST archive primer, version 4.1
[NASA-CR-189370] p 4349 N94-36280
GRAPHITE
Developments in carbon materials
p 4231 N94-36409
GRAPHITE-EPOXY COMPOSITES
Manufacturing and testing of a magnetically suspended composite flywheel energy storage system
p 4224 N94-35910
GRAPHS (CHARTS)
Representing spatial information in a computational model for network management
[NASA-CR-191669] p 4306 N94-36040
Graphing techniques for materials laboratory using Excel p 4232 N94-36414
GRASSLANDS
Methane production and consumption in grassland and boreal ecosystems
[NASA-CR-196085] p 4284 N94-35486
GRAVITATION
Progress in the development of the GMM-2 gravity field model for Mars p 4371 N94-36155
Preliminary solutions for the lunar gravity field from analysis of lunar orbiter tracking data
p 4371 N94-36156
Primordial nucleosynthesis in conformal Weyl gravity
[DE94-003002] p 4327 N94-36241
GRAVITATION THEORY
Primordial nucleosynthesis in conformal Weyl gravity
[DE94-003002] p 4327 N94-36241
GRAVITATIONAL EFFECTS
Effect of microgravity on plant growth
[NASA-CR-196004] p 4296 N94-35257
GRAVITATIONAL FIELDS
The topography of Mars: A re-evaluation of current data p 4364 N94-35460
The mass of Mars, Phobos, and Deimos, from the analysis of the Mariner 9 and Viking Orbiter tracking data p 4364 N94-35461
Measuring attitude with a gradiometer
p 4206 N94-35630
Progress in the development of the GMM-2 gravity field model for Mars p 4371 N94-36155
Preliminary solutions for the lunar gravity field from analysis of lunar orbiter tracking data
p 4371 N94-36156
GRAVITATIONAL WAVE ANTENNAS
Lunar LIGO and gravitational wave astronomy on the Moon p 4366 N94-35472
GRAVITATIONAL WAVES
Lunar LIGO and gravitational wave astronomy on the Moon p 4366 N94-35472
GRAVITY GRADIOMETERS
Measuring attitude with a gradiometer
p 4206 N94-35630
GRAVITY WAVES
JPRS report: Science and technology. Central Eurasia
[JPRS-UST-94-006] p 4249 N94-35226
Non-linear interaction of gravity waves with average jet flows, instabilities, and turbulence
[PB94-170586] p 4291 N94-36214
GRAY SCALE
Subpixel resolution from multiple images
p 4281 N94-35417
GREEN'S FUNCTIONS
Green's functions for an anisotropic medium: Part 1: Unbounded case
[AD-A278767] p 4256 N94-35694
Green's functions for an anisotropic medium. Part 2: Two-layer case
[AD-A278788] p 4256 N94-35713
GREENHOUSE EFFECT
Asymetric change of daily temperature range: Proceedings
[DE94-010102] p 4293 N94-35703
Extraction of cloud statistics from whole sky imaging cameras
[DE94-009867] p 4294 N94-35766
The computation of cloud base height from paired whole-sky imaging cameras
[DE94-009868] p 4294 N94-35767
Anthropogenic sulfate and organic aerosols, CCN, and cloud project concentration at a marine site
[DE94-004210] p 4286 N94-36025
Integrated science model for assessment of climate change
[DE94-011758] p 4288 N94-36286
GRID GENERATION (MATHEMATICS)
Three-dimensional unstructured grid refinement and optimization using edge-swapping
[NASA-TM-103966] p 4299 N94-35393
An efficient, intelligent solution for viscous flows inside solid rocket motors
[AD-A278629] p 4228 N94-36255
An adaptive, unstructured, finite-element, multi-material, thermal analysis
[AD-A278632] p 4343 N94-36256
Overset grid applications on distributed memory MIMD computers
[NASA-CR-196081] p 4268 N94-36397
GROOVES
Transient body force effects on the dryout and rewet of a heated capillary structure
[AD-A278677] p 4264 N94-35690
Propellant stress relief groove for the Titan 4 SRMU
[AD-A278628] p 4228 N94-36254
GROUND EFFECT (AERODYNAMICS)
The case for surface effect research, platform applications and technology development opportunities
p 4194 N94-36325
GROUND EFFECT MACHINES
Data reduction, analysis and results of LACV-30-07 air cushion vehicle tests, Fort Story, VA, August - September 1993
[AD-A278859] p 4190 N94-35826
GROUND STATE
Periodicity and peculiarity in 120 first and second row diatomic molecules
[AD-A278836] p 4323 N94-35793
Anionic and neutral states of Li3O
[AD-A278833] p 4323 N94-35798
T-odd, P-even photon-fermion interactions
[DE94-616869] p 4327 N94-36246
GROUND STATIONS
A new presentation of complex voltage data for Goldstone radar astronomy p 4255 N94-35561
GROUND SUPPORT SYSTEMS
Budget estimates, fiscal year 1995. Volume 2: Mission support and Inspector General
[NASA-TM-109792] p 4348 N94-35900
GROUND TESTS
Experience with Ada on the F-18 High Alpha Research Vehicle flight test program p 4310 N94-35968
Ground vibration test of the XV-15 Tiltrotor Research Aircraft and pretest predictions p 4200 N94-35972
GROUND TRACKS
Tracking system options for future altimeter satellite missions p 4205 N94-35622
GROUND WATER
Groundwater penetrating radar and high resolution seismic for locating shallow faults in unconsolidated sediments
[DE94-007284] p 4257 N94-36366
GROUP THEORY
Entropy of graphs, semigroups and groups
[PB94-167749] p 4314 N94-35763
Quantum groups, non-commutative differential geometry and applications
[DE94-011358] p 4315 N94-36270
N = 4 supersymmetry from the quantum affine algebra U(sub q)(A-circumflex(sup 1)(sub 3))
[DE94-611145] p 4317 N94-36307
GUANIDINES
A novel method for depositing precious metal films on difficult surfaces
[NASA-TM-106607] p 4243 N94-35260
GUIDANCE SENSORS
The in-flight calibration of the Hubble Space Telescope fine guidance sensors, 2 (a success story)
p 4204 N94-35615
Hubble Space Telescope Fine Guidance Sensors Instrument Handbook, version 4.0
[NASA-CR-189366] p 4349 N94-36281
GULF OF MEXICO
Proceedings: Integrated Research Planning Meeting for Gulf of Mexico Estuaries
[PB94-157799] p 4296 N94-35738
GUN PROPELLANTS
The 30th JANNAF Combustion Subcommittee Meeting, volume 1
[AD-A278793] p 4247 N94-35655
The 30th JANNAF Combustion Subcommittee Meeting, volume 2
[AD-A278794] p 4247 N94-35656
GUSTS
Non-linear interaction of gravity waves with average jet flows, instabilities, and turbulence
[PB94-170586] p 4291 N94-36214
GYROSCOPES
A long-baseline method for HST gyro drift rate bias calibration p 4203 N94-35614
In-flight estimation of gyro noise on the Upper Atmosphere Research Satellite (UARS) and Extreme Ultraviolet Explorer (EUVE) missions
p 4204 N94-35616
Operational support for Upper Atmosphere Research Satellite (UARS) attitude sensors p 4204 N94-35617
Overview of the Miniature Sensor Technology Integration (MSTI) spacecraft attitude control system
p 4206 N94-35627
Overview of the MSTI 2 on-orbit alignment
p 4206 N94-35629
Parameter estimation of the vibrational model for the SCOLE experimental facility p 4219 N94-35878

GYROSCOPIC STABILITY
A long-baseline method for HST gyro drift rate bias calibration p 4203 N94-35614

H

H-INFINITY CONTROL
Robust tracking control of a magnetically suspended rigid body p 4225 N94-35913
HADRONS
Beam tests of a prototype level-1 calorimeter trigger for LHC experiments [PB94-170495] p 4269 N94-35599
Isoscalar vector bosons at LEP 2 [DE94-611253] p 4323 N94-35787
P-matrix approach and three-nucleon problem [DE94-616887] p 4326 N94-36131
Alternating series fit to the total cross sections [DE94-616888] p 4326 N94-36132
SCATTER program of cross section calculation of the hadron and lepton interactions with nuclei [DE94-617006] p 4326 N94-36134
Summary: Hadron dynamics sessions [DE94-003011] p 4328 N94-36303
HAFNIUM COMPOUNDS
Metal cluster alloys and oxides: Elucidating structural and electronic effects in governing the reactivity and catalytic role of matter in finite dimensions [DE94-010224] p 4328 N94-36298
HAFNIUM ISOTOPES
Progress in the production of samples of gamma ray laser candidate materials [AD-A278961] p 4272 N94-35721
HALF LIFE
Calculations on some properties of the pion in the framework of Schwinger-Dyson and Bethe-Salpeter equations [DE94-611232] p 4322 N94-35786
Measurement of the decay rate of the SiH feature as a function of temperature p 4318 N94-36171
HAMILTONIAN FUNCTIONS
Modal decomposition of Hamiltonian variational equations p 4202 N94-35606
About mid-infrared optical spectrum of high-Tc superconducting compounds [DE94-615646] p 4340 N94-36030
On quantization of time-dependent systems with constraints [DE94-611114] p 4343 N94-36351
Pairing and low temperature properties of 2D Fermi-systems with attraction between particles [DE94-615510] p 4329 N94-36434
HANDBOOKS
Implementation of the military handbook 17 for polymer matrix composites and metal matrix composites [AD-A278795] p 4244 N94-35757
Fuel Cell Handbook update [DE94-002958] p 4282 N94-36021
Hubble Space Telescope Fine Guidance Sensors Instrument Handbook, version 4.0 [NASA-CR-189366] p 4349 N94-36281
Collection, processing, and reporting of damage tolerant design data for non-aerospace structural materials [NASA-CR-196046] p 4347 N94-36435
HARDWARE
NAVSPACECOM space surveillance sensor system digital signal processing receiver. Volume 4: Hardware interfaces [AD-A278845] p 4212 N94-35801
HARDWARE DESCRIPTION LANGUAGES
Rapid and accurate timing simulation of radiation-hardened digital microelectronics using VHDL [AD-A278644] p 4261 N94-36361
HARMONIC CONTROL
Selected topics on the active control of helicopter aeromechanical and vibration problems p 4200 N94-35874
HARMONIC GENERATIONS
Synthesis of novel composite Platinum-DNA films by way of wet-spinning [AD-A278763] p 4243 N94-35494
HARTREE APPROXIMATION
Magnetic metallic multilayers [DE94-011913] p 4341 N94-36274
HASTELLOY (TRADEMARK)
Analysis of high speed flow, thermal and structural interactions [NASA-CR-196017] p 4268 N94-36420
HEAD MOVEMENT
Visual-vestibular interaction [NASA-CR-196097] p 4297 N94-35379
HEART RATE
Further studies of 60-Hz exposure effects on human function [DE94-010192] p 4297 N94-36223
HEAT ENGINES
Coal-fueled diesels for modular power generation [DE94-002960] p 4275 N94-36348
HEAT FLUX
Fundamental studies in blow-down and cryogenic cooling [AD-A278967] p 4250 N94-35524
Measurement of a surface heat flux and temperature p 4231 N94-36407
HEAT MEASUREMENT
Calorimetric thermometry of meteoritic troilite: Preliminary thermometer relationships p 4355 N94-35399
Calorimetric thermobarometry of experimentally shocked quartz p 4240 N94-36174
Measurement of a surface heat flux and temperature p 4231 N94-36407
HEAT PUMPS
Performance analysis of reciprocating regenerative magnetic heat pumping [DE94-009488] p 4264 N94-35683
HEAT RESISTANT ALLOYS
High-temperature, bellows hybrid seal [NASA-CASE-LEW-15570-1] p 4274 N94-35373
High temperature creep and oxidation resistant chromium silicide matrix alloy containing molybdenum [NASA-CASE-LEW-15697-1] p 4241 N94-36275
HEAT TRANSFER
Fundamental studies in blow-down and cryogenic cooling [AD-A278967] p 4250 N94-35524
Thermodynamic behaviour of tellurium at high temperatures [DE94-612823] p 4240 N94-35960
Demonstration of a high heat removal CVD diamond substrate edge-cooled multichip module [DE94-010748] p 4260 N94-36245
Analysis of high speed flow, thermal and structural interactions [NASA-CR-196017] p 4268 N94-36420
HEAT TRANSMISSION
Performance analysis of reciprocating regenerative magnetic heat pumping [DE94-009488] p 4264 N94-35683
Properties and applications of powder-filled evacuated-panel superinsulations [DE94-009169] p 4233 N94-35932
HEAT TREATMENT
Testing of the fracture resistance of rails p 4279 N94-35353
Calorimetric thermometry of meteoritic troilite: Preliminary thermometer relationships p 4355 N94-35399
HEATING
Mineralogy of artificially heated carbonaceous chondrites p 4352 N94-35477
The new features of Ion Bernstein Wave Heating in JIPP T-2U tokamak [DE94-718978] p 4338 N94-36247
On the physics of waves in the solar atmosphere: Wave heating and wind acceleration [NASA-CR-194119] p 4375 N94-36395
HEAVY ELEMENTS
Stellar alchemy: The origin of the chemical elements [DE94-011903] p 4350 N94-36229
HEAVY IONS
ILSE combiner study [DE94-011009] p 4331 N94-36202
HELICAL WINDINGS
Review of slow-wave structures [NASA-TM-106639] p 4258 N94-35270
HELICOPTER DESIGN
EH101: A new helicopter capable of long range missions p 4194 N94-36330
HELICOPTERS
Selected topics on the active control of helicopter aeromechanical and vibration problems p 4200 N94-35874
EH101: A new helicopter capable of long range missions p 4194 N94-36330
HELIOSPHERE
Catalog of Helios 90 deg photometer events [PL-TR-94-2040] p 4375 N94-36264
HELIOTRONS
LHD helical divertor [DE94-727626] p 4336 N94-35752
Particle orbit analysis for LHD helical axis configurations [DE94-718995] p 4336 N94-35773
Neoclassical current and related MHD stability, gap modes, and radial electric field effects in heliotron and torsatron plasmas [DE94-718987] p 4337 N94-35938
Improved models of beta-limit, anomalous transport and radial electric field with loss cone loss in heliotron/torsatron [DE94-718976] p 4324 N94-35984
Design study of LHD helical divertor and high temperature divertor plasma operation [DE94-718975] p 4338 N94-36352
MHD and confinement characteristics in the high-beta regime on the CHS low-aspect-ratio heliotron/torsatron [DE94-718981] p 4339 N94-36357
HELIUM
State-to-state dynamics of molecular energy transfer [DE94-009651] p 4324 N94-35816
First measurement of helium on Mars: Implications for the problem of radiogenic gases on the terrestrial planets p 4370 N94-36153
Primordial nucleosynthesis in conformal Weyl gravity [DE94-003002] p 4327 N94-36241
HELIUM ISOTOPES
Spatio-temporal properties of centrifugal instabilities: Abstracts of 8th Couette-Taylor Meeting [PB94-150240] p 4266 N94-35981
Dissociative recombination of stored and phase-spaced cooled molecular ions in CRYRING [DE94-002459] p 4327 N94-36267
Elastic p(4)He scattering at intermediate energies [DE94-618544] p 4328 N94-36287
HEMATITE
High resolution visible to short-wave near-infrared CCD spectra of Mars during 1990 p 4356 N94-35403
High Resolution Transmission Electron Microscopy (HRTEM) of nanophase ferric oxides p 4239 N94-35433
Transmission measurements (4000-400 cm(exp -1), 2.5-25 microns) of crystalline ferric oxides and ferric oxyhydroxides: Implications for Mars p 4292 N94-35454
Hematite formed from pyroxene on Mars by meteoritic impact p 4372 N94-36165
HERMETIC SEALS
Designing aluminum sealing glasses for manufacturability [DE94-010081] p 4244 N94-35699
HETEROGENEITY
Reformulating query plans for multidatabase systems [AD-A278688] p 4345 N94-35663
A note on high order schemes for one dimensional wave equation [PB94-171006] p 4315 N94-35821
Estimation with multisensor/multiscan detection fusion [AD-A278753] p 4256 N94-36092
The relationship between hydroxyl groups on oxide surfaces and the properties of supported metals [DE94-010786] p 4241 N94-36233
Heterogeneous catalytic process for alcohol fuels from syngas [DE94-010263] p 4248 N94-36299
HIERARCHIES
Parallel algorithms for LU decomposition on a shared memory multiprocessor [PB94-167798] p 4314 N94-35531
Priorities and nonmonotonic reasoning [PB94-171170] p 4346 N94-35959
HIGGS BOSONS
Universal SU(2/1) and the Higgs and fermion masses [DE94-009182] p 4323 N94-35814
HIGH ALTITUDE
High Altitude Long Endurance aircraft design studies p 4193 N94-36322
Technological challenges of High Altitude Long Endurance unmanned configurations p 4193 N94-36323
HIGH ENERGY INTERACTIONS
Proceedings of 2nd Working meeting: Physics at VLEPP, volume 1 [DE94-616200] p 4320 N94-35569
Spin effects in high energy quark-quark scattering [DE94-616800] p 4330 N94-36080
HIGH FREQUENCIES
The new features of Ion Bernstein Wave Heating in JIPP T-2U tokamak [DE94-718978] p 4338 N94-36247
Measurements of spatial and frequency coherence of an equatorial hf path during spread-F [DE93-016615] p 4257 N94-36316
HIGH POWER LASERS
High power diode laser Master Oscillator-Power Amplifier (MOPA) [NASA-CR-196095] p 4271 N94-35488
Progress in the production of samples of gamma ray laser candidate materials [AD-A278961] p 4272 N94-35721
Specification for the TITANIA krF laser system [PB94-167103] p 4272 N94-36062

HIGH PRESSURE
Structures and properties of materials recovered from high shock pressures
[DE94-010057] p 4232 N94-35696
X ray and gamma ray spectroscopy of solids under pressure
[DE94-011207] p 4238 N94-36203
Effects of 5 MPa heliox pressure on dopaminer gic pathway: An in vivo neurochemical study
[PB94-170693] p 4297 N94-36220
Equations of state valid continuously from zero to extreme pressures with H2O and CO2 as examples
[DE94-011907] p 4238 N94-36230
Electrical conductivity of hydrogen shocked to megabar pressures
[DE93-019632] p 4238 N94-36237
Portable high precision pressure transducer system
[DE94-010137] p 4270 N94-36389

HIGH RESOLUTION
High spatial resolution telescopic multispectral imaging and spectroscopy of the Moon. 1: The Serenitatis/Tranquillitatis border region
p 4356 N94-35402
High resolution visible to short-wave near-infrared CCD spectra of Mars during 1990 p 4356 N94-35403
Absolute calibration and atmospheric versus mineralogic origin of absorption features in 2.0 to 2.5 micron Mars spectra obtained during 1993 p 4356 N94-35404
First Galileo image of asteroid 243 Ida
p 4351 N94-35416
High Resolution Transmission Electron Microscopy (HRTEM) of nanophase ferric oxides
p 4239 N94-35433
A 1- to 10-GHz downconverter for high-resolution microwave survey p 4253 N94-35551
High-resolution subsurface imaging and neural network recognition
[DE94-009546] p 4290 N94-35666
High-resolution imaging using Z-contrast Scanning Transmission Electron Microscopy
[DE94-008510] p 4333 N94-36055
A survey of reflectometry techniques with applications to TFTR
[DE94-010202] p 4338 N94-36093
Determination of grain boundary volume expansion by HREM
[DE94-010452] p 4241 N94-36231
The iWarp display module
[AD-A278610] p 4260 N94-36248
Hubble Space Telescope Goddard High Resolution Spectrograph (GHRS) Instrument Handbook (for the Post-COSTAR Observatory), version 5.0
[NASA-CR-189369] p 4349 N94-36282

HIGH REYNOLDS NUMBER
A multilevel adaptive projection method for unsteady incompressible flow
[DE93-016418] p 4267 N94-36315

HIGH SPEED
High-speed digital project, HSD test capability
[DE94-010885] p 4260 N94-36197

HIGH SPEED PHOTOGRAPHY
Debris/ice/TPS assessment and integrated photographic analysis for Shuttle Mission STS-59
[NASA-TM-109203] p 4211 N94-35523
Transformation of a Cranz-Schardin camera
[PB94-170685] p 4270 N94-36219

HIGH STRENGTH
Tough, processable semi-interpenetrating polymer networks from monomer reactants
[NASA-CASE-LAR-14838-1] p 4242 N94-35233

HIGH STRENGTH STEELS
Transformation plasticity in ductile solids
[DE94-010420] p 4240 N94-35953

HIGH TEMPERATURE
Experimental and theoretical studies of a high temperature cesium-barium tacitron, with application to low voltage-high current inversion
[DE94-008182] p 4228 N94-35349
Processing and properties of high temperature metal/fiber-reinforced-thermoplastic laminates
[AD-A278791] p 4232 N94-35654
Thermodynamic behaviour of tellurium at high temperatures
[DE94-612823] p 4240 N94-35960
Effect of niobium interlayer on high-temperature sliding friction and wear of silver films on alumina
[DE94-010462] p 4275 N94-36232
High temperature creep and oxidation resistant chromium silicide matrix alloy containing molybdenum
[NASA-CASE-LEW-15697-1] p 4241 N94-36275
Wear-resisting oxide films for 900 C
[DE94-010093] p 4246 N94-36306
High temperature heterojunction bipolar transistors
[AD-A278605] p 4261 N94-36360

HIGH TEMPERATURE ENVIRONMENTS
High temperature sorbents for oxygen
[NASA-CASE-NPO-18409-1-CU] p 4235 N94-35255

HIGH TEMPERATURE PLASMAS
LHD helical divertor
[DE94-727626] p 4336 N94-35752
A triggering mechanism of fast crash in sawtooth oscillation
[DE94-718974] p 4336 N94-35772
Hot-ion plasma in the quadrupole trap
[DE94-617216] p 4337 N94-36082
Design study of LHD helical divertor and high temperature divertor plasma operation
[DE94-718975] p 4338 N94-36352
High temperature heterojunction bipolar transistors
[AD-A278605] p 4261 N94-36360
New calculations of Fe spectra in high-temperature plasmas
[DE94-009919] p 4339 N94-36386

HIGH TEMPERATURE SUPERCONDUCTORS
Advanced technology lunar telescope
p 4350 N94-35473
Report on a SQUID made from high temperature superconductor
[PB94-169307] p 4339 N94-35598
Structures and properties of materials recovered from high shock pressures
[DE94-010057] p 4232 N94-35696
Flywheel energy storage using superconducting magnetic bearings
[DE94-009817] p 4282 N94-35829
High temperature superconductors for magnetic suspension applications p 4214 N94-35843
Measurement and characterization of force dynamics in high T(sub c) superconductors p 4214 N94-35844
Superconducting rebalance acceleration and rate sensor p 4223 N94-35904
Concepts of flywheels for energy storage using autostable high-T(sub c) superconducting magnetic bearings p 4224 N94-35909
Twin spacing versus size of a monocrystal for the nonstoichiometric 1:2:3 superconductors
[DE94-615511] p 4340 N94-36029
About mid-infrared optical spectrum of high-Tc superconducting compounds
[DE94-615646] p 4340 N94-36030
Twin spacing and the structural phase transitions in 1:2:3 high-Tc superconductors
[DE94-615647] p 4340 N94-36041
Temperature dependence of superconduction bands in HTSC
[DE94-617361] p 4341 N94-36312
Flux-pinning related defects in YBa2Cu3O(7-x) thin films grown on miscut LaAlO3 (001) substrates
[DE94-011463] p 4342 N94-36377

HIGH VACUUM
Digital control programmer for temperature control
[DE94-615584] p 4309 N94-36382

HIGH VOLTAGES
Study of point defect mobilities in zirconium during electron irradiation in a HVEM
[DE94-619028] p 4242 N94-36289

HILSCH TUBES
Vortex tubes in turbulent flows: Identification, representation, reconstruction
[NASA-CR-194900] p 4267 N94-35992

HISTOGRAMS
The capacity of color histogram indexing
[AD-A279031] p 4345 N94-35732

HISTORIES
Space educators' handbook
[NASA-TM-109779] p 4343 N94-35339
Space and the American imagination
[NASA-CR-196131] p 4376 N94-35356
Apollo 11 at twenty-five, version 1.0
[NASA-CR-193380] p 4376 N94-35363
Introduction to USRA
[NASA-CR-195980] p 4376 N94-35590
A biased historical perspective of women in the engineering field at Dryden from 1946 to November 1992 p 4251 N94-35967
In-flight simulation studies at the NASA Dryden Flight Research Facility p 4198 N94-35969
The history of space exploration
[NASA-TM-109888] p 4201 N94-36440

HOLES (ELECTRON DEFICIENCIES)
Enhanced charge trapping in bipolar spacer oxides during low-dose-rate irradiation
[DE94-007863] p 4260 N94-36268

HOLLOW CATHODES
Analysis of recent agile mirror data
[AD-A278758] p 4318 N94-36427

HOMOGENEOUS TURBULENCE
Dynamic and thermal turbulent time scale modelling for homogeneous shear flows
[NASA-TM-106635] p 4263 N94-35253
K-epsilon model of anomalous transport in resistive interchange turbulence
[DE94-718983] p 4337 N94-35937

HORIZONTAL FLIGHT
Computation of helicopter rotor acoustics in forward flight
[NASA-CR-196132] p 4319 N94-36031

HOT CORROSION
Hot Corrosion Test Facility at the NASA Lewis Special Projects Laboratory
[NASA-CR-195323] p 4200 N94-35267

HOVERING
Tipjet 80-inch model rotor hover test: Test no. 1198
[AD-A279680] p 4191 N94-36261

HUBBLE SPACE TELESCOPE
Design and simulation of EVA tools for first servicing mission of HST
[NASA-CR-196030] p 4298 N94-35266
Fixed-head star tracker attitude updates on the Hubble Space Telescope p 4203 N94-35612
In-flight scale/distortion calibration of the Hubble Space Telescope fixed-head star trackers
p 4203 N94-35613
A long-baseline method for HST gyro drift rate bias calibration p 4203 N94-35614
The in-flight calibration of the Hubble Space Telescope fine guidance sensors, 2 (a success story)
p 4204 N94-35615
Hubble Space Telescope cycle 5 call for proposals
[NASA-CR-189363] p 4349 N94-36279
HST archive primer, version 4.1
[NASA-CR-189370] p 4349 N94-36280
Hubble Space Telescope Fine Guidance Sensors Instrument Handbook, version 4.0
[NASA-CR-189366] p 4349 N94-36281
Hubble Space Telescope Goddard High Resolution Spectrograph (GHRS) Instrument Handbook (for the Post-COSTAR Observatory), version 5.0
[NASA-CR-189369] p 4349 N94-36282

HUMAN BEINGS
Further studies of 60-Hz exposure effects on human function
[DE94-010192] p 4297 N94-36223

HUMAN CENTRIFUGES
A database to evaluate acceleration (+Gz) induced loss of consciousness (G-LOC) in the human centrifuge
[AD-A278769] p 4299 N94-35707

HUMAN FACTORS ENGINEERING
International Space Station alpha remote manipulator system workstation controls test report
[NASA-TM-104796] p 4274 N94-35481
The influence of data link-provided graphical weather on pilot decision-making
[AD-A278871] p 4293 N94-35596
The prediction of pilot opinion ratings using optimal and sub-optimal pilot models
[AD-A278679] p 4298 N94-35692
Bibliography of research reports and publications issued by the Human Engineering Division
[AD-A278787] p 4299 N94-35712
Final-Approach Spacing Aids (FASA) evaluation for terminal-area, time-based air traffic control
[NASA-TP-3399] p 4192 N94-36048
Review of human factors problems related to long distance and long endurance operation of aircraft
p 4195 N94-36336

HUMAN REACTIONS
The prediction of pilot opinion ratings using optimal and sub-optimal pilot models
[AD-A278679] p 4298 N94-35692

HUMAN RESOURCES
Women as a resource for the flexibility required for high technology innovation p 4348 N94-35966

HUMAN-COMPUTER INTERFACE
A software architecture for adding new interaction techniques to a command and control based testbed
[AD-A278760] p 4302 N94-35491
The influence of data link-provided graphical weather on pilot decision-making
[AD-A278871] p 4293 N94-35596
MMI(exp 2) demonstrator systems: A multi-modal interface for man machine interaction with knowledge based systems. Deliverable D17 (TA 2) ESPRIT project 2474 MMI(exp 2)
[PB94-170537] p 4298 N94-35600
Multi-window dialogue system of data processing for experimental setup VASSILISSA in PAW environment
[DE94-612439] p 4345 N94-35790
North American ISDN Users' Forum agreements on Integrated Services Digital Network
[PB94-162559] p 4305 N94-35940
An environment for visualization, reliability, and knowledge acquisition in equational programming
[AD-A278639] p 4308 N94-36258

HURRICANES
Doppler weather radar studies of precipitation systems
[AD-A279417] p 4295 N94-36262

HYBRID PROPULSION
Bus application of oxygen-enrichment technology and diesel-electric hybrid systems
[DE94-009835] p 4285 N94-35765

HYDRATES
Be3(AsO4)2.2H2O, a new berylloarsenate phase containing bridged tetrahedral 3-rings
[AD-A278826] p 4340 N94-35677

HYDRATION
A quick look method of detecting water of hydration in small solar system bodies p 4352 N94-35470

HYDRAULIC EQUIPMENT
Separation tool for multipin electrical connectors
[NASA-CASE-NPO-18786-1-CU] p 4274 N94-35375

HYDRIDES
Measurement of the decay rate of the SiH feature as a function of temperature p 4318 N94-36171
Dissociative recombination of stored and phase-spaced cooled molecular ions in CRYRING
[DE94-002459] p 4327 N94-36267

HYDROCARBON COMBUSTION
Detailed studies of soot formation in laminar diffusion flames for application to modeling studies
[AD-A278941] p 4235 N94-35604
Infrared multiphoton ignition and combustion enhancement of natural gas.
[PB94-165438] p 4236 N94-35755
A new comprehensive reaction mechanism for combustion of hydrocarbon fuels
[DE94-008288] p 4238 N94-36205

HYDROCARBON FUELS
The effect of alternative fuels on the stability and lubricity of crankcase lubricants
[DE94-010353] p 4245 N94-36108
A new comprehensive reaction mechanism for combustion of hydrocarbon fuels
[DE94-008288] p 4238 N94-36205

HYDROCARBONS
Morphological aspects of surface reactions
[DE94-010184] p 4236 N94-35685
A new association-model for binary VLE of alcohol/hydrocarbon and amine/hydrocarbon mixtures
[DE94-011012] p 4248 N94-36034

HYDRODYNAMICS
Experimental studies of very-high Mach number hydrodynamics
[AD-A278761] p 4263 N94-35492
Solitary waves and homoclinic orbits
[DE94-009428] p 4264 N94-35681
Hydrodynamically induced loads on components submerged in high-level waste-storage tanks
[DE94-009663] p 4264 N94-35756
Hydrodynamics of maneuvering bodies: LDRD Final Report
[DE94-009970] p 4265 N94-35769
X ray radiographic imaging of hydrodynamic phenomena in radiation driven materials: Shock propagation, material compression and shear flow
[DE94-009515] p 4266 N94-35982
Boson spectra and correlations in thermal locally equilibrium systems
[DE94-616799] p 4325 N94-36079
A comparison of artificial neural networks and statistical analyses
[DE94-010846] p 4312 N94-36195
X ray radiographic imaging of hydrodynamic phenomena in radiation driven materials: Shock propagation and shear flow
[DE94-010891] p 4318 N94-36201
Taking into account dissipative processes in relativistic superfluid systems
[DE94-617391] p 4267 N94-36313

HYDROGEN
A two-dimensional model for collisional energy transfer in bimolecular ion-molecule dynamics
[AD-A278913] p 4321 N94-35589
Theoretical and experimental study of air and hydrogen electrodes
[DE94-763308] p 4283 N94-36060
Ferromagnetic resonance spectra of H2-reduced minerals and glasses p 4240 N94-36164
Electrical conductivity of hydrogen shocked to megabar pressures
[DE93-019632] p 4238 N94-36237
Primordial nucleosynthesis in conformal Weyl gravity
[DE94-003002] p 4327 N94-36241

HYDROGEN BONDS
Structural investigations of 1-ethyl-3-methylimidazolium hydrogen dichloride: Neutron diffraction studies of an ambient-temperature molten salt
[DE94-009680] p 4237 N94-35777

HYDROGEN EMBRITTLEMENT
Investigation of moisture-induced embrittlement of iron aluminides
[DE94-010881] p 4241 N94-36196

HYDROGEN IONS
Dissociative recombination of stored and phase-spaced cooled molecular ions in CRYRING
[DE94-002459] p 4327 N94-36267

HYDROLYSIS
Cross-condensation reactions in an organically modified silica sol-gel
[DE94-010086] p 4244 N94-35701
Spinnability of silica sols: The role of alkoxy group exchange
[DE94-010087] p 4244 N94-35702

HYDROTHERMAL CRYSTAL GROWTH
Be3(AsO4)2.2H2O, a new berylloarsenate phase containing bridged tetrahedral 3-rings
[AD-A278826] p 4340 N94-35677

HYDROTHERMAL SYSTEMS
Exopaleontology and the search for a fossil record on Mars p 4360 N94-35425

HYDROXIDES
High Resolution Transmission Electron Microscopy (HRTEM) of nanophase ferric oxides
p 4239 N94-35433
Transmission measurements (4000-400 cm(exp -1), 2.5-25 microns) of crystalline ferric oxides and ferric oxyhydroxides: Implications for Mars
p 4292 N94-35454

HYPERBOLIC FUNCTIONS
Optimal disturbance rejecting control of hyperbolic systems p 4220 N94-35882

HYPERCUBE MULTIPROCESSORS
Task allocation for parallel real-time execution
[AD-A278789] p 4310 N94-35653

HYPERONS
Sigma minus-nucleus interactions in emulsion at 350 GeV
[DE94-616886] p 4326 N94-36130

HYPERSONIC FLOW
A review and development of correlations for base pressure and base heating in supersonic flow
[SAND93-0280] p 4189 N94-35360
Development and application of computational aerothermodynamics flowfield computer codes
[NASA-CR-196136] p 4189 N94-35498
Investigation of Burnett equations for two-dimensional hypersonic flow
[AD-A278942] p 4190 N94-35717

HYPERSONIC SHOCK
Investigation of Burnett equations for two-dimensional hypersonic flow
[AD-A278942] p 4190 N94-35717

HYPERSONIC SPEED
Future ultra-speed tube-flight p 4225 N94-35918

HYPERSONIC VEHICLES
A review and development of correlations for base pressure and base heating in supersonic flow
[SAND93-0280] p 4189 N94-35360

HYPERSONICS
Investigation of Burnett equations for two-dimensional hypersonic flow
[AD-A278942] p 4190 N94-35717

HYPERVELOCITY IMPACT
Radiative signals from impact of Shoemaker-Levy on Jupiter p 4355 N94-35396
Purity and cleanness of aerogel as a cosmic dust capture medium p 4247 N94-35469
Experimental impacts into Teflon targets and LDEF thermal blankets p 4352 N94-36141
Hematite formed from pyroxene on Mars by meteoritic impact p 4372 N94-36165

HYPERVELOCITY PROJECTILES
Morphology of meteoroid and space debris craters on LDEF metal targets p 4353 N94-36159

HYSTERESIS
Structures and properties of materials recovered from high shock pressures
[DE94-010057] p 4232 N94-35696
Superconducting rebalance acceleration and rate sensor p 4223 N94-35904

I

ICE
The structural changes of water ice I during warmup
p 4239 N94-36144

ICE ENVIRONMENTS
Antarctic weathering of the CK chondrites EET90004, 90007, and 90022: Nickel and sulfur mobility
p 4351 N94-35451
Environmental measurements in the Beaufort Sea, Spring 1993
[AD-A278718] p 4296 N94-36293

ICE FLOES
Environmental measurements in the Beaufort Sea, Spring 1993
[AD-A278718] p 4296 N94-36293

ICE FORMATION
Debris/ice/TPS assessment and integrated photographic analysis for Shuttle Mission STS-59
[NASA-TM-109203] p 4211 N94-35523

IDAHO
Environmental resource document for the Idaho National Engineering Laboratory, volume 1
[DE94-008522] p 4287 N94-36207
Environmental resource document for the Idaho National Engineering Laboratory, volume 2
[DE94-008523] p 4287 N94-36208

IDENTIFYING
Developing interpretable models with optimized set reduction for identifying high risk software components
p 4301 N94-35435

IDENTITIES
Identity for propagator in four-fermion theory
[DE94-611104] p 4342 N94-35781
Recent progress in irrational conformal field theory
[DE94-011908] p 4317 N94-36234

IGNEOUS ROCKS
Thermal emission measurements (5-25 microns) of Hawaiian palagonitic soils with implications for Mars
p 4292 N94-35452
The parent magma of xenoliths in shergottite EETA79001: Bulk and trace element composition inferred from magmatic inclusions p 4352 N94-35467

IGNITION
Infrared multiphoton ignition and combustion enhancement of natural gas.
[PB94-165438] p 4236 N94-35755
A comparison between direct spark ignition and prechamber ignition in an internal combustion engine
[DE94-008218] p 4275 N94-36206
The reaction of hydroperoxy-propyl radicals with molecular oxygen
[DE94-006392] p 4239 N94-36319
Effects of natural gas composition on ignition delay under diesel conditions
[DE94-006405] p 4276 N94-36378

ILLUMINATING
Color center laser with transverse auxiliary illumination
[AD-D016201] p 4273 N94-36365

ILMENITE
Reduction of lunar mare soil and pyroclastic glass
p 4355 N94-35398
Lunar mineral feedstocks from rocks and soils: X-ray digital imaging in resource evaluation
p 4358 N94-35415
Grain rims on ilmenite in the lunar regolith: Comparison to vapor deposits on regolith silicates
p 4359 N94-35418
Mossbauer and spectral (visible and near-IR) data for Fe(3+)-substituted rutile p 4240 N94-36154

IMAGE ANALYSIS
Modeling of the magnetosphere-ionosphere-atmosphere system
[NASA-CR-195157] p 4288 N94-35244
Computer image analysis of etched tracks from ionizing radiation
[NASA-CR-196025] p 4319 N94-35264
Measuring track densities in lunar grains using image analysis p 4357 N94-35409
First Galileo image of asteroid 243 Ida
p 4351 N94-35416

IMAGE CLASSIFICATION
The effects of cloud inhomogeneities upon radiative fluxes, and the supply of a cloud truth validation dataset
[NASA-CR-196080] p 4293 N94-35391

IMAGE ENHANCEMENT
Subpixel resolution from multiple images
p 4281 N94-35417
Reduction procedures for accurate analysis of MSX surveillance experiment data p 4203 N94-35611

IMAGE PROCESSING
Subpixel resolution from multiple images
p 4281 N94-35417
Unsteady structure of leading-edge vortices on a delta wing
[AD-A278988] p 4190 N94-35529
Evaluation of synthetic aperture radar for oil-spill response
[AD-A278796] p 4284 N94-35674
The polygon-ellipse method of data compression of weather maps
[AD-A278958] p 4293 N94-35719
Task and environment-sensitive tracking
[AD-A278846] p 4312 N94-35802
The CMU task parallel program suite
[AD-A278951] p 4311 N94-36015

Combining nonlinear multiresolution system and vector quantization for still image compression
[DE94-009422] p 4305 N94-36017

Estimation of fractal dimensions from transect data
[DE94-009808] p 4281 N94-36018

X ray radiographic imaging of hydrodynamic phenomena in radiation driven materials: Shock propagation and shear flow
[DE94-010891] p 4318 N94-36201

Error reduction in images with the use of additional information
[AD-A278636] p 4334 N94-36257

IMAGE RESOLUTION

Combining nonlinear multiresolution system and vector quantization for still image compression
[DE94-009422] p 4305 N94-36017

IMAGERY

The capacity of color histogram indexing
[AD-A279031] p 4345 N94-35732

IMAGING TECHNIQUES

Plasma arc welding weld imaging
[NASA-CASE-MFS-28797-1] p 4273 N94-35367

Lunar mineral feedstocks from rocks and soils: X-ray digital imaging in resource evaluation
p 4358 N94-35415

Obtaining coincident image observations for Mission to Planet Earth science data return p 4202 N94-35609

In-flight scale/distortion calibration of the Hubble Space Telescope fixed-head star trackers
p 4203 N94-35613

High-resolution subsurface imaging and neural network recognition
[DE94-009546] p 4290 N94-35666

Evaluation of synthetic aperture radar for oil-spill response
[AD-A278796] p 4284 N94-35674

Extraction of cloud statistics from whole sky imaging cameras
[DE94-009867] p 4294 N94-35766

The computation of cloud base height from paired whole-sky imaging cameras
[DE94-009868] p 4294 N94-35767

High-resolution imaging using Z-contrast Scanning Transmission Electron Microscopy
[DE94-008510] p 4333 N94-36055

NMR imaging of components and materials for DOE application
[DE94-010664] p 4238 N94-36084

Petrographic characterization of lunar soils: Application of x ray digital-imaging to quantitative and automated analysis p 4368 N94-36138

X ray radiographic imaging of hydrodynamic phenomena in radiation driven materials: Shock propagation and shear flow
[DE94-010891] p 4318 N94-36201

Recursive recovery of Markov transition probabilities from boundary value data
[DE94-011914] p 4317 N94-36235

Method and apparatus for imaging an object in or through a scattering medium by using multiple-wave mixing
[AD-D016212] p 4334 N94-36368

IMPACT DAMAGE

The surface and interior of Phobos
p 4355 N94-35400

Craters in aluminum 1100 targets using glass projectiles at 1-7 km/s p 4280 N94-35407

Energy partitioning in high speed impact of analog solid rocket motors
[AD-A278771] p 4228 N94-35825

Experimental impacts into Teflon targets and LDEF thermal blankets p 4352 N94-36141

IMPACT LOADS

More shock recovery experiments on mesosiderite analogs p 4351 N94-35455

Energy partitioning in high speed impact of analog solid rocket motors
[AD-A278771] p 4228 N94-35825

IMPACT MELTS

Single agglutinates: A comparative study of compositions of agglutinitic glass, whole-grain, bulk soil, and FMR p 4355 N94-35401

Distribution of siderophile and other trace elements in melt rock at the Chicxulub impact structure
p 4352 N94-35456

Hematite formed from pyroxene on Mars by meteoritic impact p 4372 N94-36165

IMPACT TESTS

Craters in aluminum 1100 targets using glass projectiles at 1-7 km/s p 4280 N94-35407

IMPACTORS

Impact basins in Southern Daedalia, Mars: Evidence for clustered impactors? p 4360 N94-35426

Morphology of meteoroid and space debris craters on LDEF metal targets p 4353 N94-36159

IMPEDANCE

Active antenna
[NASA-CASE-GSC-13309-1] p 4251 N94-35231

IMPEDANCE MATCHING

Thin-ribbon tapered coupler for dielectric waveguides
p 4253 N94-35547

IMPEDANCE MEASUREMENT

Impedance and instability threshold estimates in the main injector 1
[DE94-010332] p 4332 N94-36431

IMPINGEMENT

Numerical simulation of shock interaction with above-ground structures
[AD-A278713] p 4279 N94-35949

IMPLOSIONS

High density implosion experiments at Nova
[DE94-010894] p 4339 N94-36375

IMPURITIES

Power balance and characterization of impurities in the Maryland Spheromak, part 2
[DE94-009603] p 4335 N94-35670

Ionic contamination detection
[DE94-010212] p 4258 N94-35686

The new features of Ion Bernstein Wave Heating in JIPP T-2U tokamak
[DE94-718978] p 4338 N94-36247

INCIDENCE

Improved performance of degraded solar arrays at non-zero sun incidence angles
[AD-A278905] p 4282 N94-35804

INCLUSIONS

Inhomogeneous distribution of materials in lodranites-acapulcoites and IAB irons and their common formation processes p 4364 N94-35463

INCOMPRESSIBLE FLOW

A multilevel adaptive projection method for unsteady incompressible flow
[DE93-016418] p 4267 N94-36315

An equal-order approximate projection FEM
[DE94-010101] p 4268 N94-36374

Numerical investigation of multi-element airfoils
[NASA-CR-194592] p 4191 N94-36394

INDEXES (DOCUMENTATION)

Aeronautical engineering: A continuing bibliography with indexes (supplement 306)
[NASA-SP-7037(306)] p 4189 N94-35338

Aerospace medicine and biology: A continuing bibliography with indexes (supplement 391)
[NASA-SP-7011(391)] p 4297 N94-35345

The capacity of color histogram indexing
[AD-A279031] p 4345 N94-35732

NASA Thesaurus. Volume 1: Hierarchical listing. Volume 2: Access vocabulary. Volume 3: Definitions
[NASA-SP-7096-VOL-1/2/3] p 4346 N94-36037

INDIAN OCEAN

Optimum satellite relay positions with application to a TDRS-1 Indian Ocean relay p 4205 N94-35624

INDIUM ARSENIDES

InP solar cell with window layer
[NASA-CASE-LEW-15606-1] p 4281 N94-35230

INDIUM COMPOUNDS

Vertical electron detachment energies for octahedral closed-shell multiply charged anions
[AD-A278835] p 4322 N94-35753

INDIUM PHOSPHIDES

Au/Zn contacts to Rho-InP: Electrical and metallurgical characteristics and the relationship between them
[NASA-TM-106590] p 4281 N94-35271

High-power CW operation of AlGaInP diode-laser arrays
[DE94-010409] p 4272 N94-36115

INDUCTION HEATING

Consolidation of zircaloy-4 end crops by induction melting
[DE94-010031] p 4240 N94-35650

INDUCTION MOTORS

Maglev crude oil pipeline p 4226 N94-35919

INDUCTORS

Optimization of turn position of tokamak inductor
[DE94-612627] p 4336 N94-35791

INDUSTRIES

National Geoscience Data Repository System
[DE94-000120] p 4344 N94-35347

Building on the foundation for an engineering career
p 4343 N94-35973

University participation in the ATS program
[DE94-003191] p 4275 N94-36022

INELASTIC SCATTERING

QCD parametrizations of the parton distribution of deep inelastic scattering
[DE94-616660] p 4325 N94-36074

Sigma minus-nucleus interactions in emulsion at 350 GeV
[DE94-616886] p 4326 N94-36130

High energy asymptotics of perturbative multi-color QCD
[DE94-001350] p 4327 N94-36238

INEQUALITIES

Successive minima on arithmetic varieties
[PB94-167699] p 4314 N94-35759

Height inequality for holomorphic curves
[PB94-167731] p 4314 N94-35762

The relativistic invariant and the Galilean mass of bodies
[DE94-616615] p 4318 N94-35956

INERTIA

The relativistic invariant and the Galilean mass of bodies
[DE94-616615] p 4318 N94-35956

INERTIAL CONFINEMENT FUSION

Inertial confinement fusion target component fabrication and technology development report
[DE94-009973] p 4335 N94-35673

Proceedings of the LLNL Technical Women's Symposium
[DE94-006616] p 4379 N94-35997

Neutron detectors for fusion reaction-rate measurements
[DE94-010407] p 4330 N94-36114

Inertial confinement fusion
[DE94-010835] p 4338 N94-36193

Beam transport
[DE94-010755] p 4331 N94-36199

INFILTRATION

Thermal performance of residential duct systems in basements
[LBL-33962] p 4250 N94-35364

INFORMATION DISSEMINATION

NASA/DOD Aerospace Knowledge Diffusion Research Project. Paper 40: Technical communications in aerospace education: A study of AIAA student members
[NASA-TM-109868] p 4344 N94-35254

Exploring hypermedia information services for disseminating software engineering information
[AD-A278765] p 4302 N94-35495

Computer Systems Laboratory
[PB94-162518] p 4333 N94-36002

INFORMATION FLOW

Synthesis of asynchronous systems from data flow specifications
[AD-A278687] p 4303 N94-35662

INFORMATION MANAGEMENT

COSMIC monthly progress report
[NASA-CR-195962] p 4302 N94-35514

INFORMATION PROCESSING (BIOLOGY)

Multidisciplinary studies of integrated neural network systems
[AD-A278774] p 4312 N94-36309

INFORMATION RETRIEVAL

Defense RDT and E online system (DROLS) retrieval reference guide
[AD-A278972] p 4344 N94-35525

Asynchronous optimistic rollback recovery using secure distributed time
[AD-A278978] p 4344 N94-35526

NASA Thesaurus. Volume 1: Hierarchical listing. Volume 2: Access vocabulary. Volume 3: Definitions
[NASA-SP-7096-VOL-1/2/3] p 4346 N94-36037

INFORMATION SYSTEMS

Exploring hypermedia information services for disseminating software engineering information
[AD-A278765] p 4302 N94-35495

ORDIT: A new methodology to assist in the process of eliciting and modelling organisational requirements
[PB94-167814] p 4345 N94-35533

Proceedings of the 4th Workshop on the Next Generation of CASE Tools
[PB94-150372] p 4302 N94-35538

The Telecommunications and Data Acquisition Report
[NASA-CR-196117] p 4252 N94-35542

The development of a statistical report software for computer system usages
[DE94-611061] p 4346 N94-35832

HST archive primer, version 4.1
[NASA-CR-189370] p 4349 N94-36280

INFRARED ABSORPTION

A quick look method of detecting water of hydration in small solar system bodies p 4352 N94-35470

INFRARED DETECTORS

Development of ultra-low noise, high performance 3 to 5 Quantum Well Infrared Photodetectors (QWIPs) for focal plane array staring image sensor systems
[AD-A278861] p 4342 N94-36385

INFRARED IMAGERY

Production of long-term global water vapor and liquid water data set using ultra-fast methods to assimilate multi-satellite and radiosonde observations
[NASA-CR-196044] p 4292 N94-35355

Reduction procedures for accurate analysis of MSX surveillance experiment data p 4203 N94-35611

Development of ultra-low noise, high performance 3 to 5 Quantum Well Infrared Photodetectors (QWIPs) for focal plane array staring image sensor systems
[AD-A278861] p 4342 N94-36385

INFRARED INSPECTION
Recursive recovery of Markov transition probabilities from boundary value data
[DE94-011914] p 4317 N94-36235

INFRARED LASERS
Infrared multiphoton ignition and combustion enhancement of natural gas.
[PB94-165438] p 4236 N94-35755
Eyesafe rare earth crystal lasers for atmosphere soudings
[AD-A279486] p 4273 N94-36227

INFRARED PHOTOMETRY
A quick look method of detecting water of hydration in small solar system bodies p 4352 N94-35470

INFRARED RADIATION
Calculations on some properties of the pion in the framework of Schwinger-Dyson and Bethe-Salpeter equations
[DE94-611232] p 4322 N94-35786
Development of ultra-low noise, high performance 3 to 5 Quantum Well Infrared Photodetectors (QWIPs) for focal plane array staring image sensor systems
[AD-A278861] p 4342 N94-36385

INFRARED RADIOMETERS
Defect detection in multi-layered, plasma sprayed zirconia by time resolved infrared radiometry: A comparison between analytical and experimental methods
[DE94-009803] p 4245 N94-35779
A precise passive narrow-beam filter infrared radiometer and its use with LIDAR in the ARM program
[DE94-004167] p 4269 N94-36085

INFRARED SPECTRA
High resolution visible to short-wave near-infrared CCD spectra of Mars during 1990 p 4356 N94-35403
Thermal emission measurements (5-25 microns) of Hawaiian palagonitic soils with implications for Mars
p 4292 N94-35452
Thermal emission measurements (5-25 microns) of palagonite/Fe-substituted montmorillonite intimate mixtures: Applications to Mars p 4292 N94-35453
Transmission measurements (4000-400 cm(exp -1), 2.5-25 microns) of crystalline ferric oxides and ferric oxyhydroxides: Implications for Mars
p 4292 N94-35454
Ferromagnetic resonance spectra of H2-reduced minerals and glasses p 4240 N94-36164
On the effects of transforming the vibrational spectra of molecular systems under microwave radiation
[DE94-617057] p 4329 N94-36310

INFRARED SPECTROMETERS
Wavelength calibration techniques and subtle surface and atmospheric absorption features in the Mariner 6, 7 IRS reflectance data p 4356 N94-35405

INFRARED SPECTROSCOPY
High spatial resolution telescopic multispectral imaging and spectroscopy of the Moon. 1: The Serenitatis/Tranquillitatis border region
p 4356 N94-35402

INGOTS
Consolidation of zircaloy-4 end crops by induction melting
[DE94-010031] p 4240 N94-35650

INJECTORS
Advanced induction accelerator designs for ground based and space based FELs
[AD-A278885] p 4271 N94-35586
ILSE combiner study
[DE94-011009] p 4331 N94-36202
Impedance and instability threshold estimates in the main injector 1
[DE94-010332] p 4332 N94-36431

INKS
Thick film fabrication of aluminum nitride microcircuits
[DE94-010107] p 4259 N94-35706

INLET FLOW
Computational methods for HSCT-inlet controls/CFD interdisciplinary research
[NASA-TM-106618] p 4198 N94-35352

INSERTION LOSS
Characterization of lithium niobate electro-optic modulators at cryogenic temperatures
[DE94-010059] p 4333 N94-35697

INSPECTION
Debris/ice/TPS assessment and integrated photographic analysis for Shuttle Mission STS-59
[NASA-TM-109203] p 4211 N94-35523
Nondestructive Inspection (NDI) of reduced strength bonds
[AD-A278745] p 4278 N94-36090

INSTALLING
An analysis of file system and installation of the file management system for NOS operating system
[DE94-611062] p 4346 N94-35833
Calculations used to optimize the installation of civil aircraft engines p 4195 N94-36332

INSTANTONS
Moduli space of monopoles and some invariants of 3-manifolds
[PB94-167756] p 4314 N94-35764

INSTRUMENT ORIENTATION
Subpixel resolution from multiple images
p 4281 N94-35417

INTEGRAL CALCULUS
On a generalized bootstrap principle
[DE94-727517] p 4314 N94-35774

INTEGRATED CIRCUITS
JPRS report: Science and technology. Central Eurasia
[JPRS-UST-94-007] p 4249 N94-35227
Ionic contamination detection
[DE94-010212] p 4258 N94-35686
BJT model in APLAC
[PB94-171022] p 4259 N94-35822
Simulation of materials processing: Fantasy or reality?
p 4230 N94-36404

INTERACTING GALAXIES
Angular momentum in the Local Group
[DE94-009322] p 4350 N94-35980

INTERACTIVE CONTROL
A software architecture for adding new interaction techniques to a command and control based testbed
[AD-A278760] p 4302 N94-35491

INTERATOMIC FORCES
Modelling of the structure and physical properties of simple disordered systems
[DE94-617087] p 4329 N94-36311

INTERCALATION
A new family of superconducting fullerides, Na(NH3)(x)C60(x = 2-8)
[DE94-011480] p 4341 N94-36272

INTERFACES
Interfacing the RAP system to real-time control, version 1
[AD-A278725] p 4312 N94-36295

INTERFEROMETERS
Development of POINTS as a planetology instrument
[NASA-CR-196026] p 4354 N94-35265
Lunar LIGO and gravitational wave astronomy on the Moon p 4366 N94-35472
Correlator data analysis for the array feed compensation system p 4253 N94-35553
High-sensitivity receiver for increasing multiplicity of measurement axes of Zygo's Heterodyne interferometer
[DE94-009916] p 4333 N94-35818

INTERFEROMETRY
The real-time display of interferometry data for Goldstone radar astronomy data acquisition
p 4255 N94-35560
Application of a Monte Carlo accuracy assessment tool to TDRS and GPS p 4207 N94-35635
NAVSPACECOM space surveillance sensor system digital signal processing receiver. Volume 3: Operating system functions
[AD-A278839] p 4212 N94-35799
NAVSPACECOM space surveillance sensor system digital signal processing receiver. Volume 4: Hardware interfaces
[AD-A278845] p 4212 N94-35801

INTERIOR BALLISTICS
The 30th JANNAF Combustion Subcommittee Meeting, volume 1
[AD-A278793] p 4247 N94-35655

INTERLAYERS
Effect of niobium interlayer on high-temperature sliding friction and wear of silver films on alumina
[DE94-010462] p 4275 N94-36232

INTERMETALLICS
Advanced composites in Japan p 4234 N94-36045
Irradiation-related amorphization and crystallization: In situ transmission electron microscope studies
[DE94-009823] p 4241 N94-36222

INTERNAL COMBUSTION ENGINES
Analysis of the injection process in direct injected natural gas engines
[PB94-156494] p 4275 N94-35931
Carbon-carbon piston development
[NASA-CR-4595] p 4233 N94-35947
Advanced hydrogen/method utilization technology demonstration
[DE94-000214] p 4248 N94-36191
A comparison between direct spark ignition and prechamber ignition in an internal combustion engine
[DE94-008218] p 4275 N94-36206
Propulsion system selection for a High Altitude Long Endurance aircraft p 4195 N94-36333

INTERNAL WAVES
JPRS report: Science and technology. Central Eurasia
[JPRS-UST-94-006] p 4249 N94-35226

INTERNATIONAL COOPERATION
AGARD highlights 93/2
[AGARD-HIGHLIGHTS-93/2] p 4376 N94-35444
Partners in space. International cooperation in space: Strategies for the new century
[ISBN-0-9629930-2-6] p 4348 N94-35901

INTERNETS
The impact of scaling on a multimedia connection architecture
[AD-A278700] p 4300 N94-35652

INTERPLANETARY DUST
Application of an alkylammonium method for characterization of phyllosilicates in CI chondrites
p 4351 N94-35432
Anatomy of a cluster IDP. Part 2: Noble gas abundances, trace element geochemistry, isotopic abundances, and trace organic chemistry of several fragments from L2008#5 p 4352 N94-35465
The anatomy of a cluster IDP. Part 1: Carbon abundance, bulk chemistry, and mineralogy of fragments from L2008#5 p 4352 N94-35466
Low encounter speed comet COMA sample return missions p 4202 N94-35607
Dust evolution from comets and asteroids: Their velocities at Earth orbit intersection
p 4352 N94-36142
Electron energy-loss spectroscopy of carbon in interplanetary dust particles p 4353 N94-36149

INTERPLANETARY MAGNETIC FIELDS
Ionospheric plasma drift and structure studies at high and mid-latitudes
[AD-A279415] p 4291 N94-36116

INTERPLANETARY MEDIUM
Catalog of Helios 90 deg photometer events
[PL-TR-94-2040] p 4375 N94-36264

INTERPOLATION
Adaptive model reduction for continuous systems via recursive rational interpolation p 4219 N94-35876
Gauss elimination by segments and multivariate polynomial interpolation
[AD-A278646] p 4315 N94-36012

INTERPROCESSOR COMMUNICATION
Combining left and right unlinking for matching a large number of learned rules
[AD-A278979] p 4311 N94-35527
The rel/REL: A family of reliable multicast protocols for distributed real-time systems
[PB94-167830] p 4310 N94-35535
Probabilities and priorities in timed CSP
[PB94-169216] p 4316 N94-35536
Mathematical theory of synchronous communication
[PB94-169224] p 4252 N94-35537
Communication and memory requirements as the basis for mapping task and data parallel programs
[AD-A278954] p 4310 N94-35806

INTERSTELLAR MATTER
The structural changes of water ice I during warmup
p 4239 N94-36144

INTERSTITIALS
Microporous structure with layered interstitial surface treatment, and method and apparatus for preparation thereof
[NASA-CASE-MSC-21487-3] p 4235 N94-35229

INTRAMOLECULAR STRUCTURES
Intramolecular energy transfer reactions in polymetallic complexes
[DE94-010114] p 4326 N94-36126

INVARIANCE
Distance dependent fractional statistics in a P, T-invariant model
[DE94-617360] p 4325 N94-36083
T-odd, P-even photon-fermion interactions
[DE94-616869] p 4327 N94-36246

INVERSE KINEMATICS
Kinematic modeling of a double octahedral Variable Geometry Truss (VGT) as an extensible gimbal
[NASA-TM-109127] p 4311 N94-35242

INVERTERS
Experimental and theoretical studies of a high temperature cesium-barium tacitron, with application to low voltage-high current inversion
[DE94-008182] p 4228 N94-35349

INVISCID FLOW
Hydrodynamics of maneuvering bodies: LDRD Final Report
[DE94-009970] p 4265 N94-35769

ION ACCELERATORS
Beam transport
[DE94-010755] p 4331 N94-36199

ION BEAMS
Beam transport
[DE94-010755] p 4331 N94-36199

Effect of niobium interlayer on high-temperature sliding friction and wear of silver films cn alumina
[DE94-010462] p 4275 N94-36232
Design and construction of a imaging instrument for studying ion emission from pure ion emitters
[DE94-010702] p 4328 N94-36302

ION CURRENTS
Ionic contamination detection
[DE94-010212] p 4258 N94-35686
Ion modulated electroactivity in thin film metallopolymers
[AD-A278618] p 4246 N94-36253

ION CYCLOTRON RADIATION
Heating experiments using neutral beams with variable injection angle and ICRF waves in CHS
[DE94-718982] p 4337 N94-35936

ION DENSITY (CONCENTRATION)
Scaling laws for TEXT plasma profiles
[DE94-010832] p 4338 N94-36200

ION EMISSION
Design and construction of a imaging instrument for studying ion emission from pure ion emitters
[DE94-010702] p 4328 N94-36302

ION ENGINES
AFOSR Contractors Propulsion Meeting
[AD-A279028] p 4198 N94-35746

ION IMPLANTATION
Non-alloyed, refractory metal contact optimization with shallow implantations of Zn and Mg
[DE94-010392] p 4240 N94-36110
Proceedings of the Twenty-First All-Union Conference on Physics of Charged Particles Interaction with Crystals
[DE94-615768] p 4341 N94-36181

ION IRRADIATION
Irradiation-related amorphization and crystallization: In situ transmission electron microscope studies
[DE94-009823] p 4241 N94-36222

ION RECOMBINATION
Dissociative recombination of stored and phase-spaced cooled molecular ions in CRYRING
[DE94-002459] p 4327 N94-36267

ION SOURCES
Design and construction of a imaging instrument for studying ion emission from pure ion emitters
[DE94-010702] p 4328 N94-36302

ION TEMPERATURE
Hot-ion plasma in the quadrupole trap
[DE94-617216] p 4337 N94-36082
Scaling laws for TEXT plasma profiles
[DE94-010832] p 4338 N94-36200
The new features of Ion Bernstein Wave Heating in JIPP T-2U tokamak
[DE94-718978] p 4338 N94-36247

IONIC COLLISIONS
A two-dimensional model for collisional energy transfer in bimolecular ion-molecule dynamics
[AD-A278913] p 4321 N94-35589

IONIC CRYSTALS
Eyesafe rare earth crystal lasers for atmosphere soudings
[AD-A279486] p 4273 N94-36227

IONIZATION
Analytic model of aurorally coupled magnetospheric and ionospheric electrostatic potentials
[NASA-CR-196130] p 4288 N94-35358
First measurement of helium on Mars: Implications for the problem of radiogenic gases on the terrestrial planets p 4370 N94-36153

IONIZATION POTENTIALS
Vertical and adiabatical ionization energies and electron affinities of new Si(n)C and Si(n)O (n=1-3) molecules
[AD-A278863] p 4324 N94-36050

IONIZING RADIATION
Computer image analysis of etched tracks from ionizing radiation
[NASA-CR-196025] p 4319 N94-35264
ROSAT/XRT-PSPC observations and the ionizing continuum of Seyfert 1 galaxy Mkn 478
[PB94-167053] p 4350 N94-35530
Rapid and accurate timing simulation of radiation-hardened digital microelectronics using VHDL
[AD-A278644] p 4261 N94-36361

IONOSONDES
A quality control package for the Digisonde Drift Analysis (DDA)
[AD-A278663] p 4289 N94-35578

IONOSPHERIC DISTURBANCES
JPRS report: Science and technology. Central Eurasia
[JPRS-UST-94-008] p 4249 N94-35228
Studies of the dayside boundary layer processes based on ground observations in the Svalbard area
[AD-A280715] p 4292 N94-36265

IONOSPHERIC DRIFT
Ionospheric plasma drift and structure studies at high and mid-latitudes
[AD-A279415] p 4291 N94-36116

IONOSPHERIC PROPAGATION
Measurements of spatial and frequency coherence of an equatorial hf path during spread-F
[DE93-016615] p 4257 N94-36316

IONOSPHERIC SOUNDING
Electromagnetic measurements of the ionosphere at the ionospheric station of Rome
[AD-A278991] p 4290 N94-35744
Ionospheric plasma drift and structure studies at high and mid-latitudes
[AD-A279415] p 4291 N94-36116

IONS
Particle orbit analysis for LHD helical axis configurations
[DE94-718995] p 4336 N94-35773
A search for energetic ion directivity in large solar flares
[NASA-CR-196036] p 4374 N94-35993

IRON
Thermal emission measurements (5-25 microns) of palagonite/Fe-substituted montmorillonite intimate mixtures: Applications to Mars p 4292 N94-35453
Transmission measurements (4000-400 cm(exp -1), 2.5-25 microns) of crystalline ferric oxides and ferric oxyhydroxides: Implications for Mars
p 4292 N94-35454
Partial melting of the St. Severin (LL) and Lost City (H) ordinary chondrites: One step backwards and two steps forward p 4353 N94-36146
The nature of agglutinitic glass in the fine-size fraction of lunar soil 10084 p 4369 N94-36148
Formation of iron metal and grain coagulation in the solar nebula p 4373 N94-36170
X ray and gamma ray spectroscopy of solids under pressure
[DE94-011207] p 4238 N94-36203
Magnetic properties of nanosize iron clusters
[DE94-011329] p 4318 N94-36204
New calculations of Fe spectra in high-temperature plasmas
[DE94-009919] p 4339 N94-36386

IRON ALLOYS
Investigation of moisture-induced embrittlement of iron aluminides
[DE94-010881] p 4241 N94-36196
Formation and stability of Fe-rich precipitates in dilute Zr(Fe) single-crystal alloys
[DE94-619027] p 4242 N94-36288

IRON OXIDES
Reduction of lunar mare soil and pyroclastic glass
p 4355 N94-35398
High Resolution Transmission Electron Microscopy (HRTEM) of nanophase ferric oxides
p 4239 N94-35433
FeO and MgO in plagioclase of lunar anorthosites: Igneous or metamorphic? p 4351 N94-35449
Thermal emission measurements (5-25 microns) of Hawaiian palagonitic soils with implications for Mars
p 4292 N94-35452

IRRADIANCE
Absolute, Extreme Ultraviolet Solar Spectral Irradiance Monitor (AESSIM)
[AD-A278709] p 4227 N94-36189

IRRADIATION
Treatment of toxic gases SO2 and NO(x) by electron beam irradiation
[DE94-615424] p 4330 N94-36028
Estimating low-dose rate irradiation response of MOSFETs
[DE94-007292] p 4342 N94-36367
Bounding the total-dose response of modern bipolar transistors
[DE94-007742] p 4261 N94-36371

ISOELECTRONIC SEQUENCE
New anionic states of the lithium trimer
[AD-A278832] p 4323 N94-35797

ISOTOPE SEPARATION
Proceedings of the LLNL Technical Women's Symposium
[DE94-006616] p 4379 N94-35997

ISOTOPES
First observation of a mass independent isotopic fractionation in a condensation reaction
p 4239 N94-35464
Anatomy of a cluster IDP. Part 2: Noble gas abundances, trace element geochemistry, isotopic abundances, and trace organic chemistry of several fragments from L2008#5 p 4352 N94-35465
The anatomy of a cluster IDP. Part 1: Carbon abundance, bulk chemistry, and mineralogy of fragments from L2008#5 p 4352 N94-35466
Isotopic and geochemical precursors of earthquakes and volcanic eruptions
[DE94-615824] p 4289 N94-35568
Mars atmospheric escape and isotopic fractionation: Synthesis of data and models p 4369 N94-36143

ITERATIVE SOLUTION
Description and use of LSODE, the Livermore Solver for Ordinary Differential Equations
[NASA-RP-1327] p 4313 N94-35259
Calculations on some properties of the pion in the framework of Schwinger-Dyson and Bethe-Salpeter equations
[DE94-611232] p 4322 N94-35786
An iterative extension of Prony's method for ARMA signal modeling
[AD-A278841] p 4319 N94-35800
Wedge scattering by the method of iteration
[DE94-010404] p 4256 N94-36112
A multilevel adaptive projection method for unsteady incompressible flow
[DE93-016418] p 4267 N94-36315

J

JAPAN
JTEC/WTEC report and program summary
p 4379 N94-36042
Information and communication technology
p 4257 N94-36043
Advanced composites in Japan p 4234 N94-36045
Space robotics in Japan p 4278 N94-36046
Space and transatmospheric propulsion technology
p 4229 N94-36047

JAPANESE SPACE PROGRAM
Space robotics in Japan p 4278 N94-36046
Space and transatmospheric propulsion technology
p 4229 N94-36047

JET ENGINE FUELS
Hot Corrosion Test Facility at the NASA Lewis Special Projects Laboratory
[NASA-CR-195323] p 4200 N94-35267

JET FLOW
Development and application of computational aerothermodynamics flowfield computer codes
[NASA-CR-196136] p 4189 N94-35498
An experimental investigation of active control of thrust vectoring nozzle flow fields
[AD-A278702] p 4229 N94-36291

JET IMPINGEMENT
Fundamental studies in blow-down and cryogenic cooling
[AD-A278967] p 4250 N94-35524

JET LAG
Some solutions to reduce the human effects of extended operation times p 4196 N94-36339

JET NOZZLES
Tipjet 80-inch model rotor hover test: Test no. 1198
[AD-A279680] p 4191 N94-36261

JET PROPULSION
Challenging the Future - Journey to Excellence. Aeropropulsion strategic plan for the 1990's
[NASA-TM-109250] p 4228 N94-35591

JOINED WINGS
Alleviation of whirl-flutter on a joined-wing tilt-rotor aircraft configuration using active controls
[NASA-CR-196103] p 4200 N94-36436

JOINTS (JUNCTIONS)
Robot friendly probe and socket assembly
[NASA-CASE-MSC-22028-1] p 4274 N94-35374
Manufacturing feasibility of several lead-free solders for electronic assembly
[DE94-007732] p 4258 N94-35564
Processing and properties of high temperature metal/fiber-reinforced-thermoplastic laminates
[AD-A278791] p 4232 N94-35654
Nondestructive Inspection (NDI) of reduced strength bonds
[AD-A278745] p 4278 N94-36090
Effect of niobium interlayer on high-temperature sliding friction and wear of silver films on alumina
[DE94-010462] p 4275 N94-36232

JUNCTION TRANSISTORS
BJT model in APLAC
[PB94-171022] p 4259 N94-35822
Non-alloyed, refractory metal contact optimization with shallow implantations of Zn and Mg
[DE94-010392] p 4240 N94-36110
High temperature heterojunction bipolar transistors
[AD-A278605] p 4261 N94-36360

JUPITER ATMOSPHERE
Radiative signals from impact of Shoemaker-Levy on Jupiter p 4355 N94-35396

K

K-EPSILON TURBULENCE MODEL
K-epsilon model of anomalous transport in resistive interchange turbulence
[DE94-718983] p 4337 N94-35937

KALMAN FILTERS
Improved solution accuracy for TDRSS-based TOPEX/Poseidon orbit determination
p 4205 N94-35620
Filter parameter tuning analysis for operational orbit determination support p 4208 N94-35637
Comparison of Kalman filter and optimal smoother estimates of spacecraft attitude p 4208 N94-35638
Advantages of estimating rate corrections during dynamic propagation of spacecraft rates: Applications to real-time attitude determination of SAMPEX
p 4209 N94-35642
KAONS
Elastic charge form factors for K mesons
[DE94-010014] p 4325 N94-36086
KINETIC ENERGY
Recovery of frozen flow losses in arcjets
[AD-A278739] p 4228 N94-36089
KINETIC EQUATIONS
The kinetics of inhomogeneous plasma
[DE94-611459] p 4336 N94-35788
KINETIC THEORY
Theoretical aspect of low pressure discharges in simple gasses
[AD-A278762] p 4335 N94-35493
Kinetic theory of runaway air breakdown and the implications for lightning initiation
[DE94-001683] p 4295 N94-36240
KINETICS
The kinetics of inhomogeneous plasma
[DE94-611459] p 4336 N94-35788
Dynamic structural effects and ultrafast biomolecular kinetics in photoinduced charge transfer reactions
[DE94-010421] p 4329 N94-36390
KLEIN-GORDON EQUATION
The 2+1-dimensional integrable generalization of the Sine-Gordon equation
[DE94-611074] p 4315 N94-36100
KLYSTRONS
State of the art in high-power microwaves: An overview
[DE94-007075] p 4272 N94-35978
KNOWLEDGE BASED SYSTEMS
Combining left and right unlinking for matching a large number of learned rules
[AD-A278979] p 4311 N94-35527
MMI(exp 2) demonstrator systems: A multi-modal interface for man machine interaction with knowledge based systems. Deliverable D17 (TA 2) ESPRIT project 2474 MMI(exp 2)
[PB94-170537] p 4298 N94-35600
Case based reasoning in engineering design
[AD-A278943] p 4305 N94-36006
KNOWLEDGE BASES (ARTIFICIAL INTELLIGENCE)
Knowledge-based systems in Japan
p 4347 N94-36044
KNOWLEDGE REPRESENTATION
Proceedings of the 4th Workshop on the Next Generation of CASE Tools
[PB94-150372] p 4302 N94-35538
KNUDSEN FLOW
Investigation of Burnett equations for two-dimensional hypersonic flow
[AD-A278942] p 4190 N94-35717
KRYPTON
Kinetics studies following state-selective laser excitation
[DE94-010305] p 4330 N94-36105
KRYPTON FLUORIDE LASERS
Specification for the TITANIA krF laser system
[PB94-167103] p 4272 N94-36062

L

LABORATORIES
A guide to research facilities at the National Renewable Energy Laboratory
[DE94-006857] p 4283 N94-36052
Environmental resource document for the Idaho National Engineering Laboratory, volume 1
[DE94-008522] p 4287 N94-36207
Environmental resource document for the Idaho National Engineering Laboratory, volume 2
[DE94-008523] p 4287 N94-36208
Network analyzer calibration for cryogenic on-wafer measurements
[DE94-010089] p 4262 N94-36430
LAGOONS
Endangered and potentially endangered wildlife on John F. Kennedy Space Center and faunal integrity as a goal for maintaining biological diversity
[NASA-TM-109204] p 4288 N94-36422
LAGRANGIAN FUNCTION
Low energy theorems from the effective Lagrangian with vector mesons
[DE94-611173] p 4322 N94-35785
Numerical methods for multibody systems
p 4222 N94-35897
Pairing and low temperature properties of 2D Fermi-systems with attraction between particles
[DE94-615510] p 4329 N94-36434
LAMINAR FLOW
Unsteady structure of leading-edge vortices on a delta wing
[AD-A278988] p 4190 N94-35529
Detailed studies of soot formation in laminar diffusion flames for application to modeling studies
[AD-A278941] p 4235 N94-35604
Boundary conditions for jet flow computations
[NASA-TM-106648] p 4266 N94-35976
Laminar flow studies at Dassault Aviation: Calculations and flight tests p 4194 N94-36328
LAMINATES
Processing and properties of high temperature metal/fiber-reinforced-thermoplastic laminates
[AD-A278791] p 4232 N94-35654
Through-the-thickness tensile strength of textile composites
[NASA-TM-109115] p 4233 N94-35946
Method for making a symmetrical layered thin film edge field-emitter-array
[AD-D016214] p 4246 N94-36121
Fatigue and residual strength behaviour of ARALL3 panels with bonded-on doublers
[AD-B181062] p 4279 N94-36226
Laminated thermoplastic composite material from recycled high density polyethylene p 4230 N94-36403
LAND SURFACE TEMPERATURE
A model of the CO2 exchanges between biosphere and atmosphere in the tundra
[NASA-CR-196008] p 4289 N94-35389
LANDFORMS
Quantifying shapes of volcanoes on Venus
p 4361 N94-35429
Volcano morphometry and volume scaling on Venus
p 4361 N94-35431
LANDING SIMULATION
Autonomous hazard detection and avoidance
[NASA-CR-188331] p 4309 N94-36439
LANDING SITES
Fluvial processes in Ma'adim Vallis and the potential of Gusev crater as a high priority site
p 4358 N94-35414
Autonomous hazard detection and avoidance
[NASA-CR-188331] p 4309 N94-36439
LANDSAT SATELLITES
Preliminary study of satellite attitude determination for the LANDSAT 7 spacecraft
[AD-A278876] p 4212 N94-35585
LANDSAT 4
Improved solution accuracy for Landsat-4 (TDRSS-user) orbit determination p 4205 N94-35623
LANTHANUM CHLORIDES
Vertical electron detachment energies ior octahedral closed-shell multiply charged anions
[AD-A278835] p 4322 N94-35753
LANTHANUM FLUORIDES
Vertical electron detachment energies for octahedral closed-shell multiply charged anions
[AD-A278835] p 4322 N94-35753
LARGE SPACE STRUCTURES
Structural assembly demonstration experiment, phase 1
[NASA-CR-193967] p 4212 N94-35484
Applying transfer matrix method to the estimation of the modal characteristics of the NASA Mini-Mass Truss
p 4218 N94-35870
LASER APPLICATIONS
JPRS report: Science and technology. Central Eurasia
[JPRS-UST-94-008] p 4249 N94-35228
Influence of an externally modulated photonic link on a microwave communications system
p 4252 N94-35544
Advanced induction accelerator designs for ground based and space based FELs
[AD-A278885] p 4271 N94-35586
Ultrafast chemical dynamics of reactions in beams
[AD-A278939] p 4323 N94-35805
A supersonic tunnel for laser and flow-seeding techniques
[NASA-TM-106588] p 4265 N94-35945
X ray radiographic imaging of hydrodynamic phenomena in radiation driven materials: Shock propagation and shear flow
[DE94-010891] p 4318 N94-36201
Molecular nitrogen fluorescence lidar for remote sensing of the auroral ionosphere
[AD-A280716] p 4291 N94-36263
Method and apparatus for imaging an object in or through a scattering medium by using multiple-wave mixing
[AD-D016212] p 4334 N94-36368
Activities of the Laser and Plasma Technology Division
[DE94-617113] p 4273 N94-36393
LASER ARRAYS
High-power CW operation of AlGaInP diode-laser arrays
[DE94-010409] p 4272 N94-36115
Phase-locked arrays of vertical-cavity surface-emitting lasers
[DE94-009279] p 4272 N94-36178
LASER BEAMS
Advanced induction accelerator designs for ground based and space based FELs
[AD-A278885] p 4271 N94-35586
LASER CAVITIES
Color center laser with transverse auxiliary illumination
[AD-D016201] p 4273 N94-36365
LASER DRILLING
Laser drilling of vertical vias in silicon
[DE94-009250] p 4270 N94-35351
LASER FUSION
Proceedings of the LLNL Technical Women's Symposium
[DE94-006616] p 4379 N94-35997
Inertial confinement fusion
[DE94-010835] p 4338 N94-36193
LASER INDUCED FLUORESCENCE
Kinetics studies following state-selective laser excitation
[DE94-010305] p 4330 N94-36105
LASER MATERIALS
Progress in the production of samples of gamma ray laser candidate materials
[AD-A278961] p 4272 N94-35721
Eyesafe rare earth crystal lasers for atmosphere soudings
[AD-A279486] p 4273 N94-36227
LASER OUTPUTS
Issues in the design and optimization of adaptive optics and laser guide stars for the Keck Telescopes
[DE94-009384] p 4349 N94-35565
Specification for the TITANIA krF laser system
[PB94-167103] p 4272 N94-36062
High-power CW operation of AlGaInP diode-laser arrays
[DE94-010409] p 4272 N94-36115
Color center laser with transverse auxiliary illumination
[AD-D016201] p 4273 N94-36365
LASER PLASMAS
High density implosion experiments at Nova
[DE94-010894] p 4339 N94-36375
Activities of the Laser and Plasma Technology Division
[DE94-617113] p 4273 N94-36393
LASER PUMPING
Improved performance of high average power semiconductor arrays for applications in diode pumped solid state lasers
[DE94-009516] p 4271 N94-35665
900-mW average power and tunability from a diode-pumped 2.94 micron Er:YAG oscillator
[DE94-009511] p 4271 N94-35679
System for end-pumping a solid state laser using a large aperture laser diode bar
[AD-D016213] p 4273 N94-36370
LASER TARGET INTERACTIONS
Experimental studies of very-high Mach number hydrodynamics
[AD-A278761] p 4263 N94-35492
LASER TARGETS
Inertial confinement fusion
[DE94-010835] p 4338 N94-36193
High density implosion experiments at Nova
[DE94-010894] p 4339 N94-36375
LASER WELDING
JPRS report: Science and technology. Central Eurasia: Materials science
[JPRS-UMS-93-007] p 4240 N94-35517
LASERS
Study and fabrication of GaSb-based laser heterostructures
[PB94-170677] p 4273 N94-36218
Activities of the Laser and Plasma Technology Division
[DE94-617113] p 4273 N94-36393
LATERAL CONTROL
Status of MSBS study at NAL p 4216 N94-35854
LATTICE PARAMETERS
A new family of superconducting fullerides, Na(NH3)(x)C60(x = 2-8)
[DE94-011480] p 4341 N94-36272

LATTICES (MATHEMATICS)
Successive minima on arithmetic varieties
[PB94-167699] p 4314 N94-35759
LAUNCH VEHICLES
Geostationary space launch vehicles and the US dilemma p 4210 N94-35377
High Earth orbit design for lunar assisted small Explorer class missions p 4202 N94-35608
Space and transatmospheric propulsion technology
p 4229 N94-36047
LAUNCH WINDOWS
The analysis of a generic air-to-air missile simulation model
[NASA-TM-109057] p 4309 N94-36438
LAUNCHING
The analysis of a generic air-to-air missile simulation model
[NASA-TM-109057] p 4309 N94-36438
LAVA
Volcano morphometry and volume scaling on Venus
p 4361 N94-35431
LEAD TITANATES
Dielectric measurements of selected ceramics at microwave frequencies p 4232 N94-36412
LEAD ZIRCONATE TITANATES
Plane shock generator explosive lens: Shock characterization of 4340 and PH13-8Mo steels, C360 brass and PZT 65/35 ferro-electric ceramic
[DE94-009254] p 4266 N94-35979
Microstructural development in solution derived PZT thin films
[DE94-008744] p 4246 N94-36209
LEADING EDGES
Unsteady structure of leading-edge vortices on a delta wing
[AD-A278988] p 4190 N94-35529
LEAST SQUARES METHOD
Block distributions on the lunar surface: A comparison between measurements obtained from surface and orbital photography p 4359 N94-35419
A simple suboptimal least-squares algorithm for attitude determination with multiple sensors
p 4210 N94-35645
A comparison of variable selection criteria for multiple linear regression: A THIRD simulation study
[AD-A278678] p 4316 N94-35691
Parameter estimation of the vibrational model for the SCOLE experimental facility p 4219 N94-35878
LECTURES
Genetic algorithms
[PB94-171048] p 4303 N94-35602
LENSES
Color center laser with transverse auxiliary illumination
[AD-D016201] p 4273 N94-36365
LEPTONS
Leptonic decay constants of heavy quarkonia in effective QCD sum rules
[DE94-611160] p 4322 N94-35784
Isoscalar vector bosons at LEP 2
[DE94-611253] p 4323 N94-35787
SCATTER program of cross section calculation of the hadron and lepton interactions with nuclei
[DE94-617006] p 4326 N94-36134
Top dilepton search at CDF
[DE94-002302] p 4327 N94-36266
LEVITATION
Measurement and characterization of force dynamics in high T(sub c) superconductors p 4214 N94-35844
Superconducting Electromagnetic Suspension (EMS) system for Grumman Maglev concept
p 4215 N94-35849
Six degree of freedom fine motion positioning stage based on magnetic levitation p 4225 N94-35916
Future ultra-speed tube-flight p 4225 N94-35918
Maglev crude oil pipeline p 4226 N94-35919
LIE GROUPS
Recent progress in irrational conformal field theory
[DE94-011908] p 4317 N94-36234
N = 4 supersymmetry from the quantum affine algebra U(sub q)(A-circumflex(sup 1)(sub 3))
[DE94-611145] p 4317 N94-36307
LIFE (DURABILITY)
Developing software for ease of change: Metrics from later in the TRALAB system life cycle
[AD-A278759] p 4302 N94-35490
Propulsion system technologies for long range and long endurance aircraft p 4195 N94-36334
LIFE SCIENCES
JPRS report: Science and technology. Central Eurasia
[JPRS-UST-94-001] p 4229 N94-35340
JPRS report: Science and technology. Central Eurasia
[JPRS-UST-94-004] p 4249 N94-35341
JPRS report: Science and technology. Central Eurasia
[JPRS-UST-94-005] p 4249 N94-35342
Aerospace medicine and biology: A continuing bibliography with indexes (supplement 391)
[NASA-SP-7011(391)] p 4297 N94-35345
Director's discretionary fund
[NASA-TM-103997] p 4376 N94-35370
JPRS report: Science and technology. Central Eurasia
[JPRS-UST-94-010] p 4250 N94-35385
JPRS report: Science and technology. Central Eurasia
[JPRS-UST-94-011] p 4250 N94-35386
JPRS report: Science and technology. Central Eurasia
[JPRS-UST-94-012] p 4250 N94-35387
Research and technology, 1993
[NASA-TM-108816] p 4380 N94-36117
LIFE SUPPORT SYSTEMS
Aerospace medicine and biology: A continuing bibliography with indexes (supplement 391)
[NASA-SP-7011(391)] p 4297 N94-35345
LIFT DEVICES
Aeroservoelastic tailoring with piezoelectric materials: Actuator optimization studies
[AD-A278640] p 4199 N94-36384
LIFT DRAG RATIO
Improvement of endurance performance by periodic optimal control of variable camber p 4194 N94-36329
Numerical investigation of multi-element airfoils
[NASA-CR-194592] p 4191 N94-36394
LIGHT (VISIBLE RADIATION)
About mid-infrared optical spectrum of high-Tc superconducting compounds
[DE94-615646] p 4340 N94-36030
LIGHT AIRCRAFT
High Altitude Long Endurance aircraft design studies
p 4193 N94-36322
LIGHT BEAMS
Method and apparatus for imaging an object in or through a scattering medium by using multiple-wave mixing
[AD-D016212] p 4334 N94-36368
LIGHT IONS
Beam transport
[DE94-010755] p 4331 N94-36199
LIGHT SCATTERING
Lunar horizon glow and the Clementine mission
p 4366 N94-35478
Analysis of regional visibility in the eastern United States using aerosol models
[PB94-158698] p 4332 N94-35584
Application of GaSe and AgGaSe2 crystal growth to non-linear optics
[PB94-170552] p 4341 N94-36212
Efficient light propagation for multiple anisotropic volume scattering
[DE94-006474] p 4334 N94-36356
Method and apparatus for imaging an object in or through a scattering medium by using multiple-wave mixing
[AD-D016212] p 4334 N94-36368
LIGHT SOURCES
Color center laser with transverse auxiliary illumination
[AD-D016201] p 4273 N94-36365
LIGHTNING
Kinetic theory of runaway air breakdown and the implications for lightning initiation
[DE94-001683] p 4295 N94-36240
LINEAR ACCELERATORS
Elastic charge form factors for K mesons
[DE94-010014] p 4325 N94-36086
Spin dynamics in storage rings and linear accelerators
[DE94-010320] p 4330 N94-36106
ILSE combiner study
[DE94-011009] p 4331 N94-36202
LINEAR PROGRAMMING
Stopping rules for a class of sampling-based stochastic programming algorithms
[AD-A278654] p 4303 N94-35577
LINEAR QUADRATIC GAUSSIAN CONTROL
Control of the SCOLE configuration using distributed parameter models p 4221 N94-35885
CSI, optimal control, and accelerometers: Trials and tribulations p 4221 N94-35888
Robustness properties of LQG optimized compensators for collocated rate sensors p 4221 N94-35890
LQG optimal compensator transfer function for the NASA LaRC CSI Evolutionary Model
p 4221 N94-35891
Rational positive real approximations for LQG optimal compensators arising in active stabilization of flexible structures p 4222 N94-35892
LINEAR QUADRATIC REGULATOR
Microgravity isolation system design: A modern control synthesis framework p 4215 N94-35851
Maneuvering and control of flexible space robots
p 4218 N94-35867
Semigroup approximation and robust stabilization of distributed parameter systems p 4222 N94-35894
LINEAR SYSTEMS
Parameter estimation of the vibrational model for the SCOLE experimental facility p 4219 N94-35878
Numerical method to study the stability of periodic solutions of particle motion in nonlinear magnetic fields
[DE94-610740] p 4325 N94-36088
Estimation with multisensor/multiscan detection fusion
[AD-A278753] p 4256 N94-36092
LINGUISTICS
Using International English to prepare technical text for translation
[DE94-002628] p 4347 N94-36102
LIQUEFIED GASES
Beam tests of a prototype level-1 calorimeter trigger for LHC experiments
[PB94-170495] p 4269 N94-35599
LIQUID CRYSTALS
Liquid crystalline thermosetting polyimides
[DE94-009939] p 4244 N94-35768
LIQUID FLOW
Transient body force effects on the dryout and rewet of a heated capillary structure
[AD-A278677] p 4264 N94-35690
LIQUID FUELS
Gasoline from natural gas by sulfur processing
[DE94-011130] p 4248 N94-36035
Heterogeneous catalytic process for alcohol fuels from syngas
[DE94-010263] p 4248 N94-36299
LIQUID HELIUM
Spatio-temporal properties of centrifugal instabilities: Abstracts of 8th Couette-Taylor Meeting
[PB94-150240] p 4266 N94-35981
LIQUID HYDROGEN
Experimental results of hydrogen slosh in a 62 cubic foot (1750 liter) tank
[NASA-TM-106625] p 4263 N94-35250
LIQUID NITROGEN
Characterization of lithium niobate electro-optic modulators at cryogenic temperatures
[DE94-010059] p 4333 N94-35697
A precise passive narrow-beam filter infrared radiometer and its use with LIDAR in the ARM program
[DE94-004167] p 4269 N94-36085
LIQUID PHASE EPITAXY
Activities of the optoelectronics laboratory
[PB94-171196] p 4334 N94-36190
Study and fabrication of GaSb-based laser heterostructures
[PB94-170677] p 4273 N94-36218
LIQUID PHASES
Liquid crystalline thermosetting polyimides
[DE94-009939] p 4244 N94-35768
Preliminary results of sulfide melt/silicate wetting experiments in a partially melted ordinary chondrite
p 4353 N94-36147
LIQUID PROPELLANT ROCKET ENGINES
AFOSR Contractors Propulsion Meeting
[AD-A279028] p 4198 N94-35746
Space and transatmospheric propulsion technology
p 4229 N94-36047
LIQUID ROCKET PROPELLANTS
The 30th JANNAF Combustion Subcommittee Meeting, volume 1
[AD-A278793] p 4247 N94-35655
LIQUID SLOSHING
Experimental results of hydrogen slosh in a 62 cubic foot (1750 liter) tank
[NASA-TM-106625] p 4263 N94-35250
LIQUID-SOLID INTERFACES
Interface shape and convection during solidification and melting of succinonitrile
[NASA-TM-106487] p 4262 N94-35248
LIQUID-VAPOR EQUILIBRIUM
Measurement of viscosity, density, and gas solubility of refrigerant blends in selected synthetic lubricants
[DE94-010426] p 4244 N94-35687
LITHIUM
Anionic states of LiFLi
[AD-A278830] p 4322 N94-35678
New anionic states of the lithium trimer
[AD-A278832] p 4323 N94-35797
LITHIUM COMPOUNDS
Anionic states of LiFLi
[AD-A278830] p 4322 N94-35678
LITHIUM NIOBATES
Characterization of lithium niobate electro-optic modulators at cryogenic temperatures
[DE94-010059] p 4333 N94-35697
LITHIUM OXIDES
Kinetics of phase transformations in glass forming systems
[NASA-CR-196082] p 4245 N94-35977
LITHOGRAPHY
Planar rotational magnetic micromotors with integrated shaft encoder and magnetic rotor levitation
p 4224 N94-35907

LITHOLOGY
The Twenty-Fifth Lunar and Planetary Science Conference. Part 1: A-G [NASA-CR-195743] p 4355 N94-35395
Mineralogy of an unusual CM clast in the Kaidun meteorite p 4352 N94-35476

LITHOSPHERE
Effects due to overlapping large impact basins on Mars p 4360 N94-35427
Rheology, tectonics, and the structure of the Venus lithosphere p 4367 N94-35479
Formation of fold and thrust belts on Venus due to horizontal shortening of a laterally heterogeneous lithosphere p 4367 N94-35480
Patterns of brittle deformation under extension on Venus p 4373 N94-36168

LOADS (FORCES)
High energy [DE94-009477] p 4331 N94-36428

LOCAL AREA NETWORKS
High level modelling and design of asynchronous interface logic [PB94-167822] p 4258 N94-35534

LOCAL GROUP (ASTRONOMY)
Angular momentum in the Local Group [DE94-009322] p 4350 N94-35980

LOCOMOTIVES
Design and operation of a medium speed 12-cylinder coal-fueled diesel engine. Phase 2: Improvements [DE94-009547] p 4275 N94-35815

LOGARITHMS
Logarithmic corrections of the two-body QED problem [DE94-611157] p 4322 N94-35783
Graphing techniques for materials laboratory using Excel p 4232 N94-36414

LOGIC CIRCUITS
High-speed digital project, HSD test capability [DE94-010885] p 4260 N94-36197

LOGIC DESIGN
High level modelling and design of asynchronous interface logic [PB94-167822] p 4258 N94-35534
The most abstract common refinement [AD-A278870] p 4305 N94-36014

LOGISTICS
NAVSPACECOM space surveillance sensor system digital signal processing receiver. Volume 3: Operating system functions [AD-A278839] p 4212 N94-35799
NAVSPACECOM space surveillance sensor system digital signal processing receiver. Volume 4: Hardware interfaces [AD-A278845] p 4212 N94-35801
The integrated model development environment [AD-A278613] p 4308 N94-36250

LONG DURATION EXPOSURE FACILITY
Results from LDEF experiment A0114: The interaction of atomic oxygen with materials surfaces at orbital altitudes [NASA-CR-196016] p 4235 N94-35388
Current activities and results of the Long Duration Exposure Facility Meteoroid and Debris Special Investigation Group p 4352 N94-35458
Morphology of meteoroid and space debris craters on LDEF metal targets p 4353 N94-36159

LONG RANGE WEATHER FORECASTING
Long range forecasts of the Northern Hemisphere anomalies with antecedent sea surface temperature patterns [NASA-CR-189358] p 4292 N94-35380

LONGITUDINAL WAVES
An electromagnetic finite difference time domain analog treatment of small signal acoustic interactions [DE94-009978] p 4319 N94-35770

LOOPS
Performance evaluation of digital phase-locked loops for advanced deep space transponders p 4254 N94-35558

LOSSES
Particle orbit analysis for LHD helical axis configurations [DE94-718995] p 4336 N94-35773

LOW ALTITUDE
Minimum performance standards: Airborne low-range radar altimeters [RTCA-DO-155] p 4198 N94-35344

LOW COST
Technology Reinvestment Project's Focus Area: Low Cost Electronic Packaging [PB94-161155] p 4259 N94-35748

LOW CURRENTS
Experimental and theoretical studies of a high temperature cesium-barium tacitron, with application to low voltage-high current inversion [DE94-008182] p 4228 N94-35349

LOW FREQUENCIES
Simulation models for computational plasma physics: Concluding report [DE94-009976] p 4335 N94-35647

LOW PASS FILTERS
Third order LPF type compensator for flexible rotor suspension p 4217 N94-35863

LOW PRESSURE
Theoretical aspect of low pressure discharges in simple gasses [AD-A278762] p 4335 N94-35493
The optimization of interfaces in InAsSb/InGaAs strained-layer superlattices grown by metal-organic chemical vapor deposition [DE94-010070] p 4340 N94-35698
Equations of state valid continuously from zero to extreme pressures with H2O and CO2 as examples [DE94-011907] p 4238 N94-36230

LOW SPEED WIND TUNNELS
Three-dimensional force data acquisition and boundary corrections for the Walter H. Beech Memorial 7 x 10 foot low speed wind tunnel [AR93-2] p 4200 N94-36437

LOW TEMPERATURE
A low temperature scanning force microscope for biological samples [DE94-011357] p 4297 N94-36269
Pairing and low temperature properties of 2D Fermi-systems with attraction between particles [DE94-615510] p 4329 N94-36434

LOW TEMPERATURE ENVIRONMENTS
Network analyzer calibration for cryogenic on-wafer measurements [DE94-010089] p 4262 N94-36430

LOWER ATMOSPHERE
Uniqueness of a solution of a steady state photochemical problem: Applications to Mars p 4370 N94-36151
First measurement of helium on Mars: Implications for the problem of radiogenic gases on the terrestrial planets p 4370 N94-36153

LUBRICANTS
Measurement of viscosity, density, and gas solubility of refrigerant blends in selected synthetic lubricants [DE94-010426] p 4244 N94-35687
Solubility, viscosity and density of refrigerant/lubricant mixtures [DE94-009996] p 4245 N94-35771
Research update: Materials Compatibility and Lubricant Research (MCLR) program [DE94-010001] p 4247 N94-36387
Sealed tube comparisons of the compatibility of desiccants with refrigerants and lubricants [DE94-010002] p 4251 N94-36388

LUBRICATING OILS
The effect of alternative fuels on the stability and lubricity of crankcase lubricants [DE94-010353] p 4245 N94-36108

LUBRICATION
The effect of alternative fuels on the stability and lubricity of crankcase lubricants [DE94-010353] p 4245 N94-36108

LUMINESCENCE
Flight testing of a luminescent surface pressure sensor [NASA-TM-103970] p 4189 N94-35394

LUNAR ATMOSPHERE
Lunar horizon glow and the Clementine mission p 4366 N94-35478

LUNAR COMPOSITION
New prospects for analyzing lunar pyroclastic glass p 4355 N94-35397
Single agglutinates: A comparative study of compositions of agglutinitic glass, whole-grain, bulk soil, and FMR p 4355 N94-35401
Luna 24 regolith breccias: A possible source of the fine size material of the Luna 24 regolith p 4362 N94-35450
Alkali element constraints on Earth-Moon relations p 4354 N94-36169

LUNAR CRATERS
The Twenty-Fifth Lunar and Planetary Science Conference. Part 1: A-G [NASA-CR-195743] p 4355 N94-35395
Block distributions on the lunar surface: A comparison between measurements obtained from surface and orbital photography p 4359 N94-35419
Preliminary description of double drive tube 68002/68001 p 4363 N94-35457

LUNAR EFFECTS
High Earth orbit design for lunar assisted small Explorer class missions p 4202 N94-35608

LUNAR EXPLORATION
Apollo 11 at twenty-five, version 1.0 [NASA-CR-193380] p 4376 N94-35363
Remote geochemical experiment package for Discovery class missions p 4350 N94-35420

LUNAR GEOLOGY
The Twenty-Fifth Lunar and Planetary Science Conference. Part 1: A-G [NASA-CR-195743] p 4355 N94-35395
High spatial resolution telescopic multispectral imaging and spectroscopy of the Moon. 1: The Serenitatis/Tranquillitatis border region p 4356 N94-35402
Lunar mineral feedstocks from rocks and soils: X-ray digital imaging in resource evaluation p 4358 N94-35415
The Twenty-Fifth Lunar and Planetary Science Conference. Part 3: P-Z [NASA-CR-195745] p 4362 N94-35448
FeO and MgO in plagioclase of lunar anorthosites: Igneous or metamorphic? p 4351 N94-35449
The Twenty-Fifth Lunar and Planetary Science Conference. Part 2: H-O [NASA-CR-195744] p 4367 N94-36136
New data supporting a Sm-146,147-Nd-142,143 formation interval for the lunar mantle p 4374 N94-36173

LUNAR GRAVITATION
Lunar LIGO and gravitational wave astronomy on the Moon p 4366 N94-35472
Preliminary solutions for the lunar gravity field from analysis of lunar orbiter tracking data p 4371 N94-36156

LUNAR LANDING SITES
Block distributions on the lunar surface: A comparison between measurements obtained from surface and orbital photography p 4359 N94-35419

LUNAR LUMINESCENCE
Lunar horizon glow and the Clementine mission p 4366 N94-35478

LUNAR MANTLE
New data supporting a Sm-146,147-Nd-142,143 formation interval for the lunar mantle p 4374 N94-36173

LUNAR MARIA
Reduction of lunar mare soil and pyroclastic glass p 4355 N94-35398
High spatial resolution telescopic multispectral imaging and spectroscopy of the Moon. 1: The Serenitatis/Tranquillitatis border region p 4356 N94-35402

LUNAR ORBITER
Preliminary solutions for the lunar gravity field from analysis of lunar orbiter tracking data p 4371 N94-36156

LUNAR PHOTOGRAPHY
Block distributions on the lunar surface: A comparison between measurements obtained from surface and orbital photography p 4359 N94-35419

LUNAR RESOURCES
Lunar mineral feedstocks from rocks and soils: X-ray digital imaging in resource evaluation p 4358 N94-35415

LUNAR ROCKS
Lunar mineral feedstocks from rocks and soils: X-ray digital imaging in resource evaluation p 4358 N94-35415
Grain rims on ilmenite in the lunar regolith: Comparison to vapor deposits on regolith silicates p 4359 N94-35418
Solar proton produced neon in shergottite meteorites p 4351 N94-35428
FeO and MgO in plagioclase of lunar anorthosites: Igneous or metamorphic? p 4351 N94-35449
Luna 24 regolith breccias: A possible source of the fine size material of the Luna 24 regolith p 4362 N94-35450
Petrographic characterization of lunar soils: Application of x ray digital-imaging to quantitative and automated analysis p 4368 N94-36138

LUNAR SOIL
Computer image analysis of etched tracks from ionizing radiation [NASA-CR-196025] p 4319 N94-35264
New prospects for analyzing lunar pyroclastic glass p 4355 N94-35397
Reduction of lunar mare soil and pyroclastic glass p 4355 N94-35398
Single agglutinates: A comparative study of compositions of agglutinitic glass, whole-grain, bulk soil, and FMR p 4355 N94-35401
Measuring track densities in lunar grains using image analysis p 4357 N94-35409
Lunar mineral feedstocks from rocks and soils: X-ray digital imaging in resource evaluation p 4358 N94-35415
Preliminary description of double drive tube 68002/68001 p 4363 N94-35457
Petrographic characterization of lunar soils: Application of x ray digital-imaging to quantitative and automated analysis p 4368 N94-36138

The nature of agglutinitic glass in the fine-size fraction of lunar soil 10084 p 4369 N94-36148

LUNAR SURFACE

Block distributions on the lunar surface: A comparison between measurements obtained from surface and orbital photography p 4359 N94-35419

Preliminary description of double drive tube 68002/68001 p 4363 N94-35457

Lunar LIGO and gravitational wave astronomy on the Moon p 4366 N94-35472

Lunar horizon glow and the Clementine mission p 4366 N94-35478

M

MACH NUMBER

Experimental studies of very-high Mach number hydrodynamics [AD-A278761] p 4263 N94-35492

MACHINE LEARNING

Developing interpretable models with optimized set reduction for identifying high risk software components p 4301 N94-35435

Combining left and right unlinking for matching a large number of learned rules [AD-A278979] p 4311 N94-35527

Prodigy planning algorithm [AD-A278900] p 4303 N94-35574

The breakdown of operators when interacting with the external world [AD-A278936] p 4299 N94-35716

Fuzzy self-learning control for magnetic servo system p 4215 N94-35852

MACHINE TRANSLATION

Good applications for crummy machine translation [AD-A278689] p 4345 N94-35651

MAGELLAN SPACECRAFT (NASA)

Magellan to Venus [NASA-CR-195779] p 4201 N94-35510

Field demonstration of X-band photonic antenna remoting in the Deep Space Network p 4252 N94-35545

MAGMA

The parent magma of xenoliths in shergottite EETA79001: Bulk and trace element composition inferred from magmatic inclusions p 4352 N94-35467

Role of magma-water interaction in very large explosive eruptions [DE94-002698] p 4291 N94-36103

MAGNESIUM

Non-alloyed, refractory metal contact optimization with shallow implantations of Zn and Mg [DE94-010392] p 4240 N94-36110

Cr, Mn, and Ca distributions for olivine in angritic systems: Constraints on the origins of Cr-rich and Ca-poor core olivine in angrite LEW87051 p 4353 N94-36162

MAGNESIUM OXIDES

FeO and MgO in plagioclase of lunar anorthosites: Igneous or metamorphic? p 4351 N94-35449

MAGNET COILS

Models for interpreting interstrand resistance measurements in Rutherford cables [DE94-010844] p 4259 N94-36194

MAGNETIC BEARINGS

Advanced technology lunar telescope p 4350 N94-35473

Influence of backup bearings and support structure dynamics on the behavior of rotors with active supports [NASA-CR-196119] p 4274 N94-35500

Flywheel energy storage using superconducting magnetic bearings [DE94-009817] p 4282 N94-35829

Second International Symposium on Magnetic Suspension Technology, part 1 [NASA-CP-3247-PT-1] p 4212 N94-35836

Aerospace applications of magnetic bearings p 4213 N94-35837

Nonlinear control of magnetic bearings p 4213 N94-35838

High performance data acquisition, identification, and monitoring for active magnetic bearings p 4213 N94-35839

High temperature superconductors for magnetic suspension applications p 4214 N94-35843

Measurement and characterization of force dynamics in high T(sub c) superconductors p 4214 N94-35844

Materials for efficient high-flux magnetic bearing actuators p 4214 N94-35845

Design, construction, and testing of a five active axes magnetic bearing system p 4214 N94-35846

Experimental measurement and calculation of losses in planar radial magnetic bearings p 4214 N94-35847

Active magnetic bearing control loop modeling for a finite element rotordynamics code p 4216 N94-35857

Modelling and control of a rotor supported by magnetic bearings p 4216 N94-35858

Dynamic analysis of a magnetic bearing system with flux control p 4216 N94-35859

Third order LPF type compensator for flexible rotor suspension p 4217 N94-35863

Second International Symposium on Magnetic Suspension Technology, part 2 [NASA-CP-3247-PT-2] p 4223 N94-35902

Integration of magnetic bearings in the design of advanced gas turbine engines p 4223 N94-35903

Electromechanical simulation and test of rotating systems with magnetic bearing or piezoelectric actuator active vibration control p 4223 N94-35905

Planar rotational magnetic micromotors with integrated shaft encoder and magnetic rotor levitation p 4224 N94-35907

Concepts of flywheels for energy storage using autostable high-T(sub c) superconducting magnetic bearings p 4224 N94-35909

Manufacturing and testing of a magnetically suspended composite flywheel energy storage system p 4224 N94-35910

Rotor dynamic behaviour of a high-speed oil-free motor compressor with a rigid coupling supported on four radial magnetic bearings p 4224 N94-35911

Magnetically suspended stepping motors for clean room and vacuum environments p 4225 N94-35915

MAGNETIC CONTROL

Magnetically operated check valve [NASA-CASE-MSC-22046-1] p 4274 N94-35661

Active magnetic bearing control loop modeling for a finite element rotordynamics code p 4216 N94-35857

Modelling and control of a rotor supported by magnetic bearings p 4216 N94-35858

Time-delay control of a magnetic levitated linear positioning system p 4217 N94-35862

Potential formation and transport in open field line systems [DE94-718910] p 4337 N94-35983

MAGNETIC DIPOLES

Limitation on the magnetic dipole moment of the reactor neutrino [DE94-611171] p 4320 N94-35566

Formation of iron metal and grain coagulation in the solar nebula p 4373 N94-36170

Beam energy absolute measurement using K-edge absorption spectrometers [DE94-010019] p 4331 N94-36192

MAGNETIC EFFECTS

Magnetic field effect on selective photoionization [DE94-611079] p 4334 N94-36180

MAGNETIC FIELD CONFIGURATIONS

LHD helical divertor [DE94-727626] p 4336 N94-35752

Analysis of recent agile mirror data [AD-A278758] p 4318 N94-36427

MAGNETIC FIELD RECONNECTION

A triggering mechanism of fast crash in sawtooth oscillation [DE94-718974] p 4336 N94-35772

Studies of the dayside boundary layer processes based on ground observations in the Svalbard area [AD-A280715] p 4292 N94-36265

MAGNETIC FIELDS

The study of the local magnetic field in the oxide alpha-Bi2O3 by the mu SR-technique [DE94-612636] p 4322 N94-35751

Particle orbit analysis for LHD helical axis configurations [DE94-718995] p 4336 N94-35773

Magnetoresistance of films and strips with the diffuse surface scattering [DE94-611100] p 4340 N94-35933

Zero modes of the two-dimensional Dirac operator on a noncompact Riemann surface in an external magnetic field [DE94-616618] p 4343 N94-36071

Functional integration method for the one-dimensional localization, the higher correlators and mean current in mesoscopic ring in the arbitrary magnetic field [DE94-616621] p 4325 N94-36073

Numerical method to study the stability of periodic solutions of particle motion in nonlinear magnetic fields [DE94-610740] p 4325 N94-36088

Magnetic field effect on selective photoionization [DE94-611079] p 4334 N94-36180

Magnetic properties of nanosize iron clusters [DE94-011329] p 4318 N94-36204

Further studies of 60-Hz exposure effects on human function [DE94-010192] p 4297 N94-36223

Magnetic metallic multilayers [DE94-011913] p 4341 N94-36274

Simultaneous observations of the westward electrojet and the cross-tail current sheet during substorms [AD-A278631] p 4292 N94-36383

MAGNETIC FLUX

On the physics of waves in the solar atmosphere: Wave heating and wind acceleration [NASA-CR-194119] p 4375 N94-36395

MAGNETIC INDUCTION

Advanced induction accelerator designs for ground based and space based FELs [AD-A278885] p 4271 N94-35586

MAGNETIC LENSES

ILSE combiner study [DE94-011009] p 4331 N94-36202

MAGNETIC LEVITATION VEHICLES

Second International Symposium on Magnetic Suspension Technology, part 1 [NASA-CP-3247-PT-1] p 4212 N94-35836

System concept definition of the Grumman superconducting Electromagnetic Suspension (EMS) Maglev design p 4213 N94-35840

Transrapid (the first high-speed Maglev train system certified ready for application): Development status and prospects for deployment p 4213 N94-35841

Control of maglev vehicles with aerodynamic and guideway disturbances p 4213 N94-35842

Fault tolerant computer control for a Maglev transportation system p 4215 N94-35848

Superconducting Electromagnetic Suspension (EMS) system for Grumman Maglev concept p 4215 N94-35849

National Maglev initiative: California line electric utility power system requirements p 4215 N94-35850

Second International Symposium on Magnetic Suspension Technology, part 2 [NASA-CP-3247-PT-2] p 4223 N94-35902

Future ultra-speed tube-flight p 4225 N94-35918

Dynamic stability of maglev systems [DE94-010451] p 4276 N94-36433

MAGNETIC MATERIALS

Advanced induction accelerator designs for ground based and space based FELs [AD-A278885] p 4271 N94-35586

MAGNETIC MIRRORS

Hot-ion plasma in the quadrupole trap [DE94-617216] p 4337 N94-36082

MAGNETIC MOMENTS

Limitation on the magnetic dipole moment of the reactor neutrino [DE94-611171] p 4320 N94-35566

Magnetic metallic multilayers [DE94-011913] p 4341 N94-36274

MAGNETIC PROPERTIES

Chondrule magnetic properties p 4352 N94-35471

Materials for efficient high-flux magnetic bearing actuators p 4214 N94-35845

Magnetic properties of nanosize iron clusters [DE94-011329] p 4318 N94-36204

MAGNETIC PUMPING

Performance analysis of reciprocating regenerative magnetic heat pumping [DE94-009488] p 4264 N94-35683

MAGNETIC SPECTROSCOPY

High Resolution Transmission Electron Microscopy (HRTEM) of nanophase ferric oxides p 4239 N94-35433

Beam energy absolute measurement using K-edge absorption spectrometers [DE94-010019] p 4331 N94-36192

MAGNETIC STORMS

Collisonless dynamics of the magnetosphere [AD-A278886] p 4290 N94-35708

Simultaneous observations of the westward electrojet and the cross-tail current sheet during substorms [AD-A278631] p 4292 N94-36383

MAGNETIC SUSPENSION

Second International Symposium on Magnetic Suspension Technology, part 1 [NASA-CP-3247-PT-1] p 4212 N94-35836

Aerospace applications of magnetic bearings p 4213 N94-35837

System concept definition of the Grumman superconducting Electromagnetic Suspension (EMS) Maglev design p 4213 N94-35840

Transrapid (the first high-speed Maglev train system certified ready for application): Development status and prospects for deployment p 4213 N94-35841

High temperature superconductors for magnetic suspension applications p 4214 N94-35843

Measurement and characterization of force dynamics in high T(sub c) superconductors p 4214 N94-35844

Fault tolerant computer control for a Maglev transportation system p 4215 N94-35848

Superconducting Electromagnetic Suspension (EMS) system for Grumman Maglev concept p 4215 N94-35849

Fuzzy self-learning control for magnetic servo system p 4215 N94-35852

Implementation of a decoupled controller for a magnetic suspension system using electromagnets mounted in a planar array p 4216 N94-35853

Status of MSBS study at NAL p 4216 N94-35854

The simulation of a propulsive jet and force measurement using a magnetically suspended wind tunnel model p 4191 N94-35855

A dynamic method for magnetic torque measurement p 4216 N94-35856

Some further developments in the dynamic modelling and control of the large angle magnetic suspension test fixture p 4217 N94-35860

Neural network controller development for a magnetically suspended flywheel energy storage system p 4217 N94-35861

Time-delay control of a magnetic levitated linear positioning system p 4217 N94-35862

Third order LPF type compensator for flexible rotor suspension p 4217 N94-35863

Second International Symposium on Magnetic Suspension Technology, part 2 [NASA-CP-3247-PT-2] p 4223 N94-35902

Electromagnetically levitated vibration isolation system for the manufacturing process of silicon monocrystals p 4223 N94-35906

Planar rotational magnetic micromotors with integrated shaft encoder and magnetic rotor levitation p 4224 N94-35907

Manufacturing and testing of a magnetically suspended composite flywheel energy storage system p 4224 N94-35910

Nonlinear feedback model attitude control using CCD in magnetic suspension system p 4225 N94-35912

Robust tracking control of a magnetically suspended rigid body p 4225 N94-35913

Magnetically suspended stepping motors for clean room and vacuum environments p 4225 N94-35915

Six degree of freedom fine motion positioning stage based on magnetic levitation p 4225 N94-35916

Analysis of achievable disturbance attenuation in a precision magnetically-suspended motion control system p 4225 N94-35917

Future ultra-speed tube-flight p 4225 N94-35918

Maglev crude oil pipeline p 4226 N94-35919

Dynamic stability of maglev systems [DE94-010451] p 4276 N94-36433

MAGNETIC TAPES

An analysis of file system and installation of the file management system for NOS operating system [DE94-611062] p 4346 N94-35833

MAGNETIZATION

Shape, size, and distribution of magnetic particles in Bjurbole chondrules p 4353 N94-36167

Magnetic metallic multilayers [DE94-011913] p 4341 N94-36274

MAGNETOHYDRODYNAMIC FLOW

A triggering mechanism of fast crash in sawtooth oscillation [DE94-718974] p 4336 N94-35772

MAGNETOHYDRODYNAMIC STABILITY

Collisonless dynamics of the magnetosphere [AD-A278886] p 4290 N94-35708

A triggering mechanism of fast crash in sawtooth oscillation [DE94-718974] p 4336 N94-35772

The kinetics of inhomogeneous plasma [DE94-611459] p 4336 N94-35788

Analysis of current diffusive ballooning mode [DE94-718992] p 4336 N94-35811

Neoclassical current and related MHD stability, gap modes, and radial electric field effects in heliotron and torsatron plasmas [DE94-718987] p 4337 N94-35938

Improved models of beta-limit, anomalous transport and radial electric field with loss cone loss in heliotron/torsatron [DE94-718976] p 4324 N94-35984

MAGNETOHYDRODYNAMIC WAVES

On the physics of waves in the solar atmosphere: Wave heating and wind acceleration [NASA-CR-194119] p 4375 N94-36395

MAGNETOHYDRODYNAMICS

Contributions of the low-latitude boundary layer to the finite width magnetotail convection model [NASA-CR-196116] p 4289 N94-35392

A triggering mechanism of fast crash in sawtooth oscillation [DE94-718974] p 4336 N94-35772

MHD and confinement characteristics in the high-beta regime on the CHS low-aspect-ratio heliotron/torsatron [DE94-718981] p 4339 N94-36357

MAGNETOMETERS

Operational support for Upper Atmosphere Research Satellite (UARS) attitude sensors p 4204 N94-35617

A new algorithm for attitude-independent magnetometer calibration p 4209 N94-35644

Magnetic properties of nanosize iron clusters [DE94-011329] p 4318 N94-36204

MAGNETORESISTIVITY

Magnetoresistance of films and strips with the diffuse surface scattering [DE94-611100] p 4340 N94-35933

Magnetic metallic multilayers [DE94-011913] p 4341 N94-36274

MAGNETOSPHERE-IONOSPHERE COUPLING

Modeling of the magnetosphere-ionosphere-atmosphere system [NASA-CR-195157] p 4288 N94-35244

MAGNETOSPHERIC INSTABILITY

ULF waves in the low-latitude boundary layer and their relationship to magnetospheric pulsations: A multisatellite observation [AD-A278906] p 4289 N94-35587

MAGNETRONS

State of the art in high-power microwaves: An overview [DE94-007075] p 4272 N94-35978

MAINTENANCE

Software architecture standard for simulation virtual machine, version 2.0 [NASA-CR-188291] p 4301 N94-35443

The development and application of composite complexity models and a relative complexity metric in a software maintenance environment p 4255 N94-35559

Implementation of a Computerized Maintenance Management System p 4343 N94-35970

MAMMALS

Multi-cellular, three-dimensional living mammalian tissue [NASA-CASE-MSC-21560-2] p 4296 N94-35232

MAN ENVIRONMENT INTERACTIONS

Asymetric change of daily temperature range: Proceedings [DE94-010102] p 4293 N94-35703

Endangered and potentially endangered wildlife on John F. Kennedy Space Center and faunal integrity as a goal for maintaining biological diversity [NASA-TM-109204] p 4288 N94-36422

MAN MACHINE SYSTEMS

Aerospace medicine and biology: A continuing bibliography with indexes (supplement 391) [NASA-SP-7011(391)] p 4297 N94-35345

International Space Station alpha remote manipulator system workstation controls test report [NASA-TM-104796] p 4274 N94-35481

MMI(exp 2) demonstrator systems: A multi-modal interface for man machine interaction with knowledge based systems. Deliverable D17 (TA 2) ESPRIT project 2474 MMI(exp 2) [PB94-170537] p 4298 N94-35600

MANAGEMENT INFORMATION SYSTEMS

COSMIC monthly progress report [NASA-CR-195962] p 4302 N94-35514

Fire data management system, FDMS 2.0, technical documentation [PB94-164019] p 4346 N94-35819

MANAGEMENT METHODS

CAirTOX: A compartment model for assessing the fate of and human exposure to toxic-chemical emissions to air [DE94-010084] p 4284 N94-35700

MANAGEMENT PLANNING

The Federal Aviation Administration plan for research, engineering and development p 4376 N94-35262

Apollo 11 at twenty-five, version 1.0 [NASA-CR-193380] p 4376 N94-35363

MANAGEMENT SYSTEMS

An analysis of file system and installation of the file management system for NOS operating system [DE94-611062] p 4346 N94-35833

Implementation of a Computerized Maintenance Management System p 4343 N94-35970

MANEUVERS

Hydrodynamics of maneuvering bodies: LDRD Final Report [DE94-009970] p 4265 N94-35769

Maneuvering and control of flexible space robots p 4218 N94-35867

MANIFOLDS (MATHEMATICS)

Generalized Fredholm determinants and Selberg zeta functions for axiom A dynamical systems [PB94-167665] p 4314 N94-35758

Some theorems on a class of harmonic manifolds [DE94-611102] p 4315 N94-35934

Quantum groups, non-commutative differential geometry and applications [DE94-011358] p 4315 N94-36270

MANIPULATORS

Kinematic modeling of a double octahedral Variable Geometry Truss (VGT) as an extensible gimbal [NASA-TM-109127] p 4311 N94-35242

MANNED SPACE FLIGHT

Space educators' handbook [NASA-TM-109779] p 4343 N94-35339

Budget estimates, fiscal year 1995. Volume 1: Agency summary, human space flight, and science, aeronautics and technology [NASA-TM-109791] p 4347 N94-35899

MANUFACTURING

Designing aluminum sealing glasses for manufacturability [DE94-010081] p 4244 N94-35699

Intelligent processing of materials, technical activities, 1993 (NAS-NRC Assessment Panel, April 21-22 1994) [PB94-164183] p 4251 N94-35737

CABPRO: An expert system for process planning multiwire cables [DE94-010213] p 4312 N94-35810

Electromagnetically levitated vibration isolation system for the manufacturing process of silicon monocrystals p 4223 N94-35906

Report on the Workshop on Manufacturing Polymer Composites by Liquid Molding [PB94-160066] p 4234 N94-36004

Design for manufacturability evaluation: Composite National Ignition Facility (NIF) pockel cell body [DE94-010669] p 4338 N94-36284

Optimisation of composite aircraft structures by direct manufacturing approaches p 4194 N94-36327

Hardness variability in commercial and hardened technologies [DE94-007270] p 4261 N94-36362

Using experimental design modules for process characterization in manufacturing/materials processes laboratories p 4230 N94-36405

Process capability determination of new and existing equipment p 4230 N94-36406

MANY BODY PROBLEM

On the theory of bounded many-particle systems with purely coulomb interactions [DE94-617215] p 4325 N94-36081

Dust evolution from comets and asteroids: Their velocities at Earth orbit intersection p 4352 N94-36142

MAPPING

Estimation of fractal dimensions from transect data [DE94-009808] p 4281 N94-36018

MARINE BIOLOGY

Proceedings: Integrated Research Planning Meeting for Gulf of Mexico Estuaries [PB94-157799] p 4296 N94-35738

MARINER SPACECRAFT

Wavelength calibration techniques and subtle surface and atmospheric absorption features in the Mariner 6, 7 IRS reflectance data p 4356 N94-35405

MARINER 6 SPACE PROBE

Wavelength calibration techniques and subtle surface and atmospheric absorption features in the Mariner 6, 7 IRS reflectance data p 4356 N94-35405

MARINER 7 SPACE PROBE

Wavelength calibration techniques and subtle surface and atmospheric absorption features in the Mariner 6, 7 IRS reflectance data p 4356 N94-35405

MARS (PLANET)

An automatic planetary vehicle for exploring Mars p 4354 N94-35336

High resolution visible to short-wave near-infrared CCD spectra of Mars during 1990 p 4356 N94-35403

Absolute calibration and atmospheric versus mineralogic origin of absorption features in 2.0 to 2.5 micron Mars spectra obtained during 1993 p 4356 N94-35404

Wavelength calibration techniques and subtle surface and atmospheric absorption features in the Mariner 6, 7 IRS reflectance data p 4356 N94-35405

Fluvial processes in Ma'adim Vallis and the potential of Gusev crater as a high priority site p 4358 N94-35414

The mass of Mars, Phobos, and Deimos, from the analysis of the Mariner 9 and Viking Orbiter tracking data p 4364 N94-35461

The real-time display of interferometry data for Goldstone radar astronomy data acquisition p 4255 N94-35560

Progress in the development of the GMM-2 gravity field model for Mars p 4371 N94-36155

MARS ATMOSPHERE

Windblown sand on Mars: The effect of saltation threshold on drift potentials derived from Mars GCM p 4366 N94-35474

Simultaneous adsorption of CO2 and H2O under Mars-like conditions and application to the evolution of the Martian climate p 4366 N94-35475

Atmospheric effects on the mapping of Martian thermal inertia and thermally derived albedo
p 4368 N94-36137

Mars atmospheric escape and isotopic fractionation: Synthesis of data and models p 4369 N94-36143

Uniqueness of a solution of a steady state photochemical problem: Applications to Mars p 4370 N94-36151

First measurement of helium on Mars: Implications for the problem of radiogenic gases on the terrestrial planets p 4370 N94-36153

MARS CRATERS

Fluvial processes in Ma'adim Vallis and the potential of Gusev crater as a high priority site
p 4358 N94-35414

Impact basins in Southern Daedalia, Mars: Evidence for clustered impactors? p 4360 N94-35426

Effects due to overlapping large impact basins on Mars p 4360 N94-35427

Noachian and Hesperian modification of the original Chryse impact basin topography p 4364 N94-35462

MARS ENVIRONMENT

Exopaleontology and the search for a fossil record on Mars p 4360 N94-35425

Simultaneous adsorption of CO2 and H2O under Mars-like conditions and application to the evolution of the Martian climate p 4366 N94-35475

MARS LANDING

Autonomous hazard detection and avoidance
[NASA-CR-188331] p 4309 N94-36439

MARS OBSERVER

The Mars Observer differential one-way range demonstration p 4210 N94-35543

The Mars Observer Ka-band link experiment
p 4255 N94-35563

MARS PHOTOGRAPHS

Subpixel resolution from multiple images
p 4281 N94-35417

MARS SURFACE

Mars aqueous chemistry experiment
[NASA-CR-196024] p 4354 N94-35263

An automatic planetary vehicle for exploring Mars
p 4354 N94-35336

Workshop on the Martian Northern Plains: Sedimentological, periglacial, and paleoclimatic evolution
[NASA-CR-196134] p 4354 N94-35359

High resolution visible to short-wave near-infrared CCD spectra of Mars during 1990 p 4356 N94-35403

Absolute calibration and atmospheric versus mineralogic origin of absorption features in 2.0 to 2.5 micron Mars spectra obtained during 1993 p 4356 N94-35404

Wavelength calibration techniques and subtle surface and atmospheric absorption features in the Mariner 6, 7 IRS reflectance data p 4356 N94-35405

Fluvial processes in Ma'adim Vallis and the potential of Gusev crater as a high priority site
p 4358 N94-35414

The fretted terrain of the Nilosyrtis Mensae region of Mars: Clues to the timing of dichotomy formation and the emplacement of the northern plains
p 4360 N94-35424

Exopaleontology and the search for a fossil record on Mars p 4360 N94-35425

Effects due to overlapping large impact basins on Mars p 4360 N94-35427

Quantifying shapes of volcanoes on Venus
p 4361 N94-35429

High Resolution Transmission Electron Microscopy (HRTEM) of nanophase ferric oxides
p 4239 N94-35433

The topography of Mars: A re-evaluation of current data p 4364 N94-35460

Noachian and Hesperian modification of the original Chryse impact basin topography p 4364 N94-35462

The parent magma of xenoliths in shergottite EETA79001: Bulk and trace element composition inferred from magmatic inclusions p 4352 N94-35467

Windblown sand on Mars: The effect of saltation threshold on drift potentials derived from Mars GCM
p 4366 N94-35474

Atmospheric effects on the mapping of Martian thermal inertia and thermally derived albedo
p 4368 N94-36137

Mossbauer and spectral (visible and near-IR) data for Fe(3+)-substituted rutile p 4240 N94-36154

MARTENSITIC TRANSFORMATION

Transformation plasticity in ductile solids
[DE94-010420] p 4240 N94-35953

MASERS

Three-photon micromasers
[DE94-611106] p 4272 N94-35782

MASS

The mass of Mars, Phobos, and Deimos, from the analysis of the Mariner 9 and Viking Orbiter tracking data p 4364 N94-35461

MASS BALANCE

Piggyback balance experiment: An illustration of Archimedes' principles and Newton's third law
[PB94-163060] p 4265 N94-35942

MASS DISTRIBUTION

Particulate and gaseous organic receptor modeling for the Southern California Air Quality Study
[PB94-156700] p 4285 N94-35735

Anthropogenic sulfate and organic aerosols, CCN, and cloud project concentration at a marine site
[DE94-004210] p 4286 N94-36025

MASS RATIOS

Applications of non-resonant RF forces for improvement of tokamak reactor performances. Part 1: Application of ponderomotive force
[DE94-718994] p 4336 N94-35813

MASS SPECTRA

Leptonic decay constants of heavy quarkonia in effective QCD sum rules
[DE94-611160] p 4322 N94-35784

MASS SPECTROMETERS

Capillary column GC-MS/MS confirmation of phosphate esters with a hybrid tandem mass spectrometer
[AD-A278748] p 4238 N94-36091

MASS SPECTROSCOPY

A combined experimental and theoretical study of the neutral, cationic and anionic Si3N cluster molecule
[AD-A278834] p 4323 N94-35792

Capillary column GC-MS/MS confirmation of phosphate esters with a hybrid tandem mass spectrometer
[AD-A278748] p 4238 N94-36091

MATERIALS RECOVERY

Consolidation of zircaloy-4 end crops by induction melting
[DE94-010031] p 4240 N94-35650

AICD: Advanced Industrial Concepts Division Biological and Chemical Technologies Research Program
[DE94-006854] p 4283 N94-36051

MATERIALS SCIENCE

Intelligent processing of materials, technical activities, 1993 (NAS-NRC Assessment Panel, April 21-22 1994)
[PB94-164183] p 4251 N94-35737

National Educators' Workshop: Update 1993. Standard Experiments in Engineering Materials Science and Technology
[NASA-CP-3259] p 4229 N94-36398

ASTM test methods for composite characterization and evaluation p 4229 N94-36399

Application of materials database (MAT.DB.) to materials education p 4230 N94-36402

Simulation of materials processing: Fantasy or reality?
p 4230 N94-36404

Using experimental design modules for process characterization in manufacturing/materials processes laboratories p 4230 N94-36405

Process capability determination of new and existing equipment p 4230 N94-36406

Graphing techniques for materials laboratory using Excel p 4232 N94-36414

Collection, processing, and reporting of damage tolerant design data for non-aerospace structural materials
[NASA-CR-196046] p 4347 N94-36435

MATERIALS TESTS

ASTM test methods for composite characterization and evaluation p 4229 N94-36399

Continuous unidirectional fiber reinforced composites: Fabrication and testing p 4229 N94-36400

Mechanical properties of crosslinked polymer coatings
p 4231 N94-36410

MATHEMATICAL LOGIC

A critique of type systems for global overloading
[AD-A278800] p 4304 N94-35676

The most abstract common refinement
[AD-A278870] p 4305 N94-36014

MATHEMATICAL MODELS

Cost and schedule estimation study report
[NASA-CR-189344] p 4300 N94-35256

Introduction to Neural Networks: Neural Network Workshop for the Hanford Community
[DE94-006526] p 4311 N94-35348

Contributions of the low-latitude boundary layer to the finite width magnetotail convection model
[NASA-CR-196116] p 4289 N94-35392

Shoemaker-Levy 9 and the tidal disruption of comets
p 4351 N94-35406

Developing interpretable models with optimized set reduction for identifying high risk software components
p 4301 N94-35435

The temperature of nitrogen on Pluto
p 4365 N94-35468

Influence of backup bearings and support structure dynamics on the behavior of rotors with active supports
[NASA-CR-196119] p 4274 N94-35500

Numerical modeling studies of wake vortex transport and evolution within the planetary boundary layer
[NASA-CR-196078] p 4192 N94-35522

Genetic algorithms
[PB94-171048] p 4303 N94-35602

Determination of extensional viscosity from capillary rheometer entrance pressure drop measurements using a numerical simulation of contraction flow
[PB94-171154] p 4263 N94-35603

Simulation models for computational plasma physics: Concluding report
[DE94-009976] p 4335 N94-35647

AFDM: An advanced fluid-dynamics model, volume 6
[DE94-009596] p 4264 N94-35669

Model documentation: Renewable Fuels Module of the National Energy Modeling System
[DE94-009962] p 4282 N94-35672

The breakdown of operators when interacting with the external world
[AD-A278936] p 4299 N94-35716

Three-photon micromasers
[DE94-611106] p 4272 N94-35782

Energy partitioning in high speed impact of analog solid rocket motors
[AD-A278771] p 4228 N94-35825

Integrated design of structures, controls, and materials
p 4218 N94-35869

Effects of noise variance model on optimal feedback design and actuator placement p 4220 N94-35883

Comparison of PDF and moment closure methods in the modeling of turbulent reacting flows
[NASA-TM-106614] p 4265 N94-35948

A three dimensional multigrid Reynolds-averaged Navier-Stokes solver for unstructured meshes
[NASA-CR-194908] p 4191 N94-35994

Analysis of mid-tropospheric carbon monoxide data using a three-dimensional global atmospheric chemistry numerical model
[DE94-004782] p 4286 N94-36026

A classical model for closed-loop diagrams of binary liquid mixtures
[DE94-011011] p 4237 N94-36033

A new association-model for binary VLE of alcohol/hydrocarbon and amine/hydrocarbon mixtures
[DE94-011012] p 4248 N94-36034

Theoretical and experimental study of air and hydrogen electrodes
[DE94-763308] p 4283 N94-36060

Classical time machine
[DE94-616616] p 4342 N94-36070

Functional integration method for the one-dimensional localization, the higher correlators and mean current in mesoscopic ring in the arbitrary magnetic field
[DE94-616621] p 4325 N94-36073

Distance dependent fractional statistics in a P, T-invariant model
[DE94-617360] p 4325 N94-36083

Progress in the development of the GMM-2 gravity field model for Mars p 4371 N94-36155

Three dimensional visualization of a coastal mesoscale model
[AD-A278576] p 4294 N94-36187

Kinetic theory of runaway air breakdown and the implications for lightning initiation
[DE94-001683] p 4295 N94-36240

An improved assessment approach for noise impacts from stationary point and traffic sources on humans and wildlife
[DE94-009728] p 4319 N94-36320

Analysis of high speed flow, thermal and structural interactions
[NASA-CR-196017] p 4268 N94-36420

Dynamic stability of maglev systems
[DE94-010451] p 4276 N94-36433

MATHEMATICS

Building on the foundation for an engineering career
p 4343 N94-35973

MATRICES (MATHEMATICS)

Three-photon micromasers
[DE94-611106] p 4272 N94-35782

Inverse problem for symmetric tridiagonal matrices. Calculation of discrete orthogonal polynomial system with arbitrary weight
[DE94-612434] p 4315 N94-35789

Modelling and control of a rotor supported by magnetic bearings p 4216 N94-35858

MATRIX MATERIALS

Tough high performance composite matrix
[NASA-CASE-LAR-14239-2] p 4232 N94-35372

Liquid crystalline thermosetting polyimides
[DE94-009939] p 4244 N94-35768

Integrated design of structures, controls, and materials
p 4218 N94-35869

Cement paste matrix composite materials center
[AD-A279017] p 4233 N94-35952

Nanochannel glass matrix used in making mesoscopic structures
[AD-D016216] p 4234 N94-36123

High temperature creep and oxidation resistant chromium silicide matrix alloy containing molybdenum [NASA-CASE-LEW-15697-1] p 4241 N94-36275

MATRIX METHODS

Applying transfer matrix method to the estimation of the modal characteristics of the NASA Mini-Mass Truss p 4218 N94-35870

Numerical method to study the stability of periodic solutions of particle motion in nonlinear magnetic fields [DE94-610740] p 4325 N94-36088

MAXIMUM LIKELIHOOD ESTIMATES

Maximum-likelihood soft-decision decoding of block codes using the A* algorithm p 4254 N94-35555

Point and interval estimation of series system reliability using small data sets [AD-A278647] p 4316 N94-35575

MEASURING INSTRUMENTS

Ionic contamination detection [DE94-010212] p 4258 N94-35686

Six degree of freedom fine motion positioning stage based on magnetic levitation p 4225 N94-35916

Measurement of a surface heat flux and temperature p 4231 N94-36407

MECHANICAL ENGINEERING

Implementation of a Computerized Maintenance Management System p 4343 N94-35970

Case based reasoning in engineering design [AD-A278943] p 4305 N94-36006

Using experimental design modules for process characterization in manufacturing/materials processes laboratories p 4230 N94-36405

MECHANICAL PROPERTIES

JPRS report: Science and technology. Central Eurasia: Materials science [JPRS-UMS-93-007] p 4240 N94-35517

Thick film fabrication of aluminum nitride microcircuits [DE94-010107] p 4259 N94-35706

Properties and bibliography of GaSe [AD-A279064] p 4340 N94-35733

Continuous unidirectional fiber reinforced composites: Fabrication and testing p 4229 N94-36400

Laminated thermoplastic composite material from recycled high density polyethylene p 4230 N94-36403

Mechanical properties of crosslinked polymer coatings p 4231 N94-36410

Collection, processing, and reporting of damage tolerant design data for non-aerospace structural materials [NASA-CR-196046] p 4347 N94-36435

MEDICAL SCIENCE

Bibliography of research reports and publications issued by the Human Engineering Division [AD-A278787] p 4299 N94-35712

Activities of National Institute of Radiological Sciences [DE94-727636] p 4296 N94-36101

MELTING

Interface shape and convection during solidification and melting of succinonitrile [NASA-TM-106487] p 4262 N94-35248

Consolidation of zircaloy-4 end crops by induction melting [DE94-010031] p 4240 N94-35650

Partial melting of the St. Severin (LL) and Lost City (H) ordinary chondrites: One step backwards and two steps forward p 4353 N94-36146

Production of ferroan andesites by the experimental partial melting of an LL chondrite p 4353 N94-36160

Partition coefficients for Al, Ca, Ti, Cr, and Ni in olivine obtained by melting experiment on an LL6 chondrite p 4353 N94-36163

MELTS (CRYSTAL GROWTH)

On the possible role of elemental carbon in the formation of reduced chondrules p 4351 N94-35421

Synthetic and natural Nakhla pyroxenes: Parent melt composition and REE partition coefficients p 4353 N94-36161

MEMBRANES

Combined SO(x)/NO(x) control via SOXAL (tm) process: An electrodialytic regenerative wet scrubbing process [DE94-009053] p 4284 N94-35346

A low temperature scanning force microscope for biological samples [DE94-011357] p 4297 N94-36269

MEMORY (COMPUTERS)

Communication and memory requirements as the basis for mapping task and data parallel programs [AD-A278954] p 4310 N94-35806

A critical examination of charge funneling and its impact on single-event upset in Si devices [DE94-007868] p 4261 N94-36373

MENISCI

Transient body force effects on the dryout and rewet of a heated capillary structure [AD-A278677] p 4264 N94-35690

MERCURY (PLANET)

The real-time display of interferometry data for Goldstone radar astronomy data acquisition p 4255 N94-35560

MERCURY SURFACE

Mercury: Mid-infrared (7.3 - 13.5 microns) spectroscopic observations showing features characteristic of plagioclase p 4370 N94-36150

MESOMETEOROLOGY

Atmospheric and dispersion modeling in areas of highly complex terrain employing a four-dimensional data assimilation technique [DE94-004041] p 4285 N94-35823

MESON RESONANCE

Hybrid mesons (Q(anti Q)g) in N(anti N) annihilation [DE94-001491] p 4327 N94-36239

MESON-MESON INTERACTIONS

Low energy theorems from the effective Lagrangian with vector mesons [DE94-611173] p 4322 N94-35785

MESONS

The silent phase transition in mesonic bags and lattice theory [DE94-616852] p 4321 N94-35583

Hybrid mesons (Q(anti Q)g) in N(anti N) annihilation [DE94-001491] p 4327 N94-36239

Decay of the D(sub s)-meson [DE94-611209] p 4329 N94-36308

MESOSCALE PHENOMENA

Mesoscale roughness of Venus p 4361 N94-35430

Atmospheric and dispersion modeling in areas of highly complex terrain employing a four-dimensional data assimilation technique [DE94-004041] p 4285 N94-35823

Three dimensional visualization of a coastal mesoscale model [AD-A278576] p 4294 N94-36187

MESSAGE PROCESSING

The rel/REL: A family of reliable multicast protocols for distributed real-time systems [PB94-167830] p 4310 N94-35535

A compile time model for composing parallel programs [AD-A278896] p 4310 N94-35597

METABOLISM

Effect of microgravity on plant growth [NASA-CR-196004] p 4296 N94-35257

METAL CLUSTERS

Nonlinear optical composites of metal cluster laden polymers [AD-D016217] p 4234 N94-36124

Metal cluster alloys and oxides: Elucidating structural and electronic effects in governing the reactivity and catalytic role of matter in finite dimensions [DE94-010224] p 4328 N94-36298

METAL COATINGS

A novel method for depositing precious metal films on difficult surfaces [NASA-TM-106607] p 4243 N94-35260

METAL FATIGUE

Fatigue and residual strength behaviour of ARALL3 panels with bonded-on doublers [AD-B181062] p 4279 N94-36226

METAL FIBERS

Continuous unidirectional fiber reinforced composites: Fabrication and testing p 4229 N94-36400

METAL FILMS

A novel method for depositing precious metal films on difficult surfaces [NASA-TM-106607] p 4243 N94-35260

Effect of niobium interlayer on high-temperature sliding friction and wear of silver films on alumina [DE94-010462] p 4275 N94-36232

METAL HYDRIDES

Theoretical and experimental study of air and hydrogen electrodes [DE94-763308] p 4283 N94-36060

METAL IONS

New calculations of Fe spectra in high-temperature plasmas [DE94-009919] p 4339 N94-36386

METAL MATRIX COMPOSITES

Implementation of the military handbook 17 for polymer matrix composites and metal matrix composites [AD-A278795] p 4244 N94-35757

Isothermal damage and fatigue behavior of SCS-6/Timetal 21S (0/90)s composite at 650 C [NASA-CR-195345] p 4234 N94-35995

Advanced composites in Japan p 4234 N94-36045

Fatigue and residual strength behaviour of ARALL3 panels with bonded-on doublers [AD-B181062] p 4279 N94-36226

METAL NITRIDES

Digital control programmer for temperature control [DE94-615584] p 4309 N94-36382

METAL OXIDE SEMICONDUCTORS

Estimating low-dose rate irradiation response of MOSFETs [DE94-007292] p 4342 N94-36367

METAL PLATES

Transient body force effects on the dryout and rewet of a heated capillary structure [AD-A278677] p 4264 N94-35690

METAL SHEETS

Transformation plasticity in ductile solids [DE94-010420] p 4240 N94-35953

METAL SURFACES

Processing and properties of high temperature metal/fiber-reinforced-thermoplastic laminates [AD-A278791] p 4232 N94-35654

Morphology of meteoroid and space debris craters on LDEF metal targets p 4353 N94-36159

Formation and stability of Fe-rich precipitates in dilute Zr(Fe) single-crystal alloys [DE94-619027] p 4242 N94-36288

METALLIZING

A novel method for depositing precious metal films on difficult surfaces [NASA-TM-106607] p 4243 N94-35260

Au/Zn contacts to Rho-InP: Electrical and metallurgical characteristics and the relationship between them [NASA-TM-106590] p 4281 N94-35271

METALORGANIC CHEMICAL VAPOR DEPOSITION

The optimization of interfaces in InAsSb/InGaAs strained-layer superlattices grown by metal-organic chemical vapor deposition [DE94-010070] p 4340 N94-35698

Development of novel II-VI solar cells [PB94-159415] p 4282 N94-35739

High temperature heterojunction bipolar transistors [AD-A278605] p 4261 N94-36360

METALS

Intelligent processing of materials, technical activities, 1993 (NAS-NRC Assessment Panel, April 21-22 1994) [PB94-164183] p 4251 N94-35737

Modeling the atmospheric input of nutrients, heavy metals, and pesticides to the Great Lakes [DE94-005481] p 4286 N94-36007

The relationship between hydroxyl groups on oxide surfaces and the properties of supported metals [DE94-010786] p 4241 N94-36233

Ion modulated electroactivity in thin film metallopolymers [AD-A278618] p 4246 N94-36253

METAMORPHISM (GEOLOGY)

FeO and MgO in plagioclase of lunar anorthosites: Igneous or metamorphic? p 4351 N94-35449

More shock recovery experiments on mesosiderite analogs p 4351 N94-35455

Shocked materials from the Dutch Peak diamictite, Utah p 4352 N94-36140

Calorimetric thermobarometry of experimentally shocked quartz p 4240 N94-36174

METASTABLE STATE

On the origin of porphyritic chondrules [DE94-010464] p 4351 N94-36418

METEORITE COLLISIONS

JPRS report: Science and technology. Central Eurasia: Space [JPRS-USP-94-001] p 4201 N94-35518

Shocked materials from the Dutch Peak diamictite, Utah p 4352 N94-36140

Hematite formed from pyroxene on Mars by meteoritic impact p 4372 N94-36165

METEORITE CRATERS

Impact basins in Southern Daedalia, Mars: Evidence for clustered impactors? p 4360 N94-35426

Effects due to overlapping large impact basins on Mars p 4360 N94-35427

Distribution of siderophile and other trace elements in melt rock at the Chicxulub impact structure p 4352 N94-35456

Current activities and results of the Long Duration Exposure Facility Meteoroid and Debris Special Investigation Group p 4352 N94-35458

Morphology of meteoroid and space debris craters on LDEF metal targets p 4353 N94-36159

METEORITES

What initiated planetesimal formation? p 4351 N94-35422

Inhomogeneous distribution of materials in lodranites-acapulcoites and IAB irons and their common formation processes p 4364 N94-35463

Pigeonholing planetary meteorites: The lessons of misclassification of EET87521 and ALH84001 p 4353 N94-36157

Synthetic and natural Nakhla pyroxenes: Parent melt composition and REE partition coefficients p 4353 N94-36161

On the origin of porphyritic chondrules [DE94-010464] p 4351 N94-36418

METEORITIC COMPOSITION
The Twenty-Fifth Lunar and Planetary Science Conference. Part 1: A-G
[NASA-CR-195743] p 4355 N94-35395
Calorimetric thermometry of meteoritic troilite: Preliminary thermometer relationships
p 4355 N94-35399
Alteration and formation of rims on the CM parent body p 4357 N94-35411
On the possible role of elemental carbon in the formation of reduced chondrules p 4351 N94-35421
The occurrence of blue luminescing enstatite in E3 and E4 chondrites p 4351 N94-35423
Antarctic weathering of the CK chondrites EET90004, 90007, and 90022: Nickel and sulfur mobility
p 4351 N94-35451
More shock recovery experiments on mesosiderite analogs p 4351 N94-35455
Distribution of siderophile and other trace elements in melt rock at the Chicxulub impact structure
p 4352 N94-35456
The parent magma of xenoliths in shergottite EETA79001: Bulk and trace element composition inferred from magmatic inclusions p 4352 N94-35467
Chondrule magnetic properties p 4352 N94-35471
Mineralogy of an unusual CM clast in the Kaidun meteorite p 4352 N94-35476
The Twenty-Fifth Lunar and Planetary Science Conference. Part 2: H-O
[NASA-CR-195744] p 4367 N94-36136
Textural constraints on the formation of alteration phases in CM chondrites p 4353 N94-36145
Partial melting of the St. Severin (LL) and Lost City (H) ordinary chondrites: One step backwards and two steps forward p 4353 N94-36146
Preliminary results of sulfide melt/silicate wetting experiments in a partially melted ordinary chondrite
p 4353 N94-36147
Pigeonholing planetary meteorites: The lessons of misclassification of EET87521 and ALH84001
p 4353 N94-36157
On the origin of enstatite chondrite chondrules based on their petrography and comparison with experimentally produced chondrules p 4353 N94-36158
Production of ferroan andesites by the experimental partial melting of an LL chondrite p 4353 N94-36160
Synthetic and natural Nakhla pyroxenes: Parent melt composition and REE partition coefficients
p 4353 N94-36161
Cr, Mn, and Ca distributions for olivine in angritic systems: Constraints on the origins of Cr-rich and Ca-poor core olivine in angrite LEW87051 p 4353 N94-36162
Partition coefficients for Al, Ca, Ti, Cr, and Ni in olivine obtained by melting experiment on an LL6 chondrite
p 4353 N94-36163
Ferromagnetic resonance spectra of H2-reduced minerals and glasses p 4240 N94-36164
Shape, size, and distribution of magnetic particles in Bjurbole chondrules p 4353 N94-36167
Pre-bombardment crystallization ages of basaltic clasts from Antarctic howardites EET87503 and EET87513
p 4354 N94-36172
On the origin of porphyritic chondrules
[DE94-010464] p 4351 N94-36418

METEORITIC DAMAGE
Impact basins in Southern Daedalia, Mars: Evidence for clustered impactors? p 4360 N94-35426
Effects due to overlapping large impact basins on Mars p 4360 N94-35427
Distribution of siderophile and other trace elements in melt rock at the Chicxulub impact structure
p 4352 N94-35456
Current activities and results of the Long Duration Exposure Facility Meteoroid and Debris Special Investigation Group p 4352 N94-35458
Shocked materials from the Dutch Peak diamictite, Utah p 4352 N94-36140

METEORITIC MICROSTRUCTURES
More shock recovery experiments on mesosiderite analogs p 4351 N94-35455
Textural constraints on the formation of alteration phases in CM chondrites p 4353 N94-36145

METEOROIDS
Eureka! Aerogel capture of meteoroids in space
p 4351 N94-35412
Current activities and results of the Long Duration Exposure Facility Meteoroid and Debris Special Investigation Group p 4352 N94-35458
Natural orbital environment definition guidelines for use in aerospace vehicle development
[NASA-TM-4527] p 4291 N94-36175

METEOROLOGICAL CHARTS
The polygon-ellipse method of data compression of weather maps
[AD-A278958] p 4293 N94-35719

METEOROLOGICAL PARAMETERS
Implementation of a low-cost, commercial orbit determination system p 4205 N94-35621
Three dimensional visualization of a coastal mesoscale model
[AD-A278576] p 4294 N94-36187
Environmental measurements in the Beaufort Sea, Spring 1993
[AD-A278718] p 4296 N94-36293

METEOROLOGICAL RADAR
Terminal Doppler Weather Radar (TDWR) Low Level Wind Shear Alert System 3 (LLWAS 3) integration studies at Orlando International Airport
[AD-A278957] p 4294 N94-35807
Doppler weather radar studies of precipitation systems
[AD-A279417] p 4295 N94-36262

METEOROLOGICAL SERVICES
The influence of data link-provided graphical weather on pilot decision-making
[AD-A278871] p 4293 N94-35596
Data requirements for ceiling and visibility products development
[AD-A278959] p 4293 N94-35720

METEOROLOGY
Computer animation of clouds
[DE94-008289] p 4292 N94-35350

METHANATION
Methane production and consumption in grassland and boreal ecosystems
[NASA-CR-196085] p 4284 N94-35486

METHANE
Methane production and consumption in grassland and boreal ecosystems
[NASA-CR-196085] p 4284 N94-35486
Novel catalysts for methane activation
[DE94-009705] p 4237 N94-35778
Gasoline from natural gas by sulfur processing
[DE94-011130] p 4248 N94-36035
Advanced hydrogen/method utilization technology demonstration
[DE94-000214] p 4248 N94-36191

METHIONINE
Stress and brain protein synthesis
[PB94-170750] p 4296 N94-35601

METHOD OF MOMENTS
Comparison of PDF and moment closure methods in the modeling of turbulent reacting flows
[NASA-TM-106614] p 4265 N94-35948

METHYL ALCOHOL
Methanol fuel additive demonstration
[PB94-156668] p 4247 N94-35941
The effect of alternative fuels on the stability and lubricity of crankcase lubricants
[DE94-010353] p 4245 N94-36108
Research and development of Proton-Exchange Membrane (PEM) fuel cell system for transportation applications: Initial conceptual design report
[DE94-010576] p 4283 N94-36243
Heterogeneous catalytic process for alcohol fuels from syngas
[DE94-010263] p 4248 N94-36299

METRIC SPACE
Successive minima on arithmetic varieties
[PB94-167699] p 4314 N94-35759
Entropy of graphs, semigroups and groups
[PB94-167749] p 4314 N94-35763

METROLOGY
The development and application of composite complexity models and a relative complexity metric in a software maintenance environment
p 4255 N94-35559
Piggyback balance experiment: An illustration of Archimedes' principles and Newton's third law
[PB94-163060] p 4265 N94-35942

MICA
Application of an alkylammonium method for characterization of phyllosilicates in CI chondrites
p 4351 N94-35432

MICROANALYSIS
New prospects for analyzing lunar pyroclastic glass
p 4355 N94-35397
Single agglutinates: A comparative study of compositions of agglutinitic glass, whole-grain, bulk soil, and FMR p 4355 N94-35401
The anatomy of a cluster IDP. Part 1: Carbon abundance, bulk chemistry, and mineralogy of fragments from L2008#5 p 4352 N94-35466
Continuum fluorescence of Cu in NbTi/Cu composite wires
[DE94-008940] p 4241 N94-36242

MICROBURSTS (METEOROLOGY)
Terminal Doppler Weather Radar (TDWR) Low Level Wind Shear Alert System 3 (LLWAS 3) integration studies at Orlando International Airport
[AD-A278957] p 4294 N94-35807

MICROCHANNEL PLATES
Neutron detectors for fusion reaction-rate measurements
[DE94-010407] p 4330 N94-36114
Design and construction of a imaging instrument for studying ion emission from pure ion emitters
[DE94-010702] p 4328 N94-36302

MICROCOMPUTERS
Digital control programmer for temperature control
[DE94-615584] p 4309 N94-36382

MICROCRACKS
Acoustical-optical fracture analysis
[PB94-170602] p 4279 N94-36216

MICROELECTRONICS
Thick film fabrication of aluminum nitride microcircuits
[DE94-010107] p 4259 N94-35706
Space-based crystal growth and thermocapillary flow
p 4342 N94-35971
Rapid and accurate timing simulation of radiation-hardened digital microelectronics using VHDL
[AD-A278644] p 4261 N94-36361
Hardness variability in commercial and hardened technologies
[DE94-007270] p 4261 N94-36362
Measurement of a surface heat flux and temperature
p 4231 N94-36407

MICROGRAVITY
Analysis of phase distribution phenomena in microgravity environments
[NASA-CR-196038] p 4249 N94-35237
Effect of microgravity on plant growth
[NASA-CR-196004] p 4296 N94-35257
The control of satellites with microgravity constraints: The COMET Control System p 4207 N94-35632
Microgravity isolation system design: A modern control synthesis framework p 4215 N94-35851
Space-based crystal growth and thermocapillary flow
p 4342 N94-35971

MICROGRAVITY APPLICATIONS
Space-based crystal growth and thermocapillary flow
p 4342 N94-35971

MICROINSTRUMENTATION
Electrostatically suspended and sensed micro-mechanical rate gyroscope p 4224 N94-35908

MICROMECHANICS
Planar rotational magnetic micromotors with integrated shaft encoder and magnetic rotor levitation
p 4224 N94-35907

MICROMETEOROIDS
Purity and cleanness of aerogel as a cosmic dust capture medium p 4247 N94-35469
Morphology of meteoroid and space debris craters on LDEF metal targets p 4353 N94-36159

MICROMINIATURIZED ELECTRONIC DEVICES
Electrostatically suspended and sensed micro-mechanical rate gyroscope p 4224 N94-35908

MICROMOTORS
Planar rotational magnetic micromotors with integrated shaft encoder and magnetic rotor levitation
p 4224 N94-35907

MICROORGANISMS
Exopaleontology and the search for a fossil record on Mars p 4360 N94-35425

MICROPARTICLES
Digital control programmer for temperature control
[DE94-615584] p 4309 N94-36382

MICROPOROSITY
Microporous structure with layered interstitial surface treatment, and method and apparatus for preparation thereof
[NASA-CASE-MSC-21487-3] p 4235 N94-35229
Atomic oxygen reactor having at least one sidearm conduit
[NASA-CASE-MSC-21487-4] p 4250 N94-35445

MICROPROCESSORS
Overview of the MSTI 2 processor-in-the-loop simulator p 4207 N94-35631

MICROSCOPY
Fluorescence detection of single molecules using pulsed near-field optical excitation and time correlated photon counting
[DE94-007553] p 4320 N94-35376

MICROSTRIP DEVICES
Experimental characterisation of gas microstrip detectors. Part 2: Counting rate characteristics
[PB94-167095] p 4269 N94-36061

MICROSTRIP TRANSMISSION LINES
Switched-beam radiometer front-end network analysis
[NASA-CR-194922] p 4252 N94-35247

MICROSTRUCTURE
Structures and properties of materials recovered from high shock pressures
[DE94-010057] p 4232 N94-35696
Integrated design of structures, controls, and materials
p 4218 N94-35869

Cement paste matrix composite materials center
[AD-A279017] p 4233 N94-35952
Investigation of moisture-induced embrittlement of iron aluminides
[DE94-010881] p 4241 N94-36196
Microstructural development in solution derived PZT thin films
[DE94-008744] p 4246 N94-36209

MICROWAVE ANTENNAS
Field demonstration of X-band photonic antenna remoting in the Deep Space Network
p 4252 N94-35545

MICROWAVE CIRCUITS
A 32-GHz solid-state power amplifier for deep space communications p 4255 N94-35562

MICROWAVE EMISSION
State of the art in high-power microwaves: An overview
[DE94-007075] p 4272 N94-35978

MICROWAVE EQUIPMENT
Influence of an externally modulated photonic link on a microwave communications system
p 4252 N94-35544
DSS-13 S-/X-band microwave feed system
p 4253 N94-35550

MICROWAVE FREQUENCIES
Dielectric measurements of selected ceramics at microwave frequencies p 4232 N94-36412

MICROWAVE IMAGERY
Production of long-term global water vapor and liquid water data set using ultra-fast methods to assimilate multi-satellite and radiosonde observations
[NASA-CR-196044] p 4292 N94-35355

MICROWAVE LANDING SYSTEMS
An analysis of operational suitability for test and evaluation of highly reliable systems
[AD-A278573] p 4192 N94-36184

MICROWAVE OSCILLATORS
A 1- to 10-GHz downconverter for high-resolution microwave survey p 4253 N94-35551

MICROWAVE PROBES
Network analyzer calibration for cryogenic on-wafer measurements
[DE94-010089] p 4262 N94-36430

MICROWAVE SOUNDING
Earth Observing System (EOS) Advanced Microwave Sounding Unit-A (AMSU-A) schedule plan
[NASA-CR-194856] p 4281 N94-35734
Application of differential inversion to DMSP microwave sounder data
[AD-A278575] p 4294 N94-36186

MICROWAVE TUBES
State of the art in high-power microwaves: An overview
[DE94-007075] p 4272 N94-35978

MICROWAVES
Influence of an externally modulated photonic link on a microwave communications system
p 4252 N94-35544
A 1- to 10-GHz downconverter for high-resolution microwave survey p 4253 N94-35551
State of the art in high-power microwaves: An overview
[DE94-007075] p 4272 N94-35978
On the effects of transforming the vibrational spectra of molecular systems under microwave radiation
[DE94-617057] p 4329 N94-36310
Astronomy in the region between 1 mm and 0.1 mm wavelength
[NASA-CR-196020] p 4349 N94-36419
Analysis of recent agile mirror data
[AD-A278758] p 4318 N94-36427
Network analyzer calibration for cryogenic on-wafer measurements
[DE94-010089] p 4262 N94-36430

MIDDLE ATMOSPHERE
Uniqueness of a solution of a steady state photochemical problem: Applications to Mars p 4370 N94-36151

MILITARY OPERATIONS
Future tanker considerations and requirements
p 4197 N94-36342
Hose-drogue versus boom receptacle air refueling
p 4197 N94-36345

MILLIMETER WAVES
A 32-GHz solid-state power amplifier for deep space communications p 4255 N94-35562
State of the art in high-power microwaves: An overview
[DE94-007075] p 4272 N94-35978

MIMD (COMPUTERS)
Overset grid applications on distributed memory MIMD computers
[NASA-CR-196081] p 4268 N94-36397

MIMO (CONTROL SYSTEMS)
Microgravity isolation system design: A modern control synthesis framework p 4215 N94-35851
Adaptive model reduction for continuous systems via recursive rational interpolation p 4219 N94-35876

MINERAL DEPOSITS
Grain rims on ilmenite in the lunar regolith: Comparison to vapor deposits on regolith silicates
p 4359 N94-35418
Petrographic characterization of lunar soils: Application of x ray digital-imaging to quantitative and automated analysis p 4368 N94-36138

MINERALOGY
Absolute calibration and atmospheric versus mineralogic origin of absorption features in 2.0 to 2.5 micron Mars spectra obtained during 1993 p 4356 N94-35404
Wavelength calibration techniques and subtle surface and atmospheric absorption features in the Mariner 6, 7 IRS reflectance data p 4356 N94-35405
A mineralogical instrument for planetary applications
p 4357 N94-35408
Grain rims on ilmenite in the lunar regolith: Comparison to vapor deposits on regolith silicates
p 4359 N94-35418
On the possible role of elemental carbon in the formation of reduced chondrules p 4351 N94-35421
Exopaleontology and the search for a fossil record on Mars p 4360 N94-35425
High Resolution Transmission Electron Microscopy (HRTEM) of nanophase ferric oxides
p 4239 N94-35433
Antarctic weathering of the CK chondrites EET90004, 90007, and 90022: Nickel and sulfur mobility
p 4351 N94-35451
Thermal emission measurements (5-25 microns) of Hawaiian palagonitic soils with implications for Mars
p 4292 N94-35452
Transmission measurements (4000-400 cm(exp -1), 2.5-25 microns) of crystalline ferric oxides and ferric oxyhydroxides: Implications for Mars
p 4292 N94-35454
Distribution of siderophile and other trace elements in melt rock at the Chicxulub impact structure
p 4352 N94-35456
Innovative instrumentation for mineralogical and elemental analyses of solid extraterrestrial surfaces: The Backscatter Moessbauer Spectrometer/X Ray Fluorescence analyzer (BaMS/XRF)
p 4239 N94-35459
Inhomogeneous distribution of materials in lodranites-acapulcoites and IAB irons and their common formation processes p 4364 N94-35463
The anatomy of a cluster IDP. Part 1: Carbon abundance, bulk chemistry, and mineralogy of fragments from L2008#5 p 4352 N94-35466
A quick look method of detecting water of hydration in small solar system bodies p 4352 N94-35470
Mineralogy of an unusual CM clast in the Kaidun meteorite p 4352 N94-35476
Mineralogy of artificially heated carbonaceous chondrites p 4352 N94-35477
The Twenty-Fifth Lunar and Planetary Science Conference. Part 2: H-O
[NASA-CR-195744] p 4367 N94-36136
Electron energy-loss spectroscopy of carbon in interplanetary dust particles p 4353 N94-36149
Synthetic and natural Nakhla pyroxenes: Parent melt composition and REE partition coefficients
p 4353 N94-36161
Cr, Mn, and Ca distributions for olivine in angritic systems: Constraints on the origins of Cr-rich and Ca-poor core olivine in angrite LEW87051 p 4353 N94-36162
Moessbauer mineralogy of calcined Murchison meteorite p 4353 N94-36166

MINERALS
National Geoscience Data Repository System
[DE94-000120] p 4344 N94-35347
Lunar mineral feedstocks from rocks and soils: X-ray digital imaging in resource evaluation
p 4358 N94-35415
Exopaleontology and the search for a fossil record on Mars p 4360 N94-35425
Application of an alkylammonium method for characterization of phyllosilicates in CI chondrites
p 4351 N94-35432
High Resolution Transmission Electron Microscopy (HRTEM) of nanophase ferric oxides
p 4239 N94-35433
Inhomogeneous distribution of materials in lodranites-acapulcoites and IAB irons and their common formation processes p 4364 N94-35463
Mossbauer and spectral (visible and near-IR) data for Fe(3+)-substituted rutile p 4240 N94-36154
Ferromagnetic resonance spectra of H2-reduced minerals and glasses p 4240 N94-36164

MINIMA
Successive minima on arithmetic varieties
[PB94-167699] p 4314 N94-35759

MINIMAX TECHNIQUE
Asymetric change of daily temperature range: Proceedings
[DE94-010102] p 4293 N94-35703

MIRRORS
Design and implementation of a beam-waveguide mirror control system for vernier pointing of the DSS-13 antenna p 4253 N94-35548
Issues in the design and optimization of adaptive optics and laser guide stars for the Keck Telescopes
[DE94-009384] p 4349 N94-35565
Analysis of recent agile mirror data
[AD-A278758] p 4318 N94-36427

MISSILE CONFIGURATIONS
User's guide for an interactive personal computer interface for the aeroprediction code
[NSWCDD/TR-94/107] p 4305 N94-35958
The analysis of a generic air-to-air missile simulation model
[NASA-TM-109057] p 4309 N94-36438

MISSILE SYSTEMS
The analysis of a generic air-to-air missile simulation model
[NASA-TM-109057] p 4309 N94-36438

MISSILE TRACKING
Overview of the Miniature Sensor Technology Integration (MSTI) spacecraft attitude control system
p 4206 N94-35627
Overview of the MSTI 2 on-orbit alignment
p 4206 N94-35629

MISSILES
Numerical simulation of shock interaction with above-ground structures
[AD-A278713] p 4279 N94-35949

MISSION PLANNING
Apollo 11 at twenty-five, version 1.0
[NASA-CR-193380] p 4376 N94-35363
Materials processing in space tasks. WBS task 5.4: Generic tasks
[NASA-CR-193979] p 4249 N94-35485
Automated maneuver planning using a fuzzy logic algorithm p 4203 N94-35610
Spacecraft attitude determination accuracy from mission experience p 4204 N94-35618
Application of star identification using pattern matching to space ground systems at GSFC
p 4209 N94-35640

MIXING RATIOS
Analysis of mid-tropospheric carbon monoxide data using a three-dimensional global atmospheric chemistry numerical model
[DE94-004782] p 4286 N94-36026
First measurement of helium on Mars: Implications for the problem of radiogenic gases on the terrestrial planets p 4370 N94-36153

MOBILE COMMUNICATION SYSTEMS
Large granularity cache coherence for intermittent connectivity
[AD-A278897] p 4345 N94-35571
Application of a Monte Carlo accuracy assessment tool to TDRS and GPS p 4207 N94-35635

MODELS
A compile time model for composing parallel programs
[AD-A278896] p 4310 N94-35597

MODULARITY
Use of formal calculation to automatically obtain adjoint programs
[PB94-170701] p 4308 N94-36259

MODULATION
Activities of the optoelectronics laboratory
[PB94-171196] p 4334 N94-36190
Attention and signal detection. A study of attention divided between visual and auditory signals
[PB94-170594] p 4298 N94-36215

MODULATORS
Characterization of lithium niobate electro-optic modulators at cryogenic temperatures
[DE94-010059] p 4333 N94-35697

MODULES
Laser drilling of vertical vias in silicon
[DE94-009250] p 4270 N94-35351
The development and application of composite complexity models and a relative complexity metric in a software maintenance environment
p 4255 N94-35559

MOISTURE CONTENT
Production of long-term global water vapor and liquid water data set using ultra-fast methods to assimilate multi-satellite and radiosonde observations
[NASA-CR-195981] p 4293 N94-35499

MOLECULAR BEAM EPITAXY
Development of ultra-low noise, high performance 3 to 5 Quantum Well Infrared Photodetectors (QWIPs) for focal plane array staring image sensor systems
[AD-A278861] p 4342 N94-36385

MOLECULAR BEAMS
Ultrafast chemical dynamics of reactions in beams
[AD-A278939] p 4323 N94-35805
MOLECULAR CLUSTERS
Metal cluster alloys and oxides: Elucidating structural and electronic effects in governing the reactivity and catalytic role of matter in finite dimensions
[DE94-010224] p 4328 N94-36298
MOLECULAR COLLISIONS
A two-dimensional model for collisional energy transfer in bimolecular ion-molecule dynamics
[AD-A278913] p 4321 N94-35589
State-to-state dynamics of molecular energy transfer
[DE94-009651] p 4324 N94-35816
MOLECULAR DYNAMICS
Vacuum ultraviolet studies of molecular dynamics
[AD-A278940] p 4321 N94-35657
Ultrafast chemical dynamics of reactions in beams
[AD-A278939] p 4323 N94-35805
State-to-state dynamics of molecular energy transfer
[DE94-009651] p 4324 N94-35816
Multicomponent glass surfaces: Structure and adsorption
[DE94-010516] p 4246 N94-36283
MOLECULAR ELECTRONICS
Electrical microengineering of redox enzymes
[AD-A279015] p 4236 N94-35745
MOLECULAR ENERGY LEVELS
Intramolecular energy transfer reactions in polymetallic complexes
[DE94-010114] p 4326 N94-36126
MOLECULAR EXCITATION
Fluorescence detection of single molecules using pulsed near-field optical excitation and time correlated photon counting
[DE94-007553] p 4320 N94-35376
Anionic states of LiFLi
[AD-A278830] p 4322 N94-35678
Periodicity and peculiarity in 120 first and second row diatomic molecules
[AD-A278836] p 4323 N94-35793
Intramolecular energy transfer reactions in polymetallic complexes
[DE94-010114] p 4326 N94-36126
Molecular nitrogen fluorescence lidar for remote sensing of the auroral ionosphere
[AD-A280716] p 4291 N94-36263
MOLECULAR GASES
Molecular nitrogen fluorescence lidar for remote sensing of the auroral ionosphere
[AD-A280716] p 4291 N94-36263
MOLECULAR IONS
A two-dimensional model for collisional energy transfer in bimolecular ion-molecule dynamics
[AD-A278913] p 4321 N94-35589
Dissociative recombination of stored and phase-spaced cooled molecular ions in CRYRING
[DE94-002459] p 4327 N94-36267
MOLECULAR ORBITALS
Anionic states of LiFLi
[AD-A278830] p 4322 N94-35678
Periodicity and peculiarity in 120 first and second row diatomic molecules
[AD-A278836] p 4323 N94-35793
MOLECULAR ROTATION
Recovery of frozen flow losses in arcjets
[AD-A278739] p 4228 N94-36089
MOLECULAR STRUCTURE
Theoretical aspect of low pressure discharges in simple gasses
[AD-A278762] p 4335 N94-35493
Structural investigations of 1-ethyl-3-methylimidazolium hydrogen dichloride: Neutron diffraction studies of an ambient-temperature molten salt
[DE94-009680] p 4237 N94-35777
MOLECULAR WEIGHT
Addition polyimides with enhanced processability
[NASA-CASE-LEW-15043-1] p 4242 N94-35234
MOLECULES
A combined experimental and theoretical study of the neutral, cationic and anionic Si3N cluster molecule
[AD-A278834] p 4323 N94-35792
MOLTEN SALTS
Structural investigations of 1-ethyl-3-methylimidazolium hydrogen dichloride: Neutron diffraction studies of an ambient-temperature molten salt
[DE94-009680] p 4237 N94-35777
Neutron diffraction study of aluminum chloride imidazolium chloride molten salts
[DE94-009679] p 4239 N94-36349
MOLYBDENUM
Design of a high activity and selectivity alcohol catalyst
[DE94-003633] p 4237 N94-36023
MOLYBDENUM ALLOYS
High temperature creep and oxidation resistant chromium silicide matrix alloy containing molybdenum
[NASA-CASE-LEW-15697-1] p 4241 N94-36275
MOMENTUM THEORY
Measuring attitude with a gradiometer
p 4206 N94-35630
MOMENTUM TRANSFER
State-to-state dynamics of molecular energy transfer
[DE94-009651] p 4324 N94-35816
MONATOMIC GASES
On the various forms of the energy equation for a dilute, monatomic mixture of nonreacting gases
[NASA-CR-4612] p 4190 N94-35864
MONITORS
Adjustable control station with movable monitors and cameras for viewing systems in robotics and teleoperations
[NASA-CASE-NPO-17837-1-CU] p 4332 N94-35384
Intelligent processing of materials, technical activities, 1993 (NAS-NRC Assessment Panel, April 21-22 1994)
[PB94-164183] p 4251 N94-35737
MONOMERS
Tough, processable semi-interpenetrating polymer networks from monomer reactants
[NASA-CASE-LAR-14838-1] p 4242 N94-35233
Addition polyimides with enhanced processability
[NASA-CASE-LEW-15043-1] p 4242 N94-35234
MONOPOLES
Moduli space of monopoles and some invariants of 3-manifolds
[PB94-167756] p 4314 N94-35764
MONOPULSE RADAR
Estimation with multisensor/multiscan detection fusion
[AD-A278753] p 4256 N94-36092
MONTE CARLO METHOD
Monolith catalysts for closed-cycle carbon dioxide lasers
[NASA-CR-196093] p 4271 N94-35489
Point and interval estimation of series system reliability using small data sets
[AD-A278647] p 4316 N94-35575
Stopping rules for a class of sampling-based stochastic programming algorithms
[AD-A278654] p 4303 N94-35577
Beam tests of a prototype level-1 calorimeter trigger for LHC experiments
[PB94-170495] p 4269 N94-35599
Application of a Monte Carlo accuracy assessment tool to TDRS and GPS p 4207 N94-35635
Computer simulations of benzene in faujasite-type zeolites
[DE94-007533] p 4242 N94-36369
Can we break intractability using randomization or the average case setting?
[AD-A278598] p 4316 N94-36425
MONTMORILLONITE
Thermal emission measurements (5-25 microns) of palagonite/Fe-substituted montmorillonite intimate mixtures: Applications to Mars p 4292 N94-35453
MOODS
Determinants of subjective fatigue for C-141 crews during Operation Desert Storm p 4196 N94-36338
MOON
High spatial resolution telescopic multispectral imaging and spectroscopy of the Moon. 1: The Serenitatis/Tranquillitatis border region
p 4356 N94-35402
MORPHOLOGY
Morphological aspects of surface reactions
[DE94-010184] p 4236 N94-35685
Computational methods for material failure processes
[AD-A278716] p 4278 N94-36292
MOSAICS
First Galileo image of asteroid 243 Ida
p 4351 N94-35416
MOTION PERCEPTION
Visual-vestibular interaction
[NASA-CR-196097] p 4297 N94-35379
MOTION STABILITY
Analysis of achievable disturbance attenuation in a precision magnetically-suspended motion control system
p 4225 N94-35917
MULTIGRID METHODS
A three dimensional multigrid Reynolds-averaged Navier-Stokes solver for unstructured meshes
[NASA-CR-194908] p 4191 N94-35994
A multilevel adaptive projection method for unsteady incompressible flow
[DE93-016418] p 4267 N94-36315
Overset grid applications on distributed memory MIMD computers
[NASA-CR-196081] p 4268 N94-36397
MULTIMEDIA
Space educators' handbook
[NASA-TM-109779] p 4343 N94-35339
Exploring hypermedia information services for disseminating software engineering information
[AD-A278765] p 4302 N94-35495
The impact of scaling on a multimedia connection architecture
[AD-A278700] p 4300 N94-35652
CAirTOX: A compartment model for assessing the fate of and human exposure to toxic-chemical emissions to air
[DE94-010084] p 4284 N94-35700
MULTIPROCESSING (COMPUTERS)
Parallel algorithms for LU decomposition on a shared memory multiprocessor
[PB94-167798] p 4314 N94-35531
MULTISENSOR APPLICATIONS
JPRS report: Science and technology. Central Eurasia
[JPRS-UST-94-007] p 4249 N94-35227
MULTISPECTRAL BAND SCANNERS
Space Shuttle orbit determination using empirical force modeling of attitude maneuvers for the German MOMS-02/D2 mission p 4207 N94-35634
MULTISPECTRAL PHOTOGRAPHY
High spatial resolution telescopic multispectral imaging and spectroscopy of the Moon. 1: The Serenitatis/Tranquillitatis border region
p 4356 N94-35402
MULTIVARIABLE CONTROL
Robust tracking control of a magnetically suspended rigid body p 4225 N94-35913
MULTIVARIATE STATISTICAL ANALYSIS
Gauss elimination by segments and multivariate polynomial interpolation
[AD-A278646] p 4315 N94-36012
MUON SPIN ROTATION
The study of the local magnetic field in the oxide alpha-Bi2O3 by the mu SR-technique
[DE94-612636] p 4322 N94-35751
MUONS
Isoscalar vector bosons at LEP 2
[DE94-611253] p 4323 N94-35787
J/psi absorption effects in the coherent production on nuclei
[DE94-616870] p 4326 N94-36129
Critical issues in muon colliders: A summary
[DE94-011382] p 4331 N94-36271
MURCHISON METEORITE
Moessbauer mineralogy of calcined Murchison meteorite p 4353 N94-36166
MUSCLE RELAXANTS
Computer automation and artificial intelligence
[DE94-611058] p 4312 N94-35831
MUSCLES
Typology of skeletal muscle in humans undergoing intense physical training or prolonged akinesia
[PB94-170644] p 4297 N94-36217
MUSCULAR STRENGTH
Typology of skeletal muscle in humans undergoing intense physical training or prolonged akinesia
[PB94-170644] p 4297 N94-36217
MUSCULOSKELETAL SYSTEM
Typology of skeletal muscle in humans undergoing intense physical training or prolonged akinesia
[PB94-170644] p 4297 N94-36217
MYOPIA
Accommodation during instrument viewing can be influenced by knowledge of object distance
[AD-A278987] p 4298 N94-35528
Is increased accommodation a necessary condition for instrument myopia?
[AD-A278962] p 4298 N94-35659

N

NAKHLITES
Pigeonholing planetary meteorites: The lessons of misclassification of EET87521 and ALH84001
p 4353 N94-36157
NASA PROGRAMS
Director's discretionary fund
[NASA-TM-103997] p 4376 N94-35370
NASA patent abstracts bibliography: A continuing bibliography. Section 1: Abstracts (supplement 45)
[NASA-SP-7039(45)-SECT-1] p 4344 N94-35382
Aerospace Safety Advisory Panel
[NASA-TM-109840] p 4201 N94-35390
Statement by Bill D. Colvin, Inspector General
[NASA-TM-109793] p 4348 N94-35446
Trace-shortened Reed-Solomon codes
p 4254 N94-35554
Challenging the Future - Journey to Excellence. Aeropropulsion strategic plan for the 1990's
[NASA-TM-109250] p 4228 N94-35591
TDRSS Onboard Navigation System (TONS) flight qualification experiment p 4206 N94-35625

NASA patent abstracts bibliography: A continuing bibliography. Section 2: Indexes (supplement 45)
[NASA-SP-7039(45)-SECT-2] p 4346 N94-35835

Budget estimates, fiscal year 1995. Volume 1: Agency summary, human space flight, and science, aeronautics and technology
[NASA-TM-109791] p 4347 N94-35899

Budget estimates, fiscal year 1995. Volume 2: Mission support and Inspector General
[NASA-TM-109792] p 4348 N94-35900

A biased historical perspective of women in the engineering field at Dryden from 1946 to November 1992 p 4251 N94-35967

Research and technology, 1993
[NASA-TM-108816] p 4380 N94-36117

National Educators' Workshop: Update 1993. Standard Experiments in Engineering Materials Science and Technology
[NASA-CP-3259] p 4229 N94-36398

NASA SPACE PROGRAMS

NASA Space Geodesy Program: GSFC data analysis, 1993. VLBI geodetic results 1979 - 1992
[NASA-TM-104605] p 4281 N94-35261

Space educators' handbook
[NASA-TM-109779] p 4343 N94-35339

Space and the American imagination
[NASA-CR-196131] p 4376 N94-35356

Planetary Rover Program
[NASA-CR-196108] p 4201 N94-35511

The history of space exploration
[NASA-TM-109888] p 4201 N94-36440

NATIONAL AIRSPACE SYSTEM

The Federal Aviation Administration plan for research, engineering and development p 4376 N94-35262

NATURAL GAS

Infrared multiphoton ignition and combustion enhancement of natural gas.
[PB94-165438] p 4236 N94-35755

Analysis of the injection process in direct injected natural gas engines
[PB94-156494] p 4275 N94-35931

Gasoline from natural gas by sulfur processing
[DE94-011130] p 4248 N94-36035

A comparison between direct spark ignition and prechamber ignition in an internal combustion engine
[DE94-008218] p 4275 N94-36206

Effects of natural gas composition on ignition delay under diesel conditions
[DE94-006405] p 4276 N94-36378

NATURAL LANGUAGE (COMPUTERS)

MMI(exp 2) demonstrator systems: A multi-modal interface for man machine interaction with knowledge based systems. Deliverable D17 (TA 2) ESPRIT project 2474 MMI(exp 2)
[PB94-170537] p 4298 N94-35600

NAVIER-STOKES EQUATION

On the nonlinear stability of viscous modes within the Rayleigh problem on an infinite flat plate
[NASA-CR-194909] p 4263 N94-35497

Boundary conditions for jet flow computations
[NASA-TM-106648] p 4266 N94-35976

A three dimensional multigrid Reynolds-averaged Navier-Stokes solver for unstructured meshes
[NASA-CR-194908] p 4191 N94-35994

An efficient, intelligent solution for viscous flows inside solid rocket motors
[AD-A278629] p 4228 N94-36255

An equal-order approximate projection FEM
[DE94-010101] p 4268 N94-36374

Numerical investigation of multi-element airfoils
[NASA-CR-194592] p 4191 N94-36394

NEAR FIELDS

Use of the sampling theorem to speed up near-field physical optics scattering calculations
p 4253 N94-35549

NEAR INFRARED RADIATION

High spatial resolution telescopic multispectral imaging and spectroscopy of the Moon. 1: The Serenitatis/Tranquillitatis border region
p 4356 N94-35402

Absolute calibration and atmospheric versus mineralogic origin of absorption features in 2.0 to 2.5 micron Mars spectra obtained during 1993 p 4356 N94-35404

Theoretical studies of ultrashort phenomena
[AD-A278938] p 4332 N94-35664

Dynamic structural effects and ultrafast biomolecular kinetics in photoinduced charge transfer reactions
[DE94-010421] p 4329 N94-36390

NEBULAE

Formation of iron metal and grain coagulation in the solar nebula p 4373 N94-36170

NEODYMIUM ISOTOPES

New data supporting a Sm-146,147-Nd-142,143 formation interval for the lunar mantle
p 4374 N94-36173

NEON

Solar proton produced neon in shergottite meteorites
p 4351 N94-35428

NEPTUNE (PLANET)

Voyager last picture show
[NASA-CR-195796] p 4367 N94-35506

NETWORK ANALYSIS

Switched-beam radiometer front-end network analysis
[NASA-CR-194922] p 4252 N94-35247

An analysis of file system and installation of the file management system for NOS operating system
[DE94-611062] p 4346 N94-35833

NETWORK CONTROL

Large granularity cache coherence for intermittent connectivity
[AD-A278897] p 4345 N94-35571

NETWORK SYNTHESIS

High level modelling and design of asynchronous interface logic
[PB94-167822] p 4258 N94-35534

NEURAL NETS

Introduction to Neural Networks: Neural Network Workshop for the Hanford Community
[DE94-006526] p 4311 N94-35348

Genetic algorithms
[PB94-171048] p 4303 N94-35602

High-resolution subsurface imaging and neural network recognition
[DE94-009546] p 4290 N94-35666

Computer automation and artificial intelligence
[DE94-611058] p 4312 N94-35831

Neural network controller development for a magnetically suspended flywheel energy storage system
p 4217 N94-35861

A comparison of artificial neural networks and statistical analyses
[DE94-010846] p 4312 N94-36195

Multidisciplinary studies of integrated neural network systems
[AD-A278774] p 4312 N94-36309

High energy
[DE94-009477] p 4331 N94-36428

NEUROLOGY

Stress and brain protein synthesis
[PB94-170750] p 4296 N94-35601

Multidisciplinary studies of integrated neural network systems
[AD-A278774] p 4312 N94-36309

NEUTRAL BEAMS

Heating experiments using neutral beams with variable injection angle and ICRF waves in CHS
[DE94-718982] p 4337 N94-35936

Feasibility study for a novel pulsed neutral beam diagnostics for tokamaks
[DE94-617129] p 4339 N94-36417

NEUTRAL BUOYANCY SIMULATION

Structural assembly demonstration experiment, phase 1
[NASA-CR-193967] p 4212 N94-35484

NEUTRAL PARTICLES

A combined experimental and theoretical study of the neutral, cationic and anionic Si3N cluster molecule
[AD-A278834] p 4323 N94-35792

NEUTRINOS

A search for radiative neutrino decay from supernovae
[NASA-CR-196011] p 4376 N94-35515

Limitation on the magnetic dipole moment of the reactor neutrino
[DE94-611171] p 4320 N94-35566

Radiatively induced electron and electron-neutrino masses
[DE94-616775] p 4321 N94-35582

Nonadiabatic neutrino oscillations revisited
[DE94-616649] p 4321 N94-35593

Some consequences in weak processes of three generations mixing in the leptonic sector
[DE94-616650] p 4321 N94-35594

Collective plasma corrections to the solar opacity
[PB94-170511] p 4375 N94-36210

NEUTRON COUNTERS

Neutron detectors for fusion reaction-rate measurements
[DE94-010407] p 4330 N94-36114

NEUTRON DIFFRACTION

Structural investigations of 1-ethyl-3-methylimidazolium hydrogen dichloride: Neutron diffraction studies of an ambient-temperature molten salt
[DE94-009680] p 4237 N94-35777

Neutron diffraction study of aluminum chloride imidazolium chloride molten salts
[DE94-009679] p 4239 N94-36349

NEUTRON EMISSION

Hot-ion plasma in the quadrupole trap
[DE94-617216] p 4337 N94-36082

NEUTRON IRRADIATION

Determination of the Fermi level position for neutron irradiated high resistivity silicon detectors and materials using the Transient Charge Technique (TChT)
[DE94-009107] p 4260 N94-36221

Study of point defect mobilities in zirconium during electron irradiation in a HVEM
[DE94-619028] p 4242 N94-36289

NEUTRON SCATTERING

Relativistic three-particle dynamical equations. 2: Application to the trinucleon system
[DE94-616653] p 4320 N94-35580

NEUTRON SOURCES

Time-of-flight diffraction at pulsed neutron sources: An introduction to the symposium
[DE94-010442] p 4327 N94-36225

NEUTRON SPECTRA

A search for energetic ion directivity in large solar flares
[NASA-CR-196036] p 4374 N94-35993

NEUTRONS

CALTRANS: A parallel, deterministic, 3D neutronics code
[DE94-010667] p 4326 N94-36127

Study of point defect mobilities in zirconium during electron irradiation in a HVEM
[DE94-619028] p 4242 N94-36289

NEWTON SECOND LAW

Piggyback balance experiment: An illustration of Archimedes' principles and Newton's third law
[PB94-163060] p 4265 N94-35942

NEWTONIAN FLUIDS

Piggyback balance experiment: An illustration of Archimedes' principles and Newton's third law
[PB94-163060] p 4265 N94-35942

NICKEL

Antarctic weathering of the CK chondrites EET90004, 90007, and 90022: Nickel and sulfur mobility
p 4351 N94-35451

Computation of dendrites using a phase field model
[PB94-160744] p 4236 N94-35736

Partition coefficients for Al, Ca, Ti, Cr, and Ni in olivine obtained by melting experiment on an LL6 chondrite
p 4353 N94-36163

NIGHT VISION

Accommodation during instrument viewing can be influenced by knowledge of object distance
[AD-A278987] p 4298 N94-35528

Is increased accommodation a necessary condition for instrument myopia?
[AD-A278962] p 4298 N94-35659

NIOBIUM

Effect of niobium interlayer on high-temperature sliding friction and wear of silver films on alumina
[DE94-010462] p 4275 N94-36232

NIOBIUM ALLOYS

Continuum fluorescence of Cu in NbTi/Cu composite wires
[DE94-008940] p 4241 N94-36242

NITRIC OXIDE

NO decomposition in non-reducing atmospheres
[DE94-011157] p 4237 N94-36036

NITRIDES

High temperature heterojunction bipolar transistors
[AD-A278605] p 4261 N94-36360

NITRILES

Interface shape and convection during solidification and melting of succinonitrile
[NASA-TM-106487] p 4262 N94-35248

NITRO COMPOUNDS

The thermochemistry and reaction mechanisms in the decomposition of energetic materials
[DE94-011420] p 4248 N94-36376

NITROGEN

Vacuum ultraviolet studies of molecular dynamics
[AD-A278940] p 4321 N94-35657

Tritiated ammonia formation
[DE94-011170] p 4237 N94-36056

Molecular nitrogen fluorescence lidar for remote sensing of the auroral ionosphere
[AD-A280716] p 4291 N94-36263

NITROGEN OXIDES

Combined SO(x)/NO(x) control via SOXAL (tm) process: An electrodialytic regenerative wet scrubbing process
[DE94-009053] p 4284 N94-35346

State-to-state dynamics of molecular energy transfer
[DE94-009651] p 4324 N94-35816

Modeling the atmospheric input of nutrients, heavy metals, and pesticides to the Great Lakes
[DE94-005481] p 4286 N94-36007

Air quality implications associated with the selection of power plants in the Pacific Northwest
[DE94-004783] p 4287 N94-36027

Treatment of toxic gases SO2 and NO(x) by electron beam irradiation
[DE94-615424] p 4330 N94-36028

NITROGEN PLASMA
The growth of silicon nitride crystalline films using microwave plasma enhanced chemical vapor deposition
[AD-A278862] p 4340 N94-35828
NITROUS OXIDES
Vacuum ultraviolet studies of molecular dynamics
[AD-A278940] p 4321 N94-35657
NOISE
In-flight estimation of gyro noise on the Upper Atmosphere Research Satellite (UARS) and Extreme Ultraviolet Explorer (EUVE) missions
p 4204 N94-35616
NOISE INTENSITY
A low temperature scanning force microscope for biological samples
[DE94-011357] p 4297 N94-36269
An improved assessment approach for noise impacts from stationary point and traffic sources on humans and wildlife
[DE94-009728] p 4319 N94-36320
NOISE MEASUREMENT
Activity report 1990-1992 and proceedings, volume 1
[DE94-610480] p 4290 N94-35830
NOISE POLLUTION
An improved assessment approach for noise impacts from stationary point and traffic sources on humans and wildlife
[DE94-009728] p 4319 N94-36320
NOISE PREDICTION (AIRCRAFT)
Engine exhaust characteristics evaluation in support of aircraft acoustic testing p 4319 N94-35963
NOISE PROPAGATION
Computation of helicopter rotor acoustics in forward flight
[NASA-CR-196132] p 4319 N94-36031
An improved assessment approach for noise impacts from stationary point and traffic sources on humans and wildlife
[DE94-009728] p 4319 N94-36320
NOISE REDUCTION
Error reduction in images with the use of additional information
[AD-A278636] p 4334 N94-36257
A low temperature scanning force microscope for biological samples
[DE94-011357] p 4297 N94-36269
NOISE TEMPERATURE
The electrical conductivities of candidate beam-waveguide antenna shroud materials
p 4252 N94-35546
Spacecraft-spacecraft radio-metric tracking: Signal acquisition requirements and application to Mars approach navigation p 4254 N94-35557
NOISE TOLERANCE
Proceedings of the Sixth International Congress on Noise as a Public Heatlh Problem, volume 3
[AD-A278218] p 4319 N94-36176
NONADIABATIC CONDITIONS
Nonadiabatic neutrino oscillations revisited
[DE94-616649] p 4321 N94-35593
NONEQUILIBRIUM FLOW
Development and application of computational aerothermodynamics flowfield computer codes
[NASA-CR-196136] p 4189 N94-35498
NEQPAK, the AEDC thermochemical nonequilibrium package: Theory and use
[AD-A279005] p 4266 N94-35951
NONINTRUSIVE MEASUREMENT
Measurement of a surface heat flux and temperature
p 4231 N94-36407
NONLINEAR EQUATIONS
Self-similar regimes of subsonic Langmuir wave collapse
[DE94-611466] p 4335 N94-35750
Variations in the modal characteristics of a telescopically deploying beam p 4218 N94-35872
NONLINEAR FEEDBACK
Nonlinear feedback model attitude control using CCD in magnetic suspension system p 4225 N94-35912
NONLINEAR OPTICS
Concurrent stabilization and imaging of a novel polymer for second harmonic generation via in situ photopolymerization
[AD-A278912] p 4243 N94-35588
Theoretical studies of ultrashort phenomena
[AD-A278936] p 4332 N94-35664
Properties and bibliography of GaSe
[AD-A279064] p 4340 N94-35733
Nonlinear optical composites of metal cluster laden polymers
[AD-D016217] p 4234 N94-36124
Application of GaSe and AgGaSe2 crystal growth to non-linear optics
[PB94-170552] p 4341 N94-36212
NONLINEAR PROGRAMMING
Application of sequential quadratic programming to large-scale structural design problems
[AD-A278574] p 4307 N94-36185
NONLINEAR SYSTEMS
Dynamic analysis of a magnetic bearing system with flux control p 4216 N94-35859
Maneuvering and control of flexible space robots
p 4218 N94-35867
Improved models of beta-limit, anomalous transport and radial electric field with loss cone loss in heliotron/torsatron
[DE94-718976] p 4324 N94-35984
Combining nonlinear multiresolution system and vector quantization for still image compression
[DE94-009422] p 4305 N94-36017
NONLINEARITY
Linear and nonlinear pattern selection in Rayleigh-Benard stability problems
[NASA-TM-104007] p 4263 N94-35371
Nonlinear control of magnetic bearings
p 4213 N94-35838
A case study in nonlinear dynamics and control of articulated spacecraft: The Space Station Freedom with a mobile remote manipulator system
p 4220 N94-35879
Numerical method to study the stability of periodic solutions of particle motion in nonlinear magnetic fields
[DE94-610740] p 4325 N94-36088
Application of GaSe and AgGaSe2 crystal growth to non-linear optics
[PB94-170552] p 4341 N94-36212
Local instabilities and the transition to chaos of non-linear waves
[PB94-170578] p 4341 N94-36213
Non-linear interaction of gravity waves with average jet flows, instabilities, and turbulence
[PB94-170586] p 4291 N94-36214
NORMAL SHOCK WAVES
A supersonic tunnel for laser and flow-seeding techniques
[NASA-TM-106588] p 4265 N94-35945
NORTH ATLANTIC TREATY ORGANIZATION (NATO)
AGARD highlights 93/2
[AGARD-HIGHLIGHTS-93/2] p 4376 N94-35444
NORTHERN HEMISPHERE
Long range forecasts of the Northern Hemisphere anomalies with antecedent sea surface temperature patterns
[NASA-CR-189358] p 4292 N94-35380
NOVA LASER SYSTEM
X ray radiographic imaging of hydrodynamic phenomena in radiation driven materials: Shock propagation, material compression and shear flow
[DE94-009515] p 4266 N94-35982
NOWCASTING
Data requirements for ceiling and visibility products development
[AD-A278959] p 4293 N94-35720
Atmospheric and dispersion modeling in areas of highly complex terrain employing a four-dimensional data assimilation technique
[DE94-004041] p 4285 N94-35823
Use of wind profiler data in short-range forcasting
[AD-A279482] p 4295 N94-36228
NOZZLE FLOW
Fundamental studies in blow-down and cryogenic cooling
[AD-A278967] p 4250 N94-35524
Tipjet 80-inch model rotor hover test: Test no. 1198
[AD-A279680] p 4191 N94-36261
An experimental investigation of active control of thrust vectoring nozzle flow fields
[AD-A278702] p 4229 N94-36291
NUCLEAR BINDING ENERGY
Relativistic three-particle dynamical equations. 2: Application to the trinucleon system
[DE94-616653] p 4320 N94-35580
NUCLEAR ELECTRIC POWER GENERATION
Logarithmic corrections of the two-body QED problem
[DE94-611157] p 4322 N94-35783
NUCLEAR EMULSIONS
Sigma minus-nucleus interactions in emulsion at 350 GeV
[DE94-616886] p 4326 N94-36130
NUCLEAR ENERGY
JPRS report: Science and technology. Central Eurasia
[JPRS-UST-94-004] p 4249 N94-35341
JPRS report: Science and technology. Central Eurasia
[JPRS-UST-94-005] p 4249 N94-35342
NUCLEAR EXPLOSIONS
A comparison of artificial neural networks and statistical analyses
[DE94-010846] p 4312 N94-36195
NUCLEAR FUSION
Applications of non-resonant RF forces for improvement of tokamak reactor performances. Part 1: Application of ponderomotive force
[DE94-718994] p 4336 N94-35813
Neutron detectors for fusion reaction-rate measurements
[DE94-010407] p 4330 N94-36114
Stellar alchemy: The origin of the chemical elements
[DE94-011903] p 4350 N94-36229
Primordial nucleosynthesis in conformal Weyl gravity
[DE94-003002] p 4327 N94-36241
NUCLEAR INTERACTIONS
Solar proton produced neon in shergottite meteorites
p 4351 N94-35428
SCATTER program of cross section calculation of the hadron and lepton interactions with nuclei
[DE94-617006] p 4326 N94-36134
NUCLEAR MAGNETIC RESONANCE
Cross-condensation reactions in an organically modified silica sol-gel
[DE94-010086] p 4244 N94-35701
NMR imaging of components and materials for DOE application
[DE94-010664] p 4238 N94-36084
NUCLEAR PHYSICS
Summary: Hadron dynamics sessions
[DE94-003011] p 4328 N94-36303
NUCLEAR POTENTIAL
P-matrix approach and three-nucleon problem
[DE94-616887] p 4326 N94-36131
NUCLEAR POWER PLANTS
Guidelines for design and development of computer/microprocessor based systems in research and power reactors
[DE94-616271] p 4300 N94-35570
Activity report 1990-1992 and proceedings, volume 1
[DE94-610480] p 4290 N94-35830
NUCLEAR RADIATION
Atomic physics and radiation processes in plasmas
[DE94-727617] p 4337 N94-35939
NUCLEAR REACTIONS
A three-body calculation of the O-16(d,p)O-17 reaction using a two-term separable potential for the s-wave nucleon-core interaction
[DE94-616652] p 4320 N94-35579
Relativistic three-particle dynamical equations. 2: Theoretical development
[DE94-616654] p 4320 N94-35581
NUCLEAR REACTORS
ONED90: 1-dimensional diffusion code
[DE94-611063] p 4305 N94-35834
Thermodynamic behaviour of tellurium at high temperatures
[DE94-612823] p 4240 N94-35960
NUCLEAR SCATTERING
Alternating series fit to the total cross sections
[DE94-616888] p 4326 N94-36132
NUCLEATION
Transformation plasticity in ductile solids
[DE94-010420] p 4240 N94-35953
Kinetics of phase transformations in glass forming systems
[NASA-CR-196082] p 4245 N94-35977
Local instabilities and the transition to chaos of non-linear waves
[PB94-170578] p 4341 N94-36213
In situ studies of zeolite syntheses using powder diffraction methods: Crystallization of instant zeolite A powder and CoAPO-5
[DE94-006570] p 4341 N94-36358
NUCLEON-NUCLEON INTERACTIONS
Complex Kohn variational principle for two-nucleon bound-state and scattering with the tensor potential
[DE94-616651] p 4321 N94-35595
The nucleon-nucleon potential in the chromodielectric soliton model
[DE94-004646] p 4329 N94-36305
NUCLEON-NUCLEON SCATTERING
Complex Kohn variational principle for two-nucleon bound-state and scattering with the tensor potential
[DE94-616651] p 4321 N94-35595
NUCLEONS
J/psi absorption effects in the coherent production on nuclei
[DE94-616870] p 4326 N94-36129
Hybrid mesons (Q(anti Q)g) in N(anti N) annihilation
[DE94-001491] p 4327 N94-36239
NUCLIDES
SYNTH: A spectrum synthesizer
[DE94-004719] p 4331 N94-36317
NUMERICAL ANALYSIS
Aspects of robust computational modeling for plain and reinforced concrete
[PB94-169240] p 4251 N94-35820

Numerical methods for multibody systems
p 4222 N94-35897

NUMERICAL CONTROL
Computational methods for HSCT-inlet controls/CFD interdisciplinary research
[NASA-TM-106618] p 4198 N94-35352
Microprocessor control of multiple peak power tracking DC/DC converters for use with solar cell arrays
[NASA-CASE-GSC-13450-2] p 4282 N94-35540
Guidelines for design and development of computer/microprocessor based systems in research and power reactors
[DE94-616271] p 4300 N94-35570
Computer automation and artificial intelligence
[DE94-611058] p 4312 N94-35831
High performance data acquisition, identification, and monitoring for active magnetic bearings
p 4213 N94-35839
Fault tolerant computer control for a Maglev transportation system p 4215 N94-35848

NUMERICAL FLOW VISUALIZATION
Vortex tubes in turbulent flows: Identification, representation, reconstruction
[NASA-CR-194900] p 4267 N94-35992

NUMERICAL INTEGRATION
Description and use of LSODE, the Livermore Solver for Ordinary Differential Equations
[NASA-RP-1327] p 4313 N94-35259

NUMERICAL WEATHER FORECASTING
Long range forecasts of the Northern Hemisphere anomalies with antecedent sea surface temperature patterns
[NASA-CR-189358] p 4292 N94-35380

O

OBJECT PROGRAMS
Symbolic debugging of globally optimized code: Data value problems and their solutions
[AD-A278898] p 4302 N94-35572

OBJECT-ORIENTED PROGRAMMING
Measuring and assessing maintainability at the end of high level design p 4301 N94-35438
Impacts of object-oriented technologies: Seven years of SEL studies p 4301 N94-35439
An object-oriented implementation of a graphical-programming system
[DE94-009298] p 4304 N94-35808
Object-oriented simulation pictures (OOSPic) for design and testing
[AD-A278798] p 4305 N94-36013

OBLATE SPHEROIDS
The Earth Satellite Program (ESP), version 2.0
[AD-A278860] p 4201 N94-35827

OBLIQUE SHOCK WAVES
Investigation of Burnett equations for two-dimensional hypersonic flow
[AD-A278942] p 4190 N94-35717
A supersonic tunnel for laser and flow-seeding techniques
[NASA-TM-106588] p 4265 N94-35945

OCCUPATION
NASA/DOD Aerospace Knowledge Diffusion Research Project. Paper 40: Technical communications in aerospace education: A study of AIAA student members
[NASA-TM-109868] p 4344 N94-35254
Mentoring for 2000 and beyond p 4343 N94-35964

OCEAN CURRENTS
Modernization of the graphics post-processors of the Hamburg German Climate Computer Center Carbon Cycle Codes
[DE94-011604] p 4288 N94-36273

OCEAN DATA ACQUISITIONS SYSTEMS
Tracking system options for future altimeter satellite missions p 4205 N94-35622

OCEAN MODELS
Modernization of the graphics post-processors of the Hamburg German Climate Computer Center Carbon Cycle Codes
[DE94-011604] p 4288 N94-36273

OCEAN SURFACE
Tracking system options for future altimeter satellite missions p 4205 N94-35622
Evaluation of synthetic aperture radar for oil-spill response
[AD-A278796] p 4284 N94-35674
Wedge scattering by the method of iteration
[DE94-010404] p 4256 N94-36112

OCEANOGRAPHIC PARAMETERS
Environmental measurements in the Beaufort Sea, Spring 1993
[AD-A278718] p 4296 N94-36293

OCEANOGRAPHY
Mission to Planet Earth. The living ocean: Observing ocean color from space
[NASA-PAM-554] p 4295 N94-35343
Tracking system options for future altimeter satellite missions p 4205 N94-35622
Evaluation of synthetic aperture radar for oil-spill response
[AD-A278796] p 4284 N94-35674

OHMIC DISSIPATION
Self-similar regimes of subsonic Langmuir wave collapse
[DE94-611466] p 4335 N94-35750
Scaling laws for TEXT plasma profiles
[DE94-010832] p 4338 N94-36200

OIL ADDITIVES
The effect of alternative fuels on the stability and lubricity of crankcase lubricants
[DE94-010353] p 4245 N94-36108

OIL SLICKS
Evaluation of synthetic aperture radar for oil-spill response
[AD-A278796] p 4284 N94-35674

OLIGOMERS
Liquid crystalline thermosetting polyimides
[DE94-009939] p 4244 N94-35768

OLIVINE
Reduction of lunar mare soil and pyroclastic glass
p 4355 N94-35398
Alteration and formation of rims on the CM parent body p 4357 N94-35411
Partial melting of the St. Severin (LL) and Lost City (H) ordinary chondrites: One step backwards and two steps forward p 4353 N94-36146
Cr, Mn, and Ca distributions for olivine in angritic systems: Constraints on the origins of Cr-rich and Ca-poor core olivine in angrite LEW87051 p 4353 N94-36162
Partition coefficients for Al, Ca, Ti, Cr, and Ni in olivine obtained by melting experiment on an LL6 chondrite
p 4353 N94-36163

ON-LINE SYSTEMS
Defense RDT and E online system (DROLS) retrieval reference guide
[AD-A278972] p 4344 N94-35525
Adaptive model reduction for continuous systems via recursive rational interpolation p 4219 N94-35876
Netlib services and resources
[DE94-010307] p 4347 N94-36300

ONBOARD DATA PROCESSING
Experience with Ada on the F-18 High Alpha Research Vehicle flight test program p 4310 N94-35968

ONBOARD EQUIPMENT
TDRSS Onboard Navigation System (TONS) flight qualification experiment p 4206 N94-35625

OPACITY
Collective plasma corrections to the solar opacity
[PB94-170511] p 4375 N94-36210

OPERATING COSTS
Future ultra-speed tube-flight p 4225 N94-35918

OPERATING SYSTEMS (COMPUTERS)
NAVSPACECOM space surveillance sensor system digital signal processing receiver. Volume 3: Operating system functions
[AD-A278839] p 4212 N94-35799
An analysis of file system and installation of the file management system for NOS operating system
[DE94-611062] p 4346 N94-35833

OPERATING TEMPERATURE
The optimization of interfaces in InAsSb/InGaAs strained-layer superlattices grown by metal-organic chemical vapor deposition
[DE94-010070] p 4340 N94-35698

OPERATIONAL AMPLIFIERS
Active antenna
[NASA-CASE-GSC-13309-1] p 4251 N94-35231
A gallium arsenide MESFET operational amplifier for use in composite operational amplifiers
[AD-A277843] p 4258 N94-35539
BJT model in APLAC
[PB94-171022] p 4259 N94-35822

OPTICAL COUPLING
High power diode laser Master Oscillator-Power Amplifier (MOPA)
[NASA-CR-196095] p 4271 N94-35488

OPTICAL EQUIPMENT
Method and apparatus for removing unwanted reflections from an interferometer
[NASA-CASE-NPO-18478-1-CU] p 4333 N94-35749

OPTICAL FIBERS
Plasma arc welding weld imaging
[NASA-CASE-MFS-28797-1] p 4273 N94-35367
Coatings for SiO2 optical fibers
[AD-D016197] p 4334 N94-36363

OPTICAL MATERIALS
Concurrent stabilization and imaging of a novel polymer for second harmonic generation via in situ photopolymerization
[AD-A278912] p 4243 N94-35588
Properties and bibliography of GaSe
[AD-A279064] p 4340 N94-35733

OPTICAL MEASUREMENT
A survey of reflectometry techniques with applications to TFTR
[DE94-010202] p 4338 N94-36093
A multi-tiered wavefront sensor using binary optics
[DE94-010393] p 4267 N94-36111

OPTICAL MEASURING INSTRUMENTS
Is increased accommodation a necessary condition for instrument myopia?
[AD-A278962] p 4298 N94-35659
A multi-tiered wavefront sensor using binary optics
[DE94-010393] p 4267 N94-36111

OPTICAL PATHS
Fabrication and phase tuning of an optical waveguide device
[AD-D016215] p 4334 N94-36122

OPTICAL PROPERTIES
The effects of cloud inhomogeneities upon radiative fluxes, and the supply of a cloud truth validation dataset
[NASA-CR-196080] p 4293 N94-35391
Properties and bibliography of GaSe
[AD-A279064] p 4340 N94-35733
Activities of the optoelectronics laboratory
[PB94-171196] p 4334 N94-36190
Selected translated abstracts of Russian-language climate-change publications. 2: Clouds
[DE94-011465] p 4295 N94-36244

OPTICAL PUMPING
Fluorescence detection of single molecules using pulsed near-field optical excitation and time correlated photon counting
[DE94-007553] p 4320 N94-35376
Chirped-pulse amplification with flashlamp-pumped Ti:Sapphire amplifiers
[DE94-010055] p 4272 N94-35695
System for end-pumping a solid state laser using a large aperture laser diode bar
[AD-D016213] p 4273 N94-36370

OPTICAL PYROMETERS
Multiwavelength pyrometer for gray and non-gray surfaces in the presence of interfering radiation
[NASA-CASE-LEW-15250-1] p 4269 N94-35383

OPTICAL RADAR
A precise passive narrow-beam filter infrared radiometer and its use with LIDAR in the ARM program
[DE94-004167] p 4269 N94-36085
Molecular nitrogen fluorescence lidar for remote sensing of the auroral ionosphere
[AD-A280716] p 4291 N94-36263
Implementation of Raman lidar for profiling of atmospheric water vapor and aerosols at the SGP CART site
[DE94-011754] p 4295 N94-36285

OPTICAL SCANNERS
Formation and stability of Fe-rich precipitates in dilute Zr(Fe) single-crystal alloys
[DE94-619027] p 4242 N94-36288

OPTICAL SWITCHING
Theoretical studies of ultrashort phenomena
[AD-A278938] p 4332 N94-35664
Molecular systems for ultrafast optical switching: Controlling electron transfer reactions with femtosecond laser pulses
[DE94-009695] p 4332 N94-35671

OPTICAL THICKNESS
Aerosol optical depth derived from solar radiometry observations at northern mid-latitude sites
[DE94-007476] p 4287 N94-36053

OPTICAL TRACKING
Task and environment-sensitive tracking
[AD-A278846] p 4312 N94-35802

OPTICAL WAVEGUIDES
Fabrication and phase tuning of an optical waveguide device
[AD-D016215] p 4334 N94-36122

OPTIMAL CONTROL
JPRS report: Science and technology. Central Eurasia
[JPRS-UST-94-007] p 4249 N94-35227
Theory and computation of optimal low- and medium-thrust transfers
[NASA-CR-196077] p 4202 N94-35487
Control of flexible structures with distributed sensing and processing p 4218 N94-35871
Optimal disturbance rejecting control of hyperbolic systems p 4220 N94-35882
Magnetically suspended stepping motors for clean room and vacuum environments p 4225 N94-35915
Improvement of endurance performance by periodic optimal control of variable camber p 4194 N94-36329

OPTIMIZATION

On optimal placement of spacers in bundled conductors p 4258 N94-35354

The development and application of composite complexity models and a relative complexity metric in a software maintenance environment p 4255 N94-35559

Symbolic debugging of globally optimized code: Data value problems and their solutions [AD-A278898] p 4302 N94-35572

Reformulating query plans for multidatabase systems [AD-A278688] p 4345 N94-35663

Optimization of turn position of tokamak inductor [DE94-612627] p 4336 N94-35791

Optimisation of composite aircraft structures by direct manufacturing approaches p 4194 N94-36327

ORBIT CALCULATION

The mass of Mars, Phobos, and Deimos, from the analysis of the Mariner 9 and Viking Orbiter tracking data p 4364 N94-35461

Flight Mechanics/Estimation Theory Symposium, 1994 [NASA-CP-3265] p 4202 N94-35605

Compatibility of TOPEX/Poseidon trajectory propagation with JPL and GSFC/FDF operational software p 4204 N94-35619

Improved solution accuracy for TDRSS-based TOPEX/Poseidon orbit determination p 4205 N94-35620

Implementation of a low-cost, commercial orbit determination system p 4205 N94-35621

Improved solution accuracy for Landsat-4 (TDRSS-user) orbit determination p 4205 N94-35623

Space Shuttle orbit determination using empirical force modeling of attitude maneuvers for the German MOMS-02/D2 mission p 4207 N94-35634

Application of a Monte Carlo accuracy assessment tool to TDRS and GPS p 4207 N94-35635

Evaluation of semiempirical atmospheric density models for orbit determination applications p 4208 N94-35636

Filter parameter tuning analysis for operational orbit determination support p 4208 N94-35637

ORBITAL ASSEMBLY

Structural assembly demonstration experiment, phase 1 [NASA-CR-193967] p 4212 N94-35484

ORBITAL ELEMENTS

Dust evolution from comets and asteroids: Their velocities at Earth orbit intersection p 4352 N94-36142

ORBITAL MANEUVERS

Theory and computation of optimal low- and medium-thrust transfers [NASA-CR-196077] p 4202 N94-35487

Automated maneuver planning using a fuzzy logic algorithm p 4203 N94-35610

ORBITAL POSITION ESTIMATION

Filter parameter tuning analysis for operational orbit determination support p 4208 N94-35637

ORBITAL VELOCITY

Dust evolution from comets and asteroids: Their velocities at Earth orbit intersection p 4352 N94-36142

ORDER-DISORDER TRANSFORMATIONS

A theoretical study of ordering phenomena in K-In and K-Sb molten alloys [DE94-611103] p 4240 N94-35935

Investigation of moisture-induced embrittlement of iron aluminides [DE94-010881] p 4241 N94-36196

Modelling of the structure and physical properties of simple disordered systems [DE94-617087] p 4329 N94-36311

ORGANIC CHEMISTRY

Anatomy of a cluster IDP. Part 2: Noble gas abundances, trace element geochemistry, isotopic abundances, and trace organic chemistry of several fragments from L2008#5 p 4352 N94-35465

ORGANIC COMPOUNDS

Morphological aspects of surface reactions [DE94-010184] p 4236 N94-35685

Particulate and gaseous organic receptor modeling for the Southern California Air Quality Study [PB94-156700] p 4285 N94-35735

Vapor-fortified QA/QC samples for the analysis of volatile organic compounds [AD-A278712] p 4229 N94-35776

Dual cure low-VOC coating process [DE94-009346] p 4245 N94-35809

ORGANIC MATERIALS

Residual Gas Analysis (RGA) and shear strength characteristics of a silver-filled epoxy and polyimide under long-term, high-temperature storage conditions [DE94-010106] p 4244 N94-35705

ORGANIC SILICON COMPOUNDS

Cross-condensation reactions in an organically modified silica sol-gel [DE94-010086] p 4244 N94-35701

Spinnability of silica sols: The role of alkoxy group exchange [DE94-010087] p 4244 N94-35702

ORGANIZATIONS

ORDIT: A new methodology to assist in the process of eliciting and modelling organisational requirements [PB94-167814] p 4345 N94-35533

Introduction to USRA [NASA-CR-195980] p 4376 N94-35590

ORTHOGONALITY

Gauss elimination by segments and multivariate polynomial interpolation [AD-A278646] p 4315 N94-36012

OSCILLATING FLOW

The velocity field created by a shallow bump in a boundary layer [NASA-CR-194899] p 4266 N94-35975

OSCILLATIONS

Nonadiabatic neutrino oscillations revisited [DE94-616649] p 4321 N94-35593

Some consequences in weak processes of three generations mixing in the leptonic sector [DE94-616650] p 4321 N94-35594

A triggering mechanism of fast crash in sawtooth oscillation [DE94-718974] p 4336 N94-35772

A procedure for oscillatory parameter identification [DE94-008047] p 4259 N94-36054

Numerical method to study the stability of periodic solutions of particle motion in nonlinear magnetic fields [DE94-610740] p 4325 N94-36088

OSCILLATORS

High power diode laser Master Oscillator-Power Amplifier (MOPA) [NASA-CR-196095] p 4271 N94-35488

900-mW average power and tunability from a diode-pumped 2.94 micron Er:YAG oscillator [DE94-009511] p 4271 N94-35679

Coherent states versus de Broglie-wavelets [DE94-611075] p 4343 N94-36381

OUTGASSING

The structural changes of water ice I during warmup p 4239 N94-36144

OXIDATION

Microporous structure with layered interstitial surface treatment, and method and apparatus for preparation thereof [NASA-CASE-MSC-21487-3] p 4235 N94-35229

Innovative instrumentation for mineralogical and elemental analyses of solid extraterrestrial surfaces: The Backscatter Moessbauer Spectrometer/X Ray Fluorescence analyzer (BaMS/XRF) p 4239 N94-35459

Methane production and consumption in grassland and boreal ecosystems [NASA-CR-196085] p 4284 N94-35486

Evaluation of Oxygen Interactions with Materials 3: Mission and induced environments [NASA-TM-109349] p 4236 N94-35680

Hematite formed from pyroxene on Mars by meteoritic impact p 4372 N94-36165

Investigation of moisture-induced embrittlement of iron aluminides [DE94-010881] p 4241 N94-36196

Simulation of materials processing: Fantasy or reality? p 4230 N94-36404

OXIDATION RESISTANCE

Analysis of the Shuttle Orbiter reinforced carbon-carbon oxidation protection system [NASA-TM-104792] p 4262 N94-35245

Atomic oxygen protective coating with resistance to undercutting at defect sites [NASA-CASE-LEW-15306-1] p 4243 N94-35502

High temperature creep and oxidation resistant chromium silicide matrix alloy containing molybdenum [NASA-CASE-LEW-15697-1] p 4241 N94-36275

OXIDATION-REDUCTION REACTIONS

Electrical microengineering of redox enzymes [AD-A279015] p 4236 N94-35745

Some perspectives on solution-phase electron-transfer processes [AD-A278616] p 4238 N94-36252

Ion modulated electroactivity in thin film metallopolymers [AD-A278618] p 4246 N94-36253

OXIDE FILMS

The relationship between hydroxyl groups on oxide surfaces and the properties of supported metals [DE94-010786] p 4241 N94-36233

Superconducting transistors [PB94-170743] p 4260 N94-36260

Wear-resisting oxide films for 900 C [DE94-010093] p 4246 N94-36306

OXIDES

The relationship between hydroxyl groups on oxide surfaces and the properties of supported metals [DE94-010786] p 4241 N94-36233

Heterogeneous catalytic process for alcohol fuels from syngas [DE94-010263] p 4248 N94-36299

OXYGEN

High temperature sorbents for oxygen [NASA-CASE-NPO-18409-1-CU] p 4235 N94-35255

Bus application of oxygen-enrichment technology and diesel-electric hybrid systems [DE94-009835] p 4285 N94-35765

The reaction of hydroperoxy-propyl radicals with molecular oxygen [DE94-006392] p 4239 N94-36319

OXYGEN ATOMS

A comparison of atomic oxygen erosion yields of carbon and selected polymers exposed in ground based facilities and in low Earth orbit [NASA-TM-106622] p 4243 N94-35243

Results from LDEF experiment A0114: The interaction of atomic oxygen with materials surfaces at orbital altitudes [NASA-CR-196016] p 4235 N94-35388

Atomic oxygen reactor having at least one sidearm conduit [NASA-CASE-MSC-21487-4] p 4250 N94-35445

Atomic oxygen protective coating with resistance to undercutting at defect sites [NASA-CASE-LEW-15306-1] p 4243 N94-35502

Evaluation of Oxygen Interactions with Materials 3: Mission and induced environments [NASA-TM-109349] p 4236 N94-35680

OXYGEN ISOTOPES

A three-body calculation of the O-16(d,p)O-17 reaction using a two-term separable potential for the s-wave nucleon-core interaction [DE94-616652] p 4320 N94-35579

OZONE

JPRS report: Science and technology. Central Eurasia: Space [JPRS-USP-94-001] p 4201 N94-35518

Vacuum ultraviolet studies of molecular dynamics [AD-A278940] p 4321 N94-35657

P

P-I-N JUNCTIONS

Development of novel II-VI solar cells [PB94-159415] p 4282 N94-35739

P-TYPE SEMICONDUCTORS

Non-alloyed, refractory metal contact optimization with shallow implantations of Zn and Mg [DE94-010392] p 4240 N94-36110

PAINTS

The electrical conductivities of candidate beam-waveguide antenna shroud materials p 4252 N94-35546

Dual cure low-VOC coating process [DE94-009346] p 4245 N94-35809

PAIR PRODUCTION

A quark model of bar Lambda production in bar Rho interactions [DE94-008071] p 4324 N94-35824

Processes of the reciprocal transformation vector charged particles pairs and electron-positron pairs [DE94-616787] p 4325 N94-36077

PALEOCLIMATOLOGY

Exopaleontology and the search for a fossil record on Mars p 4360 N94-35425

Mars atmospheric escape and isotopic fractionation: Synthesis of data and models p 4369 N94-36143

PALEONTOLOGY

Exopaleontology and the search for a fossil record on Mars p 4360 N94-35425

PANELS

Frequency domain analysis of the random loading of cracked panels [NASA-CR-196021] p 4279 N94-35974

Fatigue and residual strength behaviour of ARALL3 panels with bonded-on doublers [AD-B181062] p 4279 N94-36226

PARALLEL FLOW

Neoclassical current and related MHD stability, gap modes, and radial electric field effects in heliotron and torsatron plasmas [DE94-718987] p 4337 N94-35938

PARALLEL PROCESSING (COMPUTERS)

Runtime support for data parallel tasks [NASA-CR-194904] p 4300 N94-35240

Parallel algorithms for LU decomposition on a shared memory multiprocessor
[PB94-167798] p 4314 N94-35531
Task allocation for parallel real-time execution
[AD-A278789] p 4310 N94-35653
Communication and memory requirements as the basis for mapping task and data parallel programs
[AD-A278954] p 4310 N94-35806
Computer automation and artificial intelligence
[DE94-611058] p 4312 N94-35831
Computationally efficient multibody simulations
p 4222 N94-35896
The most abstract common refinement
[AD-A278870] p 4305 N94-36014
CALTRANS: A parallel, deterministic, 3D neutronics code
[DE94-010667] p 4326 N94-36127
The EASE Visualization Community Club
[PB94-170529] p 4308 N94-36211
Computational methods for material failure processes
[AD-A278716] p 4278 N94-36292
Overset grid applications on distributed memory MIMD computers
[NASA-CR-196081] p 4268 N94-36397

PARALLEL PROGRAMMING
Parallel algorithms for LU decomposition on a shared memory multiprocessor
[PB94-167798] p 4314 N94-35531
A compile time model for composing parallel programs
[AD-A278896] p 4310 N94-35597
Communication and memory requirements as the basis for mapping task and data parallel programs
[AD-A278954] p 4310 N94-35806
The CMU task parallel program suite
[AD-A278951] p 4311 N94-36015

PARAMETER IDENTIFICATION
High performance data acquisition, identification, and monitoring for active magnetic bearings
p 4213 N94-35839
NASA Workshop on Distributed Parameter Modeling and Control of Flexible Aerospace Systems
[NASA-CP-3242] p 4217 N94-35865
Parameter estimation of the vibrational model for the SCOLE experimental facility p 4219 N94-35878
A procedure for oscillatory parameter identification
[DE94-008047] p 4259 N94-36054

PARAMETERIZATION
The Atmospheric Radiation Measurement Program and interfaces with external data sources
[DE94-003699] p 4286 N94-36024

PARKING ORBITS
A geometric model of a V-slit Sun sensor correcting for spacecraft wobble p 4206 N94-35628

PARTIAL DIFFERENTIAL EQUATIONS
Variations in the modal characteristics of a telescopically deploying beam p 4218 N94-35872
Computational Mathematics Laboratory for multiscale analysis
[AD-A278597] p 4315 N94-36424

PARTICLE ACCELERATORS
Beam tests of a prototype level-1 calorimeter trigger for LHC experiments
[PB94-170495] p 4269 N94-35599
Critical issues in muon colliders: A summary
[DE94-011382] p 4331 N94-36271

PARTICLE COLLISIONS
Theoretical aspect of low pressure discharges in simple gasses
[AD-A278762] p 4335 N94-35493
Proceedings of 2nd Working Meeting on Physics at VLEPP, volume 2
[DE94-616167] p 4326 N94-36182

PARTICLE DECAY
A search for radiative neutrino decay from supernovae
[NASA-CR-196011] p 4376 N94-35515
Low energy theorems from the effective Lagrangian with vector mesons
[DE94-611173] p 4322 N94-35785
Pseudogoldstone boson decay induced by light and search for the solar axion radiation
[DE94-616907] p 4326 N94-36133
Decay of the D(sub s)-meson
[DE94-611209] p 4329 N94-36308

PARTICLE DIFFUSION
Dynamic aperture and transverse proton diffusion in HERA
[DE94-010309] p 4331 N94-36224

PARTICLE ENERGY
JPRS report: Science and technology. Central Eurasia: Space
[JPRS-USP-94-001] p 4201 N94-35518

PARTICLE INTENSITY
Application of higher-order multipoint statistics to the ideal spray
[DE94-005104] p 4268 N94-36318

PARTICLE INTERACTIONS
The kinetics of inhomogeneous plasma
[DE94-611459] p 4336 N94-35788
On the theory of bounded many-particle systems with purely coulomb interactions
[DE94-617215] p 4325 N94-36081
P-matrix approach and three-nucleon problem
[DE94-616887] p 4326 N94-36131
Alternating series fit to the total cross sections
[DE94-616888] p 4326 N94-36132
Proceedings of the Twenty-First All-Union Conference on Physics of Charged Particles Interaction with Crystals
[DE94-615768] p 4341 N94-36181
P-matrix description of charged particles interaction
[DE94-616853] p 4329 N94-36391

PARTICLE MASS
Goldstone pion and other mesons using a scalar confining interaction
[DE94-010016] p 4321 N94-35649
Universal SU(2/1) and the Higgs and fermion masses
[DE94-009182] p 4323 N94-35814
Top dilepton search at CDF
[DE94-002302] p 4327 N94-36266

PARTICLE MOTION
Magnetoresistance of films and strips with the diffuse surface scattering
[DE94-611100] p 4340 N94-35933
Numerical method to study the stability of periodic solutions of particle motion in nonlinear magnetic fields
[DE94-610740] p 4325 N94-36088
Application of higher-order multipoint statistics to the ideal spray
[DE94-005104] p 4268 N94-36318

PARTICLE PRODUCTION
Proceedings of 2nd Working meeting: Physics at VLEPP, volume 1
[DE94-616200] p 4320 N94-35569
Low energy theorems from the effective Lagrangian with vector mesons
[DE94-611173] p 4322 N94-35785
Isoscalar vector bosons at LEP 2
[DE94-611253] p 4323 N94-35787
Support of hadroproduction of bottom using the 800 GeV/c primary photon beam at the Fermilab tevatron
[DE94-009411] p 4324 N94-36016
CDF electroweak studies and the search for the top quark
[DE94-010333] p 4326 N94-36107
Proceedings of 2nd Working Meeting on Physics at VLEPP, volume 2
[DE94-616167] p 4326 N94-36182
Precise measurement of the left-right cross section asymmetry in Z boson production by electron-positron collisions
[DE94-010751] p 4326 N94-36198
Hybrid mesons (Q(anti Q)g) in N(anti N) annihilation
[DE94-001491] p 4327 N94-36239
Top dilepton search at CDF
[DE94-002302] p 4327 N94-36266

PARTICLE SIZE DISTRIBUTION
Shape, size, and distribution of magnetic particles in Bjurbole chondrules p 4353 N94-36167

PARTICLE SPIN
Periodicity and peculiarity in 120 first and second row diatomic molecules
[AD-A278836] p 4323 N94-35793
Spin dynamics in storage rings and linear accelerators
[DE94-010320] p 4330 N94-36106

PARTICLE THEORY
Summary: Hadron dynamics sessions
[DE94-003011] p 4328 N94-36303
Decay of the D(sub s)-meson
[DE94-611209] p 4329 N94-36308

PARTICLE TRACKS
Computer image analysis of etched tracks from ionizing radiation
[NASA-CR-196025] p 4319 N94-35264
Measuring track densities in lunar grains using image analysis p 4357 N94-35409
Eureka! Aerogel capture of meteoroids in space
p 4351 N94-35412

PARTICLE TRAJECTORIES
Q-deformations of the Veneziano model
[DE94-616769] p 4315 N94-36076

PARTICULATES
Current activities and results of the Long Duration Exposure Facility Meteoroid and Debris Special Investigation Group p 4352 N94-35458
Particulate and gaseous organic receptor modeling for the Southern California Air Quality Study
[PB94-156700] p 4285 N94-35735

PARTITIONS (MATHEMATICS)
Identity for propagator in four-fermion theory
[DE94-611104] p 4342 N94-35781
Partition coefficients for Al, Ca, Ti, Cr, and Ni in olivine obtained by melting experiment on an LL6 chondrite
p 4353 N94-36163

PARTONS
QCD parametrizations of the parton distribution of deep inelastic scattering
[DE94-616660] p 4325 N94-36074

PASSENGER AIRCRAFT
A review of computer evacuation models and their data needs
[DOT/FAA/AM-94/11] p 4191 N94-35236

PASSENGERS
Future ultra-speed tube-flight p 4225 N94-35918

PASTES
Cement paste matrix composite materials center
[AD-A279017] p 4233 N94-35952

PATENT POLICY
NASA patent abstracts bibliography: A continuing bibliography. Section 1: Abstracts (supplement 45)
[NASA-SP-7039(45)-SECT-1] p 4344 N94-35382
NASA patent abstracts bibliography: A continuing bibliography. Section 2: Indexes (supplement 45)
[NASA-SP-7039(45)-SECT-2] p 4346 N94-35835

PATHOLOGY
Activities of National Institute of Radiological Sciences
[DE94-727636] p 4296 N94-36101

PATTERN RECOGNITION
Application of star identification using pattern matching to space ground systems at GSFC
p 4209 N94-35640
Clustering techniques in speaker recognition
[AD-A278676] p 4255 N94-35689
Estimation of fractal dimensions from transect data
[DE94-009808] p 4281 N94-36018

PATTERN REGISTRATION
Subpixel resolution from multiple images
p 4281 N94-35417

PAYLOADS
Maneuvering and control of flexible space robots
p 4218 N94-35867

PEAT
Methane production and consumption in grassland and boreal ecosystems
[NASA-CR-196085] p 4284 N94-35486

PENDULUMS
An automated digital data collection and analysis system for the Charpy Impact Tester p 4232 N94-36415

PERCEPTION
The role of emotion in believable agents
[AD-A278952] p 4312 N94-35658

PERFORMANCE TESTS
Performance evaluation of digital phase-locked loops for advanced deep space transponders
p 4254 N94-35558
Concept for an algorithm testing and evaluation program at NIST
[PB94-163029] p 4304 N94-35740
Carbon-carbon piston development
[NASA-CR-4595] p 4233 N94-35947
A solid oxide fuel cell power system: 1992-1993 field operation
[DE94-010383] p 4283 N94-36109
Flight test certification of a 480 gallon composite fuel tank on CF-18 p 4196 N94-36340
In-flight refueling: Dassault Aviation research on the Rafale aircraft p 4196 N94-36341
CC-130H(T) tactical aerial refuelling tanker development flight test programme p 4198 N94-36347

PERIGEES
High Earth orbit design for lunar assisted small Explorer class missions p 4202 N94-35608

PERIODIC FUNCTIONS
Cauchy and invariant measure problem for the periodic Zakharov system
[PB94-167707] p 4317 N94-35760

PERIODIC VARIATIONS
Periodicity and peculiarity in 120 first and second row diatomic molecules
[AD-A278836] p 4323 N94-35793

PERMAFROST
A model of the CO2 exchanges between biosphere and atmosphere in the tundra
[NASA-CR-196008] p 4289 N94-35389

PERMANENT MAGNETS
Maglev crude oil pipeline p 4226 N94-35919

PEROVSKITES
X ray and gamma ray spectroscopy of solids under pressure
[DE94-011207] p 4238 N94-36203

PERSONAL COMPUTERS
Computer virus information update CIAC-2301
[DE94-011916] p 4308 N94-36236

PERSONNEL DEVELOPMENT
Women as a resource for the flexibility required for high technology innovation p 4348 N94-35966

PERSONNEL MANAGEMENT
Telecommuting (work-at-home) at NASA Lewis Research Center
[NASA-CR-195334] p 4347 N94-36396

PERTURBATION
Maneuvering and control of flexible space robots
p 4218 N94-35867
Air quality implications associated with the selection of power plants in the Pacific Northwest
[DE94-004783] p 4287 N94-36027

PERTURBATION THEORY
Linear and nonlinear pattern selection in Rayleigh-Benard stability problems
[NASA-TM-104007] p 4263 N94-35371
High energy asymptotics of perturbative multi-color QCD
[DE94-001350] p 4327 N94-36238

PESTICIDES
Modeling the atmospheric input of nutrients, heavy metals, and pesticides to the Great Lakes
[DE94-005481] p 4286 N94-36007

PETRI NETS
High level modelling and design of asynchronous interface logic
[PB94-167822] p 4258 N94-35534

PETROGRAPHY
The Twenty-Fifth Lunar and Planetary Science Conference. Part 1: A-G
[NASA-CR-195743] p 4355 N94-35395
Lunar mineral feedstocks from rocks and soils: X-ray digital imaging in resource evaluation
p 4358 N94-35415
Petrographic characterization of lunar soils: Application of x ray digital-imaging to quantitative and automated analysis p 4368 N94-36138
Shocked materials from the Dutch Peak diamictite, Utah p 4352 N94-36140
On the origin of enstatite chondrite chondrules based on their petrography and comparison with experimentally produced chondrules p 4353 N94-36158
Cr, Mn, and Ca distributions for olivine in angritic systems: Constraints on the origins of Cr-rich and Ca-poor core olivine in angrite LEW87051 p 4353 N94-36162

PETROLOGY
The Twenty-Fifth Lunar and Planetary Science Conference. Part 1: A-G
[NASA-CR-195743] p 4355 N94-35395
On the possible role of elemental carbon in the formation of reduced chondrules p 4351 N94-35421
The Twenty-Fifth Lunar and Planetary Science Conference. Part 3: P-Z
[NASA-CR-195745] p 4362 N94-35448
FeO and MgO in plagioclase of lunar anorthosites: Igneous or metamorphic? p 4351 N94-35449
More shock recovery experiments on mesosiderite analogs p 4351 N94-35455
The Twenty-Fifth Lunar and Planetary Science Conference. Part 2: H-O
[NASA-CR-195744] p 4367 N94-36136
Partial melting of the St. Severin (LL) and Lost City (H) ordinary chondrites: One step backwards and two steps forward p 4353 N94-36146
Synthetic and natural Nakhla pyroxenes: Parent melt composition and REE partition coefficients
p 4353 N94-36161
Cr, Mn, and Ca distributions for olivine in angritic systems: Constraints on the origins of Cr-rich and Ca-poor core olivine in angrite LEW87051 p 4353 N94-36162

PH
Methane production and consumption in grassland and boreal ecosystems
[NASA-CR-196085] p 4284 N94-35486

PH FACTOR
Coatings for SiO2 optical fibers
[AD-D016197] p 4334 N94-36363

PHASE DIAGRAMS
A classical model for closed-loop diagrams of binary liquid mixtures
[DE94-011011] p 4237 N94-36033

PHASE LOCKED SYSTEMS
Performance evaluation of digital phase-locked loops for advanced deep space transponders
p 4254 N94-35558
Phase-locked arrays of vertical-cavity surface-emitting lasers
[DE94-009279] p 4272 N94-36178

PHASE MODULATION
Spacecraft-spacecraft radio-metric tracking: Signal acquisition requirements and application to Mars approach navigation p 4254 N94-35557
Fabrication and phase tuning of an optical waveguide device
[AD-D016215] p 4334 N94-36122

PHASE SHIFT
A three-body calculation of the O-16(d,p)O-17 reaction using a two-term separable potential for the s-wave nucleon-core interaction
[DE94-616652] p 4320 N94-35579
Elastic p(4)He scattering at intermediate energies
[DE94-618544] p 4328 N94-36287

PHASE STABILITY (MATERIALS)
The effect of alternative fuels on the stability and lubricity of crankcase lubricants
[DE94-010353] p 4245 N94-36108

PHASE TRANSFORMATIONS
Calorimetric thermometry of meteoritic troilite: Preliminary thermometer relationships
p 4355 N94-35399
Mineralogy of artificially heated carbonaceous chondrites p 4352 N94-35477
The silent phase transition in mesonic bags and lattice theory
[DE94-616852] p 4321 N94-35583
An indigenously developed photoacoustic spectrometer for study of actinide spectroscopy
[DE94-616508] p 4235 N94-35592
Kinetics of phase transformations in glass forming systems
[NASA-CR-196082] p 4245 N94-35977
Twin spacing versus size of a monocrystal for the nonstoichiometric 1:2:3 superconductors
[DE94-615511] p 4340 N94-36029
Twin spacing and the structural phase transitions in 1:2:3 high-Tc superconductors
[DE94-615647] p 4340 N94-36041
The structural changes of water ice I during warmup
p 4239 N94-36144
Calorimetric thermobarometry of experimentally shocked quartz p 4240 N94-36174
Irradiation-related amorphization and crystallization: In situ transmission electron microscope studies
[DE94-009823] p 4241 N94-36222
Electrical conductivity of hydrogen shocked to megabar pressures
[DE93-019632] p 4238 N94-36237

PHENOMENOLOGY
Local instabilities and the transition to chaos of non-linear waves
[PB94-170578] p 4341 N94-36213

PHOBOS
The surface and interior of Phobos
p 4355 N94-35400
The mass of Mars, Phobos, and Deimos, from the analysis of the Mariner 9 and Viking Orbiter tracking data p 4364 N94-35461

PHOSPHATES
Capillary column GC-MS/MS confirmation of phosphate esters with a hybrid tandem mass spectrometer
[AD-A278748] p 4238 N94-36091

PHOTOACOUSTIC SPECTROSCOPY
An indigenously developed photoacoustic spectrometer for study of actinide spectroscopy
[DE94-616508] p 4235 N94-35592

PHOTOCATHODES
Streak tube photocathode development program
[DE94-009905] p 4270 N94-36350

PHOTOCHEMICAL REACTIONS
Concurrent stabilization and imaging of a novel polymer for second harmonic generation via in situ photopolymerization
[AD-A278912] p 4243 N94-35588
Uniqueness of a solution of a steady state photochemical problem: Applications to Mars p 4370 N94-36151
H2O-H2SO4 system in Venus' clouds and OCS, CO, and H2SO4 profiles in Venus' troposphere
p 4370 N94-36152

PHOTODETACHMENT
Anionic states of LiFLi
[AD-A278830] p 4322 N94-35678

PHOTODIODES
High-sensitivity receiver for increasing multiplicity of measurement axes of Zygo's Heterodyne interferometer
[DE94-009916] p 4333 N94-35818

PHOTODISSOCIATION
Vacuum ultraviolet studies of molecular dynamics
[AD-A278940] p 4321 N94-35657
Infrared multiphoton ignition and combustion enhancement of natural gas.
[PB94-165438] p 4236 N94-35755

PHOTOELECTRIC EMISSION
Two-photon photoemission and the dynamics of electrons at interfaces
[DE94-011373] p 4324 N94-36058

PHOTOELECTRON SPECTROSCOPY
Two-photon photoemission and the dynamics of electrons at interfaces
[DE94-011373] p 4324 N94-36058

PHOTOEXCITATION
Infrared multiphoton ignition and combustion enhancement of natural gas.
[PB94-165438] p 4236 N94-35755

PHOTOGEOLOGY
Noachian and Hesperian modification of the original Chryse impact basin topography p 4364 N94-35462

PHOTOIONIZATION
Magnetic field effect on selective photoionization
[DE94-611079] p 4334 N94-36180

PHOTOLITHOGRAPHY
Materials for efficient high-flux magnetic bearing actuators p 4214 N94-35845

PHOTOMAPPING
Subpixel resolution from multiple images
p 4281 N94-35417
Noachian and Hesperian modification of the original Chryse impact basin topography p 4364 N94-35462
Lunar horizon glow and the Clementine mission
p 4366 N94-35478

PHOTOMETERS
High-sensitivity receiver for increasing multiplicity of measurement axes of Zygo's Heterodyne interferometer
[DE94-009916] p 4333 N94-35818
Catalog of Helios 90 deg photometer events
[PL-TR-94-2040] p 4375 N94-36264
Development of ultra-low noise, high performance 3 to 5 Quantum Well Infrared Photodetectors (QWIPs) for focal plane array staring image sensor systems
[AD-A278861] p 4342 N94-36385

PHOTOMULTIPLIER TUBES
X-ray remote sensing and in-situ spectroscopy for planetary exploration missions and gamma-ray remote sensing and in-situ spectroscopy for planetary exploration missions
[NASA-CR-189352] p 4375 N94-35381
Ultrafast readout of scintillating fibers using upgraded position-sensitive photomultipliers
[DE94-010419] p 4269 N94-36095

PHOTON BEAMS
Support of hadroproduction of bottom using the 800 GeV/c primary photon beam at the Fermilab tevatron
[DE94-009411] p 4324 N94-36016

PHOTONICS
Influence of an externally modulated photonic link on a microwave communications system
p 4252 N94-35544
Field demonstration of X-band photonic antenna remoting in the Deep Space Network
p 4252 N94-35545

PHOTONS
Morphological aspects of surface reactions
[DE94-010184] p 4236 N94-35685
First measurement of helium on Mars: Implications for the problem of radiogenic gases on the terrestrial planets p 4370 N94-36153
Primordial nucleosynthesis in conformal Weyl gravity
[DE94-003002] p 4327 N94-36241
T-odd, P-even photon-fermion interactions
[DE94-616869] p 4327 N94-36246

PHOTONUCLEAR REACTIONS
J/psi absorption effects in the coherent production on nuclei
[DE94-616870] p 4326 N94-36129

PHYSICAL CHEMISTRY
Mars aqueous chemistry experiment
[NASA-CR-196024] p 4354 N94-35263
Application of an alkylammonium method for characterization of phyllosilicates in CI chondrites
p 4351 N94-35432

PHYSICAL FACTORS
An electromagnetic finite difference time domain analog treatment of small signal acoustic interactions
[DE94-009978] p 4319 N94-35770

PHYSICAL OPTICS
Use of the sampling theorem to speed up near-field physical optics scattering calculations
p 4253 N94-35549

PHYSICS
Proceedings of the LLNL Technical Women's Symposium
[DE94-006616] p 4379 N94-35997
Activities of National Institute of Radiological Sciences
[DE94-727636] p 4296 N94-36101

PHYSIOLOGICAL EFFECTS
A database to evaluate acceleration (+Gz) induced loss of consciousness (G-LOC) in the human centrifuge
[AD-A278769] p 4299 N94-35707

PHYSIOLOGICAL FACTORS
Extended range operations: A review of recent developments p 4195 N94-36337
Determinants of subjective fatigue for C-141 crews during Operation Desert Storm p 4196 N94-36338

PHYSIOLOGICAL RESPONSES
Extended range operations: A review of recent developments p 4195 N94-36337

PHYSIOLOGICAL TESTS
Further studies of 60-Hz exposure effects on human function
[DE94-010192] p 4297 N94-36223
PHYSIOLOGY
Activities of National Institute of Radiological Sciences
[DE94-727636] p 4296 N94-36101
PIEZOELECTRIC CERAMICS
Active vibration damping using smart material
p 4221 N94-35886
PIEZOELECTRICITY
Aeroservoelastic tailoring with piezoelectric materials: Actuator optimization studies
[AD-A278640] p 4199 N94-36384
PILOT ERROR
Safety study: A review of flightcrew-involved, major accidents of US air carriers, 1978 through 1990
[PB94-917001] p 4191 N94-35482
Aircraft accident report: Uncontrolled collision with terrain, American International Airways Flight 808, Douglas DC-8-61, N814CK, US Naval Air Station, Guantanamo Bay, Cuba, 18 August 1993
[PB94-910406] p 4192 N94-35521
PILOT PERFORMANCE
Safety study: A review of flightcrew-involved, major accidents of US air carriers, 1978 through 1990
[PB94-917001] p 4191 N94-35482
Aircraft accident report: Uncontrolled collision with terrain, American International Airways Flight 808, Douglas DC-8-61, N814CK, US Naval Air Station, Guantanamo Bay, Cuba, 18 August 1993
[PB94-910406] p 4192 N94-35521
The prediction of pilot opinion ratings using optimal and sub-optimal pilot models
[AD-A278679] p 4298 N94-35692
Review of human factors problems related to long distance and long endurance operation of aircraft
p 4195 N94-36336
PILOTLESS AIRCRAFT
Technological challenges of High Altitude Long Endurance unmanned configurations
p 4193 N94-36323
PIONS
Goldstone pion and other mesons using a scalar confining interaction
[DE94-010016] p 4321 N94-35649
Calculations on some properties of the pion in the framework of Schwinger-Dyson and Bethe-Salpeter equations
[DE94-611232] p 4322 N94-35786
Elastic charge form factors for K mesons
[DE94-010014] p 4325 N94-36086
PIPELINES
Maglev crude oil pipeline p 4226 N94-35919
Role of magma-water interaction in very large explosive eruptions
[DE94-002698] p 4291 N94-36103
PIPES (TUBES)
Atomic oxygen reactor having at least one sidearm conduit
[NASA-CASE-MSC-21487-4] p 4250 N94-35445
PISTON ENGINES
Unleaded AVGAS program
[AD-A278650] p 4247 N94-35795
The STRATO 2C propulsion system: A low cost approach for a High Altitude Long Endurance aircraft
p 4195 N94-36335
PISTONS
Carbon-carbon piston development
[NASA-CR-4595] p 4233 N94-35947
PITCH (INCLINATION)
Data reduction, analysis and results of LACV-30-07 air cushion vehicle tests, Fort Story, VA, August - September 1993
[AD-A278859] p 4190 N94-35826
PIXELS
Subpixel resolution from multiple images
p 4281 N94-35417
The iWarp display module
[AD-A278610] p 4260 N94-36248
PLAINS
Workshop on the Martian Northern Plains: Sedimentological, periglacial, and paleoclimatic evolution
[NASA-CR-196134] p 4354 N94-35359
PLAN POSITION INDICATORS
Color-coded radar plan position indicator
[AD-D016200] p 4257 N94-36364
PLANE STRAIN
An energy method approach to the problem of elastic strip
[PB94-171014] p 4279 N94-36000
PLANE STRESS
An energy method approach to the problem of elastic strip
[PB94-171014] p 4279 N94-36000
PLANE WAVES
Plane shock generator explosive lens: Shock characterization of 4340 and PH13-8Mo steels, C360 brass and PZT 65/35 ferro-electric ceramic
[DE94-009254] p 4266 N94-35979
PLANETARY BOUNDARY LAYER
ULF waves in the low-latitude boundary layer and their relaticnship to magnetospheric pulsations: A multisatellite observation
[AD-A278906] p 4289 N94-35587
PLANETARY COMPOSITION
The Twenty-Fifth Lunar and Planetary Science Conference. Part 1: A-G
[NASA-CR-195743] p 4355 N94-35395
High resolution visible to short-wave near-infrared CCD spectra of Mars during 1990 p 4356 N94-35403
Low encounter speed comet COMA sample return missions p 4202 N94-35607
The Twenty-Fifth Lunar and Planetary Science Conference. Part 2: H-O
[NASA-CR-195744] p 4367 N94-36136
PLANETARY CRATERS
The Twenty-Fifth Lunar and Planetary Science Conference. Part 1: A-G
[NASA-CR-195743] p 4355 N94-35395
The Twenty-Fifth Lunar and Planetary Science Conference. Part 3: P-Z
[NASA-CR-195745] p 4362 N94-35448
Rheology, tectonics, and the structure of the Venus lithosphere p 4367 N94-35479
Magellan collection of radar calibration results
[NASA-CR-194753] p 4367 N94-35509
Mercury: Mid-infrared (7.3 - 13.5 microns) spectroscopic observations showing features characteristic of plagioclase p 4370 N94-36150
PLANETARY CRUSTS
Mars aqueous chemistry experiment
[NASA-CR-196024] p 4354 N94-35263
The Twenty-Fifth Lunar and Planetary Science Conference. Part 1: A-G
[NASA-CR-195743] p 4355 N94-35395
Quantifying shapes of volcanoes on Venus
p 4361 N94-35429
Volcano morphometry and volume scaling on Venus
p 4361 N94-35431
The parent magma of xenoliths in shergottite EETA79001: Bulk and trace element composition inferred from magmatic inclusions p 4352 N94-35467
Rheology, tectonics, and the structure of the Venus lithosphere p 4367 N94-35479
PLANETARY EVOLUTION
What initiated planetesimal formation?
p 4351 N94-35422
The fretted terrain of the Nilosyrtis Mensae region of Mars: Clues to the timing of dichotomy formation and the emplacement of the northern plains
p 4360 N94-35424
Noachian and Hesperian modification of the original Chryse impact basin topography p 4364 N94-35462
A quick look method of detecting water of hydration in small solar system bodies p 4352 N94-35470
Mars atmospheric escape and isotopic fractionation: Synthesis of data and models p 4369 N94-36143
PLANETARY GEOLOGY
Mars aqueous chemistry experiment
[NASA-CR-196024] p 4354 N94-35263
Workshop on the Martian Northern Plains: Sedimentological, periglacial, and paleoclimatic evolution
[NASA-CR-196134] p 4354 N94-35359
The Twenty-Fifth Lunar and Planetary Science Conference. Part 1: A-G
[NASA-CR-195743] p 4355 N94-35395
What initiated planetesimal formation?
p 4351 N94-35422
Exopaleontology and the search for a fossil record on Mars p 4360 N94-35425
The Twenty-Fifth Lunar and Planetary Science Conference. Part 3: P-Z
[NASA-CR-195745] p 4362 N94-35448
The topography of Mars: A re-evaluation of current data p 4364 N94-35460
Noachian and Hesperian modification of the original Chryse impact basin topography p 4364 N94-35462
The parent magma of xenoliths in shergottite EETA79001: Bulk and trace element composition inferred from magmatic inclusions p 4352 N94-35467
Formation of fold and thrust belts on Venus due to horizontal shortening of a laterally heterogeneous lithosphere p 4367 N94-35480
The Twenty-Fifth Lunar and Planetary Science Conference. Part 2: H-O
[NASA-CR-195744] p 4367 N94-36136
Mossbauer and spectral (visible and near-IR) data for Fe(3+)-substituted rutile p 4240 N94-36154
PLANETARY LANDING
Autonomous hazard detection and avoidance
[NASA-CR-188331] p 4309 N94-36439
PLANETARY MAPPING
The fretted terrain of the Nilosyrtis Mensae region of Mars: Clues to the timing of dichotomy formation and the emplacement of the northern plains
p 4360 N94-35424
Noachian and Hesperian modification of the original Chryse impact basin topography p 4364 N94-35462
PLANETARY NEBULAE
Application of an alkylammonium method for characterization of phyllosilicates in CI chondrites
p 4351 N94-35432
PLANETARY SURFACES
A mineralogical instrument for planetary applications
p 4357 N94-35408
The Twenty-Fifth Lunar and Planetary Science Conference. Part 3: P-Z
[NASA-CR-195745] p 4362 N94-35448
The temperature of nitrogen on Pluto
p 4365 N94-35468
The Twenty-Fifth Lunar and Planetary Science Conference. Part 2: H-O
[NASA-CR-195744] p 4367 N94-36136
PLANETARY TEMPERATURE
The temperature of nitrogen on Pluto
p 4365 N94-35468
PLANETARY WAVES
Non-linear interaction of gravity waves with average jet flows, instabilities, and turbulence
[PB94-170586] p 4291 N94-36214
PLANNING
Prodigy planning algorithm
[AD-A278900] p 4303 N94-35574
PLASMA ARC WELDING
Plasma arc welding weld imaging
[NASA-CASE-MFS-28797-1] p 4273 N94-35367
PLASMA CLOUDS
Catalog of Helios 90 deg photometer events
[PL-TR-94-2040] p 4375 N94-36264
PLASMA CONTROL
Power balance and characterization of impurities in the Maryland Spheromak, part 2
[DE94-009603] p 4335 N94-35670
A triggering mechanism of fast crash in sawtooth oscillation
[DE94-718974] p 4336 N94-35772
Particle orbit analysis for LHD helical axis configurations
[DE94-718995] p 4336 N94-35773
Applications of non-resonant RF forces for improvement of tokamak reactor performances. Part 1: Application of ponderomotive force
[DE94-718994] p 4336 N94-35813
Potential formation and transport in open field line systems
[DE94-718910] p 4337 N94-35983
Design study of LHD helical divertor and high temperature divertor plasma operation
[DE94-718975] p 4338 N94-36352
Modelling of ELMs and dynamic responses of the H-mode
[DE94-718977] p 4339 N94-36353
MHD and confinement characteristics in the high-beta regime on the CHS low-aspect-ratio heliotron/torsatron
[DE94-718981] p 4339 N94-36357
PLASMA DENSITY
Contributions of the low-latitude boundary layer to the finite width magnetotail convection model
[NASA-CR-196116] p 4289 N94-35392
PLASMA DIAGNOSTICS
New calculations of Fe spectra in high-temperature plasmas
[DE94-009919] p 4339 N94-36386
Feasibility study for a novel pulsed neutral beam diagnostics for tokamaks
[DE94-617129] p 4339 N94-36417
PLASMA DIFFUSION
The kinetics of inhomogeneous plasma
[DE94-611459] p 4336 N94-35788
PLASMA DRIFT
Collisonless dynamics of the magnetosphere
[AD-A278886] p 4290 N94-35708
Thickness of the layer of strong radial electric field in JFT-2M H-mode plasmas
[DE94-718993] p 4336 N94-35812
Ionospheric plasma drift and structure studies at high and mid-latitudes
[AD-A279415] p 4291 N94-36116
PLASMA DYNAMICS
Collisonless dynamics of the magnetosphere
[AD-A278886] p 4290 N94-35708
The kinetics of inhomogeneous plasma
[DE94-611459] p 4336 N94-35788

Improved models of beta-limit, anomalous transport and radial electric field with loss cone loss in heliotron/torsatron
[DE94-718976] p 4324 N94-35984
Modelling of ELMs and dynamic responses of the H-mode
[DE94-718977] p 4339 N94-36353

PLASMA FREQUENCIES
The fine structure of Langmuir waves observed upstream of the bow shock at Venus
[NASA-CR-196123] p 4354 N94-35378

PLASMA HEATING
A triggering mechanism of fast crash in sawtooth oscillation
[DE94-718974] p 4336 N94-35772
Heating experiments using neutral beams with variable injection angle and ICRF waves in CHS
[DE94-718982] p 4337 N94-35936

PLASMA INTERACTIONS
JPRS report: Science and technology. Central Eurasia
[JPRS-UST-94-008] p 4249 N94-35228

PLASMA LAYERS
Contributions of the low-latitude boundary layer to the finite width magnetotail convection model
[NASA-CR-196116] p 4289 N94-35392
Design study of LHD helical divertor and high temperature divertor plasma operation
[DE94-718975] p 4338 N94-36352

PLASMA OSCILLATIONS
The fine structure of Langmuir waves observed upstream of the bow shock at Venus
[NASA-CR-196123] p 4354 N94-35378
Modelling of ELMs and dynamic responses of the H-mode
[DE94-718977] p 4339 N94-36353

PLASMA PHYSICS
Simulation models for computational plasma physics: Concluding report
[DE94-009976] p 4335 N94-35647
NIFS Symposium: Toward the research of fusion burning plasmas, present status and future strategy
[DE94-727618] p 4336 N94-35775
Potential formation and transport in open field line systems
[DE94-718910] p 4337 N94-35983
Improved models of beta-limit, anomalous transport and radial electric field with loss cone loss in heliotron/torsatron
[DE94-718976] p 4324 N94-35984
Recovery of frozen flow losses in arcjets
[AD-A278739] p 4228 N94-36089
A survey of reflectometry techniques with applications to TFTR
[DE94-010202] p 4338 N94-36093

PLASMA POTENTIALS
Thickness of the layer of strong radial electric field in JFT-2M H-mode plasmas
[DE94-718993] p 4336 N94-35812
Potential formation and transport in open field line systems
[DE94-718910] p 4337 N94-35983

PLASMA PRESSURE
Contributions of the low-latitude boundary layer to the finite width magnetotail convection model
[NASA-CR-196116] p 4289 N94-35392

PLASMA SHEATHS
Theoretical aspect of low pressure discharges in simple gasses
[AD-A278762] p 4335 N94-35493

PLASMA TURBULENCE
K-epsilon model of anomalous transport in resistive interchange turbulence
[DE94-718983] p 4337 N94-35937

PLASMA WAVES
The fine structure of Langmuir waves observed upstream of the bow shock at Venus
[NASA-CR-196123] p 4354 N94-35378
ULF waves in the low-latitude boundary layer and their relationship to magnetospheric pulsations: A multisatellite observation
[AD-A278906] p 4289 N94-35587
Self-similar regimes of subsonic Langmuir wave collapse
[DE94-611466] p 4335 N94-35750
The kinetics of inhomogeneous plasma
[DE94-611459] p 4336 N94-35788
Initial perturbations and Langmuir waves in electron-positron plasma
[DE94-617190] p 4338 N94-36097
The energy density of fluctuative electromagnetic field near the semi-bounded plasma
[DE94-617188] p 4256 N94-36099

PLASMA-PARTICLE INTERACTIONS
Participation in the definition, conduct, and analysis of particle accelerator experiments for the first Spacelab Mission
[NASA-CR-193974] p 4330 N94-35483

PLASMAS (PHYSICS)
Theoretical aspect of low pressure discharges in simple gasses
[AD-A278762] p 4335 N94-35493
Simulation models for computational plasma physics: Concluding report
[DE94-009976] p 4335 N94-35647
Analysis of current diffusive ballooning mode
[DE94-718992] p 4336 N94-35811
Applications of non-resonant RF forces for improvement of tokamak reactor performances. Part 1: Application of ponderomotive force
[DE94-718994] p 4336 N94-35813
Atomic physics and radiation processes in plasmas
[DE94-727617] p 4337 N94-35939
A survey of reflectometry techniques with applications to TFTR
[DE94-010202] p 4338 N94-36093
The pressure of fluctuative electromagnetic field in inhomogeneous medium
[DE94-617189] p 4256 N94-36096
The energy density of fluctuative electromagnetic field near the semi-bounded plasma
[DE94-617188] p 4256 N94-36099
Collective plasma corrections to the solar opacity
[PB94-170511] p 4375 N94-36210
The new features of Ion Bernstein Wave Heating in JIPP T-2U tokamak
[DE94-718978] p 4338 N94-36247
Catalog of Helios 90 deg photometer events
[PL-TR-94-2040] p 4375 N94-36264
Studies of the dayside boundary layer processes based on ground observations in the Svalbard area
[AD-A280715] p 4292 N94-36265
Experiments in diamond film fabrication in table-top plasma apparatus p 4231 N94-36411

PLASTIC PROPERTIES
Aspects of robust computational modeling for plain and reinforced concrete
[PB94-169240] p 4251 N94-35820
Transformation plasticity in ductile solids
[DE94-010420] p 4240 N94-35953

PLASTICIZERS
Diffusion and sorption of 1,4-dioxane into polychloroprene
[ARL-TR-338] p 4229 N94-35361

PLASTICS
Laminated thermoplastic composite material from recycled high density polyethylene p 4230 N94-36403

PLATEAUS
Fluvial processes in Ma'adim Vallis and the potential of Gusev crater as a high priority site
p 4358 N94-35414

PLATING
The electrical conductivities of candidate beam-waveguide antenna shroud materials
p 4252 N94-35546

PLATINUM
High temperature sorbents for oxygen
[NASA-CASE-NPO-18409-1-CU] p 4235 N94-35255
A novel method for depositing precious metal films on difficult surfaces
[NASA-TM-106607] p 4243 N94-35260
Multicomponent glass surfaces: Structure and adsorption
[DE94-010516] p 4246 N94-36283

PLATINUM COMPOUNDS
Synthesis of novel composite Platinum-DNA films by way of wet-spinning
[AD-A278763] p 4243 N94-35494

PLUMES
Instrumentation for in-flight SSME rocket engine plume spectroscopy
[NASA-TM-106596] p 4268 N94-35268
Radiative signals from impact of Shoemaker-Levy on Jupiter p 4355 N94-35396

PLUTO (PLANET)
The temperature of nitrogen on Pluto
p 4365 N94-35468

PNEUMATIC CONTROL
The reduction of takeoff ground roll by the application of a nose gear jump strut
[NASA-TM-108822] p 4198 N94-36380

PNEUMATIC EQUIPMENT
Tipjet 80-inch model rotor hover test: Test no. 1198
[AD-A279680] p 4191 N94-36261

PODS (EXTERNAL STORES)
Aerial refueling interoperability from a receiver flying qualities perspective p 4197 N94-36343

POINT DEFECTS
Study of point defect mobilities in zirconium during electron irradiation in a HVEM
[DE94-619028] p 4242 N94-36289

POINTING CONTROL SYSTEMS
Design and implementation of a beam-waveguide mirror control system for vernier pointing of the DSS-13 antenna p 4253 N94-35548
Overview of the Miniature Sensor Technology Integration (MSTI) spacecraft attitude control system
p 4206 N94-35627
Input shaping for three-dimensional slew maneuvers of a precision pointing flexible spacecraft
[DE94-008937] p 4226 N94-36001
Estimation with multisensor/multiscan detection fusion
[AD-A278753] p 4256 N94-36092

POISSON DENSITY FUNCTIONS
A new association-model for binary VLE of alcohol/hydrocarbon and amine/hydrocarbon mixtures
[DE94-011012] p 4248 N94-36034

POISSON RATIO
Shoemaker-Levy 9 and the tidal disruption of comets
p 4351 N94-35406

POLAR CAPS
Studies of the dayside boundary layer processes based on ground observations in the Svalbard area
[AD-A280715] p 4292 N94-36265

POLAR REGIONS
Analytic model of aurorally coupled magnetospheric and ionospheric electrostatic potentials
[NASA-CR-196130] p 4288 N94-35358
The effects of cloud inhomogeneities upon radiative fluxes, and the supply of a cloud truth validation dataset
[NASA-CR-196080] p 4293 N94-35391
Ionospheric plasma drift and structure studies at high and mid-latitudes
[AD-A279415] p 4291 N94-36116

POLARIZATION (CHARGE SEPARATION)
Intramolecular energy transfer reactions in polymetallic complexes
[DE94-010114] p 4326 N94-36126

POLARIZATION CHARACTERISTICS
Synthesis of novel composite Platinum-DNA films by way of wet-spinning
[AD-A278763] p 4243 N94-35494
Center for seismic studies
[AD-A278682] p 4290 N94-35693
Modelling of the structure and physical properties of simple disordered systems
[DE94-617087] p 4329 N94-36311

POLARIZED LIGHT
Magnetic field effect on selective photoionization
[DE94-611079] p 4334 N94-36180

POLICIES
Partners in space. International cooperation in space: Strategies for the new century
[ISBN-0-9629930-2-6] p 4348 N94-35901
JPRS report: Science and technology. Central Eurasia: Space
[JPRS-USP-93-005] p 4201 N94-36011

POLITICS
Space and the American imagination
[NASA-CR-196131] p 4376 N94-35356

POLLUTION CONTROL
How to develop a long term CO2 reduction plan
[DE94-009559] p 4284 N94-35668
Final regulatory impact analysis: Refueling emission regulations for light duty vehicles and trucks and heavy duty vehicles
[PB94-164027] p 4285 N94-35754
Dual cure low-VOC coating process
[DE94-009346] p 4245 N94-35809
Design and operation of a medium speed 12-cylinder coal-fueled diesel engine. Phase 2: Improvements
[DE94-009547] p 4275 N94-35815
Methanol fuel additive demonstration
[PB94-156668] p 4247 N94-35941
Treatment of toxic gases SO2 and NO(x) by electron beam irradiation
[DE94-615424] p 4330 N94-36028

POLLUTION MONITORING
Aerosol optical depth derived from solar radiometry observations at northern mid-latitude sites
[DE94-007476] p 4287 N94-36053

POLLUTION TRANSPORT
Atmospheric and dispersion modeling in areas of highly complex terrain employing a four-dimensional data assimilation technique
[DE94-004041] p 4285 N94-35823
Modeling the atmospheric input of nutrients, heavy metals, and pesticides to the Great Lakes
[DE94-005481] p 4286 N94-36007

POLYACETYLENE
Syntheses and studies of acetylenic polymers
[DE94-011201] p 4245 N94-36057

POLYETHYLENES
A comparison of atomic oxygen erosion yields of carbon and selected polymers exposed in ground based facilities and in low Earth orbit
[NASA-TM-106622] p 4243 N94-35243
Laminated thermoplastic composite material from recycled high density polyethylene p 4230 N94-36403
Microscale synthesis and characterization of polystyrene: NSF-POLYED scholars project
p 4231 N94-36408

POLYIMIDE RESINS
Addition polyimides with enhanced processability
[NASA-CASE-LEW-15043-1] p 4242 N94-35234
Tough high performance composite matrix
[NASA-CASE-LAR-14239-2] p 4232 N94-35372

POLYIMIDES
Tough, processable semi-interpenetrating polymer networks from monomer reactants
[NASA-CASE-LAR-14838-1] p 4242 N94-35233
Tough high performance composite matrix
[NASA-CASE-LAR-14239-2] p 4232 N94-35372
Residual Gas Analysis (RGA) and shear strength characteristics of a silver-filled epoxy and polyimide under long-term, high-temperature storage conditions
[DE94-010106] p 4244 N94-35705
Liquid crystalline thermosetting polyimides
[DE94-009939] p 4244 N94-35768
Third European Technical Symposium on Polyimides and High Performance Polymers: STEPI 3
[PB94-148491] p 4246 N94-36177

POLYMER BLENDS
Intelligent processing of materials, technical activities, 1993 (NAS-NRC Assessment Panel, April 21-22 1994)
[PB94-164183] p 4251 N94-35737

POLYMER CHEMISTRY
Syntheses and studies of acetylenic polymers
[DE94-011201] p 4245 N94-36057

POLYMER MATRIX COMPOSITES
Implementation of the military handbook 17 for polymer matrix composites and metal matrix composites
[AD-A278795] p 4244 N94-35757
Report on the Workshop on Manufacturing Polymer Composites by Liquid Molding
[PB94-160066] p 4234 N94-36004
Continuous unidirectional fiber reinforced composites: Fabrication and testing p 4229 N94-36400

POLYMERIC FILMS
Mechanical properties of crosslinked polymer coatings
p 4231 N94-36410

POLYMERIZATION
Addition polyimides with enhanced processability
[NASA-CASE-LEW-15043-1] p 4242 N94-35234
Concurrent stabilization and imaging of a novel polymer for second harmonic generation via in situ photopolymerization
[AD-A278912] p 4243 N94-35588
Novel catalysts for methane activation
[DE94-009705] p 4237 N94-35778
Syntheses and studies of acetylenic polymers
[DE94-011201] p 4245 N94-36057
Nonlinear optical composites of metal cluster laden polymers
[AD-D016217] p 4234 N94-36124
Third European Technical Symposium on Polyimides and High Performance Polymers: STEPI 3
[PB94-148491] p 4246 N94-36177
Microscale synthesis and characterization of polystyrene: NSF-POLYED scholars project
p 4231 N94-36408

POLYMERS
Atomic oxygen protective coating with resistance to undercutting at defect sites
[NASA-CASE-LEW-15306-1] p 4243 N94-35502
Intelligent processing of materials, technical activities, 1993 (NAS-NRC Assessment Panel, April 21-22 1994)
[PB94-164183] p 4251 N94-35737

POLYMORPHISM
A critique of type systems for global overloading
[AD-A278800] p 4304 N94-35676
The structural changes of water ice I during warmup
p 4239 N94-36144

POLYNOMIALS
Cramer-von Mises variance estimators for simulations
[AD-A278799] p 4316 N94-35675
Inverse problem for symmetric tridiagonal matrices. Calculation of discrete orthogonal polynomial system with arbitrary weight
[DE94-612434] p 4315 N94-35789
Priorities and nonmonotonic reasoning
[PB94-171170] p 4346 N94-35959
Gauss elimination by segments and multivariate polynomial interpolation
[AD-A278646] p 4315 N94-36012

POLYPHENYLS
Addition polyimides with enhanced processability
[NASA-CASE-LEW-15043-1] p 4242 N94-35234

POLYSTYRENE
Microscale synthesis and characterization of polystyrene: NSF-POLYED scholars project
p 4231 N94-36408

POLYURETHANE RESINS
Concurrent stabilization and imaging of a novel polymer for second harmonic generation via in situ photopolymerization
[AD-A278912] p 4243 N94-35588

POMERONS
High energy asymptotics of perturbative multi-color QCD
[DE94-001350] p 4327 N94-36238

PONDEROMOTIVE FORCES
Applications of non-resonant RF forces for improvement of tokamak reactor performances. Part 1: Application of ponderomotive force
[DE94-718994] p 4336 N94-35813
The pressure of fluctuative electromagnetic field in inhomogeneous medium
[DE94-617189] p 4256 N94-36096

PONTRYAGIN PRINCIPLE
A combined algorithm for minimum time slewing of flexible spacecraft p 4220 N94-35881

POROSITY
NMR imaging of components and materials for DOE application
[DE94-010664] p 4238 N94-36084

POROUS MATERIALS
Microporous structure with layered interstitial surface treatment, and method and apparatus for preparation thereof
[NASA-CASE-MSC-21487-3] p 4235 N94-35229
Theoretical and experimental study of air and hydrogen electrodes
[DE94-763308] p 4283 N94-36060

POSEIDON SATELLITE
Compatibility of TOPEX/Poseidon trajectory propagation with JPL and GSFC/FDF operational software
p 4204 N94-35619
Improved solution accuracy for TDRSS-based TOPEX/Poseidon orbit determination
p 4205 N94-35620
Tracking system options for future altimeter satellite missions p 4205 N94-35622

POSITION (LOCATION)
Mesoscale roughness of Venus p 4361 N94-35430
Transformation plasticity in ductile solids
[DE94-010420] p 4240 N94-35953
Analysis of mid-tropospheric carbon monoxide data using a three-dimensional global atmospheric chemistry numerical model
[DE94-004782] p 4286 N94-36026
Extrapolating storm location using the Integrated Terminal Weather System (ITWS) storm motion algorithm
[AD-A278611] p 4295 N94-36249
Computational methods for material failure processes
[AD-A278716] p 4278 N94-36292
Aerial refueling interoperability from a receiver flying qualities perspective p 4197 N94-36343

POSITION ERRORS
In-flight scale/distortion calibration of the Hubble Space Telescope fixed-head star trackers
p 4203 N94-35613

POSITION SENSING
Integration of magnetic bearings in the design of advanced gas turbine engines p 4223 N94-35903

POSITIONING
Materials for efficient high-flux magnetic bearing actuators p 4214 N94-35845
Magnetically suspended stepping motors for clean room and vacuum environments p 4225 N94-35915
Six degree of freedom fine motion positioning stage based on magnetic levitation p 4225 N94-35916
Analysis of achievable disturbance attenuation in a precision magnetically-suspended motion control system
p 4225 N94-35917

POSITIONING DEVICES (MACHINERY)
Fuzzy self-learning control for magnetic servo system
p 4215 N94-35852

POSITRON ANNIHILATION
T-odd, P-even photon-fermion interactions
[DE94-616869] p 4327 N94-36246

POSITRONIUM
Logarithmic corrections of the two-body QED problem
[DE94-611157] p 4322 N94-35783

POSITRONS
Precise measurement of the left-right cross section asymmetry in Z boson production by electron-positron collisions
[DE94-010751] p 4326 N94-36198

POSTLAUNCH REPORTS
Debris/ice/TPS assessment and integrated photographic analysis for Shuttle Mission STS-59
[NASA-TM-109203] p 4211 N94-35523

POSTMISSION ANALYSIS (SPACECRAFT)
STS-58 Space Shuttle Mission Report
[NASA-TM-109867] p 4211 N94-35251
STS-51 Space Shuttle Mission Report
[NASA-TM-109866] p 4211 N94-35252

POTENTIAL FIELDS
Self-similar regimes of subsonic Langmuir wave collapse
[DE94-611466] p 4335 N94-35750

POTENTIAL THEORY
The nucleon-nucleon potential in the chromodielectric soliton model
[DE94-004646] p 4329 N94-36305

POTTING COMPOUNDS
NMR imaging of components and materials for DOE application
[DE94-010664] p 4238 N94-36084

POWDER (PARTICLES)
Structures and properties of materials recovered from high shock pressures
[DE94-010057] p 4232 N94-35696
Properties and applications of powder-filled evacuated-panel superinsulations
[DE94-009169] p 4233 N94-35932

POWER AMPLIFIERS
High power diode laser Master Oscillator-Power Amplifier (MOPA)
[NASA-CR-196095] p 4271 N94-35488
A 32-GHz solid-state power amplifier for deep space communications p 4255 N94-35562
Chirped-pulse amplification with flashlamp-pumped Ti:Sapphire amplifiers
[DE94-010055] p 4272 N94-35695

POWER CONVERTERS
Microprocessor control of multiple peak power tracking DC/DC converters for use with solar cell arrays
[NASA-CASE-GSC-13450-2] p 4282 N94-35540

POWER LINES
On optimal placement of spacers in bundled conductors p 4258 N94-35354
CABPRO: An expert system for process planning multiwire cables
[DE94-010213] p 4312 N94-35810
National Maglev initiative: California line electric utility power system requirements p 4215 N94-35850

POWER PLANTS
Air quality implications associated with the selection of power plants in the Pacific Northwest
[DE94-004783] p 4287 N94-36027

POWER REACTORS
Guidelines for design and development of computer/microprocessor based systems in research and power reactors
[DE94-616271] p 4300 N94-35570

POWER SPECTRA
In-flight estimation of gyro noise on the Upper Atmosphere Research Satellite (UARS) and Extreme Ultraviolet Explorer (EUVE) missions
p 4204 N94-35616
Measuring attitude with a gradiometer
p 4206 N94-35630

PREAMPLIFIERS
Influence of an externally modulated photonic link on a microwave communications system
p 4252 N94-35544

PRECIPITATES
Formation and stability of Fe-rich precipitates in dilute Zr(Fe) single-crystal alloys
[DE94-619027] p 4242 N94-36288

PRECIPITATION (METEOROLOGY)
Production of long-term global water vapor and liquid water data set using ultra-fast methods to assimilate multi-satellite and radiosonde observations
[NASA-CR-196044] p 4292 N94-35355

PREDICTION ANALYSIS TECHNIQUES
The development and application of composite complexity models and a relative complexity metric in a software maintenance environment
p 4255 N94-35559

PREDICTIONS
The computation of cloud base height from paired whole-sky imaging cameras
[DE94-009868] p 4294 N94-35767

PREDICTOR-CORRECTOR METHODS
Description and use of LSODE, the Livermore Solver for Ordinary Differential Equations
[NASA-RP-1327] p 4313 N94-35259
Theory and computation of optimal low- and medium-thrust transfers
[NASA-CR-196077] p 4202 N94-35487
Vortex tubes in turbulent flows: Identification, representation, reconstruction
[NASA-CR-194900] p 4267 N94-35992

PREFORMS
A review of radial forging technology including preform design for process optimization
[AD-A278770] p 4250 N94-35711

PREPREGS
Through-the-thickness tensile strength of textile composites
[NASA-TM-109115] p 4233 N94-35946

PREPROCESSING
ML partial evaluation using set-based analysis
[AD-A278955] p 4304 N94-35718

PRESSURE DISTRIBUTION
A supersonic tunnel for laser and flow-seeding techniques
[NASA-TM-106588] p 4265 N94-35945
Expansion effects on supersonic turbulent boundary layers
[AD-A278989] p 4190 N94-35950
Propellant stress relief groove for the Titan 4 SRMU
[AD-A278628] p 4228 N94-36254

PRESSURE EFFECTS
X ray and gamma ray spectroscopy of solids under pressure
[DE94-011207] p 4238 N94-36203

PRESSURE MEASUREMENT
Method for making a dynamic pressure sensor and a pressure sensor made according to the method
[NASA-CASE-LAR-14029-1] p 4269 N94-35369
Flight testing of a luminescent surface pressure sensor
[NASA-TM-103970] p 4189 N94-35394
Determination of extensional viscosity from capillary rheometer entrance pressure drop measurements using a numerical simulation of contraction flow
[PB94-171154] p 4263 N94-35603
Portable high precision pressure transducer system
[DE94-010137] p 4270 N94-36389

PRESSURE REDUCTION
Determination of extensional viscosity from capillary rheometer entrance pressure drop measurements using a numerical simulation of contraction flow
[PB94-171154] p 4263 N94-35603

PRESSURE SENSORS
Method for making a dynamic pressure sensor and a pressure sensor made according to the method
[NASA-CASE-LAR-14029-1] p 4269 N94-35369
Flight testing of a luminescent surface pressure sensor
[NASA-TM-103970] p 4189 N94-35394
Portable high precision pressure transducer system
[DE94-010137] p 4270 N94-36389

PRIMERS (COATINGS)
Dual cure low-VOC coating process
[DE94-009346] p 4245 N94-35809

PRINTED CIRCUITS
Manufacturing feasibility of several lead-free solders for electronic assembly
[DE94-007732] p 4258 N94-35564
Ionic contamination detection
[DE94-010212] p 4258 N94-35686
Capillary flow solderability test for printed wiring boards
[DE94-010321] p 4259 N94-36094

PRIORITIES
Probabilities and priorities in timed CSP
[PB94-169216] p 4316 N94-35536
Priorities and nonmonotonic reasoning
[PB94-171170] p 4346 N94-35959

PROBABILITY DENSITY FUNCTIONS
Comparison of PDF and moment closure methods in the modeling of turbulent reacting flows
[NASA-TM-106614] p 4265 N94-35948

PROBABILITY THEORY
Probabilities and priorities in timed CSP
[PB94-169216] p 4316 N94-35536
Point and interval estimation of series system reliability using small data sets
[AD-A278647] p 4316 N94-35575
Integral characteristics of the magnetic bremsstrahlung
[DE94-616788] p 4256 N94-36078
High energy
[DE94-009477] p 4331 N94-36428

PROBLEM SOLVING
The weakest failure detector for solving Consensus
[NASA-CR-190545] p 4300 N94-35365
Prodigy planning algorithm
[AD-A278900] p 4303 N94-35574
Case based reasoning in engineering design
[AD-A278943] p 4305 N94-36006
Can we break intractability using randomization or the average case setting?
[AD-A278598] p 4316 N94-36425

PROCESS CONTROL (INDUSTRY)
Robust requirements specifications for safety-critical systems
[PB94-167806] p 4250 N94-35532
AICD: Advanced Industrial Concepts Division Biological and Chemical Technologies Research Program
[DE94-006854] p 4283 N94-36051
Process capability determination of new and existing equipment p 4230 N94-36406

PROCUREMENT MANAGEMENT
Statement by Bill D. Colvin, Inspector General
[NASA-TM-109793] p 4348 N94-35446
Budget estimates, fiscal year 1995. Volume 1: Agency summary, human space flight, and science, aeronautics and technology
[NASA-TM-109791] p 4347 N94-35899
Budget estimates, fiscal year 1995. Volume 2: Mission support and Inspector General
[NASA-TM-109792] p 4348 N94-35900

PRODUCT DEVELOPMENT
Designing aluminum sealing glasses for manufacturability
[DE94-010081] p 4244 N94-35699

PRODUCTIVITY
A practical guide to the technology and adoption of software process automation
[AD-A278719] p 4308 N94-36294

PROGRAM VERIFICATION (COMPUTERS)
Developing interpretable models with optimized set reduction for identifying high risk software components
p 4301 N94-35435
Symbolic debugging of globally optimized code: Data value problems and their solutions
[AD-A278898] p 4302 N94-35572
Concept for an algorithm testing and evaluation program at NIST
[PB94-163029] p 4304 N94-35740

PROGRAMMING ENVIRONMENTS
Symbolic debugging of globally optimized code: Data value problems and their solutions
[AD-A278898] p 4302 N94-35572
Environment/tool integrator for software development, version 1.2
[AD-A278965] p 4303 N94-35660
An object-oriented implementation of a graphical-programming system
[DE94-009298] p 4304 N94-35808
An environment for visualization, reliability, and knowledge acquisition in equational programming
[AD-A278639] p 4308 N94-36258

PROGRAMMING LANGUAGES
Probabilities and priorities in timed CSP
[PB94-169216] p 4316 N94-35536
A lower bound for the intersection of regular forests
[AD-A278653] p 4303 N94-35576
A critique of type systems for global overloading
[AD-A278800] p 4304 N94-35676
Task networks for controlling continuous processes
[AD-A278683] p 4312 N94-35710

PROJECT MANAGEMENT
Apollo 11 at twenty-five, version 1.0
[NASA-CR-193380] p 4376 N94-35363
Statement by Bill D. Colvin, Inspector General
[NASA-TM-109793] p 4348 N94-35446
Earth Observing System (EOS) Advanced Microwave Sounding Unit-A (AMSU-A) schedule plan
[NASA-CR-194856] p 4281 N94-35734

PROJECT PLANNING
Cost and schedule estimation study report
[NASA-CR-189344] p 4300 N94-35256
Budget estimates, fiscal year 1995. Volume 2: Mission support and Inspector General
[NASA-TM-109792] p 4348 N94-35900

PROJECTILE CRATERING
Craters in aluminum 1100 targets using glass projectiles at 1-7 km/s p 4280 N94-35407
Impact basins in Southern Daedalia, Mars: Evidence for clustered impactors? p 4360 N94-35426
Distribution of siderophile and other trace elements in melt rock at the Chicxulub impact structure
p 4352 N94-35456
Experimental impacts into Teflon targets and LDEF thermal blankets p 4352 N94-36141

PROJECTILES
Eureka! Aerogel capture of meteoroids in space
p 4351 N94-35412
Energy partitioning in high speed impact of analog solid rocket motors
[AD-A278771] p 4228 N94-35825

PRONY SERIES
An iterative extension of Prony's method for ARMA signal modeling
[AD-A278841] p 4319 N94-35800

PROPANE
The reaction of hydroperoxy-propyl radicals with molecular oxygen
[DE94-006392] p 4239 N94-36319

PROPELLANT TANKS
Experimental results of hydrogen slosh in a 62 cubic foot (1750 liter) tank
[NASA-TM-106625] p 4263 N94-35250

PROPELLANTS
The thermochemistry and reaction mechanisms in the decomposition of energetic materials
[DE94-011420] p 4248 N94-36376

PROPORTIONAL COUNTERS
Experimental characterisation of gas microstrip detectors. Part 2: Counting rate characteristics
[PB94-167095] p 4269 N94-36061

PROPULSION
AFOSR Contractors Propulsion Meeting
[AD-A279028] p 4198 N94-35746

PROPULSION SYSTEM CONFIGURATIONS
The 30th JANNAF Combustion Subcommittee Meeting, volume 2
[AD-A278794] p 4247 N94-35656
Technological challenges of High Altitude Long Endurance unmanned configurations
p 4193 N94-36323
Propulsion system selection for a High Altitude Long Endurance aircraft p 4195 N94-36333
Propulsion system technologies for long range and long endurance aircraft p 4195 N94-36334
The STRATO 2C propulsion system: A low cost approach for a High Altitude Long Endurance aircraft
p 4195 N94-36335

PROPULSION SYSTEM PERFORMANCE
The 30th JANNAF Combustion Subcommittee Meeting, volume 2
[AD-A278794] p 4247 N94-35656
Recent Advances in Long Range and Long Endurance Operation of Aircraft
[AGARD-CP-547] p 4193 N94-36321
Technological challenges of High Altitude Long Endurance unmanned configurations
p 4193 N94-36323

PROPYL COMPOUNDS
The reaction of hydroperoxy-propyl radicals with molecular oxygen
[DE94-006392] p 4239 N94-36319

PROTECTIVE CLOTHING
Aerospace medicine and biology: A continuing bibliography with indexes (supplement 391)
[NASA-SP-7011(391)] p 4297 N94-35345

PROTECTIVE COATINGS
Analysis of the Shuttle Orbiter reinforced carbon-carbon oxidation protection system
[NASA-TM-104792] p 4262 N94-35245
Atomic oxygen protective coating with resistance to undercutting at defect sites
[NASA-CASE-LEW-15306-1] p 4243 N94-35502
Coatings for SiO2 optical fibers
[AD-D016197] p 4334 N94-36363

PROTEIN SYNTHESIS
Stress and brain protein synthesis
[PB94-170750] p 4296 N94-35601

PROTEINS
Stress and brain protein synthesis
[PB94-170750] p 4296 N94-35601
A low temperature scanning force microscope for biological samples
[DE94-011357] p 4297 N94-36269

PROTOCOL (COMPUTERS)
Asynchronous optimistic rollback recovery using secure distributed time
[AD-A278978] p 4344 N94-35526
The rel/REL: A family of reliable multicast protocols for distributed real-time systems
[PB94-167830] p 4310 N94-35535
Probabilities and priorities in timed CSP
[PB94-169216] p 4316 N94-35536
Mathematical theory of synchronous communication
[PB94-169224] p 4252 N94-35537
The development and application of composite complexity models and a relative complexity metric in a software maintenance environment
p 4255 N94-35559
Large granularity cache coherence for intermittent connectivity
[AD-A278897] p 4345 N94-35571
Synthesis of asynchronous systems from data flow specifications
[AD-A278687] p 4303 N94-35662
SandiaXTP, an object-oriented implementation of XTP 3.7
[DE94-011752] p 4257 N94-36354

PROTON BEAMS
Spin dynamics in storage rings and linear accelerators
[DE94-010320] p 4330 N94-36106

PROTONS
Electron and Proton Wide-Angle Spectrometer (EPAS) on the CRRES spacecraft
[AD-A278630] p 4227 N94-35362
Particle orbit analysis for LHD helical axis configurations
[DE94-718995] p 4336 N94-35773
Dynamic aperture and transverse proton diffusion in HERA
[DE94-010309] p 4331 N94-36224

PROTOPLANETS
What initiated planetesimal formation?
p 4351 N94-35422

PROTOTYPES
Applying observations of work activity in designing prototype data analysis tools
[DE94-010206] p 4347 N94-36297

PROVING
Capillary column GC-MS/MS confirmation of phosphate esters with a hybrid tandem mass spectrometer
[AD-A278748] p 4238 N94-36091

PSEUDONOISE
Spacecraft-spacecraft radio-metric tracking: Signal acquisition requirements and application to Mars approach navigation p 4254 N94-35557

PSYCHOLOGICAL FACTORS
Extended range operations: A review of recent developments p 4195 N94-36337
Determinants of subjective fatigue for C-141 crews during Operation Desert Storm p 4196 N94-36338

PSYCHOMOTOR PERFORMANCE
Some solutions to reduce the human effects of extended operation times p 4196 N94-36339

PSYCHOPHARMACOLOGY
Some solutions to reduce the human effects of extended operation times p 4196 N94-36339

PUBLIC HEALTH
Proceedings of the Sixth International Congress on Noise as a Public Heatlh Problem, volume 3
[AD-A278218] p 4319 N94-36176

PULSAR MAGNETOSPHERES
GRO: Studies of high energy pulsars with EGRET
[NASA-CR-196003] p 4349 N94-35516

PULSARS
GRO: Studies of high energy pulsars with EGRET
[NASA-CR-196003] p 4349 N94-35516

PULSE DURATION MODULATION
Microprocessor control of multiple peak power tracking DC/DC converters for use with solar cell arrays
[NASA-CASE-GSC-13450-2] p 4282 N94-35540

PULSE GENERATORS
Analysis of recent agile mirror data
[AD-A278758] p 4318 N94-36427

PULSED LASERS
Molecular systems for ultrafast optical switching: Controlling electron transfer reactions with femtosecond laser pulses
[DE94-009695] p 4332 N94-35671
Chirped-pulse amplification with flashlamp-pumped Ti:Sapphire amplifiers
[DE94-010055] p 4272 N94-35695

PULSED RADIATION
Time-of-flight diffraction at pulsed neutron sources: An introduction to the symposium
[DE94-010442] p 4327 N94-36225

PURITY
Purity and cleanness of aerogel as a cosmic dust capture medium p 4247 N94-35469

PYROXENES
Reduction of lunar mare soil and pyroclastic glass
p 4355 N94-35398
Partial melting of the St. Severin (LL) and Lost City (H) ordinary chondrites: One step backwards and two steps forward p 4353 N94-36146
Synthetic and natural Nakhla pyroxenes: Parent melt composition and REE partition coefficients
p 4353 N94-36161
Hematite formed from pyroxene on Mars by meteoritic impact p 4372 N94-36165

Q

Q SWITCHED LASERS
Chirped-pulse amplification with flashlamp-pumped Ti:Sapphire amplifiers
[DE94-010055] p 4272 N94-35695

QUADRATIC EQUATIONS
Recent progress in irrational conformal field theory
[DE94-011908] p 4317 N94-36234

QUADRATIC PROGRAMMING
Application of sequential quadratic programming to large-scale structural design problems
[AD-A278574] p 4307 N94-36185

QUADRATURES
Correlator data analysis for the array feed compensation system p 4253 N94-35553

QUADRUPOLES
Hot-ion plasma in the quadrupole trap
[DE94-617216] p 4337 N94-36082

QUALITY CONTROL
A quality control package for the Digisonde Drift Analysis (DDA)
[AD-A278663] p 4289 N94-35578
Using experimental design modules for process characterization in manufacturing/materials processes laboratories p 4230 N94-36405

QUANTITATIVE ANALYSIS
Study on contaminants on flight and other critical surfaces
[NASA-CR-193975] p 4235 N94-35447
Petrographic characterization of lunar soils: Application of x ray digital-imaging to quantitative and automated analysis p 4368 N94-36138

QUANTUM CHEMISTRY
A combined experimental and theoretical study of the neutral, cationic and anionic Si3N cluster molecule
[AD-A278834] p 4323 N94-35792
New anionic states of the lithium trimer
[AD-A278832] p 4323 N94-35797

QUANTUM CHROMODYNAMICS
Proceedings of 2nd Working meeting: Physics at VLEPP, volume 1
[DE94-616200] p 4320 N94-35569
Leptonic decay constants of heavy quarkonia in effective QCD sum rules
[DE94-611160] p 4322 N94-35784
Proceedings of 2nd Working Meeting on Physics at VLEPP, volume 2
[DE94-616167] p 4326 N94-36182
High energy asymptotics of perturbative multi-color QCD
[DE94-001350] p 4327 N94-36238
Summary: Hadron dynamics sessions
[DE94-003011] p 4328 N94-36303
Collapse of flux tubes
[DE94-004645] p 4328 N94-36304
The nucleon-nucleon potential in the chromodielectric soliton model
[DE94-004646] p 4329 N94-36305

QUANTUM COUNTERS
Quantum groups, non-commutative differential geometry and applications
[DE94-011358] p 4315 N94-36270

QUANTUM ELECTRODYNAMICS
Logarithmic corrections of the two-body QED problem
[DE94-611157] p 4322 N94-35783

QUANTUM MECHANICS
Identity for propagator in four-fermion theory
[DE94-611104] p 4342 N94-35781
Inverse problem for symmetric tridiagonal matrices. Calculation of discrete orthogonal polynomial system with arbitrary weight
[DE94-612434] p 4315 N94-35789
Quantum mechanics and thermodynamics of particles with distance dependent statistics
[DE94-616620] p 4343 N94-36072
Exact multiplicities in the three-anion spectrum
[DE94-616768] p 4325 N94-36075
Boson spectra and correlations in thermal locally equilibrium systems
[DE94-616799] p 4325 N94-36079
Quantum groups, non-commutative differential geometry and applications
[DE94-011358] p 4315 N94-36270

QUANTUM NUMBERS
Periodicity and peculiarity in 120 first and second row diatomic molecules
[AD-A278836] p 4323 N94-35793

QUANTUM STATISTICS
Exact multiplicities in the three-anion spectrum
[DE94-616768] p 4325 N94-36075

QUANTUM THEORY
This non-axiomatizable quantum theory. From Hilbert's sixth problem to the recent viewpoint of Gell-mann and Hartle
[PB94-167715] p 4342 N94-35761
The 2+1-dimensional integrable generalization of the Sine-Gordon equation
[DE94-611074] p 4315 N94-36100
Quantum groups, non-commutative differential geometry and applications
[DE94-011358] p 4315 N94-36270
N = 4 supersymmetry from the quantum affine algebra U(sub q)(A-circumflex(sup 1)(sub 3))
[DE94-611145] p 4317 N94-36307
On quantization of time-dependent systems with constraints
[DE94-611114] p 4343 N94-36351

QUANTUM WELL LASERS
High power diode laser Master Oscillator-Power Amplifier (MOPA)
[NASA-CR-196095] p 4271 N94-35488

QUANTUM WELLS
Activities of the optoelectronics laboratory
[PB94-171196] p 4334 N94-36190
Development of ultra-low noise, high performance 3 to 5 Quantum Well Infrared Photodetectors (QWIPs) for focal plane array staring image sensor systems
[AD-A278861] p 4342 N94-36385

QUARK MODELS
Baryonic currents and their correlators in the heavy quark effective theory
[DE94-612496] p 4320 N94-35567
The silent phase transition in mesonic bags and lattice theory
[DE94-616852] p 4321 N94-35583
A quark model of bar Lambda production in bar Rho interactions
[DE94-008071] p 4324 N94-35824
Collapse of flux tubes
[DE94-004645] p 4328 N94-36304

QUARK PARTON MODEL
QCD parametrizations of the parton distribution of deep inelastic scattering
[DE94-616660] p 4325 N94-36074

QUARKS
Goldstone pion and other mesons using a scalar confining interaction
[DE94-010016] p 4321 N94-35649
Leptonic decay constants of heavy quarkonia in effective QCD sum rules
[DE94-611160] p 4322 N94-35784
Calculations on some properties of the pion in the framework of Schwinger-Dyson and Bethe-Salpeter equations
[DE94-611232] p 4322 N94-35786
A quark model of bar Lambda production in bar Rho interactions
[DE94-008071] p 4324 N94-35824
Spin effects in high energy quark-quark scattering
[DE94-616800] p 4330 N94-36080
CDF electroweak studies and the search for the top quark
[DE94-010333] p 4326 N94-36107
Top dilepton search at CDF
[DE94-002302] p 4327 N94-36266
Collapse of flux tubes
[DE94-004645] p 4328 N94-36304

QUARTZ
Calorimetric thermobarometry of experimentally shocked quartz p 4240 N94-36174

QUARTZITE
Mercury: Mid-infrared (7.3 - 13.5 microns) spectroscopic observations showing features characteristic of plagioclase p 4370 N94-36150

QUATERNIONS
Modelling and control of a rotor supported by magnetic bearings p 4216 N94-35858

R

RADAR ASTRONOMY
The Telecommunications and Data Acquisition Report
[NASA-CR-196117] p 4252 N94-35542
The real-time display of interferometry data for Goldstone radar astronomy data acquisition
p 4255 N94-35560
A new presentation of complex voltage data for Goldstone radar astronomy p 4255 N94-35561

RADAR DATA
NAVSPACECOM space surveillance sensor system digital signal processing receiver. Volume 3: Operating system functions
[AD-A278839] p 4212 N94-35799
NAVSPACECOM space surveillance sensor system digital signal processing receiver. Volume 4: Hardware interfaces
[AD-A278845] p 4212 N94-35801

RADAR DETECTION
Terminal Doppler Weather Radar (TDWR) Low Level Wind Shear Alert System 3 (LLWAS 3) integration studies at Orlando International Airport
[AD-A278957] p 4294 N94-35807

RADAR IMAGERY
Quantifying shapes of volcanoes on Venus
p 4361 N94-35429
Magellan collection of radar calibration results
[NASA-CR-194753] p 4367 N94-35509
The polygon-ellipse method of data compression of weather maps
[AD-A278958] p 4293 N94-35719

RADAR MAPS

The polygon-ellipse method of data compression of weather maps
[AD-A278958] p 4293 N94-35719

RADAR MEASUREMENT

Use of wind profiler data in short-range forcasting
[AD-A279482] p 4295 N94-36228

Groundwater penetrating radar and high resolution seismic for locating shallow faults in unconsolidated sediments
[DE94-007284] p 4257 N94-36366

RADAR RANGE

The real-time display of interferometry data for Goldstone radar astronomy data acquisition
p 4255 N94-35560

RADAR RECEIVERS

NAVSPACECOM space surveillance sensor system digital signal processing receiver. Volume 3: Operating system functions
[AD-A278839] p 4212 N94-35799

NAVSPACECOM space surveillance sensor system digital signal processing receiver. Volume 4: Hardware interfaces
[AD-A278845] p 4212 N94-35801

An analysis of operational suitability for test and evaluation of highly reliable systems
[AD-A278573] p 4192 N94-36184

RADAR TARGETS

The real-time display of interferometry data for Goldstone radar astronomy data acquisition
p 4255 N94-35560

Estimation with multisensor/multiscan detection fusion
[AD-A278753] p 4256 N94-36092

Color-coded radar plan position indicator
[AD-D016200] p 4257 N94-36364

RADARSCOPES

Final-Approach Spacing Aids (FASA) evaluation for terminal-area, time-based air traffic control
[NASA-TP-3399] p 4192 N94-36048

RADIAL DISTRIBUTION

Improved models of beta-limit, anomalous transport and radial electric field with loss cone loss in heliotron/torsatron
[DE94-718976] p 4324 N94-35984

RADIATION BELTS

Global changes of radiation situation at heights less than 1000 km
[DE94-610504] p 4290 N94-35780

RADIATION COUNTERS

Beam tests of a prototype level-1 calorimeter trigger for LHC experiments
[PB94-170495] p 4269 N94-35599

Determination of the Fermi level position for neutron irradiated high resistivity silicon detectors and materials using the Transient Charge Technique (TChT)
[DE94-009107] p 4260 N94-36221

RADIATION DETECTORS

Multiwavelength pyrometer for gray and non-gray surfaces in the presence of interfering radiation
[NASA-CASE-LEW-15250-1] p 4269 N94-35383

RADIATION EFFECTS

Measuring track densities in lunar grains using image analysis p 4357 N94-35409

Improved performance of degraded solar arrays at non-zero sun incidence angles
[AD-A278905] p 4282 N94-35804

Irradiation-related amorphization and crystallization: In situ transmission electron microscope studies
[DE94-009823] p 4241 N94-36222

Enhanced charge trapping in bipolar spacer oxides during low-dose-rate irradiation
[DE94-007863] p 4260 N94-36268

On the effects of transforming the vibrational spectra of molecular systems under microwave radiation
[DE94-617057] p 4329 N94-36310

Hardness variability in commercial and hardened technologies
[DE94-007270] p 4261 N94-36362

Estimating low-dose rate irradiation response of MOSFETs
[DE94-007292] p 4342 N94-36367

Bounding the total-dose response of modern bipolar transistors
[DE94-007742] p 4261 N94-36371

A critical examination of charge funneling and its impact on single-event upset in Si devices
[DE94-007868] p 4261 N94-36373

RADIATION HARDENING

Rapid and accurate timing simulation of radiation-hardened digital microelectronics using VHDL
[AD-A278644] p 4261 N94-36361

Hardness variability in commercial and hardened technologies
[DE94-007270] p 4261 N94-36362

A critical examination of charge funneling and its impact on single-event upset in Si devices
[DE94-007868] p 4261 N94-36373

RADIATION MEASUREMENT

The Atmospheric Radiation Measurement Program and interfaces with external data sources
[DE94-003699] p 4286 N94-36024

RADIATION PRESSURE

The Earth Satellite Program (ESP), version 2.0
[AD-A278860] p 4201 N94-35827

RADIATION PYROMETERS

Multiwavelength pyrometer for gray and non-gray surfaces in the presence of interfering radiation
[NASA-CASE-LEW-15250-1] p 4269 N94-35383

RADIATION TRANSPORT

Recursive recovery of Markov transition probabilities from boundary value data
[DE94-011914] p 4317 N94-36235

RADIATIVE HEAT TRANSFER

JPRS report: Science and technology. Central Eurasia
[JPRS-UST-94-008] p 4249 N94-35228

Selected translated abstracts of Russian-language climate-change publications. 2: Clouds
[DE94-011465] p 4295 N94-36244

RADIATIVE TRANSFER

Venus climate stability and volcanic resurfacing rates
p 4358 N94-35413

First measurement of helium on Mars: Implications for the problem of radiogenic gases on the terrestrial planets p 4370 N94-36153

RADICALS

The reaction of hydroperoxy-propyl radicals with molecular oxygen
[DE94-006392] p 4239 N94-36319

RADIO ALTIMETERS

Minimum performance standards: Airborne low-range radar altimeters
[RTCA-DO-155] p 4198 N94-35344

Mesoscale roughness of Venus p 4361 N94-35430

RADIO ANTENNAS

Switched-beam radiometer front-end network analysis
[NASA-CR-194922] p 4252 N94-35247

RADIO ASTRONOMY

The Telecommunications and Data Acquisition Report
[NASA-CR-196117] p 4252 N94-35542

RADIO COMMUNICATION

The Mars Observer Ka-band link experiment
p 4255 N94-35563

RADIO EQUIPMENT

Minimum performance standards: Airborne low-range radar altimeters
[RTCA-DO-155] p 4198 N94-35344

RADIO FREQUENCIES

Applications of non-resonant RF forces for improvement of tokamak reactor performances. Part 1: Application of ponderomotive force
[DE94-718994] p 4336 N94-35813

RADIO NAVIGATION

The Telecommunications and Data Acquisition Report
[NASA-CR-196117] p 4252 N94-35542

RADIO RECEIVERS

Spacecraft-spacecraft radio-metric tracking: Signal acquisition requirements and application to Mars approach navigation p 4254 N94-35557

RADIO TELEMETRY

The Mars Observer Ka-band link experiment
p 4255 N94-35563

RADIOACTIVE DECAY

Measurement of the decay rate of the SiH feature as a function of temperature p 4318 N94-36171

RADIOACTIVE ISOTOPES

Solar proton produced neon in shergottite meteorites
p 4351 N94-35428

Isotopic and geochemical precursors of earthquakes and volcanic eruptions
[DE94-615824] p 4289 N94-35568

RADIOACTIVE WASTES

Decision and systems analysis for underground storage tank waste retrieval systems and tank waste remediation system
[SAND94-0065] p 4286 N94-35957

RADIOGENIC MATERIALS

First measurement of helium on Mars: Implications for the problem of radiogenic gases on the terrestrial planets p 4370 N94-36153

RADIOGRAPHY

X ray radiographic imaging of hydrodynamic phenomena in radiation driven materials: Shock propagation and shear flow
[DE94-010891] p 4318 N94-36201

RADIOISOTOPE BATTERIES

GPHS-RTGs in support of the Cassini mission
[DE94-009994] p 4212 N94-35648

RADIOLOGY

Activities of National Institute of Radiological Sciences
[DE94-727636] p 4296 N94-36101

RADIOMETERS

Switched-beam radiometer front-end network analysis
[NASA-CR-194922] p 4252 N94-35247

Controller for the Electronically Scanned Thinned Array Radiometer (ESTAR) instrument
[NASA-TM-104608] p 4259 N94-36049

Absolute, Extreme Ultraviolet Solar Spectral Irradiance Monitor (AESSIM)
[AD-A278709] p 4227 N94-36189

Astronomy in the region between 1 mm and 0.1 mm wavelength
[NASA-CR-196020] p 4349 N94-36419

RADIOMETRIC CORRECTION

Reduction procedures for accurate analysis of MSX surveillance experiment data p 4203 N94-35611

RADIOSONDES

Production of long-term global water vapor and liquid water data set using ultra-fast methods to assimilate multi-satellite and radiosonde observations
[NASA-CR-196044] p 4292 N94-35355

Production of long-term global water vapor and liquid water data set using ultra-fast methods to assimilate multi-satellite and radiosonde observations
[NASA-CR-195981] p 4293 N94-35499

RADON ISOTOPES

Isotopic and geochemical precursors of earthquakes and volcanic eruptions
[DE94-615824] p 4289 N94-35568

RAIL TRANSPORTATION

System concept definition of the Grumman superconducting Electromagnetic Suspension (EMS) Maglev design p 4213 N94-35840

Transrapid (the first high-speed Maglev train system certified ready for application): Development status and prospects for deployment p 4213 N94-35841

Control of maglev vehicles with aerodynamic and guideway disturbances p 4213 N94-35842

Fault tolerant computer control for a Maglev transportation system p 4215 N94-35848

Superconducting Electromagnetic Suspension (EMS) system for Grumman Maglev concept
p 4215 N94-35849

National Maglev initiative: California line electric utility power system requirements p 4215 N94-35850

RAILS

Testing of the fracture resistance of rails
p 4279 N94-35353

RAMAN LASERS

Specification for the TITANIA krF laser system
[PB94-167103] p 4272 N94-36062

RAMAN SPECTRA

Implementation of Raman lidar for profiling of atmospheric water vapor and aerosols at the SGP CART site
[DE94-011754] p 4295 N94-36285

RANDOM LOADS

Frequency domain analysis of the random loading of cracked panels
[NASA-CR-196021] p 4279 N94-35974

RANDOM NOISE

Effects of noise variance model on optimal feedback design and actuator placement p 4220 N94-35883

RANDOM WALK

Recursive recovery of Markov transition probabilities from boundary value data
[DE94-011914] p 4317 N94-36235

RANGEFINDING

The Mars Observer differential one-way range demonstration p 4210 N94-35543

Spacecraft-spacecraft radio-metric tracking: Signal acquisition requirements and application to Mars approach navigation p 4254 N94-35557

The real-time display of interferometry data for Goldstone radar astronomy data acquisition
p 4255 N94-35560

The Mars Observer Ka-band link experiment
p 4255 N94-35563

Application of a Monte Carlo accuracy assessment tool to TDRS and GPS p 4207 N94-35635

Nondestructive Inspection (NDI) of reduced strength bonds
[AD-A278745] p 4278 N94-36090

RARE GASES

Anatomy of a cluster IDP. Part 2: Noble gas abundances, trace element geochemistry, isotopic abundances, and trace organic chemistry of several fragments from L2008#5 p 4352 N94-35465

RATS

Stress and brain protein synthesis
[PB94-170750] p 4296 N94-35601

RAYLEIGH NUMBER

Linear and nonlinear pattern selection in Rayleigh-Benard stability problems
[NASA-TM-104007] p 4263 N94-35371

RAYLEIGH WAVES
Acoustical-optical fracture analysis
[PB94-170602] p 4279 N94-36216
RAYLEIGH-BENARD CONVECTION
Linear and nonlinear pattern selection in Rayleigh-Benard stability problems
[NASA-TM-104007] p 4263 N94-35371
Spatio-temporal properties of centrifugal instabilities: Abstracts of 8th Couette-Taylor Meeting
[PB94-150240] p 4266 N94-35981
REACTING FLOW
Comparison of PDF and moment closure methods in the modeling of turbulent reacting flows
[NASA-TM-106614] p 4265 N94-35948
REACTION BONDING
Chemical reactions of chlorine on a vicinal Si(100) surface studied by ESDIAD
[AD-A279059] p 4236 N94-35731
REACTION KINETICS
A two-dimensional model for collisional energy transfer in bimolecular ion-molecule dynamics
[AD-A278913] p 4321 N94-35589
Ultrafast chemical dynamics of reactions in beams
[AD-A278939] p 4323 N94-35805
Comparison of PDF and moment closure methods in the modeling of turbulent reacting flows
[NASA-TM-106614] p 4265 N94-35948
NEQPAK, the AEDC thermochemical nonequilibrium package: Theory and use
[AD-A279005] p 4266 N94-35951
CSTL technical activities, 1991
[PB94-160769] p 4318 N94-36003
Heterogeneous reaction mechanisms and kinetics relevant to the CVD of semiconductor materials
[DE94-011001] p 4340 N94-36032
Tritiated ammonia formation
[DE94-011170] p 4237 N94-36056
Kinetics studies following state-selective laser excitation
[DE94-010305] p 4330 N94-36105
Neutron detectors for fusion reaction-rate measurements
[DE94-010407] p 4330 N94-36114
A new comprehensive reaction mechanism for combustion of hydrocarbon fuels
[DE94-008288] p 4238 N94-36205
The thermochemistry and reaction mechanisms in the decomposition of energetic materials
[DE94-011420] p 4248 N94-36376
Effects of natural gas composition on ignition delay under diesel conditions
[DE94-006405] p 4276 N94-36378
REACTION PRODUCTS
Stellar alchemy: The origin of the chemical elements
[DE94-011903] p 4350 N94-36229
REACTION WHEELS
Overview of the Miniature Sensor Technology Integration (MSTI) spacecraft attitude control system
p 4206 N94-35627
The control of satellites with microgravity constraints: The COMET Control System p 4207 N94-35632
REACTIVITY
Evaluation of Oxygen Interactions with Materials 3: Mission and induced environments
[NASA-TM-109349] p 4236 N94-35680
Chemical reactions of chlorine on a vicinal Si(100) surface studied by ESDIAD
[AD-A279059] p 4236 N94-35731
Metal cluster alloys and oxides: Elucidating structural and electronic effects in governing the reactivity and catalytic role of matter in finite dimensions
[DE94-010224] p 4328 N94-36298
REACTOR CORES
Consolidation of zircaloy-4 end crops by induction melting
[DE94-010031] p 4240 N94-35650
REAL TIME OPERATION
Adjustable control station with movable monitors and cameras for viewing systems in robotics and teleoperations
[NASA-CASE-NPO-17837-1-CU] p 4332 N94-35384
Software architecture standard for simulation virtual machine, version 2.0
[NASA-CR-188291] p 4301 N94-35443
The rel/REL: A family of reliable multicast protocols for distributed real-time systems
[PB94-167830] p 4310 N94-35535
Correlator data analysis for the array feed compensation system p 4253 N94-35553
The real-time display of interferometry data for Goldstone radar astronomy data acquisition
p 4255 N94-35560
A new presentation of complex voltage data for Goldstone radar astronomy p 4255 N94-35561
Operational support for Upper Atmosphere Research Satellite (UARS) attitude sensors p 4204 N94-35617
TDRSS Onboard Navigation System (TONS) flight qualification experiment p 4206 N94-35625
Advantages of estimating rate corrections during dynamic propagation of spacecraft rates: Applications to real-time attitude determination of SAMPEX
p 4209 N94-35642
Task allocation for parallel real-time execution
[AD-A278789] p 4310 N94-35653
A determinizable class of timed automata
[AD-A278858] p 4317 N94-35743
A taxonomy of coordination mechanisms used in real-time software based on domain analysis
[AD-A279014] p 4304 N94-35794
NAVSPACECOM space surveillance sensor system digital signal processing receiver. Volume 3: Operating system functions
[AD-A278839] p 4212 N94-35799
NAVSPACECOM space surveillance sensor system digital signal processing receiver. Volume 4: Hardware interfaces
[AD-A278845] p 4212 N94-35801
Task and environment-sensitive tracking
[AD-A278846] p 4312 N94-35802
Doppler weather radar studies of precipitation systems
[AD-A279417] p 4295 N94-36262
Interfacing the RAP system to real-time control, version 1
[AD-A278725] p 4312 N94-36295
RECEIVERS
A quality control package for the Digisonde Drift Analysis (DDA)
[AD-A278663] p 4289 N94-35578
High-sensitivity receiver for increasing multiplicity of measurement axes of Zygo's Heterodyne interferometer
[DE94-009916] p 4333 N94-35818
RECIPROCATION
Performance analysis of reciprocating regenerative magnetic heat pumping
[DE94-009488] p 4264 N94-35683
RECOGNITION
High-resolution subsurface imaging and neural network recognition
[DE94-009546] p 4290 N94-35666
RECOMMENDATIONS
Partners in space. International cooperation in space: Strategies for the new century
[ISBN-0-9629930-2-6] p 4348 N94-35901
RECYCLING
Laminated thermoplastic composite material from recycled high density polyethylene p 4230 N94-36403
Microscale synthesis and characterization of polystyrene: NSF-POLYED scholars project
p 4231 N94-36408
RED SHIFT
GRO: Studies of high energy pulsars with EGRET
[NASA-CR-196003] p 4349 N94-35516
REDUCTION (CHEMISTRY)
Reduction of lunar mare soil and pyroclastic glass
p 4355 N94-35398
REED-SOLOMON CODES
Trace-shortened Reed-Solomon codes
p 4254 N94-35554
REFLECTANCE
Multiwavelength pyrometer for gray and non-gray surfaces in the presence of interfering radiation
[NASA-CASE-LEW-15250-1] p 4269 N94-35383
New prospects for analyzing lunar pyroclastic glass
p 4355 N94-35397
High Resolution Transmission Electron Microscopy (HRTEM) of nanophase ferric oxides
p 4239 N94-35433
The nature of agglutinitic glass in the fine-size fraction of lunar soil 10084 p 4369 N94-36148
Mercury: Mid-infrared (7.3 - 13.5 microns) spectroscopic observations showing features characteristic of plagioclase p 4370 N94-36150
REFLECTING TELESCOPES
Issues in the design and optimization of adaptive optics and laser guide stars for the Keck Telescopes
[DE94-009384] p 4349 N94-35565
REFRACTIVITY
Method and apparatus for removing unwanted reflections from an interferometer
[NASA-CASE-NPO-18478-1-CU] p 4333 N94-35749
REFRACTORY MATERIALS
Tough, processable semi-interpenetrating polymer networks from monomer reactants
[NASA-CASE-LAR-14838-1] p 4242 N94-35233
Tough high performance composite matrix
[NASA-CASE-LAR-14239-2] p 4232 N94-35372
Carbon-carbon piston development
[NASA-CR-4595] p 4233 N94-35947
Advanced composites in Japan p 4234 N94-36045
REFRIGERANTS
Measurement of viscosity, density, and gas solubility of refrigerant blends in selected synthetic lubricants
[DE94-010426] p 4244 N94-35687
Solubility, viscosity and density of refrigerant/lubricant mixtures
[DE94-009996] p 4245 N94-35771
Thermophysical properties of HFC-143a and HFC-152a
[DE94-009995] p 4251 N94-36008
Research update: Materials Compatibility and Lubricant Research (MCLR) program
[DE94-010001] p 4247 N94-36387
Sealed tube comparisons of the compatibility of desiccants with refrigerants and lubricants
[DE94-010002] p 4251 N94-36388
REFRIGERATING
Research update: Materials Compatibility and Lubricant Research (MCLR) program
[DE94-010001] p 4247 N94-36387
Sealed tube comparisons of the compatibility of desiccants with refrigerants and lubricants
[DE94-010002] p 4251 N94-36388
REFRIGERATORS
Properties and applications of powder-filled evacuated-panel superinsulations
[DE94-009169] p 4233 N94-35932
REFUELING
Final regulatory impact analysis: Refueling emission regulations for light duty vehicles and trucks and heavy duty vehicles
[PB94-164027] p 4285 N94-35754
REGGE POLES
Alternating series fit to the total cross sections
[DE94-616888] p 4326 N94-36132
High energy asymptotics of perturbative multi-color QCD
[DE94-001350] p 4327 N94-36238
REGIONAL PLANNING
National Maglev initiative: California line electric utility power system requirements p 4215 N94-35850
REGOLITH
Mars aqueous chemistry experiment
[NASA-CR-196024] p 4354 N94-35263
Grain rims on ilmenite in the lunar regolith: Comparison to vapor deposits on regolith silicates
p 4359 N94-35418
Luna 24 regolith breccias: A possible source of the fine size material of the Luna 24 regolith
p 4362 N94-35450
REGRESSION ANALYSIS
A comparison of variable selection criteria for multiple linear regression: A THIRD simulation study
[AD-A278678] p 4316 N94-35691
Scaling laws for TEXT plasma profiles
[DE94-010832] p 4338 N94-36200
Graphing techniques for materials laboratory using Excel p 4232 N94-36414
RELATIVISTIC EFFECTS
Variational method in relativistic two-body problem
[DE94-612462] p 4315 N94-36416
RELATIVISTIC ELECTRON BEAMS
State of the art in high-power microwaves: An overview
[DE94-007075] p 4272 N94-35978
RELATIVISTIC THEORY
The relativistic invariant and the Galilean mass of bodies
[DE94-616615] p 4318 N94-35956
First, second and fourth sound in relativistic superfluidity theory with account for dissipative effects
[DE94-617393] p 4267 N94-36314
RELATIVITY
Classical time machine
[DE94-616616] p 4342 N94-36070
RELAXATION (MECHANICS)
The study of the local magnetic field in the oxide alpha-Bi2O3 by the mu SR-technique
[DE94-612636] p 4322 N94-35751
RELIABILITY
Point and interval estimation of series system reliability using small data sets
[AD-A278647] p 4316 N94-35575
RELIABILITY ANALYSIS
Developing interpretable models with optimized set reduction for identifying high risk software components
p 4301 N94-35435
Robust requirements specifications for safety-critical systems
[PB94-167806] p 4250 N94-35532
RELIABILITY ENGINEERING
Robust requirements specifications for safety-critical systems
[PB94-167806] p 4250 N94-35532

REMANENCE
Shape, size, and distribution of magnetic particles in Bjurbole chondrules p 4353 N94-36167
REMOTE CONTROL
An electronic interface for a fiber optic tethered unmanned underwater vehicle [AD-A279046] p 4333 N94-35747
REMOTE MANIPULATOR SYSTEM
International Space Station alpha remote manipulator system workstation controls test report [NASA-TM-104796] p 4274 N94-35481
Dynamic analysis of Space Shuttle/RMS configuration using continuum approach p 4221 N94-35887
REMOTE SENSING
Remote geochemical experiment package for Discovery class missions p 4350 N94-35420
Insight to global change: EOS/SAR mission [NASA-CR-196133] p 4284 N94-35503
Obtaining coincident image observations for Mission to Planet Earth science data return p 4202 N94-35609
A precise passive narrow-beam filter infrared radiometer and its use with LIDAR in the ARM program [DE94-004167] p 4269 N94-36085
Selected translated abstracts of Russian-language climate-change publications. 2: Clouds [DE94-011465] p 4295 N94-36244
Molecular nitrogen fluorescence lidar for remote sensing of the auroral ionosphere [AD-A280716] p 4291 N94-36263
REMOTE SENSORS
X-ray remote sensing and in-situ spectroscopy for planetary exploration missions and gamma-ray remote sensing and in-situ spectroscopy for planetary exploration missions [NASA-CR-189352] p 4375 N94-35381
REPLACING
Sealed tube comparisons of the compatibility of desiccants with refrigerants and lubricants [DE94-010002] p 4251 N94-36388
REQUIREMENTS
Robust requirements specifications for safety-critical systems [PB94-167806] p 4250 N94-35532
RESCUE OPERATIONS
Self-rescue strategies for EVA crewmembers equipped with the SAFER backpack p 4207 N94-35633
EH101: A new helicopter capable of long range missions p 4194 N94-36330
RESEARCH
Introduction to USRA [NASA-CR-195980] p 4376 N94-35590
Activities of the optoelectronics laboratory [PB94-171196] p 4334 N94-36190
RESEARCH AIRCRAFT
Ground vibration test of the XV-15 Tiltrotor Research Aircraft and pretest predictions p 4200 N94-35972
The reduction of takeoff ground roll by the application of a nose gear jump strut [NASA-TM-108822] p 4198 N94-36380
RESEARCH AND DEVELOPMENT
The Federal Aviation Administration plan for research, engineering and development p 4376 N94-35262
JPRS report: Science and technology. Central Eurasia [JPRS-UST-94-001] p 4229 N94-35340
JPRS report: Science and technology. Central Eurasia [JPRS-UST-94-004] p 4249 N94-35341
JPRS report: Science and technology. Central Eurasia [JPRS-UST-94-005] p 4249 N94-35342
Director's discretionary fund [NASA-TM-103997] p 4376 N94-35370
JPRS report: Science and technology. Central Eurasia [JPRS-UST-94-010] p 4250 N94-35385
JPRS report: Science and technology. Central Eurasia [JPRS-UST-94-011] p 4250 N94-35386
JPRS report: Science and technology. Central Eurasia [JPRS-UST-94-012] p 4250 N94-35387
AGARD highlights 93/2 [AGARD-HIGHLIGHTS-93/2] p 4376 N94-35444
JPRS report: Science and technology. Central Eurasia: Space [JPRS-USP-94-003] p 4201 N94-35520
Challenging the Future - Journey to Excellence. Aeropropulsion strategic plan for the 1990's [NASA-TM-109250] p 4228 N94-35591
Budget estimates, fiscal year 1995. Volume 1: Agency summary, human space flight, and science, aeronautics and technology [NASA-TM-109791] p 4347 N94-35899
CSTL technical activities, 1991 [PB94-160769] p 4318 N94-36003
JPRS report: Science and technology. Central Eurasia: Space [JPRS-USP-93-005] p 4201 N94-36011
Earthquake Engineering Research Center: 25th anniversry edition [PB94-160645] p 4291 N94-36019
JTEC/WTEC report and program summary p 4379 N94-36042
Research and technology, 1993 [NASA-TM-108816] p 4380 N94-36117
Research and development of Proton-Exchange Membrane (PEM) fuel cell system for transportation applications: Initial conceptual design report [DE94-010576] p 4283 N94-36243
Activities of the Laser and Plasma Technology Division [DE94-617113] p 4273 N94-36393
National Educators' Workshop: Update 1993. Standard Experiments in Engineering Materials Science and Technology [NASA-CP-3259] p 4229 N94-36398
RESEARCH FACILITIES
Data acquisition systems [DE94-009848] p 4345 N94-35817
A guide to research facilities at the National Renewable Energy Laboratory [DE94-006857] p 4283 N94-36052
Environmental resource document for the Idaho National Engineering Laboratory, volume 1 [DE94-008522] p 4287 N94-36207
Environmental resource document for the Idaho National Engineering Laboratory, volume 2 [DE94-008523] p 4287 N94-36208
RESEARCH MANAGEMENT
The Federal Aviation Administration plan for research, engineering and development p 4376 N94-35262
RESEARCH PROJECTS
Director's discretionary fund [NASA-TM-103997] p 4376 N94-35370
RESEARCH VEHICLES
An automatic planetary vehicle for exploring Mars p 4354 N94-35336
The reduction of takeoff ground roll by the application of a nose gear jump strut [NASA-TM-108822] p 4198 N94-36380
RESIDUAL GAS
Residual Gas Analysis (RGA) and shear strength characteristics of a silver-filled epoxy and polyimide under long-term, high-temperature storage conditions [DE94-010106] p 4244 N94-35705
RESIDUAL STRENGTH
Fatigue and residual strength behaviour of ARALL3 panels with bonded-on doublers [AD-B181062] p 4279 N94-36226
RESIDUAL STRESS
Optimization of residual stresses in MMC's using compensating/compliant interfacial layers. Part 2: OPTCOMP user's guide [NASA-CR-195337] p 4278 N94-35239
Testing of the fracture resistance of rails p 4279 N94-35353
RESIN MATRIX COMPOSITES
Processing and properties of high temperature metal/fiber-reinforced-thermoplastic laminates [AD-A278791] p 4232 N94-35654
RESINS
Third European Technical Symposium on Polyimides and High Performance Polymers: STEPI 3 [PB94-148491] p 4246 N94-36177
RESISTANCE HEATING
Scaling laws for TEXT plasma profiles [DE94-010832] p 4338 N94-36200
RESISTORS
Models for interpreting interstrand resistance measurements in Rutherford cables [DE94-010844] p 4259 N94-36194
RESONANCE
On the effects of transforming the vibrational spectra of molecular systems under microwave radiation [DE94-617057] p 4329 N94-36310
Notes on possible S-wave resonances in relativistic two-particle systems [DE94-616889] p 4329 N94-36392
RESONANT FREQUENCIES
Applying transfer matrix method to the estimation of the modal characteristics of the NASA Mini-Mass Truss p 4218 N94-35870
Rotor dynamic behaviour of a high-speed oil-free motor compressor with a rigid coupling supported on four radial magnetic bearings p 4224 N94-35911
RETRACTABLE EQUIPMENT
Attitude stability of a spinning spacecraft during appendage deployment/retraction p 4208 N94-35639
REUSE
Case based reasoning in engineering design [AD-A278943] p 4305 N94-36006
REYNOLDS NUMBER
Experimental studies of very-high Mach number hydrodynamics [AD-A278761] p 4263 N94-35492
Numerical investigation of multi-element airfoils [NASA-CR-194592] p 4191 N94-36394
RHEOLOGY
Rheology, tectonics, and the structure of the Venus lithosphere p 4367 N94-35479
Patterns of brittle deformation under extension on Venus p 4373 N94-36168
RHEOMETERS
Determination of extensional viscosity from capillary rheometer entrance pressure drop measurements using a numerical simulation of contraction flow [PB94-171154] p 4263 N94-35603
RHODAMINE
Fluorescence detection of single molecules using pulsed near-field optical excitation and time correlated photon counting [DE94-007553] p 4320 N94-35376
RIBONUCLEIC ACIDS
A low temperature scanning force microscope for biological samples [DE94-011357] p 4297 N94-36269
RIDING QUALITY
Control of maglev vehicles with aerodynamic and guideway disturbances p 4213 N94-35842
Fault tolerant computer control for a Maglev transportation system p 4215 N94-35848
RIEMANN MANIFOLD
Moduli space of monopoles and some invariants of 3-manifolds [PB94-167756] p 4314 N94-35764
Some theorems on a class of harmonic manifolds [DE94-611102] p 4315 N94-35934
Zero modes of the two-dimensional Dirac operator on a noncompact Riemann surface in an external magnetic field [DE94-616618] p 4343 N94-36071
RIGID STRUCTURES
Applying transfer matrix method to the estimation of the modal characteristics of the NASA Mini-Mass Truss p 4218 N94-35870
Robust tracking control of a magnetically suspended rigid body p 4225 N94-35913
RIMS
Alteration and formation of rims on the CM parent body p 4357 N94-35411
RISK
Modeling and managing risk early in software development p 4301 N94-35436
CAirTOX: A compartment model for assessing the fate of and human exposure to toxic-chemical emissions to air [DE94-010084] p 4284 N94-35700
Residual Gas Analysis (RGA) and shear strength characteristics of a silver-filled epoxy and polyimide under long-term, high-temperature storage conditions [DE94-010106] p 4244 N94-35705
ROBOT CONTROL
Adjustable control station with movable monitors and cameras for viewing systems in robotics and teleoperations [NASA-CASE-NPO-17837-1-CU] p 4332 N94-35384
Interfacing the RAP system to real-time control, version 1 [AD-A278725] p 4312 N94-36295
ROBOT DYNAMICS
Task and environment-sensitive tracking [AD-A278846] p 4312 N94-35802
ROBOTICS
Robot friendly probe and socket assembly [NASA-CASE-MSC-22028-1] p 4274 N94-35374
Adjustable control station with movable monitors and cameras for viewing systems in robotics and teleoperations [NASA-CASE-NPO-17837-1-CU] p 4332 N94-35384
Space robotics in Japan p 4278 N94-36046
ROBOTS
Robot friendly probe and socket assembly [NASA-CASE-MSC-22028-1] p 4274 N94-35374
Genetic algorithms [PB94-171048] p 4303 N94-35602
Task and environment-sensitive tracking [AD-A278846] p 4312 N94-35802
Maneuvering and control of flexible space robots p 4218 N94-35867
Space robotics in Japan p 4278 N94-36046
ROBUSTNESS (MATHEMATICS)
Robust requirements specifications for safety-critical systems [PB94-167806] p 4250 N94-35532
Aspects of robust computational modeling for plain and reinforced concrete [PB94-169240] p 4251 N94-35820
Robustness properties of LQG optimized compensators for collocated rate sensors p 4221 N94-35890
Semigroup approximation and robust stabilization of distributed parameter systems p 4222 N94-35894
Robust tracking control of a magnetically suspended rigid body p 4225 N94-35913

ROCKET ENGINE CASES
Study on contaminants on flight and other critical surfaces
[NASA-CR-193975] p 4235 N94-35447

ROCKET LAUNCHERS
Feasibility study of superconducting LSM rocket launcher system p 4225 N94-35914

ROCKS
Distribution of siderophile and other trace elements in melt rock at the Chicxulub impact structure
p 4352 N94-35456

RODS
Chirped-pulse amplification with flashlamp-pumped Ti:Sapphire amplifiers
[DE94-010055] p 4272 N94-35695

ROLL
Data reduction, analysis and results of LACV-30-07 air cushion vehicle tests, Fort Story, VA, August - September 1993
[AD-A278859] p 4190 N94-35826
The reduction of takeoff ground roll by the application of a nose gear jump strut
[NASA-TM-108822] p 4198 N94-36380

ROSAT MISSION
ROSAT/XRT-PSPC observations and the ionizing continuum of Seyfert 1 galaxy Mkn 478
[PB94-167053] p 4350 N94-35530

ROTARY WINGS
Selected topics on the active control of helicopter aeromechanical and vibration problems
p 4200 N94-35874
Computation of helicopter rotor acoustics in forward flight
[NASA-CR-196132] p 4319 N94-36031

ROTATING PLASMAS
Thickness of the layer of strong radial electric field in JFT-2M H-mode plasmas
[DE94-718993] p 4336 N94-35812

ROTATING SHAFTS
Planar rotational magnetic micromotors with integrated shaft encoder and magnetic rotor levitation
p 4224 N94-35907

ROTATION
Modelling and control of a rotor supported by magnetic bearings p 4216 N94-35858

ROTOR AERODYNAMICS
Ground vibration test of the XV-15 Tiltrotor Research Aircraft and pretest predictions p 4200 N94-35972
Computation of helicopter rotor acoustics in forward flight
[NASA-CR-196132] p 4319 N94-36031

ROTOR DYNAMICS
Active magnetic bearing control loop modeling for a finite element rotordynamics code p 4216 N94-35857
Rotor dynamic behaviour of a high-speed oil-free motor compressor with a rigid coupling supported on four radial magnetic bearings p 4224 N94-35911

ROTORS
Influence of backup bearings and support structure dynamics on the behavior of rotors with active supports
[NASA-CR-196119] p 4274 N94-35500
Design, construction, and testing of a five active axes magnetic bearing system p 4214 N94-35846
Third order LPF type compensator for flexible rotor suspension p 4217 N94-35863
Electromechanical simulation and test of rotating systems with magnetic bearing or piezoelectric actuator active vibration control p 4223 N94-35905
Planar rotational magnetic micromotors with integrated shaft encoder and magnetic rotor levitation
p 4224 N94-35907
Rotor dynamic behaviour of a high-speed oil-free motor compressor with a rigid coupling supported on four radial magnetic bearings p 4224 N94-35911
Magnetically suspended stepping motors for clean room and vacuum environments p 4225 N94-35915
Tipjet 80-inch model rotor hover test: Test no. 1198
[AD-A279680] p 4191 N94-36261

ROVING VEHICLES
An automatic planetary vehicle for exploring Mars
p 4354 N94-35336
Planetary Rover Program
[NASA-CR-196108] p 4201 N94-35511

RUBIDIUM
X ray and gamma ray spectroscopy of solids under pressure
[DE94-011207] p 4238 N94-36203

RUN TIME (COMPUTERS)
Runtime support for data parallel tasks
[NASA-CR-194904] p 4300 N94-35240

RUSSIAN FEDERATION
JPRS Report: Science and Technology. Central Eurasia: Space. Russian federation law on space
[JPRS-USP-94-002] p 4348 N94-35519
JTEC/WTEC report and program summary
p 4379 N94-36042
Information and communication technology
p 4257 N94-36043

RUTILE
Mossbauer and spectral (visible and near-IR) data for Fe(3+)-substituted rutile p 4240 N94-36154

S

S WAVES
A three-body calculation of the O-16(d,p)O-17 reaction using a two-term separable potential for the s-wave nucleon-core interaction
[DE94-616652] p 4320 N94-35579
Notes on possible S-wave resonances in relativistic two-particle systems
[DE94-616889] p 4329 N94-36392

SAFETY
Robust requirements specifications for safety-critical systems
[PB94-167806] p 4250 N94-35532

SAFETY MANAGEMENT
Aerospace Safety Advisory Panel
[NASA-TM-109840] p 4201 N94-35390
Implementation of a Computerized Maintenance Management System p 4343 N94-35970

SAMARIUM ISOTOPES
New data supporting a Sm-146,147-Nd-142,143 formation interval for the lunar mantle
p 4374 N94-36173

SAMPLES
Vapor-fortified QA/QC samples for the analysis of volatile organic compounds
[AD-A278712] p 4229 N94-35776

SAMPLING
Use of the sampling theorem to speed up near-field physical optics scattering calculations
p 4253 N94-35549

SANDS
Windblown sand on Mars: The effect of saltation threshold on drift potentials derived from Mars GCM
p 4366 N94-35474

SATELLITE ALTIMETRY
Mesoscale roughness of Venus p 4361 N94-35430

SATELLITE ATTITUDE CONTROL
Spacecraft attitude determination accuracy from mission experience p 4204 N94-35618
MME-based attitude dynamics identification and estimation for SAMPEX p 4209 N94-35643
A simple suboptimal least-squares algorithm for attitude determination with multiple sensors
p 4210 N94-35645

SATELLITE COMMUNICATION
Optimum satellite relay positions with application to a TDRS-1 Indian Ocean relay p 4205 N94-35624
Application of a Monte Carlo accuracy assessment tool to TDRS and GPS p 4207 N94-35635
North American ISDN Users' Forum agreements on Integrated Services Digital Network
[PB94-162559] p 4305 N94-35940
Information and communication technology
p 4257 N94-36043

SATELLITE CONSTELLATIONS
Obtaining coincident image observations for Mission to Planet Earth science data return p 4202 N94-35609
The Earth Satellite Program (ESP), version 2.0
[AD-A278860] p 4201 N94-35827

SATELLITE DESIGN
Natural orbital environment definition guidelines for use in aerospace vehicle development
[NASA-TM-4527] p 4291 N94-36175
Computer graphics tools for the visualization of spacecraft dynamics
[AD-A278615] p 4226 N94-36251

SATELLITE DRAG
Evaluation of semiempirical atmospheric density models for orbit determination applications
p 4208 N94-35636

SATELLITE GROUND TRACKS
The Earth Satellite Program (ESP), version 2.0
[AD-A278860] p 4201 N94-35827

SATELLITE IMAGERY
Preliminary study of satellite attitude determination for the LANDSAT 7 spacecraft
[AD-A278876] p 4212 N94-35585
Theoretical and experimental studies relevant to interpretation of auroral emissions
[NASA-CR-196032] p 4376 N94-36421

SATELLITE INSTRUMENTS
Earth Observing System (EOS) Advanced Microwave Sounding Unit-A (AMSU-A) schedule plan
[NASA-CR-194856] p 4281 N94-35734

SATELLITE NETWORKS
North American ISDN Users' Forum agreements on Integrated Services Digital Network
[PB94-162559] p 4305 N94-35940

SATELLITE OBSERVATION
CATLAC: Calibration and validation analysis tool of local area coverage for the SeaWiFS mission
[NASA-TM-104603] p 4211 N94-35269
Production of long-term global water vapor and liquid water data set using ultra-fast methods to assimilate multi-satellite and radiosonde observations
[NASA-CR-196044] p 4292 N94-35355
The Mars Observer differential one-way range demonstration p 4210 N94-35543
Obtaining coincident image observations for Mission to Planet Earth science data return p 4202 N94-35609
Estimation with multisensor/multiscan detection fusion
[AD-A278753] p 4256 N94-36092

SATELLITE ORBITS
Evaluation of semiempirical atmospheric density models for orbit determination applications
p 4208 N94-35636
Filter parameter tuning analysis for operational orbit determination support p 4208 N94-35637
The Earth Satellite Program (ESP), version 2.0
[AD-A278860] p 4201 N94-35827

SATELLITE ORIENTATION
Flight Mechanics/Estimation Theory Symposium, 1994
[NASA-CP-3265] p 4202 N94-35605
Fixed-head star tracker attitude updates on the Hubble Space Telescope p 4203 N94-35612
Comparison of Kalman filter and optimal smoother estimates of spacecraft attitude p 4208 N94-35638
Application of star identification using pattern matching to space ground systems at GSFC
p 4209 N94-35640
Advantages of estimating rate corrections during dynamic propagation of spacecraft rates: Applications to real-time attitude determination of SAMPEX
p 4209 N94-35642
MME-based attitude dynamics identification and estimation for SAMPEX p 4209 N94-35643
A new algorithm for attitude-independent magnetometer calibration p 4209 N94-35644
A simple suboptimal least-squares algorithm for attitude determination with multiple sensors
p 4210 N94-35645
Motion models in attitude estimation
p 4210 N94-35646

SATELLITE ROTATION
Attitude stability of a spinning spacecraft during appendage deployment/retraction p 4208 N94-35639
Advantages of estimating rate corrections during dynamic propagation of spacecraft rates: Applications to real-time attitude determination of SAMPEX
p 4209 N94-35642
MME-based attitude dynamics identification and estimation for SAMPEX p 4209 N94-35643
A simple suboptimal least-squares algorithm for attitude determination with multiple sensors
p 4210 N94-35645
Motion models in attitude estimation
p 4210 N94-35646

SATELLITE SOUNDING
Production of long-term global water vapor and liquid water data set using ultra-fast methods to assimilate multi-satellite and radiosonde observations
[NASA-CR-195981] p 4293 N94-35499

SATELLITE SURFACES
Results from LDEF experiment A0114: The interaction of atomic oxygen with materials surfaces at orbital altitudes
[NASA-CR-196016] p 4235 N94-35388

SATELLITE TRACKING
CATLAC: Calibration and validation analysis tool of local area coverage for the SeaWiFS mission
[NASA-TM-104603] p 4211 N94-35269
Flight Mechanics/Estimation Theory Symposium, 1994
[NASA-CP-3265] p 4202 N94-35605
Improved solution accuracy for TDRSS-based TOPEX/Poseidon orbit determination
p 4205 N94-35620
A genetic algorithm approach to automating satellite range scheduling
[AD-A278577] p 4226 N94-36188

SATELLITE-BORNE INSTRUMENTS
Development of POINTS as a planetology instrument
[NASA-CR-196026] p 4354 N94-35265
Theoretical and experimental studies relevant to interpretation of auroral emissions
[NASA-CR-196032] p 4376 N94-36421

SATELLITE-BORNE PHOTOGRAPHY
Lunar horizon glow and the Clementine mission
p 4366 N94-35478

SCALING LAWS
Experimental studies of very-high Mach number hydrodynamics
[AD-A278761] p 4263 N94-35492

Leptonic decay constants of heavy quarkonia in effective QCD sum rules
[DE94-611160] p 4322 N94-35784
Scaling laws for TEXT plasma profiles
[DE94-010832] p 4338 N94-36200

SCANNERS
Design and implementation of a beam-waveguide mirror control system for vernier pointing of the DSS-13 antenna p 4253 N94-35548
Overview of the MSTI 2 on-orbit alignment
p 4206 N94-35629
A low temperature scanning force microscope for biological samples
[DE94-011357] p 4297 N94-36269

SCANNING ELECTRON MICROSCOPY
Computer image analysis of etched tracks from ionizing radiation
[NASA-CR-196025] p 4319 N94-35264
High-resolution imaging using Z-contrast Scanning Transmission Electron Microscopy
[DE94-008510] p 4333 N94-36055

SCATTERING
The temperature of nitrogen on Pluto
p 4365 N94-35468
Use of the sampling theorem to speed up near-field physical optics scattering calculations
p 4253 N94-35549
Magnetoresistance of films and strips with the diffuse surface scattering
[DE94-611100] p 4340 N94-35933
X ray and gamma ray spectroscopy of solids under pressure
[DE94-011207] p 4238 N94-36203

SCATTERING AMPLITUDE
On a generalized bootstrap principle
[DE94-727517] p 4314 N94-35774
Low energy theorems from the effective Lagrangian with vector mesons
[DE94-611173] p 4322 N94-35785
Q-deformations of the Veneziano model
[DE94-616769] p 4315 N94-36076
Spin effects in high energy quark-quark scattering
[DE94-616800] p 4330 N94-36080
T-odd, P-even photon-fermion interactions
[DE94-616869] p 4327 N94-36246
Elastic p(4)He scattering at intermediate energies
[DE94-618544] p 4328 N94-36287

SCATTERING CROSS SECTIONS
SCATTER program of cross section calculation of the hadron and lepton interactions with nuclei
[DE94-617006] p 4326 N94-36134

SCHEDULES
Earth Observing System (EOS) Advanced Microwave Sounding Unit-A (AMSU-A) schedule plan
[NASA-CR-194856] p 4281 N94-35734

SCHEDULING
Cost and schedule estimation study report
[NASA-CR-189344] p 4300 N94-35256
A genetic algorithm approach to automating satellite range scheduling
[AD-A278577] p 4226 N94-36188

SCHLIEREN PHOTOGRAPHY
A supersonic tunnel for laser and flow-seeding techniques
[NASA-TM-106588] p 4265 N94-35945

SCHOOLS
Building on the foundation for an engineering career
p 4343 N94-35973

SCHROEDINGER EQUATION
Self-similar regimes of subsonic Langmuir wave collapse
[DE94-611466] p 4335 N94-35750
Coherent states versus de Broglie-wavelets
[DE94-611075] p 4343 N94-36381

SCIENCE
Proceedings of the LLNL Technical Women's Symposium
[DE94-006616] p 4379 N94-35997

SCIENTIFIC VISUALIZATION
Representing spatial information in a computational model for network management
[NASA-CR-191669] p 4306 N94-36040

SCIENTISTS
Women as a resource for the flexibility required for high technology innovation p 4348 N94-35966

SCINTILLATING FIBERS
Ultrafast readout of scintillating fibers using upgraded position-sensitive photomultipliers
[DE94-010419] p 4269 N94-36095

SCINTILLATION COUNTERS
X-ray remote sensing and in-situ spectroscopy for planetary exploration missions and gamma-ray remote sensing and in-situ spectroscopy for planetary exploration missions
[NASA-CR-189352] p 4375 N94-35381
Electronics for the SND scintillation counter system
[DE94-616453] p 4259 N94-36104
Neutron detectors for fusion reaction-rate measurements
[DE94-010407] p 4330 N94-36114

SEA ICE
Environmental measurements in the Beaufort Sea, Spring 1993
[AD-A278718] p 4296 N94-36293

SEA SURFACE TEMPERATURE
Long range forecasts of the Northern Hemisphere anomalies with antecedent sea surface temperature patterns
[NASA-CR-189358] p 4292 N94-35380
JPRS report: Science and technology. Central Eurasia: Space
[JPRS-USP-94-003] p 4201 N94-35520

SEALERS
Analysis of the Shuttle Orbiter reinforced carbon-carbon oxidation protection system
[NASA-TM-104792] p 4262 N94-35245

SEALING
Designing aluminum sealing glasses for manufacturability
[DE94-010081] p 4244 N94-35699

SEALS (STOPPERS)
High-temperature, bellows hybrid seal
[NASA-CASE-LEW-15570-1] p 4274 N94-35373
Rotor dynamic behaviour of a high-speed oil-free motor compressor with a rigid coupling supported on four radial magnetic bearings p 4224 N94-35911
Wear-resisting oxide films for 900 C
[DE94-010093] p 4246 N94-36306
Streak tube photocathode development program
[DE94-009905] p 4270 N94-36350

SECONDARY FLOW
The aerodynamic and heat transfer effects of an endwall boundary layer fence in a 90 degree turning square duct
[AD-A278903] p 4265 N94-35803

SEDIMENTARY ROCKS
Shocked materials from the Dutch Peak diamictite, Utah p 4352 N94-36140

SEDIMENTS
Groundwater penetrating radar and high resolution seismic for locating shallow faults in unconsolidated sediments
[DE94-007284] p 4257 N94-36366

SEISMIC WAVES
Center for seismic studies
[AD-A278682] p 4290 N94-35693
Hydrodynamically induced loads on components submerged in high-level waste-storage tanks
[DE94-009663] p 4264 N94-35756

SEISMOLOGY
Center for seismic studies
[AD-A278682] p 4290 N94-35693
Activity report 1990-1992 and proceedings, volume 1
[DE94-610480] p 4290 N94-35830
Activity Report, 1990 - 1992 and proceedings, volume 2
[DE94-610481] p 4291 N94-36087
Groundwater penetrating radar and high resolution seismic for locating shallow faults in unconsolidated sediments
[DE94-007284] p 4257 N94-36366

SELF CONSISTENT FIELDS
New anionic states of the lithium trimer
[AD-A278832] p 4323 N94-35797
Anionic and neutral states of Li3O
[AD-A278833] p 4323 N94-35798

SELF LUBRICATING MATERIALS
Wear-resisting oxide films for 900 C
[DE94-010093] p 4246 N94-36306

SEMANTICS
Probabilities and priorities in timed CSP
[PB94-169216] p 4316 N94-35536
Mathematical theory of synchronous communication
[PB94-169224] p 4252 N94-35537
Task networks for controlling continuous processes
[AD-A278683] p 4312 N94-35710

SEMICONDUCTOR DEVICES
Nanochannel glass matrix used in making mesoscopic structures
[AD-D016216] p 4234 N94-36123
A critical examination of charge funneling and its impact on single-event upset in Si devices
[DE94-007868] p 4261 N94-36373

SEMICONDUCTOR DIODES
Improved performance of high average power semiconductor arrays for applications in diode pumped solid state lasers
[DE94-009516] p 4271 N94-35665
System for end-pumping a solid state laser using a large aperture laser diode bar
[AD-D016213] p 4273 N94-36370

SEMICONDUCTOR LASERS
Improved performance of high average power semiconductor arrays for applications in diode pumped solid state lasers
[DE94-009516] p 4271 N94-35665
The optimization of interfaces in InAsSb/InGaAs strained-layer superlattices grown by metal-organic chemical vapor deposition
[DE94-010070] p 4340 N94-35698
High-power CW operation of AlGaInP diode-laser arrays
[DE94-010409] p 4272 N94-36115
Phase-locked arrays of vertical-cavity surface-emitting lasers
[DE94-009279] p 4272 N94-36178
Activities of the optoelectronics laboratory
[PB94-171196] p 4334 N94-36190
System for end-pumping a solid state laser using a large aperture laser diode bar
[AD-D016213] p 4273 N94-36370

SEMICONDUCTORS (MATERIALS)
InP solar cell with window layer
[NASA-CASE-LEW-15606-1] p 4281 N94-35230
The optimization of interfaces in InAsSb/InGaAs strained-layer superlattices grown by metal-organic chemical vapor deposition
[DE94-010070] p 4340 N94-35698
Heterogeneous reaction mechanisms and kinetics relevant to the CVD of semiconductor materials
[DE94-011001] p 4340 N94-36032
Activities of the optoelectronics laboratory
[PB94-171196] p 4334 N94-36190
High temperature heterojunction bipolar transistors
[AD-A278605] p 4261 N94-36360

SENSITIVITY
Collective plasma corrections to the solar opacity
[PB94-170511] p 4375 N94-36210
Use of formal calculation to automatically obtain adjoint programs
[PB94-170701] p 4308 N94-36259
Astronomy in the region between 1 mm and 0.1 mm wavelength
[NASA-CR-196020] p 4349 N94-36419

SENSORS
Intelligent processing of materials, technical activities, 1993 (NAS-NRC Assessment Panel, April 21-22 1994)
[PB94-164183] p 4251 N94-35737

SENSORY STIMULATION
Visual-vestibular interaction
[NASA-CR-196097] p 4297 N94-35379

SEPAC (PAYLOAD)
Participation in the definition, conduct, and analysis of particle accelerator experiments for the first Spacelab Mission
[NASA-CR-193974] p 4330 N94-35483

SEPARATORS
Separation tool for multipin electrical connectors
[NASA-CASE-NPO-18786-1-CU] p 4274 N94-35375

SEQUENCING
Synthesis of asynchronous systems from data flow specifications
[AD-A278687] p 4303 N94-35662

SERVICE LIFE
On optimal placement of spacers in bundled conductors p 4258 N94-35354

SERVOMECHANISMS
Design and implementation of a beam-waveguide mirror control system for vernier pointing of the DSS-13 antenna p 4253 N94-35548
Fuzzy self-learning control for magnetic servo system
p 4215 N94-35852

SEYFERT GALAXIES
ROSAT/XRT-PSPC observations and the ionizing continuum of Seyfert 1 galaxy Mkn 478
[PB94-167053] p 4350 N94-35530

SHAFTS (MACHINE ELEMENTS)
Robot friendly probe and socket assembly
[NASA-CASE-MSC-22028-1] p 4274 N94-35374
Rotor dynamic behaviour of a high-speed oil-free motor compressor with a rigid coupling supported on four radial magnetic bearings p 4224 N94-35911

SHAPES
Quantifying shapes of volcanoes on Venus
p 4361 N94-35429

SHEAR FLOW
Dynamic and thermal turbulent time scale modelling for homogeneous shear flows
[NASA-TM-106635] p 4263 N94-35253
X ray radiographic imaging of hydrodynamic phenomena in radiation driven materials: Shock propagation, material compression and shear flow
[DE94-009515] p 4266 N94-35982
X ray radiographic imaging of hydrodynamic phenomena in radiation driven materials: Shock propagation and shear flow
[DE94-010891] p 4318 N94-36201

SHEAR LAYERS
An experimental investigation of active control of thrust vectoring nozzle flow fields
[AD-A278702] p 4229 N94-36291

SHEAR PROPERTIES
A mechanics mode tor the compressive response of fiber reinforced composites
[AD-A278866] p 4233 N94-35715

SHEAR STRENGTH
Residual Gas Analysis (RGA) and shear strength characteristics of a silver-filled epoxy and polyimide under long-term, high-temperature storage conditions
[DE94-010106] p 4244 N94-35705

SHEATHS
High-temperature, bellows hybrid seal
[NASA-CASE-LEW-15570-1] p 4274 N94-35373

SHELTERS
Thermal performance of residential duct systems in basements
[LBL-33962] p 4250 N94-35364

SHERGOTTITES
Solar proton produced neon in shergottite meteorites
p 4351 N94-35428
The parent magma of xenoliths in shergottite EETA79001: Bulk and trace element composition inferred from magmatic inclusions p 4352 N94-35467
Pigeonholing planetary meteorites: The lessons of misclassification of EET87521 and ALH84001
p 4353 N94-36157

SHOCK LOADS
Structures and properties of materials recovered from high shock pressures
[DE94-010057] p 4232 N94-35696
X ray radiographic imaging of hydrodynamic phenomena in radiation driven materials: Shock propagation, material compression and shear flow
[DE94-009515] p 4266 N94-35982
Shocked materials from the Dutch Peak diamictite, Utah p 4352 N94-36140
Calorimetric thermobarometry of experimentally shocked quartz p 4240 N94-36174
X ray radiographic imaging of hydrodynamic phenomena in radiation driven materials: Shock propagation and shear flow
[DE94-010891] p 4318 N94-36201
Electrical conductivity of hydrogen shocked to megabar pressures
[DE93-019632] p 4238 N94-36237

SHOCK TESTS
More shock recovery experiments on mesosiderite analogs p 4351 N94-35455

SHOCK WAVE GENERATORS
Plane shock generator explosive lens: Shock characterization of 4340 and PH13-8Mo steels, C360 brass and PZT 65/35 ferro-electric ceramic
[DE94-009254] p 4266 N94-35979

SHOCK WAVE INTERACTION
Investigation of Burnett equations for two-dimensional hypersonic flow
[AD-A278942] p 4190 N94-35717
Analysis of high speed flow, thermal and structural interactions
[NASA-CR-196017] p 4268 N94-36420

SHOCK WAVES
The fine structure of Langmuir waves observed upstream of the bow shock at Venus
[NASA-CR-196123] p 4354 N94-35378
Experimental studies of very-high Mach number hydrodynamics
[AD-A278761] p 4263 N94-35492
Numerical simulation of shock interaction with above-ground structures
[AD-A278713] p 4279 N94-35949
Plane shock generator explosive lens: Shock characterization of 4340 and PH13-8Mo steels, C360 brass and PZT 65/35 ferro-electric ceramic
[DE94-009254] p 4266 N94-35979
X ray radiographic imaging of hydrodynamic phenomena in radiation driven materials: Shock propagation and shear flow
[DE94-010891] p 4318 N94-36201

SHOEMAKER-LEVY 9 COMET
Radiative signals from impact of Shoemaker-Levy on Jupiter p 4355 N94-35396
Shoemaker-Levy 9 and the tidal disruption of comets
p 4351 N94-35406

SHORT HAUL AIRCRAFT
The reduction of takeoff ground roll by the application of a nose gear jump strut
[NASA-TM-108822] p 4198 N94-36380

SHORT TAKEOFF AIRCRAFT
Direct reduced order mixed H2/H infinity control for the Short Take-Off and Landing/Maneuver Technology Demonstrator (STOL/MTD)
[AD-A278675] p 4199 N94-35796
The reduction of takeoff ground roll by the application of a nose gear jump strut
[NASA-TM-108822] p 4198 N94-36380

SHORT WAVE RADIO TRANSMISSION
Measurements of spatial and frequency coherence of an equatorial hf path during spread-F
[DE93-016615] p 4257 N94-36316

SHROUDS
The electrical conductivities of candidate beam-waveguide antenna shroud materials
p 4252 N94-35546

SIDE-LOOKING RADAR
Evaluation of synthetic aperture radar for oil-spill response
[AD-A278796] p 4284 N94-35674

SIDERITES
More shock recovery experiments on mesosiderite analogs p 4351 N94-35455

SIDESLIP
Wind tunnel measurements on a full-scale F/A-18 with a tangentially blowing slot --- conducted in the Ames 80 by 120 foot wind tunnel p 4191 N94-35965

SIEVES
Be3(AsO4)2.2H2O, a new berylloarsenate phase containing bridged tetrahedral 3-rings
[AD-A278826] p 4340 N94-35677

SIGNAL DETECTION
Spacecraft-spacecraft radio-metric tracking: Signal acquisition requirements and application to Mars approach navigation p 4254 N94-35557
Attention and signal detection. A study of attention divided between visual and auditory signals
[PB94-170594] p 4298 N94-36215

SIGNAL DISTORTION
Measurements of spatial and frequency coherence of an equatorial hf path during spread-F
[DE93-016615] p 4257 N94-36316

SIGNAL FADING
Measurements of spatial and frequency coherence of an equatorial hf path during spread-F
[DE93-016615] p 4257 N94-36316

SIGNAL PROCESSING
A closed-loop time-alignment system for baseband combining p 4253 N94-35552
NAVSPACECOM space surveillance sensor system digital signal processing receiver. Volume 3: Operating system functions
[AD-A278839] p 4212 N94-35799
NAVSPACECOM space surveillance sensor system digital signal processing receiver. Volume 4: Hardware interfaces
[AD-A278845] p 4212 N94-35801
The CMU task parallel program suite
[AD-A278951] p 4311 N94-36015
Computational Mathematics Laboratory for multiscale analysis
[AD-A278597] p 4315 N94-36424

SIGNAL TO NOISE RATIOS
Fluorescence detection of single molecules using pulsed near-field optical excitation and time correlated photon counting
[DE94-007553] p 4320 N94-35376
A closed-loop time-alignment system for baseband combining p 4253 N94-35552
Correlator data analysis for the array feed compensation system p 4253 N94-35553

SILANES
Spinnability of silica sols: The role of alkoxy group exchange
[DE94-010087] p 4244 N94-35702

SILICA GLASS
Multicomponent glass surfaces: Structure and adsorption
[DE94-010516] p 4246 N94-36283

SILICATES
Grain rims on ilmenite in the lunar regolith: Comparison to vapor deposits on regolith silicates
p 4359 N94-35418
Application of an alkylammonium method for characterization of phyllosilicates in CI chondrites
p 4351 N94-35432
Inhomogeneous distribution of materials in lodranites-acapulcoites and IAB irons and their common formation processes p 4364 N94-35463
Kinetics of phase transformations in glass forming systems
[NASA-CR-196082] p 4245 N94-35977
Textural constraints on the formation of alteration phases in CM chondrites p 4353 N94-36145
Preliminary results of sulfide melt/silicate wetting experiments in a partially melted ordinary chondrite
p 4353 N94-36147
On the origin of porphyritic chondrules
[DE94-010464] p 4351 N94-36418

SILICIDES
High temperature creep and oxidation resistant chromium silicide matrix alloy containing molybdenum
[NASA-CASE-LEW-15697-1] p 4241 N94-36275

SILICON
Laser drilling of vertical vias in silicon
[DE94-009250] p 4270 N94-35351
Large scale atomistic first principles study of adsorption and surface diffusion
[DE94-009450] p 4322 N94-35682
Chemical reactions of chlorine on a vicinal Si(100) surface studied by ESDIAD
[AD-A279059] p 4236 N94-35731
Electromagnetically levitated vibration isolation system for the manufacturing process of silicon monocrystals
p 4223 N94-35906
Space-based crystal growth and thermocapillary flow
p 4342 N94-35971
Determination of the Fermi level position for neutron irradiated high resistivity silicon detectors and materials using the Transient Charge Technique (TChT)
[DE94-009107] p 4260 N94-36221
Simulation of materials processing: Fantasy or reality?
p 4230 N94-36404

SILICON CARBIDES
Vertical and adiabatical ionization energies and electron affinities of new Si(n)C and Si(n)O (n=1-3) molecules
[AD-A278863] p 4324 N94-36050
Method of thermochemically treating silicon carbide fibers derived from polymers
[AD-D016218] p 4246 N94-36125

SILICON COMPOUNDS
Measurement of the decay rate of the SiH feature as a function of temperature p 4318 N94-36171

SILICON DIOXIDE
Purity and cleanness of aerogel as a cosmic dust capture medium p 4247 N94-35469
Cross-condensation reactions in an organically modified silica sol-gel
[DE94-010086] p 4244 N94-35701
Spinnability of silica sols: The role of alkoxy group exchange
[DE94-010087] p 4244 N94-35702
Kinetics of phase transformations in glass forming systems
[NASA-CR-196082] p 4245 N94-35977
Coatings for SiO2 optical fibers
[AD-D016197] p 4334 N94-36363

SILICON JUNCTIONS
A critical examination of charge funneling and its impact on single-event upset in Si devices
[DE94-007868] p 4261 N94-36373

SILICON NITRIDES
A combined experimental and theoretical study of the neutral, cationic and anionic Si3N cluster molecule
[AD-A278834] p 4323 N94-35792
The growth of silicon nitride crystalline films using microwave plasma enhanced chemical vapor deposition
[AD-A278862] p 4340 N94-35828

SILICON OXIDES
Vertical and adiabatical ionization energies and electron affinities of new Si(n)C and Si(n)O (n=1-3) molecules
[AD-A278863] p 4324 N94-36050
Enhanced charge trapping in bipolar spacer oxides during low-dose-rate irradiation
[DE94-007863] p 4260 N94-36268

SILICONES
Syntheses and studies of acetylenic polymers
[DE94-011201] p 4245 N94-36057

SILVER
Effect of niobium interlayer on high-temperature sliding friction and wear of silver films on alumina
[DE94-010462] p 4275 N94-36232

SIMULATION
Purity and cleanness of aerogel as a cosmic dust capture medium p 4247 N94-35469
Bit-wise arithmetic coding for data compression
p 4254 N94-35556
Determination of grain boundary volume expansion by HREM
[DE94-010452] p 4241 N94-36231

SINGLE CRYSTALS
Be3(AsO4)2.2H2O, a new berylloarsenate phase containing bridged tetrahedral 3-rings
[AD-A278826] p 4340 N94-35677
Electromagnetically levitated vibration isolation system for the manufacturing process of silicon monocrystals
p 4223 N94-35906
Space-based crystal growth and thermocapillary flow
p 4342 N94-35971
Twin spacing versus size of a monocrystal for the nonstoichiometric 1:2:3 superconductors
[DE94-615511] p 4340 N94-36029
Application of GaSe and AgGaSe2 crystal growth to non-linear optics
[PB94-170552] p 4341 N94-36212

Formation and stability of Fe-rich precipitates in dilute Zr(Fe) single-crystal alloys
[DE94-619027] p 4242 N94-36288

SINGLE EVENT UPSETS
A critical examination of charge funneling and its impact on single-event upset in Si devices
[DE94-007868] p 4261 N94-36373

SINGULARITY (MATHEMATICS)
Self-similar regimes of subsonic Langmuir wave collapse
[DE94-611466] p 4335 N94-35750
On a generalized bootstrap principle
[DE94-727517] p 4314 N94-35774
Local instabilities and the transition to chaos of non-linear waves
[PB94-170578] p 4341 N94-36213

SINTERING
Digital control programmer for temperature control
[DE94-615584] p 4309 N94-36382

SISO (CONTROL SYSTEMS)
Implementation of a decoupled controller for a magnetic suspension system using electromagnets mounted in a planar array p 4216 N94-35853
Adaptive model reduction for continuous systems via recursive rational interpolation p 4219 N94-35876

SITE SELECTION
Fluvial processes in Ma'adim Vallis and the potential of Gusev crater as a high priority site
p 4358 N94-35414
Autonomous hazard detection and avoidance
[NASA-CR-188331] p 4309 N94-36439

SIZE DISTRIBUTION
Anthropogenic sulfate and organic aerosols, CCN, and cloud project concentration at a marine site
[DE94-004210] p 4286 N94-36025

SLEEP DEPRIVATION
Some solutions to reduce the human effects of extended operation times p 4196 N94-36339

SLEWING
A combined algorithm for minimum time slewing of flexible spacecraft p 4220 N94-35881
Input shaping for three-dimensional slew maneuvers of a precision pointing flexible spacecraft
[DE94-008937] p 4226 N94-36001

SLIDING FRICTION
Effect of niobium interlayer on high-temperature sliding friction and wear of silver films on alumina
[DE94-010462] p 4275 N94-36232
Wear-resisting oxide films for 900 C
[DE94-010093] p 4246 N94-36306

SLURRIES
Determination of extensional viscosity from capillary rheometer entrance pressure drop measurements using a numerical simulation of contraction flow
[PB94-171154] p 4263 N94-35603
Coal-fueled diesels for modular power generation
[DE94-002960] p 4275 N94-36348

SLUSH HYDROGEN
Experimental results of hydrogen slosh in a 62 cubic foot (1750 liter) tank
[NASA-TM-106625] p 4263 N94-35250

SMALL PERTURBATION FLOW
The velocity field created by a shallow bump in a boundary layer
[NASA-CR-194899] p 4266 N94-35975

SMALL SCIENTIFIC SATELLITES
Controller for the Electronically Scanned Thinned Array Radiometer (ESTAR) instrument
[NASA-TM-104608] p 4259 N94-36049

SOCIOLOGY
Space and the American imagination
[NASA-CR-196131] p 4376 N94-35356

SODIUM
X ray and gamma ray spectroscopy of solids under pressure
[DE94-011207] p 4238 N94-36203

SODIUM COMPOUNDS
A new family of superconducting fullerides, Na(NH3)(x)C60(x = 2-8)
[DE94-011480] p 4341 N94-36272

SOFTWARE ENGINEERING
Annotated bibliography of Software Engineering Laboratory literature
[NASA-CR-189350] p 4300 N94-35238
Cost and schedule estimation study report
[NASA-CR-189344] p 4300 N94-35256
Collected software engineering papers, volume 11
[NASA-CR-189347] p 4301 N94-35434
Modeling and managing risk early in software development p 4301 N94-35436
An information model for use in software management estimation and prediction p 4301 N94-35437
Measuring and assessing maintainability at the end of high level design p 4301 N94-35438
Impacts of object-oriented technologies: Seven years of SEL studies p 4301 N94-35439
Software architecture standard for simulation virtual macnine, version 2.0
[NASA-CR-188291] p 4301 N94-35443
Developing software for ease of change: Metrics from later in the TRALAB system life cycle
[AD-A278759] p 4302 N94-35490
A software architecture for adding new interaction techniques to a command and control based testbed
[AD-A278760] p 4302 N94-35491
Exploring hypermedia information services for disseminating software engineering information
[AD-A278765] p 4302 N94-35495
Robust requirements specifications for safety-critical systems
[PB94-167806] p 4250 N94-35532
Proceedings of the 4th Workshop on the Next Generation of CASE Tools
[PB94-150372] p 4302 N94-35538
The development and application of composite complexity models and a relative complexity metric in a software maintenance environment
p 4255 N94-35559
Overview of the MSTI 2 processor-in-the-loop simulator p 4207 N94-35631
Environment/tool integrator for software development, version 1.2
[AD-A278965] p 4303 N94-35660
Model engineering concepts for air quality models in an integrated environmental modeling system
[PB94-158623] p 4298 N94-35688
A taxonomy of coordination mechanisms used in real-time software based on domain analysis
[AD-A279014] p 4304 N94-35794
An object-oriented implementation of a graphical-programming system
[DE94-009298] p 4304 N94-35808
Experience with Ada on the F-18 High Alpha Research Vehicle flight test program p 4310 N94-35968
Object-oriented simulation pictures (OOSPic) for design and testing
[AD-A278798] p 4305 N94-36013
Certification of computational results
p 4306 N94-36064
Certification trails and software design for testability
p 4306 N94-36066
Using certification trails to achieve software fault tolerance p 4307 N94-36068
The EASE Visualization Community Club
[PB94-170529] p 4308 N94-36211
An environment for visualization, reliability, and knowledge acquisition in equational programming
[AD-A278639] p 4308 N94-36258
A practical guide to the technology and adoption of software process automation
[AD-A278719] p 4308 N94-36294

SOFTWARE RELIABILITY
Modeling and managing risk early in software development p 4301 N94-35436
Certification trails for data structures
p 4307 N94-36069
An environment for visualization, reliability, and knowledge acquisition in equational programming
[AD-A278639] p 4308 N94-36258

SOFTWARE REUSE
A taxonomy of coordination mechanisms used in real-time software based on domain analysis
[AD-A279014] p 4304 N94-35794

SOFTWARE TOOLS
Space educators' handbook
[NASA-TM-109779] p 4343 N94-35339
A compile time model for composing parallel programs
[AD-A278896] p 4310 N94-35597
Environment/tool integrator for software development, version 1.2
[AD-A278965] p 4303 N94-35660
A collection of tools in support of automatic differentiation
[DE94-010104] p 4314 N94-35704
An object-oriented implementation of a graphical-programming system
[DE94-009298] p 4304 N94-35808
CABPRO: An expert system for process planning multiwire cables
[DE94-010213] p 4312 N94-35810

SOIL MOISTURE
A model of the CO2 exchanges between biosphere and atmosphere in the tundra
[NASA-CR-196008] p 4289 N94-35389

SOILS
Thermal emission measurements (5-25 microns) of palagonite/Fe-substituted montmorillonite intimate mixtures: Applications to Mars p 4292 N94-35453
Vapor-fortified QA/QC samples for the analysis of volatile organic compounds
[AD-A278712] p 4229 N94-35776

SOL-GEL PROCESSES
Cross-condensation reactions in an organically modified silica sol-gel
[DE94-010086] p 4244 N94-35701
Spinnability of silica sols: The role of alkoxy group exchange
[DE94-010087] p 4244 N94-35702

SOLAR ACTIVITY EFFECTS
Automated maneuver planning using a fuzzy logic algorithm p 4203 N94-35610

SOLAR ARRAYS
Microprocessor control of multiple peak power tracking DC/DC converters for use with solar cell arrays
[NASA-CASE-GSC-13450-2] p 4282 N94-35540
Improved performance of degraded solar arrays at non-zero sun incidence angles
[AD-A278905] p 4282 N94-35804
Software for continuum modeling of controls-structures interactions p 4223 N94-35898

SOLAR ATMOSPHERE
On the physics of waves in the solar atmosphere: Wave heating and wind acceleration
[NASA-CR-194119] p 4375 N94-36395

SOLAR CELLS
InP solar cell with window layer
[NASA-CASE-LEW-15606-1] p 4281 N94-35230
Microprocessor control of multiple peak power tracking DC/DC converters for use with solar cell arrays
[NASA-CASE-GSC-13450-2] p 4282 N94-35540
Development of novel II-VI solar cells
[PB94-159415] p 4282 N94-35739
Improved performance of degraded solar arrays at non-zero sun incidence angles
[AD-A278905] p 4282 N94-35804

SOLAR COSMIC RAYS
JPRS report: Science and technology. Central Eurasia: Space
[JPRS-USP-94-001] p 4201 N94-35518

SOLAR CYCLES
ATLAS solar pointing operations
p 4201 N94-35626
Global changes of radiation situation at heights less than 1000 km
[DE94-610504] p 4290 N94-35780

SOLAR ELECTRONS
Solar-geophysical data number 594, February 1994. Part 2: (Comprehensive reports). Data for August 1993, and miscellaneous
[PB94-164001] p 4374 N94-36009

SOLAR ENERGY
Model documentation: Renewable Fuels Module of the National Energy Modeling System
[DE94-009962] p 4282 N94-35672

SOLAR FLARES
A search for energetic ion directivity in large solar flares
[NASA-CR-196036] p 4374 N94-35993
Solar-geophysical data number 594, February 1994. Part 1: (Prompt reports). Data for December 1993, January 1994, and late data
[PB94-163995] p 4375 N94-36020

SOLAR FLUX
Collective plasma corrections to the solar opacity
[PB94-170511] p 4375 N94-36210

SOLAR INSTRUMENTS
ATLAS solar pointing operations
p 4201 N94-35626

SOLAR MAGNETIC FIELD
Solar-geophysical data number 594, February 1994. Part 2: (Comprehensive reports). Data for August 1993, and miscellaneous
[PB94-164001] p 4374 N94-36009
Solar-geophysical data number 594, February 1994. Part 1: (Prompt reports). Data for December 1993, January 1994, and late data
[PB94-163995] p 4375 N94-36020

SOLAR ORBITS
Catalog of Helios 90 deg photometer events
[PL-TR-94-2040] p 4375 N94-36264

SOLAR PHYSICS
ATLAS solar pointing operations
p 4201 N94-35626
Solar-geophysical data number 594, February 1994. Part 2: (Comprehensive reports). Data for August 1993, and miscellaneous
[PB94-164001] p 4374 N94-36009
Solar-geophysical data number 594, February 1994. Part 1: (Prompt reports). Data for December 1993, January 1994, and late data
[PB94-163995] p 4375 N94-36020
Collective plasma corrections to the solar opacity
[PB94-170511] p 4375 N94-36210

SOLAR PROTONS
Solar proton produced neon in shergottite meteorites
p 4351 N94-35428

Solar-geophysical data number 594, February 1994. Part 2: (Comprehensive reports). Data for August 1993, and miscellaneous
[PB94-164001] p 4374 N94-36009

SOLAR RADIATION

Pseudogoldstone boson decay induced by light and search for the solar axion radiation
[DE94-616907] p 4326 N94-36133

Absolute, Extreme Ultraviolet Solar Spectral Irradiance Monitor (AESSIM)
[AD-A278709] p 4227 N94-36189

SOLAR RADIO EMISSION

Solar-geophysical data number 594, February 1994. Part 1: (Prompt reports). Data for December 1993, January 1994, and late data
[PB94-163995] p 4375 N94-36020

SOLAR SENSORS

Operational support for Upper Atmosphere Research Satellite (UARS) attitude sensors p 4204 N94-35617

Spacecraft attitude determination accuracy from mission experience p 4204 N94-35618

ATLAS solar pointing operations
p 4201 N94-35626

Overview of the Miniature Sensor Technology Integration (MSTI) spacecraft attitude control system
p 4206 N94-35627

A geometric model of a V-slit Sun sensor correcting for spacecraft wobble p 4206 N94-35628

Overview of the MSTI 2 on-orbit alignment
p 4206 N94-35629

SOLAR SYSTEM

Application of an alkylammonium method for characterization of phyllosilicates in CI chondrites
p 4351 N94-35432

First observation of a mass independent isotopic fractionation in a condensation reaction
p 4239 N94-35464

A quick look method of detecting water of hydration in small solar system bodies p 4352 N94-35470

SOLAR TERRESTRIAL INTERACTIONS

Solar-geophysical data number 594, February 1994. Part 1: (Prompt reports). Data for December 1993, January 1994, and late data
[PB94-163995] p 4375 N94-36020

SOLDERING

Manufacturing feasibility of several lead-free solders for electronic assembly
[DE94-007732] p 4258 N94-35564

Capillary flow solderability test for printed wiring boards
[DE94-010321] p 4259 N94-36094

SOLDERS

Manufacturing feasibility of several lead-free solders for electronic assembly
[DE94-007732] p 4258 N94-35564

Capillary flow solderability test for printed wiring boards
[DE94-010321] p 4259 N94-36094

SOLENOIDS

Time-delay control of a magnetic levitated linear positioning system p 4217 N94-35862

SOLID ELECTROLYTES

A solid oxide fuel cell power system: 1992-1993 field operation
[DE94-010383] p 4283 N94-36109

SOLID LUBRICANTS

Wear-resisting oxide films for 900 C
[DE94-010093] p 4246 N94-36306

SOLID NITROGEN

The temperature of nitrogen on Pluto
p 4365 N94-35468

SOLID PROPELLANT COMBUSTION

AFOSR Contractors Propulsion Meeting
[AD-A279028] p 4198 N94-35746

SOLID PROPELLANT IGNITION

The 30th JANNAF Combustion Subcommittee Meeting, volume 1
[AD-A278793] p 4247 N94-35655

SOLID PROPELLANT ROCKET ENGINES

AFOSR Contractors Propulsion Meeting
[AD-A279028] p 4198 N94-35746

Energy partitioning in high speed impact of analog solid rocket motors
[AD-A278771] p 4228 N94-35825

Propellant stress relief groove for the Titan 4 SRMU
[AD-A278628] p 4228 N94-36254

An efficient, intelligent solution for viscous flows inside solid rocket motors
[AD-A278629] p 4228 N94-36255

SOLID PROPELLANTS

The 30th JANNAF Combustion Subcommittee Meeting, volume 1
[AD-A278793] p 4247 N94-35655

SOLID ROCKET PROPELLANTS

Propellant stress relief groove for the Titan 4 SRMU
[AD-A278628] p 4228 N94-36254

SOLID STATE

NMR imaging of components and materials for DOE application
[DE94-010664] p 4238 N94-36084

SOLID STATE DEVICES

Electron and Proton Wide-Angle Spectrometer (EPAS) on the CRRES spacecraft
[AD-A278630] p 4227 N94-35362

A 32-GHz solid-state power amplifier for deep space communications p 4255 N94-35562

SOLID STATE LASERS

Improved performance of high average power semiconductor arrays for applications in diode pumped solid state lasers
[DE94-009516] p 4271 N94-35665

System for end-pumping a solid state laser using a large aperture laser diode bar
[AD-D016213] p 4273 N94-36370

SOLID SURFACES

Innovative instrumentation for mineralogical and elemental analyses of solid extraterrestrial surfaces: The Backscatter Moessbauer Spectrometer/X Ray Fluorescence analyzer (BaMS/XRF)
p 4239 N94-35459

SOLID WASTES

Model documentation: Renewable Fuels Module of the National Energy Modeling System
[DE94-009962] p 4282 N94-35672

SOLIDIFICATION

Interface shape and convection during solidification and melting of succinonitrile
[NASA-TM-106487] p 4262 N94-35248

Computation of dendrites using a phase field model
[PB94-160744] p 4236 N94-35736

SOLIDS

X ray and gamma ray spectroscopy of solids under pressure
[DE94-011207] p 4238 N94-36203

SOLIDUS

Partial melting of the St. Severin (LL) and Lost City (H) ordinary chondrites: One step backwards and two steps forward p 4353 N94-36146

SOLITARY WAVES

Theoretical studies of ultrashort phenomena
[AD-A278938] p 4332 N94-35664

Solitary waves and homoclinic orbits
[DE94-009428] p 4264 N94-35681

The 2+1-dimensional integrable generalization of the Sine-Gordon equation
[DE94-611074] p 4315 N94-36100

The nucleon-nucleon potential in the chromodielectric soliton model
[DE94-004646] p 4329 N94-36305

SOLUBILITY

Measurement of viscosity, density, and gas solubility of refrigerant blends in selected synthetic lubricants
[DE94-010426] p 4244 N94-35687

Solubility, viscosity and density of refrigerant/lubricant mixtures
[DE94-009996] p 4245 N94-35771

A classical model for closed-loop diagrams of binary liquid mixtures
[DE94-011011] p 4237 N94-36033

SOLUTES

Solvent acidity and basicity in polar media and their role in solvation
[AD-A278604] p 4239 N94-36426

SOLVENTS

Cleaning up our act: Alternatives for hazardous solvents used in cleaning
[DE94-006624] p 4285 N94-35943

Some perspectives on solution-phase electron-transfer processes
[AD-A278616] p 4238 N94-36252

Solvent acidity and basicity in polar media and their role in solvation
[AD-A278604] p 4239 N94-36426

SOOT

Detailed studies of soot formation in laminar diffusion flames for application to modeling studies
[AD-A278941] p 4235 N94-35604

SORBENTS

High temperature sorbents for oxygen
[NASA-CASE-NPO-18409-1-CU] p 4235 N94-35255

SORPTION

High temperature sorbents for oxygen
[NASA-CASE-NPO-18409-1-CU] p 4235 N94-35255

Diffusion and sorption of 1,4-dioxane into polychloroprene
[ARL-TR-338] p 4229 N94-35361

SOUND WAVES

An electromagnetic finite difference time domain analog treatment of small signal acoustic interactions
[DE94-009978] p 4319 N94-35770

First, second and fourth sound in relativistic superfluidity theory with account for dissipative effects
[DE94-617393] p 4267 N94-36314

On the physics of waves in the solar atmosphere: Wave heating and wind acceleration
[NASA-CR-194119] p 4375 N94-36395

SOURCE PROGRAMS

Symbolic debugging of globally optimized code: Data value problems and their solutions
[AD-A278898] p 4302 N94-35572

SPACE COMMERCIALIZATION

Geostationary space launch vehicles and the US dilemma p 4210 N94-35377

SPACE COMMUNICATION

The Telecommunications and Data Acquisition Report
[NASA-CR-196117] p 4252 N94-35542

A 32-GHz solid-state power amplifier for deep space communications p 4255 N94-35562

SPACE DEBRIS

Morphology of meteoroid and space debris craters on LDEF metal targets p 4353 N94-36159

Natural orbital environment definition guidelines for use in aerospace vehicle development
[NASA-TM-4527] p 4291 N94-36175

SPACE ENVIRONMENT SIMULATION

Design and simulation of EVA tools for first servicing mission of HST
[NASA-CR-196030] p 4298 N94-35266

Theoretical and experimental studies relevant to interpretation of auroral emissions
[NASA-CR-196032] p 4376 N94-36421

SPACE EXPLORATION

An automatic planetary vehicle for exploring Mars
p 4354 N94-35336

Space educators' handbook
[NASA-TM-109779] p 4343 N94-35339

Space and the American imagination
[NASA-CR-196131] p 4376 N94-35356

Remote geochemical experiment package for Discovery class missions p 4350 N94-35420

Galileo: The Jovian laboratory
[NASA-CR-196043] p 4367 N94-35504

Voyager: National Air and Space Museum
[NASA-CR-195905] p 4367 N94-35505

Voyager last picture show
[NASA-CR-195796] p 4367 N94-35506

Magellan to Venus
[NASA-CR-195779] p 4201 N94-35510

Voyager science summary tape
[NASA-CR-195909] p 4367 N94-35513

Partners in space. International cooperation in space: Strategies for the new century
[ISBN-0-9629930-2-6] p 4348 N94-35901

The history of space exploration
[NASA-TM-109888] p 4201 N94-36440

SPACE HEATING (BUILDINGS)

Thermal performance of residential duct systems in basements
[LBL-33962] p 4250 N94-35364

SPACE LAW

JPRS Report: Science and Technology. Central Eurasia: Space. Russian federation law on space
[JPRS-USP-94-002] p 4348 N94-35519

SPACE MAINTENANCE

Design and simulation of EVA tools for first servicing mission of HST
[NASA-CR-196030] p 4298 N94-35266

SPACE MISSIONS

STS-58 Space Shuttle Mission Report
[NASA-TM-109867] p 4211 N94-35251

STS-51 Space Shuttle Mission Report
[NASA-TM-109866] p 4211 N94-35252

X-ray remote sensing and in-situ spectroscopy for planetary exploration missions and gamma-ray remote sensing and in-situ spectroscopy for planetary exploration missions
[NASA-CR-189352] p 4375 N94-35381

A 32-GHz solid-state power amplifier for deep space communications p 4255 N94-35562

NAVSPACECOM space surveillance sensor system digital signal processing receiver. Volume 3: Operating system functions
[AD-A278839] p 4212 N94-35799

NAVSPACECOM space surveillance sensor system digital signal processing receiver. Volume 4: Hardware interfaces
[AD-A278845] p 4212 N94-35801

SPACE NAVIGATION

Spacecraft-spacecraft radio-metric tracking: Signal acquisition requirements and application to Mars approach navigation p 4254 N94-35557

Improved solution accuracy for TDRSS-based TOPEX/Poseidon orbit determination
p 4205 N94-35620

TDRSS Onboard Navigation System (TONS) flight qualification experiment p 4206 N94-35625

SPACE PLASMAS

The fine structure of Langmuir waves observed upstream of the bow shock at Venus [NASA-CR-196123] p 4354 N94-35378

Spatial fluctuations of particle fluxes within the auroral zone inferred from the Intercosmos-Bulgaria-1300 satellite data [DE94-615858] p 4350 N94-36128

SPACE PLATFORMS

Theoretical and experimental studies relevant to interpretation of auroral emissions [NASA-CR-196032] p 4376 N94-36421

SPACE PROCESSING

Materials processing in space tasks. WBS task 5.4: Generic tasks [NASA-CR-193979] p 4249 N94-35485

1993 Technical Paper Contest for Women. Gear Up 2000: Women in Motion [NASA-CP-10134] p 4377 N94-35961

SPACE PROGRAMS

Partners in space. International cooperation in space: Strategies for the new century [ISBN-0-9629930-2-6] p 4348 N94-35901

SPACE SHUTTLE MAIN ENGINE

Instrumentation for in-flight SSME rocket engine plume spectroscopy [NASA-TM-106596] p 4268 N94-35268

SPACE SHUTTLE MISSIONS

Debris/ice/TPS assessment and integrated photographic analysis for Shuttle Mission STS-59 [NASA-TM-109203] p 4211 N94-35523

SPACE SHUTTLE ORBITERS

Analysis of the Shuttle Orbiter reinforced carbon-carbon oxidation protection system [NASA-TM-104792] p 4262 N94-35245

SPACE SHUTTLE PAYLOADS

STS-58 Space Shuttle Mission Report [NASA-TM-109867] p 4211 N94-35251

STS-51 Space Shuttle Mission Report [NASA-TM-109866] p 4211 N94-35252

Structural assembly demonstration experiment, phase 1 [NASA-CR-193967] p 4212 N94-35484

SPACE SHUTTLES

STS-58 Space Shuttle Mission Report [NASA-TM-109867] p 4211 N94-35251

STS-51 Space Shuttle Mission Report [NASA-TM-109866] p 4211 N94-35252

Aerospace Safety Advisory Panel [NASA-TM-109840] p 4201 N94-35390

Space Shuttle orbit determination using empirical force modeling of attitude maneuvers for the German MOMS-02/D2 mission p 4207 N94-35634

SPACE SIMULATORS

Overview of the MSTI 2 processor-in-the-loop simulator p 4207 N94-35631

SPACE STATION FREEDOM

Aerospace Safety Advisory Panel [NASA-TM-109840] p 4201 N94-35390

Dynamic analysis of Space Shuttle/RMS configuration using continuum approach p 4221 N94-35887

SPACE STATION PAYLOADS

Materials processing in space tasks. WBS task 5.4: Generic tasks [NASA-CR-193979] p 4249 N94-35485

SPACE STATIONS

International Space Station alpha remote manipulator system workstation controls test report [NASA-TM-104796] p 4274 N94-35481

Materials processing in space tasks. WBS task 5.4: Generic tasks [NASA-CR-193979] p 4249 N94-35485

Field demonstration of X-band photonic antenna remoting in the Deep Space Network p 4252 N94-35545

Self-rescue strategies for EVA crewmembers equipped with the SAFER backpack p 4207 N94-35633

SPACE SURVEILLANCE (SPACEBORNE)

Reduction procedures for accurate analysis of MSX surveillance experiment data p 4203 N94-35611

SPACE TOOLS

Design and simulation of EVA tools for first servicing mission of HST [NASA-CR-196030] p 4298 N94-35266

SPACE TRANSPORTATION

Geostationary space launch vehicles and the US dilemma p 4210 N94-35377

Space and transatmospheric propulsion technology p 4229 N94-36047

SPACE TRANSPORTATION SYSTEM FLIGHTS

STS-58 Space Shuttle Mission Report [NASA-TM-109867] p 4211 N94-35251

STS-51 Space Shuttle Mission Report [NASA-TM-109866] p 4211 N94-35252

SPACEBORNE ASTRONOMY

Hubble Space Telescope cycle 5 call for proposals [NASA-CR-189363] p 4349 N94-36279

SPACEBORNE EXPERIMENTS

Effect of microgravity on plant growth [NASA-CR-196004] p 4296 N94-35257

Results from LDEF experiment A0114: The interaction of atomic oxygen with materials surfaces at orbital altitudes [NASA-CR-196016] p 4235 N94-35388

Purity and cleanness of aerogel as a cosmic dust capture medium p 4247 N94-35469

Participation in the definition, conduct, and analysis of particle accelerator experiments for the first Spacelab Mission [NASA-CR-193974] p 4330 N94-35483

Structural assembly demonstration experiment, phase 1 [NASA-CR-193967] p 4212 N94-35484

Materials processing in space tasks. WBS task 5.4: Generic tasks [NASA-CR-193979] p 4249 N94-35485

Reduction procedures for accurate analysis of MSX surveillance experiment data p 4203 N94-35611

The control of satellites with microgravity constraints: The COMET Control System p 4207 N94-35632

Evaluation of Oxygen Interactions with Materials 3: Mission and induced environments [NASA-TM-109349] p 4236 N94-35680

Microgravity isolation system design: A modern control synthesis framework p 4215 N94-35851

SPACECRAFT ANTENNAS

The Mars Observer Ka-band link experiment p 4255 N94-35563

SPACECRAFT COMMUNICATION

Field demonstration of X-band photonic antenna remoting in the Deep Space Network p 4252 N94-35545

Spacecraft-spacecraft radio-metric tracking: Signal acquisition requirements and application to Mars approach navigation p 4254 N94-35557

The Mars Observer Ka-band link experiment p 4255 N94-35563

SPACECRAFT COMPONENTS

Aerospace applications of magnetic bearings p 4213 N94-35837

SPACECRAFT CONSTRUCTION MATERIALS

Results from LDEF experiment A0114: The interaction of atomic oxygen with materials surfaces at orbital altitudes [NASA-CR-196016] p 4235 N94-35388

Experimental impacts into Teflon targets and LDEF thermal blankets p 4352 N94-36141

SPACECRAFT CONTROL

Automated maneuver planning using a fuzzy logic algorithm p 4203 N94-35610

Overview of the Miniature Sensor Technology Integration (MSTI) spacecraft attitude control system p 4206 N94-35627

A geometric model of a V-slit Sun sensor correcting for spacecraft wobble p 4206 N94-35628

Distributed parameter modelling of flexible spacecraft: Where's the beef? p 4217 N94-35866

Parameter estimation of the vibrational model for the SCOLE experimental facility p 4219 N94-35878

A case study in nonlinear dynamics and control of articulated spacecraft: The Space Station Freedom with a mobile remote manipulator system p 4220 N94-35879

A combined algorithm for minimum time slewing of flexible spacecraft p 4220 N94-35881

Control of the SCOLE configuration using distributed parameter models p 4221 N94-35885

An optimization-based approach for integrated controls-structures design of flexible spacecraft p 4221 N94-35889

Rational positive real approximations for LQG optimal compensators arising in active stabilization of flexible structures p 4222 N94-35892

Software for continuum modeling of controls-structures interactions p 4223 N94-35898

Input shaping for three-dimensional slew maneuvers of a precision pointing flexible spacecraft [DE94-008937] p 4226 N94-36001

SPACECRAFT DESIGN

Materials processing in space tasks. WBS task 5.4: Generic tasks [NASA-CR-193979] p 4249 N94-35485

The control of satellites with microgravity constraints: The COMET Control System p 4207 N94-35632

GPHS-RTGs in support of the Cassini mission [DE94-009994] p 4212 N94-35648

An optimization-based approach for integrated controls-structures design of flexible spacecraft p 4221 N94-35889

SPACECRAFT ELECTRONIC EQUIPMENT

Effects of combined stressing on the electrical properties of film and ceramic capacitors [NASA-TM-106605] p 4257 N94-35249

SPACECRAFT LAUNCHING

Geostationary space launch vehicles and the US dilemma p 4210 N94-35377

SPACECRAFT MAINTENANCE

Design and simulation of EVA tools for first servicing mission of HST [NASA-CR-196030] p 4298 N94-35266

SPACECRAFT ORBITS

High Earth orbit design for lunar assisted small Explorer class missions p 4202 N94-35608

Automated maneuver planning using a fuzzy logic algorithm p 4203 N94-35610

Space Shuttle orbit determination using empirical force modeling of attitude maneuvers for the German MOMS-02/D2 mission p 4207 N94-35634

SPACECRAFT POWER SUPPLIES

GPHS-RTGs in support of the Cassini mission [DE94-009994] p 4212 N94-35648

SPACECRAFT RECOVERY

Attitude stability of a spinning spacecraft during appendage deployment/retraction p 4208 N94-35639

SPACECRAFT STABILITY

A geometric model of a V-slit Sun sensor correcting for spacecraft wobble p 4206 N94-35628

Attitude stability of a spinning spacecraft during appendage deployment/retraction p 4208 N94-35639

SPACECRAFT STRUCTURES

Advances in parameter estimation techniques applied to flexible structures p 4219 N94-35877

Software for continuum modeling of controls-structures interactions p 4223 N94-35898

SPACECRAFT TRACKING

The Mars Observer differential one-way range demonstration p 4210 N94-35543

Spacecraft-spacecraft radio-metric tracking: Signal acquisition requirements and application to Mars approach navigation p 4254 N94-35557

Improved solution accuracy for Landsat-4 (TDRSS-user) orbit determination p 4205 N94-35623

SPACECRAFT TRAJECTORIES

Spacecraft-spacecraft radio-metric tracking: Signal acquisition requirements and application to Mars approach navigation p 4254 N94-35557

Modal decomposition of Hamiltonian variational equations p 4202 N94-35606

Compatibility of TOPEX/Poseidon trajectory propagation with JPL and GSFC/FDF operational software p 4204 N94-35619

Improved solution accuracy for TDRSS-based TOPEX/Poseidon orbit determination p 4205 N94-35620

SPACECREWS

Self-rescue strategies for EVA crewmembers equipped with the SAFER backpack p 4207 N94-35633

SPACELAB

ATLAS solar pointing operations p 4201 N94-35626

SPACELAB PAYLOADS

Participation in the definition, conduct, and analysis of particle accelerator experiments for the first Spacelab Mission [NASA-CR-193974] p 4330 N94-35483

SPACERS

On optimal placement of spacers in bundled conductors p 4258 N94-35354

SPACING

On optimal placement of spacers in bundled conductors p 4258 N94-35354

SPALLATION

Time-of-flight diffraction at pulsed neutron sources: An introduction to the symposium [DE94-010442] p 4327 N94-36225

SPARK IGNITION

A comparison between direct spark ignition and prechamber ignition in an internal combustion engine [DE94-008218] p 4275 N94-36206

SPATIAL DEPENDENCIES

Representing spatial information in a computational model for network management [NASA-CR-191669] p 4306 N94-36040

SPATIAL DISTRIBUTION

Global changes of radiation situation at heights less than 1000 km [DE94-610504] p 4290 N94-35780

SPATIAL RESOLUTION

Ultrafast readout of scintillating fibers using upgraded position-sensitive photomultipliers [DE94-010419] p 4269 N94-36095

SPECIFICATIONS

Robust requirements specifications for safety-critical systems [PB94-167806] p 4250 N94-35532

SPECTRA
High Resolution Transmission Electron Microscopy (HRTEM) of nanophase ferric oxides p 4239 N94-35433

SPECTRAL METHODS
Periodized wavelets [DE94-010365] p 4316 N94-36432

SPECTRAL REFLECTANCE
Absolute calibration and atmospheric versus mineralogic origin of absorption features in 2.0 to 2.5 micron Mars spectra obtained during 1993 p 4356 N94-35404
Wavelength calibration techniques and subtle surface and atmospheric absorption features in the Mariner 6, 7 IRS reflectance data p 4356 N94-35405
Possible spinel absorption bands in S-asteroid visible reflectance spectra p 4368 N94-36139
Hematite formed from pyroxene on Mars by meteoritic impact p 4372 N94-36165
Moessbauer mineralogy of calcined Murchison meteorite p 4353 N94-36166

SPECTRAL SIGNATURES
The effects of cloud inhomogeneities upon radiative fluxes, and the supply of a cloud truth validation dataset [NASA-CR-196080] p 4293 N94-35391
Thermal emission measurements (5-25 microns) of Hawaiian palagonitic soils with implications for Mars p 4292 N94-35452

SPECTRAL THEORY
Determination of extensional viscosity from capillary rheometer entrance pressure drop measurements using a numerical simulation of contraction flow [PB94-171154] p 4263 N94-35603

SPECTROGRAPHS
Hubble Space Telescope Goddard High Resolution Spectrograph (GHRS) Instrument Handbook (for the Post-COSTAR Observatory), version 5.0 [NASA-CR-189369] p 4349 N94-36282

SPECTROMETERS
Instrumentation for in-flight SSME rocket engine plume spectroscopy [NASA-TM-106596] p 4268 N94-35268
Innovative instrumentation for mineralogical and elemental analyses of solid extraterrestrial surfaces: The Backscatter Moessbauer Spectrometer/X Ray Fluorescence analyzer (BaMS/XRF) p 4239 N94-35459
An indigenously developed photoacoustic spectrometer for study of actinide spectroscopy [DE94-616508] p 4235 N94-35592

SPECTROPHOTOMETRY
A quick look method of detecting water of hydration in small solar system bodies p 4352 N94-35470

SPECTROSCOPIC ANALYSIS
Instrumentation for in-flight SSME rocket engine plume spectroscopy [NASA-TM-106596] p 4268 N94-35268

SPECTROSCOPY
Study on contaminants on flight and other critical surfaces [NASA-CR-193975] p 4235 N94-35447
Mercury: Mid-infrared (7.3 - 13.5 microns) spectroscopic observations showing features characteristic of plagioclase p 4370 N94-36150
X ray and gamma ray spectroscopy of solids under pressure [DE94-011207] p 4238 N94-36203

SPECTRUM ANALYSIS
Absolute calibration and atmospheric versus mineralogic origin of absorption features in 2.0 to 2.5 micron Mars spectra obtained during 1993 p 4356 N94-35404
Wavelength calibration techniques and subtle surface and atmospheric absorption features in the Mariner 6, 7 IRS reflectance data p 4356 N94-35405
The temperature of nitrogen on Pluto p 4365 N94-35468
ROSAT/XRT-PSPC observations and the ionizing continuum of Seyfert 1 galaxy Mkn 478 [PB94-167053] p 4350 N94-35530
Ferromagnetic resonance spectra of H2-reduced minerals and glasses p 4240 N94-36164
Studies of the dayside boundary layer processes based on ground observations in the Svalbard area [AD-A280715] p 4292 N94-36265
SYNTH: A spectrum synthesizer [DE94-004719] p 4331 N94-36317

SPEECH RECOGNITION
Clustering techniques in speaker recognition [AD-A278676] p 4255 N94-35689

SPHERICAL TANKS
Experimental results of hydrogen slosh in a 62 cubic foot (1750 liter) tank [NASA-TM-106625] p 4263 N94-35250

SPHEROMAKS
Power balance and characterization of impurities in the Maryland Spheromak, part 2 [DE94-009603] p 4335 N94-35670

SPIN
Spin effects in high energy quark-quark scattering [DE94-616800] p 4330 N94-36080

SPIN DYNAMICS
Spin dynamics in storage rings and linear accelerators [DE94-010320] p 4330 N94-36106

SPIN REDUCTION
Overview of the Miniature Sensor Technology Integration (MSTI) spacecraft attitude control system p 4206 N94-35627

SPIN STABILIZATION
A geometric model of a V-slit Sun sensor correcting for spacecraft wobble p 4206 N94-35628

SPINDLES
Design, construction, and testing of a five active axes magnetic bearing system p 4214 N94-35846

SPINEL
Possible spinel absorption bands in S-asteroid visible reflectance spectra p 4368 N94-36139

SPLINE FUNCTIONS
TransFit: Finite element analysis data fitting software [NASA-CR-193988] p 4307 N94-36118

SPONTANEOUS EMISSION
Fluorescence detection of single molecules using pulsed near-field optical excitation and time correlated photon counting [DE94-007553] p 4320 N94-35376

SPRAY CHARACTERISTICS
Analysis of a High Velocity Oxygen-Fuel (HVOF) thermal spray torch. Part 1: Numerical formulation [DE94-005590] p 4267 N94-35996
Application of higher-order multipoint statistics to the ideal spray [DE94-005104] p 4268 N94-36318

SPRAYED COATINGS
Defect detection in multi-layered, plasma sprayed zirconia by time resolved infrared radiometry: A comparison between analytical and experimental methods [DE94-009803] p 4245 N94-35779

SPRAYERS
Fundamental studies in blow-down and cryogenic cooling [AD-A278967] p 4250 N94-35524
Analysis of a High Velocity Oxygen-Fuel (HVOF) thermal spray torch. Part 1: Numerical formulation [DE94-005590] p 4267 N94-35996

SPREAD F
Measurements of spatial and frequency coherence of an equatorial hf path during spread-F [DE93-016615] p 4257 N94-36316

SQUID (DETECTORS)
Report on a SQUID made from high temperature superconductor [PB94-169307] p 4339 N94-35598
Magnetic properties of nanosize iron clusters [DE94-011329] p 4318 N94-36204

STABILITY
A note on high order schemes for one dimensional wave equation [PB94-171006] p 4315 N94-35821
Numerical method to study the stability of periodic solutions of particle motion in nonlinear magnetic fields [DE94-610740] p 4325 N94-36088
Local instabilities and the transition to chaos of non-linear waves [PB94-170578] p 4341 N94-36213
Non-linear interaction of gravity waves with average jet flows, instabilities, and turbulence [PB94-170586] p 4291 N94-36214
Formation and stability of Fe-rich precipitates in dilute Zr(Fe) single-crystal alloys [DE94-619027] p 4242 N94-36288
Impedance and instability threshold estimates in the main injector 1 [DE94-010332] p 4332 N94-36431

STABILIZATION
Concurrent stabilization and imaging of a novel polymer for second harmonic generation via in situ photopolymerization [AD-A278912] p 4243 N94-35588
Estimation with multisensor/multiscan detection fusion [AD-A278753] p 4256 N94-36092

STAINLESS STEELS
Plane shock generator explosive lens: Shock characterization of 4340 and PH13-8Mo steels, C360 brass and PZT 65/35 ferro-electric ceramic [DE94-009254] p 4266 N94-35979

STANDARD DEVIATION
Process capability determination of new and existing equipment p 4230 N94-36406

STANDARDS
Minimum performance standards: Airborne low-range radar altimeters [RTCA-DO-155] p 4198 N94-35344
Software architecture standard for simulation virtual machine, version 2.0 [NASA-CR-188291] p 4301 N94-35443

STAR TRACKERS
Fixed-head star tracker attitude updates on the Hubble Space Telescope p 4203 N94-35612
In-flight scale/distortion calibration of the Hubble Space Telescope fixed-head star trackers p 4203 N94-35613
Operational support for Upper Atmosphere Research Satellite (UARS) attitude sensors p 4204 N94-35617
Spacecraft attitude determination accuracy from mission experience p 4204 N94-35618
Application of star identification using pattern matching to space ground systems at GSFC p 4209 N94-35640
Color/magnitude calibration for National Aeronautics and Space Administration (NASA) standard Fixed-Head Star Trackers (FHST) p 4209 N94-35641

STATE ESTIMATION
Comparison of Kalman filter and optimal smoother estimates of spacecraft attitude p 4208 N94-35638
Advantages of estimating rate corrections during dynamic propagation of spacecraft rates: Applications to real-time attitude determination of SAMPEX p 4209 N94-35642
MME-based attitude dynamics identification and estimation for SAMPEX p 4209 N94-35643
Motion models in attitude estimation p 4210 N94-35646

STATE VECTORS
Overview of the MSTI 2 on-orbit alignment p 4206 N94-35629
Advantages of estimating rate corrections during dynamic propagation of spacecraft rates: Applications to real-time attitude determination of SAMPEX p 4209 N94-35642

STATIC LOADS
Hydrodynamically induced loads on components submerged in high-level waste-storage tanks [DE94-009663] p 4264 N94-35756

STATISTICAL ANALYSIS
Point and interval estimation of series system reliability using small data sets [AD-A278647] p 4316 N94-35575
Improved solution accuracy for TDRSS-based TOPEX/Poseidon orbit determination p 4205 N94-35620
Environmental Monitoring and Assessment Program assessment framework [PB94-158862] p 4285 N94-35741
Activity report 1990-1992 and proceedings, volume 1 [DE94-610480] p 4290 N94-35830
The development of a statistical report software for computer system usages [DE94-611061] p 4346 N94-35832
A comparison of artificial neural networks and statistical analyses [DE94-010846] p 4312 N94-36195
Application of higher-order multipoint statistics to the ideal spray [DE94-005104] p 4268 N94-36318

STATISTICAL DISTRIBUTIONS
Application of a Monte Carlo accuracy assessment tool to TDRS and GPS p 4207 N94-35635

STEADY STATE
Three-photon micromasers [DE94-611106] p 4272 N94-35782
Uniqueness of a solution of a steady state photochemical problem: Applications to Mars p 4370 N94-36151

STEAM
Combined SO(x)/NO(x) control via SOXAL (tm) process: An electrodialytic regenerative wet scrubbing process [DE94-009053] p 4284 N94-35346

STEELS
Testing of the fracture resistance of rails p 4279 N94-35353
The electrical conductivities of candidate beam-waveguide antenna shroud materials p 4252 N94-35546

STEERABLE ANTENNAS
Switched-beam radiometer front-end network analysis [NASA-CR-194922] p 4252 N94-35247

STELLAR COLOR
Color/magnitude calibration for National Aeronautics and Space Administration (NASA) standard Fixed-Head Star Trackers (FHST) p 4209 N94-35641

STELLAR COMPOSITION
Stellar alchemy: The origin of the chemical elements [DE94-011903] p 4350 N94-36229

STELLAR EVOLUTION
Ferromagnetic resonance spectra of H2-reduced minerals and glasses p 4240 N94-36164
Stellar alchemy: The origin of the chemical elements [DE94-011903] p 4350 N94-36229

STELLAR MAGNITUDE
Color/magnitude calibration for National Aeronautics and Space Administration (NASA) standard Fixed-Head Star Trackers (FHST) p 4209 N94-35641
STELLAR MASS EJECTION
Catalog of Helios 90 deg photometer events
[PL-TR-94-2040] p 4375 N94-36264
STELLAR PHYSICS
Stellar alchemy: The origin of the chemical elements
[DE94-011903] p 4350 N94-36229
STELLAR SPECTRA
Ferromagnetic resonance spectra of H2-reduced minerals and glasses p 4240 N94-36164
STELLARATORS
Particle orbit analysis for LHD helical axis configurations
[DE94-718995] p 4336 N94-35773
Neoclassical current and related MHD stability, gap modes, and radial electric field effects in heliotron and torsatron plasmas
[DE94-718987] p 4337 N94-35938
Improved models of beta-limit, anomalous transport and radial electric field with loss cone loss in heliotron/torsatron
[DE94-718976] p 4324 N94-35984
Design study of LHD helical divertor and high temperature divertor plasma operation
[DE94-718975] p 4338 N94-36352
MHD and confinement characteristics in the high-beta regime on the CHS low-aspect-ratio heliotron/torsatron
[DE94-718981] p 4339 N94-36357
STEPPING MOTORS
Magnetically suspended stepping motors for clean room and vacuum environments p 4225 N94-35915
STIFFENING
Fatigue and residual strength behaviour of ARALL3 panels with bonded-on doublers
[AD-B181062] p 4279 N94-36226
STIFFNESS MATRIX
Distributed parameter modeling of repeated truss structures p 4218 N94-35868
STIRLING CYCLE
A precise passive narrow-beam filter infrared radiometer and its use with LIDAR in the ARM program
[DE94-004167] p 4269 N94-36085
STOCHASTIC PROCESSES
Developing interpretable models with optimized set reduction for identifying high risk software components
p 4301 N94-35435
Stopping rules for a class of sampling-based stochastic programming algorithms
[AD-A278654] p 4303 N94-35577
Cramer-von Mises variance estimators for simulations
[AD-A278799] p 4316 N94-35675
Effects of noise variance model on optimal feedback design and actuator placement p 4220 N94-35883
STONY-IRON METEORITES
More shock recovery experiments on mesosiderite analogs p 4351 N94-35455
STORAGE RINGS (PARTICLE ACCELERATORS)
Spin dynamics in storage rings and linear accelerators
[DE94-010320] p 4330 N94-36106
Dynamic aperture and transverse proton diffusion in HERA
[DE94-010309] p 4331 N94-36224
STORAGE STABILITY
Unleaded AVGAS program
[AD-A278650] p 4247 N94-35795
STORAGE TANKS
Decision and systems analysis for underground storage tank waste retrieval systems and tank waste remediation system
[SAND94-0065] p 4286 N94-35957
STORMS (METEOROLOGY)
Extrapolating storm location using the Integrated Terminal Weather System (ITWS) storm motion algorithm
[AD-A278611] p 4295 N94-36249
STRAKES
F/A-18 forebody vortex control. Volume 1: Static tests
[NASA-CR-4582] p 4190 N94-35991
STRANGENESS
A quark model of bar Lambda production in bar Rho interactions
[DE94-008071] p 4324 N94-35824
STRATIFIED FLOW
JPRS report: Science and technology. Central Eurasia
[JPRS-UST-94-006] p 4249 N94-35226
STREAK CAMERAS
Neutron detectors for fusion reaction-rate measurements
[DE94-010407] p 4330 N94-36114
Streak tube photocathode development program
[DE94-009905] p 4270 N94-36350
STRESS (PHYSIOLOGY)
Stress and brain protein synthesis
[PB94-170750] p 4296 N94-35601
STRESS ANALYSIS
Can the compressive response of fiber-reinforced composites be modelled by means of layered arrays?
[AD-A278864] p 4233 N94-35944
Propellant stress relief groove for the Titan 4 SRMU
[AD-A278628] p 4228 N94-36254
STRESS CONCENTRATION
Graphing techniques for materials laboratory using Excel p 4232 N94-36414
STRESS INTENSITY FACTORS
Frequency domain analysis of the random loading of cracked panels
[NASA-CR-196021] p 4279 N94-35974
STRESS-STRAIN RELATIONSHIPS
Graphing techniques for materials laboratory using Excel p 4232 N94-36414
STRONTIUM TITANATES
Dielectric measurements of selected ceramics at microwave frequencies p 4232 N94-36412
STRUCTURAL ANALYSIS
Aspects of robust computational modeling for plain and reinforced concrete
[PB94-169240] p 4251 N94-35820
Integrated design of structures, controls, and materials
p 4218 N94-35869
Neutron diffraction study of aluminum chloride imidazolium chloride molten salts
[DE94-009679] p 4239 N94-36349
STRUCTURAL BASINS
Impact basins in Southern Daedalia, Mars: Evidence for clustered impactors? p 4360 N94-35426
Effects due to overlapping large impact basins on Mars p 4360 N94-35427
Noachian and Hesperian modification of the original Chryse impact basin topography p 4364 N94-35462
STRUCTURAL DESIGN
Integrated design of structures, controls, and materials
p 4218 N94-35869
An optimization-based approach for integrated controls-structures design of flexible spacecraft
p 4221 N94-35889
Application of sequential quadratic programming to large-scale structural design problems
[AD-A278574] p 4307 N94-36185
High Altitude Long Endurance aircraft design studies
p 4193 N94-36322
STRUCTURAL ENGINEERING
Earthquake Engineering Research Center: 25th anniversry edition
[PB94-160645] p 4291 N94-36019
STRUCTURAL RELIABILITY
Collection, processing, and reporting of damage tolerant design data for non-aerospace structural materials
[NASA-CR-196046] p 4347 N94-36435
STRUCTURAL STABILITY
Alleviation of whirl-flutter on a joined-wing tilt-rotor aircraft configuration using active controls
[NASA-CR-196103] p 4200 N94-36436
STRUCTURAL VIBRATION
Optimal disturbance rejecting control of hyperbolic systems p 4220 N94-35882
Transfer function modeling of damping mechanisms in distributed parameter models p 4222 N94-35895
Software for continuum modeling of controls-structures interactions p 4223 N94-35898
Frequency domain analysis of the random loading of cracked panels
[NASA-CR-196021] p 4279 N94-35974
STRUTS
The reduction of takeoff ground roll by the application of a nose gear jump strut
[NASA-TM-108822] p 4198 N94-36380
STUDENTS
NASA/DOD Aerospace Knowledge Diffusion Research Project. Paper 40: Technical communications in aerospace education: A study of AIAA student members
[NASA-TM-109868] p 4344 N94-35254
SUBMERGING
Piggyback balance experiment: An illustration of Archimedes' principles and Newton's third law
[PB94-163060] p 4265 N94-35942
SUBROUTINE LIBRARIES (COMPUTERS)
Review of Mathematical Function Library for Microsoft-FORTRAN, John Wiley and Sons, 1989
[PB94-160793] p 4305 N94-36010
SUBROUTINES
Description and use of LSODE, the Livermore Solver for Ordinary Differential Equations
[NASA-RP-1327] p 4313 N94-35259
SUBSONIC FLUTTER
Alleviation of whirl-flutter on a joined-wing tilt-rotor aircraft configuration using active controls
[NASA-CR-196103] p 4200 N94-36436
SUBSONIC SPEED
Wind tunnel measurements on a full-scale F/A-18 with a tangentially blowing slot --- conducted in the Ames 80 by 120 foot wind tunnel p 4191 N94-35965
SUBSONIC WIND TUNNELS
Langley 14- by 22-foot subsonic tunnel test engineer's data acquisition and reduction manual
[NASA-TM-4563] p 4189 N94-35246
SUBSTRATES
Morphological aspects of surface reactions
[DE94-010184] p 4236 N94-35685
Thick film fabrication of aluminum nitride microcircuits
[DE94-010107] p 4259 N94-35706
Study and fabrication of GaSb-based laser heterostructures
[PB94-170677] p 4273 N94-36218
Effect of niobium interlayer on high-temperature sliding friction and wear of silver films on alumina
[DE94-010462] p 4275 N94-36232
Demonstration of a high heat removal CVD diamond substrate edge-cooled multichip module
[DE94-010748] p 4260 N94-36245
SULFATES
Modeling the atmospheric input of nutrients, heavy metals, and pesticides to the Great Lakes
[DE94-005481] p 4286 N94-36007
Anthropogenic sulfate and organic aerosols, CCN, and cloud project concentration at a marine site
[DE94-004210] p 4286 N94-36025
SULFIDES
Gasoline from natural gas by sulfur processing
[DE94-011130] p 4248 N94-36035
Preliminary results of sulfide melt/silicate wetting experiments in a partially melted ordinary chondrite
p 4353 N94-36147
SULFUR
Antarctic weathering of the CK chondrites EET90004, 90007, and 90022: Nickel and sulfur mobility
p 4351 N94-35451
SULFUR DIOXIDES
Combined SO(x)/NO(x) control via SOXAL (tm) process: An electrodialytic regenerative wet scrubbing process
[DE94-009053] p 4284 N94-35346
State-to-state dynamics of molecular energy transfer
[DE94-009651] p 4324 N94-35816
Air quality implications associated with the selection of power plants in the Pacific Northwest
[DE94-004783] p 4287 N94-36027
Treatment of toxic gases SO2 and NO(x) by electron beam irradiation
[DE94-615424] p 4330 N94-36028
SULFURIC ACID
H2O-H2SO4 system in Venus' clouds and OCS, CO, and H2SO4 profiles in Venus' troposphere
p 4370 N94-36152
SUM RULES
Leptonic decay constants of heavy quarkonia in effective QCD sum rules
[DE94-611160] p 4322 N94-35784
SUN
Formation of iron metal and grain coagulation in the solar nebula p 4373 N94-36170
On the physics of waves in the solar atmosphere: Wave heating and wind acceleration
[NASA-CR-194119] p 4375 N94-36395
SUPERCONDUCTING FILMS
Report on a SQUID made from high temperature superconductor
[PB94-169307] p 4339 N94-35598
Flux-pinning related defects in YBa2Cu3O(7-x) thin films grown on miscut LaAlO3 (001) substrates
[DE94-011463] p 4342 N94-36377
SUPERCONDUCTING MAGNETS
Second International Symposium on Magnetic Suspension Technology, part 1
[NASA-CP-3247-PT-1] p 4212 N94-35836
System concept definition of the Grumman superconducting Electromagnetic Suspension (EMS) Maglev design p 4213 N94-35840
Measurement and characterization of force dynamics in high T(sub c) superconductors p 4214 N94-35844
Superconducting Electromagnetic Suspension (EMS) system for Grumman Maglev concept
p 4215 N94-35849
Second International Symposium on Magnetic Suspension Technology, part 2
[NASA-CP-3247-PT-2] p 4223 N94-35902
Concepts of flywheels for energy storage using autostable high-T(sub c) superconducting magnetic bearings p 4224 N94-35909
Models for interpreting interstrand resistance measurements in Rutherford cables
[DE94-010844] p 4259 N94-36194

SUPERCONDUCTING SUPER COLLIDER
Models for interpreting interstrand resistance measurements in Rutherford cables
[DE94-010844] p 4259 N94-36194

SUPERCONDUCTIVITY
Superconducting rebalance acceleration and rate sensor p 4223 N94-35904
Feasibility study of superconducting LSM rocket launcher system p 4225 N94-35914
Distance dependent fractional statistics in a P, T-invariant model
[DE94-617360] p 4325 N94-36083
Superconducting transistors
[PB94-170743] p 4260 N94-36260
A new family of superconducting fullerides, Na(NH3)(x)C60(x = 2-8)
[DE94-011480] p 4341 N94-36272
Temperature dependence of superconduction bands in HTSC
[DE94-617361] p 4341 N94-36312
Pairing and low temperature properties of 2D Fermi-systems with attraction between particles
[DE94-615510] p 4329 N94-36434

SUPERCONDUCTORS
Data reduction, analysis and results of LACV-30-07 air cushion vehicle tests, Fort Story, VA, August - September 1993
[AD-A278859] p 4190 N94-35826
Continuum fluorescence of Cu in NbTi/Cu composite wires
[DE94-008940] p 4241 N94-36242
A new family of superconducting fullerides, Na(NH3)(x)C60(x = 2-8)
[DE94-011480] p 4341 N94-36272

SUPERCRITICAL FLUIDS
Dynamic structural effects and ultrafast biomolecular kinetics in photoinduced charge transfer reactions
[DE94-010421] p 4329 N94-36390

SUPERFLUIDITY
Spatio-temporal properties of centrifugal instabilities: Abstracts of 8th Couette-Taylor Meeting
[PB94-150240] p 4266 N94-35981
On possible types of vortexes in relativistic superfluid system
[DE94-617392] p 4267 N94-36098
Taking into account dissipative processes in relativistic superfluid systems
[DE94-617391] p 4267 N94-36313
First, second and fourth sound in relativistic superfluidity theory with account for dissipative effects
[DE94-617393] p 4267 N94-36314

SUPERHIGH FREQUENCIES
Field demonstration of X-band photonic antenna remoting in the Deep Space Network
p 4252 N94-35545
DSS-13 S-/X-band microwave feed system
p 4253 N94-35550
The Mars Observer Ka-band link experiment
p 4255 N94-35563
Analysis of recent agile mirror data
[AD-A278758] p 4318 N94-36427

SUPERLATTICES
The optimization of interfaces in InAsSb/InGaAs strained-layer superlattices grown by metal-organic chemical vapor deposition
[DE94-010070] p 4340 N94-35698
Activities of the optoelectronics laboratory
[PB94-171196] p 4334 N94-36190

SUPERNOVAE
A search for radiative neutrino decay from supernovae
[NASA-CR-196011] p 4376 N94-35515

SUPERSONIC BOUNDARY LAYERS
Expansion effects on supersonic turbulent boundary layers
[AD-A278989] p 4190 N94-35950

SUPERSONIC COMBUSTION
AFOSR Contractors Propulsion Meeting
[AD-A279028] p 4198 N94-35746

SUPERSONIC FLOW
A review and development of correlations for base pressure and base heating in supersonic flow
[SAND93-0280] p 4189 N94-35360
A supersonic tunnel for laser and flow-seeding techniques
[NASA-TM-106588] p 4265 N94-35945
Recovery of frozen flow losses in arcjets
[AD-A278739] p 4228 N94-36089

SUPERSONIC INLETS
Computational methods for HSCT-inlet controls/CFD interdisciplinary research
[NASA-TM-106618] p 4198 N94-35352

SUPERSONIC JET FLOW
Boundary conditions for jet flow computations
[NASA-TM-106648] p 4266 N94-35976
An experimental investigation of active control of thrust vectoring nozzle flow fields
[AD-A278702] p 4229 N94-36291

SUPERSONIC NOZZLES
A supersonic tunnel for laser and flow-seeding techniques
[NASA-TM-106588] p 4265 N94-35945

SUPERSONIC SPEED
Expansion effects on supersonic turbulent boundary layers
[AD-A278989] p 4190 N94-35950
An experimental investigation of active control of thrust vectoring nozzle flow fields
[AD-A278702] p 4229 N94-36291

SUPERSONIC TRANSPORTS
Computational methods for HSCT-inlet controls/CFD interdisciplinary research
[NASA-TM-106618] p 4198 N94-35352
Future supersonic commercial transport aircraft: A technological challenge for long haul traffic
p 4193 N94-36324

SUPERSONIC WIND TUNNELS
A supersonic tunnel for laser and flow-seeding techniques
[NASA-TM-106588] p 4265 N94-35945

SUPERSYMMETRY
Proceedings of 2nd Working meeting: Physics at VLEPP, volume 1
[DE94-616200] p 4320 N94-35569
Universal SU(2/1) and the Higgs and fermion masses
[DE94-009182] p 4323 N94-35814
Exact multiplicities in the three-anion spectrum
[DE94-616768] p 4325 N94-36075
Proceedings of 2nd Working Meeting on Physics at VLEPP, volume 2
[DE94-616167] p 4326 N94-36182
N = 4 supersymmetry from the quantum affine algebra U(sub q)(A-circumflex(sup 1)(sub 3))
[DE94-611145] p 4317 N94-36307

SUPPORTS
The electrical conductivities of candidate beam-waveguide antenna shroud materials
p 4252 N94-35546

SURFACE DIFFUSION
Large scale atomistic first principles study of adsorption and surface diffusion
[DE94-009450] p 4322 N94-35682

SURFACE DISTORTION
TransFit: Finite element analysis data fitting software
[NASA-CR-193988] p 4307 N94-36118

SURFACE EMITTING LASERS
Phase-locked arrays of vertical-cavity surface-emitting lasers
[DE94-009279] p 4272 N94-36178

SURFACE PROPERTIES
Block distributions on the lunar surface: A comparison between measurements obtained from surface and orbital photography p 4359 N94-35419
Exopaleontology and the search for a fossil record on Mars p 4360 N94-35425
Innovative instrumentation for mineralogical and elemental analyses of solid extraterrestrial surfaces: The Backscatter Moessbauer Spectrometer/X Ray Fluorescence analyzer (BaMS/XRF)
p 4239 N94-35459

SURFACE REACTIONS
Morphological aspects of surface reactions
[DE94-010184] p 4236 N94-35685
Chemical reactions of chlorine on a vicinal Si(100) surface studied by ESDIAD
[AD-A279059] p 4236 N94-35731
Heterogeneous reaction mechanisms and kinetics relevant to the CVD of semiconductor materials
[DE94-011001] p 4340 N94-36032

SURFACE ROUGHNESS
Mesoscale roughness of Venus p 4361 N94-35430

SURFACE TEMPERATURE
Multiwavelength pyrometer for gray and non-gray surfaces in the presence of interfering radiation
[NASA-CASE-LEW-15250-1] p 4269 N94-35383
The temperature of nitrogen on Pluto
p 4365 N94-35468
Measurement of a surface heat flux and temperature
p 4231 N94-36407

SURFACE TREATMENT
Microporous structure with layered interstitial surface treatment, and method and apparatus for preparation thereof
[NASA-CASE-MSC-21487-3] p 4235 N94-35229
The electrical conductivities of candidate beam-waveguide antenna shroud materials
p 4252 N94-35546
Processing and properties of high temperature metal/fiber-reinforced-thermoplastic laminates
[AD-A278791] p 4232 N94-35654

SURFACE WATER
Fluvial processes in Ma'adim Vallis and the potential of Gusev crater as a high priority site
p 4358 N94-35414
Exopaleontology and the search for a fossil record on Mars p 4360 N94-35425

SURVEYS
A 1- to 10-GHz downconverter for high-resolution microwave survey p 4253 N94-35551
Good applications for crummy machine translation
[AD-A278689] p 4345 N94-35651

SUSPENSION SYSTEMS (VEHICLES)
System concept definition of the Grumman superconducting Electromagnetic Suspension (EMS) Maglev design p 4213 N94-35840
Transrapid (the first high-speed Maglev train system certified ready for application): Development status and prospects for deployment p 4213 N94-35841
Control of maglev vehicles with aerodynamic and guideway disturbances p 4213 N94-35842
Fault tolerant computer control for a Maglev transportation system p 4215 N94-35848
Superconducting Electromagnetic Suspension (EMS) system for Grumman Maglev concept
p 4215 N94-35849

SWEPT WINGS
The reduction of takeoff ground roll by the application of a nose gear jump strut
[NASA-TM-108822] p 4198 N94-36380

SWITCHES
Experimental and theoretical studies of a high temperature cesium-barium tacitron, with application to low voltage-high current inversion
[DE94-008182] p 4228 N94-35349
Molecular systems for ultrafast optical switching: Controlling electron transfer reactions with femtosecond laser pulses
[DE94-009695] p 4332 N94-35671

SWITCHING
Experimental and theoretical studies of a high temperature cesium-barium tacitron, with application to low voltage-high current inversion
[DE94-008182] p 4228 N94-35349

SWITCHING CIRCUITS
Switched-beam radiometer front-end network analysis
[NASA-CR-194922] p 4252 N94-35247

SYMBOLIC PROGRAMMING
Combining symbolic computation and theorem proving: Some problems of Ramanujan
[AD-A278899] p 4303 N94-35573
Computationally efficient multibody simulations
p 4222 N94-35896

SYNCHRONISM
Runtime support for data parallel tasks
[NASA-CR-194904] p 4300 N94-35240
The weakest failure detector for solving Consensus
[NASA-CR-190545] p 4300 N94-35365
Mathematical theory of synchronous communication
[PB94-169224] p 4252 N94-35537
Obtaining coincident image observations for Mission to Planet Earth science data return p 4202 N94-35609
Synthesis of asynchronous systems from data flow specifications
[AD-A278687] p 4303 N94-35662

SYNCHRONOUS MOTORS
Feasibility study of superconducting LSM rocket launcher system p 4225 N94-35914

SYNCHRONOUS PLATFORMS
Geostationary space launch vehicles and the US dilemma p 4210 N94-35377

SYNCHROTRON RADIATION
Integral characteristics of the magnetic bremsstrahlung
[DE94-616788] p 4256 N94-36078
X ray and gamma ray spectroscopy of solids under pressure
[DE94-011207] p 4238 N94-36203
In situ studies of zeolite syntheses using powder diffraction methods: Crystallization of instant zeolite A powder and CoAPO-5
[DE94-006570] p 4341 N94-36358

SYNCHROTRONS
Activities of the optoelectronics laboratory
[PB94-171196] p 4334 N94-36190
X ray and gamma ray spectroscopy of solids under pressure
[DE94-011207] p 4238 N94-36203

SYNTAX
Probabilities and priorities in timed CSP
[PB94-169216] p 4316 N94-35536
Mathematical theory of synchronous communication
[PB94-169224] p 4252 N94-35537
Refinement types ML
[AD-A278937] p 4304 N94-35709

SYNTHESIS (CHEMISTRY)
Be3(AsO4)2.2H2O, a new berylloarsenate phase containing bridged tetrahedral 3-rings
[AD-A278826] p 4340 N94-35677
Third European Technical Symposium on Polyimides and High Performance Polymers: STEPI 3
[PB94-148491] p 4246 N94-36177

SYNTHESIZERS
High-speed digital project, HSD test capability
[DE94-010885] p 4260 N94-36197
SYNTH: A spectrum synthesizer
[DE94-004719] p 4331 N94-36317

SYNTHETIC APERTURE RADAR
Quantifying shapes of volcanoes on Venus
p 4361 N94-35429
Insight to global change: EOS/SAR mission
[NASA-CR-196133] p 4284 N94-35503
Evaluation of synthetic aperture radar for oil-spill response
[AD-A278796] p 4284 N94-35674
Controller for the Electronically Scanned Thinned Array Radiometer (ESTAR) instrument
[NASA-TM-104608] p 4259 N94-36049

SYNTHETIC FUELS
Heterogeneous catalytic process for alcohol fuels from syngas
[DE94-010263] p 4248 N94-36299

SYSTEM EFFECTIVENESS
The Federal Aviation Administration plan for research, engineering and development p 4376 N94-35262
An analysis of operational suitability for test and evaluation of highly reliable systems
[AD-A278573] p 4192 N94-36184

SYSTEM FAILURES
Flight testing a propulsion-controlled aircraft emergency flight control system on an F-15 airplane
[NASA-TM-4590] p 4199 N94-35258
Asynchronous optimistic rollback recovery using secure distributed time
[AD-A278978] p 4344 N94-35526

SYSTEM IDENTIFICATION
Defense RDT and E online system (DROLS) retrieval reference guide
[AD-A278972] p 4344 N94-35525
Advances in parameter estimation techniques applied to flexible structures p 4219 N94-35877
An overview of recent advances in system identification p 4220 N94-35880

SYSTEMS ANALYSIS
Developing software for ease of change: Metrics from later in the TRALAB system life cycle
[AD-A278759] p 4302 N94-35490
Decision and systems analysis for underground storage tank waste retrieval systems and tank waste remediation system
[SAND94-0065] p 4286 N94-35957

SYSTEMS ENGINEERING
Materials processing in space tasks. WBS task 5.4: Generic tasks
[NASA-CR-193979] p 4249 N94-35485
ORDIT: A new methodology to assist in the process of eliciting and modelling organisational requirements
[PB94-167814] p 4345 N94-35533
DSS-13 S-/X-band microwave feed system
p 4253 N94-35550

SYSTEMS INTEGRATION
Terminal Doppler Weather Radar (TDWR) Low Level Wind Shear Alert System 3 (LLWAS 3) integration studies at Orlando International Airport
[AD-A278957] p 4294 N94-35807
North American ISDN Users' Forum agreements on Integrated Services Digital Network
[PB94-162559] p 4305 N94-35940
Fuel Cell Handbook update
[DE94-002958] p 4282 N94-36021
Multidisciplinary studies of integrated neural network systems
[AD-A278774] p 4312 N94-36309

T

TABS (CONTROL SURFACES)
Numerical investigation of multi-element airfoils
[NASA-CR-194592] p 4191 N94-36394

TAKEOFF
Direct reduced order mixed H2/H infinity control for the Short Take-Off and Landing/Maneuver Technology Demonstrator (STOL/MTD)
[AD-A278675] p 4199 N94-35796
The reduction of takeoff ground roll by the application of a nose gear jump strut
[NASA-TM-108822] p 4198 N94-36380

TANDEM MIRRORS
Potential formation and transport in open field line systems
[DE94-718910] p 4337 N94-35983

TANKER AIRCRAFT
Future tanker considerations and requirements
p 4197 N94-36342
Tanker system and technology requirements definition: A tanker technology road map p 4197 N94-36344
Hose-drogue versus boom receptacle air refueling
p 4197 N94-36345
The KDC-10 programme of the Royal Netherlands Air Force p 4197 N94-36346
CC-130H(T) tactical aerial refuelling tanker development flight test programme p 4198 N94-36347

TANTALUM COMPOUNDS
Vertical electron detachment energies for octahedral closed-shell multiply charged anions
[AD-A278835] p 4322 N94-35753

TARGET RECOGNITION
Color-coded radar plan position indicator
[AD-D016200] p 4257 N94-36364

TARGETS
Inertial confinement fusion target component fabrication and technology development report
[DE94-009973] p 4335 N94-35673

TASK COMPLEXITY
Attention and signal detection. A study of attention divided between visual and auditory signals
[PB94-170594] p 4298 N94-36215

TASKS
Refinement types ML
[AD-A278937] p 4304 N94-35709

TAXONOMY
A taxonomy of coordination mechanisms used in real-time software based on domain analysis
[AD-A279014] p 4304 N94-35794

TAYLOR INSTABILITY
Spatio-temporal properties of centrifugal instabilities: Abstracts of 8th Couette-Taylor Meeting
[PB94-150240] p 4266 N94-35981

TDR SATELLITES
Improved solution accuracy for TDRSS-based TOPEX/Poseidon orbit determination
p 4205 N94-35620
Improved solution accuracy for Landsat-4 (TDRSS-user) orbit determination p 4205 N94-35623
Optimum satellite relay positions with application to a TDRS-1 Indian Ocean relay p 4205 N94-35624
TDRSS Onboard Navigation System (TONS) flight qualification experiment p 4206 N94-35625
Application of a Monte Carlo accuracy assessment tool to TDRS and GPS p 4207 N94-35635

TEARING MODES (PLASMAS)
Collisonless dynamics of the magnetosphere
[AD-A278886] p 4290 N94-35708

TECHNICAL WRITING
Using International English to prepare technical text for translation
[DE94-002628] p 4347 N94-36102

TECHNOLOGIES
JPRS report: Science and technology. Central Eurasia
[JPRS-UST-94-006] p 4249 N94-35226
JPRS report: Science and technology. Central Eurasia
[JPRS-UST-94-001] p 4229 N94-35340
JPRS report: Science and technology. Central Eurasia
[JPRS-UST-94-004] p 4249 N94-35341
JPRS report: Science and technology. Central Eurasia
[JPRS-UST-94-005] p 4249 N94-35342
JPRS report: Science and technology. Central Eurasia
[JPRS-UST-94-010] p 4250 N94-35385
JPRS report: Science and technology. Central Eurasia
[JPRS-UST-94-011] p 4250 N94-35386
JPRS report: Science and technology. Central Eurasia
[JPRS-UST-94-012] p 4250 N94-35387
JPRS report: Science and technology. Central Eurasia: Space
[JPRS-USP-93-005] p 4201 N94-36011
National Educators' Workshop: Update 1993. Standard Experiments in Engineering Materials Science and Technology
[NASA-CP-3259] p 4229 N94-36398

TECHNOLOGY ASSESSMENT
State of the art in high-power microwaves: An overview
[DE94-007075] p 4272 N94-35978
JTEC/WTEC report and program summary
p 4379 N94-36042
Information and communication technology
p 4257 N94-36043
Advanced composites in Japan p 4234 N94-36045
Space robotics in Japan p 4278 N94-36046
Space and transatmospheric propulsion technology
p 4229 N94-36047
Phase-locked arrays of vertical-cavity surface-emitting lasers
[DE94-009279] p 4272 N94-36178
Tanker system and technology requirements definition: A tanker technology road map p 4197 N94-36344
Activities of the Laser and Plasma Technology Division
[DE94-617113] p 4273 N94-36393
Feasibility study for a novel pulsed neutral beam diagnostics for tokamaks
[DE94-617129] p 4339 N94-36417

TECHNOLOGY TRANSFER
Computer Systems Laboratory
[PB94-162518] p 4333 N94-36002

TECHNOLOGY UTILIZATION
Technology Reinvestment Project's Focus Area: Low Cost Electronic Packaging
[PB94-161155] p 4259 N94-35748
Knowledge-based systems in Japan
p 4347 N94-36044

TECTONICS
NASA Space Geodesy Program: GSFC data analysis, 1993. VLBI geodetic results 1979 - 1992
[NASA-TM-104605] p 4281 N94-35261
Rheology, tectonics, and the structure of the Venus lithosphere p 4367 N94-35479
Formation of fold and thrust belts on Venus due to horizontal shortening of a laterally heterogeneous lithosphere p 4367 N94-35480
Activity Report, 1990 - 1992 and proceedings, volume 2
[DE94-610481] p 4291 N94-36087
Patterns of brittle deformation under extension on Venus p 4373 N94-36168

TEFLON (TRADEMARK)
A comparison of atomic oxygen erosion yields of carbon and selected polymers exposed in ground based facilities and in low Earth orbit
[NASA-TM-106622] p 4243 N94-35243
Effects of combined stressing on the electrical properties of film and ceramic capacitors
[NASA-TM-106605] p 4257 N94-35249
Experimental impacts into Teflon targets and LDEF thermal blankets p 4352 N94-36141

TELECOMMUNICATION
JPRS report: Science and technology. Central Eurasia
[JPRS-UST-94-001] p 4229 N94-35340
Trace-shortened Reed-Solomon codes
p 4254 N94-35554
SandiaXTP, an object-oriented implementation of XTP 3.7
[DE94-011752] p 4257 N94-36354
Telecommuting (work-at-home) at NASA Lewis Research Center
[NASA-CR-195334] p 4347 N94-36396

TELECONFERENCING
The impact of scaling on a multimedia connection architecture
[AD-A278700] p 4300 N94-35652

TELEMETRY
The Mars Observer differential one-way range demonstration p 4210 N94-35543
A closed-loop time-alignment system for baseband combining p 4253 N94-35552

TELEOPERATORS
Adjustable control station with movable monitors and cameras for viewing systems in robotics and teleoperations
[NASA-CASE-NPO-17837-1-CU] p 4332 N94-35384
Teleoperation and supervised autonomy for ORU exchange
[NASA-CR-196101] p 4274 N94-35512

TELEPHONES
North American ISDN Users' Forum agreements on Integrated Services Digital Network
[PB94-162559] p 4305 N94-35940

TELEROBOTICS
Adjustable control station with movable monitors and cameras for viewing systems in robotics and teleoperations
[NASA-CASE-NPO-17837-1-CU] p 4332 N94-35384
Teleoperation and supervised autonomy for ORU exchange
[NASA-CR-196101] p 4274 N94-35512

TELESCOPES
Advanced technology lunar telescope
p 4350 N94-35473
Predicted optical performance of the High-Altitude Balloon Experiment (HABE) telescope in an adverse thermal environment
[DE94-008949] p 4349 N94-35998

TELLURIUM
Thermodynamic behaviour of tellurium at high temperatures
[DE94-612823] p 4240 N94-35960

TEMPERATE REGIONS
Aerosol optical depth derived from solar radiometry observations at northern mid-latitude sites [DE94-007476] p 4287 N94-36053
Ionospheric plasma drift and structure studies at high and mid-latitudes [AD-A279415] p 4291 N94-36116

TEMPERATURE CONTROL
Demonstration of a high heat removal CVD diamond substrate edge-cooled multichip module [DE94-010748] p 4260 N94-36245
Digital control programmer for temperature control [DE94-615584] p 4309 N94-36382

TEMPERATURE DEPENDENCE
Methane production and consumption in grassland and boreal ecosystems [NASA-CR-196085] p 4284 N94-35486
Alkali element constraints on Earth-Moon relations p 4354 N94-36169
Temperature dependence of superconduction bands in HTSC [DE94-617361] p 4341 N94-36312
Portable high precision pressure transducer system [DE94-010137] p 4270 N94-36389

TEMPERATURE DISTRIBUTION
An adaptive, unstructured, finite-element, multi-material, thermal analysis [AD-A278632] p 4343 N94-36256

TEMPERATURE EFFECTS
Analysis of the Shuttle Orbiter reinforced carbon-carbon oxidation protection system [NASA-TM-104792] p 4262 N94-35245
Thermal performance of residential duct systems in basements [LBL-33962] p 4250 N94-35364
Mineralogy of artificially heated carbonaceous chondrites p 4352 N94-35477
Improved performance of degraded solar arrays at non-zero sun incidence angles [AD-A278905] p 4282 N94-35804
Properties and applications of powder-filled evacuated-panel superinsulations [DE94-009169] p 4233 N94-35932
Thermodynamic behaviour of tellurium at high temperatures [DE94-612823] p 4240 N94-35960
Predicted optical performance of the High-Altitude Balloon Experiment (HABE) telescope in an adverse thermal environment [DE94-008949] p 4349 N94-35998
Twin spacing and the structural phase transitions in 1:2:3 high-Tc superconductors [DE94-615647] p 4340 N94-36041
Moessbauer mineralogy of calcined Murchison meteorite p 4353 N94-36166
Measurement of the decay rate of the SiH feature as a function of temperature p 4318 N94-36171

TEMPERATURE GRADIENTS
Rheology, tectonics, and the structure of the Venus lithosphere p 4367 N94-35479
Predicted optical performance of the High-Altitude Balloon Experiment (HABE) telescope in an adverse thermal environment [DE94-008949] p 4349 N94-35998

TEMPERATURE INVERSIONS
Application of differential inversion to DMSP microwave sounder data [AD-A278575] p 4294 N94-36186

TEMPERATURE MEASUREMENT
Multiwavelength pyrometer for gray and non-gray surfaces in the presence of interfering radiation [NASA-CASE-LEW-15250-1] p 4269 N94-35383
Measurement of a surface heat flux and temperature p 4231 N94-36407

TEMPLATES
A collection of tools in support of automatic differentiation [DE94-010104] p 4314 N94-35704

TEMPORAL RESOLUTION
Computation of dendrites using a phase field model [PB94-160744] p 4236 N94-35736
Ultrafast readout of scintillating fibers using upgraded position-sensitive photomultipliers [DE94-010419] p 4269 N94-36095

TENSILE STRENGTH
Through-the-thickness tensile strength of textile composites [NASA-TM-109115] p 4233 N94-35946
Method of thermochemically treating silicon carbide fibers derived from polymers [AD-D016218] p 4246 N94-36125
Design and construction of a tensile tester for the testing of simple composites p 4230 N94-36401

TENSILE STRESS
Through-the-thickness tensile strength of textile composites [NASA-TM-109115] p 4233 N94-35946

TENSILE TESTS
Investigation of moisture-induced embrittlement of iron aluminides [DE94-010881] p 4241 N94-36196
Design and construction of a tensile tester for the testing of simple composites p 4230 N94-36401

TENSORS
Complex Kohn variational principle for two-nucleon bound-state and scattering with the tensor potential [DE94-616651] p 4321 N94-35595

TERMINAL BALLISTICS
The surface and interior of Phobos p 4355 N94-35400
Energy partitioning in high speed impact of analog solid rocket motors [AD-A278771] p 4228 N94-35825

TERRAIN
The fretted terrain of the Nilosyrtis Mensae region of Mars: Clues to the timing of dichotomy formation and the emplacement of the northern plains p 4360 N94-35424
Space Shuttle orbit determination using empirical force modeling of attitude maneuvers for the German MOMS-02/D2 mission p 4207 N94-35634
Atmospheric and dispersion modeling in areas of highly complex terrain employing a four-dimensional data assimilation technique [DE94-004041] p 4285 N94-35823

TERRESTRIAL RADIATION
Theoretical and experimental studies relevant to interpretation of auroral emissions [NASA-CR-196032] p 4376 N94-36421

TEST EQUIPMENT
Atomic oxygen reactor having at least one sidearm conduit [NASA-CASE-MSC-21487-4] p 4250 N94-35445
High-speed digital project, HSD test capability [DE94-010885] p 4260 N94-36197
Design and construction of a tensile tester for the testing of simple composites p 4230 N94-36401

TEST FACILITIES
Data acquisition systems [DE94-009848] p 4345 N94-35817

TETHERING
An electronic interface for a fiber optic tethered unmanned underwater vehicle [AD-A279046] p 4333 N94-35747

TETRAETHYL ORTHOSILICATE
Cross-condensation reactions in an organically modified silica sol-gel [DE94-010086] p 4244 N94-35701

TETRAHEDRONS
Be3(AsO4)2.2H2O, a new berylloarsenate phase containing bridged tetrahedral 3-rings [AD-A278826] p 4340 N94-35677

TEXTILES
Through-the-thickness tensile strength of textile composites [NASA-TM-109115] p 4233 N94-35946
ASTM test methods for composite characterization and evaluation p 4229 N94-36399

TEXTS
A collection of tools in support of automatic differentiation [DE94-010104] p 4314 N94-35704

TEXTURES
Alteration and formation of rims on the CM parent body p 4357 N94-35411
On the possible role of elemental carbon in the formation of reduced chondrules p 4351 N94-35421
Textural constraints on the formation of alteration phases in CM chondrites p 4353 N94-36145

THALLIUM COMPOUNDS
Vertical electron detachment energies for octahedral closed-shell multiply charged anions [AD-A278835] p 4322 N94-35753

THEOREM PROVING
Combining symbolic computation and theorem proving: Some problems of Ramanujan [AD-A278899] p 4303 N94-35573
Priorities and nonmonotonic reasoning [PB94-171170] p 4346 N94-35959

THEOREMS
Combining symbolic computation and theorem proving: Some problems of Ramanujan [AD-A278899] p 4303 N94-35573
Some theorems on a class of harmonic manifolds [DE94-611102] p 4315 N94-35934

THEORETICAL PHYSICS
Three-photon micromasers [DE94-611106] p 4272 N94-35782

THERMAL ANALYSIS
A 32-GHz solid-state power amplifier for deep space communications p 4255 N94-35562
Demonstration of a high heat removal CVD diamond substrate edge-cooled multichip module [DE94-010748] p 4260 N94-36245
An adaptive, unstructured, finite-element, multi-material, thermal analysis [AD-A278632] p 4343 N94-36256

THERMAL BUCKLING
Analysis of high speed flow, thermal and structural interactions [NASA-CR-196017] p 4268 N94-36420

THERMAL CONDUCTIVITY
Analysis of current diffusive ballooning mode [DE94-718992] p 4336 N94-35811

THERMAL DIFFUSIVITY
Dynamic and thermal turbulent time scale modelling for homogeneous shear flows [NASA-TM-106635] p 4263 N94-35253
MHD and confinement characteristics in the high-beta regime on the CHS low-aspect-ratio heliotron/torsatron [DE94-718981] p 4339 N94-36357

THERMAL EMISSION
Thermal emission measurements (5-25 microns) of Hawaiian palagonitic soils with implications for Mars p 4292 N94-35452
Thermal emission measurements (5-25 microns) of palagonite/Fe-substituted montmorillonite intimate mixtures: Applications to Mars p 4292 N94-35453
Atmospheric effects on the mapping of Martian thermal inertia and thermally derived albedo p 4368 N94-36137

THERMAL ENVIRONMENTS
Predicted optical performance of the High-Altitude Balloon Experiment (HABE) telescope in an adverse thermal environment [DE94-008949] p 4349 N94-35998

THERMAL FATIGUE
Isothermal damage and fatigue behavior of SCS-6/Timetal 21S (0/90)s composite at 650 C [NASA-CR-195345] p 4234 N94-35995

THERMAL INSULATION
Thermal performance of residential duct systems in basements [LBL-33962] p 4250 N94-35364
Properties and applications of powder-filled evacuated-panel superinsulations [DE94-009169] p 4233 N94-35932
Experimental impacts into Teflon targets and LDEF thermal blankets p 4352 N94-36141

THERMAL MAPPING
Atmospheric effects on the mapping of Martian thermal inertia and thermally derived albedo p 4368 N94-36137

THERMAL PLASMAS
Activities of the Laser and Plasma Technology Division [DE94-617113] p 4273 N94-36393

THERMAL PROTECTION
Debris/ice/TPS assessment and integrated photographic analysis for Shuttle Mission STS-59 [NASA-TM-109203] p 4211 N94-35523

THERMAL RADIATION
Radiative signals from impact of Shoemaker-Levy on Jupiter p 4355 N94-35396

THERMAL RESISTANCE
JPRS report: Science and technology. Central Eurasia: Materials science [JPRS-UMS-93-007] p 4240 N94-35517
Properties and applications of powder-filled evacuated-panel superinsulations [DE94-009169] p 4233 N94-35932
Third European Technical Symposium on Polyimides and High Performance Polymers: STEPI 3 [PB94-148491] p 4246 N94-36177
Measurement of a surface heat flux and temperature p 4231 N94-36407

THERMAL STABILITY
Effects of combined stressing on the electrical properties of film and ceramic capacitors [NASA-TM-106605] p 4257 N94-35249

THERMAL STRESSES
Effects of combined stressing on the electrical properties of film and ceramic capacitors [NASA-TM-106605] p 4257 N94-35249

THERMOCHEMISTRY
NEQPAK, the AEDC thermochemical nonequilibrium package: Theory and use [AD-A279005] p 4266 N94-35951
CSTL technical activities, 1991 [PB94-160769] p 4318 N94-36003
Method of thermochemically treating silicon carbide fibers derived from polymers [AD-D016218] p 4246 N94-36125

The thermochemistry and reaction mechanisms in the decomposition of energetic materials
[DE94-011420] p 4248 N94-36376

THERMOCOUPLES
Digital control programmer for temperature control
[DE94-615584] p 4309 N94-36382
Measurement of a surface heat flux and temperature
p 4231 N94-36407

THERMODYNAMIC EQUILIBRIUM
Boson spectra and correlations in thermal locally equilibrium systems
[DE94-616799] p 4325 N94-36079

THERMODYNAMIC PROPERTIES
AFDM: An advanced fluid-dynamics model, volume 6
[DE94-009596] p 4264 N94-35669
Performance analysis of reciprocating regenerative magnetic heat pumping
[DE94-009488] p 4264 N94-35683
Chirped-pulse amplification with flashlamp-pumped Ti:Sapphire amplifiers
[DE94-010055] p 4272 N94-35695
Properties and bibliography of GaSe
[AD-A279064] p 4340 N94-35733
NEQPAK, the AEDC thermochemical nonequilibrium package: Theory and use
[AD-A279005] p 4266 N94-35951
Thermodynamic behaviour of tellurium at high temperatures
[DE94-612823] p 4240 N94-35960
Thermophysical properties of HFC-143a and HFC-152a
[DE94-009995] p 4251 N94-36008
A new association-model for binary VLE of alcohol/hydrocarbon and amine/hydrocarbon mixtures
[DE94-011012] p 4248 N94-36034
Quantum mechanics and thermodynamics of particles with distance dependent statistics
[DE94-616620] p 4343 N94-36072
NMR imaging of components and materials for DOE application
[DE94-010664] p 4238 N94-36084
On the origin of porphyritic chondrules
[DE94-010464] p 4351 N94-36418

THERMODYNAMICS
CSTL technical activities, 1991
[PB94-160769] p 4318 N94-36003
Determination of grain boundary volume expansion by HREM
[DE94-010452] p 4241 N94-36231

THERMOELECTRIC GENERATORS
GPHS-RTGs in support of the Cassini mission
[DE94-009994] p 4212 N94-35648

THERMOPHYSICAL PROPERTIES
AFDM: An advanced fluid-dynamics model, volume 6
[DE94-009596] p 4264 N94-35669
Thermophysical properties of HFC-143a and HFC-152a
[DE94-009995] p 4251 N94-36008
Research update: Materials Compatibility and Lubricant Research (MCLR) program
[DE94-010001] p 4247 N94-36387

THERMOPILES
Measurement of a surface heat flux and temperature
p 4231 N94-36407

THERMOPLASTIC RESINS
Tough high performance composite matrix
[NASA-CASE-LAR-14239-2] p 4232 N94-35372
Processing and properties of high temperature metal/fiber-reinforced-thermoplastic laminates
[AD-A278791] p 4232 N94-35654
Design for manufacturability evaluation: Composite National Ignition Facility (NIF) pockel cell body
[DE94-010669] p 4338 N94-36284
Laminated thermoplastic composite material from recycled high density polyethylene p 4230 N94-36403

THERMOSETTING RESINS
Tough high performance composite matrix
[NASA-CASE-LAR-14239-2] p 4232 N94-35372

THERMOSPHERE
Modeling of the magnetosphere-ionosphere-atmosphere system
[NASA-CR-195157] p 4288 N94-35244
Natural orbital environment definition guidelines for use in aerospace vehicle development
[NASA-TM-4527] p 4291 N94-36175

THESAURI
NASA Thesaurus. Volume 1: Hierarchical listing. Volume 2: Access vocabulary. Volume 3: Definitions
[NASA-SP-7096-VOL-1/2/3] p 4346 N94-36037

THICK FILMS
Thick film fabrication of aluminum nitride microcircuits
[DE94-010107] p 4259 N94-35706

THIN AIRFOILS
Robust control design techniques for active flutter suppression p 4200 N94-35875

THIN FILMS
The growth of silicon nitride crystalline films using microwave plasma enhanced chemical vapor deposition
[AD-A278862] p 4340 N94-35828
Method for making a symmetrical layered thin film edge field-emitter-array
[AD-D016214] p 4246 N94-36121
Microstructural development in solution derived PZT thin films
[DE94-008744] p 4246 N94-36209
Ion modulated electroactivity in thin film metallopolymers
[AD-A278618] p 4246 N94-36253
Multicomponent glass surfaces: Structure and adsorption
[DE94-010516] p 4246 N94-36283
High temperature heterojunction bipolar transistors
[AD-A278605] p 4261 N94-36360
Flux-pinning related defects in YBa2Cu3O(7-x) thin films grown on miscut LaAlO3 (001) substrates
[DE94-011463] p 4342 N94-36377
Measurement of a surface heat flux and temperature
p 4231 N94-36407
Mechanical properties of crosslinked polymer coatings
p 4231 N94-36410

THORIUM COMPOUNDS
Digital control programmer for temperature control
[DE94-615584] p 4309 N94-36382

THREE BODY PROBLEM
A three-body calculation of the O-16(d,p)O-17 reaction using a two-term separable potential for the s-wave nucleon-core interaction
[DE94-616652] p 4320 N94-35579
Relativistic three-particle dynamical equations. 2: Application to the trinucleon system
[DE94-616653] p 4320 N94-35580
Relativistic three-particle dynamical equations. 2: Theoretical development
[DE94-616654] p 4320 N94-35581
Exact multiplicities in the three-anion spectrum
[DE94-616768] p 4325 N94-36075
P-matrix approach and three-nucleon problem
[DE94-616887] p 4326 N94-36131

THREE DIMENSIONAL COMPOSITES
Can the compressive response of fiber-reinforced composites be modelled by means of layered arrays?
[AD-A278864] p 4233 N94-35944

THREE DIMENSIONAL FLOW
A three dimensional multigrid Reynolds-averaged Navier-Stokes solver for unstructured meshes
[NASA-CR-194908] p 4191 N94-35994

THREE DIMENSIONAL MODELS
Space Shuttle orbit determination using empirical force modeling of attitude maneuvers for the German MOMS-02/D2 mission p 4207 N94-35634
Distributed parameter modeling of repeated truss structures p 4218 N94-35868
Three-dimensional force data acquisition and boundary corrections for the Walter H. Beech Memorial 7 x 10 foot low speed wind tunnel
[AR93-2] p 4200 N94-36437

THREE DIMENSIONAL MOTION
Input shaping for three-dimensional slew maneuvers of a precision pointing flexible spacecraft
[DE94-008937] p 4226 N94-36001

THRESHOLD CURRENTS
Study and fabrication of GaSb-based laser heterostructures
[PB94-170677] p 4273 N94-36218

THRESHOLD VOLTAGE
Estimating low-dose rate irradiation response of MOSFETs
[DE94-007292] p 4342 N94-36367

THROTTLING
Flight testing a propulsion-controlled aircraft emergency flight control system on an F-15 airplane
[NASA-TM-4590] p 4199 N94-35258

THRUST
Evaluating the dynamic response of in-flight thrust calculation techniques during throttle transients
[NASA-TM-4591] p 4193 N94-35241

THRUST VECTOR CONTROL
Direct reduced order mixed H2/H infinity control for the Short Take-Off and Landing/Maneuver Technology Demonstrator (STOL/MTD)
[AD-A278675] p 4199 N94-35796
Experience with Ada on the F-18 High Alpha Research Vehicle flight test program p 4310 N94-35968
An experimental investigation of active control of thrust vectoring nozzle flow fields
[AD-A278702] p 4229 N94-36291

THRUST-WEIGHT RATIO
The reduction of takeoff ground roll by the application of a nose gear jump strut
[NASA-TM-108822] p 4198 N94-36380

THUNDERSTORMS
Kinetic theory of runaway air breakdown and the implications for lightning initiation
[DE94-001683] p 4295 N94-36240

TILT ROTOR AIRCRAFT
The convertible (helicopter/airplane) EUROFAR: General considerations on the technical progress and on future advances p 4195 N94-36331
Alleviation of whirl-flutter on a joined-wing tilt-rotor aircraft configuration using active controls
[NASA-CR-196103] p 4200 N94-36436

TILT WING AIRCRAFT
1993 Technical Paper Contest for Women. Gear Up 2000: Women in Motion
[NASA-CP-10134] p 4377 N94-35961
Piloted simulation study of two tilt-wing control concepts p 4200 N94-35962

TIME DEPENDENCE
Magnetoresistance of films and strips with the diffuse surface scattering
[DE94-611100] p 4340 N94-35933
Classical time machine
[DE94-616616] p 4342 N94-36070
On quantization of time-dependent systems with constraints
[DE94-611114] p 4343 N94-36351

TIME LAG
Time-delay control of a magnetic levitated linear positioning system p 4217 N94-35862

TIME MEASUREMENT
Electronics for the SND scintillation counter system
[DE94-616453] p 4259 N94-36104
X ray radiographic imaging of hydrodynamic phenomena in radiation driven materials: Shock propagation and shear flow
[DE94-010891] p 4318 N94-36201

TIME OF FLIGHT SPECTROMETERS
Time-of-flight diffraction at pulsed neutron sources: An introduction to the symposium
[DE94-010442] p 4327 N94-36225

TIME SERIES ANALYSIS
Workshop on the Martian Northern Plains: Sedimentological, periglacial, and paleoclimatic evolution
[NASA-CR-196134] p 4354 N94-35359
A new presentation of complex voltage data for Goldstone radar astronomy p 4255 N94-35561
Cramer-von Mises variance estimators for simulations
[AD-A278799] p 4316 N94-35675
A comparison of artificial neural networks and statistical analyses
[DE94-010846] p 4312 N94-36195

TIN ALLOYS
Manufacturing feasibility of several lead-free solders for electronic assembly
[DE94-007732] p 4258 N94-35564

TIN TELLURIDES
Thermodynamic behaviour of tellurium at high temperatures
[DE94-612823] p 4240 N94-35960

TIP SPEED
Tipjet 80-inch model rotor hover test: Test no. 1198
[AD-A279680] p 4191 N94-36261

TISSUES (BIOLOGY)
Multi-cellular, three-dimensional living mammalian tissue
[NASA-CASE-MSC-21560-2] p 4296 N94-35232
High density cell culture system
[NASA-CASE-MSC-22060-1] p 4296 N94-35366

TITAN 4 LAUNCH VEHICLE
Propellant stress relief groove for the Titan 4 SRMU
[AD-A278628] p 4228 N94-36254

TITANIUM
Isothermal damage and fatigue behavior of SCS-6/Timetal 21S (0/90)s composite at 650 C
[NASA-CR-195345] p 4234 N94-35995
Partition coefficients for Al, Ca, Ti, Cr, and Ni in olivine obtained by melting experiment on an LL6 chondrite
p 4353 N94-36163

TITANIUM ALLOYS
Continuum fluorescence of Cu in NbTi/Cu composite wires
[DE94-008940] p 4241 N94-36242

TITANIUM COMPOUNDS
Metal cluster alloys and oxides: Elucidating structural and electronic effects in governing the reactivity and catalytic role of matter in finite dimensions
[DE94-010224] p 4328 N94-36298

TOKAMAK DEVICES
A triggering mechanism of fast crash in sawtooth oscillation
[DE94-718974] p 4336 N94-35772
NIFS Symposium: Toward the research of fusion burning plasmas, present status and future strategy
[DE94-727618] p 4336 N94-35775
Optimization of turn position of tokamak inductor
[DE94-612627] p 4336 N94-35791

Analysis of current diffusive ballooning mode
[DE94-718992] p 4336 N94-35811
Thickness of the layer of strong radial electric field in JFT-2M H-mode plasmas
[DE94-718993] p 4336 N94-35812
Applications of non-resonant RF forces for improvement of tokamak reactor performances. Part 1: Application of ponderomotive force
[DE94-718994] p 4336 N94-35813
Atomic physics and radiation processes in plasmas
[DE94-727617] p 4337 N94-35939
A survey of reflectometry techniques with applications to TFTR
[DE94-010202] p 4338 N94-36093
Scaling laws for TEXT plasma profiles
[DE94-010832] p 4338 N94-36200
The new features of Ion Bernstein Wave Heating in JIPP T-2U tokamak
[DE94-718978] p 4338 N94-36247
Feasibility study for a novel pulsed neutral beam diagnostics for tokamaks
[DE94-617129] p 4339 N94-36417

TOLERANCES (MECHANICS)
Tough, processable semi-interpenetrating polymer networks from monomer reactants
[NASA-CASE-LAR-14838-1] p 4242 N94-35233

TOMOGRAPHY
Recursive recovery of Markov transition probabilities from boundary value data
[DE94-011914] p 4317 N94-36235

TOPEX
Compatibility of TOPEX/Poseidon trajectory propagation with JPL and GSFC/FDF operational software
p 4204 N94-35619
Improved solution accuracy for TDRSS-based TOPEX/Poseidon orbit determination
p 4205 N94-35620
Tracking system options for future altimeter satellite missions p 4205 N94-35622

TOPOGRAPHY
Mesoscale roughness of Venus p 4361 N94-35430
The Twenty-Fifth Lunar and Planetary Science Conference. Part 3: P-Z
[NASA-CR-195745] p 4362 N94-35448
The topography of Mars: A re-evaluation of current data p 4364 N94-35460
Noachian and Hesperian modification of the original Chryse impact basin topography p 4364 N94-35462
Formation of fold and thrust belts on Venus due to horizontal shortening of a laterally heterogeneous lithosphere p 4367 N94-35480
Tracking system options for future altimeter satellite missions p 4205 N94-35622
Preliminary solutions for the lunar gravity field from analysis of lunar orbiter tracking data
p 4371 N94-36156

TORCHES
Plasma arc welding weld imaging
[NASA-CASE-MFS-28797-1] p 4273 N94-35367
Analysis of a High Velocity Oxygen-Fuel (HVOF) thermal spray torch. Part 1: Numerical formulation
[DE94-005590] p 4267 N94-35996

TOROIDAL PLASMAS
Power balance and characterization of impurities in the Maryland Spheromak, part 2
[DE94-009603] p 4335 N94-35670
Improved models of beta-limit, anomalous transport and radial electric field with loss cone loss in heliotron/torsatron
[DE94-718976] p 4324 N94-35984
Scaling laws for TEXT plasma profiles
[DE94-010832] p 4338 N94-36200

TORQUE
The control of satellites with microgravity constraints: The COMET Control System p 4207 N94-35632
A dynamic method for magnetic torque measurement
p 4216 N94-35856

TORQUEMETERS
A dynamic method for magnetic torque measurement
p 4216 N94-35856

TORSIONAL VIBRATION
A procedure for oscillatory parameter identification
[DE94-008047] p 4259 N94-36054
Vibration reduction in helicopter rotors using an actively controlled partial span trailing edge flap located on the blade
[NASA-CR-4611] p 4280 N94-36423

TOUGHNESS
Tough, processable semi-interpenetrating polymer networks from monomer reactants
[NASA-CASE-LAR-14838-1] p 4242 N94-35233

TOWED BODIES
Hose-drogue versus boom receptacle air refueling
p 4197 N94-36345

TOXICITY
CAirTOX: A compartment model for assessing the fate of and human exposure to toxic-chemical emissions to air
[DE94-010084] p 4284 N94-35700
Treatment of toxic gases SO2 and NO(x) by electron beam irradiation
[DE94-615424] p 4330 N94-36028

TRACE CONTAMINANTS
Global tropospheric chemistry models for radiatively important trace species: Design and research recommendations
[DE94-007089] p 4288 N94-36359

TRACE ELEMENTS
Ar-39-Ar-40 ages of four ureilites
p 4357 N94-35410
Distribution of siderophile and other trace elements in melt rock at the Chicxulub impact structure
p 4352 N94-35456
Anatomy of a cluster IDP. Part 2: Noble gas abundances, trace element geochemistry, isotopic abundances, and trace organic chemistry of several fragments from L2008#5 p 4352 N94-35465
The anatomy of a cluster IDP. Part 1: Carbon abundance, bulk chemistry, and mineralogy of fragments from L2008#5 p 4352 N94-35466
Synthetic and natural Nakhla pyroxenes: Parent melt composition and REE partition coefficients
p 4353 N94-36161
Integrated science model for assessment of climate change
[DE94-011758] p 4288 N94-36286

TRACKING (POSITION)
Tracking system options for future altimeter satellite missions p 4205 N94-35622
Estimation with multisensor/multiscan detection fusion
[AD-A278753] p 4256 N94-36092

TRACKING STATIONS
A genetic algorithm approach to automating satellite range scheduling
[AD-A278577] p 4226 N94-36188

TRAILING EDGE FLAPS
Selected topics on the active control of helicopter aeromechanical and vibration problems
p 4200 N94-35874
Vibration reduction in helicopter rotors using an actively controlled partial span trailing edge flap located on the blade
[NASA-CR-4611] p 4280 N94-36423

TRAILING EDGES
Numerical investigation of multi-element airfoils
[NASA-CR-194592] p 4191 N94-36394

TRAINING DEVICES
Using experimental design modules for process characterization in manufacturing/materials processes laboratories p 4230 N94-36405
Graphing techniques for materials laboratory using Excel p 4232 N94-36414

TRAINING SIMULATORS
The application of fuzzy logic to SAFOR in SIMNET
[AD-A279058] p 4312 N94-35730

TRAJECTORIES
Low encounter speed comet COMA sample return missions p 4202 N94-35607
Self-rescue strategies for EVA crewmembers equipped with the SAFER backpack p 4207 N94-35633

TRAJECTORY ANALYSIS
Compatibility of TOPEX/Poseidon trajectory propagation with JPL and GSFC/FDF operational software
p 4204 N94-35619
Improved solution accuracy for TDRSS-based TOPEX/Poseidon orbit determination
p 4205 N94-35620
Angular momentum in the Local Group
[DE94-009322] p 4350 N94-35980

TRANSCENDENTAL FUNCTIONS
Variations in the modal characteristics of a telescopically deploying beam p 4218 N94-35872
Review of Mathematical Function Library for Microsoft-FORTRAN, John Wiley and Sons, 1989
[PB94-160793] p 4305 N94-36010

TRANSDUCERS
Smart accelerometer --- vibration damage detection
[NASA-CASE-MSC-21951-1] p 4268 N94-35235
Analysis of achievable disturbance attenuation in a precision magnetically-suspended motion control system
p 4225 N94-35917

TRANSFER FUNCTIONS
Adaptive model reduction for continuous systems via recursive rational interpolation p 4219 N94-35876
LQG optimal compensator transfer function for the NASA LaRC CSI Evolutionary Model
p 4221 N94-35891
Transfer function modeling of damping mechanisms in distributed parameter models p 4222 N94-35895

TRANSFER ORBITS
Theory and computation of optimal low- and medium-thrust transfers
[NASA-CR-196077] p 4202 N94-35487
A geometric model of a V-slit Sun sensor correcting for spacecraft wobble p 4206 N94-35628

TRANSFERRING
Attention and signal detection. A study of attention divided between visual and auditory signals
[PB94-170594] p 4298 N94-36215

TRANSFORMATIONS (MATHEMATICS)
Entropy of graphs, semigroups and groups
[PB94-167749] p 4314 N94-35763
Executable transformational rules from Core ELLA to the Kernel
[DRA-MEMO-4629] p 4307 N94-36113

TRANSFORMERS
Experimental measurement and calculation of losses in planar radial magnetic bearings p 4214 N94-35847

TRANSIENT HEATING
Performance analysis of reciprocating regenerative magnetic heat pumping
[DE94-009488] p 4264 N94-35683

TRANSIENT OSCILLATIONS
Modelling of ELMs and dynamic responses of the H-mode
[DE94-718977] p 4339 N94-36353

TRANSIENT RESPONSE
Modelling of ELMs and dynamic responses of the H-mode
[DE94-718977] p 4339 N94-36353

TRANSISTORS
Superconducting transistors
[PB94-170743] p 4260 N94-36260

TRANSITION POINTS
The silent phase transition in mesonic bags and lattice theory
[DE94-616852] p 4321 N94-35583
ILSE combiner study
[DE94-011009] p 4331 N94-36202

TRANSITION PROBABILITIES
Recursive recovery of Markov transition probabilities from boundary value data
[DE94-011914] p 4317 N94-36235

TRANSITION TEMPERATURE
Calorimetric thermometry of meteoritic troilite: Preliminary thermometer relationships
p 4355 N94-35399
A new family of superconducting fullerides, Na(NH3)(x)C60(x = 2-8)
[DE94-011480] p 4341 N94-36272

TRANSLATING
Priorities and nonmonotonic reasoning
[PB94-171170] p 4346 N94-35959
Using International English to prepare technical text for translation
[DE94-002628] p 4347 N94-36102
Determination of grain boundary volume expansion by HREM
[DE94-010452] p 4241 N94-36231

TRANSMISSION ELECTRON MICROSCOPY
High Resolution Transmission Electron Microscopy (HRTEM) of nanophase ferric oxides
p 4239 N94-35433
High-resolution imaging using Z-contrast Scanning Transmission Electron Microscopy
[DE94-008510] p 4333 N94-36055
Irradiation-related amorphization and crystallization: In situ transmission electron microscope studies
[DE94-009823] p 4241 N94-36222

TRANSMITTANCE
Transmission measurements (4000-400 cm(exp -1), 2.5-25 microns) of crystalline ferric oxides and ferric oxyhydroxides: Implications for Mars
p 4292 N94-35454

TRANSMITTER RECEIVERS
A 32-GHz solid-state power amplifier for deep space communications p 4255 N94-35562

TRANSPONDERS
Performance evaluation of digital phase-locked loops for advanced deep space transponders
p 4254 N94-35558

TRANSPORT AIRCRAFT
The future of large capacity/long range multipurpose air cargo fleets p 4194 N94-36326
Tanker system and technology requirements definition: A tanker technology road map p 4197 N94-36344

TRANSPORT PROPERTIES
Diffusion and sorption of 1,4-dioxane into polychloroprene
[ARL-TR-338] p 4229 N94-35361
Determination of extensional viscosity from capillary rheometer entrance pressure drop measurements using a numerical simulation of contraction flow
[PB94-171154] p 4263 N94-35603

On the various forms of the energy equation for a dilute, monatomic mixture of nonreacting gases
[NASA-CR-4612] p 4190 N94-35864
K-epsilon model of anomalous transport in resistive interchange turbulence
[DE94-718983] p 4337 N94-35937
NEQPAK, the AEDC thermochemical nonequilibrium package: Theory and use
[AD-A279005] p 4266 N94-35951
Improved models of beta-limit, anomalous transport and radial electric field with loss cone loss in heliotron/torsatron
[DE94-718976] p 4324 N94-35984
Thermophysical properties of HFC-143a and HFC-152a
[DE94-009995] p 4251 N94-36008
Beam transport
[DE94-010755] p 4331 N94-36199

TRANSPORTATION
Future ultra-speed tube-flight p 4225 N94-35918

TRANSPUTERS
Computer automation and artificial intelligence
[DE94-611058] p 4312 N94-35831

TRANSVERSE WAVES
An electromagnetic finite difference time domain analog treatment of small signal acoustic interactions
[DE94-009978] p 4319 N94-35770

TRAPPED PARTICLES
Collisionless dynamics of the magnetosphere
[AD-A278886] p 4290 N94-35708
Particle orbit analysis for LHD helical axis configurations
[DE94-718995] p 4336 N94-35773

TRAPPING
Enhanced charge trapping in bipolar spacer oxides during low-dose-rate irradiation
[DE94-007863] p 4260 N94-36268

TRAVELING WAVES
Solitary waves and homoclinic orbits
[DE94-009428] p 4264 N94-35681
Spatio-temporal properties of centrifugal instabilities: Abstracts of 8th Couette-Taylor Meeting
[PB94-150240] p 4266 N94-35981

TRIANGULATION
Three-dimensional unstructured grid refinement and optimization using edge-swapping
[NASA-TM-103966] p 4299 N94-35393

TRIBOLOGY
The effect of alternative fuels on the stability and lubricity of crankcase lubricants
[DE94-010353] p 4245 N94-36108
Wear-resisting oxide films for 900 C
[DE94-010093] p 4246 N94-36306

TRIGGER CIRCUITS
Beam tests of a prototype level-1 calorimeter trigger for LHC experiments
[PB94-170495] p 4269 N94-35599

TRIMERS
New anionic states of the lithium trimer
[AD-A278832] p 4323 N94-35797

TRITIUM
Tritiated ammonia formation
[DE94-011170] p 4237 N94-36056

TROILITE
Calorimetric thermometry of meteoritic troilite: Preliminary thermometer relationships
p 4355 N94-35399

TROPICAL REGIONS
Contributions of the low-latitude boundary layer to the finite width magnetotail convection model
[NASA-CR-196116] p 4289 N94-35392
ULF waves in the low-latitude boundary layer and their relationship to magnetospheric pulsations: A multisatellite observation
[AD-A278906] p 4289 N94-35587

TROPOSPHERE
H2O-H2SO4 system in Venus' clouds and OCS, CO, and H2SO4 profiles in Venus' troposphere
p 4370 N94-36152
Global tropospheric chemistry models for radiatively important trace species: Design and research recommendations
[DE94-007089] p 4288 N94-36359

TRUCKS
Final regulatory impact analysis: Refueling emission regulations for light duty vehicles and trucks and heavy duty vehicles
[PB94-164027] p 4285 N94-35754

TRUSSES
Kinematic modeling of a double octahedral Variable Geometry Truss (VGT) as an extensible gimbal
[NASA-TM-109127] p 4311 N94-35242
Distributed parameter modeling of repeated truss structures p 4218 N94-35868
Applying transfer matrix method to the estimation of the modal characteristics of the NASA Mini-Mass Truss
p 4218 N94-35870

TUMBLING MOTION
Self-rescue strategies for EVA crewmembers equipped with the SAFER backpack p 4207 N94-35633

TUNABLE LASERS
900-mW average power and tunability from a diode-pumped 2.94 micron Er:YAG oscillator
[DE94-009511] p 4271 N94-35679

TUNDRA
A model of the CO2 exchanges between biosphere and atmosphere in the tundra
[NASA-CR-196008] p 4289 N94-35389

TUNGSTEN
Non-alloyed, refractory metal contact optimization with shallow implantations of Zn and Mg
[DE94-010392] p 4240 N94-36110
X ray and gamma ray spectroscopy of solids under pressure
[DE94-011207] p 4238 N94-36203

TUNING
Filter parameter tuning analysis for operational orbit determination support p 4208 N94-35637
Fabrication and phase tuning of an optical waveguide device
[AD-D016215] p 4334 N94-36122

TURBINE ENGINES
Propulsion system selection for a High Altitude Long Endurance aircraft p 4195 N94-36333

TURBINES
University participation in the ATS program
[DE94-003191] p 4275 N94-36022
Tipjet 80-inch model rotor hover test: Test no. 1198
[AD-A279680] p 4191 N94-36261

TURBULENCE
Experimental studies of very-high Mach number hydrodynamics
[AD-A278761] p 4263 N94-35492
Expansion effects on supersonic turbulent boundary layers
[AD-A278989] p 4190 N94-35950
Non-linear interaction of gravity waves with average jet flows, instabilities, and turbulence
[PB94-170586] p 4291 N94-36214
On the physics of waves in the solar atmosphere: Wave heating and wind acceleration
[NASA-CR-194119] p 4375 N94-36395

TURBULENCE EFFECTS
Spatial fluctuations of particle fluxes within the auroral zone inferred from the Intercosmos-Bulgaria-1300 satellite data
[DE94-615858] p 4350 N94-36128

TURBULENCE MODELS
Dynamic and thermal turbulent time scale modelling for homogeneous shear flows
[NASA-TM-106635] p 4263 N94-35253
Comparison of PDF and moment closure methods in the modeling of turbulent reacting flows
[NASA-TM-106614] p 4265 N94-35948

TURBULENT BOUNDARY LAYER
A review and development of correlations for base pressure and base heating in supersonic flow
[SAND93-0280] p 4189 N94-35360
The aerodynamic and heat transfer effects of an endwall boundary layer fence in a 90 degree turning square duct
[AD-A278903] p 4265 N94-35803
Expansion effects on supersonic turbulent boundary layers
[AD-A278989] p 4190 N94-35950

TURBULENT COMBUSTION
AFOSR Contractors Propulsion Meeting
[AD-A279028] p 4198 N94-35746
Comparison of PDF and moment closure methods in the modeling of turbulent reacting flows
[NASA-TM-106614] p 4265 N94-35948

TURBULENT FLOW
Comparison of PDF and moment closure methods in the modeling of turbulent reacting flows
[NASA-TM-106614] p 4265 N94-35948
Vortex tubes in turbulent flows: Identification, representation, reconstruction
[NASA-CR-194900] p 4267 N94-35992
A three dimensional multigrid Reynolds-averaged Navier-Stokes solver for unstructured meshes
[NASA-CR-194908] p 4191 N94-35994
Analysis of a High Velocity Oxygen-Fuel (HVOF) thermal spray torch. Part 1: Numerical formulation
[DE94-005590] p 4267 N94-35996

TWO BODY PROBLEM
Relativistic three-particle dynamical equations. 2: Theoretical development
[DE94-616654] p 4320 N94-35581
Logarithmic corrections of the two-body QED problem
[DE94-611157] p 4322 N94-35783
Quantum mechanics and thermodynamics of particles with distance dependent statistics
[DE94-616620] p 4343 N94-36072
Notes on possible S-wave resonances in relativistic two-particle systems
[DE94-616889] p 4329 N94-36392
Variational method in relativistic two-body problem
[DE94-612462] p 4315 N94-36416

TWO DIMENSIONAL FLOW
Investigation of Burnett equations for two-dimensional hypersonic flow
[AD-A278942] p 4190 N94-35717

TWO DIMENSIONAL MODELS
Local instabilities and the transition to chaos of non-linear waves
[PB94-170578] p 4341 N94-36213
Numerical investigation of multi-element airfoils
[NASA-CR-194592] p 4191 N94-36394

TWO FLUID MODELS
Analysis of phase distribution phenomena in microgravity environments
[NASA-CR-196038] p 4249 N94-35237

TWO PHASE FLOW
Analysis of phase distribution phenomena in microgravity environments
[NASA-CR-196038] p 4249 N94-35237
Analysis of a High Velocity Oxygen-Fuel (HVOF) thermal spray torch. Part 1: Numerical formulation
[DE94-005590] p 4267 N94-35996

U

ULTRAHIGH FREQUENCIES
DSS-13 S-/X-band microwave feed system
p 4253 N94-35550

ULTRAHIGH VACUUM
Heterogeneous reaction mechanisms and kinetics relevant to the CVD of semiconductor materials
[DE94-011001] p 4340 N94-36032

ULTRASONIC RADIATION
Absolute calibration technique for broadband ultrasonic transducers
[NASA-CASE-LAR-14672-1] p 4268 N94-35368

ULTRASONIC WAVE TRANSDUCERS
Absolute calibration technique for broadband ultrasonic transducers
[NASA-CASE-LAR-14672-1] p 4268 N94-35368

ULTRAVIOLET RADIATION
Absolute, Extreme Ultraviolet Solar Spectral Irradiance Monitor (AESSIM)
[AD-A278709] p 4227 N94-36189
Theoretical and experimental studies relevant to interpretation of auroral emissions
[NASA-CR-196032] p 4376 N94-36421

ULTRAVIOLET SPECTRA
ROSAT/XRT-PSPC observations and the ionizing continuum of Seyfert 1 galaxy Mkn 478
[PB94-167053] p 4350 N94-35530

UMBILICAL CONNECTORS
Microgravity isolation system design: A modern control synthesis framework p 4215 N94-35851

UNDERGROUND EXPLOSIONS
A comparison of artificial neural networks and statistical analyses
[DE94-010846] p 4312 N94-36195

UNDERGROUND STORAGE
Hydrodynamically induced loads on components submerged in high-level waste-storage tanks
[DE94-009663] p 4264 N94-35756
Decision and systems analysis for underground storage tank waste retrieval systems and tank waste remediation system
[SAND94-0065] p 4286 N94-35957

UNDERWATER COMMUNICATION
An electronic interface for a fiber optic tethered unmanned underwater vehicle
[AD-A279046] p 4333 N94-35747

UNDERWATER VEHICLES
An electronic interface for a fiber optic tethered unmanned underwater vehicle
[AD-A279046] p 4333 N94-35747

UNITED STATES
Proceedings of the Workshop on the Federal Criteria for Information Technology Security
[PB94-162583] p 4346 N94-36005

UNIVERSE
Primordial nucleosynthesis in conformal Weyl gravity
[DE94-003002] p 4327 N94-36241

UNIVERSITY PROGRAM
Introduction to USRA
[NASA-CR-195980] p 4376 N94-35590
National Educators' Workshop: Update 1993. Standard Experiments in Engineering Materials Science and Technology
[NASA-CP-3259] p 4229 N94-36398

UNSTEADY AERODYNAMICS
Robust control design techniques for active flutter suppression p 4200 N94-35875
UNSTEADY FLOW
On the nonlinear stability of viscous modes within the Rayleigh problem on an infinite flat plate [NASA-CR-194909] p 4263 N94-35497
Unsteady structure of leading-edge vortices on a delta wing [AD-A278988] p 4190 N94-35529
A multilevel adaptive projection method for unsteady incompressible flow [DE93-016418] p 4267 N94-36315
UPPER ATMOSPHERE RESEARCH SATELLITE (UARS)
In-flight estimation of gyro noise on the Upper Atmosphere Research Satellite (UARS) and Extreme Ultraviolet Explorer (EUVE) missions p 4204 N94-35616
Operational support for Upper Atmosphere Research Satellite (UARS) attitude sensors p 4204 N94-35617
Color/magnitude calibration for National Aeronautics and Space Administration (NASA) standard Fixed-Head Star Trackers (FHST) p 4209 N94-35641
UPPER SURFACE BLOWING
The reduction of takeoff ground roll by the application of a nose gear jump strut [NASA-TM-108822] p 4198 N94-36380
URANIUM
An indigenously developed photoacoustic spectrometer for study of actinide spectroscopy [DE94-616508] p 4235 N94-35592
URANIUM CARBIDES
Digital control programmer for temperature control [DE94-615584] p 4309 N94-36382
URBAN TRANSPORTATION
Bus application of oxygen-enrichment technology and diesel-electric hybrid systems [DE94-009835] p 4285 N94-35765
UREILITES
Ar-39-Ar-40 ages of four ureilites p 4357 N94-35410
USER MANUALS (COMPUTER PROGRAMS)
Optimization of residual stresses in MMC's using compensating/compliant interfacial layers. Part 2: OPTCOMP user's guide [NASA-CR-195337] p 4278 N94-35239
Langley 14- by 22-foot subsonic tunnel test engineer's data acquisition and reduction manual [NASA-TM-4563] p 4189 N94-35246
Description and use of LSODE, the Livermore Solver for Ordinary Differential Equations [NASA-RP-1327] p 4313 N94-35259
Defense RDT and E online system (DROLS) retrieval reference guide [AD-A278972] p 4344 N94-35525
Environment/tool integrator for software development, version 1.2 [AD-A278965] p 4303 N94-35660
Fire data management system, FDMS 2.0, technical documentation [PB94-164019] p 4346 N94-35819
ONED90: 1-dimensional diffusion code [DE94-611063] p 4305 N94-35834
User's guide for an interactive personal computer interface for the aeroprediction code [NSWCDD/TR-94/107] p 4305 N94-35958
HST archive primer, version 4.1 [NASA-CR-189370] p 4349 N94-36280
SandiaXTP, an object-oriented implementation of XTP 3.7 [DE94-011752] p 4257 N94-36354
UTILIZATION
Classification of advanced technical ceramics [REPT-15] p 4243 N94-35335

V

VACUUM
On new theories of physical vacuum [DE94-616613] p 4318 N94-35955
Network analyzer calibration for cryogenic on-wafer measurements [DE94-010089] p 4262 N94-36430
VACUUM FURNACES
Digital control programmer for temperature control [DE94-615584] p 4309 N94-36382
VALENCE
Periodicity and peculiarity in 120 first and second row diatomic molecules [AD-A278836] p 4323 N94-35793
New anionic states of the lithium trimer [AD-A278832] p 4323 N94-35797
VANADIUM COMPOUNDS
Metal cluster alloys and oxides: Elucidating structural and electronic effects in governing the reactivity and catalytic role of matter in finite dimensions [DE94-010224] p 4328 N94-36298
VAPOR DEPOSITION
Grain rims on ilmenite in the lunar regolith: Comparison to vapor deposits on regolith silicates p 4359 N94-35418
The optimization of interfaces in InAsSb/InGaAs strained-layer superlattices grown by metal-organic chemical vapor deposition [DE94-010070] p 4340 N94-35698
Development of novel II-VI solar cells [PB94-159415] p 4262 N94-35739
The growth of silicon nitride crystalline films using microwave plasma enhanced chemical vapor deposition [AD-A278862] p 4340 N94-35828
Heterogeneous reaction mechanisms and kinetics relevant to the CVD of semiconductor materials [DE94-011001] p 4340 N94-36032
Nonlinear optical composites of metal cluster laden polymers [AD-D016217] p 4234 N94-36124
Demonstration of a high heat removal CVD diamond substrate edge-cooled multichip module [DE94-010748] p 4260 N94-36245
Experiments in diamond film fabrication in table-top plasma apparatus p 4231 N94-36411
VAPOR PHASES
Development of atmospheric characteristics of chlorine-free alternative fluorocarbons [DE94-009791] p 4287 N94-36179
VAPOR PRESSURE
Unleaded AVGAS program [AD-A278650] p 4247 N94-35795
VAPORS
Final regulatory impact analysis: Refueling emission regulations for light duty vehicles and trucks and heavy duty vehicles [PB94-164027] p 4285 N94-35754
Solubility, viscosity and density of refrigerant/lubricant mixtures [DE94-009996] p 4245 N94-35771
Vapor-fortified QA/QC samples for the analysis of volatile organic compounds [AD-A278712] p 4229 N94-35776
Unleaded AVGAS program [AD-A278650] p 4247 N94-35795
VARIABLE GEOMETRY STRUCTURES
Kinematic modeling of a double octahedral Variable Geometry Truss (VGT) as an extensible gimbal [NASA-TM-109127] p 4311 N94-35242
VARIATIONAL PRINCIPLES
Complex Kohn variational principle for two-nucleon bound-state and scattering with the tensor potential [DE94-616651] p 4321 N94-35595
Variational method in relativistic two-body problem [DE94-612462] p 4315 N94-36416
VAX COMPUTERS
The development of a statistical report software for computer system usages [DE94-611061] p 4346 N94-35832
VECTOR MESONS
Low energy theorems from the effective Lagrangian with vector mesons [DE94-611173] p 4322 N94-35785
VECTOR QUANTIZATION
Combining nonlinear multiresolution system and vector quantization for still image compression [DE94-009422] p 4305 N94-36017
VEGETATION GROWTH
Effect of microgravity on plant growth [NASA-CR-196004] p 4296 N94-35257
VELOCITY DISTRIBUTION
Thickness of the layer of strong radial electric field in JFT-2M H-mode plasmas [DE94-718993] p 4336 N94-35812
The velocity field created by a shallow bump in a boundary layer [NASA-CR-194899] p 4266 N94-35975
Doppler weather radar studies of precipitation systems [AD-A279417] p 4295 N94-36262
VELOCITY MEASUREMENT
Purity and cleanness of aerogel as a cosmic dust capture medium p 4247 N94-35469
A dynamic method for magnetic torque measurement p 4216 N94-35856
VENEZIANO MODEL
Q-deformations of the Veneziano model [DE94-616769] p 4315 N94-36076
VENTILATION
Thermal performance of residential duct systems in basements [LBL-33962] p 4250 N94-35364
VENTS
Role of magma-water interaction in very large explosive eruptions [DE94-002698] p 4291 N94-36103
VENUS (PLANET)
The fine structure of Langmuir waves observed upstream of the bow shock at Venus [NASA-CR-196123] p 4354 N94-35378
Venus climate stability and volcanic resurfacing rates p 4358 N94-35413
Quantifying shapes of volcanoes on Venus p 4361 N94-35429
Volcano morphometry and volume scaling on Venus p 4361 N94-35431
Rheology, tectonics, and the structure of the Venus lithosphere p 4367 N94-35479
Atmosphere of Venus [NASA-CR-194214] p 4367 N94-35507
Magellan collection of radar calibration results [NASA-CR-194753] p 4367 N94-35509
Magellan to Venus [NASA-CR-195779] p 4201 N94-35510
Patterns of brittle deformation under extension on Venus p 4373 N94-36168
VENUS ATMOSPHERE
Venus climate stability and volcanic resurfacing rates p 4358 N94-35413
Atmosphere of Venus [NASA-CR-194214] p 4367 N94-35507
VENUS CLOUDS
H2O-H2SO4 system in Venus' clouds and OCS, CO, and H2SO4 profiles in Venus' troposphere p 4370 N94-36152
VENUS SURFACE
Quantifying shapes of volcanoes on Venus p 4361 N94-35429
Mesoscale roughness of Venus p 4361 N94-35430
Volcano morphometry and volume scaling on Venus p 4361 N94-35431
Rheology, tectonics, and the structure of the Venus lithosphere p 4367 N94-35479
Formation of fold and thrust belts on Venus due to horizontal shortening of a laterally heterogeneous lithosphere p 4367 N94-35480
VERTICAL TAKEOFF AIRCRAFT
Tipjet 80-inch model rotor hover test: Test no. 1198 [AD-A279680] p 4191 N94-36261
VERY LARGE SCALE INTEGRATION
High level modelling and design of asynchronous interface logic [PB94-167822] p 4258 N94-35534
VERY LONG BASE INTERFEROMETRY
NASA Space Geodesy Program: GSFC data analysis, 1993. VLBI geodetic results 1979 - 1992 [NASA-TM-104605] p 4281 N94-35261
Correlator data analysis for the array feed compensation system p 4253 N94-35553
VESTIBULAR TESTS
Visual-vestibular interaction [NASA-CR-196097] p 4297 N94-35379
VHSIC (CIRCUITS)
Rapid and accurate timing simulation of radiation-hardened digital microelectronics using VHDL [AD-A278644] p 4261 N94-36361
VIBRATION
High temperature superconductors for magnetic suspension applications p 4214 N94-35843
Maneuvering and control of flexible space robots p 4218 N94-35867
Variations in the modal characteristics of a telescopically deploying beam p 4218 N94-35872
Selected topics on the active control of helicopter aeromechanical and vibration problems p 4200 N94-35874
Parameter estimation of the vibrational model for the SCOLE experimental facility p 4219 N94-35878
Analysis of achievable disturbance attenuation in a precision magnetically-suspended motion control system p 4225 N94-35917
Recovery of frozen flow losses in arcjets [AD-A278739] p 4228 N94-36089
VIBRATION DAMPING
Data reduction, analysis and results of LACV-30-07 air cushion vehicle tests, Fort Story, VA, August - September 1993 [AD-A278859] p 4190 N94-35826
High temperature superconductors for magnetic suspension applications p 4214 N94-35843
Measurement and characterization of force dynamics in high T(sub c) superconductors p 4214 N94-35844
Distributed parameter modelling of flexible spacecraft: Where's the beef? p 4217 N94-35866
Control of flexible structures with distributed sensing and processing p 4218 N94-35871
Flutter suppression digital control law design and testing for the AFW wind tunnel model p 4200 N94-35873

Selected topics on the active control of helicopter aeromechanical and vibration problems
p 4200 N94-35874
Robust control design techniques for active flutter suppression p 4200 N94-35875
Optimal disturbance rejecting control of hyperbolic systems p 4220 N94-35882
Vibration suppression in flexible structures via the sliding-mode control approach p 4220 N94-35884
Active vibration damping using smart material
p 4221 N94-35886
Software for continuum modeling of controls-structures interactions p 4223 N94-35898
Electromechanical simulation and test of rotating systems with magnetic bearing or piezoelectric actuator active vibration control p 4223 N94-35905
Vibration reduction in helicopter rotors using an actively controlled partial span trailing edge flap located on the blade
[NASA-CR-4611] p 4280 N94-36423

VIBRATION EFFECTS
Dynamic structural effects and ultrafast biomolecular kinetics in photoinduced charge transfer reactions
[DE94-010421] p 4329 N94-36390

VIBRATION ISOLATORS
Microgravity isolation system design: A modern control synthesis framework p 4215 N94-35851
Electromagnetically levitated vibration isolation system for the manufacturing process of silicon monocrystals
p 4223 N94-35906

VIBRATION MEASUREMENT
Smart accelerometer --- vibration damage detection
[NASA-CASE-MSC-21951-1] p 4268 N94-35235

VIBRATION METERS
Smart accelerometer --- vibration damage detection
[NASA-CASE-MSC-21951-1] p 4268 N94-35235

VIBRATION MODE
Applying transfer matrix method to the estimation of the modal characteristics of the NASA Mini-Mass Truss
p 4218 N94-35870
Variations in the modal characteristics of a telescopically deploying beam p 4218 N94-35872
Vibration suppression in flexible structures via the sliding-mode control approach p 4220 N94-35884
Ground vibration test of the XV-15 Tiltrotor Research Aircraft and pretest predictions p 4200 N94-35972
A procedure for oscillatory parameter identification
[DE94-008047] p 4259 N94-36054

VIBRATION TESTS
Ground vibration test of the XV-15 Tiltrotor Research Aircraft and pretest predictions p 4200 N94-35972

VIBRATIONAL SPECTRA
On the effects of transforming the vibrational spectra of molecular systems under microwave radiation
[DE94-617057] p 4329 N94-36310

VIDEO SIGNALS
The iWarp display module
[AD-A278610] p 4260 N94-36248

VIGNETTING
AXAF-I ghost ray study: On orbit case
[NASA-CR-193987] p 4333 N94-36119

VISCOELASTIC DAMPING
Transfer function modeling of damping mechanisms in distributed parameter models p 4222 N94-35895

VISCOSITY
Determination of extensional viscosity from capillary rheometer entrance pressure drop measurements using a numerical simulation of contraction flow
[PB94-171154] p 4263 N94-35603
Measurement of viscosity, density, and gas solubility of refrigerant blends in selected synthetic lubricants
[DE94-010426] p 4244 N94-35687
Solubility, viscosity and density of refrigerant/lubricant mixtures
[DE94-009996] p 4245 N94-35771
Analysis of current diffusive ballooning mode
[DE94-718992] p 4336 N94-35811

VISCOUS FLOW
An efficient, intelligent solution for viscous flows inside solid rocket motors
[AD-A278629] p 4228 N94-36255
Computational Mathematics Laboratory for multiscale analysis
[AD-A278597] p 4315 N94-36424

VISIBILITY
Analysis of regional visibility in the eastern United States using aerosol models
[PB94-158698] p 4332 N94-35584
Data requirements for ceiling and visibility products development
[AD-A278959] p 4293 N94-35720

VISIBLE SPECTRUM
High resolution visible to short-wave near-infrared CCD spectra of Mars during 1990 p 4356 N94-35403

VISUAL PERCEPTION
Visual-vestibular interaction
[NASA-CR-196097] p 4297 N94-35379
Accommodation during instrument viewing can be influenced by knowledge of object distance
[AD-A278987] p 4298 N94-35528

VISUAL STIMULI
Visual-vestibular interaction
[NASA-CR-196097] p 4297 N94-35379

VITERBI DECODERS
Issues in the development of a 10 MBPS K=15 Viterbi decoder
[NASA-CR-196083] p 4211 N94-35357
Maximum-likelihood soft-decision decoding of block codes using the A* algorithm p 4254 N94-35555

VOLATILITY
Vapor-fortified QA/QC samples for the analysis of volatile organic compounds
[AD-A278712] p 4229 N94-35776
Alkali element constraints on Earth-Moon relations
p 4354 N94-36169

VOLCANOES
Quantifying shapes of volcanoes on Venus
p 4361 N94-35429
Volcano morphometry and volume scaling on Venus
p 4361 N94-35431
The topography of Mars: A re-evaluation of current data p 4364 N94-35460
Role of magma-water interaction in very large explosive eruptions
[DE94-002698] p 4291 N94-36103

VOLCANOLOGY
The Twenty-Fifth Lunar and Planetary Science Conference. Part 1: A-G
[NASA-CR-195743] p 4355 N94-35395
Volcano morphometry and volume scaling on Venus
p 4361 N94-35431
The Twenty-Fifth Lunar and Planetary Science Conference. Part 3: P-Z
[NASA-CR-195745] p 4362 N94-35448
Isotopic and geochemical precursors of earthquakes and volcanic eruptions
[DE94-615824] p 4289 N94-35568
The Twenty-Fifth Lunar and Planetary Science Conference. Part 2: H-O
[NASA-CR-195744] p 4367 N94-36136

VOLTAGE CONVERTERS (DC TO DC)
Microprocessor control of multiple peak power tracking DC/DC converters for use with solar cell arrays
[NASA-CASE-GSC-13450-2] p 4282 N94-35540

VORTEX BREAKDOWN
Unsteady structure of leading-edge vortices on a delta wing
[AD-A278988] p 4190 N94-35529

VORTICES
Unsteady structure of leading-edge vortices on a delta wing
[AD-A278988] p 4190 N94-35529
Hydrodynamics of maneuvering bodies: LDRD Final Report
[DE94-009970] p 4265 N94-35769
F/A-18 forebody vortex control. Volume 1: Static tests
[NASA-CR-4582] p 4190 N94-35991
Vortex tubes in turbulent flows: Identification, representation, reconstruction
[NASA-CR-194900] p 4267 N94-35992
On possible types of vortexes in relativistic superfluid system
[DE94-617392] p 4267 N94-36098
Superconducting transistors
[PB94-170743] p 4260 N94-36260

VORTICITY
Unsteady structure of leading-edge vortices on a delta wing
[AD-A278988] p 4190 N94-35529
Spatio-temporal properties of centrifugal instabilities: Abstracts of 8th Couette-Taylor Meeting
[PB94-150240] p 4266 N94-35981
Vortex tubes in turbulent flows: Identification, representation, reconstruction
[NASA-CR-194900] p 4267 N94-35992

VOYAGER PROJECT
Voyager: National Air and Space Museum
[NASA-CR-195905] p 4367 N94-35505
Voyager last picture show
[NASA-CR-195796] p 4367 N94-35506
Voyager science summary tape
[NASA-CR-195909] p 4367 N94-35513

W

WAFERS
Laser drilling of vertical vias in silicon
[DE94-009250] p 4270 N94-35351
Materials for efficient high-flux magnetic bearing actuators p 4214 N94-35845

WAKES
Hydrodynamics of maneuvering bodies: LDRD Final Report
[DE94-009970] p 4265 N94-35769

WALL FLOW
The aerodynamic and heat transfer effects of an endwall boundary layer fence in a 90 degree turning square duct
[AD-A278903] p 4265 N94-35803

WALL PRESSURE
Method for making a dynamic pressure sensor and a pressure sensor made according to the method
[NASA-CASE-LAR-14029-1] p 4269 N94-35369

WALL TEMPERATURE
Compliant metal enhanced convection cooled reverse-flow annular combustor
[NASA-TM-106626] p 4199 N94-36379

WAR GAMES
The application of fuzzy logic to SAFOR in SIMNET
[AD-A279058] p 4312 N94-35730

WARNING SYSTEMS
Terminal Doppler Weather Radar (TDWR) Low Level Wind Shear Alert System 3 (LLWAS 3) integration studies at Orlando International Airport
[AD-A278957] p 4294 N94-35807

WASTE DISPOSAL
Decision and systems analysis for underground storage tank waste retrieval systems and tank waste remediation system
[SAND94-0065] p 4286 N94-35957

WATER
Fluvial processes in Ma'adim Vallis and the potential of Gusev crater as a high priority site
p 4358 N94-35414
A quick look method of detecting water of hydration in small solar system bodies p 4352 N94-35470
Role of magma-water interaction in very large explosive eruptions
[DE94-002698] p 4291 N94-36103
The structural changes of water ice I during warmup
p 4239 N94-36144
Uniqueness of a solution of a steady state photochemical problem: Applications to Mars p 4370 N94-36151
Equations of state valid continuously from zero to extreme pressures with H2O and CO2 as examples
[DE94-011907] p 4238 N94-36230
Coal-fueled diesels for modular power generation
[DE94-002960] p 4275 N94-36348

WATER COLOR
Mission to Planet Earth. The living ocean: Observing ocean color from space
[NASA-PAM-554] p 4295 N94-35343

WATER EROSION
Fluvial processes in Ma'adim Vallis and the potential of Gusev crater as a high priority site
p 4358 N94-35414

WATER VAPOR
Production of long-term global water vapor and liquid water data set using ultra-fast methods to assimilate multi-satellite and radiosonde observations
[NASA-CR-196044] p 4292 N94-35355
Simultaneous adsorption of CO2 and H2O under Mars-like conditions and application to the evolution of the Martian climate p 4366 N94-35475
Production of long-term global water vapor and liquid water data set using ultra-fast methods to assimilate multi-satellite and radiosonde observations
[NASA-CR-195981] p 4293 N94-35499
H2O-H2SO4 system in Venus' clouds and OCS, CO, and H2SO4 profiles in Venus' troposphere
p 4370 N94-36152
Investigation of moisture-induced embrittlement of iron aluminides
[DE94-010881] p 4241 N94-36196

WAVE DIFFRACTION
Numerical simulation of shock interaction with above-ground structures
[AD-A278713] p 4279 N94-35949

WAVE DISPERSION
The energy density of fluctuative electromagnetic field near the semi-bounded plasma
[DE94-617188] p 4256 N94-36099

WAVE EQUATIONS
Goldstone pion and other mesons using a scalar confining interaction
[DE94-010016] p 4321 N94-35649
Theoretical studies of ultrashort phenomena
[AD-A278938] p 4332 N94-35664
A note on high order schemes for one dimensional wave equation
[PB94-171006] p 4315 N94-35821

WAVE FRONT DEFORMATION
Predicted optical performance of the High-Altitude Balloon Experiment (HABE) telescope in an adverse thermal environment
[DE94-008949] p 4349 N94-35998
WAVE FRONT RECONSTRUCTION
A multi-tiered wavefront sensor using binary optics
[DE94-010393] p 4267 N94-36111
WAVE FRONTS
A multi-tiered wavefront sensor using binary optics
[DE94-010393] p 4267 N94-36111
WAVE FUNCTIONS
Calculations on some properties of the pion in the framework of Schwinger-Dyson and Bethe-Salpeter equations
[DE94-611232] p 4322 N94-35786
Elastic p(4)He scattering at intermediate energies
[DE94-618544] p 4328 N94-36287
WAVE GENERATION
ULF waves in the low-latitude boundary layer and their relationship to magnetospheric pulsations: A multisatellite observation
[AD-A278906] p 4289 N94-35587
On the physics of waves in the solar atmosphere: Wave heating and wind acceleration
[NASA-CR-194119] p 4375 N94-36395
WAVE PACKETS
JPRS report: Science and technology. Central Eurasia
[JPRS-UST-94-006] p 4249 N94-35226
Coherent states versus de Broglie-wavelets
[DE94-611075] p 4343 N94-36381
WAVE PROPAGATION
Review of slow-wave structures
[NASA-TM-106639] p 4258 N94-35270
Initial perturbations and Langmuir waves in electron-positron plasma
[DE94-617190] p 4338 N94-36097
X ray radiographic imaging of hydrodynamic phenomena in radiation driven materials: Shock propagation and shear flow
[DE94-010891] p 4318 N94-36201
TSAR modeling of a TEM horn and surrounding structure
[DE94-010668] p 4256 N94-36301
On the physics of waves in the solar atmosphere: Wave heating and wind acceleration
[NASA-CR-194119] p 4375 N94-36395
Computational Mathematics Laboratory for multiscale analysis
[AD-A278597] p 4315 N94-36424
WAVE REFLECTION
Green's functions for an anisotropic medium. Part 2: Two-layer case
[AD-A278788] p 4256 N94-35713
WAVE SCATTERING
Relativistic three-particle dynamical equations. 2: Theoretical development
[DE94-616654] p 4320 N94-35581
WAVEFORMS
Center for seismic studies
[AD-A278682] p 4290 N94-35693
Coherent states versus de Broglie-wavelets
[DE94-611075] p 4343 N94-36381
WAVEGUIDE ANTENNAS
The electrical conductivities of candidate beam-waveguide antenna shroud materials
p 4252 N94-35546
Thin-ribbon tapered coupler for dielectric waveguides
p 4253 N94-35547
Design and implementation of a beam-waveguide mirror control system for vernier pointing of the DSS-13 antenna p 4253 N94-35548
Use of the sampling theorem to speed up near-field physical optics scattering calculations
p 4253 N94-35549
DSS-13 S-/X-band microwave feed system
p 4253 N94-35550
WAVEGUIDES
Thin-ribbon tapered coupler for dielectric waveguides
p 4253 N94-35547
Characterization of lithium niobate electro-optic modulators at cryogenic temperatures
[DE94-010059] p 4333 N94-35697
WAVELET ANALYSIS
Coherent states versus de Broglie-wavelets
[DE94-611075] p 4343 N94-36381
Computational Mathematics Laboratory for multiscale analysis
[AD-A278597] p 4315 N94-36424
Periodized wavelets
[DE94-010365] p 4316 N94-36432
WEAK INTERACTIONS (FIELD THEORY)
Radiatively induced electron and electron-neutrino masses
[DE94-616775] p 4321 N94-35582
Some consequences in weak processes of three generations mixing in the leptonic sector
[DE94-616650] p 4321 N94-35594
WEAR
Durability testing of medium speed diesel engine components designed for operating on coal/water slurry fuel
[DE94-009550] p 4275 N94-35667
WEAR RESISTANCE
Durability testing of medium speed diesel engine components designed for operating on coal/water slurry fuel
[DE94-009550] p 4275 N94-35667
Wear-resisting oxide films for 900 C
[DE94-010093] p 4246 N94-36306
WEATHER FORECASTING
Extrapolating storm location using the Integrated Terminal Weather System (ITWS) storm motion algorithm
[AD-A278611] p 4295 N94-36249
Use of formal calculation to automatically obtain adjoint programs
[PB94-170701] p 4308 N94-36259
Doppler weather radar studies of precipitation systems
[AD-A279417] p 4295 N94-36262
WEATHERING
Antarctic weathering of the CK chondrites EET90004, 90007, and 90022: Nickel and sulfur mobility
p 4351 N94-35451
WEDGES
Wedge scattering by the method of iteration
[DE94-010404] p 4256 N94-36112
WEIGHT INDICATORS
Piggyback balance experiment: An illustration of Archimedes' principles and Newton's third law
[PB94-163060] p 4265 N94-35942
WEIGHT MEASUREMENT
Piggyback balance experiment: An illustration of Archimedes' principles and Newton's third law
[PB94-163060] p 4265 N94-35942
WEIGHTING FUNCTIONS
Cramer-von Mises variance estimators for simulations
[AD-A278799] p 4316 N94-35675
WETLANDS
Methane production and consumption in grassland and boreal ecosystems
[NASA-CR-196085] p 4284 N94-35486
WETTABILITY
Manufacturing feasibility of several lead-free solders for electronic assembly
[DE94-007732] p 4258 N94-35564
WETTING
Preliminary results of sulfide melt/silicate wetting experiments in a partially melted ordinary chondrite
p 4353 N94-36147
WILDLIFE
Endangered and potentially endangered wildlife on John F. Kennedy Space Center and faunal integrity as a goal for maintaining biological diversity
[NASA-TM-109204] p 4288 N94-36422
WIND EFFECTS
Windblown sand on Mars: The effect of saltation threshold on drift potentials derived from Mars GCM
p 4366 N94-35474
WIND MEASUREMENT
Use of wind profiler data in short-range forcasting
[AD-A279482] p 4295 N94-36228
Doppler weather radar studies of precipitation systems
[AD-A279417] p 4295 N94-36262
WIND PROFILES
Use of wind profiler data in short-range forcasting
[AD-A279482] p 4295 N94-36228
WIND SHEAR
Terminal Doppler Weather Radar (TDWR) Low Level Wind Shear Alert System 3 (LLWAS 3) integration studies at Orlando International Airport
[AD-A278957] p 4294 N94-35807
WIND TUNNEL APPARATUS
Langley 14- by 22-foot subsonic tunnel test engineer's data acquisition and reduction manual
[NASA-TM-4563] p 4189 N94-35246
Status of MSBS study at NAL p 4216 N94-35854
Three-dimensional force data acquisition and boundary corrections for the Walter H. Beech Memorial 7 x 10 foot low speed wind tunnel
[AR93-2] p 4200 N94-36437
WIND TUNNEL CALIBRATION
Three-dimensional force data acquisition and boundary corrections for the Walter H. Beech Memorial 7 x 10 foot low speed wind tunnel
[AR93-2] p 4200 N94-36437
WIND TUNNEL MODELS
Status of MSBS study at NAL p 4216 N94-35854
The simulation of a propulsive jet and force measurement using a magnetically suspended wind tunnel model p 4191 N94-35855
Flutter suppression digital control law design and testing for the AFW wind tunnel model p 4200 N94-35873
Three-dimensional force data acquisition and boundary corrections for the Walter H. Beech Memorial 7 x 10 foot low speed wind tunnel
[AR93-2] p 4200 N94-36437
WIND TUNNEL NOZZLES
A supersonic tunnel for laser and flow-seeding techniques
[NASA-TM-106588] p 4265 N94-35945
WIND TUNNEL TESTS
The aerodynamic and heat transfer effects of an endwall boundary layer fence in a 90 degree turning square duct
[AD-A278903] p 4265 N94-35803
The simulation of a propulsive jet and force measurement using a magnetically suspended wind tunnel model p 4191 N94-35855
Flutter suppression digital control law design and testing for the AFW wind tunnel model p 4200 N94-35873
Wind tunnel measurements on a full-scale F/A-18 with a tangentially blowing slot — conducted in the Ames 80 by 120 foot wind tunnel p 4191 N94-35965
The velocity field created by a shallow bump in a boundary layer
[NASA-CR-194899] p 4266 N94-35975
F/A-18 forebody vortex control. Volume 1: Static tests
[NASA-CR-4582] p 4190 N94-35991
WIND VELOCITY
Doppler weather radar studies of precipitation systems
[AD-A279417] p 4295 N94-36262
WINDING
Feasibility study of superconducting LSM rocket launcher system p 4225 N94-35914
WINDOWS (COMPUTER PROGRAMS)
Multi-window dialogue system of data processing for experimental setup VASSILISSA in PAW environment
[DE94-612439] p 4345 N94-35790
Netlib services and resources
[DE94-010307] p 4347 N94-36300
WINDPOWER UTILIZATION
Model documentation: Renewable Fuels Module of the National Energy Modeling System
[DE94-009962] p 4282 N94-35672
WING LOADING
The reduction of takeoff ground roll by the application of a nose gear jump strut
[NASA-TM-108822] p 4198 N94-36380
WING TANKS
Flight test certification of a 480 gallon composite fuel tank on CF-18 p 4196 N94-36340
WING TIP VORTICES
Numerical modeling studies of wake vortex transport and evolution within the planetary boundary layer
[NASA-CR-196078] p 4192 N94-35522
WINGS
Ground vibration test of the XV-15 Tiltrotor Research Aircraft and pretest predictions p 4200 N94-35972
Aeroservoelastic tailoring with piezoelectric materials: Actuator optimization studies
[AD-A278640] p 4199 N94-36384
WORDS (LANGUAGE)
Good applications for crummy machine translation
[AD-A278689] p 4345 N94-35651
WORKING FLUIDS
Solubility, viscosity and density of refrigerant/lubricant mixtures
[DE94-009996] p 4245 N94-35771
Sealed tube comparisons of the compatibility of desiccants with refrigerants and lubricants
[DE94-010002] p 4251 N94-36388
WORKLOADS (PSYCHOPHYSIOLOGY)
The influence of data link-provided graphical weather on pilot decision-making
[AD-A278871] p 4293 N94-35596
Direct reduced order mixed H2/H infinity control for the Short Take-Off and Landing/Maneuver Technology Demonstrator (STOL/MTD)
[AD-A278675] p 4199 N94-35796
Final-Approach Spacing Aids (FASA) evaluation for terminal-area, time-based air traffic control
[NASA-TP-3399] p 4192 N94-36048
WORKSTATIONS
International Space Station alpha remote manipulator system workstation controls test report
[NASA-TM-104796] p 4274 N94-35481
North American ISDN Users' Forum agreements on Integrated Services Digital Network
[PB94-162559] p 4305 N94-35940
WOVEN COMPOSITES
Through-the-thickness tensile strength of textile composites
[NASA-TM-109115] p 4233 N94-35946

X

X RAY ASTRONOMY

ROSAT/XRT-PSPC observations and the ionizing continuum of Seyfert 1 galaxy Mkn 478
[PB94-167053] p 4350 N94-35530

X RAY ASTROPHYSICS FACILITY

AXAF-I ghost ray study: On orbit case
[NASA-CR-193987] p 4333 N94-36119

X RAY DETECTORS

X-ray remote sensing and in-situ spectroscopy for planetary exploration missions and gamma-ray remote sensing and in-situ spectroscopy for planetary exploration missions
[NASA-CR-189352] p 4375 N94-35381

X RAY DIFFRACTION

A mineralogical instrument for planetary applications
p 4357 N94-35408

The growth of silicon nitride crystalline films using microwave plasma enhanced chemical vapor deposition
[AD-A278862] p 4340 N94-35828

In situ studies of zeolite syntheses using powder diffraction methods: Crystallization of instant zeolite A powder and CoAPO-5
[DE94-006570] p 4341 N94-36358

X RAY FLUORESCENCE

A mineralogical instrument for planetary applications
p 4357 N94-35408

Remote geochemical experiment package for Discovery class missions p 4350 N94-35420

Innovative instrumentation for mineralogical and elemental analyses of solid extraterrestrial surfaces: The Backscatter Moessbauer Spectrometer/X Ray Fluorescence analyzer (BaMS/XRF)
p 4239 N94-35459

Continuum fluorescence of Cu in NbTi/Cu composite wires
[DE94-008940] p 4241 N94-36242

X RAY IMAGERY

Lunar mineral feedstocks from rocks and soils: X-ray digital imaging in resource evaluation
p 4358 N94-35415

X ray radiographic imaging of hydrodynamic phenomena in radiation driven materials: Shock propagation, material compression and shear flow
[DE94-009515] p 4266 N94-35982

X ray radiographic imaging of hydrodynamic phenomena in radiation driven materials: Shock propagation and shear flow
[DE94-010891] p 4318 N94-36201

X RAY IRRADIATION

Enhanced charge trapping in bipolar spacer oxides during low-dose-rate irradiation
[DE94-007863] p 4260 N94-36268

X RAY SPECTRA

ROSAT/XRT-PSPC observations and the ionizing continuum of Seyfert 1 galaxy Mkn 478
[PB94-167053] p 4350 N94-35530

X RAY SPECTROSCOPY

Remote geochemical experiment package for Discovery class missions p 4350 N94-35420

Petrographic characterization of lunar soils: Application of x ray digital-imaging to quantitative and automated analysis p 4368 N94-36138

X RAYS

X-ray remote sensing and in-situ spectroscopy for planetary exploration missions and gamma-ray remote sensing and in-situ spectroscopy for planetary exploration missions
[NASA-CR-189352] p 4375 N94-35381

AXAF-I ghost ray study: On orbit case
[NASA-CR-193987] p 4333 N94-36119

Activities of the optoelectronics laboratory
[PB94-171196] p 4334 N94-36190

Scaling laws for TEXT plasma profiles
[DE94-010832] p 4338 N94-36200

X ray radiographic imaging of hydrodynamic phenomena in radiation driven materials: Shock propagation and shear flow
[DE94-010891] p 4318 N94-36201

Kinetic theory of runaway air breakdown and the implications for lightning initiation
[DE94-001683] p 4295 N94-36240

X WING ROTORS

Vibration reduction in helicopter rotors using an actively controlled partial span trailing edge flap located on the blade
[NASA-CR-4611] p 4280 N94-36423

XENON

Kinetics studies following state-selective laser excitation
[DE94-010305] p 4330 N94-36105

XV-15 AIRCRAFT

Ground vibration test of the XV-15 Tiltrotor Research Aircraft and pretest predictions p 4200 N94-35972

Y

YAG LASERS

900-mW average power and tunability from a diode-pumped 2.94 micron Er:YAG oscillator
[DE94-009511] p 4271 N94-35679

Eyesafe rare earth crystal lasers for atmosphere soudings
[AD-A279486] p 4273 N94-36227

YAWING MOMENTS

Wind tunnel measurements on a full-scale F/A-18 with a tangentially blowing slot --- conducted in the Ames 80 by 120 foot wind tunnel p 4191 N94-35965

YBCO SUPERCONDUCTORS

Report on a SQUID made from high temperature superconductor
[PB94-169307] p 4339 N94-35598

Flux-pinning related defects in YBa2Cu3O(7-x) thin films grown on miscut LaAlO3 (001) substrates
[DE94-011463] p 4342 N94-36377

Z

ZEOLITES

NO decomposition in non-reducing atmospheres
[DE94-011157] p 4237 N94-36036

In situ studies of zeolite syntheses using powder diffraction methods: Crystallization of instant zeolite A powder and CoAPO-5
[DE94-006570] p 4341 N94-36358

Computer simulations of benzene in faujasite-type zeolites
[DE94-007533] p 4242 N94-36369

ZERO SOUND

First, second and fourth sound in relativistic superfluidity theory with account for dissipative effects
[DE94-617393] p 4267 N94-36314

ZINC

Au/Zn contacts to Rho-InP: Electrical and metallurgical characteristics and the relationship between them
[NASA-TM-106590] p 4281 N94-35271

Non-alloyed, refractory metal contact optimization with shallow implantations of Zn and Mg
[DE94-010392] p 4240 N94-36110

ZINC TELLURIDES

Development of novel II-VI solar cells
[PB94-159415] p 4282 N94-35739

ZIRCALOYS (TRADEMARK)

Consolidation of zircaloy-4 end crops by induction melting
[DE94-010031] p 4240 N94-35650

Thermodynamic behaviour of tellurium at high temperatures
[DE94-612823] p 4240 N94-35960

ZIRCONATES

Dielectric measurements of selected ceramics at microwave frequencies p 4232 N94-36412

ZIRCONIUM

Study of point defect mobilities in zirconium during electron irradiation in a HVEM
[DE94-619028] p 4242 N94-36289

ZIRCONIUM ALLOYS

Formation and stability of Fe-rich precipitates in dilute Zr(Fe) single-crystal alloys
[DE94-619027] p 4242 N94-36288

ZIRCONIUM COMPOUNDS

Vertical electron detachment energies for octahedral closed-shell multiply charged anions
[AD-A278835] p 4322 N94-35753

Metal cluster alloys and oxides: Elucidating structural and electronic effects in governing the reactivity and catalytic role of matter in finite dimensions
[DE94-010224] p 4328 N94-36298

ZIRCONIUM OXIDES

Defect detection in multi-layered, plasma sprayed zirconia by time resolved infrared radiometry: A comparison between analytical and experimental methods
[DE94-009803] p 4245 N94-35779

ZODIACAL LIGHT

Catalog of Helios 90 deg photometer events
[PL-TR-94-2040] p 4375 N94-36264

PERSONAL AUTHOR INDEX

SCIENTIFIC AND TECHNICAL AEROSPACE REPORTS VOLUME 32 NUMBER 11

Typical Personal Author Index Listing

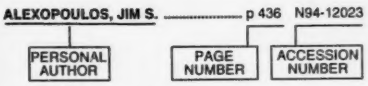

Listings in this index are arranged alphabetically by personal author. The page number helps you locate the citation in the abstract section. The accession number denotes the number by which the citation is identified.

A

ABBOT, RICK I.	p 4203	N94-35611
ABBOUD, R. G.	p 4282	N94-35829
ABRAMOWICZ-REED, L.	p 4204	N94-35615
ABRAMSON, MARK A.	p 4307	N94-36185
ABREGO, ANITA	p 4200	N94-35972
ABUSITTA, A. M. M.	p 4272	N94-35782
ACHACHE, JOSE	p 4354	N94-35336
ACOSTA, WALDO A.	p 4199	N94-36379
ADAMS, B. E.	p 4244	N94-35705
ADATI, K.	p 4338	N94-36247
ADHIKARI, S. K.	p 4320	N94-35580
	p 4320	N94-35581
	p 4321	N94-35595
ADL-TABATABAI, ALI-REZA	p 4302	N94-35572
AFUGGLAS, M.	p 4327	N94-36267
AFZAL, ROBERT S.	p 4273	N94-36365
AGRESTI, D. G.	p 4239	N94-35459
AHMED, N. U.	p 4220	N94-35882
AHRENS, THOMAS J.	p 4355	N94-35396
AITHAL, S.	p 4228	N94-36089
AKAISHI, K.	p 4336	N94-35752
	p 4338	N94-36352
AKAO, H.	p 4336	N94-35752
	p 4338	N94-36352
AKAU, R. L.	p 4349	N94-35998
AKIN, DAVID L.	p 4212	N94-35484
AKINLADE, O.	p 4240	N94-35935
AKIYAMA, R.	p 4338	N94-36247
	p 4339	N94-36357
ALANDER, J. T.	p 4303	N94-35602
ALBEE, A. L.	p 4202	N94-35607
ALBERG, M. A.	p 4324	N94-35824
ALLAIRE, P. E.	p 4214	N94-35847
	p 4215	N94-35851
ALLEN, C. C.	p 4355	N94-35397
	p 4355	N94-35398
ALLEN, C. T.	p 4260	N94-36197
ALLEN, C. W.	p 4241	N94-36222
ALLEN, CARLTON C.	p 4240	N94-36164
ALLEN, PETER	p 4278	N94-36046
ALLEN, R. P.	p 4275	N94-36022
ALLMEN, M. C.	p 4294	N94-35767
ALLTON, J. H.	p 4351	N94-35451
ALLTON, JUDITH H.	p 4355	N94-35399
ALONSO, ROBERTO	p 4209	N94-35644
ALTAN, TAYLAN	p 4250	N94-35711
ALUR, RAJEEV	p 4317	N94-35743
ALVAREZ, L. S.	p 4253	N94-35548
AMADOR, M.	p 4347	N94-36102
AMANO, T.	p 4337	N94-35936
AMBROSE, W. P.	p 4320	N94-35376
AMBUEL, L. M.	p 4346	N94-36005
AMOS, ANTHONY K.	p 4218	N94-35872
ANAGNOSTOPOULOS, GEORGE	p 4215	N94-35848
ANAND, DAVINDER K.	p 4217	N94-35861
ANDALEON, D. D.	p 4260	N94-36245
ANDERSON, B. JEFFREY	p 4291	N94-36175
ANDERSON, K. K.	p 4312	N94-36195
ANDERSON, T.	p 4250	N94-35532
ANDERSSON, M.	p 4259	N94-35822
ANDO, A.	p 4338	N94-36247
ANDREEV, A. N.	p 4345	N94-35790
ANDRES, E.	p 4253	N94-35548
ANDREWS, JOHN R.	p 4271	N94-35488
ANGOOD, S.	p 4272	N94-36062
ANKENMAN, BRUCE	p 4230	N94-36405
ANTOINE, G. J.	p 4231	N94-36407
ANTONIO, JOHN K.	p 4310	N94-35653
ANTONISHEK, T. A.	p 4305	N94-35940
ANTONOVA, E. E.	p 4350	N94-36128
AQUINO, V. M.	p 4321	N94-35593
ARENDALE, WILLIAM F.	p 4235	N94-35447
ARGO, P. E.	p 4257	N94-36316
ARIMOTO, H.	p 4337	N94-35936
	p 4339	N94-36357
ARISTOV, YU. A.	p 4336	N94-35791
ARLING, R. W.	p 4225	N94-35916
ARMSTRONG, E. S.	p 4221	N94-35889
ARNAL, D.	p 4194	N94-36328
ARNETTE, STEPHEN A.	p 4190	N94-35950
ARONOV, A. G.	p 4340	N94-35933
ARTAKL, I.	p 4258	N94-35564
ARYA, S. PAL	p 4192	N94-35522
ASH, RICHARD D.	p 4351	N94-35421
ASKARI, BRUCE	p 4343	N94-35970
ASPHAUG, E.	p 4355	N94-35400
	p 4351	N94-35406
ASSINK, R. A.	p 4244	N94-35701
	p 4244	N94-35702
ATWOOD, DAVID	p 4247	N94-35795
AXLINE, R. M.	p 4284	N94-35674
AYERS, BERT F.	p 4190	N94-35991
AZUMI, M.	p 4336	N94-35811

B

BABENKO, V. A.	p 4326	N94-36131
	p 4329	N94-36391
BABU, V.	p 4228	N94-36089
BACA, A. G.	p 4240	N94-36110
BACHMANN, GLEN R.	p 4200	N94-35875
BADIRKHAN, Z.	p 4240	N94-35935
BAECHLER, M. C.	p 4287	N94-36027
BAFFES, PAUL T.	p 4311	N94-35501
BAIK, DAE HYUN	p 4334	N94-36180
BAILEY, MICHAEL P.	p 4305	N94-36013
BAINUM, P. M.	p 4220	N94-35881
BAIR, K.	p 4283	N94-36051
BAJBUSINOV, B. O.	p 4259	N94-36104
BAJER, V. N.	p 4256	N94-36078
BAKER, D. F.	p 4209	N94-35642
BALAKRISHNAN, A. V.	p 4221	N94-35890
	p 4221	N94-35891
BALKO, BOHDAN	p 4312	N94-35730
BALMFORTH, N. J.	p 4264	N94-35681
BALS, TERESA	p 4295	N94-36262
BANKS, BRUCE A.	p 4243	N94-35243
	p 4243	N94-35502
BANKS, DAVID C.	p 4267	N94-35992
BANSAL, B. M.	p 4354	N94-36172
	p 4374	N94-36173
BAR-SHALOM, Y.	p 4256	N94-36092
BARANOV, A.	p 4273	N94-36218
BARAS, JOHN S.	p 4221	N94-35886
BARASHENKOV, V. S.	p 4318	N94-35955
BARCHET, W. R.	p 4288	N94-36359
BARCLAY, REBECCA O.	p 4344	N94-35254
BARGETTO, R.	p 4193	N94-36323
BARKASZI, MARY JO	p 4288	N94-36422
BARLETTA, W.	p 4331	N94-36271
BARNES, J. E.	p 4252	N94-35537
BARRETT, R. A.	p 4352	N94-35476
BARRETT, TIM	p 4223	N94-35905
BART, S.	p 4224	N94-35908
BARTH, M.	p 4319	N94-35770
BARTH, TIMOTHY	p 4299	N94-35393
BARTHELEMY-REQUIN, M.	p 4297	N94-36220
BARUT, A. O.	p 4343	N94-36381
BASHKANSKY, MARK	p 4334	N94-36368
BASILI, VICTOR R.	p 4301	N94-35435
	p 4301	N94-35438
BASS, B. R.	p 4279	N94-35684
BASU, A.	p 4355	N94-35401
BATEJAT, D.	p 4196	N94-36339
BATEMAN, J. E.	p 4269	N94-36061
BATES, JOSEPH	p 4312	N94-35658
BATTISSON, C. J.	p 4194	N94-36330
BATTISTA, R. A.	p 4276	N94-36355
BAUCOM, K. C.	p 4340	N94-35698
BAUGHMAN, DAVID	p 4207	N94-35633
BAUM, JOSEPH D.	p 4279	N94-35949
BAUM, S.	p 4349	N94-36280
BAUMANN, ERIC D.	p 4257	N94-35249
BEACH, R.	p 4271	N94-35665
BEACH, R. J.	p 4271	N94-35679
	p 4272	N94-36115
BECKWITH, J. F.	p 4333	N94-35818
BEECHER, JODY E.	p 4243	N94-35588
BEHROUZJOU, ROXANA	p 4225	N94-35917
BEJCZY, ANTAL	p 4278	N94-36046
BELISLE, F. H.	p 4276	N94-36355
BELL, J. H.	p 4189	N94-35394
BELL, JAMES F., III	p 4356	N94-35402
	p 4356	N94-35403
	p 4356	N94-35404
	p 4356	N94-35405
	p 4292	N94-35452
	p 4292	N94-35454
	p 4372	N94-36165
BELLANDO, J.	p 4321	N94-35593
BELTON, M. J. S.	p 4351	N94-35416
BELYTSCHKO, TED	p 4278	N94-36292
BENCOE, D. N.	p 4244	N94-35699
BENDER, BARRY A.	p 4246	N94-36125
BENDER, DOUGLAS J.	p 4210	N94-35645
BENETT, W.	p 4271	N94-35665
BENETT, W. J.	p 4272	N94-36115
BENFORD, J.	p 4272	N94-35978
BENJAMIN, BRIAN J.	p 4221	N94-35888
BENKOVICH, M. G.	p 4258	N94-35686
BENNETT, WILLIAM H.	p 4220	N94-35879
BENZ, W.	p 4355	N94-35400
	p 4351	N94-35406
BERCHTOLD, G.	p 4194	N94-36327
BERG, OTTO	p 4373	N94-36170
BERKOWITZ, C. M.	p 4288	N94-36359
BERNHARD, R. P.	p 4280	N94-35407
	p 4357	N94-35409
	p 4352	N94-36141
BERNHARD, RONALD P.	p 4352	N94-35458
BERNSTEIN, P.	p 4260	N94-36260
BERRY, DENNIS L.	p 4286	N94-35957
BHATTACHARJEE, AMITAVA	p 4290	N94-35708
BIBRING, JEAN-PIERRE	p 4354	N94-35336
BICKFORD, RANDALL L.	p 4268	N94-35268
BIEFELD, R. M.	p 4340	N94-35698
BIGARD, A. X.	p 4297	N94-36217
BIGELOW, T.	p 4338	N94-36093
BILBRO, G. L.	p 4252	N94-35247
BINGHAM, R.	p 4375	N94-36210
BINKOWSKI, F. S.	p 4332	N94-35584
BIRCKELBAW, LOURDES G.	p 4200	N94-35962
BIRD, E. L.	p 4240	N94-35650
BIRKAN, M. A.	p 4198	N94-35746
BIRNBAUM, MILTON	p 4273	N94-36227
BIRX, DANIEL	p 4271	N94-35586
BISH, DAVID L.	p 4357	N94-35408
BISSON, ROGER U.	p 4196	N94-36338
BISSON, S. E.	p 4295	N94-36285
BISWAS, RUPAK	p 4319	N94-36031
BISWAS, SAROJ K.	p 4220	N94-35882
BITZ, DENNIS A.	p 4286	N94-35957
BJARKE, L.	p 4189	N94-35394
BLAIR, F. H.	p 4295	N94-36285
BLAISDELL, JAMES H.	p 4306	N94-36040
BLAKE, D.	p 4247	N94-35469
BLAKE, DAVID F.	p 4357	N94-35408
	p 4239	N94-36144
BLANC, MICHEL	p 4354	N94-35336
BLANCHARD, D. P.	p 4355	N94-35401
BLANDER, M.	p 4351	N94-36418

BLANFORD, G. E. .... p 4357 N94-35409
p 4352 N94-35466
BLANFORD, GEORGE E. .... p 4319 N94-35264
BLANKENSHIP, G. L. .... p 4218 N94-35869
BLANKENSHIP, GILMER .... p 4220 N94-35879
BLOUGH, D. K. .... p 4312 N94-36195
BLYCKER, G. .... p 4285 N94-35943
BLYTH, A. J. C. .... p 4345 N94-35533
BOBILLIER, G. .... p 4296 N94-35601
BOEGLER, P. .... p 4224 N94-35909
BOGARD, D. D. .... p 4357 N94-35410
p 4351 N94-35428
BOIA, JOHN J. .... p 4203 N94-35613
p 4203 N94-35614
BOLDYREV, A. I. .... p 4322 N94-35753
p 4323 N94-35792
p 4323 N94-35793
BOLDYREV, ALEXANDER I. .... p 4324 N94-36050
BOLL, PATRICIA .... p 4196 N94-36338
BOLTON, S. J. .... p 4354 N94-35378
BOLTON, S. M. .... p 4270 N94-36389
BOLVIN, D. T. .... p 4205 N94-35620
BOLVIN, DAVE .... p 4204 N94-35619
BOND, HOWARD E. .... p 4349 N94-36279
BONETTO, F. .... p 4249 N94-35237
BONLIE, J. D. .... p 4272 N94-35695
BONNEL, A. M. .... p 4298 N94-36215
BONNER, B. E. .... p 4331 N94-36428
BORDER, J. S. .... p 4210 N94-35543
BORNEMANN, HANS J. .... p 4224 N94-35909
BORNHOEFT, KARL .... p 4356 N94-35403
BORST, MARK A. .... p 4230 N94-36401
BOSTIAN, CHARLES W. .... p 4257 N94-36043
BOURGAIN, J. .... p 4317 N94-35760
BOWDEN, MARY L. .... p 4212 N94-35484
BOWEN, BARRY C. .... p 4211 N94-35523
BOWYER, S. .... p 4370 N94-36153
BOZEMAN, RICHARD J., JR. .... p 4268 N94-35235
p 4274 N94-35661
BOZZELLI, J. W. .... p 4239 N94-36319
BRADLEY, J. D. .... p 4284 N94-35674
BRADLEY, J. P. .... p 4355 N94-35397
BRADLEY, JOHN P. .... p 4353 N94-36149
BRANDON, WILLIAM T. .... p 4257 N94-36043
BRASOVEANU, D. .... p 4204 N94-35618
BRAVENEC, R. V. .... p 4338 N94-36200
BRAWN, I. P. .... p 4269 N94-35599
BREININGER, DAVID R. .... p 4288 N94-36422
BRENNAN, T. M. .... p 4272 N94-36178
BRETZ, N. .... p 4338 N94-36093
BRIAND, LIONEL C. .... p 4301 N94-35435
p 4301 N94-35436
p 4301 N94-35438
BRIGGS, M. MICHAEL .... p 4206 N94-35629
BRIGHT, VICTOR M. .... p 4230 N94-36404
BRINKER, C. J. .... p 4244 N94-35701
BRINKGREVE, PAUL R. .... p 4197 N94-36346
BRINKKEMPER, S. .... p 4302 N94-35538
BRITCHER, COLIN P. .... p 4212 N94-35836
p 4217 N94-35860
p 4223 N94-35902
BRODLIE, K. W. .... p 4308 N94-36211
BROSTROEM, L. .... p 4327 N94-36267
BROTHERS, A. J. .... p 4288 N94-36359
BROTHERS, CHARLES P., JR. .... p 4261 N94-36361
BROW, R. K. .... p 4244 N94-35699
BROWN, GERALD .... p 4223 N94-35905
BROWN, JAMES R. .... p 4229 N94-36047
BROWN, R. H. .... p 4365 N94-35468
BROWNE, S. V. .... p 4347 N94-36300
BROWNFIELD, THOMAS F. .... p 4306 N94-36040
BROWNING, L. .... p 4352 N94-35476
BROWNING, L. B. .... p 4353 N94-36145
BROWNING, LAUREN B. .... p 4357 N94-35411
BROWNLEE, D. E. .... p 4355 N94-35397
p 4351 N94-35412
p 4353 N94-36159
BROZENEC, THOMAS F. .... p 4210 N94-35645
BRUCKNER, ROBERT J. .... p 4265 N94-35945
BRUSCHKE, M. V. .... p 4234 N94-36004
BRYANT, CAROLYN F. .... p 4212 N94-35799
p 4212 N94-35801
BRYSON, J. W. .... p 4279 N94-35684
BUCHELNIKOVA, N. S. .... p 4338 N94-36097
BUCK, W. W. .... p 4325 N94-36086
BUCKETT, M. I. .... p 4241 N94-36231
BUCKINGHAM, ALFRED .... p 4263 N94-35492
BUI, D. T. .... p 4236 N94-35680
BUICAN, I. .... p 4347 N94-36102
BULGUBURE, C. .... p 4194 N94-36328
BULLOCK, M. A. .... p 4358 N94-35413
BULMER, CATHERINE H. .... p 4334 N94-36122
BUNCH, T. E. .... p 4352 N94-36140
BUND, G. W. .... p 4320 N94-35579
BURCH, J. L. .... p 4330 N94-35483
BURCHAM, F. W., JR. .... p 4199 N94-35258
BURCHELL, TIMOTHY D. .... p 4231 N94-36409
BURKA, MICHAEL .... p 4291 N94-36263
BURKE, INGRID C. .... p 4284 N94-35486
BURKEN, JOHN .... p 4199 N94-35258
BURKETT, P. J. .... p 4353 N94-36158
BURNS, WILLIAM K. .... p 4334 N94-36122
BURTIS, M. D. .... p 4295 N94-36244
BUSSOLARI, STEVEN R. .... p 4293 N94-35596
BUTMAN, S. .... p 4255 N94-35563
BYUN, D. W. .... p 4298 N94-35688

C

CABLE, M. D. .... p 4339 N94-36375
CABROL, NATHALIE .... p 4358 N94-35414
CAI, Y. .... p 4276 N94-36433
CALDWELL, R. B. .... p 4262 N94-36430
CALES, MICHAEL .... p 4243 N94-35243
CALLWOOD, R. .... p 4201 N94-35827
CALVEL, P. .... p 4342 N94-36367
CANTRELL, JOHN H. .... p 4268 N94-35368
CAPRETTE, DOUGLAS S. .... p 4281 N94-35261
CAPRON, WILLIAM R. .... p 4192 N94-36048
CARABELLI, STEFANO .... p 4214 N94-35846
p 4216 N94-35857
CARLIN, R. T. .... p 4237 N94-35777
CARLOS, R. C. .... p 4257 N94-36316
CARLSON, M. .... p 4327 N94-36267
CARLSON, N. .... p 4271 N94-35665
CARLSON, N. W. .... p 4272 N94-36115
CARNEY, R. E. .... p 4269 N94-35599
CARROLL, A. S. .... p 4328 N94-36303
CARSON, L. .... p 4326 N94-36127
CASTAGNA, A. .... p 4241 N94-36196
CASTELLI, MICHAEL G. .... p 4234 N94-35995
CASTLEMAN, A. W., JR. .... p 4328 N94-36298
CASWELL, RUTH .... p 4213 N94-35842
CAVESTRI, R. C. .... p 4244 N94-35687
CHA, HYUNG KI .... p 4334 N94-36180
CHACON-TAYLOR, MONIQUE R. p 4321 N94-35589
CHAKRABARTI, S. .... p 4370 N94-36153
CHALLA, M. S. .... p 4209 N94-35642
CHALMERS, S. A. .... p 4272 N94-36178
CHAMBERS, JOHN G. .... p 4358 N94-35415
p 4368 N94-36138
CHAN, S. T. .... p 4268 N94-36374
CHAN, VINCENT W. S. .... p 4257 N94-36043
CHANCE, RICHARD .... p 4278 N94-36090
CHANDRA, A. K. .... p 4300 N94-35570
CHANDRA, TUSHAR DEEPAK .... p 4300 N94-35365
CHANG, I.-SHIH .... p 4228 N94-36254
p 4228 N94-36255
p 4343 N94-36256
CHANG, JONG HWA .... p 4305 N94-35834
CHANG, R. P. .... p 4340 N94-35828
CHANG, YOUNG-SOO .... p 4319 N94-36320
CHAO, DENNIS .... p 4262 N94-35245
CHAPMAN, C. R. .... p 4351 N94-35416
CHAPMAN, DEAN R. .... p 4190 N94-35717
CHAPMAN, E. G. .... p 4286 N94-36026
CHAPPELL, ALAN R. .... p 4309 N94-36438
CHATTOPADHYAY, S. .... p 4331 N94-36271
CHAWLA, KALPANA .... p 4268 N94-36397
CHEESEMAN, PETER .... p 4281 N94-35417
CHEETHAM, A. K. .... p 4242 N94-36369
CHEN, D. T. .... p 4264 N94-35683
CHEN, F. C. .... p 4264 N94-35683
CHEN, J. Y. .... p 4338 N94-36200
CHEN, PETER C. .... p 4350 N94-35473
CHEN, Q. Y. .... p 4214 N94-35843
CHEN, S. S. .... p 4276 N94-36433
CHEN, WEIHUAN .... p 4315 N94-35934
CHENG, C. Z. .... p 4337 N94-35938
CHEREDNICHENKO, V. A. .... p 4325 N94-36077
CHEVY, A. .... p 4341 N94-36212
CHICATELLI, AMY K. .... p 4198 N94-35352
CHMURA, LOUIS J., JR. .... p 4302 N94-35490
CHOE, ANG SUNG .... p 4334 N94-36180
CHORNOBOY, E. S. .... p 4295 N94-36249
CHOUDHURY, AJIT K. .... p 4220 N94-35883
CHOW, J. Q. .... p 4285 N94-35735
CHOW, L. C. .... p 4250 N94-35524
CHOYKE, W. J. .... p 4236 N94-35731
CHREN, WILLIAM A., JR. .... p 4259 N94-36049
CHRISTEN, D. K. .... p 4342 N94-36377
CHRISTENSEN, A. N. .... p 4341 N94-36358
CHRISTENSON, T. R. .... p 4224 N94-35907
CHRISTIE, ALAN M. .... p 4308 N94-36294
CHRISTOFFERSEN, R. .... p 4359 N94-35418
CHRISTON, M. .... p 4268 N94-36374
CHRISTOPHER, P. .... p 4205 N94-35624
CHU, C. W. .... p 4214 N94-35843
CHU, D. .... p 4210 N94-35646
CHU, W. K. .... p 4214 N94-35843
CHU, WEI-KAN .... p 4350 N94-35473
CHUANG, C.-H. .... p 4202 N94-35487
CHUANG, CHUN-HUA K. .... p 4242 N94-35234
CHUDGE, J. .... p 4345 N94-35533
CHUN, K. C. .... p 4319 N94-36320
CHUNG, I. .... p 4233 N94-35714
p 4233 N94-35715
p 4233 N94-35944
CHUNG, JOONGKEE .... p 4198 N94-35352
CHURCH, KENNETH W. .... p 4345 N94-35651
CIARLO, D. .... p 4271 N94-35665
CINTALA, M. J. .... p 4280 N94-35407
p 4352 N94-36141
CINTALA, MARK J. .... p 4359 N94-35419
CLAPP, WILLIAM G. .... p 4210 N94-35377
CLARK, BENTON C. .... p 4354 N94-35263
CLARK, PAMELA E. .... p 4350 N94-35420
CLARK, PATRICK K. .... p 4308 N94-36250
CLARKE, EDMUND .... p 4303 N94-35573
CLEMETT, S. J. .... p 4352 N94-35465
CLOUTMAN, L. D. .... p 4275 N94-36206
CLUM, JAMES A. .... p 4230 N94-36405
COATS, C. .... p 4298 N94-35688
COFFEY, H. E. .... p 4374 N94-36009
p 4375 N94-36020
COHEN, H. D. .... p 4297 N94-36223
COLE, GARY L. .... p 4198 N94-35352
COLE, RODNEY E. .... p 4294 N94-35807
COLIN, PH. .... p 4195 N94-36332
COLLAN, H. .... p 4334 N94-36190
COLLAZO, I. .... p 4338 N94-36093
COLLINS, C. B. .... p 4272 N94-35721
COLLINS, MARTIN J. .... p 4201 N94-36440
COLTRIN, M. E. .... p 4340 N94-36032
COMBS, CYNTHIA L. .... p 4292 N94-35355
p 4293 N94-35499
COMBS, W. E. .... p 4261 N94-36371
CONDON, STEVE .... p 4300 N94-35256
CONFER, G. L. .... p 4275 N94-35815
CONNOLLY, HAROLD C., JR. .... p 4351 N94-35421
CONNOLLY, J. F. .... p 4269 N94-36061
CONWAY, D. .... p 4203 N94-35610
COOK, JEFFREY .... p 4232 N94-35654
COOLEY, J. .... p 4202 N94-35608
COOLEY, R. S. .... p 4214 N94-35843
COPELAND, DONALD .... p 4197 N94-36345
CORLISS, LLOYD D. .... p 4200 N94-35962
CORNWALL, J. M. .... p 4288 N94-35358
CORRIGAN, E. .... p 4314 N94-35774
CORRIGAN, JIM .... p 4205 N94-35621
COSTARD, FRANCOIS .... p 4354 N94-35336
COSTRELL, L. .... p 4345 N94-35817
COTE, C. .... p 4335 N94-35670
COTTRON, M. .... p 4270 N94-36219
COURTY, J. C. .... p 4194 N94-36328
COUTIN-FAYE, SOPHIE .... p 4354 N94-35336
COVINO-HRBACEK, JOSEPHINE p 4334 N94-36363
COX, C. .... p 4208 N94-35637
COX, C. M. .... p 4205 N94-35620
p 4208 N94-35636
COX, D. E. .... p 4216 N94-35853
COX, DAVID E. .... p 4225 N94-35913
CRAIG, A. Y. .... p 4247 N94-35469
CRAMER, P. W. .... p 4253 N94-35549
CRASSIDIS, JOHN L. .... p 4209 N94-35643
CRAWFORD, DANIEL J. .... p 4192 N94-36048
CREDEUR, LEONARD .... p 4192 N94-36048
CREIGHTON, J. R. .... p 4340 N94-36032
CRESS, T. S. .... p 4286 N94-36024
CROSS, J. B. .... p 4236 N94-35680
CROTTS, B. D. .... p 4219 N94-35878
CROUSE, P. .... p 4204 N94-35616
CROWDER, S. V. .... p 4244 N94-35699
CROWLEY, GEOFFREY .... p 4291 N94-36116
CRUIKSHANK, D. P. .... p 4365 N94-35468
p 4370 N94-36150
CRUIKSHANK, DALE P. .... p 4356 N94-35404
CRULL, ROBERT .... p 4249 N94-35485
CSERNICA, JEFFREY .... p 4231 N94-36410
CUGINI, J. A. .... p 4346 N94-36005
CUMMINGS, RUSSELL M. .... p 4191 N94-36394
CUNEO, M. E. .... p 4331 N94-36199
CUNNINGHAM, G. S. .... p 4304 N94-35808
CURRY, DONALD M. .... p 4262 N94-35245
CURTIS, J. T. .... p 4266 N94-35951
CUY, MICHAEL D. .... p 4200 N94-35267
CUZZI, J. N. .... p 4351 N94-35422
CYRUS, JOHN D. .... p 4195 N94-36333

D

DAGOSTINO, PAUL A. .... p 4238 N94-36091
DAHIYA, J. N. .... p 4232 N94-36412
DAMERELL, A. R. .... p 4272 N94-36062
DANARED, H. .... p 4327 N94-36267
DANSON, C. N. .... p 4272 N94-36062

DANVY, OLIVER p 4304 N94-35718
DAVIES, A. R. p 4263 N94-35603
DAVIS, G. W. p 4205 N94-35622
DAVIS, J. BRADLEY p 4211 N94-35523
DAVIS, M. H. p 4376 N94-35590
DAVIS, R. M. p 4231 N94-36407
DAVIS, SANFORD S. p 4263 N94-35371
DAVIS, W. p 4204 N94-35616
DAVYDENKO, V. I. p 4339 N94-36417
DEANGELIS, U. p 4375 N94-36210
DEARAUJO, C. F., JR. p 4321 N94-35595
DEARAUJO, CARLOS F., JR. p 4321 N94-35583
DEBOOR, C. p 4315 N94-36012
DEBORST, R. p 4251 N94-35820
DECAMPOS, CLELIA APARECIDA
p 4330 N94-36028
DEFAZIO, R. p 4203 N94-35610
DEFREVILLE, CHARLES p 4196 N94-36341
DEGROH, HENRY C., III p 4262 N94-35248
DEHART, JOHN M. p 4351 N94-35423
p 4353 N94-36158
DEHOFF, P. H. p 4298 N94-35266
DELEMOS, R. p 4250 N94-35532
DELPECH, JEAN-FRANCOIS p 4348 N94-35901
DELPRETE, CRISTIANA p 4214 N94-35846
p 4216 N94-35857
DEMANDANTE, C. G. N. p 4189 N94-35394
DENKER, C. M. p 4284 N94-35346
DEPENA, JUAN p 4209 N94-35643
DERAAD, L. L., JR. p 4256 N94-36112
DERBIN, A. V. p 4320 N94-35566
DERSHOWITZ, ADAM p 4293 N94-35596
DESANTIS, A. p 4222 N94-35892
DESJARLAIS, M. P. p 4331 N94-36199
DESMARAIS, D. J. p 4360 N94-35425
DETROYE, JEFF E. p 4360 N94-35424
DEUTSCHMANN, J. K. p 4209 N94-35642
DEY, J. p 4321 N94-35583
DEY, M. p 4321 N94-35583
DHOBALE, A. R. p 4235 N94-35592
DHODAPKAR, S. D. p 4300 N94-35570
DIAMONDSTONE, B. I. p 4318 N94-36003
DIAZ, C. p 4304 N94-35740
DIEFENDORF, R. JUDD p 4234 N94-36045
DIJULIO, S. S. p 4276 N94-36378
DILLER, T. E. p 4231 N94-36407
DIMOV, G. I. p 4337 N94-36082
DINDA, PETER p 4311 N94-36015
DINDA, PETER A. p 4310 N94-35806
DINER, DANIEL B. p 4332 N94-35384
DING, YI-WEI p 4245 N94-36057
DIRUSSO, ELISEO p 4223 N94-35905
DOBROVOLSKIS, A. R. p 4351 N94-35422
DOBROWOLSKI, JAMES P. p 4287 N94-36120
DOBSON, J. E. p 4345 N94-35533
DODD, P. E. p 4261 N94-36373
DOHNALEK, Z. p 4236 N94-35731
DOHRMANN, C. R. p 4226 N94-36001
DOLINAR, S. p 4254 N94-35555
DOLL, C. E. p 4205 N94-35620
p 4205 N94-35623
p 4208 N94-35636
DOMBLESKY, JOSEPH P. p 4250 N94-35711
DONALDSON, RALPH J. p 4295 N94-36262
DONG, Q. W. p 4239 N94-35464
DONGARRA, J. J. p 4347 N94-36300
DONNELLY, M. K. p 4259 N94-36054
DOORENBOS, ROBERT B. p 4311 N94-35527
DOREY, P. E. p 4314 N94-35774
DOVER, C. B. p 4327 N94-36239
DOVEY, D. J. p 4309 N94-36429
DOWNER, JAMES p 4213 N94-35837
DOWNS, CORNELL p 4305 N94-35958
DOYLE, JAMES F. p 4279 N94-35974
DOZOIS, CLAUDE p 4291 N94-36116
DRAKE, M. J. p 4354 N94-36169
DRAKUNOV, S. p 4220 N94-35884
DRUZHININ, D. P. p 4259 N94-36104
DUBROVSKIJ, V. G. p 4315 N94-36100
DUC, DUONG ANH p 4329 N94-36308
DUCKETT, SOPHIE p 4377 N94-35961
DUDA, J. L. p 4245 N94-36108
DUGINOV, V. N. p 4322 N94-35751
DUNCAN, DAVID B. p 4288 N94-35268
DUNHAM, J. p 4208 N94-35637
DUNN, A. p 4350 N94-35980

E

EARLS, MICHAEL p 4310 N94-35968
EASTER, R. C. p 4286 N94-36028
p 4288 N94-36359
EASTMAN, D. R. p 4349 N94-35998
EDELMEN, P. C. p 4287 N94-36027
EDELSON, BURTON I. p 4257 N94-36043
EDKINS, CRAIG R. p 4298 N94-35692
EDWARDS, C. p 4254 N94-35557
EDWARDS, C. B. p 4272 N94-36062
EDWARDS, C. F. p 4268 N94-36318
EGELAND, A. p 4292 N94-36265
EHRENSTROM, WILLIAM A. p 4274 N94-35481
EKROOT, L. p 4254 N94-35555
EKSTROM, T. E. p 4276 N94-36355
EL-GENK, M. S. p 4228 N94-35349
ELARTON, J. L. p 4260 N94-36197
ELHASSOUNI, A. p 4317 N94-36307
ELKHOVSKIJ, A. S. p 4322 N94-35783
ELLINGSON, W. A. p 4245 N94-35779
ELLIOTT, GREGORY S. p 4190 N94-35950
ELLISON, A. J. G. p 4237 N94-35777
EMANUEL, M. p 4271 N94-35665
EMANUEL, M. A. p 4272 N94-36115
ENGELMORE, ROBERT S. p 4347 N94-36044
ENGLEMAN, R. R., JR. p 4282 N94-36021
ENNIX, KIMBERLY A. p 4319 N94-35963
EPPEL, JOSEPH C. p 4198 N94-36380
ERCK, R. A. p 4275 N94-36232
ERDEMIR, A. p 4275 N94-36232
EREKSON, E. J. p 4248 N94-36035
EREMIN, A. V. p 4345 N94-35790
EREMIN, V. p 4260 N94-36221
ERICKSSON, G. p 4351 N94-36418
ERMAKOV, V. N. p 4341 N94-36312
ERMER, DONALD p 4230 N94-36405
EROFEEV, V. I. p 4336 N94-35788
ESPINA, J. p 4189 N94-35394
ESTEROWITZ, LEON p 4273 N94-36370
EVANS, LARRY G. p 4350 N94-35420
EZHILCHELVAN, P. D. p 4310 N94-35535

F

FABIANO, R. p 4222 N94-35894
FAESSLER, A. p 4327 N94-36239
FANICK, E. R. p 4247 N94-35941
FARAH, I. A. p 4263 N94-35603
FARMER, JACK p 4358 N94-35414
FARMER, JACK D. p 4360 N94-35425
FARRANCE, M. A. p 4343 N94-35964
FARRELL, JAMES P. p 4202 N94-35609
FAST, J. D. p 4285 N94-35823
FATEMI, NAVID S. p 4281 N94-35271
FAWCETT, W. R. p 4239 N94-36426
FEDOTOV, YU. S. p 4325 N94-36088
FEENSTRA, P. H. p 4251 N94-35820
FEIERTAG, R. J. p 4208 N94-35636
FEIGENBAUM, EDWARD p 4347 N94-36044
FELL, PATRICK J. p 4212 N94-35585
FERGUSON, J. p 4326 N94-36127
FERIA, Y. p 4253 N94-35552
FERNANDEZ, JOSE L. p 4304 N94-35794
FERNELIUS, NILS C. p 4340 N94-35733
FERRARA, AUGUSTO p 4247 N94-35795
FIELD, J. E. p 4251 N94-36388
FINK, D. p 4209 N94-35640
FINK, EUGENE p 4303 N94-35574
FIRBY, R. J. p 4312 N94-35710
p 4310 N94-35742
p 4312 N94-36295
FITTRO, ROGER L. p 4217 N94-35861
FITZ-COY, NORMAN p 4208 N94-35639
FITZGERALD, T. J. p 4257 N94-36316
FIX, LIMOR p 4317 N94-35743
p 4305 N94-36014
FLEETWOOD, D. M. p 4260 N94-36268
p 4342 N94-36367
p 4261 N94-36371
FLEMING, R. H. p 4247 N94-35469
FLOWERS, GEORGE T. p 4274 N94-35500
FLUECKIGER, KARL p 4213 N94-35842
FLYNN, G. J. p 4352 N94-35465
FOLEY, H. C. p 4237 N94-36023
FOLTA, D. p 4203 N94-35610
FOLTA, D. C. p 4206 N94-35625
FOLTA, DAVID C. p 4202 N94-35609
FOMIN, P. I. p 4267 N94-36098
FORRESTER, PATRICK p 4274 N94-35481
FORSTER, ESTRELLA M. p 4299 N94-35707
FORT, D. p 4253 N94-35553
FOSTER, LUCAS E. p 4217 N94-35860
FOSTER, M. S. p 4338 N94-36200
FRANCO, M. M. p 4252 N94-35546
FRANK, W. p 4242 N94-36289
FRANZ, JOSEPH p 4195 N94-36333
FRAWLEY, JAMES J. p 4361 N94-35430
FRECHET, JEAN M. p 4243 N94-35588
FREDERICK, MARTIN E. p 4282 N94-35540
FREDERICO, T. p 4320 N94-35581
FREEDMAN, R. p 4356 N94-35405
FREEDMAN, RICHARD p 4356 N94-35404
FREEMAN, MARK p 4307 N94-36118
FREEMAN, TIM p 4304 N94-35709
FREESLAND, DOUGLAS p 4207 N94-35632
FREITAS, B. p 4271 N94-35665
FREITAS, B. L. p 4272 N94-36115
FRENCH, JONATHAN p 4196 N94-36338
FREY, HERBERT p 4360 N94-35426
p 4360 N94-35427
p 4364 N94-35462
FREY, R. E. p 4326 N94-36198
FRICKE, ROBERT W., JR. p 4211 N94-35251
p 4211 N94-35252
FRICKE, S. K. p 4364 N94-35461
p 4371 N94-36156
FRIEDLAND, PETER E. p 4347 N94-36044
FRIEDLAND, S. p 4314 N94-35763
FRIEDMANN, P. P. p 4280 N94-36423
FRIEDMANN, PERETZ P. p 4200 N94-35874
FRISCH, H. J. p 4326 N94-36107
FRUCHTER, A. p 4349 N94-36280
FUJIWARA, M. p 4337 N94-35936
p 4339 N94-36357
FUKUYAMA, A. p 4336 N94-35811
p 4336 N94-35812
p 4324 N94-35984
FUKUYAMA, ATSUSHI p 4339 N94-36353
FULLERTON, WAYNE p 4208 N94-35639
FULTON, J. p 4248 N94-36191
FUNCHAL, R. Z. p 4321 N94-35594
FURU, L. p 4271 N94-35679

G

GAETZ, T. J. p 4333 N94-36119
GAFFNEY, L. M. p 4201 N94-35827
GAFFURI, P. p 4238 N94-36205
GAKENHEIMER, MARTIN F. p 4203 N94-35613
p 4203 N94-35614
GAL, E. p 4275 N94-35815
GALLAGHER, J. P. p 4347 N94-36435
GALLERY, J. p 4189 N94-35394
GALLIGO, A. p 4308 N94-36259
GALLOP, J. R. p 4308 N94-36211
GALLOWAY, K. F. p 4342 N94-36367
GALVANI, J.-L. p 4193 N94-36324
GAMBHIR, S. S. p 4206 N94-35628
GANDHI, AMAR p 4299 N94-35393
GANNAWAY, MARY T. p 4247 N94-35655
p 4247 N94-35656
GAO, Q. p 4236 N94-35731
GAPOSCHKIN, E. MIKE p 4203 N94-35611
GARBER, A. p 4204 N94-35617
p 4209 N94-35641
GARBUTT, K. S. p 4191 N94-35855
GARDINER, T. p 4245 N94-35779
GARDNER, JAMES E. p 4229 N94-36398
GARDNER, THOMAS G. p 4206 N94-35630
GARISTO, F. p 4240 N94-35960
GARNER, RICHARD p 4291 N94-36263
GAROFALINI, S. H. p 4246 N94-36283
GARRETT, H. p 4333 N94-35697
GARRISON, D. H. p 4357 N94-35410
p 4351 N94-35428
GARVEY, J. p 4269 N94-35599
GARVIN, J. B. p 4361 N94-35429
p 4361 N94-35430
p 4361 N94-35431
GARWOOD, K. R. p 4195 N94-36334
GASSMAN, R. A. p 4270 N94-35351
GASTER, MICHAEL p 4266 N94-35975
GAUTIER, CATHERINE p 4289 N94-35389
GAVEL, D. T. p 4349 N94-35585
GEBALLE, THOMAS R. p 4356 N94-35404
GELFAND, JACK p 4312 N94-36309
GENTA, GIANCARLO p 4214 N94-35846
p 4216 N94-35857
GENTRY, W. R. p 4324 N94-35816
GERASIMOV, O. I. p 4329 N94-36311
GERSHTEJN, S. S. p 4323 N94-35787
GERTLER, A. W. p 4285 N94-35735
GERTZ, J. L. p 4293 N94-35719
GERVER, M. p 4223 N94-35904
p 4224 N94-35908
GHAN, S. J. p 4288 N94-36359
GHOSH, DAVE p 4218 N94-35871
GIAMMARISE, A. W. p 4275 N94-35867
GIBONI, K. L. p 4375 N94-35381
GIBSON, E. K., JR. p 4351 N94-35451
GIER, T. E. p 4340 N94-35677
GILEV, E. A. p 4337 N94-36082
GIVLER, R. C. p 4349 N94-35998
GLADSTONE, G. R. p 4370 N94-36153
GLANTZ, C. S. p 4287 N94-36027
GLOWINSKI, ROLAND p 4222 N94-35897
GOLAN, L. P. p 4275 N94-36022

GOLDBERG, N. p 4323 N94-35792
GOLDEN, D. C. p 4351 N94-35432
p 4239 N94-35433
GOLDIE, JAMES p 4213 N94-35837
GOLDSMAN, DAVID p 4316 N94-35675
GOLDSMITH, J. E. M. p 4295 N94-36285
GOLOSKOKOV, S. V. p 4330 N94-36080
GONDHALEKAR, P. M. p 4350 N94-35530
GONDHALEKAR, V. p 4223 N94-35904
p 4224 N94-35908
GONDHALEKAR, VIJAY p 4213 N94-35837
GONZALES, N. p 4323 N94-35793
GOODING, JAMES L. p 4355 N94-35399
p 4240 N94-36174
GOODRICH, P. p 4285 N94-35943
GOODWIN, P. M. p 4320 N94-35376
GOODWIN, THOMAS J. p 4296 N94-35232
GOODYER, M. J. p 4191 N94-35855
GORBAR, E. V. p 4325 N94-36083
p 4329 N94-36434
GORTON, MARK P. p 4233 N94-35947
GOSZTOLA, D. J. p 4332 N94-35671
GOTTFELDT, P. p 4272 N94-36062
GOURLEY, P. L. p 4272 N94-36178
GOUTERMAN, M. p 4189 N94-35394
GRAHAM, C. p 4297 N94-36223
GRAMLING, C. J. p 4206 N94-35625
GRANNEN, K. J. p 4340 N94-35828
GRAY, HENRY F. p 4246 N94-36121
GREBINNIK, V. G. p 4322 N94-35751
GREELEY, R. p 4366 N94-35474
GREELEY, RONALD p 4358 N94-35414
p 4351 N94-35416
GREEN, REBECCA J. p 4299 N94-35712
GREEN, S. C. p 4347 N94-36300
GREENBLATT, ARTHUR S. p 4334 N94-36122
GREENFIELD, S. R. p 4332 N94-35671
GREENWALD, THOMAS J. p 4292 N94-35355
p 4293 N94-35499
GREGG, WATSON W. p 4211 N94-35269
GREGOR, J. A. p 4318 N94-36427
GREGORY, JOHN C. p 4235 N94-35388
GRESHO, P. M. p 4268 N94-36374
GRIFFITHS, M. p 4242 N94-36289
GRINSPOON, D. H. p 4358 N94-35413
GRISAFFE, SALVATORE J. p 4234 N94-36045
GRODSINSKY, C. M. p 4215 N94-35851
GROOM, N. J. p 4216 N94-35853
GROOM, NELSON J. p 4212 N94-35836
p 4223 N94-35902
GROSCH, CHESTER E. p 4266 N94-35975
GROSS, F. p 4321 N94-35649
GROSS, THOMAS p 4302 N94-35572
p 4310 N94-35806
p 4311 N94-36015
GROSSMAN, WALTER p 4207 N94-35632
GROZIN, A. G. p 4320 N94-35567
GRUETZNER, J. K. p 4267 N94-36111
GRUN, JACOB p 4263 N94-35492
GUASP, J. p 4336 N94-35773
GUCKEL, HENRY p 4224 N94-35907
GUERRA, K. M. p 4343 N94-35964
GUETTLER, W. p 4227 N94-35362
GUHA, A. p 4204 N94-35615
GUINN, JOSEPH p 4204 N94-35619
GULATI, S. K. p 4236 N94-35755
GUREVICH, A. V. p 4295 N94-36240
GURNETT, D. A. p 4354 N94-35378
GURUMOORTHY, R. p 4213 N94-35838
p 4216 N94-35858
GUSCHIN, A. G. p 4287 N94-36179
GUSEV, A. A. p 4290 N94-35780
GUSTAFSSON, M. G. L. p 4297 N94-36269
GUSYNIN, V. P. p 4329 N94-36434
GUTOWSKI, MACIEJ p 4322 N94-35678
p 4322 N94-35753
p 4323 N94-35797
p 4323 N94-35798
GUTSCHE, T. p 4327 N94-36239
GUZZO, M. M. p 4321 N94-35593

H

HABERBUSCH, MARK S. p 4263 N94-35250
HABERLE, R. M. p 4368 N94-36137
HADJIALIEVA, F. G. p 4343 N94-36351
HADLEY, G. R. p 4272 N94-36178
HADZILACOS, VASSOS p 4300 N94-35365
HAGEDORN, P. p 4258 N94-35354
HAGER, E. PAUL p 4257 N94-36043
HAGER, JAMES A. p 4302 N94-35490
HAHN, K. p 4331 N94-36202
HAHN, O. J. p 4250 N94-35524
HAINES, MATTHEW p 4300 N94-35240
HAKES, C. L. p 4236 N94-35680
HALLOCK, L. p 4203 N94-35613
p 4204 N94-35615
HALLOCK, LOU p 4203 N94-35612
HALPERN, M. B. p 4317 N94-36234
HAMADA, Y. p 4338 N94-36247
HAMANN, DONALD p 4295 N94-36262
HAMETZ, M. p 4202 N94-35608
HAMILL, THOMAS M. p 4295 N94-36228
HAMILTON, C. E. p 4271 N94-35679
HAMMEL, B. A. p 4266 N94-35982
p 4318 N94-36201
HAMMONS, B. E. p 4272 N94-36178
HAMMOUD, AHMAD N. p 4257 N94-35249
HAMPTON, R. D. p 4215 N94-35851
HANATANI, K. p 4337 N94-35936
HANNA, A. F. p 4332 N94-35584
p 4298 N94-35688
HANSON, G. p' 4338 N94-36093
HANSON, J. C. p 4341 N94-36358
HANSON, K. M. p 4304 N94-35808
HANTAO, H. p 4338 N94-36352
HANTAO, JI. p 4336 N94-35752
HAPPOLDT, P. G. p 4245 N94-35779
HARMAN, R. p 4204 N94-35616
HARMSEN, F. p 4302 N94-35538
HARRIS, C. B. p 4324 N94-36058
HARRIS, F. IAN p 4295 N94-36262
HARRISON, L. C. p 4287 N94-36053
HARRISON, W. T. p 4340 N94-35677
HART, R. p 4208 N94-35637
HART, R. C. p 4205 N94-35620
p 4205 N94-35623
p 4206 N94-35625
HARTLEY, TOM T. p 4198 N94-35352
HARTMAN, KATHY R. p 4202 N94-35605
HARVEY, J. E. p 4296 N94-35738
HASHMALL, J. p 4204 N94-35618
HASSOUNI, Y. p 4317 N94-36307
HATCHETT, S. P. p 4339 N94-36375
HATORI, TADATSUGU p 4337 N94-35983
HAUER, J. F. p 4259 N94-36054
HAWKE, B. R. p 4356 N94-35402
HAWORTH, D. p 4237 N94-35777
HAYASHI, J. N. p 4368 N94-36137
HAYDER, M. E. p 4266 N94-35976
HAYNES, KEITH L. p 4226 N94-36251
HEAD, J. p 4351 N94-35416
HEADLEY, T. J. p 4246 N94-36209
p 4241 N94-36242
HEFLEY, WILLIAM E. p 4302 N94-35495
HEINTZE, NEVIN p 4304 N94-35718
HEINZINGER, K. p 4325 N94-36081
HELLER, ADAM p 4236 N94-35745
HELM, NEIL R. p 4257 N94-36043
HENDERSON, D. R. p 4245 N94-35771
HENLEY, E. M. p 4324 N94-35824
HENNEGES, G. p 4264 N94-35669
HENSLEY, W. K. p 4331 N94-36317
HENSON, ANNE p 4290 N94-35693
HENSON, N. J. p 4242 N94-36369
HENZINGER, THOMAS A. p 4317 N94-35743
p 4305 N94-36014
HERMAN, R. G. p 4237 N94-36036
HERNANDEZ, C. L. p 4259 N94-36094
HERTZ, H. S. p 4318 N94-36003
HERZ, RICHARD K. p 4271 N94-35489
HERZOG, RAOUL p 4213 N94-35839
HESS, BRYAN p 4300 N94-35240
HESSER, F. p 4270 N94-36219
HETMANSKI, CHRISTOPHER J. p 4301 N94-35435
p 4301 N94-35436
HEUNG, L. K. p 4237 N94-36056
HEWETT, D. W. p 4335 N94-35647
HEWINS, ROGER H. p 4351 N94-35421
HEWITT, ALAN D. p 4229 N94-35776
HICK, PAUL L. p 4375 N94-36264
HIETALA, V. M. p 4262 N94-36430
HIGGINS, STEFAN J. p 4358 N94-35415
p 4368 N94-36138
HIGUCHI, TOSHIRO p 4214 N94-35844
p 4225 N94-35915
HILL, M. G. p 4307 N94-36113
HILLIG, WILLIAM G. p 4234 N94-36045
HINDMARSH, ALAN C. p 4313 N94-35259
HINEDI, S. M. p 4254 N94-35558
HINRICHS, SUSAN p 4310 N94-35597
HIROI, T. p 4352 N94-35477
p 4368 N94-36139
p 4353 N94-36166
HIROI, TAKAHIRO p 4364 N94-35463
HIRSCHENHOFER, J. H. p 4282 N94-36021
HIRSCHON, A. S. p 4237 N94-35778
HIX, DEBORAH p 4302 N94-35491
HLAVA, P. F. p 4241 N94-36242
HOCKNEY, RICHARD p 4213 N94-35837
HOERZ, F. p 4280 N94-35407
p 4352 N94-36140
p 4352 N94-36141
p 4353 N94-36159
HOERZ, FRIEDRICH p 4240 N94-36174
HOGAN, R. C. p 4351 N94-35422
HOHLFELD, ROBERT G. p 4294 N94-36186
HOLDRIDGE, GEOFFREY M. p 4379 N94-36042
HOLFELTZ, S. T. p 4349 N94-36281
HOLLIDAY, D. p 4256 N94-36112
HOLMES, MICHAEL L. p 4225 N94-35917
HOLTET, J. A. p 4292 N94-36265
HOOD, G. M. p 4242 N94-36288
HOOD, R. Q. p 4341 N94-36274
HOPE, R. W. p 4214 N94-35847
HOPS, J. M. p 4255 N94-35559
HORZ, F. p 4351 N94-35412
HORZELA, A. p 4318 N94-35956
p 4342 N94-36070
HOSKING, F. M. p 4259 N94-36094
HOSOKAWA, M. p 4337 N94-35936
HOSPODARSKY, G. B. p 4354 N94-35378
HOU, ANN-SAN p 4225 N94-35912
HOUSEL, M. S. p 4262 N94-36430
HOUSER, ALAN R. p 4344 N94-35337
HOUSTON, PAUL L. p 4321 N94-35657
HOVER, G. L. p 4284 N94-35674
HOWARD, S. D. p 4255 N94-35560
p 4255 N94-35561
HOWELL, L. H. p 4267 N94-36315
HOY, ERIC p 4190 N94-35826
HOYT, A. E. p 4244 N94-35768
HRISCU, V. p 4347 N94-36102
HRUBSCH, L. p 4351 N94-35412
HSIAO, MIN-HUNG p 4221 N94-35885
HSU, ANDREW T. p 4265 N94-35948
HSU, B. D. p 4275 N94-35815
HSU, CHU-NAN p 4345 N94-35663
HSU, S. p 4222 N94-35894
HUA, GRACE C. p 4311 N94-35501
HUANG, JEN-KUANG p 4221 N94-35885
HUANG, S. J. p 4244 N94-35768
HUBER, P. D. p 4347 N94-36435
HUDSON, BENJAMIN L. p 4258 N94-35539
HUDSON, D. p 4272 N94-36115
HUGHES, CHARLES p 4235 N94-35447
HULL, J. p 4282 N94-35829
HUMPHRIS, R. R. p 4214 N94-35847
HUPA, M. p 4237 N94-36059
HUPP, J. T. p 4329 N94-36390
HUPP, JOSEPH T. p 4238 N94-36252
p 4246 N94-36253
HUSNAIN, S. B. p 4312 N94-35831
HWANG, D. p 4298 N94-35688
HWANG, IN AH p 4346 N94-35832
p 4346 N94-35833
HYATT, D. E. p 4285 N94-35741
HYLAND, D. C. p 4217 N94-35866
HYMER, THOMAS C. p 4305 N94-35958

I

ICHIGUCHI, K. p 4337 N94-35938
p 4324 N94-35984
IDA, K. p 4336 N94-35812
p 4337 N94-35936
p 4339 N94-36357
IDEI, H. p 4337 N94-35936
IFJU, PETER G. p 4233 N94-35946
IGUCHI, H. p 4337 N94-35936
p 4339 N94-36357
IIJIMA, B. p 4253 N94-35553
IKEDA, NOBUKAZU p 4216 N94-35854
ILIN, YU. p 4326 N94-36132
IMBRIALE, W. A. p 4253 N94-35549
INGALLS, R. L. p 4238 N94-36203
INMAN, D. J. p 4222 N94-35895
INOUE, N. p 4336 N94-35752
IRAQI, M. p 4323 N94-35792
IRVING, J. S. p 4287 N94-36207
p 4287 N94-36208
IRWIN, A. D. p 4244 N94-35702
IRWIN, J. p 4330 N94-36106
ISRAELSSON, HANS p 4290 N94-35693
ITO, HIROSHI p 4325 N94-36086
ITOH, K. p 4336 N94-35811
p 4336 N94-35812
p 4337 N94-35939
p 4324 N94-35984
ITOH, KIMITAKA p 4339 N94-36353
ITOH, MAMORU p 4306 N94-36065
ITOH, S.-I p 4324 N94-35984
ITOH, S.-I. p 4336 N94-35811
p 4336 N94-35812
ITOH, SANAE-I. p 4336 N94-35775
p 4339 N94-36353
IVANOV, A. A. p 4339 N94-36417

IVANOV, A. V. p 4352 N94-35476
IVANOV, V. V. p 4345 N94-35790

J

JAANIMAGI, P. A. p 4330 N94-36114
JACKSON, A. A. p 4352 N94-36142
JACKSON, A. H. p 4205 N94-35624
JACKSON, A. M. p 4258 N94-35564
JACKSON, BERNARD V. p 4375 N94-36264
JACKSON, THOMAS L. p 4266 N94-35975
JACKSON, WADE C. p 4233 N94-35946
JACOB, ROBERT J. p 4302 N94-35491
JACOBS, JAMES A. p 4229 N94-36398
JAFAROV, R. G. p 4343 N94-36351
JAIN, A. K. p 4288 N94-36286
JAIN, RAJ K. p 4281 N94-35230
JAKOSKY, B. M. p 4368 N94-36137
JAKOSKY, BRUCE M. p 4369 N94-36143
JARDINE, LESLIE J. p 4286 N94-35957
JENKINS, THOMAS J. p 4230 N94-36404
JENKOVSZKY, L. L. p 4315 N94-36076
JENNINGS, G. R., JR. p 4304 N94-35808
JENNINGS, M. J. p 4275 N94-35931
JENNINGS, RAYMOND D. p 4257 N94-36043
JENNISKENS, PETER p 4239 N94-36144
JENSEN, W. A. p 4338 N94-36284
JEONG, DO YOUNG p 4334 N94-36180
JERMAKIAN, JOEL B. p 4282 N94-35540
JESKE, F. R. p 4275 N94-35931
JESSON, D. E. p 4322 N94-35682
JOHNSON, BONNIE L. p 4200 N94-36437
JOHNSON, BRUCE B. p 4347 N94-36044
JOHNSON, D. R. p 4260 N94-36245
JOHNSON, DAVID B. p 4344 N94-35526
JOHNSON, R. N. p 4275 N94-35667
JOHNSTON, CAROL p 4284 N94-35486
JOHNSTON, NORMAN J. p 4232 N94-35372
JONES, J. H. p 4353 N94-36146
p 4353 N94-36160
p 4354 N94-36169
JONES, JOHN H. p 4369 N94-36143
p 4353 N94-36147
JORDAN, LAVON p 4197 N94-36342
JORDAN, R. E. p 4324 N94-36058
JORGENSEN, J. D. p 4327 N94-36225
JOSEPH, L. H. p 4353 N94-36145
JOSHI, S. M. p 4221 N94-35889
JOU, H. L. p 4216 N94-35856
JUANG, JER-NAN p 4220 N94-35880
JUANG, K. Y. p 4215 N94-35852
p 4217 N94-35862
JULYK, J. L. p 4264 N94-35756
JUREWICZ, A. J. G. p 4353 N94-36146
p 4353 N94-36160
JUREWICZ, STEPHEN R. p 4353 N94-36147
JUSTUS, BRIAN L. p 4234 N94-36123

K

KAASTRA, J. S. p 4339 N94-36386
KABANTSEV, A. A. p 4337 N94-36082
KAELLBERG, A. p 4327 N94-36267
KAFAFI, ZAKA H. p 4234 N94-36124
KAHN, R. D. p 4254 N94-35557
KAHN, ROGER E. p 4310 N94-35742
p 4312 N94-35802
KAKAD, Y. P. p 4219 N94-35878
KALDOR, S. p 4275 N94-35815
KALSI, SWARN S. p 4215 N94-35849
KANADE, TAKEO p 4278 N94-36046
KANEFSKY, ROB p 4281 N94-35417
KANEKO, H. p 4338 N94-36352
KANEKO, O. p 4338 N94-36247
KANEKO, S. p 4283 N94-36109
KANEMITSU, YOICHI p 4223 N94-35906
KANG, KEEBOM p 4316 N94-35675
KAPLAN, JOSEPH A. p 4309 N94-36438
KAPLAN, MICHAEL L. p 4192 N94-35522
KAPUSCIK, E. p 4318 N94-35956
p 4342 N94-36070
KARABEKOV, I. P. p 4331 N94-36192
KARAMCHANDANI, PRAKASH p 4287 N94-36183
KARGEL, J. S. p 4354 N94-35359
KARIG, F. p 4296 N94-36293
KARL, JEFFREY B. p 4203 N94-35612
KARNAUKHOV, S. p 4342 N94-35781
KARNOWSKY, M. p 4224 N94-35907
KASARDA, M. E. F. p 4214 N94-35847
KASCAK, ALBERT F. p 4223 N94-35905
KASIMOVSKAYA, E. E. p 4287 N94-36179
KATANUMA, I. p 4338 N94-36352
KATKOV, V. M. p 4256 N94-36078
KATNIK, GREGORY N. p 4211 N94-35523
KATO, T. p 4337 N94-35939
KAWAMURA, T. p 4336 N94-35752
KAY, IRVIN W. p 4312 N94-35730
KAY, JONATHAN S. p 4306 N94-36065
KAYA, D. p 4314 N94-35531
KAYSER, R. F. p 4251 N94-36008
KAZIMIERCZYK, P. p 4258 N94-35354
KECKLER, CLAUDE R. p 4217 N94-35865
KEFFER, CHARLES E. p 4376 N94-36421
KEGELMEYER, W. P., JR. p 4294 N94-35766
p 4294 N94-35767
KEICHER, D. M. p 4270 N94-35351
KELLER, J. L. p 4293 N94-35720
KELLER, L. P. p 4355 N94-35397
p 4359 N94-35418
p 4352 N94-35465
p 4352 N94-35466
KELLER, LINDSAY P. p 4369 N94-36148
p 4353 N94-36149
KELLER, P. E. p 4311 N94-35348
KELLER, R. A. p 4320 N94-35376
KELLETT, B. J. p 4350 N94-35530
KELLEY, ALLAN J. p 4214 N94-35844
KEMPCZYNSKI, J. p 4318 N94-35956
p 4342 N94-36070
KEMPKA, S. N. p 4265 N94-35769
KENDALL, K. N. p 4234 N94-36004
KENNEDY, CHRISTOPHER A. p 4190 N94-35864
KENNEDY, JOHN M. p 4344 N94-35254
KETO, J. W. p 4330 N94-36105
KHAMAGANOV, V. G. p 4287 N94-36179
KHASANOV, A. M. p 4345 N94-35790
KHESHGI, H. S. p 4288 N94-36286
KHODYREV, V. A. p 4341 N94-36181
KHOSROPOUR, P. p 4342 N94-36367
KHRIPLOVICH, I. B. p 4322 N94-35783
p 4327 N94-36246
KHUDIK, V. N. p 4335 N94-35750
KIELY, A. B. p 4254 N94-35556
KILKENNY, J. D. p 4266 N94-35982
p 4318 N94-36201
KIM, CHAESIL p 4223 N94-35905
KIM, HEE KYUNG p 4346 N94-35833
KIM, SI YONG p 4305 N94-35834
KIMMER, E. p 4203 N94-35613
p 4204 N94-35615
KING, N. L. p 4353 N94-36159
KINZER, K. E. p 4245 N94-35809
KISELEV, V. V. p 4322 N94-35784
KIVELSON, M. G. p 4354 N94-35378
p 4289 N94-35392
KLAASEN, K. p 4351 N94-35416
KLABUNDE, C. E. p 4342 N94-36377
KLAUS, E. E. p 4245 N94-36108
KLEIN, J. p 4224 N94-35907
KLEINHEINS, S. p 4264 N94-35669
KLEM, J. F. p 4240 N94-36110
KLENNER, J. p 4194 N94-36327
KLIER, K. p 4237 N94-36036
KLOCK, W. p 4352 N94-35466
KLUSMAN, STEVE p 4223 N94-35905
KNIGHT, JOSIAH p 4216 N94-35859
KNOBLOCK, CRAIG p 4345 N94-35663
KNOLL, M. G. p 4261 N94-36362
KNOLLE, ERNST G. p 4226 N94-35919
KNOSPE, C. R. p 4215 N94-35851
KNOWLTON, LAWRENCE W. p 4295 N94-36228
KNOX, L. p 4327 N94-36241
KOELMANS, A. M. p 4258 N94-35534
KOEPF, W. p 4329 N94-36305
KOGA, R. p 4227 N94-35362
KOHLBERG, IRA p 4263 N94-35492
KOHLER, S. M. p 4225 N94-35916
KOHNE, GLENN S. p 4232 N94-36415
KOLLIE, T. G. p 4233 N94-35932
KOLOKOLOV, I. V. p 4325 N94-36073
KOMORI, A. p 4336 N94-35752
KONOPELCHENKO, B. G. p 4315 N94-36100
KOONTZ, S. L. p 4236 N94-35680
KOONTZ, STEVEN L. p 4235 N94-35229
p 4250 N94-35445
KORENYI-BOTH, ANDRAS L. p 4281 N94-35271
KORIAGIN, JOHN p 4197 N94-36344
KORNBLUM, H. N. p 4266 N94-35982
KOROTEV, RANDY L. p 4363 N94-35457
KORTH, A. p 4227 N94-35362
KOSIER, S. L. p 4260 N94-36268
p 4261 N94-36371
KOSOWSKY, A. p 4327 N94-36241
KOTIKOV, A. V. p 4325 N94-36074
KOTTNAUER, ING. PAVEL p 4291 N94-36087
KOTULAK, JOHN C. p 4298 N94-35528
p 4298 N94-35659
KOURA, N. p 4239 N94-36349
KOVACHEV, V. p 4259 N94-36194
KOVACIC, L. p 4244 N94-35699
KOZLOWSKI, R. W. H. p 4370 N94-36150
KRAEMER, SYLVIA K. p 4201 N94-36440
KRAFT, RICHARD p 4281 N94-35417
KRAMER, BRIAN R. p 4190 N94-35991
KRASNOPOLSKY, V. A. p 4370 N94-36151
p 4370 N94-36152
KRAUS, GEORGE F. p 4318 N94-36171
KREMSER, G. p 4227 N94-35362
KRIMMER, MICHAEL p 4197 N94-36342
KROEGER, D. M. p 4342 N94-36377
KROGER, P. M. p 4210 N94-35543
KROTHAPALLI, A. p 4229 N94-36291
KRUEGER, J. p 4245 N94-35779
KRUPKE, W. F. p 4271 N94-35679
KUDLAC, MAUREEN T. p 4263 N94-35250
KUKLA, G. p 4293 N94-35703
KUMAR, MANOJ p 4222 N94-35896
KUMAR, MITHLESH p 4235 N94-35592
KUMAR, S. V. p 4309 N94-36382
KUMAZAWA, R. p 4336 N94-35813
p 4338 N94-36247
KUNDU, NIKHIL K. p 4232 N94-36414
KUNG, ERNEST C. p 4292 N94-35380
KUNZ, K. p 4319 N94-35770
KUNZ, P. D. p 4324 N94-35824
KUO, L. T. p 4215 N94-35852
KURDILA, A. J. p 4222 N94-35894
KURTH, W. S. p 4354 N94-35378
KURTZ, S. R. p 4340 N94-35698
KUSUNOKI, A. p 4283 N94-36109
KUZIN, ALEXANDER V. p 4225 N94-35917
KUZNETSOV, A. V. p 4336 N94-35791
KWAN, ROBERT K. p 4257 N94-36043
KWATNY, HARRY G. p 4220 N94-35879
KWOK, A. p 4255 N94-35563
KYRIACOU, C. p 4254 N94-35558

L

LABGAA, RACHID R. p 4289 N94-35389
LAFAVE, NORMAN p 4366 N94-35472
LAFLAMME, R. p 4350 N94-35980
LAGARDE, A. p 4270 N94-36219
LAGARDE, D. p 4196 N94-36339
LAGRANGE, MARIO B. J. p 4196 N94-36340
LAHEY, RICHARD T., JR. p 4249 N94-35237
LAKSHMINARAYANA, BUDUGUR
p 4263 N94-35253
LALA, JAYNARAYAN H. p 4215 N94-35848
LAMB, J. PARKER p 4189 N94-35360
LAMB, M. A. p 4214 N94-35843
LAMBERTSON, M. p 4204 N94-35617
LANDEN, O. L. p 4330 N94-36114
LANDHEIM, RAGNILD p 4358 N94-35414
LANDIS, GEOFFREY A. p 4281 N94-35230
LANDIS, J. p 4209 N94-35641
LANDRUM, C. p 4319 N94-35770
LANE, MARK T. p 4203 N94-35611
LANGEVIN, YVES p 4354 N94-35336
LANSER, WENDY R. p 4191 N94-35965
LANSING, F. S. p 4255 N94-35562
LARIN, I. K. p 4287 N94-36179
LARSON, N. R. p 4287 N94-36053
LARSSON, M. p 4327 N94-36267
LAUER, H. V., JR. p 4239 N94-35433
p 4240 N94-36154
p 4372 N94-36165
LAULAINEN, N. S. p 4287 N94-36053
LAVAGNO, L. p 4258 N94-35534
LAVID, M. p 4236 N94-35755
LAVIGNA, CHRIS p 4220 N94-35879
LE, JEANETTE p 4310 N94-35968
LE, L. p 4353 N94-36161
p 4353 N94-36162
LEAF, G. K. p 4316 N94-36432
LEAGO, KIMBERLY S. p 4352 N94-35458
LEAR, K. L. p 4272 N94-36178
LEAVITT, ROBERT p 4204 N94-35619
LEE, HAE CHO p 4346 N94-35832
LEE, JONG MIN p 4334 N94-36180
LEE, K. A. p 4255 N94-35562
LEE, KI BOG p 4305 N94-35834
LEE, M. p 4204 N94-35616
p 4204 N94-35617
p 4209 N94-35641
LEE, M. H. p 4322 N94-35682
LEE, SANG HOON p 4305 N94-35834
LEE, SCOTT A. p 4243 N94-35494
LEE, YOUNG JAI p 4346 N94-35832
p 4346 N94-35833
LEE, YOUNG JOO p 4334 N94-36180
LEGER, L. J. p 4236 N94-35680
LEHMAN, JILL F. p 4299 N94-35716
LEID, TERRY p 4204 N94-35616
p 4209 N94-35641

LEIGH, JAMES E. p 4200 N94-36437
LEMOINE, F. G. p 4364 N94-35461
p 4371 N94-36155
p 4371 N94-36156
LEMPERT, W. R. p 4236 N94-35755
LENDEL, A. p 4326 N94-36132
LENNON, E. B. p 4333 N94-36002
LEPICOVSKY, JAN p 4265 N94-35945
LERCH, F. J. p 4371 N94-36155
LERCHE, R. A. p 4330 N94-36114
p 4339 N94-36375
LESNIAK, L. p 4326 N94-36129
LEVINE, S. M. p 4242 N94-36369
LEWIS, K. p 4319 N94-35770
LEWIS, NORMAN G. p 4296 N94-35257
LI, F. p 4220 N94-35881
LI, NINGDA R. p 4301 N94-35437
LI, S. Z. p 4246 N94-36306
LI, SHENG S. p 4342 N94-36385
LI, W. L. p 4338 N94-36200
LI, Z. p 4260 N94-36221
LIEDAHL, D. A. p 4339 N94-36386
LIKHODED, A. A. p 4323 N94-35787
LILLEY, G. M. p 4263 N94-35497
LILLY, JOHN H. p 4219 N94-35876
LIM, KYONG B. p 4225 N94-35913
LIM, SEUNGCHUL p 4218 N94-35867
LIN, C. E. p 4215 N94-35852
p 4216 N94-35856
p 4217 N94-35862
LIN, CHIN-E. p 4225 N94-35912
LIN, YUH-LANG p 4192 N94-35522
LIND, ANN-MARIE T. p 4293 N94-35596
LINDE, GEORGE J. p 4257 N94-36364
LINDLEY, P. M. p 4247 N94-35469
LINDSTROM, D. J. p 4352 N94-35456
LINDSTROM, DAVID J. p 4352 N94-35467
LINDSTROM, M. M. p 4362 N94-35450
p 4353 N94-36157
LINDSTROM, TIFFANY p 4262 N94-35248
LINGLE, R. L., JR. p 4324 N94-36058
LIPATOV, L. N. p 4327 N94-36238
LIPSCHUTZ, M. E. p 4352 N94-35477
p 4353 N94-36166
LIU, PING p 4230 N94-36402
p 4230 N94-36403
LLOYD, BRADLEY A. p 4308 N94-36250
LOEHLE, C. p 4281 N94-36018
LOFGREN, GARY E. p 4351 N94-35421
p 4351 N94-35423
p 4353 N94-36158
LOFTIN, R. BOWEN p 4311 N94-35501
LOGAN, R. T., JR. p 4252 N94-35545
LOGNONNE, PHILIPPE p 4354 N94-35336
LOGSDON, JOHN M. p 4348 N94-35901
LOHNER, RAINALD p 4279 N94-35949
LOHR, GARY W. p 4192 N94-36048
LOKTEV, V. M. p 4340 N94-36030
p 4329 N94-36434
LONDERGAN, J. T. p 4328 N94-36303
LONG, A. C. p 4206 N94-35625
LOPEZ, R. E. p 4292 N94-36383
LORD, J. J. p 4326 N94-36130
LOTT, J. A. p 4272 N94-36178
LOVE, S. G. p 4353 N94-36159
LOVEJOY, M. L. p 4240 N94-36110
LOWE, G. p 4316 N94-35536
LOWNDES, D. H. p 4342 N94-36377
LOWRIE, JAMES W. p 4278 N94-36046
LOWRY, M. p 4333 N94-35697
LOZIER, D. W. p 4305 N94-36010
LU, W. F. p 4250 N94-35524
LU, Z. p 4285 N94-35735
LUBELL, M. S. p 4264 N94-35683
LUBIN, JEFFREY p 4312 N94-36309
LUCE, W. p 4198 N94-36380
LUCEY, PAUL G. p 4356 N94-35403
LUDWIG, D. J. p 4197 N94-36343
LUE, J. W. p 4264 N94-35683
LUERKEN, REINHARD F. p 4213 N94-35841
LUHMANN, JANET G. p 4369 N94-36143
LUTES, G. p 4252 N94-35545
LYNCH, F. p 4248 N94-36191
LYNN, JAMES G. p 4273 N94-36370
LYON, L. A. p 4246 N94-36253
LYONS, JAMES P. p 4223 N94-35903

M

MA, CHOPO p 4281 N94-35261
MA, K. B. p 4214 N94-35843
MABEN, EGBERT p 4219 N94-35877
MACCORMACK, ROBERT W. p 4190 N94-35717
MADZSAR, GEORGE C. p 4268 N94-35268
MAGHAMI, P. G. p 4221 N94-35889
MAHDAVI, M. p 4375 N94-35381
MAHLE, CHRISTOPH E. p 4257 N94-36043
MAINE, TRINDEL A. p 4199 N94-35258
MAISEL, MARTIN D. p 4198 N94-36380
MAKHOV, A. M. p 4326 N94-36134
MAKSIMOV, S. J. p 4325 N94-36074
MALCOLM, GERALD N. p 4190 N94-35991
MALEKI, L. p 4252 N94-35544
p 4252 N94-35545
MALHOTRA, R. p 4237 N94-35778
MALKIN, V. M. p 4335 N94-35750
MALMKJAER, KAROLINE p 4304 N94-35718
MANAENKOV, S. I. p 4328 N94-36287
MANCHALA, DANIEL p 4223 N94-35905
MANHEIMER, WALLACE M. p 4335 N94-35493
MANITIUS, ANDRE p 4222 N94-35893
MANKA, CHARLES p 4263 N94-35492
MANNERVIK, S. p 4327 N94-36267
MANSHADI, F. p 4253 N94-35550
MARCHANT, N. J. p 4270 N94-36389
MARCHYWKA, MICHAEL J. p 4239 N94-36372
MARCUS, JEFFREY H. p 4191 N94-35236
MARIN, L. E. p 4352 N94-35456
MARK, STEVE p 4213 N94-35842
MARKLEY, R. E. p 4260 N94-36197
MARKS, VIRGINIA B. p 4217 N94-35865
MARLAIRE, RUTH DASSO p 4348 N94-35966
MARR, W. W. p 4285 N94-35765
MARTENS, M. A. p 4332 N94-36431
MARTIN, J. C. p 4320 N94-35376
MARTIN, T. Z. p 4356 N94-35405
MARTINEZ, R. R. p 4352 N94-35456
MARTINEZ, RENE R. p 4352 N94-35467
MARTINI, A. p 4195 N94-36331
MARUSKA, H. P. p 4261 N94-36360
MARVIN, D. C. p 4282 N94-35804
MARX, K. D. p 4268 N94-36318
MASHKEVICH, S. V. p 4343 N94-36072
p 4325 N94-36075
p 4325 N94-36083
MASI, JAMES V. p 4231 N94-36411
MASON, LARRY W. p 4354 N94-35263
MASQUELIER, D. p 4333 N94-35697
MASSON, GERALD M. p 4306 N94-36063
p 4306 N94-36064
p 4306 N94-36065
p 4306 N94-36066
p 4307 N94-36067
p 4307 N94-36068
p 4307 N94-36069
MASSON, PHILIPPE p 4354 N94-35336
MASTERS, JOHN E. p 4229 N94-36399
MASTIN, G. A. p 4284 N94-35674
MATHEW, J. p 4318 N94-36427
MATHEWS, M. p 4202 N94-35608
MATINLINNA, J. p 4237 N94-36059
MATLIN, A. p 4295 N94-36249
MATOCHKIN, E. P. p 4338 N94-36097
MATSON, CHARLES L. p 4334 N94-36257
MATSUSHITA, OSAMI p 4217 N94-35863
MATTHEWS, L. p 4350 N94-35530
MAUER, A. p 4314 N94-35704
MAURY, S. p 4331 N94-36271
MAVRIPLIS, D. J. p 4191 N94-35994
MAX, C. E. p 4349 N94-35565
MAX, N. p 4292 N94-35350
p 4334 N94-36356
MAXWELL, B. p 4223 N94-35904
p 4224 N94-35908
MAXWELL, G. P. p 4276 N94-36355
MAYER-ROSA, D. p 4290 N94-35830
MAYER, F. p 4346 N94-36005
MAYER, F. L. p 4296 N94-35738
MCAFEE, W. J. p 4279 N94-35684
MCBRIDE, KATHLEEN M. p 4359 N94-35419
MCCAIN, HARRY p 4278 N94-36046
MCCALLUM, DUNCAN p 4213 N94-35842
MCCAMMON, K. p 4333 N94-35697
MCCARTY, JOHN P. p 4229 N94-36047
MCCLAIN, J. GREER p 4198 N94-36380
MCCLELLAND, H. T. p 4230 N94-36406
MCCONAGHY, C. p 4333 N94-35697
MCCONNELL, THOMAS p 4197 N94-36345
MCCOOL, S. C. p 4338 N94-36200
MCCURDY, HOWARD E. p 4376 N94-35356
MCCUTCHEON, R. p 4203 N94-35613
MCDONALD, J. S. p 4370 N94-36153
MCDONNELL, J. A. M. p 4351 N94-35412
MCDOWELL, R. E. p 4275 N94-35667
p 4275 N94-35815
MCELIECE, R. J. p 4254 N94-35554
MCEWEN, ROB p 4206 N94-35627
MCGEE, WILLIAM F. p 4273 N94-35367
MCGUIRE, J. C. p 4353 N94-36160
MCKAY, D. S. p 4355 N94-35397
p 4355 N94-35398
p 4355 N94-35401
p 4357 N94-35409
p 4359 N94-35418
MCKAY, DAVID S. p 4358 N94-35415
p 4352 N94-35465
p 4352 N94-35466
p 4368 N94-36138
p 4369 N94-36148
p 4353 N94-36149
MCKAY, G. p 4353 N94-36161
p 4353 N94-36162
MCKAY, G. A. p 4353 N94-36163
MCKECHNIE, T. S. p 4267 N94-36111
MCKINNON, A. D. p 4331 N94-36317
MCKONE, T. E. p 4284 N94-35700
MCLACHLAN, B. G. p 4189 N94-35394
MCMANUS, JOHN W. p 4309 N94-36438
MCMARTIN, W. P. p 4206 N94-35628
MCMICHAEL, C. K. p 4214 N94-35843
MCNEILL, J. D. p 4324 N94-36058
MCNEILLY, G. S. p 4288 N94-36273
MCNELIS, NANCY B. p 4263 N94-35250
MCPARTLAND, MICHAEL D. p 4209 N94-35643
MCQUILLAN, M. p 4314 N94-35762
MCSWEEN, HARRY Y., JR. p 4357 N94-35411
MCWATTERS, D. p 4253 N94-35551
MEGER, R. A. p 4318 N94-36427
MEHLHORN, R. p 4194 N94-36329
MEHROTRA, PIYUSH p 4300 N94-35240
MEI, V. C. p 4264 N94-35683
MEIROVITCH, LEONARD p 4218 N94-35867
MEISENHEIMER, T. L. p 4261 N94-36362
MELCHER, KEVIN J. p 4198 N94-35352
MELFI, S. H. p 4295 N94-36285
MELIUS, C. F. p 4248 N94-36376
MELTON, R. B. p 4286 N94-36024
MELTZER, M. p 4285 N94-35943
MENG, C. I. p 4292 N94-36383
MENG, R. L. p 4214 N94-35843
MENGEL, M. p 4275 N94-35815
MERFELD, D. p 4297 N94-35379
MERKLE, CHARLES p 4229 N94-36047
MERKLE, K. L. p 4241 N94-36231
MERRILL, DEANE W. p 4344 N94-35337
MERRY, W. R. p 4324 N94-36058
MESLIN, BRAD M. p 4348 N94-35901
MESSENGER, S. p 4352 N94-35465
METZGER, RICHARD C. p 4310 N94-35653
MEWE, R. p 4339 N94-36386
MEYER, STEPHAN S. p 4349 N94-36419
MEYER, THOMAS J. p 4209 N94-35643
MIAO, F. Q. p 4248 N94-36035
MICHAEL, J. R. p 4246 N94-36209
p 4241 N94-36242
MICHALSKY, J. J. p 4287 N94-36053
MIKOUCHI, T. p 4353 N94-36162
p 4353 N94-36163
MILANA, J. p 4321 N94-35649
MILEY, H. S. p 4331 N94-36317
MILIKH, G. M. p 4295 N94-36240
MILLER, RENE H. p 4212 N94-35484
MILLER, W. D. p 4270 N94-35351
MILLING, M. E. p 4344 N94-35347
MILLOTT, T. A. p 4280 N94-36423
MILLS, G. A. p 4237 N94-36023
MILMAN, V. p 4322 N94-35682
MILSHTEJN, A. I. p 4322 N94-35783
MINEEV, YU. V. p 4290 N94-35780
MING, D. W. p 4351 N94-35432
p 4239 N94-35433
MISCOVICH, D. p 4285 N94-35943
MISHCHENKO, A. V. p 4343 N94-36071
p 4315 N94-36076
MISTRETTA, G. p 4208 N94-35637
MISTRETTA, G. D. p 4205 N94-35620
p 4205 N94-35623
MITCHELL, A. C. p 4238 N94-36237
MITTLEFEHLDT, D. W. p 4351 N94-35455
p 4353 N94-36146
p 4353 N94-36157
MIURA, Y. p 4336 N94-35812
MIYAMOTO, M. p 4364 N94-35463
p 4353 N94-36163
MIZUNO, TAKAYUKI p 4223 N94-35906
MODERA, MARK p 4250 N94-35364
MOGILKA, PH. p 4195 N94-36332
MOLBAY-ARSAN, A. p 4195 N94-36332
MONTAGUE, GERALD p 4223 N94-35905
MONTGOMERY, RAYMOND C. p 4218 N94-35871
MONTHUS, X. p 4195 N94-36332
MONTOYA, D. p 4285 N94-35943
MOOK, D. JOSEPH p 4209 N94-35643
MOORE, FRANK G. p 4305 N94-35958
MOORE, J. M. p 4354 N94-35359
MOORE, K. p 4347 N94-36300
MOORE, KEVIN A. p 4200 N94-36437
MOORE, M. p 4253 N94-35548

MORAN, MATTHEW E. p 4263 N94-35250
MORASCA, SANDRO p 4301 N94-35438
MORGAN, J. P. p 4270 N94-36389
MORISON, J. D. p 4307 N94-36113
MORITA, S. p 4339 N94-36357
MORRIS, BRIAN G. p 4274 N94-35661
MORRIS, CARL J. p 4212 N94-35799
p 4212 N94-35801
MORRIS, R. V. p 4355 N94-35398
p 4355 N94-35401
p 4239 N94-35433
p 4240 N94-36154
MORRIS, RICHARD V. p 4292 N94-35454
p 4363 N94-35457
p 4239 N94-35459
p 4240 N94-36164
p 4372 N94-36165
p 4353 N94-36166
MORRISON, D. p 4351 N94-35416
MORSE, J. p 4333 N94-35697
MORSE, STEPHEN E. p 4298 N94-35528
p 4298 N94-35659
MORTON, DAVID P. p 4303 N94-35577
MORUSIEWICZ, LINDA p 4300 N94-35238
MOTOJIMA, O. p 4336 N94-35773
MOUROULIS, P. p 4271 N94-35488
MUDALIAR, SABA p 4256 N94-35694
p 4256 N94-35713
MUKHOPADHYAY, VIVEK p 4200 N94-35873
MULCAHY, T. p 4282 N94-35829
MULCAHY, T. M. p 4276 N94-36433
MUMM, R. H. p 4303 N94-35660
MUMMERT, L. p 4345 N94-35571
MUNRO, D. p 4266 N94-35982
p 4318 N94-36201
MURPHY, P. W. p 4338 N94-36193
MURPHY, R. W. p 4264 N94-35683
MURPHY, S. p 4203 N94-35613
MURPHY, T. J. p 4330 N94-36114
p 4339 N94-36375
MURRAY, B. T. p 4236 N94-35736
MURRAY, C. S. p 4228 N94-35349
MURRAY, S. F. p 4246 N94-36306
MUSIELAK, Z. E. p 4375 N94-36395
MUTLU, ERTEM p 4316 N94-35691
MUTOH, T. p 4336 N94-35813
MYERS, IRA T. p 4257 N94-35249
MYERS, TAMARA A. p 4212 N94-35799

N

NABER, J. D. p 4276 N94-36378
NACLERIO, N. p 4259 N94-35748
NADELMAN, MATTHEW S. p 4203 N94-35612
NAGLE, GAIL A. p 4215 N94-35848
NAIK, DIPAK p 4298 N94-35266
NAKAJIMA, N. p 4337 N94-35938
NAKAMURA, Y. p 4337 N94-35938
NANDI, S. p 4210 N94-35543
NASH, M. p 4259 N94-35748
NASSER, MAHMOUD G. p 4222 N94-35897
NATANSON, G. A. p 4209 N94-35642
NAVA, DAVID F. p 4353 N94-36167
NEAL, D. R. p 4267 N94-36111
NEAL, M. p 4259 N94-36194
NEEMAN, Y. p 4323 N94-35814
NEHRKORN, THOMAS p 4295 N94-36228
NEIL, G. R. p 4331 N94-36192
NELLIS, W. J. p 4232 N94-35696
p 4238 N94-36237
NELSON, G. C. p 4241 N94-36242
NELSON, JESSICA L. p 4375 N94-36264
NELSON, M. B. p 4339 N94-36375
NELSON, R. p 4239 N94-35464
NEMESURE, M. p 4205 N94-35620
NEMESURE, MICHAEL p 4204 N94-35619
NENOFF, T. M. p 4340 N94-35677
NEUFFER, D. p 4331 N94-36271
NEUKUM, G. p 4351 N94-35416
NEUMANN, G. A. p 4367 N94-35480
p 4373 N94-36168
NEVILLE, KELLY J. p 4196 N94-36338
NEWCOMER, P. P. p 4318 N94-36204
NEWELL, P. T. p 4289 N94-35587
NEWMAN, LAURI KRAFT p 4202 N94-35609
NEWSAM, J. M. p 4242 N94-36369
NEWTON, CRYSTAL H. p 4244 N94-35757
NG, DANIEL L. P. p 4269 N94-35383
NG, K. Y. p 4332 N94-36431
NG, W. C. p 4256 N94-36301
NGUYEN, T. p 4239 N94-35459
NGUYEN, T. M. p 4254 N94-35558
NIER, A. O. p 4352 N94-35465
NII, H. PENNY p 4347 N94-36044
NIKLEWSKI, D. p 4208 N94-35637
NIKLEWSKI, D. J. p 4205 N94-35620
p 4205 N94-35623
NIKOLAEV, V. S. p 4340 N94-36029
p 4340 N94-36041
NISHIMURA, K. p 4336 N94-35813
p 4337 N94-35936
p 4339 N94-36357
NOH, JAE MAN p 4305 N94-35834
NORBY, P. p 4341 N94-36358
NORMAN, E. B. p 4350 N94-36229
NORMAN, M. D. p 4354 N94-36169
NORRIS, ANDREW T. p 4265 N94-35948
NORTHAM, G. BURTON p 4229 N94-36047
NORTON, D. P. p 4342 N94-36377
NOVAKAO, T. p 4286 N94-36025
NOWLIN, R. N. p 4260 N94-36268
NUTH, JOSEPH A., III p 4239 N94-35464
p 4373 N94-36170
p 4318 N94-36171
NYBERG, KAREN L. p 4274 N94-35374
NYQUIST, L. E. p 4354 N94-36172
p 4374 N94-36173

O

OBADA, A. S. F. p 4272 N94-35782
OBERBECK, V. R. p 4352 N94-36140
OBERKAMPF, W. L. p 4267 N94-35996
OBERKAMPF, WILLIAM L. p 4189 N94-35360
OBRAZTSOV, V. F. p 4323 N94-35787
OBRYAN, M. V. p 4352 N94-35471
OCKER, KATHERINE D. p 4240 N94-36174
ODDY, DONNA M. p 4288 N94-36422
OEZGUENER, UEMIT p 4220 N94-35884
OHALLARON, DAVID p 4311 N94-36015
OHALLORON, DAVID R. p 4310 N94-35806
OHASHI, TAKAAKI p 4225 N94-35914
OHYABU, N. p 4336 N94-35752
p 4338 N94-36352
OKA, Y. p 4338 N94-36247
OKAMOTO, M. p 4337 N94-35937
p 4337 N94-35938
OKAMURA, S. p 4337 N94-35936
p 4339 N94-36357
OKEEFE, JOHN D. p 4355 N94-35396
OLIVIER, S. S. p 4349 N94-35565
OLSEN, ALLAN W. p 4234 N94-36124
OLSON, C. L. p 4331 N94-36199
OLSON, G. B. p 4240 N94-35953
OLSON, J. E. p 4328 N94-36302
OLVER, F. W. J. p 4305 N94-36010
ONEL, Y. p 4269 N94-36095
ONO, T. p 4336 N94-35752
p 4338 N94-36352
ORANS, ROBIN p 4377 N94-35961
ORENBERG, JAMES B. p 4292 N94-35453
ORIE, NETTIE M. p 4189 N94-35246
ORKIN, V. L. p 4287 N94-36179
ORTIZ, J. V. p 4322 N94-35753
ORTON, GLENN S. p 4355 N94-35396
ORVIS, W. J. p 4308 N94-36236
OSBORNE, WILLIAM P. p 4211 N94-35357
OSTEEN, B. L. p 4285 N94-35823
OSTERHELD, A. L. p 4339 N94-36386
OTOSHI, T. Y. p 4252 N94-35546
p 4253 N94-35547
OTSUKI, MASAYUKI p 4364 N94-35463
OTSUKI, MAYUMI p 4364 N94-35463
OTTO, S. R. p 4263 N94-35497
OUROURA, A. p 4338 N94-36200
OVASKAINEN, O. p 4279 N94-36000
OVERTON, ERIC p 4257 N94-35249
OWEN, T. C. p 4365 N94-35468
OWENS, W. R. p 4282 N94-36021
OZA, D. H. p 4205 N94-35620
p 4205 N94-35623
p 4208 N94-35636
OZBAY, HITAY p 4200 N94-35875

P

PADOWITZ, D. F. p 4324 N94-36058
PAGE, A. G. p 4235 N94-35592
PAIS, M. R. p 4250 N94-35524
PALAZZOLO, ALAN B. p 4223 N94-35905
PANG, DA-CHEN p 4217 N94-35861
p 4224 N94-35910
PANISKO, M. E. p 4331 N94-36317
PARISH, DONALD A. p 4226 N94-36188
PARK, BONG SIK p 4346 N94-35832
PARK, JEONG SEOK p 4346 N94-35832
PARK, SOO JIN p 4346 N94-35832
PARK, SUN HEE p 4346 N94-35832
p 4346 N94-35833
PARKER, T. J. p 4354 N94-35359
PARKINSON, W. H. p 4227 N94-36189
PARMENTIER, E. M. p 4367 N94-35480
PARNAS, R. S. p 4234 N94-36004
PAROBIJ, I. S. p 4325 N94-36074
PASKIN, MARC D. p 4199 N94-36379
PASTOR, JOHN p 4284 N94-35486
PATCH, S. K. p 4317 N94-36235
PATCHEN, ALLAN p 4358 N94-35415
p 4368 N94-36138
PATEL, G. B. p 4371 N94-36155
PATER, RUTH H. p 4242 N94-35233
p 4232 N94-35372
PATT, FREDERICK S. p 4211 N94-35269
PATTIPATI, K. R. p 4256 N94-36092
PAVLOFF, MICHAEL S. p 4207 N94-35635
PAYNE, M. C. p 4322 N94-35682
PEARSON, JOHN p 4312 N94-36309
PELTON, A. p 4351 N94-36418
PELTON, GARRETT A. p 4299 N94-35716
PELTON, JOSEPH N. p 4257 N94-36043
PENNATI, G. p 4238 N94-36205
PENNELL, W. E. p 4279 N94-35684
PENNER, J. E. p 4286 N94-36025
PENNOCK, S. T. p 4256 N94-36301
PENNYCOOK, S. J. p 4322 N94-35682
p 4333 N94-36055
PEPIN, S. p 4329 N94-36305
PERDIEU, L. H. p 4259 N94-35706
PEREPEZKO, JOHN H. p 4234 N94-36045
PERES, O. L. G. p 4321 N94-35594
PERRY, T. S. p 4266 N94-35982
PETERSEN, G. p 4283 N94-36051
PETERSEN, J. p 4326 N94-36126
PETERSON, D. W. p 4260 N94-36245
PETERSON, M. B. p 4246 N94-36306
PETIT, JOCELYN I. p 4232 N94-36413
PETROV, N. M. p 4326 N94-36131
p 4329 N94-36391
PHAM, VUONG T. p 4262 N94-35245
PHI, DUONG VAN p 4329 N94-36308
PHILLION, D. W. p 4266 N94-35982
p 4330 N94-36114
PHILLIP, F. p 4242 N94-36289
PHILLIP, W. H. p 4243 N94-35260
PHILLIPS, P. E. p 4338 N94-36200
PHINNEY, W. C. p 4351 N94-35449
PHIPPS, MICKIE A. p 4260 N94-36296
PIEN, HOMER p 4309 N94-36439
PILINIS, CHRISTODOULOS p 4287 N94-36183
PINDERA, MAREK-JERZY p 4278 N94-35239
PINELLI, THOMAS E. p 4344 N94-35254
PIPER, T. C. p 4270 N94-36389
PIPES, R. BYRON p 4234 N94-36045
PISANO, F. p 4321 N94-35582
PITKAERANTA, J. p 4279 N94-36000
PITZ, W. J. p 4238 N94-36205
p 4239 N94-36319
PITZER, K. S. p 4238 N94-36230
PLATT, C. M. R. p 4269 N94-36085
PLEITEZ, V. p 4321 N94-35582
p 4321 N94-35594
POISSON-QUINTON, PHILIPPE p 4194 N94-36326
POLI, DORA DECASTRO RUBIO p 4330 N94-36028
POLLACK, J. B. p 4358 N94-35413
p 4366 N94-35474
p 4370 N94-36152
POLLACK, JAMES B. p 4356 N94-35404
p 4356 N94-35405
PONEZHA, E. A. p 4341 N94-36312
POPOVIC, R. p 4308 N94-36211
PORTIER, R. W. p 4346 N94-35819
POTASKE, M. J. p 4332 N94-35664
POTTER, A. E. p 4366 N94-35478
POULOS, A. T. p 4236 N94-35755
POULTON, M. M. p 4290 N94-35686
POUNDS, K. A. p 4350 N94-35530
POVINELLI, LOUIS A. p 4229 N94-36047
POWELL, H. T. p 4338 N94-36193
POWERS, SHERYLL GOECKE p 4251 N94-35967
PRABAKAR, S. p 4244 N94-35701
p 4244 N94-35702
PRADEEP, A. K. p 4213 N94-35838
p 4216 N94-35858
PRADETTO, J. C. p 4224 N94-35911
PRAUSNITZ, J. M. p 4237 N94-36033
p 4248 N94-36034
PRESCOTT, DOUGLAS N. p 4255 N94-35689
PRESTON, MARK A. p 4223 N94-35903
PRICE, D. F. p 4272 N94-35695
PRICE, D. L. p 4237 N94-35777
PROISE, M. p 4213 N94-35840
PROKOPOWICZ, PETER N. p 4312 N94-35802
PROVANCHA, JANE A. p 4288 N94-36422
PROVOST, LIONEL R. p 4238 N94-36091
PRYWES, NOAH p 4308 N94-36258

PUGACHEVA, G. I. p 4290 N94-35780

Q

QUAAL, KAREN S. p 4231 N94-36408
QUENBY, J. J. p 4350 N94-35530
QUINCEY, P. G. p 4339 N94-35598
QUINN, RICHARD p 4366 N94-35475
QUINTO, P. FRANK p 4189 N94-35246
QURESHI, A. HAQ p 4258 N94-35270

R

RADACK, S. M. p 4333 N94-36002
RADHAKRISHNAN, KRISHNAN p 4313 N94-35259
RAHMAN, M. S. p 4315 N94-35934
RAINA, P. p 4204 N94-35617
RAJ, SAI V. p 4241 N94-36275
RAJORE, S. B. p 4309 N94-36382
RAMAKRISHNAN, JAYANT p 4221 N94-35887
p 4222 N94-35896
RAMAN, N. K. p 4244 N94-35701
RANDEL, DAVID L. p 4292 N94-35355
p 4293 N94-35499
RANZI, E. p 4238 N94-36205
RAO, A. K. p 4275 N94-36348
RAO, M. C. p 4279 N94-35684
RAO, M. N. p 4351 N94-35428
RASCOE, D. L. p 4255 N94-35562
RASMUSSEN, G. ALLEN p 4287 N94-36120
RATNER, MARK A. p 4246 N94-36253
RAY, CHANDRA S. p 4245 N94-35977
RAY, RONALD J. p 4193 N94-35241
REAGAN, MICHAEL K. p 4264 N94-35690
REASENBERG, ROBERT D. p 4354 N94-35265
REBER, R. A., JR. p 4260 N94-36268
REBOLD, T. A. p 4255 N94-35563
REDONDO, A. p 4242 N94-36369
REED, CHARLES E. p 4344 N94-35525
REEVES, J. M. L. p 4194 N94-36325
REGARDIE, MYRNA p 4300 N94-35256
REGENIE, VICTORIA A. p 4310 N94-35968
REIDY, ANNE MARIE p 4360 N94-35427
REIF, ANDREW p 4198 N94-36347
REIGBER, CHRISTOPH p 4207 N94-35634
REIGELSPERGER, WILLIAM C., JR.
p 4199 N94-35796
REINISCH, BODO W. p 4291 N94-36116
REINKE, DONALD L. p 4292 N94-35355
p 4293 N94-35499
REINTJES, JOHN F. p 4334 N94-36368
REITZE, D. H. p 4272 N94-35695
REMINGTON, B. A. p 4266 N94-35982
p 4318 N94-36201
RENAUD, J. p 4195 N94-36331
RENSFELT, K. G. p 4327 N94-36267
RENZI, R. F. p 4260 N94-36245
RESS, D. B. p 4339 N94-36375
RESTREPO, J. M. p 4316 N94-36432
REZVANI, M. A. p 4264 N94-35756
RHO, SI PYO p 4334 N94-36180
RICHARDS, B. p 4338 N94-36200
RICHARDSON, B. R. p 4238 N94-36084
RICHON, K. p 4203 N94-35610
RICKMAN, S. L. p 4236 N94-35680
RIDES, M. p 4263 N94-35603
RIEGER, D. J. p 4240 N94-36110
RIES, J. C. p 4205 N94-35622
RIETSCHEL, H. p 4224 N94-35909
RIEU, M. p 4297 N94-36217
RIM, H. J. p 4205 N94-35622
RINGEBACH, PAULA p 4247 N94-35795
RINGERUD, MARK A. p 4292 N94-35355
p 4293 N94-35499
RINTAHEN, J. p 4346 N94-35959
RISSO, J. J. p 4297 N94-36220
RIVERA-CARPIO, C. p 4286 N94-36025
RIZZO, DEAN H. p 4265 N94-35803
ROACH, R. K. p 4333 N94-36002
ROARK, JAMES H. p 4360 N94-35426
p 4360 N94-35427
ROBBINS, WILLIAM E. p 4269 N94-35369
ROBELLO, DOUGLAS R. p 4243 N94-35588
ROBERTS, J. B., JR. p 4331 N94-36428
ROBINETT, R. D. p 4226 N94-36001
ROBINS, GLENN M. p 4269 N94-35369
ROBINSON, R. p 4355 N94-35401
ROBINSON, RAYMOND C. p 4200 N94-35267
ROCKWELL, DONALD O. p 4190 N94-35529
RODE, O. D. p 4362 N94-35450
RODGERS, WILLIAM G., JR. p 4192 N94-36048
ROESKE, S. B. p 4261 N94-36362
ROGERS, C. F. p 4286 N94-36025
ROGERS, J. p 4326 N94-36127
ROMANEK, C. S. p 4351 N94-35451
ROSENTHAL, R. R. p 4267 N94-36111
ROSS, J. p 4283 N94-36051
ROSTAING, N. p 4308 N94-36259
ROTE, D. M. p 4276 N94-36433
ROTEA, MARIO A. p 4199 N94-36384
ROUSH, T. L. p 4356 N94-35405
ROUSH, TED L. p 4292 N94-35452
p 4292 N94-35453
p 4292 N94-35454
ROUSSEL-DUPRE, R. A. p 4295 N94-36240
ROWAN, L. R. p 4351 N94-35455
ROWAN, THOMAS H. p 4347 N94-36300
ROWLANDS, D. D. p 4371 N94-36156
ROY, J. A. p 4242 N94-36288
RUAN, MIFANG p 4220 N94-35883
RUDERMAN, MALVIN p 4349 N94-35516
RUGH, H. H. p 4314 N94-35758
RUND, BERTON B. p 4197 N94-36344
RUTLEDGE, SHARON K. p 4243 N94-35243
p 4243 N94-35502
RYAN, JAMES W. p 4281 N94-35261
RYBICKI, DANIEL J. p 4273 N94-35367
RYGAARD, CHRISTOPHER A. p 4206 N94-35629
p 4207 N94-35631

S

SABOUNGI, M. L. p 4239 N94-36349
SACHS, G. p 4194 N94-36329
SACKINGER, S. J. p 4259 N94-36094
SAEED, A. p 4250 N94-35532
SAKAKIBARA, S. p 4339 N94-36357
SALAMA, AHMED p 4204 N94-35619
SALEM, A. J. p 4234 N94-36004
SALIKOVA, T. V. p 4346 N94-35954
SALTER, ROBERT M. p 4225 N94-35918
SALZAR, ROBERT S. p 4278 N94-35239
SALZMANN, D. p 4337 N94-35939
SAMEL, A. p 4195 N94-36337
SAMII, M. V. p 4205 N94-35620
SAMIMY, MO p 4190 N94-35950
SAMPSON, MARK R. p 4294 N94-36187
SANDHOLT, P. E. p 4292 N94-36265
SANTORO, ROBERT J. p 4235 N94-35604
SANUKI, H. p 4324 N94-35984
SASAKI, R. p 4314 N94-35774
SASTRY, M. D. p 4235 N94-35592
SATO, T. p 4336 N94-35772
SATORNINO, GEORGE A. p 4263 N94-35250
SATYANARAYANAN, M. p 4345 N94-35571
SAUL, G. E. p 4285 N94-35741
SAVARD, R. M. p 4331 N94-36317
SAVE, PHIL p 4215 N94-35850
SAWADA, HIDEO p 4216 N94-35854
SAYLOR, R. D. p 4286 N94-36026
p 4288 N94-36359
SCALI, JAMES L. p 4289 N94-35578
p 4291 N94-36116
SCHAEFER, R. J. p 4236 N94-35736
SCHAEFER, R. M. p 4312 N94-35810
SCHIFFRIES, C. M. p 4344 N94-35347
SCHIMEL, DAVID S. p 4284 N94-35486
SCHLEICH, D. P. p 4338 N94-36193
SCHLOSSNAGLE, G. p 4316 N94-36432
SCHLUETER, J. A. p 4341 N94-36272
SCHLUTTER, D. J. p 4352 N94-35465
SCHMIED, J. p 4224 N94-35911
SCHNEIDER, IRWIN p 4273 N94-36365
SCHNEIDER, SAMUEL, JR. p 4243 N94-35335
SCHNITZLER, J. V. p 4237 N94-36033
p 4248 N94-36034
SCHONBERG, WILLIAM P. p 4228 N94-35825
SCHOOLER, EVE M. p 4300 N94-35652
SCHOONOVER, R. M. p 4265 N94-35942
SCHORR, HERBERT p 4347 N94-36044
SCHRIMPF, R. D. p 4260 N94-36268
p 4342 N94-36367
p 4261 N94-36371
SCHRODT, DARLA p 4246 N94-36125
SCHULTZ, R. J. p 4242 N94-36288
SCHULZ, C. K. p 4357 N94-35409
SCHUPP, P. p 4315 N94-36270
SCHURAYTZ, B. C. p 4352 N94-35456
SCHWAB, JOHN R. p 4263 N94-35253
SCHWARTZ, ALAN W. p 4191 N94-36261
SCHWARZ, CAROL p 4363 N94-35457
SCHWARZ, H. p 4323 N94-35792
SCHWARZ, J. A. p 4241 N94-36233
SCHWEITZER, J. p 4375 N94-35381
SEDLAK, J. p 4208 N94-35638
p 4210 N94-35646
SEE, T. H. p 4280 N94-35407
p 4352 N94-36141
SEE, THOMAS H. p 4352 N94-35458
SEFER, N. R. p 4247 N94-35941
SEGALL, EDWARD p 4311 N94-36015
SEHMBEY, M. S. p 4250 N94-35524
SEILA, ANDREW F. p 4316 N94-35675
SEKAR, R. R. p 4285 N94-35765
SEKI, T. p 4336 N94-35813
p 4338 N94-36247
SELVIN, STEVE p 4344 N94-35337
SELYUGIN, O. V. p 4330 N94-36080
SERDYUKOVA, S. I. p 4315 N94-35789
SERIKOV, A. A. p 4329 N94-36310
SERPA, JAMES N. p 4192 N94-36184
SESAK, JOHN R. p 4221 N94-35888
SESSLER, A. p 4331 N94-36271
SEVERE, GERALDA p 4229 N94-35361
SEXTON, F. W. p 4261 N94-36362
p 4261 N94-36373
SHAFER, MARY F. p 4198 N94-35969
SHAH, JITENDRA p 4287 N94-36183
SHAH, R. J. p 4245 N94-36108
SHANEYFELT, M. R. p 4261 N94-36362
SHANKAR, U. p 4332 N94-35584
SHANNON, J. p 4286 N94-36007
SHAPOVAL, D. V. p 4329 N94-36392
SHARMA, PRAMOD K. p 4235 N94-35255
SHARPTON, V. L. p 4352 N94-35456
SHATILOV, D. N. p 4330 N94-35999
SHEAKOSKI, J. R. p 4333 N94-35747
SHEEHAN, JAMES E. p 4234 N94-36045
SHELFER, T. D. p 4239 N94-35459
SHEN, JI-YAO p 4218 N94-35870
SHEN, YONG-HONG p 4343 N94-35970
p 4342 N94-35971
SHERIDAN, TOM p 4278 N94-36046
SHERIF, J. S. p 4255 N94-35559
SHERWIN, M. E. p 4240 N94-36110
SHEVLYAGIN, M. V. p 4323 N94-35787
SHIH, C.-Y. p 4354 N94-36172
p 4374 N94-36173
SHIMABUKURO, F. I. p 4253 N94-35547
SHIMPO, F. p 4336 N94-35813
SHIN, YOUNG S. p 4190 N94-35826
SHIRAISHI, KATSUTO p 4225 N94-35914
SHIVPURI, RAJIV p 4250 N94-35711
SHOEMAKER, J. D. p 4285 N94-35943
SHOUP, D. p 4209 N94-35640
SHRIVASTAVA, S. K. p 4310 N94-35535
SHROBE, HOWARD p 4347 N94-36044
SHUL, R. J. p 4240 N94-36110
SHUSTER, MALCOLM D. p 4209 N94-35644
SIBECK, D. G. p 4289 N94-35587
SIEBERS, D. L. p 4276 N94-36378
SIEGWART, ROLAND p 4213 N94-35839
SIGRAY, P. p 4327 N94-36267
SILAGADZE, Z. K. p 4322 N94-35785
SIMENOG, I. V. p 4329 N94-36392
SIMONS, J. p 4323 N94-35793
SIMONS, JACK p 4321 N94-35589
p 4322 N94-35678
p 4322 N94-35753
p 4323 N94-35792
p 4323 N94-35797
p 4323 N94-35798
p 4324 N94-36050
SIMONS, RIES M. p 4195 N94-36336
SINGER, BART A. p 4267 N94-35992
SINGY, A. p 4376 N94-35590
SINYUKOV, YU. M. p 4325 N94-36079
SIROCKY, PAUL J. p 4274 N94-35373
SITENKO, O. G. p 4329 N94-36392
SITENKO, YU. A. p 4343 N94-36071
SKIDMORE, J. p 4271 N94-35665
SKIDMORE, J. A p 4272 N94-36115
SKILLMAN, D. p 4202 N94-35608
SKROBIS, K. J. p 4224 N94-35907
SLATER, J. C. p 4222 N94-35895
SMALLEY, DAVID J. p 4295 N94-36262
SMART, J. L. p 4341 N94-36272
SMITH, D. E. p 4364 N94-35460
p 4364 N94-35461
p 4371 N94-36155
p 4371 N94-36156
SMITH, FRED W. p 4206 N94-35629
SMITH, LARRY D. p 4274 N94-35375
SMITH, PETER L. p 4227 N94-36189
SMITH, R. p 4247 N94-35941
SMITH, REBECCA B. p 4288 N94-36422
SMITH, ROBERT E. p 4291 N94-36175
SMITH, SEAN W. p 4344 N94-35526
SMITH, T. G. p 4267 N94-36111
SMITH, W. C. p 4275 N94-36348
SMITH, WARREN W. p 4306 N94-36065
SNYDER, K. D. p 4370 N94-36150
SOCKI, R. A. p 4351 N94-35451
SODERBLOM, D. R. p 4349 N94-36282
SOGARO, A. p 4238 N94-36205

SOHN, JAE MIN p 4346 N94-35832
SOKOLOV, V. G. p 4337 N94-36082
SOLARZ, R. p 4271 N94-35665
SOLOMON, G. p 4254 N94-35554
SONG, KYU SEOK p 4334 N94-36180
SONNABEND, DAVID p 4206 N94-35630
SOOD, DEVENDRA K. p 4223 N94-35903
SOPER, A. K. p 4237 N94-35777
SOULE, C. p 4314 N94-35759
SPAULDING, GLENN F. p 4296 N94-35366
SPELCE, T. E. p 4309 N94-36429
SPELLMAN, G. P. p 4338 N94-36284
SPENCE, CLAY p 4312 N94-36309
SPENCE, H. E. p 4289 N94-35392
p 4289 N94-35587
p 4292 N94-36383
SPERLING, R. p 4203 N94-35610
SPEZZAFERRO, R. p 4193 N94-36323
SPIEGEL, F. X. p 4229 N94-36400
SPIEGEL, F. XAVIER p 4230 N94-36401
p 4232 N94-36415
SPRAGUE, A. L. p 4370 N94-36150
SPRINGMEYER, R. R. p 4347 N94-36297
SRINIDHI, SARAGUR M. p 4347 N94-36396
ST.CYR, G. J. p 4256 N94-36112
STACEY, W. M. p 4338 N94-36093
STALEY, R. J. p 4269 N94-35599
STANCU, F. p 4329 N94-36305
STANGELAND, MAYNARD L. p 4229 N94-36047
STARK, MIKE p 4300 N94-35256
p 4301 N94-35439
STAUFFER, D. B. p 4282 N94-36021
STEICH, D. p 4319 N94-35770
STEIMLE, LAWRENCE J. p 4333 N94-35749
STEINETZ, BRUCE M. p 4274 N94-35373
STEINMAN, D. p 4335 N94-35673
STEPANOVA, M. V. p 4350 N94-36128
STEPHENS, GRAEME L. p 4292 N94-35355
p 4293 N94-35499
STERNBERG, B. K. p 4290 N94-35666
STERNER, S. M. p 4238 N94-36230
STEVENS, E. J. p 4288 N94-36273
STEVENS, J. G. p 4236 N94-35755
STICH, I. p 4322 N94-35682
STOCKMAN, STEPHANIE p 4360 N94-35427
p 4364 N94-35462
STOKES, G. M. p 4286 N94-36024
STOKESBERRY, D. P. p 4305 N94-35940
STOLOFF, N. S. p 4241 N94-36196
STONEMAN, C. p 4273 N94-36370
STORACE, ALBERT F. p 4223 N94-35903
STORM, WILLIAM F. p 4196 N94-36338
STRAKHOVENKO, V. M. p 4256 N94-36078
STRANGEWAY, R. J. p 4354 N94-35378
STRAWN, ROGER p 4319 N94-36031
STRAYER, T. p 4257 N94-36354
STRENS, M. R. p 4345 N94-35533
STRGANAC, T. p 4222 N94-35894
STRICKER, MARKUS A. p 4345 N94-35732
STRICKLAND, J. H. p 4265 N94-35769
STRUMINSKIJ, B. V. p 4315 N94-36076
STRYKOWSKI, P. J. p 4229 N94-36291
STUCKY, G. D. p 4340 N94-35677
STUDEBAKER, KAREN p 4200 N94-35972
STURTEVANT, ROBERT p 4301 N94-35443
STUTZ, JOHN p 4281 N94-35417
STYLES, R. C. p 4242 N94-36289
SU, PENWEN p 4230 N94-36406
SUAREZ, CARLOS J. p 4190 N94-35991
SUBHLOK, JASPAL p 4310 N94-35806
SUBRAMANIAM, V. V. p 4228 N94-36089
SUENAGA, HISASHI p 4216 N94-35854
SUGAMA, H. p 4337 N94-35937
p 4337 N94-35938
SUHADOLC, P. p 4290 N94-35830
SULLIVAN, GREGORY F. p 4306 N94-36064
p 4306 N94-36065
p 4306 N94-36066
p 4307 N94-36067
p 4307 N94-36068
p 4307 N94-36069
SULLIVAN, WILLIAMS E. p 4312 N94-36309
SUNDSTROEM, G. p 4327 N94-36267
SUNSHINE, J. M. p 4368 N94-36139
SUTTON, JOHN F. p 4251 N94-35231
SUTTON, S. p 4271 N94-35665
SUTTON, S. B. p 4271 N94-35679
SUTTON, S. R. p 4352 N94-35465
SUZUKI, TAKAYUKI p 4216 N94-35854
SUZUYA, K. p 4239 N94-36349
SVOBODA, ROBERT C. p 4376 N94-35515
SWAIN, MICHAEL J. p 4345 N94-35732
p 4310 N94-35742
p 4312 N94-35802
SWANEY, COLIN p 4274 N94-35481
SWEET, J. N. p 4260 N94-36245
SWEGLE, J. p 4272 N94-35978
SWIDERSKI, ZDZISLAW p 4279 N94-35353
SYCARA, K. p 4305 N94-36006
SYMANSKI, J. J. p 4260 N94-36248
SZARSKA, M. p 4326 N94-36130
SZYMURSKI, S. R. p 4247 N94-36387

T

TAKABE, H. p 4337 N94-35939
TAKAGI, MICHIYUKI p 4217 N94-35863
TAKAHASHI, K. p 4289 N94-35587
TAKAHASHI, NAOHIKO p 4217 N94-35863
TAKAHASHI, S. p 4239 N94-36349
TAKAMI, HIROSHI p 4225 N94-35914
TAKATA, TOSHIKO p 4355 N94-35396
TAKEDA, HIROSHI p 4364 N94-35463
TAKEUCHI, S. p 4283 N94-36109
TALPALLIKAR, M. p 4267 N94-35996
TANG, DERSHUEN A. p 4192 N94-36048
TANG, PUNAN p 4223 N94-35905
TAPLEY, B. D. p 4205 N94-35622
TARN, J. H. p 4215 N94-35852
p 4217 N94-35862
TARTAKOVSKIJ, V. K. p 4325 N94-36077
TASKAEV, S. YU. p 4337 N94-36082
TATTON-BROWN, H. E. p 4194 N94-36330
TAYLOR, LAWRENCE A. p 4358 N94-35415
p 4368 N94-36138
TAYLOR, LAWRENCE W., JR. p 4218 N94-35870
p 4221 N94-35887
p 4223 N94-35898
TELTZOV, M. V. p 4350 N94-36128
TEMES, CLIFFORD L. p 4257 N94-36364
TEMPLEMAN, JAMES N. p 4302 N94-35491
TEMPLETON, C. K. p 4232 N94-36412
TENEVA, G. N. p 4326 N94-36131
THEISS, T. J. p 4279 N94-35684
THERRIEN, CHARLES W. p 4319 N94-35800
THIEMENS, M. H. p 4239 N94-35464
THIESSEN, DAVID L. p 4333 N94-35749
THOMAS, C. E. p 4338 N94-36093
THOMAS, K. p 4263 N94-35603
THOMAS, K. L. p 4352 N94-35465
p 4352 N94-35466
THOMAS, KATHIE L. p 4353 N94-36149
THOMAS, WILLIAM M. p 4301 N94-35436
THOMSON, MICHAEL p 4310 N94-35968
THORNTON, EARL A. p 4268 N94-36420
THORNTON, K. W. p 4285 N94-35741
THURMAN, S. p 4254 N94-35557
TISCHLER, V. A. p 4193 N94-36322
TISHKOFF, J. M. p 4198 N94-35746
TODD, RUSSELL F. p 4294 N94-35807
TODOROKI, J. p 4324 N94-35984
TOENSKOETTER, H. p 4195 N94-36335
TOLSTAYA, E. D. p 4290 N94-35780
TOMIO, L. p 4320 N94-35580
p 4320 N94-35581
p 4321 N94-35583
p 4321 N94-35595
TOMOBUCHI, M. p 4364 N94-35463
TOMPA, G. S. p 4282 N94-35739
TONASSE, M. D. p 4321 N94-35582
TONUCCI, RONALD J. p 4234 N94-36123
TORTI, R. p 4223 N94-35904
p 4224 N94-35908
TOTH, P. p 4346 N94-36005
TOUEG, SAM p 4300 N94-35365
TRAMEL, R. W. p 4266 N94-35951
TRAN, N. T. p 4303 N94-35660
TRAUB, JOSEPH F. p 4316 N94-36425
TREIDLER, BURKE p 4250 N94-35364
TREIMAN, A. H. p 4353 N94-36157
TREIMAN, ALLAN H. p 4352 N94-35467
TREMBLAY, MARC p 4198 N94-36347
TREW, R. J. p 4252 N94-35247
TROMBKA, JACOB I. p 4350 N94-35420
TROY, G. p 4346 N94-36005
TRUDNOWSKI, D. J. p 4259 N94-36054
TRULOVE, P. C. p 4237 N94-35777
TRUMPER, D. L. p 4214 N94-35845
TRUMPER, DAVID L. p 4225 N94-35917
TRYKA, K. A. p 4365 N94-35468
TSIRELSON, B. S. p 4342 N94-35761
TSOU, P. p 4351 N94-35412
p 4247 N94-35469
p 4202 N94-35607
TSUTSUI, YUKIO p 4214 N94-35844
TSYTOVICH, V. N. p 4375 N94-36210
TULINOV, A. F. p 4341 N94-36181
TUNNELL, T. p 4295 N94-36240
TUOMELA, J. p 4315 N94-35821
TUOMI, T. p 4334 N94-36190
TURKEL, E. p 4266 N94-35976
TUTTLE, B. A. p 4246 N94-36209
TYGAR, J. D. p 4344 N94-35526
TYLER, C. A. p 4201 N94-35626

U

UETA, K. p 4320 N94-35579
UHERKA, K. p 4282 N94-35829
ULLALAND, S. L. p 4227 N94-35362
UNDERWOOD, S. p 4204 N94-35616
p 4204 N94-35617
UNGER, L. p 4351 N94-36418
URBAN, C. p 4224 N94-35909
USENKO, A. S. p 4256 N94-36096
p 4256 N94-36099
USOV, YU. V. p 4259 N94-36104

V

VAJDA, S. p 4375 N94-35381
VAKATOV, D. V. p 4345 N94-35790
VALENTINE, G. A. p 4291 N94-36103
VALETT, JON p 4300 N94-35238
VALK, PIERRE J. L. p 4195 N94-36336
VALLET, MICHEL p 4319 N94-36176
VALTONEN, M. p 4259 N94-35822
VANAKEN, JOHANNES M. p 4200 N94-36436
VANDERHOEVEN, W. p 4279 N94-36226
VANIMAN, DAVID T. p 4357 N94-35408
VANKLEUNEN, W. p 4275 N94-35815
VANNUCCI, RAYMOND D. p 4242 N94-35234
VANROSENDALE, JOHN p 4300 N94-35240
VAWTER, G. A. p 4272 N94-36178
VEITCH, L. C. p 4243 N94-35260
VELASCO, CARLOS H. p 4319 N94-35800
VELOSO, MANUELA p 4303 N94-35574
VEMPATI, R. K. p 4240 N94-36154
VENKATAPATHY, ETHIRAJ p 4189 N94-35498
VENKATRAMANI, N. p 4273 N94-36393
VENKAYYA, V. B. p 4193 N94-36322
VENTURINI, E. L. p 4318 N94-36204
VERMA, R. L. p 4273 N94-36393
VERUTTIPONG, W. p 4253 N94-35548
VESELSKI, M. p 4345 N94-35790
VESTRAND, W. THOMAS p 4374 N94-35993
VEVERKA, J. p 4351 N94-35416
VEYO, S. E. p 4283 N94-36109
VIANCO, P. T. p 4258 N94-35564
VIEIRA, JOSE MAURO p 4330 N94-36028
VIITANEN, M. p 4283 N94-36060
VILAS, F. p 4352 N94-35470
p 4368 N94-36139
VILCHINSKIJ, S. I. p 4267 N94-36098
p 4267 N94-36313
VILNROTTER, V. p 4253 N94-35553
VINOGRADOV, V. M. p 4315 N94-36416
VIRGIN, LAWRENCE p 4216 N94-35859
VOIGT, J. A. p 4246 N94-36209
VOLPANO, DENNIS M. p 4303 N94-35576
p 4304 N94-35676
VONBRAUN, C. p 4207 N94-35634
VONDERHAAR, T. H. p 4293 N94-35499
VONDERHAAR, THOMAS H. p 4292 N94-35355
VONHOLTZ, E. p 4379 N94-35997
VOROBEV, G. M. p 4336 N94-35791
VOROBEV, P. V. p 4326 N94-36133
VRUDHULA, SARMA B. p 4303 N94-35662
VYILCHINSKIJ, S. YI. p 4267 N94-36314

W

WADDELL, M. G. p 4257 N94-36366
WADE, R. C. p 4347 N94-36300
WAGSTAFF, J. p 4353 N94-36161
WAKATANI, M. p 4337 N94-35937
p 4337 N94-35938
WALIGORA, SHARON p 4300 N94-35256
WALKER, R. M. p 4352 N94-35465
WALLACE, JAY S. p 4246 N94-36125
WALLACE, R. J. p 4266 N94-35982
p 4318 N94-36201
WALLETT, THOMAS M. p 4258 N94-35270
WALLIN, BECKY L. p 4344 N94-35337
WALSH, THOMAS p 4216 N94-35859
WAMHOF, P. D. p 4255 N94-35562
WAN, SHAO-LONG p 4322 N94-35786
WANG, H. H. p 4341 N94-36272
WANG, HAN-CHING p 4218 N94-35868
WANG, KE-LIN p 4322 N94-35786
WANG, LUI p 4311 N94-35501
WANG, R. G. p 4314 N94-35764
WANG, Z. L. p 4342 N94-36377
WANIEK, L. p 4290 N94-35830
WARREN, J. p 4352 N94-35466

WARREN, JACK L. p 4352 N94-35458
WARREN, M. E. p 4267 N94-36111
p 4272 N94-36178
WASIELEWSKI, M. R. p 4332 N94-35671
WASILEWSKI, P. J. p 4352 N94-35471
WASKOM, TOMMY L. p 4230 N94-36402
p 4230 N94-36403
WATANABE, K. p 4336 N94-35772
p 4337 N94-35938
p 4338 N94-36352
WATANABE, KATSUHIDE p 4223 N94-35906
WATANABE, T. p 4336 N94-35752
p 4338 N94-36352
WATARI, T. p 4336 N94-35813
p 4338 N94-36247
WATSON, A. T. p 4269 N94-35599
WATSON, J. G. p 4285 N94-35735
WAX, S. p 4259 N94-35748
WAYMAN, RICHARD J. p 4344 N94-35525
WEAVER, MICHAEL J. p 4238 N94-36252
WEBB, DAVID F. p 4375 N94-36264
WEBB, J. C. p 4263 N94-35497
WEBB, JON p 4310 N94-35806
p 4311 N94-36015
WEBER, M. D. p 4229 N94-36400
WEERATUNGA, SISIRA p 4268 N94-36397
WEGMANN, H. M. p 4195 N94-36337
WEI, A. p 4261 N94-36371
WEINER, E. O. p 4264 N94-35756
WEIR, S. T. p 4238 N94-36237
WEIRICK, L. J. p 4266 N94-35979
WEISS, RAINER p 4349 N94-36419
WEISSHAAR, TERRENCE A. p 4199 N94-36384
WEITSMAN, Y. J. p 4233 N94-35714
p 4233 N94-35715
WEITSMAN, Y. JACK p 4233 N94-35944
WEIZER, VICTOR G. p 4281 N94-35271
WELLS, RAYMOND, JR. p 4315 N94-36424
WELLS, STEPHEN p 4224 N94-35910
WELTER, GARY L. p 4203 N94-35613
p 4203 N94-35614
p 4204 N94-35615
WEN, T. p 4296 N94-36293
WENTWORTH, SUSAN J. p 4355 N94-35399
p 4355 N94-35401
WENZEL, K. W. p 4338 N94-36200
WESSALE, WILLIAM p 4301 N94-35443
WEST, HARVEY A. p 4229 N94-36400
WESTBROOK, C. K. p 4238 N94-36205
p 4276 N94-36378
WHEELER, A. A. p 4236 N94-35736
WHEELER, Z. p 4210 N94-35646
WHITE, J. M. p 4236 N94-35685
WHITE, RUTH p 4343 N94-35973
WHITE, SUSAN p 4377 N94-35961
p 4343 N94-35973
WHITE, W. E. p 4272 N94-35695
WHITEMAN, D. N. p 4295 N94-36285
WHITTAKER, WILLIAM p 4278 N94-36046
WICKS, A. L. p 4231 N94-36407
WICKS, G. p 4271 N94-35488
WIESEL, WILLIAM E. p 4202 N94-35606
WIESMANN, H. p 4354 N94-36172
p 4374 N94-36173
WILCOXON, J. P. p 4318 N94-36204
WILCZYNSKI, H. p 4326 N94-36130
WILETS, L. p 4324 N94-35824
p 4328 N94-36304
p 4329 N94-36305
WILEY, ROGER W. p 4298 N94-35528
WILGEN, J. p 4338 N94-36093
WILKEN, B. p 4227 N94-35362
WILKES, R. J. p 4326 N94-36130
WILLAND, CRAIG S. p 4243 N94-35588
WILLIAMS, DAVID J. p 4243 N94-35588
WILLIAMS, J. p 4351 N94-35412
WILLIAMS, M. E. p 4214 N94-35845
WILLIAMS, R. A. p 4325 N94-36086
WILLIAMS, R. S., JR. p 4361 N94-35431
WILLIAMS, ROBERT L., II p 4311 N94-35242
WILLIAMS, S. p 4366 N94-35474
WILLIAMS, S. D. p 4262 N94-35245
WILLIAMS, STEVEN H. p 4360 N94-35424
WILLIAMS, TODD O. p 4278 N94-35239
WILLIAMS, TREVOR p 4207 N94-35633
WILLITS, CRAIG J. p 4316 N94-35575
WILLS, E. L. p 4239 N94-35459
WILSON, DWIGHT S. p 4306 N94-36064
p 4306 N94-36065
p 4306 N94-36066
p 4307 N94-36067
WILSON, HOLLY J. p 4344 N94-35525
WILSON, M. D. p 4298 N94-35600
WILSON, R. B. p 4237 N94-35778
WILSON, R. P. p 4275 N94-36348
WILSON, THOMAS L. p 4366 N94-35472
p 4350 N94-35473
WINOKUR, P. S. p 4260 N94-36268
p 4261 N94-36362
p 4261 N94-36373
WITTEBORN, F. C. p 4370 N94-36150
WITTMEYER, IAN L. p 4292 N94-35355
p 4293 N94-35499
WOLF, D. R. p 4304 N94-35808
WOLF, DAVID A. p 4296 N94-35232
WOLTER, W. p 4326 N94-36130
WONG, Y. p 4305 N94-36017
WOO, C. H. p 4242 N94-36289
WOOD, G. E. p 4255 N94-35563
WOODEN, D. p 4370 N94-36150
WOODFILL, JERRY p 4343 N94-35339
WOODRUFF, C. p 4204 N94-35617
WOODWARD, ROBERT H. p 4211 N94-35269
WORKMAN, GARY L. p 4235 N94-35447
WOZNIAK, K. p 4326 N94-36130
WRIGHT, K. p 4314 N94-35531
WU, CHANG-NING p 4231 N94-36408
WU, H. J. p 4237 N94-35778
WUEBBLES, D. J. p 4288 N94-36286
WUU, TZYH-YUNG p 4303 N94-35662
WYATT, D. E. p 4257 N94-36366

X

XIA, HONG-XING p 4222 N94-35893
XIONG, F. p 4340 N94-35828
XU, J. p 4220 N94-35881
XU, P. p 4366 N94-35474

Y

YAGI, M. p 4336 N94-35811
YAKIMENKO, I. P. p 4325 N94-36081
p 4256 N94-36096
p 4256 N94-36099
YAKOVLEV, A. V. p 4258 N94-35534
YAKOVLEV, O. I. p 4320 N94-35567
YAMADA, H. p 4339 N94-36357
YAMAGUCHI, A. p 4364 N94-35463
YAMAZAKI, K. p 4336 N94-35752
p 4336 N94-35773
p 4338 N94-36352
YAN, ZHUANG p 4221 N94-35886
YANG, S. V. p 4351 N94-35432
p 4352 N94-35476
YANO, KENICHI p 4223 N94-35906
YAO, X. S. p 4252 N94-35544
p 4252 N94-35545
YARBROUGH, D. W. p 4233 N94-35932
YASAKA, Y. p 4338 N94-36247
YASIN, O. M. p 4272 N94-35782
YATES, J. T., JR. p 4236 N94-35731
YATSU, KIYOSHI p 4337 N94-35983
YEH, C. p 4253 N94-35547
YEH, H.-G. p 4254 N94-35558
YEN, C. W. p 4202 N94-35607
YI, JONG HOON p 4334 N94-36180
YOKOYAMA, H. p 4283 N94-36109
YOO, BYUNG DUK p 4334 N94-36180
YOSHIDA, KINJIRO p 4225 N94-35914
YOST, F. G. p 4259 N94-36094
YOST, WILLIAM T. p 4268 N94-35368
YOUNG, J. F. p 4233 N94-35952
YOUNG, LAURENCE R. p 4297 N94-35379
YUEN, JOSEPH H. p 4252 N94-35542
YUREV, M. Z. p 4318 N94-35955
YUSHCHENKO, O. P. p 4323 N94-35787

Z

ZABKA, R. p 4224 N94-35909
ZAGORODNIJ, A. G. p 4325 N94-36081
p 4256 N94-36096
p 4256 N94-36099
p 4329 N94-36311
ZAKKARI, M. p 4317 N94-36307
ZANDA, BRIGITTE p 4351 N94-35421
ZEE, SUNG KYUN p 4305 N94-35834
ZELKOWITZ, MARVIN V. p 4301 N94-35437
ZENT, AARON P. p 4366 N94-35475
ZEWAIL, AHMED H. p 4323 N94-35805
ZHANG, Z. M. p 4338 N94-36200
ZHAO, XUDONG p 4303 N94-35573
ZHUKOV, V. A. p 4322 N94-35751
ZIMA, HANS p 4300 N94-35240
ZIMMERMAN, C. J. p 4201 N94-35626
ZIMMERMAN, DAVID C. p 4219 N94-35877
ZIMMERMANN, F. p 4331 N94-36224
ZOLENSKY, M. E. p 4351 N94-35432
p 4352 N94-35476
p 4352 N94-35477
p 4352 N94-36141
p 4353 N94-36145
p 4353 N94-36166
ZOLENSKY, MICHAEL p 4357 N94-35411
ZOLENSKY, MICHAEL E. p 4352 N94-35458
ZOLPER, J. C. p 4240 N94-36110
p 4272 N94-36178
ZOMBERG, BRIAN G. p 4259 N94-36049
ZOOK, H. A. p 4366 N94-35478
p 4352 N94-36142
ZOU, H. p 4242 N94-36288
ZUBER, M. T. p 4364 N94-35460
p 4367 N94-35479
p 4367 N94-35480
p 4371 N94-36155
p 4371 N94-36156
p 4373 N94-36168
ZUCKERWAR, ALLAN J. p 4269 N94-35369
ZUKOSKI, EDWARD E. p 4229 N94-36047

CORPORATE SOURCE INDEX

Typical Corporate Source Index Listing

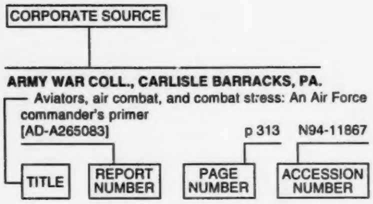

CORPORATE SOURCE
ARMY WAR COLL., CARLISLE BARRACKS, PA.
Aviators, air combat, and combat stress: An Air Force commander's primer
[AD-A265083] p 313 N94-11867
TITLE
REPORT NUMBER
PAGE NUMBER
ACCESSION NUMBER

Listings in this index are arranged alphabetically by corporate source. The title of the document provides the user with a brief description of the subject matter. The report number helps to indicate the type of document cited (e.g., NASA report, translation, NASA contractor report). The accession number denotes the number by which the citation is identified. The page number helps you locate the citation in the abstract section. The titles are arranged under each corporate source in ascending accession number order.

A

ABO AKADEMI, TURKU (FINLAND).

LIEKKI Combustion Research Program
[DE94-763298] p 4237 N94-36059

ACADEMY OF SCIENCES OF THE UKRAINE, KIEV.

Twin spacing versus size of a monocrystal for the nonstoichiometric 1:2:3 superconductors
[DE94-615511] p 4340 N94-36029

About mid-infrared optical spectrum of high-Tc superconducting compounds
[DE94-615646] p 4340 N94-36030

Twin spacing and the structural phase transitions in 1:2:3 high-Tc superconductors
[DE94-615647] p 4340 N94-36041

Zero modes of the two-dimensional Dirac operator on a noncompact Riemann surface in an external magnetic field
[DE94-616618] p 4343 N94-36071

Quantum mechanics and thermodynamics of particles with distance dependent statistics
[DE94-616620] p 4343 N94-36072

Exact multiplicities in the three-anion spectrum
[DE94-616768] p 4325 N94-36075

Q-deformations of the Veneziano model
[DE94-616769] p 4315 N94-36076

Processes of the reciprocal transformation vector charged particles pairs and electron-positron pairs
[DE94-616787] p 4325 N94-36077

Boson spectra and correlations in thermal locally equilibrium systems
[DE94-616799] p 4325 N94-36079

P-matrix approach and three-nucleon problem
[DE94-616887] p 4326 N94-36131

Alternating series fit to the total cross sections
[DE94-616888] p 4326 N94-36132

P-matrix description of charged particles interaction
[DE94-616853] p 4329 N94-36391

Pairing and low temperature properties of 2D Fermi-systems with attraction between particles
[DE94-615510] p 4329 N94-36434

ACADEMY OF SCIENCES (USSR), KIEV (USSR).

QCD parametrizations of the parton distribution of deep inelastic scattering
[DE94-616660] p 4325 N94-36074

On the theory of bounded many-particle systems with purely coulomb interactions
[DE94-617215] p 4325 N94-36081

Distance dependent fractional statistics in a P, T-invariant model
[DE94-617360] p 4325 N94-36083

The pressure of fluctuative electromagnetic field in inhomogeneous medium
[DE94-617189] p 4256 N94-36096

On possible types of vortexes in relativistic superfluid system
[DE94-617392] p 4267 N94-36098

The energy density of fluctuative electromagnetic field near the semi-bounded plasma
[DE94-617188] p 4256 N94-36099

On the effects of transforming the vibrational spectra of molecular systems under microwave radiation
[DE94-617057] p 4329 N94-36310

Modelling of the structure and physical properties of simple disordered systems
[DE94-617087] p 4329 N94-36311

Temperature dependence of superconduction bands in HTSC
[DE94-617361] p 4341 N94-36312

Taking into account dissipative processes in relativistic superfluid systems
[DE94-617391] p 4267 N94-36313

First, second and fourth sound in relativistic superfluidity theory with account for dissipative effects
[DE94-617393] p 4267 N94-36314

Notes on possible S-wave resonances in relativistic two-particle systems
[DE94-616889] p 4329 N94-36392

ACADEMY OF SCIENCES (USSR), LENINGRAD (USSR).

Limitation on the magnetic dipole moment of the reactor neutrino
[DE94-611171] p 4320 N94-35566

Elastic p(4)He scattering at intermediate energies
[DE94-618544] p 4328 N94-36287

ACADEMY OF SCIENCES (USSR), MOSCOW (USSR).

Development of atmospheric characteristics of chlorine-free alternative fluorocarbons
[DE94-009791] p 4287 N94-36179

Collective plasma corrections to the solar opacity
[PB94-170511] p 4375 N94-36210

ACADEMY OF SCIENCES (USSR), NOVOSIBIRSK (USSR).

Baryonic currents and their correlators in the heavy quark effective theory
[DE94-612496] p 4320 N94-35567

Self-similar regimes of subsonic Langmuir wave collapse
[DE94-611466] p 4335 N94-35750

Logarithmic corrections of the two-body QED problem
[DE94-611157] p 4322 N94-35783

Low energy theorems from the effective Lagrangian with vector mesons
[DE94-611173] p 4322 N94-35785

The kinetics of inhomogeneous plasma
[DE94-611459] p 4336 N94-35788

Data acquisition system of the GDL facility
[DE94-616604] p 4346 N94-35954

Computer simulation of beam-beam effects at large amplitudes and determination of life time
[DE94-616235] p 4330 N94-35999

Functional integration method for the one-dimensional localization, the higher correlators and mean current in mesoscopic ring in the arbitrary magnetic field
[DE94-616621] p 4325 N94-36073

Integral characteristics of the magnetic bremsstrahlung
[DE94-616788] p 4256 N94-36078

Hot-ion plasma in the quadrupole trap
[DE94-617216] p 4337 N94-36082

Initial perturbations and Langmuir waves in electron-positron plasma
[DE94-617190] p 4338 N94-36097

The 2+1-dimensional integrable generalization of the Sine-Gordon equation
[DE94-611074] p 4315 N94-36100

Electronics for the SND scintillation counter system
[DE94-616453] p 4259 N94-36104

Pseudogoldstone boson decay induced by light and search for the solar axion radiation
[DE94-616907] p 4326 N94-36133

SCATTER program of cross section calculation of the hadron and lepton interactions with nuclei
[DE94-617006] p 4326 N94-36134

T-odd, P-even photon-fermion interactions
[DE94-616869] p 4327 N94-36246

Feasibility study for a novel pulsed neutral beam diagnostics for tokamaks
[DE94-617129] p 4339 N94-36417

ADVISORY GROUP FOR AEROSPACE RESEARCH AND DEVELOPMENT, NEUILLY-SUR-SEINE (FRANCE).

AGARD highlights 93/2
[AGARD-HIGHLIGHTS-93/2] p 4376 N94-35444

Recent Advances in Long Range and Long Endurance Operation of Aircraft
[AGARD-CP-547] p 4193 N94-36321

AEROJET-GENERAL CORP., AZUSA, CA.

Earth Observing System (EOS) Advanced Microwave Sounding Unit-A (AMSU-A) schedule plan
[NASA-CR-194856] p 4281 N94-35734

AEROSPACE CORP., EL SEGUNDO, CA.

Analytic model of aurorally coupled magnetospheric and ionospheric electrostatic potentials
[NASA-CR-196130] p 4288 N94-35358

Electron and Proton Wide-Angle Spectrometer (EPAS) on the CRRES spacecraft
[AD-A278630] p 4227 N94-35362

Contributions of the low-latitude boundary layer to the finite width magnetotail convection model
[NASA-CR-196116] p 4289 N94-35392

ULF waves in the low-latitude boundary layer and their relationship to magnetospheric pulsations: A multisatellite observation
[AD-A278906] p 4289 N94-35587

Improved performance of degraded solar arrays at non-zero sun incidence angles
[AD-A278905] p 4282 N94-35804

Propellant stress relief groove for the Titan 4 SRMU
[AD-A278628] p 4228 N94-36254

An efficient, intelligent solution for viscous flows inside solid rocket motors
[AD-A278629] p 4228 N94-36255

An adaptive, unstructured, finite-element, multi-material, thermal analysis
[AD-A278632] p 4343 N94-36256

Simultaneous observations of the westward electrojet and the cross-tail current sheet during substorms
[AD-A278631] p 4292 N94-36383

AEROSPACE ENGINEERING TEST ESTABLISHMENT, COLD LAKE (ALBERTA).

Flight test certification of a 480 gallon composite fuel tank on CF-18 p 4196 N94-36340

CC-130H(T) tactical aerial refuelling tanker development flight test programme p 4198 N94-36347

AEROSPACE MEDICAL RESEARCH LABS., BROOKS AFB, TX.

Determinants of subjective fatigue for C-141 crews during Operation Desert Storm p 4196 N94-36338

AEROSPACE MEDICAL RESEARCH LABS., WRIGHT-PATTERSON AFB, OH.

Bibliography of research reports and publications issued by the Human Engineering Division
[AD-A278787] p 4299 N94-35712

AEROSPATIALE, TOULOUSE (FRANCE).

Future supersonic commercial transport aircraft: A technological challenge for long haul traffic
p 4193 N94-36324

Calculations used to optimize the installation of civil aircraft engines p 4195 N94-36332

AIR-CONDITIONING AND REFRIGERATION TECHNOLOGY INST., INC., ARLINGTON, VA.

Research update: Materials Compatibility and Lubricant Research (MCLR) program
[DE94-010001] p 4247 N94-36387

Sealed tube comparisons of the compatibility of desiccants with refrigerants and lubricants
[DE94-010002] p 4251 N94-36388

AIR FORCE INST. OF TECH., WRIGHT-PATTERSON AFB, OH.

Point and interval estimation of series system reliability using small data sets
[AD-A278647] p 4316 N94-35575

Modal decomposition of Hamiltonian variational equations p 4202 N94-35606

Clustering techniques in speaker recognition
[AD-A278676] p 4255 N94-35689

Transient body force effects on the dryout and rewet of a heated capillary structure
[AD-A278677] p 4264 N94-35690

A comparison of variable selection criteria for multiple linear regression: A THIRD simulation study
[AD-A278678] p 4316 N94-35691

The prediction of pilot opinion ratings using optimal and sub-optimal pilot models
[AD-A278679] p 4298 N94-35692

Direct reduced order mixed H2/H infinity control for the Short Take-Off and Landing/Maneuver Technology Demonstrator (STOL/MTD)
[AD-A278675] p 4199 N94-35796

An analysis of operational suitability for test and evaluation of highly reliable systems
[AD-A278573] p 4192 N94-36184

Application of sequential quadratic programming to large-scale structural design problems
[AD-A278574] p 4307 N94-36185

A genetic algorithm approach to automating satellite range scheduling
[AD-A278577] p 4226 N94-36188

Rapid and accurate timing simulation of radiation-hardened digital microelectronics using VHDL
[AD-A278644] p 4261 N94-36361

Simulation of materials processing: Fantasy or reality?
p 4230 N94-36404

AIR FORCE OFFICE OF SCIENTIFIC RESEARCH, BOLLING AFB, WASHINGTON, DC.

AFOSR Contractors Propulsion Meeting
[AD-A279028] p 4198 N94-35746

ALABAMA UNIV., HUNTSVILLE, AL.

Results from LDEF experiment A0114: The interaction of atomic oxygen with materials surfaces at orbital altitudes
[NASA-CR-196016] p 4235 N94-35388

Study on contaminants on flight and other critical surfaces
[NASA-CR-193975] p 4235 N94-35447

Energy partitioning in high speed impact of analog solid rocket motors
[AD-A278771] p 4228 N94-35825

On the physics of waves in the solar atmosphere: Wave heating and wind acceleration
[NASA-CR-194119] p 4375 N94-36395

Theoretical and experimental studies relevant to interpretation of auroral emissions
[NASA-CR-196032] p 4376 N94-36421

ALASKA UNIV., FAIRBANKS, AK.

Modeling of the magnetosphere-ionosphere-atmosphere system
[NASA-CR-195157] p 4288 N94-35244

ALENIA AERONAUTICA, TURIN (ITALY).

Technological challenges of High Altitude Long Endurance unmanned configurations
p 4193 N94-36323

ALLIED-SIGNAL AEROSPACE CO., KANSAS CITY, MO.

Ionic contamination detection
[DE94-010212] p 4258 N94-35686

Residual Gas Analysis (RGA) and shear strength characteristics of a silver-filled epoxy and polyimide under long-term, high-temperature storage conditions
[DE94-010106] p 4244 N94-35705

Thick film fabrication of aluminum nitride microcircuits
[DE94-010107] p 4259 N94-35706

CABPRO: An expert system for process planning multiwire cables
[DE94-010213] p 4312 N94-35810

High-speed digital project, HSD test capability
[DE94-010885] p 4260 N94-36197

ALUMINUM CO. OF AMERICA, ALCOA CENTER, PA.

New developments in aluminum for aircraft and automobiles p 4232 N94-36413

AMERICAN GEOLOGICAL INST., ALEXANDRIA, VA.

National Geoscience Data Repository System
[DE94-000120] p 4344 N94-35347

AMERICAN UNIV., WASHINGTON, DC.

Space and the American imagination
[NASA-CR-196131] p 4376 N94-35356

AMES LAB., IA.

Syntheses and studies of acetylenic polymers
[DE94-011201] p 4245 N94-36057

ANALYTIC SCIENCES CORP., FAIRBORN, OH.

The integrated model development environment
[AD-A278613] p 4308 N94-36250

ANALYTIC SCIENCES CORP., RESTON, VA.

A geometric model of a V-slit Sun sensor correcting for spacecraft wobble p 4206 N94-35628

ANALYTICAL ENGINEERING CORP., BOULDER, CO.

Measuring attitude with a gradiometer
p 4206 N94-35630

AQUATECH SYSTEMS, WARREN, NJ.

Combined SO(x)/NO(x) control via SOXAL (tm) process: An electrodialytic regenerative wet scrubbing process
[DE94-009053] p 4284 N94-35346

ARCON CORP., WALTHAM, MA.

Green's functions for an anisotropic medium: Part 1: Unbounded case
[AD-A278767] p 4256 N94-35694

Green's functions for an anisotropic medium. Part 2: Two-layer case
[AD-A278788] p 4256 N94-35713

ARGONNE NATIONAL LAB., IL.

Molecular systems for ultrafast optical switching: Controlling electron transfer reactions with femtosecond laser pulses
[DE94-009695] p 4332 N94-35671

A collection of tools in support of automatic differentiation
[DE94-010104] p 4314 N94-35704

Bus application of oxygen-enrichment technology and diesel-electric hybrid systems
[DE94-009835] p 4285 N94-35765

Structural investigations of 1-ethyl-3-methylimidazolium hydrogen dichloride: Neutron diffraction studies of an ambient-temperature molten salt
[DE94-009680] p 4237 N94-35777

Defect detection in multi-layered, plasma sprayed zirconia by time resolved infrared radiometry: A comparison between analytical and experimental methods
[DE94-009803] p 4245 N94-35779

Flywheel energy storage using superconducting magnetic bearings
[DE94-009817] p 4282 N94-35829

Modeling the atmospheric input of nutrients, heavy metals, and pesticides to the Great Lakes
[DE94-005481] p 4286 N94-36007

Estimation of fractal dimensions from transect data
[DE94-009808] p 4281 N94-36018

Irradiation-related amorphization and crystallization: In situ transmission electron microscope studies
[DE94-009823] p 4241 N94-36222

Time-of-flight diffraction at pulsed neutron sources: An introduction to the symposium
[DE94-010442] p 4327 N94-36225

Determination of grain boundary volume expansion by HREM
[DE94-010452] p 4241 N94-36231

Effect of niobium interlayer on high-temperature sliding friction and wear of silver films on alumina
[DE94-010462] p 4275 N94-36232

High energy asymptotics of perturbative multi-color QCD
[DE94-001350] p 4327 N94-36238

A new family of superconducting fullerides, Na(NH3)(x)C60(x = 2-8)
[DE94-011480] p 4341 N94-36272

Wear-resisting oxide films for 900 C
[DE94-010093] p 4246 N94-36306

An improved assessment approach for noise impacts from stationary point and traffic sources on humans and wildlife
[DE94-009728] p 4319 N94-36320

Neutron diffraction study of aluminum chloride imidazolium chloride molten salts
[DE94-009679] p 4239 N94-36349

On the origin of porphyritic chondrules
[DE94-010464] p 4351 N94-36418

Periodized wavelets
[DE94-010365] p 4316 N94-36432

Dynamic stability of maglev systems
[DE94-010451] p 4276 N94-36433

ARIZONA UNIV., TUCSON, AZ.

High-resolution subsurface imaging and neural network recognition
[DE94-009546] p 4290 N94-35666

ARLING (R. W.), WINDHAM, NH.

Six degree of freedom fine motion positioning stage based on magnetic levitation p 4225 N94-35916

ARMY AEROMEDICAL RESEARCH LAB., FORT RUCKER, AL.

Accommodation during instrument viewing can be influenced by knowledge of object distance
[AD-A278987] p 4298 N94-35528

Is increased accommodation a necessary condition for instrument myopia?
[AD-A278962] p 4298 N94-35659

ARMY COLD REGIONS RESEARCH AND ENGINEERING LAB., HANOVER, NH.

Vapor-fortified QA/QC samples for the analysis of volatile organic compounds
[AD-A278712] p 4229 N94-35776

ARMY RESEARCH LAB., WATERTOWN, MA.

Diffusion and sorption of 1,4-dioxane into polychloroprene
[ARL-TR-338] p 4229 N94-35361

ARNOLD ENGINEERING DEVELOPMENT CENTER, ARNOLD AFS, TN.

NEQPAK, the AEDC thermochemical nonequilibrium package: Theory and use
[AD-A279005] p 4266 N94-35951

ATMOSPHERIC AND ENVIRONMENTAL RESEARCH, INC., CAMBRIDGE, MA.

Use of wind profiler data in short-range forcasting
[AD-A279482] p 4295 N94-36228

ATOMIC ENERGY OF CANADA LTD., CHALK RIVER (ONTARIO).

Formation and stability of Fe-rich precipitates in dilute Zr(Fe) single-crystal alloys
[DE94-619027] p 4242 N94-36288

Study of point defect mobilities in zirconium during electron irradiation in a HVEM
[DE94-619028] p 4242 N94-36289

ATOMIC ENERGY OF CANADA LTD., PINAWA (MANITOBA).

Thermodynamic behaviour of tellurium at high temperatures
[DE94-612823] p 4240 N94-35960

AUBURN UNIV., AL.

Influence of backup bearings and support structure dynamics on the behavior of rotors with active supports
[NASA-CR-196119] p 4274 N94-35500

B

BHABHA ATOMIC RESEARCH CENTRE, BOMBAY (INDIA).

Guidelines for design and development of computer/microprocessor based systems in research and power reactors
[DE94-616271] p 4300 N94-35570

An indigenously developed photoacoustic spectrometer for study of actinide spectroscopy
[DE94-616508] p 4235 N94-35592

Digital control programmer for temperature control
[DE94-615584] p 4309 N94-36382

Activities of the Laser and Plasma Technology Division
[DE94-617113] p 4273 N94-36393

BOSTON COLL., NEWTON, MA.

Catalog of Helios 90 deg photometer events
[PL-TR-94-2040] p 4375 N94-36264

BOSTON UNIV., MA.

Application of differential inversion to DMSP microwave sounder data
[AD-A278575] p 4294 N94-36186

BROOKHAVEN NATIONAL LAB., UPTON, NY.

Determination of the Fermi level position for neutron irradiated high resistivity silicon detectors and materials using the Transient Charge Technique (TChT)
[DE94-009107] p 4260 N94-36221

Hybrid mesons (Q(anti Q)g) in N(anti N) annihilation
[DE94-001491] p 4327 N94-36239

Summary: Hadron dynamics sessions
[DE94-003011] p 4328 N94-36303

In situ studies of zeolite syntheses using powder diffraction methods: Crystallization of instant zeolite A powder and CoAPO-5
[DE94-006570] p 4341 N94-36358

BUCKNELL UNIV., LEWISBURG, PA.

Mechanical properties of crosslinked polymer coatings
p 4231 N94-36410

C

CAE-LINK CORP., HOUSTON, TX.

Software architecture standard for simulation virtual machine, version 2.0
[NASA-CR-188291] p 4301 N94-35443

CALIFORNIA INST. OF TECH., PASADENA, CA.

Radiative signals from impact of Shoemaker-Levy on Jupiter p 4355 N94-35396

Trace-shortened Reed-Solomon codes
p 4254 N94-35554

Ultrafast chemical dynamics of reactions in beams
[AD-A278939] p 4323 N94-35805

CALIFORNIA POLYTECHNIC STATE UNIV., SAN LUIS OBISPO, CA.
Numerical investigation of multi-element airfoils
[NASA-CR-194592] p 4191 N94-36394

CALIFORNIA UNIV., BERKELEY, CA.
First measurement of helium on Mars: Implications for the problem of radiogenic gases on the terrestrial planets p 4370 N94-36153

CALIFORNIA UNIV., BERKELEY. LAWRENCE BERKELEY LAB, CA.
Data available from birth and death registries and cancer registries in the US
[LBL-30971] p 4344 N94-35337
Thermal performance of residential duct systems in basements
[LBL-33962] p 4250 N94-35364
A classical model for closed-loop diagrams of binary liquid mixtures
[DE94-011011] p 4237 N94-36033
A new association-model for binary VLE of alcohol/hydrocarbon and amine/hydrocarbon mixtures
[DE94-011012] p 4248 N94-36034
Two-photon photoemission and the dynamics of electrons at interfaces
[DE94-011373] p 4324 N94-36058
ILSE combiner study
[DE94-011009] p 4331 N94-36202
Stellar alchemy: The origin of the chemical elements
[DE94-011903] p 4350 N94-36229
Equations of state valid continuously from zero to extreme pressures with H2O and CO2 as examples
[DE94-011907] p 4238 N94-36230
Recent progress in irrational conformal field theory
[DE94-011908] p 4317 N94-36234
Recursive recovery of Markov transition probabilities from boundary value data
[DE94-011914] p 4317 N94-36235
A low temperature scanning force microscope for biological samples
[DE94-011357] p 4297 N94-36269
Quantum groups, non-commutative differential geometry and applications
[DE94-011358] p 4315 N94-36270
Critical issues in muon colliders: A summary
[DE94-011382] p 4331 N94-36271
Magnetic metallic multilayers
[DE94-011913] p 4341 N94-36274

CALIFORNIA UNIV., DAVIS, CA.
Solvent acidity and basicity in polar media and their role in solvation
[AD-A278604] p 4239 N94-36426

CALIFORNIA UNIV., LOS ANGELES, CA.
Distributed parameter modeling of repeated truss structures p 4218 N94-35868
Selected topics on the active control of helicopter aeromechanical and vibration problems
p 4200 N94-35874
Robustness properties of LQG optimized compensators for collocated rate sensors p 4221 N94-35890
LQG optimal compensator transfer function for the NASA LaRC CSI Evolutionary Model
p 4221 N94-35891
Vibration reduction in helicopter rotors using an actively controlled partial span trailing edge flap located on the blade
[NASA-CR-4611] p 4280 N94-36423

CALIFORNIA UNIV., RICHMOND, CA.
Earthquake Engineering Research Center: 25th anniversry edition
[PB94-160645] p 4291 N94-36019

CALIFORNIA UNIV., SAN DIEGO, CA.
Monolith catalysts for closed-cycle carbon dioxide lasers
[NASA-CR-196093] p 4271 N94-35489

CALIFORNIA UNIV., SAN DIEGO, LA JOLLA, CA.
On the various forms of the energy equation for a dilute, monatomic mixture of nonreacting gases
[NASA-CR-4612] p 4190 N94-35864

CALIFORNIA UNIV., SANTA BARBARA, CA.
A model of the CO2 exchanges between biosphere and atmosphere in the tundra
[NASA-CR-196008] p 4289 N94-35389
Be3(AsO4)2.2H2O, a new beryllloarsenate phase containing bridged tetrahedral 3-rings
[AD-A278826] p 4340 N94-35677

CALSPAN-BUFFALO UNIV. RESEARCH CENTER, NY.
Task allocation for parallel real-time execution
[AD-A278789] p 4310 N94-35653

CARNEGIE-MELLON UNIV., PITTSBURGH, PA.
Exploring hypermedia information services for disseminating software engineering information
[AD-A278765] p 4302 N94-35495
Asynchronous optimistic rollback recovery using secure distributed time
[AD-A278978] p 4344 N94-35526
Combining left and right unlinking for matching a large number of learned rules
[AD-A278979] p 4311 N94-35527
Large granularity cache coherence for intermittent connectivity
[AD-A278897] p 4345 N94-35571
Symbolic debugging of globally optimized code: Data value problems and their solutions
[AD-A278898] p 4302 N94-35572
Combining symbolic computation and theorem proving: Some problems of Ramanujan
[AD-A278899] p 4303 N94-35573
Prodigy planning algorithm
[AD-A278900] p 4303 N94-35574
A compile time model for composing parallel programs
[AD-A278896] p 4310 N94-35597
The role of emotion in believable agents
[AD-A278952] p 4312 N94-35658
Refinement types ML
[AD-A278937] p 4304 N94-35709
The breakdown of operators when interacting with the external world
[AD-A278936] p 4299 N94-35716
ML partial evaluation using set-based analysis
[AD-A278955] p 4304 N94-35718
A taxonomy of coordination mechanisms used in real-time software based on domain analysis
[AD-A279014] p 4304 N94-35794
Communication and memory requirements as the basis for mapping task and data parallel programs
[AD-A278954] p 4310 N94-35806
Case based reasoning in engineering design
[AD-A278943] p 4305 N94-36006
The CMU task parallel program suite
[AD-A278951] p 4311 N94-36015
A practical guide to the technology and adoption of software process automation
[AD-A278719] p 4308 N94-36294

CENTRE D'ETUDES ET DE RECHERCHES BIO-PHYSIOLOGIQUES APPLIQUEES A LA MARINE, TOULON (FRANCE).
Effects of 5 MPa heliox pressure on dopaminer gic pathway: An in vivo neurochemical study
[PB94-170693] p 4297 N94-36220
Superconducting transistors
[PB94-170743] p 4260 N94-36260

CENTRE D'ETUDES ET DE RECHERCHES DE MEDECINE AEROSPATIALE, BRETIGNY SUR ORGE (FRANCE).
Some solutions to reduce the human effects of extended operation times p 4196 N94-36339

CENTRE NATIONAL D'ETUDES SPATIALES, TOULOUSE (FRANCE).
An automatic planetary vehicle for exploring Mars
p 4354 N94-35336

CESKOSLOVENSKA AKADEMIE VED, PRAGUE.
Activity report 1990-1992 and proceedings, volume 1
[DE94-610480] p 4290 N94-35830
Activity Report, 1990 - 1992 and proceedings, volume 2
[DE94-610481] p 4291 N94-36087

CHICAGO UNIV., CHICAGO, IL.
Task networks for controlling continuous processes
[AD-A278683] p 4312 N94-35710
The capacity of color histogram indexing
[AD-A279031] p 4345 N94-35732
The DataCube server. Animate agent project working note 2, version 1.0
[AD-A278847] p 4310 N94-35742
Task and environment-sensitive tracking
[AD-A278846] p 4312 N94-35802
Interfacing the RAP system to real-time control, version 1
[AD-A278725] p 4312 N94-36295

CINCINNATI UNIV., OH.
Self-rescue strategies for EVA crewmembers equipped with the SAFER backpack p 4207 N94-35633

CLEMSON UNIV., SC.
University participation in the ATS program
[DE94-003191] p 4275 N94-36022
Intramolecular energy transfer reactions in polymetallic complexes
[DE94-010114] p 4326 N94-36126

COAST GUARD, WASHINGTON, DC.
Evaluation of synthetic aperture radar for oil-spill response
[AD-A278796] p 4284 N94-35674

COLLEGE OF WESTERN NEW ENGLAND, SPRINGFIELD, MA.
Experiments in diamond film fabrication in table-top plasma apparatus p 4231 N94-36411

COLORADO STATE UNIV., FORT COLLINS, CO.
Methane production and consumption in grassland and boreal ecosystems
[NASA-CR-196085] p 4284 N94-35486

COLORADO UNIV., BOULDER, CO.
Measuring attitude with a gradiometer
p 4206 N94-35630

COLUMBIA UNIV., NEW YORK, NY.
GRO: Studies of high energy pulsars with EGRET
[NASA-CR-196003] p 4349 N94-35516
Theoretical studies of ultrashort phenomena
[AD-A278938] p 4332 N94-35664
Collisonless dynamics of the magnetosphere
[AD-A278886] p 4290 N94-35708
Can we break intractability using randomization or the average case setting?
[AD-A278598] p 4316 N94-36425

COLUMBIA UNIV., PALISADES, NY.
Asymetric change of daily temperature range: Proceedings
[DE94-010102] p 4293 N94-35703

COMISSAO NACIONAL DE ATIVIDADES ESPACIAIS, SAO JOSE DOS CAMPOS (BRAZIL).
A new algorithm for attitude-independent magnetometer calibration p 4209 N94-35644

COMMITTEE ON GOVERNMENT OPERATIONS (U.S. HOUSE).
Statement by Bill D. Colvin, Inspector General
[NASA-TM-109793] p 4348 N94-35446

COMMONWEALTH SCIENTIFIC AND INDUSTRIAL RESEARCH ORGANIZATION, MORDIALOC (AUSTRALIA).
A precise passive narrow-beam filter infrared radiometer and its use with LIDAR in the ARM program
[DE94-004167] p 4269 N94-36085

COMPUTER SCIENCES CORP., GREENBELT, MD.
Collected software engineering papers, volume 11
[NASA-CR-189347] p 4301 N94-35434

COMPUTER SCIENCES CORP., LANHAM, MD.
Spacecraft attitude determination accuracy from mission experience p 4204 N94-35618
Comparison of Kalman filter and optimal smoother estimates of spacecraft attitude p 4208 N94-35638
Application of star identification using pattern matching to space ground systems at GSFC
p 4209 N94-35640
Motion models in attitude estimation
p 4210 N94-35646

COMPUTER SCIENCES CORP., LAUREL, MD.
A long-baseline method for HST gyro drift rate bias calibration p 4203 N94-35614

COMPUTER SOFTWARE MANAGEMENT AND INFORMATION CENTER, ATHENS, GA.
COSMIC monthly progress report
[NASA-CR-195962] p 4302 N94-35514

CONNECTICUT UNIV., STORRS, CT.
Estimation with multisensor/multiscan detection fusion
[AD-A278753] p 4256 N94-36092

CONSIGLIO NAZIONALE DELLE RICERCHE, ROME (ITALY).
Rational positive real approximations for LQG optimal compensators arising in active stabilization of flexible structures p 4222 N94-35892

CORNELL UNIV., ITHACA, NY.
The weakest failure detector for solving Consensus
[NASA-CR-190545] p 4300 N94-35365
Concurrent stabilization and imaging of a novel polymer for second harmonic generation via in situ photopolymerization
[AD-A278912] p 4243 N94-35588
Vacuum ultraviolet studies of molecular dynamics
[AD-A278940] p 4321 N94-35657
A determinizable class of timed automata
[AD-A278858] p 4317 N94-35743
The most abstract common refinement
[AD-A278870] p 4305 N94-36014

CSP ASSOCIATES, INC., CAMBRIDGE, MA.
Partners in space. International cooperation in space: Strategies for the new century
[ISBN-0-9629930-2-6] p 4348 N94-35901

D

DASSAULT AVIATION, SAINT-CLOUD (FRANCE).
Laminar flow studies at Dassault Aviation: Calculations and flight tests p 4194 N94-36328
In-flight refueling: Dassault Aviation research on the Rafale aircraft p 4196 N94-36341

DAVID SARNOFF RESEARCH CENTER, PRINCETON, NJ.
Multidisciplinary studies of integrated neural network systems
[AD-A278774] p 4312 N94-36309

DAYTON UNIV. RESEARCH INST., OH.
Collection, processing, and reporting of damage tolerant design data for non-aerospace structural materials
[NASA-CR-196046] p 4347 N94-36435

DEFENCE RESEARCH AGENCY, MALVERN (ENGLAND).
Executable transformational rules from Core ELLA to the Kernel
[DRA-MEMO-4629] p 4307 N94-36113

DEFENCE RESEARCH ESTABLISHMENT SUFFIELD, RALSTON (ALBERTA).
Capillary column GC-MS/MS confirmation of phosphate esters with a hybrid tandem mass spectrometer
[AD-A278748] p 4238 N94-36091

DEFENSE ADVANCED RESEARCH PROJECTS AGENCY, ARLINGTON, VA.
Technology Reinvestment Project's Focus Area: Low Cost Electronic Packaging
[PB94-161155] p 4259 N94-35748

DEFENSE TECHNICAL INFORMATION CENTER, ALEXANDRIA, VA.
Defense RDT and E online system (DROLS) retrieval reference guide
[AD-A278972] p 4344 N94-35525

DELAWARE UNIV., NEWARK, DE.
Design of a high activity and selectivity alcohol catalyst
[DE94-003633] p 4237 N94-36023

DEPARTMENT OF ENERGY, WASHINGTON, DC.
Model documentation: Renewable Fuels Module of the National Energy Modeling System
[DE94-009962] p 4282 N94-35672

DEPARTMENT OF THE NAVY, WASHINGTON, DC.
Method for making a symmetrical layered thin film edge field-emitter-array
[AD-D016214] p 4246 N94-36121
Fabrication and phase tuning of an optical waveguide device
[AD-D016215] p 4334 N94-36122
Nanochannel glass matrix used in making mesoscopic structures
[AD-D016216] p 4234 N94-36123
Nonlinear optical composites of metal cluster laden polymers
[AD-D016217] p 4234 N94-36124
Method of thermochemically treating silicon carbide fibers derived from polymers
[AD-D016218] p 4246 N94-36125
Coatings for SiO2 optical fibers
[AD-D016197] p 4334 N94-36363
Color-coded radar plan position indicator
[AD-D016200] p 4257 N94-36364
Color center laser with transverse auxiliary illumination
[AD-D016201] p 4273 N94-36365
Method and apparatus for imaging an object in or through a scattering medium by using multiple-wave mixing
[AD-D016212] p 4334 N94-36368
System for end-pumping a solid state laser using a large aperture laser diode bar
[AD-D016213] p 4273 N94-36370
Electrochemical process and product therefrom
[AD-D016211] p 4239 N94-36372

DETROIT DIESEL ALLISON, MI.
Research and development of Proton-Exchange Membrane (PEM) fuel cell system for transportation applications: Initial conceptual design report
[DE94-010576] p 4283 N94-36243

DEUTSCHE AEROSPACE A.G., MUNICH (GERMANY).
Optimisation of composite aircraft structures by direct manufacturing approaches p 4194 N94-36327

DEUTSCHE FORSCHUNGS- UND VERSUCHSANSTALT FUER LUFT- UND RAUMFAHRT, COLOGNE (GERMANY).
Extended range operations: A review of recent developments p 4195 N94-36337

DIRECTION DES RECHERCHES ET MOYENS D'ESSAIS, PARIS (FRANCE).
Spatio-temporal properties of centrifugal instabilities: Abstracts of 8th Couette-Taylor Meeting
[PB94-150240] p 4266 N94-35981

DIRECTION DES RECHERCHES, ETUDES ET TECHNIQUES, PARIS (FRANCE).
Stress and brain protein synthesis
[PB94-170750] p 4296 N94-35601
Third European Technical Symposium on Polyimides and High Performance Polymers: STEPI 3
[PB94-148491] p 4246 N94-36177
Non-linear interaction of gravity waves with average jet flows, instabilities, and turbulence
[PB94-170586] p 4291 N94-36214
Attention and signal detection. A study of attention divided between visual and auditory signals
[PB94-170594] p 4298 N94-36215
Acoustical-optical fracture analysis
[PB94-170602] p 4279 N94-36216

DRAPER (CHARLES STARK) LAB., INC., CAMBRIDGE, MA.
Control of maglev vehicles with aerodynamic and guideway disturbances p 4213 N94-35842
Fault tolerant computer control for a Maglev transportation system p 4215 N94-35848
Autonomous hazard detection and avoidance
[NASA-CR-188331] p 4309 N94-36439

DUKE UNIV., DURHAM, NC.
Dynamic analysis of a magnetic bearing system with flux control p 4216 N94-35859

DYNACS ENGINEERING CO., INC., PALM HARBOR, FL.
Computationally efficient multibody simulations
p 4222 N94-35896

E

EBARA RESEARCH CO. LTD., KANAGAWA (JAPAN).
Electromagnetically levitated vibration isolation system for the manufacturing process of silicon monocrystals
p 4223 N94-35906

ECK RESEARCH CO., COLUMBIA, MO.
Long range forecasts of the Northern Hemisphere anomalies with antecedent sea surface temperature patterns
[NASA-CR-189358] p 4292 N94-35380

ECOLE POLYTECHNIQUE, PARIS (FRANCE).
Partners in space. International cooperation in space: Strategies for the new century
[ISBN-0-9629930-2-6] p 4348 N94-35901

EDGERTON, GERMESHAUSEN AND GRIER, INC., IDAHO FALLS, ID.
Environmental resource document for the Idaho National Engineering Laboratory, volume 1
[DE94-008522] p 4287 N94-36207
Environmental resource document for the Idaho National Engineering Laboratory, volume 2
[DE94-008523] p 4287 N94-36208
Design and construction of a imaging instrument for studying ion emission from pure ion emitters
[DE94-010702] p 4328 N94-36302

EIDETICS INTERNATIONAL, INC., TORRANCE, CA.
F/A-18 forebody vortex control. Volume 1: Static tests
[NASA-CR-4582] p 4190 N94-35991

EIDGENOESSISCHE TECHNISCHE HOCHSCHULE, ZURICH (SWITZERLAND).
High performance data acquisition, identification, and monitoring for active magnetic bearings
p 4213 N94-35839

ELORET CORP., PALO ALTO, CA.
Development and application of computational aerothermodynamics flowfield computer codes
[NASA-CR-196136] p 4189 N94-35498

EMCORE CORP., SOMERSET, NJ.
Development of novel II-VI solar cells
[PB94-159415] p 4282 N94-35739

EMR-PHOTOELECTRIC, PRINCETON, NJ.
X-ray remote sensing and in-situ spectroscopy for planetary exploration missions and gamma-ray remote sensing and in-situ spectroscopy for planetary exploration missions
[NASA-CR-189352] p 4375 N94-35381

ENERGIA, INC., PRINCETON, NJ.
Infrared multiphoton ignition and combustion enhancement of natural gas.
[PB94-165438] p 4236 N94-35755

ENSR CONSULTING AND ENGINEERING, CAMARILLO, CA.
Regional source-receptor relationships for atmospheric acidity and acid deposition in California
[PB94-156676] p 4287 N94-36183

ENVIRONMENTAL PROTECTION AGENCY, ANN ARBOR, MI.
Final regulatory impact analysis: Refueling emission regulations for light duty vehicles and trucks and heavy duty vehicles
[PB94-164027] p 4285 N94-35754

ENVIRONMENTAL RESEARCH LAB., GULF BREEZE, FL.
Proceedings: Integrated Research Planning Meeting for Gulf of Mexico Estuaries
[PB94-157799] p 4296 N94-35738

EUROCOPTER FRANCE, MARIGNANE (FRANCE).
The convertible (helicopter/airplane) EUROFAR: General considerations on the technical progress and on future advances p 4195 N94-36331

F

FARE, INC., COLLEGE PARK, MD.
Manufacturing and testing of a magnetically suspended composite flywheel energy storage system
p 4224 N94-35910

FEDERAL AVIATION ADMINISTRATION, OKLAHOMA CITY, OK.
A review of computer evacuation models and their data needs
[DOT/FAA/AM-94/11] p 4191 N94-35236

FEDERAL AVIATION ADMINISTRATION, WASHINGTON, DC.
The Federal Aviation Administration plan for research, engineering and development p 4376 N94-35262

FERMI NATIONAL ACCELERATOR LAB., BATAVIA, IL.
CDF electroweak studies and the search for the top quark
[DE94-010333] p 4326 N94-36107
Primordial nucleosynthesis in conformal Weyl gravity
[DE94-003002] p 4327 N94-36241
Top dilepton search at CDF
[DE94-002302] p 4327 N94-36266
Impedance and instability threshold estimates in the main injector 1
[DE94-010332] p 4332 N94-36431

FLORIDA UNIV., GAINESVILLE, FL.
Attitude stability of a spinning spacecraft during appendage deployment/retraction p 4208 N94-35639
Advances in parameter estimation techniques applied to flexible structures p 4219 N94-35877
Development of ultra-low noise, high performance 3 to 5 Quantum Well Infrared Photodetectors (QWIPs) for focal plane array staring image sensor systems
[AD-A278861] p 4342 N94-36385

FRONTIER TECHNOLOGY, INC., BEAVERCREEK, OH.
Future tanker considerations and requirements
p 4197 N94-36342
Hose-drogue versus boom receptacle air refueling
p 4197 N94-36345

FTN AND ASSOCIATE LTD. LITTLE ROCK, AR.
Environmental Monitoring and Assessment Program assessment framework
[PB94-158862] p 4285 N94-35741

G

GALAXY SCIENTIFIC CORP., PLEASANTVILLE, NJ.
Unleaded AVGAS program
[AD-A278650] p 4247 N94-35795

GENERAL ATOMIC CO., SAN DIEGO, CA.
Inertial confinement fusion target component fabrication and technology development report
[DE94-009973] p 4335 N94-35673

GENERAL COHERENT TECHNOLOGY, INC., RICHARDSON, TX.
Progress in the production of samples of gamma ray laser candidate materials
[AD-A278961] p 4272 N94-35721

GENERAL ELECTRIC CO., ERIE, PA.
Durability testing of medium speed diesel engine components designed for operating on coal/water slurry fuel
[DE94-009550] p 4275 N94-35667
Design and operation of a medium speed 12-cylinder coal-fueled diesel engine. Phase 2: Improvements
[DE94-009547] p 4275 N94-35815

GENERAL ELECTRIC CO., LYNN, MA.
Integration of magnetic bearings in the design of advanced gas turbine engines p 4223 N94-35903

GENERAL ELECTRIC CO., SCHENECTADY, NY.
Nonlinear control of magnetic bearings
p 4213 N94-35838
Modelling and control of a rotor supported by magnetic bearings p 4216 N94-35858
Heavy duty gas turbine combustion tests with simulated low BTU coal gas
[DE94-002970] p 4276 N94-36355

GEORGE MASON UNIV., FAIRFAX, VA.
Dynamical observer for a flexible beam via finite element approximations p 4222 N94-35893

GEORGIA INST. OF TECH., ATLANTA, GA.
Theory and computation of optimal low- and medium-thrust transfers
[NASA-CR-196077] p 4202 N94-35487
A survey of reflectometry techniques with applications to TFTR
[DE94-010202] p 4338 N94-36093

GEORGIA UNIV., ATHENS.
Estimation of fractal dimensions from transect data
[DE94-009808] p 4281 N94-36018

GILBERT/COMMONWEALTH, READING, PA.
Fuel Cell Handbook update
[DE94-002958] p 4282 N94-36021

GOSUDARSTVENNYI KOMITET PO ISPOLZOVANIYU ATOMNOI ENERGII, SERPUKHOV (USSR).
Proceedings of 2nd Working meeting: Physics at VLEPP, volume 1
[DE94-616200] p 4320 N94-35569
Leptonic decay constants of heavy quarkonia in effective QCD sum rules
[DE94-611160] p 4322 N94-35784
Isoscalar vector bosons at LEP 2
[DE94-611253] p 4323 N94-35787

Numerical method to study the stability of periodic solutions of particle motion in nonlinear magnetic fields
[DE94-610740] p 4325 N94-36088
Proceedings of 2nd Working Meeting on Physics at VLEPP, volume 2
[DE94-616167] p 4326 N94-36182

GRUMMAN AEROSPACE CORP., BETHPAGE, NY.
System concept definition of the Grumman superconducting Electromagnetic Suspension (EMS) Maglev design p 4213 N94-35840
Superconducting Electromagnetic Suspension (EMS) system for Grumman Maglev concept
p 4215 N94-35849
Nondestructive Inspection (NDI) of reduced strength bonds
[AD-A278745] p 4278 N94-36090

H

HARRIS CORP., MELBOURNE, FL.
Distributed parameter modelling of flexible spacecraft: Where's the beef? p 4217 N94-35866

HARVARD COLL. OBSERVATORY, CAMBRIDGE, MA.
Absolute, Extreme Ultraviolet Solar Spectral Irradiance Monitor (AESSIM)
[AD-A278709] p 4227 N94-36189

HELSINKI UNIV. OF TECHNOLOGY, ESPOO (FINLAND).
Genetic algorithms
[PB94-171048] p 4303 N94-35602
A note on high order schemes for one dimensional wave equation
[PB94-171006] p 4315 N94-35821
BJT model in APLAC
[PB94-171022] p 4259 N94-35822
Priorities and nonmonotonic reasoning
[PB94-171170] p 4346 N94-35959
An energy method approach to the problem of elastic strip
[PB94-171014] p 4279 N94-36000
Activities of the optoelectronics laboratory
[PB94-171196] p 4334 N94-36190

HOUSTON UNIV., CLEAR LAKE, TX.
Computer image analysis of etched tracks from ionizing radiation
[NASA-CR-196025] p 4319 N94-35264

HOUSTON UNIV., TX.
High temperature superconductors for magnetic suspension applications p 4214 N94-35843
Numerical methods for multibody systems
p 4222 N94-35897

HOWARD UNIV., WASHINGTON, DC.
A combined algorithm for minimum time slewing of flexible spacecraft p 4220 N94-35881
Effects of noise variance model on optimal feedback design and actuator placement p 4220 N94-35883

HUGHES AIRCRAFT CO., LOS ANGELES, CA.
A simple suboptimal least-squares algorithm for attitude determination with multiple sensors
p 4210 N94-35645

HUGHES STX, INC., LEXINGTON, MA.
Doppler weather radar studies of precipitation systems
[AD-A279417] p 4295 N94-36262

HUMBOLDT STATE UNIV., ARCATA, CA.
Representing spatial information in a computational model for network management
[NASA-CR-191669] p 4306 N94-36040

HYDROGEN CONSULTANTS, INC., LITTLETON, CO.
Advanced hydrogen/method utilization technology demonstration
[DE94-000214] p 4248 N94-36191

I

ILLINOIS UNIV., URBANA, IL.
Cement paste matrix composite materials center
[AD-A279017] p 4233 N94-35952

IMAGINATION RESOURCES, INC., DUBLIN, OH.
Measurement of viscosity, density, and gas solubility of refrigerant blends in selected synthetic lubricants
[DE94-010426] p 4244 N94-35687

IMPERIAL COLL. OF SCIENCE AND TECHNOLOGY, LONDON (ENGLAND).
ROSAT/XRT-PSPC observations and the ionizing continuum of Seyfert 1 galaxy Mkn 478
[PB94-167053] p 4350 N94-35530

INDUSTRIEANLAGEN-BETRIEBSGESELLSCHAFT M.B.H., OTTOBRUNN (GERMANY).
The STRATO 2C propulsion system: A low cost approach for a High Altitude Long Endurance aircraft
p 4195 N94-36335

INSTITUT DE RECHERCHE DE TRANSPORTS, BRON (FRANCE).
Proceedings of the Sixth International Congress on Noise as a Public Heatlh Problem, volume 3
[AD-A278218] p 4319 N94-36176

INSTITUT DES HAUTES ETUDES SCIENTIFIQUES, BURES-SUR-YVETTE (FRANCE).
Generalized Fredholm determinants and Selberg zeta functions for axiom A dynamical systems
[PB94-167665] p 4314 N94-35758
Successive minima on arithmetic varieties
[PB94-167699] p 4314 N94-35759
Cauchy and invariant measure problem for the periodic Zakharov system
[PB94-167707] p 4317 N94-35760
This non-axiomatizable quantum theory. From Hilbert's sixth problem to the recent viewpoint of Gell-mann and Hartle
[PB94-167715] p 4342 N94-35761
Height inequality for holomorphic curves
[PB94-167731] p 4314 N94-35762
Entropy of graphs, semigroups and groups
[PB94-167749] p 4314 N94-35763
Moduli space of monopoles and some invariants of 3-manifolds
[PB94-167756] p 4314 N94-35764

INSTITUT NATIONAL DE LA SANTE ET DE LA RECHERCHE MEDICALE, PARIS (FRANCE).
Typology of skeletal muscle in humans undergoing intense physical training or prolonged akinesia
[PB94-170644] p 4297 N94-36217

INSTITUTE FOR COMPUTER APPLICATIONS IN SCIENCE AND ENGINEERING, HAMPTON, VA.
Runtime support for data parallel tasks
[NASA-CR-194904] p 4300 N94-35240
On the nonlinear stability of viscous modes within the Rayleigh problem on an infinite flat plate
[NASA-CR-194909] p 4263 N94-35497
The velocity field created by a shallow bump in a boundary layer
[NASA-CR-194899] p 4266 N94-35975
Vortex tubes in turbulent flows: Identification, representation, reconstruction
[NASA-CR-194900] p 4267 N94-35992
A three dimensional multigrid Reynolds-averaged Navier-Stokes solver for unstructured meshes
[NASA-CR-194908] p 4191 N94-35994

INSTITUTE FOR DEFENSE ANALYSES, ALEXANDRIA, VA.
The application of fuzzy logic to SAFOR in SIMNET
[AD-A279058] p 4312 N94-35730

INSTITUTE OF GAS TECHNOLOGY, CHICAGO, IL.
Gasoline from natural gas by sulfur processing
[DE94-011130] p 4248 N94-36035

INSTITUTE OF NUCLEAR PHYSICS, KRAKOW (POLAND).
The relativistic invariant and the Galilean mass of bodies
[DE94-616615] p 4318 N94-35956
Classical time machine
[DE94-616616] p 4342 N94-36070

INSTITUTE OF NUCLEAR TECHNIQUES, KRACOW (POLAND).
J/psi absorption effects in the coherent production on nuclei
[DE94-616870] p 4326 N94-36129
Sigma minus-nucleus interactions in emulsion at 350 GeV
[DE94-616886] p 4326 N94-36130

INSTITUTO DE FISICA TEORICA, SAO PAULO (BRAZIL).
A three-body calculation of the O-16(d,p)O-17 reaction using a two-term separable potential for the s-wave nucleon-core interaction
[DE94-616652] p 4320 N94-35579
Relativistic three-particle dynamical equations. 2: Application to the trinucleon system
[DE94-616653] p 4320 N94-35580
Relativistic three-particle dynamical equations. 2: Theoretical development
[DE94-616654] p 4320 N94-35581
Radiatively induced electron and electron-neutrino masses
[DE94-616775] p 4321 N94-35582
The silent phase transition in mesonic bags and lattice theory
[DE94-616852] p 4321 N94-35583
Nonadiabatic neutrino oscillations revisited
[DE94-616649] p 4321 N94-35593
Some consequences in weak processes of three generations mixing in the leptonic sector
[DE94-616650] p 4321 N94-35594
Complex Kohn variational principle for two-nucleon bound-state and scattering with the tensor potential
[DE94-616651] p 4321 N94-35595

INSTITUTO DE PESQUISAS ENERGETICAS E NUCLEARES, SAO PAULO (BRAZIL).
Treatment of toxic gases SO2 and NO(x) by electron beam irradiation
[DE94-615424] p 4330 N94-36028

INTEGRATED SYSTEMS, INC., SANTA CLARA, CA.
Overview of the Miniature Sensor Technology Integration (MSTI) spacecraft attitude control system
p 4206 N94-35627
Overview of the MSTI 2 on-orbit alignment
p 4206 N94-35629
Overview of the MSTI 2 processor-in-the-loop simulator p 4207 N94-35631

INTERNATIONAL ATOMIC ENERGY AGENCY, VIENNA (AUSTRIA).
Isotopic and geochemical precursors of earthquakes and volcanic eruptions
[DE94-615824] p 4289 N94-35568

INTERNATIONAL CENTRE FOR THEORETICAL PHYSICS, TRIESTE (ITALY).
Identity for propagator in four-fermion theory
[DE94-611104] p 4342 N94-35781
Three-photon micromasers
[DE94-611106] p 4272 N94-35782
Calculations on some properties of the pion in the framework of Schwinger-Dyson and Bethe-Salpeter equations
[DE94-611232] p 4322 N94-35786
Magnetoresistance of films and strips with the diffuse surface scattering
[DE94-611100] p 4340 N94-35933
Some theorems on a class of harmonic manifolds
[DE94-611102] p 4315 N94-35934
A theoretical study of ordering phenomena in K-In and K-Sb molten alloys
[DE94-611103] p 4240 N94-35935
N = 4 supersymmetry from the quantum affine algebra U(sub q)(A-circumflex(sup 1)(sub 3))
[DE94-611145] p 4317 N94-36307
Decay of the D(sub s)-meson
[DE94-611209] p 4329 N94-36308
On quantization of time-dependent systems with constraints
[DE94-611114] p 4343 N94-36351
Coherent states versus de Broglie-wavelets
[DE94-611075] p 4343 N94-36381

INTEVAC, PALO ALTO, CA.
Streak tube photocathode development program
[DE94-009905] p 4270 N94-36350

IOWA UNIV., IOWA CITY, IA.
The fine structure of Langmuir waves observed upstream of the bow shock at Venus
[NASA-CR-196123] p 4354 N94-35378
Ultrafast readout of scintillating fibers using upgraded position-sensitive photomultipliers
[DE94-010419] p 4269 N94-36095

ISTITUTO NAZIONALE DI GEOFISICA, ROME (ITALY).
Electromagnetic measurements of the ionosphere at the ionospheric station of Rome
[AD-A278991] p 4290 N94-35744

J

JET PROPULSION LAB., CALIFORNIA INST. OF TECH., PASADENA, CA.
High temperature sorbents for oxygen
[NASA-CASE-NPO-18409-1-CU] p 4235 N94-35255
Separation tool for multipin electrical connectors
[NASA-CASE-NPO-18786-1-CU] p 4274 N94-35375
Adjustable control station with movable monitors and cameras for viewing systems in robotics and teleoperations
[NASA-CASE-NPO-17837-1-CU] p 4332 N94-35384
Insight to global change: EOS/SAR mission
[NASA-CR-196133] p 4284 N94-35503
Galileo: The Jovian laboratory
[NASA-CR-196043] p 4367 N94-35504
Voyager: National Air and Space Museum
[NASA-CR-195905] p 4367 N94-35505
Voyager last picture show
[NASA-CR-195796] p 4367 N94-35506
Atmosphere of Venus
[NASA-CR-194214] p 4367 N94-35507
Galileo Earth/Moon 1 encounter
[NASA-CR-195545] p 4367 N94-35508
Magellan collection of radar calibration results
[NASA-CR-194753] p 4367 N94-35509
Magellan to Venus
[NASA-CR-195779] p 4201 N94-35510
Planetary Rover Program
[NASA-CR-196108] p 4201 N94-35511
Teleoperation and supervised autonomy for ORU exchange
[NASA-CR-196101] p 4274 N94-35512

Voyager science summary tape
[NASA-CR-195909] p 4367 N94-35513
The Telecommunications and Data Acquisition Report
[NASA-CR-196117] p 4252 N94-35542
The Mars Observer differential one-way range demonstration p 4210 N94-35543
Influence of an externally modulated photonic link on a microwave communications system
p 4252 N94-35544
Field demonstration of X-band photonic antenna remoting in the Deep Space Network
p 4252 N94-35545
The electrical conductivities of candidate beam-waveguide antenna shroud materials
p 4252 N94-35546
Thin-ribbon tapered coupler for dielectric waveguides
p 4253 N94-35547
Design and implementation of a beam-waveguide mirror control system for vernier pointing of the DSS-13 antenna p 4253 N94-35548
Use of the sampling theorem to speed up near-field physical optics scattering calculations
p 4253 N94-35549
DSS-13 S-/X-band microwave feed system
p 4253 N94-35550
A 1- to 10-GHz downconverter for high-resolution microwave survey p 4253 N94-35551
A closed-loop time-alignment system for baseband combining p 4253 N94-35552
Correlator data analysis for the array feed compensation system p 4253 N94-35553
Maximum-likelihood soft-decision decoding of block codes using the A* algorithm p 4254 N94-35555
Bit-wise arithmetic coding for data compression
p 4254 N94-35556
Spacecraft-spacecraft radio-metric tracking: Signal acquisition requirements and application to Mars approach navigation p 4254 N94-35557
Performance evaluation of digital phase-locked loops for advanced deep space transponders
p 4254 N94-35558
The development and application of composite complexity models and a relative complexity metric in a software maintenance environment
p 4255 N94-35559
The real-time display of interferometry data for Goldstone radar astronomy data acquisition
p 4255 N94-35560
A new presentation of complex voltage data for Goldstone radar astronomy p 4255 N94-35561
A 32-GHz solid-state power amplifier for deep space communications p 4255 N94-35562
The Mars Observer Ka-band link experiment
p 4255 N94-35563
Low encounter speed comet COMA sample return missions p 4202 N94-35607
Compatibility of TOPEX/Poseidon trajectory propagation with JPL and GSFC/FDF operational software
p 4204 N94-35619
Method and apparatus for removing unwanted reflections from an interferometer
[NASA-CASE-NPO-18478-1-CU] p 4333 N94-35749
Information and communication technology
p 4257 N94-36043

JOHNS HOPKINS UNIV., BALTIMORE, MD.
Transient Faults in Computer Systems
[NASA-CR-194717] p 4306 N94-36063
Certification of computational results
p 4306 N94-36064
Experimental evaluation of the certification-trail method p 4306 N94-36065
Certification trails and software design for testability
p 4306 N94-36066
Experimental evaluation of certification trails using abstract data type validation p 4307 N94-36067
Using certification trails to achieve software fault tolerance p 4307 N94-36068
Certification trails for data structures
p 4307 N94-36069

JOHNS HOPKINS UNIV., COLUMBIA, MD.
The 30th JANNAF Combustion Subcommittee Meeting, volume 1
[AD-A278793] p 4247 N94-35655
The 30th JANNAF Combustion Subcommittee Meeting, volume 2
[AD-A278794] p 4247 N94-35656

JOINT INST. FOR NUCLEAR RESEARCH, DUBNA (USSR).
The study of the local magnetic field in the oxide alpha-Bi2O3 by the mu SR-technique
[DE94-612636] p 4322 N94-35751
Inverse problem for symmetric tridiagonal matrices. Calculation of discrete orthogonal polynomial system with arbitrary weight
[DE94-612434] p 4315 N94-35789
Multi-window dialogue system of data processing for experimental setup VASSILISSA in PAW environment
[DE94-612439] p 4345 N94-35790
On new theories of physical vacuum
[DE94-616613] p 4318 N94-35955
Spin effects in high energy quark-quark scattering
[DE94-616800] p 4330 N94-36080
Variational method in relativistic two-body problem
[DE94-612462] p 4315 N94-36416

JOINT PUBLICATIONS RESEARCH SERVICE, ARLINGTON, VA.
JPRS report: Science and technology. Central Eurasia
[JPRS-UST-94-006] p 4249 N94-35226
JPRS report: Science and technology. Central Eurasia
[JPRS-UST-94-007] p 4249 N94-35227
JPRS report: Science and technology. Central Eurasia
[JPRS-UST-94-008] p 4249 N94-35228
JPRS report: Science and technology. Central Eurasia
[JPRS-UST-94-001] p 4229 N94-35340
JPRS report: Science and technology. Central Eurasia
[JPRS-UST-94-004] p 4249 N94-35341
JPRS report: Science and technology. Central Eurasia
[JPRS-UST-94-005] p 4249 N94-35342
JPRS report: Science and technology. Central Eurasia
[JPRS-UST-94-010] p 4250 N94-35385
JPRS report: Science and technology. Central Eurasia
[JPRS-UST-94-011] p 4250 N94-35386
JPRS report: Science and technology. Central Eurasia
[JPRS-UST-94-012] p 4250 N94-35387
JPRS report: Science and technology. Central Eurasia: Materials science
[JPRS-UMS-93-007] p 4240 N94-35517
JPRS report: Science and technology. Central Eurasia: Space
[JPRS-USP-94-001] p 4201 N94-35518
JPRS Report: Science and Technology. Central Eurasia: Space. Russian federation law on space
[JPRS-USP-94-002] p 4348 N94-35519
JPRS report: Science and technology. Central Eurasia: Space
[JPRS-USP-94-003] p 4201 N94-35520
JPRS report: Science and technology. Central Eurasia: Space
[JPRS-USP-93-005] p 4201 N94-36011

K

KANAGAWA ACADEMY OF SCIENCE AND TECHNOLOGY, KAWASAKI (JAPAN).
Magnetically suspended stepping motors for clean room and vacuum environments p 4225 N94-35915

KANAZAWA INST. OF TECH. (JAPAN).
Measurement and characterization of force dynamics in high T(sub c) superconductors p 4214 N94-35844

KENTUCKY UNIV., LEXINGTON, KY.
Fundamental studies in blow-down and cryogenic cooling
[AD-A278967] p 4250 N94-35524

KERNFORSCHUNGSZENTRUM G.M.B.H., KARLSRUHE (GERMANY).
Concepts of flywheels for energy storage using autostable high-T(sub c) superconducting magnetic bearings p 4224 N94-35909

KNOLLE MAGNETRANS, SAN FRANCISCO, CA.
Maglev crude oil pipeline p 4226 N94-35919

KOREAN ATOMIC ENERGY RESEARCH INST., DAEDUK (REPUBLIC OF KOREA).
The development of a statistical report software for computer system usages
[DE94-611061] p 4346 N94-35832
An analysis of file system and installation of the file management system for NOS operating system
[DE94-611062] p 4346 N94-35833
ONED90: 1-dimensional diffusion code
[DE94-611063] p 4305 N94-35834
Magnetic field effect on selective photoionization
[DE94-611079] p 4334 N94-36180

KYOTO UNIV., UJI (JAPAN).
On a generalized bootstrap principle
[DE94-727517] p 4314 N94-35774

KYUSHU UNIV., FUKUOKA (JAPAN).
Feasibility study of superconducting LSM rocket launcher system p 4225 N94-35914

L

LAWRENCE LIVERMORE NATIONAL LAB., CA.
Computer animation of clouds
[DE94-008289] p 4292 N94-35350
Issues in the design and optimization of adaptive optics and laser guide stars for the Keck Telescopes
[DE94-009384] p 4349 N94-35565
Simulation models for computational plasma physics: Concluding report
[DE94-009976] p 4335 N94-35647
Improved performance of high average power semiconductor arrays for applications in diode pumped solid state lasers
[DE94-009516] p 4271 N94-35665
900-mW average power and tunability from a diode-pumped 2.94 micron Er:YAG oscillator
[DE94-009511] p 4271 N94-35679
Chirped-pulse amplification with flashlamp-pumped Ti:Sapphire amplifiers
[DE94-010055] p 4272 N94-35695
Structures and properties of materials recovered from high shock pressures
[DE94-010057] p 4232 N94-35696
Characterization of lithium niobate electro-optic modulators at cryogenic temperatures
[DE94-010059] p 4333 N94-35697
CAirTOX: A compartment model for assessing the fate of and human exposure to toxic-chemical emissions to air
[DE94-010084] p 4284 N94-35700
An electromagnetic finite difference time domain analog treatment of small signal acoustic interactions
[DE94-009978] p 4319 N94-35770
High-sensitivity receiver for increasing multiplicity of measurement axes of Zygo's Heterodyne interferometer
[DE94-009916] p 4333 N94-35818
Cleaning up our act: Alternatives for hazardous solvents used in cleaning
[DE94-006624] p 4285 N94-35943
State of the art in high-power microwaves: An overview
[DE94-007075] p 4272 N94-35978
X ray radiographic imaging of hydrodynamic phenomena in radiation driven materials: Shock propagation, material compression and shear flow
[DE94-009515] p 4266 N94-35982
Proceedings of the LLNL Technical Women's Symposium
[DE94-006616] p 4379 N94-35997
Combining nonlinear multiresolution system and vector quantization for still image compression
[DE94-009422] p 4305 N94-36017
Anthropogenic sulfate and organic aerosols, CCN, and cloud project concentration at a marine site
[DE94-004210] p 4286 N94-36025
Wedge scattering by the method of iteration
[DE94-010404] p 4256 N94-36112
Neutron detectors for fusion reaction-rate measurements
[DE94-010407] p 4330 N94-36114
High-power CW operation of AlGaInP diode-laser arrays
[DE94-010409] p 4272 N94-36115
CALTRANS: A parallel, deterministic, 3D neutronics code
[DE94-010667] p 4326 N94-36127
Inertial confinement fusion
[DE94-010835] p 4338 N94-36193
X ray radiographic imaging of hydrodynamic phenomena in radiation driven materials: Shock propagation and shear flow
[DE94-010891] p 4318 N94-36201
A new comprehensive reaction mechanism for combustion of hydrocarbon fuels
[DE94-008288] p 4238 N94-36205
A comparison between direct spark ignition and prechamber ignition in an internal combustion engine
[DE94-008218] p 4275 N94-36206
Computer virus information update CIAC-2301
[DE94-011916] p 4308 N94-36236
Electrical conductivity of hydrogen shocked to megabar pressures
[DE93-019632] p 4238 N94-36237
Design for manufacturability evaluation: Composite National Ignition Facility (NIF) pockel cell body
[DE94-010669] p 4338 N94-36284
Integrated science model for assessment of climate change
[DE94-011758] p 4288 N94-36286
Applying observations of work activity in designing prototype data analysis tools
[DE94-010206] p 4347 N94-36297
TSAR modeling of a TEM horn and surrounding structure
[DE94-010668] p 4256 N94-36301
A multilevel adaptive projection method for unsteady incompressible flow
[DE93-016418] p 4267 N94-36315
The reaction of hydroperoxy-propyl radicals with molecular oxygen
[DE94-006392] p 4239 N94-36319
Streak tube photocathode development program
[DE94-009905] p 4270 N94-36350

Efficient light propagation for multiple anisotropic volume scattering
[DE94-006474] p 4334 N94-36356
An equal-order approximate projection FEM
[DE94-010101] p 4268 N94-36374
High density implosion experiments at Nova
[DE94-010894] p 4339 N94-36375
Effects of natural gas composition on ignition delay under diesel conditions
[DE94-006405] p 4276 N94-36378
New calculations of Fe spectra in high-temperature plasmas
[DE94-009919] p 4339 N94-36386
GRIZ: Finite element analysis results visualization for unstructured grids
[DE94-010066] p 4309 N94-36429

LEEDS UNIV. (ENGLAND).
The EASE Visualization Community Club
[PB94-170529] p 4308 N94-36211

LEHIGH UNIV., BETHLEHEM, PA.
Unsteady structure of leading-edge vortices on a delta wing
[AD-A278988] p 4190 N94-35529
NO decomposition in non-reducing atmospheres
[DE94-011157] p 4237 N94-36036

LEICESTER UNIV. (ENGLAND).
ROSAT/XRT-PSPC observations and the ionizing continuum of Seyfert 1 galaxy Mkn 478
[PB94-167053] p 4350 N94-35530

LITTLE (ARTHUR D.), INC., CAMBRIDGE, MA.
Coal-fueled diesels for modular power generation
[DE94-002960] p 4275 N94-36348

LOCKHEED ENGINEERING AND SCIENCES CO., HAMPTON, VA.
Carbon-carbon piston development
[NASA-CR-4595] p 4233 N94-35947
ASTM test methods for composite characterization and evaluation p 4229 N94-36399

LOCKHEED ENGINEERING AND SCIENCES CO., HOUSTON, TX.
STS-58 Space Shuttle Mission Report
[NASA-TM-109867] p 4211 N94-35251
STS-51 Space Shuttle Mission Report
[NASA-TM-109866] p 4211 N94-35252

LOCKHEED MISSILES AND SPACE CO., SUNNYVALE, CA.
CSI, optimal control, and accelerometers: Trials and tribulations p 4221 N94-35888

LOGICON R AND D ASSOCIATES, LOS ANGELES, CA.
Wedge scattering by the method of iteration
[DE94-010404] p 4256 N94-36112

LOS ALAMOS NATIONAL LAB., NM.
Fluorescence detection of single molecules using pulsed near-field optical excitation and time correlated photon counting
[DE94-007553] p 4320 N94-35376
AFDM: An advanced fluid-dynamics model, volume 6
[DE94-009596] p 4264 N94-35669
Liquid crystalline thermosetting polyimides
[DE94-009939] p 4244 N94-35768
An object-oriented implementation of a graphical-programming system
[DE94-009298] p 4304 N94-35808
Angular momentum in the Local Group
[DE94-009322] p 4350 N94-35980
Using International English to prepare technical text for translation
[DE94-002628] p 4347 N94-36102
Role of magma-water interaction in very large explosive eruptions
[DE94-002698] p 4291 N94-36103
Kinetic theory of runaway air breakdown and the implications for lightning initiation
[DE94-001683] p 4295 N94-36240
Measurements of spatial and frequency coherence of an equatorial hf path during spread-F
[DE93-016615] p 4257 N94-36316
Computer simulations of benzene in faujasite-type zeolites
[DE94-007533] p 4242 N94-36369

LOUISIANA STATE UNIV., BATON ROUGE, LA.
A search for radiative neutrino decay from supernovae
[NASA-CR-196011] p 4376 N94-35515

LOUISVILLE UNIV., KY.
Adaptive model reduction for continuous systems via recursive rational interpolation p 4219 N94-35876

LOYOLA COLL., BALTIMORE, MD.
JTEC/WTEC report and program summary
p 4379 N94-36042
Design and construction of a tensile tester for the testing of simple composites p 4230 N94-36401
An automated digital data collection and analysis system for the Charpy Impact Tester p 4232 N94-36415

LUNAR AND PLANETARY INST., HOUSTON, TX.
Workshop on the Martian Northern Plains: Sedimentological, periglacial, and paleoclimatic evolution
[NASA-CR-196134] p 4354 N94-35359
The Twenty-Fifth Lunar and Planetary Science Conference. Part 1: A-G
[NASA-CR-195743] p 4355 N94-35395
The Twenty-Fifth Lunar and Planetary Science Conference. Part 3: P-Z
[NASA-CR-195745] p 4362 N94-35448
The Twenty-Fifth Lunar and Planetary Science Conference. Part 2: H-O
[NASA-CR-195744] p 4367 N94-36136

M

MADISON GUIDANCE, NAVIGATION AND CONTROL, YORKTOWN HEIGHTS, NY.
The control of satellites with microgravity constraints: The COMET Control System p 4207 N94-35632

MARTIN MARIETTA ASTRO SPACE, PHILADELPHIA, PA.
GPHS-RTGs in support of the Cassini mission
[DE94-009994] p 4212 N94-35648

MARTIN MARIETTA CORP., DENVER, CO.
Mars aqueous chemistry experiment
[NASA-CR-196024] p 4354 N94-35263

MARYLAND UNIV., COLLEGE PARK, MD.
Collected software engineering papers, volume 11
[NASA-CR-189347] p 4301 N94-35434
Developing interpretable models with optimized set reduction for identifying high risk software components
p 4301 N94-35435
Modeling and managing risk early in software development p 4301 N94-35436
An information model for use in software management estimation and prediction p 4301 N94-35437
Measuring and assessing maintainability at the end of high level design p 4301 N94-35438
Power balance and characterization of impurities in the Maryland Spheromak, part 2
[DE94-009603] p 4335 N94-35670
Active vibration damping using smart material
p 4221 N94-35886

MASON AND HANGER-SILAS MASON CO., INC., AMARILLO, TX.
NMR imaging of components and materials for DOE application
[DE94-010664] p 4238 N94-36084

MASSACHUSETTS INST. OF TECH., CAMBRIDGE.
Visual-vestibular interaction
[NASA-CR-196097] p 4297 N94-35379
Structural assembly demonstration experiment, phase 1
[NASA-CR-193967] p 4212 N94-35484
Astronomy in the region between 1 mm and 0.1 mm wavelength
[NASA-CR-196020] p 4349 N94-36419

MASSACHUSETTS INST. OF TECH., LEXINGTON.
The influence of data link-provided graphical weather on pilot decision-making
[AD-A278871] p 4293 N94-35596
Reduction procedures for accurate analysis of MSX surveillance experiment data p 4203 N94-35611
Space Shuttle orbit determination using empirical force modeling of attitude maneuvers for the German MOMS-02/D2 mission p 4207 N94-35634
The polygon-ellipse method of data compression of weather maps
[AD-A278958] p 4293 N94-35719
Data requirements for ceiling and visibility products development
[AD-A278959] p 4293 N94-35720
Terminal Doppler Weather Radar (TDWR) Low Level Wind Shear Alert System 3 (LLWAS 3) integration studies at Orlando International Airport
[AD-A278957] p 4294 N94-35807
Extrapolating storm location using the Integrated Terminal Weather System (ITWS) storm motion algorithm
[AD-A278611] p 4295 N94-36249

MASSACHUSETTS UNIV., LOWELL, MA.
A quality control package for the Digisonde Drift Analysis (DDA)
[AD-A278663] p 4289 N94-35578
Ionospheric plasma drift and structure studies at high and mid-latitudes
[AD-A279415] p 4291 N94-36116

MATERIALS SCIENCES CORP., FORT WASHINGTON, PA.
Implementation of the military handbook 17 for polymer matrix composites and metal matrix composites
[AD-A278795] p 4244 N94-35757

MCDONNELL-DOUGLAS AEROSPACE, LONG BEACH, CA.
Tanker system and technology requirements definition: A tanker technology road map p 4197 N94-36344

METSAT, INC., FORT COLLINS, CO.
Production of long-term global water vapor and liquid water data set using ultra-fast methods to assimilate multi-satellite and radiosonde observations
[NASA-CR-196044] p 4292 N94-35355
Production of long-term global water vapor and liquid water data set using ultra-fast methods to assimilate multi-satellite and radiosonde observations
[NASA-CR-195981] p 4293 N94-35499

MICROELECTRONICS CENTER OF NORTH CAROLINA, RESEARCH TRIANGLE PARK, NC.
Model engineering concepts for air quality models in an integrated environmental modeling system
[PB94-158623] p 4298 N94-35688

MIDWEST RESEARCH INST., GOLDEN, CO.
AICD: Advanced Industrial Concepts Division Biological and Chemical Technologies Research Program
[DE94-006854] p 4283 N94-36051
A guide to research facilities at the National Renewable Energy Laboratory
[DE94-006857] p 4283 N94-36052
Advanced hydrogen/method utilization technology demonstration
[DE94-000214] p 4248 N94-36191

MIDWEST RESEARCH INST., KANSAS CITY, MO.
Further studies of 60-Hz exposure effects on human function
[DE94-010192] p 4297 N94-36223

MINNESOTA MINING AND MFG. CO., SAINT PAUL, MN.
Dual cure low-VOC coating process
[DE94-009346] p 4245 N94-35809

MINNESOTA UNIV., MINNEAPOLIS, MN.
State-to-state dynamics of molecular energy transfer
[DE94-009651] p 4324 N94-35816

MISSOURI UNIV., ROLLA, MO.
Kinetics of phase transformations in glass forming systems
[NASA-CR-196082] p 4245 N94-35977

MITRE CORP., BEDFORD, MA.
Application of a Monte Carlo accuracy assessment tool to TDRS and GPS p 4207 N94-35635
The Earth Satellite Program (ESP), version 2.0
[AD-A278860] p 4201 N94-35827

MONTPELLIER-2 UNIV. (FRANCE)
Study and fabrication of GaSb-based laser heterostructures
[PB94-170677] p 4273 N94-36218

MOSCOW STATE UNIV. (RUSSIA).
Global changes of radiation situation at heights less than 1000 km
[DE94-610504] p 4290 N94-35780
Spatial fluctuations of particle fluxes within the auroral zone inferred from the Intercosmos-Bulgaria-1300 satellite data
[DE94-615858] p 4350 N94-36128
Proceedings of the Twenty-First All-Union Conference on Physics of Charged Particles Interaction with Crystals
[DE94-615768] p 4341 N94-36181

N

NAPLES UNIV. (ITALY).
Collective plasma corrections to the solar opacity
[PB94-170511] p 4375 N94-36210

NASA CENTER FOR AEROSPACE INFORMATION, LINTHICUM HEIGHTS, MD.
NASA Thesaurus. Volume 1: Hierarchical listing. Volume 2: Access vocabulary. Volume 3: Definitions
[NASA-SP-7096-VOL-1/2/3] p 4346 N94-36037

NATIONAL AERONAUTICS AND SPACE ADMINISTRATION, WASHINGTON, DC.
Aeronautical engineering: A continuing bibliography with indexes (supplement 306)
[NASA-SP-7037(306)] p 4189 N94-35338
Mission to Planet Earth. The living ocean: Observing ocean color from space
[NASA-PAM-554] p 4295 N94-35343
Aerospace medicine and biology: A continuing bibliography with indexes (supplement 391)
[NASA-SP-7011(391)] p 4297 N94-35345
NASA patent abstracts bibliography: A continuing bibliography. Section 1: Abstracts (supplement 45)
[NASA-SP-7039(45)-SECT-1] p 4344 N94-35382
Aerospace Safety Advisory Panel
[NASA-TM-109840] p 4201 N94-35390
Statement by Bill D. Colvin, Inspector General
[NASA-TM-109793] p 4348 N94-35446
NASA patent abstracts bibliography: A continuing bibliography. Section 2: Indexes (supplement 45)
[NASA-SP-7039(45)-SECT-2] p 4346 N94-35835

Budget estimates, fiscal year 1995. Volume 1: Agency summary, human space flight, and science, aeronautics and technology
[NASA-TM-109791] p 4347 N94-35899

Budget estimates, fiscal year 1995. Volume 2: Mission support and Inspector General
[NASA-TM-109792] p 4348 N94-35900

The history of space exploration
[NASA-TM-109888] p 4201 N94-36440

NATIONAL AERONAUTICS AND SPACE ADMINISTRATION. AMES RESEARCH CENTER, MOFFETT FIELD, CA.

Director's discretionary fund
[NASA-TM-103997] p 4376 N94-35370

Linear and nonlinear pattern selection in Rayleigh-Benard stability problems
[NASA-TM-104007] p 4263 N94-35371

Three-dimensional unstructured grid refinement and optimization using edge-swapping
[NASA-TM-103966] p 4299 N94-35393

Flight testing of a luminescent surface pressure sensor
[NASA-TM-103970] p 4189 N94-35394

The surface and interior of Phobos
p 4355 N94-35400

High spatial resolution telescopic multispectral imaging and spectroscopy of the Moon. 1: The Serenitatis/Tranquillitatis border region
p 4356 N94-35402

High resolution visible to short-wave near-infrared CCD spectra of Mars during 1990 p 4356 N94-35403

Absolute calibration and atmospheric versus mineralogic origin of absorption features in 2.0 to 2.5 micron Mars spectra obtained during 1993 p 4356 N94-35404

Wavelength calibration techniques and subtle surface and atmospheric absorption features in the Mariner 6, 7 IRS reflectance data p 4356 N94-35405

Shoemaker-Levy 9 and the tidal disruption of comets
p 4351 N94-35406

A mineralogical instrument for planetary applications
p 4357 N94-35408

Venus climate stability and volcanic resurfacing rates
p 4358 N94-35413

Fluvial processes in Ma'adim Vallis and the potential of Gusev crater as a high priority site
p 4358 N94-35414

First Galileo image of asteroid 243 Ida
p 4351 N94-35416

Subpixel resolution from multiple images
p 4281 N94-35417

What initiated planetesimal formation?
p 4351 N94-35422

Exopaleontology and the search for a fossil record on Mars p 4360 N94-35425

Thermal emission measurements (5-25 microns) of Hawaiian palagonitic soils with implications for Mars
p 4292 N94-35452

Thermal emission measurements (5-25 microns) of palagonite/Fe-substituted montmorillonite intimate mixtures: Applications to Mars p 4292 N94-35453

Transmission measurements (4000-400 cm(exp -1), 2.5-25 microns) of crystalline ferric oxides and ferric oxyhydroxides: Implications for Mars
p 4292 N94-35454

The temperature of nitrogen on Pluto
p 4365 N94-35468

Purity and cleanness of aerogel as a cosmic dust capture medium p 4247 N94-35469

Windblown sand on Mars: The effect of saltation threshold on drift potentials derived from Mars GCM
p 4366 N94-35474

Simultaneous adsorption of CO2 and H2O under Mars-like conditions and application to the evolution of the Martian climate p 4366 N94-35475

1993 Technical Paper Contest for Women. Gear Up 2000: Women in Motion
[NASA-CP-10134] p 4377 N94-35961

Piloted simulation study of two tilt-wing control concepts p 4200 N94-35962

Mentoring for 2000 and beyond p 4343 N94-35964

Wind tunnel measurements on a full-scale F/A-18 with a tangentially blowing slot p 4191 N94-35965

Implementation of a Computerized Maintenance Management System p 4343 N94-35970

Space-based crystal growth and thermocapillary flow
p 4342 N94-35971

Ground vibration test of the XV-15 Tiltrotor Research Aircraft and pretest predictions p 4200 N94-35972

Building on the foundation for an engineering career
p 4343 N94-35973

Knowledge-based systems in Japan
p 4347 N94-36044

Research and technology, 1993
[NASA-TM-108816] p 4380 N94-36117

Atmospheric effects on the mapping of Martian thermal inertia and thermally derived albedo
p 4368 N94-36137

The structural changes of water ice I during warmup
p 4239 N94-36144

Mercury: Mid-infrared (7.3 - 13.5 microns) spectroscopic observations showing features characteristic of plagioclase p 4370 N94-36150

The reduction of takeoff ground roll by the application of a nose gear jump strut
[NASA-TM-108822] p 4198 N94-36380

NATIONAL AERONAUTICS AND SPACE ADMINISTRATION. GODDARD SPACE FLIGHT CENTER, GREENBELT, MD.

Active antenna
[NASA-CASE-GSC-13309-1] p 4251 N94-35231

Annotated bibliography of Software Engineering Laboratory literature
[NASA-CR-189350] p 4300 N94-35238

Cost and schedule estimation study report
[NASA-CR-189344] p 4300 N94-35256

NASA Space Geodesy Program: GSFC data analysis, 1993. VLBI geodetic results 1979 - 1992
[NASA-TM-104605] p 4281 N94-35261

CATLAC: Calibration and validation analysis tool of local area coverage for the SeaWiFS mission
[NASA-TM-104603] p 4211 N94-35269

Mission to Planet Earth. The living ocean: Observing ocean color from space
[NASA-PAM-554] p 4295 N94-35343

Remote geochemical experiment package for Discovery class missions p 4350 N94-35420

Impact basins in Southern Daedalia, Mars: Evidence for clustered impactors? p 4360 N94-35426

Effects due to overlapping large impact basins on Mars p 4360 N94-35427

Quantifying shapes of volcanoes on Venus
p 4361 N94-35429

Mesoscale roughness of Venus p 4361 N94-35430

Volcano morphometry and volume scaling on Venus
p 4361 N94-35431

Collected software engineering papers, volume 11
[NASA-CR-189347] p 4301 N94-35434

Impacts of object-oriented technologies: Seven years of SEL studies p 4301 N94-35439

The topography of Mars: A re-evaluation of current data p 4364 N94-35460

The mass of Mars, Phobos, and Deimos, from the analysis of the Mariner 9 and Viking Orbiter tracking data p 4364 N94-35461

Noachian and Hesperian modification of the original Chryse impact basin topography p 4364 N94-35462

First observation of a mass independent isotopic fractionation in a condensation reaction
p 4239 N94-35464

Chondrule magnetic properties p 4352 N94-35471

Rheology, tectonics, and the structure of the Venus lithosphere p 4367 N94-35479

Formation of fold and thrust belts on Venus due to horizontal shortening of a laterally heterogeneous lithosphere p 4367 N94-35480

Microprocessor control of multiple peak power tracking DC/DC converters for use with solar cell arrays
[NASA-CASE-GSC-13450-2] p 4282 N94-35540

Flight Mechanics/Estimation Theory Symposium, 1994
[NASA-CP-3265] p 4202 N94-35605

High Earth orbit design for lunar assisted small Explorer class missions p 4202 N94-35608

Obtaining coincident image observations for Mission to Planet Earth science data return p 4202 N94-35609

Automated maneuver planning using a fuzzy logic algorithm p 4203 N94-35610

Fixed-head star tracker attitude updates on the Hubble Space Telescope p 4203 N94-35612

In-flight scale/distortion calibration of the Hubble Space Telescope fixed-head star trackers
p 4203 N94-35613

The in-flight calibration of the Hubble Space Telescope fine guidance sensors, 2 (a success story)
p 4204 N94-35615

In-flight estimation of gyro noise on the Upper Atmosphere Research Satellite (UARS) and Extreme Ultraviolet Explorer (EUVE) missions
p 4204 N94-35616

Operational support for Upper Atmosphere Research Satellite (UARS) attitude sensors p 4204 N94-35617

Improved solution accuracy for TDRSS-based TOPEX/Poseidon orbit determination
p 4205 N94-35620

Improved solution accuracy for Landsat-4 (TDRSS-user) orbit determination p 4205 N94-35623

Optimum satellite relay positions with application to a TDRS-1 Indian Ocean relay p 4205 N94-35624

TDRSS Onboard Navigation System (TONS) flight qualification experiment p 4206 N94-35625

Evaluation of semiempirical atmospheric density models for orbit determination applications
p 4208 N94-35636

Filter parameter tuning analysis for operational orbit determination support p 4208 N94-35637

Color/magnitude calibration for National Aeronautics and Space Administration (NASA) standard Fixed-Head Star Trackers (FHST) p 4209 N94-35641

Advantages of estimating rate corrections during dynamic propagation of spacecraft rates: Applications to real-time attitude determination of SAMPEX
p 4209 N94-35642

Space robotics in Japan p 4278 N94-36046

Controller for the Electronically Scanned Thinned Array Radiometer (ESTAR) instrument
[NASA-TM-104608] p 4259 N94-36049

Uniqueness of a solution of a steady state photochemical problem: Applications to Mars p 4370 N94-36151

H2O-H2SO4 system in Venus' clouds and OCS, CO, and H2SO4 profiles in Venus' troposphere
p 4370 N94-36152

Progress in the development of the GMM-2 gravity field model for Mars p 4371 N94-36155

Preliminary solutions for the lunar gravity field from analysis of lunar orbiter tracking data
p 4371 N94-36156

Shape, size, and distribution of magnetic particles in Bjurbole chondrules p 4353 N94-36167

Patterns of brittle deformation under extension on Venus p 4373 N94-36168

Formation of iron metal and grain coagulation in the solar nebula p 4373 N94-36170

Measurement of the decay rate of the SiH feature as a function of temperature p 4318 N94-36171

NATIONAL AERONAUTICS AND SPACE ADMINISTRATION. HUGH L. DRYDEN FLIGHT RESEARCH FACILITY, EDWARDS, CA.

Evaluating the dynamic response of in-flight thrust calculation techniques during throttle transients
[NASA-TM-4591] p 4193 N94-35241

Flight testing a propulsion-controlled aircraft emergency flight control system on an F-15 airplane
[NASA-TM-4590] p 4199 N94-35258

Engine exhaust characteristics evaluation in support of aircraft acoustic testing p 4319 N94-35963

A biased historical perspective of women in the engineering field at Dryden from 1946 to November 1992 p 4251 N94-35967

Experience with Ada on the F-18 High Alpha Research Vehicle flight test program p 4310 N94-35968

In-flight simulation studies at the NASA Dryden Flight Research Facility p 4198 N94-35969

NATIONAL AERONAUTICS AND SPACE ADMINISTRATION. JOHN F. KENNEDY SPACE CENTER, COCOA BEACH, FL.

Debris/ice/TPS assessment and integrated photographic analysis for Shuttle Mission STS-59
[NASA-TM-109203] p 4211 N94-35523

Endangered and potentially endangered wildlife on John F. Kennedy Space Center and faunal integrity as a goal for maintaining biological diversity
[NASA-TM-109204] p 4288 N94-36422

NATIONAL AERONAUTICS AND SPACE ADMINISTRATION. LYNDON B. JOHNSON SPACE CENTER, HOUSTON, TX.

Microporous structure with layered interstitial surface treatment, and method and apparatus for preparation thereof
[NASA-CASE-MSC-21487-3] p 4235 N94-35229

Multi-cellular, three-dimensional living mammalian tissue
[NASA-CASE-MSC-21560-2] p 4296 N94-35232

Smart accelerometer
[NASA-CASE-MSC-21951-1] p 4268 N94-35235

Analysis of the Shuttle Orbiter reinforced carbon-carbon oxidation protection system
[NASA-TM-104792] p 4262 N94-35245

Space educators' handbook
[NASA-TM-109779] p 4343 N94-35339

High density cell culture system
[NASA-CASE-MSC-22060-1] p 4296 N94-35366

Robot friendly probe and socket assembly
[NASA-CASE-MSC-22028-1] p 4274 N94-35374

New prospects for analyzing lunar pyroclastic glass
p 4355 N94-35397

Reduction of lunar mare soil and pyroclastic glass
p 4355 N94-35398

Calorimetric thermometry of meteoritic troilite: Preliminary thermometer relationships
p 4355 N94-35399

Single agglutinates: A comparative study of compositions of agglutinitic glass, whole-grain, bulk soil, and FMR p 4355 N94-35401

Craters in aluminum 1100 targets using glass projectiles at 1-7 km/s p 4280 N94-35407

Measuring track densities in lunar grains using image analysis p 4357 N94-35409
Ar-39-Ar-40 ages of four ureilites p 4357 N94-35410
Alteration and formation of rims on the CM parent body p 4357 N94-35411
Eureka! Aerogel capture of meteoroids in space p 4351 N94-35412
Lunar mineral feedstocks from rocks and soils: X-ray digital imaging in resource evaluation p 4358 N94-35415
Grain rims on ilmenite in the lunar regolith: Comparison to vapor deposits on regolith silicates p 4359 N94-35418
Block distributions on the lunar surface: A comparison between measurements obtained from surface and orbital photography p 4359 N94-35419
On the possible role of elemental carbon in the formation of reduced chondrules p 4351 N94-35421
The occurrence of blue luminescing enstatite in E3 and E4 chondrites p 4351 N94-35423
The fretted terrain of the Nilosyrtis Mensae region of Mars: Clues to the timing of dichotomy formation and the emplacement of the northern plains p 4360 N94-35424
Solar proton produced neon in shergottite meteorites p 4351 N94-35428
Application of an alkylammonium method for characterization of phyllosilicates in CI chondrites p 4351 N94-35432
High Resolution Transmission Electron Microscopy (HRTEM) of nanophase ferric oxides p 4239 N94-35433
Atomic oxygen reactor having at least one sidearm conduit
[NASA-CASE-MSC-21487-4] p 4250 N94-35445
FeO and MgO in plagioclase of lunar anorthosites: Igneous or metamorphic? p 4351 N94-35449
Luna 24 regolith breccias: A possible source of the fine size material of the Luna 24 regolith p 4362 N94-35450
Antarctic weathering of the CK chondrites EET90004, 90007, and 90022: Nickel and sulfur mobility p 4351 N94-35451
More shock recovery experiments on mesosiderite analogs p 4351 N94-35455
Distribution of siderophile and other trace elements in melt rock at the Chicxulub impact structure p 4352 N94-35456
Preliminary description of double drive tube 68002/68001 p 4363 N94-35457
Current activities and results of the Long Duration Exposure Facility Meteoroid and Debris Special Investigation Group p 4352 N94-35458
Innovative instrumentation for mineralogical and elemental analyses of solid extraterrestrial surfaces: The Backscatter Moessbauer Spectrometer/X Ray Fluorescence analyzer (BaMS/XRF) p 4239 N94-35459
Inhomogeneous distribution of materials in lodranites-acapulcoites and IAB irons and their common formation processes p 4364 N94-35463
Anatomy of a cluster IDP. Part 2: Noble gas abundances, trace element geochemistry, isotopic abundances, and trace organic chemistry of several fragments from L2008#5 p 4352 N94-35465
The anatomy of a cluster IDP. Part 1: Carbon abundance, bulk chemistry, and mineralogy of fragments from L2008#5 p 4352 N94-35466
The parent magma of xenoliths in shergottite EETA79001: Bulk and trace element composition inferred from magmatic inclusions p 4352 N94-35467
A quick look method of detecting water of hydration in small solar system bodies p 4352 N94-35470
Lunar LIGO and gravitational wave astronomy on the Moon p 4366 N94-35472
Advanced technology lunar telescope p 4350 N94-35473
Mineralogy of an unusual CM clast in the Kaidun meteorite p 4352 N94-35476
Mineralogy of artificially heated carbonaceous chondrites p 4352 N94-35477
Lunar horizon glow and the Clementine mission p 4366 N94-35478
International Space Station alpha remote manipulator system workstation controls test report
[NASA-TM-104796] p 4274 N94-35481
General purpose architecture for intelligent computer-aided training
[NASA-CASE-MSC-21381-1] p 4311 N94-35501
Magnetically operated check valve
[NASA-CASE-MSC-22046-1] p 4274 N94-35661
Evaluation of Oxygen Interactions with Materials 3: Mission and induced environments
[NASA-TM-109349] p 4236 N94-35680
Petrographic characterization of lunar soils: Application of x ray digital-imaging to quantitative and automated analysis p 4368 N94-36138
Possible spinel absorption bands in S-asteroid visible reflectance spectra p 4368 N94-36139
Shocked materials from the Dutch Peak diamictite, Utah p 4352 N94-36140
Experimental impacts into Teflon targets and LDEF thermal blankets p 4352 N94-36141
Dust evolution from comets and asteroids: Their velocities at Earth orbit intersection p 4352 N94-36142
Mars atmospheric escape and isotopic fractionation: Synthesis of data and models p 4369 N94-36143
Textural constraints on the formation of alteration phases in CM chondrites p 4353 N94-36145
Partial melting of the St. Severin (LL) and Lost City (H) ordinary chondrites: One step backwards and two steps forward p 4353 N94-36146
Preliminary results of sulfide melt/silicate wetting experiments in a partially melted ordinary chondrite p 4353 N94-36147
The nature of agglutinitic glass in the fine-size fraction of lunar soil 10084 p 4369 N94-36148
Electron energy-loss spectroscopy of carbon in interplanetary dust particles p 4353 N94-36149
Mossbauer and spectral (visible and near-IR) data for Fe(3+)-substituted rutile p 4240 N94-36154
Pigeonholing planetary meteorites: The lessons of misclassification of EET87521 and ALH84001 p 4353 N94-36157
On the origin of enstatite chondrite chondrules based on their petrography and comparison with experimentally produced chondrules p 4353 N94-36158
Morphology of meteoroid and space debris craters on LDEF metal targets p 4353 N94-36159
Production of ferroan andesites by the experimental partial melting of an LL chondrite p 4353 N94-36160
Synthetic and natural Nakhla pyroxenes: Parent melt composition and REE partition coefficients p 4353 N94-36161
Cr, Mn, and Ca distributions for olivine in angritic systems: Constraints on the origins of Cr-rich and Ca-poor core olivine in angrite LEW87051 p 4353 N94-36162
Partition coefficients for Al, Ca, Ti, Cr, and Ni in olivine obtained by melting experiment on an LL6 chondrite p 4353 N94-36163
Ferromagnetic resonance spectra of H2-reduced minerals and glasses p 4240 N94-36164
Hematite formed from pyroxene on Mars by meteoritic impact p 4372 N94-36165
Moessbauer mineralogy of calcined Murchison meteorite p 4353 N94-36166
Alkali element constraints on Earth-Moon relations p 4354 N94-36169
Pre-bombardment crystallization ages of basaltic clasts from Antarctic howardites EET87503 and EET87513 p 4354 N94-36172
New data supporting a Sm-146,147-Nd-142,143 formation interval for the lunar mantle p 4374 N94-36173
Calorimetric thermobarometry of experimentally shocked quartz p 4240 N94-36174

NATIONAL AERONAUTICS AND SPACE ADMINISTRATION. LANGLEY RESEARCH CENTER, HAMPTON, VA.
InP solar cell with window layer
[NASA-CASE-LEW-15606-1] p 4281 N94-35230
Tough, processable semi-interpenetrating polymer networks from monomer reactants
[NASA-CASE-LAR-14838-1] p 4242 N94-35233
Kinematic modeling of a double octahedral Variable Geometry Truss (VGT) as an extensible gimbal
[NASA-TM-109127] p 4311 N94-35242
Langley 14- by 22-foot subsonic tunnel test engineer's data acquisition and reduction manual
[NASA-TM-4563] p 4189 N94-35246
NASA/DOD Aerospace Knowledge Diffusion Research Project. Paper 40: Technical communications in aerospace education: A study of AIAA student members
[NASA-TM-109868] p 4344 N94-35254
Absolute calibration technique for broadband ultrasonic transducers
[NASA-CASE-LAR-14672-1] p 4268 N94-35368
Method for making a dynamic pressure sensor and a pressure sensor made according to the method
[NASA-CASE-LAR-14029-1] p 4269 N94-35369
Tough high performance composite matrix
[NASA-CASE-LAR-14239-2] p 4232 N94-35372
Second International Symposium on Magnetic Suspension Technology, part 1
[NASA-CP-3247-PT-1] p 4212 N94-35836
Implementation of a decoupled controller for a magnetic suspension system using electromagnets mounted in a planar array p 4216 N94-35853
NASA Workshop on Distributed Parameter Modeling and Control of Flexible Aerospace Systems
[NASA-CP-3242] p 4217 N94-35865
Applying transfer matrix method to the estimation of the modal characteristics of the NASA Mini-Mass Truss p 4218 N94-35870
Control of flexible structures with distributed sensing and processing p 4218 N94-35871
Flutter suppression digital control law design and testing for the AFW wind tunnel model p 4200 N94-35873
An overview of recent advances in system identification p 4220 N94-35880
Dynamic analysis of Space Shuttle/RMS configuration using continuum approach p 4221 N94-35887
An optimization-based approach for integrated controls-structures design of flexible spacecraft p 4221 N94-35889
Software for continuum modeling of controls-structures interactions p 4223 N94-35898
Second International Symposium on Magnetic Suspension Technology, part 2
[NASA-CP-3247-PT-2] p 4223 N94-35902
Robust tracking control of a magnetically suspended rigid body p 4225 N94-35913
Through-the-thickness tensile strength of textile composites
[NASA-TM-109115] p 4233 N94-35946
Final-Approach Spacing Aids (FASA) evaluation for terminal-area, time-based air traffic control
[NASA-TP-3399] p 4192 N94-36048
National Educators' Workshop: Update 1993. Standard Experiments in Engineering Materials Science and Technology
[NASA-CP-3259] p 4229 N94-36398
The analysis of a generic air-to-air missile simulation model
[NASA-TM-109057] p 4309 N94-36438

NATIONAL AERONAUTICS AND SPACE ADMINISTRATION. LEWIS RESEARCH CENTER, CLEVELAND, OH.
Addition polyimides with enhanced processability
[NASA-CASE-LEW-15043-1] p 4242 N94-35234
A comparison of atomic oxygen erosion yields of carbon and selected polymers exposed in ground based facilities and in low Earth orbit
[NASA-TM-106622] p 4243 N94-35243
Interface shape and convection during solidification and melting of succinonitrile
[NASA-TM-106487] p 4262 N94-35248
Effects of combined stressing on the electrical properties of film and ceramic capacitors
[NASA-TM-106605] p 4257 N94-35249
Experimental results of hydrogen slosh in a 62 cubic foot (1750 liter) tank
[NASA-TM-106625] p 4263 N94-35250
Dynamic and thermal turbulent time scale modelling for homogeneous shear flows
[NASA-TM-106635] p 4263 N94-35253
Description and use of LSODE, the Livermore Solver for Ordinary Differential Equations
[NASA-RP-1327] p 4313 N94-35259
A novel method for depositing precious metal films on difficult surfaces
[NASA-TM-106607] p 4243 N94-35260
Instrumentation for in-flight SSME rocket engine plume spectroscopy
[NASA-TM-106596] p 4268 N94-35268
Review of slow-wave structures
[NASA-TM-106639] p 4258 N94-35270
Au/Zn contacts to Rho-InP: Electrical and metallurgical characteristics and the relationship between them
[NASA-TM-106590] p 4281 N94-35271
Computational methods for HSCT-inlet controls/CFD interdisciplinary research
[NASA-TM-106618] p 4198 N94-35352
High-temperature, bellows hybrid seal
[NASA-CASE-LEW-15570-1] p 4274 N94-35373
Multiwavelength pyrometer for gray and non-gray surfaces in the presence of interfering radiation
[NASA-CASE-LEW-15250-1] p 4269 N94-35383
Atomic oxygen protective coating with resistance to undercutting at defect sites
[NASA-CASE-LEW-15306-1] p 4243 N94-35502
Challenging the Future - Journey to Excellence. Aeropropulsion strategic plan for the 1990's
[NASA-TM-109250] p 4228 N94-35591
Microgravity isolation system design: A modern control synthesis framework p 4215 N94-35851
Electromechanical simulation and test of rotating systems with magnetic bearing or piezoelectric actuator active vibration control p 4223 N94-35905
A supersonic tunnel for laser and flow-seeding techniques
[NASA-TM-106588] p 4265 N94-35945

Comparison of PDF and moment closure methods in the modeling of turbulent reacting flows
[NASA-TM-106614] p 4265 N94-35948

Boundary conditions for jet flow computations
[NASA-TM-106648] p 4266 N94-35976

Information and communication technology
p 4257 N94-36043

Advanced composites in Japan p 4234 N94-36045

High temperature creep and oxidation resistant chromium silicide matrix alloy containing molybdenum
[NASA-CASE-LEW-15697-1] p 4241 N94-36275

Compliant metal enhanced convection cooled reverse-flow annular combustor
[NASA-TM-106626] p 4199 N94-36379

NATIONAL AERONAUTICS AND SPACE ADMINISTRATION. MARSHALL SPACE FLIGHT CENTER, HUNTSVILLE, AL.

Plasma arc welding weld imaging
[NASA-CASE-MFS-28797-1] p 4273 N94-35367

ATLAS solar pointing operations
p 4201 N94-35626

Space and transatmospheric propulsion technology
p 4229 N94-36047

Natural orbital environment definition guidelines for use in aerospace vehicle development
[NASA-TM-4527] p 4291 N94-36175

NATIONAL AERONAUTICS AND SPACE ADMINISTRATION. PASADENA OFFICE, CA.

High temperature sorbents for oxygen
[NASA-CASE-NPO-18409-1-CU] p 4235 N94-35255

Separation tool for multipin electrical connectors
[NASA-CASE-NPO-18786-1-CU] p 4274 N94-35375

Adjustable control station with movable monitors and cameras for viewing systems in robotics and teleoperations
[NASA-CASE-NPO-17837-1-CU] p 4332 N94-35384

Method and apparatus for removing unwanted reflections from an interferometer
[NASA-CASE-NPO-18478-1-CU] p 4333 N94-35749

NATIONAL AEROSPACE LAB., AMSTERDAM (NETHERLANDS).

Fatigue and residual strength behaviour of ARALL3 panels with bonded-on doublers
[AD-B181062] p 4279 N94-36226

NATIONAL AEROSPACE LAB., TOKYO (JAPAN).

Status of MSBS study at NAL p 4216 N94-35854

NATIONAL CHENG KUNG UNIV., TAINAN (TAIWAN).

Fuzzy self-learning control for magnetic servo system
p 4215 N94-35852

A dynamic method for magnetic torque measurement
p 4216 N94-35856

Time-delay control of a magnetic levitated linear positioning system p 4217 N94-35862

Nonlinear feedback model attitude control using CCD in magnetic suspension system p 4225 N94-35912

NATIONAL DEFENCE ACADEMY, TOKYO (JAPAN).

Third order LPF type compensator for flexible rotor suspension p 4217 N94-35863

NATIONAL GEOPHYSICAL DATA CENTER, BOULDER, CO.

Solar-geophysical data number 594, February 1994. Part 2: (Comprehensive reports). Data for August 1993, and miscellaneous
[PB94-164001] p 4374 N94-36009

Solar-geophysical data number 594, February 1994. Part 1: (Prompt reports). Data for December 1993, January 1994, and late data
[PB94-163995] p 4375 N94-36020

NATIONAL INST. FOR FUSION SCIENCE, NAGOYA (JAPAN).

LHD helical divertor
[DE94-727626] p 4336 N94-35752

A triggering mechanism of fast crash in sawtooth oscillation
[DE94-718974] p 4336 N94-35772

Particle orbit analysis for LHD helical axis configurations
[DE94-718995] p 4336 N94-35773

NIFS Symposium: Toward the research of fusion burning plasmas, present status and future strategy
[DE94-727618] p 4336 N94-35775

Analysis of current diffusive ballooning mode
[DE94-718992] p 4336 N94-35811

Thickness of the layer of strong radial electric field in JFT-2M H-mode plasmas
[DE94-718993] p 4336 N94-35812

Applications of non-resonant RF forces for improvement of tokamak reactor performances. Part 1: Application of ponderomotive force
[DE94-718994] p 4336 N94-35813

Heating experiments using neutral beams with variable injection angle and ICRF waves in CHS
[DE94-718982] p 4337 N94-35936

K-epsilon model of anomalous transport in resistive interchange turbulence
[DE94-718983] p 4337 N94-35937

Neoclassical current and related MHD stability, gap modes, and radial electric field effects in heliotron and torsatron plasmas
[DE94-718987] p 4337 N94-35938

Atomic physics and radiation processes in plasmas
[DE94-727617] p 4337 N94-35939

Potential formation and transport in open field line systems
[DE94-718910] p 4337 N94-35983

Improved models of beta-limit, anomalous transport and radial electric field with loss cone loss in heliotron/torsatron
[DE94-718976] p 4324 N94-35984

The new features of Ion Bernstein Wave Heating in JIPP T-2U tokamak
[DE94-718978] p 4338 N94-36247

Design study of LHD helical divertor and high temperature divertor plasma operation
[DE94-718975] p 4338 N94-36352

Modelling of ELMs and dynamic responses of the H-mode
[DE94-718977] p 4339 N94-36353

MHD and confinement characteristics in the high-beta regime on the CHS low-aspect-ratio heliotron/torsatron
[DE94-718981] p 4339 N94-36357

NATIONAL INST. OF RADIOLOGICAL SCIENCES, CHIBA (JAPAN).

Activities of National Institute of Radiological Sciences
[DE94-727636] p 4296 N94-36101

NATIONAL INST. OF STANDARDS AND TECHNOLOGY, GAITHERSBURG, MD.

Classification of advanced technical ceramics
[REPT-15] p 4243 N94-35335

Computation of dendrites using a phase field model
[PB94-160744] p 4236 N94-35736

Intelligent processing of materials, technical activities, 1993 (NAS-NRC Assessment Panel, April 21-22 1994)
[PB94-164183] p 4251 N94-35737

Concept for an algorithm testing and evaluation program at NIST
[PB94-163029] p 4304 N94-35740

Data acquisition systems
[DE94-009848] p 4345 N94-35817

Fire data management system, FDMS 2.0, technical documentation
[PB94-164019] p 4346 N94-35819

North American ISDN Users' Forum agreements on Integrated Services Digital Network
[PB94-162559] p 4305 N94-35940

Piggyback balance experiment: An illustration of Archimedes' principles and Newton's third law
[PB94-163060] p 4265 N94-35942

Computer Systems Laboratory
[PB94-162518] p 4333 N94-36002

CSTL technical activities, 1991
[PB94-160769] p 4318 N94-36003

Report on the Workshop on Manufacturing Polymer Composites by Liquid Molding
[PB94-160066] p 4234 N94-36004

Proceedings of the Workshop on the Federal Criteria for Information Technology Security
[PB94-162583] p 4346 N94-36005

Thermophysical properties of HFC-143a and HFC-152a
[DE94-009995] p 4251 N94-36008

Review of Mathematical Function Library for Microsoft-FORTRAN, John Wiley and Sons, 1989
[PB94-160793] p 4305 N94-36010

NATIONAL OCEANIC AND ATMOSPHERIC ADMINISTRATION, RESEARCH TRIANGLE PARK, NC.

Analysis of regional visibility in the eastern United States using aerosol models
[PB94-158698] p 4332 N94-35584

NATIONAL PHYSICAL LAB., TEDDINGTON (ENGLAND).

Report on a SQUID made from high temperature superconductor
[PB94-169307] p 4339 N94-35598

Determination of extensional viscosity from capillary rheometer entrance pressure drop measurements using a numerical simulation of contraction flow
[PB94-171154] p 4263 N94-35603

NATIONAL TRANSPORTATION SAFETY BOARD, WASHINGTON, DC.

Safety study: A review of flightcrew-involved, major accidents of US air carriers, 1978 through 1990
[PB94-917001] p 4191 N94-35482

Annual review of aircraft accident data. US general aviation, calendar year 1992
[PB94-181054] p 4192 N94-35496

Aircraft accident report: Uncontrolled collision with terrain, American International Airways Flight 808, Douglas DC-8-61, N814CK, US Naval Air Station, Guantanamo Bay, Cuba, 18 August 1993
[PB94-910406] p 4192 N94-35521

NAUCHNO-ISSLEDOVATELSKII INST. EHLEKTROFIZICHESKOJ APPARATURY, LENINGRAD (USSR).

Optimization of turn position of tokamak inductor
[DE94-612627] p 4336 N94-35791

NAVAL AIR WARFARE CENTER, PATUXENT RIVER, MD.

Aerial refueling interoperability from a receiver flying qualities perspective p 4197 N94-36343

NAVAL AIR WARFARE CENTER, WARMINSTER, PA.

Processing and properties of high temperature metal/fiber-reinforced-thermoplastic laminates
[AD-A278791] p 4232 N94-35654

A database to evaluate acceleration (+Gz) induced loss of consciousness (G-LOC) in the human centrifuge
[AD-A278769] p 4299 N94-35707

The case for surface effect research, platform applications and technology development opportunities
p 4194 N94-36325

Propulsion system selection for a High Altitude Long Endurance aircraft p 4195 N94-36333

NAVAL COMMAND, CONTROL AND OCEAN SURVEILLANCE CENTER, SAN DIEGO, CA.

Environment/tool integrator for software development, version 1.2
[AD-A278965] p 4303 N94-35660

The iWarp display module
[AD-A278610] p 4260 N94-36248

NAVAL POSTGRADUATE SCHOOL, MONTEREY, CA.

A gallium arsenide MESFET operational amplifier for use in composite operational amplifiers
[AD-A277843] p 4258 N94-35539

A lower bound for the intersection of regular forests
[AD-A278653] p 4303 N94-35576

Stopping rules for a class of sampling-based stochastic programming algorithms
[AD-A278654] p 4303 N94-35577

Cramer-von Mises variance estimators for simulations
[AD-A278799] p 4316 N94-35675

A critique of type systems for global overloading
[AD-A278800] p 4304 N94-35676

An iterative extension of Prony's method for ARMA signal modeling
[AD-A278841] p 4319 N94-35800

Data reduction, analysis and results of LACV-30-07 air cushion vehicle tests, Fort Story, VA, August - September 1993
[AD-A278859] p 4190 N94-35826

Object-oriented simulation pictures (OOSPic) for design and testing
[AD-A278798] p 4305 N94-36013

Three dimensional visualization of a coastal mesoscale model
[AD-A278576] p 4294 N94-36187

Computer graphics tools for the visualization of spacecraft dynamics
[AD-A278615] p 4226 N94-36251

NAVAL RESEARCH LAB., WASHINGTON, DC.

Developing software for ease of change: Metrics from later in the TRALAB system life cycle
[AD-A278759] p 4302 N94-35490

A software architecture for adding new interaction techniques to a command and control based testbed
[AD-A278760] p 4302 N94-35491

Experimental studies of very-high Mach number hydrodynamics
[AD-A278761] p 4263 N94-35492

Theoretical aspect of low pressure discharges in simple gasses
[AD-A278762] p 4335 N94-35493

NAVSPACECOM space surveillance sensor system digital signal processing receiver. Volume 3: Operating system functions
[AD-A278839] p 4212 N94-35799

NAVSPACECOM space surveillance sensor system digital signal processing receiver. Volume 4: Hardware interfaces
[AD-A278845] p 4212 N94-35801

Analysis of recent agile mirror data
[AD-A278758] p 4318 N94-36427

NAVAL SURFACE WARFARE CENTER, BETHESDA, MD.

Tipjet 80-inch model rotor hover test: Test no. 1198
[AD-A279680] p 4191 N94-36261

NAVAL SURFACE WARFARE CENTER, DAHLGREN, VA.

Preliminary study of satellite attitude determination for the LANDSAT 7 spacecraft
[AD-A278876] p 4212 N94-35585

User's guide for an interactive personal computer interface for the aeroprediction code
[NSWCDD/TR-94/107] p 4305 N94-35958

NAVAL WAR COLL., NEWPORT, RI.

Geostationary space launch vehicles and the US dilemma p 4210 N94-35377

NETHERLANDS AEROSPACE MEDICAL CENTRE, SOESTERBERG.
Review of human factors problems related to long distance and long endurance operation of aircraft
p 4195 N94-36336

NEVADA UNIV. SYSTEM, RENO, NV.
Particulate and gaseous organic receptor modeling for the Southern California Air Quality Study
[PB94-156700] p 4285 N94-35735

NEW HAMPSHIRE UNIV., DURHAM.
A search for energetic ion directivity in large solar flares
[NASA-CR-196036] p 4374 N94-35993

NEW MEXICO STATE UNIV., LAS CRUCES, NM.
Issues in the development of a 10 MBPS K=15 Viterbi decoder
[NASA-CR-196083] p 4211 N94-35357

NEW MEXICO UNIV., ALBUQUERQUE, NM.
Experimental and theoretical studies of a high temperature cesium-barium tacitron, with application to low voltage-high current inversion
[DE94-008182] p 4228 N94-35349

NEWCASTLE-UPON-TYNE UNIV., NEWCASTLE (ENGLAND).
Parallel algorithms for LU decomposition on a shared memory multiprocessor
[PB94-167798] p 4314 N94-35531
Robust requirements specifications for safety-critical systems
[PB94-167806] p 4250 N94-35532
ORDIT: A new methodology to assist in the process of eliciting and modelling organisational requirements
[PB94-167814] p 4345 N94-35533
High level modelling and design of asynchronous interface logic
[PB94-167822] p 4258 N94-35534
The rel/REL: A family of reliable multicast protocols for distributed real-time systems
[PB94-167830] p 4310 N94-35535

NICE UNIV. (FRANCE).
Use of formal calculation to automatically obtain adjoint programs
[PB94-170701] p 4308 N94-36259

NORTH CAROLINA STATE UNIV., RALEIGH, NC.
Switched-beam radiometer front-end network analysis
[NASA-CR-194922] p 4252 N94-35247
Numerical modeling studies of wake vortex transport and evolution within the planetary boundary layer
[NASA-CR-196078] p 4192 N94-35522

NORTH CAROLINA UNIV., CHARLOTTE, NC.
Design and simulation of EVA tools for first servicing mission of HST
[NASA-CR-196030] p 4298 N94-35266
Materials for efficient high-flux magnetic bearing actuators p 4214 N94-35845
Parameter estimation of the vibrational model for the SCOLE experimental facility p 4219 N94-35878
Analysis of achievable disturbance attenuation in a precision magnetically-suspended motion control system
p 4225 N94-35917

NORTHWESTERN UNIV., EVANSTON, IL.
The growth of silicon nitride crystalline films using microwave plasma enhanced chemical vapor deposition
[AD-A278862] p 4340 N94-35828
Transformation plasticity in ductile solids
[DE94-010420] p 4240 N94-35953
Some perspectives on solution-phase electron-transfer processes
[AD-A278616] p 4238 N94-36252
Ion modulated electroactivity in thin film metallopolymers
[AD-A278618] p 4246 N94-36253
Computational methods for material failure processes
[AD-A278716] p 4278 N94-36292
Dynamic structural effects and ultrafast biomolecular kinetics in photoinduced charge transfer reactions
[DE94-010421] p 4329 N94-36390

NYMA, INC., BROOK PARK, OH.
Isothermal damage and fatigue behavior of SCS-6/Timetal 21S (0/90)s composite at 650 C
[NASA-CR-195345] p 4234 N94-35995

O

OAK RIDGE NATIONAL LAB., TN.
Large scale atomistic first principles study of adsorption and surface diffusion
[DE94-009450] p 4322 N94-35682
Performance analysis of reciprocating regenerative magnetic heat pumping
[DE94-009488] p 4264 N94-35683
Biaxial loading and shallow-flaw effects on crack-tip constraint and fracture-toughness
[DE94-010128] p 4279 N94-35684
Properties and applications of powder-filled evacuated-panel superinsulations
[DE94-009169] p 4233 N94-35932
High-resolution imaging using Z-contrast Scanning Transmission Electron Microscopy
[DE94-008510] p 4333 N94-36055
Development of atmospheric characteristics of chlorine-free alternative fluorocarbons
[DE94-009791] p 4287 N94-36179
Investigation of moisture-induced embrittlement of iron aluminides
[DE94-010881] p 4241 N94-36196
Selected translated abstracts of Russian-language climate-change publications. 2: Clouds
[DE94-011465] p 4295 N94-36244
Dissociative recombination of stored and phase-spaced cooled molecular ions in CRYRING
[DE94-002459] p 4327 N94-36267
Modernization of the graphics post-processors of the Hamburg German Climate Computer Center Carbon Cycle Codes
[DE94-011604] p 4288 N94-36273
Netlib services and resources
[DE94-010307] p 4347 N94-36300
Flux-pinning related defects in YBa2Cu3O(7-x) thin films grown on miscut LaAlO3 (001) substrates
[DE94-011463] p 4342 N94-36377
Developments in carbon materials
p 4231 N94-36409

OAK RIDGE Y-12 PLANT, TN.
Consolidation of zircaloy-4 end crops by induction melting
[DE94-010031] p 4240 N94-35650

OFFICE NATIONAL D'ETUDES ET DE RECHERCHES AEROSPATIALES, PARIS (FRANCE).
The future of large capacity/long range multipurpose air cargo fleets p 4194 N94-36326

OHIO STATE UNIV., COLUMBUS.
A review of radial forging technology including preform design for process optimization
[AD-A278770] p 4250 N94-35711
Robust control design techniques for active flutter suppression p 4200 N94-35875
Vibration suppression in flexible structures via the sliding-mode control approach p 4220 N94-35884
Expansion effects on supersonic turbulent boundary layers
[AD-A278989] p 4190 N94-35950
Recovery of frozen flow losses in arcjets
[AD-A278739] p 4228 N94-36089

OLD DOMINION UNIV., NORFOLK, VA.
Some further developments in the dynamic modelling and control of the large angle magnetic suspension test fixture p 4217 N94-35860
Control of the SCOLE configuration using distributed parameter models p 4221 N94-35885

OSLO UNIV. (NORWAY).
Studies of the dayside boundary layer processes based on ground observations in the Svalbard area
[AD-A280715] p 4292 N94-36265

OVERSET METHODS, INC., LOS ALTOS, CA.
Overset grid applications on distributed memory MIMD computers
[NASA-CR-196081] p 4268 N94-36397

OXFORD UNIV. (ENGLAND).
Probabilities and priorities in timed CSP
[PB94-169216] p 4316 N94-35536
Mathematical theory of synchronous communication
[PB94-169224] p 4252 N94-35537

P

PACIFIC NORTHWEST LAB., RICHLAND, WA.
Introduction to Neural Networks: Neural Network Workshop for the Hanford Community
[DE94-006526] p 4311 N94-35348
The Atmospheric Radiation Measurement Program and interfaces with external data sources
[DE94-003699] p 4286 N94-36024
Analysis of mid-tropospheric carbon monoxide data using a three-dimensional global atmospheric chemistry numerical model
[DE94-004782] p 4286 N94-36026
Air quality implications associated with the selection of power plants in the Pacific Northwest
[DE94-004783] p 4287 N94-36027
Aerosol optical depth derived from solar radiometry observations at northern mid-latitude sites
[DE94-007476] p 4287 N94-36053
A procedure for oscillatory parameter identification
[DE94-008047] p 4259 N94-36054
A comparison of artificial neural networks and statistical analyses
[DE94-010846] p 4312 N94-36195
SYNTH: A spectrum synthesizer
[DE94-004719] p 4331 N94-36317
Global tropospheric chemistry models for radiatively important trace species: Design and research recommendations
[DE94-007089] p 4288 N94-36359

PAKISTAN INST. OF NUCLEAR SCIENCE AND TECHNOLOGY, ISLAMABAD.
Computer automation and artificial intelligence
[DE94-611058] p 4312 N94-35831

PARIS VI UNIV. (FRANCE).
Application of GaSe and AgGaSe2 crystal growth to non-linear optics
[PB94-170552] p 4341 N94-36212

PARIS XI UNIV., ORSAY (FRANCE).
Local instabilities and the transition to chaos of non-linear waves
[PB94-170578] p 4341 N94-36213

PENNSYLVANIA STATE UNIV., UNIVERSITY PARK, PA.
Detailed studies of soot formation in laminar diffusion flames for application to modeling studies
[AD-A278941] p 4235 N94-35604
An electronic interface for a fiber optic tethered unmanned underwater vehicle
[AD-A279046] p 4333 N94-35747
The aerodynamic and heat transfer effects of an endwall boundary layer fence in a 90 degree turning square duct
[AD-A278903] p 4265 N94-35803
Variations in the modal characteristics of a telescopically deploying beam p 4218 N94-35872
The effect of alternative fuels on the stability and lubricity of crankcase lubricants
[DE94-010353] p 4245 N94-36108
Metal cluster alloys and oxides: Elucidating structural and electronic effects in governing the reactivity and catalytic role of matter in finite dimensions
[DE94-010224] p 4328 N94-36298
Continuous unidirectional fiber reinforced composites: Fabrication and testing p 4229 N94-36400

PENNSYLVANIA UNIV., PHILADELPHIA, PA.
An environment for visualization, reliability, and knowledge acquisition in equational programming
[AD-A278639] p 4308 N94-36258

PHOTOMETRICS, INC., WOBURN, MA.
Molecular nitrogen fluorescence lidar for remote sensing of the auroral ionosphere
[AD-A280716] p 4291 N94-36263

PITTSBURGH UNIV., PITTSBURGH, PA.
Chemical reactions of chlorine on a vicinal Si(100) surface studied by ESDIAD
[AD-A279059] p 4236 N94-35731

POITIERS UNIV. (FRANCE).
Transformation of a Cranz-Schardin camera
[PB94-170685] p 4270 N94-36219

POLISH ACADEMY OF SCIENCES, WARSAW.
Testing of the fracture resistance of rails
p 4279 N94-35353
On optimal placement of spacers in bundled conductors p 4258 N94-35354

POLITECNICO DI TORINO (ITALY).
Design, construction, and testing of a five active axes magnetic bearing system p 4214 N94-35846
Active magnetic bearing control loop modeling for a finite element rotordynamics code p 4216 N94-35857

PRAIRIE VIEW AGRICULTURAL AND MECHANICAL COLL., TX.
Support of hadroproduction of bottom using the 800 GeV/c primary photon beam at the Fermilab tevatron
[DE94-009411] p 4324 N94-36016

PRINCETON UNIV., NJ.
Multidisciplinary studies of integrated neural network systems
[AD-A278774] p 4312 N94-36309

PURDUE UNIV., ELKHART, IN.
Graphing techniques for materials laboratory using Excel p 4232 N94-36414

PURDUE UNIV., WEST LAFAYETTE, IN.
Frequency domain analysis of the random loading of cracked panels
[NASA-CR-196021] p 4279 N94-35974
Aeroservoelastic tailoring with piezoelectric materials: Actuator optimization studies
[AD-A278640] p 4199 N94-36384

R

RADIO TECHNICAL COMMISSION FOR AERONAUTICS, WASHINGTON, DC.
Minimum performance standards: Airborne low-range radar altimeters
[RTCA-DO-155] p 4198 N94-35344

RENSSELAER POLYTECHNIC INST., TROY, NY.
Analysis of phase distribution phenomena in microgravity environments
[NASA-CR-196038] p 4249 N94-35237

Investigation of moisture-induced embrittlement of iron aluminides
[DE94-010881] p 4241 N94-36196

RESEARCH INST. FOR ADVANCED COMPUTER SCIENCE, MOFFETT FIELD, CA.
Computation of helicopter rotor acoustics in forward flight
[NASA-CR-196132] p 4319 N94-36031

RICARDO NORTH AMERICA, INC., BURR RIDGE, IL.
Analysis of the injection process in direct injected natural gas engines
[PB94-156494] p 4275 N94-35931

RICE UNIV., HOUSTON, TX.
Computational Mathematics Laboratory for multiscale analysis
[AD-A278597] p 4315 N94-36424
High energy
[DE94-009477] p 4331 N94-36428

ROBICON, INC., PRINCETON, NJ.
Multidisciplinary studies of integrated neural network systems
[AD-A278774] p 4312 N94-36309

ROCHESTER INST. OF TECH., NY.
High power diode laser Master Oscillator-Power Amplifier (MOPA)
[NASA-CR-196095] p 4271 N94-35488

ROLLS-ROYCE LTD., BRISTOL (ENGLAND).
Propulsion system technologies for long range and long endurance aircraft p 4195 N94-36334

ROYAL NETHERLANDS AIR FORCE, THE HAGUE.
The KDC-10 programme of the Royal Netherlands Air Force p 4197 N94-36346

RUTGERS - THE STATE UNIV., PISCATAWAY, NJ.
Multicomponent glass surfaces: Structure and adsorption
[DE94-010516] p 4246 N94-36283

RUTHERFORD APPLETON LAB., CHILTON (ENGLAND).
ROSAT/XRT-PSPC observations and the ionizing continuum of Seyfert 1 galaxy Mkn 478
[PB94-167053] p 4350 N94-35530
Beam tests of a prototype level-1 calorimeter trigger for LHC experiments
[PB94-170495] p 4269 N94-35599
MMI(exp 2) demonstrator systems: A multi-modal interface for man machine interaction with knowledge based systems. Deliverable D17 (TA 2) ESPRIT project 2474 MMI(exp 2)
[PB94-170537] p 4298 N94-35600
Experimental characterisation of gas microstrip detectors. Part 2: Counting rate characteristics
[PB94-167095] p 4269 N94-36061
Specification for the TITANIA krF laser system
[PB94-167103] p 4272 N94-36062
Collective plasma corrections to the solar opacity
[PB94-170511] p 4375 N94-36210
The EASE Visualization Community Club
[PB94-170529] p 4308 N94-36211

S

SANDIA NATIONAL LABS., ALBUQUERQUE, NM.
Laser drilling of vertical vias in silicon
[DE94-009250] p 4270 N94-35351
A review and development of correlations for base pressure and base heating in supersonic flow
[SAND93-0280] p 4189 N94-35360
Manufacturing feasibility of several lead-free solders for electronic assembly
[DE94-007732] p 4258 N94-35564
Evaluation of synthetic aperture radar for oil-spill response
[AD-A278796] p 4284 N94-35674
The optimization of interfaces in InAsSb/InGaAs strained-layer superlattices grown by metal-organic chemical vapor deposition
[DE94-010070] p 4340 N94-35698
Designing aluminum sealing glasses for manufacturability
[DE94-010081] p 4244 N94-35699
Cross-condensation reactions in an organically modified silica sol-gel
[DE94-010086] p 4244 N94-35701
Spinnability of silica sols: The role of alkoxy group exchange
[DE94-010087] p 4244 N94-35702
Extraction of cloud statistics from whole sky imaging cameras
[DE94-009867] p 4294 N94-35766
The computation of cloud base height from paired whole-sky imaging cameras
[DE94-009868] p 4294 N94-35767
Hydrodynamics of maneuvering bodies: LDRD Final Report
[DE94-009970] p 4265 N94-35769
Decision and systems analysis for underground storage tank waste retrieval systems and tank waste remediation system
[SAND94-0065] p 4286 N94-35957
Plane shock generator explosive lens: Shock characterization of 4340 and PH13-8Mo steels, C360 brass and PZT 65/35 ferro-electric ceramic
[DE94-009254] p 4266 N94-35979
Analysis of a High Velocity Oxygen-Fuel (HVOF) thermal spray torch. Part 1: Numerical formulation
[DE94-005590] p 4267 N94-35996
Predicted optical performance of the High-Altitude Balloon Experiment (HABE) telescope in an adverse thermal environment
[DE94-008949] p 4349 N94-35998
Input shaping for three-dimensional slew maneuvers of a precision pointing flexible spacecraft
[DE94-008937] p 4226 N94-36001
Heterogeneous reaction mechanisms and kinetics relevant to the CVD of semiconductor materials
[DE94-011001] p 4340 N94-36032
Capillary flow solderability test for printed wiring boards
[DE94-010321] p 4259 N94-36094
Non-alloyed, refractory metal contact optimization with shallow implantations of Zn and Mg
[DE94-010392] p 4240 N94-36110
A multi-tiered wavefront sensor using binary optics
[DE94-010393] p 4267 N94-36111
Phase-locked arrays of vertical-cavity surface-emitting lasers
[DE94-009279] p 4272 N94-36178
Beam transport
[DE94-010755] p 4331 N94-36199
Magnetic properties of nanosize iron clusters
[DE94-011329] p 4318 N94-36204
Microstructural development in solution derived PZT thin films
[DE94-008744] p 4246 N94-36209
Continuum fluorescence of Cu in NbTi/Cu composite wires
[DE94-008940] p 4241 N94-36242
Demonstration of a high heat removal CVD diamond substrate edge-cooled multichip module
[DE94-010748] p 4260 N94-36245
Enhanced charge trapping in bipolar spacer oxides during low-dose-rate irradiation
[DE94-007863] p 4260 N94-36268
Implementation of Raman lidar for profiling of atmospheric water vapor and aerosols at the SGP CART site
[DE94-011754] p 4295 N94-36285
Application of higher-order multipoint statistics to the ideal spray
[DE94-005104] p 4268 N94-36318
SandiaXTP, an object-oriented implementation of XTP 3.7
[DE94-011752] p 4257 N94-36354
Hardness variability in commercial and hardened technologies
[DE94-007270] p 4261 N94-36362
Estimating low-dose rate. irradiation response of MOSFETs
[DE94-007292] p 4342 N94-36367
Bounding the total-dose response of modern bipolar transistors
[DE94-007742] p 4261 N94-36371
A critical examination of charge funneling and its impact on single-event upset in Si devices
[DE94-007868] p 4261 N94-36373
Network analyzer calibration for cryogenic on-wafer measurements
[DE94-010089] p 4262 N94-36430

SANDIA NATIONAL LABS., LIVERMORE, CA.
The thermochemistry and reaction mechanisms in the decomposition of energetic materials
[DE94-011420] p 4248 N94-36376

SATCON TECHNOLOGY CORP., CAMBRIDGE, MA.
Aerospace applications of magnetic bearings
p 4213 N94-35837
Superconducting rebalance acceleration and rate sensor p 4223 N94-35904
Electrostatically suspended and sensed micro-mechanical rate gyroscope p 4224 N94-35908

SCIENCE APPLICATIONS INTERNATIONAL CORP., ARLINGTON, VA.
Center for seismic studies
[AD-A278682] p 4290 N94-35693

SCIENCE APPLICATIONS INTERNATIONAL CORP., MCLEAN, VA.
Numerical simulation of shock interaction with above-ground structures
[AD-A278713] p 4279 N94-35949

SCIENCE RESEARCH COUNCIL, CHILTON (ENGLAND).
Beam tests of a prototype level-1 calorimeter trigger for LHC experiments
[PB94-170495] p 4269 N94-35599

SCIENCE RESEARCH LAB., INC., SOMERVILLE, MA.
Advanced induction accelerator designs for ground based and space based FELs
[AD-A278685] p 4271 N94-35586

SEATTLE PACIFIC COLL., WA.
Error reduction in images with the use of additional information
[AD-A278636] p 4334 N94-36257

SI DIAMOND TECHNOLOGY, INC., HOUSTON, TX.
An experimental investigation of active control of thrust vectoring nozzle flow fields
[AD-A278702] p 4229 N94-36291

SIENA COLL., LONDONVILLE, NY.
Microscale synthesis and characterization of polystyrene: NSF-POLYED scholars project
p 4231 N94-36408

SMITHSONIAN ASTROPHYSICAL OBSERVATORY, CAMBRIDGE, MA.
Development of POINTS as a planetology instrument
[NASA-CR-196026] p 4354 N94-35265
TransFit: Finite element analysis data fitting software
[NASA-CR-193988] p 4307 N94-36118
AXAF-I ghost ray study: On orbit case
[NASA-CR-193987] p 4333 N94-36119

SOUTH DAKOTA SCHOOL OF MINES AND TECHNOLOGY, RAPID CITY, SD.
The effects of cloud inhomogeneities upon radiative fluxes, and the supply of a cloud truth validation dataset
[NASA-CR-196080] p 4293 N94-35391

SOUTHAMPTON UNIV. (ENGLAND).
The simulation of a propulsive jet and force measurement using a magnetically suspended wind tunnel model p 4191 N94-35855

SOUTHEASTERN UNIV. RESEARCH ASSOCIATION, NEWPORT NEWS, VA.
Goldstone pion and other mesons using a scalar confining interaction
[DE94-010016] p 4321 N94-35649
Elastic charge form factors for K mesons
[DE94-010014] p 4325 N94-36086
Beam energy absolute measurement using K-edge absorption spectrometers
[DE94-010019] p 4331 N94-36192

SOUTHERN CALIFORNIA EDISON CO., ROSEMEAD, CA.
National Maglev initiative: California line electric utility power system requirements p 4215 N94-35850

SOUTHWEST RESEARCH INST., SAN ANTONIO, TX.
Participation in the definition, conduct, and analysis of particle accelerator experiments for the first Spacelab Mission
[NASA-CR-193974] p 4330 N94-35483
Methanol fuel additive demonstration
[PB94-156668] p 4247 N94-35941

SPACE TELESCOPE SCIENCE INST., BALTIMORE, MD.
Apollo 11 at twenty-five, version 1.0
[NASA-CR-193380] p 4376 N94-35363
Hubble Space Telescope cycle 5 call for proposals
[NASA-CR-189363] p 4349 N94-36279
HST archive primer, version 4.1
[NASA-CR-189370] p 4349 N94-36280
Hubble Space Telescope Fine Guidance Sensors Instrument Handbook, version 4.0
[NASA-CR-189366] p 4349 N94-36281
Hubble Space Telescope Goddard High Resolution Spectrograph (GHRS) Instrument Handbook (for the Post-COSTAR Observatory), version 5.0
[NASA-CR-189369] p 4349 N94-36282

SPAUSCHUS ASSOCIATES, INC., STOCKBRIDGE, GA.
Solubility, viscosity and density of refrigerant/lubricant mixtures
[DE94-009996] p 4245 N94-35771

SPIRE CORP., BEDFORD, MA.
High temperature heterojunction bipolar transistors
[AD-A278605] p 4261 N94-36360

SRI INTERNATIONAL CORP., MENLO PARK, CA.
Novel catalysts for methane activation
[DE94-009705] p 4237 N94-35778

STANFORD LINEAR ACCELERATOR CENTER, CA.
Spin dynamics in storage rings and linear accelerators
[DE94-010320] p 4330 N94-36106
Precise measurement of the left-right cross section asymmetry in Z boson production by electron-positron collisions
[DE94-010751] p 4326 N94-36198
Dynamic aperture and transverse proton diffusion in HERA
[DE94-010309] p 4331 N94-36224

STANFORD UNIV., CA.
Investigation of Burnett equations for two-dimensional hypersonic flow
[AD-A278942] p 4190 N94-35717

STATE UNIV. OF NEW YORK, BUFFALO, NY.
MME-based attitude dynamics identification and estimation for SAMPEX p 4209 N94-35643
Transfer function modeling of damping mechanisms in distributed parameter models p 4222 N94-35895

STATE UNIV. OF SOUTHEAST MISSOURI, CAPE GIRARDEAU, MO.
Dielectric measurements of selected ceramics at microwave frequencies p 4232 N94-36412

STERLING SOFTWARE, INC., CLEVELAND, OH.
Telecommuting (work-at-home) at NASA Lewis Research Center
[NASA-CR-195334] p 4347 N94-36396

STERLING SOFTWARE, INC., MOFFETT FIELD, CA.
Alleviation of whirl-flutter on a joined-wing tilt-rotor aircraft configuration using active controls
[NASA-CR-196103] p 4200 N94-36436

STICHTING VOOR FUNDAMENTEEL ONDERZOEK DER MATERIE, UTRECHT (NETHERLANDS).
Aspects of robust computational modeling for plain and reinforced concrete
[PB94-169240] p 4251 N94-35820

STORM INTEGRATION, INC., SAN JOSE, CA.
Implementation of a low-cost, commercial orbit determination system p 4205 N94-35621

SULZER-ESCHER WYSS LTD., ZURICH (SWITZERLAND).
Rotor dynamic behaviour of a high-speed oil-free motor compressor with a rigid coupling supported on four radial magnetic bearings p 4224 N94-35911

SUPERCONDUCTING SUPER COLLIDER LAB., DALLAS, TX.
Models for interpreting interstrand resistance measurements in Rutherford cables
[DE94-010844] p 4259 N94-36194

SVERDRUP TECHNOLOGY, INC., BROOK PARK, OH.
Hot Corrosion Test Facility at the NASA Lewis Special Projects Laboratory
[NASA-CR-195323] p 4200 N94-35267

SYRACUSE UNIV., NY.
The relationship between hydroxyl groups on oxide surfaces and the properties of supported metals
[DE94-010786] p 4241 N94-36233

SYRE CORP., MOFFETT FIELD, CA.
Women as a resource for the flexibility required for high technology innovation p 4348 N94-35966

T

TECHNICAL RESEARCH CENTRE OF FINLAND, ESPOO.
BJT model in APLAC
[PB94-171022] p 4259 N94-35822

TECHNISCHE UNIV., DELFT (NETHERLANDS).
Aspects of robust computational modeling for plain and reinforced concrete
[PB94-169240] p 4251 N94-35820

TECHNISCHE UNIV., MUNICH (GERMANY).
Improvement of endurance performance by periodic optimal control of variable camber p 4194 N94-36329

TECHNISCHE UNIV., TWENTE (NETHERLANDS).
Proceedings of the 4th Workshop on the Next Generation of CASE Tools
[PB94-150372] p 4302 N94-35538

TECHNO-SCIENCES, INC., GREENBELT, MD.
Integrated design of structures, controls, and materials p 4218 N94-35869
A case study in nonlinear dynamics and control of articulated spacecraft: The Space Station Freedom with a mobile remote manipulator system p 4220 N94-35879

TELEDYNE BROWN ENGINEERING, HUNTSVILLE, AL.
Materials processing in space tasks. WBS task 5.4: Generic tasks
[NASA-CR-193979] p 4249 N94-35485

TEMPLE UNIV., PHILADELPHIA, PA.
Optimal disturbance rejecting control of hyperbolic systems p 4220 N94-35882

TENNESSEE UNIV., KNOXVILLE, TN.
On the Buckling/Kinking compressive failure of fibrous composites
[AD-A278865] p 4233 N94-35714
A mechanics mode for the compressive response of fiber reinforced composites
[AD-A278866] p 4233 N94-35715
Can the compressive response of fiber-reinforced composites be modelled by means of layered arrays?
[AD-A278864] p 4233 N94-35944

TEXAS A&M UNIV., COLLEGE STATION, TX.
Semigroup approximation and robust stabilization of distributed parameter systems p 4222 N94-35894

TEXAS UNIV., AUSTIN, TX.
Tracking system options for future altimeter satellite missions p 4205 N94-35622
Solitary waves and homoclinic orbits
[DE94-009428] p 4264 N94-35681
Morphological aspects of surface reactions
[DE94-010184] p 4236 N94-35685
Electrical microengineering of redox enzymes
[AD-A279015] p 4236 N94-35745
Universal SU(2/1) and the Higgs and fermion masses
[DE94-009182] p 4323 N94-35814
Kinetics studies following state-selective laser excitation
[DE94-010305] p 4330 N94-36105
Scaling laws for TEXT plasma profiles
[DE94-010832] p 4338 N94-36200

THYSSEN HENSCHEL AMERICA, INC.
Transrapid (the first high-speed Maglev train system certified ready for application): Development status and prospects for deployment p 4213 N94-35841

TOKYO UNIV. (JAPAN).
Magnetically suspended stepping motors for clean room and vacuum environments p 4225 N94-35915

TOLEDO UNIV., OH.
Synthesis of novel composite Platinum-DNA films by way of wet-spinning
[AD-A278763] p 4243 N94-35494

TURKU UNIV. (FINLAND).
Theoretical and experimental study of air and hydrogen electrodes
[DE94-763308] p 4283 N94-36060

U

UNION CARBIDE CORP., SOUTH CHARLESTON, WV.
Heterogeneous catalytic process for alcohol fuels from syngas
[DE94-010263] p 4248 N94-36299

UNIVERSITIES SPACE RESEARCH ASSOCIATION, BOULDER, CO.
Introduction to USRA
[NASA-CR-195980] p 4376 N94-35590

UNIVERSITY COLL. OF WALES, ABERYSTWYTH.
Determination of extensional viscosity from capillary rheometer entrance pressure drop measurements using a numerical simulation of contraction flow
[PB94-171154] p 4263 N94-35603

UNIVERSITY OF EASTERN ILLINOIS, CHARLESTON, IL.
Application of materials database (MAT.DB.) to materials education p 4230 N94-36402
Laminated thermoplastic composite material from recycled high density polyethylene p 4230 N94-36403

UNIVERSITY OF SOUTHERN CALIFORNIA, LOS ANGELES, CA.
Eyesafe rare earth crystal lasers for atmosphere soudings
[AD-A279486] p 4273 N94-36227

UNIVERSITY OF SOUTHERN CALIFORNIA, MARINA DEL REY, CA.
Good applications for crummy machine translation
[AD-A278689] p 4345 N94-35651
The impact of scaling on a multimedia connection architecture
[AD-A278700] p 4300 N94-35652
Synthesis of asynchronous systems from data flow specifications
[AD-A278687] p 4303 N94-35662
Reformulating query plans for multidatabase systems
[AD-A278688] p 4345 N94-35663

URBAN CONSORTIUM FOR TECHNOLOGY INITIATIVES.
How to develop a long term CO2 reduction plan
[DE94-009559] p 4284 N94-35668

US CENTER FOR RESEARCH AND EDUCATION ON STRATEGY AND TECHNOLOGY, ARLINGTON, VA.
Partners in space. International cooperation in space: Strategies for the new century
[ISBN-0-9629930-2-6] p 4348 N94-35901

UTAH STATE UNIV., LOGAN, UT.
Natural resources and environmental issues. Volume 1: Riparian Resources: A Symposium on the Disturbances, Management, Economics, and Conflicts Associated with Riparian Ecosystems p 4287 N94-36120

UTAH UNIV., SALT LAKE CITY, UT.
A two-dimensional model for collisional energy transfer in bimolecular ion-molecule dynamics
[AD-A278913] p 4321 N94-35589
Anionic states of LiFLi
[AD-A278830] p 4322 N94-35678
Vertical electron detachment energies for octahedral closed-shell multiply charged anions
[AD-A278835] p 4322 N94-35753
A combined experimental and theoretical study of the neutral, cationic and anionic Si3N cluster molecule
[AD-A278834] p 4323 N94-35792
Periodicity and peculiarity in 120 first and second row diatomic molecules
[AD-A278836] p 4323 N94-35793
New anionic states of the lithium trimer
[AD-A278832] p 4323 N94-35797
Anionic and neutral states of Li3O
[AD-A278833] p 4323 N94-35798
Vertical and adiabatical ionization energies and electron affinities of new Si(n)C and Si(n)O (n=1-3) molecules
[AD-A278863] p 4324 N94-36050

V

VIRGINIA POLYTECHNIC INST. AND STATE UNIV., BLACKSBURG, VA.
Maneuvering and control of flexible space robots p 4218 N94-35867
Measurement of a surface heat flux and temperature p 4231 N94-36407

VIRGINIA UNIV., CHARLOTTESVILLE, VA.
Optimization of residual stresses in MMC's using compensating/compliant interfacial layers. Part 2: OPTCOMP user's guide
[NASA-CR-195337] p 4278 N94-35239
Experimental measurement and calculation of losses in planar radial magnetic bearings p 4214 N94-35847
Neural network controller development for a magnetically suspended flywheel energy storage system p 4217 N94-35861
Analysis of high speed flow, thermal and structural interactions
[NASA-CR-196017] p 4268 N94-36420

W

WASHINGTON STATE UNIV., PULLMAN, WA.
Effect of microgravity on plant growth
[NASA-CR-196004] p 4296 N94-35257

WASHINGTON UNIV., SEATTLE, WA.
A quark model of bar Lambda production in bar Rho interactions
[DE94-008071] p 4324 N94-35824
X ray and gamma ray spectroscopy of solids under pressure
[DE94-011207] p 4238 N94-36203
Environmental measurements in the Beaufort Sea, Spring 1993
[AD-A278718] p 4296 N94-36293
Collapse of flux tubes
[DE94-004645] p 4328 N94-36304
The nucleon-nucleon potential in the chromodielectric soliton model
[DE94-004646] p 4329 N94-36305

WESTFIELD COLL., LONDON (ENGLAND).
Beam tests of a prototype level-1 calorimeter trigger for LHC experiments
[PB94-170495] p 4269 N94-35599

WESTINGHOUSE HANFORD CO., RICHLAND, WA.
Hydrodynamically induced loads on components submerged in high-level waste-storage tanks
[DE94-009663] p 4264 N94-35756

WESTINGHOUSE IDAHO NUCLEAR CO., INC., IDAHO FALLS, ID.
Portable high precision pressure transducer system
[DE94-010137] p 4270 N94-36389

WESTINGHOUSE SAVANNAH RIVER CO., AIKEN, SC.
Atmospheric and dispersion modeling in areas of highly complex terrain employing a four-dimensional data assimilation technique
[DE94-004041] p 4285 N94-35823
Tritiated ammonia formation
[DE94-011170] p 4237 N94-36056
Groundwater penetrating radar and high resolution seismic for locating shallow faults in unconsolidated sediments
[DE94-007284] p 4257 N94-36366

WESTINGHOUSE SCIENCE AND TECHNOLOGY CENTER, PITTSBURGH, PA.
A solid oxide fuel cell power system: 1992-1993 field operation
[DE94-010383] p 4283 N94-36109

WESTLAND HELICOPTERS LTD., YEOVIL (ENGLAND).
EH101: A new helicopter capable of long range missions p 4194 N94-36330

WICHITA STATE UNIV., KS.
Three-dimensional force data acquisition and boundary corrections for the Walter H. Beech Memorial 7 x 10 foot low speed wind tunnel
[AR93-2] p 4200 N94-36437

WISCONSIN-STOUT UNIV., MENOMONIE, WI.
Process capability determination of new and existing equipment p 4230 N94-36406

WISCONSIN UNIV., MADISON, WI.
Planar rotational magnetic micromotors with integrated shaft encoder and magnetic rotor levitation
p 4224 N94-35907
Gauss elimination by segments and multivariate polynomial interpolation
[AD-A278646] p 4315 N94-36012
Using experimental design modules for process characterization in manufacturing/materials processes laboratories p 4230 N94-36405
WRIGHT LAB., EGLIN AFB, FL.
An overview of multichip modules
[AD-A278730] p 4260 N94-36296
WRIGHT LAB., WRIGHT-PATTERSON AFB, OH.
Properties and bibliography of GaSe
[AD-A279064] p 4340 N94-35733
High Altitude Long Endurance aircraft design studies
p 4193 N94-36322

X

XERAD, INC., SANTA MONICA, CA.
Future ultra-speed tube-flight p 4225 N94-35918

CONTRACT NUMBER INDEX

SCIENTIFIC AND TECHNICAL AEROSPACE REPORTS VOLUME 32 NUMBER 11

Typical Contract Number Index Listing

AF PROJ. 2306 .... p 92 N94-11866

CONTRACT NUMBER
PAGE NUMBER
ACCESSION NUMBER

Listings in this index are arranged alphanumerically by contract number. Under each contract number the accession numbers denoting documents that have been produced as a result of research done under that contract are arranged in ascending order. The page number helps to locate the citation in the abstract section. The accession number denotes the number by which the citation is identified.

AF PROJ. 2295 .... p 4291 N94-36263
AF PROJ. 2308 .... p 4198 N94-35746
AF PROJ. 2310 .... p 4292 N94-36265
AF PROJ. 2311 .... p 4375 N94-36264
AF PROJ. 2688 .... p 4295 N94-36228
AF PROJ. 2781 .... p 4295 N94-36262
AF PROJ. 4600 .... p 4256 N94-35694
p 4256 N94-35713
AF PROJ. 4643 .... p 4291 N94-36116
AF PROJ. 7013 .... p 4312 N94-36309
AF PROJ. 7670 .... p 4273 N94-36227
AF-AFOSR-0005-91 .... p 4190 N94-35529
AF-AFOSR-0014-90 .... p 4323 N94-35805
AF-AFOSR-0063-90 .... p 4227 N94-36189
AF-AFOSR-0155-91 .... p 4218 N94-35872
AF-AFOSR-0237-85 .... p 4227 N94-35362
AF-AFOSR-0242-90 .... p 4233 N94-35952
AF-AFOSR-0318-91 .... p 4228 N94-36089
AF-AFOSR-0334-90 .... p 4315 N94-36424
AF-AFOSR-0335-90 .... p 4308 N94-36258
AF-AFOSR-0340-90 .... p 4278 N94-36292
AF-AFOSR-0347-91 .... p 4316 N94-36425
AF-AFOSR-0386-91 .... p 4199 N94-36384
AF-AFOSR-0412-91 .... p 4190 N94-35950
AF-AFOSR-1054-90 .... p 4221 N94-35886
ARB-A032-189 .... p 4287 N94-36183
ARB-A832-123 .... p 4247 N94-35941
ARB-A832-132 .... p 4285 N94-35735
ARPA ORDER 7013 .... p 4312 N94-36309
ARPA ORDER 7330 .... p 4310 N94-35597
ARPA ORDER 7597 .... p 4344 N94-35526
p 4303 N94-35573
ARPA ORDER 8313 .... p 4304 N94-35709
p 4304 N94-35718
CEC-BRE2-CT92-0274 .... p 4224 N94-35909
DA PROJ. 1L1-62211-A-47-A .... p 4199 N94-36379
DAAA22-89-M-0081 .... p 4250 N94-35711
DAAH04-93-C-0040 .... p 4261 N94-36360
DAAJ02-92-C-0055 .... p 4223 N94-35903
DAAL01-93-C-4064 .... p 4244 N94-35757
DAAL03-90-G-0090 .... p 4315 N94-36012
DABT63-91-C-0001 .... p 4300 N94-35652
DAJA45-93-C-0036 .... p 4290 N94-35744
DASG60-89-C-0129 .... p 4228 N94-35825
DE-AC01-88FE-61684 .... p 4282 N94-36021
DE-AC02-76CH-00016 .... p 4260 N94-36221
p 4327 N94-36239
p 4328 N94-36303
p 4341 N94-36358
DE-AC02-76CH-03000 .... p 4326 N94-36107
p 4327 N94-36241
p 4327 N94-36266
p 4332 N94-36431
DE-AC02-83CH-10093 .... p 4283 N94-36051
p 4283 N94-36052
p 4248 N94-36191
DE-AC02-90CH-10435 .... p 4283 N94-36243
DE-AC03-76SF-00098 .... p 4344 N94-35337
p 4250 N94-35364
p 4286 N94-36025
p 4237 N94-36033
p 4248 N94-36034
p 4324 N94-36058
p 4331 N94-36202
p 4350 N94-36229
p 4238 N94-36230
p 4317 N94-36234
p 4317 N94-36235
p 4297 N94-36269
p 4315 N94-36270
p 4331 N94-36271
p 4341 N94-36274
DE-AC03-76SF-00515 .... p 4330 N94-36106
p 4326 N94-36198
p 4331 N94-36224
DE-AC03-91SF-18601 .... p 4335 N94-35673
DE-AC03-91SF-18852 .... p 4212 N94-35648
DE-AC04-76DP-00613 .... p 4258 N94-35686
p 4244 N94-35705
p 4259 N94-35706
p 4312 N94-35810
p 4260 N94-36197
DE-AC04-76DP-00789 .... p 4225 N94-35916
DE-AC04-76DR-00789 .... p 4295 N94-36285
p 4268 N94-36318
p 4257 N94-36354
DE-AC04-88ID-12692 .... p 4245 N94-35809
DE-AC04-91AL-65030 .... p 4238 N94-36084
DE-AC04-94AL-85000 .... p 4270 N94-35351
p 4189 N94-35360
p 4258 N94-35564
p 4340 N94-35698
p 4244 N94-35699
p 4244 N94-35701
p 4244 N94-35702
p 4294 N94-35766
p 4294 N94-35767
p 4265 N94-35769
p 4286 N94-35957
p 4266 N94-35979
p 4267 N94-35996
p 4349 N94-35998
p 4226 N94-36001
p 4340 N94-36032
p 4259 N94-36094
p 4240 N94-36110
p 4267 N94-36111
p 4272 N94-36178
p 4331 N94-36199
p 4318 N94-36204
p 4246 N94-36209
p 4241 N94-36242
p 4260 N94-36245
p 4260 N94-36268
p 4261 N94-36362
p 4342 N94-36367
p 4261 N94-36371
p 4261 N94-36373
p 4248 N94-36376
p 4262 N94-36430
DE-AC05-84ER-40150 .... p 4321 N94-35649
p 4325 N94-36086
p 4331 N94-36192
DE-AC05-84OR-21400 .... p 4240 N94-35650
p 4322 N94-35682
p 4264 N94-35683
p 4279 N94-35684
p 4293 N94-35703
p 4233 N94-35932
p 4333 N94-36055
p 4338 N94-36093
p 4287 N94-36179
p 4241 N94-36196
p 4295 N94-36244
p 4327 N94-36267
p 4288 N94-36273
p 4347 N94-36300
p 4342 N94-36377
DE-AC06-76RL-01830 .... p 4311 N94-35348
p 4286 N94-36024
p 4286 N94-36026
p 4287 N94-36027
p 4287 N94-36053
p 4259 N94-36054
p 4312 N94-36195
p 4331 N94-36317
p 4288 N94-36359
DE-AC06-87RL-10930 .... p 4264 N94-35756
DE-AC07-76ID-01570 .... p 4287 N94-36207
p 4287 N94-36208
p 4328 N94-36302
DE-AC07-84ID-12435 .... p 4270 N94-36389
DE-AC09-76SR-00819 .... p 4281 N94-36018
DE-AC09-89SR-18035 .... p 4285 N94-35823
p 4237 N94-36056
p 4257 N94-36366
DE-AC21-88MC-23174 .... p 4275 N94-35667
p 4275 N94-35815
DE-AC21-88MC-25124 .... p 4275 N94-36348
DE-AC21-92MC-29101 .... p 4290 N94-35666
DE-AC22-91PC-90046 .... p 4248 N94-36299
DE-AC22-91PC-91347 .... p 4284 N94-35346
DE-AC22-92PC-92112 .... p 4237 N94-35778
DE-AC22-93PC-92114 .... p 4248 N94-36035
DE-AC35-89ER-40486 .... p 4259 N94-36194
p 4241 N94-36242
DE-AI05-91ER-40616 .... p 4345 N94-35817
DE-FC02-92CE-16067 .... p 4284 N94-35668
DE-FC21-91MC-27221 .... p 4276 N94-36355
DE-FC21-91MC-28055 .... p 4283 N94-36109
DE-FC21-92MC-29061 .... p 4275 N94-36022
DE-FG01-89CE-34025 .... p 4297 N94-36223
DE-FG02-85ER-60372 .... p 4293 N94-35703
DE-FG02-86ER-13515 .... p 4324 N94-35816
DE-FG02-87ER-13808 .... p 4329 N94-36390
DE-FG02-88ER-45365 .... p 4240 N94-35953
DE-FG02-91CE-23810 .... p 4244 N94-35687
p 4245 N94-35771
p 4251 N94-36008
p 4247 N94-36387
p 4251 N94-36388
DE-FG02-91ER-40664 .... p 4269 N94-36095
DE-FG02-92ER-14258 .... p 4328 N94-36298
DE-FG02-92ER-14268 .... p 4241 N94-36233
DE-FG02-92ER-61373 .... p 4269 N94-36085
DE-FG02-92ER-75708 .... p 4228 N94-35349
DE-FG05-80ET-53088 .... p 4264 N94-35681
DE-FG05-84ER-13191 .... p 4330 N94-36105
DE-FG05-85ER-40200 .... p 4323 N94-35814
DE-FG05-86ER-13626 .... p 4236 N94-35685
DE-FG05-86ER-53241 .... p 4335 N94-35670
DE-FG05-88ER-45368 .... p 4246 N94-36283
DE-FG05-88ER-53267 .... p 4338 N94-36200
DE-FG05-92ER-40717 .... p 4331 N94-36428
DE-FG05-92ER-40728 .... p 4324 N94-36016
DE-FG06-84ER-45163 .... p 4238 N94-36203
DE-FG06-88ER-40427 .... p 4324 N94-35824
p 4328 N94-36304
p 4329 N94-36305
DE-FG09-87ER-13768 .... p 4326 N94-36126
DE-FG22-90PC-90291 .... p 4237 N94-36023
DE-FG22-93BC-14968 .... p 4344 N94-35347
DE-FG22-93PC-93222 .... p 4237 N94-36036
DNA001-89-C-0098 .... p 4279 N94-35949
DRET-88-1011 .... p 4297 N94-36220
DRET-911496 .... p 4308 N94-36259
DTFA01-91-Z-02036 .... p 4295 N94-36249
DTFA01-93-Z-02012 .... p 4293 N94-35596
p 4293 N94-35719
p 4293 N94-35720
p 4294 N94-35807
DTFA03-88-C-00016 .... p 4278 N94-36090
DTFR53-91-C-00043 .... p 4215 N94-35848
DTFR53-92-C-00004 .... p 4215 N94-35849
EPA-R-816496 .... p 4298 N94-35688
EPA-68-DO-0093 .... p 4285 N94-35741
EPA-68-01-7365 .... p 4298 N94-35688
F04701-88-C-0089 .... p 4227 N94-35362
p 4289 N94-35587
p 4282 N94-35804
p 4228 N94-36254
p 4228 N94-36255
p 4343 N94-36256
p 4292 N94-36383
F19628-89-C-0186 .... p 4256 N94-35694
p 4256 N94-35713
F19628-89-K-0038 .... p 4273 N94-36227

F19628-90-C-0002 .... p 4203 N94-35611
p 4293 N94-35719
p 4293 N94-35720
p 4294 N94-35807
F19628-90-C-0003 .... p 4302 N94-35495
p 4304 N94-35794
p 4308 N94-36294
F19628-90-C-0088 .... p 4295 N94-36262
F19628-90-K-0005 .... p 4289 N94-35578
p 4291 N94-36116
F19628-90-K-0006 .... p 4375 N94-36264
F19628-91-C-0168 .... p 4304 N94-35709
p 4304 N94-35718
F19628-92-C-0014 .... p 4295 N94-36228
F19628-92-C-0160 .... p 4291 N94-36263
F19628-93-C-0193 .... p 4345 N94-35571
F19628-94-C-0001 .... p 4201 N94-35827
F29601-92-C-0005 .... p 4290 N94-35693
F30602-91-C-0081 .... p 4345 N94-35663
F30602-93-D-0075 .... p 4310 N94-35653
F33615--91-C-2152 .... p 4250 N94-35524
F33615-90-C-0007 .... p 4308 N94-36250
F33615-90-C-1465 .... p 4344 N94-35526
p 4303 N94-35573
F33615-93-1-1330 .... p 4311 N94-35527
p 4303 N94-35574
F49620-90-C-0003 .... p 4305 N94-36006
F49620-90-C-0010 .... p 4312 N94-36309
F49620-92-J-0012 .... p 4190 N94-35717
F49620-92-J-0080 .... p 4321 N94-35657
F49620-92-J-0131 .... p 4310 N94-35806
p 4311 N94-36015
F49620-92-J-0161 .... p 4235 N94-35604
F49620-92-J-0228 .... p 4334 N94-36257
F49620-92-J-0426 .... p 4229 N94-36291
F49620-92-J-0444 .... p 4294 N94-36186
F49620-92-J-0450 .... p 4222 N94-35894
F49620-92-J-0507 .... p 4292 N94-36265
F49620-93-1-0056 .... p 4305 N94-36014
F49620-93-1-0071 .... p 4290 N94-35708
F49620-93-1-0164 .... p 4256 N94-36092
F49620-93-1-0277 .... p 4332 N94-35664
GRI-5089-298-1897 .... p 4236 N94-35755
GRI-5092-291-2304 .... p 4275 N94-35931
JPL-958694 .... p 4354 N94-35378
JPL-958779 .... p 4354 N94-35378
JPL-959737 .... p 4205 N94-35622
MDA903-87-C-0064 .... p 4345 N94-35651
MDA903-92-D-0020 .... p 4303 N94-35662
MDA972-90-C-0035 .... p 4310 N94-35597
MDA972-90-J-1001 .... p 4214 N94-35843
MIPR-Z51100-2-E00467 .... p 4284 N94-35674
NAGW-1828 .... p 4284 N94-35486
NAGW-1841 .... p 4349 N94-36419
NAGW-2126 .... p 4288 N94-35358
p 4289 N94-35392
NAGW-2212 .... p 4292 N94-35452
NAGW-2497 .... p 4354 N94-35265
NAGW-2737 .... p 4289 N94-35389
NAGW-2756 .... p 4374 N94-35993
NAGW-3048 .... p 4376 N94-35363
NAGW-3834 .... p 4376 N94-35590
NAGW-748 .... p 4368 N94-36139
NAG1-1013 .... p 4268 N94-36420
NAG1-1051 .... p 4271 N94-35489
NAG1-1056 .... p 4217 N94-35860
NAG1-1147 .... p 4271 N94-35488
NAG1-1173 .... p 4279 N94-35974
NAG1-1193 .... p 4190 N94-35864
NAG1-1228 .... p 4235 N94-35388
NAG1-225 .... p 4218 N94-35867
NAG1-943 .... p 4252 N94-35247
NAG10-0086 .... p 4296 N94-35257
NAG2-445 .... p 4297 N94-35379
NAG2-477 .... p 4200 N94-35874
p 4280 N94-36423
NAG2-593 .... p 4300 N94-35365
NAG3-1400 .... p 4249 N94-35237
NAG3-1446 .... p 4262 N94-35248
NAG3-1450 .... p 4198 N94-35352
NAG3-1507 .... p 4274 N94-35500
NAG5-1097 .... p 4288 N94-35244
NAG5-1491 .... p 4211 N94-35357
NAG5-2016 .... p 4349 N94-35516
NAG5-2038 .... p 4298 N94-35266
NAG5-2062 .... p 4376 N94-35515
NAG5-2181 .... p 4209 N94-35643
NAG8-834 .... p 4376 N94-36421
NAG8-839 .... p 4375 N94-36395
NAG8-898 .... p 4245 N94-35977
NAG8-921 .... p 4202 N94-35487
NAG9-600 .... p 4347 N94-36435
NAG9-718 .... p 4319 N94-35264
NASW-4574 .... p 4354 N94-35359
p 4355 N94-35395
p 4362 N94-35448
p 4367 N94-36136
NASW-4670 .... p 4302 N94-35514
NASW-4698 .... p 4354 N94-35263
NASW-4715 .... p 4292 N94-35355
p 4293 N94-35499
NASW-4798 .... p 4376 N94-35356
NAS1-19000 .... p 4233 N94-35947
NAS1-19241 .... p 4221 N94-35888
NAS1-19299 .... p 4267 N94-35992
NAS1-19480 .... p 4300 N94-35240
p 4263 N94-35497
p 4266 N94-35975
p 4267 N94-35992
p 4191 N94-35994
NAS10-11624 .... p 4288 N94-36422
NAS2-13383 .... p 4190 N94-35991
NAS2-13721 .... p 4319 N94-36031
NAS3-24226 .... p 4199 N94-36379
NAS3-25266 .... p 4313 N94-35259
p 4200 N94-35267
NAS3-25517 .... p 4263 N94-35250
NAS3-25883 .... p 4268 N94-35268
NAS3-26100 .... p 4347 N94-36396
NAS3-26571 .... p 4278 N94-35239
NAS3-27186 .... p 4257 N94-35249
p 4265 N94-35945
p 4265 N94-35948
p 4234 N94-35995
NAS5-26555 .... p 4349 N94-36279
p 4349 N94-36280
p 4349 N94-36281
p 4349 N94-36282
NAS5-30957 .... p 4292 N94-35380
NAS5-31000 .... p 4203 N94-35613
p 4204 N94-35615
NAS5-31500 .... p 4202 N94-35608
p 4203 N94-35610
p 4203 N94-35612
p 4203 N94-35613
p 4203 N94-35614
p 4204 N94-35615
p 4204 N94-35617
p 4204 N94-35618
p 4205 N94-35620
p 4205 N94-35623
p 4206 N94-35625
p 4208 N94-35636
p 4208 N94-35637
p 4208 N94-3 338
p 4209 N94-35640
p 4209 N94-35641
p 4209 N94-35642
p 4210 N94-35646
NAS5-31704 .... p 4224 N94-35910
NAS5-31718 .... p 4293 N94-35391
NAS5-31786 .... p 4204 N94-35615
NAS5-32314 .... p 4281 N94-35734
NAS5-32486 .... p 4375 N94-35381
NAS5-32500 .... p 4204 N94-35616
NAS8-32488 .... p 4330 N94-35483
NAS8-34501 .... p 4212 N94-35484
NAS8-36123 .... p 4307 N94-36118
p 4333 N94-36119
NAS8-38079 .... p 4249 N94-35485
NAS8-38609 .... p 4235 N94-35447
NAS8-41000 .... p 4201 N94-35626
NAS9-17900 .... p 4222 N94-35897
NAS9-18181 .... p 4301 N94-35443
NAS9-18426 .... p 4309 N94-36439
NATO-CRG-900164 .... p 4266 N94-35975
NCC1-188 .... p 4192 N94-35522
NCC2-417 .... p 4200 N94-36436
NCC2-420 .... p 4189 N94-35498
NCC2-700 .... p 4306 N94-36040
NCC2-761 .... p 4191 N94-36394
NCC2-806 .... p 4268 N94-36397
NCC3-19 .... p 4243 N94-35243
NCC3-233 .... p 4198 N94-35352
p 4265 N94-35948
p 4266 N94-35976
NGT-50444 .... p 4280 N94-36423
NGT-50541 .... p 4222 N94-35895
NR PROJ. RS3-4-J-77 .... p 4260 N94-36248
NSC-82-0424-E0006-040 .... p 4225 N94-35912
NSC81-0424-E005-040 .... p 4216 N94-35856
NSF ATM-91-15557 .... p 4289 N94-35392
NSF CCR-87-01103 .... p 4305 N94-36014
NSF CCR-89-01780 .... p 4300 N94-35365
NSF CCR-89-08092 .... p 4306 N94-36064
p 4306 N94-36065
p 4306 N94-36066
p 4307 N94-36067
p 4307 N94-36068
p 4307 N94-36069
NSF CCR-89-10569 .... p 4306 N94-36064
p 4306 N94-36065
p 4306 N94-36066
p 4307 N94-36067
p 4307 N94-36068
p 4307 N94-36069
NSF CCR-90-14363 .... p 4305 N94-36014
NSF CCR-91-02231 .... p 4300 N94-35365
NSF CCR-92-00794 .... p 4305 N94-36014
NSF CDA-90-15667 .... p 4306 N94-36064
NSF CDR-88-03012 .... p 4221 N94-35886
NSF DMR-88-21625 .... p 4224 N94-35907
NSF DUE-93-50629 .... p 4230 N94-36403
NSF ECS-89-02528 .... p 4379 N94-36042
NSF ECS-89-22947 .... p 4379 N94-36042
NSF ECS-91-16566 .... p 4224 N94-35907
NSF ENG-91-11333 .... p 4379 N94-36042
NSF ENG-92-17849 .... p 4379 N94-36042
NSF ISI-89-61518 .... p 4282 N94-35739
NSG-1414 .... p 4220 N94-35881
NSG-1442 .... p 4306 N94-36063
NSG-5123 .... p 4301 N94-35435
p 4301 N94-35436
p 4301 N94-35437
p 4301 N94-35438
N00014-89-J-1497 .... p 4321 N94-35589
p 4322 N94-35678
p 4322 N94-35753
p 4323 N94-35792
p 4323 N94-35793
p 4323 N94-35797
p 4323 N94-35798
p 4324 N94-36050
N00014-89-J-1848 .... p 4340 N94-35828
N00014-90-C-0099 .... p 4271 N94-35586
N00014-90-J-1159 .... p 4340 N94-35677
N00014-90-J-1556 .... p 4233 N94-35714
p 4233 N94-35715
p 4233 N94-35944
N00014-91-C-0001 .... p 4247 N94-35655
p 4247 N94-35656
N00014-91-J-1035 .... p 4238 N94-36252
p 4246 N94-36253
N00014-91-J-1219 .... p 4317 N94-35743
p 4305 N94-36014
N00014-91-J-1338 .... p 4243 N94-35588
N00014-91-J-1457 .... p 4243 N94-35494
N00014-91-J-1641 .... p 4236 N94-35731
N00014-91-J-1656 .... p 4236 N94-35745
N00014-91-J-1876 .... p 4224 N94-35907
N00014-91-J-1976 .... p 4342 N94-36385
N00014-93-C-2091 .... p 4272 N94-35721
N00014-93-K-2036 .... p 4354 N94-35265
N00014-93-1-0332 .... p 4312 N94-35710
N00014-93-1-0351 .... p 4239 N94-36426
N00014-93-1-1394 .... p 4312 N94-35710
N00039-88-C-0051 .... p 4333 N94-35747
N00039-91-C-0072 .... p 4296 N94-36293
N00039-93-C-0152 .... p 4302 N94-35572
p 4310 N94-35806
p 4311 N94-36015
PROJ. RR22-M59 .... p 4191 N94-36261
RNA PROJ. G93109 .... p 4275 N94-35931
RTOP 151-01-60-01 .... p 4292 N94-35452
p 4292 N94-35453
RTOP 152-14-40-22 .... p 4352 N94-35467
RTOP 152-17-40-23 .... p 4353 N94-36149
RTOP 185-52-62-07 .... p 4292 N94-35452
p 4292 N94-35453
RTOP 199-52-11-02 .... p 4353 N94-36149
RTOP 233-01-0E .... p 4243 N94-35243
RTOP 233-01-01-05 .... p 4217 N94-35865
RTOP 233-03-01-01 .... p 4212 N94-35836
p 4223 N94-35902
RTOP 233-03-03-02 .... p 4311 N94-35242
RTOP 235-01-1C .... p 4258 N94-35270
RTOP 307-51-50 .... p 4376 N94-35370
RTOP 310-10-61-90-01 .... p 4210 N94-35543
RTOP 310-10-62-16 .... p 4252 N94-35544
p 4252 N94-35545
RTOP 310-20-65-86-08 .... p 4252 N94-35546
p 4253 N94-35547
RTOP 310-20-65-89-01 .... p 4253 N94-35549
RTOP 310-20-65-92-02 .... p 4253 N94-35548
RTOP 310-30-69-91-05 .... p 4253 N94-35550
RTOP 310-30-70-89-01 .... p 4253 N94-35553
RTOP 310-30-70-93-01 .... p 4253 N94-35552
RTOP 310-30-71-83-02 .... p 4254 N94-35554
p 4254 N94-35555
RTOP 310-30-71-83-04 .... p 4254 N94-35556
RTOP 314-30-61-04-54 .... p 4253 N94-35551
RTOP 314-40-41-21-03 .... p 4255 N94-35559
RTOP 314-40-52-29-26 .... p 4255 N94-35560
p 4255 N94-35561
RTOP 315-90-81-41-07 .... p 4254 N94-35557
RTOP 315-91-10-13-08 .... p 4254 N94-35558
RTOP 315-91-50-20-02 .... p 4255 N94-35562
RTOP 315-91-60-10-05 .... p 4255 N94-35563

RTOP 323-01-0B .... p 4268 N94-35268
RTOP 505-10-11 .... p 4299 N94-35393
RTOP 505-59-36 .... p 4198 N94-36380
RTOP 505-59-50-05 .... p 4190 N94-35864
RTOP 505-59-50 .... p 4263 N94-35371
RTOP 505-62-10 .... p 4265 N94-35945
RTOP 505-62-52 .... p 4263 N94-35253
p 4313 N94-35259
p 4198 N94-35352
RTOP 505-63-12 .... p 4278 N94-35239
RTOP 505-63-50-01 .... p 4229 N94-36398
RTOP 505-63-50-04 .... p 4233 N94-35946
RTOP 505-64-12-02 .... p 4252 N94-35247
RTOP 505-64-13-01 .... p 4192 N94-36048
RTOP 505-68-00 .... p 4193 N94-35241
RTOP 505-70-63-01 .... p 4233 N94-35947
RTOP 505-90-5K .... p 4265 N94-35948
p 4266 N94-35976
RTOP 505-90-52-01 .... p 4300 N94-35240
p 4263 N94-35497
p 4266 N94-35975
p 4267 N94-35992
p 4191 N94-35994
RTOP 505-90-53 .... p 4309 N94-36438
RTOP 506-41-11 .... p 4281 N94-35271
RTOP 506-41-41 .... p 4257 N94-35249
RTOP 510-01-01 .... p 4243 N94-35260
RTOP 533-02-34 .... p 4199 N94-35258
RTOP 535-03-10-02 .... p 4189 N94-35246
RTOP 537-03-23 .... p 4189 N94-35394
RTOP 537-04-20 .... p 4200 N94-35267
p 4199 N94-36379
RTOP 550-00-00 .... p 4202 N94-35605
RTOP 552-00-00 .... p 4300 N94-35238
p 4300 N94-35256
p 4301 N94-35434
RTOP 633-00-00 .... p 4349 N94-36279
p 4349 N94-36280
p 4349 N94-36281
p 4349 N94-36282
RTOP 674-21-05 .... p 4262 N94-35248
RTOP 691-00-00 .... p 4375 N94-35381
RTOP 740-00-00 .... p 4259 N94-36049
RTOP 763-22-41 .... p 4234 N94-35995
RTOP 889-62-10-41 .... p 4361 N94-35429
p 4361 N94-35430
p 4361 N94-35431
RTOP 910-40-00 .... p 4292 N94-35380
RTOP 926-00-00 .... p 4281 N94-35261
RTOP 960-30-02 .... p 4347 N94-36396
RTOP 970-00-00 .... p 4211 N94-35269
SRC-88-MC-507 .... p 4224 N94-35907
SRI PROJ. 4069 .... p 4237 N94-35778
SWRI PROJ. 15-4865 .... p 4330 N94-35483
W-31-109-ENG-38 .... p 4332 N94-35671
p 4314 N94-35704
p 4285 N94-35765
p 4237 N94-35777
p 4245 N94-35779
p 4282 N94-35829
p 4286 N94-36007
p 4281 N94-36018
p 4245 N94-36108
p 4241 N94-36222
p 4327 N94-36225
p 4241 N94-36231
p 4275 N94-36232
p 4327 N94-36238
p 4341 N94-36272
p 4246 N94-36306
p 4319 N94-36320
p 4239 N94-36349
p 4351 N94-36418
p 4316 N94-36432
p 4276 N94-36433
W-7405-ENG-36 .... p 4320 N94-35376
p 4264 N94-35669
p 4236 N94-35680
p 4244 N94-35768
p 4304 N94-35808
p 4350 N94-35980
p 4347 N94-36102
p 4291 N94-36103
p 4295 N94-36240
p 4257 N94-36316
p 4242 N94-36369
W-7405-ENG-48 .... p 4313 N94-35259
p 4292 N94-35350
p 4349 N94-35565
p 4335 N94-35647
p 4271 N94-35665
p 4271 N94-35679
p 4272 N94-35695
p 4232 N94-35696
p 4333 N94-35697
p 4284 N94-35700
p 4319 N94-35770
p 4333 N94-35818
p 4285 N94-35943
p 4286 N94-35957
p 4272 N94-35978
p 4266 N94-35982
p 4379 N94-35997
p 4305 N94-36017
p 4286 N94-36025
p 4256 N94-36112
p 4330 N94-36114
p 4272 N94-36115
p 4326 N94-36127
p 4338 N94-36193
p 4318 N94-36201
p 4238 N94-36205
p 4275 N94-36206
p 4308 N94-36236
p 4238 N94-36237
p 4338 N94-36284
p 4288 N94-36286
p 4347 N94-36297
p 4256 N94-36301
p 4267 N94-36315
p 4239 N94-36319
p 4270 N94-36350
p 4334 N94-36356
p 4268 N94-36374
p 4339 N94-36375
p 4276 N94-36378
p 4339 N94-36386
p 4309 N94-36429
W-7405-ENG-82 .... p 4245 N94-36057

REPORT NUMBER INDEX

SCIENTIFIC AND TECHNICAL AEROSPACE REPORTS VOLUME 32 NUMBER 11

.Typical Report Number Index Listing

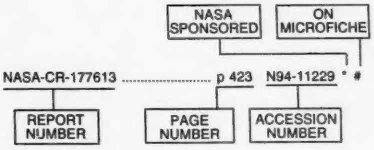

Listings in this index are arranged alphanumerically by report number. The accession number denotes the number by which the citation is identified. The page number helps to locate the citation in the abstract section. An asterisk (*) indicates that the item is a NASA report. A pound sign (#) indicates that the item is available on microfiche.

A-92169 .... p 4299 N94-35393 * #
A-92175 .... p 4189 N94-35394 * #
A-93031 .... p 4376 N94-35370 * #
A-93034 .... p 4377 N94-35961 * #
A-93048 .... p 4263 N94-35371 * #
A-94041 .... p 4380 N94-36117 * #
A-94056 .... p 4190 N94-35991 * #
A-94082 .... p 4198 N94-36380 * #
A-94096 .... p 4280 N94-36423 * #

AAA-LIEKKI-L93-1 .... p 4237 N94-36059 #

AD-A253611 .... p 4300 N94-35365 * #
AD-A277843 .... p 4258 N94-35539
AD-A278218 .... p 4319 N94-36176
AD-A278573 .... p 4192 N94-36184
AD-A278574 .... p 4307 N94-36185
AD-A278575 .... p 4294 N94-36186
AD-A278576 .... p 4294 N94-36187
AD-A278577 .... p 4226 N94-36188
AD-A278597 .... p 4315 N94-36424
AD-A278598 .... p 4316 N94-36425
AD-A278604 .... p 4239 N94-36426
AD-A278605 .... p 4261 N94-36360
AD-A278610 .... p 4260 N94-36248
AD-A278611 .... p 4295 N94-36249
AD-A278613 .... p 4308 N94-36250
AD-A278615 .... p 4226 N94-36251
AD-A278616 .... p 4238 N94-36252
AD-A278618 .... p 4246 N94-36253
AD-A278628 .... p 4228 N94-36254
AD-A278629 .... p 4228 N94-36255
AD-A278630 .... p 4227 N94-35362 #
AD-A278631 .... p 4292 N94-36383
AD-A278632 .... p 4343 N94-36256
AD-A278636 .... p 4334 N94-36257
AD-A278639 .... p 4308 N94-36258
AD-A278640 .... p 4199 N94-36384
AD-A278644 .... p 4261 N94-36361
AD-A278646 .... p 4315 N94-36012
AD-A278647 .... p 4316 N94-35575
AD-A278650 .... p 4247 N94-35795
AD-A278653 .... p 4303 N94-35576
AD-A278654 .... p 4303 N94-35577
AD-A278663 .... p 4289 N94-35578
AD-A278675 .... p 4199 N94-35796
AD-A278676 .... p 4255 N94-35689
AD-A278677 .... p 4264 N94-35690
AD-A278678 .... p 4316 N94-35691
AD-A278679 .... p 4298 N94-35692
AD-A278682 .... p 4290 N94-35693
AD-A278683 .... p 4312 N94-35710
AD-A278687 .... p 4303 N94-35662
AD-A278688 .... p 4345 N94-35663
AD-A278689 .... p 4345 N94-35651
AD-A278700 .... p 4300 N94-35652
AD-A278702 .... p 4229 N94-36291
AD-A278709 .... p 4227 N94-36189
AD-A278712 .... p 4229 N94-35776
AD-A278713 .... p 4279 N94-35949
AD-A278716 .... p 4278 N94-36292
AD-A278718 .... p 4296 N94-36293
AD-A278719 .... p 4308 N94-36294
AD-A278725 .... p 4312 N94-36295
AD-A278730 .... p 4260 N94-36296
AD-A278739 .... p 4228 N94-36089
AD-A278745 .... p 4278 N94-36090
AD-A278748 .... p 4238 N94-36091
AD-A278753 .... p 4256 N94-36092
AD-A278758 .... p 4318 N94-36427
AD-A278759 .... p 4302 N94-35490
AD-A278760 .... p 4302 N94-35491
AD-A278761 .... p 4263 N94-35492
AD-A278762 .... p 4335 N94-35493
AD-A278763 .... p 4243 N94-35494
AD-A278765 .... p 4302 N94-35495
AD-A278767 .... p 4256 N94-35694
AD-A278769 .... p 4299 N94-35707
AD-A278770 .... p 4250 N94-35711
AD-A278771 .... p 4228 N94-35825
AD-A278774 .... p 4312 N94-36309
AD-A278787 .... p 4299 N94-35712
AD-A278788 .... p 4256 N94-35713
AD-A278789 .... p 4310 N94-35653
AD-A278791 .... p 4232 N94-35654
AD-A278793 .... p 4247 N94-35655
AD-A278794 .... p 4247 N94-35656
AD-A278795 .... p 4244 N94-35757
AD-A278796 .... p 4284 N94-35674
AD-A278798 .... p 4305 N94-36013
AD-A278799 .... p 4316 N94-35675
AD-A278800 .... p 4304 N94-35676
AD-A278826 .... p 4340 N94-35677
AD-A278830 .... p 4322 N94-35678
AD-A278832 .... p 4323 N94-35797
AD-A278833 .... p 4323 N94-35798
AD-A278834 .... p 4323 N94-35792
AD-A278835 .... p 4322 N94-35753
AD-A278836 .... p 4323 N94-35793
AD-A278839 .... p 4212 N94-35799
AD-A278841 .... p 4319 N94-35800
AD-A278845 .... p 4212 N94-35801
AD-A278846 .... p 4312 N94-35802
AD-A278847 .... p 4310 N94-35742
AD-A278858 .... p 4317 N94-35743
AD-A278859 .... p 4190 N94-35826
AD-A278860 .... p 4201 N94-35827
AD-A278861 .... p 4342 N94-36385
AD-A278862 .... p 4340 N94-35828
AD-A278863 .... p 4324 N94-36050
AD-A278864 .... p 4233 N94-35944
AD-A278865 .... p 4233 N94-35714
AD-A278866 .... p 4233 N94-35715
AD-A278870 .... p 4305 N94-36014
AD-A278871 .... p 4293 N94-35596
AD-A278876 .... p 4212 N94-35585
AD-A278885 .... p 4271 N94-35586
AD-A278886 .... p 4290 N94-35708
AD-A278896 .... p 4310 N94-35597
AD-A278897 .... p 4345 N94-35571
AD-A278898 .... p 4302 N94-35572
AD-A278899 .... p 4303 N94-35573
AD-A278900 .... p 4303 N94-35574
AD-A278903 .... p 4265 N94-35803
AD-A278905 .... p 4282 N94-35804
AD-A278906 .... p 4289 N94-35587
AD-A278912 .... p 4243 N94-35588
AD-A278913 .... p 4321 N94-35589
AD-A278936 .... p 4299 N94-35716
AD-A278937 .... p 4304 N94-35709
AD-A278938 .... p 4332 N94-35664
AD-A278939 .... p 4323 N94-35805
AD-A278940 .... p 4321 N94-35657
AD-A278941 .... p 4235 N94-35604
AD-A278942 .... p 4190 N94-35717
AD-A278943 .... p 4305 N94-36006
AD-A278951 .... p 4311 N94-36015
AD-A278952 .... p 4312 N94-35658
AD-A278954 .... p 4310 N94-35806
AD-A278955 .... p 4304 N94-35718
AD-A278957 .... p 4294 N94-35807
AD-A278958 .... p 4293 N94-35719
AD-A278959 .... p 4293 N94-35720
AD-A278961 .... p 4272 N94-35721
AD-A278962 .... p 4298 N94-35659
AD-A278965 .... p 4303 N94-35660
AD-A278967 .... p 4250 N94-35524
AD-A278972 .... p 4344 N94-35525
AD-A278978 .... p 4344 N94-35526
AD-A278979 .... p 4311 N94-35527
AD-A278987 .... p 4298 N94-35528
AD-A278988 .... p 4190 N94-35529
AD-A278989 .... p 4190 N94-35950
AD-A278991 .... p 4290 N94-35744
AD-A279005 .... p 4266 N94-35951
AD-A279014 .... p 4304 N94-35794
AD-A279015 .... p 4236 N94-35745
AD-A279017 .... p 4233 N94-35952
AD-A279028 .... p 4198 N94-35746
AD-A279031 .... p 4345 N94-35732
AD-A279046 .... p 4333 N94-35747
AD-A279058 .... p 4312 N94-35730
AD-A279059 .... p 4236 N94-35731
AD-A279064 .... p 4340 N94-35733
AD-A279415 .... p 4291 N94-36116 #
AD-A279417 .... p 4295 N94-36262 #
AD-A279482 .... p 4295 N94-36228 #
AD-A279486 .... p 4273 N94-36227 #
AD-A279680 .... p 4191 N94-36261 #
AD-A280715 .... p 4292 N94-36265 #
AD-A280716 .... p 4291 N94-36263 #

AD-B168325 .... p 4337 N94-35938 #
AD-B168925 .... p 4339 N94-36357 #
AD-B168930 .... p 4324 N94-35984 #
AD-B168932 .... p 4338 N94-36352 #
AD-B168944 .... p 4339 N94-36353 #
AD-B168945 .... p 4337 N94-35937 #
AD-B169199 .... p 4337 N94-35936 #
AD-B173715 .... p 4337 N94-35983 #
AD-B178352L .... p 4344 N94-35254 * #
AD-B179180 .... p 4337 N94-35939 #
AD-B179444 .... p 4336 N94-35752 #
AD-B181062 .... p 4279 N94-36226 #

AD-D016197 .... p 4334 N94-36363
AD-D016200 .... p 4257 N94-36364
AD-D016201 .... p 4273 N94-36365
AD-D016211 .... p 4239 N94-36372
AD-D016212 .... p 4334 N94-36368
AD-D016213 .... p 4273 N94-36370
AD-D016214 .... p 4246 N94-36121
AD-D016215 .... p 4334 N94-36122
AD-D016216 .... p 4234 N94-36123
AD-D016217 .... p 4234 N94-36124
AD-D016218 .... p 4246 N94-36125

AD-E201889 .... p 4289 N94-35578
AD-E501776 .... p 4312 N94-35730

AECL-10691 .... p 4240 N94-35960 #
AECL-10798 .... p 4242 N94-36288 #
AECL-10801 .... p 4242 N94-36289 #

AEDC-TR-93-20 .... p 4266 N94-35951

AERO-3 .... p 4199 N94-36384

AFIT/DS/AA/94-1 .... p 4264 N94-35690

AFIT/DS/ENG/94-01 .... p 4261 N94-36361

AFIT/GAE/ENY/94M-2 .... p 4298 N94-35692
AFIT/GAE/ENY/94M-3 .... p 4199 N94-35796

AFIT/GE/ENG/94M-05 .... p 4255 N94-35689

AFIT/GOR/ENC/ENS/94M-19 .... p 4316 N94-35575

AFIT/GOR/ENS/94M-08 .... p 4316 N94-35691
AFIT/GOR/ENS/94M-10 .... p 4226 N94-36188

REPORT

AFIT/GOR/ENS/94M-13 .... p 4192 N94-36184

AFOSR-TR-94-0275 .... p 4198 N94-35746
AFOSR-TR-94-0276 .... p 4323 N94-35805

AFOSR-94-0162TR .... p 4229 N94-36291
AFOSR-94-0201TR .... p 4294 N94-36186
AFOSR-94-0245TR .... p 4316 N94-36425
AFOSR-94-0249TR .... p 4315 N94-36424
AFOSR-94-0251TR .... p 4256 N94-36092
AFOSR-94-0252TR .... p 4312 N94-36309
AFOSR-94-0253TR .... p 4278 N94-36292
AFOSR-94-0254TR .... p 4227 N94-36189
AFOSR-94-0255TR .... p 4308 N94-36258
AFOSR-94-0256TR .... p 4334 N94-36257
AFOSR-94-0259TR .... p 4228 N94-36089
AFOSR-94-0263TR .... p 4199 N94-36384
AFOSR-94-0264TR .... p 4235 N94-35604
AFOSR-94-0268TR .... p 4190 N94-35950
AFOSR-94-0269TR .... p 4190 N94-35529
AFOSR-94-0270TR .... p 4233 N94-35952
AFOSR-94-0271TR .... p 4290 N94-35708
AFOSR-94-0272TR .... p 4332 N94-35664
AFOSR-94-0277TR .... p 4321 N94-35657
AFOSR-94-0278TR .... p 4190 N94-35717
AFOSR-94-0280TR .... p 4305 N94-36006

AGARD-CP-547 .... p 4193 N94-36321 #

AGARD-HIGHLIGHTS-93/2 .... p 4376 N94-35444 #

AIAA PAPER 94-0858 .... p 4344 N94-35254 * #
AIAA PAPER 94-1825 .... p 4265 N94-35945 * #
AIAA PAPER 94-2115 .... p 4193 N94-35241 * #
AIAA PAPER 94-2123 .... p 4199 N94-35258 * #
AIAA PAPER 94-2195 .... p 4266 N94-35976 * #
AIAA PAPER 94-2628 .... p 4243 N94-35243 * #
AIAA PAPER 94-2710 .... p 4199 N94-36379 * #
AIAA PAPER 94-2985 .... p 4268 N94-35268 * #
AIAA PAPER 94-3209 .... p 4198 N94-35352 * #
AIAA PAPER 94-3259 .... p 4263 N94-35250 * #
AIAA PAPER 94-3356 .... p 4265 N94-35948 * #

AL/CF-SR-1994-0003 .... p 4299 N94-35712

AL/HR-TR-1994-0009 .... p 4308 N94-36250

ANL-HEP-CP-93-67 .... p 4327 N94-36238

ANL-93/34 .... p 4316 N94-36432 #

ANL/CHM/CP-81871 .... p 4332 N94-35671 #

ANL/CHM/PP-81405 .... p 4341 N94-36272 #

ANL/CMT/PP-77577 .... p 4351 N94-36418 #

ANL/EA/CP-82328 .... p 4319 N94-36320

ANL/ER/CP-81722 .... p 4286 N94-36007 #

ANL/ER/PP-74994 .... p 4281 N94-36018

ANL/ESD/TM-58 .... p 4285 N94-35765

ANL/ET/CP-81839 .... p 4275 N94-36232 #
ANL/ET/CP-82049 .... p 4245 N94-35779
ANL/ET/CP-82361 .... p 4282 N94-35829

ANL/MCS-TM-185 .... p 4314 N94-35704 #

ANL/MCT/PP-78088 .... p 4276 N94-36433 #

ANL/MSD/CP-81522 .... p 4239 N94-36349
ANL/MSD/CP-82168 .... p 4237 N94-35777
ANL/MSD/CP-82380 .... p 4241 N94-36222 #
ANL/MSD/CP-82465 .... p 4241 N94-36231 #
ANL/MSD/CP-82631 .... p 4327 N94-36225 #

ANL/OTM/CR-5 .... p 4246 N94-36306
ANL/OTM/CR-6 .... p 4245 N94-36108 #

APL-UW-TM-4-93 .... p 4296 N94-36293

ARB-R-94/512 .... p 4247 N94-35941

ARCCB-CR-94004 .... p 4250 N94-35711

ARL-MR-151 .... p 4199 N94-36379 * #

ARL-TR-338 .... p 4229 N94-35361 #

AR93-2 .... p 4200 N94-36437 #

ATC-212 .... p 4293 N94-35720
ATC-213 .... p 4293 N94-35719

ATC-216 .... p 4294 N94-35807

ATR-91(7234)-1 .... p 4289 N94-35392 * #
ATR-93(7251)-1 .... p 4288 N94-35358 * #

BARC-1993/E/017 .... p 4309 N94-36382 #
BARC-1993/E/020 .... p 4235 N94-35592 #
BARC-1993/E/023 .... p 4300 N94-35570
BARC-1993/P/004 .... p 4273 N94-36393 #

BNL-49501 .... p 4327 N94-36239
BNL-49650 .... p 4328 N94-36303
BNL-60041 .... p 4341 N94-36358 #
BNL-60072 .... p 4260 N94-36221 #

BUDKERINP-92-1 .... p 4315 N94-36100
BUDKERINP-92-55 .... p 4327 N94-36246
BUDKERINP-92-57 .... p 4322 N94-35783 #
BUDKERINP-92-58 .... p 4335 N94-35750 #
BUDKERINP-92-59 .... p 4320 N94-35567
BUDKERINP-92-60 .... p 4336 N94-35788 #
BUDKERINP-92-61 .... p 4322 N94-35785 #
BUDKERINP-93-10 .... p 4339 N94-36417 #

CA-93-00955 .... p 4240 N94-35960 #

CAL-2198 .... p 4349 N94-35516 * #

CDRKNSWC/SSD-93/54 .... p 4191 N94-36261 #

CEBAF-PR-94-003 .... p 4331 N94-36192 #

CEBAF-TH-94-01 .... p 4321 N94-35649
CEBAF-TH-94-02 .... p 4325 N94-36086

CERB-92-12 .... p 4297 N94-36220

CMOTT-94-3 .... p 4265 N94-35948 * #

CMS-TSR-94-10 .... p 4315 N94-36012

CMU-CS-94-100 .... p 4345 N94-35571
CMU-CS-94-103 .... p 4303 N94-35573
CMU-CS-94-105 .... p 4302 N94-35572
CMU-CS-94-106 .... p 4310 N94-35806
CMU-CS-94-108 .... p 4310 N94-35597
CMU-CS-94-110 .... p 4304 N94-35709
CMU-CS-94-121 .... p 4299 N94-35716
CMU-CS-94-123 .... p 4303 N94-35574
CMU-CS-94-129 .... p 4304 N94-35718
CMU-CS-94-130 .... p 4344 N94-35526
CMU-CS-94-131 .... p 4311 N94-36015
CMU-CS-94-132 .... p 4311 N94-35527
CMU-CS-94-136 .... p 4312 N94-35658

CMU/SEI-93-TR-34 .... p 4304 N94-35794
CMU/SEI-94-TR-007 .... p 4308 N94-36294
CMU/SEI-94-TR-3 .... p 4302 N94-35495

COG-92-248 .... p 4240 N94-35960 #
COG-92-409 .... p 4242 N94-36288 #
COG-92-40 .... p 4242 N94-36289 #

CONF-9105436 .... p 4341 N94-36181 #
CONF-9109529 .... p 4289 N94-35568 #
CONF-9204276 .... p 4312 N94-35831 #
CONF-9206427-VOL-1 .... p 4320 N94-35569
CONF-9206427-VOL-2 .... p 4326 N94-36182 #
CONF-9207225 .... p 4336 N94-35775 #
CONF-9209396 .... p 4336 N94-35772 #
CONF-9209396 .... p 4337 N94-35936 #
CONF-9209396 .... p 4337 N94-35937 #
CONF-9209396 .... p 4337 N94-35938 #
CONF-9209396 .... p 4324 N94-35984 #
CONF-9209396 .... p 4338 N94-36247 #
CONF-9209396 .... p 4338 N94-36352 #
CONF-9209396 .... p 4339 N94-36353 #
CONF-9209396 .... p 4339 N94-36357 #
CONF-9209428-VOL-1 .... p 4290 N94-35830 #
CONF-9209428 .... p 4291 N94-36087
CONF-9210457-1 .... p 4331 N94-36224 #
CONF-930389-25 .... p 4328 N94-36303
CONF-9304164-1 .... p 4267 N94-36315
CONF-9305257 .... p 4379 N94-35997
CONF-9305317-2 .... p 4317 N94-36234 #
CONF-9305320-1-VUGRAPHS .... p 4286 N94-36007 #
CONF-9306190-1 .... p 4257 N94-36316 #
CONF-9306221-7 .... p 4327 N94-36238
CONF-930637-7 .... p 4327 N94-36239
CONF-930676-46 .... p 4238 N94-36237
CONF-930711-4 .... p 4327 N94-36267
CONF-930767-6 .... p 4330 N94-36106 #
CONF-930767-7 .... p 4326 N94-36198 #
CONF-930823-14 .... p 4327 N94-36266
CONF-930893-19 .... p 4276 N94-36355
CONF-930893-31 .... p 4275 N94-36022 #
CONF-930893-33 .... p 4282 N94-36021 #
CONF-9309297-10 .... p 4326 N94-36107 #
CONF-9309302-1 .... p 4329 N94-36305
CONF-9309350 .... p 4293 N94-35703
CONF-9309352-1 .... p 4324 N94-35824
CONF-930999-3 .... p 4328 N94-36304
CONF-931006-3 .... p 4275 N94-36348 #
CONF-9310193-12 .... p 4331 N94-36271 #
CONF-9310212-1 .... p 4347 N94-36102 #
CONF-9310222-1 .... p 4291 N94-36103 #
CONF-9310241-1 .... p 4286 N94-36024 #
CONF-931048-12 .... p 4330 N94-36114 #
CONF-931048-13 .... p 4339 N94-36375 #
CONF-931048-14 .... p 4331 N94-36199 #
CONF-931080-6 .... p 4347 N94-36297 #
CONF-931107-26 .... p 4331 N94-36317 #
CONF-9311137-3 .... p 4236 N94-35680 * #
CONF-931117-2 .... p 4286 N94-36026 #
CONF-931132-3-REV-1 .... p 4266 N94-35982 #
CONF-931132-4 .... p 4318 N94-36201 #
CONF-931165-2 .... p 4287 N94-36027 #
CONF-931237-5 .... p 4272 N94-35978 #
CONF-940113-10 .... p 4275 N94-35815 #
CONF-940113-8 .... p 4275 N94-35667 #
CONF-940115-14 .... p 4286 N94-36025 #
CONF-940115-16 .... p 4285 N94-35823
CONF-940115-29 .... p 4287 N94-36053 #
CONF-940142-21 .... p 4320 N94-35376 #
CONF-940142-31-REV-1 .... p 4272 N94-35695
CONF-940142-32 .... p 4272 N94-36178 #
CONF-940142-33 .... p 4271 N94-35665 #
CONF-940142-34 .... p 4333 N94-35697 #
CONF-940142-35 .... p 4324 N94-36058 #
CONF-940159-1 .... p 4311 N94-35348 #
CONF-940179-1 .... p 4350 N94-35980 #
CONF-940226-6 .... p 4271 N94-35679 #
CONF-940247-3 .... p 4305 N94-36017
CONF-940254-2 .... p 4304 N94-35808 #
CONF-940263-1 .... p 4259 N94-36054 #
CONF-940272-1 .... p 4322 N94-35682 #
CONF-940275-1 .... p 4241 N94-36222 #
CONF-940275-2 .... p 4241 N94-36231 #
CONF-940277-2 .... p 4295 N94-36285 #
CONF-940301-30 .... p 4350 N94-36229 #
CONF-9403100-1 .... p 4339 N94-36386 #
CONF-940353-5 .... p 4290 N94-35666 #
CONF-940380-2 .... p 4232 N94-35696
CONF-940391-4 .... p 4267 N94-36111 #
CONF-940395-1 .... p 4349 N94-35565 #
CONF-940411-13 .... p 4318 N94-36204 #
CONF-940411-7 .... p 4244 N94-35702 #
CONF-940411-8 .... p 4244 N94-35701
CONF-940411-9 .... p 4340 N94-35698
CONF-9404118-2 .... p 4260 N94-36245 #
CONF-9404131-1 .... p 4333 N94-35818 #
CONF-940416-3 .... p 4244 N94-35699
CONF-940440-1 .... p 4240 N94-36110 #
CONF-940440-2 .... p 4275 N94-36232 #
CONF-940445-2 .... p 4282 N94-35829
CONF-940445-5 .... p 4283 N94-36109 #
CONF-940449-4 .... p 4349 N94-35998 #
CONF-940483-4 .... p 4245 N94-35779
CONF-9405113-1 .... p 4292 N94-35350 #
CONF-9405121-1 .... p 4247 N94-36387 #
CONF-9405121-2 .... p 4251 N94-36388 #
CONF-9405127-1 .... p 4262 N94-36430 #
CONF-9405136-1 .... p 4248 N94-36376 #
CONF-9405140-1 .... p 4327 N94-36225 #
CONF-940529-5 .... p 4237 N94-35777
CONF-940529-7 .... p 4239 N94-36349
CONF-940582-3 .... p 4272 N94-36115 #
CONF-940593-7 .... p 4332 N94-35671 #
CONF-940613-5 .... p 4264 N94-35756
CONF-940613-7 .... p 4279 N94-35684 #
CONF-9406133-1 .... p 4226 N94-36001
CONF-940625-3 .... p 4233 N94-35932
CONF-940632-10 .... p 4288 N94-36286 #
CONF-940632-8 .... p 4319 N94-36320
CONF-940633-2 .... p 4238 N94-36230 #
CONF-940658-1 .... p 4258 N94-35564 #
CONF-940684-1-PT-1 .... p 4267 N94-35996 #
CONF-940711-11 .... p 4275 N94-36206 #
CONF-940711-12 .... p 4238 N94-36205 #
CONF-940711-5 .... p 4276 N94-36378 #
CONF-940711-6 .... p 4239 N94-36319 #
CONF-940726-1 .... p 4261 N94-36362 #
CONF-940726-3 .... p 4342 N94-36367 #
CONF-940726-5 .... p 4261 N94-36371 #
CONF-940726-6 .... p 4261 N94-36373 #
CONF-940726-7 .... p 4260 N94-36268
CONF-940726-9 .... p 4260 N94-36221 #
CONF-940734-1 .... p 4268 N94-36318 #
CONF-940742-4 .... p 4268 N94-36374
CONF-940743-1 .... p 4334 N94-36356 #
CONF-940744-1 .... p 4341 N94-36358 #
CONF-940744-2 .... p 4242 N94-36369 #

CONF-940753-1 .... p 4246 N94-36209 #
CONF-940753-2 .... p 4241 N94-36242 #
CONF-940753-3 .... p 4342 N94-36377 #

CPIA-606-VOL-1 .... p 4247 N94-35655
CPIA-606-VOL-2 .... p 4247 N94-35656

CRREL-SR-94-2 .... p 4229 N94-35776

CSDL-C-6303 .... p 4309 N94-36439 * #

CSP-93-1009-VOL-3 .... p 4319 N94-36176

CT-17 .... p 4259 N94-35822

CU-TR-92-1293 .... p 4300 N94-35365 * #

DE93-016418 .... p 4267 N94-36315
DE93-016615 .... p 4257 N94-36316 #
DE93-019632 .... p 4238 N94-36237
DE94-000120 .... p 4344 N94-35347 #
DE94-000214 .... p 4248 N94-36191 #
DE94-001350 .... p 4327 N94-36238
DE94-001491 .... p 4327 N94-36239
DE94-001683 .... p 4295 N94-36240
DE94-002302 .... p 4327 N94-36266
DE94-002459 .... p 4327 N94-36267
DE94-002628 .... p 4347 N94-36102 #
DE94-002698 .... p 4291 N94-36103 #
DE94-002958 .... p 4282 N94-36021 #
DE94-002960 .... p 4275 N94-36348 #
DE94-002970 .... p 4276 N94-36355
DE94-003002 .... p 4327 N94-36241
DE94-003011 .... p 4328 N94-36303
DE94-003191 .... p 4275 N94-36022 #
DE94-003633 .... p 4237 N94-36023 #
DE94-003699 .... p 4286 N94-36024 #
DE94-004041 .... p 4285 N94-35823
DE94-004167 .... p 4269 N94-36085 #
DE94-004210 .... p 4286 N94-36025 #
DE94-004645 .... p 4328 N94-36304
DE94-004646 .... p 4329 N94-36305
DE94-004719 .... p 4331 N94-36317 #
DE94-004782 .... p 4286 N94-36026 #
DE94-004783 .... p 4287 N94-36027 #
DE94-005104 .... p 4268 N94-36318 #
DE94-005481 .... p 4286 N94-36007 #
DE94-005590 .... p 4267 N94-35996 #
DE94-006392 .... p 4239 N94-36319 #
DE94-006405 .... p 4276 N94-36378 #
DE94-006474 .... p 4334 N94-36356 #
DE94-006526 .... p 4311 N94-35348 #
DE94-006570 .... p 4341 N94-36358 #
DE94-006616 .... p 4379 N94-35997
DE94-006624 .... p 4285 N94-35943 #
DE94-006854 .... p 4283 N94-36051 #
DE94-006857 .... p 4283 N94-36052 #
DE94-007075 .... p 4272 N94-35978 #
DE94-007089 .... p 4288 N94-36359 #
DE94-007270 .... p 4261 N94-36362 #
DE94-007284 .... p 4257 N94-36366 #
DE94-007292 .... p 4342 N94-36367 #
DE94-007476 .... p 4287 N94-36053 #
DE94-007533 .... p 4242 N94-36369 #
DE94-007553 .... p 4320 N94-35376 #
DE94-007732 .... p 4258 N94-35564 #
DE94-007742 .... p 4261 N94-36371 #
DE94-007863 .... p 4260 N94-36268
DE94-007868 .... p 4261 N94-36373 #
DE94-008047 .... p 4259 N94-36054 #
DE94-008071 .... p 4324 N94-35824
DE94-008182 .... p 4228 N94-35349 #
DE94-008218 .... p 4275 N94-36206 #
DE94-008288 .... p 4238 N94-36205 #
DE94-008289 .... p 4292 N94-35350 #
DE94-008510 .... p 4333 N94-36055 #
DE94-008522 .... p 4287 N94-36207 #
DE94-008523 .... p 4287 N94-36208 #
DE94-008744 .... p 4246 N94-36209 #
DE94-008937 .... p 4226 N94-36001
DE94-008940 .... p 4241 N94-36242 #
DE94-008949 .... p 4349 N94-35998 #
DE94-009053 .... p 4284 N94-35346 #
DE94-009107 .... p 4260 N94-36221 #
DE94-009169 .... p 4233 N94-35932
DE94-009182 .... p 4323 N94-35814 #
DE94-009250 .... p 4270 N94-35351 #
DE94-009254 .... p 4266 N94-35979 #
DE94-009279 .... p 4272 N94-36178 #
DE94-009298 .... p 4304 N94-35808 #
DE94-009302 .... p 4236 N94-35680 * #
DE94-009322 .... p 4350 N94-35980 #
DE94-009346 .... p 4245 N94-35809 #
DE94-009384 .... p 4349 N94-35565 #
DE94-009411 .... p 4324 N94-36016
DE94-009422 .... p 4305 N94-36017
DE94-009428 .... p 4264 N94-35681 #
DE94-009450 .... p 4322 N94-35682 #
DE94-009477 .... p 4331 N94-36428 #
DE94-009488 .... p 4264 N94-35683 #
DE94-009511 .... p 4271 N94-35679 #
DE94-009515 .... p 4266 N94-35982 #
DE94-009516 .... p 4271 N94-35665 #
DE94-009546 .... p 4290 N94-35666 #
DE94-009547 .... p 4275 N94-35815 #
DE94-009550 .... p 4275 N94-35667 #
DE94-009559 .... p 4284 N94-35668 #
DE94-009596 .... p 4264 N94-35669 #
DE94-009603 .... p 4335 N94-35670 #
DE94-009651 .... p 4324 N94-35816 #
DE94-009663 .... p 4264 N94-35756
DE94-009679 .... p 4239 N94-36349
DE94-009680 .... p 4237 N94-35777
DE94-009695 .... p 4332 N94-35671 #
DE94-009705 .... p 4237 N94-35778
DE94-009728 .... p 4319 N94-36320
DE94-009791 .... p 4287 N94-36179
DE94-009803 .... p 4245 N94-35779
DE94-009808 .... p 4281 N94-36018
DE94-009817 .... p 4282 N94-35829
DE94-009823 .... p 4241 N94-36222 #
DE94-009835 .... p 4285 N94-35765
DE94-009848 .... p 4345 N94-35817 #
DE94-009867 .... p 4294 N94-35766
DE94-009868 .... p 4294 N94-35767
DE94-009905 .... p 4270 N94-36350
DE94-009916 .... p 4333 N94-35818 #
DE94-009919 .... p 4339 N94-36386 #
DE94-009939 .... p 4244 N94-35768
DE94-009962 .... p 4282 N94-35672 #
DE94-009970 .... p 4265 N94-35769
DE94-009973 .... p 4335 N94-35673 #
DE94-009976 .... p 4335 N94-35647 #
DE94-009978 .... p 4319 N94-35770
DE94-009994 .... p 4212 N94-35648 #
DE94-009995 .... p 4251 N94-36008 #
DE94-009996 .... p 4245 N94-35771
DE94-010001 .... p 4247 N94-36387 #
DE94-010002 .... p 4251 N94-36388 #
DE94-010014 .... p 4325 N94-36086
DE94-010016 .... p 4321 N94-35649
DE94-010019 .... p 4331 N94-36192 #
DE94-010031 .... p 4240 N94-35650
DE94-010055 .... p 4272 N94-35695
DE94-010057 .... p 4232 N94-35696
DE94-010059 .... p 4333 N94-35697 #
DE94-010066 .... p 4309 N94-36429 #
DE94-010070 .... p 4340 N94-35698
DE94-010081 .... p 4244 N94-35699
DE94-010084 .... p 4284 N94-35700
DE94-010086 .... p 4244 N94-35701
DE94-010087 .... p 4244 N94-35702 #
DE94-010089 .... p 4262 N94-36430 #
DE94-010093 .... p 4246 N94-36306
DE94-010101 .... p 4268 N94-36374
DE94-010102 .... p 4293 N94-35703
DE94-010104 .... p 4314 N94-35704 #
DE94-010106 .... p 4244 N94-35705
DE94-010107 .... p 4259 N94-35706 #
DE94-010114 .... p 4326 N94-36126 #
DE94-010128 .... p 4279 N94-35684 #
DE94-010137 .... p 4270 N94-36389 #
DE94-010184 .... p 4236 N94-35685
DE94-010192 .... p 4297 N94-36223 #
DE94-010202 .... p 4338 N94-36093 #
DE94-010206 .... p 4347 N94-36297 #
DE94-010212 .... p 4258 N94-35686 #
DE94-010213 .... p 4312 N94-35810
DE94-010224 .... p 4328 N94-36298 #
DE94-010263 .... p 4248 N94-36299 #
DE94-010305 .... p 4330 N94-36105 #
DE94-010307 .... p 4347 N94-36300 #
DE94-010309 .... p 4331 N94-36224 #
DE94-010320 .... p 4330 N94-36106 #
DE94-010321 .... p 4259 N94-36094 #
DE94-010332 .... p 4332 N94-36431 #
DE94-010333 .... p 4326 N94-36107 #
DE94-010353 .... p 4245 N94-36108 #
DE94-010365 .... p 4316 N94-36432 #
DE94-010383 .... p 4283 N94-36109 #
DE94-010392 .... p 4240 N94-36110 #
DE94-010393 .... p 4267 N94-36111 #
DE94-010404 .... p 4256 N94-36112 #
DE94-010407 .... p 4330 N94-36114 #
DE94-010409 .... p 4272 N94-36115 #
DE94-010419 .... p 4269 N94-36095 #
DE94-010420 .... p 4240 N94-35953 #
DE94-010421 .... p 4329 N94-36390 #
DE94-010426 .... p 4244 N94-35687 #
DE94-010442 .... p 4327 N94-36225 #
DE94-010451 .... p 4276 N94-36433 #
DE94-010452 .... p 4241 N94-36231 #
DE94-010462 .... p 4275 N94-36232 #
DE94-010464 .... p 4351 N94-36418 #
DE94-010516 .... p 4246 N94-36283 #
DE94-010576 .... p 4283 N94-36243 #
DE94-010664 .... p 4238 N94-36084 #
DE94-010667 .... p 4326 N94-36127 #
DE94-010668 .... p 4256 N94-36301 #
DE94-010669 .... p 4338 N94-36284 #
DE94-010702 .... p 4328 N94-36302 #
DE94-010748 .... p 4260 N94-36245 #
DE94-010751 .... p 4326 N94-36198 #
DE94-010755 .... p 4331 N94-36199 #
DE94-010786 .... p 4241 N94-36233 #
DE94-010832 .... p 4338 N94-36200 #
DE94-010835 .... p 4338 N94-36193 #
DE94-010844 .... p 4259 N94-36194 #
DE94-010846 .... p 4312 N94-36195 #
DE94-010881 .... p 4241 N94-36196 #
DE94-010885 .... p 4260 N94-36197 #
DE94-010891 .... p 4318 N94-36201 #
DE94-010894 .... p 4339 N94-36375 #
DE94-011001 .... p 4340 N94-36032 #
DE94-011009 .... p 4331 N94-36202 #
DE94-011011 .... p 4237 N94-36033 #
DE94-011012 .... p 4248 N94-36034 #
DE94-011130 .... p 4248 N94-36035 #
DE94-011157 .... p 4237 N94-36036 #
DE94-011170 .... p 4237 N94-36056 #
DE94-011201 .... p 4245 N94-36057 #
DE94-011207 .... p 4238 N94-36203 #
DE94-011329 .... p 4318 N94-36204 #
DE94-011357 .... p 4297 N94-36269
DE94-011358 .... p 4315 N94-36270 #
DE94-011373 .... p 4324 N94-36058 #
DE94-011382 .... p 4331 N94-36271 #
DE94-011420 .... p 4248 N94-36376 #
DE94-011463 .... p 4342 N94-36377 #
DE94-011465 .... p 4295 N94-36244 #
DE94-011480 .... p 4341 N94-36272 #
DE94-011604 .... p 4288 N94-36273 #
DE94-011752 .... p 4257 N94-36354 #
DE94-011754 .... p 4295 N94-36285 #
DE94-011758 .... p 4288 N94-36286 #
DE94-011903 .... p 4350 N94-36229 #
DE94-011907 .... p 4238 N94-36230 #
DE94-011908 .... p 4317 N94-36234 #
DE94-011913 .... p 4341 N94-36274 #
DE94-011914 .... p 4317 N94-36235 #
DE94-011916 .... p 4308 N94-36236 #
DE94-610480 .... p 4290 N94-35830 #
DE94-610481 .... p 4291 N94-36087
DE94-610504 .... p 4290 N94-35780
DE94-610740 .... p 4325 N94-36088
DE94-611058 .... p 4312 N94-35831 #
DE94-611061 .... p 4346 N94-35832 #
DE94-611062 .... p 4346 N94-35833 #
DE94-611063 .... p 4305 N94-35834 #
DE94-611074 .... p 4315 N94-36100
DE94-611075 .... p 4343 N94-36381 #
DE94-611079 .... p 4334 N94-36180 #
DE94-611100 .... p 4340 N94-35933 #
DE94-611102 .... p 4315 N94-35934 #
DE94-611103 .... p 4240 N94-35935 #
DE94-611104 .... p 4342 N94-35781 #
DE94-611106 .... p 4272 N94-35782 #
DE94-611114 .... p 4343 N94-36351 #
DE94-611145 .... p 4317 N94-36307 #
DE94-611157 .... p 4322 N94-35783 #
DE94-611160 .... p 4322 N94-35784 #
DE94-611171 .... p 4320 N94-35566
DE94-611173 .... p 4322 N94-35785 #
DE94-611209 .... p 4329 N94-36308 #
DE94-611232 .... p 4322 N94-35786 #
DE94-611253 .... p 4323 N94-35787 #
DE94-611459 .... p 4336 N94-35788 #
DE94-611466 .... p 4335 N94-35750 #
DE94-612434 .... p 4315 N94-35789 #
DE94-612439 .... p 4345 N94-35790 #
DE94-612462 .... p 4315 N94-36416 #
DE94-612496 .... p 4320 N94-35567
DE94-612627 .... p 4336 N94-35791 #
DE94-612636 .... p 4322 N94-35751 #
DE94-612823 .... p 4240 N94-35960 #
DE94-615424 .... p 4330 N94-36028 #
DE94-615510 .... p 4329 N94-36434 #
DE94-615511 .... p 4340 N94-36029 #
DE94-615584 .... p 4309 N94-36382 #
DE94-615646 .... p 4340 N94-36030 #
DE94-615647 .... p 4340 N94-36041 #
DE94-615768 .... p 4341 N94-36181 #
DE94-615824 .... p 4289 N94-35568 #
DE94-615858 .... p 4350 N94-36128 #
DE94-616167 .... p 4326 N94-36182 #
DE94-616200 .... p 4320 N94-35569
DE94-616235 .... p 4330 N94-35999 #
DE94-616271 .... p 4300 N94-35570

DE94-616453 p 4259 N94-36104 #
DE94-616508 p 4235 N94-35592 #
DE94-616604 p 4346 N94-35954 #
DE94-616613 p 4318 N94-35955 #
DE94-616615 p 4318 N94-35956 #
DE94-616616 p 4342 N94-36070 #
DE94-616618 p 4343 N94-36071 #
DE94-616620 p 4343 N94-36072 #
DE94-616621 p 4325 N94-36073
DE94-616649 p 4321 N94-35593
DE94-616650 p 4321 N94-35594
DE94-616651 p 4321 N94-35595
DE94-616652 p 4320 N94-35579 #
DE94-616653 p 4320 N94-35580 #
DE94-616654 p 4320 N94-35581 #
DE94-616660 p 4325 N94-36074
DE94-616768 p 4325 N94-36075 #
DE94-616769 p 4315 N94-36076 #
DE94-616775 p 4321 N94-35582 #
DE94-616787 p 4325 N94-36077 #
DE94-616788 p 4256 N94-36078 #
DE94-616799 p 4325 N94-36079 #
DE94-616800 p 4330 N94-36080 #
DE94-616852 p 4321 N94-35583 #
DE94-616853 p 4329 N94-36391 #
DE94-616869 p 4327 N94-36246
DE94-616870 p 4326 N94-36129 #
DE94-616886 p 4326 N94-36130 #
DE94-616887 p 4326 N94-36131 #
DE94-616888 p 4326 N94-36132 #
DE94-616889 p 4329 N94-36392 #
DE94-616907 p 4326 N94-36133 #
DE94-617006 p 4326 N94-36134 #
DE94-617057 p 4329 N94-36310 #
DE94-617087 p 4329 N94-36311 #
DE94-617113 p 4273 N94-36393 #
DE94-617129 p 4339 N94-36417 #
DE94-617188 p 4256 N94-36099 #
DE94-617189 p 4256 N94-36096
DE94-617190 p 4338 N94-36097
DE94-617215 p 4325 N94-36081
DE94-617216 p 4337 N94-36082 #
DE94-617360 p 4325 N94-36083
DE94-617361 p 4341 N94-36312 #
DE94-617391 p 4267 N94-36313 #
DE94-617392 p 4267 N94-36098 #
DE94-617393 p 4267 N94-36314 #
DE94-618544 p 4328 N94-36287 #
DE94-619027 p 4242 N94-36288 #
DE94-619028 p 4242 N94-36289 #
DE94-718910 p 4337 N94-35983 #
DE94-718974 p 4336 N94-35772 #
DE94-718975 p 4338 N94-36352 #
DE94-718976 p 4324 N94-35984 #
DE94-718977 p 4339 N94-36353 #
DE94-718978 p 4338 N94-36247 #
DE94-718981 p 4339 N94-36357 #
DE94-718982 p 4337 N94-35936 #
DE94-718983 p 4337 N94-35937 #
DE94-718987 p 4337 N94-35938 #
DE94-718992 p 4336 N94-35811 #
DE94-718993 p 4336 N94-35812 #
DE94-718994 p 4336 N94-35813 #
DE94-718995 p 4336 N94-35773 #
DE94-727517 p 4314 N94-35774 #
DE94-727617 p 4337 N94-35939 #
DE94-727618 p 4336 N94-35775 #
DE94-727626 p 4336 N94-35752 #
DE94-727636 p 4296 N94-36101
DE94-763298 p 4237 N94-36059 #
DE94-763308 p 4283 N94-36060 #

DMM(A)-121 p 4263 N94-35603

DNA-TR-93-4 p 4279 N94-35949

DOE/AL-65030/9328 p 4238 N94-36084 #

DOE/BC-14968/1 p 4344 N94-35347 #

DOE/CE-16067/2 p 4284 N94-35668 #
DOE/CE-23810/20A p 4251 N94-36008 #
DOE/CE-23810/20B p 4245 N94-35771
DOE/CE-23810/38B p 4244 N94-35687 #
DOE/CE-23810/40A p 4247 N94-36387 #
DOE/CE-23810/40B p 4251 N94-36388 #
DOE/CE-34025/T12 p 4297 N94-36223 #

DOE/CH-10435/T15 p 4283 N94-36243 #

DOE/EIA-M069 p 4282 N94-35672 #

DOE/ER-13191/14 p 4330 N94-36105 #
DOE/ER-13515/9 p 4324 N94-35816 #
DOE/ER-13626/T1 p 4236 N94-35685
DOE/ER-13768/4 p 4326 N94-36126 #
DOE/ER-13808/6 p 4329 N94-36390 #
DOE/ER-14258/T1 p 4328 N94-36298 #
DOE/ER-14268/2 p 4241 N94-36233 #
DOE/ER-40150/258 p 4325 N94-36086
DOE/ER-40150/261 p 4321 N94-35649
DOE/ER-40150/264 p 4331 N94-36192 #
DOE/ER-40200/319 p 4323 N94-35814 #
DOE/ER-40427/20-N93 p 4329 N94-36305
DOE/ER-40427/21-N93 p 4328 N94-36304
DOE/ER-40427/31-N93 p 4324 N94-35824
DOE/ER-40616/T1 p 4345 N94-35817 #
DOE/ER-40664/T1 p 4269 N94-36095 #
DOE/ER-40717/10 p 4331 N94-36428 #
DOE/ER-40728/T1 p 4324 N94-36016
DOE/ER-45163/40 p 4238 N94-36203 #
DOE/ER-45365/6 p 4240 N94-35953 #
DOE/ER-45368/T1 p 4246 N94-36283 #
DOE/ER-53241/7-PT-2 p 4335 N94-35670 #
DOE/ER-53267/129 p 4338 N94-36200 #
DOE/ER-61373/2 p 4269 N94-36085 #
DOE/ER-75708/T2 p 4228 N94-35349 #

DOE/ER/40762-025 p 4321 N94-35649

DOE/ET-53088/651 p 4264 N94-35681 #

DOE/FE-61684/94/C0264 p 4282 N94-36021 #

DOE/ID-12692/6 p 4245 N94-35809 #

DOE/MC-23174/94/C0329 p 4275 N94-35667 #
DOE/MC-23174/94/C0332 p 4275 N94-35815 #
DOE/MC-25124/94/C0273 p 4275 N94-36348 #
DOE/MC-27221/94/C0243 p 4276 N94-36355
DOE/MC-28055/94/C0334 p 4283 N94-36109 #
DOE/MC-29061/94/C0269 p 4275 N94-36022 #
DOE/MC-29101/94/C0333 p 4290 N94-35666 #

DOE/PC-90046/T9 p 4248 N94-36299 #
DOE/PC-90291/T12 p 4237 N94-36023 #
DOE/PC-91347/T6 p 4284 N94-35346 #
DOE/PC-92112/T3 p 4237 N94-35778
DOE/PC-92114/T2 p 4248 N94-36035 #
DOE/PC-93222/1 p 4237 N94-36036 #

DOE/SF-18852/T38 p 4212 N94-35648 #

DOT/FAA/AM-94/11 p 4191 N94-35236 #

DOT/FAA/CT-93/42 p 4278 N94-36090
DOT/FAA/CT-93/65 p 4247 N94-35795

DOT/FAA/RD-94/12 p 4294 N94-35807
DOT/FAA/RD-94/2 p 4295 N94-36249
DOT/FAA/RD-94/5 p 4293 N94-35720
DOT/FAA/RD-94/6 p 4293 N94-35719
DOT/FAA/RD-94/9 p 4293 N94-35596

DRA-MEMO-4629 p 4307 N94-36113 #

DRC-TH-05/93 p 4321 N94-35593

DRES-SM-1400 p 4238 N94-36091

DRET/DS/SR-93/1311 p 4291 N94-36214

DTIC-TR-94/21 p 4344 N94-35525

DTP-93/19 p 4314 N94-35774 #

E-5843 p 4313 N94-35259 * #
E-8474 p 4262 N94-35248 * #
E-8770 p 4200 N94-35267 * #
E-8852 p 4265 N94-35945 * #
E-8857 p 4281 N94-35271 * #
E-8865 p 4347 N94-36396 * #
E-8881 p 4257 N94-35249 * #
E-8884 p 4278 N94-35239 * #
E-8886 p 4243 N94-35260 * #
E-8897 p 4265 N94-35948 * #
E-8903 p 4198 N94-35352 * #
E-8910 p 4243 N94-35243 * #
E-8911 p 4268 N94-35268 * #
E-8916 p 4263 N94-35250 * #
E-8917 p 4199 N94-36379 * #
E-8927 p 4234 N94-35995 * #
E-8936 p 4263 N94-35253 * #
E-8943 p 4258 N94-35270 * #
E-8956 p 4266 N94-35976 * #

EDR-16194 p 4283 N94-36243 #

EGG-MS-10992 p 4328 N94-36302 #

EGG-WMO-10279-VOL-1 p 4287 N94-36207 #
EGG-WMO-10279-VOL-2 p 4287 N94-36208 #

EPA/600/A-94/036 p 4298 N94-35688
EPA/600/A-94/043 p 4332 N94-35584
EPA/600/R-94/013 p 4296 N94-35738 #
EPA/620/R-94/016 p 4285 N94-35741

ESC-TR-93-321 p 4304 N94-35794
ESC-TR-94-003 p 4302 N94-35495
ESC-TR-94-007 p 4308 N94-36294

ESDP-4129 p 4295 N94-36244 #

ESM93-2.0-CM p 4233 N94-35715
ESM94-1.0-CM p 4233 N94-35944
ESM94-2.0-CM p 4233 N94-35714

FNAL-TM-1880 p 4332 N94-36431 #

FNAL/C-93/212-E p 4327 N94-36266
FNAL/C-94/044-E p 4326 N94-36107 #

FNAL/PUB-93/322-A p 4327 N94-36241

FRCR-444 p 4338 N94-36200 #

GA-A-21647 p 4335 N94-35673 #

GCT/9401 p 4272 N94-35721

GRI-93/0398 p 4275 N94-35931
GRI-93/0443 p 4236 N94-35755

GTFR-112 p 4338 N94-36093 #

H-1988 p 4199 N94-35258 * #
H-1990 p 4193 N94-35241 * #

IAEA-CN-56/C-1-4 p 4324 N94-35984 #
IAEA-CN-56/C-2-2 p 4339 N94-36357 #
IAEA-CN-56/C-2-4 p 4337 N94-35936 #
IAEA-CN-56/C-4-2 p 4338 N94-36352 #
IAEA-CN-56/D-3-2 p 4336 N94-35772 #
IAEA-CN-56/D-4-15(CP) p 4337 N94-35938 #
IAEA-CN-56/D-4-19 p 4339 N94-36353 #
IAEA-CN-56/D-4-20 p 4337 N94-35937 #
IAEA-CN-56/E-2-3 p 4338 N94-36247 #

IAEA-TECDOC-726 p 4289 N94-35568 #

IC-93/188 p 4343 N94-36351 #
IC-93/211 p 4317 N94-36307 #
IC-93/231 p 4329 N94-36308 #
IC-93/233 p 4343 N94-36381 #
IC-93/242 p 4322 N94-35786 #
IC-93/252 p 4340 N94-35933 #
IC-93/268 p 4315 N94-35934 #
IC-93/269 p 4240 N94-35935 #
IC-93/276 p 4342 N94-35781 #

ICASE-94-21 p 4266 N94-35975 * #
ICASE-94-22 p 4267 N94-35992 * #
ICASE-94-26 p 4300 N94-35240 * #
ICASE-94-29 p 4191 N94-35994 * #
ICASE-94-30 p 4263 N94-35497 * #

ICOMP-94-10 p 4198 N94-35352 * #
ICOMP-94-12 p 4266 N94-35976 * #
ICOMP-94-9 p 4265 N94-35948 * #

IDA-P-2940 p 4312 N94-35730

IDA/HQ-93-44868 p 4312 N94-35730

IFSR-651 p 4264 N94-35681 #

IFT-P-051/93 p 4321 N94-35593
IFT-P-059-93 p 4321 N94-35582 #
IFT-P-060-93 p 4321 N94-35594
IFT-P-064-93 p 4321 N94-35595
IFT-P-066-93 p 4321 N94-35583 #
IFT-P-068-93 p 4320 N94-35579 #
IFT-P-069-93 p 4320 N94-35580 #
IFT-P-070-93 p 4320 N94-35581 #

IFUSP-P-1074 p 4321 N94-35594
IFUSP-P-1075 p 4321 N94-35582 #

IFVE-UNK-92-22 p 4325 N94-36088

IHEP-OTF-92-149 p 4322 N94-35784 #
IHEP-OTF-92-53 p 4323 N94-35787 #

IHES/M/93/63 p 4317 N94-35760
IHES/M/93/69 p 4314 N94-35759
IHES/M/94/2 p 4342 N94-35761
IHES/M/94/4 p 4314 N94-35762
IHES/M/94/8 p 4314 N94-35763

IHES/M/94/9 .... p 4314 N94-35764

IHES/P/94/7 .... p 4314 N94-35758

INIS-MF-13733-VOL-1 .... p 4290 N94-35830 #
INIS-MF-13734-VOL-2 .... p 4291 N94-36087
INIS-MF-13741 .... p 4312 N94-35831 #

INIS-RU-361 .... p 4341 N94-36181 #
INIS-RU-362-VOL-1 .... p 4320 N94-35569
INIS-RU-363-VOL-2 .... p 4326 N94-36182 #

INP-MSU-93-3-295 .... p 4350 N94-36128 #

INP-1577/PH .... p 4318 N94-35956 #
INP-1578/PH .... p 4342 N94-36070 #
INP-1596/PH .... p 4326 N94-36130 #
INP-1608/PH .... p 4326 N94-36129 #

INT-PATENT-CLASS-B01J-29/06 p 4235 N94-35255 *
INT-PATENT-CLASS-B01J-37/30 p 4235 N94-35255 *
INT-PATENT-CLASS-B23K-10/02 p 4273 N94-35367 *
INT-PATENT-CLASS-B23K-9/095 p 4273 N94-35367 *

INT-PATENT-CLASS-C08J-5/08 .. p 4242 N94-35233 *
INT-PATENT-CLASS-C08L-79/08 p 4232 N94-35372 * #

INT-PATENT-CLASS-F16D-1/00 . p 4274 N94-35374 *
INT-PATENT-CLASS-F16J-15/16 p 4274 N94-35373 *
INT-PATENT-CLASS-F16K-15/02 p 4274 N94-35661 *

INT-PATENT-CLASS-G01B-11/00 p 4333 N94-35749 *
INT-PATENT-CLASS-G01B-9/02 . p 4333 N94-35749 *
INT-PATENT-CLASS-G01D-18/00 p 4268 N94-35368 *
INT-PATENT-CLASS-G01J-5/62 . p 4269 N94-35383 *
INT-PATENT-CLASS-G01L-7/08 . p 4269 N94-35369 *
INT-PATENT-CLASS-G01M-9/00 p 4269 N94-35369 *
INT-PATENT-CLASS-G05F-5/00 . p 4282 N94-35540 * #
INT-PATENT-CLASS-G06F-15/52 p 4311 N94-35501 *
INT-PATENT-CLASS-G08B-21/00 p 4268 N94-35235 *

INT-PATENT-CLASS-H01L-31/06 p 4281 N94-35230 *
INT-PATENT-CLASS-H01Q-1/24 . p 4251 N94-35231 *
INT-PATENT-CLASS-H01R-43/00 p 4274 N94-35375 *
INT-PATENT-CLASS-H04B-17/00 p 4268 N94-35368 *
INT-PATENT-CLASS-H04N-7/18 . p 4332 N94-35384 *

IPEN-PUB-381 .... p 4330 N94-36028 #

IS-T-1680 .... p 4245 N94-36057 #

ISBN-0-88363-893-2 .... p 4201 N94-36440 * #
ISBN-0-9629930-2-6 .... p 4348 N94-35901
ISBN-92-835-0726-6 .... p 4193 N94-36321 #
ISBN-951-22-1533-0 .... p 4259 N94-35822
ISBN-951-22-1915-8 .... p 4346 N94-35959
ISBN-951-22-1927-1 .... p 4315 N94-35821
ISBN-951-22-1955-7 .... p 4279 N94-36000
ISBN-951-29-0125-0 .... p 4283 N94-36060 #

ISI-RR-93-366 .... p 4303 N94-35662

ISI/RR-93-368 .... p 4345 N94-35663
ISI/RR-93-369 .... p 4345 N94-35651

ISI/RS-93-360 .... p 4300 N94-35652

ITF-92-10R .... p 4343 N94-36071 #
ITF-92-32R .... p 4267 N94-36313 #
ITF-92-37R .... p 4256 N94-36099 #
ITF-92-47R .... p 4267 N94-36098 #
ITF-93-18U .... p 4267 N94-36314 #
ITF-93-2R .... p 4256 N94-36096
ITF-93-3R .... p 4325 N94-36077 #

ITP-92-40E .... p 4329 N94-36391 #
ITP-92-54E .... p 4329 N94-36434 #
ITP-93-12E .... p 4340 N94-36029 #
ITP-93-13E .... p 4325 N94-36081
ITP-93-14E .... p 4326 N94-36131 #
ITP-93-16E .... p 4325 N94-36083
ITP-93-18E .... p 4341 N94-36312 #
ITP-93-21E .... p 4325 N94-36074
ITP-93-25E .... p 4326 N94-36132 #
ITP-93-30E .... p 4340 N94-36030 #
ITP-93-31E .... p 4329 N94-36392 #
ITP-93-32E .... p 4325 N94-36075 #
ITP-93-36E .... p 4315 N94-36076 #
ITP-93-37E .... p 4340 N94-36041 #
ITP-93-4E .... p 4329 N94-36311 #
ITP-93-40E .... p 4329 N94-36310 #
ITP-93-5E .... p 4343 N94-36072 #
ITP-93-8E .... p 4325 N94-36079 #

IYAF-91-96 .... p 4259 N94-36104 #

IYAF-92-16 .... p 4338 N94-36097

IYAF-92-2 .... p 4256 N94-36078 #
IYAF-92-42 .... p 4346 N94-35954 #
IYAF-92-57 .... p 4322 N94-35783 #
IYAF-92-58 .... p 4335 N94-35750 #
IYAF-92-60 .... p 4336 N94-35788 #
IYAF-92-61 .... p 4322 N94-35785 #
IYAF-92-66 .... p 4326 N94-36134 #
IYAF-92-79 .... p 4330 N94-35999 #
IYAF-92-94 .... p 4326 N94-36133 #
IYAF-93-12 .... p 4325 N94-36073
IYAF-93-5 .... p 4337 N94-36082 #

JINR-E-2-93-164 .... p 4330 N94-36080 #

JINR-R-10-92-449 .... p 4345 N94-35790 #
JINR-R-11-92-434 .... p 4315 N94-35789 #
JINR-R-14-92-334 .... p 4322 N94-35751 #
JINR-R-2-92-485 .... p 4318 N94-35955 #
JINR-R-4-92-405 .... p 4315 N94-36416 #

JPL-TDA-PR-42-117 .... p 4252 N94-35542 * #

JPRS-UMS-93-007 .... p 4240 N94-35517 #

JPRS-USP-93-005 .... p 4201 N94-36011 #
JPRS-USP-94-001 .... p 4201 N94-35518 #
JPRS-USP-94-002 .... p 4348 N94-35519 #
JPRS-USP-94-003 .... p 4201 N94-35520 #

JPRS-UST-94-001 .... p 4229 N94-35340 #
JPRS-UST-94-004 .... p 4249 N94-35341 #
JPRS-UST-94-005 .... p 4249 N94-35342 #
JPRS-UST-94-006 .... p 4249 N94-35226 #
JPRS-UST-94-007 .... p 4249 N94-35227 #
JPRS-UST-94-008 .... p 4249 N94-35228 #
JPRS-UST-94-010 .... p 4250 N94-35385 #
JPRS-UST-94-011 .... p 4250 N94-35386 #
JPRS-UST-94-012 .... p 4250 N94-35387 #

JSC-26704 .... p 4274 N94-35481 * #

KAERI/TR-277/92 .... p 4346 N94-35832 #
KAERI/TR-278/92 .... p 4346 N94-35833 #
KAERI/TR-353/93 .... p 4305 N94-35834 #
KAERI/TR-367/93 .... p 4334 N94-36180 #

KCP-613-5271 .... p 4258 N94-35686 #
KCP-613-5283 .... p 4259 N94-35706 #
KCP-613-5291 .... p 4312 N94-35810
KCP-613-5292 .... p 4260 N94-36197 #
KCP-613-5377 .... p 4244 N94-35705

L-17260 .... p 4192 N94-36048 * #
L-17263 .... p 4189 N94-35246 * #
L-17362 .... p 4217 N94-35865 * #
L-17369-PT-1 .... p 4212 N94-35836 * #
L-17369-PT-2 .... p 4223 N94-35902 * #
L-17396 .... p 4229 N94-36398 * #

LA-SUB-93-307 .... p 4244 N94-35768

LA-UR-93-2140 .... p 4257 N94-36316 #
LA-UR-93-3546 .... p 4347 N94-36102 #
LA-UR-93-3699 .... p 4291 N94-36103 #
LA-UR-94-1118 .... p 4350 N94-35980 #
LA-UR-94-491 .... p 4242 N94-36369 #
LA-UR-94-695 .... p 4320 N94-35376 #
LA-UR-94-759 .... p 4304 N94-35808 #
LA-UR-94-789 .... p 4236 N94-35680 * #

LA-11692-MS-VOL-6 .... p 4264 N94-35669 #
LA-12601-MS .... p 4295 N94-36240

LAMP-93/3 .... p 4272 N94-35782 #

LBL-30971 .... p 4344 N94-35337 #
LBL-33962 .... p 4250 N94-35364 #
LBL-34182 .... p 4297 N94-36269
LBL-34610 .... p 4317 N94-36234 #
LBL-34942 .... p 4315 N94-36270 #
LBL-35194 .... p 4324 N94-36058 #
LBL-35232 .... p 4331 N94-36271 #
LBL-35335 .... p 4331 N94-36202 #
LBL-35354 .... p 4238 N94-36230 #
LBL-35431 .... p 4248 N94-36034 #
LBL-35432 .... p 4237 N94-36033 #
LBL-35438 .... p 4350 N94-36229 #
LBL-35491 .... p 4341 N94-36274 #
LBL-35495 .... p 4317 N94-36235 #

LC-79-640375 .... p 4374 N94-36009
LC-79-640375 .... p 4375 N94-36020

LIYAF-1765 .... p 4320 N94-35566

LPI-TR-93-04-PT-2 .... p 4354 N94-35359 * #

M-729 .... p 4291 N94-36175 * #

MCR-93-1339-ISSUE-2 .... p 4354 N94-35263 * #

ME/ES-TR-94-1 .... p 4298 N94-35266 * #

MEMO-INF-93-32 .... p 4302 N94-35538

MEMS-94-101 .... p 4190 N94-35950

MIT-ATC-208 .... p 4295 N94-36249
MIT-ATC-215 .... p 4293 N94-35596

MSC-TPR-3417/CA07 .... p 4244 N94-35757

MTR-93B0000070-V2 .... p 4201 N94-35827

NAS 1.15:103966 .... p 4299 N94-35393 * #
NAS 1.15:103970 .... p 4189 N94-35394 * #
NAS 1.15:103997 .... p 4376 N94-35370 * #
NAS 1.15:104007 .... p 4263 N94-35371 * #
NAS 1.15:104603 .... p 4211 N94-35269 * #
NAS 1.15:104605 .... p 4281 N94-35261 * #
NAS 1.15:104608 .... p 4259 N94-36049 * #
NAS 1.15:104792 .... p 4262 N94-35245 * #
NAS 1.15:104796 .... p 4274 N94-35481 * #
NAS 1.15:106487 .... p 4262 N94-35248 * #
NAS 1.15:106588 .... p 4265 N94-35945 * #
NAS 1.15:106590 .... p 4281 N94-35271 * #
NAS 1.15:106596 .... p 4268 N94-35268 * #
NAS 1.15:106605 .... p 4257 N94-35249 * #
NAS 1.15:106607 .... p 4243 N94-35260 * #
NAS 1.15:106614 .... p 4265 N94-35948 * #
NAS 1.15:106618 .... p 4198 N94-35352 * #
NAS 1.15:106622 .... p 4243 N94-35243 * #
NAS 1.15:106625 .... p 4263 N94-35250 * #
NAS 1.15:106626 .... p 4199 N94-36379 * #
NAS 1.15:106635 .... p 4263 N94-35253 * #
NAS 1.15:106639 .... p 4258 N94-35270 * #
NAS 1.15:106648 .... p 4266 N94-35976 * #
NAS 1.15:108816 .... p 4380 N94-36117 * #
NAS 1.15:108822 .... p 4198 N94-36380 * #
NAS 1.15:109057 .... p 4309 N94-36438 * #
NAS 1.15:109115 .... p 4233 N94-35946 * #
NAS 1.15:109127 .... p 4311 N94-35242 * #
NAS 1.15:109203 .... p 4211 N94-35523 * #
NAS 1.15:109204 .... p 4288 N94-36422 * #
NAS 1.15:109250 .... p 4228 N94-35591 * #
NAS 1.15:109349 .... p 4236 N94-35680 * #
NAS 1.15:109779 .... p 4343 N94-35339 *
NAS 1.15:109791 .... p 4347 N94-35899 * #
NAS 1.15:109792 .... p 4348 N94-35900 * #
NAS 1.15:109793 .... p 4348 N94-35446 * #
NAS 1.15:109840 .... p 4201 N94-35390 * #
NAS 1.15:109866 .... p 4211 N94-35252 * #
NAS 1.15:109867 .... p 4211 N94-35251 * #
NAS 1.15:109868 .... p 4344 N94-35254 * #
NAS 1.15:109888 .... p 4201 N94-36440 * #
NAS 1.15:4527 .... p 4291 N94-36175 * #
NAS 1.15:4563 .... p 4189 N94-35246 * #
NAS 1.15:4590 .... p 4199 N94-35258 * #
NAS 1.15:4591 .... p 4193 N94-35241 * #
NAS 1.21:7011(391) .... p 4297 N94-35345 *
NAS 1.21:7037(306) .... p 4189 N94-35338 *
NAS 1.21:7039(45)-SECT-1 .... p 4344 N94-35382 *
NAS 1.21:7039(45)-SECT-2 .... p 4346 N94-35835 *
NAS 1.21:7096-VOL-1/2/3 .... p 4346 N94-36037 *
NAS 1.26:188291 .... p 4301 N94-35443 * #
NAS 1.26:188331 .... p 4309 N94-36439 * #
NAS 1.26:189344 .... p 4300 N94-35256 * #
NAS 1.26:189347 .... p 4301 N94-35434 * #
NAS 1.26:189350 .... p 4300 N94-35238 * #
NAS 1.26:189352 .... p 4375 N94-35381 * #
NAS 1.26:189358 .... p 4292 N94-35380 * #
NAS 1.26:189363 .... p 4349 N94-36279 * #
NAS 1.26:189366 .... p 4349 N94-36281 * #
NAS 1.26:189369 .... p 4349 N94-36282 * #
NAS 1.26:189370 .... p 4349 N94-36280 * #
NAS 1.26:190545 .... p 4300 N94-35365 * #
NAS 1.26:191669 .... p 4306 N94-36040 * #
NAS 1.26:193380 .... p 4376 N94-35363 * #
NAS 1.26:193967 .... p 4212 N94-35484 * #
NAS 1.26:193974 .... p 4330 N94-35483 * #
NAS 1.26:193975 .... p 4235 N94-35447 * #
NAS 1.26:193979 .... p 4249 N94-35485 * #
NAS 1.26:193987 .... p 4333 N94-36119 * #
NAS 1.26:193988 .... p 4307 N94-36118 * #
NAS 1.26:194119 .... p 4375 N94-36395 * #
NAS 1.26:194592 .... p 4191 N94-36394 * #
NAS 1.26:194717 .... p 4306 N94-36063 * #
NAS 1.26:194856 .... p 4281 N94-35734 * #
NAS 1.26:194899 .... p 4266 N94-35975 * #
NAS 1.26:194900 .... p 4267 N94-35992 * #
NAS 1.26:194904 .... p 4300 N94-35240 * #
NAS 1.26:194908 .... p 4191 N94-35994 * #
NAS 1.26:194909 .... p 4263 N94-35497 * #

NAS 1.26:194922 .... p 4252 N94-35247 * #
NAS 1.26:195157 .... p 4288 N94-35244 * #
NAS 1.26:195323 .... p 4200 N94-35267 * #
NAS 1.26:195334 .... p 4347 N94-36396 * #
NAS 1.26:195337 .... p 4278 N94-35239 * #
NAS 1.26:195345 .... p 4234 N94-35995 * #
NAS 1.26:195743 .... p 4355 N94-35395 * #
NAS 1.26:195744 .... p 4367 N94-36136 * #
NAS 1.26:195745 .... p 4362 N94-35448 * #
NAS 1.26:195962 .... p 4302 N94-35514 * #
NAS 1.26:195980 .... p 4376 N94-35590 * #
NAS 1.26:195981 .... p 4293 N94-35499 * #
NAS 1.26:196003 .... p 4349 N94-35516 * #
NAS 1.26:196004 .... p 4296 N94-35257 * #
NAS 1.26:196008 .... p 4289 N94-35389 * #
NAS 1.26:196011 .... p 4376 N94-35515 * #
NAS 1.26:196016 .... p 4235 N94-35388 * #
NAS 1.26:196017 .... p 4268 N94-36420 * #
NAS 1.26:196020 .... p 4349 N94-36419 * #
NAS 1.26:196021 .... p 4279 N94-35974 * #
NAS 1.26:196024 .... p 4354 N94-35263 * #
NAS 1.26:196025 .... p 4319 N94-35264 * #
NAS 1.26:196026 .... p 4354 N94-35265 * #
NAS 1.26:196030 .... p 4298 N94-35266 * #
NAS 1.26:196032 .... p 4376 N94-36421 * #
NAS 1.26:196036 .... p 4374 N94-35993 * #
NAS 1.26:196038 .... p 4249 N94-35237 * #
NAS 1.26:196044 .... p 4292 N94-35355 * #
NAS 1.26:196046 .... p 4347 N94-36435 * #
NAS 1.26:196077 .... p 4202 N94-35487 * #
NAS 1.26:196078 .... p 4192 N94-35522 * #
NAS 1.26:196080 .... p 4293 N94-35391 * #
NAS 1.26:196081 .... p 4268 N94-36397 * #
NAS 1.26:196082 .... p 4245 N94-35977 * #
NAS 1.26:196083 .... p 4211 N94-35357 * #
NAS 1.26:196085 .... p 4284 N94-35486 * #
NAS 1.26:196093 .... p 4271 N94-35489 * #
NAS 1.26:196095 .... p 4271 N94-35488 * #
NAS 1.26:196097 .... p 4297 N94-35379 * #
NAS 1.26:196103 .... p 4200 N94-36436 * #
NAS 1.26:196116 .... p 4289 N94-35392 * #
NAS 1.26:196117 .... p 4252 N94-35542 * #
NAS 1.26:196119 .... p 4274 N94-35500 * #
NAS 1.26:196123 .... p 4354 N94-35378 * #
NAS 1.26:196130 .... p 4288 N94-35358 * #
NAS 1.26:196131 .... p 4376 N94-35356 * #
NAS 1.26:196132 .... p 4319 N94-36031 * #
NAS 1.26:196134 .... p 4354 N94-35359 * #
NAS 1.26:196136 .... p 4189 N94-35498 * #
NAS 1.26:4582 .... p 4190 N94-35991 * #
NAS 1.26:4595 .... p 4233 N94-35947 * #
NAS 1.26:4611 .... p 4280 N94-36423 * #
NAS 1.26:4612 .... p 4190 N94-35864 * #
NAS 1.55:10134 .... p 4377 N94-35961 * #
NAS 1.55:3242 .... p 4217 N94-35865 * #
NAS 1.55:3247-PT-1 .... p 4212 N94-35836 * #
NAS 1.55:3247-PT-2 .... p 4223 N94-35902 * #
NAS 1.55:3259 .... p 4229 N94-36398 * #
NAS 1.55:3265 .... p 4202 N94-35605 * #
NAS 1.60:3399 .... p 4192 N94-36048 * #
NAS 1.61:1327 .... p 4313 N94-35259 * #
NAS 1.75:554 .... p 4295 N94-35343 * #

NASA-CASE-GSC-13309-1 .... p 4251 N94-35231 *
NASA-CASE-GSC-13450-2 .... p 4282 N94-35540 * #

NASA-CASE-LAR-14029-1 .... p 4269 N94-35369 *
NASA-CASE-LAR-14239-2 .... p 4232 N94-35372 * #
NASA-CASE-LAR-14672-1 .... p 4268 N94-35368 *
NASA-CASE-LAR-14838-1 .... p 4242 N94-35233 *

NASA-CASE-LEW-15043-1 .... p 4242 N94-35234 *
NASA-CASE-LEW-15250-1 .... p 4269 N94-35383 *
NASA-CASE-LEW-15306-1 .... p 4243 N94-35502 *
NASA-CASE-LEW-15570-1 .... p 4274 N94-35373 *
NASA-CASE-LEW-15606-1 .... p 4281 N94-35230 *
NASA-CASE-LEW-15697-1 .... p 4241 N94-36275 *

NASA-CASE-MFS-28797-1 .... p 4273 N94-35367 *

NASA-CASE-MSC-21381-1 .... p 4311 N94-35501 *
NASA-CASE-MSC-21487-3 .... p 4235 N94-35229 *
NASA-CASE-MSC-21487-4 .... p 4250 N94-35445 *
NASA-CASE-MSC-21560-2 .... p 4296 N94-35232 *
NASA-CASE-MSC-21951-1 .... p 4268 N94-35235 *
NASA-CASE-MSC-22028-1 .... p 4274 N94-35374 *
NASA-CASE-MSC-22046-1 .... p 4274 N94-35661 *
NASA-CASE-MSC-22060-1 .... p 4296 N94-35366 *

NASA-CASE-NPO-17837-1-CU .... p 4332 N94-35384 *
NASA-CASE-NPO-18409-1-CU .... p 4235 N94-35255 *
NASA-CASE-NPO-18478-1-CU .... p 4333 N94-35749 *
NASA-CASE-NPO-18786-1-CU .... p 4274 N94-35375 *

NASA-CP-10134 .... p 4377 N94-35961 * #
NASA-CP-3242 .... p 4217 N94-35865 * #
NASA-CP-3247-PT-1 .... p 4212 N94-35836 * #
NASA-CP-3247-PT-2 .... p 4223 N94-35902 * #
NASA-CP-3259 .... p 4229 N94-36398 * #
NASA-CP-3265 .... p 4202 N94-35605 * #

NASA-CR-188291 .... p 4301 N94-35443 * #
NASA-CR-188331 .... p 4309 N94-36439 * #
NASA-CR-189344 .... p 4300 N94-35256 * #
NASA-CR-189347 .... p 4301 N94-35434 * #
NASA-CR-189350 .... p 4300 N94-35238 * #
NASA-CR-189352 .... p 4375 N94-35381 * #
NASA-CR-189358 .... p 4292 N94-35380 * #
NASA-CR-189363 .... p 4349 N94-36279 * #
NASA-CR-189366 .... p 4349 N94-36281 * #
NASA-CR-189369 .... p 4349 N94-36282 * #
NASA-CR-189370 .... p 4349 N94-36280 * #
NASA-CR-190545 .... p 4300 N94-35365 * #
NASA-CR-191669 .... p 4306 N94-36040 * #
NASA-CR-193380 .... p 4376 N94-35363 * #
NASA-CR-193967 .... p 4212 N94-35484 * #
NASA-CR-193974 .... p 4330 N94-35483 * #
NASA-CR-193975 .... p 4235 N94-35447 * #
NASA-CR-193979 .... p 4249 N94-35485 * #
NASA-CR-193987 .... p 4333 N94-36119 * #
NASA-CR-193988 .... p 4307 N94-36118 * #
NASA-CR-194119 .... p 4375 N94-36395 * #
NASA-CR-194214 .... p 4367 N94-35507 *
NASA-CR-194592 .... p 4191 N94-36394 * #
NASA-CR-194717 .... p 4306 N94-36063 * #
NASA-CR-194753 .... p 4367 N94-35509 *
NASA-CR-194856 .... p 4281 N94-35734 * #
NASA-CR-194899 .... p 4266 N94-35975 * #
NASA-CR-194900 .... p 4267 N94-35992 * #
NASA-CR-194904 .... p 4300 N94-35240 * #
NASA-CR-194908 .... p 4191 N94-35994 * #
NASA-CR-194909 .... p 4263 N94-35497 * #
NASA-CR-194922 .... p 4252 N94-35247 * #
NASA-CR-195157 .... p 4288 N94-35244 * #
NASA-CR-195323 .... p 4200 N94-35267 * #
NASA-CR-195334 .... p 4347 N94-36396 * #
NASA-CR-195337 .... p 4278 N94-35239 * #
NASA-CR-195345 .... p 4234 N94-35995 * #
NASA-CR-195545 .... p 4367 N94-35508 *
NASA-CR-195743 .... p 4355 N94-35395 * #
NASA-CR-195744 .... p 4367 N94-36136 * #
NASA-CR-195745 .... p 4362 N94-35448 * #
NASA-CR-195779 .... p 4201 N94-35510 *
NASA-CR-195796 .... p 4367 N94-35506 *
NASA-CR-195905 .... p 4367 N94-35505 *
NASA-CR-195909 .... p 4367 N94-35513 *
NASA-CR-195962 .... p 4302 N94-35514 * #
NASA-CR-195980 .... p 4376 N94-35590 * #
NASA-CR-195981 .... p 4293 N94-35499 * #
NASA-CR-196003 .... p 4349 N94-35516 * #
NASA-CR-196004 .... p 4296 N94-35257 * #
NASA-CR-196008 .... p 4289 N94-35389 * #
NASA-CR-196011 .... p 4376 N94-35515 * #
NASA-CR-196016 .... p 4235 N94-35388 * #
NASA-CR-196017 .... p 4268 N94-36420 * #
NASA-CR-196020 .... p 4349 N94-36419 * #
NASA-CR-196021 .... p 4279 N94-35974 * #
NASA-CR-196024 .... p 4354 N94-35263 * #
NASA-CR-196025 .... p 4319 N94-35264 * #
NASA-CR-196026 .... p 4354 N94-35265 * #
NASA-CR-196030 .... p 4298 N94-35266 * #
NASA-CR-196032 .... p 4376 N94-36421 * #
NASA-CR-196036 .... p 4374 N94-35993 * #
NASA-CR-196038 .... p 4249 N94-35237 * #
NASA-CR-196043 .... p 4367 N94-35504 *
NASA-CR-196044 .... p 4292 N94-35355 * #
NASA-CR-196046 .... p 4347 N94-36435 * #
NASA-CR-196077 .... p 4202 N94-35487 * #
NASA-CR-196078 .... p 4192 N94-35522 * #
NASA-CR-196080 .... p 4293 N94-35391 * #
NASA-CR-196081 .... p 4268 N94-36397 * #
NASA-CR-196082 .... p 4245 N94-35977 * #
NASA-CR-196083 .... p 4211 N94-35357 * #
NASA-CR-196085 .... p 4284 N94-35486 * #
NASA-CR-196093 .... p 4271 N94-35489 * #
NASA-CR-196095 .... p 4271 N94-35488 * #
NASA-CR-196097 .... p 4297 N94-35379 * #
NASA-CR-196101 .... p 4274 N94-35512 *
NASA-CR-196103 .... p 4200 N94-36436 * #
NASA-CR-196108 .... p 4201 N94-35511 *
NASA-CR-196116 .... p 4289 N94-35392 * #
NASA-CR-196117 .... p 4252 N94-35542 * #
NASA-CR-196119 .... p 4274 N94-35500 * #
NASA-CR-196123 .... p 4354 N94-35378 * #
NASA-CR-196130 .... p 4288 N94-35358 * #
NASA-CR-196131 .... p 4376 N94-35356 * #
NASA-CR-196132 .... p 4319 N94-36031 * #
NASA-CR-196133 .... p 4284 N94-35503 *
NASA-CR-196134 .... p 4354 N94-35359 * #
NASA-CR-196136 .... p 4189 N94-35498 * #
NASA-CR-4582 .... p 4190 N94-35991 * #
NASA-CR-4595 .... p 4233 N94-35947 * #
NASA-CR-4611 .... p 4280 N94-36423 * #
NASA-CR-4612 .... p 4190 N94-35864 * #

NASA-PAM-554 .... p 4295 N94-35343 * #

NASA-RP-1327 .... p 4313 N94-35259 * #

NASA-SP-7011(391) .... p 4297 N94-35345 *
NASA-SP-7037(306) .... p 4189 N94-35338 *
NASA-SP-7039(45)-SECT-1 .... p 4344 N94-35382 *
NASA-SP-7039(45)-SECT-2 .... p 4346 N94-35835 *
NASA-SP-7096-VOL-1/2/3 .... p 4346 N94-36037 *

NASA-TM-103966 .... p 4299 N94-35393 * #
NASA-TM-103970 .... p 4189 N94-35394 * #
NASA-TM-103997 .... p 4376 N94-35370 * #
NASA-TM-104007 .... p 4263 N94-35371 * #
NASA-TM-104603 .... p 4211 N94-35269 * #
NASA-TM-104605 .... p 4281 N94-35261 * #
NASA-TM-104608 .... p 4259 N94-36049 * #
NASA-TM-104792 .... p 4262 N94-35245 * #
NASA-TM-104796 .... p 4274 N94-35481 * #
NASA-TM-106487 .... p 4262 N94-35248 * #
NASA-TM-106588 .... p 4265 N94-35945 * #
NASA-TM-106590 .... p 4281 N94-35271 * #
NASA-TM-106596 .... p 4268 N94-35268 * #
NASA-TM-106605 .... p 4257 N94-35249 * #
NASA-TM-106607 .... p 4243 N94-35260 * #
NASA-TM-106614 .... p 4265 N94-35948 * #
NASA-TM-106618 .... p 4198 N94-35352 * #
NASA-TM-106622 .... p 4243 N94-35243 * #
NASA-TM-106625 .... p 4263 N94-35250 * #
NASA-TM-106626 .... p 4199 N94-36379 * #
NASA-TM-106635 .... p 4263 N94-35253 * #
NASA-TM-106639 .... p 4258 N94-35270 * #
NASA-TM-106648 .... p 4266 N94-35976 * #
NASA-TM-108816 .... p 4380 N94-36117 * #
NASA-TM-108822 .... p 4198 N94-36380 * #
NASA-TM-109057 .... p 4309 N94-36438 * #
NASA-TM-109115 .... p 4233 N94-35946 * #
NASA-TM-109127 .... p 4311 N94-35242 * #
NASA-TM-109203 .... p 4211 N94-35523 * #
NASA-TM-109204 .... p 4288 N94-36422 * #
NASA-TM-109250 .... p 4228 N94-35591 * #
NASA-TM-109349 .... p 4236 N94-35680 * #
NASA-TM-109779 .... p 4343 N94-35339 *
NASA-TM-109791 .... p 4347 N94-35899 * #
NASA-TM-109792 .... p 4348 N94-35900 * #
NASA-TM-109793 .... p 4348 N94-35446 * #
NASA-TM-109840 .... p 4201 N94-35390 * #
NASA-TM-109866 .... p 4211 N94-35252 * #
NASA-TM-109867 .... p 4211 N94-35251 * #
NASA-TM-109868 .... p 4344 N94-35254 * #
NASA-TM-109888 .... p 4201 N94-36440 * #
NASA-TM-4527 .... p 4291 N94-36175 * #
NASA-TM-4563 .... p 4189 N94-35246 * #
NASA-TM-4590 .... p 4199 N94-35258 * #
NASA-TM-4591 .... p 4193 N94-35241 * #

NASA-TP-3399 .... p 4192 N94-36048 * #

NAWCADWAR-93079-60 .... p 4232 N94-35654
NAWCADWAR-93089-60 .... p 4299 N94-35707

NIFS-MEMO-11 .... p 4337 N94-35939 #
NIFS-MEMO-9 .... p 4337 N94-35983 #

NIFS-PROC-13 .... p 4336 N94-35775 #

NIFS-167 .... p 4336 N94-35772 #
NIFS-169 .... p 4337 N94-35938 #
NIFS-170 .... p 4337 N94-35937 #
NIFS-175 .... p 4339 N94-36353 #
NIFS-176 .... p 4324 N94-35984 #
NIFS-177 .... p 4338 N94-36352 #
NIFS-181 .... p 4338 N94-36247 #
NIFS-184 .... p 4337 N94-35936 #
NIFS-185 .... p 4339 N94-36357 #
NIFS-215 .... p 4336 N94-35812 #
NIFS-216 .... p 4336 N94-35811 #
NIFS-217 .... p 4336 N94-35773 #
NIFS-220 .... p 4336 N94-35813 #
NIFS-239 .... p 4336 N94-35752 #

NIIEFA-P-0905 .... p 4336 N94-35791 #

NIIYAF-MGU-92-31-280 .... p 4290 N94-35780
NIIYAF-MGU-93-3-295 .... p 4350 N94-36128 #

NIRS-31 .... p 4296 N94-36101

NIST/SP-823/5 .... p 4305 N94-35940

NIST/TN-1407 .... p 4346 N94-35819

NISTIR-4490 .... p 4305 N94-36010

NISTIR-4894 .... p 4236 N94-35736
NISTIR-5312 .... p 4251 N94-35737
NISTIR-5342 .... p 4333 N94-36002
NISTIR-5366 .... p 4304 N94-35740 #
NISTIR-5373 .... p 4234 N94-36004
NISTIR-5377 .... p 4265 N94-35942
NISTIR-5386 .... p 4346 N94-36005

NLR-TP-92467U .... p 4279 N94-36226 #

NONP-NASA-DK-94-15961 .... p 4376 N94-35363 * #
NONP-NASA-DK-94-5859 .... p 4343 N94-35339 *

NONP-NASA-VT-94-15911 .... p 4284 N94-35503 *
NONP-NASA-VT-94-15912 .... p 4367 N94-35504 *
NONP-NASA-VT-94-15913 .... p 4367 N94-35505 *
NONP-NASA-VT-94-15914 .... p 4367 N94-35506 *
NONP-NASA-VT-94-15915 .... p 4367 N94-35507 *
NONP-NASA-VT-94-15916 .... p 4367 N94-35508 *
NONP-NASA-VT-94-15917 .... p 4367 N94-35509 *
NONP-NASA-VT-94-15918 .... p 4201 N94-35510 *
NONP-NASA-VT-94-15919 .... p 4201 N94-35511 *
NONP-NASA-VT-94-15920 .... p 4274 N94-35512 *
NONP-NASA-VT-94-15921 .... p 4367 N94-35513 *

NP-SEC-93-025 .... p 4319 N94-35800

NPL-DES-132 .... p 4339 N94-35598

NPS-AS-93-028 .... p 4316 N94-35675

NPS-CS-94-005 .... p 4303 N94-35576
NPS-CS-94-006 .... p 4304 N94-35676

NPS-ME-94-002 .... p 4190 N94-35826

NPS-OR-94-003 .... p 4303 N94-35577
NPS-OR-94-006 .... p 4305 N94-36013

NRAD-TD-2610 .... p 4260 N94-36248

NRAD-TR-1548-REV-1 .... p 4303 N94-35660

NREL/SP-280-5794 .... p 4283 N94-36052 #
NREL/SP-6506 .... p 4283 N94-36051 #

NREL/TP-425-6357 .... p 4248 N94-36191 #

NRL/FR/8150-94-9714-VOL-3 .... p 4212 N94-35799
NRL/FR/8150-94-9715-VOL-4 .... p 4212 N94-35801

NRL/MR/5530-94-7464 .... p 4302 N94-35491
NRL/MR/6707-94-7462 .... p 4335 N94-35493
NRL/MR/6750-94-7461 .... p 4318 N94-36427
NRL/MR/6790-94-7366 .... p 4263 N94-35492
NRL/MR/8140-94-7479 .... p 4302 N94-35490

NSF/ISI-90086 .... p 4282 N94-35739

NSTS-08286 .... p 4211 N94-35252 * #
NSTS-08287 .... p 4211 N94-35251 * #

NSWCDD/TR-94/107 .... p 4305 N94-35958 #
NSWCDD/TR-94/15 .... p 4212 N94-35585

NTSB/AAR-94/04 .... p 4192 N94-35521 #

NTSB/ARG-94/02 .... p 4192 N94-35496 #

NTSB/SS-94/01 .... p 4191 N94-35482 #

OMI-02-93 .... p 4268 N94-36397 * #

ONR-TR-8 .... p 4239 N94-36426

ORNL/CDIAC-64 .... p 4295 N94-36244 #

ORNL/FTR-4912 .... p 4333 N94-36055 #

ORNL/SUB-86-SL103 .... p 4287 N94-36179
ORNL/SUB-90-SF521/02 .... p 4241 N94-36196 #

ORNL/TM-12630 .... p 4264 N94-35683 #
ORNL/TM-12666 .... p 4288 N94-36273 #
ORNL/TM-12680 .... p 4347 N94-36300 #

PATENTS-US-A7868149 .... p 4270 N94-36389 #

PB94-148491 .... p 4246 N94-36177
PB94-150240 .... p 4266 N94-35981
PB94-150372 .... p 4302 N94-35538
PB94-156494 .... p 4275 N94-35931
PB94-156668 .... p 4247 N94-35941
PB94-156676 .... p 4287 N94-36183
PB94-156700 .... p 4285 N94-35735
PB94-157799 .... p 4296 N94-35738 #
PB94-158623 .... p 4298 N94-35688
PB94-158698 .... p 4332 N94-35584
PB94-158862 .... p 4285 N94-35741
PB94-159415 .... p 4282 N94-35739
PB94-160066 .... p 4234 N94-36004
PB94-160645 .... p 4291 N94-36019
PB94-160744 .... p 4236 N94-35736
PB94-160769 .... p 4318 N94-36003
PB94-160793 .... p 4305 N94-36010
PB94-161155 .... p 4259 N94-35748
PB94-162518 .... p 4333 N94-36002
PB94-162559 .... p 4305 N94-35940
PB94-162583 .... p 4346 N94-36005
PB94-163029 .... p 4304 N94-35740 #
PB94-163060 .... p 4265 N94-35942
PB94-163995 .... p 4375 N94-36020
PB94-164001 .... p 4374 N94-36009
PB94-164019 .... p 4346 N94-35819
PB94-164027 .... p 4285 N94-35754
PB94-164183 .... p 4251 N94-35737
PB94-165438 .... p 4236 N94-35755
PB94-167053 .... p 4350 N94-35530
PB94-167095 .... p 4269 N94-36061
PB94-167103 .... p 4272 N94-36062
PB94-167665 .... p 4314 N94-35758
PB94-167699 .... p 4314 N94-35759
PB94-167707 .... p 4317 N94-35760
PB94-167715 .... p 4342 N94-35761
PB94-167731 .... p 4314 N94-35762
PB94-167749 .... p 4314 N94-35763
PB94-167756 .... p 4314 N94-35764
PB94-167798 .... p 4314 N94-35531
PB94-167806 .... p 4250 N94-35532
PB94-167814 .... p 4345 N94-35533
PB94-167822 .... p 4258 N94-35534
PB94-167830 .... p 4310 N94-35535
PB94-169216 .... p 4316 N94-35536
PB94-169224 .... p 4252 N94-35537
PB94-169240 .... p 4251 N94-35820
PB94-169307 .... p 4339 N94-35598
PB94-170495 .... p 4269 N94-35599
PB94-170511 .... p 4375 N94-36210
PB94-170529 .... p 4308 N94-36211
PB94-170537 .... p 4298 N94-35600
PB94-170552 .... p 4341 N94-36212
PB94-170578 .... p 4341 N94-36213
PB94-170586 .... p 4291 N94-36214
PB94-170594 .... p 4298 N94-36215
PB94-170602 .... p 4279 N94-36216
PB94-170644 .... p 4297 N94-36217
PB94-170677 .... p 4273 N94-36218
PB94-170685 .... p 4270 N94-36219
PB94-170693 .... p 4297 N94-36220
PB94-170701 .... p 4308 N94-36259
PB94-170743 .... p 4260 N94-36260
PB94-170750 .... p 4296 N94-35601
PB94-171006 .... p 4315 N94-35821
PB94-171014 .... p 4279 N94-36000
PB94-171022 .... p 4259 N94-35822
PB94-171048 .... p 4303 N94-35602
PB94-171154 .... p 4263 N94-35603
PB94-171170 .... p 4346 N94-35959
PB94-171196 .... p 4334 N94-36190
PB94-181054 .... p 4192 N94-35496 #
PB94-910406 .... p 4192 N94-35521 #
PB94-917001 .... p 4191 N94-35482 #

PIYAF-1795 .... p 4328 N94-36287 #

PL-TR-2009 .... p 4295 N94-36228 #
PL-TR-93-2167 .... p 4273 N94-36227 #
PL-TR-93-2168 .... p 4295 N94-36262 #
PL-TR-93-2220 .... p 4289 N94-35578
PL-TR-94-2002(1) .... p 4291 N94-36116 #
PL-TR-94-2032 .... p 4292 N94-36265 #
PL-TR-94-2040 .... p 4375 N94-36264 #
PL-TR-94-2044 .... p 4291 N94-36263 #

PNL-SA-22412 .... p 4331 N94-36317 #
PNL-SA-22853 .... p 4287 N94-36027 #
PNL-SA-22883 .... p 4259 N94-36054 #
PNL-SA-22899 .... p 4287 N94-36053 #
PNL-SA-23164 .... p 4286 N94-36024 #
PNL-SA-23289 .... p 4286 N94-36026 #
PNL-SA-23624 .... p 4311 N94-35348 #

PNL-9012 .... p 4288 N94-36359 #
PNL-9050 .... p 4312 N94-36195 #

PREPRINT 92-1 .... p 4315 N94-36100

PRG-111 .... p 4316 N94-35536
PRG-112 .... p 4252 N94-35537

PSU/ARL-TR-94-08 .... p 4333 N94-35747

R/D-7132-EE-01 .... p 4290 N94-35744

RAL-93-096 .... p 4269 N94-36061
RAL-94-014 .... p 4272 N94-36062
RAL-94-016 .... p 4298 N94-35600
RAL-94-018 .... p 4350 N94-35530
RAL-94-020 .... p 4269 N94-35599
RAL-94-023 .... p 4375 N94-36210
RAL-94-024 .... p 4308 N94-36211

RDA-TR-1910001-002 .... p 4256 N94-36112 #

REPT-10392A .... p 4281 N94-35734 * #
REPT-15 .... p 4243 N94-35335 #
REPT-93-103 .... p 4293 N94-35499 * #
REPT-94B00060 .... p 4202 N94-35605 * #
REPT-94B00079 .... p 4211 N94-35269 * #
REPT-94B00084 .... p 4281 N94-35261 * #
REPT-94B00089 .... p 4259 N94-36049 * #

RIACS-TR-94-06 .... p 4319 N94-36031 * #

RL-TR-93-264-PT-1 .... p 4256 N94-35694
RL-TR-93-265 .... p 4256 N94-35713
RL-TR-94-7 .... p 4310 N94-35653

RNA-93-232 .... p 4275 N94-35931

RR-A327, ... p 4315 N94-35821
RR-A328 .... p 4279 N94-36000

RTCA-DO-155 .... p 4198 N94-35344 #

S-677 .... p 4343 N94-35339 *
S-763 .... p 4262 N94-35245 * #
S-770 .... p 4274 N94-35481 * #

SAIC-C94-02 .... p 4290 N94-35693

SAND-93-1613C .... p 4267 N94-35996 #
SAND-93-1772 .... p 4270 N94-35351 #
SAND-93-2048C .... p 4244 N94-35699
SAND-93-2198C .... p 4331 N94-36199 #
SAND-93-2510C .... p 4240 N94-36110 #
SAND-93-2546C .... p 4244 N94-35701
SAND-93-2547C .... p 4244 N94-35702 #
SAND-93-2617C .... p 4340 N94-35698
SAND-93-2711C .... p 4318 N94-36204 #
SAND-93-2778C .... p 4260 N94-36245 #
SAND-93-3836 .... p 4259 N94-36094 #
SAND-93-3919 .... p 4266 N94-35979 #
SAND-93-3989C .... p 4272 N94-36178 #
SAND-94-0033 .... p 4340 N94-36032 #
SAND-94-0048 .... p 4265 N94-35769
SAND-94-0131C .... p 4349 N94-35998 #
SAND-94-0367C .... p 4261 N94-36373 #
SAND-94-0382C .... p 4260 N94-36268
SAND-94-0457C .... p 4342 N94-36367 #
SAND-94-0458C .... p 4261 N94-36371 #
SAND-94-0470C .... p 4258 N94-35564 #
SAND-94-0532C .... p 4261 N94-36362 #
SAND-94-0575C .... p 4262 N94-36430 #
SAND-94-0577C .... p 4267 N94-36111 #
SAND-94-0732C .... p 4246 N94-36209 #
SAND-94-0776C .... p 4241 N94-36242 #
SAND-94-0783C .... p 4226 N94-36001
SAND-94-1224C .... p 4248 N94-36376 #
SAND-94-8222 .... p 4294 N94-35766
SAND-94-8223 .... p 4294 N94-35767
SAND-94-8493C .... p 4268 N94-36318 #
SAND-94-8597 .... p 4295 N94-36285 #
SAND-94-8646 .... p 4257 N94-36354 #

SAND93-0280 .... p 4189 N94-35360 #
SAND94-0065 .... p 4286 N94-35957 #

SAO-AXAF-DR-93-052 .... p 4307 N94-36118 * #
SAO-AXAF-DR-93-053 .... p 4333 N94-36119 * #

SEL-82-1206 .... p 4300 N94-35238 * #
SEL-93-001 .... p 4301 N94-35434 * #
SEL-93-002 .... p 4300 N94-35256 * #

SFIM-AEC-TS-CR-94030 .... p 4229 N94-35776

SGD-594-PT-1 .... p 4375 N94-36020
SGD-594-PT-2 .... p 4374 N94-36009

SMC-TR-94-15 .... p 4227 N94-35362 #
SMC-TR-94-19 .... p 4292 N94-36383
SMC-TR-94-20 .... p 4289 N94-35587
SMC-TR-94-23 .... p 4343 N94-36256
SMC-TR-94-24 .... p 4228 N94-36254
SMC-TR-94-25 .... p 4228 N94-36255
SMC-TR-94-27 .... p 4282 N94-35804

SPIRE-FR-60296 .... p 4261 N94-36360

SR-3 .... p 4289 N94-35578

SRL-04-F-1994 .... p 4271 N94-35586

SSCL-666 .... p 4259 N94-36194 #

SSL-10-83 .... p 4212 N94-35484 * #

SST-115 .... p 4301 N94-35443 * #

STC-TR-2833 .... p 4292 N94-35355 * #

SU-SLAC-PUB-6448 .... p 4330 N94-36106 #
SU-SLAC-PUB-6458 .... p 4331 N94-36224 #
SU-SLAC-PUB-6470 .... p 4326 N94-36198 #

TKK-F-C139 .... p 4334 N94-36190

TKO-C53 .... p 4303 N94-35602

TR-0091(6940-05)-11 .... p 4227 N94-35362 #
TR-0091(6940-06)-1 .... p 4289 N94-35587
TR-0091(6940-06)-3 .... p 4292 N94-36383
TR-14-ONR .... p 4243 N94-35588
TR-15 .... p 4340 N94-35828
TR-17 .... p 4246 N94-36253
TR-18 .... p 4238 N94-36252
TR-40 .... p 4324 N94-36050
TR-41 .... p 4322 N94-35678
TR-43 .... p 4322 N94-35753
TR-44 .... p 4323 N94-35797
TR-45 .... p 4323 N94-35798
TR-46 .... p 4323 N94-35792
TR-47-ONR .... p 4321 N94-35589
TR-48 .... p 4323 N94-35793
TR-93(3530)-2 .... p 4228 N94-36254
TR-93(3530)-3 .... p 4228 N94-36255
TR-93(3530)-4 .... p 4343 N94-36256
TR-93(3925)-4 .... p 4282 N94-35804

TRS-450 .... p 4314 N94-35531
TRS-451 .... p 4250 N94-35532
TRS-456 .... p 4345 N94-35533
TRS-460 .... p 4258 N94-35534
TRS-461 .... p 4310 N94-35535

TURKU-SFL-D1 .... p 4283 N94-36060 #

T17-ONR .... p 4340 N94-35677

U-OF-IOWA-93-21 .... p 4354 N94-35378 * #

UC-350 .... p 4250 N94-35364 #
UC-605 .... p 4344 N94-35337 #
UC-706 .... p 4189 N94-35360 #

UCB-PTH-93/35 .... p 4315 N94-36270 #

UCRL-CR-115619 .... p 4284 N94-35700
UCRL-CR-116204 .... p 4256 N94-36112 #
UCRL-CR-116329 .... p 4270 N94-36350

UCRL-ID-113855 .... p 4313 N94-35259 * #
UCRL-ID-115730 .... p 4256 N94-36301 #
UCRL-ID-115831 .... p 4285 N94-35943 #
UCRL-ID-116827 .... p 4335 N94-35647 #
UCRL-ID-116945 .... p 4319 N94-35770
UCRL-ID-116958 .... p 4326 N94-36127 #
UCRL-ID-117135 .... p 4338 N94-36284 #

UCRL-JC-107799 .... p 4339 N94-36375 #
UCRL-JC-112327 .... p 4267 N94-36315
UCRL-JC-114300 .... p 4347 N94-36297 #
UCRL-JC-114456-REV-1 .... p 4266 N94-35982 #
UCRL-JC-114456 .... p 4318 N94-36201 #
UCRL-JC-114575 .... p 4238 N94-36237
UCRL-JC-114963 .... p 4330 N94-36114 #
UCRL-JC-115308 .... p 4286 N94-36025 #
UCRL-JC-115513 .... p 4271 N94-35679 #
UCRL-JC-115654 .... p 4334 N94-36356 #
UCRL-JC-115802 .... p 4239 N94-36319 #
UCRL-JC-115803 .... p 4275 N94-36206 #
UCRL-JC-115804 .... p 4276 N94-36378 #
UCRL-JC-115807 .... p 4238 N94-36205 #
UCRL-JC-115838 .... p 4305 N94-36017
UCRL-JC-115863 .... p 4292 N94-35350 #
UCRL-JC-115897 .... p 4268 N94-36374
UCRL-JC-115945 .... p 4272 N94-36115 #
UCRL-JC-115980 .... p 4232 N94-35696
UCRL-JC-116059 .... p 4271 N94-35665 #
UCRL-JC-116078 .... p 4333 N94-35697 #
UCRL-JC-116292-REV-1 .... p 4272 N94-35695
UCRL-JC-116324 .... p 4272 N94-35978 #
UCRL-JC-116505 .... p 4349 N94-35565 #
UCRL-JC-116526 .... p 4288 N94-36286 #
UCRL-JC-116866 .... p 4339 N94-36386 #
UCRL-JC-116931 .... p 4333 N94-35818 #

UCRL-LR-105821-94-1 .... p 4338 N94-36193 #

UCRL-MA-115696 .... p 4309 N94-36429 #
UCRL-MA-115896 .... p 4308 N94-36236 #

UDR-TR-94-88 .... p 4347 N94-36435 * #

UK-ME-93-04 .... p 4250 N94-35524

UNM-ISNPS-1-1994 .... p 4228 N94-35349 #

US-PATENT-APPL-SN-007874 ..... p 4274 N94-35373 *
US-PATENT-APPL-SN-038748 ..... p 4274 N94-35661 *
US-PATENT-APPL-SN-048871 ..... p 4274 N94-35375 *
US-PATENT-APPL-SN-067184 ..... p 4241 N94-36275 *
US-PATENT-APPL-SN-098918 ..... p 4273 N94-35367 *
US-PATENT-APPL-SN-117511 ..... p 4268 N94-35368 *
US-PATENT-APPL-SN-127886 ..... p 4282 N94-35540 * #
US-PATENT-APPL-SN-138046 ..... p 4269 N94-35369 *
US-PATENT-APPL-SN-213558 ..... p 4296 N94-35232 *
US-PATENT-APPL-SN-213559 ..... p 4296 N94-35232 *
US-PATENT-APPL-SN-317931 ..... p 4296 N94-35232 *
US-PATENT-APPL-SN-429514 ..... p 4232 N94-35372 * #
US-PATENT-APPL-SN-429739 ..... p 4235 N94-35229 *
US-PATENT-APPL-SN-429739 ..... p 4250 N94-35445 *
US-PATENT-APPL-SN-430470 ..... p 4242 N94-35233 *
US-PATENT-APPL-SN-545235 ..... p 4311 N94-35501 *
US-PATENT-APPL-SN-571060 ..... p 4251 N94-35231 *
US-PATENT-APPL-SN-772181 ..... p 4242 N94-35234 *
US-PATENT-APPL-SN-772804 ..... p 4257 N94-36364
US-PATENT-APPL-SN-787993 ..... p 4282 N94-35540 * #
US-PATENT-APPL-SN-788674 ..... p 4273 N94-36370
US-PATENT-APPL-SN-831763 ..... p 4242 N94-35233 *
US-PATENT-APPL-SN-834451 ..... p 4268 N94-35235 *
US-PATENT-APPL-SN-837014 ..... p 4246 N94-36125
US-PATENT-APPL-SN-868149 ..... p 4270 N94-36389 #
US-PATENT-APPL-SN-868806 ..... p 4273 N94-36365
US-PATENT-APPL-SN-883957 ..... p 4333 N94-35749 *
US-PATENT-APPL-SN-892914 ..... p 4234 N94-36124
US-PATENT-APPL-SN-894505 ..... p 4235 N94-35229 *
US-PATENT-APPL-SN-894505 ..... p 4250 N94-35445 *
US-PATENT-APPL-SN-897638 ..... p 4234 N94-36123
US-PATENT-APPL-SN-901649 ..... p 4334 N94-36363
US-PATENT-APPL-SN-909345 ..... p 4243 N94-35502 *
US-PATENT-APPL-SN-939791 ..... p 4296 N94-35232 *
US-PATENT-APPL-SN-954109 ..... p 4332 N94-35384 *
US-PATENT-APPL-SN-955512 ..... p 4281 N94-35230 *
US-PATENT-APPL-SN-968082 ..... p 4232 N94-35372 * #
US-PATENT-APPL-SN-976742 ..... p 4334 N94-36122
US-PATENT-APPL-SN-983334 ..... p 4334 N94-36368
US-PATENT-APPL-SN-983356 ..... p 4246 N94-36121
US-PATENT-APPL-SN-991003 ..... p 4235 N94-35255 *
US-PATENT-APPL-SN-991403 ..... p 4269 N94-35383 *
US-PATENT-APPL-SN-993477 ..... p 4274 N94-35374 *
US-PATENT-APPL-SN-995612 ..... p 4235 N94-35229 *
US-PATENT-APPL-SN-996263 ..... p 4296 N94-35366 *
US-PATENT-APPL-SN-997265 ..... p 4250 N94-35445 *
US-PATENT-APPL-SN-999629 ..... p 4239 N94-36372

US-PATENT-CLASS-136-252 .... p 4281 N94-35230 *
US-PATENT-CLASS-136-256 .... p 4281 N94-35230 *
US-PATENT-CLASS-136-293 .... p 4282 N94-35540 * #
US-PATENT-CLASS-137-516.29 .. p 4274 N94-35661 *
US-PATENT-CLASS-137-528 .... p 4274 N94-35661 *
US-PATENT-CLASS-148-423 .... p 4241 N94-36275 *
US-PATENT-CLASS-148-442 .... p 4241 N94-36275 *
US-PATENT-CLASS-156-345 .... p 4250 N94-35445 *
US-PATENT-CLASS-156-643 .... p 4250 N94-35445 *
US-PATENT-CLASS-156-651 .... p 4246 N94-36121
US-PATENT-CLASS-204-146 .... p 4239 N94-36372
US-PATENT-CLASS-219-121.45 .. p 4273 N94-35367 *
US-PATENT-CLASS-219-121.48 .. p 4273 N94-35367 *
US-PATENT-CLASS-219-121.54 .. p 4273 N94-35367 *
US-PATENT-CLASS-219-130.01 .. p 4273 N94-35367 *
US-PATENT-CLASS-244-158R .... p 4243 N94-35502 *
US-PATENT-CLASS-244-163 .... p 4243 N94-35502 *
US-PATENT-CLASS-250-338.1 .... p 4269 N94-35383 *
US-PATENT-CLASS-251-65 .... p 4274 N94-35661 *
US-PATENT-CLASS-257-434 .... p 4281 N94-35230 *
US-PATENT-CLASS-257-443 .... p 4234 N94-36123
US-PATENT-CLASS-257-631 .... p 4281 N94-35230 *
US-PATENT-CLASS-257-76 .... p 4281 N94-35230 *
US-PATENT-CLASS-264-82 .... p 4246 N94-36125
US-PATENT-CLASS-277-230 .... p 4274 N94-35373 *
US-PATENT-CLASS-277-75 .... p 4274 N94-35373 *
US-PATENT-CLASS-29-252 .... p 4274 N94-35375 *
US-PATENT-CLASS-29-454 .... p 4269 N94-35369 *
US-PATENT-CLASS-29-764 .... p 4274 N94-35375 *
US-PATENT-CLASS-323-299 .... p 4282 N94-35540 * #
US-PATENT-CLASS-323-906 .... p 4282 N94-35540 * #
US-PATENT-CLASS-340-683 .... p 4268 N94-35235 *
US-PATENT-CLASS-342-181 .... p 4257 N94-36364
US-PATENT-CLASS-343-701 .... p 4251 N94-35231 *
US-PATENT-CLASS-348-114 .... p 4332 N94-35384 *
US-PATENT-CLASS-348-143 .... p 4332 N94-35384 *
US-PATENT-CLASS-348-159 .... p 4332 N94-35384 *
US-PATENT-CLASS-356-345 .... p 4333 N94-35749 *
US-PATENT-CLASS-356-354 .... p 4333 N94-35749 *
US-PATENT-CLASS-356-359 .... p 4333 N94-35749 *
US-PATENT-CLASS-356-360 .... p 4333 N94-35749 *
US-PATENT-CLASS-359-326 .... p 4334 N94-36368
US-PATENT-CLASS-364-401 .... p 4311 N94-35501 *
US-PATENT-CLASS-364-557 .... p 4269 N94-35383 *
US-PATENT-CLASS-364-578 .... p 4311 N94-35501 *
US-PATENT-CLASS-367-13 .... p 4268 N94-35368 *
US-PATENT-CLASS-372-42 .... p 4273 N94-36365
US-PATENT-CLASS-372-71 .... p 4273 N94-36370
US-PATENT-CLASS-374-126 .... p 4269 N94-35383 *
US-PATENT-CLASS-374-128 .... p 4269 N94-35383 *
US-PATENT-CLASS-374-129 .... p 4269 N94-35383 *
US-PATENT-CLASS-374-9 .... p 4269 N94-35383 *
US-PATENT-CLASS-385-132 .... p 4334 N94-36122
US-PATENT-CLASS-395-94 .... p 4332 N94-35384 *
US-PATENT-CLASS-403-325 .... p 4274 N94-35374 *
US-PATENT-CLASS-403-327 .... p 4274 N94-35374 *
US-PATENT-CLASS-403-328 .... p 4274 N94-35374 *
US-PATENT-CLASS-403-359 .... p 4274 N94-35374 *
US-PATENT-CLASS-403-378 .... p 4274 N94-35374 *
US-PATENT-CLASS-403-379 .... p 4274 N94-35374 *
US-PATENT-CLASS-420-428 .... p 4241 N94-36275 *
US-PATENT-CLASS-420-429 .... p 4241 N94-36275 *
US-PATENT-CLASS-420-578 .... p 4241 N94-36275 *
US-PATENT-CLASS-420-588 .... p 4241 N94-36275 *
US-PATENT-CLASS-422-129 .... p 4250 N94-35445 *
US-PATENT-CLASS-422-186.04 .. p 4250 N94-35445 *
US-PATENT-CLASS-422-186.05 .. p 4250 N94-35445 *
US-PATENT-CLASS-428-323 .... p 4234 N94-36124
US-PATENT-CLASS-428-336 .... p 4243 N94-35502 *
US-PATENT-CLASS-428-421 .... p 4243 N94-35502 *
US-PATENT-CLASS-428-422 .... p 4243 N94-35502 *
US-PATENT-CLASS-428-432 .... p 4243 N94-35502 *
US-PATENT-CLASS-428-433 .... p 4243 N94-35502 *
US-PATENT-CLASS-428-473.5 .... p 4242 N94-35233 *
US-PATENT-CLASS-435-1 .... p 4296 N94-35232 *
US-PATENT-CLASS-435-240.24 .. p 4296 N94-35232 *
US-PATENT-CLASS-435-240.24 .. p 4296 N94-35366 *
US-PATENT-CLASS-435-240.25 .. p 4296 N94-35232 *
US-PATENT-CLASS-435-240.25 .. p 4296 N94-35366 *
US-PATENT-CLASS-435-240.2 .... p 4296 N94-35232 *
US-PATENT-CLASS-435-286 .... p 4296 N94-35366 *
US-PATENT-CLASS-435-296 .... p 4296 N94-35366 *
US-PATENT-CLASS-435-312 .... p 4296 N94-35366 *
US-PATENT-CLASS-435-313 .... p 4296 N94-35366 *
US-PATENT-CLASS-435-818 .... p 4296 N94-35366 *
US-PATENT-CLASS-437-5 .... p 4281 N94-35230 *
US-PATENT-CLASS-439-158 .... p 4274 N94-35375 *
US-PATENT-CLASS-455-291 .... p 4251 N94-35231 *
US-PATENT-CLASS-501-12 .... p 4334 N94-36363
US-PATENT-CLASS-502-258 .... p 4235 N94-35229 *
US-PATENT-CLASS-502-259 .... p 4235 N94-35229 *
US-PATENT-CLASS-502-260 .... p 4235 N94-35229 *
US-PATENT-CLASS-502-332 .... p 4235 N94-35229 *
US-PATENT-CLASS-502-335 .... p 4235 N94-35229 *
US-PATENT-CLASS-502-66 .... p 4235 N94-35255 *
US-PATENT-CLASS-502-74 .... p 4235 N94-35255 *
US-PATENT-CLASS-525-421 .... p 4242 N94-35233 *
US-PATENT-CLASS-525-421 .... p 4232 N94-35372 * #
US-PATENT-CLASS-525-426 .... p 4232 N94-35372 * #
US-PATENT-CLASS-525-432 .... p 4242 N94-35233 *
US-PATENT-CLASS-525-432 .... p 4232 N94-35372 * #
US-PATENT-CLASS-525-436 .... p 4242 N94-35233 *
US-PATENT-CLASS-525-436 .... p 4232 N94-35372 * #
US-PATENT-CLASS-525-903 .... p 4242 N94-35233 *
US-PATENT-CLASS-525-903 .... p 4232 N94-35372 * #
US-PATENT-CLASS-528-125 .... p 4242 N94-35234 *
US-PATENT-CLASS-528-126 .... p 4242 N94-35234 *
US-PATENT-CLASS-528-128 .... p 4242 N94-35234 *
US-PATENT-CLASS-528-172 .... p 4242 N94-35234 *
US-PATENT-CLASS-528-173 .... p 4242 N94-35234 *
US-PATENT-CLASS-528-174 .... p 4242 N94-35234 *
US-PATENT-CLASS-528-353 .... p 4242 N94-35234 *
US-PATENT-CLASS-73-147 .... p 4269 N94-35369 *
US-PATENT-CLASS-73-715 .... p 4269 N94-35369 *
US-PATENT-CLASS-73-756 .... p 4269 N94-35369 *
US-PATENT-CLASS-75-230 .... p 4241 N94-36275 *
US-PATENT-CLASS-901-47 .... p 4332 N94-35384 *
US-PATENT-CLASS-92-103M ...... p 4269 N94-35369 *

US-PATENT-5,230,848 .... p 4246 N94-36125
US-PATENT-5,234,758 .... p 4234 N94-36124
US-PATENT-5,250,954 .... p 4257 N94-36364
US-PATENT-5,259,061 .... p 4334 N94-36122
US-PATENT-5,262,362 .... p 4334 N94-36363
US-PATENT-5,264,722 .... p 4234 N94-36123
US-PATENT-5,266,155 .... p 4246 N94-36121
US-PATENT-5,267,254 .... p 4273 N94-36365
US-PATENT-5,268,920 .... p 4273 N94-36370
US-PATENT-5,269,890 .... p 4239 N94-36372

US-PATENT-5,270,853 .... p 4334 N94-36368
US-PATENT-5,306,784 .... p 4242 N94-35233 *
US-PATENT-5,308,764 .... p 4296 N94-35232 *
US-PATENT-5,309,149 .... p 4268 N94-35235 *
US-PATENT-5,311,198 .... p 4251 N94-35231 *
US-PATENT-5,311,422 .... p 4311 N94-35501 *
US-PATENT-5,312,685 .... p 4243 N94-35502 *
US-PATENT-5,314,853 .... p 4235 N94-35255 *
US-PATENT-5,314,857 .... p 4235 N94-35229 *
US-PATENT-5,320,136 .... p 4274 N94-35661 *
US-PATENT-5,322,573 .... p 4281 N94-35230 *
US-PATENT-5,322,924 .... p 4242 N94-35234 *
US-PATENT-5,325,339 .... p 4268 N94-35368 *
US-PATENT-5,325,720 .... p 4269 N94-35369 *
US-PATENT-5,326,172 .... p 4269 N94-35383 *
US-PATENT-5,326,186 .... p 4274 N94-35374 *
US-PATENT-5,327,071 .... p 4282 N94-35540 * #
US-PATENT-5,327,219 .... p 4333 N94-35749 *
US-PATENT-5,329,089 .... p 4273 N94-35367 *
US-PATENT-5,329,693 .... p 4274 N94-35375 *
US-PATENT-5,330,590 .... p 4241 N94-36275 *
US-PATENT-5,330,908 .... p 4296 N94-35366 *
US-PATENT-5,331,063 .... p 4232 N94-35372 * #
US-PATENT-5,331,413 .... p 4332 N94-35384 *
US-PATENT-5,332,239 .... p 4274 N94-35373 *
US-PATENT-5,332,551 .... p 4250 N94-35445 *

USAARL-94-13 .... p 4298 N94-35528
USAARL-94-14 .... p 4298 N94-35659

USCG-D-02-94 .... p 4284 N94-35674

USGC-R/DC-27/93 .... p 4284 N94-35674

UVA/528308/MANE94/101 .... p 4268 N94-36420 * #

WHC-SA-2118 .... p 4264 N94-35756

WL-TR-93-2128 .... p 4250 N94-35524
WL-TR-94-4013 .... p 4340 N94-35733
WL-TR-94-7023 .... p 4260 N94-36296

WM-94-102 .... p 4321 N94-35649

WSRC-MS-93-456 .... p 4257 N94-36366 #
WSRC-MS-93-502 .... p 4285 N94-35823

WSRC-TR-94-0132 .... p 4237 N94-36056 #

Y/DV-1272 .... p 4240 N94-35650

YITP/U-93-9 .... p 4314 N94-35774 #

APPENDIX

NASA SCIENTIFIC AND TECHNICAL INFORMATION PROGRAM PRODUCTS AND SERVICES

The NASA Scientific and Technical Information (STI) Program provides for the collection and announcement of aerospace-related reports and literature obtained worldwide through agreements and exchanges. The result of the collection is the comprehensive NASA STI Database that covers aeronautics, space, and supporting disciplines.

The STI Database, documents generated or obtained by NASA, and products and services derived from or supporting the database are made available to the NASA research community and to the public. Descriptions and sources of these items are presented in the following pages.

Scientific and Technical Aerospace Reports (STAR) is an abstract journal, listing citations with abstracts for aerospace-related reports obtained from worldwide sources. *STAR* is issued on the first of each month, and announces current documents that have been entered into the NASA STI Database during the previous month. The reports are of the following types:

- NASA, NASA contractor, and NASA grantee reports;
- Reports issued by other U.S. Government agencies, domestic and foreign institutions, universities, and private firms;
- Translations in report form;
- NASA-owned patents and patent applications
- Other U.S. Government agency and foreign patents and patent applications
- Domestic and foreign dissertations and theses.

Journal, book, and conference literature, journal translations, and certain foreign dissertations having the same subject scope as *STAR* are announced in a companion journal, *NASA Open Volumes on Aerospace (NOVA). NOVA* is issued on the 15th of each month and is available from the NASA Center for AeroSpace Information, at the address below.

ELIGIBILITY AND REGISTRATION FOR NASA STI PRODUCTS AND SERVICES

Organizations of the type listed below that have registered with NASA can receive products and services.

- NASA offices and installations, contractors, subcontractors, grantees, and consultants;
- Other U.S. Government agencies and their contractors;
- Libraries in the United States that have arrangements with NASA to maintain collections of NASA documents for public reference;
- Other organizations in the United States having a need for NASA documents in work related to aeronautics and space research;
- Organizations abroad that have established reciprocal documents exchange arrangements with NASA.

The central service points—central points of document acquisition and control within qualified organizations—or individuals are eligible to register for NASA STI products and services. Domestic organizations or individuals may be eligible to receive various classes of NASA publications and services and should address their requests for registration or further information to:

ATTN: Registration Services
NASA Center for AeroSpace Information
800 Elkridge Landing Road
Linthicum Heights, MD 21090-2934
301-621-0390

Organizations abroad should direct requests to:
National Aeronautics and Space Administration
Scientific and Technical Information Program (JTT)
International STI Program
Washington, DC 20546-0001
USA
703-271-5640

SUBJECT SCOPE

The subject scope of *STAR* and *NOVA* includes all aspects of aeronautics and space research and development, supporting basic and applied research, and applications. Aerospace aspects of Earth resources, energy development, conservation, oceanography, environmental protection, urban transportation, and other topics of high national priority are also covered.

HOW TO USE *STAR* SUBJECT CATEGORIES

Abstracts in *STAR* are categorized by 10 major subject divisions that are divided further into 76 specific subject categories. The subject divisions and categories are listed in the Table of Contents together with a note for each that defines its scope and provides any cross-references. For example:

> **16 SPACE TRANSPORTATION**
>
> Includes passenger and cargo space transportation, e.g., shuttle operations; and space rescue techniques. For related information see also *03 Air Transportation and Safety* and *18 Spacecraft Design, Testing and Performance*. For space suits see *54 Man/System Technology and Life Support.*

CROSS-REFERENCES

Individual *STAR* abstracts are not ordinarily cross-referenced, except for certain conference reports or book translations that have had separate abstracts written for their component papers or chapters. Citations and abstracts of the components follow immediately after those of the parent document. When the subject content of a component differs sufficiently from the general content of the parent, a cross-reference citation also is printed at the end of the category to which it normally would have been assigned if it were independent.

DOCUMENTS ON MICROFICHE

Documents available on microfiche are designated by a pound sign (#) following the accession number.

LIMITED REPRODUCIBILITY

A note of limited reproducibility appears in the citation, if there are factors affecting the reproducibility of more than 20% of the document. These factors include faint or broken type, color photographs, black and white photographs, foldouts, dot matrix print, or some other factor that limits the reproducibility of the document. This notation also appears on the microfiche header.

NASA PATENTS AND PATENT APPLICATIONS

Patents and patent applications owned by NASA are announced in *STAR* under appropriate subject categories and are referenced in the *STAR* indexes. In the Report Number Index, patents are indexed by the NASA Case Number, and the U.S. Patent Class. Patent applications are indexed by the NASA Case Number and the U.S. Patent Application Serial Number.

Printed copies of patents (which are not microfiched) are available for purchase from the U.S. Patent and Trademark Office.

When ordering patents, the U.S. Patent Number should be used, and payment must be remitted in advance, by money order or check payable to the Commissioner of Patents and Trademarks. Prepaid purchase coupons for ordering are also available from the U.S. Patent and Trademark Office.

NASA patent application specifications are sold in both paper copy and microfiche by the NASA Center for AeroSpace Information (CASI). The N accession number should be used in ordering either paper copy or microfiche from CASI.

The patents and patent applications announced in *STAR* are owned by NASA and are available for royalty-free licensing. Requests for licensing terms and further information should be addressed to:

National Aeronautics and Space Administration
Associate General Counsel for Intellectual Property
Code GP
Washington, DC 20546-0001

SOURCES FOR DOCUMENTS

One or more sources from which a document announced in *STAR* is available to the public is ordinarily given on the last line of the citation. The most commonly indicated sources and their acronyms or abbreviations are listed below, and their addresses are listed on page A-6. If the publication is available from a source other than those listed, the publisher and his address will be displayed on the availability line or in combination with the corporate source line.

Avail: CASI. Sold by the NASA Center for AeroSpace Information. Prices for hard copy (HC) and microfiche (MF) are indicated by a price code following the letters HC or MF in the *STAR* citation. Current values for the price codes are given in the tables on page A-7.

NOTE ON ORDERING DOCUMENTS: When ordering publications from CASI, use the N accession number or other report number. It is also advisable to cite the title and other bibliographic identification.

Avail: SOD (or GPO). Sold by the Superintendent of Documents, U.S. Government Printing Office, in hard copy.

Avail: BLL (formerly NLL): British Library Lending Division, Boston Spa, Wetherby, Yorkshire, England. Photocopies available from this organization at the price shown. (If none is given, inquiry should be addressed to the BLL.)

Avail: DOE Depository Libraries. Organizations in U.S. cities and abroad that maintain collections of Department of Energy reports, usually in microfiche form, are listed in *Energy Research Abstracts*. Services available from the DOE and its depositories are described in a booklet, *DOE Technical Information Center - Its Functions and Services* (TID-4660), which may be obtained without charge from the DOE Technical Information Center.

Avail: ESDU. Pricing information on specific data, computer programs, and details on Engineering Sciences Data Unit (ESDU) topic categories can be obtained from ESDU International Ltd. Requesters in North America should use the Virginia address while all other requesters should use the London address, both of which are on page A-6.

Avail: Fachinformationszentrum Karlsruhe. Gesellschaft für wissenschaftlich-technische Information mbH 76344 Eggenstein-Leopoldshafen, Germany.

Avail: HMSO. Publications of Her Majesty's Stationery Office are sold in the U.S. by Pendragon House, Inc. (PHI), Redwood City, CA. The U.S. price (including a service and mailing charge) is given, or a conversion table may be obtained from PHI.

Avail: Issuing Activity, or Corporate Author, or no indication of availability. Inquiries as to the availability of these documents should be addressed to the organization shown in the citation as the corporate author of the document.

Avail: NASA Public Document Rooms. Documents so indicated may be examined at or purchased from the National Aeronautics and Space Administration (JBD-4), Public Documents Room (Room 1H23), Washington, DC 20546-0001, or public document rooms located at NASA installations, and the NASA Pasadena Office at the Jet Propulsion Laboratory.

Avail: NTIS. Sold by the National Technical Information Service. Initially distributed microfiche under the NTIS SRIM (Selected Research in Microfiche) are available. For information concerning this service, consult the NTIS Subscription Section, Springfield, VA 22161.

Avail: Univ. Microfilms. Documents so indicated are dissertations selected from *Dissertation Abstracts* and are sold by University Microfilms as xerographic copy (HC) and microfilm. All requests should cite the author and the Order Number as they appear in the citation.

Avail: US Patent and Trademark Office. Sold by Commissioner of Patents and Trademarks, U.S. Patent and Trademark Office, at the standard price of $1.50 each, postage free. (See discussion of NASA patents and patent applications on page A-3.)

Avail: (US Sales Only). These foreign documents are available to users within the United States from the National Technical Information Service (NTIS). They are available to users outside the United States through the International Nuclear Information Service (INIS) representative in their country, or by applying directly to the issuing organization.

Avail: USGS. Originals of many reports from the U.S. Geological Survey, which may contain color illustrations, or otherwise may not have the quality of illustrations preserved in the microfiche or facsimile reproduction, may be examined by the public at the libraries of the USGS field offices whose addresses are listed on page A-6. The libraries may be queried concerning the availability of specific documents and the possible utilization of local copying services, such as color reproduction.

FEDERAL DEPOSITORY LIBRARY PROGRAM

In order to provide the general public with greater access to U.S. Government publications, Congress established the Federal Depository Library Program under the Government Printing Office (GPO), with 53 regional depositories responsible for permanent retention of material, inter-library loan, and reference services. At least one copy of nearly every NASA and NASA-sponsored publication, either in printed or microfiche format, is received and retained by the 53 regional depositories. A list of the regional GPO libraries, arranged alphabetically by state, appears on page A-8. These libraries are *not* sales outlets. A local library can contact a regional depository to help locate specific reports, or direct contact may be made by an individual.

PUBLIC COLLECTION OF NASA DOCUMENTS

An extensive collection of NASA and NASA-sponsored publications is maintained by the British Library Lending Division, Boston Spa, Wetherby, Yorkshire, England for public access. The British Library Lending Division also has available many of the non-NASA publications cited in *STAR*. European requesters may purchase facsimile copy or microfiche of NASA and NASA-sponsored documents, those identified by both the symbols # and * from ESA — Information Retrieval Service European Space Agency, 8-10 rue Mario-Nikis, 75738 CEDEX 15, France.

SUBMITTING DOCUMENTS

All users of this abstract service are urged to forward reports to be considered for announcement in *STAR*. This will aid NASA in its efforts to provide the fullest possible coverage of all scientific and technical publications that might support aeronautics and space research and development. If you have prepared relevant reports (other than those you will transmit to NASA, DOD, or DOE through the usual contract- or grant-reporting channels), please send them for consideration to the NASA Center for AeroSpace Information, 800 Elkridge Landing Road, Linthicum Heights, MD 21090-2934.

Reprints of journal articles, book chapters, and conference papers are also welcome. These will be considered for announcement in *STAR's* companion journal, *NOVA*.

You may specify a particular source to be included in a report announcement if you wish; otherwise the report will be placed on a public sale at the NASA Center for AeroSpace Information. Copyrighted publications will be announced but not distributed or sold.

PURCHASE OF *STAR*

STAR is publicly available on annual subscription from the NASA Center for AeroSpace Information (CASI). The 1994 subscription price of $94.00/domestic, $117.00/foreign will be applied on a prorated basis, through 1994. 1995 *STAR* subscription prices are $100.00/domestic and $125.00/foreign. Single copy prices: $33.00/domestic, $41.00/foreign.

An annual, cumulative *STAR Index* is also available at $54.00/domestic, $65.00/foreign.

STAR is available to registered users on annual subscription from the NASA Center for AeroSpace Information, ATTN: Registration Services, 800 Elkridge Landing Road, Linthicum Heights, MD 21090-2934.

ADDRESSES OF ORGANIZATIONS

British Library Lending Division
Boston Spa, Wetherby, Yorkshire
England

Commissioner of Patents and Trademarks
U.S. Patent and Trademark Office
Washington, DC 20231

Department of Energy
Technical Information Center
P.O. Box 62
Oak Ridge, TN 37830

European Space Agency-
Information Retrieval Service ESRIN
Via Galileo Galilei
00044 Frascati (Rome) Italy

Engineering Sciences Data Unit International
P.O. Box 1633
Manassas, VA 22110

Engineering Sciences Data Unit
International, Ltd.
251-259 Regent Street
London, W1R 7AD, England

Fachinformationszentrum Karlsruhe
Gesellschaft für wissenschaftlich-technische
Information mbH
76344 Eggenstein-Leopoldshafen, Germany

Her Majesty's Stationery Office
P.O. Box 569, S.E. 1
London, England

NASA Center for AeroSpace Information
800 Elkridge Landing Road
Linthicum Heights, MD 21090-2934

National Aeronautics and Space Administration
Scientific and Technical Information Program
(JTT)
Washington, DC 20546-0001

National Technical Information Service
5285 Port Royal Road
Springfield, VA 22161

Pendragon House, Inc.
899 Broadway Avenue
Redwood City, CA 94063

Superintendent of Documents
U.S. Government Printing Office
Washington, DC 20402

University Microfilms
A Xerox Company
300 North Zeeb Road
Ann Arbor, MI 48106

University Microfilms, Ltd.
Tylers Green
London, England

U.S. Geological Survey Library National Center
MS 950
12201 Sunrise Valley Drive
Reston, VA 22092

U.S. Geological Survey Library
2255 North Gemini Drive
Flagstaff, AZ 86001

U.S. Geological Survey
345 Middlefield Road
Menlo Park, CA 94025

U.S. Geological Survey Library
Box 25046
Denver Federal Center, MS914
Denver, CO 80225

CASI PRICE TABLES

(Effective August 1, 1993)

STANDARD PRICE DOCUMENTS

PRICE CODE	NORTH AMERICAN PRICE	FOREIGN PRICE
A01	$ 9.00	$ 18.00
A02	12.50	25.00
A03	17.50	35.00
A04-A05	19.50	39.00
A06-A09	27.00	54.00
A10-A13	36.50	73.00
A14-A17	44.50	89.00
A18-A21	52.00	104.00
A22-A25	61.00	122.00
A99	Call For Price	Call For Price

MICROFICHE

PRICE CODE	NORTH AMERICAN PRICE	FOREIGN PRICE
A01	$ 9.00	$ 18.00
A02	12.50	25.00
A03	17.50	35.00
A04	19.50	39.00
A06	27.00	54.00
A10	36.50	73.00

IMPORTANT NOTICE

CASI Shipping and Handling Charges
U.S.—ADD $3.00 per TOTAL ORDER
Canada and Mexico—ADD $3.50 per TOTAL ORDER
All Other Countries—ADD $7.50 per TOTAL ORDER
Does NOT apply to orders
requesting CASI RUSH HANDLING.
CASI accepts most credit/charge cards.

NASA Center for AeroSpace Information
800 Elkridge Landing Road
Linthicum Heights, MD 21090-2934
Telephone: (301) 621-0390
E-mail: help@sti.nasa.gov
Fax: (301) 621-0134

FEDERAL REGIONAL DEPOSITORY LIBRARIES

ALABAMA

AUBURN UNIV. AT MONTGOMERY LIBRARY
Documents Dept.
7300 University Dr.
Montgomery, AL 36117-3596
(205) 244-3650 Fax: (205) 244-0678

UNIV. OF ALABAMA
Amelia Gayle Gorgas Library
Govt. Documents
Box 870266
Tuscaloosa, AL 35487-0266
(205) 348-6046 Fax: (205) 348-8833

ARIZONA

DEPT. OF LIBRARY, ARCHIVES, AND PUBLIC RECORDS
Federal Documents
Third Floor State Capitol
1700 West Washington
Phoenix, AZ 85007
(602) 542-4121 Fax: (602) 542-4400, 542-4500

ARKANSAS

ARKANSAS STATE LIBRARY
State Library Services
One Capitol Mall
Little Rock, AR 72201
(501) 682-2869

CALIFORNIA

CALIFORNIA STATE LIBRARY
Govt. Publications Section
914 Capitol Mall - P.O. Box 942837
Sacramento, CA 94237-0001
(916) 322-4572 Fax: (916) 324-8120

COLORADO

UNIV. OF COLORADO - BOULDER
Norlin Library
Govt. Publications
Campus Box 184
Boulder, CO 83309-0184
(303) 492-8834 Fax: (303) 492-2185

DENVER PUBLIC LIBRARY
Govt. Publications Dept. BS/GPD
1357 Broadway
Denver, CO 80203
(303) 571-2135

CONNECTICUT

CONNECTICUT STATE LIBRARY
231 Capitol Avenue
Hartford, CT 06106
(203) 566-4971 Fax: (203) 566-3322

FLORIDA

UNIV. OF FLORIDA LIBRARIES
Documents Dept.
Library West
Gainesville, FL 32611-2048
(904) 392-0366 Fax: (904) 392-7251

GEORGIA

UNIV. OF GEORGIA LIBRARIES
Govt. Documents Dept.
Jackson Street
Athens, GA 30602
(404) 542-8949 Fax: (404) 542-6522

HAWAII

UNIV. OF HAWAII
Hamilton Library
Govt. Documents Collection
2550 The Mall
Honolulu, HI 96822
(808) 948-8230 Fax: (808) 956-5968

IDAHO

UNIV. OF IDAHO LIBRARY
Documents Section
Moscow, ID 83843
(208) 885-6344 Fax: (208) 885-6817

ILLINOIS

ILLINOIS STATE LIBRARY
Reference Dept.
300 South Second
Springfield, IL 62701-1796
(217) 782-7596 Fax: (217) 524-0041

INDIANA

INDIANA STATE LIBRARY
Serials/Documents Section
140 North Senate Avenue
Indianapolis, IN 46204
(317) 232-3678 Fax: (317) 232-3728

IOWA

UNIV. OF IOWA LIBRARIES
Govt. Publications Dept.
Washington & Madison Streets
Iowa City, IA 52242
(319) 335-5926 Fax: (319) 335-5830

KANSAS

UNIV. OF KANSAS
Govt. Documents & Map Library
6001 Malatt Hall
Lawrence, KS 66045-2800
(913) 864-4660 Fax: (913) 864-5380

KENTUCKY

UNIV. OF KENTUCKY LIBRARIES
Govt. Publications/Maps Dept.
Lexington, KY 40506-0039
(606) 257-3139 Fax: (606) 257-1563, 257-8379

LOUISIANA

LOUISIANA STATE UNIV.
Middleton Library
Govt. Documents Dept.
Baton Rouge, LA 70803
(504) 388-2570 Fax: (504) 388-6992

LOUISIANA TECHNICAL UNIV.
Prescott Memorial Library
Govt. Documents Dept.
305 Wisteria Street
Ruston, LA 71270-9985
(318) 257-4962 Fax: (318) 257-2447

MAINE

TRI-STATE DOCUMENTS DEPOS.
Raymond H. Fogler Library
Govt. Documents & Microforms Dept.
Univ. of Maine
Orono, ME 04469
(207) 581-1680

MARYLAND

UNIV. OF MARYLAND
Hornbake Library
Govt. Documents/Maps Unit
College Park, MD 20742
(301) 454-3034 Fax: (301) 454-4985

MASSACHUSETTS

BOSTON PUBLIC LIBRARY
Govt. Documents Dept.
666 Boylston Street
Boston, MA 02117
(617) 536-5400 ext. 226
Fax: (617) 267-8273, 267-8248

MICHIGAN

DETROIT PUBLIC LIBRARY
5201 Woodward Avenue
Detroit, MI 48202-4093
(313) 833-1440, 833-1409
Fax: (313) 833-5039

LIBRARY OF MICHIGAN
Govt. Documents Unit
P.O. Box 30007
Lansing, MI 48909
(517) 373-0640 Fax: (517) 373-3381

MINNESOTA

UNIV. OF MINNESOTA
Wilson Library
Govt. Publications Library
309 19th Avenue South
Minneapolis, MN 55455
(612) 624-5073 Fax: (612) 626-9353

MISSISSIPPI

UNIV. OF MISSISSIPPI
J.D. Williams Library
Federal Documents Dept.
106 Old Gym Bldg.
University, MS 38677
(601) 232-5857 Fax: (601) 232-5453

MISSOURI

UNIV. OF MISSOURI - COLUMBIA
Ellis Library
Govt. Documents
Columbia, MO 65201
(314) 882-6733 Fax: (314) 882-8044

MONTANA

UNIV. OF MONTANA
Maureen & Mike Mansfield Library
Documents Div.
Missoula, MT 59812-1195
(406)243-6700 Fax: (406) 243-2060

NEBRASKA

UNIV. OF NEBRASKA - LINCOLN
D.L. Love Memorial Library
Documents Dept.
Lincoln, NE 68588
(402) 472-2562

NEVADA

UNIV. OF NEVADA
Reno Library
Govt. Publications Dept.
Reno, NV 89557
(702) 784-6579 Fax: (702) 784-1751

NEW JERSEY

NEWARK PUBLIC LIBRARY
U.S. Documents Div.
5 Washington Street - P.O. Box 630
Newark, NJ 07101-0630
(201) 733-7812 Fax: (201) 733-5648

NEW MEXICO

UNIV. OF NEW MEXICO
General Library
Govt. Publications Dept.
Albuquerque, NM 87131-1466
(505) 277-5441 Fax: (505) 277-6019

NEW MEXICO STATE LIBRARY
325 Don Gaspar Avenue
Santa Fe, NM 87503
(505) 827-3826 Fax: (505) 827-3820

NEW YORK

NEW YORK STATE LIBRARY
Documents/Gift & Exchange Section
Federal Depository Program
Cultural Education Center
Albany, NY 12230
(518) 474-5563 Fax: (518) 474-5786

NORTH CAROLINA

UNIV. OF NORTH CAROLINA - CHAPEL HILL
CB#3912, Davis Library
BA/SS Dept. - Documents
Chapel Hill, NC 27599
(919) 962-1151 Fax: (919) 962-0484

NORTH DAKOTA

NORTH DAKOTA STATE UNIV. LIB.
Documents Office
Fargo, ND 58105
(701) 237-8886 Fax: (701) 237-7138
In cooperation with Univ. of North Dakota, Chester Fritz Library Grand Forks

OHIO

STATE LIBRARY OF OHIO
Documents Dept.
65 South Front Street
Columbus, OH 43266
(614) 644-7051 Fax: (614) 752-9178

OKLAHOMA

OKLAHOMA DEPT. OF LIBRARIES
U.S. Govt. Information Div.
200 NE 18th Street
Oklahoma City, OK 73105-3298
(405) 521-2502, ext. 252, 253
Fax: (405) 525-7804

OKLAHOMA STATE UNIV.
Edmon Low Library
Documents Dept.
Stillwater, OK 74078
(405) 744-6546 Fax: (405) 744-5183

OREGON

PORTLAND STATE UNIV.
Millar Library
934 SW Harrison - P.O. Box 1151
Portland, OR 97207
(503) 725-3673 Fax: (503) 725-4527

PENNSYLVANIA

STATE LIBRARY OF PENN.
Govt. Publications Section
Walnut St. & Commonwealth Ave. - P.O. Box 1601
Harrisburg, PA 17105
(717) 787-3752

SOUTH CAROLINA

CLEMSON UNIV.
Cooper Library
Public Documents Unit
Clemson, SC 29634-3001
(803) 656-5174 Fax: (803) 656-3025
In cooperation with Univ. of South Carolina, Thomas Cooper Library, Columbia

TENNESSEE

MEMPHIS STATE UNIV. LIBRARIES
Govt. Documents
Memphis, TN 38152
(901) 678-2586 Fax: (901) 678-2511

TEXAS

TEXAS STATE LIBRARY
United States Documents
P.O. Box 12927 - 1201 Brazos
Austin, TX 78711
(512) 463-5455 Fax: (512) 463-5436

TEXAS TECH. UNIV. LIBRARY
Documents Dept.
Lubbock, TX 79409
(806) 742-2268 Fax: (806) 742-1920

UTAH

UTAH STATE UNIV.
Merrill Library & Learning Resources Center, UMC-3000
Documents Dept.
Logan, UT 84322-3000
(801) 750-2684 Fax: (801) 750-2677

VIRGINIA

UNIV. OF VIRGINIA
Aldermman Library
Govt. Documents
Charlottesville, VA 22903-2498
(804) 824-3133 Fax: (804) 924-4337

WASHINGTON

WASHINGTON STATE LIBRARY
Document Section
MS AJ-11
Olympia, WA 98504-0111
(206) 753-4027 Fax: (206) 753-3546

WEST VIRGINIA

WEST VIRGINIA UNIV. LIBRARY
Govt. Documents Section
P.O. Box 6069
Morgantown, WV 26506
(304) 293-3640

WISCONSIN

ST. HIST. SOC. OF WISCONSIN LIBRARY
Govt. Publications Section
816 State Street
Madison, WI 53706
(608) 262-2781 Fax: (608) 262-4711
In cooperation with Univ. of Wisconsin - Madison, Memorial Library

MILWAUKEE PUBLIC LIBRARY
Documents Div.
814 West Wisconsin Avenue
Milwaukee, WI 53233
(414) 278-2167 Fax: (414) 278-2137

*U.S. GOVERNMENT PRINTING OFFICE:1994-387-253/00010

SCAN Goes Electronic!

*I*f you have NASA Mail or if you can access the Internet you can get biweekly issues of *SCAN* delivered to your desktop — absolutely *free*!

Electronic SCAN takes advantage of computer technology to alert you to the latest aerospace-related, worldwide scientific and technical information that has been published.

*N*o more waiting while the paper copy is printed and mailed to you. You can review *Electronic SCAN* the same day it is released! And you get all 191 — or any combination of — subject areas of announcements with abstracts to browse at your leisure. When you locate a publication of interest, you can print the announcement or electronically add it to your publication order list.

Electronic SCAN.
Timely.
Flexible.
Complete.
Free!

*S*tart your free access to *Electronic SCAN* today. Over 1,000 announcements of new reports, books, conference proceedings, journal articles . . . and more — delivered to your computer every two weeks.

*F*or instant access via Internet:
ftp.sti.nasa.gov
gopher.sti.nasa.gov
listserv@sti.nasa.gov

*F*or additional information:
e-mail: help@sti.nasa.gov
scan@sti.nasa.gov
(Enter this address on the "To" line. Leave the subject line blank and send. You will receive an automatic reply with instructions in minutes.)
phone: 301-621-0390
fax: 301-621-0134
write: NASA Access Help Desk
NASA STI Program
NASA Center for AeroSpace Information
800 Elkridge Landing Road
Linthicum Heights, MD 21090-2934

NASA STI PROGRAM
SCIENTIFIC &
TECHNICAL
INFORMATION

SCAN *and* Electronic SCAN *are products of the NASA Scientific & Technical Information Program.*

9/93

POSTMASTER
Address Correction Requested
(Sections 137 and 159 Post Manual)

National Aeronautics and
Space Administration
Code JTT
Washington, DC 20546-0001

Official Business
Penalty for Private Use, $300

BULK RATE
POSTAGE & FEES PAID
NASA
PERMIT No. G-27

NASA

POSTMASTER: If Undeliverable (Section 158
Postal Manual) Do Not Return

Please circulate this publication to other colleagues within your organization.

____________________ ____________________
____________________ ____________________
____________________ ____________________
____________________ ____________________
____________________ ____________________
____________________ ____________________

NASA
STI PROGRAM
SCIENTIFIC &
TECHNICAL
INFORMATION